Textbook of Echocardiography for Intensivists and Emergency Physicians

Armando Sarti
F. Luca Lorini

Editors

Second Edition

Springer

Textbook of Echocardiography for Intensivists and Emergency Physicians

Armando Sarti • F. Luca Lorini
Editors

Textbook of Echocardiography for Intensivists and Emergency Physicians

Second Edition

Springer

Editors
Armando Sarti
Rianimazione
Ospedale Santa Maria Nuova
Firenze
Italy

F. Luca Lorini
Dipartimento di Anestesia e
Rianimazione
Az. Osp. Ospedali Riuniti di Bergamo
Bergamo
Italy

Preface

The first edition of this book, *Echocardiography for Intensivists*, was published six years ago. At that time, the use of ultrasound machines was not yet a routine for many intensivists around the world. Today, many doctors, who are involved in the management of unstable or critically ill patients, are simply unable to practice without it. Echocardiography is now firmly considered to be the most useful diagnostic tool for the evaluation of patients with acute cardiovascular disorders in the ICU, the operating theatre and the emergency department. Ultrasound examination of the heart and great vessels provides reliable functional anatomy and hemodynamic assessment of the cardiovascular system. There is no alternative way to assist and guide the clinicians so that, within just a few minutes, they may understand the cause of cardiocirculatory shock and accordingly treat hemodynamic derangement at the bedside.

Today, more than 60 years after its initial conception, echocardiography is established enough to be in a widespread use even outside the cardiology unit. Ultrasound assessment of the cardiovascular system is continuously being refined according to advances in research and technology. However, the appropriate clinical application of this unique diagnostic technique in the acute setting requires specific education with constant updates and training.

The first edition of the book was developed from awareness of the need for a text specifically written for intensivists, emergency physicians and anaesthesiologist who wished to incorporate the ultrasound technique into their clinical practice. Thanks to the contributions made by all the authors, the first edition of the book has been well-received all around the world, and a Chinese language edition has also been published. This second edition has been completely revised and expanded with the aim of becoming a *Textbook of Echocardiography for Intensivist and Emergency Physicians*. Each existing chapter has been updated, with the addition of many new figures and references, and ten entirely new chapters have been added.

We wish to express our gratitude to all of the authors of both editions for their invaluable contributions, and we would also like to thank Springer for their skilful production of this textbook. Last, but not least, we are indebted to our families for their understanding and support.

Finally, we wish to dedicate our efforts to all the patients who have to face critical medical conditions and to the doctors, nurses and caregivers who do their best to provide them with the care they need.

We will feel greatly rewarded if this book helps to improve, in some way, the care of such patients.

Firenze, Italy   Armando Sarti
Bergamo, Italy   F. Luca Lorini

Contents

Part I

Ultrasound and Use of the Echo Machine

Essential Physics of Ultrasound and Use of the Ultrasound Machine

Dionisio F. Colella, Paolo Prati, and Armando Sarti

1.1 Ultrasound

Sound is a mechanical wave made up of compressions and rarefactions of molecules in a medium (solid, liquid, or gas) (Fig. 1.1).

Sounds is characterized by some parameters:

- *Frequency* is the number of cycle per unit time (1 s), measured in hertz (Hz). The higher the frequency, the better the resolution, but the lower the penetration (Fig. 1.2).
- *Period* is the duration of a cycle (the inverse of frequency).
- *Wavelength* is the distance that sound travels in one cycle. The wavelength depends on the size of the piezoelectric crystals in the transducer and the medium through which the sound wave travels (Table 1.1).
- *Amplitude* is the amount of change in the oscillating variable. Amplitude decreases as the wave travels (attenuation), leading to echoes from deeper structures being weaker
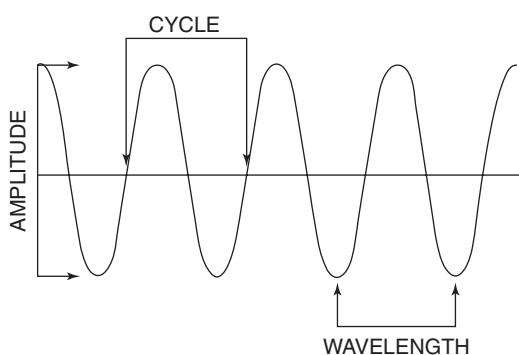
Fig. 1.1 A sound wave

than those from superficial structures. It is measured in decibels:

$$\text{Decibel}(\text{dB}) = 20\log_{10} A^2 / A_r^2,$$

where A is the sound amplitude of interest and A_r is a standard reference sound level.

- *Intensity* is the measure of the energy in a sound beam. It is related to potential tissue damage. For example, ultrasound used for lithotripsy has high intensity to fragment renal stones. It is measured in watts per square meter.
- *Power* is the amount of energy transferred. It is expressed in watts.
- The power or the intensity levels are not represented on the ultrasound machine, but there are two other variables that indirectly change those two parameters: mechanical index and

D. F. Colella (✉)
Department of Anesthesia and Intensive Care,
Tor Vergata University, Rome, Italy

P. Prati
Policlinico Tor Vergata, Rome, Italy

A. Sarti
Department of Anesthesia and Intensive Care,
Tor Vergata University, Rome, Italy

Policlinico Tor Vergata, Rome, Italy

Fig. 1.2 Relationship between transducer frequency, penetration, and wavelength. As the transducer frequency increases, resolution increases and penetration decreases
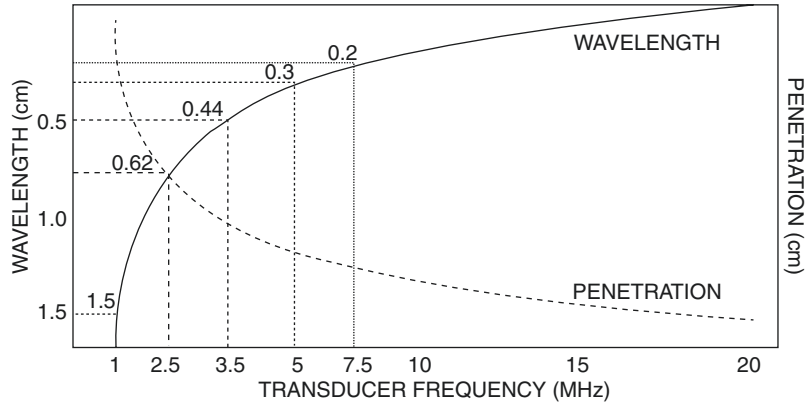
Table 1.1 Relationship between frequency and wavelength

Frequency (MHz)	Wavelength (mm)
1.25	1.2
2.5	0.60
5.0	0.30
7.5	0.20
10.0	0.15

Table 1.2 Ultrasound velocities in different mediums

Material	Velocity (m/s)
Air	330
Water	1497
Fat	1440
Blood	1570
Soft tissue	1540

thermal index. The first one represents the risk of cavitation. The second one is related to the increase of temperature of the tissues (Table 1.1, Fig. 1.2).

- *Propagation velocity* is the velocity determined by the medium that the sound passes through. It is related to the tissue's resistance to compression. Velocity is the product of frequency and wavelength. The propagation velocity through a medium is increased by increasing stiffness of the medium and is reduced by increasing density of the medium (Table 1.2).

Velocity is the product of wavelength and frequency:

$$v = \lambda \times f.$$

1.2 Interaction of Ultrasound with Tissues

1.2.1 Attenuation

When the ultrasound beam passes through uniform tissues, its energy is attenuated by dispersion and absorption.

Absorption is the conversion of ultrasound energy into heat. The attenuation coefficient relates the amount of attenuation to the frequency of the ultrasound beam and the distance that beam travels.

Dispersion occurs because of reflection, refraction, and scattering. The attenuation of the sound wave is increased at higher frequencies, so in order to have better penetration of deeper tissues, a lower frequency is used.

Attenuation involves less energy returning to the transducer, resulting in a poor image.

As the sound traveling through a tissue reaches another tissue with different acoustic properties, the sound energy can be reflected or change its direction, depending on the acoustic impedance of the second interface.

Acoustic impedance is the ability of a tissue to transmit sound and depends on:

- The density of the medium
- The propagation velocity of ultrasound through the medium:

$$Z = \rho \times v,$$

Fig. 1.3 The left ventricular wall is hidden behind a calcified posterior mitral leaflet
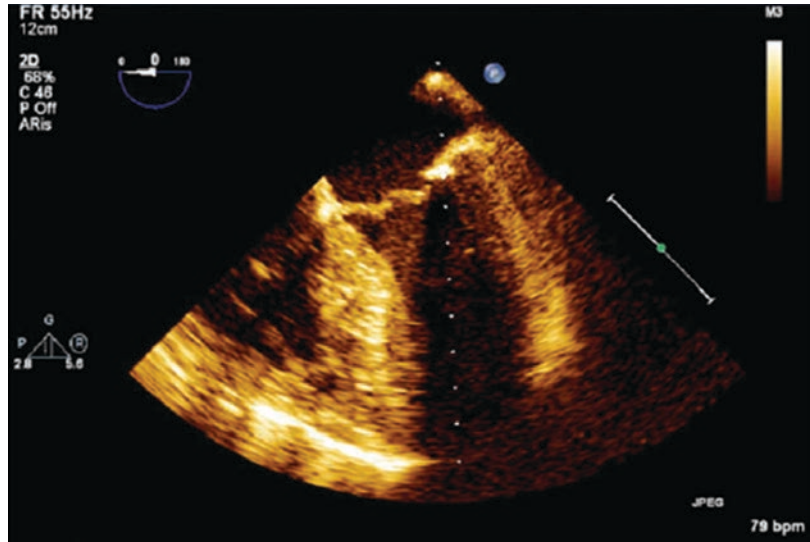
where Z is the acoustic impedance, ρ is the density of the material, and v is the speed of ultrasound.

If different mediums have a large difference in acoustic impedance, there is an acoustic impedance mismatch. The greater the acoustic mismatch, the greater the percentage of ultrasound reflected and the lower the percentage transmitted.

1.2.2 Reflection

When a sound wave reaches a smooth surface, it is reflected with an angle that is opposite the incident angle. *The more the angle is near 90°, the lower the amount of energy that is lost.*

There are two types of *reflection*:

1. *Specular* reflection
2. *Scattering* reflection

If the sound wave reaches a small and irregularly shaped surface (such as red blood cells), the ultrasound energy is scattered in all directions.

Reflection can be measured by the reflection coefficient:

$$R = \left(Z_2 - Z_1\right)^2 / \left(Z_2 + Z_1\right)^2,$$

where R is the reflection coefficient and Z is the acoustic impedance.

When the second medium encountered is a strong reflector, some phenomena can occur:

- Acoustic shadowing (Fig. 1.3)
- Reverberation (Fig. 1.4)
- A side lobe (Fig. 1.5)

1.2.3 Refraction

When a sound beam reaches the interface between two mediums, some of it is not reflected but passes through the interface, and its direction is altered. This is called refraction. The amount of refraction is proportional to the difference in the velocity of sound in the two tissues and to the angle of incidence:

$$n_1 / n_2 = \sin\theta_1 / \sin\theta_2,$$

where n is the refraction coefficient and θ is the angle of incidence.

It is possible to see some refraction artifact (Figs. 1.6 and 1.7).

Fig. 1.4 Comet tail. Mirror image: double-barred aorta
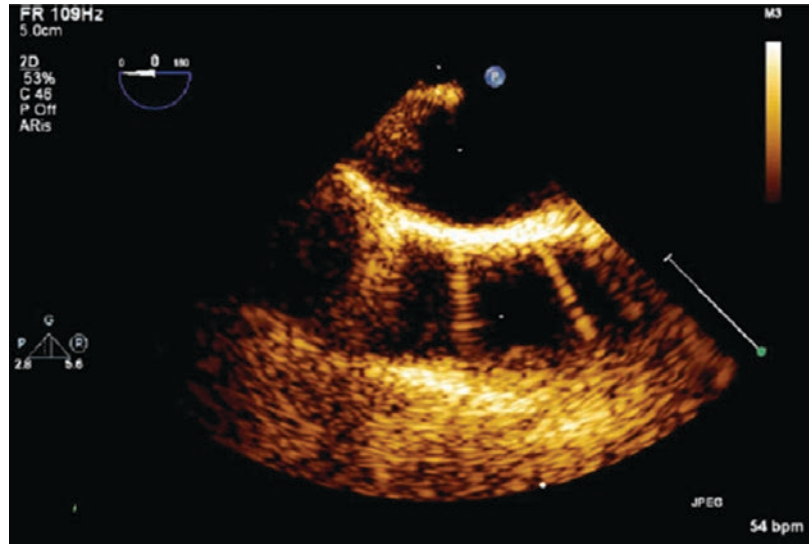
Fig. 1.5 Side lobe artifacts can create a false aortic flap
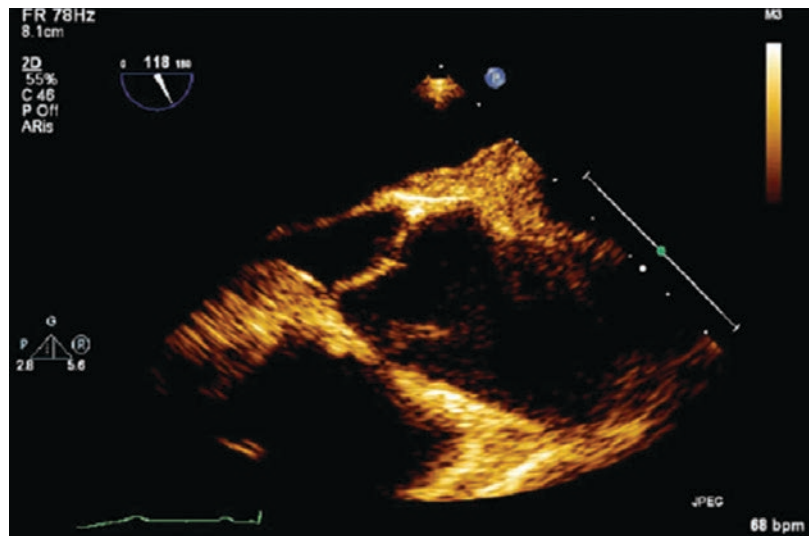
1.3 Ultrasound Wave Formation

Ultrasound waves are generated by *piezoelectric crystals*. An electrical current applied to a crystal causes vibration and consequent expansion and contraction. These changes are transmitted into the body as ultrasound waves. Modern transducers are both transmitters and receivers.

There is a strict relationship between time, distance, and velocity of ultrasound propagation.

Knowing the time required for sound to travel from the transducer to an object, the time needed for the returning echo from that object to the transducer, and the propagation velocity in that medium allows one to calculate the distance the ultrasound waves have crossed. This is the basis of ultrasonic imaging.

Electrical energy is not applied to the transducer in a continuous way: ultrasound waves are produced at regular intervals with a pulsed

Fig. 1.6 Grading lobe. The pulmonary catheter seems to be in the aorta
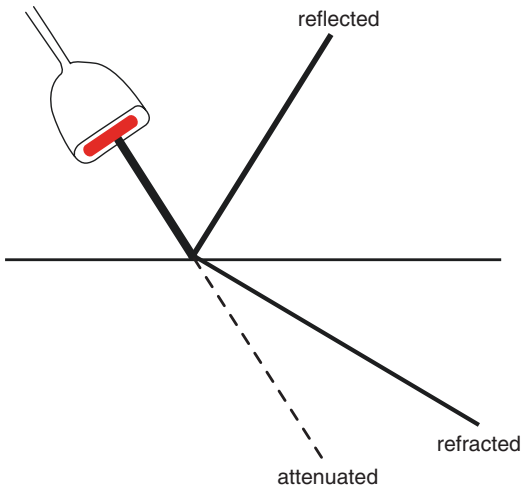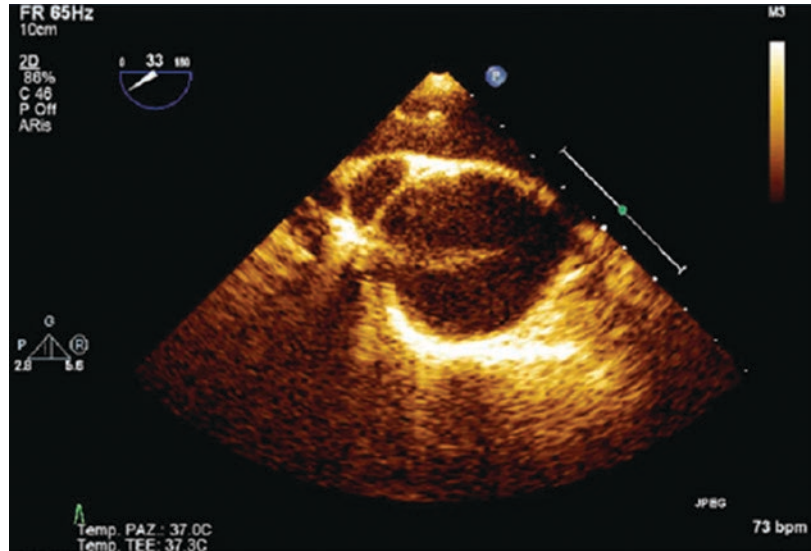
Fig. 1.7 Reflection, refraction, and attenuation

repetition period, leading to a defined *pulse repetition frequency* (PRF; in kilohertz). The wavelength of the ultrasound generated is inversely related to the thickness of the piezoelectric elements.

The piezoelectric elements cannot emit a second pulse until the first has returned to the transducer: the ability to recognize different objects is related to the frequency of emission of the ultrasound wave pulse.

The ultrasound beam emitted from the transducer has a particular shape: it begins with a narrow beam (near field), and then the ultrasound beam diverges in the far field. The length of the near field (or Fresnel zone) is related to the diameter of the transducer (*D*) and the wavelength:

$$L_n = D^2 / 4\lambda.$$

Even the angle of divergence, forming the far field (or Fraunhofer zone), is related to the diameter of the transducer (*D*) and the wavelength:

$$\sin\theta = 1.22\lambda / D.$$

The resolution is improved in the near field because of the narrower diameter of the ultrasound beam. It is easy to understand that a high-diameter transducer with high frequency (short wavelength) can produce the best ultrasound beam.

There is another way to reduce the diameter of the ultrasound beam and thus improve the resolution: focusing the beam. This produces a reduction of the beam size at a particular point, ameliorating the image.

1.3.1 Resolution

This is the ability to recognize two objects. Spatial resolution is the ability to differentiate two separate objects that are close together. Temporal resolution is the ability to place structures at a particular time.

1.3.2 Axial Resolution

This is the ability to recognize two different objects at different depths from the transducer along the axis of the ultrasound beam (Figs. 1.8 and 1.9):
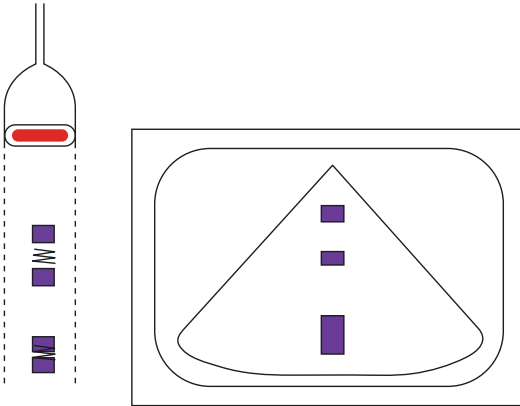
Fig. 1.8 Axial resolution. The spatial pulse length is short enough to be placed within two different structures, so they are resolved
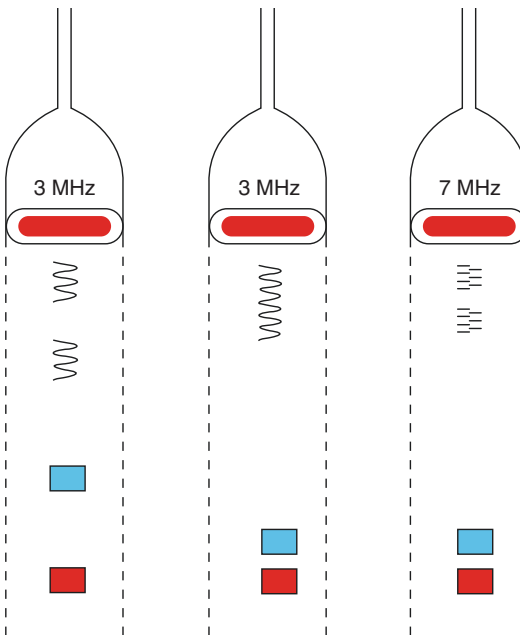
Fig. 1.9 Axial resolution and transducer frequency. Closer objects cannot be resolved by a low transducer frequency. Increasing the transducer frequency (shortening the spatial pulse length and duration) is required to resolve the objects

$$\text{Axial resolution} = \frac{\text{spatial pulse length (SPL)}}{2},$$

where SPL = λ × no. of cycles.

It is improved by higher-frequency (shorter-wavelength) transducers but at the expense of penetration. Higher frequencies are therefore used to image structures close to the transducer.

1.3.3 Lateral Resolution

This is the ability to distinguish objects that are side by side. It is dependent on the beam width because two objects side by side cannot be distinguished if they are separated by less than the beam width. It is improved by the use of higher-frequency transducer (which increases the beam width) and an optimized focal zone (Figs. 1.10 and 1.11).
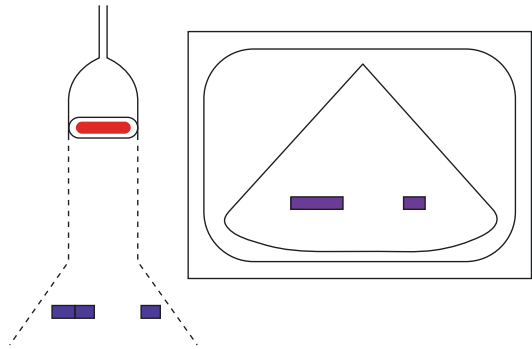
Fig. 1.10 Lateral resolution. Wider beams cannot resolve near objects
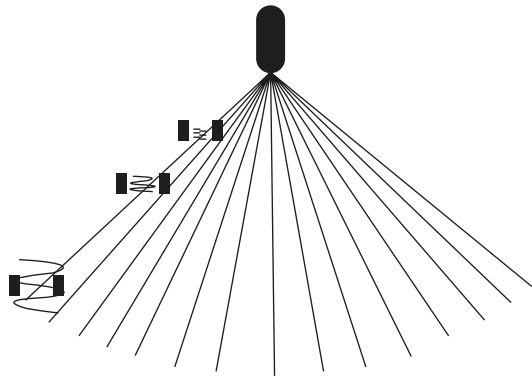
Fig. 1.11 Lateral resolution. At low depth, lateral resolution is worsened

1.3.4   Temporal Resolution

This is dependent on the frame rate. It is improved by:

- Minimizing depth—the maximum distance from the transducer as this affects the PRF
- Narrowing the sector to the area of interest—narrowing the sector angle
- Minimizing the line density (but at the expense of lateral resolution)

1.4   Doppler Echocardiography

Doppler echocardiography is a method for detecting the direction and velocity of moving blood within the heart.

The *Doppler effect* (or *Doppler shift*) is the change in frequency of a wave for an observer moving relative to the source of the wave (Fig. 1.12).

When the source of the sound wave is moving toward the observer, each successive wave is emitted from a position closer to the observer than the previous wave, and it takes less time than the previous wave to reach the observer. Then the time between the arrival of successive waves is reduced, resulting in a higher frequency. If the source of waves is moving away from the observer, the opposite effect can be seen, with increased time between the arrival of successive waves, giving them a lower frequency.

The amount of that change in frequency is the Doppler shift. Blood flow velocity (V) is related to the Doppler shift by the speed of sound in blood (C) and the intercept angle (θ) between the ultrasound beam and the direction of blood flow:

$$\text{Doppler shift} = 2 \times F\left(\text{transmitted}\right) \times \left[\left(V \times \cos\theta\right)\right] / C$$

A factor of 2 is used because the sound wave has a "round-trip" transit time to and from the transducer. If the ultrasound beam is not parallel to blood flow, an angle of incidence greater than 30° can underestimate the Doppler shift.

There are two kinds of Doppler application: pulsed-wave Doppler and continuous-wave Doppler.

In the *continuous-wave Doppler* technique, the transducer continuously transmits and receives ultrasound waves (Fig. 1.13).

The continuous-wave Doppler technique measures all velocities along the ultrasound beam. It cannot discriminate the time interval from the emission and the reflection, giving no information about the depth of the received signal. The continuous-wave Doppler technique is able to detect very high velocities, and it can be useful to evaluate the high velocity flow through a stenotic aortic valve.

In the *pulsed-wave Doppler* technique, the transducer alternately transmits and receives the ultrasound wave and its returning echo (Fig. 1.14).

Fig. 1.12 Doppler shift
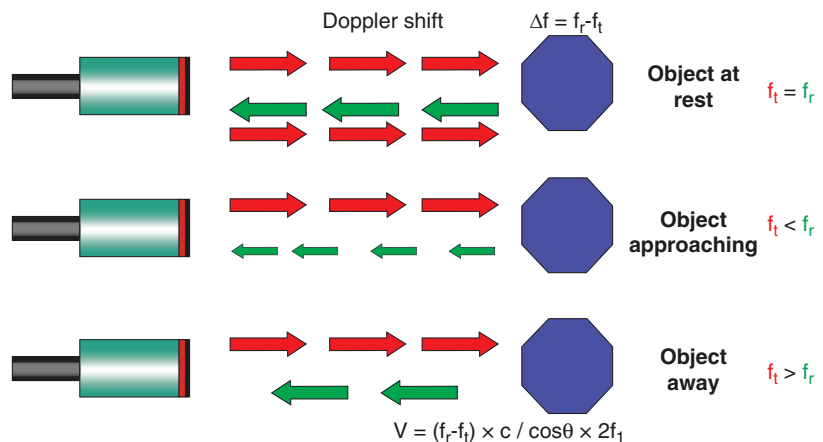
Fig. 1.13 Continuous-wave Doppler imaging
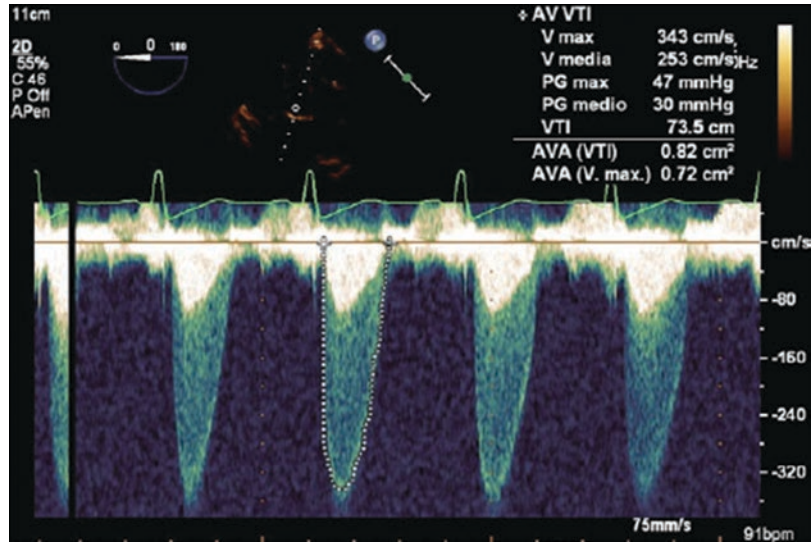
Fig. 1.14 Pulsed-wave Doppler echocardiography
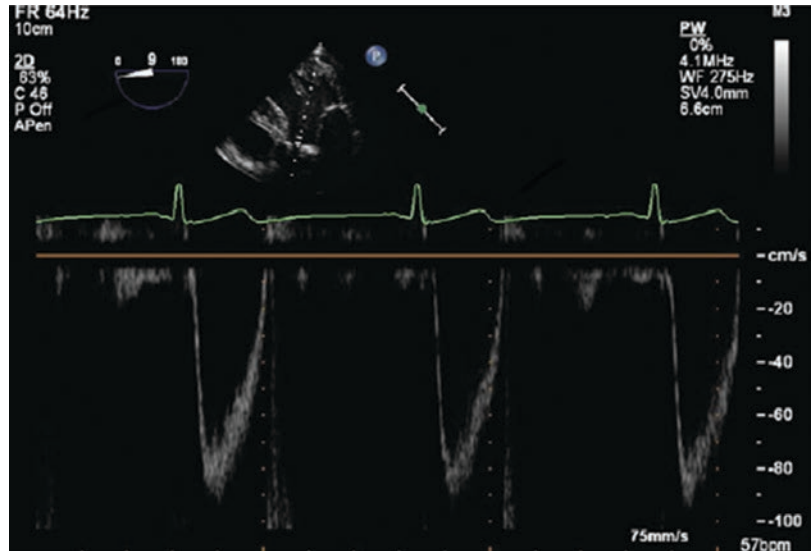
The transducer must wait for the returning echo before sending out another ultrasound wave. The pulsed-wave Doppler technique samples velocities at a specific point (sample volume) of the ultrasound beam.

The number of pulses transmitted from a Doppler transducer each second is called the pulse repetition frequency (PRF). The sampling rate determinates the acquisition of information. If the Doppler shift frequency is higher than the PRF, the Doppler signal is displayed on the other side of the baseline. This is the alias artifact.

Aliasing occurs when the measured velocity is greater than half of the PRF (Figs. 1.15 and 1.16). This velocity is called the *Nyquist limit*.

There are some ways to improve the velocity performance of the pulsed-wave Doppler technique:

1. Decrease the distance between the transducer and the sample volume. Reducing the distance the ultrasound beam has to travel will increase the frequency of emission of the pulsed wave (PRF).

Fig. 1.15 Aliasing
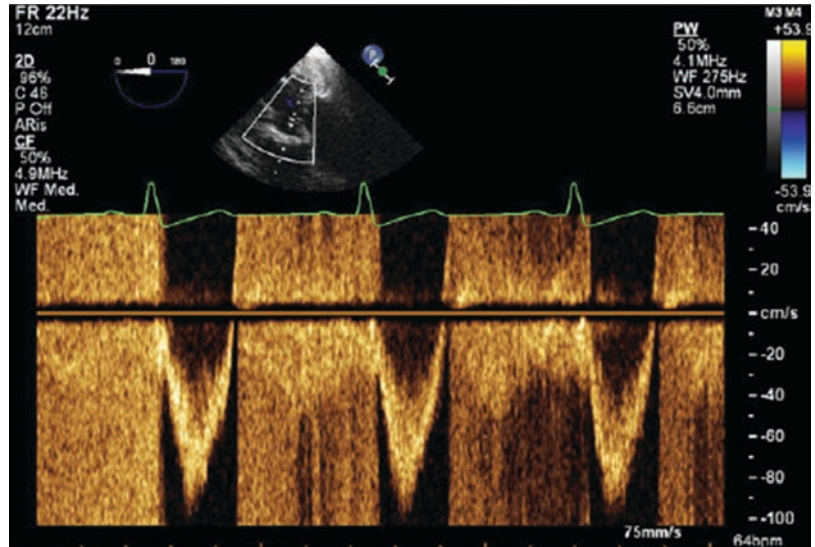
Fig. 1.16 Aliasing
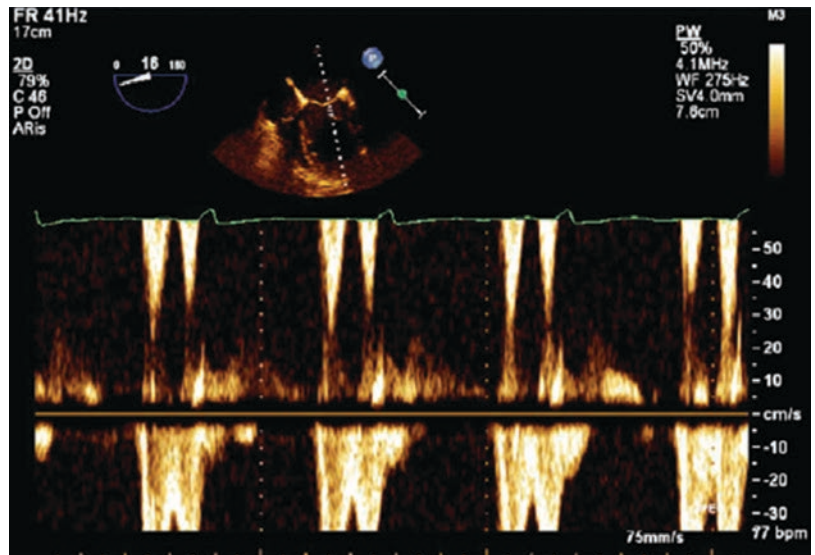
2. Choose a low frequency of emission.
3. Set the baseline to display a greater range of velocities (Fig. 1.17).

In *tissue Doppler* imaging (Fig. 1.18), a low-pass filter is used to measure only the velocity of myocardial tissues. Tissue Doppler imaging uses a small pulsed-wave sample volume showing low velocity–high amplitude signals.

Color Doppler imaging combines a 2D image with a Doppler method to visualize the velocity of blood flow within an image plane. The Doppler shift of thousands of sample volumes displays the directions of the blood cells: blue for away from and red for toward the transducer (Fig. 1.19).

High-flow velocities are displayed in yellow (toward the transducer) and cyan (away from the transducer); green is used to visualize areas of turbulence. As with the pulsed-wave Doppler technique, the color flow Doppler technique suffers from the Nyquist limit, and aliasing can occur (Fig. 1.20).

Color M-mode Doppler imaging combines the spatiotemporal graphic representation of M-mode

Fig. 1.17 Aliasing
resolved by setting the
right baseline
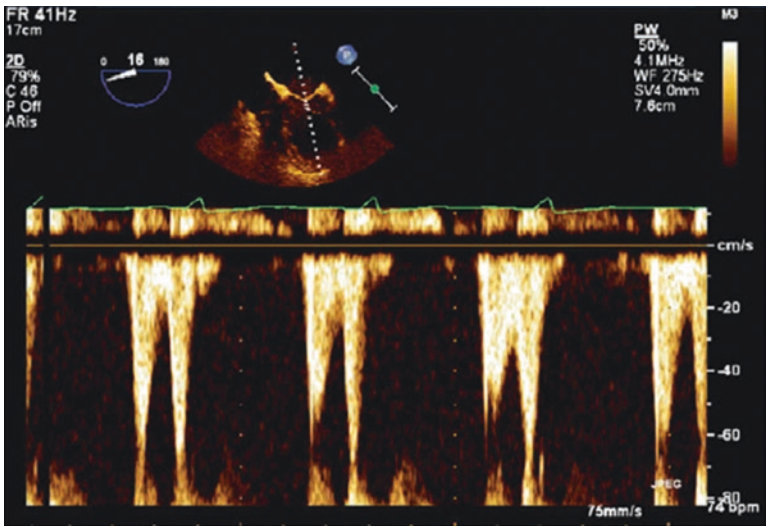
Fig. 1.18 Tissue
Doppler imaging
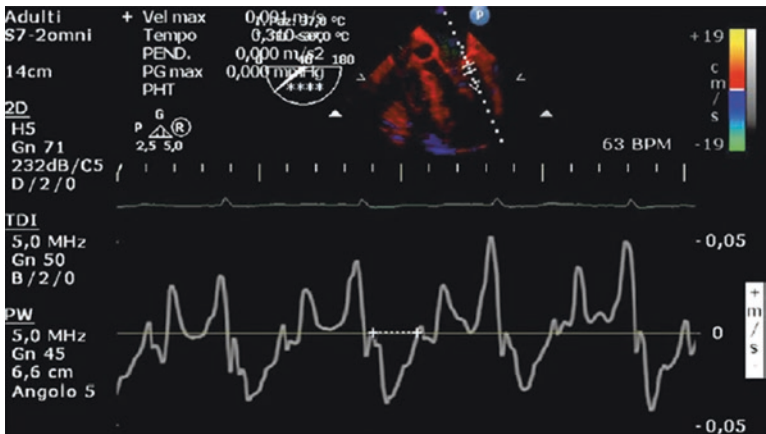
Fig. 1.19 Color
Doppler imaging. *Blue*
away from and *red*
toward the transducer
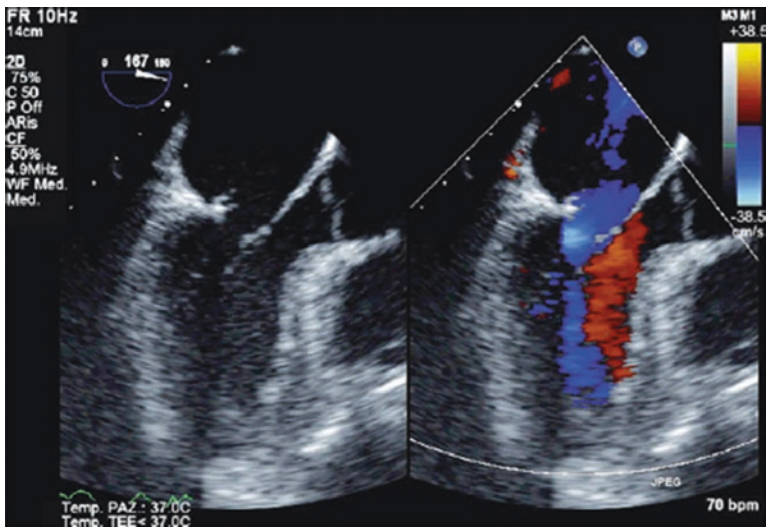
Fig. 1.20 Color Doppler aliasing
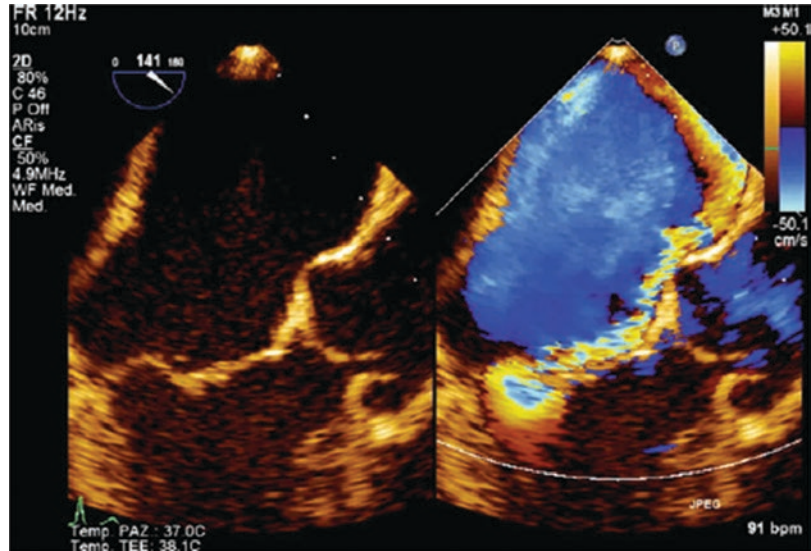
Fig. 1.21 Color M-mode imaging
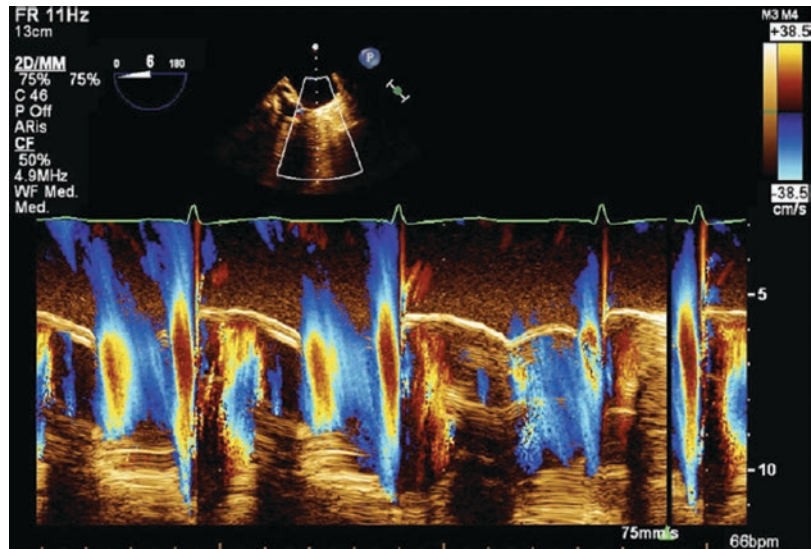
and color codification. It shows at the same time a one-dimensional view of anatomic structures and color flow visualization. It is useful to assess transmitral flow (Fig. 1.21).

lar patient to be examined. The positioning of the patient and the probe is discussed in Chap. 2, together with all transthoracic views. First, it is essential to study well the instruction manual of the device at one's disposal to use it optimally.

1.5 Use of the Ultrasound Machine: Optimizing the Picture

The image quality depends on the operator's skill and also on the adjustment of the ultrasound machine according to the features of the particu-

1.5.1 Environment

The brightness of the environment where the examination is done should be reduced. The examination is performed in the ICU at the bedside, so it is preferable to have beds that can be

easily arranged with Trendelenburg positioning, anti-Trendelenburg positioning, head and trunk lifting, and side tilting.

1.5.2 Ultrasonograph Setting

1.5.2.1 Electrocardiogram
Despite often being omitted to save time, it is important to always connect the electrocardiogram (ECG) wire of the ultrasound device to the patient electrodes. The ECG trace, recorded at the base of the display with a "marker" of time coinciding with the moving image, allows establishment of the phases of the cardiac cycle based on electrical activity of the heart, apart from monitoring the ECG. The mechanical systole usually begins immediately after the R wave and ends at about half of the T wave. The end of diastole coincides with the R-wave peak of the ECG (Fig. 1.22).

1.5.2.2 Probes
The probes used for adult echocardiography emit ultrasound with a frequency of about 3 MHz, whereas the probes used in pediatric echocardiography emit higher frequencies, from 5 to 7.5 MHz. These emissions represent the best compromise for use according to different types of patients, given that the higher the frequency, the better the image definition, but the lower the penetration of ultrasound into the tissues. Modern equipment

Fig. 1.23 Ultrasound probes. From *left* to *right*: vascular and soft tissue linear probe, cardiac phased-array probe, abdominal convex probe

can produce sharper images through "tissue harmonic imaging": in a nutshell, the harmonics produced by the interaction of the ultrasound beam with the tissues are enhanced, and the fundamental harmonic frequencies are suppressed, resulting in better far-field quality. The image quality is better, but the very echo-reflective structures, such as pericardium and valves, can thus appear thicker than they really are. The probes have a touch and often light marker, defining the scanning plane and laterality. Figure 1.23 shows the various probes used for the study of the heart with transthoracic approaches, the vessels, and the thoracic and abdominal organs.

1.5.2.3 Sector Depth
The depth can be adjusted by the operator. The machine starts with a default standard depth so that the whole heart is displayed, but the depth of the field can be varied in order to position the structures of interest in the middle of the image. If the outer edges of the heart in the default image exceed the limits of the display, the heart as a whole or some part of it is certainly enlarged.

1.5.2.4 Width of the Scanning Beam
The maximum amplitude ensures that the most lateral structures are seen, but a reduction of the amplitude may sometimes be preferable to produce greater definition of the central structures; this is because a shorter time is needed to scan a narrower angle.
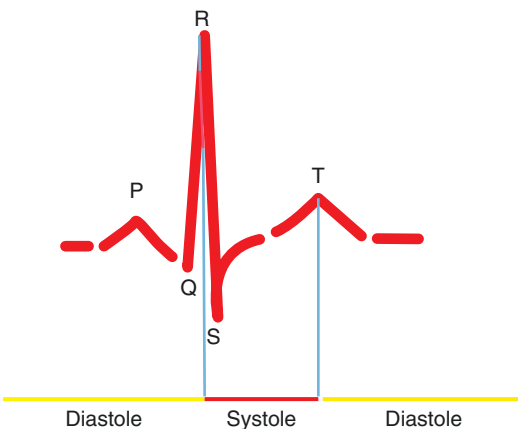
Fig. 1.22 ECG systolic and diastolic phases

1.5.2.5 Gain

The construction of the image as grayscale or monochrome images depends on the intensity of the return signal, which depends on the distance traveled and on the reflective properties of the tissues encountered (see earlier). Therefore, the gain can be adjusted for different depths in order to compensate for the reduction of the return signal. This adjustment (time gain compensation), which is automatic in modern equipment, usually occurs through a system of levers that correspond to vertical depths of the field. Observing the display as the default, the operator improves the image manually by moving the levers that correspond to different levels of depth. In some devices there is also a system of horizontal adjustment for adjusting the image in the lateral fields (lateral gain compensation). However, these adjustments must be done with care since excess gain produces brighter images, leading to poor definition between close structures and even artifacts. In contrast, too dark images are produced with not enough gain, hiding some low-echo-reflective structures. Even though it depends somewhat on operator preference, a well-adjusted image (Fig. 1.24) is one that has:

- Fairly uniform intensity of solid structures
- A slight speckling in the dark cavities full of blood

1.5.2.6 Focus

The focus of the image is usually by default in the central part of the display, but one can move the focus to higher or lower levels for further research on particular structures.

1.5.2.7 Regulating Continuous-Wave Doppler and Pulsed-Wave Doppler Imaging

As already mentioned, continuous-wave Doppler imaging is used for the measurement of high flow rate in line with the cursor all along the stream to be examined. Pulsed-wave Doppler imaging is not suitable for high-speed flows but reproduces the flow in a specific area to be examined. The operator can adjust the gain of the Doppler signal. The optimal image is one that shows well the shape of the wave flow (changes in speed over time). By convention, the blood flow movement toward the transducer is represented above the baseline. In contrast, the movement away from the transducer is represented below the baseline. The scale of reproduction of the Doppler signal (*y*-axis) can be adjusted to avoid cutting high-speed-flow waves. The speed, usually 50 mm/s (*x*-axis), can be adjusted to better fit the times for special measures. The alignment of the ultrasound beam with the flow remains paramount for both continuous-wave and pulsed-wave interrogation. An angle of more than 30° between the blood flow

Fig. 1.24 Echocardiographic image (apical five-chamber view) with good contrast adjustment
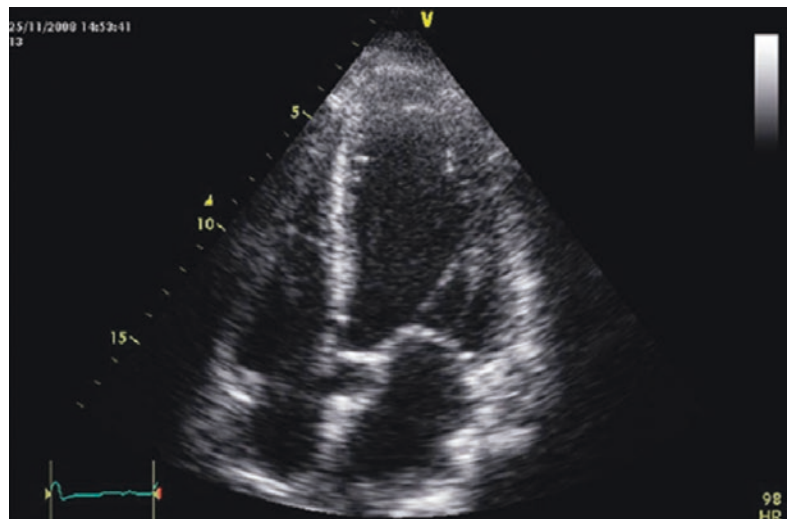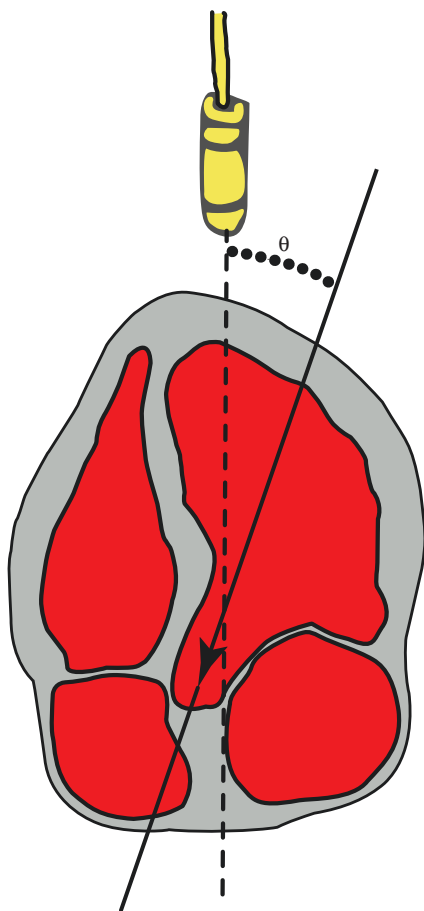
Fig. 1.25 Apical five-chamber view. Note the angle between the ultrasound beam (*dotted line*) and the blood flow through the left ventricular outflow tract (*continuous line*)

and the Doppler cursor is not considered acceptable for reliable Doppler measurements (Fig. 1.25). A previous look with color flow mapping helps to get the proper alignment. In the evaluation of valvular regurgitation flows, the cursor is placed through the narrowest part of the jet, as previously assessed by color flow mapping.

1.5.2.8 Regulating Color Doppler Imaging (Color Flow Mapping)

The assessment area is located by the operator usually using a "trackball" to reach the structures of interest. The default width, height, and gain signal of the color area can be increased or decreased by the operator. After an initial comprehensive assessment to study the various streams, the field can be narrowed to obtain better definition of the single flow to be studied. Blanking out the 2D imaging sector either side of the color sector produces a better image of the flow. The gain of the color signal can also be increased in order to define small jets, even if the excess of gain alters the image by creating artifacts. A good rule is a gain that produces a minimum of speckling in areas outside the colored stream. Some assessment techniques of valvular regurgitation such as proximal isovelocity surface area are based on the phenomenon of aliasing, and it is therefore necessary to adjust the base map of the color reproduction, represented in the display at the top right as a rectangle in two-tone red and blue scale graduation.

1.6 Artifacts

The shadow is an artifact produced as ultrasound reaches an object with high acoustic impedance. Attenuation of the acoustic beam occurs, and ultrasound will not be able to penetrate beyond the object any further. This linear hypoechoic or anechoic area covers deeper structures that cannot be visualized. Thus below the very echo-reflective object, such as a prosthetic valve or calcium deposit, little or nothing can be seen. This shadowing can be useful for the differential diagnosis between high-attenuation objects. In contrast, as ultrasound passes through an area of very low attenuation, it produces an acoustic enhancement, and structures located beneath this area appear hyperechoic. Under other conditions ultrasound can produce solid hyperechoic rebound lines which start from the echo-reflective structure and run until the end at the bottom of the image. In the chest ultrasound assessment, these reverberation artifacts, called comet tails (B lines), originate from the pleura, producing vertical hyperechoic stripes, which are used to diagnose and quantify lung water (Fig. 1.26). An area of very high acoustic impedance may also produce an acoustic mirror, which deflects the ultrasound beam to the side. The false mirror image will be deeper than the correct anatomical reflector. Reflecting structures affected by lateral

Fig. 1.26 Lung ultrasound: comet tails
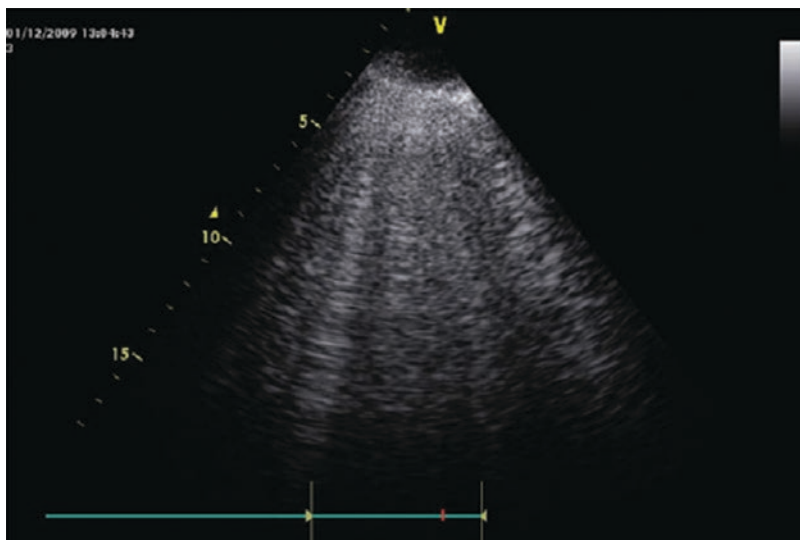
beams can also produce arcs, which appear as horizontal lines on the display. When in doubt if a structure visible in the image is an artifact, it is always useful to search for this structure using different planes since it is not likely that an artifact will be created in the same way by the ultrasound beam in different views.

Further Reading

Feigenbaum H, Armstrong WF, Ryan T. Feigenbaum's echocardiography. Philadelphia: Lippincott Williams & Wilkins; 2005.

Oh JK, Steward JB, Tajik AJ. The echo manual. 3rd ed. Philadelphia: Lippincott Williams & Wilkins; 2007.

Perrino AC. A practical approach to transesophageal echocardiography. 2nd ed. Philadelphia: Lippincott Williams & Wilkins; 2008.

Quiñones MA, et al. Recommendations for quantification of Doppler echocardiography: a report from the Doppler Quantification Task Force of the Nomenclature and Standards Committee of the American Society of Echocardiography. J Am Soc Echocardiogr. 2002;15:167–84.

Savage RM. Comprehensive textbook of intraoperative transesophageal echocardiography. Philadelphia: Lippincott Williams & Wilkins; 2004.

Part II

Standard Echocardiographic Examination

Ultrasound Morphology of the Heart: Transthoracic Examination

2

Armando Sarti, Simone Cipani, and Costanza Innocenti

2.1 Morphology Ultrasound of the Heart: Standard Transthoracic Examination

2.1.1 Echocardiographic Anatomy

The heart is located within the chest between the lungs and in front of the esophagus. From the base toward the apex, the heart is positioned:

- From top to bottom
- From back to front
- From right to left

Recalling the different structures on ultrasound images appears very complicated for the beginner operator if the various projections of the different structures are not kept in mind, according to the position of the heart within the chest under the section plane of the ultrasound scan. It

should be noted that the echo image shows a thin slice of the structures crossed by the ultrasound beam. The structures first encountered by ultrasound, near the probe, are displayed at the top corner of the image, and deeper structures are displayed proportionally lower on the screen, according to the progressive distance from the probe.

2.1.2 Patient Positioning

In the intensive care unit (ICU), it is not always possible to position the patient as desired. However, even small shifts can dramatically improve image acquisition. The patient should be kept with the trunk raised to 45° as is normally done in the ICU. The position on the left side or midway between the supine and the left lateral approach generally allows the heart to draw near to the chest wall, thus gaining the best acoustic windows. The patient's left arm must be raised and brought toward the head, so as to widen the left-sided intercostal spaces (Fig. 2.1) since the rib absorbs ultrasound. Aside from the ribs, aerated lung tissue is the major obstacle to the penetration of ultrasound. Therefore, patients with chronic pulmonary disease and emphysema are usually more difficult to study with transthoracic windows. Sometimes, for these patients, the only approach that produces clear images is the subcostal approach. If the patient does not have acoustic

A. Sarti
Department of Anesthesia and Intensive Care, Santa Maria Annunziata Hospital, Florence, Italy

S. Cipani (✉)
Department of Anesthesia and Intensive Care, Santa Maria Nuova Hospital, Florence, Italy
e-mail: simone.cipani@uslcentro.toscana.it

C. Innocenti
Department of Anesthesia and Intensive Care, Nuovo ospedale San Giovanni di Dio, Florence, Italy
e-mail: costanza.innocenti@uslcentro.toscana.it

Fig. 2.1 Position of the operator and the patient for echocardiography in the intensive care unit. (From Sarti [1] with permission)

Fig. 2.2 Position of the probe for the parasternal long-axis view. Note the probe marker. (From Sarti [1] with permission)

windows on the chest wall and if the subcostal area is not accessible, often because of the presence of surgical wound dressings, it is essential to turn to transesophageal echocardiography. Nevertheless, the skillful operator, with a little patience, is almost always able to get acceptable and usable transthoracic echocardiographic images for most patients even in the emergency and intensive care settings. Depth, size, and gain settings must be adjusted frequently during the examination to get the best possible ultrasound imaging. Zoomed images are better for precise quantitative measuring. During 2D, CFM, and Doppler examinations, the gain should be increased to the point that it generates background noise and then decreased to the level that produces optimal imaging.

Fig. 2.3 Position of the probe for the apical four-chamber view. Note the probe marker. (From Sarti [1] with permission)

2.1.3   Positioning of the Probe (Acoustic Windows)

The probe, with a stream of acoustic gel at the end, is held not too tightly between the thumb and first two fingers of the gloved right hand, while maintaining contact with the chest wall with the other fingers, without causing pain or discomfort from excessive pressure, in two main locations:

1. *Left parasternal* at the second to fourth intercostal spaces (Fig. 2.2)

2. *Around the area of the apical beat*, at the fifth or sixth intercostal space along the anterior axillary line or more laterally (Fig. 2.3)

Another possible transthoracic location is parasternal right, which is used either in pediatrics or to assess the aortic valve (see Chap. 23).

The other basic positions of the probe, outside the chest wall, are:

- *Subcostal* central level, just below the xiphoid process (Fig. 2.4)
- *Suprasternal* level, at the jugular notch (Fig. 2.5)

Fig. 2.4 Position of the probe for the subcostal views. (From Sarti [1] with permission)

Fig. 2.5 Position of the probe for the suprasternal views. (From Sarti [1] with permission)

2.1.4   Positioning of the Operator and the Ultrasound Machine

Most operators stay at the right side of the patient and keep the probe in the right hand. Others prefer to set themselves at the patient's left, holding the probe with the left hand, thus avoiding much contact with the patient's body. In any case, the position must be convenient, stable, and relaxed. Sitting is comfortable, but it is sometimes necessary to stand, lean, or even sit on the edge of the patient's bed; in this case a disposable gown should be worn. The ultrasound machine is usually placed to the right side of the patient's head, so that only small movements of the opera-

tor's head are needed to shift from the patient to the display and vice versa. In this arrangement the left hand is used to operate the controls. It is always useful to keep in mind the ultrasound section plane within the chest before looking at the images. The movement of the probe, as positioning, pointing, angling, or rotation (see Table 2.1), should be regulated while always considering what happens to the section plane inside the thorax.

2.1.5   Parasternal Long-Axis View

This is a longitudinal section of the heart (Fig. 2.6). The probe is in the left parasternal position, and the marker is placed toward the right shoulder (Fig. 2.2). Initially, instead of insisting on a single point, different intercostal spaces should be tried, sliding from the second to the fourth, sometimes down to the fifth, to find the best acoustic window. The proper image is a section that shows part of the right ventricle, the septum, in a more or less horizontal position which continues toward the aortic upper wall. Below it the aortic valve and the left atrium are on the right side of the display. The left ventricle is found in the center (Figs. 2.6 and 2.7). If more than one intercostal space allows one to obtain valid images, it is often preferable to use higher spaces. The parasternal long-axis view is usually the first image sought at the beginning of the examination since it highlights many structures and provides a first general idea of the heart. Positioning the cursor on the basis of the 2D image, one can obtain M-mode echograms, which are useful for measuring the size of the cardiac chambers and the thickness and the kinetics of the anterior septum (anterior descending artery) and the posterior wall (circumflex and right coronary arteries to the apex). The diameter of the left ventricular outflow tract is also measured during the systole just before the fully opened aortic cusps. The functional anatomy of aortic and mitral valves can be studied, including forward flow and any possible regurgitation, with color Doppler imaging (color flow mapping, CFM). Continuous-wave and pulsed-wave trans-

Table 2.1 Standard views, landmarks, rotation, and angling of the probe (structures and measures)

View	Probe position	Probe marker	Probe rotation	Probe angulation	Structures	Measurements
PSLAX	Parasternal second to fourth intercostal space	Right shoulder	–	Variable	Left ventricle (except apex), LV septal and posterior walls, mitral and aortic valves, mitral subvalvular structures, LA, ascending aorta, RV outflow tract	LV and RV size and thickness, LV and RV kinetics, LV outflow tract and ascending aorta sizes, CFM of mitral and aortic flows
PSLAX modified for right ventricle (tricuspid plane)	Parasternal second to fourth intercostal space	Right shoulder	Slightly clockwise	Inferomedial tilting from PSLAX	RV inflow, RA, tricuspid valve	CFM, PW, and CW Doppler imaging of transtricuspid flow
PSLAX modified for right ventricle (pulmonary valve)	Parasternal second to fourth intercostal space	Right shoulder	Slightly clockwise	Upward tilting from PSLAX-modified RV tricuspid plane	RV outflow, pulmonary valve	CFM, PW, and CW imaging of transpulmonary flow, pulmonary VTI
PSSAX papillary muscle plane	Parasternal second to fourth intercostal space	Left shoulder	90° clockwise from PSLAX	–	LV and RV sizes, LV walls, papillary muscles	LV and RV kinetics, FS, FAC
PSSAX mitral plane	Parasternal second to fourth intercostal space	Left shoulder	90° clockwise from PSLAX	Upward tilting from PSSAX papillary muscles	Mitral valve, let ventricle, and LV sizes	Mitral valve (P1, P2, P3 and A1, A2, A3), mitral area, LV and RV kinetics
PSSAX aortic plane	Parasternal second to fourth intercostal space	Left shoulder	90° clockwise from PSLAX	Upward tilting from PSSAX mitral plane	Aortic, tricuspid, and pulmonary valves, RV outflow, pulmonary trunk	Aortic valve (all cusps), aortic valve area, CFM and PW transpulmonary Doppler imaging
A4C	Apical fourth to sixth intercostal space along the left mid-clavicular or anterior axillary line (apical beat)	Left leg	–	–	Global vision of the heart, left ventricle, right ventricle, LA, RA, LV septal and lateral walls, RV free wall, mitral and tricuspid valves	LV and RV kinetics, EF, TAPSE, CFM, PW and CW transvalvular mitral and tricuspid flows, pulmonary pressure assessment
A5C	Apical fourth to sixth intercostal space along the left midclavicular or anterior axillary line	Left leg	Variable	Upward tilting	Global vision of the heart plus aortic outflow valve and ascending aorta	CFM, CW, and PW Doppler imaging of LV outflow, VTI
A2C	Apical fourth to sixth intercostal space along the left midclavicular or anterior axillary line	Right shoulder	90° counterclockwise from A4C	–	LV, LA, LV inferior and anterior walls, mitral valve	LV kinetics, EF, CFM, CW, and PW Doppler imaging of transmitral flow

View	Probe position	Probe marker	Probe rotation	Probe angulation	Structures	Measurements
A3C	Apical fourth to sixth intercostal space along the left mid-clavicular or anterior axillary line	Right hand	45° counterclockwise from A2C	–	Left ventricle, LA, mitral valve, LV anteroseptal and posterior walls	LV kinetics, CFM, CW, and PW Doppler imaging of transaortic flow, VTI
SC4C	Subcostal	Left shoulder	Variable	Variable	Global vision of the heart, left ventricle, right ventricle, LA, RA, LV septal and posterolateral walls, interatrial septum, liver, and intrahepatic veins	LV and RV kinetics, possible interatrial shunt
Subcostal abdominal aorta	Subcostal	Left shoulder	Variable	Downward from SC4C	Abdominal aorta	Aortic diameter
Subcostal RV and LV outflows	Subcostal	Left shoulder	Variable	Upward from SC4C	LV and RV outflow	CFM, CW, and PW imaging of LV and RV outflows (if in line)
Subcostal IVC	Subcostal, shifted a little to the left from SC4C	Left shoulder or head	Variable	Leftward tilting	IVC, RA	IVC diameter and respiratory variations
Subcostal short axis	Subcostal	Left shoulder	Variable	90° counterclockwise from SC4C	LV and RV short axis, LV and RV kinetics	–
Subcostal apical short axis	Subcostal	Left shoulder	Variable	Right tilting	LV apex	–
Subcostal basal short axis	Subcostal	Left shoulder	Variable	Left tilting	Basal LV and RV short axis	–
Suprasternal	Jugular notch	Left shoulder	Variable	Variable	Ascending aorta and aortic arch	Aortic diameter

PSLAX parasternal long axis, *RV* right ventricular, *PSSAX* parasternal short axis, *A4C* apical four chamber, *A5C* apical five chamber, *A2C* apical two chamber, *A3C* apical five chamber, *SC4C* subcostal four chamber, *IVC* inferior vena cava, *LV* left ventricular, *LA* left atrium, *RA* right atrium, *CFM* color flow mapping, *PW* pulsed wave, *CW* continuous wave, *VTI* velocity–time integral, *FS* fractional shortening, *FAC* fractional area change, *EF* ejection fraction, *TAPSE* tricuspid annular plane systolic excursion

valvular flow measurements are not possible since the blood flows more or less perpendicular to the ultrasound beam. Except for the outflow part of the right ventricle, the right side of the heart is not generally visible. However, a broader view of the right atrium, the tricuspid valve, and the inflow tract of the right ventricle can be obtained by angling the probe down under the sternum and a fraction more medial, with a slight clockwise or, more rarely, counterclockwise rota-

tion (Fig. 2.8), whereas an upward (cranial) angling and slight clockwise rotation from the basic parasternal long-axis view may show the right ventricular outflow tract with the pulmonary valve and the pulmonary trunk (Fig. 2.9).

2.1.6 Parasternal Short-Axis View

The probe remains in the same position as shown to obtain the parasternal long-axis view but is rotated 90° clockwise with the marker now pointing to the left shoulder in order to obtain a cross section of the heart (Fig. 2.10). The image shows the left ventricle as a ring, more or less thick according to the thickness of the walls, with a section of the right ventricle that presents itself as a cap attached to the left ventricle by the septum, on the upper left of the display (Fig. 2.11). We must aim to produce a well-shaped circular section, avoiding oblong or oval images of the left ventricle. The assessment of the left ventricular kinetics is best performed in a plane that highlights the sections of the largest section of the papillary muscles inside the ventricular cavity (Fig. 2.12). This section examines all the walls of the left ventricle, which thickens and moves toward the center in systole, with visibility of the myocardial tissue perfused by all three major coronary trunks. The upper part of
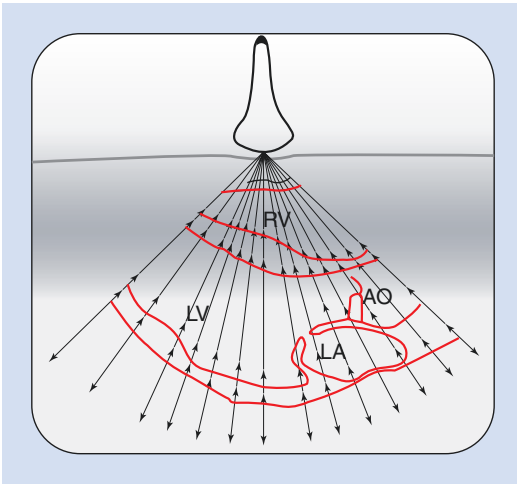
Fig. 2.6 Section plane and ultrasound beam for the parasternal long-axis view. *AO* aorta, *LA* left atrium, *LV* left ventricle, *RV* right ventricle. (From Sarti [1] with permission)

Fig. 2.7 Parasternal long-axis view
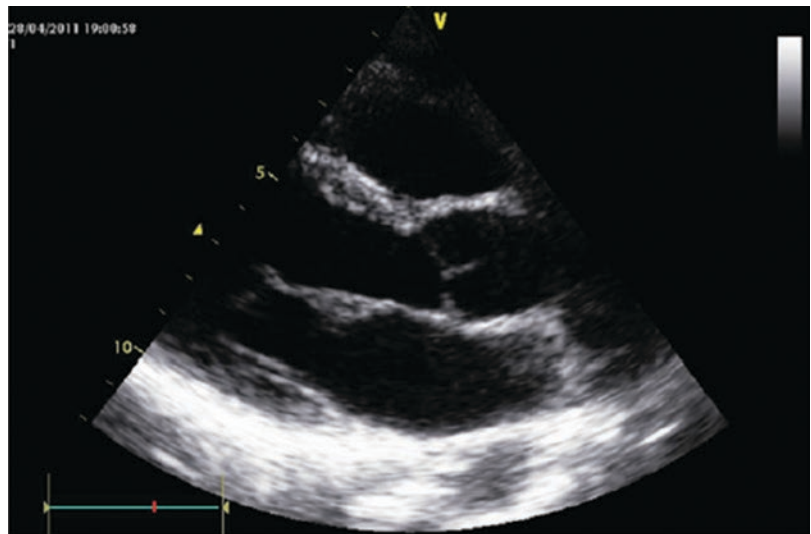
Fig. 2.8 Parasternal long-axis view modified for the right ventricular inflow tract
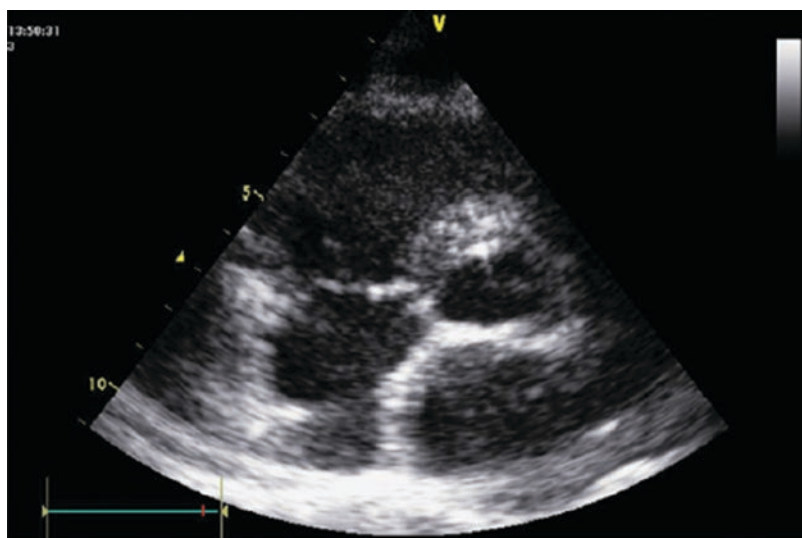
Fig. 2.9 Parasternal long-axis view modified for the right ventricular outflow tract and the right pulmonary artery. *RV* right ventricle
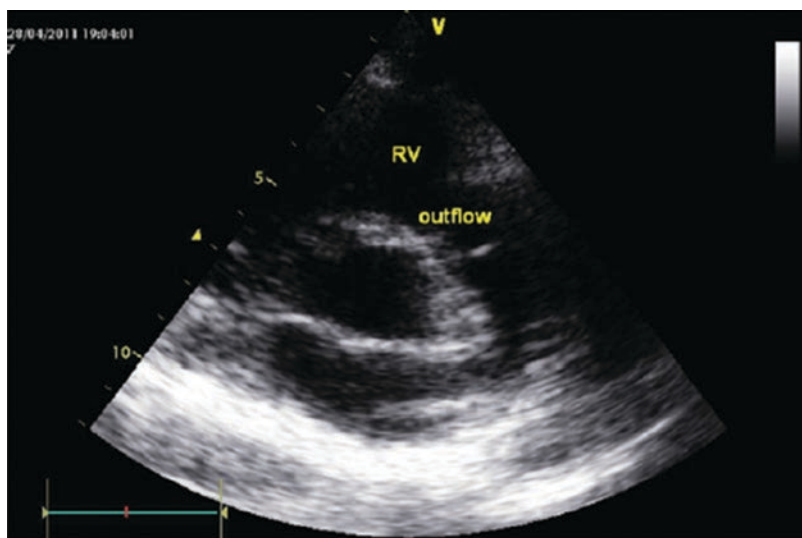
the ring, starting at the eight o'clock to ten o'clock position to the two o'clock position, is attributable to the anterior descending artery. The tissue on the right side of the ventricular ring, from the two o'clock position to the six o'clock to seven o'clock position, coincides with the circumflex artery perfusion, and the bottom of the ring, shifted slightly to the left of the image, from the six o'clock to seven o'clock position to the eight o'clock to ten o'clock position, represents the myocardium perfused by the right coronary artery.

Downward (caudally) angling of the probe shows the base of the papillary muscles and then the apex of the left ventricle. An upward angulation (cranial) of the probe moves instead of the section plane to cross the mitral valve, which is cut through the opening and closing motion (Fig. 2.11). A further upward angulation (Fig. 2.13) shows a central section of the aortic outflow with the valve (the aortic box, shaped as a "Mercedes star") and its three moving cusps. On the left, the tricuspid valve and the right outflow can be seen, with the pulmonary valve and

Fig. 2.10 Probe position for the parasternal short-axis view and the section line of the marker. (Modified from Sarti [1] with permission)

Fig. 2.11 Parasternal short-axis view at the level of the mitral valve (diastole)
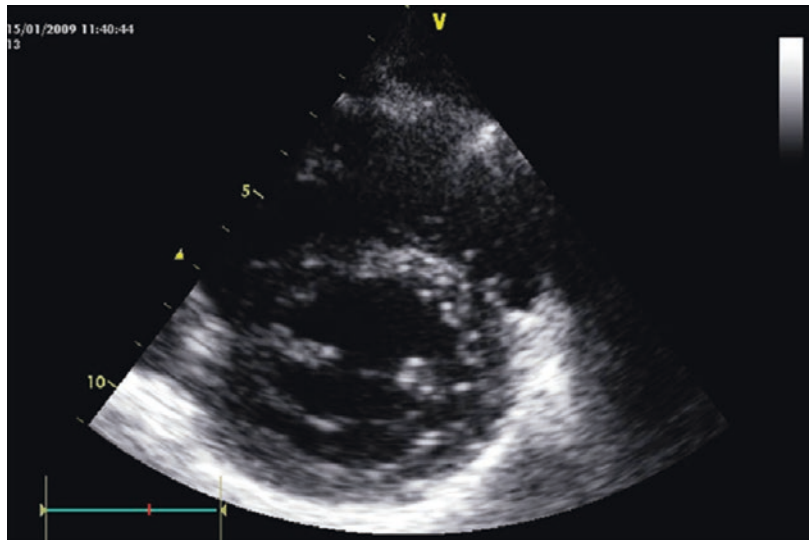
the pulmonary trunk at the top of the image, above the aortic valve.

Sweeping with the probe, from an upward left side angle progressively down toward the right side, shows the various sections in succession with the structures from the base toward the apex of the heart.

2.1.7 Right Parasternal View

The probe is placed on the right side of the sternum, at the third intercostal space or one intercostal space above or below. This view is used to get a better image of the aortic valve and to measure transaortic blood flow in line with the ultra-

Fig. 2.12 Parasternal short-axis view at the level of the papillary muscles
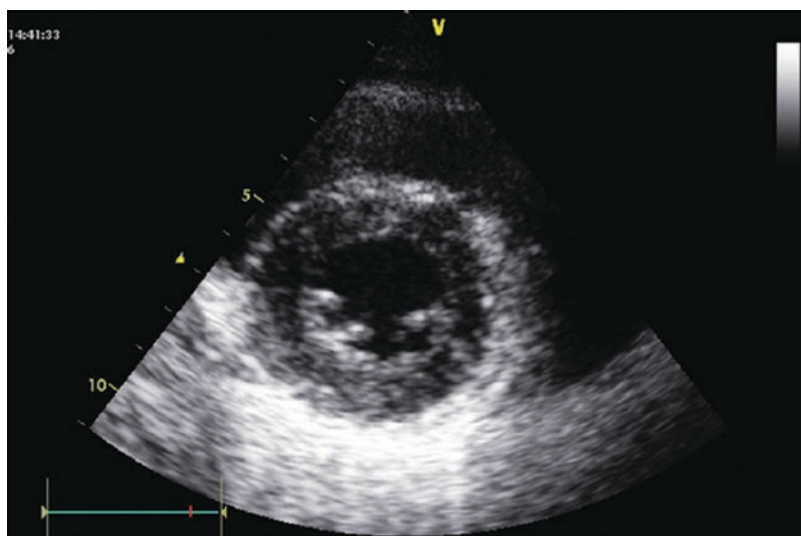
Fig. 2.13 Parasternal short-axis view at the level of the aortic valve ("Mercedes sign" in diastole) and right ventricle
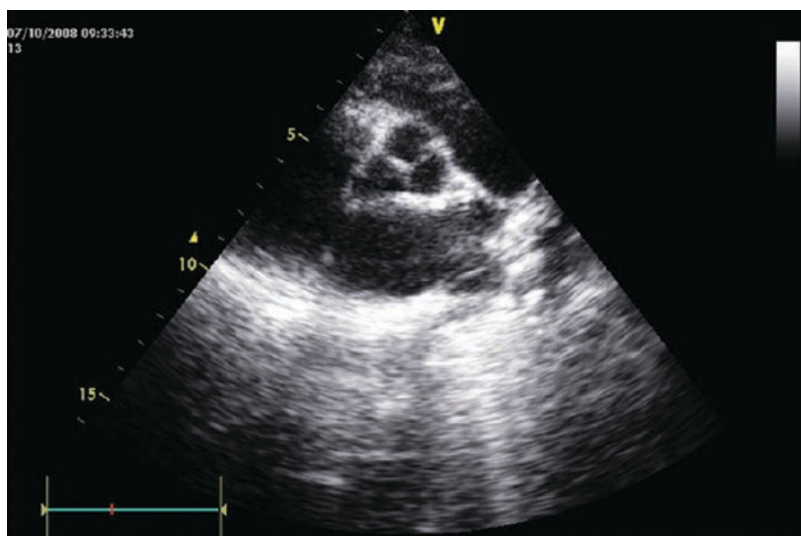
sound beam. To bring the aorta forward near the anterior thoracic wall, the patient is rolled on to the right side. The 2D image shows the aortic valve and the ascending aorta. CFM can be used as a guide to place the cursor along the transaortic flow for continuous-wave Doppler interrogation. In pediatric practice, a high right parasternal view with the marker pointing at the left leg enables examination of the right atrium, superior vena cava, and left atrium. The right pulmonary artery and upper right pulmonary vein may also be visible.

2.1.8   Apical Four-Chamber View

The probe is placed in the area of the apical cardiac beat with the marker pointing toward the left hand (raised to the head) of the patient (Fig. 2.14). The probe is slid up and down and to the side in the search for an image that dissects the heart into its four chambers with the interventricular septum in the middle; the apex at the top; the left ventricle, with its normal rugby ball shape, on the right side; and the right ventricle, with its triangular shape, on the left of the display (Fig. 2.15).

This image shows the left ventricular septal and lateral walls. Toward the bottom of the image, the atrial septum can be seen, with the two atrioventricular valves horizontal, the mitral valve on the right and the tricuspid valve on the left. The atrial chambers, the left chamber on the right and right chamber on the left, take up the bottom of the image. The bottom right of the image often reveals one or two pulmonary veins draining into the left atrium.

Small movements and small changes of angles are made to try and obtain the maximum possible length of the left ventricle and evidence of both endocardial and epicardial edges of the apex. The apex thickens in systole but does not move toward the base of the heart. If the image shows that the apex actually moves toward the atrioventricular valves, the section plane is not correct.

This view is used for various measurements, including ejection fraction, septal kinetics (right coronary artery for a short distance baseline and anterior descending artery up to the apex), and lateral wall kinetics (circumflex artery) of the left ventricle, kinetics and measurements of the right ventricle, and the morphological and Doppler study of the valves and transvalvular flows.

2.1.8.1 Apical Five-Chamber View

From the position for the apical four-chamber view, the probe is angled up slightly and sometimes rotated a little to highlight the left ventricular outflow tract (fifth chamber) with the aortic valve. This apical five-chamber view (Fig. 2.16) is used to evaluate the aortic outflow chamber and the flow toward the aorta or an aortic regurgitation because of good alignment of the ultrasound beam and thus reliable Doppler measurements.

2.1.8.2 Apical Two-Chamber View

From the position for the apical four-chamber view, the probe is rotated about 90° counterclockwise, resulting in a section plane perpendicular to the four-chamber view. Sections of the right side of the heart disappear, and only the left

Fig. 2.14 Probe position for the apical four-chamber view and the section plane. (Modified from Sarti [1] with permission)

Fig. 2.15 Apical four-chamber view
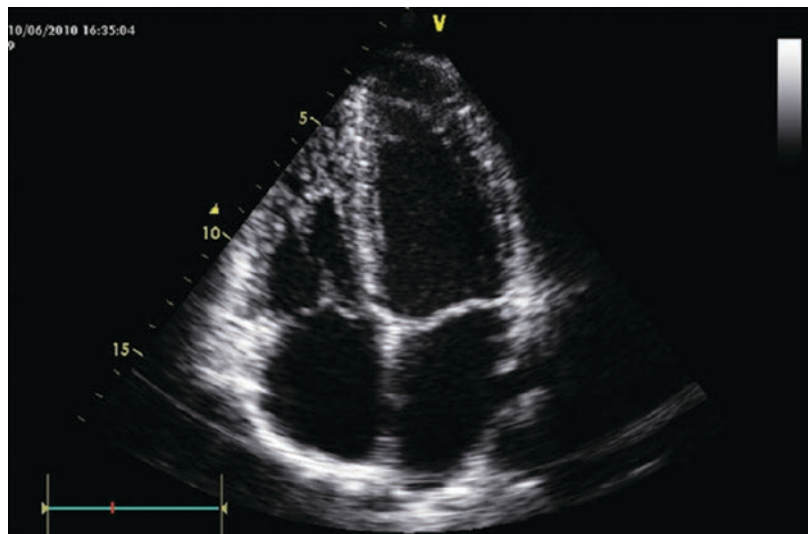
Fig. 2.16 Apical five-chamber view. (From Sarti [1] with permission).
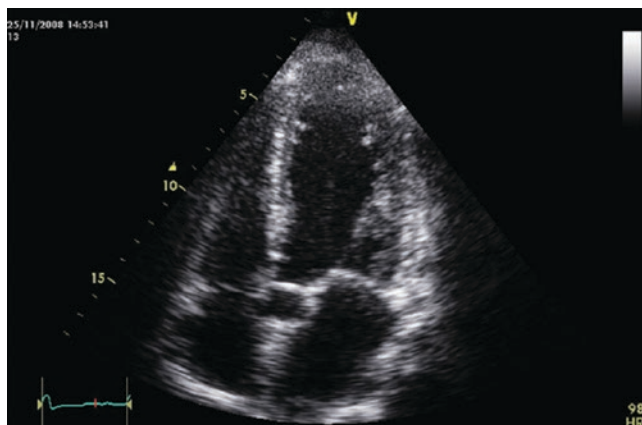
Fig. 2.17 Apical two-chamber view
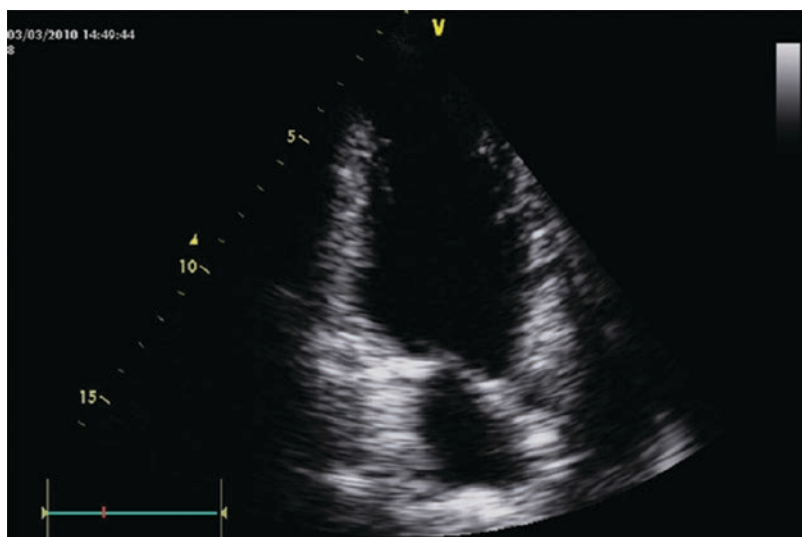
side of the heart is now visible. The left atrium is at the bottom of the image and the left ventricle is at the top, with the mitral valve in between the two (Fig. 2.17).

The inferior wall of the left ventricle (right coronary artery from the base to the top of the apex) is on the left side of the image, and the anterior wall is on the right side (anterior descending artery).

For the biplane method, the left ventricular measurement of the ejection fraction, already done in the apical four-chamber view, is repeated in the apical two-chamber view. The mitral valve is examined in the apical two-chamber view with

another plane and at a different level in relation to the apical four-chamber view.

2.1.8.3 Apical Three-Chamber View

Further rotation of the probe, approximately 45° counterclockwise from the position for the apical two-chamber view, still shows the left ventricle and left atrium (Fig. 2.18). Furthermore, on the right of the display, the left ventricular outflow tract can be seen (third chamber). This section is similar to the parasternal long-axis view but is oriented with the apex at the top and the base of the heart at the bottom. However, in contrast to the apical three-chamber view, the
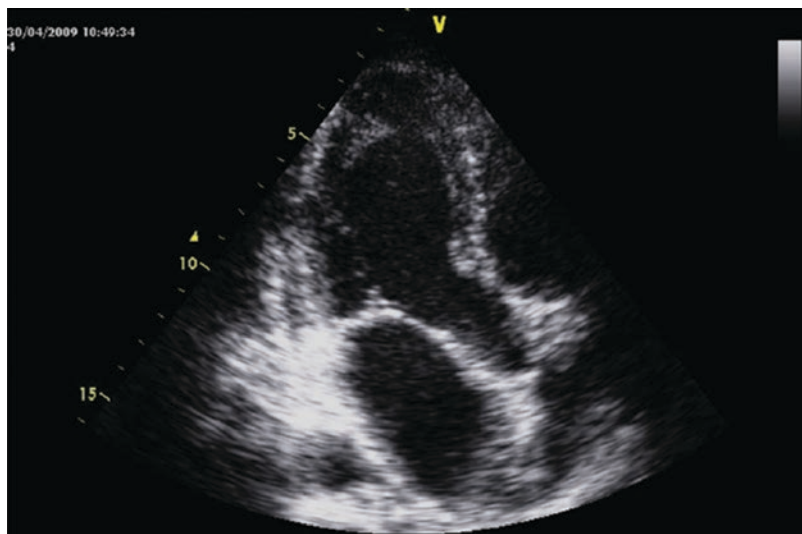
parasternal long-axis view does not normally show the apex. The anteroseptal wall of the left ventricle is on the right, and the posterior wall is on the left.

2.1.9 Subcostal View

This fundamental projection must never be omitted, particularly in emergency and intensive care practice. In patients on mechanical ventilation or with emphysema and in cases where the patient cannot be moved to the side, the subcostal approach may be the only approach which allows assessable images to be obtained. The patient lies in the supine position with the trunk raised to 45°, the knees bent, and the hips flexed slightly to relax the abdominal wall. The probe, held flat with the thumb and forefinger of the right hand, is placed under the xiphoid process (Fig. 2.4), with the marker toward the left shoulder and a variable angle, moving slightly left or right of the midline, in the search for a subcostal four-chamber view (Fig. 2.19). The liver, with its characteristic echo structure, is the essential reference. The right side of the heart is placed at the top of the image, and the left side is placed at the bottom. The observable walls of the left ventricle are the septal and posterolateral walls. The interatrial septum is seen here in its full length with good definition of the thin foramen ovale. Any possible shunt through the open foramen ovale can be studied with this approach with CFM and pulsed-wave imaging. A right-to-left shunt can also be demonstrated with the microbubble contrast produced by the quick injection of agitated saline into a vein, flowing from the right atrium to the left atrium.

A greater upward angulation of the probe shows the outflow of the left ventricle and the structures of the right side of the heart with the inflow and outflow of the right ventricle and valves. In contrast, angling the probe downward toward the abdomen may show the abdominal aorta. A shift of the probe to the left, toward the right side of the patient, brings out the inferior cava vein and hepatic veins, which enter horizontally into the right atrium (Fig. 2.20). The size of the inferior cava vein and the respiratory changes of its caliber provide information on the venous filling and blood volume of the patient. In this view, the intrahepatic veins run vertically down to reach the inferior vena cava in line with the ultrasound beam. Thus, pulsed-wave Doppler echocardiography can be used to show venous intrahepatic blood flow.

A rotation of 90° counterclockwise starting from the baseline subcostal four-chamber view produces subcostal cross sections of the heart, similar to those obtained with the parasternal

Fig. 2.19 Subcostal four-chamber view
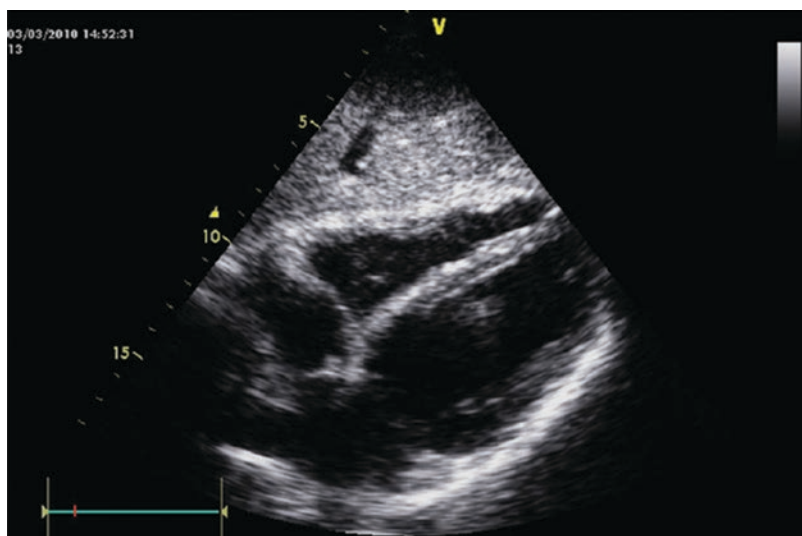
Fig. 2.20 Subcostal view modified for the inferior vena cava
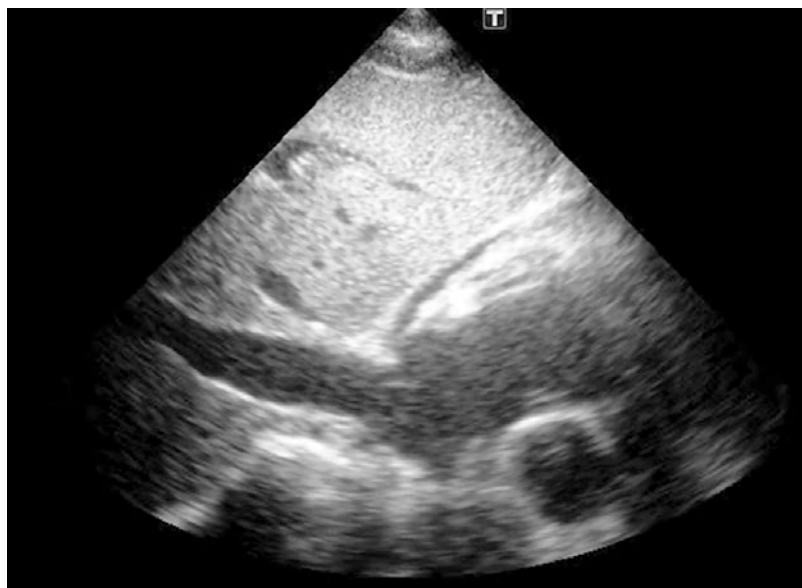
short-axis view. An inclination to the right gives sections toward the apex of the heart, whereas an inclination to the left explores sections of the base.

2.1.10 Suprasternal View

To obtain suprasternal images, the patient is raised to at least 45°, with the head extended on the neck. In certain circumstances this approach is not easily done in the ICU or is clearly contra-indicated (neck trauma). The probe is placed on the supraclavicular area just above the sternal manubrium, directed toward the chest with the marker pointing at the left shoulder (Fig. 2.5). A little movement or angulation is used to find part of the aortic arch and descending aorta (Fig. 2.21). Manipulating the probe to the right can show the ascending aorta. CFM is then used to define the aorta and its branches. A slight rotation of the probe may show the left atrium and pulmonary
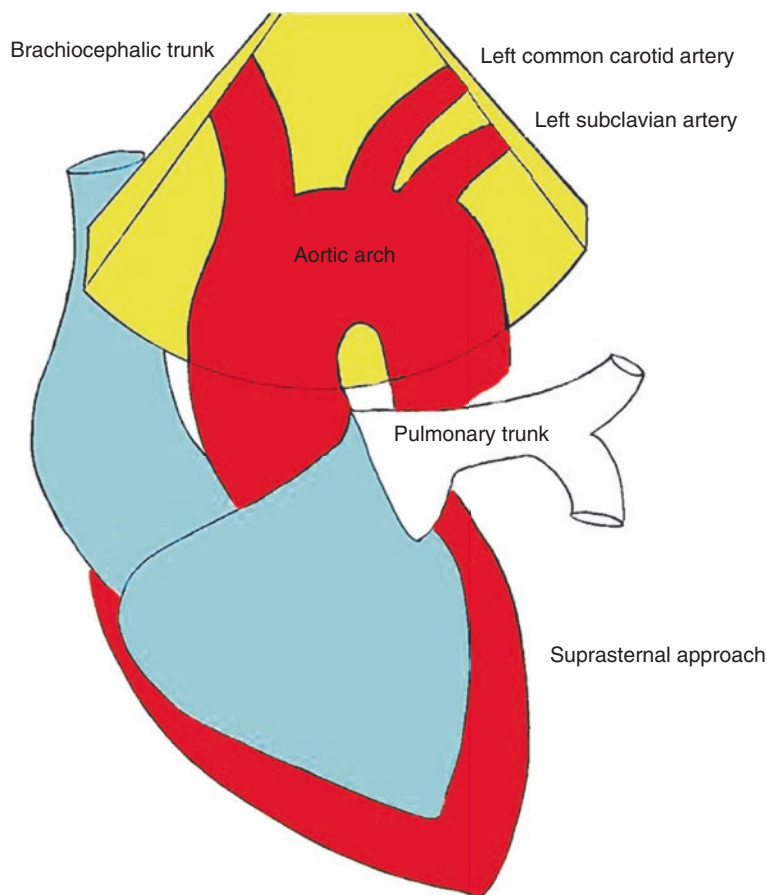
veins. The right branch of the pulmonary artery often appears below the aortic arch. This view is not always used. It may allow evaluation of the aorta in thoracic trauma or suspicion of dissection, but transesophageal echocardiography is far more effective for this purpose.

2.1.11 Overview

Figure 2.22 shows a summary diagram of the various probe positions with corresponding images. Figure 2.23 outlines the main transthoracic views according to the section planes. Table 2.1 describes the movement of the probe, as position, pointing, angling, and rotation, the

structures to be seen, and the main measurements to be done.

The first echo examination of an ICU patient should include most of these views in regular sequence. Even if not all views are obtainable, a routine sequence must be tried all the same to avoid missing important unexpected information. All the structures should be identified to discriminate between normal and any deviation from normal using each usable echo modality, including M-mode echocardiography, Doppler echocardiography, and tissue Doppler imaging. Afterward, at the end of the first examination or during another assessment, the examiner focuses on particular views for specific purposes or monitoring.
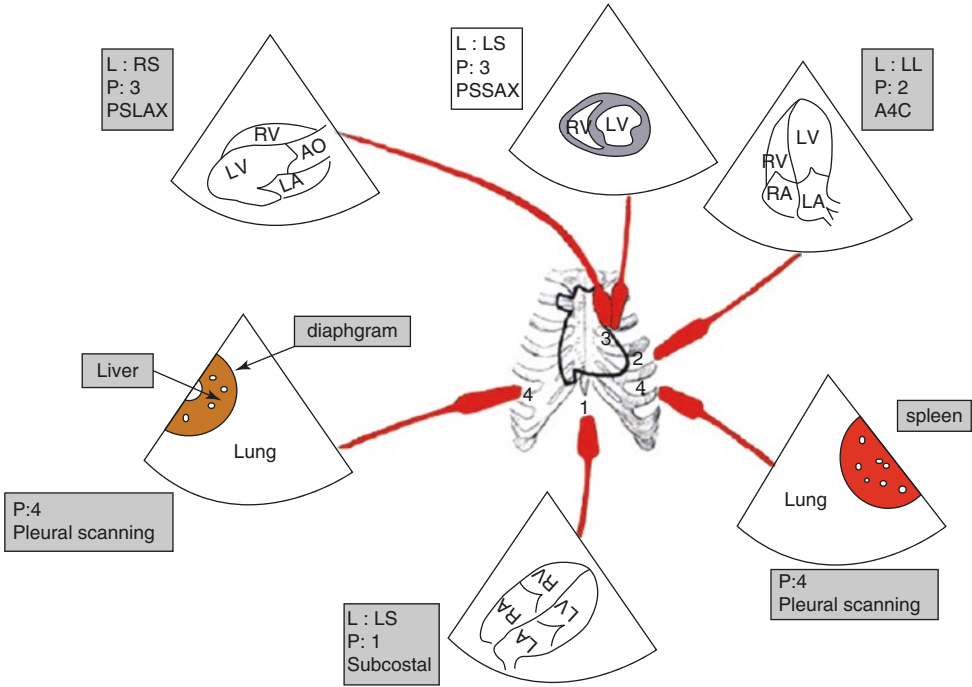
Fig. 2.22 Outline of the probe positions and main views. *L* probe landmark, *P* probe position, *RS* right shoulder, *LS* left shoulder, *LL* left leg, *PSLAX* parasternal long axis, *PSSAX* parasternal short axis, *A4C* apical four chamber
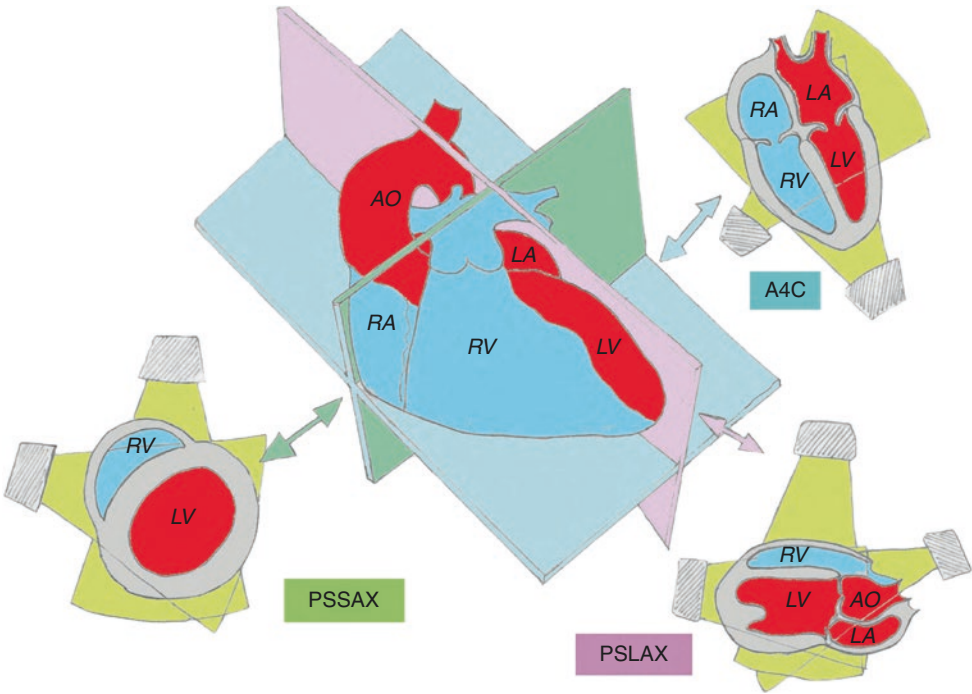
Fig. 2.23 Outline of the echocardiographic section planes and views. *A4C* apical four chamber, *AO* aorta, *LA* left atrium, *LV* left ventricle, *PSLAX* parasternal long axis, *PSSAX* parasternal short axis, *RA* right atrium, *RV* right ventricle. (Modified from Sarti [1] with permission)

Reference

1. Sarti A. Ecocardiografia per l'intensivista. Milan: Springer; 2009.

Further Reading

Feigenbaum H, Armstrong WF, Ryan T. Feigenbaum's echocardiography. Philadelphia: Lippincott Williams & Wilkins; 2009.

Oh JK, Steward JB, Tajik AJ. The Echo manual. 3rd ed. Philadelphia: Lippincott Williams & Wilkins; 2007.

Otto C. The practice of clinical echocardiography. 5th ed. New York: Elsevier; 2017.

Transthoracic Echocardiography in the ICU: The Patient Who Is Difficult to Study

Piercarlo Ballo

Key Points
- Transthoracic echocardiography is of major clinical importance in the management of intensive care unit patients.
- Since these patients often have suboptimal echocardiographic windows, methods aimed at optimizing images should be correctly applied. These include techniques to minimize patient's related disturbing factors, optimize instrumental settings, study the patient using alternative views, and measure indexes that are less sensitive to image quality.
- For patients in whom the transthoracic approach does not allow to obtain adequate data, transoesophageal echocardiography often provides additional information. However, care is needed to avoid inappropriate requests of transoesophageal examinations.

3.1 Introduction

Prompt and accurate diagnostic assessment of critically ill patients is crucial in the intensive care unit (ICU). Transthoracic echocardiography (TTE) is of major clinical value in this setting, due to its widespread availability and rapid diagnostic capability. However, it is well known that critically ill patients are often relatively difficult to study by echocardiography because of unsatisfactory acoustic windows. Both factors related to patient's condition (e.g. supine decubitus, chest wall interference) and instrumentation (e.g. artefacts due to mechanical ventilation) contribute to this technical difficulty. Early studies reported a failure rate >30% for the transthoracic approach in the ICU setting, with higher values among patients with significant body weight gain from admission, those supported with relatively high positive end-expiratory pressure, and those with chest tubes.

Thanks to dramatic technical improvements in the recent years, including harmonics, contrast, and digital technologies, the failure rate is to date considerably reduced. In 2004, an evaluation of 100 consecutive requests by critical care physicians for urgent echocardiograms to identify the aetiology of shock in ICU patients found that TTE was feasible in 99% of cases. More recently, studies have confirmed that adequate imaging in the ICUs can be obtained in the large majority of patients, even using portable echocardiographs,

P. Ballo (✉)
Cardiology Unit, Santa Maria Annunziata Hospital, Florence, Italy
e-mail: piercarlo.ballo@uslcentro.toscana.it

provided that care is given to optimize technical settings on the echocardiograph and to minimize disturbing factors. However, when TTE does not provide adequate diagnostic information, the use of transesophageal echocardiography (TEE) is indicated. TEE can provide adequate and conclusive images in the large majority of patients and in some conditions is currently recommended as the first-line approach (Table 3.1). In a recent analysis of mechanically ventilated patients, critical care TEE was found to be feasible and safe and to have significant clinical utility by yielding a change in clinical management in nearly 40% of cases. However, efforts to optimize images and to achieve adequate TTE examinations should always be made to avoid inappropriate requests of TEE. These efforts should be considered mandatory particularly for patients in whom immediate availability of echocardiographic information is of major clinical importance.

Based on these considerations, the practical approach to the patient difficult to study should include the following steps: (1) minimizing patient's related disturbing factors, (2) optimizing machine settings, (3) approaching the patient using multiple and alternative views, and (4) utilizing echocardiographic indexes that are less dependent on image quality.

3.2　Minimizing Patient's Related Disturbing Factors

Patients in the ICUs typically lie in the supine position. This position moves the heart behind the sternum and away from the chest anterior

Table 3.1 Indications to transesophageal echocardiography

TEE as initial or supplemental test: general uses	
Use of TEE when there is a high likelihood of a nondiagnostic TTE due to patient characteristics or inadequate visualization of relevant structures	A(8)
Routine use of TEE when a diagnostic TTE is reasonably anticipated to resolve all diagnostic and management concerns	I (1)
Re-evaluation of prior TEE finding for interval change (e.g. resolution of thrombus after anticoagulation, resolution of vegetation after antibiotic therapy) when a change in therapy is anticipated	A(8)
Surveillance of prior TEE finding for interval change (e.g. resolution of thrombus after anticoagulation, resolution of vegetation after antibiotic therapy) when no change in therapy is anticipated	I (2)
Guidance during percutaneous noncoronary cardiac interventions including but not limited to closure device placement, radiofrequency ablation, and percutaneous valve procedures	A(9)
Suspected acute aortic pathology including but not limited to dissection/transection	A(9)
Routine assessment of pulmonary veins in an asymptomatic patient status post-pulmonary vein isolation	I (3)
TEE as initial or supplemental test: valvular disease	
Evaluation of valvular structure and function to assess suitability for, and assist in planning of, an intervention	A(9)
To diagnose infective endocarditis with a low pretest probability (e.g. transient fever, known alternative source of infection, or negative blood cultures/atypical pathogen for endocarditis)	I(3)
To diagnose infective endocarditis with a moderate or high pretest probability (e.g. staph bacteraemia, fungaemia, prosthetic heart valve, or intracardiac device)	A(9)
TEE as initial or supplemental test: embolic event	
Evaluation for cardiovascular source of embolus with no identified noncardiac source	A (7)
Evaluation for cardiovascular source of embolus with a previously identified noncardiac source	U (5)
Evaluation for cardiovascular source of embolus with a known cardiac source in which a TEE would not change management	I (1)
TEE as initial test: atrial fibrillation/flutter	
Evaluation to facilitate clinical decision-making with regard to anticoagulation, cardioversion, and/or radiofrequency ablation	A (9)
Evaluation when a decision has been made to anticoagulate and not to perform cardioversion	I(2)

wall, thus increasing the distance with the probe and favouring tissue artefacts. Most beds in the ICUs can be regulated to obtain a partial left lateral inclination. This inclination leads to relative leftward and anterior shifting of the heart, reduces the artefacts related to the sternum interposition, and decreases the distance with the probe, often yielding an improvement in echocardiographic image quality. Mechanical ventilation systems and chest tubes often lead to considerable image artefacts. When clinically possible in relation to the safety of the patient, transient interruption or reduction of mechanical respiratory assistance (e.g. by decreasing the positive end-expiratory pressure) eliminates or reduces these artefacts, improving image quality. In some cases, image artefacts can also be produced by electrical interference with monitors or other electrical devices that are placed nearby the patient. Again, when clinically possible, turning off these devices in a safe manner (e.g. by using the monitor system of the echocardiograph during the examination after turning off an external monitor that produces artefacts) may further improve image quality.

3.3   Optimizing Machine Settings

Sonographers working in clinics with ICUs should be trained in optimizing machine settings, in order to be able to obtain the best possible echocardiographic images of the patient's heart. A number of parameters can be changed and modulated to achieve this. *Probe frequency* should be chosen by reminding the inverse relation between resolution and penetration. High frequencies correspond to small beam amplitudes which allow higher axial and lateral resolution, but their penetration capability is reduced and less suitable for deeper structures. Conversely, low frequencies correspond to high beam amplitudes which yield worse resolution but with higher their penetration capability that allows adequate exploration of deeper structures. Most echocardiographs have preset controls, allowing rapid selection of a configuration that enhances a particular characteristic, e.g. penetration or resolution. A correct *focus distance* should also be chosen. Adjusting the focus of the beam leads to narrowing of the ultrasound beam at the desired depth, allowing optimization of spatial resolution and improving visualization of the focused structures.

When adequate probe frequency and focus are used, care should be given to optimize signal processing. This can be made by adjusting a number of controls, including pulse repetition frequency, frame rate, system gain, time gain compensation, lateral gain compensation, compression, smoothing, and postprocessing settings (which act on image display). Among these, *pulse repetition frequency* corresponds to the triggering frequency and determines the number of scan lines for time unit. Increasing this number enhances motion display. An increase in pulse repetition frequency can also be obtained by narrowing the sector depth. The *frame rate* corresponds to the scanning frequency of the whole sector. Increasing the frame rate leads to better temporal resolution. Frame rate is inversely related to both sector depth and width. Thus, a reduction in sector depth or width increases frame rate and temporal resolution.

In clinical practice, in the patient difficult to study, after identification of the most appropriate probe frequency, the focus should be positioned at the level of the structure to be explored to increase spatial resolution, and both sector depth and width should be reduced to increase temporal resolution. Gain controls, compression, smoothing, and postprocessing settings should then be manually adjusted to further improve image quality. Figure 3.1 shows an example of echocardiographic images before and after accurate optimization of settings. Some high-level echocardiographs have a command that activates an automatic detection of the best overall control configuration to optimize image quality. However, the choice of the most adequate setting still remains dependent on the experience and the preferences of the sonographer.
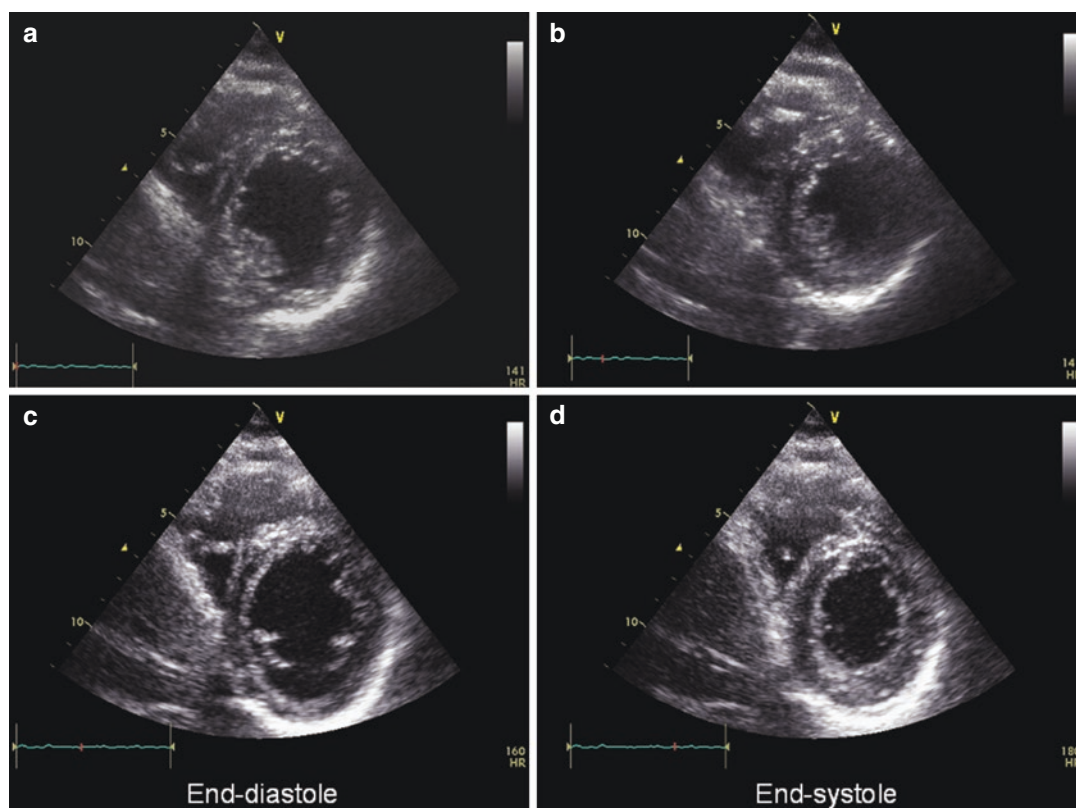
Fig. 3.1 Example of image optimization in a parasternal short-axis view at the midventricular level. Before optimization (panels **a** and **b**), detection of endocardial borders was problematic in the end-systolic frame. A subsequent acquisition after setting optimization (panels **c** and **d**) allowed improvement in overall image quality and adequate detection of endocardial borders at end-systole. Optimization was achieved by choosing a different two-dimensional map and changing gain, compression, and rejection controls

3.4 Approaching the Patient Using Multiple and Alternative Views

After elimination of patient's related disturbing factors and optimization of machine settings, the third step is to approach the patient using both standard and alternative views. The use of off-axis views may facilitate visualization of heart structures not easily visualized from conventional windows. Most of these views are commonly used even in standard examinations, so that the term "off-axis" may also be inappropriate for most of them. For example, a long-axis of the right ventricle can be well visualized starting from a parasternal long-axis of the left ventricle and inclining the probe so that the direction of the ultrasonic beam moves towards the patient's right side. This view may be of particular utility when right-sided chambers cannot be adequately visualized from apical views. A typical application of this view is related to the estimation of pulmonary artery systolic pressure from the peak velocity of the tricuspid regurgitant flow when imaging or correct alignment of the tricuspid regurgitation is not adequate from the apical four-chamber view. Starting from the parasternal long-axis of the left ventricle and inclining the probe to move the ultrasonic beam towards the patient's left side allow visualization of the right ventricular outflow tract, the pulmonary valve, and the pulmonary artery on a tomographic plane that is approximately perpendicular to that seen by the standard short-axis view at the level of

great vessels. This alternative view may be useful to explore both pulmonary outflow and regurgitation when imaging is not adequate from the standard view and can allow measurements of indexes related to pulmonary artery pressure and pulmonary bed resistance (Fig. 3.2). An alternative two-chamber visualization of the right ventricular inflow tract can also be obtained from the apical approach, starting from the standard two-chamber view for the left ventricle and again inclining the probe so that the direction of the ultrasonic beam moves towards the patient's right side. The subxiphoidal approach is of particular utility in the ICUs, as it often allows good visual-
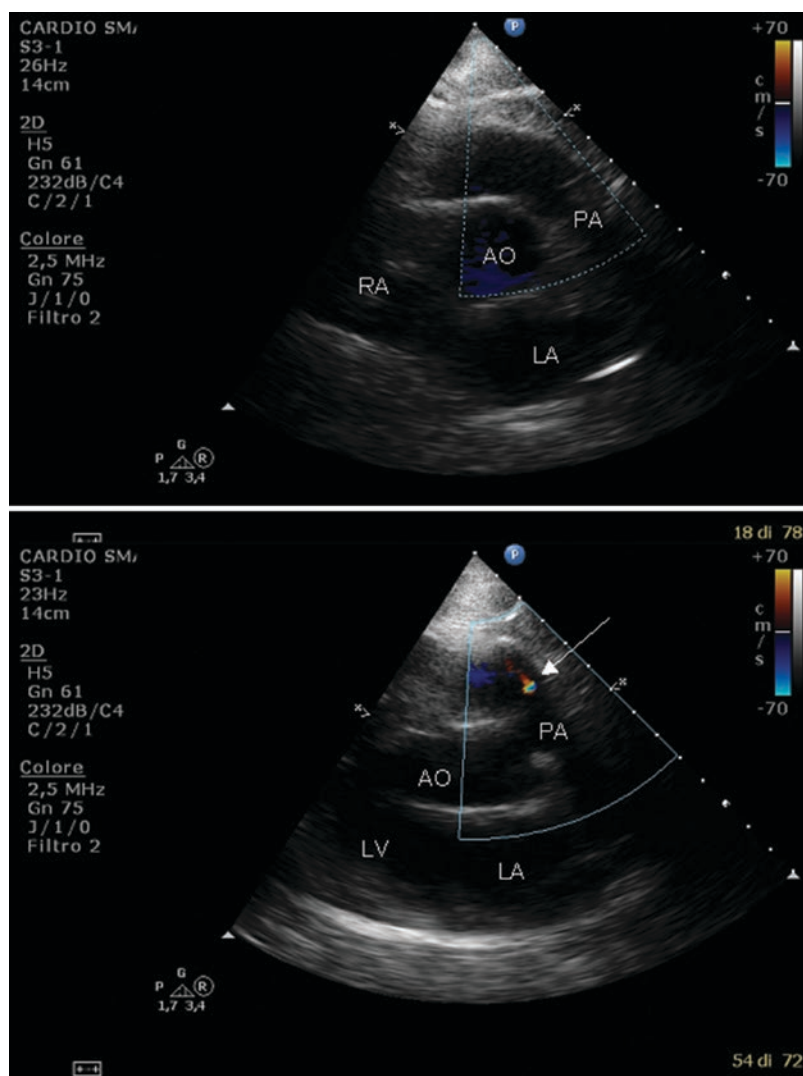
Fig. 3.2 Example of alternative view for the imaging of pulmonary valve. From the standard short-axis view at the level of great vessels (top panel), no pulmonary regurgitation was recorded. Using an alternative view obtained starting from the parasternal long-axis of the left ventricle and inclining the probe to move the ultrasonic beam towards the patient's left side, a pulmonary regurgitant flow appeared (arrow). This view explores the pulmonary valve and the pulmonary artery on a tomographic plane that is approximately perpendicular to that used in the classic short-axis, so that it can be used to detect eccentric regurgitant flow not seen in the standard view. Accurate detection of pulmonary regurgitation may be of clinical importance for the estimation of pulmonary artery mean and diastolic pressure. AO aorta, LA left atrium, LV left ventricle, PA pulmonary artery; RA right atrium

ization of the heart in patients with poor parasternal and apical windows (e.g. related to chronic obstructive pulmonary disease or increased chest anteroposterior dimension), even when mechanical respiratory support is ongoing, and without the need of changing the supine decubitus of the patient. Several alternative views may also be used to image other structures often difficult to explore using the standard approach, e.g. the right parasternal view for the distal ascending tract of the aorta and modified parasternal short-axis and apical views for its proximal and distal intrathoracic descending tract. Overall, a large number of alternative and off-axis views exist. However, the choice of using one or more of them is strictly dependent on the experience and the preference of the sonographer and is dictated by each individual examination.

3.5   Utilizing Echocardiographic Indexes That Are Less Dependent on Image Quality

An additional step in the approach to patients technically difficult to explore includes the use of indexes that are relatively less sensitive on the quality of acoustic windows. A typical example of this is represented by the use of indexes of longitudinal function for the assessment of left ventricular (LV) and right ventricular (RV) function.

3.5.1   LV Systolic Function

Accurate evaluation of LV systolic function is a key aspect for the management of patients in the ICUs. LV ejection fraction as an overall index of LV systolic function is often quantitatively assessed using two-dimensional approaches aimed at measuring LV volumes (e.g. the modified Simpson's rule). A rough evaluation of global LV function can also be qualitatively obtained by visual inspection alone. However, both methods rely on adequate visualization of LV endocardial border, which is often not obtainable in critically ill patients despite appropriate harmonic imaging and efforts in optimizing images. Assessment of

LV segmental wall motion is dependent on detection of endocardial border as well and therefore suffers from similar limitations. Contrast techniques can dramatically improve visualization of the endocardial border, but they are not routinely used in critical practice. In these cases, measurement of left atrioventricular plane displacement by standard M-mode or peak mitral annulus systolic velocity by tissue Doppler (s') (Figs. 3.3 and 3.4), usually calculated by averaging values measured in at least two sites of the annulus (e.g. septal and lateral from the apical four-chamber view), provides accurate indexes of LV longitudinal systolic function that are less dependent on image quality and that can often be well measured even in patients with suboptimal acoustic windows. Moreover, compared to ejection fraction, measurement of atrioventricular plane displacement and s' are more reproducible, less time-consuming, and relatively less sensitive to loading conditions.

3.5.2   LV Diastolic Function

Adequate information about LV diastolic performance can be obtained in most patients even in case of suboptimal windows. Recording of LV inflow pattern by pulsed Doppler after placing the sample volume at the level of mitral tip from the apical four-chamber view is feasible in the large majority of critically ill patients. LV inflow imaging provides valuable information regarding LV diastolic dysfunction by identification of diastolic pattern (normal, impaired relaxation, pseudonormal, and restrictive). However, it should be stressed that the simple use of LV inflow as an index of LV diastolic function is strongly limited by its strict load dependence. More reliable information regarding LV relaxation properties can be obtained by considering the peak early diastolic velocity of mitral annulus by tissue Doppler (e'). As for systolic annulus velocity, diastolic velocities are usually calculated by averaging values measured in at least two sites of the annulus (e.g. septal and lateral from the apical four-chamber view). Average e' is a relatively load-independent
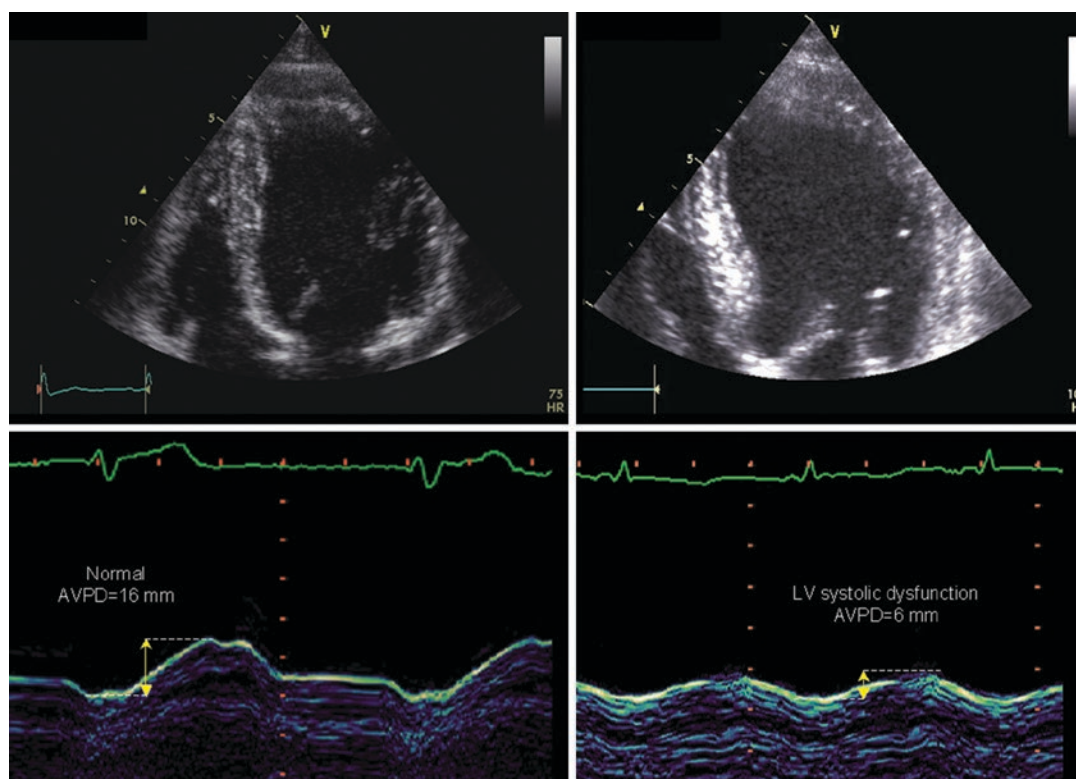
Fig. 3.3 Utility of left atrioventricular plane displacement in two patients with suboptimal quality of four-chamber view (top panels), in whom accurate detection of subendocardial border for the determination of left ventricular (LV) ejection fraction was difficult. Displacement of the annulus was normal in the first subject (left), but reduced in the second one (right), indicating considerable LV systolic dysfunction

measure of LV relaxation. The ratio between early diastolic peak velocity of LV inflow (E) measured by standard pulsed Doppler and e' provides a reliable non-invasive estimate of LV filling pressures (Fig. 3.5). Determination of e' and the E/e' ratio allows rapid and accurate assessment of LV diastolic function in the ICUs, with relatively high feasibility even in case of suboptimal windows.

3.5.3 RV Systolic Function

The same considerations made for the assessment of LV systolic function can be applied to the evaluation of RV systolic function. Assessment of RV ejection fraction by two-dimensional echocardiography is even more difficult than LV ejection fraction and relies on geometrical assumptions that are less validated due to the irregular crescent/triangular shape of the right ventricle. As the use of three-dimensional echocardiography for the assessment of RV ejection fraction is still not applicable to daily practice and is affected by image quality similarly to two-dimensional methods, in practice, most sonographers use indexes of RV longitudinal systolic function. M-mode tricuspid annulus systolic excursion and tissue Doppler peak systolic velocity of tricuspid annulus are commonly used to quantify RV systolic performance and can often be measured even in patients with poor acoustic windows (Fig. 3.6). Both indexes show a good relationship with RV ejection fraction. Their advantages resemble those already explained for LV longitudinal indexes.

Fig. 3.4 Examples of pulsed tissue Doppler imaging of mitral annulus systolic velocity in a normal subject (top panel) and in a patient with left ventricular (LV) systolic dysfunction (bottom panel)
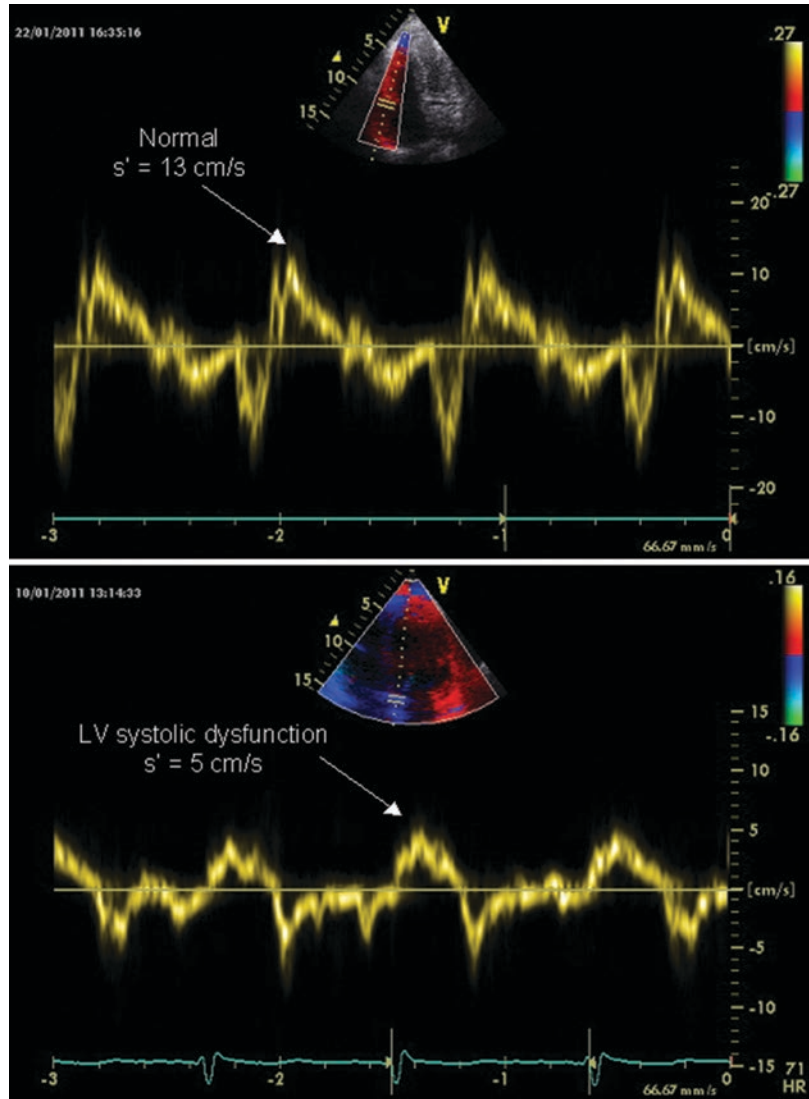
3.5.4　Other Applications

The opportunity of using indexes that are less dependent on image quality should be constantly taken into account for all aspects of echocardiographic examination when images are of suboptimal quality. Accordingly, in addition to the assessment of ventricular function, this concept can be applied to a number of echocardiographic evaluations (e.g. determination of pulmonary artery pressures, calculation of cardiac output, estimation of valve regurgitation or stenosis severity, analysis of prosthetic valve haemodynamic, and so on).
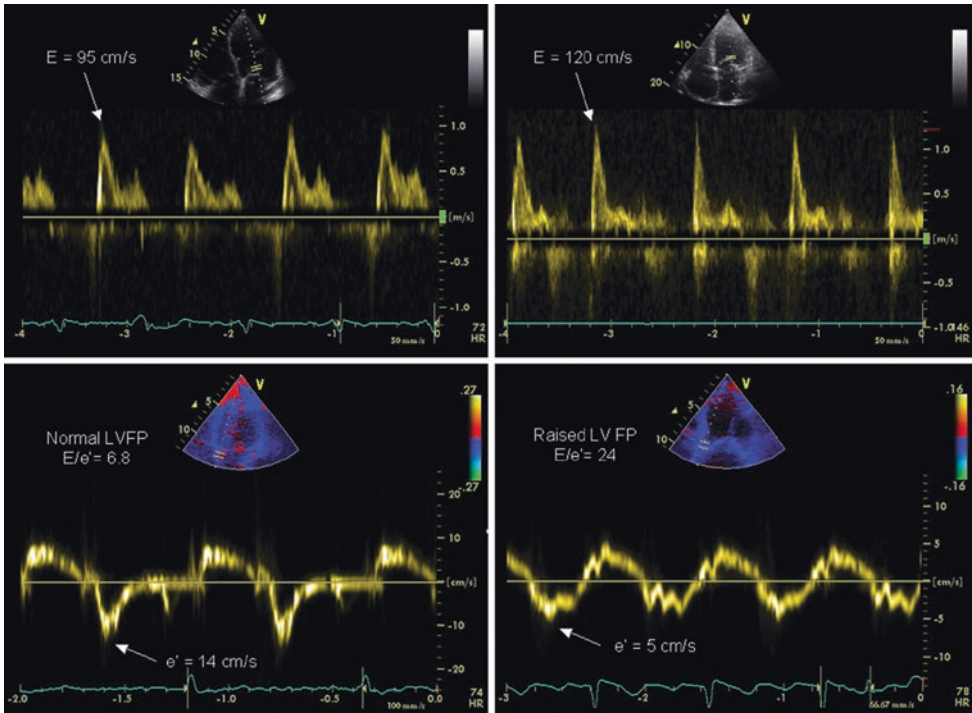
Fig. 3.5 Assessment of left ventricular diastolic function using standard pulsed Doppler of transmitral flow and tissue Doppler imaging of diastolic mitral annulus motion. Left panels were recorded in a normal subject. Right panels were recorded in a subject with advanced left ventricular dysfunction. LVFP left ventricular filling pressure

Fig. 3.6 Tricuspid annulus plane systolic excursion (TAPSE) (top panel) and pulsed tissue Doppler pattern of tricuspid annulus motion (bottom panel) in a normal subject
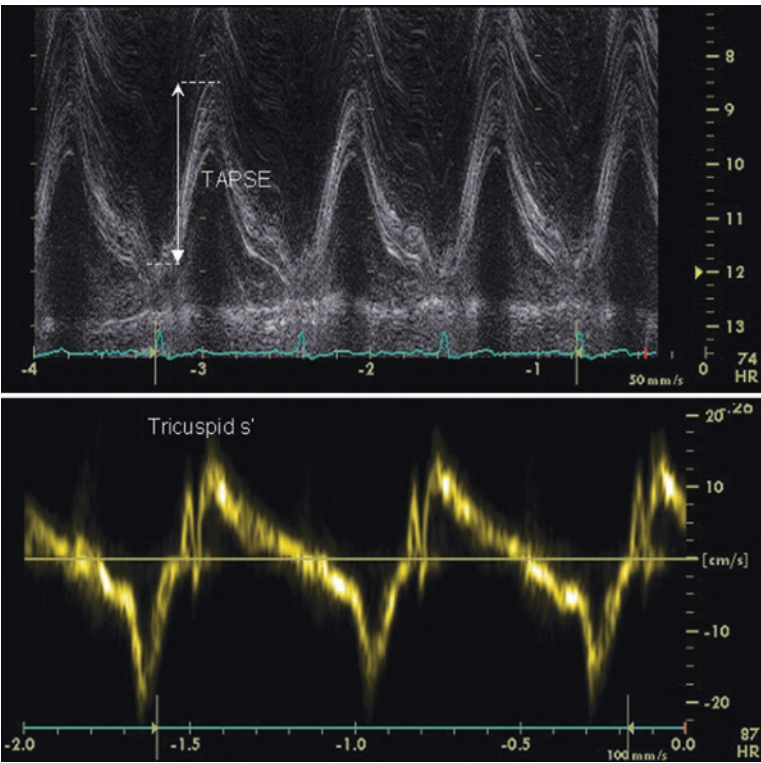
Further Reading

Aguilera Garcia Y, Quintero L, Singh K, Lakticova V, Iakovou A, Koenig S, et al. Feasibility, safety, and utility of advanced critical care transesophageal echocardiography performed by pulmonary/critical care fellows in a Medical Intensive Care Unit. Chest. 2017;152(4):736–41.

Cook CH, Praba AC, Beery PR, Martin LC. Transthoracic echocardiography is not cost effective in critically ill surgical patients. J Trauma. 2002;52:280–4.

Culp BC, Mock JD, Ball TR, Chiles CD, Culp WC Jr. The pocket echocardiograph: a pilot study of its validation and feasibility in intubated patients. Echocardiography. 2011;28:371–7.

Douglas PS, Garcia MJ, Haines DE, Lai WW, Manning WJ, Patel AR, et al. ACCF/ASE/AHA/ASNC/HFSA/HRS/SCAI/SCCM/SCCT/SCMR 2011 appropriate use criteria for echocardiography a report of the American College of Cardiology Foundation Appropriate Use Criteria Task Force, American Society of Echocardiography, American Heart Association, American Society of Nuclear Cardiology, Heart Failure Society of America, Heart Rhythm Society, Society for Cardiovascular Angiography and Interventions, Society of Critical Care Medicine, Society of Cardiovascular Computed Tomography, and Society for Cardiovascular Magnetic Resonance Endorsed by the American College of Chest Physicians. J Am Coll Cardiol. 2001;57:1126–66.

Hwang JJ, Shyu KG, Chen JJ, Tseng YZ, Kuan P, Lien WP. Usefulness of transesophageal echocardiography in the treatment of critically ill patients. Chest. 1993;104:861–6.

Joseph MX, Disney PJS, Da Costa R, Hutchison SJ. Transthoracic echocardiography to identify or exclude cardiac cause of shock. Chest. 2004;126:1592–7.

Nagueh SF, Smiseth OA, Appleton CP, Byrd BF 3rd, Dokainish H, Edvardsen T, et al. Recommendations for the evaluation of left ventricular diastolic function by echocardiography: an update from the American Society of Echocardiography and the European Association of Cardiovascular Imaging. J Am Soc Echocardiogr. 2016;29:277–314.

Rudski LG, Lai WW, Afilalo J, Hua L, Handschumacher MD, Chandrasekaran K, et al. Guidelines for the echocardiographic assessment of the right heart in adults: a report from the American Society of Echocardiography endorsed by the European Association of Echocardiography, a registered branch of the European Society of Cardiology, and the Canadian Society of Echocardiography. J Am Soc Echocardiogr. 2010;23:685–713; quiz 786–8.

Ultrasound Morphology of the Heart: Transesophageal Examination

4

Ferdinando Luca Lorini, Carlo Sorbara,
and Sergio Cattaneo

4.1 Introduction

A transesophageal echocardiography (TEE) examination is effective to assist in the hemodynamic treatment of patients during cardiovascular anesthesia and to make a diagnosis in the operating room during cardiac operations and in the intensive care unit. More and more anesthesiologists are involved in this practice, and they provide a remarkable contribution to scientific and practical progress of perioperative echocardiography. Executing TEE requires time, but there are a lot of advantages for hemodynamic monitoring and diagnosis, which explain the increasing interest in TEE for many years.

The heart is a very complex three-dimensional structure with a lot of anatomic components bound together; therefore, perfect knowledge of the anatomy is very important to understand two-dimensional echo images of the heart. The operator's experience is very important; we think that TEE should be used in all cardiac surgery

patients without contraindications, especially at the beginning of the learning curve. The simplified TEE examination usually requires 5–10 min. During the examination, the TEE operator or an anesthesiologist or a nurse can check the stability of the patient.

Sometimes images are very bad because of anatomic conditions (cardiac cavity dilatation) or air in stomach (it is possible to improve the image after suction). Instrument settings and adjustments are important for optimizing image quality and the diagnostic capabilities of TEE. Many TEE probes can obtain an image with more than one transducer frequency. Increasing the imaging frequency improves resolution but decreases penetration. Structures closer to the probe, such as the aortic valve (AV), are imaged best at a higher frequency, whereas structures farther away from the probe, such as the apical regions of the left ventricle (LV), are imaged best at a lower frequency. The depth is adjusted so that the structure being examined is centered in the display, and the focus is moved to the area of interest. Overall image gain and dynamic range (compression) are adjusted so that the blood in the chambers appears nearly black and is distinct from the gray scales representing tissue. Time compensation gain adjustments are set to create uniform brightness and contrast throughout the imaging field. The color flow Doppler (CFD) gain is set to a threshold that just eliminates any background noise within the color sector. Decreasing the

F. L. Lorini (✉) · S. Cattaneo
Department of Anesthesia and Intensive Care
Medicine, ASST Papa Giovanni XXIII,
Bergamo, Italy
e-mail: llorini@asst-pg23.it; scattaneo@asst-pg23.it

C. Sorbara
Anesthesia and Intensive Care Department, Regional
Teaching Hospital, Azienda ULSS 9, Veneto,
Treviso, Italy

size and depth of the color sector increases the aliasing velocity and frame rate. Decreasing the width of the two-dimensional imaging sector also increases the frame rate.

4.2 Patient Safety

Rarely TEE can cause serious and even fatal complications; effort should be made to detect preexisting esophageal or gastric problems before performing TEE. Contraindications to TEE include esophageal stricture, diverticulum, tumor, and recent esophageal or gastric surgery. The TEE transducer should be inspected for defects and cracks in the waterproof covering before insertion. The mouth should be examined for preexisting injuries and loose teeth. The TEE probe may be inserted into an anesthetized, tracheally intubated patient with or without the use of a laryngoscope by displacing the mandible anteriorly and inserting the probe gently in the midline. Flexing the neck will help in some cases. If insertion of the probe is not easy, a laryngoscope can be used to expose the glottis and permit direct passage of the probe posteriorly into the esophagus. Once the transducer is in the esophagus, it should never be forced through a resistance. The tip of the transducer should be allowed to return to the neutral position before the probe is advanced or withdrawn, and excessive force should never be applied when the transducer is moved in the esophagus or when the tip is flexed with the control wheels. Cleaning and decontamination of the probe should be performed after each use.

4.3 The Simplified TEE Examination

The comprehensive, intraoperative TEE examination, recommended in the guidelines written by the American Society of Echocardiography and the Society of Cardiovascular Anesthesiologists in 1999, consists of a series of 20 cross-sectional views of the heart and great vessels. The views are designated by the transducer location (i.e.,

the echo window), a description of the imaging plane (e.g., short axis, long axis), and the main anatomic structure in the image.

One should not start to study immediately a pathological element (surgical indication); one should use a standard protocol to practice the TEE examination. One should get only one cardiac structure (valve or cavity) in focus and analyze it and its relationship to other structures. It is very important to move the scan plane and build up a three-dimensional structure from the two-dimensional image. Everyone has to develop a personal approach to the intraoperative TEE examination; we suggest a simplified intraoperative TEE examination that reduces the number of views from the 20 standard views and is able to analyze all the main heart structures. The main advantage of this systematic approach is the minimization of the manipulation of the TEE probe to perform a complete examination of major cardiac structures.

The cardiac examination is performed at three locations. The first location is the mid-esophagus at the AV level, the second is a few centimeters distal in the mid-esophagus at the level of the mitral valve, and the final location is in the stomach at the level of the LV. After completion of the cardiac examination, the aorta is evaluated throughout its thoracic course.

4.3.1 Mid-esophageal AV Level

4.3.1.1 Mid-esophageal AV Short-Axis View

After the probe has been inserted, it is advanced until the leaflets of the AV are seen. The imaging plane is then rotated to approximately 45° to obtain the mid-esophageal AV short-axis view. The primary structure visualized is the AV in the short axis. The size of the AV in comparison with the atrial chambers in addition to the mobility of the aortic leaflets and any leaflet calcification is carefully noted (Fig. 4.1). The primary diagnostic goals of this view are to define the general morphology of the AV (e.g., bicuspid vs. tricuspid) and to determine if aortic stenosis is present. The intra-atrial septum can be observed for openings,

Depth: mid-esophageal (30-40 cm from the dental rhyme)
              advancing or retreating until the aortic valve

Angle: 30°-60°

Flex: none

Laterality: none

Goals: aortic valve, left atrium, right atrium, right ventricle,
              pulmonary valve, right ventricular outflow tract

Legend: LA: left atrium
           RA: right atrium
           RV: right ventricle
           PV: pulmonary value
           nc: non-coronary aortic cusp
           rc: right coronary aortic cusp
           lc: left coronary aortic cusp
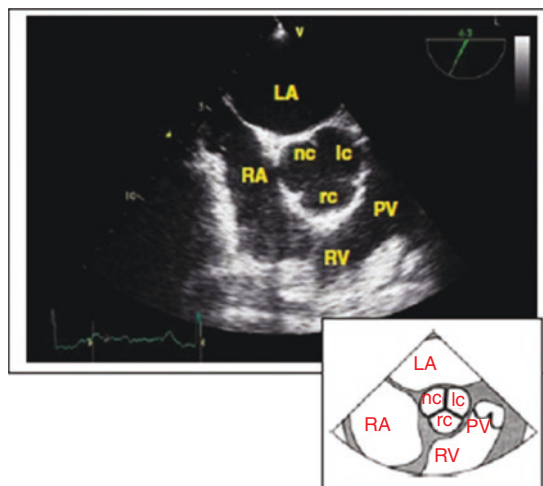
Fig. 4.1 Mid-esophageal aortic valve short-axis view

consistent with an atrial septal defect or patent foramen ovale.

4.3.1.2 Mid-esophageal AV Long-Axis View

The mid-esophageal AV long-axis view is obtained by further rotating the imaging angle to approximately 110–130°. A slight turn of the probe toward the patient's right may be necessary to optimize this image. The view is complete when the left ventricular outflow tract, AV, and proximal ascending aorta are displayed together. Additional structures to observe are the outflow tract itself, the sinus of Valsalva, and the sinotubular junction (Fig. 4.2). The primary diagnostic goal of this view is to evaluate AV function. The proximal ascending aorta should be inspected for calcification, enlargement, and protruding atheroma. An important limitation of this view is that the aortic cannulation site in the distal ascending aorta cannot be visualized. After completion of a two-dimensional examination, AV function is evaluated further with CFD imaging.

4.3.1.3 Mid-esophageal Right Ventricular Inflow–Outflow View

The next view obtained at the level of the AV is the mid-esophageal right ventricular inflow–

outflow view. One starts at the mid-esophageal AV short axis and, without moving the probe, changes the rotation of the imaging angle to approximately 60–90°. The desired imaging plane will visualize the tricuspid valve, the right ventricular outflow tract, and the proximal pulmonary artery (Fig. 4.3). The primary diagnostic goals of this view are to gauge the right ventricular chamber and pulmonary artery size and to evaluate the pulmonary valve. This view is often superior to the mid-esophageal four-chamber view for Doppler interrogation of the tricuspid valve.

4.3.1.4 Mid-esophageal Bicaval View

The mid-esophageal bicaval view is then obtained by turning the probe further to the patient's right. This image is often best with 5–15° less rotation than in the mid-esophageal AV long-axis view. The key structures in this view are the left atrium, right atrium, superior vena cava, intra-atrial septum, and right atrial appendage (Fig. 4.4). The primary diagnostic goals of this view are to examine for atrial chamber enlargements and the presence of a patent foramen ovale or an atrial septal defect and to detect intra-atrial air. If the integrity of the intra-atrial septum is questioned, CFD imaging or bubble contrast imaging should be performed.

Depth: mid-esophageal (30-40 cm from the dental rhyme)
            advancing or retreating until the aortic valve

Angle: 120°-160°

Flex: none

Laterality: none

Rotation: right-left to bring the aortic valve in the center

Goals: aortic valve, left atrium, left ventricular outflow tract

Legend: LA: left atrium
            LV: right ventricle
            AV: aortic value
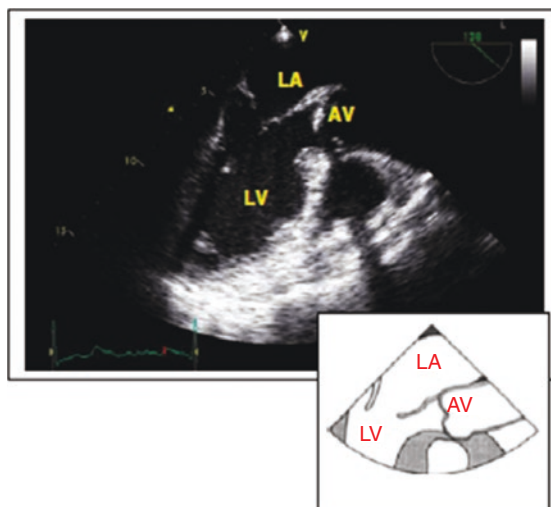
Fig. 4.2 Mid-esophageal aortic valve long-axis view

Depth: mid-esophageal (30-40 cm from the dental rhyme)

Angle: 60°-90°

Flex: none

Laterality: none

Goals: right atrium, left atrium, atrial septum, tricuspid valve,
            right ventricle, pulmonary value, aortic valve

Legend: RA: right atrium
            TV: tricuspid value
            PV: pulmonary value
            AV: Aortic valve
            RV: right ventricle
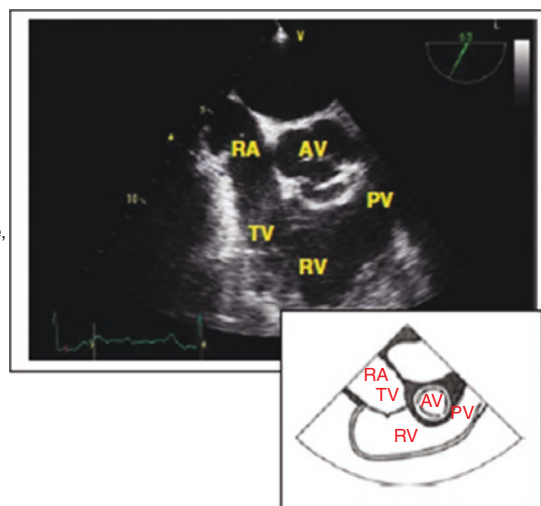
Fig. 4.3 Mid-esophageal right ventricular inflow–outflow view

4.3.2 Mid-esophageal Mitral Valve Level

4.3.2.1 Mid-esophageal Four-Chamber View

After completion of the mid-esophageal bicaval view, the imaging angle is returned to 0° and the TEE probe is advanced to the mitral valve level. In the transverse plane, the mid-esopha-geal four-chamber view is obtained. This view allows visualization of all the chambers of the heart. The image rotation is approximately 0–10° with some posterior flexion of the probe. The key structures to observe are the left atrium, the LV, the right atrium, the right ventricle, the mitral and tricuspid valves, and the septal and lateral walls of the myocardium. If a portion of the left ventricular outflow tract and AV is displayed (called the five-chamber view), retroflexion of the probe and slight advancement or rotation of

<u>Depth:</u>   mid-esophageal (30-40 cm from the dental rhyme)

<u>Angle:</u>   80°-110°

<u>Flex:</u>   none

<u>Laterality:</u>   none

<u>Rotation:</u>   the right to place the right atrium in the center

<u>Goals:</u>   right atrium, left atrium, atrial septum, inferior vena cave and superior vena cava

<u>Legend:</u>   LA: left atrium
                  RV: right atrium
                  IVC: inferior vena cava
                  SVC: superior vena cava
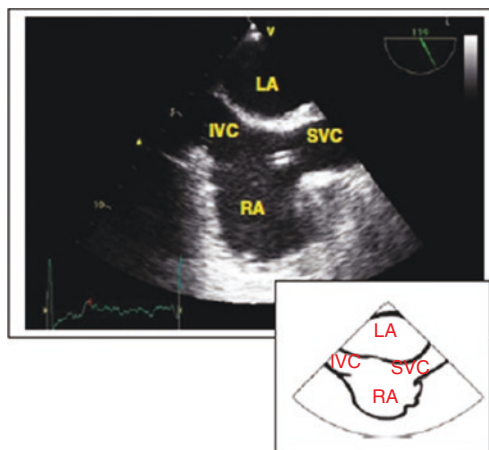
Fig. 4.4 Mid-esophageal bicaval view

<u>Depth:</u>   mid-esophageal (30-40 cm from the dental rhyme)

<u>Angle:</u>   0°-20°

<u>Laterality:</u>   none

<u>Goals:</u>   right atrium, right ventricle, left atrium, left ventricle, mitral value, tricuspid valve

<u>Legend:</u>   RA: right atrium
                  RV: right ventricle
                  LA: left atrium
                  LV: left ventricle
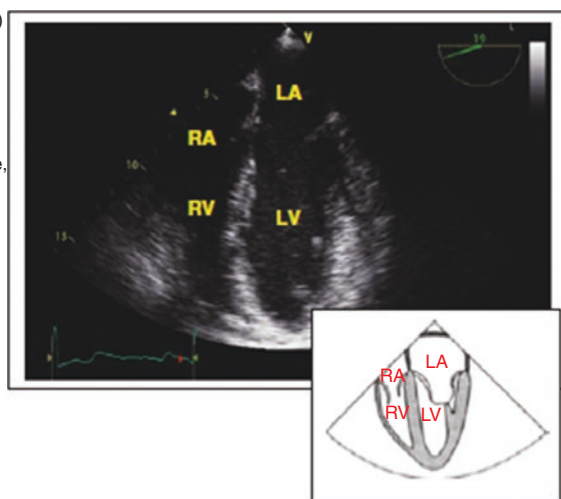
Fig. 4.5 Mid-esophageal four-chamber view

the imaging plane to 5–10° should produce the mid-esophageal four-chamber view (Fig. 4.5). The mid-esophageal four-chamber view is one of the most diagnostically valuable views in TEE. The diagnostic goals of this view include evaluation of chamber size and function, valvular function (both mitral and tricuspid), biventricular interdependence, and regional motion of the septal and lateral walls of the LV. An additional important use of this view is to look for intraventricular air following cardiopulmonary bypass. After two-dimensional interrogation of this view, CFD imaging should be applied to the mitral and tricuspid valves to detect valvular insufficiency and stenosis.

4.3.2.2 Mid-esophageal Two-Chamber View

From the mid-esophageal four-chamber view, the imaging angle is rotated to approximately 60–90° to obtain the mid-esophageal two-chamber view. This view is characterized by the presence of the left atrial appendage and the absence of right-sided heart structures, and it allows visualization of the anterior and inferior walls of the LV. Occasionally, turning the probe shaft

to the right will improve chamber alignment and visualization of the true left ventricular apex. Ventricular thrombus or hypokinesis at the apex is often best appreciated in this view (Fig. 4.6). The primary goals of this view are to evaluate left ventricular function (especially the apex) and anterior and inferior regional wall motion. It can also be used to look for thrombus of the left ventricular apex and left atrial appendage.

4.3.3   Transgastric Level: Transgastric Mid-papillary Short-Axis View

After completion of the interrogation of the heart at the aortic and mitral valve levels, the imaging plane is returned to 0°, and the probe is advanced into the stomach to obtain the transgastric views. The first is the transgastric mid short-axis view. The probe is then anteflexed and withdrawn until contact is made with the wall of the stomach. The key structures to visualize are the left ventricular walls and cavity in addition to the posteromedial and anterolateral papillary muscles. A true short-axis cross section of the LV is confirmed when the two papillary muscles are approximately of equal size. Fine-tuning this image may be dif-

ficult (Fig. 4.7). The primary diagnostic goals of this view are assessment of left ventricular systolic function, left ventricular volume, and regional wall motion.

4.3.4   Aortic Examination

4.3.4.1 Descending Aortic Short-Axis View

After completion of the preliminary evaluation of the heart, the aorta is examined. From the transgastric two-chamber view, the imaging angle is rotated to 0°, and the probe shaft is turned to the patient's left and slightly withdrawn until a transverse view of the descending aorta is obtained (the descending aortic short-axis view). Key factors in imaging the aorta are its small size and its proximity to the TEE probe head in the esophagus. Consequently, the following maneuvers are necessary to optimize aortic imaging. First, the image depth is reduced to enlarge the displayed aortic image. Then, the frequency of the transducer can be increased to enhance resolution. The aorta is then visualized along its course as the probe is slowly withdrawn. When the aorta begins to appear elongated, the level of the aortic arch has been reached (Fig. 4.8).

Depth: mid-esophageal (30-40 cm from the dental rhyme)

Angle: 80°-100°

Deflection: none

Laterality: none

Goals: left atrium, mitral value, left ventricle

Legend: LA: left atrium
            LV: left ventricle
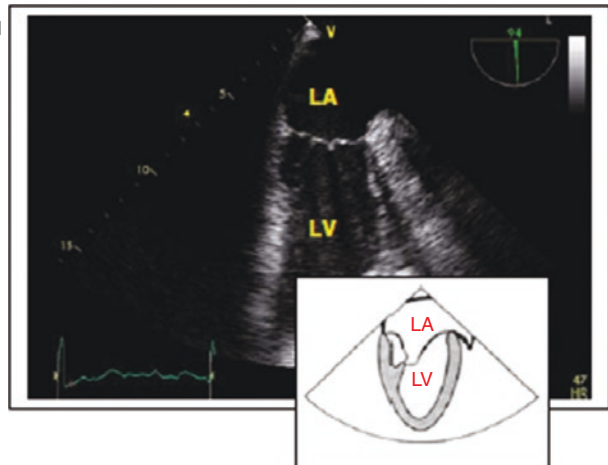
Fig. 4.6 Mid-esophageal two-chamber view

Depth: transgastric

Angle: 0°

Flex: anteflex

Laterality: none

Goals: left atrium, left ventricle

Legend: LV: left ventricle
             pmPM: posteromedial papillary muscle
             alPM: anterolateral papillary muscle
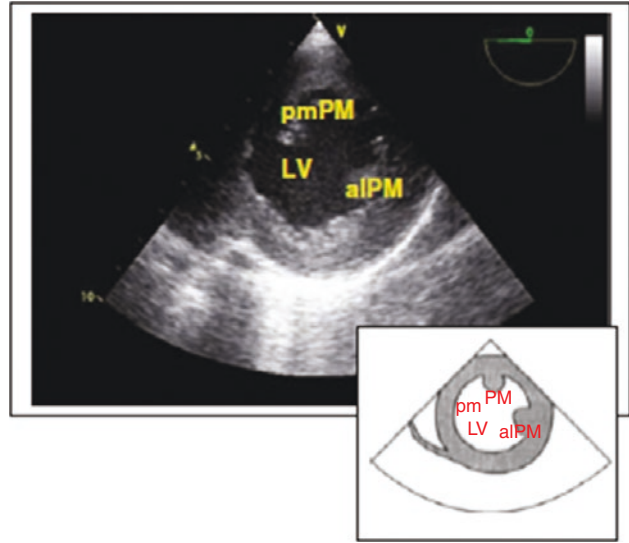
Fig. 4.7   Transgastric mid-papillary short-axis view

Depth: mid-esophageal (30-40 cm from the dental rhyme)

Angle: 0°

Flex: none

Laterality: none

Goals: descending thoracic aorta

Legend: DAo: descending aorta
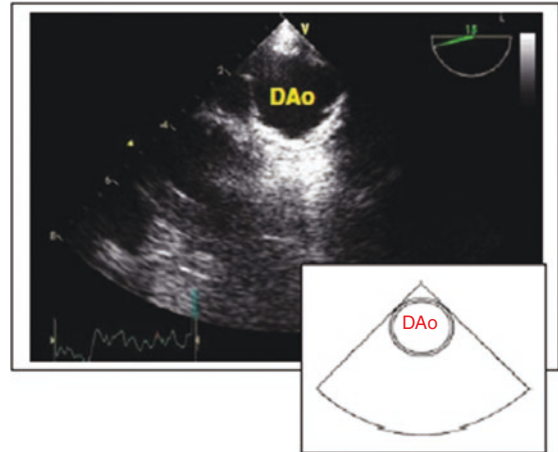
Fig. 4.8   Descending aortic short-axis view

4.3.4.2 Upper Esophageal Aortic Arch Short-Axis View

From the level of the aortic arch, the imaging angle is turned to 90° to obtain the upper esophageal aortic arch short-axis view. Small left and right turns of the probe shaft will allow the arch to be interrogated for calcification, enlargement, and foreign bodies. The origins of the great vessels may be at approximately three o'clock in the short axis of the aortic arch. The origin of the left subclavian artery is visualized in this view.

4.3.4.3 Descending Aortic Long-Axis View

From the upper esophageal aortic arch short-axis view with the imaging plane maintained at 90°, the probe is advanced to obtain the longitudinal view of the descending aorta (the descend-
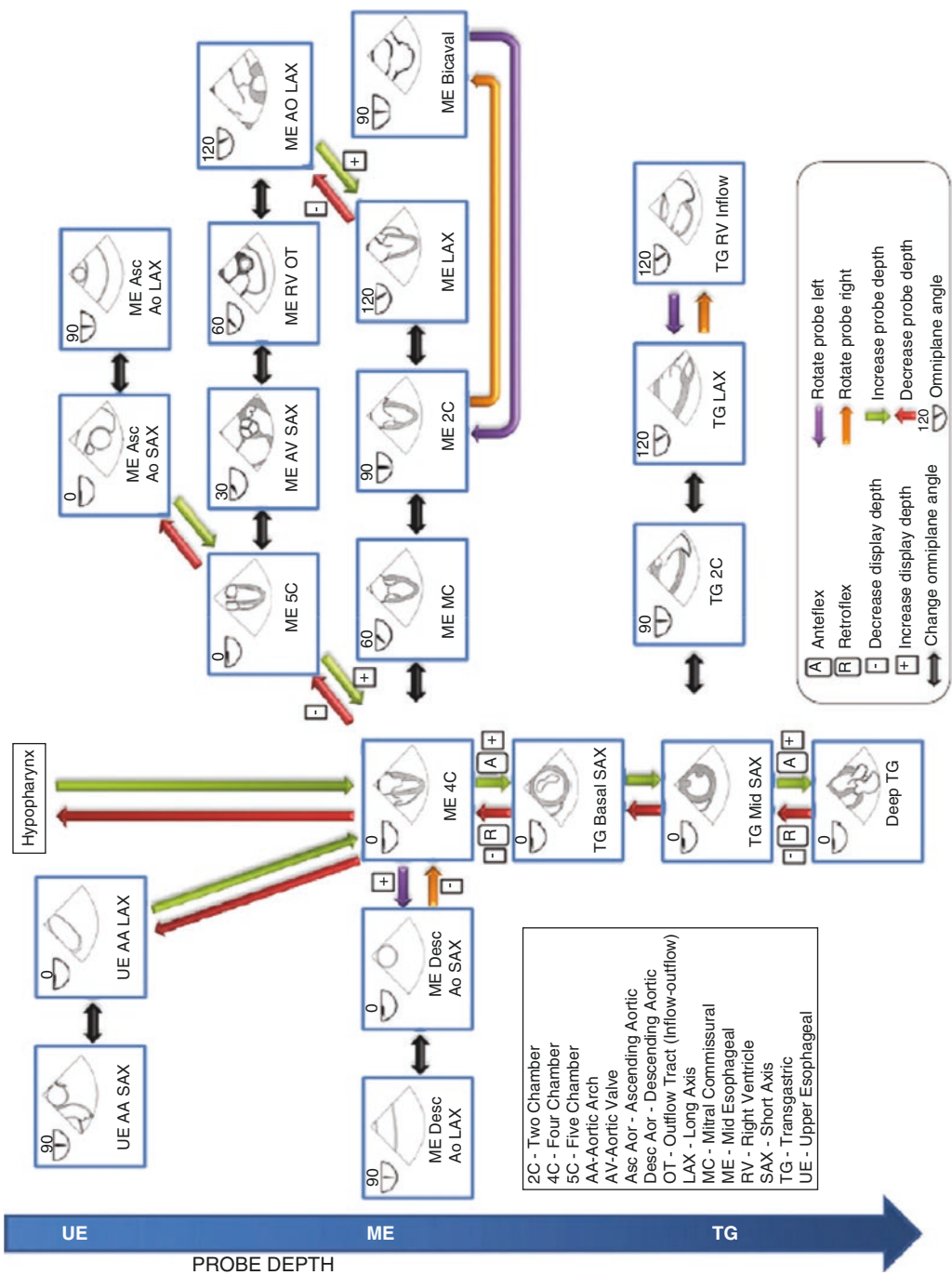
Fig. 4.9 The 21 standard transesophageal echocardiography views

ing aortic long-axis view). Again, as the probe is advanced, small left and right turns of the probe permit better interrogation of the aortic walls.

4.4   Summary

To help understand the relationships between the various echocardiographic sections, Fig. 4.9 summarizes all standard views and movements of the transesophageal probe to move from one view to another.

Suggested Reading

Miller JP, Lambert SA, Shapiro WA, et al. The adequacy of basic intraoperative transesophageal echocardiography performed by experienced anesthesiologists. Anesth Analg. 2001;92:1103–10.

Shanewise JS, Cheung AT, Aronson S, et al. ASE/SCA guidelines for performing a comprehensive intraoperative multiplane transesophageal echocardiographic examination: recommendations of the American Society of Echocardiography Council for Intraoperative Echocardiography and the Society of Cardiovascular Anesthesiologists Task Force for Certification in Perioperative Transesophageal Echocardiography. Anesth Analg. 1999;89:870–84.

Stevenson JG. Adherence to physician training guidelines for pediatric transesophageal echocardiography affects the outcome of patients undergoing repair of congenital cardiac defects. J Am Soc Echocardiogr. 1999;12:165–72.

Thys DM, Abel M, Bollen BA, et al. Practice guidelines for perioperative transesophageal echocardiography. A report by the American Society of Anesthesiologists and the Society of Cardiovascular Anesthesiologists Task Force on Transesophageal Echocardiography. Anesthesiology. 1996;84:986–1006.

Ungerleider RM, Kisslo JA, Greeley WJ, et al. Intraoperative echocardiography during congenital heart operations: experience from 1,000 cases. Ann Thorac Surg. 1995;60:S539–42.

Three-Dimensional Echocardiography

5

Mauro Pepi and Gloria Tamborini

5.1 Introduction

Three-dimensional (3D) echocardiographic (3DE) imaging represents a major innovation in cardiovascular ultrasound. Advancements in computer and transducer technologies permit real-time 3DE acquisition and presentation of cardiac structures from any spatial point of view.

Progress in three-dimensional echocardiography (3D) has been rather slow in the 1980s and 1990s due mainly to technical reasons, but nowadays this technique is simple and rapid and allows additional clinical information in different cardiovascular fields. This chapter details the current status of 3D technology and in particular recent advances in 3D live methods (either transthoracic -3DTTE- or transesophageal -3DTEE-) with its clinical applications in main heart diseases.

5.2 Methods and New Technologies

Several methods including random and sequential scanning and free-hand techniques by both transthoracic and transesophageal echocardiography have been proposed in the past, and all of them

required an off-line reconstruction. Real-time volumetric imaging and ultrasound developed in the early 1990s by the group of Von Ram of the Duke University was based on novel matrix phased array transducer technology. However the first-generation instrument had several practice limitations despite its potential very promising clinical applications were clearly demonstrated. In the early 2000, the second-generation real-time live 3D (and nowadays the new probe and software technologies) allowed a true routine application of the method in different fields: it is simple and rapid and may be easily integrated and associated with the standard 2D examination. In brief these new transducers (with 3000/4000 ultrasound elements) generate multidirectional beam steering and signal processing which take place automatically in the scanning probe itself. This technology generates in the display true pyramidal volumes of data and creates online rendered images; since this pyramidal data set is still limited in terms of volumes (generally $60° \times 30°$), it is alternatively possible to obtain a larger volume data set of up to $100° \times 100°$ (the so-called full-volume data set) acquiring together up to seven (generally 4 or 7) sub-volumes over consecutive cardiac cycles. Moreover new software allow to utilize zoom methods, to acquire 3D images also in the presence or arrhythmias, and to improve spatial and temporal resolution. Images acquired may be immediately sliced in several planes and rotated in order to visualize cardiac structures from any plane and multiple prospectives. As concerns the

M. Pepi (✉) · G. Tamborini
Centro Cardiologico Monzino, IRCCS, Milan, Italy
e-mail: Mauro.pepi@ccfm.it

"old technologies," 3D sequential transesophageal acquisition (multiplane TEE with ECG and respiratory gating) is now abandoned. A new generation of TEE echocardiography probes with a novel matrix array technique has been introduced in 2008, allowing 3D presentation of cardiac structures in real time. This toll provides fast and complete 3D information about cardiac structures improving spatial orientation and overcoming limitations of off-line 3D technologies. Therefore we refer to real-time transthoracic (RT3DTTE), transesophageal sequential acquisition (3DTEE), and real-time transesophageal (RT3DTEE) echocardiography. Finally we also refer to the very new introduction of a single beat acquisition which allows a complete full volume acquired in a single beat.

5.3   Image Display and Analysis

In contrast to cross-sectional (i.e., tomographic) modalities, 3D echocardiography requires that the "viewing perspective" be in the chamber that is in immediate continuity with the region of interest. Volume rendering is a process whereby the cardiac structures area reconstructed by the computer so that volumetric data set can be sectioned electronically in any plane. Once part of the data set is cropped away, you can see inside the heart. By this method the display and analysis of size, shape, and motion of cardiac structures may be examined from any desired perspective. Moreover the image may be manipulated and rotated, and as an example, mitral and tricuspid valves may be viewed from above (simulating atriotomy, the so-called surgical view) or from below. Thanks to advances in shading techniques, an impression of perspective and depth is created. Other methods of analysis focused on the evaluation and display of cardiac chambers such as the left ventricle. Wire frame rendering or surface rendering results in displaying the surfaces of the analyzed object facing the observer as solid structure. These images may be obtained from manually or electronically derived contours from the data set. This method allows the assessment of the shape providing the visualization of the chamber in terms of volume, shape, and function.

Table 5.1 Transthoracic and transesophageal 3D main clinical applications

Quantification of left ventricular volumes and function (and shape)
Quantification of left ventricular mass
Assessment of regional wall motion of the LV (rest and stress)
Assessment of left ventricular dyssynchrony
Quantification of right ventricular volumes and function
Evaluation of valve diseases
Evaluation of cardiac masses
Guidance of intracardiac interventions
Monitoring of cardiac surgery
Congenital heart diseases

5.4   Different Clinical Applications

Table 5.1 reports the main clinical applications of 3D echocardiography (either 3DTTE or 3DTEE).

5.5   Quantification of Left Ventricular (LV) Volumes and Function (and Shape)

The biggest advancement of 3D echocardiography is the lack of dependence on geometric modeling resulting in more accurate chamber quantification. Several studies have directly compared the accuracy of 3D vs 2D measurements of LV volumes and have demonstrated the superiority of 3D method (less underestimation, superior reproducibility, and intra- and interobserver variability). It is nowadays possible with different software on board on the ultrasound units or off-line to detect endocardial surfaces from the 3D data sets and rapidly obtain volumes and ejection fraction. Despite this advantage the method still slightly underestimates the LV volume in comparison with the MRI considered as the gold standard. Several reasons may explain this underestimation including resolution of 3D echo, trabeculations of the LV, and methods of measurements with the two different techniques. Very recently novel-automated software have been developed that provide LV and LA volumetric quantification, based on an adaptive analytics

algorithm, which was trained on a large number of 3DE data sets obtained in patients with a variety of normal and abnormal hearts. This allows a very rapid and completely automated LV quantification.

5.6 Quantification of Left Ventricular Mass

Left ventricular mass measurements rely not only to endocardial but also to epicardial boundary identification. It is therefore challenging. Nevertheless several studies based on 3D echo showed a good accuracy of the method in normal and pathologic hearts. In this regard contrast enhancement 3D echocardiography may further improve both LV volume and mass measurements.

5.7 Assessment of Regional Wall Motion of the LV (Rest and Stress)

Several studies have assessed the role of 3D echocardiography for the evaluation of regional

LV function. With both the full-volume acquisition and the new single beat acquisition, 3D allows direct displacement of endocardial surfaces therefore leading to an objective dynamic quantification of global and regional function. Despite limitation in temporal and spatial resolution and the dependence on optimal quality of images, this method (through the utilization of specific software on board on the ultrasound units or off-line) may overcome the subjective interpretation of regional analysis performed in standard examinations. Real-time 3D-derived regional motion was validated against a CMR reference. 3D regional motion may be potentially very useful in different fields: more objective quantification of number of segments involved in regional dysfunction, echo-stress, and guidance of resynchronization therapy. In echo-stress study the main advantage is the unique possibility of visualizing all LV segments during one breath hold. The majority of echo-stress studies demonstrated an accuracy similar to standard 2D techniques but significant advantages in terms of acquisition time and evaluation of all segments during each step of the stress (Fig. 5.1).
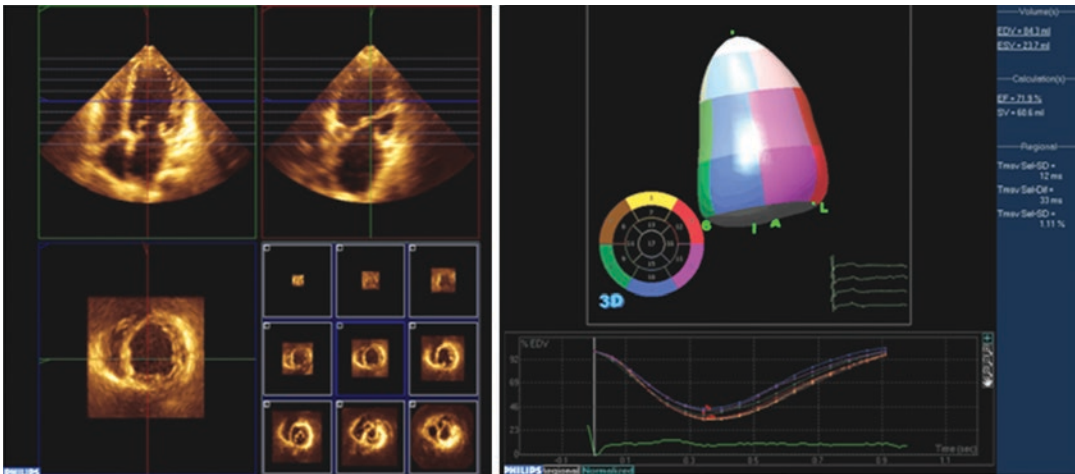
Fig. 5.1 Left panel shows 3D data set as well as short axis of the left ventricle at different cut planes of the chamber facilitating wall motion analysis. Right panel: a color-coded segment analysis, and derived curves of the LV wall motion analysis are shown

5.8 Left Ventricular Dyssynchrony

Cardiac resynchronization therapy (CRT) is a very important and expanding technique in patients with symptomatic heart failure, poor LV function, and QRS duration >120 ms. 3D real-time echocardiography is an emerging tool to provide new indicators of myocardial dyssynchrony in selecting and monitoring patients with heart failure undergoing biventricular pacing. Several methods have been proposed. Kapetanakis et al. studied a large cohort of normal subjects and patients with real-time transthoracic 3D echo proposing a new systolic dyssynchrony index (SDI) derived by the dispersion of time to minimum regional volume for all 16 segments of the left ventricle. Normal subjects had a well-synchronized segmental function (SDI 3.5%). On the contrary patients may have SDI which increased with worsening of LV dysfunction (severe dysfunction SDI 14.7%). At long-term follow-up, patients undergoing CRT showed in case of positive response a marked reduction of SDI, associated with increase in ejection fraction and decrease of LV volumes. Soliman et al. also confirmed these data. An SDI > 10% predicted CRT response with good sensitivity and specificity. Marsan et al. demonstrated that a cutoff value of SDI of 6.4% has high sensitivity and specificity (88% and 85%, respectively, in a long-term follow-up) and good reproducibility.

5.9 Quantification of Right Ventricular Volumes and Function

Due to the peculiar right ventricular morphology and function, 2DE has several limitations in the evaluation of the right ventricle (RV) which can be readily overcome by of a 3DE-gated wide-angled acquisition which enables a complete assessment geometry, volumes, and ejection fraction displaying the surfaces of the entire RV including the inflow, apex, and outflow tract.

Several methods and software have been used to evaluate the RV. 3D data are acquired in a full-volume set from the four-chamber apical view adapted to improve the visualization of the entire RV. 3DE data set are typically digitally stored, and then post-processed off-line or more recently on-cart dedicated RV analysis software packages are now available further facilitating the use of these measurements in clinical practice. Current RV analysis software display 2D cut planes of the RV sagittal, four chamber, and coronal views obtained from the full-volume 3DE data set. The majority of the currently used method of analysis automatically display these three views which are checked for consistency by toggling back and forth. The anatomy and pathology of the tricuspid valve and the RV are best visualized using volume-rendered images. The right atrium and RV can be visualized using multiple cut planes. A variety of options for online or off-line 3D reconstruction of the RV exist. After acquisition and automatic display of the RV end-diastolic and end-systolic frames, the operator in the different planes traces a contour of the endocardial border. Recent available software calculate RV volumes from end-diastolic and end-systolic endocardial border tracings of sagittal (to outline the tricuspid valve in the best possible view), four chamber (to outline the apex), and coronal (to outline the RVOT) 3DE-derived cross-sectional planes. The operator frequently needs to manually adjust the traced contours in each frame prior to cast reconstruction and quantitative analysis. This software analysis, which uses a semiautomated border detection algorithm with manual correction options, was validated using in vitro models as well as in vivo using cardiac magnetic resonance as the gold standard. The different software packages create a surface-rendering cast of the right ventricle. The end-diastolic and end-systolic volumes as well as RV ejection fraction are measured and automatically displayed (Fig. 5.2). Curves of global and regional RV function may be generated and analyzed.

Data on RV volumes and function are of diagnostic and prognostic importance in a variety of cardiac disease including valve disease, congenital heart disease, pulmonary hypertension, and heart failure. 3DE not only allows the evaluation of volumes and function in normal subjects and
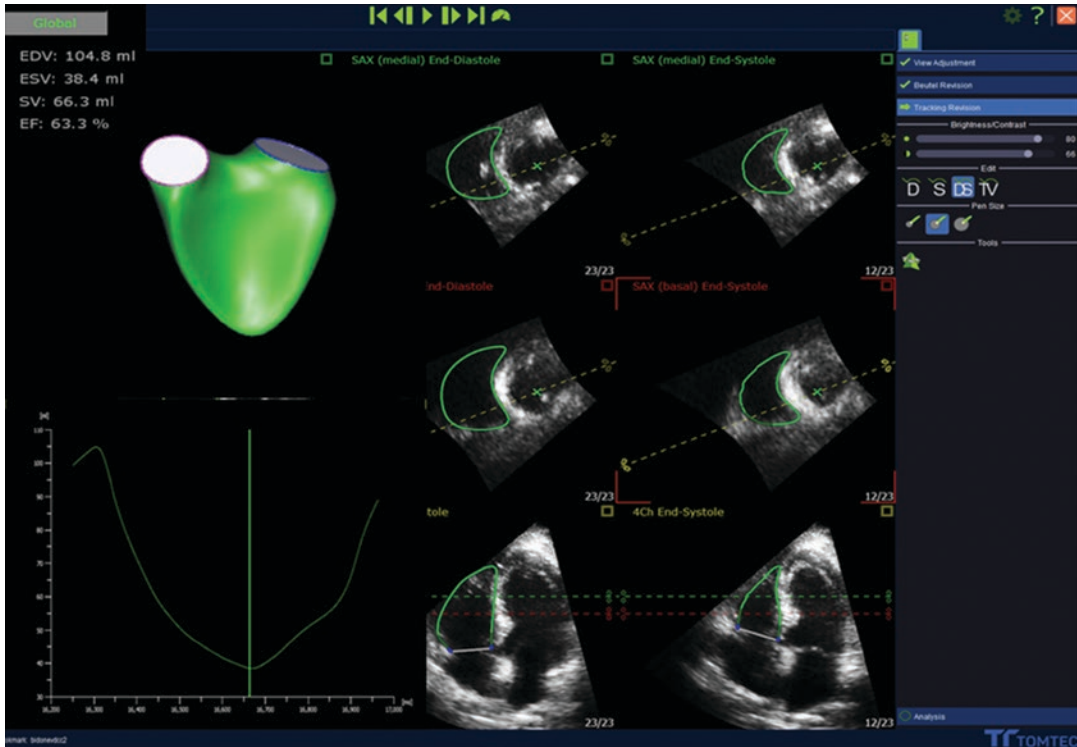
Fig. 5.2 End-diastolic and end-systolic RV surface volumes are depicted in different orientations showing the inflow, outflow, and apex segments of the right ventricle allowing a 3D morphologic display of the RV (upper left panel) . The bottom left panel also shows quantitative analysis of the curve with RV volumes, stroke volume, and ejection fraction

patients, allowing identification of patients with different severities of RV dilatation and dysfunction. Several clinical studies have shown a good correlation between magnetic resonance and 3DE volumes and ejection fraction of the RV in selected populations with the majority of studies showing a slight underestimation of volumes compared to the reference technique. Differences in RV volumes have been demonstrated between men (129 ± 25 ml) and women (102 ± 33 ml); however adjusting to lean body mass (but not to body surface area or height) eliminated this difference. The 3DTTE RV ejection fraction shows a high correlation with MRI values.

The use of TT 3DE has been validated in patients with several pathologies: heart failure, pulmonary hypertension, LV and RV cardiomyopathy, and congenital heart diseases. The feasibility and utility of TT 3DE for the guidance of RV endomyocardial biopsies in children has been demonstrated. Assessment of RV function is of great interest in cardiovascular surgery because right-sided heart failure is one of the most frequent causes of morbidity and mortality postvalvular and congenital surgery, coronary artery bypass, and heart transplantation. This highlights the importance of an accurate preoperative assessment of the RV to improve risk stratification and an early and precise postoperative follow-up to optimize treatment. In this regard 2DE and Doppler parameters (TAPSE, DTI of the annulus) have several limitations particularly in the postoperative follow-up. The evaluation of RV volumes and ejection fraction using 3DE overcomes many of the limitations of 2DE methods. Recently reference values of RV volumes and ejection fraction have been published. Finally preliminary data on TEE 3D acquisition

and reconstruction of the RV have been published, and the prognostic role of 3DTTE ejection fraction is demonstrated.

5.10 Evaluation of Valve Diseases

Both qualitative and quantitative evaluation of valvular heart disease can be improved by 3D echocardiography. Anyplane and paraplane analysis of a stenotic valve allows an accurate planimetry of the smallest orifice area. Zamorano et al. demonstrated that 3DTTE is a feasible, accurate, and highly reproducible technique for assessing mitral valve (MV) area in patients with rheumatic MV stenosis. In a consecutive series of 80 patients, compared with all other echo-Doppler methods, 3DTTE had the best agreement with the invasively determined MV area, and intra- and interobserver variability of the method was very good. The same author also studied 29 patients undergoing percutaneous balloon mitral valvuloplasty. 3DTTE had the best agreement with the invasively determined MV area particularly in the immediate post-procedural period; thus the method may be proposed as an ideal one throughout this procedure and makes invasive evaluation unnecessary in this setting.

A part with these very important quantitative data, 3DTTE may be integrated to 2D evaluation in the assessment of qualitative morphology of the MV. Commissures, leaflets, annulus calcifications, and subvalvular structures may be visualized from different and unique planes facilitating the understanding of this complex apparatus. Each of the atrioventricular valves may be in fact depicted both from the atrium or ventricle with access to "en face" views and from any other angle. Vegetations, commissural diseases, subvalvular pathologies (tip of the leaflets/cordae/papillary muscles), and clefts may be accurately diagnosed. MV prolapse is visualized as a bulging or protrusion on the atrial site, and in this regard, 3D is the ideal method to demonstrate the pathology.

Several studies showed that 3D (either transthoracic or transesophageal) echocardiography is superior in comparison with the corresponding 2D techniques in the description of MV pathology. In particular since real-time transthoracic 3D echocardiography has an accuracy similar to that of 2D transesophageal echocardiography, this new technique (which is also simple and rapid) may be integrated in the standard 2D examination and should be regarded as an important examination in decision regarding MV repair. Mitral valve (MV) prolapse is the most frequent etiology of mitral regurgitation in industrialized countries. Since the 1970s MV repair has become preferential to replacement and is now possible in the overwhelming majority of patients with MV prolapse. Recent studies and guidelines have underlined the importance of early surgical intervention to preserve long-term left ventricular function in severe mitral regurgitation. In this regard a noninvasive preoperative assessment of MV anatomy is essential to define feasibility and complexity of repair differentiating cases with simple or complex lesions and to plan the ideal surgical strategy. For all these reasons, 3DTTE and 3DTEE should be regarded as an important examination in decision regarding MV repair particularly in cases with complex diseases and in the light of these new early surgical strategies. Recently a large series of cases with mitral valve prolapse evaluated with different echo methods has been published. One-hundred twelve consecutive patients with severe mitral regurgitation due to degenerative MV prolapse underwent a complete 2D and 3DTTE the day before surgery and a complete 2D and 3DTEE in the operating room. Echocardiographic data obtained by the different techniques (including scallops, commissures, chordal rupture identification) were compared with MV surgical inspection. Three-dimensional techniques were feasible in a relatively short time (3DTTE, 7 ± 4 min; 3DTEE, 8 ± 3 min), with good (3DTTE 55%; 3D TEE 35%) and optimal (3DTTE 21%; 3DTEE 45%) imaging quality in the majority of cases. 3DTEE allowed more accurate identification (95.6% accuracy) of all MV lesions in comparison with other techniques. 3DTTE and 2DTEE had similar accuracies (90% and 87%, respectively), while the accuracy of 2DTT (77%) was significantly lower. Thus these data showed that 3DTTE and 3DTEE are feasible, not time-

consuming and useful methods in identifying the location of MV prolapse in patients undergoing MV repair. They were superior in the description of pathology in comparison with the corresponding 2D techniques and should be regarded as an important adjunct to standard 2D examinations in decisions regarding MV repair. 3D live TEE technologies (miniaturization technology of the matrix array transducer) allow nowadays to have similar results in real time with obvious advances in clinical applications mainly in the operating room, giving immediate data to anesthesiologists and surgeons in the pre- and postoperative periods. Salcedo et al. published a "State-of-the-art" paper on systematic characterization of the mitral valve by real-time 3D TEE confirming that several studies showed that this new technique not only provides spectacular (and immediate) images of the mitral valve but also adds clinical value particularly in cases with complex mitral
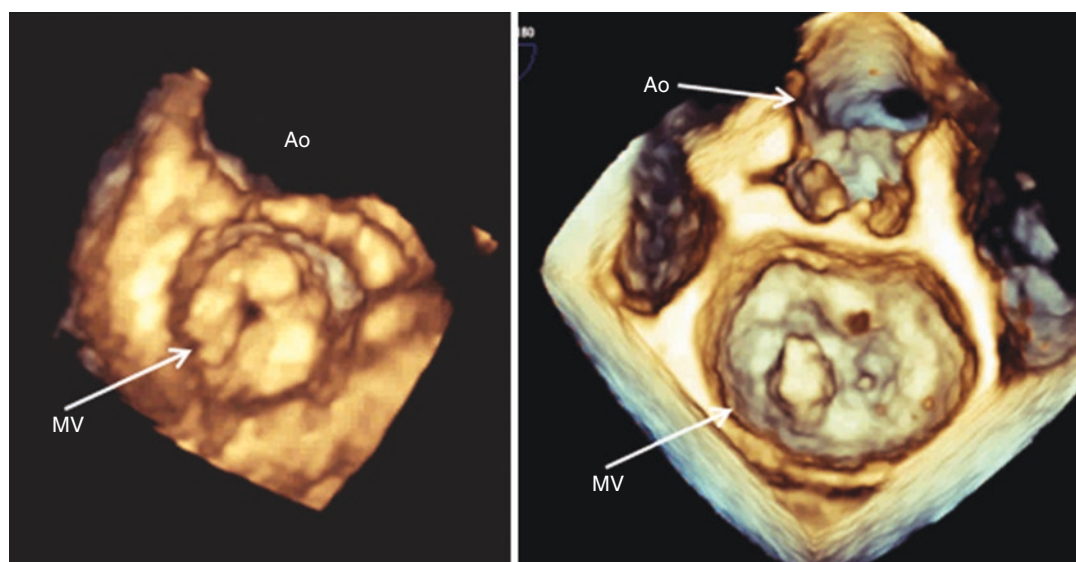
Fig. 5.3 Surgical views of a severe mitral stenosis (left panel) and of a P2 prolapse (right panel) evaluated by real-time 3DTEE. AV aortic valve, MV mitral valve
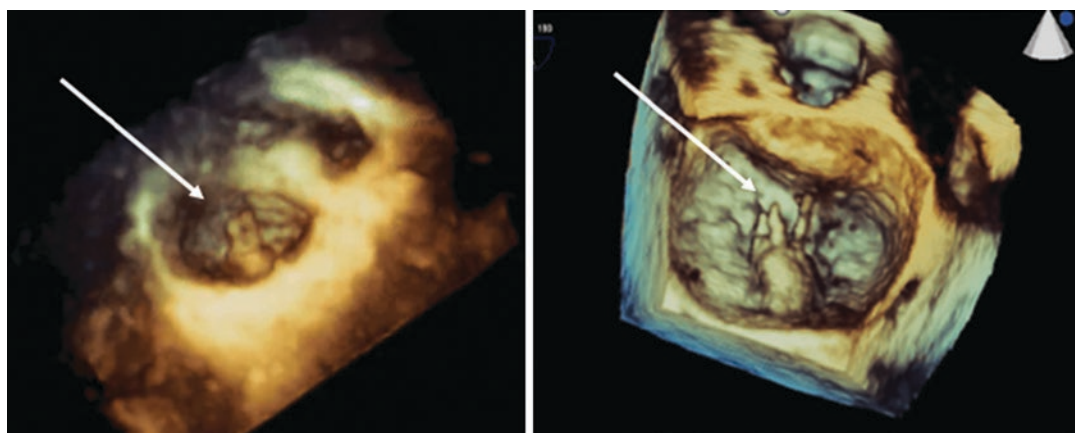
Fig. 5.4 Surgical view of the mitral valve with transthoracic (left panel) and transesophageal (right pane) echocardiography of the same patient. With both approaches a flail P2 prolapse with ruptured chordae is clearly defined
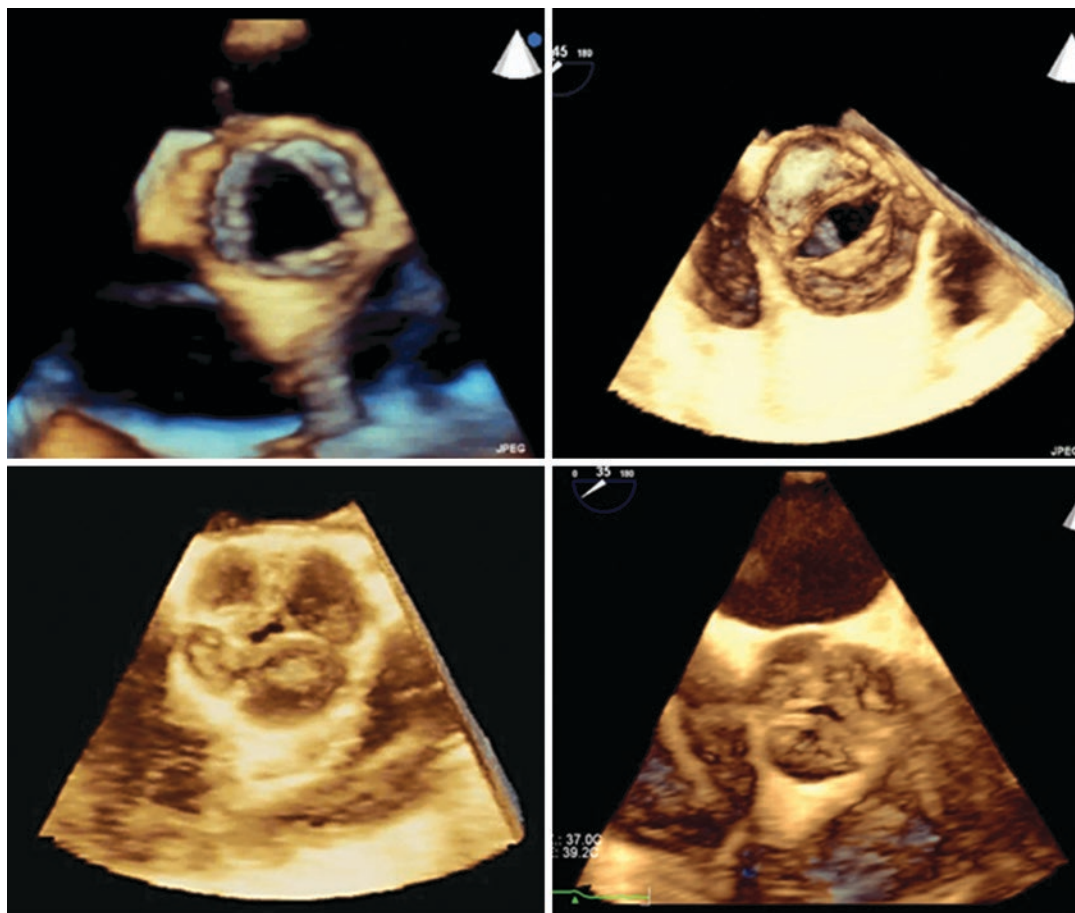
Fig. 5.5 Real-time 3DTEE of the aortic valve of four different cases. Upper left panel: normal opening of a tricuspid valve. Upper right panel, systolic frame of a bicuspid valve; bottom left panel, quadricuspid valve in diastolic frame; bottom right panel, systolic frame of a stenotic tricuspid valve

valve prolapsed. In this regard Tamborini et al. demonstrated that it is also true with transthoracic real-time 3D echocardiography in patients undergoing mitral valve repair. Overall accuracy in identification of mitral valve scallop was 95% (vs surgical inspection), and the method may predict the complexity of surgical procedures. Figures 5.3 and 5.4 show cases of MV stenosis and prolapse examined by 3DTEE and 3DTTE, respectively. Recently matrix technology offers all modalities (2DTTE with Doppler, 3DTTE with color Doppler) in a single transducer, similarly to the TEE probes, therefore avoiding the disadvantages of utilizing a dedicated 3DTTE probe.

The aortic valve may be easily evaluated by 3DTTE or 3DTEE. The morphology of the valve may be defined with high accuracy demonstrating normality or of the cusps, congenital abnormalities (bicuspid aortic valve), or acquired pathologies (Figs. 5.5 and 5.6). Few data have been concentrated on the accuracy of 3D in the assessment of the severity of aortic valve stenosis. Goland et al. evaluated the reproducibility and accuracy of real-time 3DTTE in 33 patients with aortic stenosis. Aortic valve area by 3DTTE was compared with 2DTTE planimetry, 2DTEE planimetry, and in 15 cases with invasive measurements showing good agreement and small absolute differences in aortic valve area between all planimetric methods. Interobserver variability was better for 3D technique. Therefore 3DTEE is a rapid and novel method that provides an accu-
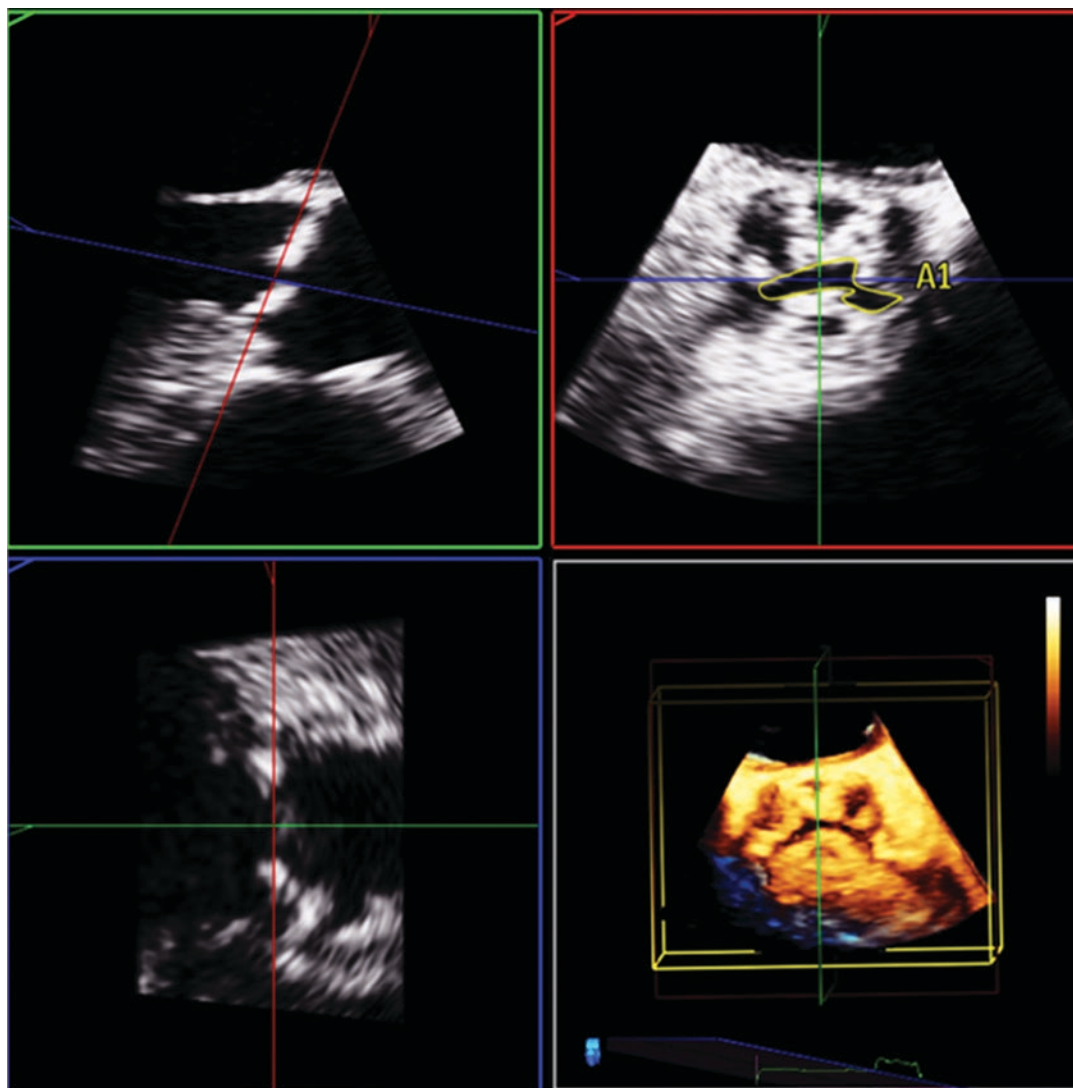
Fig. 5.6 These panels show steps of measurements of an aortic valve orifice based on a 3D data set (right bottom panel). By allying planes in different axes (left upper and bottom panels), the correct systolic orifice of an aortic stenosis may be analyzed by planimetry (right upper panel)

rate and reliable quantitative assessment of aortic stenosis.

Three-dimensional echocardiography offers a direct view to evaluate the leaflet surface of the tricuspid valve, a unique method to visualize the three leaflets simultaneously. Potentially this offers the opportunity to study every tricuspid pathology by different prospectives such as from the right ventricle, from the right atrium, or from oblique planes. Leaflet coaptation and separation may be therefore visualized easily. Even

though consecutive series of cases with tricuspid valve disease has not been published and no data demonstrate an additional clinical value of the method, several case reports showed the importance of this technique in Ebstein's anomaly, tricuspid stenosis, and other tricuspid pathologies. This potentiality in different tricuspid pathologies may be further completed by the measurement of right ventricular volumes and function (ejection fraction) by off-line 3DTTE analysis. In fact in all tricuspid pathologies, a crucial point

is represented by right ventricular function, and calculation of right ventricular volumes is not feasible by conventional 2D echocardiography. Full-volume analysis by 3DTTE allows in few seconds the acquisition of a complete data set of the right ventricle that allow off-line calculation of right ventricular volume as well as recognition of tricuspid diseases.

5.11   Congenital Heart Diseases

Main current clinical applications of real-time 3DTTE and 3DTEE include atrial and ventricular septal defects, several complex congenital pathologies, and bicuspid aortic valve. In children and young adults, 3DTTE (due to their excellent acoustic window) represents an ideal technique to visualize the complex anatomy of these pathologies. Position, morphology, and relation with other cardiac structures are better defined. In atrial or ventricular septal defects, location, size configuration, type, and measurement of rims are easily imaged by 3DTTE and 3DTEE in the majority of cases, thus impacting with the indication of percutaneous or surgical procedures (Fig. 5.7). Moreover these methods allow an in vivo 3D assessment of devices providing new insights, positioning, and interferences with the adjacent structures.
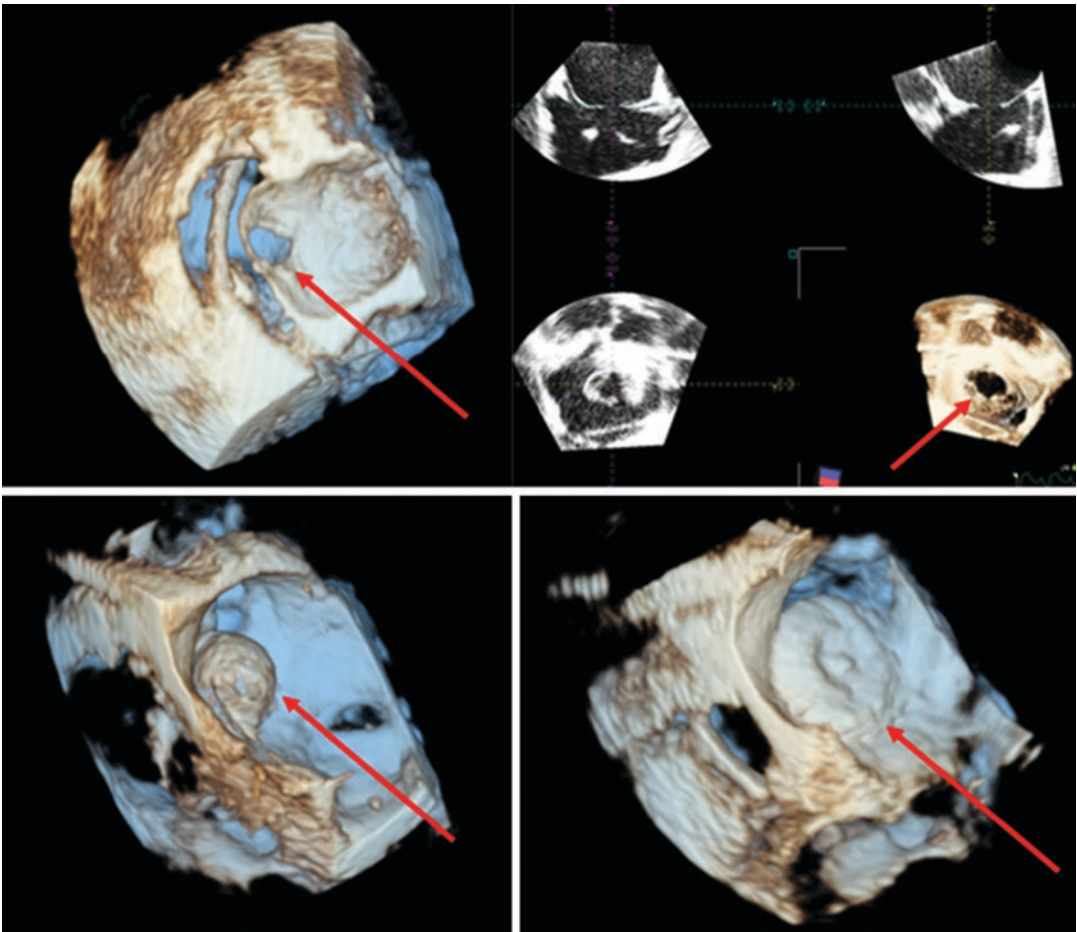
Fig. 5.7 Percutaneous closure of an atrial septal defect. Upper left panel: catheter advanced into the right atrium; the arrow shows the ASD. Upper right panel: en face reconstruction of the ASD (arrow). Bottom left panel: expansion of the balloon (arrow) to measure the correct sizing of the defect. Bottom right panel: the arrow shows the Amplatzer device correctly implanted

5.12   Cardiac Masses

3DTTE and 3DTEE are also emerging techniques for the evaluation (particularly in the preoperative assessment) of cardiac masses including vegetations, thrombi, and tumors. Morphology, size, and location of masses may be defined accurately, and 3D approach facilitates the understanding of relationships with the adjacent anatomical structures. Identification of the attachment points of vegetations and tumors may improve clinical and procedural decisions. Initial experience with the real-time 3DTEE in the operating room also supports the use of the real-time 3DTEE in this field.

5.13   Monitoring of Percutaneous Procedures

Some fields of echocardiography are under rapid evolution, in particular the use of TOE in the context of catheter-based interventions. For these interventions TOE data are crucial both in informing management decisions by the interdisciplinary Heart Team and during or after the procedure. While no fundamental changes in TOE hardware have recently occurred, the use of 3D-capable transducers has expanded, and software related to 3D data sets continues to evolve, allowing more complex processing, e.g., measurements of linear dimensions or curved areas of valvular structures or linking TOE data sets with simultaneous fluoroscopic images.

The new generation of real-time 3DTEE provides a unique new imaging technique to monitor invasive percutaneous or surgical procedures. Pathomorphology of cardiac structures may be in fact evaluated as well as catheters and devices during procedures. Therefore new surgical procedures, atrial septal or PFO percutaneous closures, aortic valve implantation (Fig. 5.8), percutaneous mitral valve repair or commissurotomy, transcatheter closure of periprosthetic regurgitation, left atrial appendage closure, and electrophysiological procedures may be monitored by real-time 3D echocardiography increasing safety, accuracy, and efficacy of these interventions. Several studies suggested that in percutaneous mitral clip procedures and transcatheter closure of periprosthetic regurgitation, 3DTEE appears to be superior in comparison with the sole 2D TEE monitoring and is nowadays considered mandatory (Fig. 5.9).

5.14   Monitoring of Cardiac Surgery

Multiplane 2D TEE introduced in the early 1990s has significantly improved TOE imaging during cardiac surgery. Real-time 3D TEE has the potentiality to become a routine application also in this field particularly in valve surgery and congenital and complex surgical procedures. Our first experience in 120 examinations clearly shows feasibility, excellent imaging quality, and an additional clinical value of these techniques mainly in valve surgery (either repair or replacement) not only in the preoperative period but also in evaluating postoperative complications, as well as in cardiac mass resection. Moreover, apart from percutaneous procedures and routine surgical procedure, other new surgical techniques such as transapical chordae tendineae implantation for mitral leaflet prolapse need 3D guidance (Fig. 5.10). Indeed 3DTEE has several advantages in this setting because of its ability to optimize the image planes throughout the entire procedure.

5.15   Future Perspectives

Advances in both micro-industrial design and computer technology will further reduce the size of transducers, improve temporal and spatial resolution, and permit single beat acquisition with simple quantitative analysis. Finally change in display of 3D images of the heart may improve virtual dynamic reality of the method facilitating communication network, training, and interventional procedures.
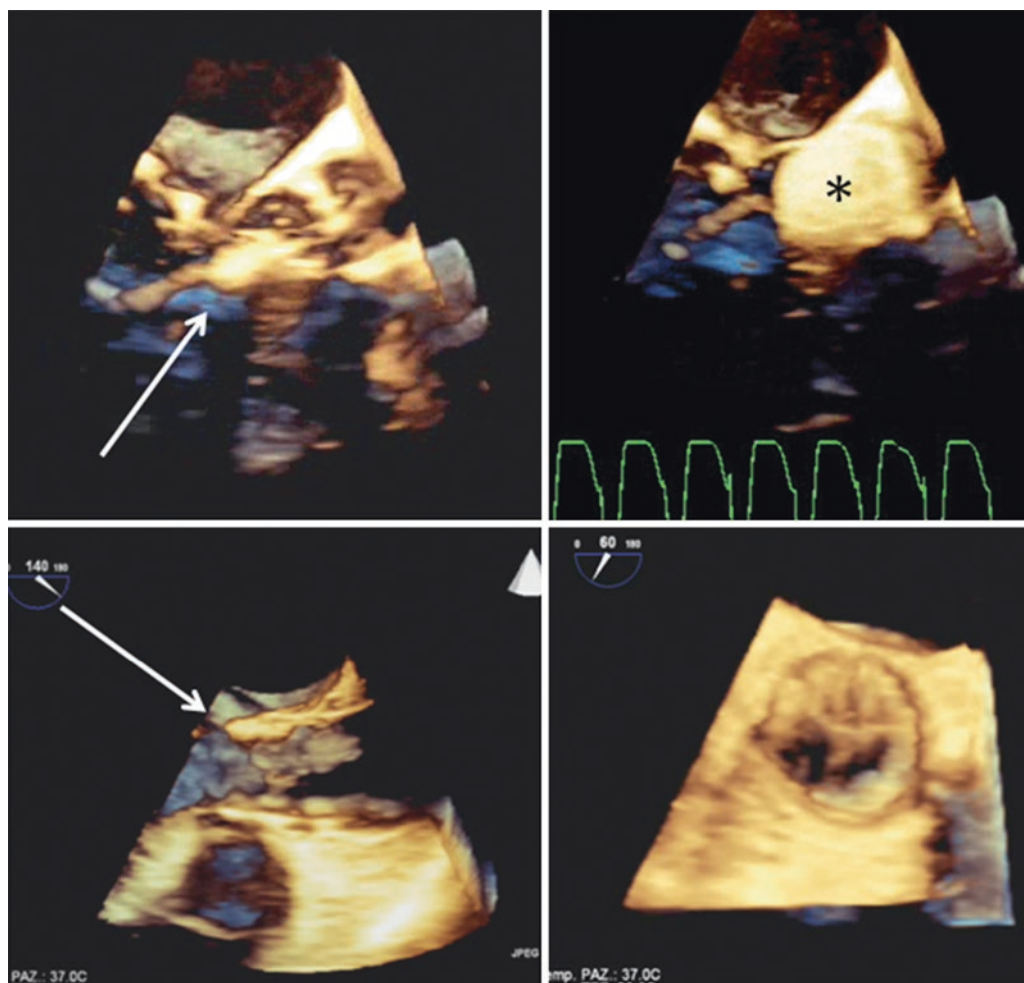
Fig. 5.8 This figure shows four main steps of a percutaneous aortic valve implantation (Edwards Sapien). Left upper panel shows the positioning of the catheter through the valve, and the corresponding right upper panel completes opening of the balloon (*). In the bottom panels, the prosthesis has been implanted and visualized in the long (left panel) and short (right panel) 3D views
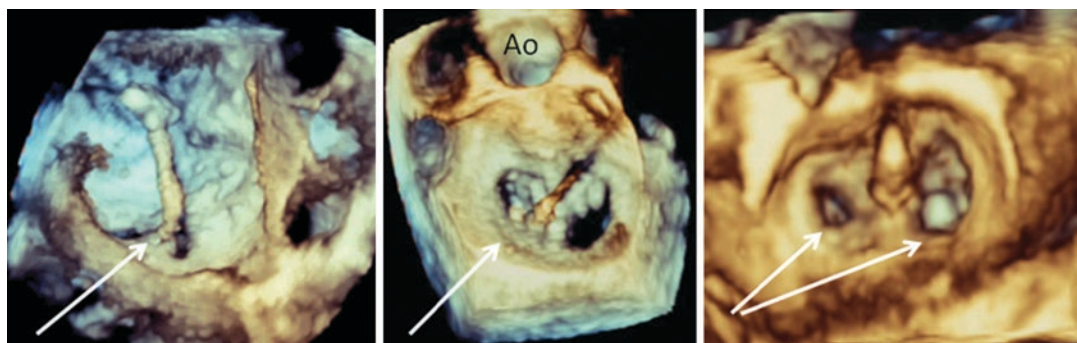
Fig. 5.9 Micro-industrial clip implantation: in the left panel, the arrow shows the passage of the device from the right to the left atrium approaching the mitral valve. In the middle panel, the device is grasping the P2-A2 scallops of the mitral leaflets. In the right panel, the two arrows show the double orifices created by the device which is clearly seen in the center of the valve
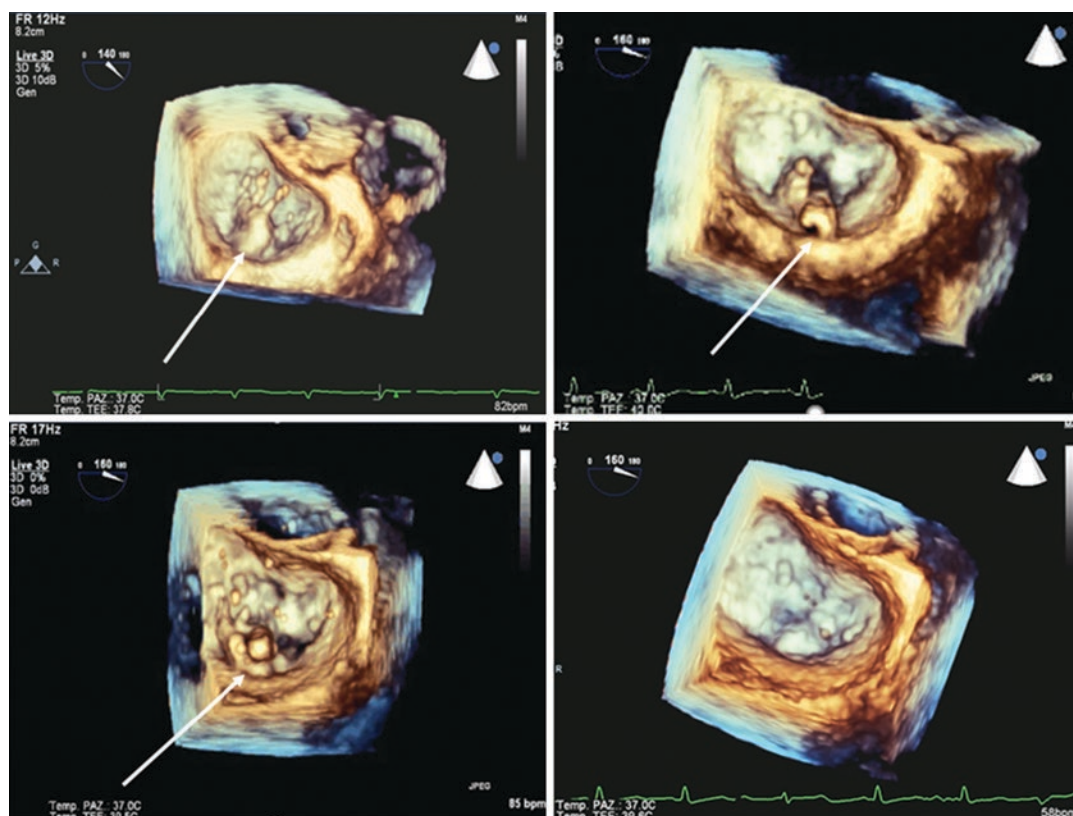
Fig. 5.10 Transapical neochordae implantation procedure. Left upper panel: surgical view of a fail P2 with ruptured chordae (arrow). Right upper panel: under 3D surgical view, monitoring the device is advanced into the left atrial cavity closed to the flail scallop (arrow), and (left bottom panel) a new chorda is implanted (arrow showing bubbles due to the implantation and the device position). Finally (bottom right panel) by external traction of the implanted chorda, operator may observe and monitor the complete resolution of the prolapse

Suggested Reading

Flachskampf FA, Wouters PF, Edvardsen T, Evangelista A, Habib G, Hoffman P, Hoffmann R, Lancellotti P, Pepi M, for the European Association of Cardiovascular Imaging. Recommendations for transoesophageal echocardiography: EACVI update 2014. Eur Heart J Cardiovasc Imaging. 2014;5(4):353–65.

Gripari P, Tamborini G, Barbier P, Maltagliati A, Galli C, Muratori M, Salvi L, Sisillo E, Alamanni F, Pepi M. Real-time three-dimensional transoesophageal echocardiography: a new intraoperative feasible and useful technology in cardiac surgery. Int J Cardiovasc Imaging. 2010;26:651–60.

Lang RM, Badano LP, Tsang W, Adams DH, Agricola E, Buck T, Faletra FF, Franke A, Hung J, Pérez de Isla L, Kamp O, Kasprzak JD, Lancellotti P, Marwick TH, McCulloch ML, Monaghan MJ, Nihoyannopoulos P, Pandian NG, Pellikka PA, Pepi M, Roberson DA, Shernan SK, Shirali GS, Sugeng L, Ten Cate FJ, Vannan MA, Zamorano JL, Zoghbi WA. EAE/ASE Recommendations for image acquisition and display using three-dimensional echocardiography. J Am Soc Echocardiogr. 2012;25(1):3–46.

Mor-Avi V, Sugeng L, Lang R. Real time 3-dimensional echocardiography. An integral component of the routine echocardiographic examination in adult patients ? Circulation. 2009;119:314–29.

Pepi M, Tamborini G, Maltagliati A, et al. Head-to-head comparison of two- and three-dimensional transthoracic and transesophageal echocardiography in the localization of mitral valve prolapse. J Am Coll Cardiol. 2006;48(12):2524–30.

Perk G, Lang R, Garcia-Fernandez M, et al. Use of real-time three-dimensional echocardiography in intracardiac catheter based interventions. J Am Soc Echocardiogr. 2009;22:865–82.

Tamborini G, Ajmone Marsan N, Gripari P, Maffessanti F, Brusoni D, Muratori M, Caiani E, Fiorentini C,

Pepi M. Reference values for right ventricular volumes and ejection fraction with real-time three-dimensional echocardiography: evaluation in a large series of normal subjects. J Am Soc Echocardiogr. 2010;23:109–15.

Tamborini G, Fusini L, Gripari P, Muratori M, Cefalù C, Maffessanti F, Alamanni F, Bartorelli A, Pontone G, Andreini A, Bertella E, Fiorentini C, Pepi M. Feasibility and accuracy of 3DTEE versus CT for the evaluation of aortic valve annulus to left main ostium distance before transcatheter aortic valve implantation. J Am Coll Cardiol Img. 2012;5:579–88.

Speckle Tracking Echocardiography (STE) for Left and Right Ventricles

6

Simone Cipani, Anna Viappiani, and Armando Sarti

Key Points
- Tissue Doppler imaging
- Speckles
- Strain
- Left ventricle deformation and functional parameters
- Right ventricle and functional parameters
- STE: advantages and disadvantages

6.1 Introduction

In recent years the study of myocardial function has led to renewed interest. This is due to the development of new ultrasound techniques such as tissue Doppler and speckle tracking imaging that have allowed to obtain new indices of both regional and global myocardial functions in addition to the traditional parameters of ventricular function.

The tissue Doppler imaging is a sensitive and accurate method for the quantitative assessment of segmental and global cardiac function, providing information related to the speed of tissue motion in a parallel direction to the ultrasound beam.

However there are two important limitations:

(a) The dependence of the Doppler measurements from the angle of incidence of the Doppler beam
(b) The dependence of heart traversing movements

STE method overcomes these limitations, allowing one to assess myocardial deformation. By the interaction of ultrasound with the myocardium, acoustic markers (*speckles*) are generated and followed during their displacement in the cardiac cycle, thanks to special software. From movement of individual speckles, by applying specific algorithms, the software is able to reconstruct the deformation dynamics of individual myocardial segments, quantifying the strain (amount of deformation) and strain rate (deformation rate).

The strain is a dimensionless parameter that reflects the variation of length of the segment considered in relation to its initial length and is expressed in percentage.

S. Cipani (✉)
Department of Anesthesia and Intensive Care, Santa Maria Nuova Hospital, Florence, Italy
e-mail: simone.cipani@uslcentro.toscana.it

A. Viappiani
Department of Anesthesia and Intensive Care, Castelfranco Veneto Hospital, Treviso, Italy

A. Sarti
Department of Anesthesia and Intensive Care, SS Maria Annunziata Hospital, Florence, Italy
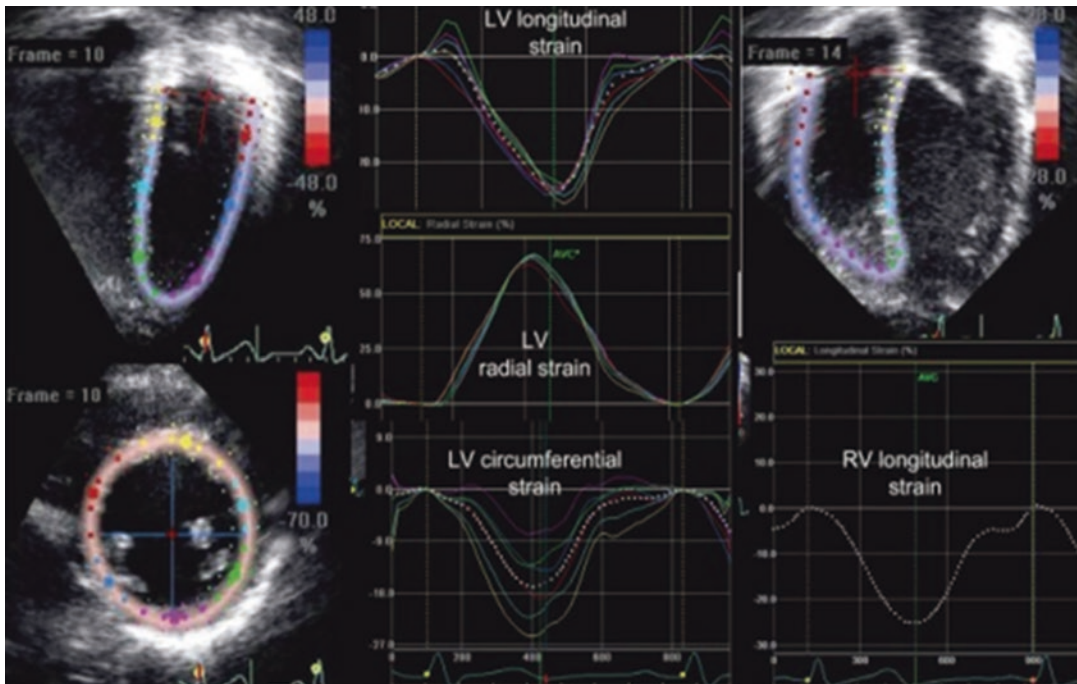
Fig. 6.1 Longitudinal strain: any reduction in the length (systole) corresponds to a negative strain, while the increase in length (diastole) corresponds to a positive strain. The radial plane shows an opposite situation: positive strain in systole (thickening) and negative in diastole (thinning)

The frequency with which this deformation is a concept in part comparable to the speed with which this occurs is defined strain rate and is expressed in s-1. The strain is a strictly load-dependent parameter, while the strain rate has a lower sensitivity to changes in preload and afterload, resulting in a relatively load-independent contractility index.

By convention, any reduction in the length along the longitudinal axis (as occurs in systole) corresponds to *a negative strain*, while the increase in length (as occurs in diastole) corresponds to *a positive strain*. The radial plane shows an opposite situation, with positive strain values in systole (thickening) and negative in diastole (thinning) (Fig. 6.1).

6.2 Left Ventricle (LV)

The myocardial wall is anatomically divided into three layers (subendocardium, intermediate layer, and subepicardium) organized with a different prevalence of muscle fibers with a specific course.

The subendocardial fibers have an orientation in the longitudinal-diagonal direction from the base toward the apex; in the middle layer, the fibers are oriented in a circular direction, while the subepicardial layer is made from the fibers of subendocardium with oblique longitudinal trend toward the base. So the subendocardial and subepicardial layers are characterized by the presence of fibers with a course along the longitudinal plane, but what characterizes these two wall components is constant change of their angle of orientation with respect to the circular fibers of the intermediate layer.

All this involves the formation of a counterclockwise spiral subepicardial level and a slot spiral at subendocardial level, which passes from the left-hand propeller to a propeller clockwise subepicardium and the subendocardium. The subendocardial component contributes substantially to the longitudinal shortening of the ventricle, while subepicardium and intermediate components contribute mainly to the circumferential deformation and rotation. All three components contribute to parietal radial thickening.

Following this architecture, the systolic contraction of the left ventricle is not attributable, as for skeletal muscle presenting tendon insertional structures, in a single direction.

In fact, the left ventricle during the systolic phase is submitted to different types of deformation which interact with each other in a very complex manner.

The main types of myocardial deformation that occur during left ventricle shortening are:

1. Longitudinal
2. Circumferential
3. Parietal thickening
4. Twisting

6.2.1   Longitudinal

1. During the ejection phase, the subendocardial and subepicardial components are shortened at the same time, even if the subendocardial change is greater than subepicardial one. This results in a reduction of the distance between the individual speckles and implies that during systole, the longitudinal shortening is represented by a *negative strain curve*.

6.2.2   Circumferential

2. According to some authors, the circumferential strain (centro-parietal shortening) is 60% of ejection fraction in normal subjects. This deformation has a base-apex gradient that is higher in apical and medium segments.

The circumferential deformation follows the shortening in the longitudinal plane so that the size of the left ventricle along the short axis increases during the isovolumic ventricular contraction and its shape becomes more spherical. Even for the circumferential shortening, there is a reduction of the distance of the individual speckles, and so we have a *negative strain curve*.

6.2.3   Parietal Thickening

3. The wall thickening of the ventricular myocardium during systole is not only due to the longitudinal shortening and circumferential mechanisms but also determined by overlap of myocyte layers that slide on each other (*shear strain*). This phenomenon results in 40% of parietal thickening that eventually will produce more than 60% of ejection fraction in a healthy heart. By convention direct radially myocardial deformation toward the center of the ventricular cavity (thickening) is expressed by a *positive strain curve*.

6.2.4   Twisting

4. The complex structural organization of the myocardium is the basis of torsional movement (twist); as previously mentioned the subendocardial fibers have a right-handed (clockwise) spiral orientation, the middle layer has a circumferential orientation, and the subepicardial fibers have a spiral clockwise direction. This results in a torsional deformation of the left ventricle to the apex which rotates in the opposite direction (counterclockwise) with respect to the basis (clockwise). This proves to be a key element in regulating the mechanics of systo-diastolic left ventricle function making possible a reduction of ventricular volume by 60% with a shortening of the myocardial fibers of only 15%. The rotation and the overlap of the subendocardial fibers determine a deformation of the intercellular matrix, creating a potential energy storage in the cellular and extracellular proteins such as titin and collagen. The subsequent rotation frees the previously stored energy, which bounces open like the energy from a spring when it is released, generating the sucking diastolic which contributes to rapid filling of the ventricle (Fig. 6.2).
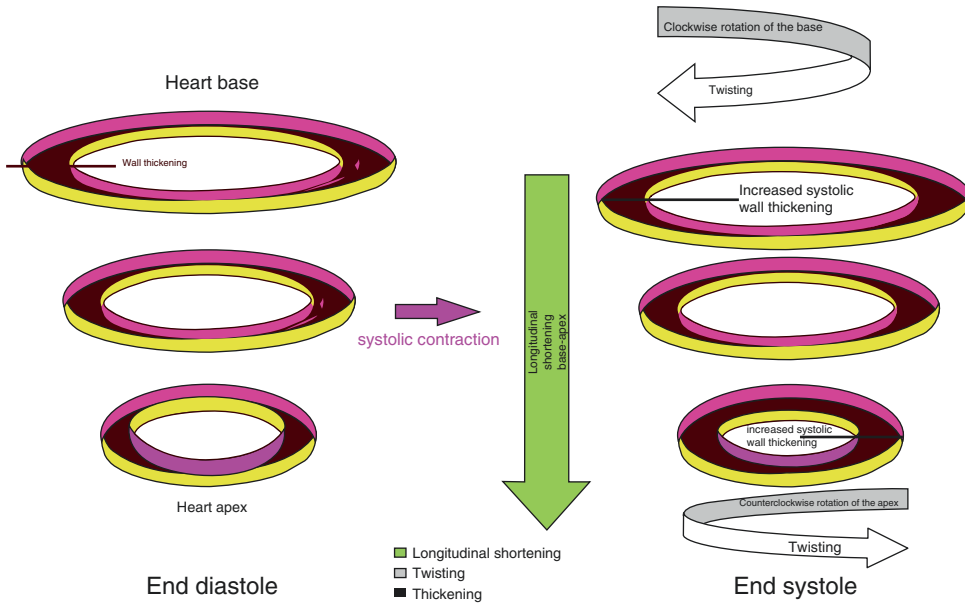
Fig. 6.2 During systole contraction 1. Radially myocardial deformation with wall thickening (black line). 2. Longitudinal shortening (green arrow). 3. Twisting with clockwise rotation of base and counterclockwise of the apex (gray arrow)
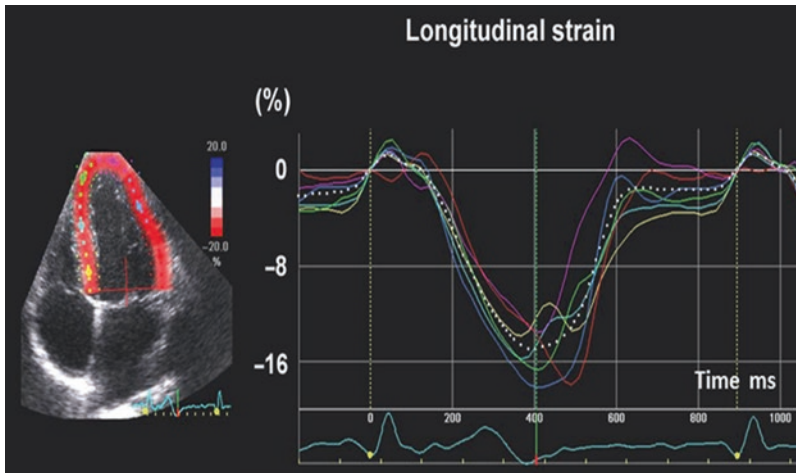
Fig. 6.3 The myocardium is shortened base-apex direction resulting in a reduction of the distance between the various points and hence is represented by a negative curve in systole. The software automatically divides each recorded section into six segments with colorimetric representation: intense red, normal systolic contraction; pale pink, reduced contraction; light blue/blue, not in phase contraction. Green line (AVC): aortic valve closure

6.3 Left Ventricle Functional Parameters with STE

6.3.1 Longitudinal Strain (LS)

The longitudinal strain is the myocardial deformation along the base-apex axis. The myocardium is shortened base-apex direction resulting in a reduction of the distance between the various points and hence is represented by a negative curve in systole (Fig. 6.3) and by a positive curve in the diastole. This parameter is applicable also to the 17 segments in which the left ventricle is divided; thus it is possible to make
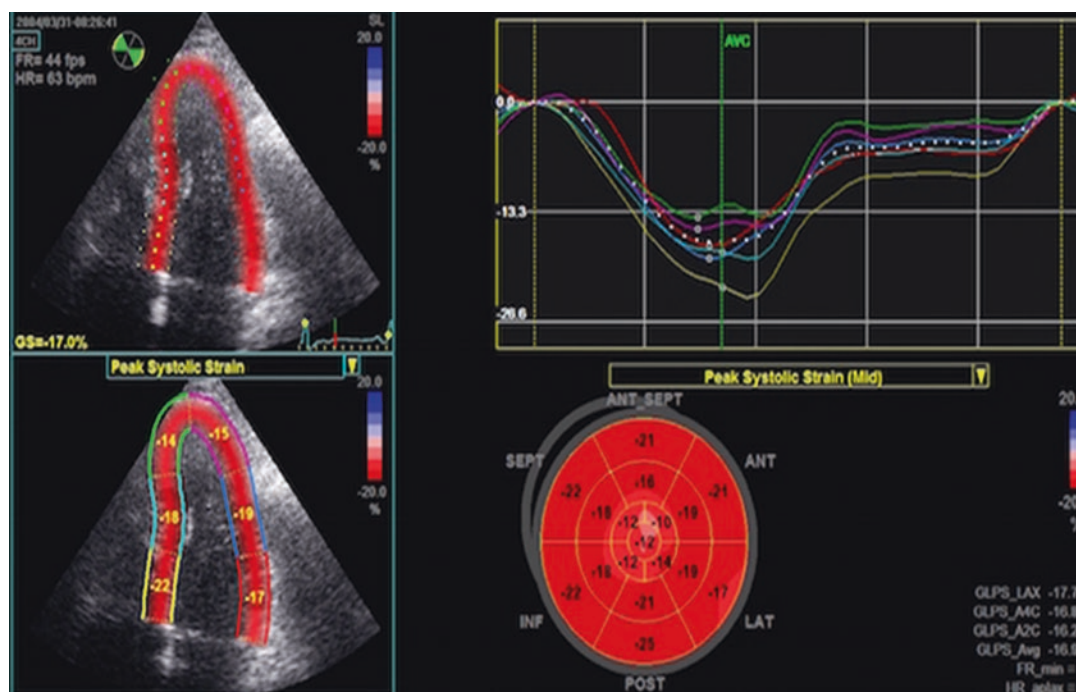
Fig. 6.4 Global longitudinal strain (GLS) and peak systolic strain of the left ventricle on the left. "Bull's eye" of longitudinal strain: global distribution vision of strain. AVC (green line), aortic valve closure

an average of the different values, obtaining the global strain that quantitatively expresses the global systolic ventricular function (Fig. 6.4 "bull's eye"). Currently the main scientific communities are not able to determine with certainty the normal value of LS. Too many turn out to be the heterogeneity in scientific studies, in the software used by the various manufacturers. In fact, the 2015 ASE guidelines report an indicative normality range of **−20%**.

6.4   Right Ventricle

The right ventricle plays an important role in terms of morbidity and mortality in patients with cardiopulmonary disease. Unfortunately, still the systematic evaluation of this important cardiac chamber is not uniformly performed. This is partly due to the enormous attention paid to the assessment of the left ventricle and the lack of familiarity with the ultrasonographic techniques of evaluation currently available for the study of the right sections. Structurally the right ventricle

has a complex geometry that prevents it from being compared to any geometric shape. In fact, proceeding from the inflow portion, where the fibers have a predominantly oblique orientation with a mean radius of curvature of about 4 cm, there is the outflow tract or infundibular cone, where the fibers have a circular plow with a small radius of curvature <1 cm. The inflow portion and the outflow are separated by the "Leonardo moderator band" and supraventricular crest. These anatomical characteristics of the right ventricle entail significant limitations in volumetric assessments and function.

An important consequence of this structural organization is the inability of the right ventricle to cope with sharply significant increases in afterload. Such acute adaptive incapacity shows in the dilatation as the expression of the high compliance of the right ventricle in response to pre- and afterload increases. This involves significant morphofunctional modifications, determining the displacement of the normal curvature of the interventricular septum that in the initial stages assumes a flattened form and then meets a

reversal of its normal convexity. This morphofunctional situation can translate into a reduction in the compliance of the left ventricle and an increase in diastolic blood pressure of the right ventricle, sometimes leading to a reduced coronary perfusion. Although the dilatation of the right ventricle is an important, initial compensation mechanism, from the moment that there is an increase of the diameter of the end-diastolic volume that compensates the reduction of cardiac output, it should be emphasized that the right ventricle is able to support this condition only for a short time.

The particular geometrical and structural characteristics of the right ventricle explain the inadequacy of conventional echocardiographic parameters in the evaluation of the contractile function of the panel. In this context, the evaluation of strain and strain rate with STE represents a very useful and convenient method. The right ventricular deformation indices obtained with STE show a good correlation with the traditional right ventricular function parameters provided by the cardiac magnetic resonance imaging. In addition, the STE method applied on the right ventricle showed high feasibility and high reproducibility. It should be noted that the deformation analysis with STE is usually applied to the portion of the right ventricular inflow; however, this constitutes a valid evaluation of global systolic function tool, in fact this ventricular portion constitutes about 85% in terms of the stroke volume of right chamber, and the longitudinal shortening is the major determinant of the overall pump function.

6.5   Right Ventricle (RV) Functional Parameters with STE

6.5.1   Global Longitudinal Strain (GLS)

The reference values for regional and global strain of RV were obtained from 100 healthy subjects. In the context of the right ventricle, GLS is a parameter borrowed from LV measurements, and software currently used to measure RV GLS from most manufacturers has been designed for LV measurements and later adapted for the right ventricle. The term RV GLS usually refers to either the average of the RV free wall and the septal segments or the free wall segments alone. Peak global longitudinal RV strain excluding the interventricular septum has been recently reported to have prognostic value in various disease states (myocardial infarction, pulmonary hypertension, amyloidosis, etc.) and to predict RV failure after LV assist device implantation.

It has been also demonstrated a good correlation between global longitudinal strain and the traditional indices of right ventricular systolic function. A global longitudinal RV free wall strain $>-20\%$ is likely normal (Fig. 6.5).

6.6   STE Advantages

Thanks to the assessment of myocardial deformation, the STE allows to obtain angle-independent measurements, relatively insensitive to cardiac translational movements (with the exception of movements of through-plane motion, which by definition also influence the STE measurements), thus exceeding the limitations of tissue Doppler.

A further extremely important advantage provided by this method, particularly with some analysis software, is the potential information about subendocardial layer.

This layer is particularly vulnerable because of its remoteness from the large epicardial coronary vessels and close contact with intracavitary pressures.

In several myocardial pathologies, the involvement is not transmural; the main components of the myocardial deformation show different degrees of alteration, and the traditional parameters of ventricular function are still in the normal range. STE is a fundamental instrument that allows early reveal structural alterations especially when the functional classic parameters are not yet altered. It is an example of the compensa-
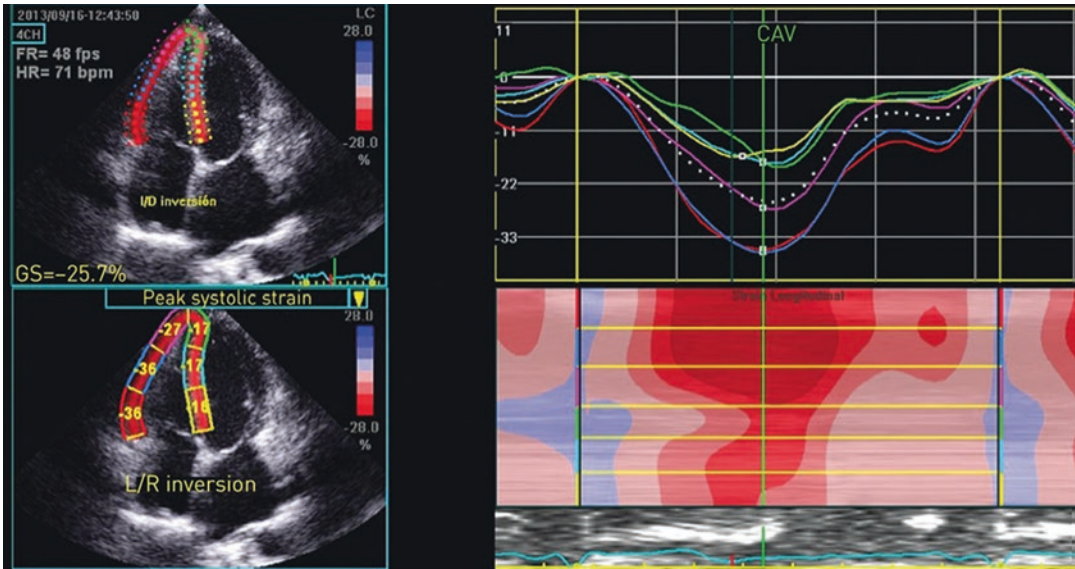
Fig. 6.5 Global longitudinal strain and peak systolic strain of the right ventricle. The software automatically divides each recorded section into six segments with colorimetric representation: intense red, normal systolic con- traction; pale pink, reduced contraction; light blue/blue, not in phase contraction. AVC (green line), aortic valve closure

tion carried out by the intermediate layer and subepicardial in order to maintain normal cardiac output through the expression of normal function of the longitudinal values.

6.7   STE Disadvantages

The limits of this method can be summarized in the following points:

1. Strict dependence of the 2D image quality
2. Image processing STE highly dependent on the frame rate: lower frame rates can lead to instability of the various patterns, while excessively high values reduce the image resolution. Optimal range between 50 and 70 Hz.
3. Reduced accuracy of the strain measures in the event of marked ventricular remodeling.
4. Possible side dropout in longitudinal movement in relation to the low resolution of the left ventricular lateral wall.

6.8   Conclusion

The ventricular myocardium has two mechanisms for ejecting stroke volume:

- Fiber shortening (longitudinal, circumferential, and torsion)
- Wall thickening

These mechanisms can be altered at different levels in the course of heart disease. One example is hypertensive heart disease where there has been a shortening of the longitudinal fibers and a thickening of the wall as a compensatory mechanism.

This mechanism has the purpose of reducing the wall tension; in fact, thanks to a multiplicative effect and / or reorganization of the myofibers are witnessing an endocardial inward shift in order to ensure a good ejection fraction also in conditions of relaxation impaired function. STE allows to highlight early endocardial alterations,

even when traditional function indices are still normal; it represents an important tool for the clinician.

Further Reading

Cameli M, et al. Speckle tracking echocardiography as a new technique to evaluate right ventricular function in patients with left ventricular assist device therapy. J Heart Lung Transplant. 2013;32:424–30.

Cameli M, et al. Speckle tracking echocardiography: a practical guide. G Ital Cardiol. 2017;18(4):253–69.

Mondillo SJ. Speckle tracking echocardiography. A new technique for assessing myocardial function. J Ultrasound Med. 2011;30:71–83.

Part III

Essential Functional Echo-Anatomy

The Left Ventricle: Frequent Imaging in ICU Patients

7

Simone Cipani, Claudio Poli, and Silvia Marchiani

7.1 Introduction

The study of left ventricular (LV) function is crucial in the emergency department and the ICU. The left ventricle comprises an inflow and an outflow tract, the papillary muscles, and the mitral subvalvular apparatus. The two papillary muscles stick to the free wall. The transthoracic views that allow the assessment of the left ventricle are the parasternal long-axis view, the parasternal short-axis view, the apical four-chamber view, the apical two-chamber view, the apical five-chamber view (outflow tract), the apical three-chamber view (outflow tract and mitral view), and the subcostal view. The main transesophageal views are the mid-esophageal four-chamber view, the mid-esophageal two-chamber view, the mid-esophageal long-axis view, and all transgastric and deep transgastric views. The myocardial echo density is usually a bit lower than that of the valves. The myocardial tissue echo structure should be uniform. Apparent marked heterogeneity of the tissue is observed in some cardiomyopathies, such as amyloidosis and

hypertrophic cardiomyopathy. The wall thickness is generally uniform, although in elderly patients, particularly if they are hypertensive, it is common to find asymmetric hypertrophy at the basal portion of the septum, proximal to the outflow tract. Ventricular interdependence must be always kept in mind. Thus, the abnormalities of LV shape and function always imply an effect on the morphology and function of the right ventricle and vice versa.

7.2 Standard Measures

Standard measurements of the left ventricle are derived in parasternal long-axis or parasternal short-axis (transthoracic echocardiography, TTE) or transgastric (transesophageal echocardiography, TEE) M-mode from the edges of the structures. If in M-mode it is impossible to achieve alignment with the largest part of the left ventricle crossing the septum and the posterior wall in a perpendicular way, one can take measurements directly in two dimensions, although this way they may be less precise and often underestimated. The thickness of the septum, the cavity diameter at the widest point just below the mitral valve, and the posterior wall thickness are measured preferably in a 2D-derived M-mode track which includes a number of cycles, both when the heart is completely filled in end diastole (ECG R wave)

S. Cipani (✉) · C. Poli
Department of Anesthesia and Intensive Care, Santa Maria Nuova Hospital, Florence, Italy
e-mail: simone.cipani@uslcentro.toscana.it; claudio.poli@uslcentro.toscana.it

S. Marchiani
Department of Neuroanesthesia and Intensive Care, Careggi University Hospital, Florence, Italy

Fig. 7.1 Parasternal long-axis (transthoracic echocardiography, TTE) M-mode image just below the mitral valve: end-diastolic measurements
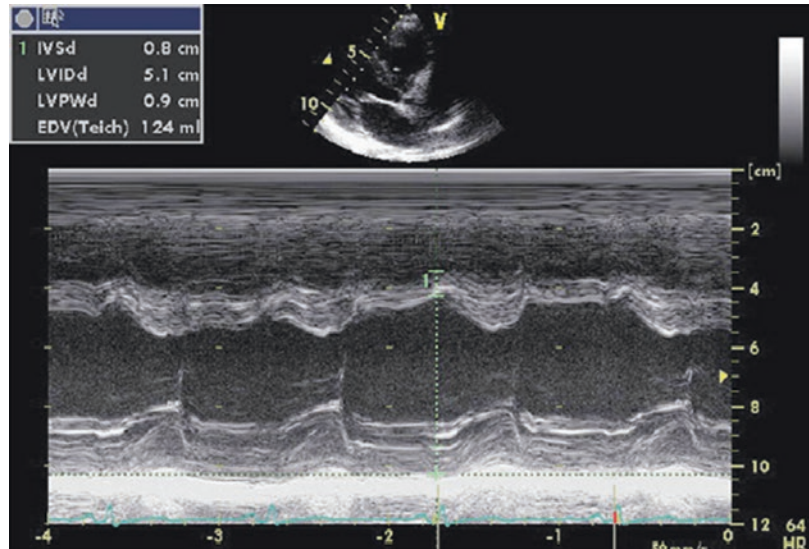
Fig. 7.2 Parasternal long-axis (TTE) M-mode image at the level of mitral valve: increased distance between the septum and the maximum diastolic excursion of the mitral valve. (From Sarti with permission)
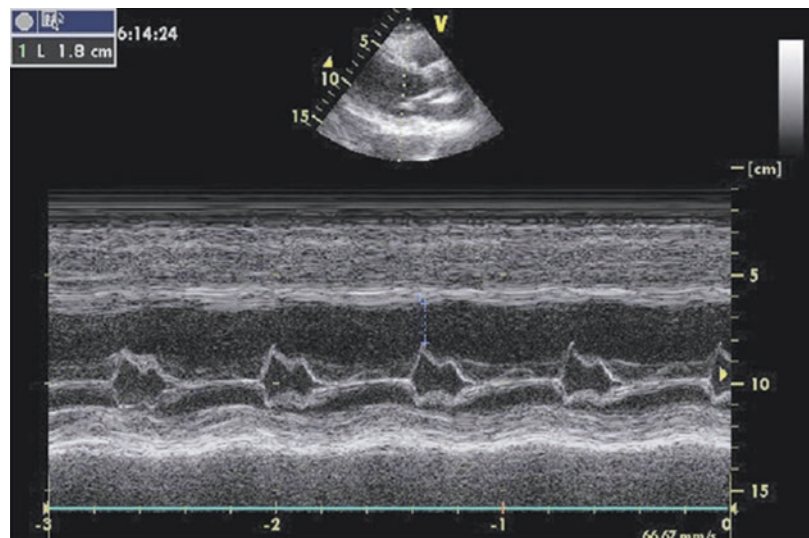
(Fig. 7.1) and at the maximum emptying in end systole (normally half of the ECG T wave). The normal septum movement is toward the LV posterior wall. An asynchrony of the septal wall movement is observed in left bundle branch block or for previous cardiac surgery. An abnormal movement, toward the right ventricular free wall in systole, is observed when there is a right ventricular systolic pressure overload or diastolic volume overload (septal dyskinesia, "right working septum"). Normal values differ with gender and size of the subject and are shown in

tables of normal values. Common values in telediastole are a LV cavity diameter of 4.2–5.9 cm in men and 3.9–5.3 cm in women and a septal and posterior wall thickness of 0.6–1.0 cm in men (males) and 0.6–0.9 cm in women. However, measures exceeding upper and lower limits must be reported considering gender, age, body surface area (BSA), and ethnicity.

In M-mode, the normal distance between the septum and the maximum diastolic excursion of the mitral valve (mitral E wave corresponding to the rapid ventricular filling) must not exceed

Fig. 7.3 Parasternal long axis: increased wall thicknesses of anterior-basal interventricular septum (19 mm)
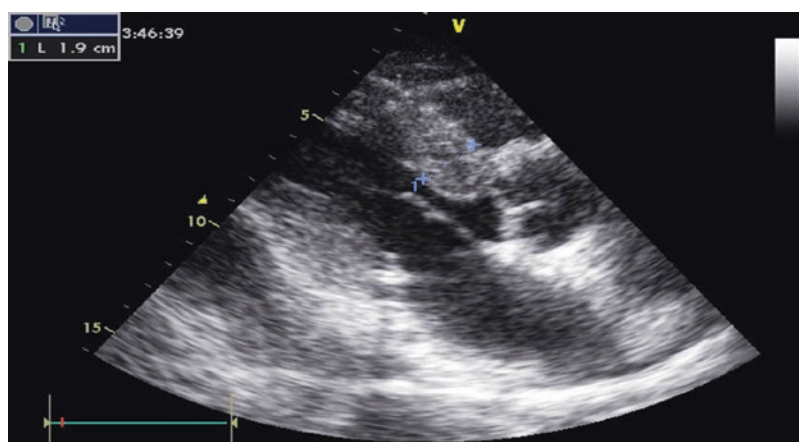
Fig. 7.4 Parasternal long axis: note (yellow arrows) the increased wall thicknesses of anterior-basal septum and the posterior wall
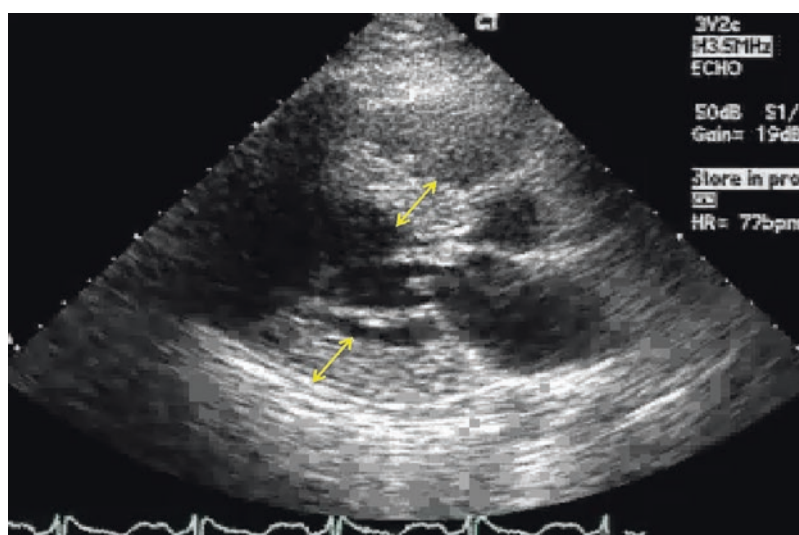
1 cm. A wider gap shows a ventricular dilatation with LV dysfunction and/or low cardiac output (Fig. 7.2).

7.2.1 Frequent Imaging in ICU Patients

Hypertrophic Cardiomyopathy Pathological condition frequently occurs especially in elderly patients with history of hypertension. Its response in young patients with a suspicious history should dif-ferentiate hypertrophic cardiomyopathy in differential diagnosis. As previously mentioned, the normal cutoff of the parietal thickness is 0.9 cm in females and 1.0 cm in males. Generally, if the hypertrophy framework is associated with normal endocavitary diameters, we are faced with a condition of concentric hypertrophy (Figs. 7.3 and 7.4). If parietal hypertrophy is associated with an increase in endocavitary diameters, we are faced with a picture of eccentric hypertrophy (RWT relative wall thickness: 2× posterior wall/end-diastolic diameter of left ventricle; if **<0.42** eccentric hypertrophy).

Fig. 7.5 Apical two chamber: note the increased volume and diameter of left ventricle
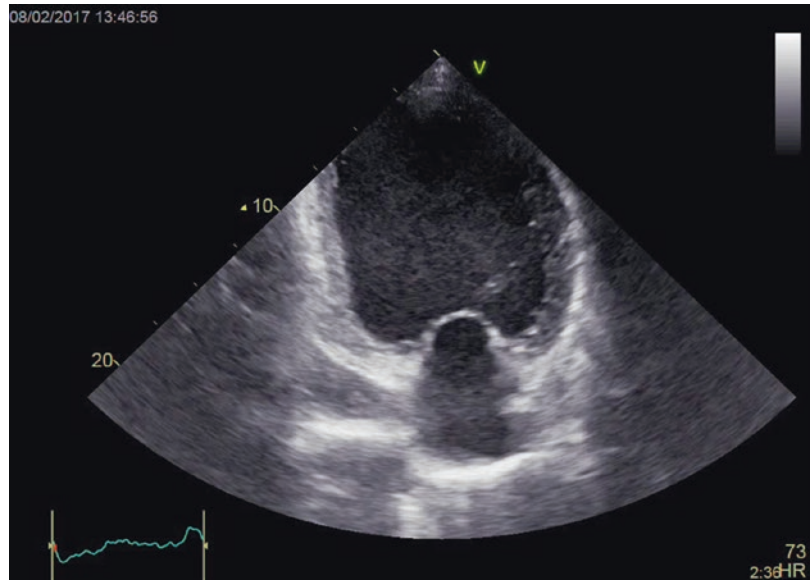
Fig. 7.6 Apical four chamber: female patient with amyloidosis; note the reduced dimension and volume of left ventricle
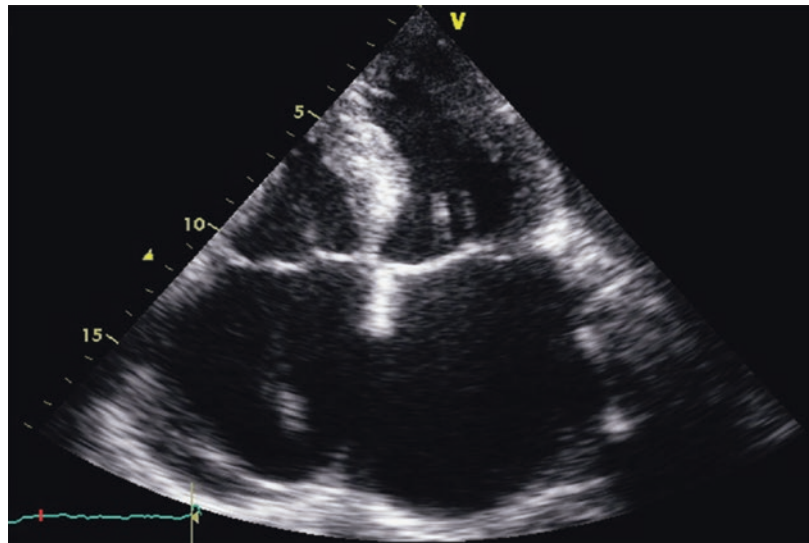
Dilatative cardiomyopathy This is a common clinical condition in patients with previous ischemic heart disease. Sometimes its presence may be the result of phlogistic myocardial involvement (myocarditis). In the absence of coronary artery disease, the differential diagnosis must be shifted to primitive dilated cardiomyopathy (Fig. 7.5).

Restrictive Cardiomyopathy (RCM) Restrictive cardiomyopathy (RCM) is a rare form of heart muscle disease that is characterized by restrictive filling of the ventricles (Fig. 7.6). In this disease the contractile function (squeeze) of the heart and wall thicknesses are usually normal, but the relaxation or filling phase of the heart is very abnormal.

Fig. 7.7 Apical four chamber: apical ballooning in Takotsubo syndrome
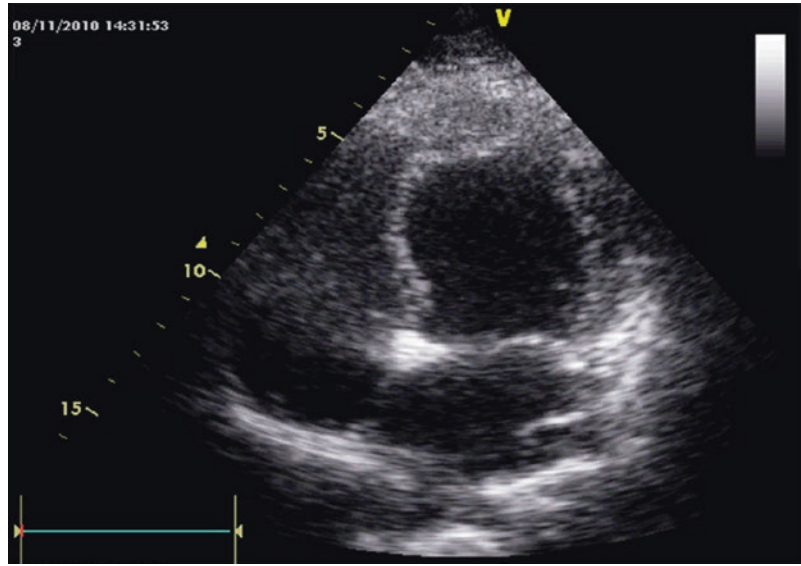
This occurs because the heart muscle is stiff and poorly compliant and does not allow the ventricular chambers to fill with blood normally. This inability to relax and fill with blood results in a "backup" of blood into the atria (top chambers of the heart), lungs, and body causing the symptoms and signs of heart failure.

7.2.2 Other Images

Takotsubo (Stress-Related Cardiomyopathy Syndrome) It is a common, transient, clinical condition in elderly female o postmenopausal age, generally triggered by acute emotional event. Takotsubo cardiomyopathy mimics acute coronary syndrome (ST-segment elevation or depression, T wave changes, mild increase in cardiac enzymes) and is accompanied by reversible left ventricular apical ballooning in the absence of angiographically significant coronary artery stenosis. In Japanese, "takotsubo" means "fishing pot for trapping octopus," and the left ventricle of a patient diagnosed with this condition resembles that shape. Echocardiographic features: apical ballooning (Fig. 7.7) with apical akinesis and basal wall hypercontraction.

Precipitant factors: acute emotional stress, acute intracranial events, bleeding trauma, stroke, sepsis, surgical procedures, overproduction of endogenous catecholamines, and administration of exogenous catecholamines.

Bicuspid Aortic Valve The aortic valve is a one-way valve between the heart and the aorta, the main artery from the heart that distributes oxygen-rich blood to the body. Normally, the aortic valve has three small flaps or leaflets that open widely and close securely to regulate blood flow, allowing blood to flow from the heart to the aorta and preventing blood from flowing backward into the heart. In bicuspid aortic valve disease (BAVD), the valve has only two leaflets. With this deformity, the valve doesn't function perfectly, but it may function adequately for years without causing symptoms or obvious signs of a problem. The latest studies suggest that bicuspid aortic valve disease is caused by a connective tissue disorder that also causes other circulatory system problems. Patients with bicuspid aortic valve disease also may have abnormal coronary arteries, aortic aneurysm or an abnormal thoracic aorta, and unstable (labile) high blood pressure (Fig. 7.8).

Fig. 7.8 Parasternal short axis: aortic box without the normal presence of three leaflets
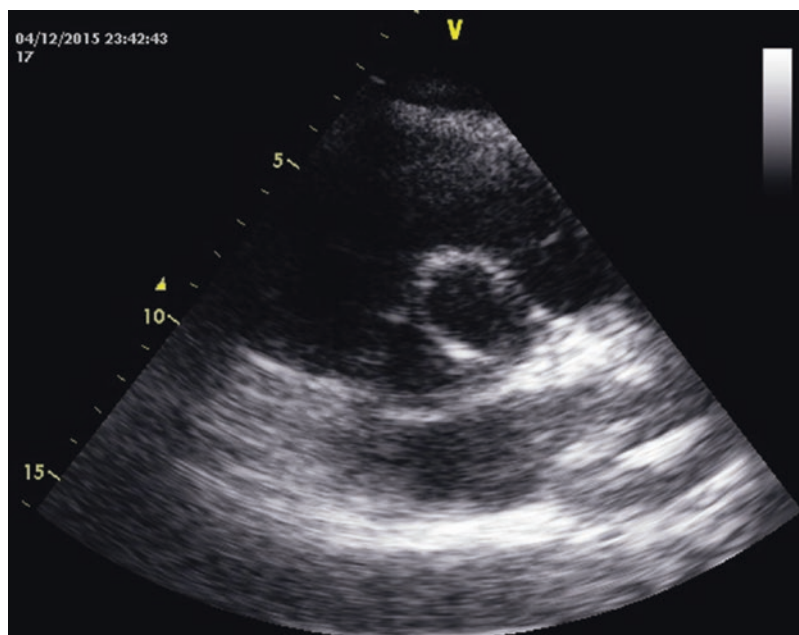
7.3 Global Systolic Function

The left ventricle is a pump that continuously changes its complex performance according to many factors. Starting from any given level of contractility (dP/dt), the left ventricle empties in a variable fraction, from diastole to systole [aortic ejection fraction (EF), systolic volume, stroke volume], depending on the degree of the cavity filling, which depends on both preload and afterload. LV preload is related to pulmonary venous return, left atrial pressure, LV wall active relaxation, and distensibility. LV afterload is related to the arterial elastic aortic distensibility (impedance), the transmural pressure, and the systemic vascular resistance. Ventricular filling is related to stroke volume by the Frank-Starling law, which accounts for an increase in stroke volume depending on increased filling of the cavity up to a plateau, which depends on the state of contraction. Beyond this plateau, further increase in filling pressure does not change the systolic ejection but overloads the pulmonary circulation. A healthy heart has significant reserve for increasing ejection according to Starling's law, whereas as LV function worsens, this reserve progressively reduces to zero. In this case, in response to a volume load, there is not an increase in stroke volume but only an increased pulmonary pressure, which increases the amount of lung water. Generally, a left ventricle that loses the normal "truncated rugby ball" shape and becomes more spherical does not exhibit a good systolic function. All ICU treatments interfere with the preload, contractility, and afterload variables. For example, lifting of the patient's legs (passive leg raising), or a rapid intravenous fluid bolus, produces an increase in preload (greater vena cava size and lowering respiratory variations). The consequent filling of cavities produces or does not produce, depending on Starling's law, a significant increase in stroke volume, the fluid responsiveness. Only repeated assessments of changes in stroke volume in response to a preload charge (administration of fluids or passive raising of the patient's legs) allow the reconstruction of the Frank-Starling curve of the patient's heart, according to the current cardiovascular condition (infusion of catecholamines, mechanical ventilation). Indeed, hemodynamic drugs act at all levels, such as contraction, the venous tone, and the arterial vascular stiffness and resistance.

Mechanical positive pressure ventilation generally worsens the right ventricular function (increasing pulmonary vascular resistance), whereas it improves the LV function because of an effect on the transmural myocardial pressure. The LV systolic function, intended as the contractility state, is not easily measurable in clinical practice. The contour of a mitral regurgitation jet, if any, both as the peak level and as the speed/time curve contour profile, is related to dP/dT, which is the "true" contractility. The EF or other less precise but conceptually similar measures such as diastolic-systolic changes in diameter (fractional shortening, FS) or in area (fractional area change, FAC) are not specific measures of contractility, since they are greatly affected by both LV preload and LV afterload. Nevertheless, EF, FS, and FAC are still considered standard measures of systolic function. EF correlates well with mortality, and it is widely used as a measure of global systolic function in a stable condition but may be misleading for a critically ill unstable patient mainly because of sudden changes of both preload and afterload.

LV wall kinetic motion and thickening are used for studying the regional systolic function (regional wall motions abnormality) (see later).

7.3.1   Left Ventricular Rotation

The human heart rotates around its longitudinal axis during the cardiac cycle. The apex rotates clockwise during early isovolumetric contraction and counterclockwise during the LV ejection period, whereas at the same time, the LV base rotates in the opposite direction. In the diastolic phase, there is untwisting, the LV recoil. Systolic LV torsion helps systolic ejection and also stores energy by twisting and shearing myofibers. Quantification of LV rotation is a sensitive tool to detect early systolic and diastolic function impairment. Nowadays it is possible to study LV rotation by using speckle tracking imaging (see Chap. 6), but a high-quality image is necessary, and the interoperator variability is still high (Fig. 7.9). Recently, a computed TEE system has been developed for quantifying automatically LV rotation.

7.3.2   Longitudinal Shortening

An immediate estimation of the systolic function is obtained in M-mode by observing the systolic shift of the lateral mitral ring toward the apex in the apical four-chamber view (TTE) or the midesophageal four-chamber view (TEE). The highest and the lowest points of the M-mode sinusoid wave are measured, having put the cursor along the mitral ring (Fig. 7.10). A value greater than 13 mm is normal, and a value below 13 mm represents beginning of a longitudinal systolic dysfunction. It has been suggested to repeat the measure three times and average.

7.3.3   Fractional Shortening

This is the simplest parameter for quantifying the global systolic function. In the M-mode parasternal long axis or parasternal short axis view (TTE) or the transgastric basal short axis view (TEE), it is difference between the LV diastolic and systolic internal diameters divided by the LV diastolic internal diameter: (LVIDd − LVIDs/LVIDd) × 100 (Fig. 7.1).

Normal values for FS range from 25% to 45%. Normally this parameter is well correlated with the EF. The major limitation is that the systolic function of an ellipsoid, such as the left ventricle, is estimated by the change of a single diameter. Any modification of shape or alteration in the regional kinetics is not considered. So, for the FS to be an expression of the global function, it is necessary for the LV kinetics to be homogeneous along the whole ventricle.

7.3.4   Fractional Area Change

Instead of the diameters, it is possible to evaluate the area changes, end systolic and end diastolic, in a cross section of the heart, in the parasternal short-axis view at the mid-papillary level (TTE) (Fig. 7.11), or in the transgastric mid-short-axis view (TEE). This measure is also expressed as a fraction: (LVEDA − LVESA/LVEDA) × 100, where LVEDA is LV end-diastolic area and

Fig. 7.9 Apical four-chamber view (TTE). Left ventricular (LV) longitudinal speckle tracking
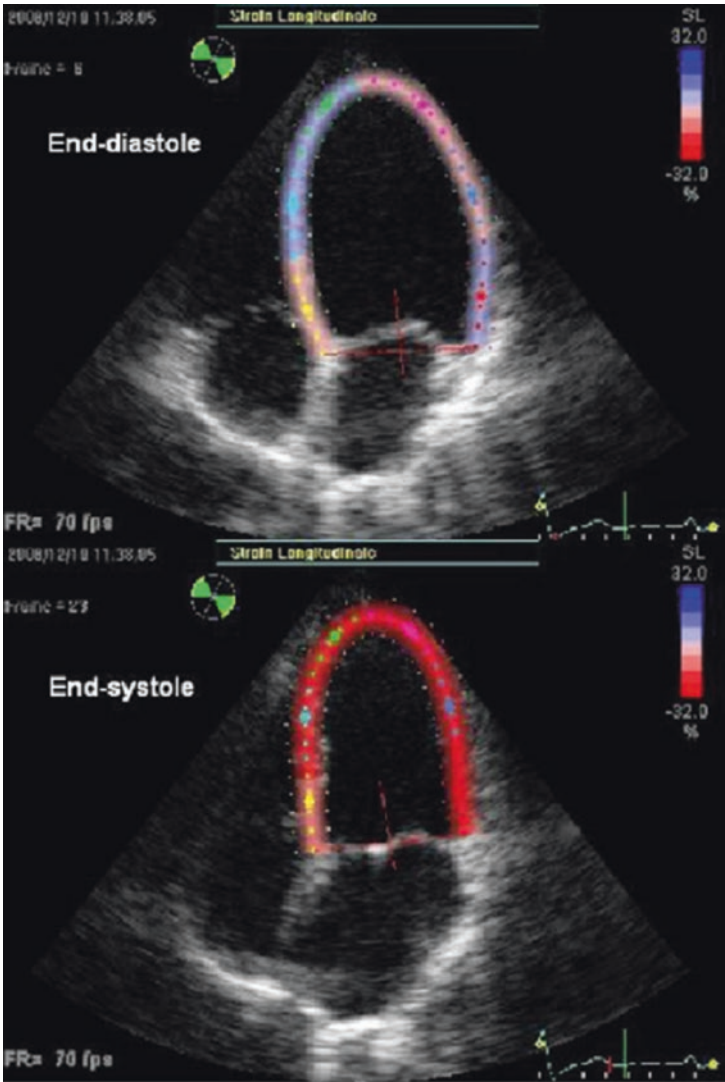
Fig. 7.10 Apical four-chamber (TTE) M-mode image. Lateral mitral ring kinetics (longitudinal shortening). (From Sarti with permission)
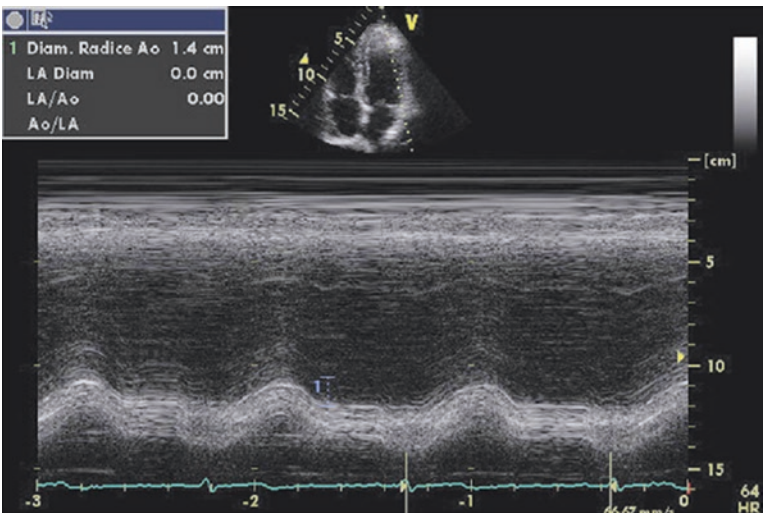
Fig. 7.11 Parasternal short-axis view (TTE). (**a**) LV end-diastolic area. (**b**) LV end-systolic area. (From Sarti with permission)
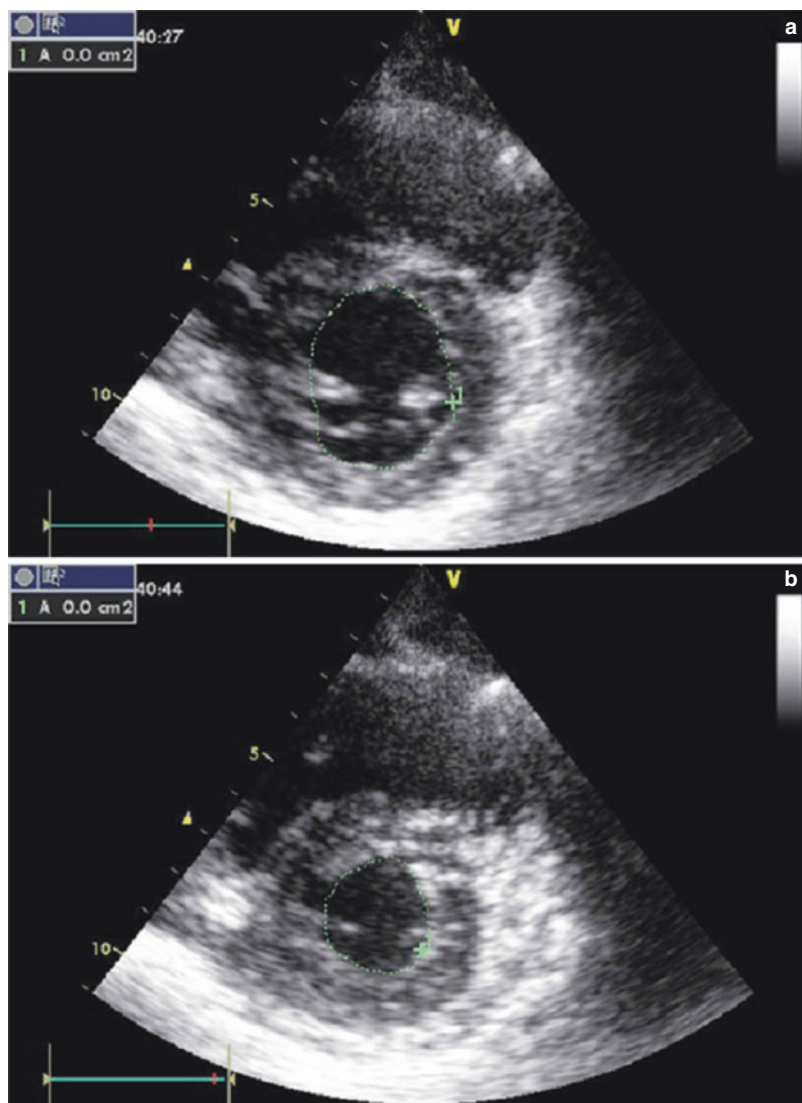
LVESA is LV end-systolic area. The normal end-diastolic area indexed for body surface area is equal to or greater than 5.5 cm^2/m^2. The normal FAC value is or exceeds 45%. Again, regional variations in shape or kinetics of the left ventricle are not recognized by this measure, which represents a single section plane of the left ventricle, at the mid-papillary level. Nevertheless, FAC and LVEDA (often in the literature end-diastolic area), although reliable only in the presence of a uniform contraction, are easy to obtain and appear in many ultrasound-guided algorithms for classification and treatment of the patient's hemodynamics.

7.3.5 Ejection Fraction

Ejection fraction (EF) is the gold standard to measure global systolic function. In fact, as already mentioned, EF is not a specific measure of contractility. Rather, it reflects the interaction between preload, contractility, and afterload. It is the amount of blood (stroke volume) pumped out of the left ventricle in each cardiac cycle, reported as a percentage of the end-diastolic volume: EF = (LVEDV − LVESV/LVEDV) × 100, where LVEDV is LV end-diastolic volume and LVESV is LV end-systolic volume. The normal value is greater than 50%. To be more precise, <52% for

men and <54% for women are suggestive of abnormal systolic dysfunction. From 50% to 40%, there is a slight decrease, whereas from 40% to 30%, there is a significant reduction of the pump function. Below 30% a severe reduction in global systolic function is diagnosed. A good emptying of the left ventricle (high EF) in a hypotensive patient, if there is no concomitant hypovolemia, evokes the suspicion that either ventricular outflow is in part ejected into a low-pressure chamber, as in mitral insufficiency, or that the ventricle empties well for a significant reduction in afterload, such as in vasoparalysis, as often happens in sepsis syndromes. In the latter case, the infusion of norepinephrine to restore vascular resistance and maintain blood pressure better shows the real state of contraction, which may be a decreased EF, unmasked by the normalized afterload. If there is severe mitral insufficiency, EF is considered normal if it exceeds 60%. The other measures of ejection based on variations of diameters and areas should be reassessed if there is significant mitral regurgitation.

It is better to consider that since EF is related to diastolic volume, even a very low EF such as 25% in a patient with dilated cardiomyopathy may reflect an adequate or only slightly reduced stroke volume, because it is 25% of a greatly increased end-diastolic volume and thus a normal or near-normal cardiac output at rest. In these cases an effort, however slight, or an acute disease, unmasks the inability of the left ventricle to increase its performance, that is, stroke volume and cardiac output, in response to increased oxygen demand. Then all the symptoms and signs of acute cardiac failure become manifest.

The only method now recommended for the measurement of EF is the modified Simpson method that estimates systolic and diastolic volumes in two different planes perpendicular to each other, in practice in the apical four-chamber and apical two-chamber projections (TTE) or the mid-esophageal four-chamber and mid-esophageal two-chamber projections (TEE). The ultrasound machine automatically calculates the values for the media. The inner edges of the LV endocardium, including the papillary muscles, are outlined using the "trackball" tracer both in end diastole and in end systole. At the mitral level, the contour is closed connecting the opposite points of the valve ring by a straight line. It is necessary, therefore, that the endocardium be visible along the entire cavity and for the entire cycle. The maximum length from the apical endocardium to the mitral annulus is also measured. The calculation, which results in a volume (area for length), is automatically computed by splitting the cavity into small cylinders (Fig. 7.12). It is important to search for the maximum length of the left ventricle, the true long axis, avoiding cutting the LV ellipsoid with an oblique section (in this case excessive mobility and altered shape of the apex are shown on the display). Also, cardiac cycles originating from extrasystoles should be avoided. For better accuracy, especially if the aortic ejection is particularly variable (i.e., changes in systolic blood pressure monitored invasively or changes in the maximum amplitude of the plethysmographic wave measured by a pulse oximeter), the measurement must be repeated for at least three cycles in sinus rhythm and for at least five cycles if there is atrial fibrillation. Note that for a skilled echocardiographer, according to data confirmed in the literature, the simple inspection of some cardiac cycles in motion ("eyeball measurement") provides a reliable estimate of EF, which correlates well with more accurate measurements.

7.3.6 Tissue Doppler Imaging

The speed wave produced by the movement of myocardial tissue at the lateral or septal mitral ring in the apical four-chamber view (TTE) or the mid-esophageal four-chamber view (TEE) is related to EF. Tissue Doppler imaging (TDI) thus allows an immediate assessment of global LV systolic function. The normal systolic velocity (S wave; Fig. 7.13) is 8–10 cm/s at the lateral ring side. Below 8 cm/s there is a systolic depression, reflecting the corresponding reduction of the EF. The function is reduced gradually between 8 and 3 cm/s. A severe alteration, corresponding to EF < 30%, is generally below 3 cm/s. Values vary a little between the lateral and the septal level at the mitral ring.

Fig. 7.12 Apical four-chamber view (TTE). (**a**) LV end-diastolic volume. (**b**) LV end-systolic volume. See the text for details
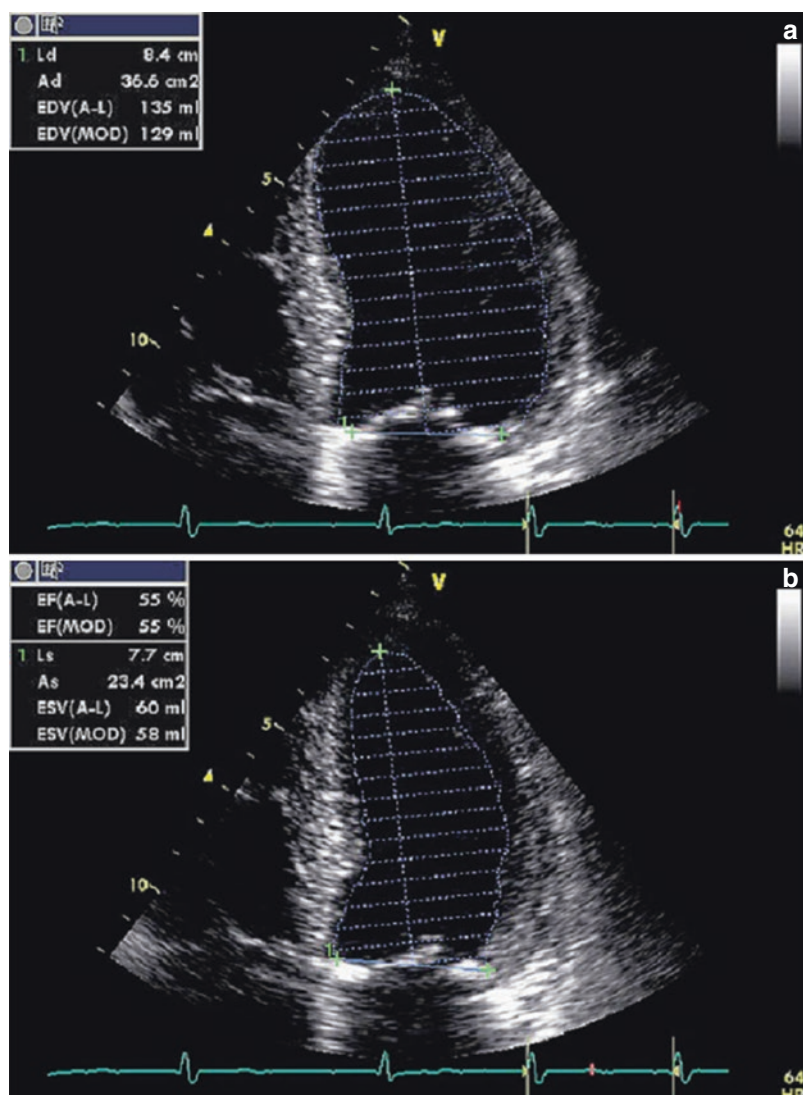
7.3.7 Ventricular Wall Kinetics

The following walls of the left ventricle are examined with TTE:

- The anteroseptal and posterior walls: parasternal long-axis and apical three-chamber views
- All the walls at mid-papillary level: parasternal short-axis view
- The septal and lateral walls: apical four-chamber view
- The inferior wall on the left of the display and the anterior wall on the right: apical two-chamber view

- The septal and posterior-lateral walls: subcostal view

The following LV walls are examined using TEE:

- The septal and lateral walls: mid-esophageal four-chamber view
- The inferior (on the left on the display) and anterior (on the right on the display) walls: mid-esophageal two-chamber view
- The posterior (on the left on the display) and anteroseptal (on the right on the display) walls: mid-esophageal long-axis view
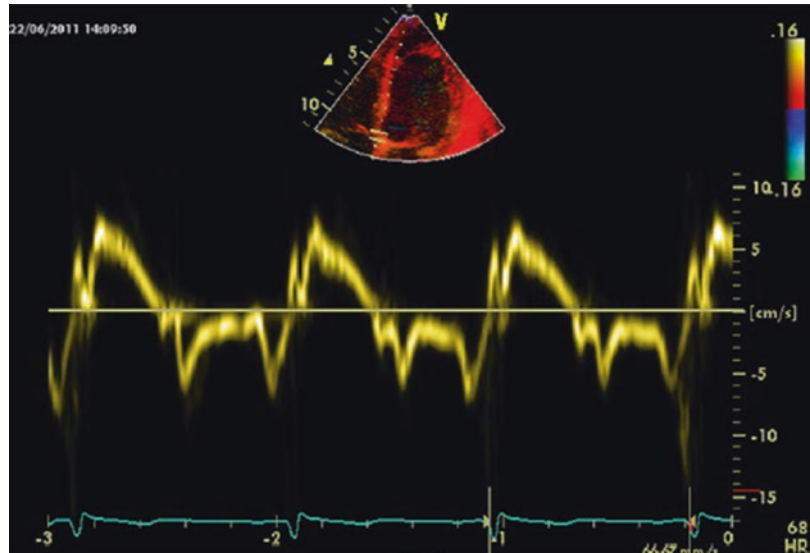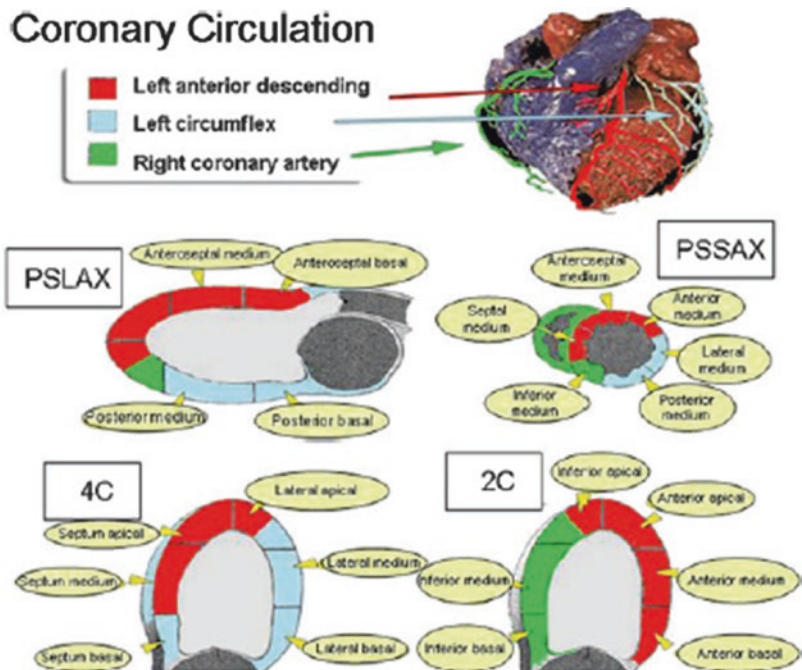
- All the walls at the mid-papillary level: transgastric mid short-axis view
- All the walls at the basal level: transgastric basal short-axis view

Although there are variations, it can be stated that:

- The anterior wall, most of the septum, and the apex are typically perfused by the left descending artery.
- The lateral wall and the posterior wall are perfused by the circumflex artery.
- The inferior wall is perfused by the right coronary artery (Fig. 7.14).

For the assessment of the wall motion, each wall in the four-chamber view and in the two-chamber view is divided into three segments: basal, medial, and apical, which are characterized by a number. We can examine these segments also in the parasternal short-axis (TTE) or transgastric (TEE) view (the only one that shows all the sections of myocardium perfused by the three main coronary trunks) at the basal (six segments), medial (six segments), and apical (four segments) levels. This 16-segment model has recently been integrated with the 17th segment, the apical cap, without myocardial endocardial borders (Fig. 7.15), which is useful for comparison with other cardiac imaging techniques (magnetic resonance imaging, scintigraphy, CT).

The wall contractility is evaluated by two simultaneous assessments:

1. Systolic thickening, which must typically be greater than 30%
2. The convergent movement of the wall toward the LV lumen

The former is prevalent in the assessment of the kinetics because the latter is also affected by tractions exerted by adjacent tissues. The study of regional kinetics may not be easy for the beginner. The index finger placed on the "display" in the center of the LV cavity, in the parasternal short-axis view (TTE) or the transgastric view (TEE), can help in the evaluation of centripetal motion and thickening. The individual segments are qualitatively evaluated for:

1. Normal contraction
2. Hypokinesia (reduction)
3. Akinesia (absence)
4. Dyskinesia (paradoxical centrifugal motion in systole)
5. Aneurysm (a visible deformation both in systole and in diastole, which causes an excessive thinning of the wall)

Changes 2–5 are defined as regional wall motion abnormalities. From the findings of the individual segments, it is then possible to indicate the affected coronary artery (Fig. 7.14). By
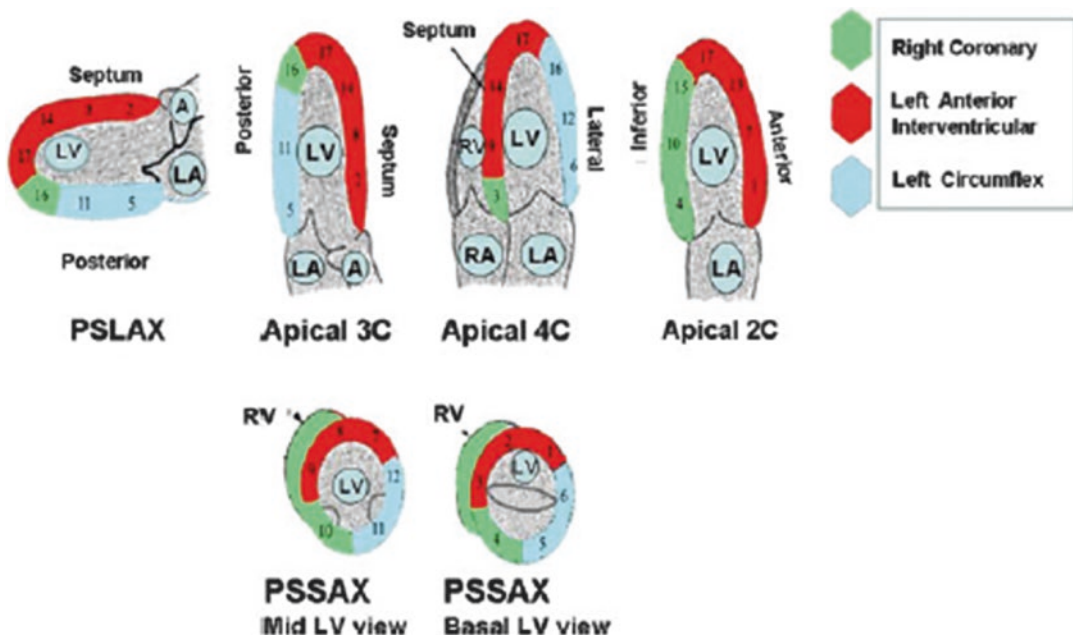
Fig. 7.15 Classification of LV myocardial segments and coronary perfusion in different TTE views. A ascending aorta, 2C two chamber, 3C three chamber, 4C four chamber, LA left atrium, LV left ventricle, PSLAX parasternal long axis, PSSAX parasternal short axis. (Modified from Sarti with permission)

Table 7.1 Wall motion scoring index

Score	definition
1	Normal. Thickening of more than 30% and movement toward the inner cavity
2	Hypokinesia. Reduction of movement and thickening of less than 30%
3	Akinesia. Absence of thickening (a remnant movement can be transmitted)
4	Dyskinesia. Paradoxical movement outward in systole
5	Aneurysm. Permanent dilation deformation in both diastole and systole with a thin and hyper-echo-reflective wall

The score is the sum of individual segment scores divided by the number of segments examined. A normal left ventricle has a wall motion scoring index of 1

assigning a score of contractility to each segment, one can calculate the wall motion scoring index. It is the sum of the scores divided by the number of segments studied (Table 7.1). The normal value is therefore 1.

7.4 Diastolic Function

7.4.1 Introduction and Background

The heart is a variable-volume pump inserted into a system of elastic tubes with one-way valves, filled with blood. So the pump function is not only related to the systolic squeeze, but it also depends on the degree of relaxation of the heart chambers, which creates the reserve volume required for an effective ejection. A normal LV is able to fill up to a regular end-diastolic volume without significant increase of left atrial pressure at rest and even during exercise or other stressors. Echocardiography is the only clinical method that allows easy assessment of LV diastolic filling. Diastolic function, which has only recently been thoroughly and regularly evaluated, may be considered "the dark side of the moon" of the cardiac function. Diastolic dysfunction, although not present at rest, often appears during myocardial stress due to myocardial ischemia or during weaning from mechanical ventilation. Many pathological conditions which are often seen in the emergency department and ICU and are characterized by impend-

ing pulmonary edema and low cardiac output with normal EF are well explained by diastolic dysfunction. As the left ventricle relaxes slowly and compliance decreases, cardiac filling is reduced, and the pressure load in the left atrium increases. The overloaded left atrium tends to enlarge. Pulmonary capillary pressure is also increased, thus facilitating interstitial edema and ultimately alveoli flooding. The increase in lung water can be easily studied by ultrasonography of the lung (comet tails; see Chaps. 30 and 35). Most of the coronary flow of the left ventricle occurs during the diastolic phase. Therefore, a deficit of coronary perfusion (e.g., when associated with a reduction in diastolic time, such as during tachycardia, atrial fibrillation, or in hypotension) is accompanied by an impaired relaxation, thus reducing cardiac output and increasing pulmonary capillary pressure. Concentric LV hypertrophy and myocardial fibrosis reduce compliance and therefore the distensibility of the cavity. These mechanisms are the most common precipitating cause of surgical perioperative ischemia, even without significant coronary obstruction, along with the increase in oxygen consumption due to tachycardia, possible high blood pressure due to pain, or reduced coronary perfusion pressure due to hypotension. In fact, perioperative myocardial infarctions do not always show a thrombotic coronary obstruction. Often, they are characterized by more or less extended subendocardial necrosis. The onset of high-frequency atrial fibrillation may suddenly worsen an ischemic borderline condition. So in these patients, the arrhythmia should be treated promptly, often combining antiarrhythmic drugs with electric shock.

In general, diastolic dysfunction is suspected in:

- Elderly patients
- Diabetic patients
- Patients with metabolic syndrome
- Hypertensive patients, especially if arterial pressure is not well controlled
- The presence of ventricular hypertrophy
- The presence of aortic stenosis
- Restrictive heart disease

7.4.2 Phases of Diastole

Diastole is divided into four stages:

1. Isovolumetric relaxation. This is an active, energy-requiring phenomenon and therefore needs good perfusion. It begins with the closure of the aortic valve and continues until the opening of the mitral valve.
2. Rapid ventricular filling. The active muscle relaxation continues, and the left ventricle is filled according to its own compliance. It starts as the ventricular pressure drops below the left atrial pressure; thus, the mitral valve opens, and most of the ventricular filling occurs (diastolic *E* wave of the transmitral pulsed wave Doppler flow). Aging can reduce the *E* wave peak.
3. Mesodiastolic phase. The flow is very slow following the minimum pressure gradient between the left atrium and the left ventricle.
4. Atrial contraction. *A* wave of the transmitral pulsed wave Doppler flow, normally 20–30% of the total filling volume. It may increase in importance, more than 50%, as the left ventricle becomes stiffer. This atrial filling contribution is obviously lost if there is atrial fibrillation, with severe clinical consequences, such as low cardiac output and/or pulmonary edema.

7.4.3 Pulsed Wave Doppler Assessment of Transmitral Flow

The transmitral diastolic flow is examined with pulsed wave Doppler echocardiography in the apical four-chamber or two-chamber view (TTE) or the mid-esophageal four-chamber or two-chamber view (TEE) according with the flow direction, 2–3 mm beyond the level of the valve's opening. To obtain a reliable assessment, it is necessary to have good alignment of the ultrasound beam with the flow. Diastolic transmitral flow presents in succession the protodiastolic rapid filling (*E* wave), the mesodiastolic pause, and the telediastolic filling, "atrial systole" (*A* wave) (Fig. 7.16).

The parameters of interest are:

- The *E* peak velocity (72 ± 14 cm/s under the age of 50 years and 62 ± 14 cm/s above the age of 50 years).
- The *E* wave deceleration time, from the apex of the *E* wave to the isoelectric line; normal below 200 ms (below 180 ± 20 ms from 20 to 50 years and below 210 ± 36 ms above 50 years).
- The *A* peak velocity (40 ± 10 cm/s below the age of 50 years and 59 ± 14 cm/s above the age of 50 years).

Fig. 7.16 Apical four-chamber view (TTE). Pulsed wave Doppler image of diastolic transmitral flow (normal pattern). (From Sarti with permission)
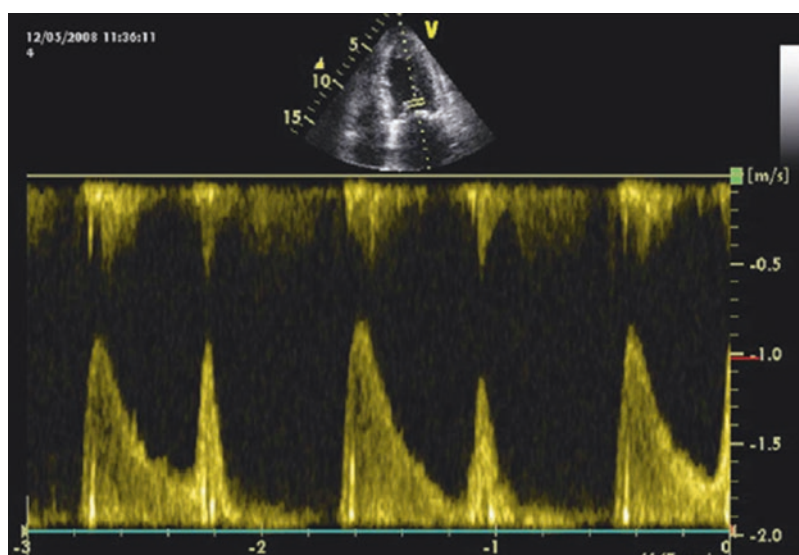
- The *E/A* ratio. Normally, $E > A$), but *E* is usually equal to *A*, or slightly less, in older people (1.9 ± 0.6 below 50 years and 1.1 ± 0.3 above 50 years).

A stiff left ventricle leads to increased end-diastolic pressure and increased left atrial pressure. Thus, the volume of the atrium augments. Diastolic function is characterized by four stages with changes in the parameters shown above (Fig. 7.17). For heart rate greater than 100 beats per minute, transmitral Doppler waves are generally less recognizable. Of course, this classification does not apply if there is atrial fibrillation because of the disappearance of the *A* wave. In the course of atrial fibrillation, it is possible to evaluate LV diastolic function by the *E* wave (Fig. 7.18) and the deceleration time, together with the TDI parameters (see below).

Pattern 1 is the normal one (Fig. 7.17). In altered relaxation (pattern 2), the *E* wave loses speed, and the *E/A* ratio is reversed (Fig. 7.19). However, as the left atrial pressure progressively increases, the *E* wave rises again, and the *E/A* ratio becomes greater than 1 again (pseudonormal, pattern 3). With advanced diastolic dysfunction, the *E/A* ratio becomes greater than 2 (restrictive pattern, pattern 4) (Fig. 7.20). It should be considered that as far as the *E/A* ratio is

Fig. 7.17 Classification of diastolic function. See the text for details. DT deceleration time. (Modified from Sarti with permission)

Transmitral diastolic flow pattern

E/A ratio	0.75–1.5	<0.75	0.75–1.5	>1.5	>1.5
DT (ms)	150–200	>200	150–200	<150	<150
E/Ea ratio	<10	<10	>10	>>10	>>10
Pattern	1	2	3	4 Reversible	4 Unreversible
Diastolic function	Normal	Impaired relaxation	Pseudo-normal	Restrictive	
				Severe dysfunction	
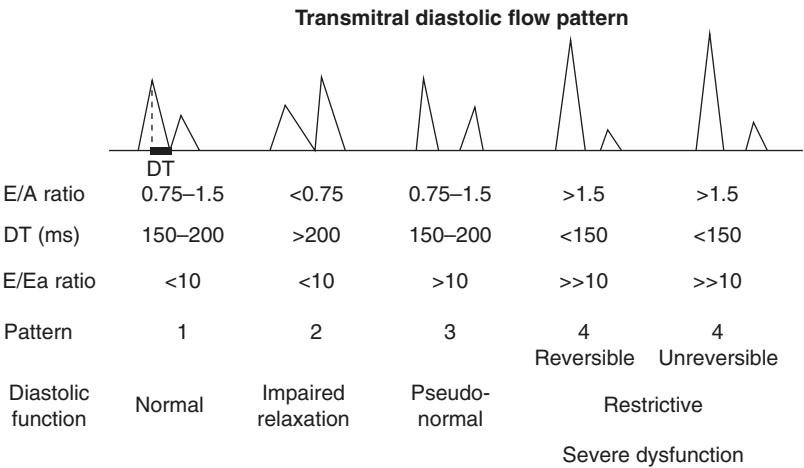
Fig. 7.18 Apical four-chamber view (TTE). Pulsed wave Doppler image of mitral flow in atrial fibrillation (absence of *A* wave). (From Sarti with permission)
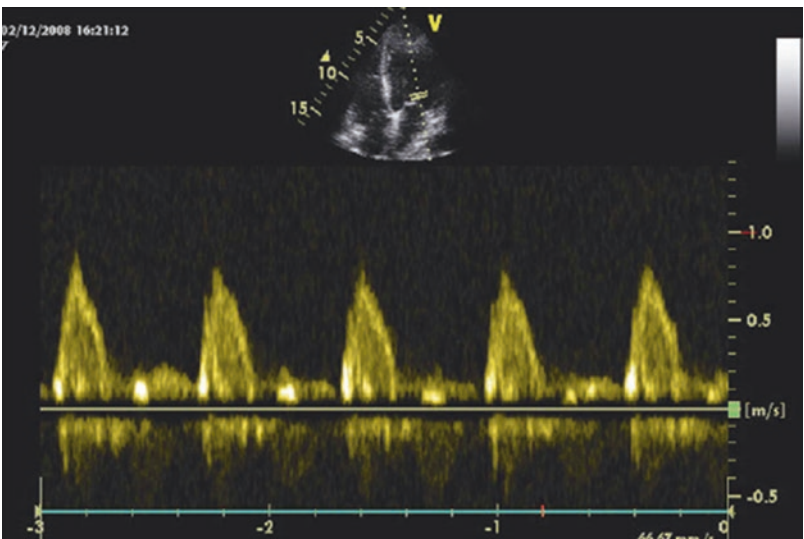
Fig. 7.19 Pulsed wave Doppler image of transmitral diastolic flow: inversion of the *E*/*A* wave. Apical four-chamber view (TTE). Pattern 2. Impaired relaxation. (From Sarti with permission)
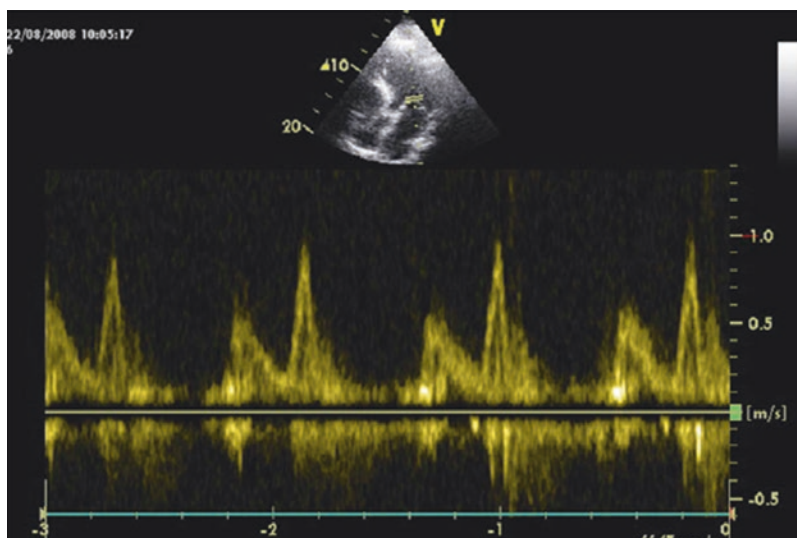
Fig. 7.20 Severe diastolic dysfunction. Transesophageal echocardiography image of a restrictive pattern

concerned, normal and pseudonormal functions are not distinguishable, but a heart with pseudonormal diastolic dysfunction also has other pathological changes as seen on ultrasonographic examination such as LV hypertrophy and atrial dilatation. Moreover, any doubt can be clarified by TDI evaluation that examines directly the speed of movement of the myocardium (see below).

The release phase of the Valsalva maneuver allows one to distinguish a reversible phase of the restrictive dysfunction from the final irreversible stage. As the restrictive pattern is still reversible, an increasing *A* wave (due to increased venous return) is observed together with an *E*/*A* ratio equal to or even greater than 1. Instead, in the irreversible phase, no significant change in the *A* wave peak is observed in the release phase of the Valsalva maneuver. In the ICU, with a mechanically ventilated patient, a sort of Valsalva maneuver may be done by stretching slowly the lungs by manual ventilation using a bag valve mask. A sudden release of the positive pressure produces the release phase of this modified Valsalva maneuver.

7.4.4 Tissue Doppler Imaging

TDI is a very sensitive technique for evaluating LV diastolic function because it directly evaluates the speed of movement of the myocardial tissue (Fig. 7.13). At the level of the lateral mitral annulus in the apical four-chamber view (TTE) or the mid-esophageal four-chamber view (TEE), a tissue Doppler wave of relaxation directed toward the base of the heart because of the LV diastolic filling expansion is recorded in diastole. This wave is called E' (sometimes Ea or Em in the less recent literature). E' is temporally correlated with the transmitral flow Doppler E wave. A further tissue stretch is then recorded as an A' (or Aa or Am) wave, which is related to further LV expansion due to atrial systole and is concomitant with the Doppler A wave of telediastolic transmitral flow. Of course, the A' wave, like the A wave, disappears if there is atrial fibrillation. The parameters of interest are:

1. The speed of early relaxation, E'. Normally this is 10 cm/s or greater. A value less than 10 cm/s (or less than 8 cm/s at the septal level of the mitral annulus) defines a diastolic dysfunction.
2. The E/E' ratio (or E/Ea, or E/Em), which is the ratio between the peak velocity of early flow (pulsed wave Doppler echocardiography) and the speed of tissue relaxation movement (TDI). It is rather intuitive that the ratio between the peak flow, which depends on the transmitral pressure gradient, and the speed of

the myocardial relaxation can represent LV filling pressure. This ratio is generally considered normal under 10 and abnormal (impaired diastolic relaxation) over 10–12. In the presence of regional wall motion abnormalities, the lateral and septal E' should be averaged. In this case, high-filling pressure is identified by E/E' greater than 13. A value greater than 15 is associated with a marked increase in left atrial pressure and pulmonary capillary wedge pressure and also with a significant increase of atrial B-type natriuretic peptide (see Chaps. 30 and 35).

7.5 Myocardial Performance Index

By placing the pulsed wave Doppler sample volume between the two streams of the mitral valve (diastolic) and aortic valve (systolic) flows in the apical five-chamber view (TTE) or the deep transgastric long-axis view (TEE), one can study these two flows and the isovolumetric diastolic and systolic phases in succession:

- The isovolumetric relaxation time at the beginning of diastole
- The isovolumetric contraction time at the beginning of systole
- The aortic ejection time between the two (Fig. 7.21)

Fig. 7.21 Pulsed wave Doppler sample volume positioned between the inflow and outflow of the left ventricle (**a**) is the time between the opening and closing of the mitral valve and (**b**) is the aortic ejection time. Apical five-chamber view (TTE) (see the text). (From Sarti with permission)
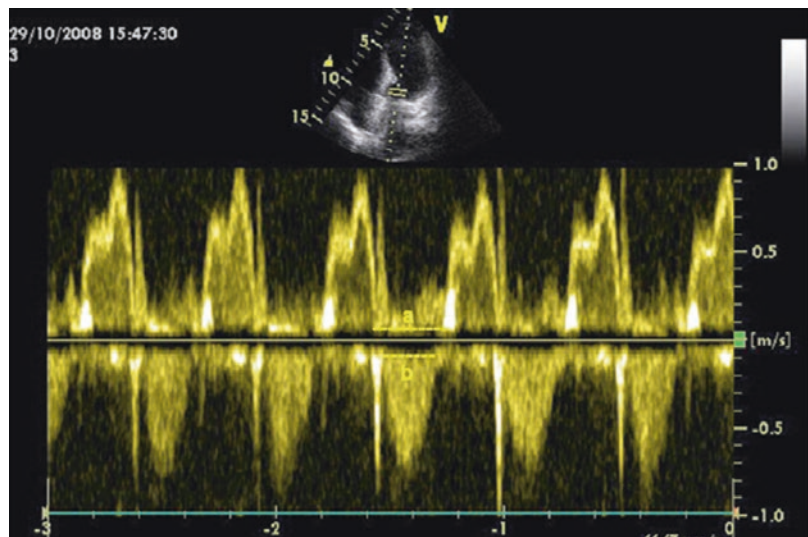
The myocardial performance index (MPI) is defined as $(a - b)/b$, where a corresponds to the time between closing of the mitral valve and its reopening in the next cycle (end of A wave and beginning of the subsequent E wave in transmitral flow Doppler measurements) and b corresponds to the aortic ejection time, as evidenced by the Doppler flow (velocity-time integral) at the LV outflow tract (Fig. 7.15). The normal value is between 0.30 and 0.38. This index is altered both by systolic dysfunction ($+dP/dt$, time of isovolumetric contraction) and by diastolic dysfunction ($-dP/dt$, isovolumetric relaxation time), and it is therefore a general index of LV performance.

Further Reading

Bloechlinger S, Grander W, Bryner J, et al. Left ventricular rotation: a neglected aspect of the cardiac cycle. Intensive Care Med. 2010;37:156–63.

Bouhemad B, Nicolas-Robin A, Arbelot C, et al. Isolated and reversible impairment of ventricular relaxation in patients with septic shock. Crit Care Med. 2008;36:766–74.

Combes A, Arnoult F, Trouillet JL. Tissue Doppler imaging estimation of pulmonary artery occlusion pressure in ICU patients. Intensive Care Med. 2004;30:75–81.

Lang RM, Badano LP, Mor-Avi V, et al. Recommendations for chamber quantification by Echocardiography in adults: An Update from the American Society of Echocardiography and the European Association of Cardiovascular Imaging. 2015. https://doi.org/10.2015/j.echo.2014.10.003.

Matyal R, Skubas NJ, Shernan SK, et al. Perioperative assessment of diastolic dysfunction. Anesth Analg. 2011;113:449–72.

Poelaert J, Osipowska E, Verborgh C. Diastolic dysfunction and cardiac failure in the intensive care unit. In: Vincent JL, editor. 2008 yearbook of intensive and emergency medicine. Berlin: Springer; 2008. p. 76–87.

Sarti A. Ecocardiografia per l'intensivista. Milan: Springer; 2009.

Slama M, Maizel J. Echocardiographic measurement of ventricular function. Curr Opin Crit Care. 2006;12:241–8.

Sturgess DJ, Marwick TH, Joyce CJ, et al. Tissue Doppler in critical illness: a retrospective cohort study. Crit Care. 2007;11:R97.

Vignon P. Ventricular diastolic abnormalities in the critically ill. Curr Opin Crit Care. 2013;19:242–9.

The Right Ventricle and Pulmonary Artery: Frequent Imaging in ICU Patients

8

Luigi Tritapepe, Mario Mezzapesa, Giulia Frasacco, Chiara Manganelli, Vincenzo De Santis, and Massimo Pacilli

8.1 The Right Ventricle: Anatomy

In the normal heart, the right ventricle is the most anteriorly situated cardiac chamber and lies immediately behind the sternum. It has a complex geometry, appearing triangular at the frontal view and semilunar when viewed in a transverse section of the heart, with the septum being the most important determinant of shape. Under normal loading and electrical conditions, the septum moves toward the right ventricle in both systole and diastole. This complex geometry cannot be simply represented with geometric models, which presents important limitations for the estimation of right ventricular (RV) volume and function based on two-dimensional (2D) tomographic views. The ventricles extend from the atrioventricular junction leftward to the apex and cephalad to the ventriculoarterial junction. For the right ventricle, the annuli of the leaflets of the tricuspid and pulmonary valves delimit the chamber at the respective junctions with the atrium and the arterial trunk. The RV can be described in terms of three components: the inlet, which consists of the tricuspid valve, chordae tendineae, and papillary muscles; the trabeculated apical myocardium; and the infundibulum or conus, which corresponds to the smooth myocardial outflow region. This division seems to be more practical than the classical division of the right ventricle into the sinus and conus components. Additionally, the RV can also be divided into anterior, lateral, and inferior walls, as well as basal, mid, and apical sections. Another important characteristic of the RV is the presence of a ventriculoinfundibular fold that separates the tricuspid and pulmonary valves. In contrast, in the LV, the aortic and mitral valves are in fibrous continuity. Although the RV is usually located on the right side of the heart and connects with the pulmonary circulation, the RV anatomy is defined by its structure rather than by its position or connections. The morphological features which identify RV are (1) the more apical hinge line of the septal leaflet of the tricuspid valve relative to the anterior leaflet of the mitral valve; (2) the presence of a moderator band; (3) the presence of more than three papillary muscles; (4) the trileaflet configuration of the tricuspid valve with septal papillary attachments; (5) and the presence of coarse trabeculations.

The right ventricle contracts in a "peristaltic" pattern that proceeds from the sinus, where fibers are mostly oriented obliquely with an average major radius of curvature of nearly 4 cm, to the

L. Tritapepe (✉) · G. Frasacco
Policlinico Casilino Hospital, Rome, Italy
e-mail: luigi.tritapepe@uniroma1.it

M. Mezzapesa · C. Manganelli · M. Pacilli
Department of Anesthesia and Intensive Care,
Cardiac Surgery ICU, Policlinico Umberto I Hospital,
Sapienza University of Rome, Rome, Italy

V. De Santis
Umberto I Hospital, Lugo, RA, Italy

infundibulum, whose fibers are circumconal with a small radius of curvature of 0.8 cm. Because of the complex shape of the right ventricle, triangular from the frontal aspect and crescentic from the apex, it is necessary to image the right ventricle from several projections, each characterized by specific anatomic landmarks. The thickness of the RV free wall is in the range of only 3–5 mm, and the RV mass is approximately one fourth/one sixth of that of the left ventricle. Still, owing to the lower impedance and greater distensibility of the pulmonary artery bed, the right ventricle can pump blood at the same rate and volume as the left ventricle. The ability of both ventricles to maintain a normal cardiac output, ensuring sufficient organ perfusion, depends on three key factors: the contractile status of myocardial tissue; the preload, which represents the initial stretching of cardiac myocytes prior to contraction; and the afterload, defined as the load against which the heart must contract to eject blood. In addition, RV performance is directly influenced by left ventricular (LV) functional status owing to ventricular interaction. The interventricular septum, the pericardium, and common muscle fibers all play an important role in facilitating the transfer of force from the left ventricle to the right ventricle during the cardiac cycle. Around one third of the pressure generated in the right ventricle is determined by LV contraction. The right ventricle is affected much by the increase in pulmonary artery pressure, which can cause the acute dilation of the right ventricle resulting in tricuspid regurgitation. The increase in RV pressure and dilation of the right ventricle may cause the interventricular septum to shift itself to the left, with decreased compliance of the left ventricle and increased LV end-diastolic pressure. In other words, the right ventricle also tolerates a large increase in volume but immediately suffers from any increase in afterload.

8.2 The Pulmonary Artery: Anatomy

The pulmonary artery is a large artery originating from the superior surface of the right ventricle and carrying deoxygenated blood from the heart to the lungs. The pulmonary artery is the exception to the rule that arteries carry oxygenated blood from the heart to other parts of the body. The pulmonary trunk (pulmonary artery or main pulmonary artery) is approximately 5 cm in length and 3 cm in diameter. It branches into two pulmonary arteries (left and right), which deliver deoxygenated blood to the corresponding lung. The right pulmonary artery commences below the arch of the aorta and runs to the right and slightly downward to reach the hilum of the right lung. In its course, it passes behind the ascending aorta and the superior vena cava and in front of the esophagus and the stem of the right bronchus. Near the lung it gives off a large branch which accompanies the eparterial bronchus. The left pulmonary artery runs to the left and backward, across the front of the descending aorta and the left bronchus, to the hilum of the left lung.

8.3 The Right Ventricle: Echocardiography

The right ventricle has been less studied than the left ventricle in terms of physiopathology and echocardiography. However, this ventricle plays an important role in morbidity and mortality of patients presenting with sign and symptoms of cardiopulmonary disease. Its functionality may determine the load response and blood volume in unstable patients, and whenever the hypotensive patient does not respond to a fluid challenge, involvement of the right ventricle is suspected. Owing to its widespread availability, echocardiography is used as the first-line imaging modality for assessment of RV size and function. The quantitative assessment of RV size and function is often difficult, because of the complex anatomy. With transthoracic echocardiography (TTE), we may explore with sufficient precision the dimension and function of the right ventricle. A qualitative evaluation of the right ventricle can be obtained by assessing the shape of the right ventricle, which can be visualized in the parasternal short-axis view, the parasternal long-axis view and its modification, and the apical four-chamber

view. The location of the right ventricle behind the sternum restricts somewhat the transthoracic parasternal windows that can be accessed by the ultrasound beam. Thick trabeculations in the chamber may occasionally be confused with a thrombus or a tumor or may be misdiagnosed as hypertrophic cardiomyopathy. Because of the triangular shape of the right ventricle, its apex is normally not well evaluated in the apical four-chamber view, so when the apex is well visible or exceeds the LV apex, this means there is enlargement or hypertrophy of the right ventricle. Then this is an important point in the echocardiographic evaluation of the RV dilation and function: immediately, we can exclude an involvement of the right ventricle in determination of contingent disease. However, we need other measures to confirm the diagnosis of RV dilation. In the apical four-chamber view, we can measure the transverse and the longitudinal diameter of the right ventricle to assess the size of the right ventricle. Two transverse diameters are measured in the apical four-chamber view: the annulus or basal diameter, which is about 3.5 cm in diastole and 2.9 cm in systole, and the mid diameter, at the mid-ventricular level, which is about 3.0 cm in diastole and 2.4 cm in systole. Finally, we measure the length of the right ventricle from the annulus to the apex, which is about 7.1 cm in diastole and 5.5 cm in systole. Still in the apical four-chamber view, it is important to measure the RV end-diastolic area (RVEDA), which, generally, is about two thirds of the LV end-diastolic area (LVEDA) and is about 20 cm^2. The relationship between the RVEDA and the LVEDA is very important to make the diagnosis of primary or secondary involvement of the right ventricle. An RVEDA/LVEDA ratio less than 0.6 is considered normal, whereas an RVEDA/LVEDA ratio between 0.6 and 1.0 is typical of RV dilation, which becomes a huge dilation for a ratio greater than 1.0.

The wall thickness of the right ventricle, as measured in the apical four-chamber view or better in the subcostal four-chamber view, is usually less than 0.5 cm. Any increase of the thickness above 0.5 cm shows hypertrophy of the right ventricle. In the parasternal long-axis view, it is also possible to measure the RV diameter at the outflow tract by 2D echocardiography and in M-mode ($RVOT_1$). $RVOT_1$ is measured at the maximal diastolic expansion of the right ventricle. Two other diameters, $RVOT_2$ and $RVOT_3$, are measured at the outflow tract of the right ventricle in the parasternal short-axis view at the basal level of the heart. $RVOT_2$ is the widest part of the outflow tract, and $RVOT_3$ is measured at the pulmonary annulus plane. These diameters are more important for the trend modifications due to loading and contractile conditions than as isolated values. Then, without difficult calculations, but almost at a glance, we can get an idea of the function of the right ventricle at that time (Figs. 8.1 and 8.2).
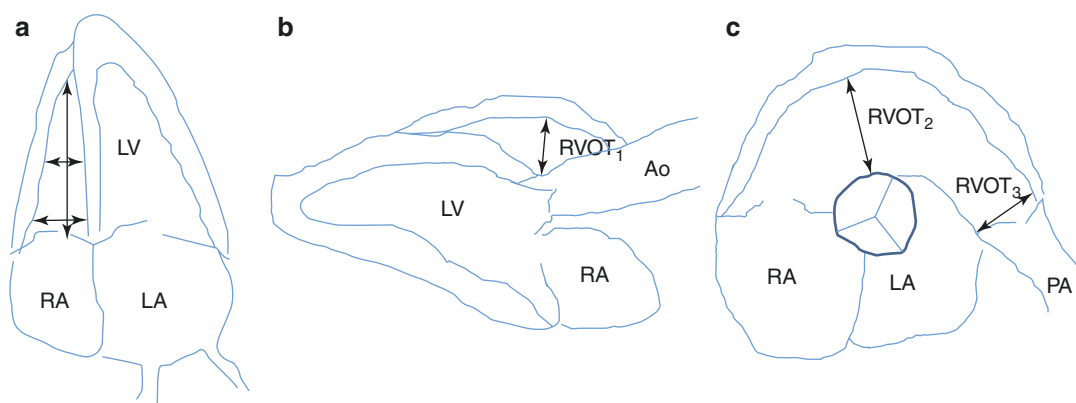
Fig. 8.1 The echocardiographic views used for evaluating the diameters of the ventricle. (**a**) apical four-chamber view, (**b**) parasternal long-axis view, and (**c**) parasternal short-axis view at the base of the heart. Ao aorta, LA left atrium, LV left ventricle, PA pulmonary artery, RV right ventricle
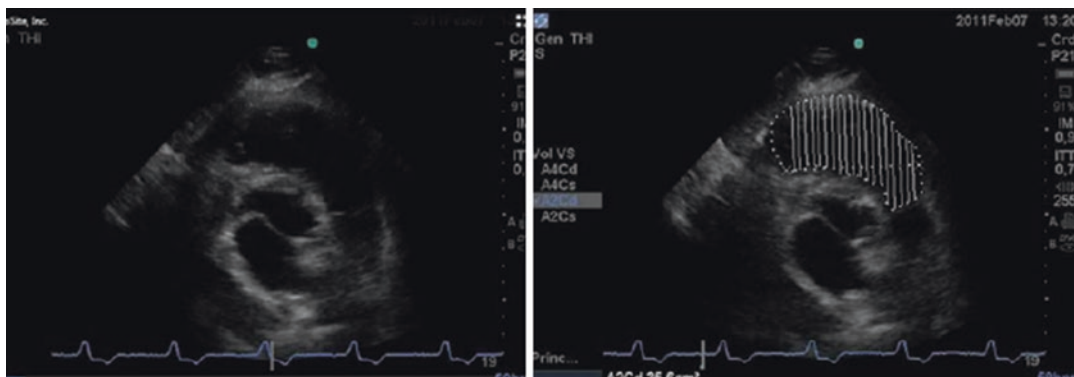
Fig. 8.2 Transthoracic echocardiography (TTE), parasternal short-axis view of the right ventricle, and its volume measurement

Fig. 8.3 Increase of the afterload of RV with D shape of LV and loss of eccentricity index
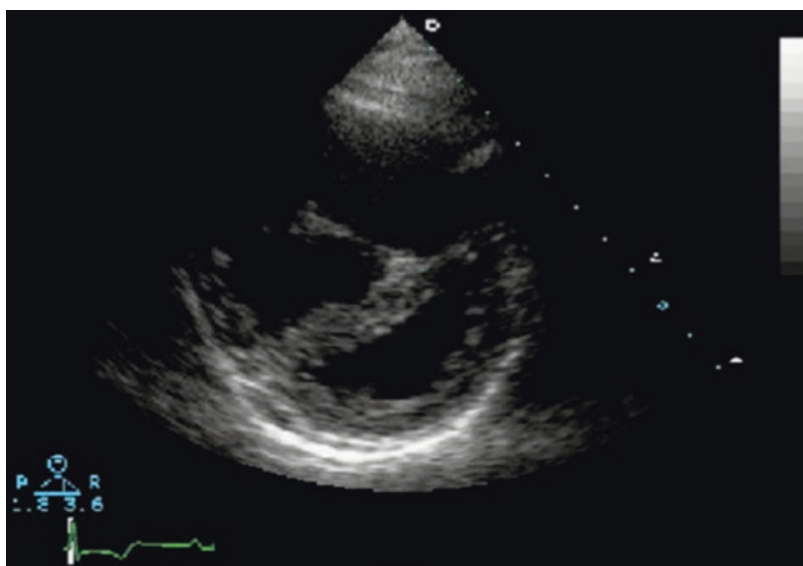
In the parasternal short-axis view, at the mid-papillary level, we can observe the short axis of the left ventricle and the right ventricle but especially the shape of the interventricular septum. The movement of the interventricular septum is very important for the diagnosis of volume overload of the right ventricle or pressure overload inside the right ventricle. In fact, the flattening of the septum can represent an increase in volume or in pressure of the RV, and the left ventricle takes the form of the letter D (Fig. 8.3).

In this condition the left ventricle is unloaded (hypodiastolic) and the right ventricle is over-

loaded. In the case of increased afterload of the right ventricle, the septum moves toward the left ventricle in systole and diastole, whereas in the case of volume overload, the movement toward the left ventricle is visible only during diastole. These circumstances should be immediately diagnosed particularly in patients ventilated with high levels of positive end-expiratory pressure in mechanical ventilation, because, while presenting all forms of dynamic change of the hemodynamic indices explored, such patients do not respond to the fluidic load during the hemodynamic instability period. The eccentricity index is

an index for grading the level of RV hypertension (i.e., in the case of pulmonary embolism or excessive positive end-expiratory pressure in the acute respiratory distress syndrome patient) and is measured in the parasternal short-axis view at the mid-ventricular level. This index is the ratio between the anteroposterior diameter of the left ventricle and the lateroseptal diameter of the same ventricle, measured in diastole. Normally the eccentricity index is 1; every elevation of this value (above 1) means an increase of the RV overload if it is measured at the end of diastole, whereas it shows an increase of pressure if it is measured at the end of systole and diastole.

With transesophageal echocardiography, however, the right-side structures are farthest from the esophagus, and the definition of the right ventricle is sufficiently good. The tomographic views in which we can recognize the shape, function, and volume of the right ventricle are the same but specular of TTE. The best evaluation of the right ventricle is obtained in the mid-esophageal four-chamber view, the mid-esophageal RV inflow–outflow view, the transgastric short-axis view, and the transgastric RV inflow view. The classic mid-esophageal four-chamber view puts the right ventricle on the left side of the screen, but the apex is far from the transducer. An optimal tomography is represented by the mid-esophageal RV inflow–outflow view, where the right ventricle is positioned on the left and at the bottom of the screen and we can obtain good alignment for Doppler investigation of tricuspid valve. In the transgastric short-axis view, we can observe, especially in ventilated patients, in which there are not good windows for exploration, the ratio between both ventricles, which is so important to manage fluid loading and diagnose RV failure in the case of hypocontractility and enlargement of the right ventricle. At this level, rotating the multiplane angle to about 100° and turning the probe slightly to the right, we obtain the transgastric RV inflow view, in which projection we can study well the subvalvular structures of the tricuspid valve and we can evaluate the movement and thickness of the inferior portion of the RV free wall.

8.4 The Pulmonary Artery: Echocardiography

The pulmonary artery is studied with TTE in the parasternal short-axis view at the base of the heart and in the modified parasternal long-axis view. In the subcostal short-axis view, it is possible to obtain useful images to study the right ventricle and the pulmonary artery. The pulmonary artery and/or its right branch are visible as a little circle below the aortic arch in suprasternal tomography. Transesophageal echocardiography allows us to completely evaluate the pulmonary artery and its right branch. The left branch is not visible because of the presence of the left main bronchus, which, with its air content, prevents the passage of the ultrasound beam. The mid-esophageal RV inflow–outflow view is a good tomographic view to evaluate the diameter of the pulmonary artery, the flow through the pulmonary valve, and the tricuspid regurgitation, which, sampled with continuous wave Doppler imaging, allows us to measure the systolic pulmonary pressure when the right atrial pressure is known [pulmonary artery pressure = 4 × (peak velocity of tricuspid regurgitation)^2 + central venous pressure] (Fig. 8.4).

Two other views are fundamental to study the pulmonary artery: the mid-esophageal ascending aortic short-axis view and the upper esophageal aortic arch short-axis view. The first one shows the trunk of the pulmonary artery and the right branch of pulmonary artery. This tomographic view is important because the trunk of the pulmonary artery is parallel to the pulsed wave Doppler beam and the pulmonary velocity–time integral can be measured, which is essential to determine the right cardiac output and to show the cyclic variation of velocity–time integral with different intrathoracic pressure levels (Fig. 8.5).

Furthermore, we can follow the positioning of a Swan–Ganz catheter and detect formation of thrombosis around the pulmonary catheter. In the case of pulmonary embolism, we can observe the thrombi throughout the pulmonary artery bed.
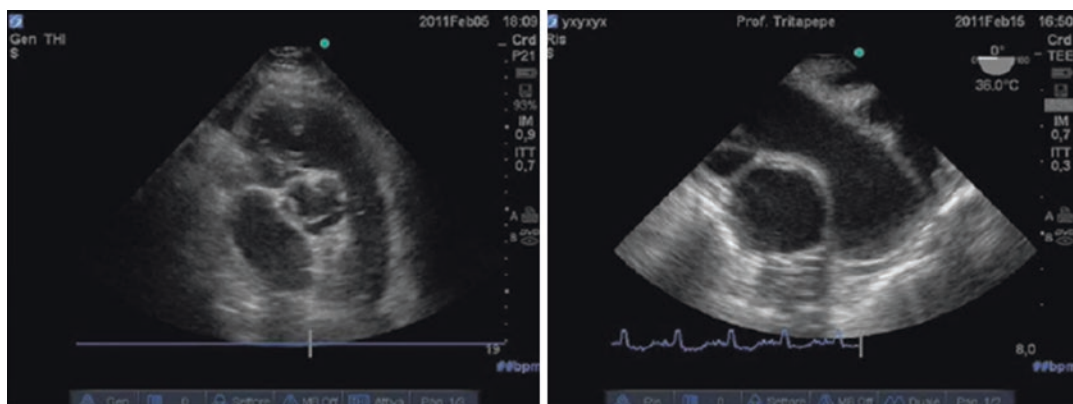
Fig. 8.4 TTE and transesophageal echocardiography of the trunk of the pulmonary artery

Fig. 8.5 Pulsed wave Doppler imaging of the pulmonary artery and variation of the velocity–time integral with the respiratory cycle
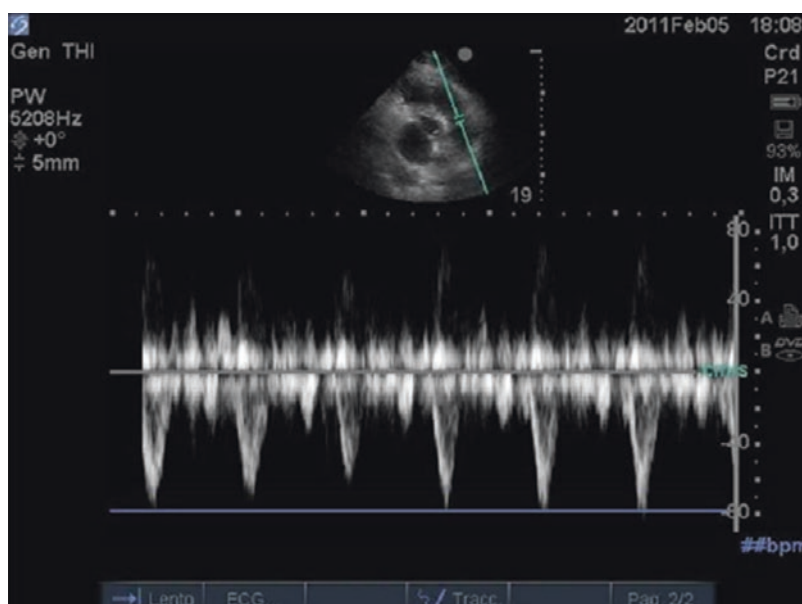
8.5 Assessment of Right Ventricular Systolic Function

Unlike the left ventricle, the assessment of systolic function of the right ventricle with the biplane method to quantify RV function is complicated by its particular shape and geometry. Nevertheless, some surrogate methods are used and now accepted because of MRI validation. The RV outflow tract shortening fraction is obtained in the parasternal short-axis view at the base of the heart, where we can measure (in M-mode) the RV outflow tract diameter in systole and diastole. The difference between the two diameters divided by the diastolic diameter gives the RV outflow tract shortening fraction. RV fractional area change describes the percentage change in RV area between diastole and systole. It is measured in the apical four-chamber view and is calculated by measuring the RV end-diastolic area (RVEDA) and the RV end-systolic area and dividing the difference between these

Table 8.1 Normal values for parameters of right ventricular systolic function

Parameter	Normal value
RVOT-SF (%) = (EDRVOTD − ESRVOTD)/EDRVOTD × 100	61 ± 13[a]
RVFAC (%) = RVEDA − RVESA/RVEDA × 100	56 ± 13[b]

EDRVOTD right ventricular outflow tract diameter in diastole, *ESRVOTD* right ventricular outflow tract diameter in systole, *RVEDA* right ventricular end-diastolic area, *RVESA* right ventricular end-systolic area, *RVFAC* right ventricular fractional area change, *RVOT-SF* right ventricular outflow tract shortening fraction
[a]Lindqvist et al.
[b]Lopez-Candales et al.

areas by the RVEDA. It is very well related to the ejection fraction calculated from MRI and is used to stratify patients after myocardial infarction, pulmonary hypertension, or cardiac surgery. Some errors are possible because the endocardial border determination of the right ventricle is complicated by the presence of widely represented trabeculae. For this reason, the RV ejection fraction is not normally measured (Table 8.1).

8.6   Tricuspid Annular Plane Systolic Excursion

A quantitative method to evaluation of RV systolic function that is well accepted and confirmed by the literature is the tricuspid annular plane systolic excursion (TAPSE). In other words, because the right ventricle contracts in a "peristaltic" pattern that proceeds from the sinus to the infundibulum, it is sufficient to measure the extent of dislodgement of the lateral portion of the tricuspid annulus toward the apex to quantify RV efficiency. The TAPSE is measured in M-mode utilizing the apical four-chamber view. The cursor is positioned on the image of the lateral tricuspid annulus, and the distance between the above and below point formed by the excursion of the tricuspid annular plane is measured. Normally, the TAPSE is more than 1.7 cm. A value below 1.7 cm is highly suggestive of RV systolic dysfunction. When TAPSE is very low

(less than 1.3 cm), the right ventricle is in a very bad condition and has a serious systolic dysfunction. Samad et al. assessed TAPSE in patients after a first acute myocardial infarction and showed that TAPSE of 15 mm or less was associated with increased mortality (45% at 2 years) compared with patients having TAPSE greater than 20 mm (4%). Special care must be taken when interpreting this parameter in longitudinal studies of patients undergoing procedures that affect the overall heart motion (i.e., cardiac surgery).

8.7   Tissue Doppler Imaging and Tei Index

Tissue Doppler imaging (TDI) allows quantitative assessment of RV systolic and diastolic function by means of measurement of myocardial velocities. Tissue velocities can be measured using pulsed wave tissue Doppler imaging at different levels of the RV free wall, but because of the difficulties to explore the apical segment of the right ventricle and because of physiological considerations, we use TDI on the basal segment of the RV free wall. The peak systolic velocities registered at this level (RV S') fit with RV systolic function and represent a good prognostic index of survival in patients with RV myocardial infarction. A peak systolic velocity greater than 11 cm/s is considered normal, but patients with myocardial infarction velocities greater than 8 cm/s have a significantly better event-free survival at 1 year than patients with systolic annular velocities below 8 cm/s. The Doppler index of myocardial performance (Tei index or myocardial performance index MPI or RIMP) is yet another parameter that can be used for evaluation of RV performance. It is expressed by the formula: (isovolumic contraction time + isovolumic relaxation time)/RV ejection time. It is established that it is actually unaffected by heart rate, loading conditions, or the presence and the severity of tricuspid regurgitation. If pulsed wave Doppler imaging is used to calculate Tei index, one needs to measure the inflow and the outflow of

the right ventricle. The velocities, sampled in conjunction with ECG registration, emphasize the isovolumic contraction time and relaxation time, and so Tei index can be calculated with the formula previously mentioned. However, the use of MPI is limited by the absence of the isovolumic relaxation and contraction times in the normal RV and by the pseudonormalization of the index in the presence of increased right atrial pressure. In fact, increased right atrial pressure causes a reduction of the isovolumic relaxation time and pseudonormalization of the myocardial performance index. The upper reference limit for the right-sided MPI is 0.40 using the pulsed Doppler method and 0.55 using the pulsed tissue Doppler method. It should not be used as the sole quantitative method for evaluation of RV function and should not be used with irregular heart rates.

8.8 Right Ventricular Strain and Strain Rate

New ultrasound methodologies have been proposed in recent years in order to make the evaluation of RV function more quantitative and robust. Strain measures myocardial tissue deformation, with strain rate measuring this deformation over time. In routine practice, strain is only measured in the longitudinal, apical four-chamber view. Longitudinal strain is calculated as the percentage of systolic shortening of the RV free wall from base to apex, while longitudinal strain rate is the rate of this shortening. RV longitudinal strain is less confounded by overall heart motion but depends on RV loading conditions as well as RV size and shape. One dimensional strain is acquired using DTI and is consequentially angle dependent. Two-dimensional strain is possible with the speckle tracking technique (STE strain). Speckle tracking measures motion in the myocardium by following speckle location and tracking them with

continued image acquisition via a complex algorithm, with derivation of strain values. This technique is relatively angle independent and allows measurement of RV strain in both the short and long axes. Two-dimensional STE-derived strain, particularly of the RV free wall, appears to be reproducible and feasible for clinical use. Peak global longitudinal RV strain excluding the interventricular septum has been recently reported to have prognostic value in various disease states, such as heart failure, acute myocardial infarction, pulmonary hypertension, and amyloidosis, and to predict RV failure after LV assist device implantation. Because of the need for additional normative data from large studies involving multivendor equipment, no definite reference ranges are currently recommended for either global or regional RV strain or strain rate.

8.9 Right Ventricular Diastolic Function

RV diastolic dysfunction may be clinically useful because it serves as an early and more easily quantifiable marker of subclinical RV dysfunction. Multiple studies have shown that RV diastolic dysfunction is usually present before apparent systolic dysfunction and before RV dilatation or RV hypertrophy. Measurement of RV filling is different from LV filling for two reasons: the time, which is shorter for the right ventricle, and the velocity, which is slower than for the left ventricle. In fact, the tricuspid valve area is greater than the mitral orifice and a large quantity of blood passes through the valve slowly. Nevertheless, it is possible, as for the left ventricle, to study the transtricuspid flow with pulsed wave Doppler imaging in the parasternal short-axis view at the base of the heart or in the apical four-chamber view, two views that present good alignment of Doppler beam. The *E* and *A* velocities can be collected, and the

E/A ratio represents the grading of RV diastolic dysfunction. Diastolic dysfunction is characterized by a decrease in the *E/A* ratio. The transtricuspid flow is affected by the loading condition, heart rate, aging, and respiration. The study of RV diastolic function is completed by TDI at the level of the tricuspid lateral annular plane and measurement of the inferior vena cava (IVC). The E1 and A1 waves measure RV diastolic function with minor influence of the loading condition. TDI should be used to differentiate normal from pseudonormal RV diastolic pattern. Besides, TDI allows to measure the *E/E′* ratio. An *E/E′* ratio >4 had a high sensitivity and specificity for predicting a right atrial pressure >10 mmHg in noncardiac surgery intensive care unit patients. Grading of RV diastolic dysfunction should be done as follows: tricuspid *E/A* ratio <0.8 suggests impaired relaxation, a tricuspid *E/A* ratio of 0.8–2.1 with an *E/E′* ratio >6 or diastolic flow predominance in the hepatic veins suggests pseudonormal filling, and a tricuspid *E/A* ratio >2.1 with a deceleration time <120 ms suggests restrictive filling. The diameter and the collapsibility of the inferior vena cava can help to identify the function of the right ventricle, especially the diastolic function. Finally, the hepatic vein change on the Doppler flow pattern can identify a RV diastolic dysfunction when the ratio of the total hepatic reverse flow integral to the total forward flow integral increases.

8.10   Right Ventricle in the ICU

Two special stress situations for RV are present in ICU. The patient with ARDS and those with septic shock suffer very early from the right ventricular insufficiency. Pulmonary vascular dysfunction is associated with ARDS and leads to increased right ventricular afterload and eventually right ventricular failure, also called acute cor pulmonale (Fig. 8.3). Interest in acute cor pulmonale and its negative impact on outcome in patients with ARDS has grown in recent years. Right ventricular function in these patients should be closely monitored, and this is helped by the widespread use of echocardiography in intensive care units. Because mechanical ventilation may worsen right ventricular failure, the interaction between the lungs and the right ventricle appears to be a key factor in the ventilation strategy. A rationale for a right ventricle-protective ventilation approach is provided, and such a strategy is described, including the reduction of lung stress (i.e., the limitation of plateau pressure and driving pressure), the reduction of PaCO2, and the improvement of oxygenation. Prone positioning seems to be a crucial part of this strategy by protecting both the lungs and the right ventricle, resulting in increased survival of patients with ARDS. Further studies are required to validate the positive impact on prognosis of right ventricle-protective mechanical ventilation. Septic shock patients invariably require life-support therapies like invasive ventilation, vasopressors, and fluids. Understanding the complex interaction between these factors, either individually or in combination, along with disease per se on RV is challenging. Understandably, previous studies have only minimally explored this issue. Ventilation increases RV afterload due to increase in pulmonary vascular resistance. Ventilated patients showed increased chamber dimensions and reduced systolic and diastolic functions of RV, though nonsignificantly. However, interpretation needs to be cautious as majority of patients were ventilated. Vasopressors inevitably have dose-dependent direct effects on the pulmonary circulation and myocardium. Noradrenaline increases pulmonary vascular resistance but does not increase RVEF. Right heart dimensional and functional abnormalities exist in high proportions in septic shock (Fig. 8.6). However, their predictability of poor outcomes remains questionable.

Fig. 8.6 Enlargement of RV. In the picture, diameters of both ventricles are similar
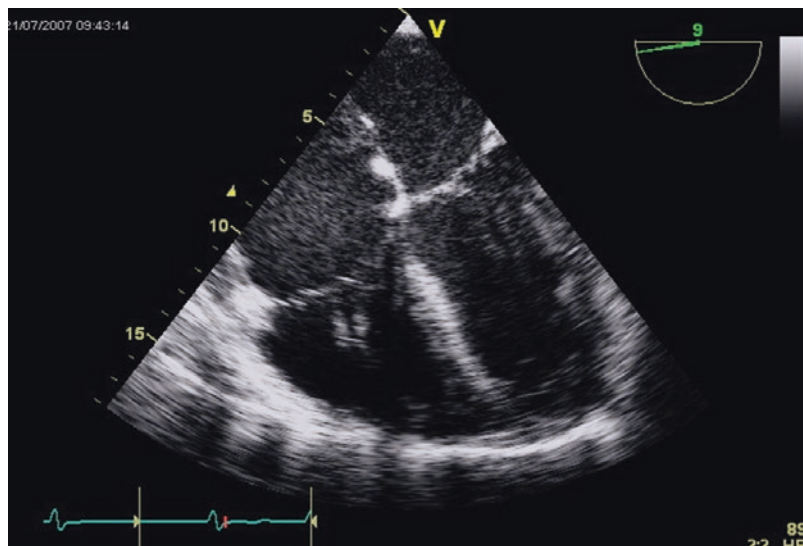
Further Reading

Bleeker GB, Steendijk P, Holman ER, et al. Assessing right ventricular function: the role of echocardiography and complementary technologies. Heart. 2006;92(1):i19–26.

D'Hooge J, Heimdal A, Jamal F, Kukulski T, Bijnens B, Rademakers F, et al. Regional strain and SR measurements by cardiac ultrasound: principles, implementation and limitations. Eur J Echocardiogr. 2000;1:154–70.

Haddad F, Hunt SA, Rosenthal DN, Murphy DJ. Right ventricular function in cardiovascular disease, Part I: anatomy, physiology, aging, and functional assessment of the right ventricle. Circulation. 2008;117(11):1436–48.

Hahn RT, Abraham T, Adams MS, Bruce CJ, et al. Guidelines for performing a comprehensive transesophageal echocardiographic examination: recommendations from the American Society of Echocardiography and the Society of Cardiovascular Anesthesiologists. Anesth Analg. 2014;118(1): 21–68.

Ho SY, Nihoyannopoulos P. Anatomy, echocardiography, and normal right ventricular dimensions. Heart. 2006;92(1):i2–i13.

Jurcut R, Giusca S, La Gerche A, et al. The echocardiographic assessment of the right ventricle: what to do in 2010? Eur J Echocardiogr. 2010;11:81–96.

Lang RM, Badano LP, Mor-Avi V, et al. Recommendations for cardiac chamber quantification by echocardiography in adults: an update from the American Society of Echocardiography and the European Association of Cardiovascular Imaging. Eur Heart J Cardiovasc Imaging. 2015;16(3):233–70.

Lindqvist P, Henein M, Kazzam E. Right ventricular outflow-tract fractional shortening: an applicable measure of right ventricular systolic function. Eur J Echocardiogr. 2003;4:29–35.

Lopez-Candales A, Rajagopalan N, Saxena N, Gulyasy B, Edelman K, Bazaz R. Right ventricular systolic function is not the sole determinant of tricuspid annular motion. Am J Cardiol. 2006;98:973–7.

Mathew JP, Ayoub CM. Clinical manual and review of transesophageal echocardiography. Columbus: McGraw-Hill; 2005.

Pleister A, Kahwash R, Haas G, Ghio S, Cittadini A, Baliga RR. Echocardiography and heart failure: a glimpse of the right heart. Echocardiography. 2015;32(Suppl 1):S95–107.

Rudski LG, Lai WW, et al. Guidelines for the echocardiographic assessment of the right heart in adults: a report from the American Society of Echocardiography. J Am Soc Echocardiogr. 2010;23:685–713.

Samad BA, Alam M, Jensen-Urstad K. Prognostic impact of right ventricular involvement as assessed by tricuspid annular motion in patients with acute myocardial infarction. Am J Cardiol. 2002;90:778–81.

Sheehan F, Redington A. The right ventricle: anatomy, physiology and clinical imaging. Heart. 2008;94:1510–5.

Sutherland GR, Di Salvo G, Claus P, D'hooge J, Bijnens B. Strain and strain rate imaging: a new clinical approach to quantifying regional myocardial function. J Am Soc Echocardiogr. 2004;17(7):788–802.

Vieillard-Baron A. Assessment of right ventricular function. Curr Opin Crit Care. 2009;15:254–60.

Left and Right Atria: Frequent Imaging in ICU Patients

9

Luigi Tritapepe, Francesca Pompei,
Maurizio Marandola, Giovanni Carriero,
Alessandra Di Persio, and Claudio Di Giovanni

9.1 Anatomy

Compared with the right atrium, the left atrium is characterized by lower volume and greater wall thickness. However, owing to its transverse axis, it forms a large part of the base of the heart and extends to the right, covering, in part, that side of the atrium. Considering the heart in situ, there are the following walls: anterosuperior wall, corresponding to the rib and sternum face that has a relationship with the ascending aorta and the pulmonary trunk, and the posterior–superior wall, which, with the interposition of the pericardium, has a relationship with the esophagus. Four pulmonary veins, two on each side, open into the posterior–superior wall of the atrium. The four orifices of the pulmonary veins have no valves; the posteroinferior wall is very large and flat and corresponds to the diaphragmatic face; the anteroinferior wall is where the mitral valve is positioned; the medial wall (or septum) corresponds to the atrial septum. The medial wall has a slight depression that corresponds to the fossa ovalis of the right atrium. In front, this depression is limited by a semilunar fold, which is the residue of the foramen ovalis valve, the lateral wall through which one accesses the left atrial (LA) appendage (LAA). The cavity of the atrium has smooth walls; trabeculae carneae are found only near the LAA anastomosed to the network. The left atrioventricular orifice is positioned low and anteriorly and leads into the ventricular cavity; it has a valve apparatus, consisting of two cusps called the bicuspid or mitral valve.

The right atrium is on the right and forward of the left atrium. It has, roughly, a cube shape and consists of six walls. Considering the heart in situ, the anterosuperior wall corresponds to the rib–sternum face; the posterior–superior wall corresponds to the base of the heart and has the openings of the cavae veins, superior and inferior; the posteroinferior wall corresponds to the diaphragmatic face where the coronary sinus ends; the anteroinferior wall corresponds to the orifice of the tricuspid valve; the medial wall is formed by the interatrial septum; and the lateral wall communicates with the right atrial appendage.

The inner surface of the right atrium, with the other chambers of the heart, is covered with endocardium and has a smooth posterior portion,

L. Tritapepe (✉) · M. Marandola · C. Di Giovanni
Department of Anesthesia and Intensive Care,
Cardiac Surgery ICU, Policlinico Umberto I Hospital,
Sapienza University of Rome, Rome, Italy
e-mail: luigi.tritapepe@uniroma1.it

F. Pompei
Azienda Ospedaliera San Camillo-Forlanini,
Rome, Italy

G. Carriero
Policlinico Casilino Hospital, Rome, Italy

A. Di. Persio
Bambino Gesù Children Hospital, Rome, Italy

the sinus of caval veins, and an anterolateral corrugate surface caused by the presence of fleshy pads that are regularly arranged, the pectinate muscles. The boundary between these two portions is marked by a ridge, the crista terminalis.

In the posterior–superior surface of the right atrium, to the limits with the anterosuperior and posteroinferior faces, are the outlets of the upper and lower caval veins. The contour of the anterolateral orifice of the superior vena cava is defined by the crista terminalis, and the flow around the mouth of the inferior vena cava (IVC) passes through a rudimentary valve, the Eustachian valve, which goes from the contour of the orifice to the edge of the fossa ovalis. To the left and in front of the orifice of the IVC, near the atrioventricular orifice, is the mouth of the coronary sinus, which carries most of the effluent blood from the walls of the heart, the coronary sinus ends with the Thebesius valve, which has the task of preventing the reflux of blood into the coronary sinus during atrial systole.

The medial wall (or septum) is smooth and has an elongated depression in the vertical direction, the fossa ovalis. This depression is bordered in front and above by a crescent-shaped pad, the flap of the fossa ovalis representing the free end of the septum secundum. The lateral wall has the atrial appendage, an appendix cavity whose walls show numerous anastomosed muscles that continue to network with those covering much of the atrial wall.

Forward and further down at the anteroinferior wall lies the atrioventricular orifice, which leads into the ventricular cavity. It has a valve apparatus which consists of three leaflets or cusps, hence the name of the tricuspid valve.

9.2   Echocardiography

The atria can go into dilation when stenosis or insufficiency of valvular apparatus occurs. The atrial kick contributes to a stroke volume of around 20%, and its contribution increases when there is diastolic dysfunction owing to the elevation of atrial pressure. When atrial fibrillation occurs, the atrial contribution to cardiac output is lost, and in this case a worsening degree of diastolic dysfunction may cause a low-output syndrome. An increased atrial volume is an independent predictor of adverse car-

diovascular events, including stroke and congestive heart failure. Accordingly, accurate measurement of the atrial size has become increasingly relevant to clinical practice. Most clinical studies have used echocardiographic measurements, because echocardiography is the most accepted and best validated modality for atrial volume quantification. The area–length method has often been chosen for atrial volume quantification, because it is simple, relatively quick, and can be done using standard acquisitions; however, since it approximates atrium to an ellipsoid, the biplane disk summation technique, which incorporates fewer geometric assumptions and is less sensitive to errors related to the irregular shape of left atrium, should be the preferred method. Transthoracic is the recommended approach for assessing left atrium size, because frequently with transesophageal examination, it cannot be fit completely in image sector. Echocardiographic apical two- and four-chamber views are used with the subject in the left lateral decubitus position to demonstrate the left ventricular apex and mitral valve.

9.3   Left Atrium

The left atrium has three important roles: it contributes 20–30% of cardiac output, is an anatomical reservoir during ventricular systole, and is a passive conduit for the flow during the early phase of diastole. All these functions can be explored with the echocardiography. With transthoracic echocardiography (TTE), the left atrium is seen in many standard projections, such as the apical four-chamber, apical two-chamber, apical three-chamber, parasternal short-axis, parasternal long-axis, and subcostal projections (Fig. 9.1). The mean longitudinal diameter of the left atrium is about 4.1 cm, and the mean transverse diameter is about 3.8 cm. The diameter is measured at the end of the systole, when the atrium is very full. An optimal view is represented by the parasternal long-axis view, where, with the help of M-mode, it is very easy to measure the LA diameter. The LA area is less than 20 cm^2 and can be easily obtained with the apical four-chamber and apical two-chamber projections. Although very simple to perform, a stronger association with outcomes in cardiac patients is proven with mea-
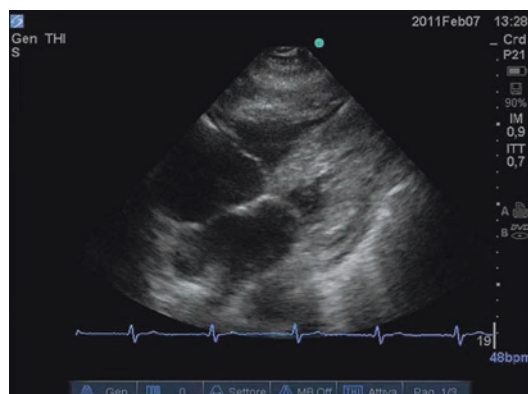
Fig. 9.1 Transthoracic echocardiography of the right and left atria at the end of systole

surement of left atrium volume rather than area. LA volume should be measured using the disk summation algorithm and BSA-indexed; recommended upper normal indexed volume is 34 mL/m^2. When planimetry is performed, the confluence of pulmonary veins and LA appendage should be excluded. 3D echocardiography compared with 2D assessment provides a more accurate assessment compared with cardiac magnetic resonance; nonetheless given the relative lack of studies, normal values are not currently available in international guidelines. The LA volume and diameters are increased in many pathological conditions, but mitral valve disease and left ventricular function are the major determinants for the enlargement and the loss of LA function. With the apical four-chamber view, we observe the ends of the pulmonary veins as the pass into the left atrium, and we can measure their flow through pulsed wave Doppler imaging, which is useful to study the degree of diastolic dysfunction, mitral valve regurgitation, and LA pressure. With transesophageal echocardiography (TEE) we may see the left atrium in most of the recommended two-dimensional tomographic views. Not only the left atrium, but especially the LAA can be visualized with TEE. The mid-esophageal four-chamber, mid-esophageal two-chamber, mid-esophageal long-axis, transgastric two-chamber, mid-esophageal mitral commissural, mid-esophageal aortic valve short-axis, mid-esophageal aortic valve long-axis, deep transgastric long-axis, mid-esophageal bicaval, and mid-esophageal right ventricular inflow–outflow views are all tomographic views that allow us to explore the dimensions and function of the left atrium and the relationship between the left atrium and the left ventricle. The mid-esophageal four-chamber view and the mid-esophageal two-chamber view are the projections used to measure the left atrium and the apical four-chamber view with TTE that allows us to visualize more accurately the superior margin of the left atrium. The LAA is an important structure that is well visualized with the mid-esophageal two-chamber between 60° and 90° or with the transgastric two-chamber view around 90°. The LAA is a triangular structure divided from the left superior pulmonary vein by a ridge called the Coumadin ridge, which is often confused with a thrombotic formation or a mass. With the use of tissue Doppler imaging, we can differentiate the ridge from a thrombus. Pulsed wave Doppler imaging is utilized to measure the different flow rates in the pulmonary vein and in the LAA. When the patient suffers of atrial fibrillation, we can explore with TEE the LAA where clots can form. The presence of slow flow (smoke effect) in the left atrium or thrombi inside the LAA can be always detected before the use of DC shock to reverse atrial fibrillation (Fig. 9.2a, b). If there is mitral regurgitation, it is possible to determine LA pressure by sampling the regurgitant jet with continuous wave Doppler imaging. In particular, LA pressure = systolic arterial blood pressure − [4 × (peak mitral regurgitant velocity)^2].

Especially in the ICU, patients with hemodynamic instability can have different degrees of mitral insufficiency. It is very important to measure the atrial diameter because this may help to differentiate between the acute and subacute or chronic forms of mitral insufficiency. It is crucial to assess the cause of the hemodynamic instability and consider other abnormalities that lead to hypotension. Some abnormalities in the zone near the left atrium, such as aortic dissection, aortic aneurysm, pericardial hematoma after cardiac surgery or after percutaneous cardiac intervention, and lung or mediastinal tumors, can cause LA compression, directly or through compression of pulmonary veins. Chronic LA compression can lead to symptoms mimicking congestive
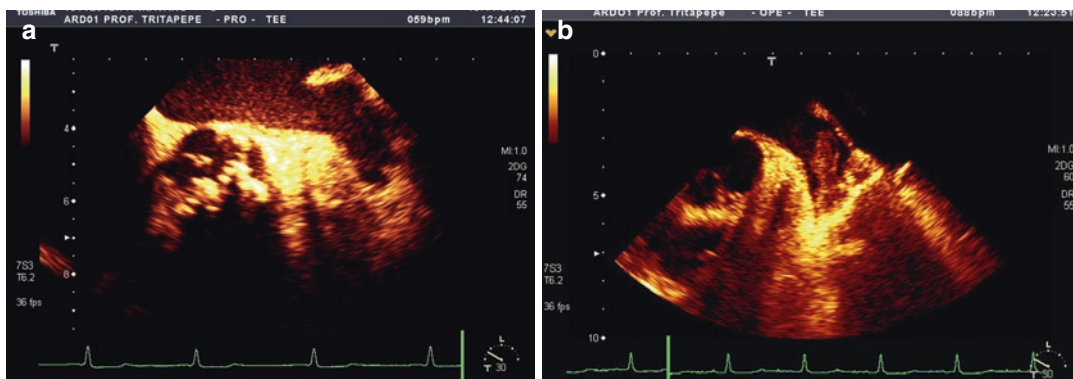
Fig. 9.2 Left atrial appendage free from thrombi (**a**). Huge thrombus in the left atrial appendage (**b**)

heart failure. Unlike LA compression, congestive heart failure is associated with an enlarged left atrium. Acute LA compression causes immediate hypotension and low-output syndrome. Analysis with TEE can be used to obtain more information about the compromising structure or can be used when TTE has limitations.

9.4 Right Atrium

With TTE, the right atrium is seen in the apical four-chamber, parasternal short-axis, and subcostal projections (Fig. 9.1). Moving the probe slightly to the right of the patient, in the subcostal position, one can see flow from the IVC into the right atrium. This is a very important view used to assess the preload of the patient and the response to volume load. The lateral diameter of the right atrium is evaluated in the apical four-chamber view and is usually less than 4.5 cm. Differently from the left atrium, right atrium size seems to be gender dependent, and normal values are available (RA minor axis dimension $1,9 \pm 0.3$ cm/m^2 both in men and women; RA major axis dimension 2.5 ± 0.3 cm/m^2 in women and 2.4 ± 0.3 cm/m^2 in men). It is not possible with TTE to estimate precisely the volume in orthogonal projections as it is when studying the left atrium; thus a single view area length or disk summation techniques are recommended, with normal values of 21 ± 6 mL/m^2 for women and 25 ± 7 mL/m^2 for men. With TEE, the right atrium

is seen in the mid-esophageal four-chamber, mid-esophageal aortic valve short-axis, mid-esophageal bicaval, mid-esophageal right ventricular inflow–outflow, and transgastric right ventricular inflow views. The right atrium can be evaluated in the mid-esophageal four-chamber view, but the mid-esophageal bicaval view is the best projection to estimate the volume of the right atrium and the ends of the superior (on the right side of the display screen) and inferior (on the left side) venae cavae. This bicaval view allows us to measure the bicaval diameters in M-mode and see the bicaval diameter modification during the respiratory cycle, which is important to define fluid responsiveness of hemodynamically unstable patients. Also, the mid-esophageal bicaval view is the crucial projection to monitor the positioning of venous cannulae in extracorporeal membrane oxygenation or extracorporeal life support procedures. Patients with atrial or ventricular catheters (Swan–Ganz or pacemaker cables) can have thrombotic masses near or on the indwelling devices that are well evaluated in the mid-esophageal bicaval view. In this projection, the atrial septum is also well visualized and may reveal pathological loss of continuity (atrial septal defects) or paraphysiological loss as a patent foramen ovale (PFO). Especially in acute lung injury/acute respiratory distress syndrome patients ventilated with positive end-expiratory pressure, the inversion of the pressure gradient between the right and left atria at the level of PFO causes shunt with hypoxia and allows passage of

air bubbles or fibrin aggregates through the PFO, with consequent paradoxical embolization. The arrangement of the septum, moved down to the right or straight or even prominent at the upper left, shows the current pressure in the right atrium and can be a sign of right ventricular failure, along with an enlarged right atrium itself.

9.5 Interatrial Septum

The interatrial septum is always a structure worth exploring, especially in the patient in the ICU. The different pressure regimes, related to high levels of intrathoracic pressure in mechanically ventilated patients, can determine the patency of the foramen ovale or reverse shunt in atrial septal defects. The subcostal four-chamber projection is easily visible with TTE, and by aligning the probe perpendicular to the septum, we can use pulsed wave Doppler imaging to study any interatrial flow. In the apical four-chamber view, we visualize the septal wall to the roof of the atria and the portion near the valve plane losing the continuity of the echoes of the septum (the phenomenon of dropout) near the fossa ovalis. This should not be confused with an atrial septal defect. It is often difficult to distinguish between a slightly redundant septum and a true aneurysm. In both cases, the wall of separation between the left atrium and right atrium rather than remaining in a fixed position during

contraction and relaxation of the heart, according to the different pressures present in the left atrium, can tend to shift to the left or right. This condition may be associated with the presence of a small permeability of the wall (atrial septum), a condition that could be the cause of the transient ischemic attack. The interatrial septum is well evaluated with TEE, especially in the mid-esophageal bicaval view (Fig. 9.3), but also in the mid-esophageal aortic valve short-axis view (Fig. 9.4a, b).

Lipomatosis of the interatrial septum is a rare benign disease characterized by accumulation of fatty tissue of the atrial septum. Typically, the thickening of the lipomatous septum saves the
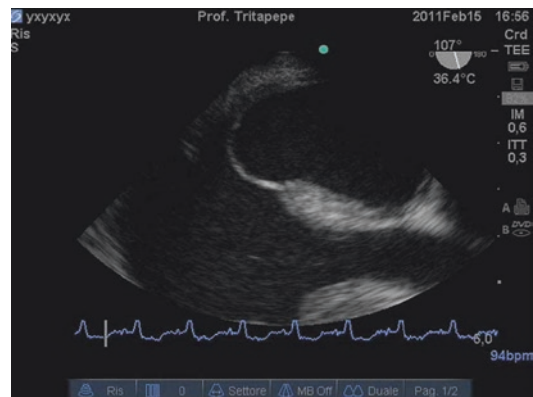
Fig. 9.3 Transesophageal echocardiography of the right atrium in the bicaval view, with the septum at the level of the fossa
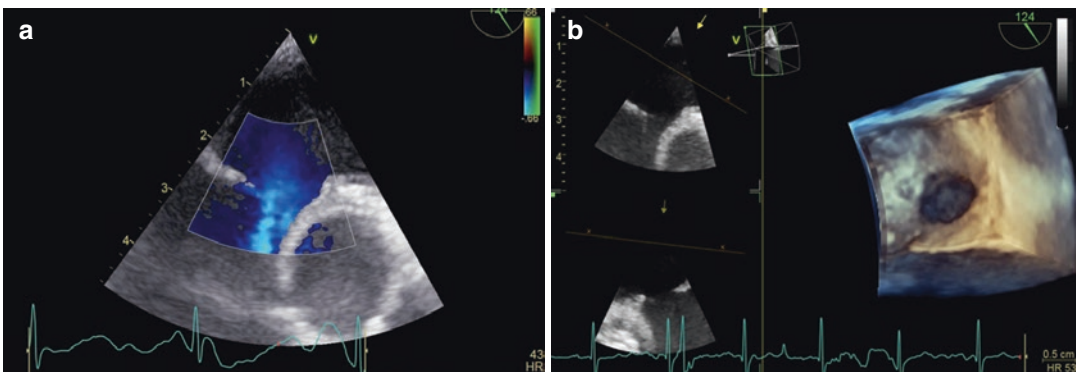
Fig. 9.4 (**a**) Interatrial septum defect with left-to-right shunt. (**b**) The same patient was studied with 3D echo. In the picture, on the right, the septal defect is well represented

fossa ovalis. It may be associated with supraventricular arrhythmias and may sometimes result in hemodynamic complications. For this reason, it is always considered in the differential diagnosis of cardiac masses.

9.6 Chiari Network

Another element found on echocardiography of the right atrium is the presence of the Chiari network, a remnant of the embryonic venous sinus valve. It has no pathological significance, but, appearing as a floating weblike structure that generates echoes in motion, it can be mistaken as a thrombus or vegetation or mass. It is well evaluated in the apical four-chamber projection.

9.7 Eustachian Valve

The Eustachian valve is an endocardial fold extending from the anteroinferior margin of the inferior vena cava to the anterior part of the limbus of the fossa ovalis. The Eustachian valve is programmed to regress completely after birth. In about 30% of adults, it persists with variable size and structure. It is well evaluated with TTE in the subcostal view, in the projection to explore the inferior vena cava. It can be confused with thrombus or vegetation and could promote the migration of thrombi or embolization toward the fossa ovalis. In case of doubt, TEE examination is recommended.

Further Reading

Kenneth KE. Anatomy of the left atrial appendage. Echocardiography. 2008;25:669–73.

Lang RM, Badano LP, Mor-Avi V, Afilalo J, Armstrong A, Ernande L, et al. Recommendations for cardiac chamber quantification by echocardiography in adults: an update from the American Society of Echocardiography and the European Association of Cardiovascular Imaging. Eur Heart J Cardiovasc Imaging. 2015;16:233–70.

Oh JK, Steward JB, Tajik AJ. The echo manual. Philadelphia: Lippincott Williams & Wilkins; 2007.

Whitlock M, Garg A, Gelow J, Jacobson T, Broberg C. Comparison of left and right atrial volume by echocardiography versus cardiac magnetic resonance imaging using the area-length method. Am J Cardiol. 2010;106:1345–50.

Pericardium and Pericardial Disease

10

Ferdinando Luca Lorini, Stefania Cerutti, and Giovanni Di Dedda

10.1 Introduction

The normal pericardium is a thin, linear structure that echocardiographically is outlined as a bright, highly echogenic line. Within the two layers of the pericardium, the inner serosal layer and the outer fibrous pericardium, accumulate physiologically about 10–50 ml of pericardial fluid, generally visualized only in systole as an echo-free space surrounding the heart.

Transthoracic echocardiography is a milestone and the first-line imaging modality for diagnosing pericardial diseases like pericardial effusion and cardiac tamponade, constrictive pericarditis, pericardial cysts and tumors, and partial and complete absence of the pericardium. The limitations of this imaging are very few, mainly represented by a poor echocardiographic window and the lack of details of the pericardium's anatomy, which in case need to be investigated with further examination. CT scan and MRI provide a larger field of view, allowing the detection of loculated pericardial effusion and pericardial thickening and masses, as well as associated chest abnormalities. Although transthoracic echocardiography is almost always the ideal technique to detect and graduate pericardial diseases, several factors in the postoperative period after cardiac surgery may contribute to the need of transesophageal echocardiography.

10.2 Pericardial Effusion

The etiology of pericardial effusions (PE) ranges from inflammatory effusions (secondary to bacterial or viral infections, myocardial infarction, trauma, or neoplasm) to hemorrhagic effusions, mostly common in the postoperative cardiac surgery setting. Different criteria are used to classify pericardial effusion: the onset (acute, subacute, chronic), the distribution (circumferential or loculated), the hemodynamic impact (none, cardiac tamponade, effusive-constrictive), the composition (exudates, transudate, blood), and especially the size. The clinical signs and symptoms are related to the etiology of the PE and to the hemodynamic significance of the effusion itself. If the PE is secondary to pericarditis, a prodrome of fever, malaise, and myalgia could precede major symptoms like retrosternal or left precordial chest pain and shortness of breath. A pericardial friction rub could be present, though it could be transient, and heart rate is usually rapid and regular. If the PE develops slowly, it can be remarkably asymptomatic, while rapidly accumulating effusions manifest clinically with tamponade (see next paragraph).

F. L. Lorini (✉) · S. Cerutti · G. Di Dedda
Department of Anesthesia and Intensive Care Medicine, ASST Papa Giovanni XXIII, Bergamo, Italy
e-mail: llorini@asst-pg23.it; scerutti@asst-pg23.it; gdidedda@asst-pg23.it

Echocardiography should be the first modality to determine the size and the hemodynamic significance of PE, as it is even a more accurate imaging technique than computed tomography in quantitative assessing of nonloculated PE, always keeping in mind the few limitations that this exam holds. The hemodynamic consequences of PE will be examined in the next paragraph. In this paragraph we will examine the classification and the characteristics of PE.

The size of the effusion has been graded by the European Society of Cardiology in small, moderate, large, and very large (Table 10.1). Pericardial effusions may be seen not only in systole (as it is common for the physiological pericardial fluid), but they become visible throughout the entire cardiac cycle. As the amount of pericardial fluid increases, fluid distributes from the posterobasilar left ventricle to the apex and anterior wall and then laterally and posteriorly to the left atrium (Fig. 10.1). It is important to emphasize that the mere presence of an effusion, even when large, does not indicate hemodynamic significance. Since the rapidity of pericardial fluid accumulation and the compliance of the pericardium influence the pressure elevation for any given fluid volume, effusion volume alone does not determine hemodynamic significance. Therefore, the presence of an effusion must be related to other echocardiographic parameters of cardiac filling and transvalvular flow and must be correlated with the clinical features (see next paragraph).

Although PE generally appears as an echo-free space encircling the heart, sometimes echo-
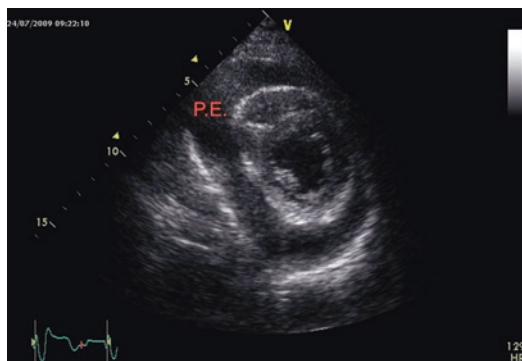
Fig. 10.1 A TEE TG short-axis left ventricle view showing a circumferential large pericardial effusion

genic materials such as fibrinous strands and shaggy exudative coating are found. These findings are important as well, because initial echocardiographic characteristics of PE determine the pericardial complication. More precisely, echogenic PE, including exudative frond-like coating and fibrinous strands in PE, are the major risk factor for pericardial complication such as constrictive pericarditis and PE recurrence. Diffuse echogenic PE results in the highest incidence of events, followed by PE with exudative coating and fibrinous strands. Echocardiography could, then, be used not only for diagnostic purposes but also for a prognostic evaluation.

PE are a possible complication of cardiac surgery, with a reported incidence that ranges between 50% and 64% of cases depending on study definitions and designs. They compromise cardiac function in 0.8–7% of cases and have a peak incidence on the 10th postoperative day. Echocardiographic monitoring of the surgical patients should be done up to 20 days–1 month after surgical intervention, because late pericardial effusions are an important cause of morbidity. Persisting PE is more frequent after undergoing CABG surgery than after undergoing valve replacement surgery, on the contrary, the incidence of late cardiac tamponade is higher in the patients undergoing valve replacement surgery. The use of TTE is important not only for the follow-up of the cardiac surgical patients, but it has been validated for the classification of postoperative pericardial effusion for predicting late postoperative cardiac tamponade. Indeed, the

Table 10.1 Classification of pericardial effusion by the European Society of Cardiology

Classification of PE	Dimension in diastole	Location
Small	<10 mm	Posterior atrioventricular groove
Moderate	10–20 mm	
Large	>20 mm	Usually extends behind the left atrium, may determine a compression of the heart
Very large	>20 mm	Extends behind the left atrium and determine a compression of the heart

incidence of late cardiac tamponade is significantly increased in patients with a TTE loculated effusion >15 mm or circumferential effusion >10 mm on postoperative day 20.

The risk of pericardial effusion has to be considered not only in the adult population but also after congenital cardiac surgery. Serial echocardiographic monitoring up to 28 days postoperatively is indicated in selected high-risk patients such as those with symptoms of postpericardiotomy syndrome and those given warfarin. Interestingly, PE that eventually becomes moderate to large in amount tends to present later and occurs more commonly after Fontan-type procedures.

Although transthoracic echocardiography is almost always the ideal technique to detect and graduate PE, several factors in the postoperative patient after cardiac surgery may contribute to the need of transesophageal echocardiography: the surgical site may preclude the use of the optimal transthoracic window, chest tubes may prevent proper positioning of the patient, and some loculated effusions or intrapericardial clots may not be amenable to transthoracic imaging.

As a final consideration, the differential diagnosis of echo-free spaces should include pericardial effusions, pleural effusions, and pericardial fat. As a rule, in the different views, pericardial fluid reflects at the posterior atrioventricular groove, whereas pleural effusion continues under the left atrium, posterior to the descending aorta. Pericardial fat can be identified as the hypoechoic space anterior to the epicardial fat; it is more prominent anteriorly but may appear circumferentially, thus mimicking effusion. Pericardial fat is slightly echogenic and tends to move with the heart; on the contrary the effusion is generally echolucent and motionless.

Echocardiography is very important not only for the diagnostic purposes but also as a guide of percutaneous needle pericardiocentesis: it has an excellent profile in simplicity, safety, and efficacy. Echocardiography identifies the shortest route where the pericardium can be entered intercostally, allows a clear localization of the needle, and shows the immediate benefit of the removal of the exceeding pericardial fluid.

Finally, approach to pericardial effusion should be selected according to the distribution of pericardial effusion in echocardiography. If the effusion is equally large in the apical position and in front of the right ventricle from the subxiphoid view, both apical and subxiphoid approach can be attempted, according to the operator's preference. However, if the effusion is significantly asymmetrically distributed, it should be approached from the side where the accumulation of fluid is largest. The reported incidence of major complication ranges from 1.3% to 1.6%.

10.3   Cardiac Tamponade

When the accumulation of pericardial fluid causes an increase in the pericardial pressure exceeding the intracardiac pressure, the positive transmural pressure gradient compresses cardiac chambers at different points in the cardiac cycle compromising cardiac filling. Depending on the type and the severity of tamponade, a variety of physical findings may be present: chest pain radiating to the neck and jaw, orthopnea, cough, and dysphagia. The jugular venous pressure is elevated; an exaggeration of the normal variation in the pulse pressure during the inspiratory phase of respiration greater than 10 mmHg is commonly found (pulsus paradoxus) as well as an elevation in the venous jugular pressure during inspiration (Kussmaul sign). In chest radiography large effusions are depicted as globular cardiomegaly with sharp margins ("water bottle" silhouette). Electrocardiography may demonstrate diminished QRS and T-wave voltages, PR-segment depression, ST-T changes, bundle-branch block, and electrical alternans. Patients after cardiac surgery provide a much more specific diagnostic challenge, since effusions may be localized, underlying cardiac pathology is present, and positive pressure ventilation is used, all factors likely to alter the classical clinical findings.

Echocardiography is a powerful tool to quickly identify the hemodynamic significance of the pericardial effusion and the cardiac

tamponade. The basic elements that allow this identification are the following:

- The low pressures of the right chambers make them the first structures susceptible to the increased transmural pressure. Right atrial wall inversion during ventricular systole (the indentation is seen near the peak of the R wave) is usually an early sign of cardiac tamponade, followed by diastolic compression of the RVOT (evaluated by both M-mode and 2D echocardiography) (Fig. 10.2). The longer is the duration of the right atrial invagination relative to the length of the cardiac cycle, the greater is the likelihood of significant hemodynamic compromise: duration of right atrial collapse exceeding one third of the cardiac cycle increases specificity without sacrificing sensitivity. Right-chamber collapse may be delayed in the setting of pulmonary hypertension; in such cases, left atrial collapse may precede the right atrial one. False-positive right ventricle diastolic collapse may be present in hypovolemic states (because of the very low RV diastolic pressure) and in patients with large pleural effusions.
- "Swinging heart": when large pericardial effusion accumulates, the heart will be swinging in the pericardial fluid beat-to-beat.
- Ventricular interdependence: during inspiration the interventricular septum bulges into the left ventricle due to increased systemic venous return to the right ventricle and limited expansion of the right ventricle free wall.
- Respiratory variation in tricuspid and pulmonary flow detected with Doppler echocardiography. Tricuspid flow increases and mitral flow decreases during inspiration: the percent respiratory variations in mitral inflow E-wave of >35% and tricuspid inflow E-wave of >40% correlate well with tamponade physiology. These respiratory variations could not be seen in the invasively ventilated patient.
- Plethora of the inferior vena cava: IVC diameter >21 mm and a lack of change in vena cava caliper (<50% reduction in diameter) during inspiration.
- Prominence of diastolic reversals in hepatic veins by pulsed Doppler: with expiration systemic venous return decreases with reversal diastolic flow in the hepatic veins.
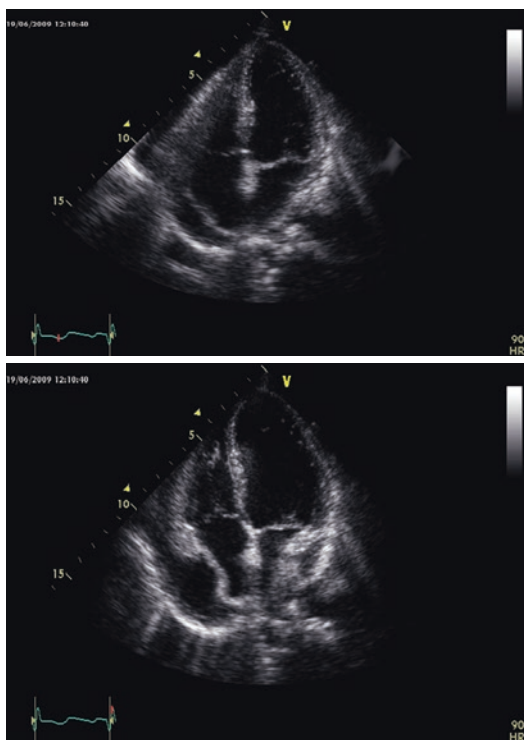
Fig. 10.2 TTE apical four-chamber view showing a large pericardial effusion with right atrial wall inversion during ventricular systole (on the bottom)

10.4 Constrictive Pericarditis

The most common reported causes of constrictive pericarditis in developed countries are idiopathic or viral (42–49%), post-cardiac surgery (11–37%), postradiation therapy (9–31%), connective tissue disorder (3–7%), post-infectious causes (3–6%), and miscellaneous causes (malignancy, trauma, drug-induced, asbestosis, sarcoidosis, uremic pericarditis in 10%). Chronic inflammation of the pericardium results in thickening fibrosis and fusion of both layers of the pericardium. Constrictive pericarditis represents the end stage of this chronic inflammatory process leading to a limit in diastolic filling and resulting in diastolic failure, with relatively

preserved global systolic function. The most common symptoms are related to either fluid overload (peripheral edema, elevated central venous pressure, hepatomegaly, pleural effusion, ascites, and anasarca) or decreased cardiac output (dyspnea, fatigue, palpitations, weakness, and exercise intolerance). The impaired ventricular filling determines particular patterns at the direct measurements of pressures: M- or W-shaped atrial pressure waveforms and "dip-and-plateau" right ventricular pressure waveforms. End-diastolic pressure equalization (typically within 5 mmHg) occurs between these cardiac chambers in constrictive pericarditis because of the fixed and limited space within the thickened and stiff pericardium. Pulmonary artery systolic pressures are usually normal in pericardial constriction; higher pulmonary pressures suggest a restrictive cardiomyopathy.

An important reason to use echocardiography early in the diagnostic process is to rule out more common causes of right-sided heart failure, including left or right ventricular systolic dysfunction, severe pulmonary hypertension, or unrecognized left-sided valvular diseases. Once these diseases are excluded, echocardiography is very useful in recognizing the pericardial thickening and the elements that characterize constrictive pericarditis. Visualization of the pericardium thickening (Fig. 10.3) could be done in a more accurate way with transesophageal echocardiography, with a significant cutoff value of 3 mm.
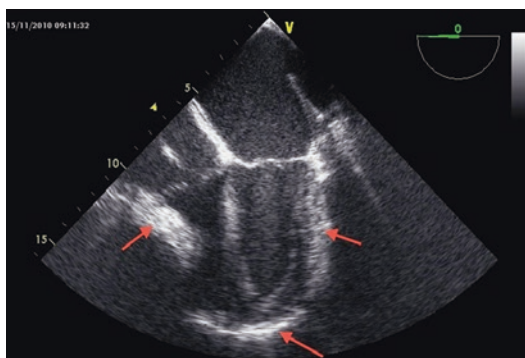
Fig. 10.3 TEE ME four-chamber view showing pericardial thickening and calcification in constrictive pericarditis

The echocardiographic characteristics of constrictive pericarditis are secondary to the impaired diastolic cardiac filling and elevated ventricular filling pressures:

- Mitral inflow assessed by Doppler echocardiography demonstrates a rapid increase in ventricular diastolic pressure that creates the dip-and-plateau pattern with an increased early diastolic filling (E-wave) velocity with a rapid deceleration time and a small or absent A-wave.
- Marked respiratory variation in left and right ventricular inflow velocities is seen with Doppler echocardiography. There is an increase in early diastolic mitral inflow of >25% during expiration and an increase of the tricuspid inflow velocity by at least 40% with inspiration. After complete pericardiectomy mitral inflow patterns return to normal, and little respiratory variation is seen.
- Tissue Doppler (TDI) of the mitral annulus shows a prominent early diastolic velocity. A lateral or septal early diastolic mitral annular velocity of >8 cm/s on pulsed tissue Doppler is in general the accepted cutoff value to diagnose constrictive pericarditis. Mitral annular velocities are particularly useful when pronounced respiratory variations in peak early mitral inflow velocities are not seen. The tethering of the lateral annulus secondary to the constrictive process causes the "annulus reversus" phenomenon: the medial mitral e' velocity becomes equal to or greater than the lateral e' velocity on average, in contrast to what is seen in other forms of heart failure and in the absence of cardiac disease.
- Increased ventricular interdependence with a classic respiratory shift in the position of the interventricular septum toward the left ventricle during inspiration ("septal bounce"). Beyond the respirophasic motion, a septal "bounce," also referred to as a "shudder" or "diastolic checking," may be present. The mechanism of this "bounce" is a combination of differential timing of filling and pericardial constraint, leading to rapid cessation of filling.

- Flow propagation velocity into the left ventricle detected by color-Doppler M-mode is greater than 45 cm/s.
- Marked diastolic flow reversal that increases in expiration is evident in the hepatic veins.
- The evaluation with the two-dimensional speckle tracking echocardiography shows a rapid flattening of the posterior wall of the left ventricle in early diastole with normal or exaggerated longitudinal deformation of the left ventricle. In general, circumferential strain, torsion, and early diastolic twisting are decreased in constrictive pericarditis. In contrast, global longitudinal strain is usually preserved. Patients with restrictive cardiomyopathy can demonstrate the converse pattern: global longitudinal strain is decreased, while circumferential strain and early diastolic untwisting are preserved.

The above criteria are important not only to diagnose constrictive pericarditis, but they help distinguishing it from restrictive cardiomyopathy. Doppler echocardiographic techniques, in particular, have been shown to be useful in differentiating between these two diseases. A marked respiratory variation in mitral inflow and pulmonary venous flow is present in patients with constrictive pericarditis but is absent in those with restrictive cardiomyopathy. Recently, the newer echocardiographic modalities of tissue Doppler echocardiography and color M-mode flow propagation have been validated as ancillary tools to distinguish between these diseases, though they are equivalent and complementary to Doppler respiratory variation in distinguishing between constrictive pericarditis and restrictive cardiomyopathy. The additive role of the new methods needs to be established in difficult cases of constrictive pericarditis where respiratory variation may be absent or decreased. Of the two newer modalities, tissue Doppler echocardiography of the mitral annulus tends to have greater specificity and sensitivity than color M-mode flow propagation and is generally easier to use. As the velocity of propagation of early ventricular inflow from color M-mode and the early mitral annular velocity from tissue Doppler imaging are markers of myocardial relaxation, their values are generally normal or supranormal in pure constrictive pericarditis, in which myocardial relaxation is normal or raised. By contrast, these values are decreased in restrictive cardiomyopathy, in which myocardial relaxation is impaired.

Patients with chronic obstructive pulmonary disease or severe right ventricle disfunction and large respiratory variations in intrathoracic pressure may also show inspiratory decreases in early mitral inflow velocities, like in constrictive pericarditis. To distinguish these two conditions, the intensivist should consider that in chronic obstructive pulmonary disease, there is a greater decrease in intrathoracic pressure in inspiration, which generates greater negative pressure changes in the thoracic cavity. This augments blood flow to the right atrium from the superior vena cava during inspiration.

10.5 Effusive-Constrictive Pericarditis

The features of cardiac tamponade and constrictive pericarditis may combine originating the effusive-constrictive pericarditis. These rare and particular cases should be diagnosed not only with the important help of the echocardiographic imaging but also taking into consideration hemodynamic variations before and after the removal of the exceeding pericardial fluid. The clinical diagnosis of this condition is based, indeed, on the demonstration that in a patient with pericardial effusion and tamponade, a clinical and hemodynamic picture consistent with pericardial constriction persists after the removal of enough pericardial fluid to lower the intrapericardial pressure to normal.

10.6 Pericardial Masses

Primary pericardial tumors are rare; secondary tumors are far most common. Primary tumors can be benign, including lipoma, hemangioma, and teratoma or malignant, including

mesothelioma, sarcoma, and lymphoma. Metastatic tumors are usually of breast, lung, and bone marrow origin.

Pericardial masses are often detected incidentally during routine echocardiography; though echocardiography should be considered important in the identification of these masses, CT scan or CMR should always be performed as they are the imaging modalities of choice when further evaluating these tumors. Currently, 2D echocardiography techniques are most often used to assess tumor characteristics such as shape, size, tumor attachment, and location as related to adjacent structures. Transesophageal echocardiography (TEE) can be a complementary diagnostic test that is especially helpful in characterizing masses in the posterior structures of the heart, particularly in the left atrium, left atrial appendage, right heart, and descending thoracic aorta. Further use of 3D echocardiography can be helpful by allowing for measurement of the entire volume of a mass, which may be underestimated by 2D echocardiography.

10.7   Pericardial Cysts

Pericardial cysts are rare, benign congenital, or inflammatory malformation; they can also be acquired after cardiothoracic surgery. They are usually found incidentally during routine x-ray or echo examinations and appear as echo-free fluid-filled loculated masses located mostly at the right costophrenic angle, less frequently in the left costophrenic angle, or in the posterior or anterior superior mediastinum. Color-flow and pulsed-Doppler interrogation at low-velocity setting can be used to ensure there is no phasic flow within the structure and to differentiate pericardial cysts from coronary aneurysm, left ventricular aneurysm, prominent left atrial appendage, aortic aneurysm, or solid tumors. Transesophageal echocardiography can be useful if transthoracic echocardiography is inadequate in delineating the diagnosis and can help identifying a pericardial cyst in atypical locations and distinguishing it from other posteriorly located lesions.

10.8   Congenital Absence of the Pericardium

Congenital absence of the pericardium is a rare anomaly whose reported prevalence is of 0.002–0.004%. This defect could be partial or complete, mostly located on the left side of the heart and more frequently asymptomatic and detected incidentally. The foramen-type defects are the most dangerous subgroup of partial defects, because they can be fatal when they allow herniation of part of the heart. The absence of the pericardium determines an exaggerated cardiac motion, particularly of the posterior wall of the left ventricle. Traditional echocardiography shows prominence of the right-sided cardiac chambers and abnormal septal motion. If the right ventricle shifts to the left, its cavity may falsely appear enlarged. Finally, there is typically a displacement of the apical imaging window into the axilla and the atria appear compressed. Echocardiogram should be useful as well in the identification of the associated heart defects such as atrial septal defects and bicuspid aortic valve.

Suggested Reading

Adler Y, Charron P, Imazio M, et al. 2015 ESC Guidelines for the diagnosis and management of pericardial diseases. The Task Force for the Diagnosis and Management of Pericardial Diseases of the European Society of Cardiology (ESC). Eur Heart J. 2015;36:2921–64.

Cosyns B, Plein S, Nihoyanopoulos P, Smiseth O, et al. On behalf of the European Association of Cardiovascular Imaging (EACVI) and European Society of Cardiology Working Group (ESC WG) on myocardial and pericardial diseases. European Association of Cardiovascular Imaging (EACVI) position paper: multimodality imaging in pericardial disease. Eur Heart J Cardiovasc Imaging. 2014;16:12–31.

Cremer PC, Kwon DH. Multimodality imaging of pericardial disease. Curr Cardiol Rep. 2015;17:24.

Zhou W, Srichai MB. Multi-modality imaging assessment of pericardial masses. Curr Cardiol Rep. 2017;19:32.

The Aorta: Frequent Imaging in ICU Patients

Luigi Tritapepe, Domenico Vitale,
Mario Mezzapesa, Emilia Delia, Ilaria Chiesa,
and Roberto Arzilla

11.1 Anatomy

The aorta is the largest and strongest artery in the body; its wall consists of three layers: the thin inner layer or intima, a thick middle layer or media, and a rather thin outer layer, or adventitia. The endothelium-lined aortic intima is a thin, delicate layer and is easily traumatized. Normally it is not very echogenic, but that can change in pathological conditions. The media is composed of smooth muscle cells and multiple layers of elastic laminae that provide not only tensile strength but also distensibility and elasticity, properties vital to the aorta's circulatory role. The adventitia contains mainly collagen as well as the vasa vasorum, which nourish the outer half of the aortic wall and a major part of the media. It arises from the left ventricle, ascends for a short distance in the thorax, then forms an arch, and finally descends through the chest and through the abdomen, in a candy cane-shaped configuration, where it ends by dividing into two arteries called the common iliac arteries. It is separated from the heart in the anterior mediastinum and turns left in front of the trachea and the left main bronchus, projecting into the posterior mediastinum, where it comes down behind the esophagus and in front of the vertebrae. The aorta consists of five main anatomic segments: the aortic root, the tubular portion of the ascending aorta, the aortic arch, the descending thoracic aorta, and the abdominal aorta. The aortic root includes the aortic valve annulus, aortic valve cusps, coronary ostia, and sinuses of Valsalva. Distally the root joins the tubular portion of the ascending aorta at an easily recognized landmark termed the sinotubular junction (STJ). The tubular portion of the ascending aorta extends from the STJ to the origin of the brachiocephalic artery. The aortic arch extends from the brachiocephalic artery to the left subclavian artery. The arch gives rise to three branches from its superior aspect, from where they course posterosuperiorly. The descending aorta begins distal to the left subclavian artery at the ligamentum arteriosum, a remnant of the fetal patent ductus arteriosus. This area is called the aortic isthmus, and it is important to visualize it in cases of coarctation of the aorta or patent ductus arteriosus. This region is also used as a landmark since the location of any disease in the descending aorta is described in relation to the isthmus. The descending thoracic aorta may be subdivided into the proximal part, which extends from the left subclavian artery to the level of the pulmonary artery, and the distal part which extends from the level of the pulmonary artery to

L. Tritapepe (✉) · M. Mezzapesa · E. Delia
I. Chiesa · R. Arzilla
Department of Anesthesia and Intensive Care,
Cardiac Surgery ICU, Policlinico Umberto I Hospital,
Sapienza University of Rome, Rome, Italy
e-mail: luigi.tritapepe@uniroma1.it

D. Vitale
Azienda Ospedaliera S. Croce e Carle, Cuneo, Italy

Table 11.1 Aortic root dimensions in normal adults

	Absolute values (cm)		Indexed values (cm/m²)	
Aortic root	Men	Women	Men	Women
Annulus	2.6 ± 0.3	2.3 ± 0.2	1.3 ± 0.1	1.3 ± 0.1
Sinuses of Valsalva	3.4 ± 0.3	3.0 ± 0.3	1.7 ± 0.2	1.8 ± 0.2
Sinotubular junction	2.9 ± 0.3	2.6 ± 0.3	1.5 ± 0.2	1.5 ± 0.2
Proximal ascending aorta	3.0 ± 0.4	2.7 ± 0.4	1.5 ± 0.2	1.6 ± 0.3

the diaphragm. The abdominal aorta may be subdivided into the proximal part, which extends from the diaphragm to the ostia of the renal arteries, and the distal part, from the renal arteries to the iliac bifurcation. The aorta gives off branches that go to the heart, the head and neck, the arms, the major organs in the chest and abdomen, and the legs. It serves to supply them all with oxygenated blood. Many aortic diseases immediately damage the organs to which it supplies blood.

In adults aortic dimensions are strongly positively correlated with age and body size. They are larger in men than in women of the same age and body size (Table 11.1).

11.2   Echocardiography

Echocardiography plays an important role in the diagnosis and follow-up of aortic diseases. Evaluation of the aorta must always be performed during the echocardiographic examination. Echocardiography is useful for every aortic disease that involves size, shape, and atherosclerotic degeneration of the thoracic aorta. With transesophageal echocardiography (TEE), we can easily visualize and study the aortic root and the proximal ascending aorta, and TEE can resolve the technical limitation of transthoracic echocardiography (TTE) in the examination of the thoracic aorta. TEE is the technique of choice in the diagnosis of aortic dissection, but in the emergency setting, TTE may be used as the initial screening mode. The discovery of an intimal flap

in the ascending aorta, pericardial effusion/tamponade, and acute aortic valve insufficiency is possible with TTE. However, a negative TTE finding does not rule out aortic dissection and other imaging techniques must be considered. TEE is more accurate in defining the location of an entry tear, the severity of aortic regurgitation, and true lumen compression. TEE is recommended in selecting and monitoring surgical and endovascular treatment especially to detect every possible complication. CT and MRI have a greater field of view and may yield complementary information, but echocardiography is portable, rapid, accurate, and cost-effective in the diagnosis of most aortic diseases. The echocardiographic view of the aorta shows it to be circular in the perpendicular sections and tube shaped in the parallel sections relative to its largest axis. The echocardiographic image shows the wall as echo-reflecting and the aortic lumen as echo-free.

11.3   TTE of the Aorta

TTE is one of the techniques most used to measure proximal aortic segments in clinical practice. The aortic root and proximal ascending aorta are best imaged in the left parasternal long-axis view. The left lung and sternum often limit imaging of the more distal portion of the ascending aorta from this transducer position. In some patients, especially those with aortic dilatation, the right parasternal long-axis view can provide supplemental information. The parasternal long-axis view allows us to correctly measure the aortic root diameters (Fig. 11.1). In the parasternal long-axis view, directly in two dimensions or in M-mode, we can study the aortic root and the proximal ascending aorta at the end of diastole with the aortic leaflets closed. We can measure the annulus, where the leaflets are attached, the Valsalva sinuses, in the maximal diameter, and the sinotubular junction, at the end of the sinuses and the beginning of tubular tract. The root and the proximal aorta measure less than 3.7 cm in an
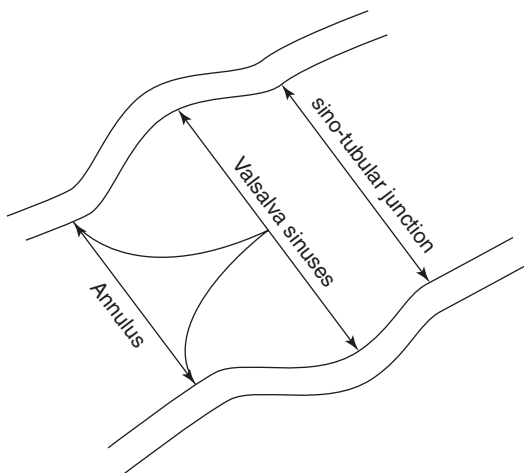
Fig. 11.1 The ascending aorta with measurement points

11.4   TEE of the Aorta

TEE has been shown to be a very sensitive diagnostic tool in the delineation and management of different aortic diseases. It is a fundamental examination to diagnose the aortic syndrome and differentiate other diseases in the case of chest pain. TEE represents a diagnostic tool for the cardiologist, intensivist, and anesthesiologist wishing to practice cardiac anesthesia. The anatomic proximity of the aorta to the esophagus allows one to have a good view of the aorta, almost entirely. The only invisible tract is the distal portion of the ascending aorta owing to the presence of air in the right main bronchus, whereas the proximal portion of the aortic arch is poorly visible because of the proximity of the trachea, which could cause a virtual blind spot in that area (Fig. 11.2).

adult of mean size. With the same view, we can observe the descending aorta as a circular image below the left atrium, posteriorly. In all patients with suspected aortic disease, the right parasternal long-axis view, also if it is not routinely performed, is recommended for estimating the true size of the ascending aorta. The ascending aorta is also visualized in the apical three-chamber and modified apical five-chamber views; however, in these views, the aortic walls are seen with suboptimal lateral resolution, and the diagnosis could be misinterpreted or unrecognized. The subcostal views may in some cases be helpful and allow one to visualize the suprarenal aorta. All these tomographies also allow us to study optimally the aortic valve, which is often involved in disorders of the ascending aorta (e.g., bicuspid valve, aortic regurgitation due to dilatation of the ascending aorta or aortic dissection, and other diseases). The suprasternal view is a crucial view to visualize, above the right pulmonary artery, the aortic arch and the three supra-aortic trunks (innominate, left carotid, and left subclavian arteries) and again a variable tract of the descending and the ascending aorta. However, if inconclusive information or abnormalities are present, another imaging modality (e.g., TEE) is required to either the complete information or add diagnostic information.

Fig. 11.2 Evaluation of the aorta by transesophageal echocardiography (TEE)

TTE	TEE
PSLAX, PSSAX (Asc + Desc Ao)	ME Asc Aortic LAX, ME Asc Aortic SAX (Asc Ao)
A4C, A2C, ALAX (Desc Ao)	UE Aortic Arch, UE Aortic Arch LAX (arch + Asc Ao)
Suprasternal (Arch, Asc, and Desc Ao)	Desc Aortic LAX, Desc Aortic SAX (Desc Ao)
Subcostal (Abdominal and Asc Ao)	

TTE transthoracic echocardiography, *TEE* transesophageal echocardiography, *PSLAX* parasternal long axis, *PSSAX* parasternal short axis, *Asc* ascending, *Desc* descending, *Ao* aorta, *A4C* apical four chamber, *A2C* apical two chamber, *ALAX* apical long axis, *ME* mid-esophageal, *LAX* long axis, *SAX* short axis, *UE* upper esophageal

In routine practice, evaluation of the aorta by TEE is possible through six views (Table 11.2): mid-esophageal ascending aortic short-axis view, mid-esophageal ascending aortic long-axis view, upper esophageal aortic arch view, upper esophageal aortic arch long-axis view, descending aortic short-axis view, and descending aortic long-axis view. In the mid-esophageal four-chamber view at 0°, the probe should be withdrawn 2 cm, and the ascending aorta can be shown in the short axis. This produces a circular image of the aortic root between the left atrium and the right atrium. Rotating the imaging plane to 90° will produce the long-axis view showing the ascending aorta. In this projection, however, the distal ascending aorta cannot be visualized owing to the dispersion of echoes due to tracheal air. The ascending aortic long-axis view is a good view to measure the wall thickness, the aortic diameter, and the turbulence of flow. To view the descending thoracic aorta, we must return to the mid-esophageal four-chamber view and then rotate the probe through 180°; we then see the aorta positioned behind the esophagus. The aorta is circular at the top of the screen, and changing the depth and frequency, we may well see it in an appropriate manner. If the probe is moved down, the aorta is no longer displayed when we reach the diaphragm muscle. With slight shifts of the probe back, we obtain the short-axis view of the thoracic aorta at various levels, making sure to rotate the probe slightly to center the image of the aorta because it runs laterally and then posteriorly to the esophagus at this level. Thus, we can fully display the descending thoracic aorta, which is very useful, for example, in the positioning of an endoluminal stent. Rotating the imaging plane to 90° will bring into view the long-axis image of the descending aorta.

To view the arch, we go back to the mid-esophageal four-chamber view at 0° and pull the probe back slowly until the aortic arch is seen. This is displayed in the upper esophageal long-axis view about 20 cm from the mouth rhymes. The proximal part of the aortic arch is not viewable because of air in the trachea; however, we have a good view of the arch that shows the proximal portion on the left of the screen and the distal part on the right, with the posterior wall near the probe and at the top of the screen and the anterior wall farther and down. To obtain short-axis images of the aortic arch, we need to rotate the probe 90° clockwise. The left subclavian artery and the left common carotid artery can also be viewed by pulling the probe further back (Fig. 11.3).

Near the aortic arch, we can see the trunk of the pulmonary artery and part of its left branch. It is impossible to see the brachiocephalic arterial trunk because of the presence of tracheal air, which prevents the penetration of the echoes. Study of the thoracic aorta should include wall thickness, tissue characteristics, dimensions, and blood flow patterns by Doppler assessment.

11.5 Aortic Atheroma

Various terms have been used to describe the appearance of atherosclerotic lesions of the aorta on imaging. The simplest lesions are usually reported as "atheroma" or "atheromatous plaque." When mobile components are seen attached to these plaques, the terms ruptured plaque, mobile plaque, mobile debris, and superimposed thrombi are used. A growing body of evidence has established an association between echocardiographically demonstrated aortic atheroma and embolic
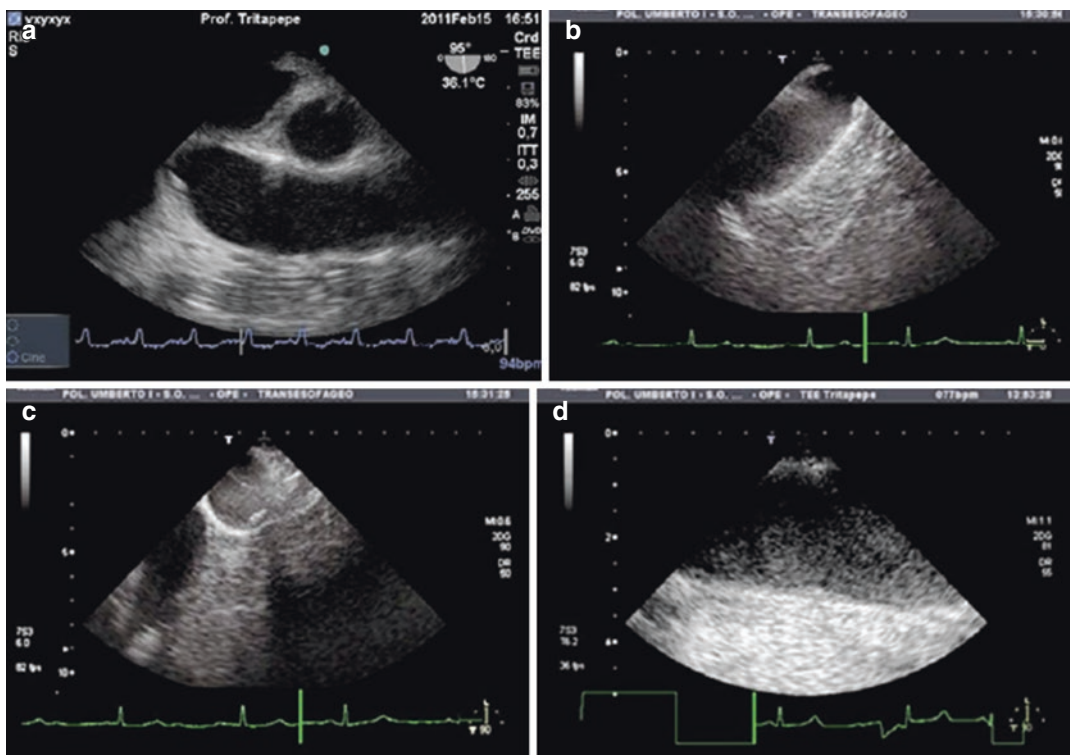
Fig. 11.3 TEE of the aorta: (**a**) ascending aorta, (**b**) arch, (**c**) at level of the origin of the subclavian artery, (**d**) descending aorta

events, both cerebral and peripheral. In addition, thoracic aortic atherosclerosis has been identified as a stronger predictor of significant coronary artery disease. Aortic atherosclerosis has also been associated with cholesterol embolization (blue toe syndrome), stroke after coronary artery bypass surgery, and catheter-related embolism after cardiac catheterization and intra-aortic balloon pump insertion. Therefore, the detection of aortic atherosclerosis on imaging has prognostic implications. On ultrasound examination, the normal aortic wall is seen as two parallel echogenic lines separated by a relatively hypoechoic space. The inner line represents the luminal-intimal interface, whereas the outer line represents the medial-adventitial border. Thus, the distance between the lines reflects the combined thickness of the intima and media, the "intimal-medial thickness," which is normally ≤1 mm. Moreover, the normal aortic wall has a smooth, continuous surface. Any irregular thickening of ≥2 mm on TEE is therefore considered to be an atheroma. For aortic disease, TEE provides real-time images that allow the evaluation of plaque morphology, ulceration, and mobility. Aortic atherosclerosis has been classified on the basis of plaque characteristics of thickness, presence or absence of mobile components, and presence or absence of ulceration. Plaque thickness is considered to be a more objective and reliable measure of atheroma severity than is plaque morphology. Therefore, most grading systems are based on the maximal plaque thickness in the most diseased segment (Fig. 11.4, Table 11.3). The major limitation of the existing classification systems is the failure to account for the overall plaque burden in terms of its extent over the length of the thoracic aorta or a segment of the aorta. Therefore, it is recommended to report whether the atheromas are localized or diffuse.

TEE has become the procedure of choice for both detecting aortic atheroma and assessing ath-
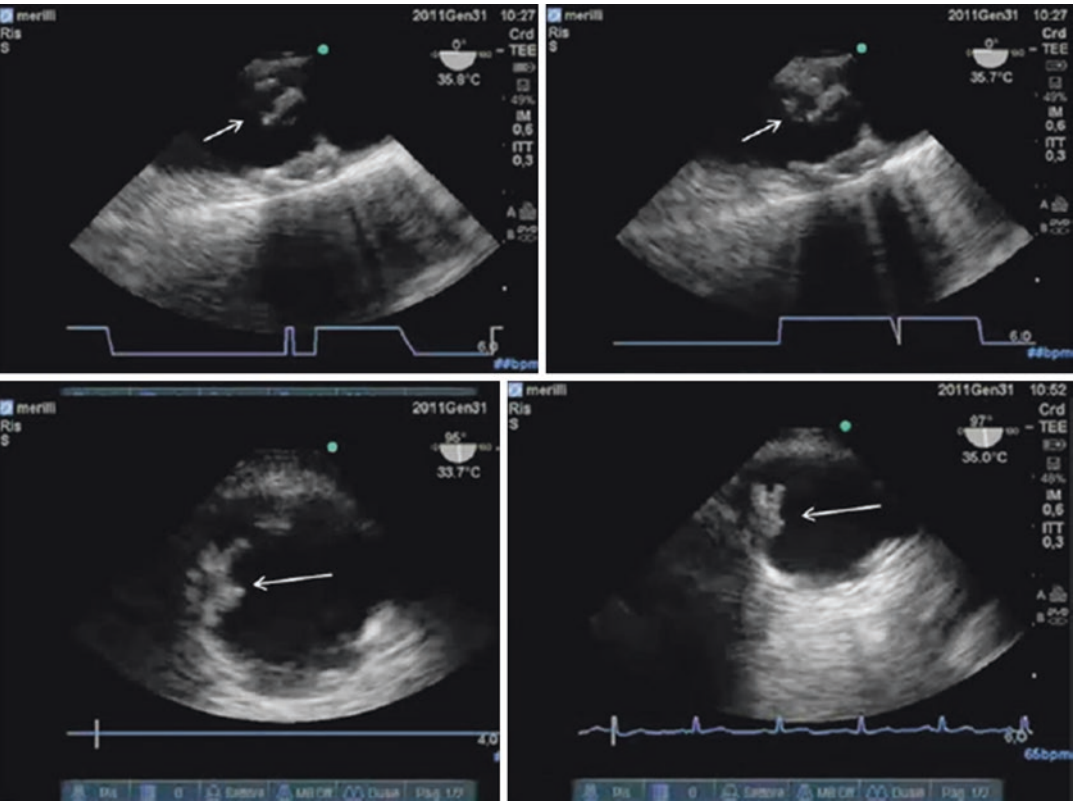
Fig. 11.4 TEE of the aorta at the level of the arch and of the origin of the subclavian artery. Note the presence of a huge mobile atheroma (*arrow*)

Table 11.3 Grading system for severity of aortic atherosclerosis

Grade	Severity (atheroma thickness)	Description
1	Normal	Intimal thickness <2 mm
2	Mild	Mild (focal or diffuse) intimal thickening of 2–3 mm
3	Moderate	Atheroma >3–5 mm (no mobile/ulcerated components)
4	Severe	Atheroma >5 mm (no mobile/ulcerated components)
5	Complex	Grade 2, 3, or 4 atheroma plus mobile or ulcerated components

eroma size and morphology. It is useful in cardiac surgery to detect the presence of aortic atheroma. In fact, many surgeons still palpate the aorta for atheroma scanning before making an aortotomy or placing a vascular clamp, but this method can only detect the most severe cases of atherosclerosis, and in some instances the palpation itself can dislodge the plaques and lead to embolic sequelae. The aortic atheroma must always be detected before intra-aortic devices (intra-aortic balloon pump, cannulae, endovascular stents) are positioned.

11.6 Aortic Aneurysm

The aneurysm is considered a dilation of an aorta whose diameter is least more than 50% the diameter of the expected normal value for age, height, and sex. True aneurysms result from stretching of the entire thickness of the aortic wall; thus, the wall of an aneurysm contains all three of its layers (intima, media, and adventitia). Aneurysms of the aorta can be classified into two morphologic
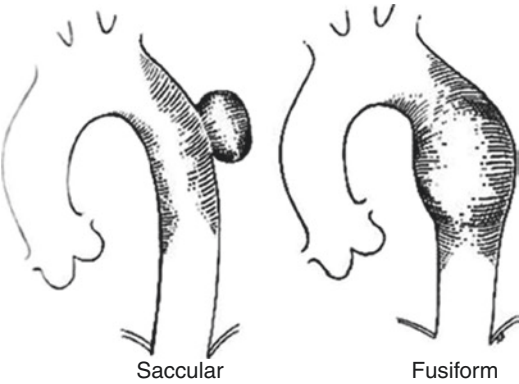
Fig. 11.5 Diagram illustrating the two morphologic types of aortic aneurysms: saccular and fusiform

types: fusiform and saccular (Fig. 11.5). Fusiform aneurysms, which are more common than saccular aneurysms, result from diffuse weakening of the aortic wall. This process leads to dilatation of the entire circumference of the aorta, producing a spindle-shaped deformity with a tapered beginning and end. Saccular aneurysms result when only a portion of the aortic circumference is weakened, producing an asymmetric, relatively focal balloon-shaped outpouching. Sixty percent of aortic aneurysm involve the aortic root and/or ascending tubular aorta, 40% involve the descending aorta, 10% involve the arch, and 10% involve the thoracoabdominal aorta. They are often related to systemic arterial hypertension and atherosclerosis, but, especially in the ascending aortic tract, also to Marfan syndrome and other collagenopathies, aortic bicuspid valve, and other aortic valve diseases.

The aneurysm of the descending thoracic aorta can be due to aortic atherosclerosis, but it can also be consequence of previous thoracic trauma with the mechanism of incomplete wall rupture or strain at the level of the isthmus tract of the aorta.

The ascending aortic aneurysm can be easily detected with TTE in the parasternal long-axis view, in which we can recognize not only the aortic diameter and the systolic expansion of the aneurysm but also the remodeling of the aortic valve with its consequent insufficiency. Aortic diameter is the principal predictor of aortic rupture or dissection. The risk for rupture or

dissection of thoracic aortic aneurysm (TAA) from different etiologies increases significantly at sizes >60 mm. The mean rupture rate is only 2% per year for aneurysms <50 mm in diameter, rising slightly to 3% for aneurysms with diameters of 50–59 mm, but increasing sharply to 7% per year for aneurysms >60 mm in diameter. The importance of echocardiography is in evaluating the growing of the aortic aneurysm, in detecting the presence of intramural thrombi, and in preventing rupture by referring the patient to the surgeon when the diameter generally exceeds more than 5 cm. Table 11.4 summarizes the main goals during the echocardiographic evaluation of an aortic aneurysm.

When patients with aortic root or ascending TAAs undergo aortic repair, the anatomy of the aorta and aortic valve has usually been defined preoperatively. Nevertheless, it is always wise to use intraoperative TEE to confirm the prior imaging findings. The initial intraoperative transesophageal echocardiographic examination should begin before the initiation of cardiopulmonary bypass, so the physiology of the aortic valve can be assessed. If the valve is bicuspid, one should determine the presence and severity of associated valvular aortic stenosis, regurgitation, or both. If there is significant AR, one should determine the mechanism, looking specifically for prolapse and/or retraction of the conjoined leaflet, as this is a common cause of bicuspid AR and may be correctable with BAV repair. One should also assess the degree of leaflet thickening, calcification, and restriction, because in the setting of significant valve dysfunction, these findings may influence the surgeon's decision

Table 11.4 Goal of imaging of thoracic aortic aneurysm

1. Confirm diagnosis
2. Measure maximal diameter of the aneurysm
3. Define longitudinal extent of the aneurysm
4. Measure the diameters of the proximal and distal margins of the aneurysm
5. Determine involvement of the aortic valve
6. Determine involvement of the arch vessel(s)
7. Detect periaortic hematoma or other sign of leakage
8. Differentiate from aortic dissection
9. Detect mural thrombus

regarding the need for valve repair or replacement. The ascending aorta, aortic arch, and descending aorta should each be inspected for the presence of associated pathology, such as an unrecognized aortic dissection, IMH, PAU, or protruding atheromas. Large atheromas in the ascending aorta or arch may prompt additional imaging of the aorta using intraoperative epiaortic echocardiography and influence decisions regarding the site of aortic cannulation and perfusion. Postoperative TEE should begin as soon as the patient comes off cardiopulmonary bypass. The examination should begin with inspection of the aortic valve, as unanticipated valve dysfunction may necessitate a return to bypass. The aim of postoperative TEE is to assess and record the recovery of an adequate physiology after the surgical treatment of the aortic aneurysm. Besides, TEE is now usually employed in all procedures of endovascular aortic stenting and recently in monitoring and guiding percutaneous aortic valve replacement. The implantation of transluminally placed endovascular grafts or stents has become an alternative to aortic surgery especially in the treatment of a thoracoabdominal aneurysm. TEE monitoring is crucial to detect, during the whole procedure, the exact positioning of stents and to search for endoleaks to exclude aortic lesions.

11.7 Aortic Dissection

Aortic dissection is characterized by an intimal tear near an aortic plaque or by an aortic penetration from an ulcerated plaque and the extension of an intramural hematoma affecting the media and allows the hematoma to expand throughout the aortic wall. The detachment of the intima from the aortic wall is a result of the thrust due to the systolic blood pressure and cardiac contractility. This mechanism promotes the formation of two lumens in the aorta: the false lumen and the true lumen. When the dissection involves the aortic root, correct functioning of the aortic valve is of importance because aortic valve insufficiency can precipitate the hemodynamics. Also, the dissection can proceed toward the coronary ostia, causing acute myocardial ischemia or infarction

that has to be accurately detected by echocardiography before these lesions are treated with antiplatelets or with percutaneous transluminal coronary angioplasty or an intra-aortic balloon pump. In the absence of a diagnosis or in the case of misinterpretation, we may have a disaster related to massive bleeding or organ malperfusion at the time of emergent surgery. TEE is the technique of choice in the diagnosis of aortic dissection, but in the emergency setting, TTE may be used as the initial screening mode. Although CT angiography and MRI images are more sensitive and specific, they cannot be used in unstable patients, which is more often the case in this clinical scenario. In the case of doubt or absence of a clear landmark with TTE, TEE is required to differentiate a dissection from the other abnormalities that cause chest pain. Depending on the location of dissection, we distinguish a dissection as Stanford type A (type I and II of the DeBakey classification) when the lesion involves the ascending aorta and arch and as Stanford type B (DeBakey type III) when it affects the descending aorta, below the emergence of the subclavian artery. Type A aortic dissection is a true surgical emergency with a mortality rate that increases from the time of onset. A criterion that determines the extreme urgency is the presence of pericardial effusion or tamponade as well as the condition of shock. In type B aortic dissection, in the absence of malperfusion of splanchnic organs, we have to treat the patient aggressively with antihypertensive drugs associated with beta blockers, and only after stabilizing the lesion can we treat the aortic dissection with endoluminal stents. Echocardiographic diagnosis is fundamental to resolve some doubts and to help the surgeon, in case of type A, or radiologist, in case of type B, to correct the aortic dissection with success. Echocardiographic diagnosis needs to detect a mobile intraluminal flap, the presence of a false lumen, and one or more entry tears where the flow goes from a true lumen into the false lumen. Doppler and color Doppler imaging may help to identify the true lumen from the false lumen and to evidence the aortic tear. Doppler imaging does not show a normal wave typical of aortic flow in the false lumen, which may have a

flat wave due to luminal thrombosis. The differences between the false lumen and the true lumen can be summarized as follows: the false lumen is bigger than the true lumen; during systole the true lumen expands, whereas the false lumen is compressed; the direction of flow is antegrade in the true lumen and reduced or absent in the false lumen. For a complete discussion, see Chap. 33.

11.8 Intramural Hematoma

Intramural hematoma is a bleeding inside the layers of the aortic wall. It can resolve spontaneously or following medical therapy or can develop into an aortic aneurysm or dissection. The diagnosis of intramural hematoma can be straightforward in typical cases, but an intramural hematoma can be confused with a thrombus or a thrombosis of the false lumen in aortic dissection. TEE may facilitate the diagnosis of intramural hematoma, whereas TTE does not have accuracy on the aortic wall. On echocardiography an intramural hematoma appears as concentric or more localized thickening (more than 5 mm) of the aortic wall without measurable flow within. The International Registry of Acute Aortic Dissection data demonstrate a 5.7% prevalence of intramural hematoma in patients with acute aortic syndromes. Like classic aortic dissection, intramural hematoma is a highly lethal condition when it involves the ascending aorta, and surgical therapy should be considered, but this condition is less critical when it is limited to the arch or the descending aorta.

11.9 Sinus of Valsalva Aneurysm

The spaces between the luminal surface of the three bulges on the aortic root and their respective valvar leaflets are known as the aortic sinuses of Valsalva. A sinus of Valsalva aneurysm is often a congenital abnormality caused by a dilation, usually of a single sinus of Valsalva, from a separation between the aortic media and the annulus fibrosus. Other disease processes that involve the

aortic root (e.g., atherosclerotic aneurysms, endocarditis, cystic medial necrosis, chest trauma) may also produce a sinus of Valsalva aneurysm, although this usually involves multiple sinuses. Rupture of the dilated sinus may lead to intracardiac shunting when a communication is established with the right atrium or directly into the right ventricle (60–90%). Cardiac tamponade may occur if the rupture involves the pericardial space. TTE and TEE are accurate in the diagnosis of a sinus of Valsalva aneurysm both in the parasternal long-axis view and the mid-esophageal aortic valve long-axis view and in the short-axis view.

11.10 Aortic Coarctation

Aortic coarctation is a relatively uncommon congenital cardiovascular disorder. It is most commonly located just distal to the left subclavian artery. Aortic coarctation causes reduced blood flow to the lower body, which can present as hypertension and congestive heart failure early in life, or may be identified when a search for a cause of hypertension is performed later in life. It typically occurs in an isolated location just after the aortic arch at the level of the aortic isthmus. It can be associated with other congenital abnormalities such as a bicuspid aortic valve. The narrowing of the aortic lumen increases the blood pressure in the upper body and reduces it in the lower part. Patients with aortic coarctation also have a form of vasculopathy with increased risk for aneurysm formation in the ascending aorta, at the site of coarctation repair, and in the intracranial vasculature. A BAV is present in >50% of patients with aortic coarctation. TEE is more sensitive than TTE in visualizing the coarctation of the aorta. In addition, apart from imaging the ridge of the aortic lumen, Doppler imaging is accurate in determining the severity of aortic coarctation. In fact, the presence of a high-velocity turbulent flow with color flow imaging and continuous wave Doppler imaging could justify the suspicion of an aortic coarctation. Nevertheless, Doppler gradients are not useful for quantification, neither in native nor in

postoperative coarctation. A diastolic "run-off" phenomenon is presumably the most reliable sign of significant coarctation or recoarctation.

11.11 Patent Ductus Arteriosus

Patent ductus arteriosus is a heart defect that occurs soon after birth in some babies. It is a persistent communication between the aorta and the pulmonary artery. It can be isolated or may be present in association with all forms of congenital heart disease (CHD). The most common associated lesions are ventricular and/or atrial septal defects. Before birth the aorta and the pulmonary artery are connected by the ductus arteriosus. This vessel is an essential part of fetal blood circulation. Within minutes or up to a few days after birth, the ductus arteriosus is closed. In some babies, however, the ductus arteriosus remains open (patent). This opening allows mixing of oxygenated blood from the aorta to the pulmonary artery. Patients are at an increased risk of developing endarteritis, heart failure, and pulmonary vascular disease. Patent ductus arteriosus can be detected with TTE in the parasternal short-axis view, in which we can observe, with color Doppler imaging, a jet from the aorta to the pulmonary artery.

11.12 Bicuspid Aortic Valve and Related Aortopathy

BAVs affect 1–2% of the population and are often associated with aortopathy. Nearly 50% of patients with BAVs have dilatation of either the aortic root or ascending aorta. Dilatation of the aortic arch and descending thoracic aorta can also occur but is less common. Recently, it has been reported that patients with BAVs also are at increased risk for intracranial aneurysms compared with the normal population, although the clinical significance of this is unknown. Progressive dilatation of the aorta may occur irrespective of the functional status of the BAV and places patients at increased risk for aortic

dissection or rupture. Patients with BAVs may also have coexisting coronary artery anomalies, including reversal of dominance, short left main coronary artery (<10 mm), and anomalous origin of the left circumflex artery from the right coronary cusp. Failure to recognize these anomalies may result in risk for coronary artery injury during aortic valve repair or replacement. TTE is the primary imaging tool for the initial diagnosis and screening as well as serial follow-up of patients with known or suspected BAVs with or without aortopathy. BAVoccurs in >50% of patients with coarctation, but coarctation is noted in <10% of patients with BAVs. Nevertheless, whenever a BAV is detected, coarctation should always be sought.

11.13 Traumatic Injury to the Thoracic Aorta

Traumatic injuries to the aorta may result from either blunt (nonpenetrating, indirect) or sharp (penetrating, direct) trauma. Blunt aortic injuries (BAIs) are far more common. In BAIs, the aortic wall is damaged from the inside to the outside, from the intima to the adventitia. The most common location of BAI is at the aortic isthmus just distal to the left subclavian artery. The second most common location is the supravalvular portion of the ascending aorta. Motor vehicle accidents account for 75% of cases in most series of BAIs, but crush injuries, explosions, motorcycle and aircraft crashes, pedestrian injuries, and direct blows to the chest are also known to produce similar injuries. The aortic isthmus is the most common location for BAIs (80–95%), followed by the ascending aorta and then the diaphragmatic aorta. Those regions represent transition points between relatively fixed and mobile aortic segments. These transition points have the greatest exposure to shear and hydrostatic forces generated by abrupt deceleration. CT is now the diagnostic test of choice. Nevertheless, because of its wide availability, portability, and accuracy, as well as the fact that no contrast medium is required, TEE is also a

powerful diagnostic tool that gained popularity as a first-line study. Furthermore, TEE may fail to adequately image the distal ascending aorta (TEE's known blind spot) and may not identify all of the branches of the aortic arch (Tables 11.5 and 11.6). Transesophageal echocardiographic findings in patients with BAIs include (1) dilatation in the region of the isthmus, (2) an abnormal aortic contour, (3) an intraluminal medial flap, (4) a pseudoaneurysm, (5) a crescentic or circumferential thickening of the aortic wall (IMH), and (6) mobile linear echodensities attached to the aortic wall consistent with an intimal tear or a thrombus. Similar findings are seen in patients with spontaneous aortic dissection, but there are some important differences. With traumatic aortic injury, the medial flap tends to be thicker, has greater mobility, and is typically perpendicular (rather than parallel) to the aortic wall so that there is an absence of two channels. The aortic contour is usually deformed because of the presence of a localized pseudoaneurysm. Last, with traumatic aortic injury, the findings are confined to the isthmus region, rather than propagating distally all the way to the iliac arteries.

Table 11.5 Advantage of TEE in blunt traumatic thoracic aortic injury

1. Highly accurate in region of aortic isthmus (most common region for BAI)
2. Can be performed at bedside or in OR
3. Can be performed in unstable patients who need emergency OR and when there is not time for CT
4. No radiation exposure
5. Does not require contrast; safe in renal insufficiency
6. Can assess other cardiac injuries and cardiac function

Table 11.6 Disadvantages of TEE in blunt traumatic thoracic aortic injury

1. Difficulty imaging distal ascending aorta
2. Difficulty evaluating arch vessels
3. Operator dependent (requires skilled operator): Training and experience required and availability
4. Not always safe in patients with facial, cervical, spine, oropharynx
5. Or esophageal injuries
6. Reverberation artifact

Further Reading

Cook CC, Gleason TG. Great vessel and cardiac trauma. Surg Clin North Am. 2009;89:797–820.

Evangelista A, Mukherjee D, Mehta RH, et al. Acute intramural hematoma of the aorta a mystery in evolution. Circulation. 2005;111:1063–70.

Evangelista A, Flachskampf FA, Erbel R, et al. Echocardiography in aortic diseases: EAE recommendations for clinical practice. Eur J Echocardiogr. 2010;11:645–58.

Goldstein SA, Evangelista A, Abbara S, et al. Multimodality imaging of diseases of the thoracic aorta in adults: from the American Society of Echocardiography and the European Association of Cardiovascular Imaging: endorsed by the Society of Cardiovascular Computed Tomography and Society for Cardiovascular Magnetic Resonance. J Am Soc Echocardiogr. 2015;28(2):119–82.

Harloff A, Simon J, Brendecke S, et al. Complex plaques in the proximal descending aorta an underestimated embolic source of stroke. Stroke. 2010;41:1145–50.

Ho SY. Structure and anatomy of the aortic root. Eur J Echocardiogr. 2009;10:i3–i10.

Kabirdas D, Scridon C, Brenes J-C, et al. Accuracy of transthoracic echocardiography for the measurement of the ascending aorta: comparison with transesophageal echocardiography. Clin Cardiol. 2010;33:502–7.

Michelena HI, Khanna AD, Mahoney D, Margaryan E, Topilsky Y, Suri RM, et al. Incidence of aortic complications in patients with bicuspid aortic valves. JAMA. 2011;306:1104–12.

Shiga T, Wajima Z, Apfel CC, Inoue T, Ohe Y. Diagnostic accuracy of transesophageal echocardiography, helical computed tomography, and magnetic resonance imaging for suspected thoracic aortic dissection. Arch Intern Med. 2006;166:1350–6.

Svensson LG, Adams DH, Bonow RO, Kouchoukos NT, Miller DC, O'Gara PT, et al. Aortic valve and ascending aorta guidelines for management and quality measures. Ann Thorac Surg. 2013;95:S1–66.

Vasaiwala S, Vidovich MI, Connolly J, Frazin L. Transesophageal echocardiography of the descending thoracic aorta: establishing an accurate anatomic marker using the celiac artery. Echocardiography. 2010;27:1093–7.

Warnes CA, Williams RG, Bashore TM, et al. ACC/AHA 2008 Guidelines for the Management of Adults with Congenital Heart Disease: a report of the American College of Cardiology/American Heart Association Task Force on Practice Guidelines (writing committee to develop guidelines on the management of adults with congenital heart disease). Circulation. 2008;118(23):e714–833.

Willoteaux S, Nedelcu C, Bouvier A, et al. Syndrome aortique: quelle imagerie réaliser? Presse Med. 2011;40:43–53.

The Vena Cava's and the Great Vessels Ultrasound

12

Silvia Laviola, Angelica Venni, and Silvio Cantini

Key Points

- Ultrasound is an important tool for physicians to assess the volume status and responsiveness in the critically ill patients.
- Ultrasound imaging of vena cava diameter fluctuation with respiration is a noninvasive method to assess fluid responsiveness in patients under controlled mechanical ventilation.
- IVC respiratory variations greater than 42% in spontaneously breathing patients are a very accurate predictive marker of fluid responsiveness.
- ΔVSC seems to have better accuracy than ΔIVC for predicting fluid responsiveness in ventilated septic patients.
- IJV distensibility is a reliable index of fluid responsiveness in mechanically ventilated patients.

In critically ill patients, the evaluation of hemodynamic status and the patient's capacity to respond to a fluid challenge are extremely important. In this context, transthoracic and abdominal ultrasound are becoming a powerful noninvasive tool in the daily care of the critically ill subject. They play a fundamental role for the assessment of static (left ventricular end diastolic area, inferior vena cava [IVC] size) and dynamic load conditions (velocity-time integral [VTI] of aortic blood flow and respiratory changes after passive leg raising [PLR], aortic peak velocity [ΔVPeak], common carotid artery [CCA] blood flow, superior vena cava [SVC] collapsibility index, IVC distensibility index). Both static measurements and dynamic variables, based on heart-lung interactions, give important data for the estimation of intravascular volume status and for the evaluation of the response to intravenous fluid resuscitation. Any information should be considered within the context of the overall clinical picture to be useful for the correct diagnosis. Fluid management is very important in the treatment of critically ill patients and those having acute circulatory failure. The unnecessary administration of fluids is associated with poor clinical outcome, prolonged mechanical ventilation, renal dysfunction, and higher mortality. It is therefore of primary importance to have reliable bedside tools to predict the efficacy of volume expansion. The goal is maintaining the right tissue perfusion without interstitial edema.

S. Laviola (✉) · A. Venni · S. Cantini
Anesthesia and Intensive Care Department, Santa Maria Annunziata Hospital, Azienda USL Toscana Centro, Florence, Italy
e-mail: silvia.laviola@uslcentro.toscana.it;
silvio.cantini@uslcentro.toscana.it;
angelica.venni@uslcentro.toscana.it

12.1 The Superior Vena Cava

The SVC is about 7 cm long, formed by the confluence of the right and left innominate veins. The SVC runs vertically down from the level of the first costal cartilage to about the level of the third costal cartilage, approximately posterior to the right sternal border, and ends by entering the right atrium (RA) at its superior pole.

The SVC has an entirely intrathoracic course, is sensitive to volume status, varies its diameter in relation to the respiratory cycle, and is affected by mechanical ventilation (MV) in an opposite way compared to the IVC. The maximal diameter is observed during expiration, and the minimal diameter during inflation (Table 12.1). In mechanically ventilated patients, the increase in pleural pressure during inflation produces complete or partial collapse of the SVC, since the external pressure exerted by the thoracic cavity on the SVC is greater than the venous pressure required to maintain the vessel fully open. The amplitude of SVC dimensional changes during MV predicts the hemodynamic effect of blood volume expansion.

Imaging of the SVC is obtained by transesophageal echocardiography (TEE) or transthoracic echocardiography (TTE).

12.1.1 Transesophageal Echocardiography

Using TEE, the SVC is examined with a multiplane probe (5 MHz) in the mid-esophageal (ME) bicaval view. The SVC is examined from a long-axis view, using two-dimensional images to correctly align the M-mode beam at the level of the maximum diameter. The SVC diameters (D_{max} and D_{min}) are measured over a single ventilatory cycle, 2–3 cm above the junction of the SVC and the right atrium, and the so-called cava collapsibility index (ΔSVC) – i.e., the inspiratory decrease in SVC diameter – is calculated as $100 \times$ (D_{max} on expiration – D_{min} on inspiration/D_{max} on expiration). The ΔSVC has been shown to be predictive of fluid responsiveness for a variation in SVC size >36%, with high specificity (100%) and good positive predictive value.

12.1.2 Transthoracic Echocardiography

TTE is able to visualize the SVC through three different scans. With the patient in the supine position, a low-frequency probe (2–5 MHz) such

Table 12.1 SVC and IVC diameter changes during positive pressure ventilation
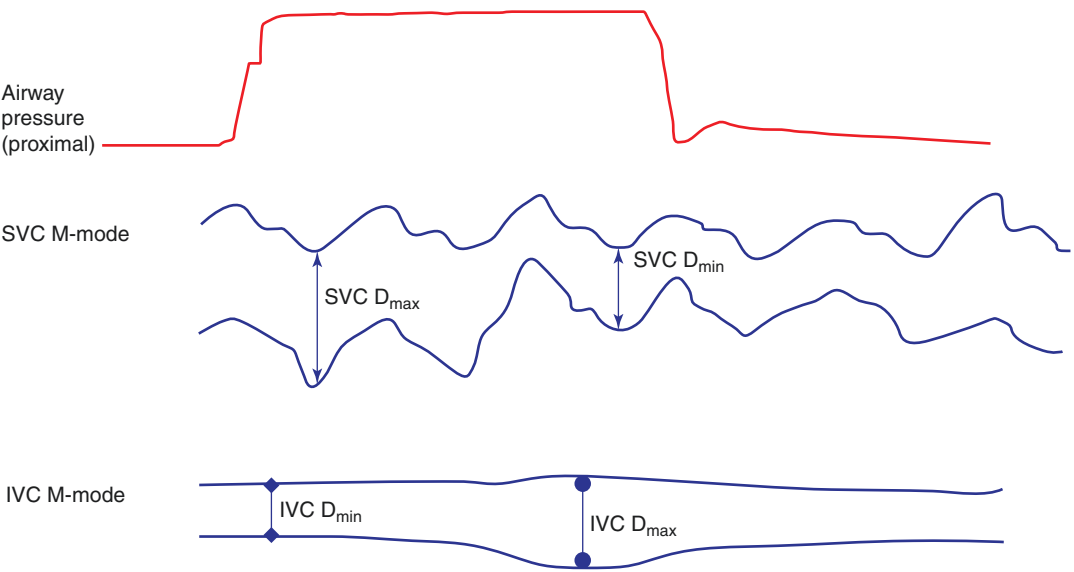
as a phased array, or a high-frequency probe (5–7.5 MHz) as a linear probe, should be selected.

- Right supraclavicular scan. The transducer is placed in the supraclavicular fossa between the sternal and clavicular heads of the sterno-mastoid muscle. From this view, not only the top 4 cm of the SVC but also the right innominate vein (Fig. 12.1), its formation by the right subclavian and internal jugular veins, and often the left innominate vein can be visualized.
- Subcostal scan. The cardiac probe is placed in the subcostal region 1–2 cm below the xiphoid process, with the indicator pointing directly to the patient's left, to create an appropriate four-chamber view. The SVC is visualized as a straight narrow tube opening into the right atrium at its upper pole. Imaging of the SVC from these two opposite windows (supraclavicular and subcostal) provides complementary information. The proximal (lower) part of the SVC is best highlighted in the subcostal view; the distal (upper) half part of the SVC is best seen in the right supraclavicular view.
- Apical five-chamber scan. The cardiac probe is placed in the cardiac apex and with the patient in the left anterior oblique position.

The lower part of SVC connecting with the right atrium is displayed.

12.2   The Inferior Vena Cava

The IVC is formed at the level of the fifth lumbar vertebra by the confluence of the right and left common iliac veins. Its course in the thoracic cavity is short and it empties into the RA, under the coronary sinus. The IVC extends 45 cm and receives many tributaries along its abdominal course. The most important are the hepatic veins. In particular, the superior hepatic vein is important to the sonographer because its course is almost parallel to the ultrasound beam during the imaging of the IVC from the subcostal views. In some patients, a prominent Eustachian valve can be seen at the junction of the IVC and the RA. When a more extensive valve is present, it forms a Chiari network, extending from the inferior to the superior vena cava. Both are considered normal variants of no clinical significance.

12.2.1   Transthoracic Echocardiography

Three approaches may be used. With the patient in the supine position, a low-frequency probe

Fig. 12.1 Right supraclavicular view of the SVC, two-dimensional image. The upper panel shows the right innominate vein (RIV), the SVC, the brachiocephalic trunk, and the aortic arch (AoAr); in the lower panel, Doppler flow of the SVC
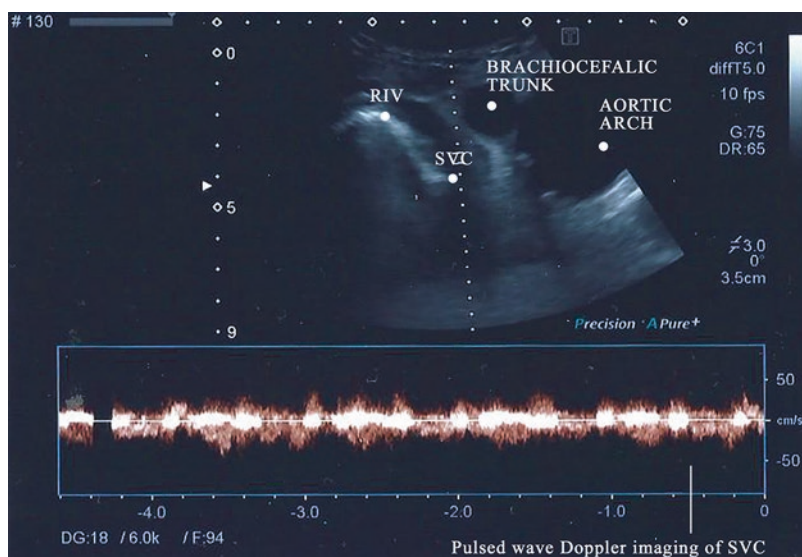
(2–5 MHz), such as a phased-array or curvilinear probe, should be selected.

- Subcostal short axis. The cardiac probe is placed on the patient's abdomen just below the xiphoid bone, with the marker toward the left shoulder of the patient. Once an appropriate subcostal four-chamber image is obtained, a slow counterclockwise rotation of the probe by 60–90° shows the IVC entering the right atrium. The M-mode cursor should be oriented perpendicular to the IVC, either 1 cm caudal to the junction of the hepatic veins or just 2–3 cm from the junction with the right atrium (Fig. 12.2). The measurement of IVC diameter close to the IVC-right atrium junction may be influenced more by contraction of the diaphragm, but this location is less susceptible to motion artifact.
- Transabdominal coronal long-axis "rescue view." The second approach is to scan using the liver as an acoustic window by placing the probe in the right mid-axillary line, the marker pointed toward the head of the patient; the IVC can be visualized running longitudinally adjacent to the liver and crossing the diaphragm, until it enters the right atrium.
- Subcostal transabdominal long axis. In this approach, the IVC is evaluated at the liver

level, the probe is placed in longitudinal scanning to the right of the epigastric midline, and the marker points to the patient's head. It is important to distinguish the IVC from the abdominal aorta (Fig. 12.3): the aorta has a systolic pulse and an incompressible thick wall, whereas the IVC is a compressible thin-wall structure with the hepatic veins draining into it.

12.2.2 The IVC Bedside Ultrasound

The IVC ultrasound helps to assess the intravascular volume status of the patient. In physiological states, the venous capacitance system contains 60% of the intravascular volume. The IVC is a compliant blood vessel subject to abdominal pressure, its short intrathoracic part is purely virtual, and its caliber is altered by blood volume, respiration, and right heart function.

Changes in intravascular volume are reflected in the ultrasonography evaluation of the IVC diameter, where increased or decreased vessel's distensibility and diameter help to guide clinical management of the patient during the respiratory cycle.

The IVC is normally 1.5–2.5 cm in diameter and a 50% inspiratory collapse is usually

Fig. 12.2 TTE, subxiphoid transabdominal short axis, two-dimensional and M-mode images of the IVC. Respiratory variations. The beam is positioned 2 cm caudal to the hepatic vein-IVC-junction
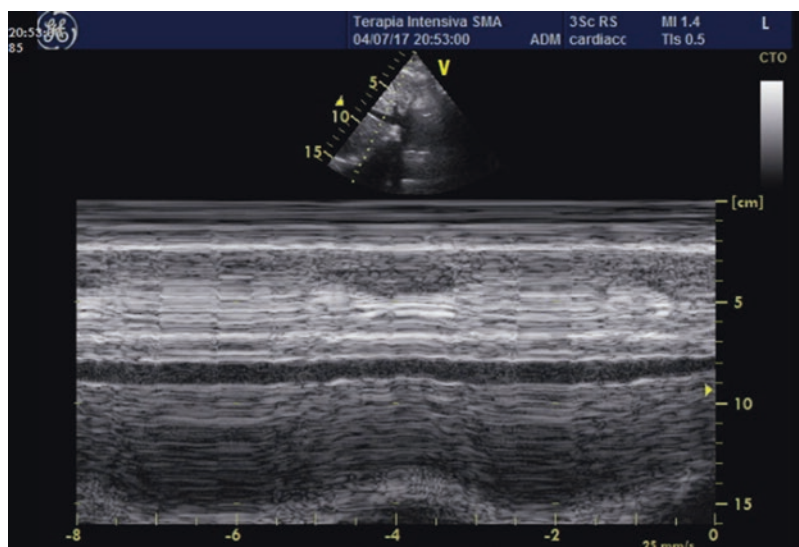
Fig. 12.3 TTE, subxiphoid transabdominal long axis, two-dimensional image of the IVC and abdominal aorta
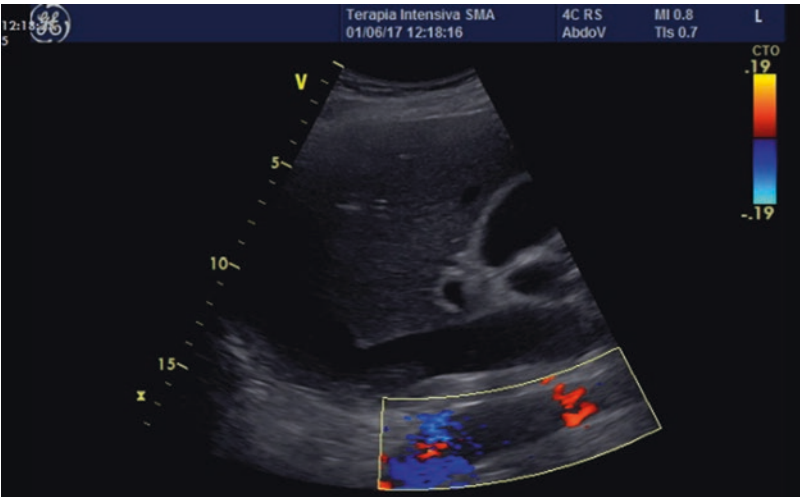
Table 12.2 Estimation of right atrial pressure

IVC diameter (cm)	Breathing variations in IVC diameter (%)	Estimated RAP
Small < 1.2	Spontaneous collapse	Volume depletion
Normal 0.5–2.5	Decrease > 50%	0–5 mmHg
Normal 1.5–2.5	Decrease < 50%	5–10 mmHg
Dilated > 2.5	Decrease < 50%	10–15 mmHg
Dilated > 2.5	No change	>15 mmHg

observed. In a healthy subject breathing spontaneously, cyclic changes in intrathoracic pressure, which are transmitted to the right atrial pressure, produce cyclic changes in venous return, yielding an inspiratory decrease in IVC diameter >50%. This cyclic change is reduced or even abolished in some conditions, e.g., cardiac tamponade or severe right ventricular failure.

The IVC size in spontaneously breathing patients, measured slightly distal to the hepatic vein, correlates with right atrial pressure (RAP) (Table 12.2). A low IVC diameter (ˊ1.0–1.2 cm) suggests volume depletion; a high IVC diameter (ˎ2.5 cm) suggests volume overload.

The variations of IVC size can be studied in both spontaneous breathing and ventilated patients.

- The IVC collapsibility index (cIVC) during spontaneous breathing is calculated as the difference between the maximum diameter on expiration and the minimum diameter on inspiration, divided by the maximum diameter and expressed as a percentage: $100 \times (D_{max}$ on expiration $- D_{min}$ on inspiration$/D_{max}$ on expiration). A reduction in IVC diameter of 42% or more is a very accurate predictive marker of fluid responsiveness in spontaneously breathing patients.

- In mechanical ventilation, the inspiratory phase produces an increase in intrathoracic pressure, which is transmitted to right atrial pressure, reducing the venous return. This produces an increase in the volume of the extra-thoracic venous blood, so the diameter of the IVC increases. The IVC dilation will be even greater if the IVC is easily distended as in hypovolemic status. The changes in IVC diameter are reversed compared with those observed during spontaneous breathing; the IVC dilates in inspiration and decreases in expiratory phase. These changes during mechanical ventilation are decreased by vena cava dilatation produced by a high volume status.

- The IVC distensibility index (DIVC) is measured during controlled mechanical ventilation and expressed as a percentage of the

difference between the value of the maximum diameter and the minimum diameter, divided by the minimum: $100 \times (D_{max}$ on inflation $- D_{min}$ on expiration$/D_{min})$. A distensibility index above 18% can predict a significant increase in cardiac output after a blood volume expansion with 90% sensitivity and 90% specificity.

12.3　The Aortic Flow Variations

In spontaneously breathing patients with suspected hypovolemia, stroke volume measurement using echocardiography (the velocity-time integral of aortic blood flow [VTI_{ao}]) before and after passive leg raising (PLR) can accurately discriminate patient who will obtain a hemodynamic benefit from fluid challenge. Variations in VTI_{ao} proved to predict fluid responsiveness in ventilated septic shock even after 100 mL of hydroxyethyl starch infusion (1 min). This finding has been confirmed in ventilated patients, also using smaller amounts of crystalloid solution (50 mL over 15 s).

The PLR test is able to determine changes in blood flow in response to preload manipulations, thus predicting the response to a fluid bolus, without exposing the patient to potential hypervolemia. The method to perform PLR is of utmost importance because it basically affects its hemodynamic effects and reliability. PLR should start from the semi-recumbent position. The trunk is at 45° and then must be lowered, raising the legs at 45°. This induces a gravitational transfer of blood from the lower limbs and splanchnic compartment toward the intrathoracic compartment. The method has the advantage of reversing its effects once the legs are tilted down. The volume of blood transferred to the heart is enough to increase the left cardiac preload, according to the Frank-Starling principle.

The variations of peak aortic velocity (ΔVPeak) during mechanical ventilation in septic patients are a good indicator for fluid responsiveness (Fig. 12.4). Respiratory variations in aortic flow, over one respiratory cycle, are calculated as the difference between the maximum aortic flow velocity and the minimum divided by the mean: [(max velocity − minimum velocity) divided by (max velocity + minimum velocity)/2)] and expressed as a percentage. A ΔVPeak of 12% during mechanical ventilation predicts fluid responsiveness in both adults and children.

Fig. 12.4 TTE, apical five-chamber view, pulsed Doppler imaging at the level of the aortic valve. Respiratory variations in aortic flow. The low speed (25 mm/s) allows visualization of several respiratory cycles
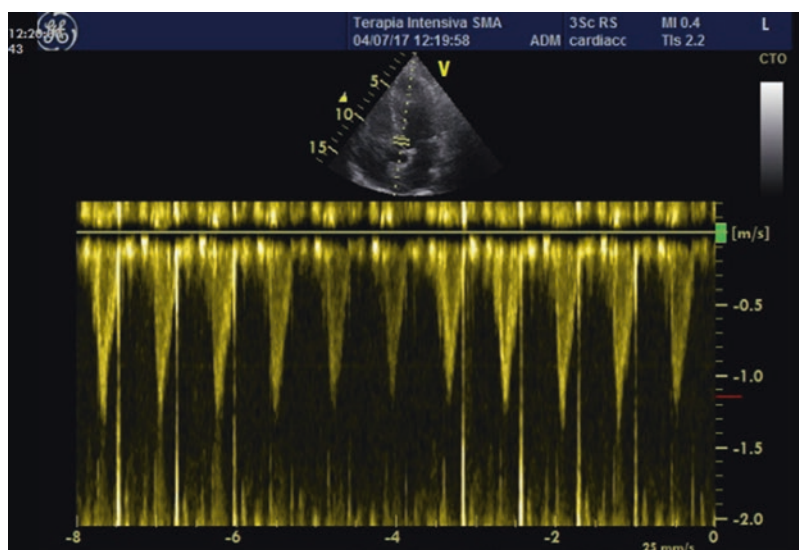
12.3.1 Echocardiography of Aortic Blood Flow

The aortic flow can be assessed by TEE and TTE.

- Using TEE, the aortic blood flow is recorded by Doppler imaging from the transgastric long-axis view at the level of aortic annulus.
- Using TTE, the aortic blood flow is recorded by the apical five-chamber view using pulsed Doppler imaging. The sample box should be placed at the level of the aortic valve, within 1 cm of it, in the LVOT. The patient should be in sinus rhythm (if the patient has atrial fibrillation, multiple consecutive beats [5–10] should be averaged). The patient is placed in the supine position at 45°; the left arm must be raised and brought toward the head, so as to widen the left-sided intercostal spaces. The phased-array probe should be selected.

12.4   Carotid Blood Flow (CBF)

The CBF have been proposed as a marker of volume status and fluid responsiveness. This approach measures the diameter of the carotid and the carotid VTI. The CBF uses the same formula that is utilized to calculate the cardiac output (CO) at the aorta outflow tract: $VTI \cdot \pi/4D^2 \cdot HR$. A variation of CBF greater than 20% after passive leg raising predicts an increase in cardiac output with 94% sensitivity and 86% specificity.

12.4.1 The Carotid Artery Bedside Ultrasound

The patient is placed in the supine position at 30°, with the head rotated away from the ultrasound operator. The carotid flow is measured by using a linear high-frequency transducer, with the vascular preset.

To obtain a clear longitudinal two-dimensional image of the common carotid artery (CCA) and the carotid bulb, the probe is placed transversely over the carotid triangle. After imaging the CCA and the IJV, a compression maneuver will help to differentiate them. Rotating the probe over the CCA, with the marker facing toward the head of the patient, the longitudinal view of the CCA will be displayed. Freezing the image, the internal diameter is measured, 1–2 cm proximal to the bulb. The Doppler sample volume is placed in the middle of the vessel lumen, 1–2 cm proximal to the bulb, while the Doppler beam is adjusted to ensure <60° of angle for the best signal (Fig. 12.5). At least three pulse cycles should be used to calculate the VTI, averaging them.

Fig. 12.5 Carotid artery Doppler flow imaging. The linear array transducer is placed in the long axis over the CCA
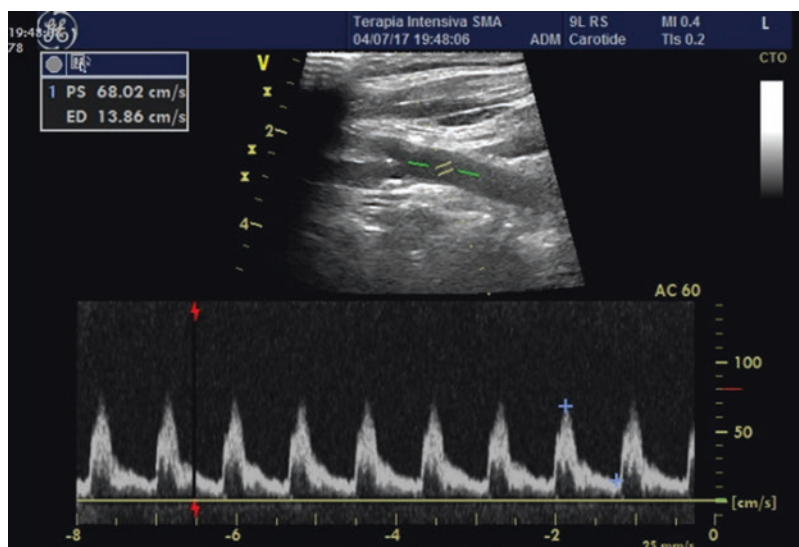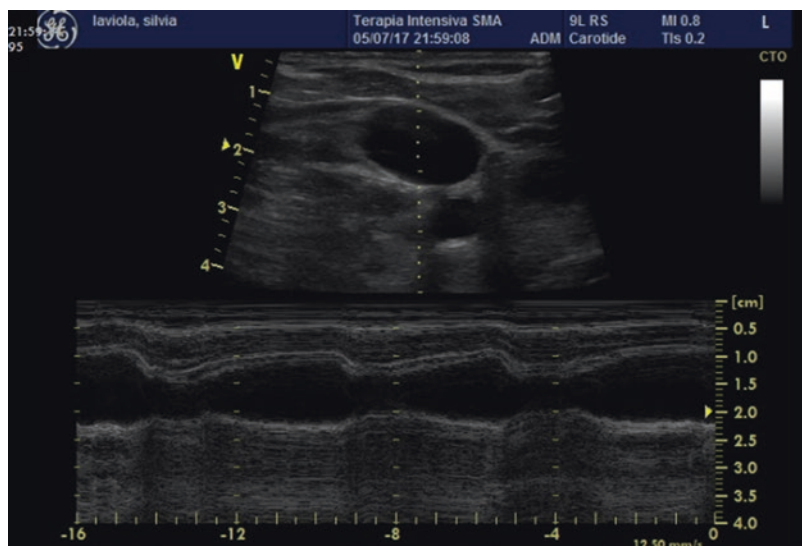
12.5 Right Internal Jugular Vein Distensibility

A new promising method to assess fluid responsiveness, which appears to be a valid alternative to measure IVC's distensibility, is the ultrasound assessment of the distensibility of the right internal jugular vein (RIJV). Particularly in septic patients subjected to invasive ventilation, this approach has shown that a distensibility greater than 18%, before a challenge volume, has 80% sensitivity and 85% specificity to predict the response to fluid challenge.

12.5.1 The Internal Jugular Vein Bedside Ultrasound

The patient is in the supine position at 30°, with head rotation of 30°. A high-frequency probe (5–7.5 MHz), as a linear probe, should be selected.

The linear probe is placed over the neck, perpendicular to the skin and oriented orthogonally to the diameter of the jugular vein in the short axis. The RIJV is displayed in 2D and M-mode at the level of the cricoid cartilage. The anteroposterior diameter is measured by M-Mode during a respiratory cycle (Fig. 12.6).

Further Reading

Cecconi M, De Backer D, Antonelli M, et al. Consensus on circulatory shock and hemodynamic monitoring. Task force of the European Society of Intensive Care Medicine. Intensive Care Med. 2014;40:1795–815.

Feissel M, Michard F, Mangin I, Ruyer O, Faller JP, Teboul JL. Respiratory changes in aortic blood velocity as an indicator of fluid responsiveness in ventilated patients with septic shock. Chest. 2001;119:867–73.

Feissel M, Michard F, Faller JP, Teboul JL. The respiratory variation in inferior vena cava diameter as a guide to fluid therapy. Intensive Care Med. 2004;30:1834–7.

Guarracino F, Ferro B, Forfori F, Bertini P, Magliacano L, Pinsky MR. Jugular vein distensibility predicts fluid responsiveness in septic patients. Crit Care. 2014;18:647.

Marik PE, Levitov A, Young A, et al. The use of bioreactance and carotid Doppler to determine volume responsiveness and blood flow redistribution following passive leg raising in hemodynamically unstable patients. Chest. 2013;143:364–70.

Veillard-Baron A, Chergui K, Rabiller A, Peyrouset O, Page B, Beauchet A, Jardin F. Superior vena caval collapsibility as a gauge of volume status in ventilated septic patients. Intensive Care Med. 2012;30:1734–9.

Ischemia and Myocardial Infarction

13

Ferdinando Luca Lorini, Marialuigia Dello Russo, and Elena Pagani

13.1 Introduction

The echocardiogram is a standard tool in the evaluation and treatment of patients with acute myocardial infarction (AMI). The role of echocardiography is to establish the diagnosis, location, and extent of myocardial infarction, to diagnose mechanical complications of infarction, and to provide prognostic information important for risk stratification and short- and long-term outcome. A 2003 task force of the American College of Cardiology, the American Heart Association, and the American Society of Echocardiography gave a class I recommendation for the use of echocardiography in the diagnosis of suspected acute ischemia or infarction not evident by standard means, but did not recommend echocardiography when the diagnosis was already apparent. The task force recommended against the routine use of echocardiography for diagnosis of chest pain in patients with electrocardiographic changes diagnostic of myocardial ischemia or infarction.

13.2 Diagnosis of AMI

The diagnosis of AMI is typically based upon the:

- History and symptoms
- Electrocardiogram
- Cardiac enzymes, particularly serum troponins and myocardial-bound creatine kinase

Although not routinely performed for diagnosis, echocardiography is an accurate, noninvasive test that is able to detect evidence of myocardial ischemia or necrosis. Severe ischemia produces regional wall motion abnormalities (RWMAs) that can be visualized echocardiographically. The RWMAs reflect a localized decrease in the amplitude and rate of myocardial excursion, as well as a blunted degree of myocardial thickening. Since ischemic RWMAs develop prior to symptoms, chest pain in the absence of RWMAs should not be due to active myocardial ischemia. However, the converse is not true; the presence of RWMAs does not establish the diagnosis of ischemia. There are a number of other causes of RWMAs, including a prior infarction, focal myocarditis, prior surgery, left bundle branch block, ventricular preexcitation via an accessory pathway, and cardiomyopathy.

F. L. Lorini (✉) · M. Dello Russo
Department of Anesthesia and Intensive Care Medicine, ASST Papa Giovanni XXIII, Bergamo, Italy
e-mail: llorini@asst-pg23.it

E. Pagani
Department of Anesthesia and Intensive Care Medicine, Azienda Ospedaliero-Universitaria Pisana, Pisa, Italy

13.3 Role of Echocardiography in Ischemic Heart Disease

The use of echocardiography in ischemic heart disease is based upon the rapid change in wall motion of a segment after an interruption or critical decrease in its blood supply. This phenomenon occurs within a few seconds of the onset of coronary occlusion, just after the onset of diastolic abnormalities and many seconds before electrocardiographic changes and angina. Experimental and clinical studies have shown that wall motion abnormalities have a high sensitivity for predicting myocardial infarction. Other studies, performed in the emergency department on patients evaluated for myocardial ischemia, have reported similar results. An important aspect is that necrosis does not cause necessary wall motion abnormalities; therefore, echocardiography can also be used to identify patients with ischemia without infarction. Importantly, the sensitivity is significantly higher than that for electrocardiography and is comparable to that for myocardial perfusion imaging. Transthoracic echocardiography (TTE) is often underutilized in this setting. TTE has the advantages of being readily accessible, portable, noninvasive, and fast; it may detect significant findings that are misdiagnosed or not detected on initial clinical evaluation. Although TTE has been most commonly used for evaluation of regional wall changes, transesophageal echocardiography (TEE) is an alternative, more invasive technique that may be of particular importance during surgery or in the patient with inadequate transthoracic echocardiographic images. As an example, the continuous high-quality imaging of the left ventricle afforded by TEE during surgical procedures makes it ideally suited for the early detection of ischemia. These intraoperative changes in wall motion are more predictive of postoperative ischemia or infarction than ECG changes or hemodynamic abnormalities as documented with Swan-Ganz catheter measurements, such as an increase in pulmonary capillary wedge pressure (PCWP). Echocardiography is a valuable, noninvasive diagnostic tool that can provide information about systolic function and valvular abnormalities and can provide alternative explanations for the causes of chest pain, such as aortic dissection, aortic stenosis, cardiac tamponade, pericarditis, and hypertrophic cardiomyopathy.

13.4 Evaluation of Regional Wall Motion

The abnormalities in wall motion associated with ischemia are characterized by:

- Diminished or absent inward endocardial motion
- Impaired systolic myocardial thickening (in the normal condition, it is greater than 30%)

TEE is highly sensitive for the detection of acute ischemia and is therefore used extensively for real-time monitoring of regional wall motion as well as global left ventricular (LV) function. Basic routine echocardiography views allow imaging of the anterior, inferior, posterior, and lateral walls from different locations in the heart (from the base of the heart in the plane of the mitral valve to the apex). Echocardiographic signs of ischemia/infarction are the following:

- Wall motion abnormalities (hypokinetic, akinetic)
- The left ventricle might have a reduced ejection fraction, with a negative correlation between EF < 40% and the short- to long-term outcome
- Mechanical complications of infarction (ischemic mitral regurgitation, ventricular septal defect, myocardial rupture)

The location of the wall motion abnormality correlates well with the involved coronary artery (Fig. 13.1):

1. Inferior wall motion abnormality is a sign of infarction involving the posterior descending artery of the right coronary artery or the distal left circumflex artery—seen best on the short-axis view and the parasternal long-axis view.
2. Septal, apical, and anterior wall motion abnormality is a sign of infarction involving
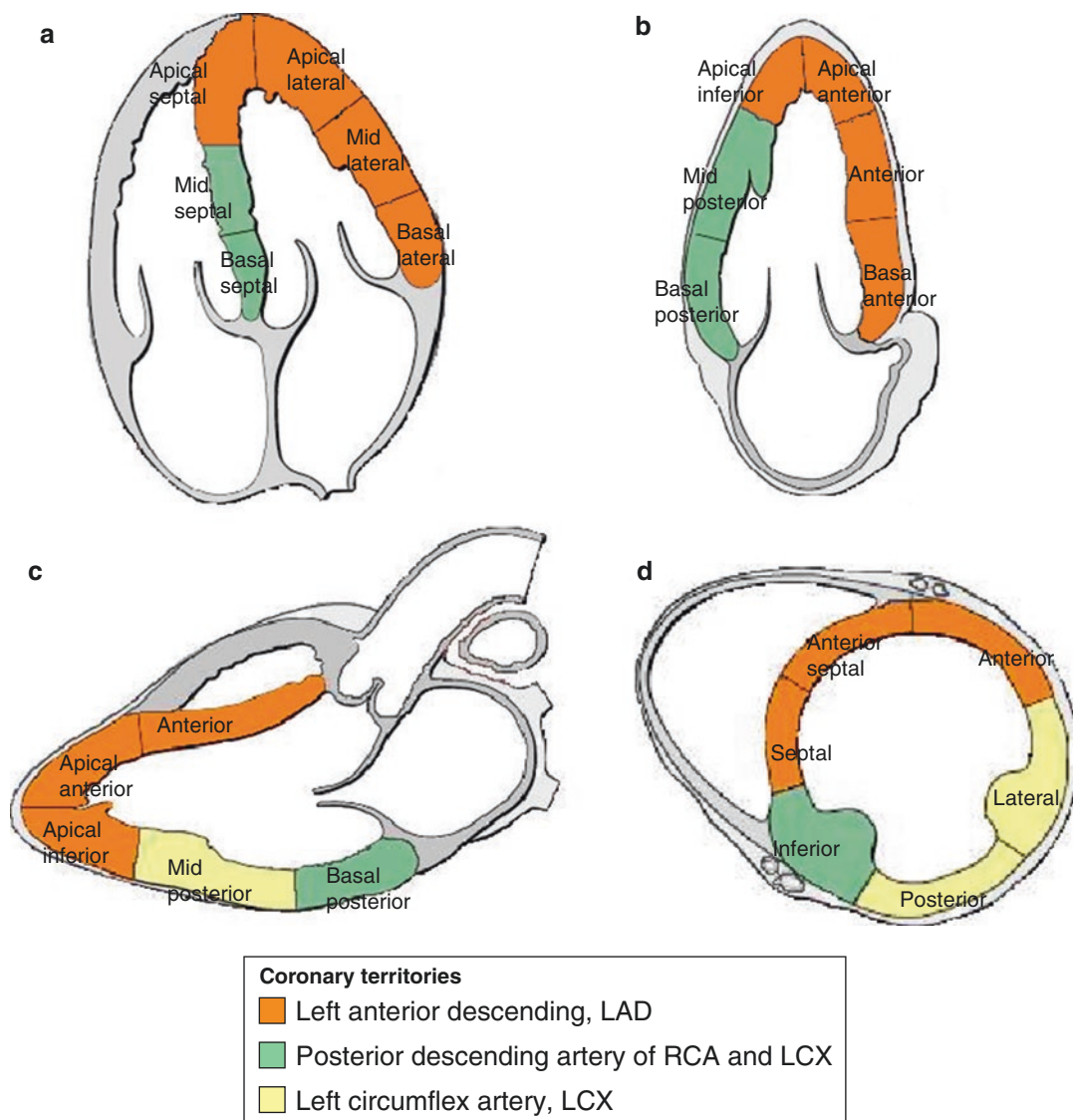
Fig. 13.1 Exemplificative scheme of main TTE views and coronary distribution: (**a**) Apical four-chamber view. (**b**) Apical two-chamber view. (**c**) Left parasternal long-axis view. (**d**) Short-axis view

the left anterior descending artery—seen best on the short-axis view and the four-chamber view.

3. Lateral and posterior wall motion abnormality is a sign of infarction involving the circumflex artery—seen best on the short-axis view.

As an adjunct to other techniques, M-Mode can be used after AMI, but it has a limitation in the analysis of RWMA, being able to evaluate

only two walls (anterior septum and posterior wall). Moreover, no information is obtainable on evidence and magnitude of LV global systolic dysfunction.

Contrast echocardiography is a challenging technique that needs further development and standardization. Its advantage is that it provides the possibility to measure myocardial perfusion at the bedside giving precious information as the nuclear perfusion imaging does.

13.5 Transthoracic Echocardiography

The main TTE views used for evaluation of AMI and RWMA are as follows:

1. Four-chamber view: septum and lateral wall (Fig. 13.2a)
2. Two-chamber view: inferior (left of display) and anterior (right of display) walls (Fig. 13.2b)
3. Parasternal short-axis view: all walls at the papillary level (Fig. 13.2c)
4. Parasternal long-axis view: septum and posterior wall (Fig. 13.2d)

13.6 Transesophageal Echocardiography

The TEE views most widely used for evaluation of AMI and RWMA (Fig. 13.3) are as follows:

1. Mid-esophageal four-chamber view
2. Mid-esophageal two-chamber view
3. Mid-esophageal long-axis view
4. Four transgastric mid short-axis view

The standard transesophageal LV short-axis view (horizontal plane) is obtained by the transgastric view at the level of the papillary muscle tips. At this level, the myocardium is supplied by all three major coronary vessels and can be divided into four or six segments for standardization purposes: anterior, anterolateral, inferolateral, inferior, inferoseptal, and anteroseptal (Fig. 13.3).

13.7 Echocardiography and Complications of AMI

Papillary muscle rupture is an infrequent but often fatal mechanical complication of AMI (Fig. 13.4). Despite its rarity, it is an important cause of severe mitral regurgitation usually proceeding to heart failure and, if not corrected, to cardiogenic shock and eventually death. Echocardiography is one of the noninvasive imaging assessment techniques that can identify
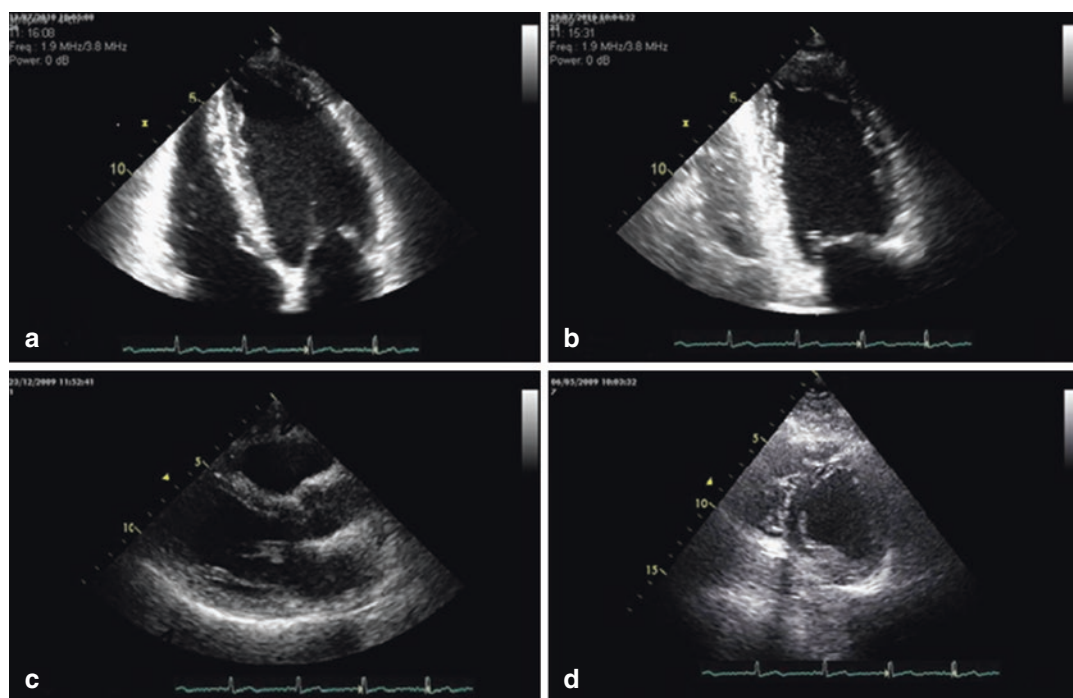
Fig. 13.2 Main TTE views used for evaluation of AMI. Four chamber (**a**), two chamber (**b**), parasternal short axis (**c**), parasternal long axis (**d**)

Four chamber view

Two chamber view

Long axis view

Mid short axis view

Basal short axis view

Basal segments
1. Basal anteroseptal
2. Basal anterior
3. Basal lateral
4. Basal posterior
5. Basal inferior
6. Basal septal

Mid segments
7. Mid anteroseptal
8. Mid anterior
9. Mid lateral
10. Mid posterior
11. Mid inferior
12. Mid septal

Apical segments
13. Apical anterior
14. Apical lateral
15. Apical inferior
16. Apical septal

Fig. 13.3 TEE views most widely used for evaluation of AMI and RWMA and selective study of 16 segments of LV
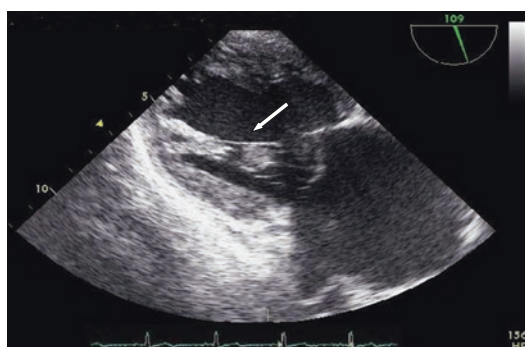
Fig. 13.4 TEE transgastric long-axis view of LV. Arrow shows papillary muscle rupture, an acute complication of AMI

mechanical complications such as acute mitral regurgitation in the setting of AMI, and it allows precise location of the papillary muscle rupture and leaflet involvement and evaluation of the modality and entity of mitral regurgitation and hemodynamic complications. TTE has an important role in diagnosing mechanical acute complications during AMI and in the decision-making for patients with sudden onset of hemodynamic compromise. Echocardiography is the imaging technique of choice for detecting complications of acute infarction, including myocardial free wall rupture, acute ventricular septal defect, and mitral regurgitation secondary to papillary mus-

cle rupture or ischemia. TTE is able to identify a papillary muscle rupture with a diagnostic sensitivity of 65–85%, but TEE is more sensitive. TTE is particularly useful in showing complications of ruptured papillary muscle such as the "flail" of mitral flaps and the papillary stump interested by the prolapsing rupture in the left atrium.

Echocardiography is also an important tool to evaluate the characteristics that are linked directly to the short- and long-term outcome of the patient:

- Standard Doppler of the mitral valve and evaluation of the diastolic pattern, knowing that a restrictive filling pattern detected early after AMI is a recognized predictor of adverse outcome.
- MR and PASP.

13.8 Assessment of Myocardial Ischemia and Viability Using Tissue Doppler and Deformation Imaging

The accurate evaluation of LV regional systolic function remains an important goal in clinical echocardiography. As explained before, conventional evaluation of LV regional function using two-dimensional echocardiography is based on the subjective assessment of endocardial excursion and myocardial thickening. However, it is mostly related to the negative effect of poor image quality, which makes interpretation difficult and observer variability high. Recent advances in ultrasound technology have enabled us to acquire regional myocardial velocities, strain, and strain rate using the tissue Doppler imaging (TDI) technique. They potentially offer new and unique ultrasonic parameters to describe the regional deformation properties of myocardial tissue, which could reveal new information about myocardial structure and function.

In echocardiography, the term "strain" is used to describe local shortening, thickening, and lengthening of the myocardium as a measure of regional LV function. Conventional assessment of contractile function is based on the measure-

ment of the transmural thickening and does not provide information regarding the transmural distribution of contractile performance. Strain in the myocardium can be measured by tissue Doppler imaging (TDI) or by speckle-tracking echocardiography (STE). The theoretical basis for measuring strain by TDI is that myocardial velocity gradient is an estimate of strain rate, and natural strain can be calculated as the temporal integral of strain rate. Speckle-tracking echocardiography utilizes the phenomenon in which natural acoustic markers in grayscale ultrasound images form interference patterns (speckles) within myocardial tissue. Strains are calculated from each LV segment in circumferential, longitudinal, or radial directions. TDI and strain rate imaging have been introduced as quantitative methods for assessing myocardial function and have been shown to overcome the limitations of current ultrasound methods for assessing the complex changes in regional myocardial function that occur in different ischemic substrates. TDI analyzes in real-time endocardial and epicardial velocities and measures the myocardial velocity gradient, which is an index of myocardial deformation. Reduction of TDI e' occurs early in myocardial ischemia. e' velocity is reduced in the segments supplied by a stenotic artery, and E'/e' negatively correlates with the number of vessels with significant stenosis. Strain/strain rate imaging has been shown to be a sensitive technique for quantifying regional myocardial deformation compared with other cardiac imaging modalities. Strain and strain rate are measures of changes in shape and therefore represent deformations. Strain, represented by the symbol ε, is a dimensionless index that refers to the amount of tissue deformation normalized to its original shape. It can be written mathematically as

$$\varepsilon = \frac{L - L0}{L0}$$

where L is the length of the myocardium after deformation and $L0$ is its original length. By convention, strain is defined as positive when the distance between the points of measurement is increasing (i.e., lengthening), whereas shortening

is represented by negative strain. When strain is acquired at the LV apex, normal LV myocardium has a negative strain in systole and a positive strain in diastole in the longitudinal direction. Strain and strain rate imaging have also been applied recently in the assessment of left atrial function. When strain is acquired at the LV apex, the left atrium has a positive strain in ventricular systole and a negative strain during ventricular diastole. Strain rate is the first derivative of strain or the speed at which deformation (i.e., strain) occurs. Strain rate can also be considered as the velocity gradient between two points in the myocardium. When strain rate is acquired at the LV apex, normal ventricular myocardium has a negative strain rate in systole and a positive strain rate during diastole (Fig. 13.5). The left atrium has a positive strain rate in ventricular systole and a negative strain rate during ventricular diastole. Peak strain, peak systolic strain, and strain rate

are the more commonly used parameters. Peak strain is the maximum strain which may occur during LV ejection (defined as the interval between aortic valve opening and closure). Strain and strain rate imaging have been shown to be able to differentiate between transmural and non-transmural infarcts. Patients with transmural infarction show significantly lower circumferential and longitudinal strain and strain rate compared with those with subendocardial infarct, with no significant differences in radial strain. In myocardial infarction, transmural extension of scar distribution in the infarct zone is proportionally related to the reduction in systolic function measured by the radial transmural velocity gradient or by strain rate imaging. Measurement of both systolic and postsystolic deformation both at rest and during a graded dobutamine infusion may help to distinguish between transmural and non-transmural infarcts. Although TDI
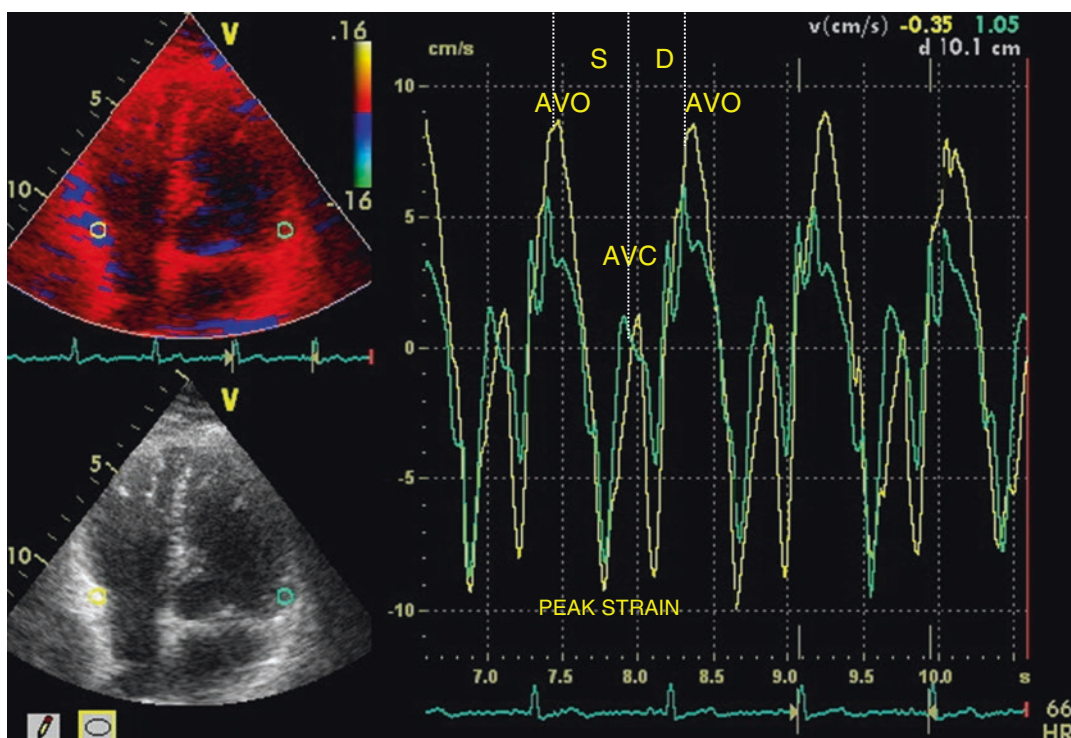
Fig. 13.5 Strain and strain rate imaging by tissue Doppler imaging. The panel is the strain rate at the basal septal wall of the left (green) and right (yellow) ventricle. Note the negative strain rate in systole (S) and the positive strain rates during diastole (D). In this example, the peak systolic strain is about 10% which occurs during LV ejection defined as the interval between aortic valve opening (AVO) and closure (AVC)

measurement of regional function by peak systolic ejection velocity is easy to perform, reproducible, and validated, and regional function is typically reduced during ischemia, many experimental studies have demonstrated its limited ability to differentiate between different grades of ischemic dysfunction and to distinguish ischemic from postischemic dysfunction. This important limitation of TDI is related to the fact that velocities in one myocardial segment are determined by function in other segments as well, which is due to tethering between segments and cardiac translational motion. Importantly, these measurements are angle dependent because radial strain has opposite polarity of longitudinal and circumferential strains. Furthermore, similar to all measures of myocardial fiber shortening, systolic strain is load dependent, and therefore, blood pressure should be considered when interpreting measurements of strain. Other sources of variation in strain are age and gender.

In conclusion, strain imaging has the ability to evaluate regional myocardial function. Strain rate has not replaced conventional grayscale imaging in the assessment of regional LV function, and the implementation of these new indices in routine clinical practice will need additional clinical and large-scale studies.

Suggested Readings

Cheitlin MD, Armstrong WF, Aurigemma GP, et al. ACC/AHA/ASE 2003 guideline update for the clinical application of echocardiography: summary article. A report of the American College of Cardiology/AmericanHeart Association Task Force on Practice Guidelines (ACC/AHA/ASE committee to update the1997 guidelines for the clinical application of echocardiography). J Am Soc Echocardiogr. 2006;16(10):1091–110.

Chen X, Nakatani S. Transmural myocardial strain gradient: a new and robust quantitative index of left ventricular wall motion based on myocardial strain imaging. Echocardiography. 2011;28(2):181–7.

Greaves SC. Role of echocardiography in acute coronary syndromes. Heart. 2010;88(4):419–25.

Kadappu KK, Thomas L. Tissue Doppler imaging in echocardiography: value and limitations. Heart Lung Circ. 2015;24:224–33.

Leung DY, Arnold CT. Emerging clinical role of strain imaging in echocardiography. Heart Lung Circ. 2010;19:161–74.

Muttreja MR, Mohler ER 3rd. Clinical use of ischemic markers and echocardiography in the emergency department. Echocardiography. 1999;16(2):187–92.

Prastaro M, Pirozzi E, Gaibazzi N, et al. Expert review on the prognostic role of echocardiography after acute myocardial infarction. J Am Soc Echocardiogr. 2017;30:430–43.

Smiseth OA, Torp H, Opdahl A, et al. Myocardial strain imaging: how useful is it in clinical decision making? Eur Heart J. 2016;37:1196–207.

The Cardiomyopathies

14

Ferdinando Luca Lorini, Alessandra Rizza,
and Francesco Ferri

14.1 Introduction

The cardiomyopathies are a heterogeneous group
of disease of the myocardium. Historically in the
WHO/International Society and Federation of
Cardiology classification of 1996, cardiomyopa-
thies were defined as primary disorders of
unknown cause. Heart muscle diseases of known
cause or associated with systemic disorders were
classified as secondary. However, this distinction
between primary and secondary heart muscle dis-
ease has become redundant, as the cause of previ-
ously idiopathic disorders has been discovered.
Recently the American Heart Association pro-
posed that cardiomyopathies are "myocardial
diseases associated with mechanical and/or elec-
trical dysfunction that usually—but not invari-
ably—exhibit inappropriate ventricular
hypertrophy or dilatation and are due to a variety
of causes that are frequently genetic." The
American Heart Association panel also suggested
that ion channelopathies and disorders of con-

duction should be considered cardiomyopathies
as well because channel mutations alter
biophysical properties and protein structure,
thereby creating structurally abnormal ion chan-
nel interfaces and architecture. The AHA defini-
tion and classification are scientific schemes that
help in the understanding of these complex disor-
ders, but are not useful for clinical diagnosis in
the clinical setting. The European Society of
Cardiology (ESC) has then assumed that the clin-
ically most useful method for diagnosing and
managing the cardiomyopathies is a classifica-
tion in which heart muscle diseases are grouped
according to ventricular morphology and func-
tion. The ESC has defined cardiomyopathies as
"myocardial disorders in which the heart muscle
is structurally and functionally abnormal, in the
absence of coronary artery disease, hypertension,
valvular disease and congenital heart disease suf-
ficient to cause the observed myocardial abnor-
mality." The ESC classification is meant to be
particularly useful in everyday clinical practice.
The ESC classification consists of the following
categories:

- Hypertrophic cardiomyopathy (HCM)
- Dilated cardiomyopathy (DCM)
- Restrictive cardiomyopathy (RCM)
- Arrhythmogenic right ventricular (RV) car-
  diomyopathy (ARVC)
- Unclassified, e.g., left ventricular (LV)
  noncompaction

F. L. Lorini (✉) · F. Ferri
Department of Anesthesia and Intensive Care
Medicine, ASST Papa Giovanni XXIII,
Bergamo, Italy
e-mail: llorini@asst-pg23.it; fferri@asst-pg23.it

A. Rizza
Department of Anesthesia and Intensive Care
Medicine, Ospedale Pediatrico Bambino Gesù,
Rome, Italy

The cause of each cardiomyopathy is taken into account by replacing the traditional division of primary and secondary by a new division into familial (or genetic) and nonfamilial (nongenetic). The nonfamilial category is subdivided into idiopathic cause and acquired cardiomyopathies in which LV dysfunction is a complication of another disorder (e.g., myocarditis, drugs, pregnancy, endocrine disorders, tachycardiomyopathy).

The MOGE(S) classification for a phenotype-genotype-based nomenclature of cardiomyopathy was endorsed by the World Heart Federation and published in 2013. This proposed system was inspired by the TNM staging of malignant tumors and does not include ion channelopathies. The clinical applicability of this system is debated. The acronym MOGE(S) is derived from the five elements this classification is made of:

- The morphofunctional (M) notation is a descriptive phenotypic diagnosis (e.g., MD = dilated cardiomyopathy).
- The organ involvement (O) notation describes if heart and/or extracardiac involvement related to the cause of heart disease is present (e.g., OH + K = heart and kidney involvement).
- The genetic or familial inheritance (G) notation indicates the nature of genetic transmission (e.g., GAD = autosomal dominant).
- The etiological annotation (E) provides description of the specific genetic cause/mutation.
- The functional status (S) term is optional and described with the New York Heart Association (NYHA) functional class.

Recent studies evaluated if MOGE (S) classification could have a prognostic value.

There is no ideal classification; however, from an echocardiographic point of view, the classification based on structure and function is the most useful. This chapter will describe HCM, DCM, RCM, ARVC, and LV noncompaction according to the ESC classification.

14.2 Hypertrophic Cardiomyopathy

HCM is clinically defined in the presence of LV hypertrophy and in the absence of hypertension and valve disease. LV hypertrophy occurs in 1 out of 500 of the general population, and this incidence includes all kinds of hypertrophy. HCM is a familial disease with an autosomal pattern of inheritance, caused by mutations in genes encoding for sarcomeric proteins, usually resulting in an asymmetrical pattern of LV hypertrophy; HCM could also be secondary to glycogen and lysosomal storage disorders, mitochondrial diseases, or cardiac amyloidosis (CA).

The echocardiographic diagnostic criteria in HCM include:

1. Left ventricular hypertrophy evaluation. In individuals with suspected HCM and in their relatives, a complete evaluation of all left ventricular (LV) segments from base to apex should be performed. Measurements of LV wall thickness (WT) must be obtained at end-diastole and in short-axis views at mitral valve level, at the base of papillary muscles, and at the apex, so that the follow-up could be performed more precisely. LV thickness, evaluated at the septum and free wall level, is considered abnormal when it is greater than 15 mm (Fig. 14.1) and an unexplained maximal wall thickness ≥13 mm in first-degree relatives of patients with HCM. A value greater than 30 mm is a risk factor for sudden cardiac death. The distribution of hypertrophy may be anterior septal, anterior and posterior septal, posterior basal wall, or apical (e.g., in Japanese people). The most common pattern in HCM is the asymmetrical thickening of the interventricular septum. The LV thickness is defined as asymmetrical when there is a septal to free wall thickness ratio between 1.3 and 1.5.
2. Systolic function. Usually ejection fraction (EF) or fractional shortening (FS) are normal or even increased due to preserved radial contractile function. However, longitudinal strain (LS) values using speckle tracking
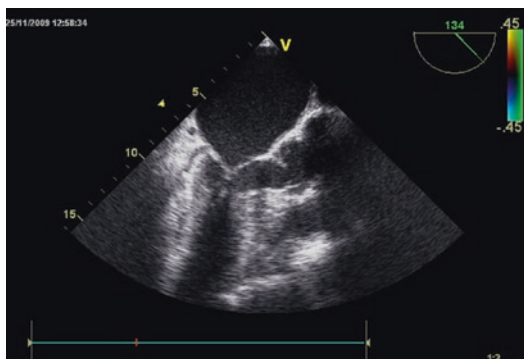
Fig. 14.1 Asymmetrical hypertrophy in hypertrophic cardiomyopathy
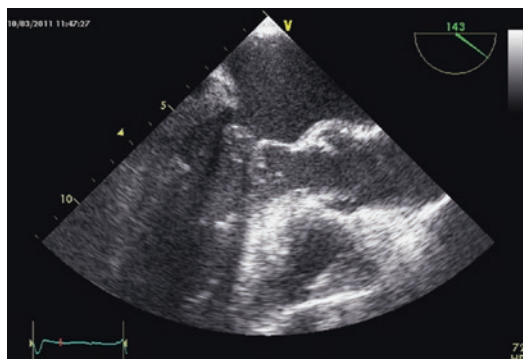
Fig. 14.2 SAM in HCM

echocardiography have been reported to be decreased. While in the initial phase of the HCM EF is normal, later on 5–10% of patients develop a burn-out phase in which LV dilates, wall thickness regresses, and EF decreases. This seems to be due to diffuse myocardial ischemia secondary to microvascular dysfunction leading to fibrosis replacement.

3. Systolic anterior motion (SAM) of the mitral valve. SAM is characterized by an abrupt anterior movement of the mitral valve in systole (Fig. 14.2), reaching its peak before maximum movement of the posterior wall (this characteristic allows one to differentiate true SAM from "pseudo SAM," which is produced by an exaggerated anterior motion of the mitral valve and reaches its peak after the full contraction of the posterior wall). A Venturi effect is thought to be responsible for dragging the anterior mitral leaflet into the LV outflow tract (LVOT). The severity of SAM is correlated with the severity of LVOT obstruction: incomplete SAM (when the anterior mitral leaflet fails to contact the interventricular septum) and complete SAM (when the anterior mitral leaflet contacts the IVS). Exercise echocardiography can help in the assessment of the dynamic component of SAM.

4. Pressure gradient across the LVOT. This gradient may be variable, because obstruction is dynamic; it should be quantified from the apical five-chamber and three-chamber view using CW Doppler. A value of 30 mmHg or greater has physiological consequences and is associated with progression to New York Heart Association classes III–IV and death from heart failure or stroke, especially in patients aged over 40 years. It is generally accepted that obstruction becomes hemodynamically relevant when it is ≥50 mmHg.

5. Dynamic mitral regurgitation. Mitral regurgitation is a consequence of SAM which induces abnormal mitral leaflet coaptation. The evaluation of the presence and degree of mitral regurgitation is performed by color Doppler echocardiography. The regurgitant jet is usually posteriorly directed, and an anterior or central jet may occur in the presence of an intrinsic mitral valve disease due to annular (calcification), chordae (anomalous insertion, fibrotic reaction), papillary (secondary to hypertrophy, to anterior and basilar displacement of the anterolateral papillary muscle, to insertion of anterolateral papillary muscle directly into the mid-anterior mitral valve leaflet), or leaflet disease (excessive tissue and elongated leaflets, prolapse, leaflet mismatch, calcification) (Fig. 14.3).

6. Small LV cavity. Mid-cavity obstruction may occur owing to muscular apposition in a small LV cavity, with excessive hypertrophy of the mid-ventricle and papillary muscles.

7. Diastolic dysfunction. Almost all patients with HCM have some degree of LV diastolic dysfunction. The mechanisms linked to
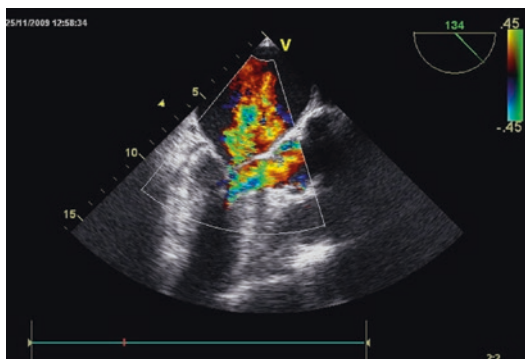
Fig. 14.3 Mitral regurgitation and SAM in HCM

diastolic dysfunction are complex and include altered contraction and relaxation of sarcomeric protein, altered sensitivity to calcium, disarray of and increased amount of extracellular matrix, increased wall thickness, and ischemia.

Diastolic dysfunction is assessed by the analysis of both transmitral spectral Doppler flow velocity (E) and mitral annular velocity (E'). Transmitral blood flow is represented by an early E wave and a late A wave on pulsed wave Doppler echocardiography, isovolumic relaxation is slowed, the rate of rapid filling is diminished, and the atrial contribution to filling is increased, as well is LV stiffness. Unfortunately in HCM, the E wave varies with preload and does not correlate well with LV hypertrophy. Tissue Doppler imaging (TDI) provides more accurate evaluation of diastolic dysfunction. Early diastolic mitral annular velocities are significantly reduced, and the ratio of transmitral velocity E/E' is higher and appears to correlate with New York Heart Association functional class. The ratio of early transmitral (E) to tissue Doppler early diastolic (e') velocities of the lateral mitral annulus accurately quantifies LV pressures, in particular before atrial contraction; $E/e' > 14$ showed the best sensitivity and specificity for identifying pre-capillary wedge pressure greater than 15 mmHg. However, that ratio shows only a modest correlation when related to mean left atrial pressure, although this parameter identifies patients with low exercise capacity. TDI has been investigated in the preclinical diagnosis of HCM,

but additional data are needed to determine TDI velocity values that provide the highest diagnostic accuracy.

Two-dimensional speckle tracking echocardiography and 3D echocardiography are not routine diagnostic exams, but can help in adding morphologic information and in the risk stratification of the patient. Two-dimensional (2D) speckle tracking echocardiography during the last few years has gained attention because of its clinical and prognostic implications in cardiomyopathies and hypertrophic cardiomyopathy (HCM) in particular. Reduced global longitudinal strain is associated with more severe disease and a higher risk for major cardiac events, independently of other clinical and echocardiographic risk factors. Left ventricular dyssynchrony also seems promising as a risk factor for sudden cardiac events.

Differential diagnosis of HCM includes:

- LV hypertrophy due to hypertension: LV hypertrophy in HCM is asymmetrical, whereas that of LV hypertrophy caused by hypertension has a concentric appearance.
- LV hypertrophy in athletes: The criteria that may be utilized to support the diagnosis of pathological HCM are LVOT obstruction, impaired diastolic function, enlarged left atrium, family history, left bundle branch block, and ST-segment depression.

The management of HCM, in addition to b-blockers, includes surgical septal myectomy (if the LVOT gradient is greater than 50 mmHg) or percutaneous alcohol septal ablation. The abnormal insertion of papillary muscle may contribute to mitral regurgitation, requiring a more extended septal myectomy or mitral valve replacement. Intraoperative echocardiography is used to check:

- Residual gradient across the LVOT
- Iatrogenic ventricular septal defect
- SAM of the mitral valve
- Residual mitral regurgitation

To note, global longitudinal strain rate does not seem to normalize after myectomy or septal

alcohol ablation, because it probably reflects more accurately the underlying molecular damage of the disease.

Echocardiography can provide important information for the appropriate diagnosis of HCM; however, it cannot distinguish conditions based on myocyte hypertrophy from those in which LV mass and wall thickness are increased by interstitial infiltration or intracellular accumulation of metabolic substrates. Cardiac magnetic resonance imaging may help in the diagnosis, even if the final diagnosis in some specific conditions can only be obtained by myocardial biopsy.

Fig. 14.4   Dilated LV in dilatative cardiomyopathy

14.3   Dilated Cardiomyopathy

Dilated cardiomyopathy (DCM) is a primary myocardial disease characterized by different degrees of LV dysfunction and dilatation in the absence of chronic increased afterload (e.g., aortic stenosis or hypertension) or volume overload (e.g., mitral regurgitation). Although there are many different causes of DCM, in most cases, it is idiopathic. DCM may be a final consequence of a variety of pathways, such as hypertension, ischemia, severe valvular disease, myocarditis, endocrine or congenital heart disorders, toxins, chemotherapy, and LV noncompaction. In the absence of these etiological factors, DCM may occur as a result of gene mutations. Echocardiography not only facilitates evaluation of strict diagnostic criteria but also provides us with a comprehensive assessment of cardiac anatomy, pathophysiological changes, and hemodynamics. The following are the echocardiographic features of DCM:

- Ventricular dilatation. The left ventricle is considered dilated if its end-diastolic volume is more than 117% of the predicted value, corrected for age and body surface area (Fig. 14.4).
- Severe ventricular dysfunction. Typically LV fractional shortening is less than 20% and LV ejection fraction is less than 35%.

- Functional mitral regurgitation with a central jet.
- Dilatation of the mitral annulus associated with an increase of the annulus dimensions.
- Tethering of both mitral leaflets by displaced papillary muscles. The degree of tethering is reflected in the angle between each leaflet and the annular plane, the height between the annular plane and leaflet point of coaptation, and the tenting area bordered by the annular plane and the two leaflets.
- Functional tricuspid regurgitation secondary to RV dilatation, RV dysfunction, or pulmonary hypertension. Peak TR velocity of more than 2.5 m/s is associated with increased mortality, increased hospitalization, and higher incidence of heart failure.
- Stress echo and contractile reserve. Assessment of contractile reserve by low-dose dobutamine stress echocardiography has a prognostic value. An increase in LV EF from rest to peak stress by ≥5% or a percentage change from baseline of ≥20% indicates the presence of contractile reserve and is associated with a better prognosis.

The differential diagnosis of DCM includes ischemic heart disease and primary mitral valve disease: in both conditions, there is a low ejection fraction, but in DCM there is a dilated mitral annulus, abnormal papillary muscle angle, leaflet tethering, and absence of severe leaflet disease (e.g., rheumatic disease, flail, or prolapse).

14.4   Restrictive Cardiomyopathy

RCM is characterized by increased stiffness of the myocardium, normal or reduced ventricular diastolic volumes, normal or mildly increased wall thickness, and preserved systolic function. Unlike the other cardiomyopathies, which are classified according to morphological criteria, RCM is a functional classification. The classic echocardiographic features include:

- A small (not dilated neither hypertrophied) left ventricle
- Marked dilatation of both atria (Fig. 14.5)
- Normal systolic function in the absence of a pericardial disease
- Mild to moderate mitral and tricuspid valve regurgitation
- Increased pulmonary pressures
- Pulmonary venous flow showing a blunted S wave and pronounced diastolic and atrial waves (with sinus rhythm)
- A restrictive filling pattern, as transmitral velocity is characterized by a rapid but ill-sustained ventricular filling on pulsed wave Doppler echocardiography (E wave), little or no late ventricular filling (A wave), an E/A ratio greater than 2, and the deceleration time of the E wave shortened to less than 150 ms. However, as in the case of HCM, transmitral velocity in the early stage of RCM is reduced; when compliance of the heart decreases, the left atrial pressure increases, leading to pseudonormalization of the diastolic pattern
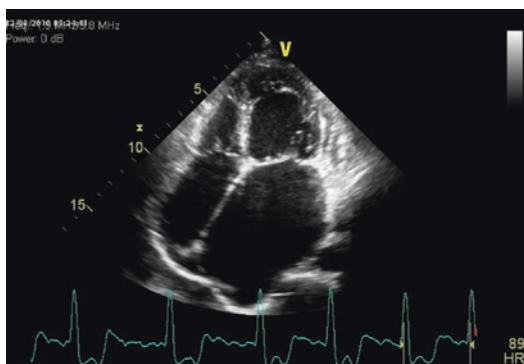
and then to a restrictive pattern. The early mitral tissue Doppler velocity may be a more reliable guide to LV filling pressure as the E/E' ratio increases with the severity of the disease. In RCM—unlike in constrictive pericarditis—E' is blunted and this reduction is consistent with the finding that RCM is a disease of the myocardium.

Systemic amyloidosis is a disorder of protein metabolism in which abnormal extracellular protein material is deposited in organs and tissue. Primary amyloidosis involves the heart in 90% of cases, and cardiac amyloidosis is the commonest cause of RCM: interstitial infiltration of the atria and ventricles leads to a firm and rubbery consistency of the myocardium. Secondary amyloidosis only rarely affects the heart. The echocardiographic features of cardiac amyloidosis include thickened RV and LV walls, granular or "sparkling" appearance of the myocardium, normal-sized or small LV, enlarged atria, depressed LV systolic and diastolic function, mild mitral regurgitation, restrictive pattern of E/A, high E/e' ratio suggestive of elevated filling pressures, and pericardial effusion in advanced disease. Tissue Doppler echocardiography can contribute to the earlier diagnosis of amyloid infiltration of the heart. Peak systolic and early diastolic mitral annular velocities, as well as myocardial velocity gradients (strain rate) in systole and early diastole, are equally reduced in patients with or without a restrictive pattern of transmitral Doppler velocities.

Three-dimensional echocardiographic imaging is not part of the routine examination and is still investigational, but can provide additive information. In RCM, such as amyloidosis, 3D echocardiography allows for determination of temporal and regional characterization of LV dyssynchrony and deformation (LV strain).

14.5   Arrhythmogenic Right Ventricular Cardiomyopathy

ARVC is an autosomal dominant inherited disease linked to mutations in genes encoding for

specialized intercellular adhesion junctions known as desmosomes and thus is mechanistically distinct from either HCM or DCM. The original descriptions of ARVC focused on the fatty replacement in the right ventricle. Replacement infers that the muscle develops normally and subsequently undergoes dysplastic degeneration with replacement of muscle by fibrous scarring and fatty tissue. The histology is characterized by an unusual distribution of fatty and fibrotic tissue within the right ventricle, preferentially affecting the apex, the inflow tract, and the outflow tract. There is important histologic evidence of fibrofatty involvement of the left ventricle in 30–75% of ARVC cases. All tissue abnormalities should be quantified by morphometry to allow a precise classification. Myocardial biopsy is not suggested because of the patchy distribution of the disease (biopsies are most often obtained from the RV septum, while diseased tissue is most often located to the RV-free wall).

ARVC is a syndrome characterized by myocardial disease, predominantly involving the right ventricle and associated with ventricular tachycardia arising from this chamber, syncope, and sudden death. Classic symptoms include palpitations, cardiac syncope, and aborted cardiac arrest due to ventricular arrhythmias. Heart failure may develop in later stages.

Three phases have been described in ARVC disease:

1. Early "concealed phase": patients are often asymptomatic, but are at risk of ventricular arrhythmias and sudden cardiac death.
2. "Electrical phase": patients present with symptomatic arrhythmias, and RV morphological abnormalities may or may not be detectable.
3. Diffuse, progressive disease: right, left, or biventricular heart failure, often combined with ventricular arrhythmias.

The progression of ARVC is characterized by periodic bursts and "hot phases." The disease progression is facilitated by environmental factors, such as exercise and inflammation.

The intrinsic difficulties in making a diagnosis of ARVC are evident from the existence of the task force criteria. Current Task Force Criteria for ARVC diagnosis (revised in 2010) combine diagnostic criteria from six categories, including repolarization or depolarization abnormalities on electrocardiography (ECG), presence of ventricular arrhythmias, morphological and functional changes, histopathology, family history, and genetic findings. Criteria are classified as major and minor criteria for ARVC. Combinations of findings establish diagnostic grades of "definite," "borderline," or "possible" ARVC. ECG may be useful, but only in the appropriate clinical context. Major criteria include Epsilon waves or inverted T waves in the right precordial leads in individuals older than 14 years in the absence of right bundle branch block. Minor criteria include inverted T waves in V1 and V2 in individuals older than 14 years of age (in the absence of complete RBBB) or in V4, V5, or V6 and inverted T waves in leads V1, V2, V3, and V4 in individuals older than 14 years of age in the presence of a complete RBBB.

Early diagnosis by echocardiography is difficult, because of the irregular shape and trabeculation of the normal right ventricle. However, some echocardiographic features suggestive of ARVC have been showed and are included in the major criteria:

- RV and RV outflow tract dilatation (>32 mm in the PLAX RVOT window or >36 mm in the PSAX RVOT window)
- Trabecular derangement
- Global RV dysfunction with right ventricle fractional area change less than 33%
- RV regional wall motion abnormality, especially of the apex and anterior wall
- Focal RV aneurysms

Echocardiographic assessment in ARVC requires considerable expertise given the complex geometry of the right ventricle, the lack of standard reference views, and the load dependence of RV function. RV function can be further assessed by strain echocardiography, even though it is not included in the diagnostic criteria of the

task force. Both RV and LV function by strain echocardiography are reduced in ARVC.

The differential diagnoses to consider are pulmonary hypertension, atrial and ventricular septal defects with left-to-right shunt, right ventricular myocardial infarction, dilated cardiomyopathy, and myocarditis. Furthermore, sarcoidosis is a well-known phenocopy of ARVC and may share potential mechanistic links.

14.6 Left Ventricular Noncompaction

LV noncompaction is a sarcomeric cardiomyopathy. Sporadic or familial adult forms are genetically distinct from X-linked infantile cases, and they are transmitted by an autosomal dominant trait. The reported prevalence is 0.014–0.05%. The major clinical manifestations in patients with reduced LV function include heart failure, arrhythmias (atrial fibrillation, ventricular tachyarrhythmias, sudden cardiac death, and Wolff–Parkinson–White syndrome in pediatric patients), and systemic embolic events. The diagnosis is often delayed (3.5–5.7 years).

Echocardiography is considered the reference standard for the diagnosis. The current criteria were developed by various groups and the features include:

- Absence of coexisting cardiac abnormalities by definition
- Morphology: typical two-layered structure of the myocardium with a thin, compacted epicardial band and a much thicker, noncompacted endocardial layer consisting of trabecular meshwork with deep endocardial spaces
- Multiple ventricular trabeculations, prominent in the middle and apical segments (Fig. 14.6)
- Predominant segmental location of the abnormality (noncompacted myocardium greater than 80%) found in the apical and mid-ventricular regions of both inferior and lateral walls
- Color Doppler evidence of deeply perfused intertrabecular recesses (not communicating
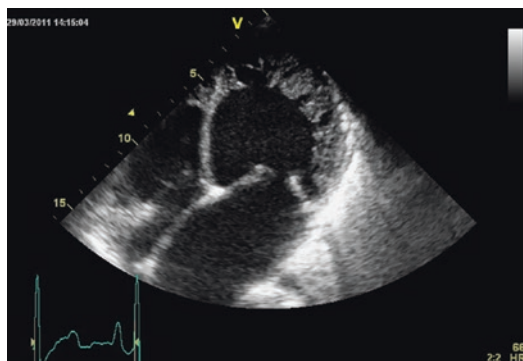
Fig. 14.6 LV noncompaction

with the coronary circulation, unlike for myocardial sinusoids)

The role of contrast echocardiography has been highlighted by multiple studies in the literature, even though its use is not part of the routine evaluation. The use of contrast echocardiography allows:

1. Identification of intertrabecular recesses
2. Identification of LV thrombi
3. Delineation of the entire length and depth of trabeculations
4. Improved localization of compacted segments

Strain analysis has proven useful in the assessment of NCCM: reduced strain values can be detected both in patients with preserved EF and impaired systolic function. This evaluation could detect impending systolic dysfunction and identify patients with increased risk of arrhythmias and sudden cardiac death.

Suggested Readings

Arbustini E, Narula N, Dec GW, et al. The MOGE(S) classification for a phenotype-genotype nomenclature of cardiomyopathy: endorsed by the World Heart Federation. J Am Coll Cardiol. 2013;62:2046–72.

Chebrolu LH, Mehta AM, Nanda NC. Noncompaction cardiomyopathy: the role of advanced multimodality imaging techniques in diagnosis and assessment. Echocardiography. 2017;34:279–89.

Dominguez F, González-López E, Padron-Barthe L, et al. Role of echocardiography in the diagnosis and management of hypertrophic cardiomyopathy. Heart. 2018;104:261–73.

Elliott P, Andersson R, Arbustini E. Classification of the cardiomyopathies: a position statement from the ESC working group on myocardial and pericardial disease. Eur Heart J. 2008;29:270–6.

Haugaa KH, Haland TF, Leren IS, et al. Arrhythmogenic right ventricular cardiomyopathy, clinical manifestations, and diagnosis. Europace. 2016;18:965–72.

Kaski JP, Elliott P. The classification concept of the ESC working group on myocardial and pericardial diseases for dilated cardiomyopathy. Herz. 2007;32:446–51.

Losi A, Nistri S, Galderisi M. Echocardiography in patients with hypertrophic cardiomyopathy: usefulness of old and new techniques in the diagnosis and pathophysiological assessment. Cardiovasc Ultrasound. 2010;8(7):1–19.

Maron BJ, Towbin JA. Contemporary definitions and classifications of the cardiomyopathies: an AHA scientific statement from the Council on Clinical Cardiology, Heart Failure and Transplantation Committee. Circulation. 2006;113:1807–16.

Nihoyannopoulos P, Dawson D. Restrictive cardiomyopathies. Eur J Echocardiogr. 2009;10:23–33.

Patrick T, Calum A, et al. Arrhythmogenic right ventricular cardiomyopathy. Heart Fail Clin. 2010;6:161–77.

Thomas DE, Wheeler R, Zaheer R, et al. The role of echocardiography in guiding management in dilated cardiomyopathy. Eur J Echocardiogr. 2009;10:iii15–21.

Cor Pulmonale and Pulmonary Hypertension

15

Ferdinando Luca Lorini, Lorenzo Grazioli, and Angelo Vavassori

15.1 Cor Pulmonale and Pulmonary Hypertension

Cor pulmonale is a condition in which there is a right ventricular enlargement secondary to a lung disorder that produces pulmonary arterial hypertension. Right ventricular (RV) failure may follow this type of condition. Cor pulmonale may be acute or chronic.

A lung disorder can cause pulmonary hypertension by several mechanisms:

- Loss of capillary bed
- Vasoconstriction (hypoxia, hypercapnia)
- Hypertrophy of arterioles in the pulmonary vessel tree

In this condition, echocardiography is a useful method for evaluation of RV function and pulmonary hypertension.

In the first phase there is only pulmonary hypertension, but with the progression of the disorder, right-sided heart failure can occur with

worsening of P_{O2} and P_{CO2} and peripheral edema. However, it has been demonstrated that in the subclinical period, COPD patients can develop the initial signs of RV failure before pulmonary hypertension.

Pulmonary hypertension complicating chronic respiratory disease, particularly COPD, is generally defined by a mean pulmonary artery pressure (PAP) greater than 20 mmHg, which is slightly different from the definition of idiopathic pulmonary arterial hypertension (mean PAP >= 25 mmHg).

Echocardiography is an important tool to identify and classify pulmonary hypertension and its degree.

15.2 Common Right Ventricular Measurements

Estimation of RV function is not so well codified as that of LV function because of the complex shape of the right ventricle—triangular when viewed from the front and a crescent wrapping partway around the left ventricle when viewed in the transverse section; the septum in the normal condition is an arch into the right ventricle both in systole and in diastole.

The right ventricle is divided into three parts: inflow tract (starting with the tricuspid valve), apex, and infundibulum (ending with the pulmonary valve). RV diameter (RVD) is the first

F. L. Lorini (✉) · L. Grazioli
Department of Anaesthesia and Intensive care, ASST Papa Giovanni XXIII, Bergamo, Italy
e-mail: llorini@asst-pg23.it; lgrazioli@asst-pg23.it

A. Vavassori
Department of Anaesthesia and Intensive care, ASST Lecco, Lecco, Italy
e-mail: a.vavassori@asst-lecco.it

measurement we perform. It is necessary to use a four-chamber view and to measure, in diastole, in the middle of the RV cavity the distance between the free wall and the septum.

The diameter of the right ventricle measured in the middle of the cavity is normally 2.7–3.3 cm. In patients with COPD, we can observe enlargement of the right ventricle. We can observe this by measuring the transverse mid-cavity diameter in the four-chamber view. This parameter is also useful for determination of right-sided heart failure, in which there is a further increase in diameter respect who have only pulmonary hypertension (Image 15.1).

The normal wall thickness (measured in diastole) is less than 5 mm; a greater thickness indicates RV hypertrophy and may suggest pressure overload.

Guidelines suggest acquiring the wall thickness using the subcostal four-chamber view and excluding epicardial fat (Image 15.2).

RV fractional area change (RV FAC) is the percentage variation between the RV end-diastolic area and the RV end-systolic area.

RV FAC is calculated as (end-diastolic area – end-systolic area)/ end-diastolic area*100.

This parameter is well correlated with MRI-derived RV ejection fraction.

In this case, the cutoff for RV myocardial dysfunction is 35%. The limitation of this method is the difficulty recognizing of endocardial border delineation.

Tricuspid annular plane systolic excursion (TAPSE) is a parameter which indicates the systolic displacement of the tricuspid annular plane; it is the expression of the RV longitudinal function. To obtain TAPSE, we need to use M-mode on the lateral tricuspid annulus in the four-chamber view. A value greater than 15 mm is correlated with normal systolic function, and a value below 8 mm is correlated with significant RV dysfunction; there is also a relation between TAPSE and RV ejection fraction (Table 15.1).

In COPD patients, TAPSE represents an independent risk factor for mortality, with a cutoff of 14 mm, and doubling of the TAPSE value is correlated with a reduction of mortality of 26% (Image 15.4).

Limitations are represented by the load and angle dependency.

Important in the definition of pulmonary hypertension is the estimation of systolic pulmonary artery pressure (PAPs) through the tricuspid
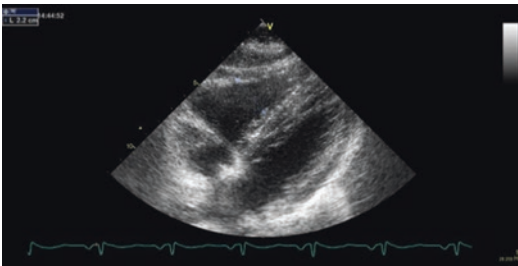
Image 15.1 Right ventricular diameter (RVD)
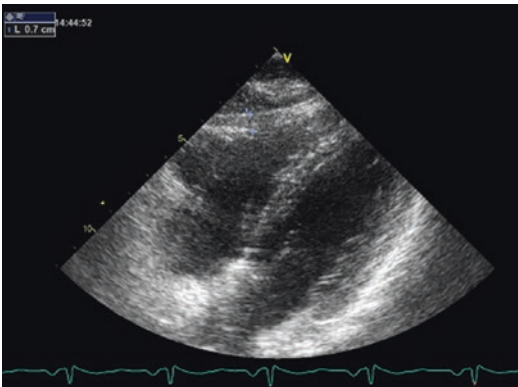
Image 15.2 Right ventricle wall thickness
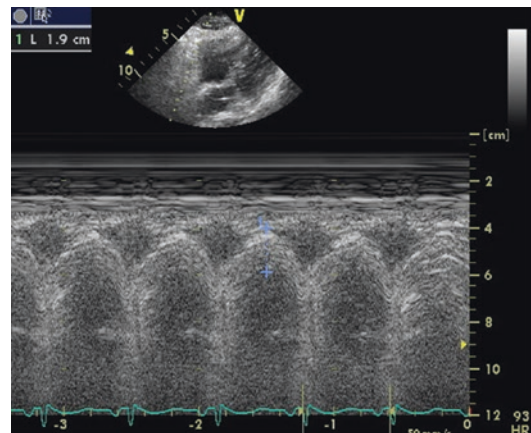
Image 15.3 Calculation of TAPSE (in red)

Table 15.1 Relation between TAPSE and RV ejection fraction

TAPSE mm	EF%
5	20
10	30
15	40
20	50
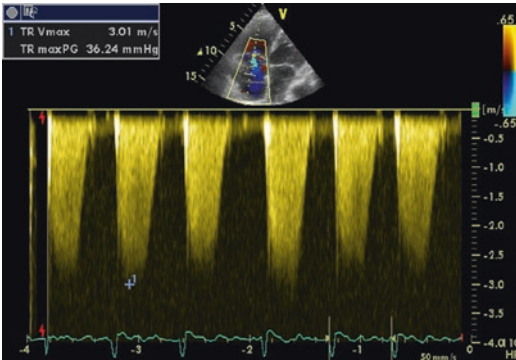
Image 15.4 For calculation of PAPs sum tricuspid gradient with atrial pressure

regurgitation with a simplified Bernoulli equation: PAPs = $(4*V^2 + $ RA pressure), where V (m/s) is the peak velocity of the regurgitant jet (Image 15.4).

Estimated RV and PA systolic pressure are the same in absence of RVOT obstruction or pulmonic valve stenosis.

We need to use a four-chamber view and continuous Doppler echocardiography of tricuspid regurgitation.

The estimation of systolic PAP is based on the peak tricuspid regurgitation velocity taking into account right atrial pressure (RAP).

For extubated patient without invasive monitoring, RAP can be estimated on the diameter and respiratory variation of the inferior vena cava (IVC):

1. An IVC diameter <2.1 cm that collapses >50% with a sniff suggests a normal RA pressure of 3 mmHg (range 0–5 mmHg)
2. An IVC diameter >2.1 cm that collapses <50% with a sniff or <20% on quiet inspiration suggests a high RA pressure of 15 mmHg (range 10–20 mmHg)

In critically ill patient, RAP can be estimated through measuring IVC diameter or evaluating IVC Doppler.

The European guidelines for the diagnosis and treatment of pulmonary hypertension consider three levels of probability the echocardiographic diagnosis of pulmonary hypertension:

- *Low probability* when peak tricuspid regurgitation velocity is less than 2.8 m/s (or systolic PAP is less than 36 mm Hg).
- *Intermediate probability* if peak tricuspid regurgitation velocity is less than 2.8 m/s but with other echocardiographic sign of PH or with a peak tricuspid regurgitation velocity between 2.9 and 3.4 m/s (or systolic PAP is between 37 and 50 mmHg) alone.
- *High probability* if peak tricuspid velocity is between 2.9 and 3.4 m/s (or systolic PAP is between 37 and 50 mmHg) with other echocardiographic sign of PH or if peak tricuspid velocity is >3.4 m/s (or systolic PAP is greater than 50 mm Hg) alone.

As echocardiographic signs suggesting pulmonary hypertension in addition to tricuspid regurgitation velocity measurement, the guidelines consider:

- Category A
  - Right ventricle/left ventricle basal diameter ratio >1.0
  - Flattening of the interventricular septum (left ventricular eccentricity index >1.1 in systole and/or diastole)
- Category B:
  - Right ventricular outflow Doppler acceleration time <105 msec and/or mid-systolic notching
  - Early diastolic pulmonary regurgitation velocity >2.2 m/sec
  - Pulmonary Artery diameter >25 mm
- Category C:
  - Inferior cava diameter >21 mm with decreased inspiratory collapse (<50% with a sniff or <20% with quiet inspiration)
  - Right atrial area (end systole) >18 cm^2

Echocardiographic signs from at least two different categories of the list should be present to alter the level of probability.

Major limitations occur in the case of severe tricuspid regurgitation or when the right ventricle is unable to generate enough pressure through the pulmonary artery, falsely underestimating the PA systolic pressure.

Because the estimation of the pressure is angle-dependent, to minimize the risk of error, the measurement has to be acquired in multiple views to be sure of using the maximum velocity.

Diastolic pulmonary pressure can be estimated by the Bernoulli equation applied to the velocity of the end-diastolic pulmonary regurgitant jet as follows: [pulmonary artery diastolic pressure = 4 * (end-diastolic pulmonary regurgitant velocity)^2 + right atrial pressure].

There are a lot of methods which can be used to estimate mean PAP by sampling the pulmonary valve regurgitation or by use of empirical formulas. A simple method which correlates well with catheter measurements has been described recently. The mean systolic gradient (between the right atrium and the right ventricle) is calculated by tracing the tricuspid regurgitation velocity-time integral.

Mean PAP = right atrial pressure + mean systolic gradient.

15.3 Advanced Right Ventricular Measurements

The function of the right ventricle can be investigated by use of novel technique such as tissue Doppler imaging (TDI), strain, and strain rate. With this type of imaging, the Doppler focus is on the myocardium and not on blood.

15.3.1 Tissue Doppler Imaging

TDI reveals the velocity of the myocardium in a region of interest, in our case, the right ventricle. The use of TDI allows us to study the right ventricle in a way that is less preload dependent compared with the conventional methods.

The conventional approach is the four-chamber view.

There are two types of TDI: pulse-based and color-based.

Pulse-based TDI is simpler to use but has poor spatial resolution owing to the movement of the heart. We can record the maximum instantaneous velocity.

Color-based TDI has better spatial resolution and enables us to analyze the waves offline and also to acquire measurements simultaneously.

It has poorer temporal resolution than pulse-based TDI, but increasing the frame rate (more than 120–150 frames per second) makes the acquisition acceptable. Other limitations are the insonation angle and translational myocardial motion.

The values we sample with color-based TDI are mean values, and on average, the values are 25% lower than those obtained by pulse-based TDI.

With TDI, we can see five distinct waveforms:

1. Isovolumic contraction time velocity: early systole; above or below the baseline.
2. Systolic peak (S^1): during RV mechanical systole, pulmonary valve opening; always above the baseline.
3. Isovolumic relaxation time velocity: early diastole (end of T wave); it can be above or below the baseline.
4. Early diastolic wave (E^1): during RV relaxation; it is usually under the baseline.
5. Late diastolic wave (A^1): represents atrial contraction (just after the P wave on ECG), always under zero (Image 15.5).

These parameters are considered at the tricuspid annulus; it is important to keep the basal

Image 15.5 TDI waves
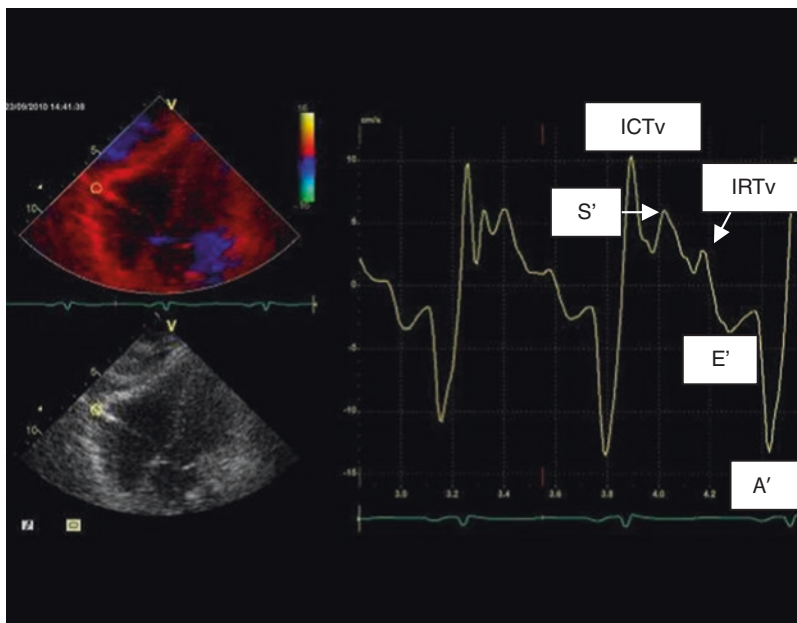
segment and the annulus aligned with the Doppler cursor to avoid velocity underestimation. Similar to TAPSE, S^1 is measured relative to the transducer and may therefore be influenced by overall heart motion.

In particular, S^1 obtained on the tricuspid annulus measures the longitudinal peak velocity of excursion, showing good correlation with radionuclide angiography right ventricular ejection fraction.

The septum should not be considered alone for the study of the right ventricle because it is not only linked to RV function.

A simple and reproducible measurement is that of the systolic peak; the cutoff used is 10 cm/s. Below this limit, there is suggestion of RV failure.

We consider the systolic peak at the annular free wall and measure it with pulsed TDI. Lower velocities are found for the mid and apical zones of the right ventricle, and the velocity can be lower with increasing age.

Color-based TDI measurements have lower velocities, but more studies are required before they can be used as a guideline.

In particular, in a study on COPD patients, the cutoff for RV failure was 9.2 cm/s, with a sensitivity of 80% and a specificity of 62%. There was also good correlation with conventional parameters such as RV diameter and systolic PAP.

Despite TDI of the free wall is not considered in normal clinical practice because of the high variability of the signal a S^1 velocity <9.5 cm/sec measured on the free wall side indicates RV systolic disfunction.

The disadvantage is that it is load-dependent and could not represent the global RV function.

S^1 can be also measured with color-based TDI; in this case, the reference value is 25% less.

Another parameter is the isovolumic acceleration (IVA), which is obtained by dividing the isovolumic velocity or the isovolumic contraction time velocity by the acceleration time (from the baseline to the peak of the isovolumic velocity).

IVA has to be sampled on the tricuspid annulus. In COPD patients, IVA is impaired and is correlated with the forced expiratory volume in the first second and with the severity of the disease.

The cutoff is quite variable in the literature, the value depending on the control population, COPD without right-sided heart failure, and COPD with right-sided heart failure.

Image 15.6 Calculation of IVA (by color –TDI waves) in red acceleration time, in white 0 line
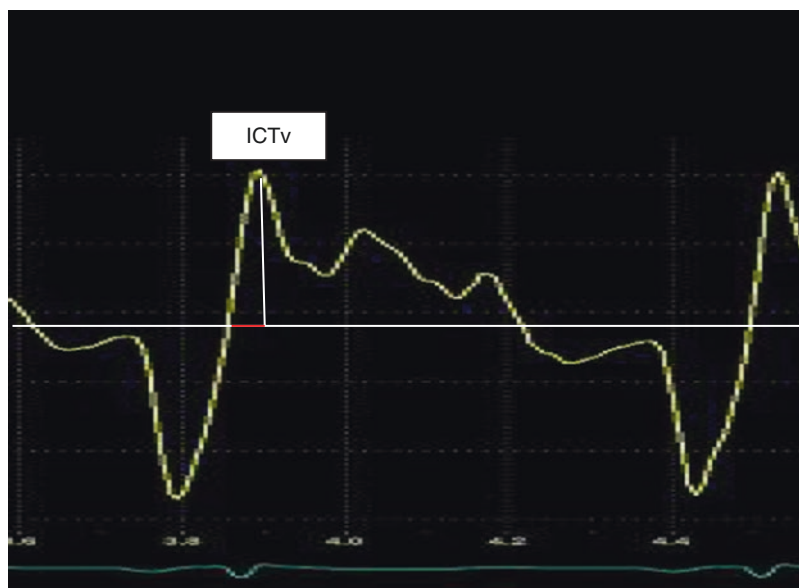
However, with pulsed TDI, a value under 1.9 m/s^2 reveals a COPD patient with right-sided heart failure with 82% sensitivity and 77% specificity; in the literature, there is not an univocal range for the lower limit of this parameter because of its variability with age.

We can consider only the range for a homogeneous population as a reference.

The color-based TDI IVA reference value is 20% lower than the pulse-based TDI value.

IVA is not affected by the loading condition and reflects RV contractility but is dependent on age and is influenced by heart rate (Image 15.6).

Is it possible to evaluate diastolic RV function.

The early, rapid filling phase of diastole is represented by the E-wave. The E-wave acceleration time reflects right ventricular relaxation. Atrial contraction occurs in late diastole and is represented by the A-wave. The early diastolic tissue Doppler velocity, commonly denoted as e', represents right ventricular relaxation. Increased E/e' ratios represent increased right ventricular filling pressures. In adults, E/e' ratios <15 are considered normal.

With normal diastolic function, the early filling velocity is higher than the atrial contraction velocity; therefore, reversal of the E/A ratio (<0.8) with increased deceleration time represents impaired ventricular relaxation.

An accentuated relationship of the rapid filling and the atrial contraction velocities (E/A > 2.1) with decreased deceleration time (<120 ms) represents restrictive physiology – a late phase of diastolic dysfunction. Short deceleration time helps discern between normal diastolic function and "pseudo-normalization" – the intermediate phase of diastolic dysfunction characterized by preserved E/A relationship (E/A ratio between 0.8 and 2.1 with E/e' ratio >6). Increased deceleration time is directly associated with tau in subjects with pulmonary arterial hypertension.

15.3.2 Strain, Strain Rate, and Speckle Tracking

Strain is defined as the change of distance between two points divided by the initial length: (L–L0)/L0. It is expressed as a percentage; conventionally, shortening or thinning has a negative value, and lengthening or thickening has a positive value.

Strain rate is the first derivative of strain and represents the change of velocity between two points divided by the distance between them. The unit of measure is reciprocal seconds. These parameters are derived from TDI. Acquisition of

the images usually has to be performed in the four-chamber view at high frame rate (more than 150 frames per second). Strain is influenced by the presence of pulmonary hypertension. Systolic strain is closely related to stroke volume and contractility.

Strain can be sampled on the tricuspid annulus, on the free wall, or on the apex. Strain and strain rate have higher values for the apical segment.

Strain and strain rate are angle-dependent, and the angle should be under 30° from the beam direction.

There is a novel technique—2D speckle tracking—that is relatively angle-independent and also is less influenced by the frame rate and the quality of the image; for this reason, 2D speckle tracking echocardiography (STE) strain becomes the method of choice.

The use of deformation imaging implies a great progress in echocardiography, as it allows assessment of segmental myocardial specific motion (i.e., longitudinal, radial, and circumferential motions; twist and rotation).

Strain imaging was initially developed as an extension of the Doppler velocity imaging. However, given the angle dependence of Doppler imaging, only longitudinal strain could be measured.

The more recently developed STE is a grayscale-based technique which is angle-independent and hence permits more comprehensive assessment of myocardial deformation.

As we know, a grayscale image on echocardiography is composed of several bright speckles that are produced as a result of the scatter of the ultrasound beam by the tissue.

The STE software identifies these speckles and then tracks them frame-by-frame using a "sum-of-the absolute-differences" algorithm. From this data, the software automatically resolves the magnitude of myocardial deformation in different directions and generates strain and strain rate curves.

The longitudinal strain is measured from the apical long-axis images, whereas the short-axis images are used for measuring radial and circumferential strain and rotation. Since STE utilizes grayscale images, the strain derived by STE is also known as two-dimensional strain, to differentiate it from the Doppler-based strain.

Speckle tracking overcomes most of the limitations inherent in conventional echocardiography, given that it is independent of cardiac translation; also it is angle- and load-independent, thus allowing accurate quantification of regional and global myocardial function.

Speckle tracking echocardiography (STE) is particularly useful for the diagnosis and management of various right heart diseases, such as right heart failure, pulmonary artery hypertension, arrhythmogenic right ventricular dysplasia, and congenital heart disease.

The peak systolic strain (at the end of the T wave on ECG) is maximum in a normal subject, decreases in pulmonary hypertension patients, and decreases further if the right ventricle is decompensated.

The systolic wave correlates well with the regional ejection fraction.

Dysfunction of the right side of the heart starts early in the COPD patient, and strain and strain rate can detect it.

The normal longitudinal strain value for the basal fraction of the right ventricle is about −27%, and for the free wall, it is −29% (± 9.9%) with regional strain.

COPD and pulmonary hypertension decrease the wave (more positive) of peak systolic wall strain in particular on the free wall (Image 15.7).

Also strain rate correlates well with the contractility of the right ventricle. It has the advantage of not being load-dependent like strain.

In particular, systolic wall strain rate (reference from −1.5 ± 0.41 to −2.23 ± 0.91) worsens in COPD patients and worsens further in cor pulmonale patients (Image 15.8).

A reduced value of strain is correlated with prognosis and RV performance in PH patients.

Strain can be measured in long axis using global longitudinal strain (GLS) calculated as the average from all six segments (basal free wall, mid-free wall, apical free wall, basal septum, mid septum, and apical septum) as a measure of global RV function.
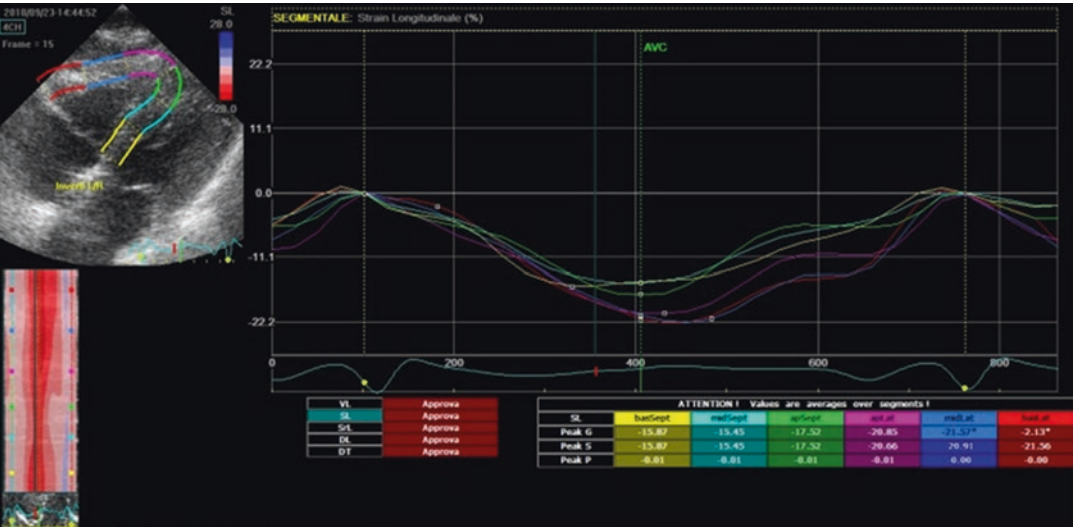
Image 15.7 Peak systolic strain (obtain by analysis of 2D strain)
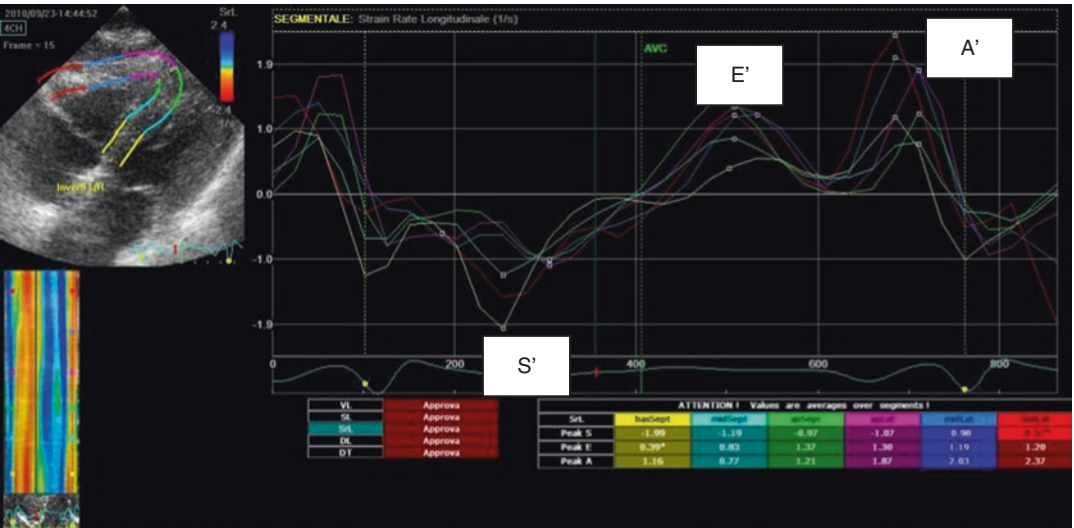
Image 15.8 SR imaging E',A',S' (peak systolic strain rate) obtain by analysis of 2D strain

Patients with pulmonary arterial hypertension (PAH), a global longitudinal strain >−19.4% allows identification of patients at high risk of adverse cardiovascular events.

15.3.3 Myocardial Performance Index or Tei Index

The myocardial performance index (MPI) is a useful method to assess the systolic and diastolic function of the right ventricle. To calculate the MPI, we can sample time intervals using pulsed Doppler echocardiography or TDI: MPI = (isovolumic relaxation time + isovolumic contraction time)/ejection time.

With pulsed Doppler echocardiography, the ejection time is measured from the onset to the cessation of the flow for the RV outflow tract. The sum of the isovolumic relaxation time and the isovolumic contraction time is the time between the E wave and the A wave of the next

beat, seen on tricuspid valve Doppler, minus the ejection time. The parasternal long-axis view is recommended for visualization of both the pulmonary valve and the tricuspid valve.

More user-friendly is the calculation of the MPI from TDI because we do not need to acquire the image of the two valves.

The upper reference of the MPI calculated with pulsed wave Doppler echocardiography is 0.43, and with TDI, it is 0.54. Patients with pulmonary hypertension and decompensation of the right side of the heart have values above these limits.

The disadvantage of this method is that it is load-dependent and is not useful in arrhythmia such as atrial fibrillation and when right atrial pressure is high.

The use of this tool is, however, recommended as a complement of other methods for evaluation of the right ventricle.

15.4 Three-Dimensional Echocardiography

The RV is unique from a functional standpoint with the inflow and outflow sections contracting perpendicularly to each other.

RV inflow contracts longitudinally, the RV outflow is circumferential.

Using full-volume image acquisition, the entire RV may be visualized and does not require geometric assumptions, which is often a problem with traditional methods.

Literature is growing and 3D echo appeared to have a good correlation with MR imaging, in particular semiautomated.

3D echocardiography can be used especially to evaluate RV end-diastolic volume, end-systolic volume, and RV ejection fraction.

In particular, 3D echo is useful in post-cardiotomic patients where conventional assessment of longitudinal function may not be reflective of global function.

Comprehensive shape analysis is also possible with 3D imaging, and such data may highlight subtle differences across different categories in PAH; RV EF value <45% is considered abnormal.

RV 3D EF is load-dependent and affected by poor acoustic images and irregular rhythms.

It requires experience and offline analysis.

Further Reading

Hamilton-Craig C, Stedman K, Maxwell R, et al. Accuracy of quantitative echocardiographic measures of right ventricular function as compared to cardiovascular magnetic resonance. IJC Heart Vasc. 2016;12:38–44.

Parasuraman S, Walker S, Loudon B, et al. Assessment of pulmonary artery pressure by echocardiography—a comprehensive review. IJC Heart Vasc. 2016;12:45–51.

Arbo J, Maslove D, Beraud A. Bedside assessment of right atrial pressure in critically ill septic patients using tissue Doppler ultrasonography. J Crit Care. 2013;28(6):1112.e1–5.

Harjola V, Mebazaa A, Čelutkienė J, et al. Contemporary management of acute right ventricular failure: a statement from the heart failure association and the working group on pulmonary circulation and right ventricular function of the European Society of Cardiology. Eur J Heart Fail. 2016;18(3):226–41.

Alsoos F, Khaddam A. Echocardiographic evaluation methods for right ventricular function. J Echocardiogr. 2015;13(2):43–51.

Pleister A, Kahwash R, Haas G, et al. Echocardiography and heart failure: a glimpse of the right heart. Echocardiography. 2014;32:S95–S107.

Bossone E, Ferrara F, Grünig E. Echocardiography in pulmonary hypertension. Curr Opin Cardiol. 2015;30(6):574–86.

Calcutteea A, Lindqvist P, Soderberg S, Henein M. Global and regional right ventricular dysfunction in pulmonary hypertension. Echocardiography. 2013;31(2):164–71.

Ishizu T, Seo Y, Atsumi A, et al. Global and regional right ventricular function assessed by novel three-dimensional speckle-tracking echocardiography. J Am Soc Echocardiogr. 2017;30(12):1203–13.

DiLorenzo M, Bhatt S, Mercer-Rosa L. How best to assess right ventricular function by echocardiography. Cardiol Young. 2015;25(08):1473–81.

Arthur M, Landolfo C, Wade M, Castresana M. Inferior Vena Cava Diameter (IVCD) measured with transesophageal echocardiography (TEE) can be used to derive the central venous pressure (CVP) in anesthetized mechanically ventilated patients. Echocardiography. 2009;26(2):140–9.

Sugeng L, Mor-Avi V, Weinert L, et al. Multimodality comparison of quantitative volumetric analysis of the right ventricle. JACC Cardiovasc Imaging. 2010;3(1):10–8.

Lu K, Chen J, Profitis K, et al. Right ventricular global longitudinal strain is an independent predictor of right ventricular function: a multimodality study of cardiac magnetic resonance imaging, real time

three-dimensional echocardiography and speckle tracking echocardiography. Echocardiography. 2014;32(6):966–74.

Allam L, Onsy A, Ghalib H. Right ventricular outflow tract systolic excursion and fractional shortening: can these echocardiographic parameters be used for the assessment of right ventricular function? J Cardiovasc Echogr. 2017;27(2):52.

Longobardo L, Suma V, Jain R, et al. Role of two-dimensional speckle-tracking echocardiography strain in the assessment of right ventricular systolic function and comparison with conventional parameters. J Am Soc Echocardiogr. 2017;30(10):937–946.e6.

Tannus-Silva D, Rabahi M. State of the art review of the right ventricle in COPD patients: it is time to look closer. Lung. 2016;195(1):9–17.

Pristera N, Musarra R, Schilz R, Hoit B. The role of echocardiography in the evaluation of pulmonary arterial hypertension. Echocardiography. 2015;33(1):105–16.

Lang R, Badano L, Mor-Avi V, et al. Recommendations for cardiac chamber quantification by echocardiography in adults: an update from the American Society of Echocardiography and the European Association of Cardiovascular Imaging. Eur Heart J Cardiovasc Imaging. 2015;16(3):233–71.

Galiè N, Humbert M, Vachiery J-L, et al. ESC/ERS guidelines for the diagnosis and treatment of pulmonary hypertension. The joint task force for the diagnosis and treatment of pulmonary hypertension of the European Society of Cardiology (ESC) and the European Respiratory Society (ERS). Eur Respir J2015; 46:903–975. (2015). Eur Respir J. 2015;46(6):1855–6.

Mitral Valve

16

Ilaria Nicoletti, Carla Avallato,
and Alessandro Locatelli

16.1 Mitral Valve Anatomy

The mitral valve apparatus includes mitral annulus, two leaflets, approximately 1 mm thick, chorde tendineae and papillary muscles. Mitral annulus is a ellipsoid, saddle-shaped structure; it's a part of the fibrous skeleton of the heart.

The anterior mitral leaflet (AML) and the posterior mitral leaflet (PML) cover approximately one-third and two-thirds, respectively, of the circumference of the annulus The AML is longer than the PML; the distance from the base to the free edge of AML is about 1.5–2.5 cm, while the distance from the base to the free edge of the PML is about 1 cm (Photo 16.1).

The PML is divided into three segments or scallops: P1, P2 and P3 (Photo 16.2). P1 is the lateral scallop and it is close to the anterolateral commissure and atrial appendage. P2 is the central scallop and generally the largest; it's more prone to prolapse and lesions. P3 is the medial scallop; it is close to the postero-medial commissure and the tricuspid valve. The AML has a semicircular shape and is anchored to the fibrous portion of the annulus and so it's more resistant to pathological dilatation. Its fibrous core is in continous with the noncoronary cusp of the aortic
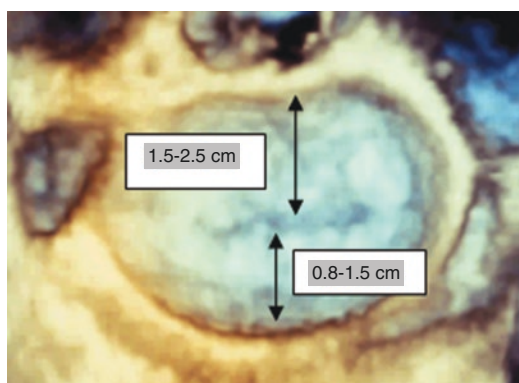
Photo 16.1 Anterior and posterior mitral leaflet
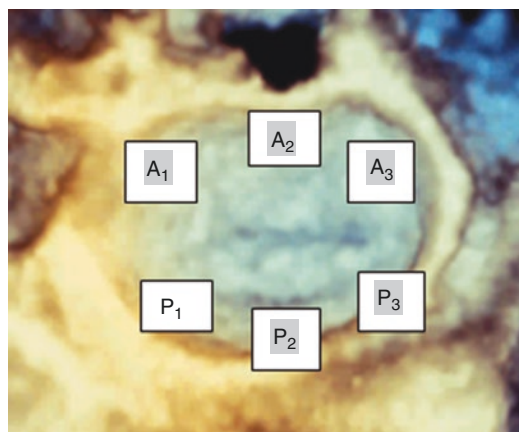
Photo 16.2 Scallops of anterior and posterior mitral valve

valve. In the AML, although it is not anatomically divided into scallops, three regions (A1, A2 and A3) have also been identified in accordance with the PML. In systole the two leaflets of the mitral

I. Nicoletti · C. Avallato · A. Locatelli (✉)
Department of Emergency and Critical Care,
Santa Croce & Carle Hospital, Cuneo, Italy
e-mail: nicoletti.i@ospedale.cuneo.it;
avallato.c@ospedale.cuneo.it;
locatelli.a@ospedale.cuneo.it

valve overlap in an area known as the "coaptation zone" that is about 7–10 mm long (Photo 16.3).

The chordae tendinae arise from the papillary muscles or directly from the ventricular walls and reach the leaflets; according to their insertion site chordae tendinae are classified in three types of chordae:

– Primary or marginal chordae: they are attached to the leaflets tip. The rupture of these chordae causes insufficiency. They serve to prevent prolapse and to align the coaptation zone. Those chordae inserted at the level of the commissures are called commissural chordae.
– Secondary chordae: they are inserted on the ventricular surface of the leaflets and relieve the tension from the leaflets by distributing it

across their ventricular surface. The "strut chordae", belong to this type; these robust chordae maintain the shape and function of the left ventricle.
– Tertiary chordae: they are attached on the base of PML and arise from the ventricular wall.

There are two papillary muscles, anterolateral and posteromedial; they arise from the left ventricle free wall, between the middle third and the apical one. They exert a dynamic force on the valve leaflets that counterbalances the pressure rise in the ventricle during systole. The anterolateral papillary muscle has a dual blood supply, from the circumflex artery and from the diagonal branches of the left anterior descending artery. The posteromedial papillary muscle is usually supply by right coronary artery and it is, therefore, more susceptible to risk of ischemic damage.

A perfect interplay among all of these structures, namely the mitral leaflets, the subvalvular apparatus, the annulus and the left ventricle, is critical for the normal functioning of the MV.

16.2 Mitral Valve Echocardiography Examination

Transthoracic Echocardiography (TTE): the windows used for studying the anatomy and function of MV are parasternal long and short axis (Photos 16.4 and 16.5); apical, 4 or 5 chamber view and apical 2 chamber views (Photos 16.6 and 16.7).
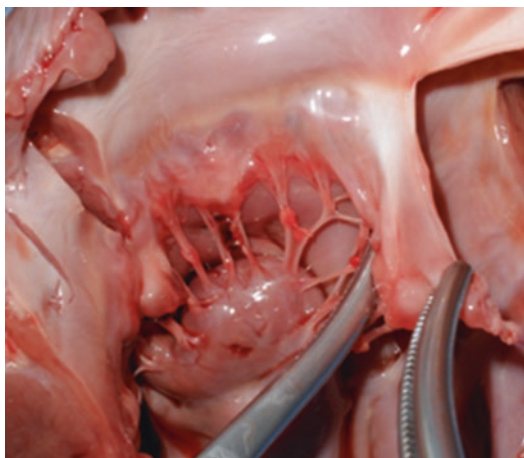
Photo 16.3 Coaptation zone

Photo 16.4 Parasternal long-axis view
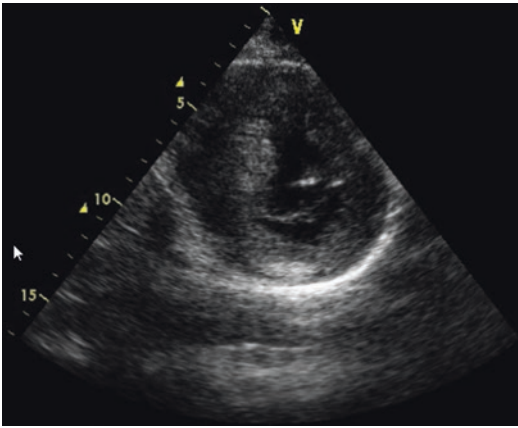
Photo 16.5 Parasternal short-axis view

Transesophageal Echocardiography (TEE): the usual windows for this examination are mid-esophageal view (4 chambers, commissural, 2 chambers, long axis) (Photos 16.8, 16.9, 16.10, and 16.11) and transgastric basal views (short axis and two-chambers) (Photos 16.12 and 16.13).

Photo 16.6 Apical four-chamber view
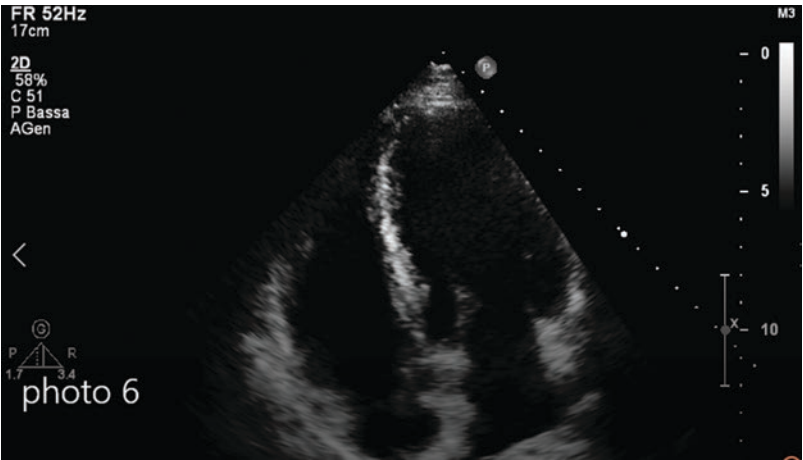
Photo 16.7 Apical two-chamber view
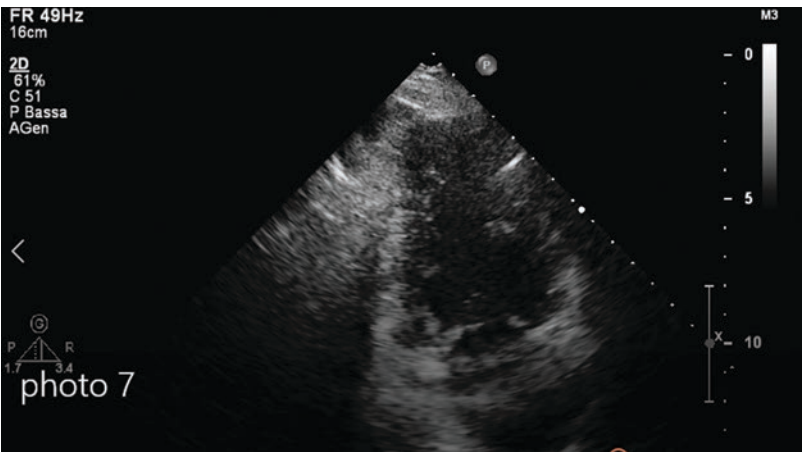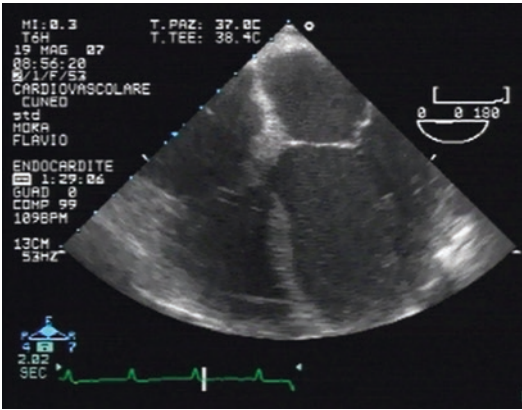
Photo 16.8 Mid-esophageal four-chamber view
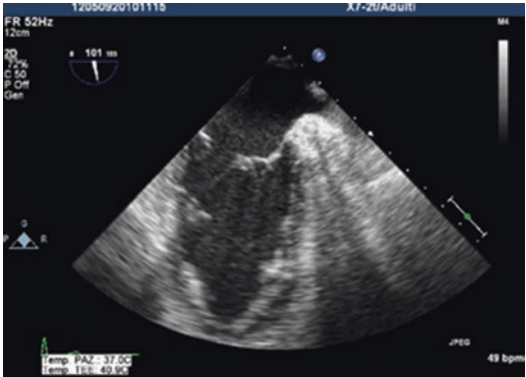
Photo 16.10 Mid-esophageal two-chamber view
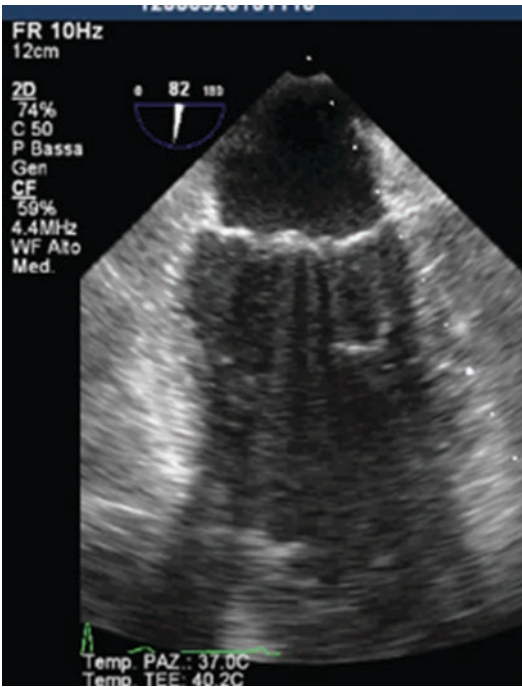
Photo 16.9 Mid-esophageal commissural view
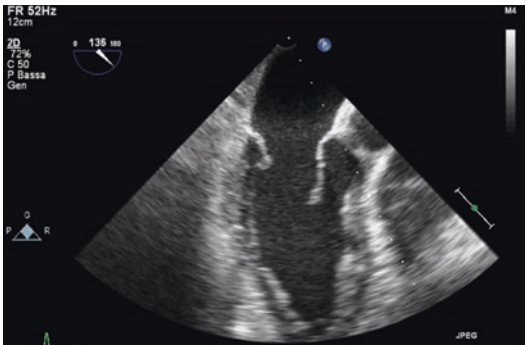
Photo 16.11 Mid-esophageal long axis view
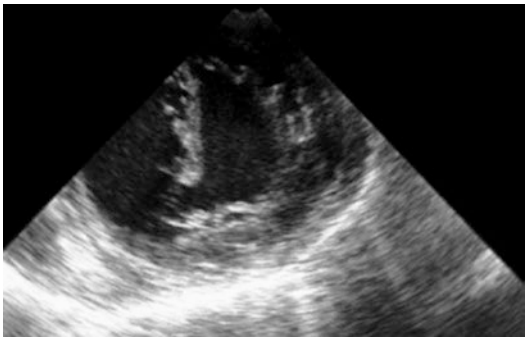
Photo 16.12 Transgastric basal short-axis view

16.3 Mitral Valvulopathy

- Mitral Stenosis
- Mitral Regurgitation

Stenosis and insufficiency of the MV, that can be coexist, are the common result of several forms of disease.

16.3.1 Mitral Regurgitation (MR)

Two types of MR are recognized: primary or organic and secondary or functional [1]. The first type is due to a structural abnormalities of the
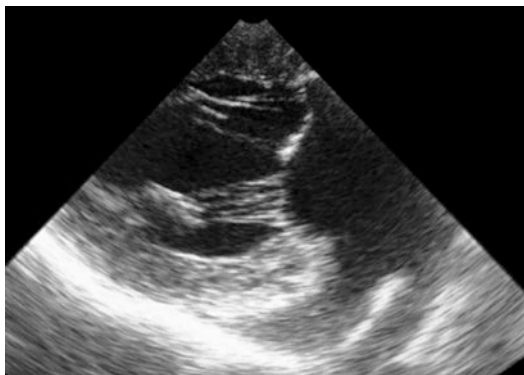
Photo 16.13 Transgastric basal two-chamber view

mitral valve apparatus; the second is due to a regional or global remodeling of the left ventricle causing a distortion of the MV apparatus.

Primary or organic MR: It is due to intrinsic valve diseases such as degenerative pathologies (Barlow's disease, fibroelastic degeneration, Marfan's syndrome, Ehlers-Danlos syndrome), rheumatic heart disease, endocarditis [1]. The myxoid degeneration involves both the leaflets and the chordae. The leaflets are redundant and thickened (>5 mm), especially in their more distal part: flail and prolapse are the most frequent scenarios. Careful assessment of annular calcifications should be performed because they may complicate surgical repair.

Secondary or functional MR: Ischemic heart disease and dilated cardiomyopathy are common underlying patologies. Functional MR is due to an alteration of the geometry of the left ventricle (dilation and spherical enlargement) followed by dilation of the mitral annulus and dislocation of the papillary muscles [1, 3]. The MV is morphologically normal but the systolic coaptation of its leaflets is impaired, due to reduced contractility and loss of synchronisation of the LV and the papillary muscles. The mitral annulus also shows an altered systolic contraction.

16.3.1.1 Mechamism of Mitral Regurgitation

Carpentier's classification is the most commonly used. It identifies three types of MR based on leaflets motion.

Type I: Normal leaflet motion with a coaptation defect.

Degenerative or ischemic annular ectasia, leaflet perforation due to endocarditis may be present

Type II: Excessive leaflet motion

Cordal stretching or rupture, papillary muscle rupture or degenerative pathology may be present.

– Billowing leaflet: mitral leaflet bulge above the annulus toward the left atrium during systole, but the coaptation line is maintained below the mitral anulus;
– Floppy valve: myxomatous valvular degeneration is present. The leaflets are thickened (more than 5 mm in diastole) and redundant. The chordae often are elongated.
– Prolapse: In this case the line of coaptation is above the mitral annulus, about 2 mm or more, but the leaflet tip is directed towards the LV. It can be assessed in the mid esophageal four or five-chamber and long axis at the end of systole (Photos 16.14 and 16.15).
– Flail: the free edge of the leaflet is upturned in the LA and its tip is directed towards the LA. Chordal rupture, due to degenerative, infective or ischemic matters, is commonly the cause; the PML, especially P2, is more often involved. The regurgitant jet is usually eccentric, moving away the side of the lesion (Photos 16.16 and 16.17).

Type III: Restricted leaflet motion.

It may be associated with rheumatic heart disease, dilated cardiomyopathy and ischemic cardiomyopathy. This type is further subdivided into type IIIa e IIIb.
• IIIa: Leaflet movement is restricted, both in systole and diastole, due to organic causes (mostly rheumatic disease).
• IIIb: Leaflet movement is restricted due to functional causes (mostly ischemic heart disease). Systolic tethering of the leaflets, papillary muscle displacement or left ventricle
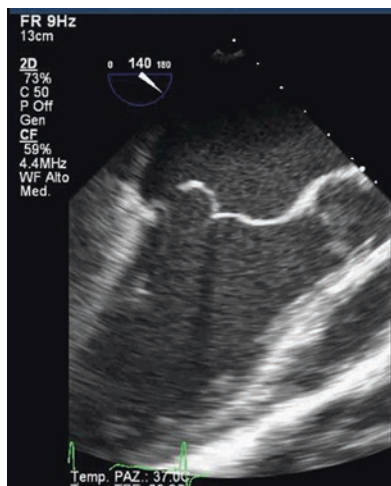
Photo 16.14 Mid esophageal long axis view: prolapse
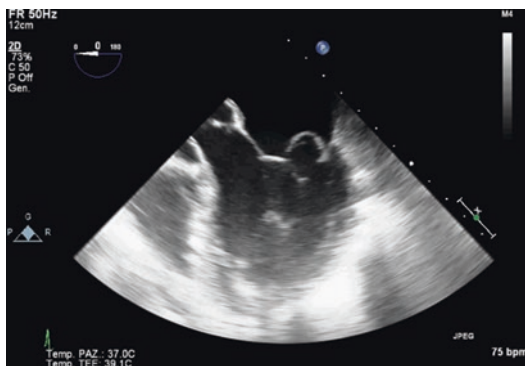
Photo 16.15 Mid esopageal five-chamber view: prolapse

dilation are present. Leaflet motion is normal during diastole.

16.3.1.2 Echocardiographic Assessment of MR Severity

Standard approach to MR evaluation uses the same views employed for morphological examination of the valve. Quantification of MR severity should integrate all avaible parameters: qualitative, semi-quantitative and quantitative (regurgitation volume, regurgitation area, regurgitation fraction) [1, 4, 5].

16.3.1.3 Qualitative Assessment

Color Flow Doppler: it's widely used to detect or rule out regurgitant jets. This method gives information about origin, size and direction of regurgitant jet but it's essential to mind that some misleadings items like gain setting, color flow scale, systolic pressure gradient between LV and LA, type of jet (central or eccentric) can impact on jet evaluation. Qualitative parameters to evaluate a mitral regurgitant jet are: color flow jet area, flow convergence zone and continuous wave Doppler signal Photo 16.18.

Color flow jet area: is the spatial representation of the velocity of the blood which regurgitates into the left atrium. This area of turbulence is influenced by the pressure gradient between the left ventricle and atrium. If LV pressure is lowered (e.g: by hypovolemia or reduced left ventricular contraction) a parallel reduction is observed in the regurgitant jet. Also a high systolic LA pressure can reduce jet expansion into the LA. A close control of color gain is essential for a good assessment; in fact too high or too low gains cause respectively a larger or smaller turbulence area; therefore it should be set just below noise level. Moreover color flow scale and Nyquist limit should be set before examination; usually a Nyquist limit (aliasing velocity) of 50–70 cm/sec is used. Color flow jet area should only be used for detecting MR, not to quantify it. However we can say that a small, central jet (area <4 cm^2), is consistent with a mild degree of IM whereas a very large jet or an eccentric jet hugging LA wall identifies a severe MI.

Proximal flow convergence: this qualitative parameter gives a visual evaluation of the severity of regurgitation. It's derived from a hydrodynamic principle: as blood flow converges towards a narrow orifice, it accelerates forming concentric emispheric shells; when aliasing velocity is reached a distinct red-blue interface occurs. By adjusting the Nyquist limit (generally lowering to 30–40 cm/sec) the most hemispheric flow convergence is obtained. Its absence usually is a sign of mild MR, but in the severe MR it's large throughout systole.

Continuous wave Doppler (CW-D) signal: the density and the shape of the CWD signal is an index of MR severity. In fact a dense signal hints at significant MR whereas a faint one suggest a
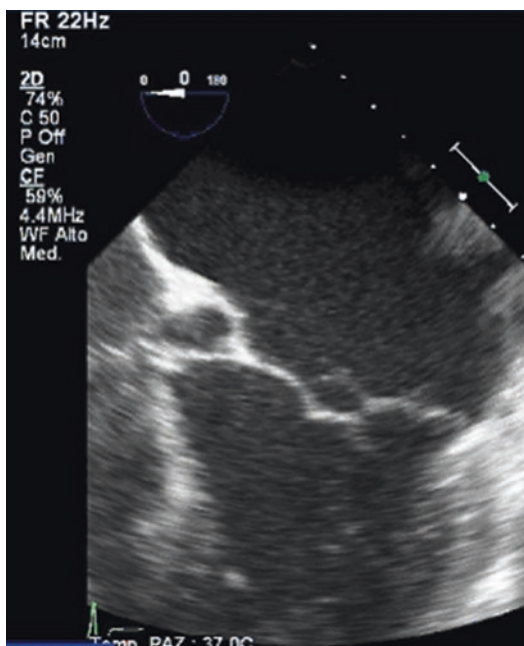
Photo 16.16 Flail
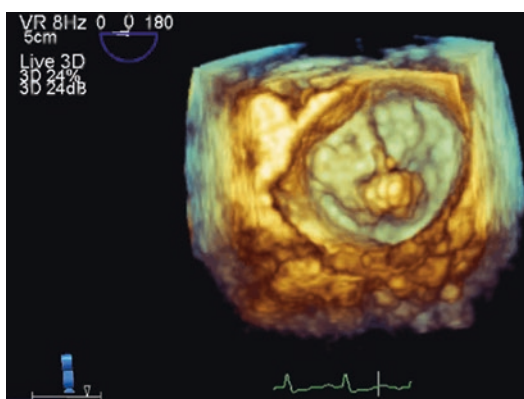
Photo 16.17 Flail in 3D view

16.3.1.4 Semi-quantitative Assessment

By Pulsed-Wave (PW) Doppler and Color Flow Doppler are obtained other parameters for evaluation of MR: pulmonary vein flow, mitral inflow and vena contracta.
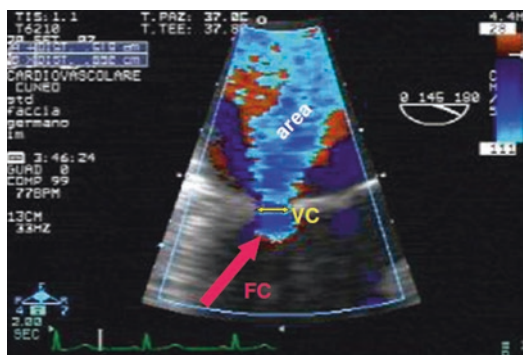
Photo 16.18 Jet area, flow convergence zone, vena contracta

Pulmonary vein flow (PVF): typical PW-Doppler profile consists of three waves: two waves are positive (an anterograde systolic wave S and an early diastolic wave D), and a retrograde wave a in late diastole due to atrial contraction. In healty people S > D but in presence of significant MR S wave is blunted until to be inverted in severe MR. A systolic blunted wave isn't specific because it can be also observed in other situations of elevated LA pressure as atrial fibrillation. However if a systolic flow reversal is found, that suggests a severe MR. It's recomended to sample through all pulmonary veins; if a systolic flow reversal is found in more than one pulmonary vein it's specific for severe MR.

Transmitral flow (TMF): it shows two waves: E (due to early diastolic filling) and A (due to atrial contraction). In severe MR a dominant early filling is present (higher E-wave) due to increased diastolic flow across the MV; E velocity is ≥1.2 m/sec. Conversely a dominant A-wave excludes significant MR.

Vena contracta width (VCw): by applying Color Flow Doppler the vena contracta is the narrowest portion of the regurgitant jet positioned just downstream of the regurgitant orifice. It is independent of hemodynamic variations and can be applied to either central jets or eccentric ones, but not for multiple jets or in case of elliptical shape of the regurgitant orifice as in secondary MR. In the case of multiple jets, the respective VC widths should not be added. The measurement of the VC area by 3D echocardiography would be a more exact parameter because by a

mild MR. Usually in chronic not severe MR the CW-D envelope is parabolic, but in severe acute MR the CW-D signal profile is truncated and triangular.

multiplanar reconstruction the narrowest VC area can be found and a manual planimetry of the color Doppler signal can be done. For measurement of VCw a perpendicular view to the commissural line should be used (ME long axis in TEE and parasternal long axis in TTE) and the three components of regurgitant flow (flow convergence, VC, jet area) should be seen in the cut-plane. In primary MR a VCw <3 mm indicates mild MR, whereas a VCw ≥7 mm defines severe MR; intermediate values require a quantitative approach. In secondary MR a VCw ≥4 mm indicates a severe MR.

Timing of regurgitation is also an important element in the assessment of the regurgitant jet. By Color M-mode, it can visualize how much of the systole is involved in regurgitation: not holosystolic jets (limited to early- or late- systole) rarely are severe.

16.3.1.5 Quantitative Assessment

The quantitative methods to assess MR are: quantitative Doppler method and flow convergence method (proximal isovelocity surface method). All these methods measure three parameters: EROA (effective regurgitant orifice area), RVol (regurgitant volume) and RF (regurgitant fraction).

Flow convergence method (PISA method): it's based on the application of flow conservation principle and continuity equation. When a flow converges towards circular orifice, it accelerates forming concentric hemispheres whose surfaces have the same velocity (isovelocity). Due to the principle of mass conversion the flow at the level of these hemispheres is the same as the flow through the regurgitant orifice. Regulating the aliasing velocity (Nyquist limit: the velocity beyond which the color is inverted, from red to blue in TEE examination), a well-defined external hemisphere is obtained. The flow throught hemisphere can be calculated as:

$Q = 2\pi r^2 \times V_{\text{aliasing}}$ (Photo 16.19).(r is the distance between the surface of the first hemisphere and the regurgitant orifice)

Similarly the flow through regurgitant orifice is given by

$$\text{FlowReg} = \text{EROA} \times V_{\text{max reg jet}}$$
$$\left(\text{EROA} = \text{effective regurgitant orifice area} \right)$$

Because the flow at the hemisphere level is the same as the flow through the regurgitant orifice

$$\text{EROA} = Q / V_{\text{max reg jet}} = 2\pi r^2 \times V_{\text{aliasing}} / V_{\text{max reg jet}}$$

($V_{\text{max reg jet}}$ is the maximum velocity of the MR measured with CW-Doppler).

Multiplying EROA by the $\text{VTI}_{\text{reg jet}}$ measured by CW-Doppler, the regurgitant volume (RV) is obtained:

$$\text{RV}\left(\text{ml}\right) = \text{EROA}\left(\text{cm}^2\right) \times \text{VTI}_{\text{reg jet}}\left(\text{cm}\right)$$

For a greater quality of these measurements it's important to assess flow and velocity at the same time of the regurgitant phase. PISA assessment is improved by reducing the depth of the image and setting Nyquist limit at 20–40 cm/sec. The radius is measured in meso-systole using the first velocity of aliasing. The presence of a flow convergence at a Nyquist limit of 50–60 cm/sec immediately suggests a significant MR. At a aliasing velocity of 40 cm/sec a PISA radius >1 indicates severe MR.

If V_{aliasing} is 40 cm/s and the V_{max} of the MR is 500 cm/s, EROA is $r^2 / 2\left(6.28 \times r^2 \times 40 / 500\right)$

PISA method has some limitations:

– It measures an instataneous regurgitant flow and orifice area;
– This method assumes that regurgitant orifice is flat and the flow convergence shape is hemispherical but it isn't always true. When the shape of the flow convergence isn't a hemi-
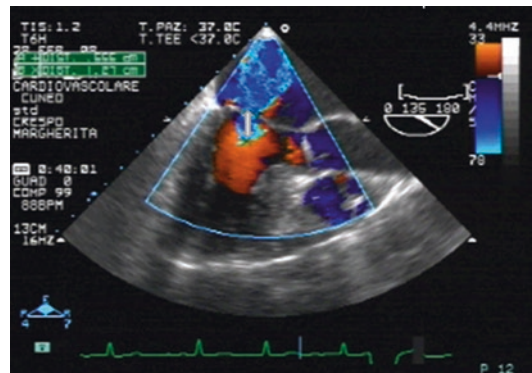
Photo 16.19 Radius: distance between the surface of the first hemisphere and the regurgitant orifice

sphere, the PISA method gives a wrong estimate of the degree of MR.

Quantitative pulsed Doppler method: The regurgitant volume (RV) is the difference between the amount of blood going into the LV in diastole and that one going out through aortic valve in systole. The flow through the regurgitant valve (MV) and the flow through the LVOT are used to calculate rigurgitant volume.

$$RV = SV_{MV} - SV_{LVOT} \left(SV = \text{stroke volume} \right)$$

$$SV = CSA \times VTI = \pi r^2 / 4 \times VTI = 0.785 \times d^2 \times VTI$$

(CSA = cross sectional$_{\text{reg jet}}$ area; d = diameter; VTI =velocity time integral).

$$RV = \left(CSA_{MV} \times TVI_{MV} \right) - \left(CSA_{LVOT} \times TVI_{LVOT} \right)$$

The diametTer of the MV is measured in mid-diastole from ME 4-chamber view in TEE and from apical 4-chamber view in TTE assuming that MV area is circular; if MV area is elliptic, the diameter in 2-chamber view has also to be measured. The diameter of the LVOT is measured in mid-systole from ME long axis view just beneath the aortic valvular plane in TEE and from parasternal long-axis view in TTE assuming that LVOT area has circular shape. To obtain the time velocity integral (TVI), PW-Doppler is used. TVI$_{MV}$ is recorded at the level of the mitral annulus and TVI$_{LVOT}$ is measured just beneath the aortic anulus. In case of aortic insufficiency the flow through the pulmonary valve is used.

$$EROA = RV / TVI_{MV} \left(TVI \text{ is recorded by CW-D} \right)$$

$$FR = \left(RV / SV_{MV} \right) \times 100$$

Doppler Volumetric method is awkward and a time-consuming approach and it isn't raccomended as a first line method to quantify MR severity.

VTI$_{MV}$/VTI$_{Ao}$: this ratio gives a quick idea on the MR severity. The transmitralic flow is sampled at the level of the mitral leaflets, and the aortic flow at the level of the aortic annulus. A VTI$_{MV}$/VTI$_{Ao}$ ratio >1.4 indicates severe MR; whereas a ratio VTI$_{MV}$/VTI$_{Ao}$ < 1 indicates mild MR.

Functional MR: Common causes are ischemic and dilated cardiopathies. In this type of insufficiency the valve and subvalvular apparatus are unaffected but there is an impaired leaflet coaptation from a reduced function and distorted geometry of the left ventricle. The remodeling of the LV is responsible for the transition from an ellipsoidal to a spherical geometry resulting in a displacement of the papillary muscles, mitral annulus and subvalvular apparatus. The papillary muscles undergo apical and posterior displacement with leaflets tethering and apical displacement of the leaflets coaptation area; the leaflets apposition is usually normal, that is the tips of the leaflets are at the same level in systole. The imbalance between the tethering forces (as result of LV distorted geometry) and the closure forces (due to the LV impaired contraction) associated with asynchronous papillary contraction and mitral annulus dilation, results in functional mitral regurgitation. The presence and degree of MR seem to be more closely related to the extent of geometric remodeling and dysfunction, than to the severity of systolic impairment of the left ventricle. Global ventricular remodeling is more evident in anterior myocardial infarction than in the inferior myocardial infarction. However, the incidence of MR is greater in inferior myocardial infarction due to the anatomical and functional involvement of the basal segment of the posterior-inferior wall adjacent to the papillary muscles. Posterior papillary muscle undergoes apical and posterior repositioning with tethering of both mitral leaflets so that their coaptation point is not at the center of the ventricular cavity but posteriorly. The AML, tethered by the secondary chords, is reshaped in a "hockey stick" figure and, during valve closure, slides toward the PML generating a posteriorly oriented, eccentric regurgitation jet. In anterior and inferior myocardial infarction and in dilated cardiomyopathy a posterior and apical papillary muscles displacement occurs, with symmetrical tenting on both leaflets. The coaptation zone is shifted toward the apex and posteriorly. Since the leaflets are similarly tethered, apposition is normal and the regurgitation jet is central. The regurgitant jet has a biphasic profile with a peak in early and late

systole, but decreases in mid-systole. It's important to evaluate hemodynamic changes because anaesthesia and vasoactive agents change the loading conditions driving to an underestimation of the regurgitant. Global LV remodeling can be assessed by measuring its volumes and by calculation of the spherical index, which is the relationship between the short and long axis in mid esophageal 4-chamber views at end systole. In mild esophageal long axis views at mid-systole the following parameters are measured:

– Coaptation depth: It is the distance between the line of coaptation of the leaflets and the mitral annulus plane. This is an index of the dislocation of the papillary muscles and of LV remodeling. In normal conditions it is ≤5 mm (Photo 16.20);
– Tenting area: This is measured in mesosystole as the space between the valve leaflets and the line which connects the two furthest points from the annulus. A tenting area of > cm^2 indicates moderate MR (Photo 16.21).

Degenerative MR: Common causes are rheumatic valve disease and myxoid degeneration.

The myxoid degeneration involves both the leaflets and the chordae. The leaflets are redundant and thickened (>5 mm), especially in their more distal part showing a clubbed shape. Flail and prolapse are the most frequent scenarios. Careful assessment of annular calcifications should be performed as they may complicate surgical repair efforts.

Evaluation of MR severity should combine multiple parameters, because all methods have some limitations. It has been suggested to distinguish between mild and severe MR and for intermediate values it's recommended to use quantitative methods.

Chronic mild MR: There are ≥4 following parameters:

- Small, narrow central jet;
- VCw ≤0.3 cm;
- PISA radius ≤0.3 cm at Nyquist limit 30–40 cm/sec or absent
- Dominant A wave in mitral inflow
- Faint or incomplete CW-Doppler signal
- Normal LV and LA size
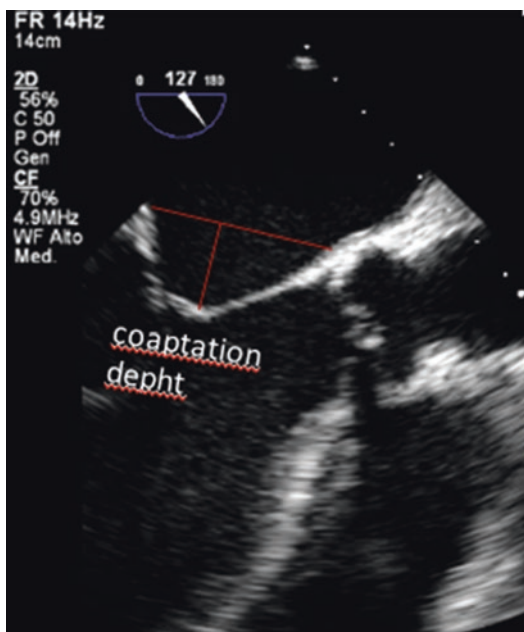
Photo 16.20 Coaptation depht
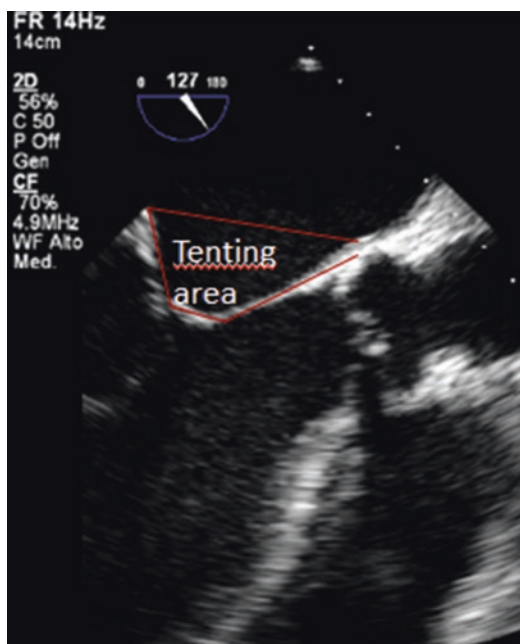
Photo 16.21 Tenting area

Chronic severe MR: There are ≥4 following parameters:

- flail leaflet
- VCw ≥0.7 cm
- PISA radius ≥1 cm at Nyquist limit 30–40 cm/sec
- Central large jet >50% of LA area
- Pulmonary vein flow reversal
- Enlarged LV but normal function

If only 2–3 parameters are positive for mild or severe MR, it is suggested to measure EROA, RVol and RF

- EROA <20 mm^2; RV <30 ml; RF <30% ➔ MR grade I (mild MR)
- EROA 20–29 mm^2; RV 30–44 ml; RF 30–39% ➔ MR grade II (moderate MR)
- EROA 30–39 mm^2; RV45–59 ml; RF40–49%➔ MR grade III (moderate MR)
- In the last case if 3 parameters of severe MR or elliptical orifice are founded the MR will be severe.
- EROA ≥40 mm^2; RV ≥60 ml; RF ≥50%➔ MR grade VI (severe MR)

In a functional MR the threshold for severe MR is lower EROA ≥20 mm^2, RV > or =30 ml). A EROA > or = 20 mm^2 is associated with a worse prognosis but it isn't clear if the worsening of prognosis depends on MR or myocardial damage [Baumgartner H, et al. 2017 ESC/EACTs Guidelines for the management of valvular heart disease. Eur heart J 2017: 1-53]

16.3.1.6   TEE and MV Surgery

TEE can be of help during two separate stages of surgical MV repair. The first stage is prior to cardiopulmonary bypass (CPB) when it is necessary to assess the regurgitation, its mechanism and the possibility of valve repair. The evaluation of regurgitation site and mechanism allows the surgeon to plan the surgical strategy. Appraising of MR severity is less reliable than that performed pre-operatively becaue both the preload and afterload conditions can be changed by anesthesia. In primary MR negative predictors of MV repair are:

large central regurgitant jet, anular dilatation (≥50 mm), wide valvular calcification, three or more abnormal scallops and involvement of LAM. In secondary MR adverse predictors of MR are: coaptation depth ≥1 cm, tenting area >2.5–3 cm^2, interpapillary muscle distance >20 mm, end-diastolic diameter >65 mm and end-systolic diameter >51 mm, systolic sphericity index >0.7. The second stage is after complete weaning-off from CPB, when the result of MV repair is evaluated. The assessment of residual regurgitant jets, possible complications such as valve stenosis, SAM (systolic anterior motion), coronary injury, left ventricular rupture, and aortic valve damage can be detected. TEE is also used in case of valve replacement, to assess the functioning of the prosthesis and possible perivalvular leaks. The most common complications are:

- Stenosis: The presence of a peak E-wave velocity >2 m/sec in TMF should point to stenosis, which can be confirmed by a mean gradient >6 mmHg and maximum gradient >16 mmHg.
- SAM (systolic anterior motion) (Photo 16.22): is most often observed after repair of a myxomatous valve. Redundant leaflets, reduced mitral-aortic angle, a small left ventricle, anterior displacement of the point of coaptation and a small annulus, are all baseline features associated with this complication. Pre-CPB TEE (mid esophageal 5-chamber and long axis views) showing AML/PML ratio <1 and a distance between the coaptation point and septum (C-sept) <2.5 cm can identify subjects who are at increased risk for SAM. Post-CPB TEE, in case of SAM, shows a dynamic obstruction of LVOT and the presence of a regurgitant jet directed posteriorly. Volume loading, vasoconstrictors and beta-blockers may help in these cases but, if conservative measures fail, surgical revision of the mitral valve repair is called for the SAM resolution.
- Coronary artery injury: the circumflex artery runs along atrioventricular groove at the level of the posterior mitral annulus. If, during mitral ring placement, the sutures are placed too deeply into the MV annulus, coronary
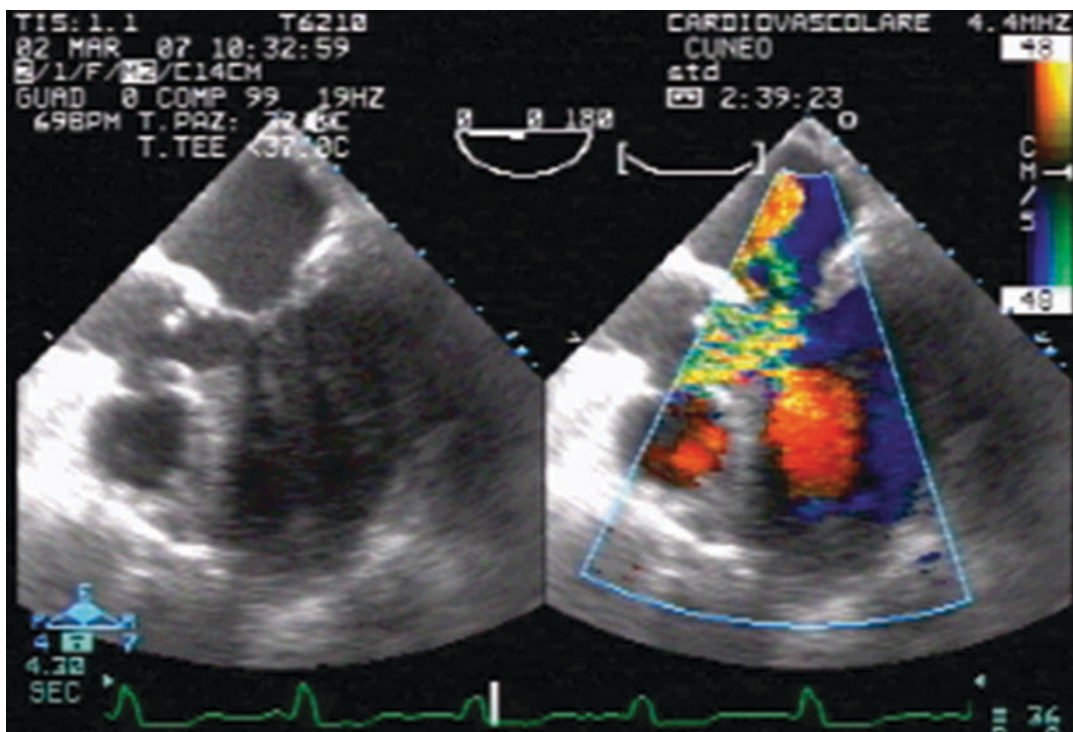
Photo 16.22 Systolic anterior motion

disruption can occur with impairment of coronary flow. TEE shows new ischemic wall motion abnormalities in the lateral or inferolateral wall.

- Left ventricular rupture: can occur at the level of the atrioventricular groove or the free wall of the left ventricle between the insertion of the papillary muscles and the AV groove. This is a much-feared and devastating complication. Female gender, advanced age and calcification of the annulus are predisposing factors. TEE shows persistent bubbling of air into the left ventricular cavity. Surgical placement of a ventricular patch is the only therapy.
- Aortic valve leaflets injury: sutures placed too deep at the level of the anterior mitral annulus can damage the aortic leaflets (mainly the left coronary or the noncoronary cusp) causing lesions or inappropriate pulling; the result is massive aortic regurgitation requiring surgical correction.

16.3.2 Mitral Stenosis

The valve area is between 4 and 6 cm^2. The most common cause of MS is rheumatic disease followed by degenerative type. Other rare causes of MS can be congenital as congenital stenosis and parachute mitral valve or acquired as malignant carcinoid disease, inflammatory disease, tumors. Careful morphological examination by echocardiography is crucial to decide if a conservative treatment can be made. Morphological analysis assesses:

- Leaflet thickening: typically more marked at the tips of the leaflets in the rheumatic disease. Later in the course of the disease thickening extends towards the base of the leaflets. In the degenerative MS calcifications involve annulus and base of the leaflets.

– Restricted leaflet movement: in particular the AML shows a characteristic "doming" or "hockey stick" deformity
– Commissural fusion
– Thickening, shortening, and different fusion degree of the chordae tendineae;

16.3.2.1 Quantification of Mitral Stenosis Severity

Quantification of MV severity is founded on pressure gradient measurement and mitral valve area (planimetry and Pht).

Pressure gradient measurement: CW-Doppler is used. By Bernoulli equation applyed to the transmitral velocity flow curve is obtained mean and peak gradient. TEE views are ME 4-chamber or ME long axis. For TTE apical 4-chamber view is applyed. The mean gradient is more relevant for assessing MS because the peak gradient is influenced by LA compliance, LV diastolic function and loading. The pressure gradient is also overestimated in case of concomitant severe MR.

Valve area calculation: the calculation can be performed by planimetry, pressure half time (PHT) method, continuity equation or PISA.

Planimetry can be performed by TEE using TG basal short-axis view and by TTE using parasternal short axis view. The valve area is measured in mid-diastole and the smallest orifice at the leaflet tips should be identified. Difficulties can be found in the correct alignment to the valve, and an oblique view will result in overestimation of the valve area.

PHT (pressure half-time method): is the time interval between the maximum early diastolic pressure gradient and the time point where the gradient is dropped to one-half. The more severe the mitral stenosis, the longer the time interval is. The volume sample is positioned through the mitral orifice, parallel to the flow; the sampling can be facilitated by using color Doppler. The PHT is calculated directly by the machine software once the deceleration slope of the E on CW-D spectrum is been traced. From PHT the valve area can be derived using the equation MVA = 220/PHT.

Other methods for evaluation of MS are:

• Continuity equation: based on the principle of mass conservation. In the absence of regurgitation and shunts, the volume of flow through the mitral valve is the same as the cardiac output. The flow through the mitral valve is obtained from $CSA_{VM} \times VTI_{VM}$. Cardiac output is mainly calculated on LVOT or, in the case of aortic regurgitation, on the pulmonary valve. The flow through the LVOT is obtained by the product $CSA_{LVOT} \times VTI_{LVOT}$

$$CSA_{VM} \times VTI_{VM} = CSA_{LVOT} \times VTI_{LVOT}$$

$$CSA_{VM} = \left(CSA_{LVOT} \times VTI_{LVOT}\right) / VTI_{VM}$$

(CSA = cross sectional area; VTI = velocity time integral)

The valve area calculated by continuity equation is independent of the transvalvular pressure gradients, left ventricle compliance and hemodynamic modifications. It's mandatory that the examined valves aren't regurgitant because, in the presence of valvular regurgitation, the forward flows are not equal.

PISA (proximal isovelocity surface area) or flow convergence method: in this method the continuity equation and color Doppler are associated to assess the flow through the stenotic MV and the same principles are used as those discussed above for insufficiency. However, in this case acceleration of blood with the formation of concentric hemispheres occurs in the atrium rather than ventricle. For the principle of flow conservation, calculated flow through these hemispheres is the same as through a stenotic valve. Flow is calculated as the product of the area of the hemisphere times the velocity of aliasing ($Q = 2\pi \times r^2 \times V_{aliasing}$). The most external hemisphere is selected because it is the easiest to identify; the radius (r) in the first hemisphere is measured from the border of the same hemisphere to the extremity of the leaflets. Using the continuity equation:

$$CSA_{VM} \times V_{max\ VM} = Area_{PISA} \times V_{aliasing}$$

$$CSA_{VM} = Area_{PISA} \times V_{aliasing} / V_{max\ VM}.$$

Current guidelines consider MS severe when MVA is ≤ than 1.5cm^2 and Pht is ≥150 ms e molto severa MS when MVA is ≤1cm^2 and Pht is

≥220 ms. Transmitral mean pressure gradient, usually between 5 and 10 mmHg in severe MS, isn't included among the criteria of severity because it's affected by heart rate and forward flow. It's also useful evaluate the possible consequence of MS like LA enlargement with spontaneous echocontrast and thrombi and pulmonary hypertension (PAPs >30 mmHg).

References

1. Zoghbi WA, Adams D, et al. Recomandation for non-invasive evaluation native valvular regurgitation. J Am Soc Echocardiogr. 2017;30(4):303–71.
2. Nishimura RA, et al. 2017 AHA/ACC Focused Update of the 2014 AHA/ACC Guideline for the Management of Patients With Valvular Heart Disease: A Report of the American College of Cardiology/American Heart Association Task Force on Clinical Practice Guidelines. Circulation. 2017;135(25):e1159–95.
3. Asgar AW, Mack MJ, et al. Secondary mitral regurgitation in heart failure. J Am Coll Card. 2015;65:1231–48.
4. Lancellotti P, Tribouilloy C, et al. Recomandations for the echocardiographic assessmet of native valvular regurgitation: an executive summary from the European Association of Cardiovascular Imaging. Eur Heart J Cardiovasc Imaging. 2013;14:611–44.
5. Lancellotti P, et al. European Association of echocardiography recommendations for the assessment of valvular regurgitation. Part 2: mitral and tricuspid regurgitation (native valve disease). Eur J Echocardiogr. 2010;11:307–32.
6. Baumgartner H. Echocardiographic assessment of valve stenosis: EAE/ASE recommendations for clinical practice. J Am Soc Echocardiogr. 2009;22(1):1–23.
7. Grayburn PA. How to measure severity of mitral regurgitation. Heart. 2008;94:376–83.
8. Lambert AS. Proximal isovelocity surface area should be routinely measured in evaluating mitral regurgitation: a core review. Anaesth Analg. 2007;105:940–3.

Aortic Valve

17

Alessandro Locatelli, Ilaria Nicoletti,
and Carla Avallato

17.1 Anatomy

The aortic valve is the anatomical structure that separates the left ventricle from the ascending aorta. It consists of three leaflets or cusps attached to a fibrous annulus along a crown-shaped line. The leaflets are semilunar and their a free edge shows a thicker central portion called nodule of Arantius. The protruding of the free edge into the lumen enables the aortic valve to close. The lowest points of the leaflets attach to the annulus define the base of the aortic valve; the sinotubular junction idis the connection between the aortic valve and the ascending aorta. The structure is completed by the sinuses of Valsalva, the small dilations located behind each leaflets and inside of aorta. The right and left coronary arteries arise in the related sinus of Valsalva and this relationship, also, identifies the three leaflets as left, right and non-coronary cusps (Photos 17.1 and 17.2). Usually, the leaflets have different size: the non-coronary cusp is wider than the right coronary cusp and the left coronary cusp is the smallest one. The portion of the aorta made up of the cusps, the annulus, the

Photo 17.1 The three leaflets of the aortic valve

A= anulus; B= valsalva sinus; C = sinuo-tubular junction

Photo 17.2 Aortic root and diameters

A. Locatelli (✉) · I. Nicoletti · C. Avallato
Department of Emergency and Critical Care,
Santa Croce & Carle Hospital, Cuneo, Italy
e-mail: locatelli.a@ospedale.cuneo.it; nicoletti.i@ospedale.cuneo.it; avallato.c@ospedale.cuneo.it

sinuses of Valsalva, the coronary artery orifices, the sinotubular junction and the proximal ascending aorta is named aortic root and its accurate, global evaluation is important for understanding the functional mechanisms of different pathologies.

17.2 Echocardiography Examination

Transthoracic (TTE) and transesophageal echocardiography (TEE) can be used to visualize the aortic valve.

By the transesophageal echocardiography, the first image is obtained with the mid-esophageal short axis view: the tip probe is at the depth of 25–35 cm, in neutral position and the ultrasound beam is rotated between 20° and 40°. During diastole, in this view, the leaflets of the aortic valve, form an image called "Mercedes-Benz sign"; the right coronary cusp is visualized at the bottom of the display, the left coronary cusp is on the right and the non-coronary cusp on the left (Photo 17.3). At the level of the left sinus of Valsalva is often seen
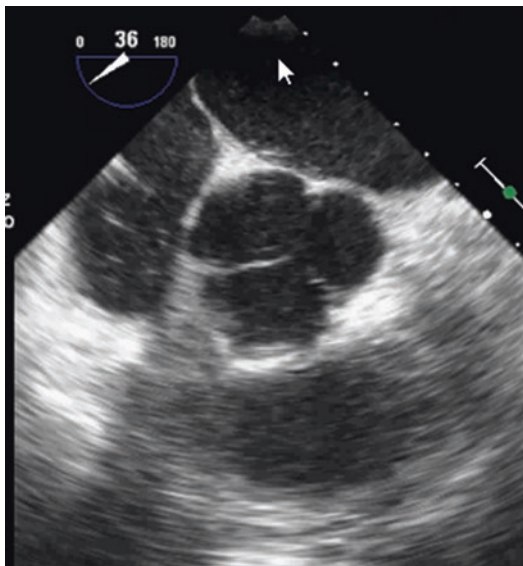
Photo 17.3 TEE: mid-esophageal short-axis view
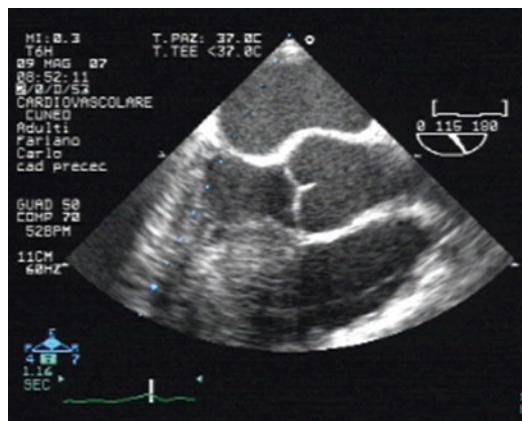
Photo 17.4 TEE: mid-esophageal long-axis view

the orifice of the left coronary artery. In this view, it is possible to observe the leaflets and their alterations like calcification, perforation or presence of vegetations. During the systole it is possible to measure the planimetry of the valve area. From this view, by the rotation of the angle of the ultrasound beams to 120° – 140° is obtained the mid-esophageal aortic valve long-axis view (ME AV LAX) (Photo 17.4). The aortic root is visible with the LVOT (left ventricle outflow tract) and the ascending aorta. In the ME AV LAX it is simple to measure all the diameters of the aortic root: the annulus, the widest cross-section at the sinuses of Valsalva, the sinotubular junction (SJ) and the ascending aorta (usually this measure is taken 1 cm beyond the SJ). Generally, in this view the aortic leaflets are the right coronary cusp at the bottom of aortic root (anteriorly) and the non-coronary cusp at the top (posteriorly); but, if the transducer is turned to the left side, the anterior leaflet could be the left coronary cusp instead of the non-coronary cusp. To obtain the correct alignment to the Doppler signal, the aortic valve must be visualize in transgastric long-axis view (TG LAX) or in deep transgastric long-axis view (deep TG LAX) (Photos 17.5 and 17.6). In this views, the ultrasound beam is almost parallel to the blood flow and it is possible to assess the
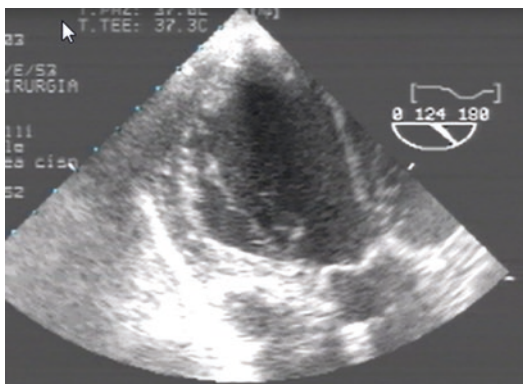
Photo 17.5 TEE: transgastric long-axis view
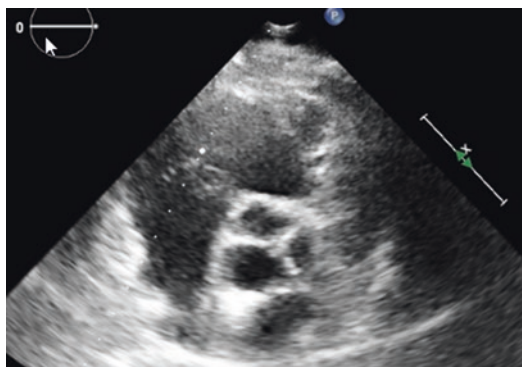
Photo 17.7 TTE: parasternal aortic valve short-axis view

Photo 17.6 TEE: deep transgastric long-axis view

Photo 17.8 TTE: parasternal long-axis view

transvalvular velocity and the pressure gradients. Analogous views with the transthoracic echocardiography are: the parasternal short axis view where all three cusps of the aortic valve should be visible with the right cusp displayed on the top; the parasternal long axis view where the full aortic root is imaged; the apical 5 chamber and the apical 3 chamber views are useful to assess the structure and mobility of the aortic valve and to correctly applied the continuous and the pulse wave Doppler (Photos 17.7, 17.8, 17.9, and 17.10).
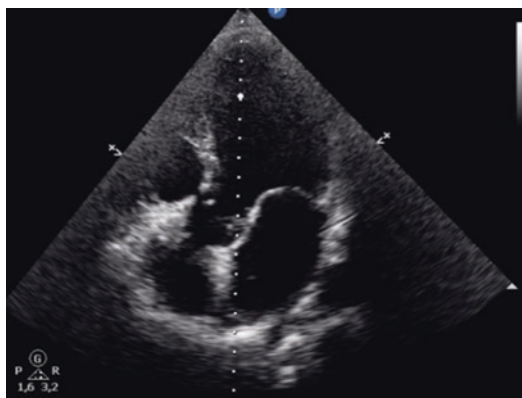
Photo 17.9 TTE: apical 5 chamber view

17.3 Aortic Stenosis (AS)

17.3.1 Etiology

There are three types of aortic stenosis:

– Calcific aortic stenosis: it's common in older adults and is consequence of calcific degeneration of the valve that starts from the anulus and extends to the body of the cusps without commissural fusion. AoValve (AoV) is tricuspid and presents thickened and calcified cusps with reduced motion (Photo 17.11).
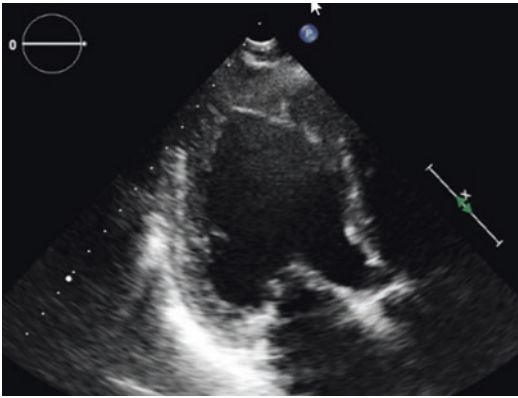
Photo 17.10   TTE: apical 3 chamber view

– Congenital aortic stenosis: it's more commonly associated with cardiac malformation called bicuspid AoV. In this malformation there is a fusion between coronary cusps; the most common form presents a fusion between left and right coronary cusp, so the bicuspid aortic valve is made by a larger anterior and a smaller posterior cusp. A raphe, which is the fusion zone between cusps, is seen on the anterior cusp. By echocardiography, in short axis during the systole, a typical "fish mouth" apparence can be seen. Bicuspid Ao valve tends to the calcific degeneration and leads to symptoms around 50 years of age (Photo 17.12).
– Rheumatic aortic stenosis: it's characterized by thickening of the cusp edges and commissural fusion.

17.3.2 Aortic Valve and Echocardiographic Views

TTE windows for studying anatomy and function of the AoV are (Photos 17.7, 17.8, 17.9, and 17.10):

– Parasternal long and short axis
– Apical 5 chamber and 3 chamber views
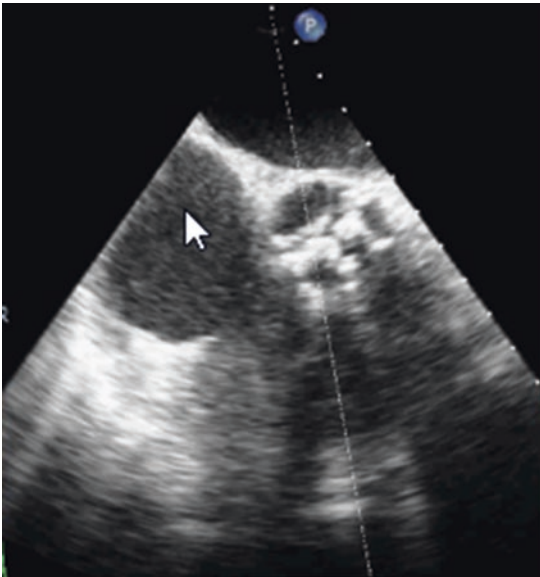
Photo 17.11   Calcific aortic stenosis

Photo 17.12 Bicuspid aortic valve

TEE windows for the Ao valve examination are (Photos 17.3, 17.4, 17.5, and 17.6):

– Mid-esophageal view (short axis, 45° and long axis, 120°)
– Transgastric view (long axis, 120°)
– Deep transgastric long axis view, 0°

In normal subjets, the aortic cusps appare thin and fine and sometimes are hard to visualize. During diastole, in short axis view, they are closed and form an image called "Mercedez-Benz sign". This view is useful for evaluation of the cusps number and if there is a fusion of one or more commissures. As the degenerative disease is proceding, the cusps become thickened, deformed and their mobility is more and more reduced. It's impossible to quantify the degree of stenosis by echocardiographic detections, but a severe stenosis can be assumed if cusps appare thickened and calcified and their mobility is slow or absent.

17.3.3 Echocardiographic Evaluation of Aortic Stenosis Severity

The quantification of the severity of Ao stenosis is based on valve area by continuity equation, peak jet velocity and mean transvalvular pressure gradient. Multiple windows have to be used to measure the peak velocity and a good alignment of the Doppler beam to the direction of the aortic flow must be searched.

Peak Jet Velocity: In normal condition AoV area is about 3–4 cm^2 and the peak transaortic velocity is less than 2 m/sec; a peak velocity ≥ 4 m/s is indicative of severe aortic stenosis. An AS is assigned moderate if a peak velocity between 2.6 and 2.9 m/s is founded. In mild AS peak velocity is ≤ 2.5 m/s. The shape of the velocity curve is also useful for a qualitative evaluation of the severity of the stenosis. In fact as aortic stenosis gets worse the peak velocity moves to late systole and the velocity curve shape become more rounded. This curve take the shape of a "dagger" with a late peak in case of dynamic subaortic obstruction.

Mean pressure gradient: The maximum gradient is obtained from maximum velocity using the simplified Bernoulli equation $\Delta P_{max} = 4(v^2_{max})$. When the proximal velocity (LVOT velocity) is over 1.5 m/s, it has to be included in the Bernoulli equation $[\Delta P_{max} = 4(v^2_{max} - v^2_{prox})]$. Mean pressure gradient is drawn by a software of the echograph that calculates it from the traced velocity curve (Photo 17.13).

Aortic valve area: Its calcultation is based on the principle of flow continuity. This principle assumes that flow through the stenotic valve is equal to proximal flow to the valve. Therefore the stroke volume through stenotic aortic valve must be equal to the stroke volume within LVOT ($SV_{Ao} = SV_{LVOT}$).

$$SV = CSA \times VTI \left(\begin{array}{l} CSA = \text{cross sectional area;} \\ VTI = \text{velocity time integral} \end{array} \right)$$

$$CSA = \pi r^2$$

$$SV_{Ao} = SV_{LVOT} \rightarrow CSA_{Ao} \times VTI_{Ao} = CSA_{LVOT} \times VTI_{LVOT}$$

$$CSA_{Ao} = \left(CSA_{LVOT} \times VTI_{LVOT} \right) / VTI_{Ao}$$

Diameter of LVOT is measured from parasternal long axis by TTE and from ME long axis
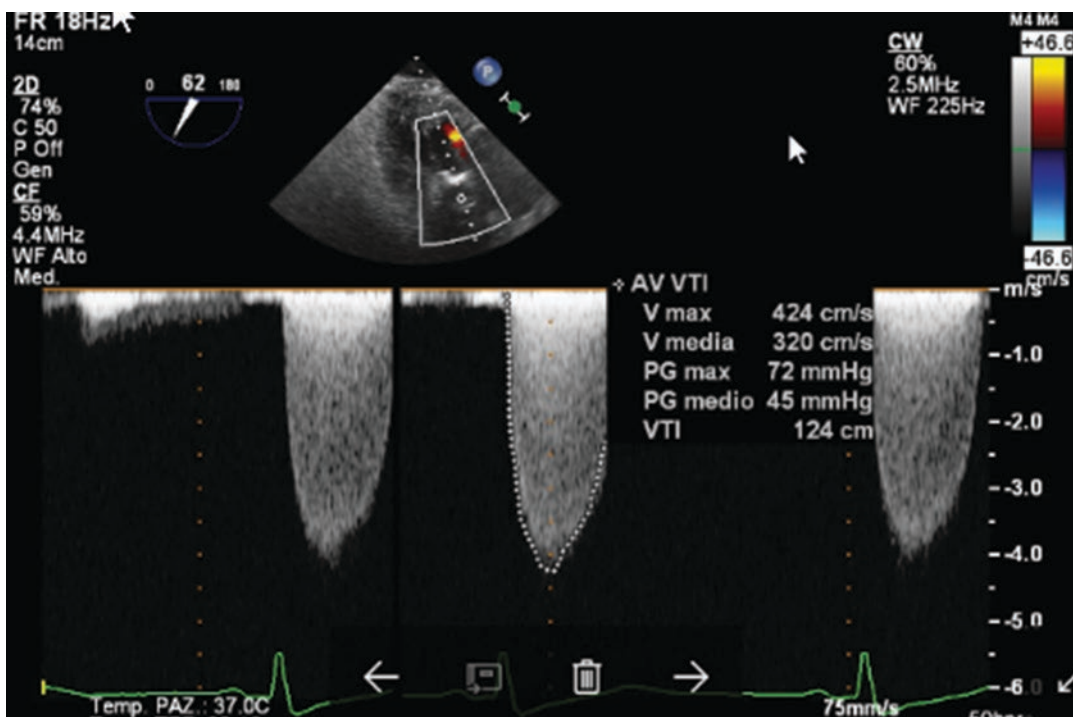
Photo 17.13 Pressure gradient of the aortic valve

view by TEE. LVOT area is assumed circular even if it is more elliptical; zoom mode may be useful to measure the diameter [Area$_{LVOT}$ = π $(d/2)^2$]. VTI is obtained tracing the outline of the jet velocity envelope through aortic valve and LVOT. CW-Doppler and PW-Doppler respectively are used. LVOT velocity is sampled proximal to the Ao valve where the flow is still laminar, whithin 1 cm because the diameter doesn't change in the most people. LVOT diameter and velocity should be measured at the same anatomic level during mid-systole or in the systolic frame where there is the largest diameter.

Other additional parameters for Ao stenosis evaluation are:

– Doppler velocity index: Is the ratio between LVOT velocity and Ao valve velocity. In normal conditions this ratio is about 1, but in case of Ao valve stenosis it is ≤0.25. Instead of LVOT and Ao valve velocity, VTI may be used.

Photo 17.14 Planimetry of the aortic valve area

– Planimetry of aortic valve area: calcifications cause reverberations and shadows that can hinder a right measurement of the area. ETE allows a more accurate measurement (Photo 17.14).

17.3.4 Criteria for Grading Ao Stenosis (AS)

Mild AS: Peak velocity (m/s) 2.6–2.9; mean gradient (mmHg) <20; AVA (cm^2) >1.5; indexed area (cm^2/m^2) >0.85; velocity ratio >0.50.

Moderate AS: Peak velocity (m/s) 3–4: Mean gradient (mmHg) 20–40; AVA (cm^2) 1–1.5; indexed area (cm^2/m^2) 0.6–0.85; velocity ratio 0.25–0.50.

Severe AS: Peak velocity (m/s) $\geq$4; mean gradient (mmHg) $\geq$40; AVA (cm^2) <1; indexed area (cm^2/m^2) <0.6; velocity ratio <0.25.

The last recommendations EACVI/ASE about assessment of aortic valve stenosis ask to use several parameters (gradients, valve area, valve morphologhy, flow rate, LV morphology and function, blood pressure and symtoms) and to do a step by step grading of AS severity. Firstly, if a AS is suspected on the basis of morphologic evaluation by echocardiography, it must be assessed velocity and gradient of the valve.

Two different conditions can be found: Low-gradient AS or high-gradient AS.

In case of low gradient (V_{max} <4 m/s e ΔP_{max} <40 mmHg) AVA assessment has to be made:

- AVA >1 cm^2: Moderate AS
- AVA $\leq$1 cm^2: It must be excluded measurement errors. The following step will be the flow assessment (stroke volume index, SVi).

If SVi is normal (>35 ml/m^2), AS isn't severe. If a low flow is present (SVi $\leq$35 ml/m^2), LV ejection fraction (LVEF) has be evaluated.

In low flow/low gradient with LVEF <50% echostress dobutamina to evaluate the contractile reserve is recommended. If a contractile reserve is present, dobutamine stress echocardiography induces an increase in SV $\geq$20%. This test allows to distinguish true severe AS from pseudosevere AS. In severe AS the dobutamine infusion increases flow and gradient but the calculated valve area doesn't change. In pseudosevere AS gradient don't change but the calculated area increases. If contractile reserve is absent, a clear distinction can't be drawn. In that case it has to rely on calcium score by MSCT (multislice CT) for the likelihood of severe AS.

- Calcium score by MSCT
- Severe AS likely: Men $\geq$2000; women $\geq$1200
- Severe AS very likely: Men $\geq$3000; women $\geq$1600
- Severe AS unlikely: Men <1600; women <800

In low flow/low gradient with LVEF $\geq$50% it is very difficult to distinguish between severe and non severe AS. Several parameters have to be considered: clinical criteria (age, symtoms), qualitative (hypertension, reduced LV longitudinal function) and quantitative data (mean gradient 30–40 mmHg, AVA $\leq$0.8 cm^2, SVi <35 mL/m^2, elevated calcium score, high BNP). In case of high gradient (Vmax $\geq$4 m/s e ΔPmax$\geq$40 mmHg) associated to an aortic area >1 it must be searched the presence of high cardiac output conditions (fever, anemia, hypertiroidism, arterio-venous shunts) that increase flow and consequently velocity and gradient. These conditions should be solved and then the gradient revalued.

17.4 Aortic Regurgitation (AR)

Aortic valve is a part of the aortic root; it's consists of three semilunar cusps (right, left and non coronary cusp), three interleflets triangles, three sinuses of Valsalva, an aortic-ventricular junction (called anulus) and a sinotubular junction. Diameter of the sinotubular junction is about 10–15% larger than diameter of anulus. The interleaflets triangole beetwen left coronary cusp (LCC) and non coronary cusp (NCC) is in fibrous continuity with the base of anterior mitral leaflet. From the right and left sinuses arise, respectively, the right and left coronary arteries.

17.4.1 Etiology

Abnormlities of AoV or aortic root can cause regurgitation. It can be acute or chronic; endocarditis and aortic dissection are the main causes of acute regurgitation (Photos 17.15 and 17.16). Chronic Regurgitation recognizes different causes:

- Degenerative AR: is the most common type. It can involve leaflets and/or aorta with leaflets prolapse, dilatation of aortic root and ascending Ao
- Calcific AR: calcification involves the central part of the cusps
- Rheumatic AR: commissural fusion, thickening and retraction of leaflets are typicaly found
- Congenital abnormalities: the most common type is bicuspid Ao where there is a fusion between right and left coronary cusps. On echocardiography examination two cusp can be seen, anterior one larger and posterior one smaller. Bicuspid AoV is often associated with aneurysm of ascending Ao
- Inflammatory disease: systemic lupus erythematosus, rheumatoid arthritis, Reiter syndrome, Takayasu arteritis

Photo 17.15 Endocarditis of the aortic valve
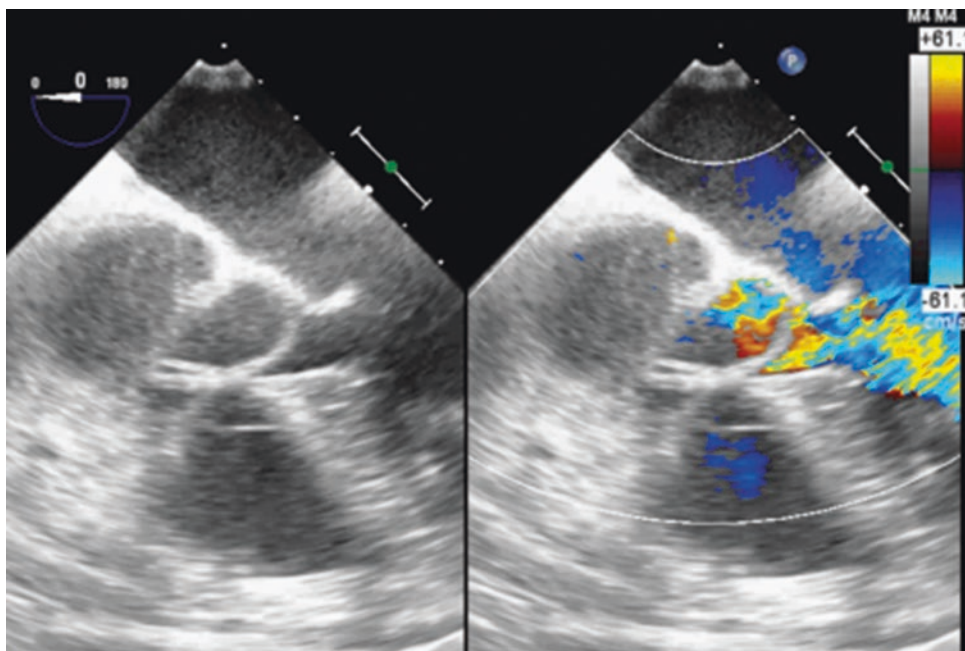
Photo 17.16 Aortic valve regurgitation in dissection of aorta

17.4.2 Mechanisms of Aortic Regurgitation (AR)

A functional classification similar to Carpentier's classification for mitral valve is been adopted to describe the mechanism of insufficiency. It identifies three types of AR:

- Type I: aortic dilatation with normal cusp motion or cusp perforation. This type is been subdivided in four subtypes (Photo 17.17):
    - Ia→ dilatation of distal ascending Ao and enlargement of sinustubular junction (SJT) with outward displacement of the commissure
    - Ib→aortic root dilatation (STJ and sinuses of Valsalva)
    - Ic→ anulus dilatation
    - Id→aortic cusp perforation
- Type II: cusp prolapse or flail due to an eccessive leaflet motion. In case of prolapse the free edge of the cusp gets over anular plane. In cusp flail there is an whole eversion of the leaflet in LVOT. In this type of AR an eccentric jet is present and it goes towards the opposite direction of affected cusp (Photo 17.18)
- Type III: there is a decreased cusp mobility with reduced valve opening. It can be due to rheumatic heart disease, degenerative calcification, connective tissue disorders, infective endocarditis (Photo 17.19)

Photo 17.17 Dilatation of ascending aorta

17.4.3 Assessment of Aortic Rigurgitation

Echocardiography is very important for the evaluation of AoV and Aortic root anatomy
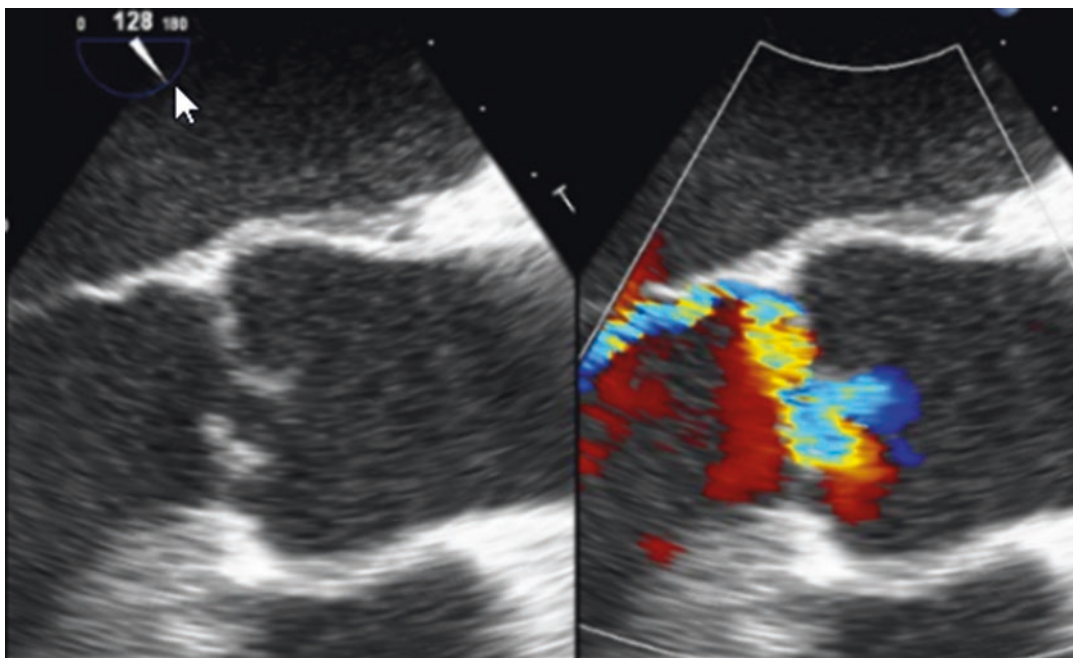
Photo 17.18 Flail of the RCC
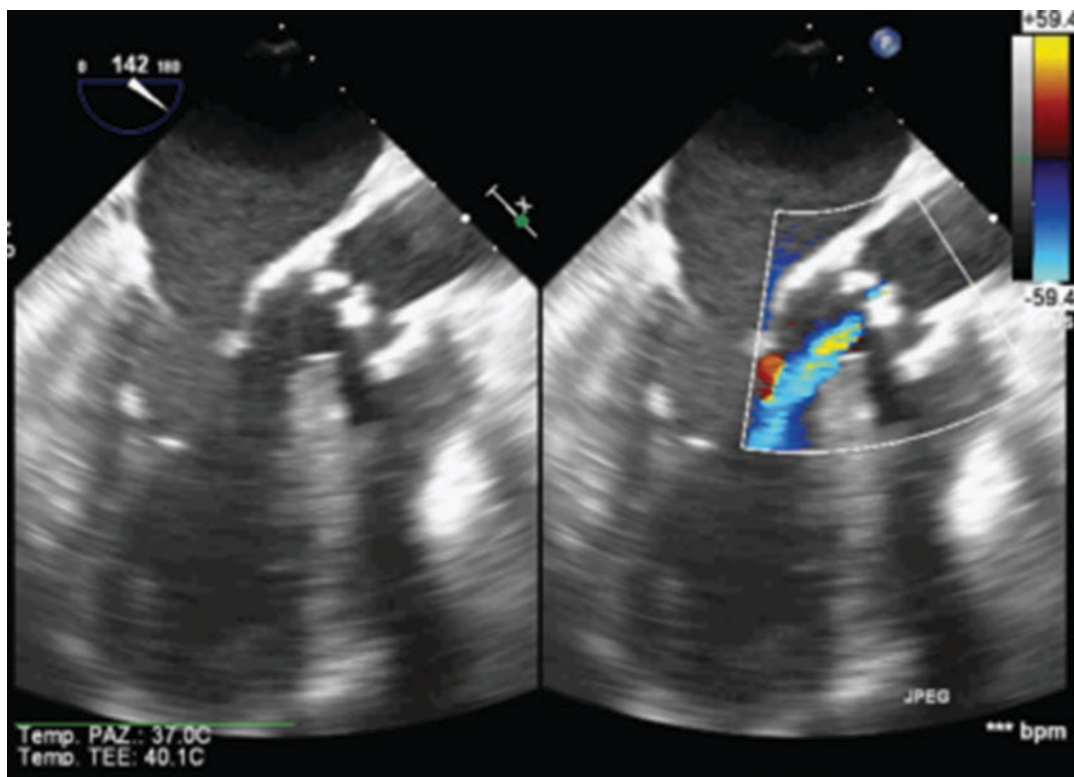
Photo 17.19 Type III of aortic valve regurgitation

because it allows to understand etiology and mechamisms of regurgitation. Moreover the consequences on LV of the regurgitation can be evaluated; in fact a chronic AR causes a volume and pressure overload that leads to LV remodeling with progressive dilatation and systolic dysfunction.

17.4.4 Echocardiographic Assessment of AR Severity

Standard approach to AR evaluation uses the same views employed for morphological examination of the valve. Doppler echocardiography (Color flow Doppler, Pulse-wave Doppler, Continuous-wave Doppler) is very useful to detect and quantify AR; qualitative, semi-quantitative and quantitative (regurgitation volume, regurgitation area, regurgitation fraction) parameters should be investigated.
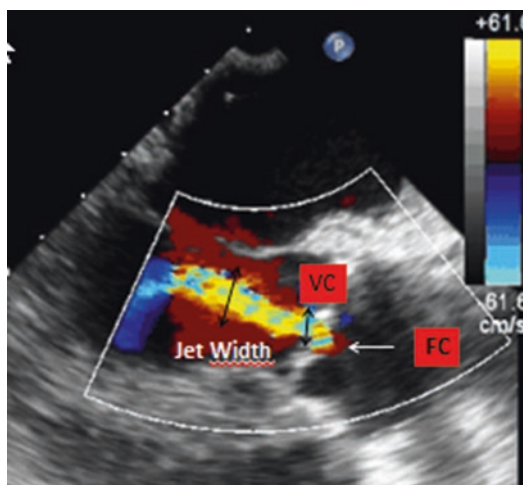
Photo 17.20 Jet width, vena contracta and flow convergence of the regurgitant jet

17.4.5 Color Doppler

We can evaluate three parameters: jet width, vena contracta and flow convergence (Photo 17.20).

Jet width: It can be both a qualitative than a semiquantitative parameter. In the first case a visual evaluation is given: a small jet width points to a mild AR but a large one indicates a severe AR. This is true for central jets. A semiquantitative assessment is given if we measured the width or the area of the jet compared with LVOT width or area. This parameter hasn't to be used in eccentric or multiple jets. A ratio <25% usually hints a mild regurgitation, while a ratio ≥65% indicates a severe AR.

Vena contracta width: It is the narrowest portion of the regurgitant jet. A VC <0.3 cm indicates mild AR; a VC >0.6 indicates severe AR. It can be used also for eccentric jets.

Flow convergence (PISA): In presence of a narrow orifice blood flow accelerates forming concentric emispheric shells; if aliasing velocity is reached a distinct red-blue interface occurs. This parameter allowes a fast visual evaluation of the rigurgitation (it's absent in mild AR and large in severe AR) but it can be also used for a quantitative assessment of the severity of AR; in fact measuring flow convergence radius, AR peak velocity and VTI of the regurgitant jet we can obtain EROA and regurgitant volume. A EROA ≥30 cm^2 and a RegVol ≥60 ml indicate a severe AR.

17.4.6 Continuous Wave Doppler

By CW-doppler can be sampled an envelope of the regurgitant jet which density is proportional to the severity of the regurgitation: the more severe the AR the more dense will be the envelope. A faint envelope indicates a mild AR, a dense one is suggestive of a severe AR. Moreover this envelope can be used to measure the Pht (the time needed for the Ao-LV pressure gradient to reduce by 50%) and the slope of the regurgitant jet envelope. A Pht >500 msec indicates a mild AR, a Pht <200 suggets a severe AR. A slope of the regurgitant jet >3 m/sec is suggestive of a severe AR (Photos 17.21 and 17.22).

17.4.7 Pulse Wave Doppler

PW-Doppler allows to investigate the presence of flow reversal in descending thoracic Ao. An early flow reversal is a normal finding, but it suggests a moderate to severe AR if it is holodiastolic. AR is certainly severe if a holodiastolic flow is found in abdominal Ao. Another parameter by PW-D is the end-diastolic velocity at the peak of R wave. If the end diastolic velocity is >20 cm/sec AR is almost undoubtedly severe.

CW-D and PW-D are also usefull to obtain quantitative measurements as regurgitation

Photo 17.21 CWD: envelope of the regurgitant jet: mild AR
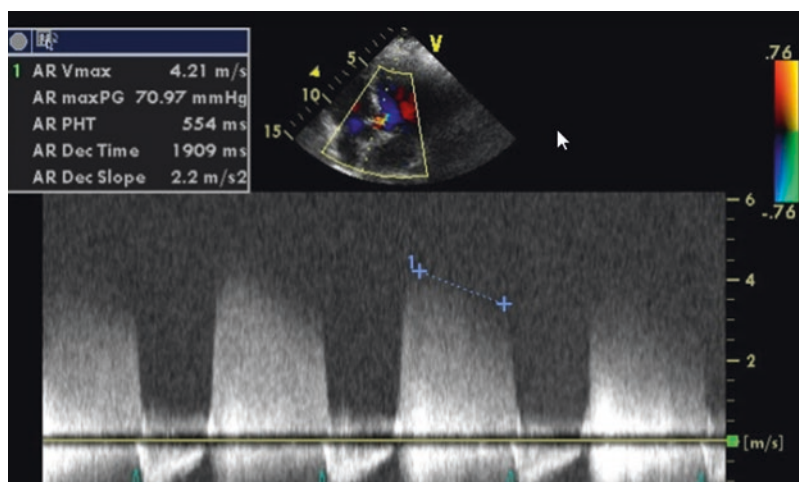
Photo 17.22 CWD: envelope of the regurgitant jet: moderate AR
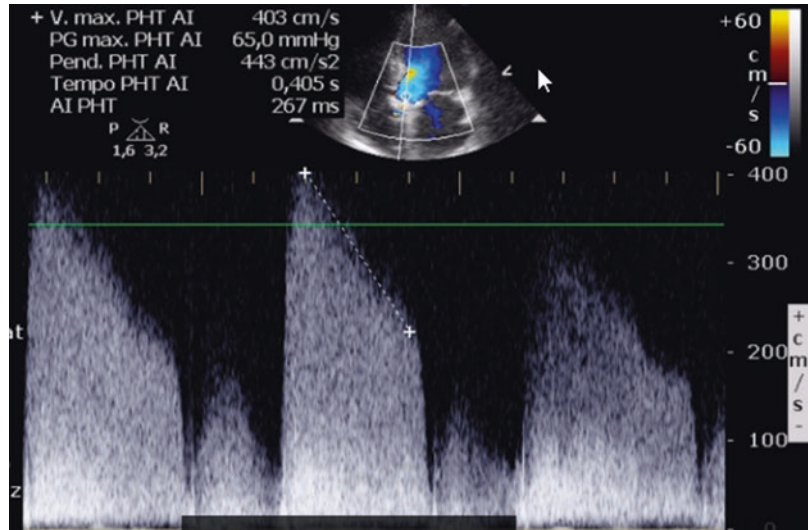
volume, regurgitation area, regurgitation fraction. The total stroke volume across the AV in case of AR is the sum of forward SV (that we can measure at the MV, if there isn't regurgitation) plus the regurgitant volume.

$$RV = SV_{AV} - SV_{MV} = \left(CSA_{MV} \times VTI_{MV} \right)$$

$$SV_{AV} = CSA_{AV} \times VTI_{AV} = 0.785 \times d^2 \times VTI_{AV}$$

$$SV_{MV} = CSA_{MV} \times VTI_{MV} = 0.785 \times d^2 \times VTI_{MV}$$

$$RV = \left(0.785 \times d^2 \times VTI_{AV} \right) - \left(0.785 \times d^2 \times VTI_{MV} \right)$$

$$EROA = RV / TVI_{AR}$$

$$RF = RV / SV_{AV} \times 100\%$$

Evaluation of AR severity should combine multiple parameters, because all methods have some limitations. It has been suggested to distinguish between mild and severe AR and to use quantitative methods for grading severity in case of intermediate values.

Chronic mild AR:
- VCw ≤0.3 cm;
- Central jet, width <25% LVOT
- Small or no flow convergence
- Faint or incomplete CW-Doppler signal
- PHT >500 ms
- Normal LV

Chronic severe AR:
- flail valve
- VCw >0.6 cm
- Central jet, width ≥65% LVOT
- Large flow convergence
- PHT <200 ms
- Holodiastolic flow reversal in the descending Ao
- Enlarged LV but normal function

If only 2–3 parameters are positive for mild or severe AR, it's suggested to measure EROA, RVol and RF

- EROA <0.1 cm^2; RV <30 ml; RF <30% → MR grade I (mild MR)
- EROA 0.10–0.19 cm^2; RV 30–44 ml; RF 30–39%→ MR grade II (moderate MR)
- EROA 0.20–0.29 cm^2; RV 45–59 ml; RF 40–49%→ MR grade III (moderate MR)
- In the last case if 3 parameters of severe MR are founded the MR will be severe
- EROA ≥0.3 cm^2; RV ≥60 ml; RF ≥50%-→ MR grade VI (severe MR)

References

1. Zoghbi WA, Adams D, et al. Recommendation for noninvasive evaluation of native valvular regurgitation. A report from the American Society of Echocardiography developed in collaboration with

the Society for Cardiovascular Magnetic Resonance. JASE. 2017;30(4):303–71.

2. Baumgartner H, et al. Recomentations on the echocardiographic assessment of the aortic valve stenosis: a focused update from the European Association of Cardiovascular Imaging and the American Society of Echocardiography. J Am Echocardiogr. 2017;30:372–92.

3. Nishimura RA, et al. AHA/ACC guideline for the management of patients with valvular heart disease: a report of the American College of Cardiology/ American Heart Association Task Forceon Practise Guidelines. Circulation. 2014;129:e521–643.

4. Pibarot P, et al. Low-flow, low-gradient aoertic stenosis with normal and depressed left ventricular ejection fraction. J Am Coll Cardiol. 2012;60: 1845–1853g.

5. Cueff C, et al. Measurement of aortic valve calcification using multislice computed tomography: correlation with emodynamic severity of aortic stenosis and clinical implication for patients with low ejection fraction. Heart. 2011;97:721–6.

Tricuspid and Pulmonary Valves

18

Claudio Poli, Armando Sarti, and Vanni Orzalesi

18.1 Tricuspid Valve Morphology and Function

The tricuspid valve (TV) as the name implies has three cusps, as well as the pulmonary valve. The TV, morphologically similar to the mitral, but it is placed downward, towards the apex of the heart. The subvalvular apparatus, including papillary muscles and chordae tendinae, sticks mainly to the septum, and it is not easily visible in the US images.

The TV is visible mainly in PSLAX modified for the right sections, in PSSAX at the "big vessels level", in A4C, and in subcostal projections by TTE. Using TEE, this valve is easily seen in ME 4C, ME RV inflow-outflow, ME AV SAX, TG RV inflow, and deep TG LAX. The cusps should not be thicker than 4 mm. The annulus, well visible in TTE A4C and TEE ME 4C, has a diameter ranging typically between 2 and 3.8 cm. Using the CFM Doppler it is possible to detect a slight tricuspidal regurgitation in most subjects. This is normal. On the other side moderate or severe regurgitations are never normal.

Basing on TV regurgitation is possible to estimate the systolic pulmonary pressure (see Chap. 14).

The respiratory changes in transtricuspidal flow are very marked, up to 40% in normal subjects, so a reliable Doppler assessment of pulmonary artery systolic pressure needs many measurements along the respiratory cycle.

By TTE it is not possible to study the Doppler flow in the inferior cava vein, which is essential to assess the right heart, because of the impossibility of a proper ultrasound alignment. However, using the PW Doppler in the subcostal projection for the inferior vena cava, it is possible to evaluate the US aligned vertical flow in an hepatic vein, about 1 cm before its merging into the inferior vena cava (see Chap. 11).

The hepatic vein's flow is a good mirror of the vena cava's flow. The normal flow pattern has

- A dominant systolic component;
- A diastolic velocity of no more than 50% of the systolic one.

If there is significant tricuspidal regurgitation the flow in the hepatic veins can be dramatically reduced in systole and even reversed, while its diastolic component becomes predominant.

The normal atrio-ventricular flow through the tricuspid valve, estimated with PW in A4C (TTE) or ME 4C (TEE), is a low-speed flow, well below 1 mt/sec.

C. Poli (✉) · A. Sarti · V. Orzalesi
Anesthesia and Intensive Care Department,
Santa Maria Nuova Hospital, Azienda Sanitaria
Firenze, Florence, Italy
e-mail: claudio.poli@uslcentro.toscana.it

18.2   Pulmonary Valve Morphology and Function

The pulmonary valve (PV) is visible by TTE in modified PSLAX projection (cranial inclination), in PSSAX and subcostal short axis at the level of the aortic valve. Using TEE this valve is mainly seen in ME RV inflow-otflow, ME AV SAX, and UE AA (aortic arch) SAX. The cusps' thickness normally does not exceed 2 mm. The transpulmonary flow is studied by TTE in PSSAX with the PW or CW doppler. Normally, the peak does not exceed 0.9 m/sec. A slight regurgitation is visible in most healthy subjects. Through the pulmonary regurgitation jet the diastolic pulmonary artery pressure can be estimated (see Chap. 14).

18.3   Carcinoid Syndrome

The serotonin-producing carcinoid tumor causes damage to the right heart valves. They gradually thicken and lose their normal mobility (Figs. 18.1 and 18.2), causing valvular insufficiency and sometimes even stenosis.

If there are no carcinoid lung metastases, left heart structures are not affected.

Alterations of TV and PV are also described in the amphetamine-addicted patients. Amphetamine-derived drugs have also been widely used in the past to reduce the sense of hunger with the purpose of weight loss.
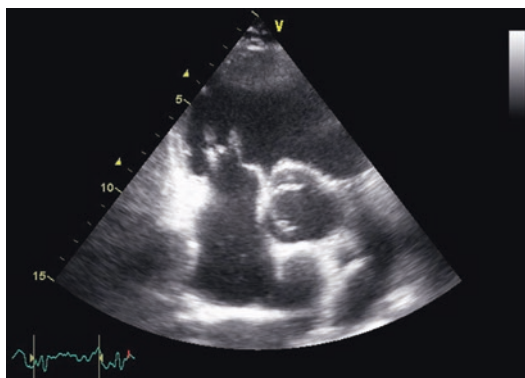
Fig. 18.1 TTE PSSAX. Carcinoid syndrome. Thickened leaflets of the tricuspid valve causing severe regurgitation and stenosis
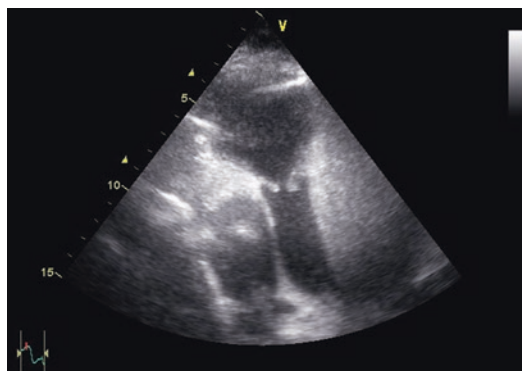
Fig. 18.2 TTE, modified PSSAX for RV outflow and pulmonary valve. Carcinoid syndrome. Thickened leaflets of the pulmonary valve leading to severe regurgitation and stenosis

18.4   Tricuspid Stenosis

It is a rare condition observed in relation to carcinoid syndrome (Fig. 18.1), rheumatic heart disease or Loeffler's endomyocardial fibrosis. The diagnostic principles are like those used for mitral stenosis. The valve has the morphological changes in relation to the causing pathology. The average gradient obtained from the Doppler CW transvalvular flow is considered severely impaired if more than 5 mmHg. Caval congestion is observed with severe tricuspid stenosis.

18.5   Pulmonary Stenosis

It is known to be associated with Noonan syndrome. Apart from the congenital forms, pulmonary stenosis can also be caused by carcinoid syndrome (Fig. 18.2) or rheumatic disease. Among the congenital forms, the most common, subvalvular, with a dynamic obstruction component, is most often related to Fallot's tetralogy. The right ventricle thickens in response to obstruction.

18.6   Tricuspid Regurgitation

The most common cause of TV regurgitation is related to TV annulus enlargement due to right ventricular cavity dilatation (by reduced RV contractility and pressure or volume overload). In this case, apart

from the annulus expansion, the valve is morphologically normal. The other most common cause of TV regurgitation is endocarditis, particularly in intravenous-drug-addicted patients, in the carcinoid syndrome, and in rheumatic disease. The congenital defect of the peri-membranous ventricular septum may be complicated by TV regurgitation. Even Ebstein's anomaly, which consists of a displacement of the septal cusp towards the apex, with right ventricle "atrialization", is associated with tricuspidal regurgitation. The valve leaflets appear dysplastic. Sometimes Ebstein anomaly is diagnosed in adulthood with the onset of right heart failure. It is not uncommon the association with the Wolff-Parkinson-White syndrome (Fig. 18.3).

The study of Doppler CFM through the tricuspid valve should not be omitted in each cardiac US assessment. First, the possible morphological alterations are considered. The simple visual observation of the regurgitant jet gives an idea of the insufficiency, despite the large fluctuations caused by breathing (Fig. 18.4). Moreover, the flow is also affected by the pressure generated by the RV. With pulmonary hypertension the high right ventricular pressure generates a well-defined, high speed jet (Fig.18.5). So, TV regurgitation cannot be measured by visual CFM jet only. The most reliable, and easy-to-apply method to estimate the amount of TV regurgitation is measuring the diameter of the narrowest

Fig. 18.3 From Sarti A. Ecocardiografia per l'intensivista. Springer Verlag Italia, Milano, 2009, with the permission of the publisher and the author. TTE Subcostal 4 C. Severe tricuspidal regurgitation
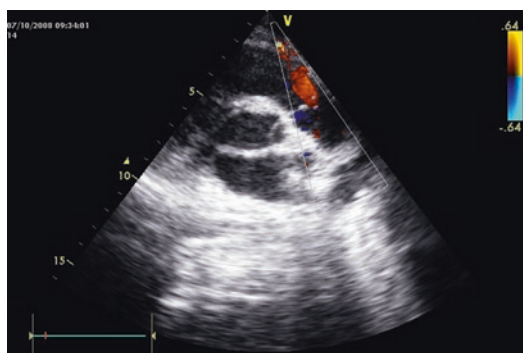
Fig. 18.5 From Sarti A. Ecocardiografia per l'intensivista. (Springer Verlag Italia, Milano, 2009, with the permission of the publisher and the author. TTE PSSAX. Pulmonary insufficiency)

Fig. 18.4 TTE A4C. CW Doppler of a high-speed tricuspid regurgitation jet
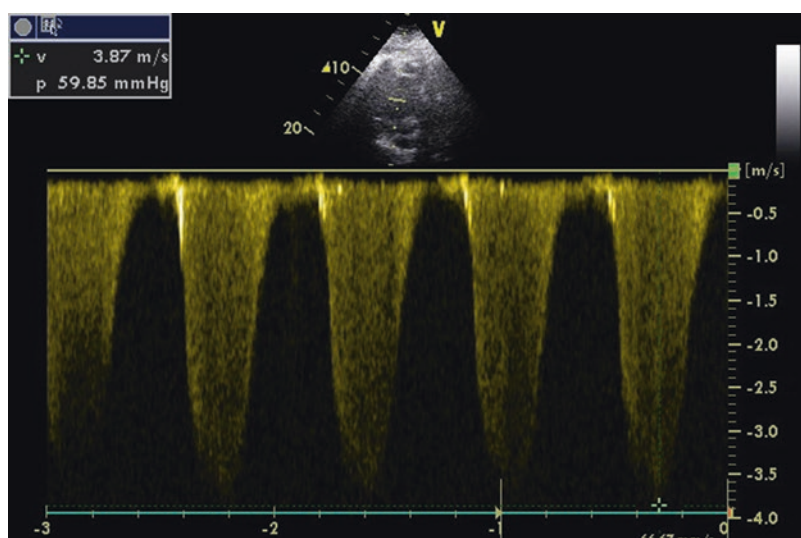
point of the jet, just beyond the valvular level (vena contracta). A diameter that exceeds 0.7 cm reveales a severe regurgitation.

18.7 Pulmonary Insufficiency (Fig. 18.5)

Pulmonary regurgitation in adults is substantially in relation with rheumatic disease, carcinoid syndrome or endocarditis. Also, pulmonary hypertension may dilate the annulus and cause valvular leakage. The anterograde flow and regurgitation is studied in PSSAX (TTE) or ME AV SAX and RV inflow-outflow (TEE) with CFM. A large jet in relation to the area of right ventricular outflow tract, with a length equal or > to 20 mm and area equal or >1.5 cm^2, shows a significant regurgitation. By CW Doppler it is possible to study the pressure half time (time of the peak to reach the half value) of pulmonary insufficiency. A value <100 mt/sec. Reveals a significant regurgitation. An important regurgitation first causes RV dilatation and later right ventricular hypertrophy.

Further Reading

Oh JK, Tajik AJ, Stewart JB. The echo manual. 3rd ed. Philadelphia: Lippincott Williams & Wilkins; 2007.

Feigenbaum H, Armstrong WF, Ryan T. Feigenbaum's echocardiography. Philadelphia: Lippincott Williams & Wilkins; 2005.

Endocarditis

19

Roger L. Click

19.1 Introduction

Endocarditis is not common but can be a life threatening inflammation of the endocardium, particulartly the heart valves, native or prosthetic. Vegetative material is the hallmark of endocarditis and may be infective or noninfective. The diagnosis can be challenging because in some cases symptoms are vague and nonspecific. The diagnosis is based on positive blood cultures, clinical and echocardiographic features. Since patients with endocarditis can become critically ill and it may be fatal, the diagnosis must be made quickly and appropriate treatment initiated. In this chapter, the role of echocardiography in the diagnosis and management of endocarditis will be reviewed.

19.2 Classification

Infective endocarditis is usually the result of a bacterial or fungal infection of the heart valves. With a transient bacteremia, i.e., dental cleaning, bacteria can seed abnormal valves and grow, form a vegetation and damage the valve, potentially be embolic or form an abscess.

R. L. Click (✉)
Division of Cardiology, Mayo Clinic,
Rochester, MN, USA
e-mail: click.roger@mayo.edu

Noninfective endocarditis, also nonbacterial thrombotic endocarditis or marantic endocarditis may occur on normal valves. Often times associated with other systemic illnesses such as cancer, hypercoagulable state and lupus (Libman-Sacks). The vegetations are sterile and usually smaller and nondestructive to the valve. The greatest risk is embolic.

19.3 Diagnostic Criteria

There are three general criteria to diagnose endocarditis: bacteremia, active endocardial pathology and predisposing heart disease. More specifically, in 1994 the Duke Clinical Criteria for the diagnosis of infective endocarditis established guidelines. There are major and minor criteria for the diagnosis (see Table 19.1).

Table 19.1 Duke criteria for diagnosis of endocarditis

Major criteria	Minor criteria
Positive blood cultures	Predisposition
Endocardial involvement	Fever
Positive echocardiogram	Vascular phenomenon
New valvular regurgitation	Immunologic phenomenon
	[a]Microbiologic evidence
	[a]Echocardiographic evidence

[a]Less than major criteria

To make the diagnosis with the Duke Criteria requires two major criteria, one major and three minor or five minor criteria.

The Duke Criteria define echocrdiographic evidence as: oscillating intracardiac mass on a heart valve or supporting structure in the path of a regurgitant jet or prosthetic material, cardiac abscess, new dehiscence of a prosthetic valve or new valvular regurgitation. Echocardiographic assessment of the patient for endocarditis can be divided into two general areas: recognize/differentiate and complications.

19.4 Recognize/Differentiate

Recognizing the presence of endocarditis refers to identifying vegetations and abnormal valve pathology and differentiating from other noninfective valve lesions or abnormalitaies. Transthoracic echocardiography (TTE) is less than half as sensitive compared to transesophageal echocardiography (TEE), 44% vs 94%. The specificity is better, TTE at 98% vs TEE at 100%. For this reason it is recommended that a TEE be performed on all patients, if possible, when suspected endocarditis is the question. Fig. 19.1 shows an example of a mitral valve with TTE and TEE and the presence of vegetations easily missed by TTE.

To recognize a vegetation the echocardiographic features have to be appreciated. Most vegetations are on left sided heart valves because of the higher pressure jet lesions from regurgitation and the more common anatomical variants of left sided valves, i.e. bicuspid aortic valve (Fig. 19.2), mitral stenosis, and prolapse.

Right heart lesions are less common but may be seen with intravenous drug use and right heart
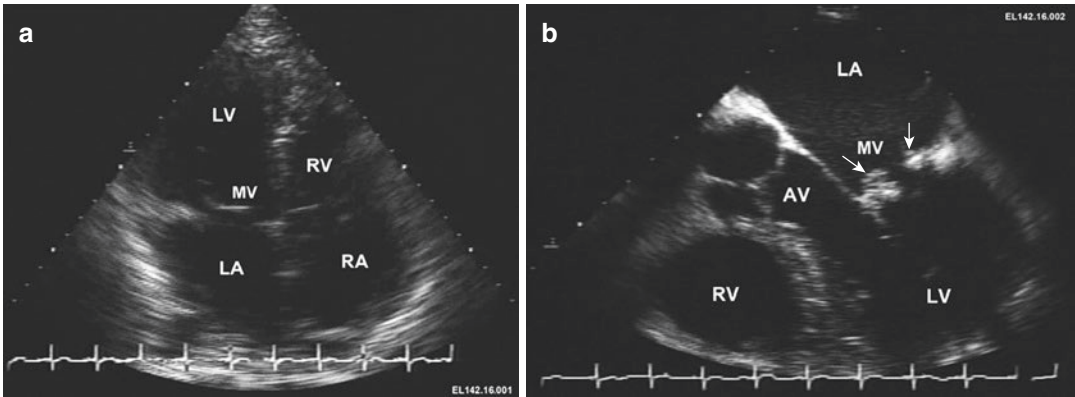
Fig. 19.1 Transthoracic echo (TTE), 4 chamber view of patient with suspected endocarditis (panel **a**). Images are difficult and no obvious vegetations seen. In panel **b**, a transesophageal long axis view of the same patient shows obvious mitral valve (MV) vegetations (arrows). LA left atrium, AV aortic valve, RV right ventricle, LV left ventricle
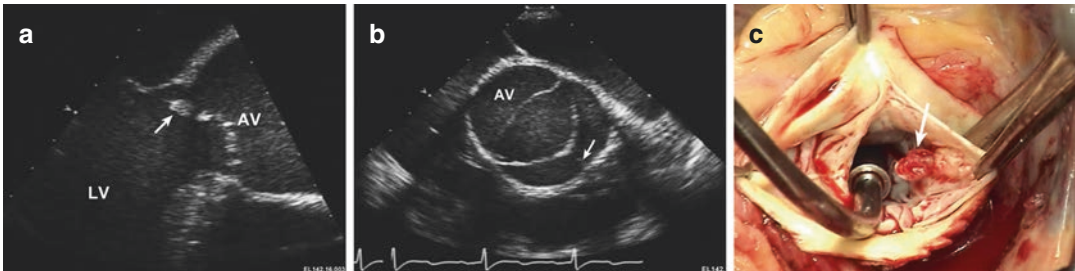
Fig. 19.2 Transesophageal echo (TEE) view long axis view (Panel **a**) of the aortic valve (AV) with a vegetation (arrow). Panel **b**-short axis view of the AV bicuspid with raphe (arrow). Panel **c** is an intraoperative photo of the valve and vegetation (arrow)

indwelling catheters and pacemakers. Vegetations tend to be irregular, bulky and may be multiple and lead to valve destruction (Figs 19.3 and 19.4). Sites of vegetations are shown in Table 19.2.

Once an abnormal mass on a valve has been identified one has to differentiate it from other types of valve masses. Endocarditis vegetations more often occur on an abnormal valve. Other lesions, i.e., fibroelastomas, more commonly are seen on normal valves. They are usually discrete, singular and do not cause valve erosion or destruction.

The strands often called degenerative strands are often seen in the older population. The main differentiator of vegetations from other valve lesions are the presence of other features

Table 19.2 Sites of vegitation

Atrial surfaces of atrioventricular valve
Ventricular surface of aortic and pulmonary valves
Prosthetic valve sewing ring
Cusps of bioprosthetic valves
Sites affected by turbulent flow
Patches, pacing wires, catheters
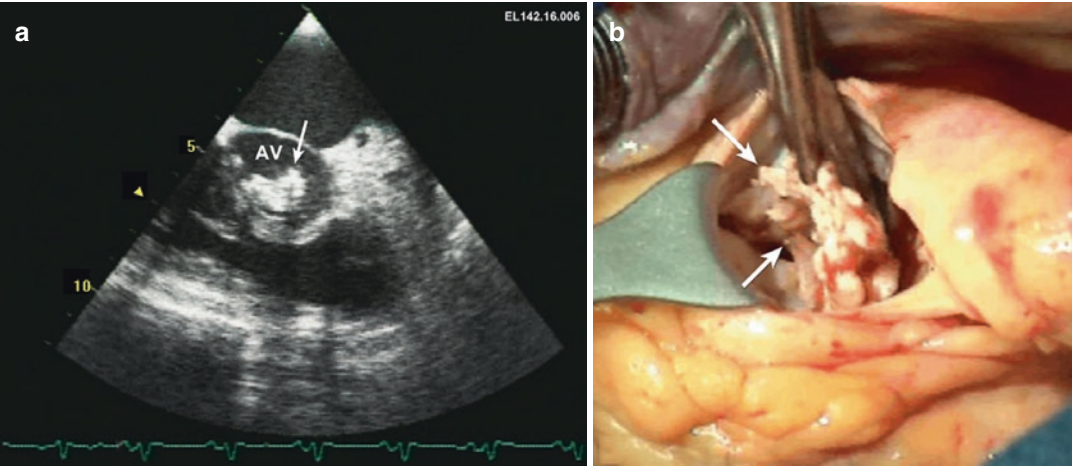
Fig. 19.3 Panel **a**-TEE short axis of the AV with vegetation (arrow). Panel **b** shows the intraoperative picture of the AV vegetation and significant valve destruction
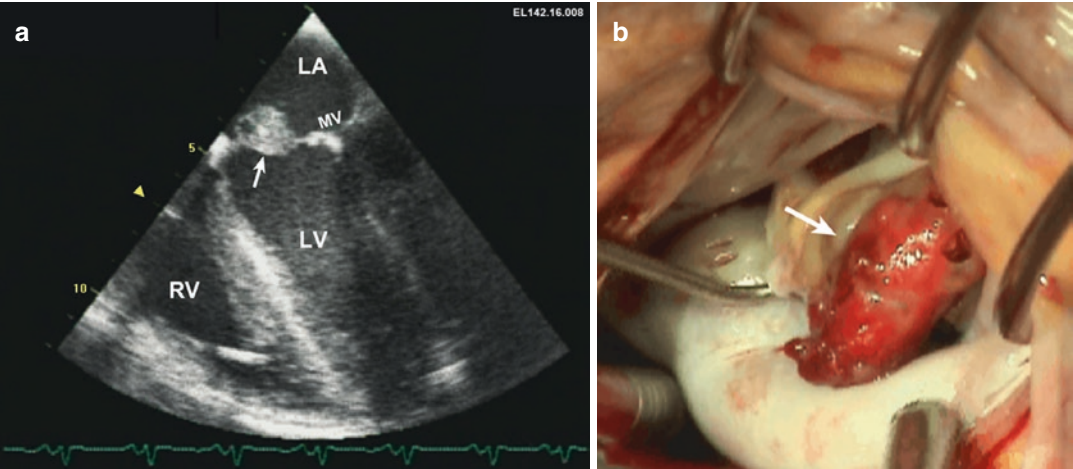
Fig. 19.4 Panel **a**-TEE four chamber of the MV with vegetation (arrow). Panel **b** shows an intraoperative picture of the MV vegetation (arrow). LA left atrium, LV left ventricle, RV right ventricle

indicating endocarditis, i.e., fever, positive blood cultures and clinical presentation. Rarely, does a patient have ongoing active endocarditis and not appear ill or have other associated features. Whereas, other types of valve lesions usually do not have accompanied features, i.e., ill patient, fever, or positive blood cultures. Table 19.3 lists other causes of lesions seen on valves.

19.5 Complications of Endocarditis

Patients with endocarditis, if diagnosed and treated promptly, can avoid many of the complications of the infection. However, many patients

are diagnosed after weeks or months of lingering illness because of vague symptoms. These patients are at significant increased risk of developing complications (see Table 19.4).

It has been shown that larger vegetations >1.0 cm^2 pose a greater risk with more complications including heart failure, emboli, and need for surgery. When vegetations seed an abnormal valve they break down the valve tissue and perforation can occur leading to significant regurgitation (Fig. 19.5).Perforations can be difficult to see echocardiographically but eccentric color flow jets may be a clue. Surgically, they may be repairable with a small pericardial patch.

Fungal vegetations tend to be larger and bulky and can be obstructive. Fungal endocarditis is more often seen in intravenous drug users and those immunocompromised or on broad-spectrum antibiotics. Fungal endocarditis may be more difficult to diagnose as blood cultures may be negative and also more of a challenge to treat. Figure 19.6 shows the typical echo and

Table 19.3 Differential diagnoses for noninfective and lesions on valve

Thrombus
Myxomatous tissue
Ruptured chordae/flail scallop
Fibroelastoma (papilloma)
Nonbacterial thrombotic endocarditis
Valve fenestration (especially torn)
Healed vegetation
Torn tissue prosthesis
Strands/excrescences

Table 19.4 Complications of endocarditis

Emboli
Abscess formation
Mycotic aneurysm
Valve destruction (regurgitation)
Valve stenosis (bulky masses, obstruction)
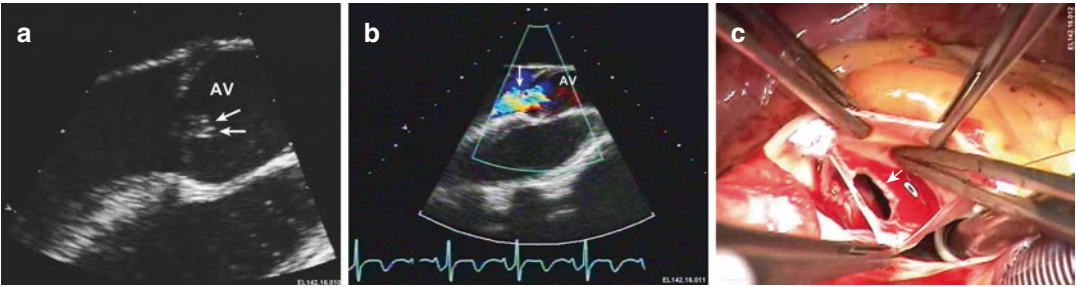
Fig. 19.5 Panel **a**-TEE of AV in the long axis with vegetation (arrows). Panel **b**-Same AV with Color Flow Doppler shows extensive aortic regurgitation (arrow). Panel **c**-Intraoperative picture of large AV leaflet perforation (arrow) from the endocarditis
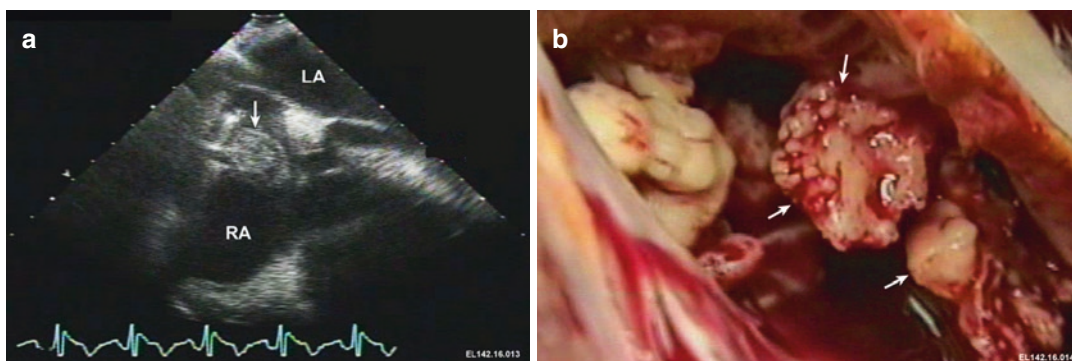
Fig. 19.6 Panel **a**-TEE of large mass (arrow) in the right atrium (RA). Panel **b**-Intraoperative photo of multiple RA masses from a fungal infection. LA left atrium
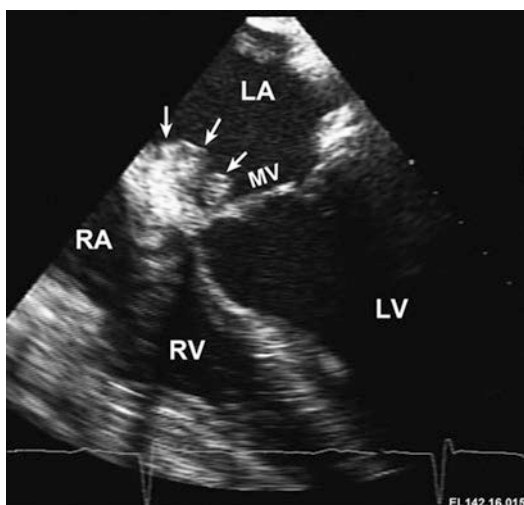
Fig. 19.7 TEE four chamber view showing MV endocarditis with extension into the intervalvaular fibrosa area (arrows). RA right atrium, RV right ventricle, LV left ventricle, LA left atrium

intraoperative picture of a fungal infection involving the right heart.

If left untreated, vegetations can extend from valves to other structures. Mitral and aortic vegetations frequently will extend into the intervalvular fibrosa (the anatomical area between the aortic root and mitral annulus). Once seeded, an abscess space may form (Fig. 19.7).

Likewise, extension from the valve leaflets can occur and cause a perivalvular abscess which may stay contained or can rupture through to an adjacent chamber and cause a perivalvular fistula (Fig. 19.8).

Valvular prostheses are particularly vulnerable to infection. Echocardiographically it may be a challenge to see infection on a prosthesis. The sewing ring is the most common location and the only clue may be "haziness". Rarely there is obstruction or stuck leaflet (Fig. 19.9).
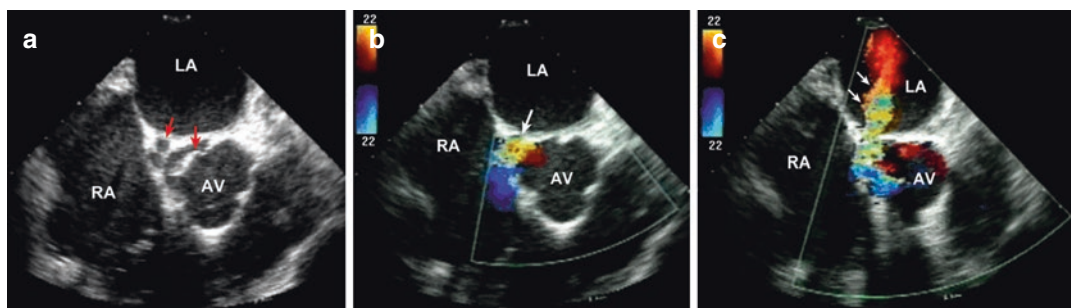
Fig. 19.8 Panel **a**-TEE of the AV with perivalvular abscess (arrows). Panel **b**-Same view with color flow Doppler. Panel **c**-Same view several days later showing on color flow Doppler perforation (arrows) of the perivalvular abscess into the LA. RA right atrium
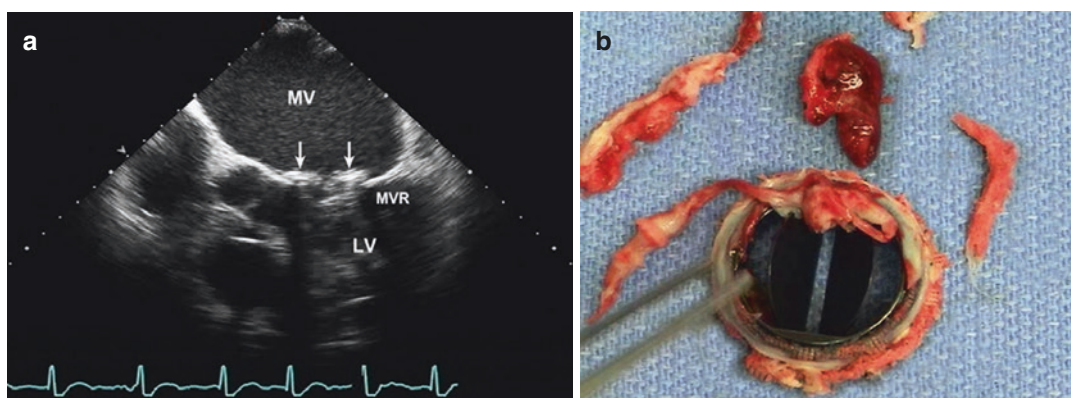
Fig. 19.9 Panel **a**-TEE 4 chamber view of a mechanical mitral valve replacement (MVR) with "shaggy" echos coming from the sewing ring (arrows). Panel **b**-Removed mitral prosthesis with vegetative material and thrombus. LA left atrium, LV left ventricle

19.6   Conclusion

Endocarditis is a serious, potentially fatal infection of cardiac valves. If treated early, complications may be avoided, however, the diagnosis is often delayed because of nonspecific symptoms. Complications are not uncommon and include emboli, valve destruction and abscess formation. If there is significant valve destruction and hemodynamic instability, emboli, or abscess formation, patients are often faced with valve replacement. Echocardiography plays a key role in diagnosis and mangement of patients with endocarditis and therefore should be one of the first tests performed if endocarditis is suspected.

Suggested Reading

Bayer AS, Bolger AF, Taubert KA, et al. Diagnosis and management of infective endocarditis and its complications. Circulation. 1998;98:2936–48.

Daniel WG, Mugge A, Martin RP, et al. Improvement in the diagnosis of abscesses associated with endocarditis by transesophageal echocardiography. N Engl J Med. 1991;324:795–800.

Durack DT, Lukes AS, Bright DK, et al. New criteria for diagnosis of infective endocarditis: utilization of specific echocardiographic findings. Am J Med. 1994;96:200–9.

Erbel R, Rohmann S, Drexler M, et al. Improved diagnostic value of echocardiography in patients with infective endocarditis by transesophageal approach: a prospective study. European Heart Journal. 1988;9:43–53.

Shively BK, Gurule FT, Roldan CA, et al. Diagnostic value of transesophageal compared with transthoracic echocardiography in infective endocarditis. JACC. 1991;18:391–7.

Prosthetic Valve Evaluation

20

Roger L. Click

20.1 Introduction

With the aging population has come an increased number of cardiac operative procedures including valve replacement, repair and percutaneous valve replacement approach. Echocardiography plays a significant role in the assessment of prosthetic valves. The primary goal for echocardiography is to determine if a prosthetic valve is normal or abnormal. All echo parameters including 2D appearance, color flow Doppler, and pressure gradients must be obtained to determine if a valve is normal. Finally, the echocardiographer has to be familiar with what is normal for a given type of valve and location. In this chapter, the echocardiographic features of prosthetic heart valves will be reviewed.

20.2 General Considerations

In many applications, 2D echocardiography, either transthoracic (TTE) or transesophageal (TEE), will provide most of the diagnostic information. To determine if a valve prosthesis is normal, one must rely as much or more on Doppler information in addition to the 2D appearance of the valve. In addition, the type of prosthetic valve

R. L. Click (✉)
Division of Cardiology, Mayo Clinic,
Rochester, MN, USA
e-mail: click.roger@mayo.edu

and Doppler characteristics of the valve in a specific location has to be appreciated. The hemodynamics of each patient has to be assessed at the time of the prosthetic assessment. Is there tachycardia, high or low cardiac output or other factors that may effect the Doppler velocities, i.e., anemia, fever or thyroid disease?

Each prosthesis has a normal appearing 2D motion and color flow Doppler pattern. Also, each prosthesis has a normal Doppler velocity range depending on the prosthesis type and location. It is always helpful to have a baseline echo of a prosthesis shortly after it has been placed to compare appearance and velocities on follow-up echos. Most patients who have had a new prosthetic valve will have a dismissal echo to establish this baseline.

20.3 Normal 2D Echo Appearance

In general, TEE is superior to TTE to assess the echocardiographic appearance and motion of prosthetic leaflets. The mitral valve leaflets are easier to see for all prostheses (Fig. 20.1) while an aortic prosthesis leaflet motion may be more difficult to see with TEE or TTE. In Many cases, an aortic prosthesis can be seen best from the transgastric view. The leaflet motion as well as parallel Doppler angle is best seen from this position and velocity assessment more accurate (Fig. 20.2).
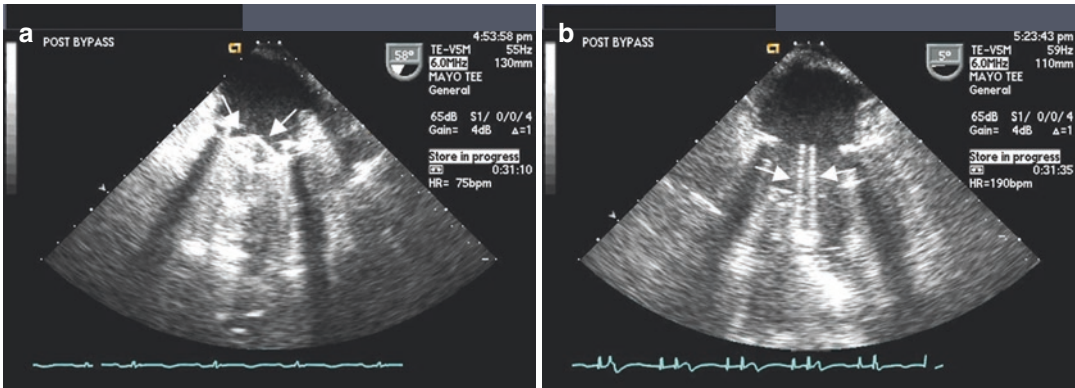
Fig. 20.1 Transesophageal (TEE) view of a normal mitral bileaflet disc prosthesis in the mitral position (MVR). The arrows show a normal closed position (Panel **a**) and open position (Panel **b**)
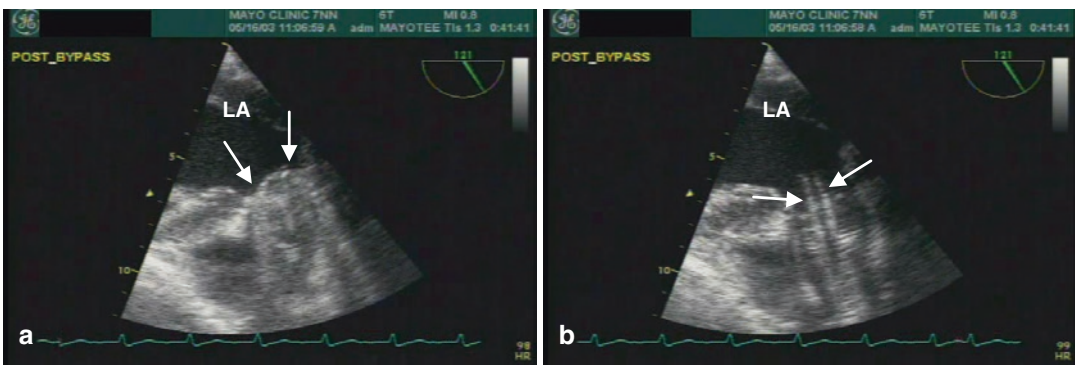
Fig. 20.2 TEE transgastric view of a normal aortic bileaflet disc prosthesis. The arrows show a normal closed position (Panel **a**) and panel **b** a normal open position. LA Left atrium

Tissue prostheses (Hancock, Ionescu-Shiley or Homograft) usually have struts and thin leaflets which may be hard to see on TTE, but easier with TEE (Fig. 20.3).

If normal opening and closing excursion of a mechanical prosthesis is not seen from multiple angles, then one has to suspect a stuck or obstructed prosthesis (see Fig. 20.4). This is usually confirmed with color flow Doppler and velocity measurements. If still not clear, fluoroscopy can determine if there is normal mechanical leaflet motion.

Likewise, tissue prostheses may have a subtle 2D appearance that shows incomplete coaptation and resulting significant regurgitation (Fig. 20.5).

20.4 Color Flow Characteristics

After one has examined a prosthesis with 2D echo, either with TTE or TEE, the next step is color flow Doppler assessment of the valve. Each type of valve has a specific color flow Doppler flow profile. Tissue prostheses usually have a small central jet, mild at most. Mechanical prostheses have closing volume jets. The more popular bileaflet tilting disc prostheses (St. Jude) have several closing volume jets (Fig. 20.6) where as, single tilting disc prosthesis will have either a single larger central jet (Hall-Medtronic) or smaller closing jets on each side (Bjork-Shiley).

Regardless of the closing volume jets one must identify the sewing ring. All closing volume
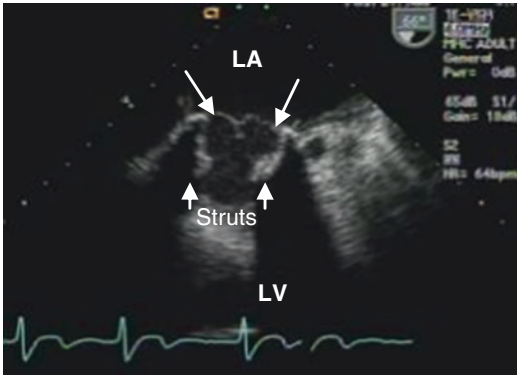
Fig. 20.3 TEE view of a normal appearing mitral tissue prosthesis. Typical thin leaflets (arrows) and supporting struts (arrows). LA left atrium, LV left ventricle
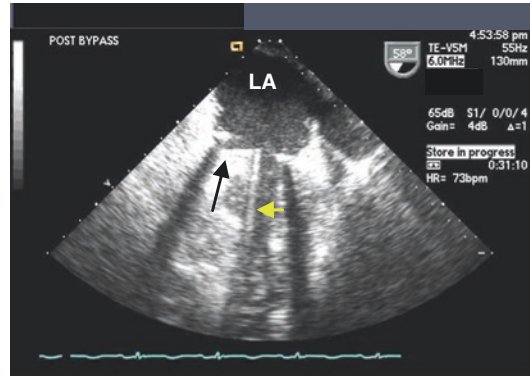
Fig. 20.4 TEE view of a bileaflet mechanical prosthesis. Only one leaflet opens (yellow arrow) while the other leaflet is frozen closed (black arrow). LA left atrium
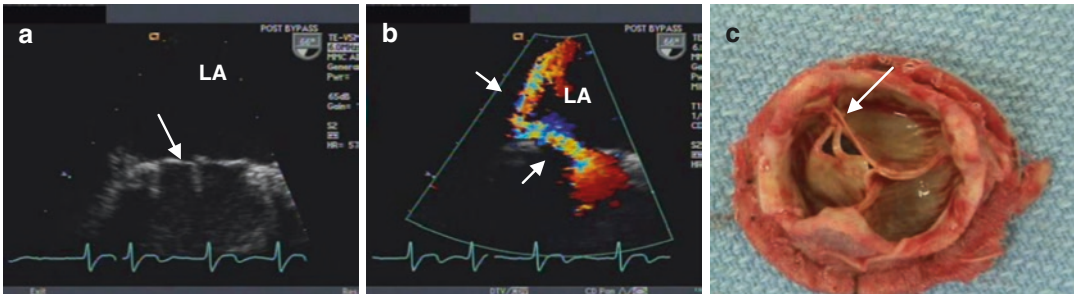
Fig. 20.5 TEE view of abnormal mitral tissue prosthesis. Panel **a** shows incomplete coaptation of the leaflets (arrow). Panel **b** shows an eccentric mitral regurgitant jet (arrows). Panel **c** shows the surgical specimen and torn leaflet (arrow). LA left atrium, LV left ventricle
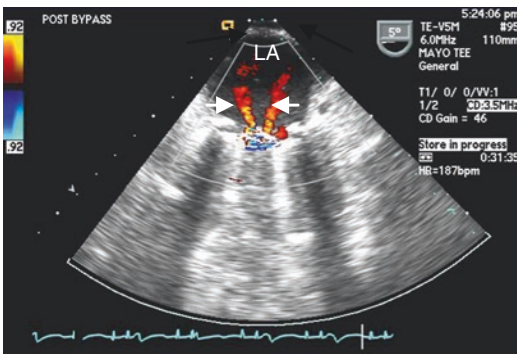
Fig. 20.6 TEE view of a mitral bileaflet mechanical prosthesis in closed position showing normal closing volume jets (arrows). LA left atrium

jets will be inside the ring. Perivalvular jets will be outside the sewing ring (Fig. 20.7). If a prosthesis 2D appearance suggests dysfunction, i.e., stuck valve or abnormal coaptation of a tissue proathesis, then a large regurgitant jet will be seen coming through the valve leaflets and would not be confused with closing velocity jets (Fig. 20.8).

20.5 Doppler

The final check on a prosthesis to determine if it is normal is to determine the hemodynamic profile. This is done with Doppler. In most cases continuous wave Doppler can be used to determine the peak and mean gradients. Using the modified Bernoulli equation (pressure gradient = $4 \times velocity^2$), pressure gradients across the prosthesis can be determined. Studies have shown a good correlation between gradients measured noninvasively by echo Doppler and those obtained by invasive catheter measurements.
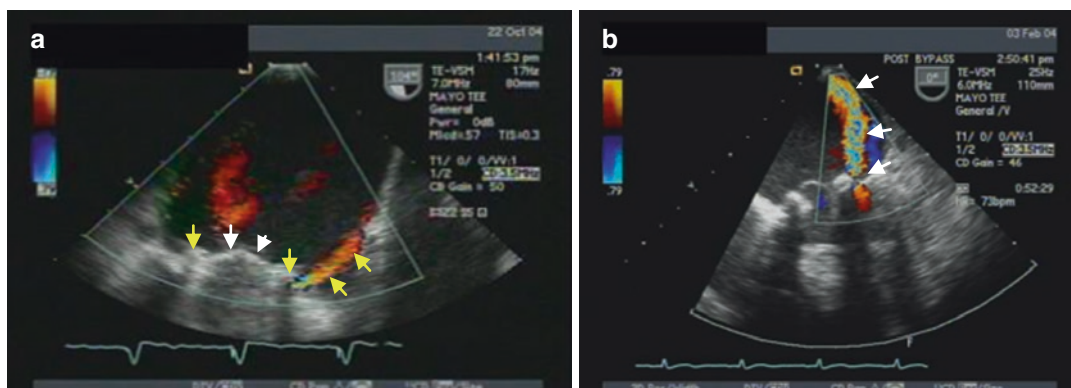
Fig. 20.7 Panel **a** – TEE view of an abnormal mitral bileaflet mechanical prosthesis. The leaflets (small white arrows) are shown in the closed position, and sewing ring seen (yellow arrows) and large perivalvular regurgitant jet (yellow arrow heads). Panel **b** – TEE view of another abnormal mitral tissue prosthesis with large perivalvular jet (arrows)
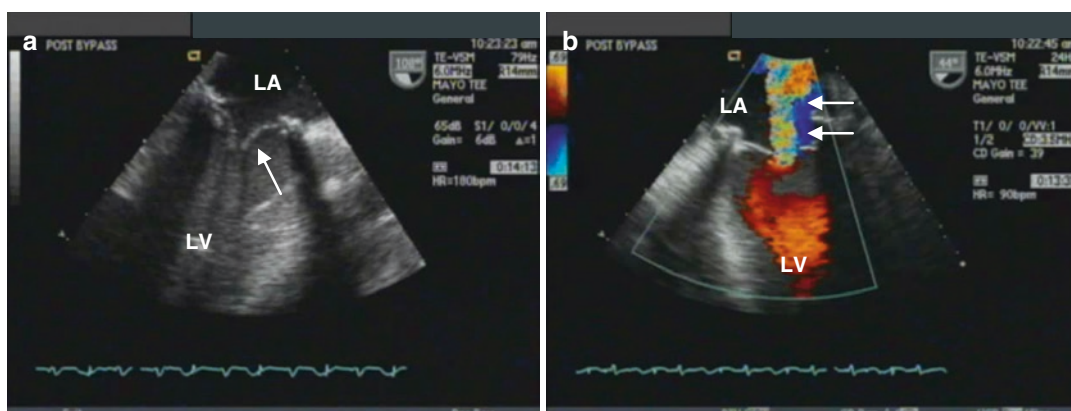
Fig. 20.8 TEE view of an abnormal mitral tissue prosthesis with incomplete coaptation of leaflets (arrow) seen in Panel **a**. Panel **b** shows large valvular regurgitation (arrows). LA left atrium, LV left ventricle

Both peak and mean gradients across a prosthesis should be determined. These values will depend on the type and location of the prosthesis. Normal ranges for all types of prostheses and locations have been established and reported from studies of the Mayo Clinic Echocardiography Laboratory (see references). Aortic mechanical prostheses, bileaflet and single tilting disc, have mean gradients in the 13–15 mmHg range. The older ball cage prostheses in the aortic position are higher, average mean gradient 23 mmHg. Aortic tissue valves have lower mean gradients with <10 mmHg for homografts, and other tissue aortic prostheses, mean gradient around 13 mmHg.

In the mitral position, there is not a lot of difference between mechanical and tissue prosthesis. Average mean gradients for all are in the 4–5 mmHg range. Normal mean gradients for tricuspid and pulmonic prostheses have also been determined (see references). These are reference guidelines for the majority of normal prostheses. It is always helpful to have the early postoperative Doppler velocities of a prosthesis. Presumably, these will be normal for that valve in that location for a given patient. If follow-up Doppler shows a significant variance from this baseline or outside the established values then the prosthesis may be abnormal.

If the Doppler gradients have changed or are increased you must determine if it is an abnormal prosthesis, i.e., stuck valve, pannus ingrowth, or stiffened tissue valve leaflets. Other issues need

to be ruled out that can result in abnormally high velocities across a prosthesis, i.e., anemia, high cardiac output, significant regurgitation, tachycardia, or thyrotoxicosis.

It is usually the combination of 2D imaging, color flow Doppler features and Doppler velocities that go into assessing a prosthesis and determining if it is malfunctioning, either obstructive or regurgitant.

20.6 Management

If a mechanical prosthesis seems abnormal, ie abnormal motion, color profile abnormal or higher than normal velocities, echo may help determine the cause. If the valve is abnormal because of thrombus, in addition to maximizing anticoagulation, lytic therapy has been successful freeing up a prosthetic leaflet. If this is unsuccessful the valve may have to be replaced.

If a tissue valve is stenotic or torn with significant regurgitation, then surgery may be the best option.

20.7 Summary

Echocardiography, 2D, color flow Doppler and Doppler gradients must all be employed to accurately assess a valve prosthesis and determine if normal or abnormal. Baseline and routine follow-up echos are helpful to determine if these features of a given prosthesis have changed. This is especially true for Doppler gradients. Finally, the echocardiographer must be familiar with all types of prostheses in various locations with regard to the normal 2D appearance, color flow pattern and Doppler gradients. Only then can they interpret the echo data accurately and determine if a prosthetic valve is normal or abnormal.

Suggested Reading

Burstow DJ, Nishimura RA, Bailey KR, et al. Continuous wave Doppler echocardiographic measurement of prosthetic valve gradients: a simultaneous Doppler-catheter correlative study. Circulation. 1990;82:1467–75.

Connolly HM, Miller FA Jr, Taylor CL, et al. Doppler hemodynamic profiles of 82 clinically and echocardiographically normal tricuspid valve prostheses. Circulation. 1993;88:2711–7.

Lengyel M, Miller F Jr, Taylor CL, et al. Doppler Hemodynamic profiles in 456 clinically and echo-normal mitral valve prostheses (abstract). Circulation. 1990;82 Suppl 3:III–43.

Miller F Jr, Callahan J, Taylor C, et al. Normal aortic valve prosthesis hemodynamics: 609 prospective Doppler examinations (abstract). Circulation. 1989;80 Suppl 2:II–169.

Novaro GM, Connolly HM, Miller FA. Doppler hemodynamics of 51 clinically and echocardiographically normal pulmonary valve prostheses. Mayo Clin Proc. 2001;76:155–60.

Cardiac Tumors and Masses

21

Roger L. Click

21.1 Introduction

Echocardiography is the imaging modality most often used to identify intracardiac masses. An echocardiogram can be quickly performed in any situation or setting, i.e., outpatient, bedside, emergency room, ICU, or operating room. The results are usually immediately available for clinical decision making. The majority of intracardiac masses found by echocardiography are thrombi and vegetations usually in the setting of cardiomyopathy, atrial fibrillation, valvular heart disesae, or endocarditis. Endocarditis and vegetations will be discussed in a separate chapter. In this chapter, the focus will be on cardiac thrombi and tumors.

Intracardiac thrombi generally have caused an embolus or have embolic potential whereas cardiac tumors are much less common, but can present with a variety of symptoms and frequently require urgent surgical removal. Most cardiac masses are found incidentally in patients referred for an echocardiogram for other reasons. Less frequently, patients are referred for an echocardiogram specifically to rule out a cardiac mass, i.e., source of embolism.

Transthoracic echocardiography (TTE) is often the first imaging modalilty when an intracardiac mass or tumor is discovered. Size, location, mobility, hemodynamic effects can all be delineated by TTE. Transesophageal echocardiography (TEE) can provide additional information in many cases or be helpful to see certain structures, i.e., the left atrial appendange.

21.2 Intracardiac Thrombi

Intracardiac thrombi are usually located in the left atrium (LA), left atrial appendage (LAA) or the left ventricle (LV). Left ventricular thrombi are usually found in the LV apex in patients with a dilated cardiomyopathy or coronary artery disease and an apical infarct. The thrombus can be laminated (Fig. 21.1), with generally low embolic potential or pedunculated (Fig. 21.2) and considered higher risk of embolization.

Sometimes, it may be difficult to determine if a "haziness" in the LV apex is a thrombus. Changing depths, gain and frequency may help sort out a true apical thrombus from an artifact. Contrast injection may also prove beneficial to determine real thrombus from artifact. Aggressive revascularization treatment with lytic agents or primary angioplasty has decreased the incidence of severe apical wall motion abnormalities and aneurysms and has lessened the likelihood of LV apical thrombus formation. Unlike other applications, a TTE may better view the LV apex than a TEE. The LV apex may be foreshortened with a

R. L. Click (✉)
Division of Cardiology, Mayo Clinic,
Rochester, MN, USA
e-mail: click.roger@mayo.edu
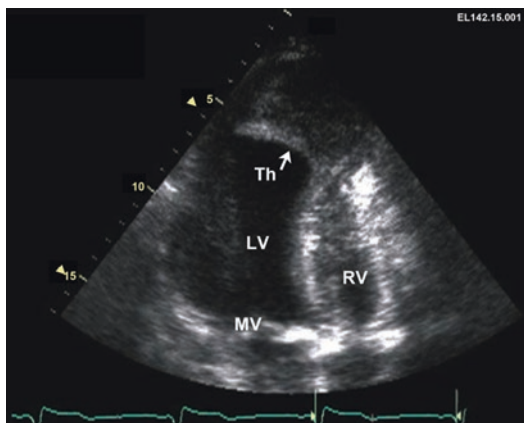
Fig. 21.1 TTE apical 4 chamber view showing an apical aneurysm and laminated thrombus (Th). LV left ventricle, MV mitral valve, RV right ventricle
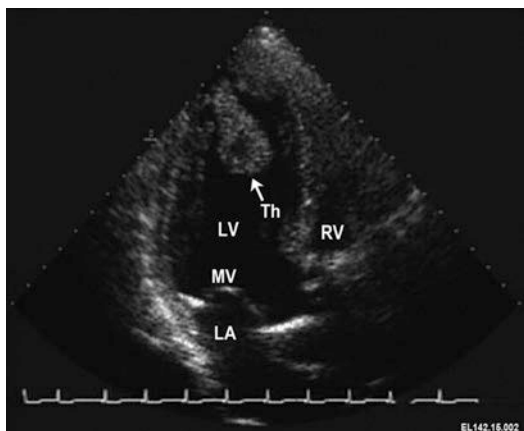
Fig. 21.2 TTE apical long axis view showing a pedunculated thormbus (Th) in the left ventriclular (LV) apex. MV mitral valve, LA left atrium, RV right ventricle

Fig. 21.3 TEE of left atrial appendage (LAA) showing LAA thrombus (Th). LA left atrium

spontaneous echo contrast and low empying velocities of the LAA by TEE may also predict the risk of thrombus and embolization.

21.3 Intracardiac Tumors

Tumors of the heart can be divided into primary, either benign or malignant, or secondary from metastases or extension from surrounding tissue. Primary intracardiac tumors are uncommon with the autopsy incidence 0.002–0.28%. Metastatic tumors to the heart are more common by about 20 times.

Table 21.1 shows the distribution of primary cardiac tumors both benign and malignant in an autopsy series.

In a surgical series (Dujardin et al.), 75 cardiac masses were surgically removed. The majority were benign. Most malignant tumors would not be managed surgically. Myxoma is the most common primary tumor of the heart accounting for 41% in the autopsy series (Table 21.1) and in the operative series. Of the 31 myxomas in the operatiave series 24 were in the left atrium. Atrial myxomas can be silent or can cause a variety of symptoms including fever, arthralgias, arrhythmias, hemodynamic obstruction, and most serious, embolization. Therefore, when discovered, most are surgically removed urgently. The echocardiographic appearance is typical. Usually a myxoma is pedunculated and attached to the atrial septum by a stalk. Most are single, but in Carney syndrome, multiple myxomas are

TEE whereas, the true LV apex is best seen by TTE to rule out an apical thrombus.

The LA and LAA are other common locations for thrombi in patients with atrial fibrillation, mitral stenosis or a prosthetic mitral valve. Unlike viewing the LV apex, the LA and especially the LAA are best viewed with a TEE. Patients with atrial fibrillation are particularly at increased risk for the development of LA and LAA thrombi. In patients with atrial fibrillation who have had a suspected embolism or precardioversion, a TEE is the imaging modalilty of choice (Fig. 21.3).

Imaging the LAA can be a challenge. Contrast can help determine if haziness or "smoke" in the LAA is a formed thrombus. The presence of

Table 21.1 Cardiac tumor distribution (autopsy series)

Benign cardiac tumors	1° Malignant tumors
N = 319	N = 125
Myxoma – 41%	Angiosarcoma – 31%
Lipoma – 14%	Rhabdomyosarcoma – 21%
Papillary Fibroelastoma – 13%	Mesothelioma – 15%
Rhabdomyoma – 11%	Fibrosarcoma – 11%
Fibroma – 5%	Other Sarcoma – 9%
Hemangioma – 5%	Lymphoma – 6%
Teratoma – 4%	Miscellaneous – 7%
Mesothelioma – 4%	
Miscellaneous – 3%	

Used with permission from Freeman et al., Transesophageal Echocardiography, modified from original from McAllister et al., Tumors of the Cardiovascular System

accompanied by lentiginosis and endocrine abnormalities. Figure 21.4 shows the typical echo features of a left atrial myxoma and the corresponding surgical specimen.

Cardiac fibromas are benign, occur more commonly in children and may cause arrhythmias, obstruction, heart failure, and chest pain. They are well demarcated masses usually within the wall of the left ventricle or septum. Figure 21.5 shows the typical echocardiographic appearance of a fibroma. Embolization is rare.

Rhabdomyomas, also benign, are the most common tumor in children. They can be associated with tuberous sclerosis and may be multiple in the left and right ventricles, right ventricular outflow or pulmonary artery (Fig. 21.6).
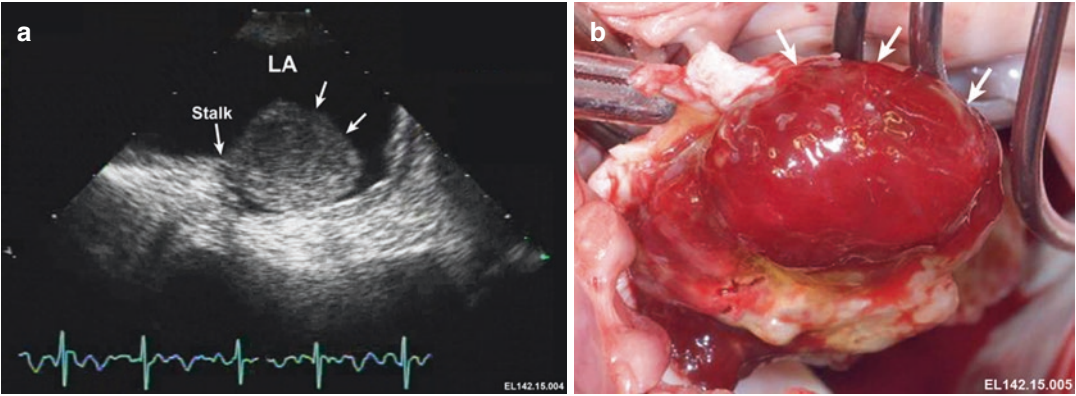
Fig. 21.4 TEE of left atrial myxoma and corresponding surgical speciman. The attachment stalk of the myxoma (arrows) is shown (**a**). In the surgical view (**b**) the myxoma is seen (arrows)
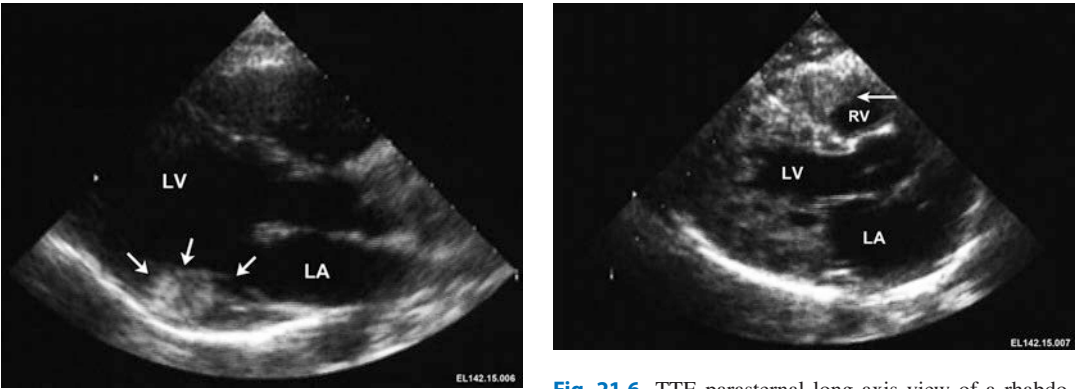
Fig. 21.5 TTE parasternal long axis view of a fibroma (arrows) in the inferior lateral wall of the left ventricle (LV). LA left atrium

Fig. 21.6 TTE parasternal long axis view of a rhabdomyoma (arrow) in the right ventricle (RV). LV left ventricle, LA left atrium
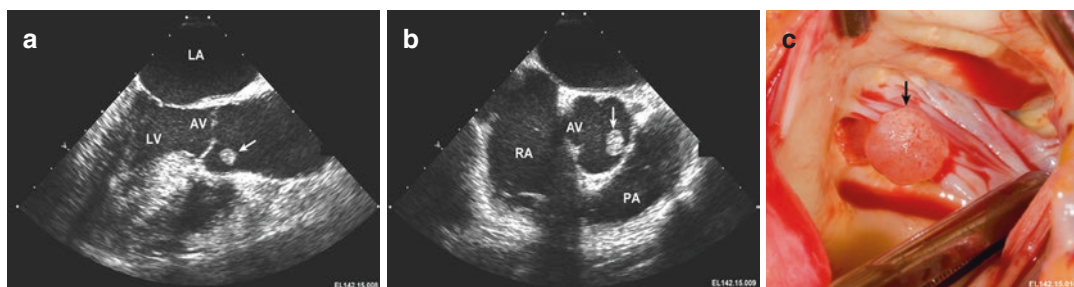
Fig. 21.7 TEE of an aortic valve (AV) fibroelastoma (arrows) shown in the long axis (**a**), short axis (**b**), and the surgical specicimen (**c**). LA left atrium, AV aortic valve, LV left ventricle, RA right atrium, PA pulmonary artery
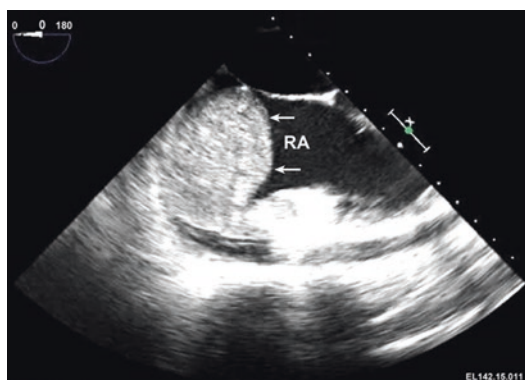
Fig. 21.8 TEE of a right atrial (RA) invasive angiosarcoma (arrows)

Fibroelastomas or papillomas are small benign tumors usually attached to the valves. They are often well demarcated and pedunculated (Fig. 21.7). Often found incidentally, the greatest risk is embolization and should be considered for surgical removal if no other embolic source is found. Fibroelastomas may at times be difficult to differentiate from other valvular masses such as vegetations, Lambl's excrescences or other degenerative strands. Other clinical features, i.e., fever and positive blood cultures, most often point to vegetation rather than fibroelastoma.

Malignant tumors can appear anywhere in the heart. Usually they have an invasive, infiltrative, irregular appearance and may be associated with pericardial involvement or a pericardial effusion. Angiosarcomas are more common and frequently in the right atrium (Fig. 21.8).

Metastatic tumors to the heart can be from any primary tumor elsewhere. Most common are from the lung, breast, kidney, liver, lymphoma, melanoma, and osteogenic sarcoma. Like other malignant tumors they have an irregular invasive appearance and often there is pericardial involvement. Malignant tumors, primary or metastatic, have a poor prognosis and often not resectable. Malignant tumors from the pelvic organs and kidney can extend up the inferior vena cava (IVC) and have a "snake" like appearance and may extend into the right atrium (RA) and appear as a mass in the RA. If surgical resection of the primary tumor is performed, intraoperatiave echo needs to be done simultaneously to ensure all the tumor is removed. These extensions are usually not adherent to the IVC or RA, and the entire extension will slide out with the primary tumor (Fig. 21.9).

Local extension into the cardiac structures from malignant mediastinal or lung tumors can occur. These can be identified by their obvious extension from the primary tumor. They are invasive and irregular with pericardial involvement (Fig. 21.10).

21.4 Management

LV thrombi if pedunculated are usually managed with maximizing anticoagulation, lytic therapy or surgery generally not recommended. Laminated LV thrombus usually does not necessitate anticoagulation. All atrial thrombi require anticoagulation. Benign intracardiac tumors such as myxomas and fibromas usually should be urgently removed surgically. The embolic risk is
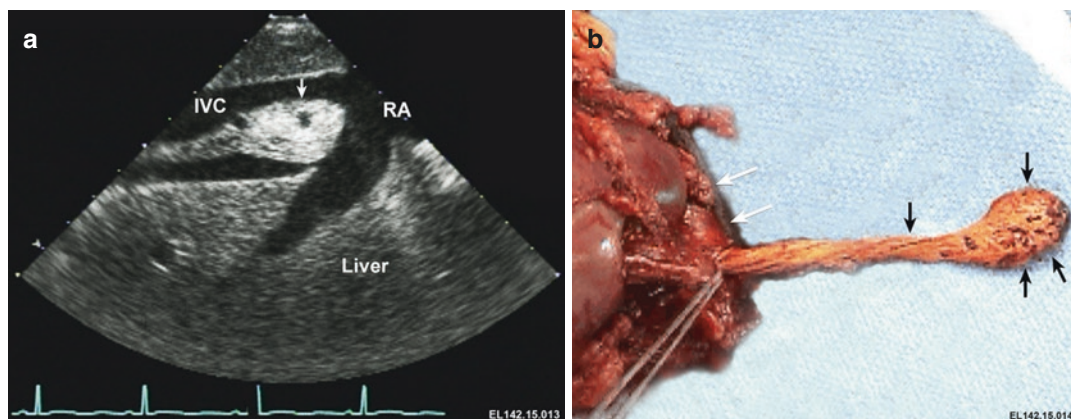
Fig. 21.9 TEE (**a**) of inferior vena cava (IVC) and hypernephroma (arrow) extending up the IVC just to outside the right atrium (RA). (**b**) shows the hypernephroma (white arrows) and the stalk and extension of tumor/thrombus (black arrows)
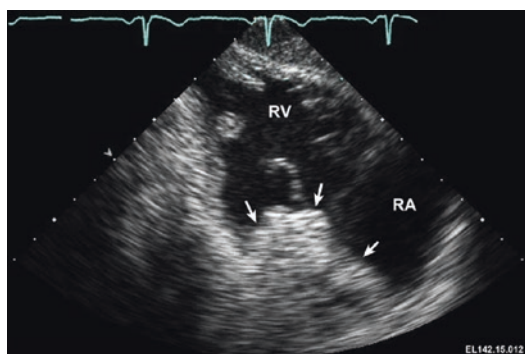
Fig. 21.10 TEE, transgastric view of an invasive right atrial (RA) tumor (arrows) from extension secondary to an adjacent lung tumor. RV right ventricle

unpredictable. Malignant or metastatic tumors of the heart most often are not resectable and the prognosis is poor.

21.5 Summary

Intracardiac masses are not common. Usually they are first discovered echocardiographically. The echocardiographic features can help distinguish the type of mass, its location, attachment site, demarcation, and invasiveness. Also, the clinical situation may aide in distinguishing masses, i.e., age of patient, history of myocardial infarction, atrial fibrillation, fever, embolization, or other primary tumor with metastases or extension. Once discovered, echocardiography is helpful in management and surgical resection and surveilance for any recurrence.

Suggested Reading

DeVille JB, Corely D, BS J, et al. Assessment of intracardiac masses by transesophageal echocardiography. Tex Heart Inst J. 1995;22(2):134–7.

Dujardin KS, Click RL, Oh JK. The role of intraoperative transesophageal echocardiography in patients undergoing cardiac mass removal. J Am Soc Echocardiogr. 2000;13(12):1080–3.

Jr MAHA, Fenoglio JJ Jr. Tumors of the cardiovascular system: Fascicle 15, 2nd series. Atlas of tumor pathology. Washington, DC: Armed Forces Institute of Pathology; 1978.

Klarich KW, Enriquez-Sarano M, Gura GM, et al. Papillary fibroelastoma: echocardiographic characteristics for diagnosis and pathologic correlation. JACC. 1997;30(3):784–90.

Wysokinski WE, Ammash NM, Soande F, et al. Predicting left atrial thrombi in atrial fibrillation. Am Heart J. 2010;159:665–71.

Congenital Septal Abnormalities in The Adult Patient

22

Ferdinando Luca Lorini, Cristian Ottavio Mirabile, and Moreno Favarato

22.1 Atrial Septal Defects

Atrial septal defect (ASD) is one of the most common adult congenital heart defects (ACHDs), accounting for 30% of all cases.

22.1.1 Anatomy and Physiopathology of ASDs

ASD is a persistent communication between atria. Ostium primum ASD (OP) results from deficiency/absence of the lower part of the atrial septum, near the crux of the heart. Ostium secundum ASD (OS) is in the region of the fossa ovale. Sinus venosus ASD (SV) may be located in the superior part of the atrial septum with connection of the right pulmonary vein to the right atrium. In some patients, the septum may be aneurysmal and/or fenestrated. ASDs are singular or associated with other lesions (Table 22.1). Shunt flow occurs in systole and diastole and can be from left to right or from right to left. Blood in each

Table 22.1 Lesions associated with ASDs

Type of ASD	Associated lesions
OS	Pulmonic stenosis, mitral valve prolapse, partial anomalous pulmonary venous connection
OP	Mitral Cleft, Subaoartic (SubAo) stenosis
SV	Partial anomalous pulmonary venous
Coronary Sinus (CS)	Partial anomalous pulmonary venous, persistent left SVC

atrium can flow either through the atrioventricular (AV) valve to the ventricle or across the defect to the opposite ventricle. Ventricular compliance affects the direction of flow through the ASD in diastole. Left ventricle has less capacitance for blood than the right ventricle; therefore, blood in the left atrium is more likely to fill the more expandable right ventricle. When the right ventricle loses its compliance because of other pathological processes (i.e., right ventricular outflow tract obstruction, RVOTO), the shunt flow is from right to left. In systole, the different compliance of atria and other abnormalities (i.e., valve regurgitation) determines shunt flow and the size of the ASD determines the volume of the shunt.

22.1.2 Clinical Aspects

In an unrepaired ASD there is left-to-right shunt with right ventricular (RV) volume overload and pulmonary over circulation. The main clinical

F. L. Lorini (✉) · M. Favarato
Department of Anesthesia and Intensive Care Medicine, ASST Papa Giovanni XXIII, Bergamo, Italy
e-mail: llorini@asst-pg23.it; mfavarato@asst-pg23.it

C. O. Mirabile
Department of Anesthesia and Intensive Care-SAMU-SMUR, Hôpital Universitaire Necker, Paris, France

features associated with it are pulmonary infections, fatigue, exercise intolerance, palpitations, cardiomegaly, new audible murmur in pregnancy, atrial arrhythmias, flow-related pulmonary arterial hypertension (PAH) and vascular obstructive disease, ictus cerebri in paradoxical embolism, atrial fibrillation, and indwelling venous catheters. ASDs should be diagnosed by demonstration of shunting across the defects, RV volume overload, and associated anomalies. Patients with unexplained RV volume overload should be referred to an ACHD center. In a repaired ASD the clinical aspects are most dependent on the original abnormality and its correction. Many patients with ASD are asymptomatic, so they may present for primary repair in adulthood. Complications such as tachyarrhythmias and paradoxical emboli increase in frequency with age, so repair is ideally performed in childhood. Closure after 5 years of age is associated with incomplete resolution of RV hypertrophy and survival is worse when the ASD is closed after 24 years of age.

22.1.3 Echocardiography

PAH and paradoxical movement of the atrial septum in patients with unexplained RV overload may be correlated with ASD.

22.1.3.1 Transthoracic Echocardiography

This is the primary diagnostic imaging modality for ASD. The study includes 2-D imaging of the atrial septum from parasternal, apical, and subcostal views with color demonstration of shunting. Subcostal views with deep inspiration and high right parasternal views are particularly helpful in adults. The atrial septum from the orifice of the superior vena cava to the orifice of the inferior vena cava should be visualized to detect SV defects or the extension of large OS in these regions.

22.1.3.2 Transesophageal Echocardiography

The recommended views for imaging the atrial septum are the mid-esophageal four-chamber view for OS and OP ASDs (Fig. 22.1), the mid-
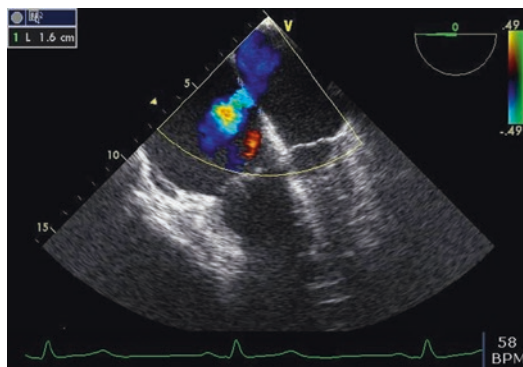
Fig. 22.1 *ASD OS:* TEE view with Color Doppler (0°, transverse, ME 4-chamber, Color Doppler)

esophageal bicaval view for an SV defect and for detection of anomalous pulmonary veins, and the mid-esophageal short-axis view at the aortic valve level to bring the atrial septum into the center of the screen. Transesophageal echocardiography (TEE) is necessary to detect connection of the pulmonary veins to the left atrium in patients with ASD. In addition, it is useful for optimal views of the atrial septum (better localization and sizing of the ASD, measurement of septal rims) and so for a good therapeutic approach. A large coronary sinus (CS) orifice with evidence of atrial shunting may indicate a defect in the roof of the CS, so the entire CS roof should be imaged when this is suspected. When a coronary sinoseptal defect is associated with lesions that cause right-to-left shunting, the orifice of the CS may not be enlarged, and the defect may not be recognized until after definitive surgery, at which time a left-to-right shunt may occur. With PAH, the low velocity of the shunt flow across the coronary sinoseptal defect may be difficult to distinguish from other low-velocity flow within the atria. Right atrial (RA) and RV enlargement with diastolic flattening and paradoxical motion of the interventricular septum are evidence of RV volume overload and significant left-to-right shunt. The RV systolic pressure should be estimated from the peak velocity of the tricuspid regurgitant jet if it is present. Two-dimensional imaging should assess associated lesions, and their functional significance should be determined by color Doppler and spectral Doppler imaging.

22.1.3.3   Doppler Echocardiography

It can be useful in the diagnosis of ASDs to evaluate the pressure gradient between atria. The pulsed wave Doppler trans-ASD shows a continuous flow with end-systolic peak flow. The pulmonary to systemic flow ratio can be used to assess patients with ASDs or ventricular septal defects (VSDs) by comparing the different stroke volumes through the left ventricular (LV) outflow tract and the RV outflow tract.

22.1.3.4   Contrast Echocardiography

Contrast echocardiography with intravenous agitated saline injection is used to confirm the presence of a right-to-left atrial shunt if the findings from imaging and color Doppler echocardiography are inconclusive. Additionally, the presence of negative contrast in the right atrium may be helpful in identifying a left-to-right shunt. If a left-to-right shunt or RV volume overload is recognized but unexplained, the patient should be referred to an ACHD center.

22.1.3.5   TEE for Closure of ASDs

The use of TEE has spread greatly because of its use in closure of OS ASD by the percutaneous technique. Factors that determine suitability for transcatheter closure of OS include the size of the defect and the presence of adequate tissue rims around the ASD. Accurate imaging of the anatomic features of the ASD is critical for case selection, planning, and guidance during the procedure. Conventionally, a margin of 5 mm is considered adequate. For a comprehensive evaluation during the percutaneous closure procedure, TEE is performed in three different planes: transverse (0°), longitudinal (90°), and at 45°; it plays a critical role for patient selection, guidance, and post-closure evaluation.

22.1.4   Patent Foramen Ovale

Patent foramen ovale (PFO) is found in up to 25% of adults in the general population, it is generally discovered accidentally, and has no consequences. However, association of PFO with various clinical conditions has been reported (embolic stroke, platypnea orthodeoxia, decompression sickness in divers, and migraine). Optimal treatment has not been established and there are contradictory results from different studies. Patients with suspected PFO should undergo a contrast study, as color Doppler echocardiography detects only 5–10% of interatrial shunts. The most widely used technique is the injection of agitated saline solution microbubbles. This should be performed at rest and during maneuvers that increase RA pressure (i.e., Valsalva), because this can improve diagnostic sensitivity. The presence of a single microbubble in the left atrium and left ventricle in the first three beats after right cavity opacification is considered diagnostic of PFO. Microbubbles after the third beat may correspond to intrapulmonary shunt. The number of microbubbles crossing the PFO enables us to quantify shunting. Instead of counting microbubbles, some echocardiography laboratories classify severity as complete to almost complete to slight left chamber opacification. The principal limitation of transthoracic echocardiography (TTE) is its relatively poor sensitivity compared with TEE (Fig. 22.2). TEE should be considered if the findings of the TTE study are negative or inconclusive but strong clinical suspicion of PFO remains. PFO morphology is heterogeneous and ranges from simple, large defects to long, oblique, and tunnel-like defects. TEE enables detailed assessment of the interatrial septum, which is important for successful transcatheter closure. For example, long tunnels represent a problem for devices with a fixed distance
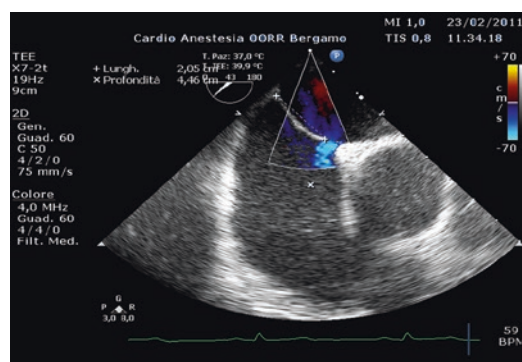
Fig. 22.2 *PFO:* TEE view before closure with Color Doppler across defect (ME 45°)

Fig. 22.3 *Patent Forame Ovale (PFO):* TEE control after closure by Amplatzer device
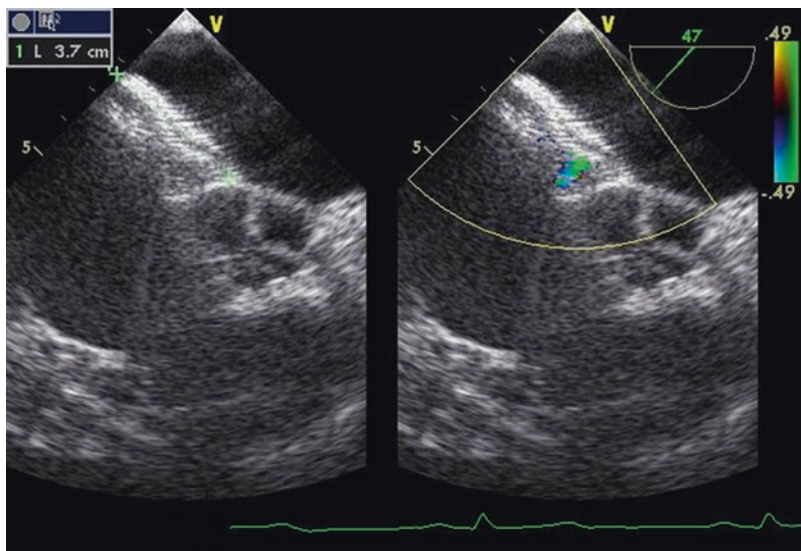
between RA and left atrial (LA) components, as there is the potential for both disks to be partially deployed within the tunnel. Long tunnels can be identified with TEE measurement of the maximum opening diameter of the communicating channel (septum primum–septum secundum distance) at the entrance to the left atrium. During intervention, TEE is useful in determining the size of the device to be implanted and provides direct visual guidance in device deployment, avoiding interference with other structures (Fig. 22.3).

22.2 Ventricular Septal Defects

VSD is the most common congenital heart defect at birth and occurs in three in every 1000 live births. There is high incidence of spontaneous closure of most small-to-moderate VSDs in the first decade of life, so the incidence is much lower in older infants and particularly in adults: VSDs account for approximately 10% of all cases of ACHD. There are four anatomic types of VSDs, with multiple synonyms for each one.

22.2.1 Anatomy and Physiopathology of VSDs

Incorrect embryological development of the ventricular septum results in VSD. Type 1 VSDs (conal, subpulmonary, infundibular, supracristal, doubly committed juxta-arterial) occur in the RV outflow tract. Spontaneous closure is uncommon. Type 2 or perimembranous VSDs are the most common defects, and nearly 80% of VSDs are of this type. The defect is in the septum membrane next to the septal tricuspid leaflet, which can become adherent to the VSD, so creating an aneurysm of the ventricular septum and limiting shunt by closure of the VSD. On the LV side of the septum, the defect is next to the aortic valve. Type 3 VSDs (inlet VSDs) occur in the lower part of the right ventricle and adjacent to the tricuspid valve. These defects typically occur in patients with Down syndrome. Type 4 or muscular VSDs can be located centrally, apically, and at the margin of the septum, near RV free wall: they result from excessive fetal muscular resorption. They are multiple in limited numbers of patients. Spontaneous closure is common in children. VSD is most often an isolated lesion. It is a component of complex abnormalities such as conotruncal defects or is associated with left-sided obstructive lesions. A subpulmonary VSD is often associated with progressive aortic valve regurgitation caused by prolapse of the aortic cusp through the defect. Another mechanism of aortic valve regurgitation is the passage of a non-coronary cusp in restrictive VSD by the Venturi principle (difference in pressure between the two chambers). The degree of VSD intracardiac

shunting depends on defect size, location, pulmonary vascular resistance, and compliance of the left and right ventricles. The volume and the route of the flow through the VSD is based on the size and the comparative resistance between the usual ventricular and the VSD outflow tracts. Left-to-right shunt may result from a large VSD along with a low pulmonary vascular resistance as compared with the systemic circulation, and vice versa; in a left-to-right shunt, there is low output of the left ventricle. To gain a normal cardiac output, the response is an elevation in LV volumes and so in LA pressure. The consequence is congestion of the pulmonary venous circulation. In addition to systolic flow, we must consider a diastolic flow through the VSD that depends on the differences in compliance, contractility, and volume between the two ventricles. It has been demonstrated that in patients with a small VSD, infective endocarditis may occur on the rim of the VSD and this event is also related with the injury of the endocardium by the turbulent flow. A progressive aortic insufficiency may result from aortic cusp prolapse. If the defects are large, these patients have the typical spectrum of symptoms of congestive heart failure. Particularly the LV overload may predispose to the development of pulmonary vascular disease, which can progress to Eisenmenger syndrome. There will be cyanosis when there is a relevant right-to-left shunt from the right ventricle to the aorta through the VSD. A physiological classification of an isolated VSD in adults is as follows: in restrictive VSD, RV pressure is lower than LV pressure and there is no RVOTO; in unrestrictive VSD, RV pressure is equal to LV pressure without RVOTO.

22.2.2 Clinical Aspects

Isolated VSDs are uncommon in adults because larger VSDs are clinically evident and repaired early; spontaneous closure is more frequent in small-to-moderate VSDs; the mortality of young patients with very large unrepaired VSDs is high. Typical clinical presentations are as follows: a patient with a VSD corrected when he/she was a child; an asymptomatic patient but with a systolic murmur; infective endocarditis with fever and bacteremia, with pulmonary embolism or cerebral abscess; diagnosis of an aortic regurgitation; a patient with right-to-left shunt and progressive development of PAH affected by cyanosis and exercise intolerance. In patients with an isolated VSD, the clinical features depend on size of the defect and the status of vascular pulmonary resistance. The clinical severity grading for isolated VSDs is as follows:

- Small VSD: less than or 25% of aortic annulus diameter, small left-to-right shunt, absent LV overload, no PAH.
- Moderate VSD: more than 25% to less than 75% of aortic diameter, with small to moderate left-to-right shunts, mild to moderate LV volume overload, absent or mild PAH. The patients remain asymptomatic or have mild congestive heart failure; symptoms are usually controlled with drugs.
- Large VSD: greater than or 75% of aortic diameter, moderate to large left-to-right shunt, volume overloading of the left ventricle, developing PAH; congestive heart failure is frequent in childhood and a change in shunt to right to left is possible, thus resulting in Eisenmenger syndrome.

22.2.3 Echocardiography

Patients with hemodynamically significant VSDs with evidence of volume overload and progressive aortic insufficiency due to chamber dilation are referred for closure of the defect.

22.2.3.1 Transthoracic Echocardiography

This remains the mainstay of diagnosis for VSDs. The windows used to investigate a VSD are subcostal and apical views (Fig. 22.4) and these are useful if there are good echocardiographic windows. TTE is fundamental in the preoperative phase to obtain information about the number and location of the VSDs, biventricular function, and size of left and right chambers, and for imaging of the aortic valve to detect possible prolapse/regurgitation, the presence/absence of RVOTO or LV outflow tract obstruction (LVOTO), and the
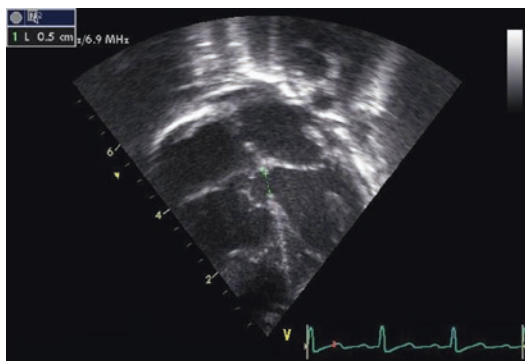
Fig. 22.4 *A perimembranous VSD:* TTE apical view, SAX
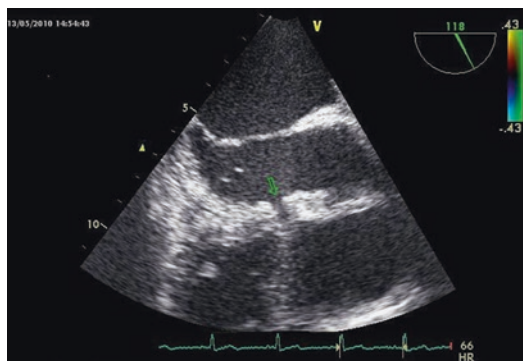
Fig.22.5 *A VSD in SubAo position (Arrow) and LVOT:* TEE view (ME, AV LAX, 120°)

presence of tricuspid valve insufficiency. By Doppler analysis, tricuspid regurgitation jet may be detected, and a Doppler study of the flow through the VSD is desirable. The description of septal configuration and movement is routine in the study. In a patient operated on for closure of a VSD with new symptoms and signs of cardiac failure and PAH, a Doppler echocardiographic analysis of possible residual shunting and evaluation of pulmonary arterial pressure by tricuspid regurgitation and pulmonary regurgitation is mandatory; in addition, for a good evaluation it is necessary to investigate if there is aortic regurgitation, ventricular function, and the presence of LVOTO and RVOTO.

22.2.3.2 Transesophageal Echocardiography

TEE is useful but not so essential for evaluating isolated defects of the interventricular septum because visualization of the defect can usually be achieved using TTE. Nevertheless TEE is useful in the evaluation of associated valvular abnormalities. The commonest defect (perimembranous) is located near the tricuspid valve just beneath the aortic valve. This kind of VSD is better seen in the five-chamber view in the low esophageal position. In the short-axis view at the aortic valve level, the defect can be seen near the tricuspid valve. Obtaining images of the membranous septum, we may see ventricular septal

aneurysms or tricuspid tissue tags. In perimembranous VSD in which there is aortic regurgitation, the aortic cusp may herniate in the defect. Perimembranous defects have been seen in subvalvular aortic stenosis. Muscular septal defects are located centrally or near the apex in the muscular part of septum: the best views are the mid-esophageal four chamber view (0–20°) and the transgastric mid short-axis view (0°). The inlet type of VSDs is generally a feature of a partial AV septal defect (AVSD): they are located in the posterior or inlet septum in close proximity to the AV valves (echocardiographically, AV valves are on the same level without offset as and are located inferior to the tricuspid valve). Defects in the outlet septum are referred to supracristal, infundibular, doubly committed or subarterial VSDs. The longitudinal plane of the outflow tract (Fig. 22.5; mid-esophageal, long axis, 120°) provides adequate visualization of this defect and anatomic/functional characterization of aortic valve. Another useful view for VSD is gained by plane rotation from 0° to 30–45°: it is similar to an inverted parasternal short-axis view. In conclusion, for an adequate TTE study of VSDs, the following must be included: identification of the region of the septum involved, the identification of all defects, assessment of the size of the defect and its borders, evaluation of chamber sizes and wall thickness, assessment of shunt size (pulmonary to systemic flow ratio), estimation of RV

pressure and pulmonary arterial pressures, and identification of additional associated lesions. By evaluation of the peak systolic velocity through the VSD velocity, we may acquire the RV systolic pressure (RVSP) and pulmonary artery systolic pressure (PASP):

$$RVSP(or\ PASP) = SBP - 4 \times PVSD2,$$

where SBP is the systolic blood pressure and PVSD is peak velocity of the VSD jet.

22.2.3.3   Contrast Echocardiography

This is employed to detect relatively small right to-left ventricular level shunts. This simple and effective technique is useful to identify small defects: only a few microbubbles in the left ventricle are required for diagnostic confirmation. Contrast echocardiography is particularly useful for suspected defects that cannot to be imaged by standard approaches, for small muscular defects in association with PAH, and in the intraoperative evaluation of post-repair residual defects. It is useful to use a deep Valsalva maneuver during intravenous injection to optimize visualization of microbubbles across the defect.

22.2.3.4   TEE for Closure of the VSDs

Advances in operative hemodynamic device engineering have permitted safe and feasible percutaneous closure of VSDs; the basic principles of TEE guiding the process of closure of these defects are similar to those for ASDs. The ACHD patients suitable to undergo a percutaneous closure procedure are those with perimembranous and muscular VSDs.

22.3   Atrioventricular Septal Defects

22.3.1   Anatomy and Physiopathology of AVSDs

The AV canal results from incomplete development of endocardial cushions. Defects in AVSDs may be only at the atrial septum (OP) or may include an inlet VSD. AV valves are abnormal, composed of five leaflets, separated into right and left AV valves, or like a common valve. The AV valve may be misaligned with respect to the ventricles and it is possibly associated with RV or LV hypoplasia. The posteromedial papillary muscle may be rotated abnormally to the lateral wall of the ventricle. Conotruncal abnormalities may be associated. In partial AVSD, the ventricular septum is intact. There is an OPASD, a cleft in the left AV valve and two separate AV valve annuli. Intermediate AVSD is a part of spectrum between complete and partial AVSD. It is characterized by OP ASD, restrictive VSD, and mitral cleft. There are due to a distinct AV valve because anterior and posterior leaflets are fused. In complete AVSD, there is an unrestrictive inlet VSD, often a primum ASD, the atrial septum is rarely intact, and the AV valve is common.

22.3.2 Clinical Aspects

Unrepaired adults may be asymptomatic or present with symptoms. The principal cause of becoming symptomatic in young patients is a significant left AV valve regurgitation. Subaortic stenosis may occur initially or may develop and progress later. Surgical correction involves closure of the ASD and VSD, division of the AV valve, and closure of a cleft in the anterior leaflet of the mitral valve. Repair is usually performed in infants because the risk of evolution in end-stage PAH is very high if the defect is closed too late.

22.3.3 Echocardiography

In a patient with a partial unrepaired AVSD, TTE is the primary imaging modality and should include demonstration of the rims of the OP (Fig. 22.6), a VSD (if present), the morphology and function of the AV valve, ventricular size, shunting, and subaortic stenosis (if present). In a

Fig. 22.6 *OP ASD in partial AVSD:* TTE apical view, without and with Color Doppler
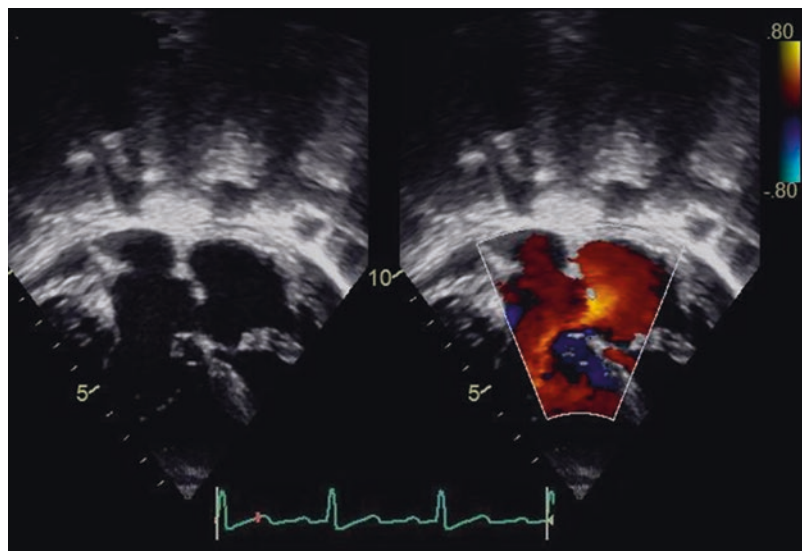
patient with a complete and unrepaired AVSD, the study must include the presence and size of the septal defect, the morphology and function of the common AV valve, and ventricular size and function. When the ventricular portion of the septal defect is large, the ventricular septum may be deficient apically and inferiorly. Pulmonary arterial pressures should be evaluated by measuring tricuspid insufficiency and pulmonary regurgitation jet velocity with simultaneous systemic blood pressure measurement. Evidence of subaortic obstruction, caused by attachment of the AV valve to the crest of the interventricular septum, should be sought by imaging and Doppler echocardiography. In the post repair patient, residua include left AV valve dysfunction, subaortic stenosis, shunt flow in the VSD patch, and uncontrolled PAH. It may be difficult to distinguish residual LV to RA shunt from tricuspid regurgitation with RV hypertension, resulting in erroneous diagnosis of PAH.

Suggested Reading

Bhatt AB, Foster E, et al. Congenital heart disease in the older adult: a scientific statement from the American Heart Association. Circulation. 2015;131(21):1884–931.

Miller-Hance WC, Silverman NH. Transesophageal echocardiography (TEE) in congenital heart disease with focus on the adult. Cardiol Clin. 2000;18(4):861–92.

Pineda AM, Mihos CG, et al. Percutaneous closure of intracardiac defects in adults: state of the art. J Invasive Cardiol. 2015;27(12):561–72.

Silvesides CK, Dore A, Poirier N, et al. Canadian Cardiovascular Society 2009 consensus conference on the management of adults with congenital heart disease: shunt lesions. Can J Cardiol. 2010;26(3):e70–9.

Warnes CA, Williams RG, Bashore TM, et al. ACC/AHA 2008 guidelines for the management of adults with congenital heart disease. A report of the American College of Cardiology/American Heart Association Task Force on practice guidelines (writing committee to develop guidelines on the management of adults with congenital heart disease). Circulation. 2008;118:e714–833.

Essential Pediatric Echocardiography

23

Ferdinando Luca Lorini, Mariavittoria Lagrotta, and Simona Marcora

23.1 Introduction

Echocardiography in intensive care settings has widespread utilization to evaluate hemodynamically unstable patients. Transthoracic echocardiography (TTE) is the easiest and less invasive way to image cardiac structures. Approaching a pediatric echo exam it is important to chose the correct probe: 10 MHz for neonates and 5 MHz for bigger children. Certain views are of added importance for pediatric examinations: subxiphoid or subcostal, suprasternal notch, and right parasternal views (Fig. 23.1a, b).

However, in many critically ill patients, low-quality images are obtained because the acoustic windows are suboptimal for the presence of chest tubes, extensive dressings, mechanical ventilation. Transesophageal echocardiography (TEE)

provides images of better quality. In addition TEE probe can be left in place for the continuous monitoring. Recently, the world's smallest multiplane transesophageal echocardiography probe has been released. The micro TEE probe can be used in newborns and infants less than 5 Kg weight.

In clinical practice echocardiography in pediatric intensive care units has different applications. It is important a strict collaboration for acquisition and interpretation of echocardiographic exams between anesthesist and pediatric cardiologist, according to the complex anatomy of congenital heart disease and the many surgical procedures used to palliate or repair them.

The recent introduction of the term "functionally echocardiography" has improved the bedside use of echocardiography to assess myocardial and pulmonary function, the changes in cardiovascular status in response to treatment, systemic and pulmonary blood flow. This chapter discusses its use in the more common diagnostic dilemmas confronting the intensivist.

F. L. Lorini (✉) · M. Lagrotta
Department of Anesthesia and Intensive Care Medicine, ASST Papa Giovanni XXIII, Bergamo, Italy
e-mail: llorini@asst-pg23.it; mlagrotta@asst-pg23.it

S. Marcora
Unit of Paediatric Cardiology and Congenital Cardiopathy, ASST Papa Giovanni XXIII, Bergamo, Italy
e-mail: smarcora@asst-pg23.it
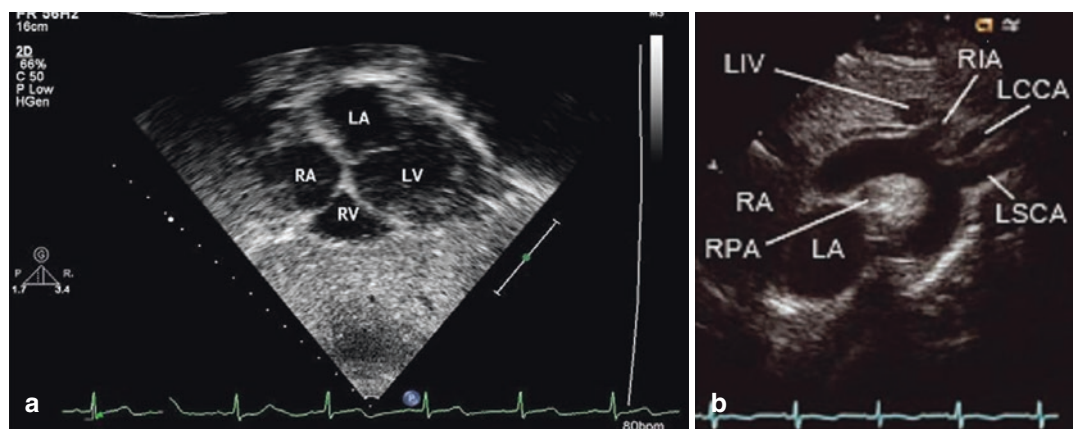
Fig. 23.1 Peculiar echo view in pediatric cardiac echo. In (**a**) subcostal view obtained by applying the transducer in the subcostal space and tilting the transducer anterior to posterior. All cardiac chambers can be seen, particulary the interatrial septum. In (**b**) suprasternal view obtained by placing the transducer in the suprasternal notch with the plane of the sound oriented between the right nipple and the left shoulder. This view is good to evaluate the arch and the ductus (rotating the probe perpendicular)

23.2 Sistolic and Diastolic Ventricular Function

Echocardiography and Doppler ultrasound are the main tools used to evaluate LV function non-invasively in children with heart disease.

The evaluation of systolic function in children can be easily obtained with the fractional shortening (FS) calculated by subtracting the left ventricular internal diameter in systole (LVESD) from the left ventricular internal diameter in diastole (LVEDD) dividing this by LVEDD and multiplying by 100. The normal value is >25%. This method has some limitations in this setting as it is not valid in case of hypokinesia/akinesia (ex. paradoxical septum in pulmonary hypertension or atrial septal defect, post-by pass septum), dependent on loading conditions and inadequate in case of abnormal LV geometry (ex. univentricular heart). Ejection fraction calculated by two dimensional echo can be a valid alternative in case of regional hypokinesia but it is dependend on loading conditions and ventricle geometry. Three-dimensional echocardiography has been recently introduced and new high-frequency matrix transducers allows a better and more reliable evaluation of ventricle function and volumes.

The methods employed for the evaluation of diastolic function include: (1) Doppler evaluation of transmitral inflow, with evaluation of peak E and peak A velocities, and the E:A ratio; (2) pulmonary vein Doppler with evaluation of peak S and D velocities; (3) tissue Doppler evaluation of the mitral valve annulus with measurement of peak e and peak a myocardial velocities, as well as isovolumic relaxation time; (4) evaluation of color M-mode Doppler of left ventricular inflow and measurement of the velocity of flow propagation. Normal references in children are available in literature but it would be preferred that every echo lab gives its normal range according to its population.

The increased availability of several newer techniques such as tissue doppler, strain and strain rate to assess ventricular function has stimulated interest for their use in congenital heart disease (CHD). Several characteristics of tissue velocity and deformation imaging make them attractive for assessment of ventricular function in CHD. These methods are independent of ventricular geometry and therefore may be useful for the evaluation of ventricles with variable morphology, in particularly right ventricular (RV) function and hearts with a functionally single ventricle. Furthermore this methods allow quantification of myocardial motion and deformation in different directions (longitudinal, radial, circumferential) while conventional techniques allow only the assessment of radial function. This is very important for the evaluation of RV, the most important ventricle in most

of CHD, where the fibers are arranged in a predominantly longitudinal orientation. Finally, these techniques quantify regional myocardial function in addition to global ventricular function.

In clinical practice the acquisition time is the fundamental to get good image and curves. Moreover it is important to use the same protocols to get reproducible data. Nowadays no pediatric guidelines exists about acquisition of Tissue Doppler and Strain. Normal value for pediatric range of TDI and strain parameters (Figs. 23.2a, b) are beginning to be present in literature but we think that it is important to collect them before and after operation in order that each patient is the control of himself.

Our protocol, made with the pediatric cardiologists, is described below.

TDI derived velocity is obtained by pulsed doppler (angle dependent) or color TDI (less angle dependent). Strain is obtained by speckle tracking strain.

Pulsed TDI

During image acquisition it is important:

1. To have good and stable QRS at ECG.
2. To optimize temporal resolution by selecting as narrow an image sector as possible(FRAME RATE >150 sec is recommended).

Fig. 23.2 (**a**, **b**) Four chamber view. Pulse TDI of left ventricle at level of septum and lateral wall. It can be evaluated a normal pattern: a case of a child with pregress LV dysfunction after myocarditis
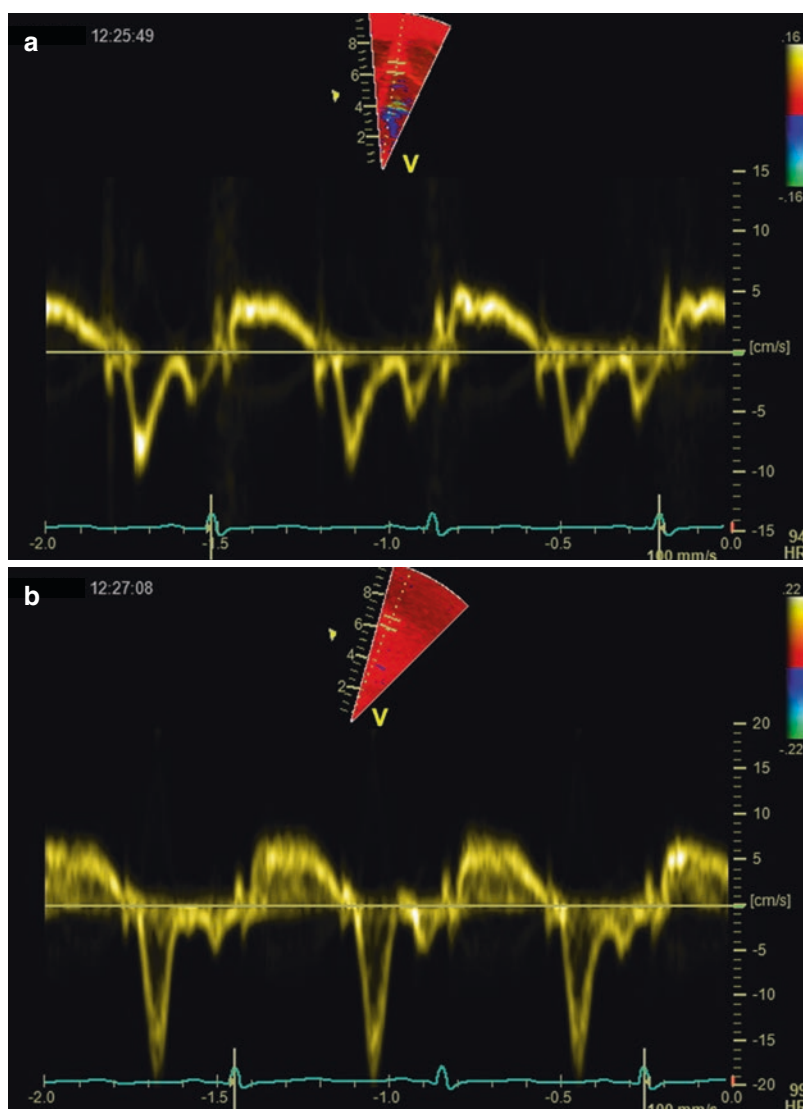
3. To select appropiate velocity scale (around 15–20 cm/sec).
4. To put the ventricle wall to be interrogated in the center of the imaging sector(tilting function).
   To select TVI function and align the pulsed Doppler perpendicular to the structure to be studied.
   Sedation of the baby to keep him still and have good images and ECG trace is almost always needed.
   Post-processing analysis is not possible.

Color TDI

During image acquisition it is important:

1. To have good and stable QRS at ECG (sedation).
2. To optimal visualize the myocardial wall with a clear delineation of myocardial tissue and extracardiac structures.
3. To optimize the FPR >180 narrowing the image sector until it is slightly wider than the investigated wall.
4. To adjust velocity scale to avoid aliasing.
5. To record three complete cycle at the same heart rate activating TVI function.
6. Post-processing is possible.

Spleckle Tracking Strain (Fig. 23.3**)**

During image acquisition is important:

1. To have a good and stable ECG (sedation)
2. To optimize a standard 2D image view (2,3,4 chamber views for longitudinal strain; parasternal short axis view for radial strain) in order to obtain a clear delineation of the myocardial walls
3. To obtain a FPR between 50 and 80; this is obtained by narrowing the imaging sector to include little than the interrogated wall segment
4. To store images in cineloop format for offline analysis (at least two cycles)

23.3 Hemodynamic Management

In cardiac disases like univentricular heart a surgical shunt or a stent in ductus arteriosus put the systemic and pulmonary circulation in parallel. In this situation maldistribution of cardiac output between the pulmonary can be one of the major cause of hemodynamic instability in ICU. Sudden shifts in the resistance ratio between the two vascular beds can have deleterious effects on the
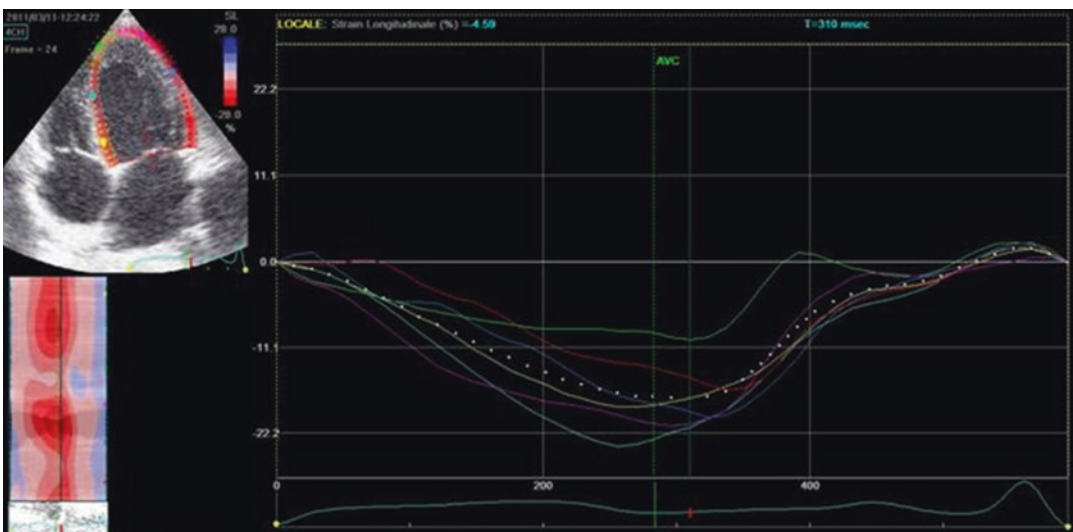
Fig. 23.3 Longitudinal strain. Strain measurement is obtained using 2D 4 chamber view with speckle tracking

distribution of flow : for example a decrease in pulmonary vascular resistance, an increase in pulmonary overcirculation or both may result in pulmonary overcirculation and systemic hypoperfusion. A Doppler index has been introduced to measure the pulmonary /flow ratio. Doppler flow ratio (DFR) (Fig. 23.4a–c) is the mean time velocity integral (VTI) of retrograde flow divided by the TVI of the antegrade flow calculate with pulsed Doppler distal to the shunt in the descending aorta using a sagittal suprasternal notch. A DFR = 1 predicts a QP:QS = 1.

Fig. 23.4 (**a**) VTI of retrograde flow. (**b**) VTI of anterograde flow. A low DFR ratio with almost absent retrograde flow in aortic arch suggest a partial closure of the shunt (**c**) in a case of Ebstein with pulmonary atresia
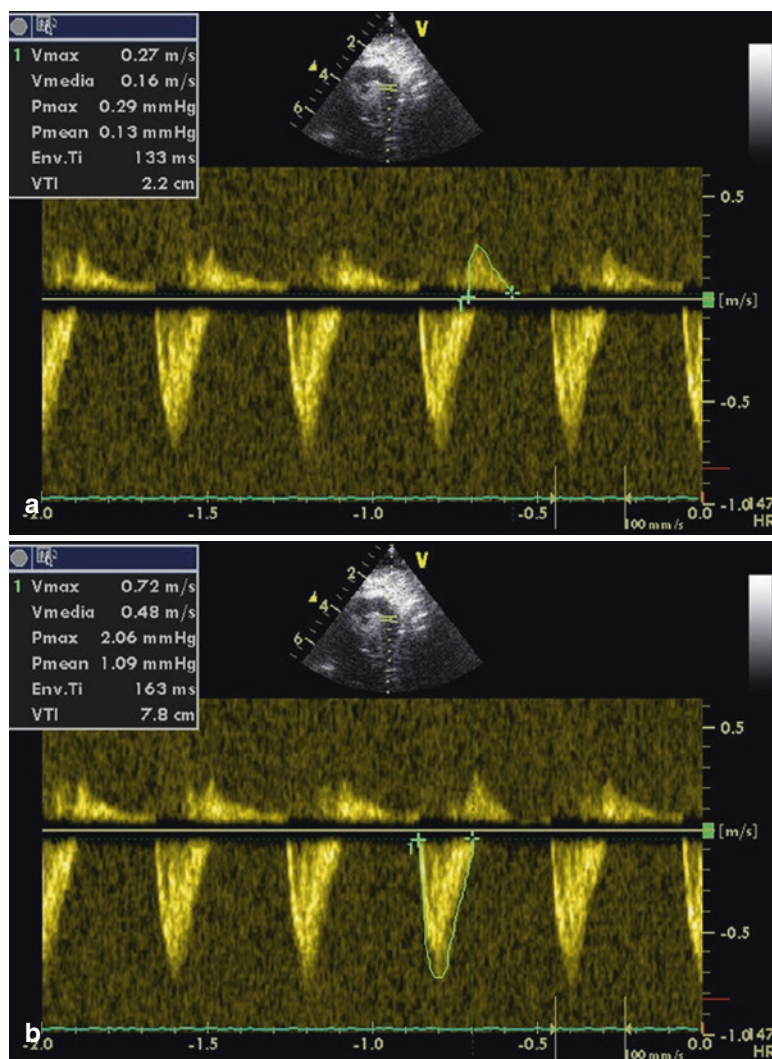
Fig. 23.4 (continued)
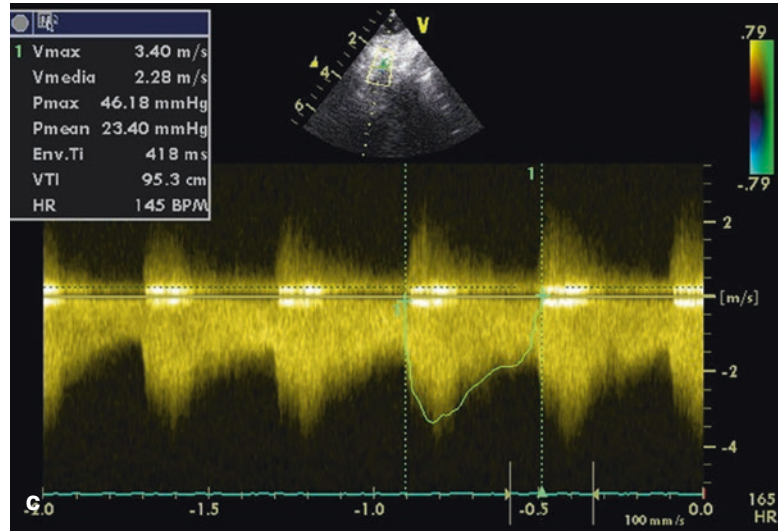
23.4 Unexplained Hypoxemia

Sometimes, ICU children have a disproportionate level of hypoxemia to the degree of disease. TEE or TTE can help to diagnose an intracardiac shunt through a patent foramen ovale or an atrial septal defect. Using normal saline solution usually agitated with two syringes and TT apical four-chamber view with color flow Doppler or TEE midesophageal bicaval and four-chamber view with color flow Doppler is possible demonstrate right-to-left intracardiac shunt. If there is right-to-left shunting, left atrial contrast is observed in three-five cardiac cycles and the density does not match that of right atrium. When intrapulmonary shunting occurs, the intensity of contrast in right side diminishes while in left side increases and the contrast passes the left atrium via the pulmonary veins. Another source of high oxygen demands is the patent ductus arteriosus with pulmonary hypertension and right-to-left ductal shunting

23.5 Pulmonary Hypertension
(Figs. 23.5, 23.6, and 23.7)

Systolic pulmonary artery pressure can be estimated with tricuspid regurgitation (TR) velocity, and pulmonary artery diastolic pressure can be estimated from the end-diastolic pulmonary regurgitation velocity. Mean PA pressure can be estimated by the PA acceleration time (AT) or derived from the systolic and the diastolic pressures. Right ventricle systolic pressure (RVSP) can be evaluated with peak TR jet velocity, using the simplified Bernoulli equation and combining this value with an estimation of RA pressure: $RVSP = 4(V)^2 + RA$ pressure, where V is the peak velocity in meters per second of the tricuspid valve regurgitant jet, and RA pressure is estimated from inferior vena cava (IVC) diameter and respiratory variation if there is not a direct measure of right atrial pressure. In absence of gradient at level of pulmonic valve or right ventricle outflow tract (RVOT), systolic blood pressure in AP is equal to RV systolic pressure. In case of RVSP elevation, obstruction at level of RVOT or pulmonary valve should be excluded, especially in patients with congenital heart disease or undergone pulmonic valve surgery. Sometimes, the simplified Bernoulli equation may underestimate the RV-RA gradient. Some cardiologists who care with patients with congenital heart disease will consider systolic pulmonary artery pressure greater than two thirds of the systolic blood pressure as impressive of severe pulmonary hypertension (PH).

Fig. 23.5 Trans-tricuspidalic CW Doppler for indirect estimation of pressure in RV, that in the absence of stenotic pulmonary valve, is = systolic pulmonary artery pressure
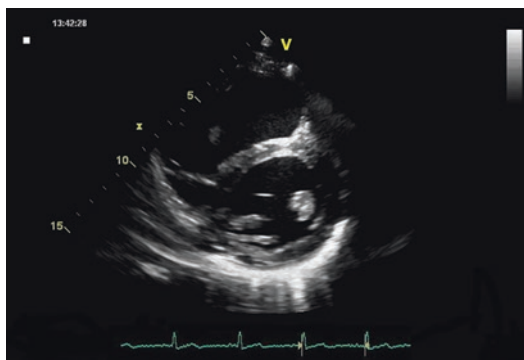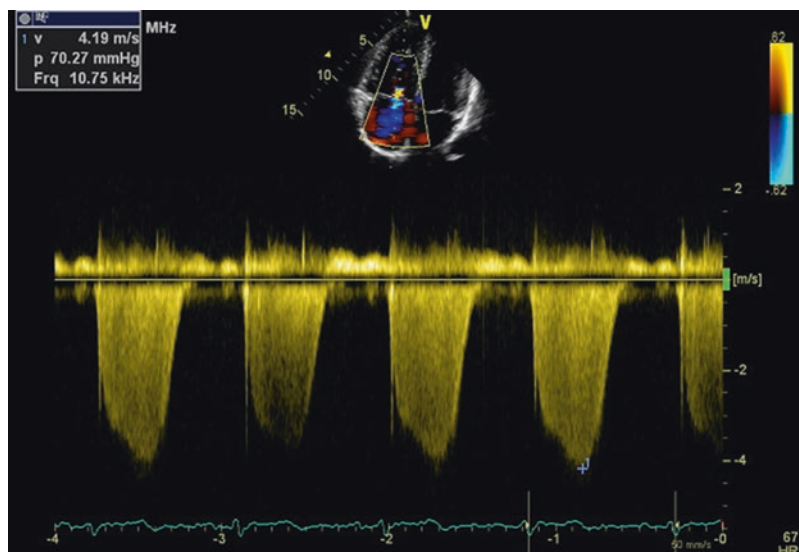
Fig. 23.6 Stop-frame in parasternal RV short axis at papillary muscle (PM) level from a patient with isolated right ventricular (RV) pressure overload due to primary pulmonary hypertension. There is a leftward ventricular septal (VS) shift and reversal of septal curvature with relative sparing of LV deformation at end-diastole

Fig. 23.7 Stop-frame in parasternal RV short axis at papillary muscle (PM) level from a patient with isolated right ventricular (RV) pressure overload due to primary pulmonary hypertension. There is a leftward ventricular septal (VS) shift and reversal of septal curvature with most marked deformation of LV at end-systole (flattening)

23.6 Intracardiac Vegetations

Suspected infective endocarditis is rather common in children with central line or endotracheal tube. With TTE is possible to obtain accurate imaging of the valves but TEE is the procedure of choice to identify complications such as abscess, perforation, mycotic aneurism. For right-sided vegetations, TEE does not offer a substantial benefit if compared with TTE. Multiplane TEE has a sensibility >90% in detecting left-sided vegetations. The image is of an echo-dense, pedunculated or adherent with different degrees of movement. The size of vegetations, mobility, position and number of valves involved are related to the complications such as systemic embolization, heart failure, response to treatment, re-surgery in patients with prosthetic valve. The pitfalls during echo examination are represented by myxomatous changes, suture material, thrombus.

23.7 Cardiac Tamponade and Pericardial Effusion

The quantity of pericardial fluid cannot be determined with echocardiography but many echocardiographers are used to quantify the pericardial fluid with terms such as trivial, moderate or severe. If this sentences does not reveal the actual quantity of fluid, on the other hand they are useful for serial evaluations. The fluid position can be anterior, posterior or circumferential. However, the most sensitive two-dimensional sign of cardiac tamponade is RV collapse during diastole. Left atrium and ventricle can collapse too, especially if LV pressures are low. M-mode includes persistence of effusion throughout the cardiac cycle, a characteristic "swinging motion" of the heart. The images can be provided with TT echocardiography in parasternal SAX, subcostal coronal cut, apical 4–5 chamber views. At the same time hemopericardium and cardiac tamponade can easily diagnosed with TEE. Two-dimensional echocardiographic identification of pericardial effusion usually reveals an echo-free space (Figs. 23.8 and 23.9). The diagnosis of pericardial tamponade includes the identification of changes with the breath in atrial and ventricular Doppler inflow profiles. As usual, during spontaneous breathing intrathoracic pressures are transmitted equally to the pericardial space and intracardiac chambers. The transmission of intrathoracic pressure is prevented by non-compliant pericardium in patients with pericardial effusion. Consequently, LA e LV filling pressure gradients are decreased during spontaneous inspi-
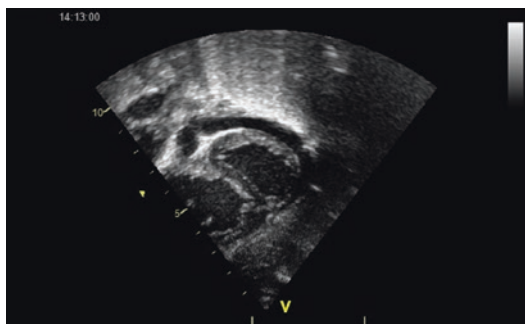
Fig. 23.8 Subcostal view is a good view to evaluate pericardial effusion

Fig. 23.9 Long axis. It is possible to detect the apex in the evaluation of pericardial effusion

ration, resulting in diminished PV forward diastolic velocities, delayed MV opening, prolonged IVRT (Isovolumic relaxation time), decreased mitral E-wave velocity. So relative increases in LA and LV filling pressure gradients during spontaneous expiration are responsible for increases in Doppler LA and LV inflow velocities. The ventricular interdependence is responsible for reciprocal changes in right-sided intracardiac flows that results in increased tricuspid E-wave velocities during spontaneous inspiration. In addition, hepatic venous forward flow decreases during espiration.

23.8 Residual Postoperative Lesion

Residual heart lesions in patients undergone cardiac surgery or lesions not previously identified can result in difficult clinical management in ICU. Echocardiography provides useful informations to the intensivist about residual intracardiac shunts, persistent mitral insufficiency following mitral valve repair, patch being dehisced, sutures coming loose. The images from transthoracic echocardiography can be limited by postoperative dressings, so TEE can be useful in ICU.

23.9 Intracardiac Thrombus

Echocardiography is useful in determining the source of emboli in patients with atrial arrhythmias, prosthetic valves, central lines, severe car-
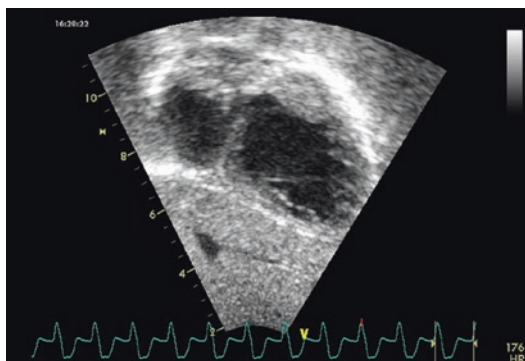
Fig. 23.10 Subxyphoid view. Thrombus at level of apex after DIV closure with patch in DORV

diac dysfunction. Findings include atrial and ventricular thrombi (Fig. 23.10), vegetations, tumors and atrial septal aneurysm. Spontaneous echo contrast ("smoke") in the atrium indicates a low flow that may lead to thrombus formation. Transesophageal echocardiography can provide increased sensitivity in the detection of intracavitary thrombi, especially those in left atrium and left atrial appendage.

23.10 Pleural Effusion, Pneumothorax and Diaphragmatic Paralysis

The chest ultrasound (US) represents a promising technique for the detection and follow-up of pleural effusion, lung embolism, pneumonia, pneumothorax, atelectasis in the adult. Recently, its use has been increased in children too, because of higher sensitivity to ionising radiation during chest x-ray. Ideally, an emission frequency of 5–7 MHz is desirable for optimizing visualisation of the lung. The probe should be small with a convex tip so it can be easily placed on intercostals spaces. Generally, a convex probe of 3–5 MHz, as available on multi-purpose ultrasound machines, allows a good visualisation of the lung. The probe is placed perpendicular, oblique and parallel to the ribs in the anterior, lateral and posterior thorax. For the examination of posterior thorax the child is positioned in lateral decubitus and in sitting position. Using anterior

and posterior axillary lines as anatomical landmarks, each chest wall can be divided in six lung regions: upper and lower parts of the anterior, posterior and lateral chest wall. Chest US also provides information about the need of additional procedures, such as thoracentesis and it may also guide the procedure. Another peculiarity of US is its ability to give some information about the type of effusion, an unorganised anechogenic effusion or an organised effusion. Despite of chest x-ray that gives more panoramic view in few time, the US takes longer to explore the entire surface of the two hemithoraces (anterior, posterior, lateral). In case of peripheral consolidation not extending to the subpleura the US is unfit to see the area due to interposition of the lung ventilated. The only regions inaccessible to US are the posterior apical regions that are covered by the scapulae. In normal chest ultrasound the ribs, on longitudinal scans, appear as curvilinear structures with posterior acoustic shadowing. The pleura appears as a regular echogenic line, pleural line, that moves with respiration. Pleural motion has described as "lung-sliding sign". Beyond the pleura-lung interface, the lung is filled with air and does not allow additional views of the normal lung. However, the large change in acoustic impedance at the pleura-lung interface results in horizontal artefacts that are seen as a series of echogenic parallel lines equidistant one from another below the pleural line. Such artefacts are known as A lines. Vertically oriented comet-tail artefacts arising from the pleural line, known as B lines according to Lichtenstein's classification, are absent in normal lung. They arise from the pleural line, move with lung sliding, reach the border of the screen and delete the A line. The presence of this artefacts is due to fluid-rich interlobular septae, which are surrounded by air and are considered pathological findings. The evidence of air inside the bronchograms that moves with respiration is defined "dynamic air bronchogram". It is a sign of patency of the bronchus and excludes atelectasis. Pleural effusion can be easily identified and appears as an anoechogenic area in the pleural space. The presence of lung sliding excludes pneumothorax. At the same time, the presence of

comet-tail excludes the diagnosis of pneumothorax. The presence of air within the pleural spaces prevents full expansion of the lung and generates parallel horizontal reverberation artefacts that are diagnosed of pneumothorax. When the question of diaphragmatic paresis or paralysis arises, fluoroscopy can be performed. Because this procedure involves transport, transthrocacic echocardiography can be performed at the bedside. TTE can evualuate movement of each hemidiaphragm.

23.11 Pediatric Sedation Management

In some children nonpainful procedures (eg echocardiography) can cause anxiety and lack cooperation with medical provider. When non pharmacologic interventions are not sufficient and mild sedation is required for nonpainful procedures, we suggest that children receive sedation with oral, sublingual or rectal midazolam.

Discussion about the risks, benefits and alternatives with parents is always necessary. Before echocardiography procedure, recommendations for duration of NPO must be followed as well as the emergency equipment must be available. Midazolam induces anxiolysis, sedation and amnesia. By mouth, 0.5 mg/Kg (maximum 20 mg); sublingual administration is more pleasant, equally rapid and effective, but requires cooperation; rectally, the dosage is 0.3–0.5 mg/Kg.

Suggested Reading

Barnes S, Yaster M, Kudchadkar SR. Pediatric sedation management. Pediatr Rev. 2016;37(5)

Guidelines for the Echocardiographic Assessment of Right Heart in Adults. A Report from the American Society of Echocardiography Endorsed by the European Association of Echocardiography, a registered branch of the European Society of Cardiology, and the Canadian Society of Echocardiography. J Am Soc Echocardiogr. 2010;23:685–713.

Jensen MB, Sloth E, Larsen KM, Schmidt B. Transthoracic echocardiography for cardiopulmonary monitoring in intensive care. Eur J Anaesthesiol. 2004;21:700–7.

Karski JM. Transesophageal echocardiography in the intensive care unit. Semin Cardiothorac Vasc Anaesth. 2006;10:162–6.

Kluckow M, Seri I, Evans N. Functional echocardiography: an emerging clinical tool for the neonatologist. J Pediatr. 2007;150:125–30.

Lai WW, Geva T, Shirali GS, Rychik J. Guidelines and standards for performance of a pediatric echocardiogram: a report from the Task Force of the Pediatric Council of the American Society of Echocardiography. J Am Soc Echocardiogr. 2006;19:1413–30.

Lichtenstein DA, Lascols N, Prin S, Mezière G. The "lung pulse": an early ultrasound sign of complete atelectasis. Intensive Care Med. 2003;29:2187–92.

Part IV

Echocardiography in the ICU and OR: Basic and Advanced Applications

Echocardiographic History, Echocardiographic Monitoring, and Goal-Directed, Focus-Oriented, and Comprehensive Examination

24

Armando Sarti, Simone Cipani, and Massimo Barattini

24.1 What Kind of Examination?

Echocardiography is applied in the emergency and ICU setting according to specific needs as follows:

1. First ultrasonographic examination of the patient. This assessment by transthoracic echocardiography (TTE) or transesophageal echocardiography (TEE) is performed systematically, according to a logical and reproducible sequence which includes all major cardiovascular structures and measurements from all ultrasound views. Chronic findings, such as hypertrophy or left-sided heart dilatation, must be distinguished from acute changes in order to reconstruct the morphofunctional history of the patient's heart.
2. Further examination to reassess the patient. This is more targeted to obtain more specific information and is done in order to follow the evolution of the clinical picture and the response to drugs and general treatment over time, including mechanical positive pressure ventilation.
3. Focus-oriented or goal-directed clinical interrogation and assessment. In the literature, a focused examination is often considered a basic assessment. Many terms are employed to designate these less-than-complete or simplified echocardiograms, such as "point-of-care," "limited," "targeted," and "functional." Here, we consider instead a cardiovascular ultrasound which occurs any time during the clinical course of hospitalization in order to resolve a specific question or problem. It implies that a comprehensive assessment has already been done or will be done. Therefore, a focus-oriented or goal-directed examination is not only a basic assessment but may be rather a patient-tailored examination specifically designed to support the making of quick decisions in relation to the diagnosis and treatment following a logical plan, algorithm, or predefined flowchart. This chapter and Chaps. 25, 26, 27, 28, 29, 30, 31, 32, 33, 34, 35, 36, 37, 38, 39, 40, 41, 42, 43, 44, 45, 46, and 47 in detail deal with many focus-oriented and goal-directed assessments.
4. Rapid emergency examination. For very unstable patients, the ultrasonographic assessment will only concentrate on the essential informa-

A. Sarti (✉)
Department of Anesthesia and Intensive Care, Santa Maria Annunziata Hospital, Florence, Italy

S. Cipani · M. Barattini
Department of Anesthesia and Intensive Care, Santa Maria Nuova Hospital, Florence, Italy
e-mail: simone.cipani@uslcentro.toscana.it;
massimo.barattini@uslcentro.toscana.it

tion that can be obtained in a few minutes or even seconds. Examples are the focused assessment with sonography in trauma (FAST) examination (see Chap. 53), designed to help in the diagnosis of and the treatment plan for the traumatized patient, and the focused emergency echocardiography in life support (FEEL) examination (see Chap. 48), used to obtain a rapid diagnosis and an immediate intervention, such as the administration of epinephrine, a pericardium drainage, or a fluid bolus during advanced life support.

24.2   Operator's Skill

An inexperienced operator will be limited in terms of what he/she is able to obtain and interpret and will need to seek help with any questions or doubts. As the intensivist's skills improve progressively, he/she will be able to enhance his/her ability to use diagnostic ultrasonography in assessing and treating critically ill or injured patients. Apart from the gained experience and skill of the examiner, echocardiography is generally considered operator-dependent. This is true in part. Intra- and inter-observer variability has been reported between 3% and 10% in the ICU practice. Standardized ICU TEE is less operator-dependent than TTE and is considered nearly operator-independent according to some authors.

Cholley et al. [1] have set out a pyramid for the progressive acquisition of echocardiographic expertise by intensivists. At the base there are the less experienced workers, ideally all ICU physicians, who are required to recognize:

- Large pericardial effusion
- The diameter of the inferior vena cava and its changes throughout the respiratory cycle
- Right ventricular (RV) dilatation
- An evident left ventricular (LV) dysfunction
- Basic ultrasonographic appearance of the pleura and lung

At the center of the pyramid, we find operators with more advanced training who are able to:

- Detect severe valvular dysfunction
- Measure RV (tricuspid annular plane systolic excursion, TAPSE) and LV (fractional shortening, fractional area change, ejection fraction, pulsed wave Doppler measurement of transmitral flow) systolic and diastolic function
- Measure the systolic pulmonary pressure
- Assess "fluid responsiveness
- Perform thoracic echography

At the top of the pyramid, we have the skilled operators, of which there is often just one or only a few in each ICU, who have a substantial "background" in cardiology and who are able to use and integrate all the techniques, including Doppler echocardiography, tissue Doppler imaging (TDI), and even speckle tracing, and who can perform the full range of echocardiographic diagnoses and hemodynamic assessments.

In our opinion, every junior intensivist should be trained and certified in performing at least basic heart and lung ultrasonography. The standard of training courses and accreditation is highly variable around the world. Acceptable competency requires both cognitive and technical knowledge of ultrasound instrumentation, image acquisition, and cardiopulmonary anatomy, physiology, and pathology. Enough evidence from the literature shows that reading a book in advance, a TTE/TEE course involving both theoretical and practical training and ongoing mentoring and supervision after the course can provide a high standard of practice. Many scientific societies define procedural competency on the basis of a minimum number of supervised echocardiographic examinations performed by the intensivist. However, regular reaccreditation and continuous comparison with adequate standards are still required to maintain competency. A recent international round table of the European Society of Intensive Care Medicine, endorsed by many other societies [2], states that there was a 100% agreement among the participants that basic critical care echocardiography and general critical care ultrasonography should be mandatory in the curriculum of ICU physicians.

Echocardiography and lung echography are currently considered a key irreplaceable tool in the ICU practice. However, merging cardiac and lung ultrasound in the ICU routine is not always achieved in many countries. A continuous training effort of the intensive and critical care societies as well as full commitment of senior and ultrasound-skilled intensivists is mandatory to extend these techniques for a better care of our patients.

24.3 First Comprehensive Examination of the Patient

A systematic assessment implies the need for substantial experience and mastery of most of the echocardiographic techniques, including B-mode, M-mode, continuous wave Doppler, pulsed wave Doppler, color flow mapping (CFM), and TDI. During the training phase, the intensivist would be better off requesting the intervention of the cardiologist, or another skillful intensivist, so as to perform the first systematic assessment in conjunction with an experienced colleague.

First, it is advisable to review all previous echocardiographic examinations, if available. The comparison is useful to determine the starting point of the patient before the episode that led him/her to the emergency department or ICU. Currently observed findings are often very different from those produced previously, even recently. In fact, the ICU ultrasound assessment is performed on patients in a critical or unstable condition due to acute changes in arterial pressure, hypovolemia or hypervolemia, hypoxemia, hypercapnia, mechanical ventilation, and high levels of circulating catecholamines. This "stress echocardiography" examination may thus show latent disorders which are not visible at rest.

Echocardiography always starts from the patient and must keep the patient at the center of clinical reasoning. Before the echocardiography machine is switched on, the patient's medical history, the physical examination without forgetting the stethoscope, and all the results of laboratory and radiographic findings should be reviewed.

Each operator may follow his or her own particular sequence of image acquisition, so as not to overlook some data. With experience, as soon as the operator places the probe on the chest, a general idea of the patient's heart will be readily obtained. Nevertheless, it is better to proceed in a systematic way and then come back to specific views and focus on specific changes in the light of the findings already detected.

A possible TTE sequence used by the author, with the elements not to be overlooked, is as follows:

- Parasternal long-axis view: examination of the whole heart, pericardium, measurements of LV outflow tract diameter, left atrium, aortic valve, mitral valve, mitral subvalvular apparatus, CFM Doppler assessment of transvalvular flows and possible regurgitation, RV outflow tract dimension and kinetics, septum, and LV posterior wall motion
- Modified parasternal long-axis view for the right side of the heart: inflow and outflow of the right ventricle, tricuspid and pulmonary valves and flows, and possible pericardial effusion
- Parasternal short-axis view: basal sections, aortic box and mitral valve, RV inflow and outflow Doppler and CFM interrogation, segmental wall thickness and kinetics at submitral level, papillary and apical segmental wall thickness and motility, and LV diastolic and systolic areas
- Apical four-chamber view: general morphology of the heart, the atria, and ventricles, RV systolic function (TAPSE), segmental wall motion of the left ventricle, atrioventricular valves with ongoing flows and possible regurgitation (continuous wave, pulsed wave, and CFM Doppler echocardiography), systolic pulmonary artery pressure, LV ejection fraction, LV diastolic function (transmitral flow peak ratio, morphology, and E/A), LV and RV TDI, E/Ea ratio, and possible pericardial effusion
- Apical two-chamber view: left atrium and left ventricle, mitral valve, LV ejection fraction, and segmental wall kinetics
- Apical five-chamber view: LV outflow tract with pulsed wave and CFM Doppler interro-

gation, aortic valve, and transaortic flow (peak velocity and velocity–time integral)

- Apical three-chamber view: LV outflow tract, mitral and aortic valves, transaortic flow, and segmental wall kinetics
- Subcostal four-chamber view: general morphology of the heart, size and thickness, atrial septum, right ventricle, and any pleural or pericardial effusion
- Subcostal short-axis view: valves, RV thickness, and LV kinetics
- Subcostal view modified for the vena cava: diameter and respiratory variations of the inferior vena cava, shape and size of the intrahepatic veins, and intrahepatic venous pulsed wave Doppler interrogation
- Suprasternal view (not always used, if feasible and not contraindicated): aortic arch, pulmonary artery, and descending aorta
- Lung ultrasonography: search for possible pleural effusion, pneumothorax (sliding and lung point), pulmonary atelectasis or consolidation, and lung water (comet tails)

24.4 Echocardiographic History: General Ultrasonographic Morphofunctional Study of the Heart

It should always be considered that, in ICU echocardiography, acute changes are often superimposed on chronic alterations and remodeling. Since new-onset modification overlaps with pre-existing alteration, the intensivist ultrasonography operator is faced with and must interpret a myriad of different and complex findings. This is more and more frequent today, with ICU patients who are often characterized by advanced age and various associated comorbidities. All the echocardiographic information must be integrated within the clinical context of the patient, putting together the physical examination, including the cardiac auscultation and the anamnesis, with all other available data. Ultrasonography of the lung further contributes to outlining the whole diagnostic picture.

Some echocardiographic findings are frequently encountered in ICU practice:

1. Diffuse hypokinesia of the left ventricle without cardiac remodeling (i.e., without hypertrophy or dilatation) suggests an acute dysfunction due to sepsis, myocarditis, or postischemic or postanoxic disturbance (stunned myocardium). Drug toxicity or other toxic substances should also be suspected. If remodeling with dilatation is associated with diffuse hypokinesia, it is natural to suspect a dilated cardiomyopathy, either postischemic or a primitive myocardial alteration.

2. Hypokinesia or akinesia of one or more LV walls is typical of acute myocardial ischemia but may also reflect chronic alterations. Even if there are individual variations, most of the septum (except for the basal part of it, which is supplied by the right coronary artery) and the LV anterior wall are supplied by the left anterior descending artery. The LV inferior wall and the RV free wall reflect the perfusion of the right coronary artery, whereas the LV lateral and posterior walls (except for a small portion near the apex supplied by the right coronary artery) are supplied by the circumflex artery. An old myocardial infarction scar appears as a hypokinetic–akinetic wall, which is also thinned and echo-hyperreflective.

3. Diffuse hyperkinesia of the left ventricle is a common finding in the ICU (Fig. 24.1). It is visible as a marked reduction, or even a collapse, of the ventricular cavity in systole (kissing ventricle). If hypovolemia is the cause, LV end-systolic obliteration is associated with:
   - Reduction of LV end-diastolic volume or area
   - Reduced diameter of the inferior vena cava (TTE) and superior vena cava (TEE) with marked respiratory variations
   - Otherwise, if the LV end-diastolic area or volume is normal or increased, LV hyperkinesia may be linked to the ventricular emptying made easier because of decreased systemic vascular resistance, as occurs with:
   - Sepsis
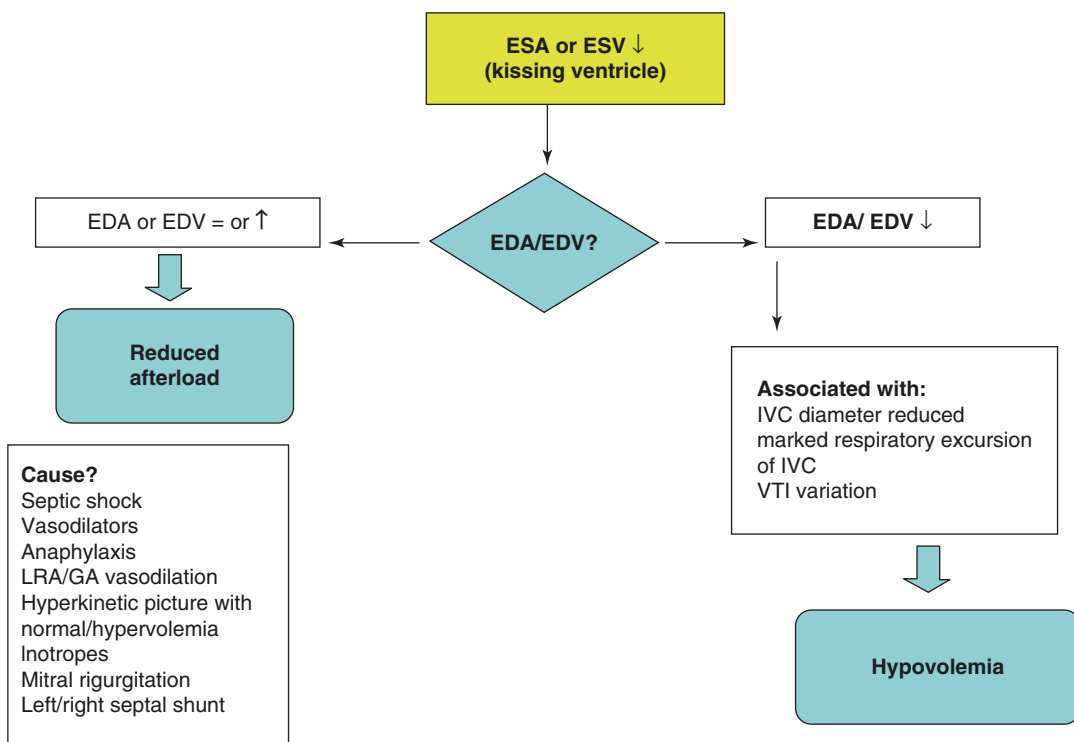
Fig. 24.1 Ultrasound-guided algorithm for the assessment of left ventricular hyperkinesia. Differential diagnosis between hypovolemia and afterload reduction. EDA end-diastolic area, EDV end-diastolic volume, ESA end-systolic area, ESV end-systolic volume, IVC inferior vena cava, GA general anesthesia, RA regional analgesia, VTI velocity–time integral. (Modified from Sarti [3] with permission)

- Anaphylaxis
- Vasodilators
- Epidural or spinal anesthesia
- Vasovagal syndrome
- Hyperthyroidism
- Cirrhosis
- Advanced pregnancy
- An easier unloading of the left ventricle (and thus a higher ejection fraction) may also be due to the systolic ejection which in part flows in a low-pressure chamber, as occurs with:
- Mitral regurgitation
- Left-to-right shunt through the ventricular septum
- To confirm the systemic vasodilatation as the cause of the hypotension associated with the left kissing ventricle, one may consider an easy algorithm (Fig. 24.2).
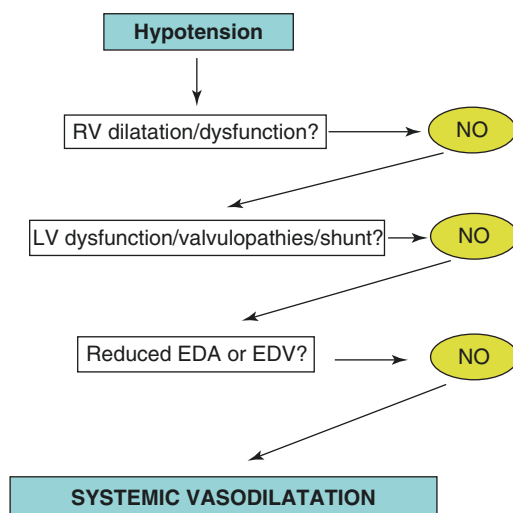
Fig. 24.2 Scheme of confirmation of vasodilatation as the cause of hypotension. EDA end-diastolic area, EDV end-diastolic volume, LV left ventricular, RV right ventricular. (Modified from Sarti [3] with permission)

4. The LV dilatation suggests an adaptation that has been shaped in months or years. It can be achieved while maintaining the elliptical shape or with an increase of lateral ventricular diameter leading to a spheroidal ventricle, almost always associated with annulus dilatation and mitral regurgitation. The patient's clinical history helps to distinguish a post-ischemic cause from a myocardial primitive disorder or valve diseases. The study of aortic and mitral valves is thus mandatory.

5. The dilatation of the left atrium is frequently found in critically ill patients, especially in the elderly. It always implies diagnostic and prognostic significance. If significant mitral valve disease can be ruled out, LV systolic and/or diastolic dysfunction should be always suspected. Right atrial dilatation is generally observed with RV dysfunction and tricuspid regurgitation. The interatrial septum tends to arch with convexity directed toward the lower-pressure chamber.

6. Acute mitral or aortic regurgitation is not accompanied by ventricular dilatation. Although CFM Doppler interrogation may show only a modest regurgitant jet, there is a significant increase in ventricular and atrial pressures. This must be kept in mind when faced with an unstable or critically ill patient with a mild valvular regurgitation and symptoms and signs of pulmonary edema and low cardiac output. The overall echocardiographic assessment is very helpful in clarifying the differential diagnostic interpretation of acute valvular insufficiency (e.g., ischemia, myocardial infarction, or endocarditis vegetations).

7. LV hypertrophy always suggests chronic remodeling. The morphology and function of all cardiac valves must never be omitted from the examination. Eccentric hypertrophy occurs with severe aortic regurgitation. Concentric hypertrophy of the septum, particularly prominent in the basal portion, is typical of hypertensive subjects, especially if they have not been adequately managed. A very thick septum or marked general LV hypertrophy is observed in hypertrophic cardiomyopathy. Aortic stenosis is another very frequent cause of concentric LV hypertrophy, particularly in the elderly. LV hypertrophy is often accompanied by diastolic dysfunction. Basal septal hypertrophy increases the risk of dynamic outflow obstruction, which is not a steady phenomenon, can be transient, and is greatly facilitated by hypovolemia, reduced LV afterload, and hypercontractility. The recognition of this disorder always has a significant therapeutic impact.

8. RV dilatation without hypertrophy is related to acute volume overload or increased impedance of the right ventricle. In the emergency and ICU setting, this is often caused by pulmonary embolism or acute lung injury/acute respiratory distress syndrome associated with positive pressure mechanical ventilation. With severe RV dysfunction, the interventricular septum progressively flattens before moving toward the left ventricle, producing the "D" image of the left ventricle in the TTE parasternal short-axis view, or the TEE transgastric 0° view. Septal dyskinesia is also observed in acute cor pulmonale. Hypokinesia of the basal part of the right ventricle, with concomitant maintenance of the kinetics of the apical part, may be seen in pulmonary embolism (McConnell sign).

9. RV free wall hypertrophy, with or without dilatation, is a chronic remodeling induced by chronic obstructive pulmonary disease, chronic pulmonary embolization, or other causes of pulmonary hypertension. With significant right-sided heart hypertrophy and dilatation, the right ventricle takes up the apex of the heart.

10. RV hypokinesia without remodeling may occur in the course of:
   - Sepsis
   - Pulmonary embolization
   - Acute respiratory distress syndrome
   - Mechanical ventilation
   - RV myocardial infarction, usually combined with the involvement of the inferior wall of the left ventricle

The right ventricle may dilate more or less in relation to central venous filling, the contractility condition, and pulmonary artery pressure. Primary RV myocardial failure must be distinguished from secondary involvement, which is associated with pulmonary hypertension.

24.5 Echocardiographic Monitoring: Serial Examinations

In the acute phase of hemodynamic instability, the echocardiographic assessment is regularly repeated to check the clinical evolution and the response to management according to specific therapeutic goals, such as central venous hemoglobin saturation greater than 75%, decreasing lactate levels, and adequate diuresis. In practice, the ultrasonographic assessment is often repeated:

- To determine the "fluid responsiveness" and follow the effect of a fluid bolus or of the passive leg raising maneuver
- After starting the infusion of vasopressors, vasodilators, or inotropes and after any significant change in their dosage
- To check the effect of mechanical ventilation, after any significant change on plateau pressure, mean airway pressure, or positive end-expiratory pressure
- To study a difficult weaning from positive pressure ventilation

So the ultrasonographic examination becomes primarily designed to follow the spontaneous evolution of the clinical condition of the patient and the results of the management plan supervising some physiological variables, such as:

- Ejection fraction, considered together with LV end-diastolic volume
- Stroke volume, or more often LV velocity–time integral (VTI), which changes according to stroke volume changes because left ventricle outflow tract does not change acutely
- Systolic and diastolic diameters, areas, or volumes of the cardiac chambers

- Size and respiratory variations of the inferior vena cava (TTE) or superior vena cava (TEE)
- LV filling pressures, including the evaluation of the E/Ea ratio
- RV area, septal dyskinesia, pulmonary artery systolic pressure, E/Ea ratio, and TAPSE
- Pleural or pericardial effusion size before and after drainage
- Lung comets (B lines) and pulmonary consolidation after a diuretic, a nitrate, or another drug therapy, the start of mechanical ventilation, or any change of the ventilator setting

Echocardiography, supplemented by chest ultrasonography, often provides all the necessary information to achieve hemodynamic stabilization of the patient. Nevertheless, a nonechocardiographic method for continuously monitoring cardiac output is normally associated with cardiovascular ultrasonography in order to monitor the patient at the bedside.

References

1. Cholley BP, Vieillard-Baron A, Mebazaa A. Echocardiography in the ICU: time for widespread use! Intensive Care Med. 2005;32:9–10.
2. Expert Round Table on Ultrasound in ICU. International expert statement on training standards for critical care ultrasonography. Intensive Care Med. 2011;37:1077–83.
3. Sarti A. Ecocardiografia per l'intensivista. Milan: Springer; 2009.

Suggested Reading

Breitkreutz R, Walcher F, Seeger F. Focused echocardiographic evaluation in resuscitation management: concept of an advanced life support-conformed algorithm. Crit Care Med. 2007;35:S150–61.

Jensen MB. Transthoracic echocardiography for cardiopulmonary monitoring in intensive care. Eur J Anaesthesiol. 2004;21:700–7.

Noble VE, Nelson B, Sutingo AN. Emergency and critical care ultrasound. Cambridge: Cambridge Medicine; 2007.

Tayal VS, Kline JA. Emergency echocardiography to detect pericardial effusion in patients in PEA and near-PEA states. Resuscitation. 2005;59:315–9.

Echocardiography in the ICU and OR: Basic and Advanced Applications

25

Alessandro Forti, Ferdinando Luca Lorini, and Carlo Sorbara

25.1 Intraoperative Echocardiography in Cardiac Surgery

Intraoperative decision-making and patient outcome could be improved by the correct performance and interpretation of the transesophageal echocardiography. Since its first use in the operating room (over 20 years ago), TEE has been used as an important diagnostic tool during cardiac surgery with a significant impact on surgical care and anesthesia management. In 1999 the American Society of Echocardiography/Society of Cardiothoracic Anesthesiologists task force published guidelines for performing a comprehensive intraoperative TOE examination. The guidelines describe 20 views of the heart and great vessels that include all four chambers and valves of the heart as well as the thoracic aorta and the pulmonary artery. However, additional views are often required to assess a particular abnormality detected during a surgical procedure.

25.2 Indication of Intraoperative TEE

There are three categories of indications for intraoperative TEE described by the ASA/SCA practice guidelines:

1. *Hemodynamic instability and valve repair surgery* (supported by the strongest evidence in the literature and expert opinion)
2. *Patient at risk for myocardial ischemia during surgery and operations to remove cardiac tumors* (supported by less evidence in the literature and expert consensus)
3. *Monitoring for emboli during orthopedic procedures and intraoperative assessment of graft patency* (supported by little evidence in the literature and expert opinion)

The management echo-tailored of hemodynamic instability is reviewed in Chaps. 26 and 29.

25.3 Warning to Avoid Complications

It is necessary before the TEE examination to review the medical history of the patient regarding the presence of dysphagia, hematemesis, or esophageal disease. In those cases an evaluation of an internist such as a gastroenterologist may be helpful to assess the risk of the TEE procedure.

A. Forti
Anesthesia and Intensive Care Department, Regional Teaching Hospital, Azienda ULSS 9, Veneto, Treviso, Italy

F. L. Lorini (✉)
Department of Anesthesia and Intensive Care, ASST Papa Giovanni XXIII, Bergamo, Italy
e-mail: llorini@asst-pg23.it

C. Sorbara
Department of Anesthesia and Intensive Care, OMCEO, Treviso, Italy

Table 25.1 Contraindication for transesophageal echocardiography

Absolute	Relative
Recent esophageal or gastric surgery	History of mediastinal radiation
Symptomatic esophageal stricture	Symptomatic hiatal hernia
Esophageal diverticulum	Coagulopathy
Esophageal tumor or abscess	Unexplained UGI bleeding
	Esophageal varices
	Cervical spine disease

An important maneuver is the probe insertion. Excessive power may never be used to insert it within the esophagus. The easiest way to perform this procedure is by grabbing the mandible with the left hand and inserting the probe with the right. The probe has to be inserted with constant gentle pressure in addition to a slight turning back and forth and from left to right to find the esophageal opening. It is very important to know when the TEE examination is contraindicated (Table 25.1).

25.4 Valve Repair Surgery

Mitral valve repair

Mitral valve reconstruction is clearly favored over prosthetic replacement for the surgical treatment of mitral regurgitation. Mitral valve repair is associated with improved operative and late mortality and with minimization of potential complications associated with mitral prostheses, such as thromboembolism, infective endocarditis, and bleeding secondary to anticoagulant therapy. Vital to the effectiveness of mitral valve repair is the intraoperative assessment of mitral competence after reconstructive procedures. Accordingly, several techniques of intraoperative echocardiography have been described. With the escalating surgical trend toward mitral valve repair for mitral regurgitation, this procedure has become the primary indication for intraoperative TEE in adult patients. This technique readily offers high-resolution real-time delineation of the functional pathoanatomy of the mitral valve leaflets, annulus, and support apparatus, aiding the surgeon in planning approaches to mitral valve repair.

In contemporary practice, degenerative mitral valve disease is clearly the most common cause of mitral regurgitation requiring operative repair. Mitral leaflet redundancy, prolapse, ruptured chordae, and flail leaflet segments caused by myxomatous degeneration of the mitral valve are readily demonstrable on TEE. The location and degree of mitral leaflet malcoaptation can be visualized on tomographic four-chamber and two-chamber scanning of the entirety of the valve with transverse and longitudinal TEE, respectively. Determination of the extent of mitral annular dilatation and calcification is possible with these imaging planes. It is also important, especially in patients with ischemic heart disease, to examine the myocardial support of the mitral apparatus. The best approach is from the transgastric window. Transverse TEE short-axis imaging delineates global and regional left ventricular function. Localized myocardial dysfunction may range from segmental hypokinesis to regional thinning with infarct expansion and may have a significant effect on the technique or even feasibility of mitral valve repair in patients with ischemic mitral regurgitation. Examination of the mitral support apparatus has also been greatly supplemented by transgastric longitudinal imaging.

Aortic valve repair

Intraoperative TEE for the evaluation of repair procedures is likely to become of use much more for aortic regurgitation than for aortic stenosis. Intraoperative two-dimensional examination is useful for the delineation of the mechanism of aortic regurgitation, such as cusp prolapse or incomplete coaptation due to enlargement of the aortic root and annulus. Semiquantitation of associated regurgitation should be performed by composite biplanar long- and short-axis color Doppler imaging. With central regurgitant jets, the ratio of subvalvular jet to outflow tract dimension (on long-axis imaging) and the ratio of subvalvular jet to outflow tract area (on short-axis imaging) correlate well with angiographic gradation of aortic regurgitation. The trajectory of the aortic regurgitant jet also aids in the clarification of the mechanism and insufficiency; defects in central coaptation cause central jets, and asymmetrical

cusp malcoaptation produces eccentric jets usually directed away from the most affected cusp. Longitudinal short-axis color Doppler imaging of the aortic valve usually can pinpoint the exact site and size of the regurgitant orifice, further guiding surgical repair efforts. Significant residual aortic regurgitation shown by intraoperative color Doppler evaluation after initial aortic valve repair was noted in 7% of patients studied by Cosgrove et al., prompting immediate successful revision of the repair in all patients in this series.

25.5   Monitoring of Myocardial Ischemia

Monitoring myocardial ischemia and segmental LV regional wall motion analysis is, in detail, reviewed in Chaps. 13 and 28. Ideally, complete evaluation of regional LV performance requires that multiple views of the left ventricle be obtained, e.g., at the base, midcavity, and apex. A qualitative impression of LV contraction is obtained by evaluating LV wall thickening and endocardial motion. Qualitative schemes describe regional wall motion as normal, hypokinetic, akinetic, or dyskinetic. Regional wall motion is normal if there are obvious systolic wall thickening and inward endocardial motion. Hypokinesia refers to abnormal systolic wall thickening or inward endocardial motion and may be graded as mild, moderate, or severe. Akinesia refers to the absence of systolic wall thickening or inward endocardial motion. Dyskinesia refers to paradoxical motion in which a portion of the wall moves in the opposite direction to the rest of the left ventricle and may even become thinner rather than thicker during systole. This is a pattern typical of transmural myocardial infarction and LV aneurysm. A scoring system based on regional systolic function can be readily applied to this schema (see Chap. 13).

25.5.1   Limitation of TEE to Diagnose Myocardial Ischemia

Errors in the interpretation of RWMA are often due to images of poor quality or to operator inex-

perience. Poor quality may be caused by inappropriate settings on the ultrasonograph or dropout in the lateral segments of the sector arc. Occasionally, a true short-axis view of the left ventricle cannot be obtained. Oblique views may produce a false impression of RWMA. Misinterpretation of regional wall motion may be related to translational or rotational changes in cardiac position throughout the cardiac or respiratory cycle that can be amplified after pericardiotomy. Omission of short-axis views at the base and apex of the left ventricle may overlook RWMA present only in these cross sections. Temporal heterogeneity of LV contraction due to abnormal LV activation (bundle-branch block or paced rhythm) may lead to a false interpretation of regional systolic function, because even though all the ventricular wall segments may contract normally, they do so at slightly different times, so that the impression given is regional dysfunction within segments with delayed electrical activation. There is also increasing uncertainty about the specificity of transient RWMA as a marker of myocardial ischemia. Intermittent myocardial ischemia can produce areas of postischemic ("stunned") myocardium. Although all methods have some limitations, TEE has provided a unique opportunity for further elucidation of the complex interactions of the heart in response to anesthesia and surgery.

25.6   Mass Lesions

Cardiac tumors and masses are reviewed in Chap. 20. Intraoperative TEE provides valuable information to the surgeon both before and after tumor resection. As also is used during surgery for intracardiac myxoma, TEE can precisely localize tumor attachment, define the tumor's effect on and potential invasion of surrounding anatomic structures, and identify multifocal tumors within the heart. After tumor resection, TEE is useful to confirm complete removal, to detect residual valvular regurgitation caused by trauma from either the tumor or surgical excision, and to exclude a possible intracardiac communication precipitated by surgical resection.

Intraoperative TEE has also been used to delineate the nature and extent of secondary neoplastic invasion of the heart, particularly in patients with renal cell carcinoma. It has been demonstrated that TEE provided highly accurate definition of intracaval neoplastic preoperative extension of renal cell carcinoma into the right heart; images were superior to characterization by preoperative computed tomography, magnetic resonance imaging, or inferior vena cavography. After tumor resection, the absence of tumor embolization, residual tumor, and inferior vena cava obstruction has been reliably confirmed by TEE in such cases. We also use intraoperative TEE to evaluate intracaval extension of other genitourinary neoplasms.

25.7 Monitoring for Intraoperative Embolism

25.7.1 Cardiac Surgery

Intracardiac air is routinely encountered in patients after cardiac operations, such as valvular or congenital heart surgery, in which the chambers of the heart are opened to air. At the end of the cardiac surgical procedure, maneuvers are undertaken to ensure that intracardiac air has been eliminated. These procedures include placement of the patient in the Trendelenburg position, transient carotid artery compression, and prolonged venting of the left ventricle. Transesophageal echocardiography is an exquisitely sensitive monitor of intracardiac air and should be used to detect intracardiac air before cardiopulmonary bypass is discontinued. Significant amounts of air necessitate prolonged venting maneuvers to avoid potential arterial air embolism.

25.7.2 Orthopedic Surgery

During surgery for total hip arthroplasty, significant hemodynamic deterioration occasionally develops during reaming of the femoral shaft or at the time of insertion of methyl methacrylate

cement. Preliminary studies have suggested that embolization of air, fat, or cement occurs at these times or later with manipulation of the joint. Because cemented total hip arthroplasty is associated with a significantly greater degree of embolism than is the noncemented operation, the increases in intramedullary pressure that occur with cementing may be the cause of embolism. Several studies suggest that TEE may have a role in monitoring selected patients undergoing major orthopedic operations; TEE is also useful for the detection of other causes of hypotension, such as venous thromboembolism and hypovolemia.

25.7.3 Liver Surgery

Occasionally, isolated right ventricular failure could account for some of the hemodynamic instability seen during liver transplantation. More often, venous, pulmonary, and paradoxical embolization of air and thrombi contributed to right ventricular failure. Air embolism during liver transplantation occurs particularly at the time of vein-to-vein bypass, and TEE is the ideal tool for recognizing this. Risk of disrupting esophageal varices in patients with portal hypertension is minimal but does exist. Hence, the potential benefit of TEE monitoring for air embolism in patients undergoing liver surgery must be weighed against the risks of variceal bleeding.

25.7.4 Neurosurgery

Transesophageal echocardiography has several intraoperative applications in neuroanesthesia and neurosurgery. Specifically, TEE can be used as a monitor of venous air embolism (VAE) and paradoxical air embolism (PAE).

Venous air embolism is a well-recognized complication of neurosurgical procedures in patients who are in the sitting position. The most important factors that limit morbidity and mortality from VAE are early diagnosis and prompt treatment. At present the most sensitive monitor for intraoperative detection of VAE is TEE two-dimensional imaging.

Paradoxical air embolism is a rare complication in patients undergoing neurosurgical procedures, but when it occurs, the results can be devastating. It has been postulated that a patent foramen ovale (PFO) predisposes patients to development of PAE during episodes of VAE. Venous air entering the pulmonary circulation results in an increase in pulmonary artery pressure secondary to obstruction of pulmonary arterial blood flow and, possibly, reflex vasoconstriction. The resultant pulmonary hypertension may yield increases in right atrial and ventricular pressures relative to left-sided pressures. Thus, a right-to-left atrial pressure gradient may occur that predisposes to development of PAE if a PFO exists. Transesophageal echocardiography may be used preoperatively to identify patients with a PFO and thus alert the clinician to the potential increased risk of PAE (see Chaps. 21 and 35). Intraoperative TEE with provocative maneuvers may be used after induction of anesthesia to detect a PFO. When a PFO is identified before the surgical procedure begins, one may choose to perform the operation in a position associated with a lower incidence of VAE than the sitting position. Performing the operation in this alternative position with lower risk of VAE might, theoretically, lower the risk of PAE.

Suggested Reading

Carpentier A, et al. Reconstructive surgery of mitral valve incompetence: ten year appraisal. J Thorac Cardiovasc Surg. 1980;79:2338–48.

Cosgrove DM, et al. Valvuloplasty for aortic insufficiency. J Thorac Cardiovasc Surg. 1991;102:571–7.

Lang RM, Bierig M, Devereux RB, et al. Recommendations for chamber quantification: a report from the American Society of Echocardiography's Guidelines and Standards Committee and the Chamber Quantification Writing Group, in conjunction with the European Association of Echocardiography. J Am Soc Echocardiogr. 2005;18:1440–63.

Zoghbi WA, Enriquez-Sarano M, Foster E, et al. Recommendations for evaluation of the severity of native valvular regurgitation with two-dimensional and Doppler echocardiography. J Am Soc Echocardiogr. 2003;16:777–802.

General Hemodynamic Assessment

26

Carla Avallato, Ilaria Nicoletti, and Alessandro Locatelli

Key Messages

- Transthoracic and transesophageal echocardiography has become a daily instrument to monitor hemodynamic parameters which are the foundation for diagnosis, decision-making, and the therapy in the critically ill patients.
- Intravascular pressures, such as the left atrial pressure, the end-diastolic pressure of the left ventricle, and the systolic pulmonary artery pressure, cannot be directly measured by echocardiography. With Doppler echocardiography, it is possible to obtain the necessary data to apply the modified Bernoulli equation and, so, calculate the value of the specific pressure.
- Left ventricular filling pressure (or pulmonary capillary wedge pressure) is a parameter obtained by combining the velocity of transmitral flow, collected by pulse wave Doppler echocardiography, and the velocity of tissue relaxation velocity, measured by the tissue Doppler imaging.
- Right atrial pressure measurement is indirected: its value is assessed by ultrasound measurement of the inferior vena cava diameter and its collapsibility during the respiratory cycle.
- The flow equation is used to determine the stroke volume, the first element to evaluate the cardiac output. Usually, the necessary data for this equation can be taken either at the mitral valve or aortic valve level.
- Echocardiography achieves its diagnosis capability using different softwares able to provide the ejection fraction, such as the Simpson's rule application, the acoustic quantification, and the 3D dataset.

26.1 Introduction

The assessment of hemodynamic parameters is the foundation for the correct diagnosis and treatment of patients hospitalized in the intensive care. Both the transthoracic echocardiography (TTE) and the transesophageal echocardiography (TEE) have proven to be versatile tools in providing a large amount of information on cardiac

C. Avallato · I. Nicoletti · A. Locatelli (✉)
Department of Emergency, Anaesthesia and Intensive Care, Santa Croce & Carle Hospital, Cuneo, Italy
e-mail: avallato.c@ospedale.cuneo.it; nicoletti.i@ospedale.cuneo.it; locatelli.a@ospedale.cuneo.it

function, in real time and directly at the bedside, also thanks to the application of the Doppler technology. Assessment of the hemodynamic parameters is based on an estimate of pressures and volumes, and we shall see how echocardiography can provide the data in a minimally invasive manner. However, the limitations of this technique should also be highlighted which are often operator-dependent and related to the quality of the images obtained. This can compromise both the accurate assessment of the parameters and the correct application of the physical principles of Doppler echocardiography, such as the proper alignment of the Doppler beam with the estimated direction of blood flow and the precise location of the sample (or sample point).

26.2   Pressure Assessment

The intravascular pressure cannot be measured directly, but, with Doppler echocardiography, it is possible to obtain the necessary data to apply the Bernoulli equation. The Bernoulli equation shows the difference in pressure generated by the passage of blood flow through a narrowed orifice as, for example, a heart valve. The estimate of the pressures inside the heart chambers assumes the presence of a jet of valvular regurgitation in the cavity ahead. In its clinical application, the equation can be simplified as follows (Fig. 26.1):

$$P1 - P2 = \frac{1}{2}\rho\left(V2^2 - V1^2\right)$$

where:
- ρ is the blood density (1.06×10^3 Kg/m³)
- $V2$ is the velocity at the distal point of the narrowed orifice
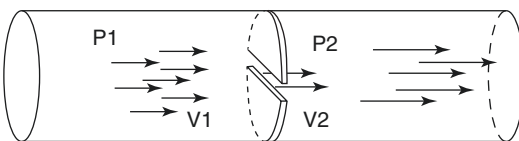
Fig. 26.1 The pressure gradient created by flow passing through a restricted orifice is correlated with the difference of the square of velocity. This is simplified in the Bernoulli equation

- $V1$ is the velocity at the proximal point of the narrowed orifice

Because $V1$ is much lower than $V2$, it can be disregarded in the final simplified formula which is:

$$\Delta P = 4 \times V2^2$$

Modern ultrasound machines automatically provide the value of the pressure gradient, which is obtained by measuring with the continuous wave Doppler echocardiography the peak velocity of the regurgitant flow. Continuous wave Doppler echocardiography is necessary to deal with high speeds (Fig. 26.2).

Considering this, using the heart valve regurgitation flow and the pressure of the heart chambers that determines it, we can calculate the left atrial pressure (LAP), the end-diastolic pressure of the left ventricle (LVEDP), and systolic pulmonary artery pressure (sPAP).

LAP is calculated using the mitral valve regurgitation. The driving pressure is the aortic systolic blood pressure (sBP) which, in the absence of stenosis of the aortic valve, is considered equal to the left ventricle pressure. The resulting equation is:

$$LAP = sBP - 4V_{MR^2}$$

where V_{MR}^2 is the peak velocity of the mitral regurgitant jet.

Several factors may make the value obtained less reliable, such as the load conditions and compliance of the left ventricle, the use of isotropic drugs, and mitral insufficiency characterized by multiple regurgitation jets.

The determination of LVEDP uses the regurgitation jet of the aortic valve. The LVEDP is calculated by measuring the difference between the driving pressure (systemic diastolic blood pressure, dBP) and the end-diastolic gradient of aortic regurgitation. The resulting equation is:

$$LVEDP = dBP - 4V_{AR\text{-}EDV^2}$$

where $V_{AR\text{-}EDV}^2$ is the end-diastolic velocity of the regurgitation jet of the aortic valve.

Fig. 26.2 Peak velocity
assessment of the mitral
regurgitant flow using
continuous wave
Doppler
echocardiography
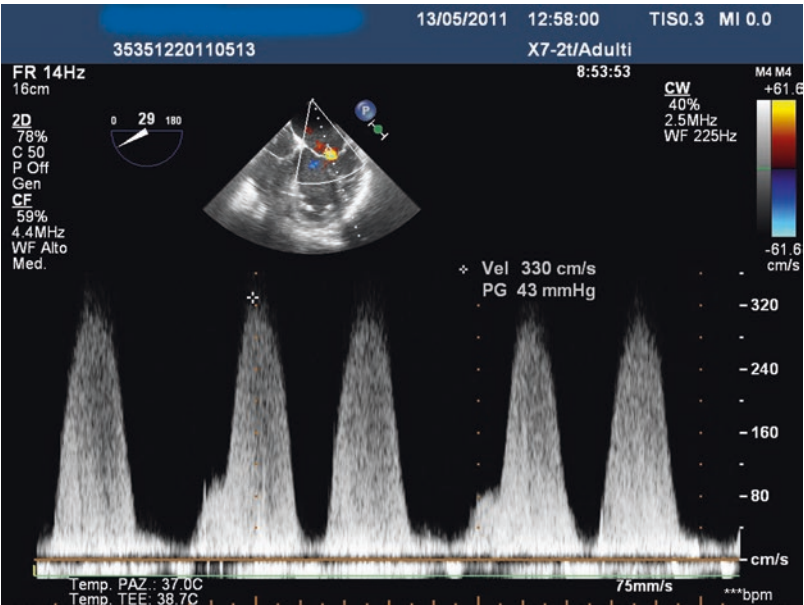
Right Atrial Pressure and	Size	Collapsibility	Values	
Inferior vena cava	< 2,1 cm	> 50 %	0-5	mmHg
size and collapsibility	> 2,1 cm	> 50 %	5-10	mmHg
during sniff	> 2,1 cm	< 50 %	10-20	mmHg

Fig. 26.3 Data from the American Society of Echocardiography

The sPAP is equal to the systolic right ventricular pressure in the absence of stenosis of the right ventricular outflow tract or of the pulmonary valve. It is determined by measuring the peak velocity of the tricuspid valve regurgitation jet, obtained with the continuous wave Doppler echocardiography. The equation is:

$$sPAP = 4V_{TR^2} + RAP$$

where RAP is the pressure in the right atrium. This pressure is 8–10 mmHg, but, if the patient shows signs of congestive heart failure or jugular venous distension, it can be estimated by ultrasound measurement of the inferior vena cava and its variations during the respiratory cycle. A dilated vena cava (diameter greater than 2.1 cm) and its variations inferior to 50% during respiration are significant for RAP >15 mmHg (Fig. 26.3).

These data are not correct in patients on positive pressure ventilation, because the reduction in venous return during the inspiration time changes the inferior vena cava collapsibility.

Mean pulmonary artery pressure can be estimated by pulsed wave Doppler echocardiography by measuring the acceleration time of the velocity-time integral (VTI) of the pulmonary artery flow, using the TTE parasternal short-axis view (Fig. 26.4) or the TEE mid-esophageal ascending aortic short-axis view. The shorter the time to reach the peak velocity, the higher the mean pressure in the pulmonary artery:

$$Mean\ PAP = 79 - 0.45 \times AT$$

where PAP is the pulmonary artery pressure and AT is the acceleration time.

Normal value is higher than 90 ms but lesser than 60 ms if pulmonary hypertension occurs. A sharp rise of pulmonary peak velocity by simple visual inspection can immediately suggest a high pulmonary pressure as the ascending velocity slope is very sharp (Fig. 26.5).

Left ventricular filling pressure (pulmonary capillary wedge pressure) is calculated by the E/E' ratio (or E/Ea ratio), which is the ratio between the peak velocity of early transmitral flow (pulse wave Doppler echocardiography)

Fig. 26.4 TEE mid-esophageal ascending aortic short-axis view and pulmonary artery velocity-time integral (VTI). AT acceleration time
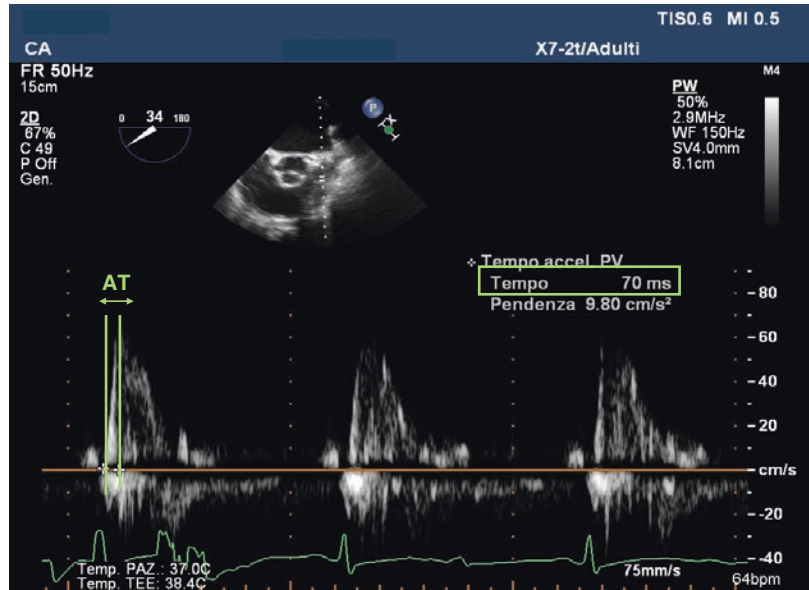
Fig. 26.5 TTE parasternal short-axis view, pulmonary artery VTI: short acceleration time in pulmonary hypertension
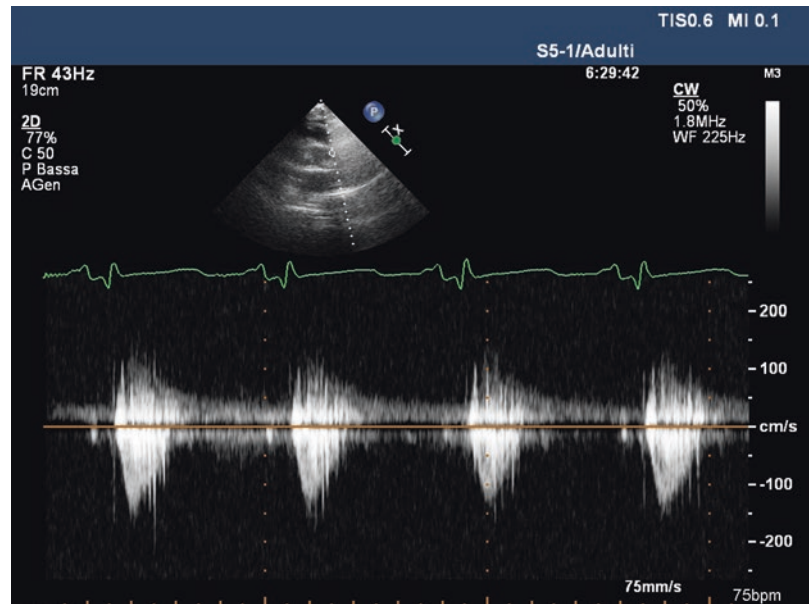
and the speed of early tissue relaxation velocity (tissue Doppler imaging) (Figs. 26.6 and 26.7). It is rather intuitive that the ratio between the peak flow, which depends on the transmitral pressure gradient, and the speed of the myocardial relaxation can represent left ventricular fill-ing pressure. This ratio is considered normal under 8–10 and abnormal (increased filling pressure) over 10. In particular, a value over 15 is associated with a marked increase in left ventricular filling pressure and pulmonary wedge pressure (Fig. 26.8) especially if the ventricular

Fig. 26.6 TEE mid-esophageal four-chamber view: *E* peak velocity of early transmitral flow (pulse wave Doppler echocardiography)
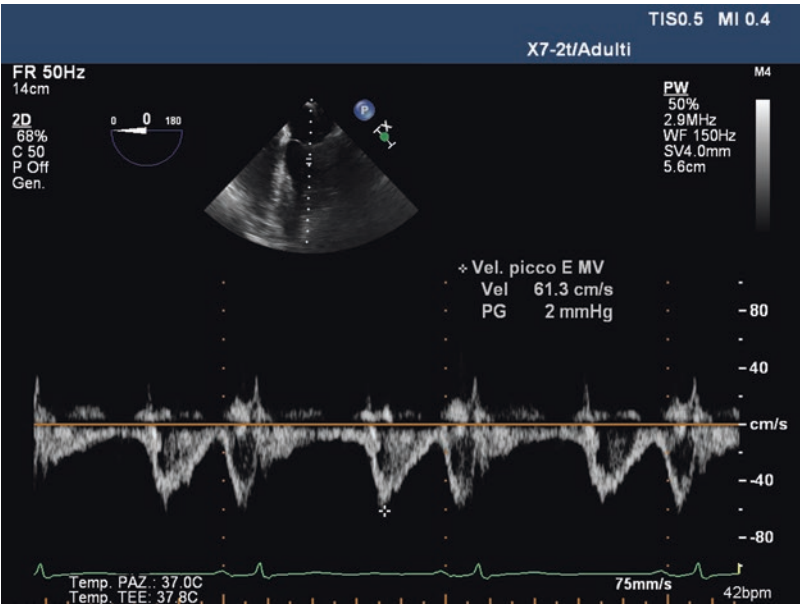
Fig. 26.7 TEE mid-esophageal four-chamber view: *E/Ea* ratio (*Ea* speed of early tissue relaxation velocity of lateral mitral ring with tissue Doppler imaging)
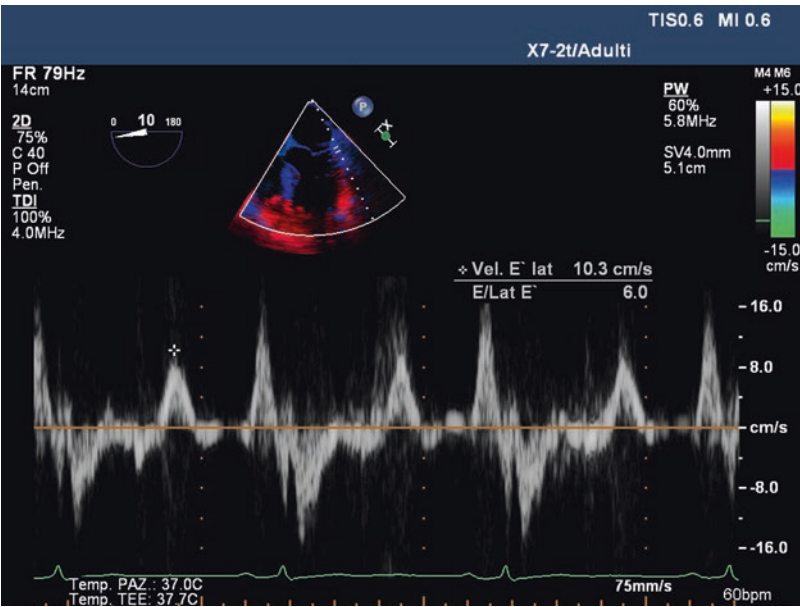
systolic function is preserved and also with a significant increase of the level of natriuretic peptide. The E wave of the mitral inflow velocity is measured in the apical four-chamber view with TTE and in the mid-esophageal four-chamber view with TEE. The best measurement of E′ velocity of the tissue Doppler imaging is obtained with the Doppler angles aligned with the lateral mitral valve annulus, in the apical four-chamber view with TTE and in the mid-esophageal four-chamber view with TEE.
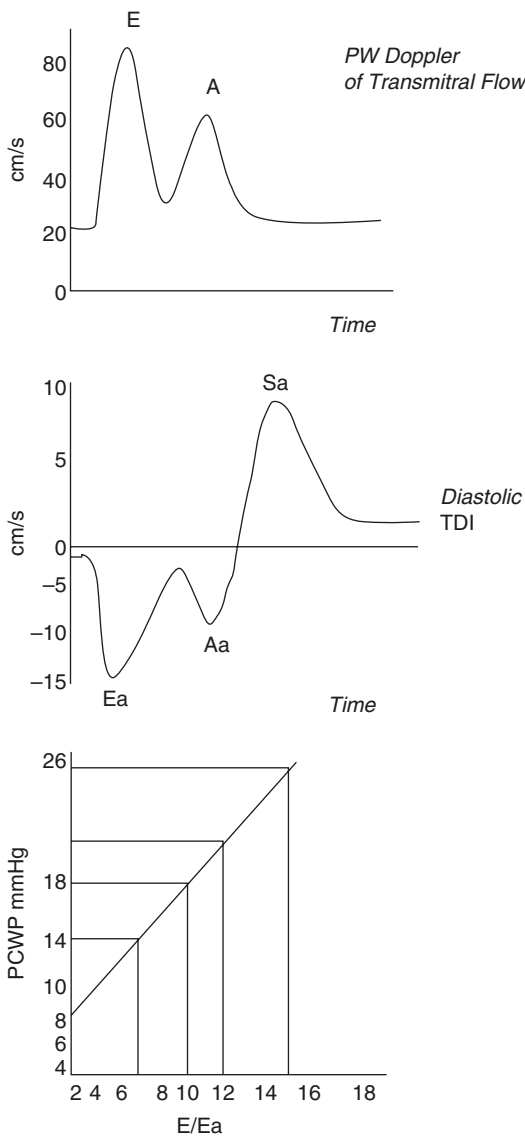
Fig. 26.8 Top to bottom: transthoracic echocardiography (TTE) apical four-chamber pulse wave (PW) Doppler measurement of transmital flow, TTE apical four-chamber lateral ring tissue Doppler imaging (TDI), and the relationship between *E/Ea* (*E/E′*) and pulmonary capillary wedge pressure (PCWP)

26.3 Cardiac Output

Echocardiography allows us to obtain qualitative and quantitative estimation of ventricular volumes and therefore measure cardiac output. This is accomplished either through the use of Doppler technology or through volumetric measurements and derived applications (e.g., acoustic quantification and real-time three-dimensional echocardiography).

The application of Doppler echocardiography in this context uses the flow equation: the flow or volume is the product of the cross-sectional area (CSA) through which the blood sample moves and the distance that this blood volume covers in a given time. In echocardiography, this distance, corresponding to the column of the blood moving through the CSA in a heartbeat, can be calculated using the velocity-time integral (VTI) of the Doppler wave (pulse wave Doppler echocardiography or continuous wave Doppler echocardiography) found in the specific CSA. All echocardiographic devices provide automatic calculation of VTI tracing the outline of the corresponding Doppler signal (Fig. 26.9).

This is illustrated by the following equation:

$$\text{Volume}\left(\text{cm}^3\right) = \text{CSA}\left(\text{cm}^2\right) \times \text{VTI}\left(\text{cm}\right)$$

In this way, the stroke volume (SV) is calculated, i.e., the volume of blood ejected with each heartbeat. With echocardiography, the SV is obtained with several methods, properly
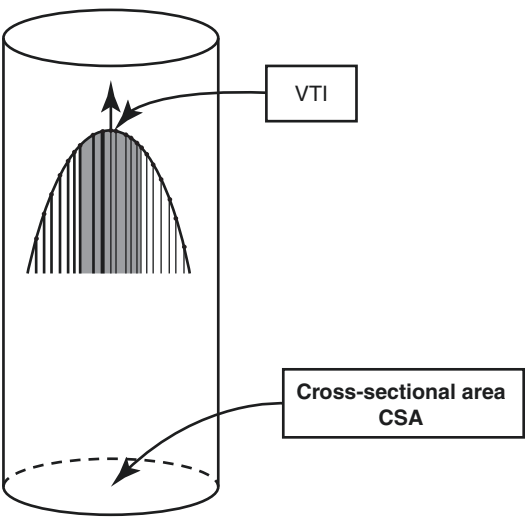
Fig. 26.9 Flow equation: the flow is the product of the cross-sectional area (CSA) and the distance that the blood volume covers in a given time, assessed by the velocity-time integral (VTI)

correlating the measure of CSA with the point of detection of the Doppler signal.

For the *left ventricular outflow tract*, the pulsed Doppler signal is used (pulse wave Doppler echocardiography). The sample is placed 5 mm below the aortic valve. The ultrasound Doppler beam must be as parallel as possible to the direction of the blood flow so that the angle of incidence between the two directions does not exceed 20° (in this way the possible error produced will be less than 6%). With TEE the best alignment is achieved with trans-gastric projections (trans-gastric long-axis view at 90–120° or deep trans-gastric view), whereas with TTE the apical five-chamber view is used. The CSA is calculated using the diameter of the left ventricular outflow tract measured with the M-mode at the aortic annulus during systole (Figs. 26.10 and 26.11).

The CSA of the aortic valve can be obtained by tracing its plane during systole or, more accurately, considering the valve like an equilateral triangle and using the same mathematical formula based on the length of one side. The aortic valve is the narrowest point through which the flow passes: a reduction of the diameter results in an increase in blood velocity. For this reason, it is necessary to use continuous wave Doppler echocardiography.

With the use of the mitral valve for SV calculation, the VTI profile is obtained more easily. The trans-mitral flow is obtained during diastole in the four-chamber long-axis view with pulse wave Doppler echocardiography. The sample is placed in the middle of the mitral valve in the annulus plane. It's more difficult to obtain a correct value of the valve area because the mitral annulus is elliptical, not circular. With the same projection, the diameter from the rise of the anterior leaflet to the posterior leaflet of the valve is measured during diastole. The mitral valve has a funnel shape. For this reason, planimetry has been validated with TTE: it is performed in the parasternal short-axis view, moving carefully from the apex to the base of the heart.

Another way to estimate the SV is to use the systolic and diastolic volumes of the left ventricle. The SV is calculated by:

$$SV = LVEDV - LVESV,$$

where LVEDV is the left ventricular end-diastolic volume and the LVESV is the left end-systolic volume.

Fig. 26.10 CSA assessment using M-mode. The diameter of the left ventricular outflow tract (LVOT) is measured at the aortic annulus during systole
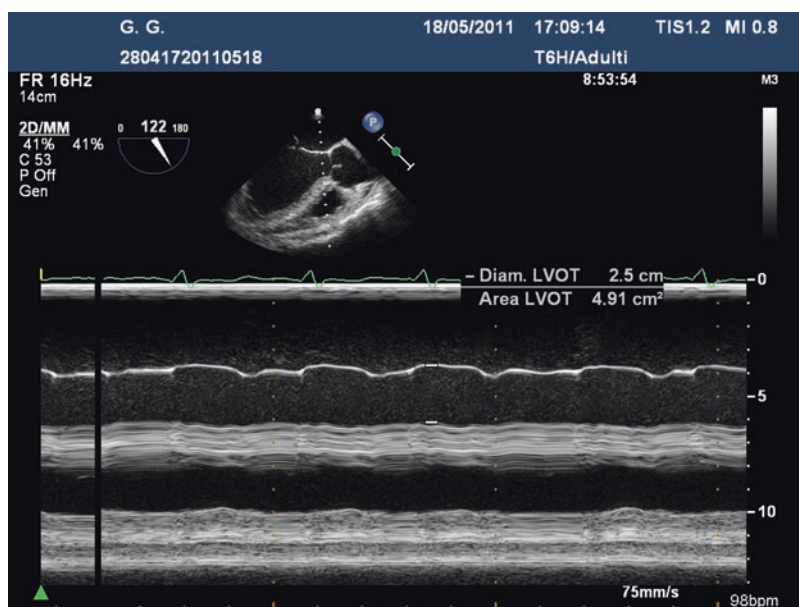
Fig. 26.11 VTI assessment using PW Doppler spectrum. The sample is placed 5 mm below the plane of the aortic valve
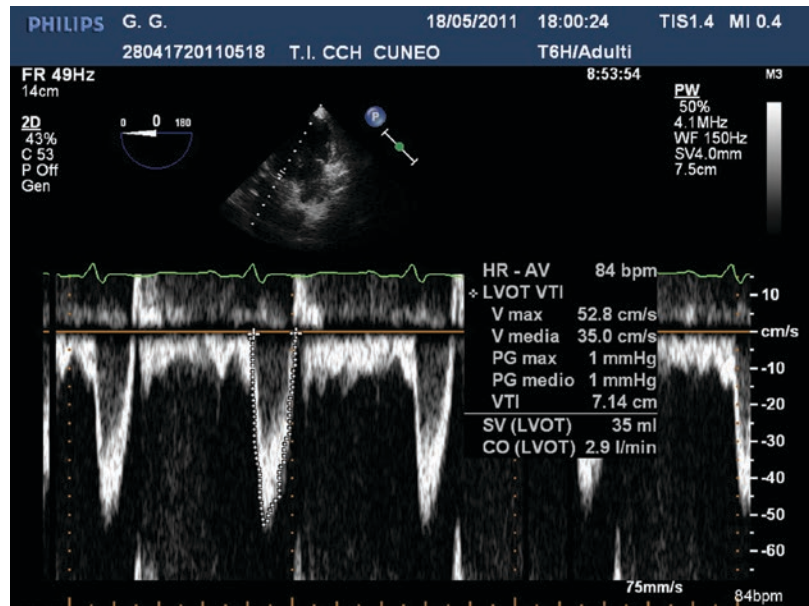
Different methods are used, but the most used ones are:

- *The area-length method*. The projection used is the four-chamber long-axis view, for both TTE and TEE. This method is based on the assumption that the left ventricle has a geometric elliptical shape. To obtain the volume, it is necessary to trace the areas and the largest longitudinal diameter of the left ventricle at the end of systole and at the end of diastole. In order to not underestimate the volume, it is also important to obtain the view of the true apex.
- *Simpson's rule*. This method is often present in echocardiography software. The ventricle is divided into multiple slices of known thickness, each considered as a cylinder. The total volume of the ventricle is obtained automatically by adding all the volume of individual slices. It is necessary to set the machine up correctly to get the best resolution and visualization of the endocardium, the inner edge of which is traced. Again, the measurements are made at the end of systole and the end of diastole. By convention, the papillary muscles are included in the cavity of the ventricle. If the patient has a sinus

rhythm, it is sufficient to perform measurements on three different heartbeats; if the patient has atrial fibrillation, the measurement needs to be repeated for seven to nine beats (Figs. 26.12 and 26.13).

The limitation of these volumetric methods is related to the echocardiographic image resolution and ventricular geometry itself. The resolution of the 2D echocardiography ranges between 0.3 and 1.5 mm, depending on the frequency and the number of cycles employed. Therefore, variations of a few millimeters are sufficient to provide significant changes in SV. Also, variations in regional contractility may lead to errors in determining the absolute value of SV and therefore of cardiac output.

26.4 New Approaches

26.4.1 Acoustic Quantification

Acoustic quantification represents an ultrasound imaging system which provides detection and tracks blood boundaries based on quantitative assessment of acoustic properties of the tissue in real time. It is a noninvasive method for online

Application of
the echocardiography
software for the
measurement of ejection
fraction by Simpson's
rule. Left ventricular
long-axis views
measuring end-diastolic
and end-systolic
volumes
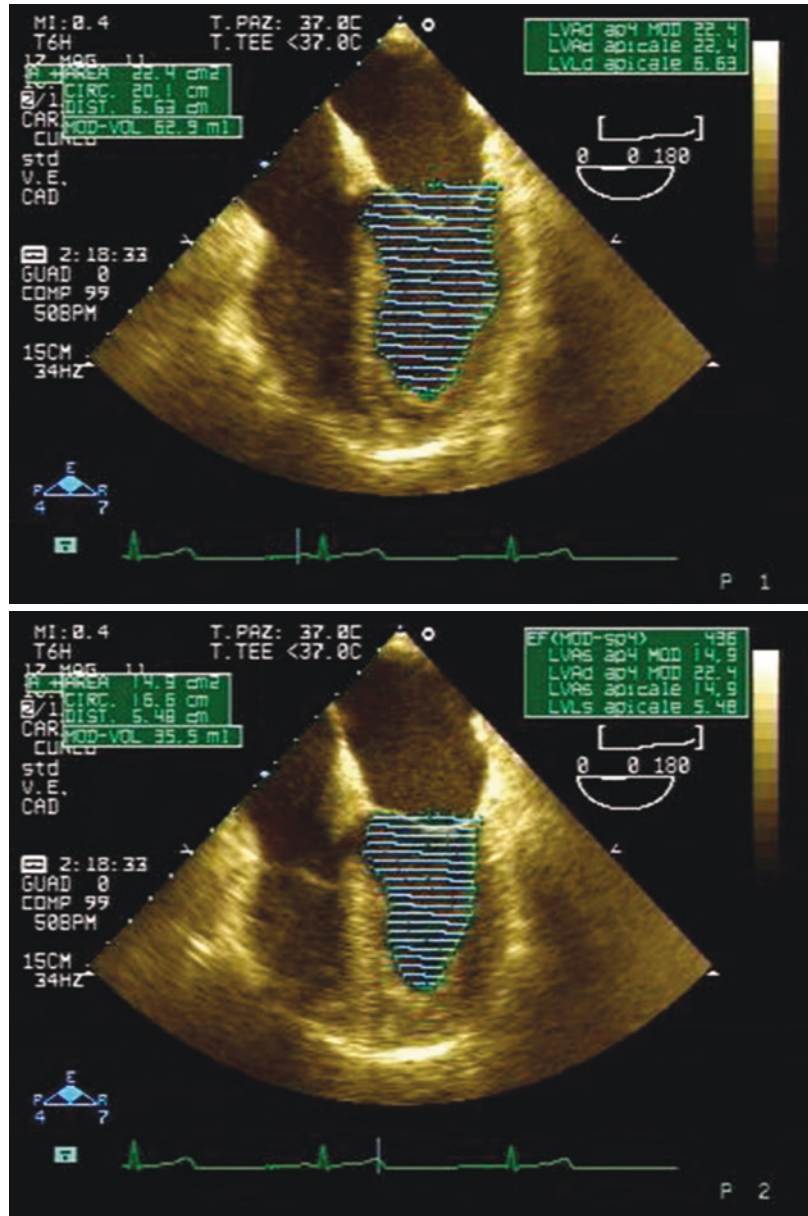
quantification of left ventricle end-diastolic vol-
ume, end-systolic volume, and ejection fraction.
The acoustic technique has the ability to identify,
view, and highlight the endocardium-blood sur-
face. The software allows one to select the area of
interest, which is the inner cavity of the left ven-
tricle. The ECG trace is needed to correlate the
area variations with the cardiac cycle. The resul-
tant waveform is associated with the value of

ejection fraction, the end-diastolic and end-
systolic volumes, and then SV (Fig. 26.14).

26.4.2   Real-Time 3D Echocardiography

The spatial limit of 2D echocardiography has
been partly surpassed by technological evolution

Fig. 26.14 Acoustic quantification (AQ). The software is used to select the region of interest (ROI), which is the inner cavity of the left ventricle. The resultant waveform is associated with the value of ejection fraction (EF)
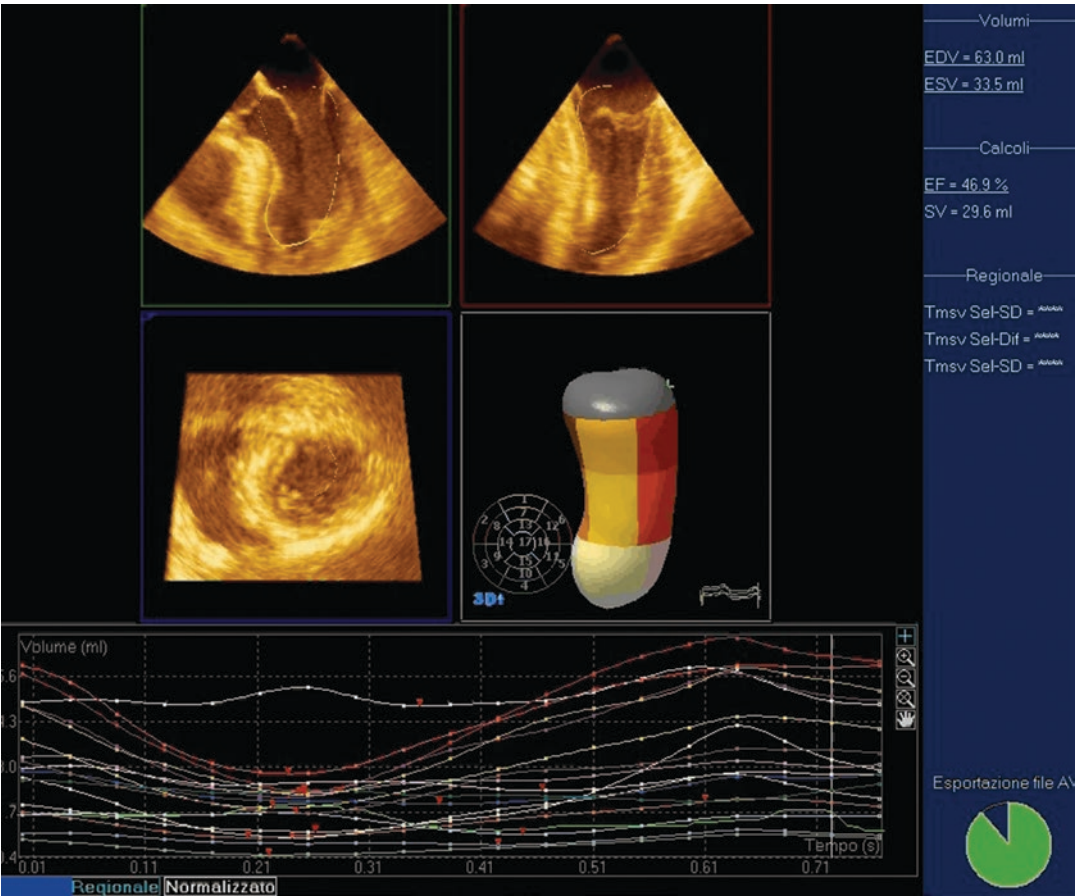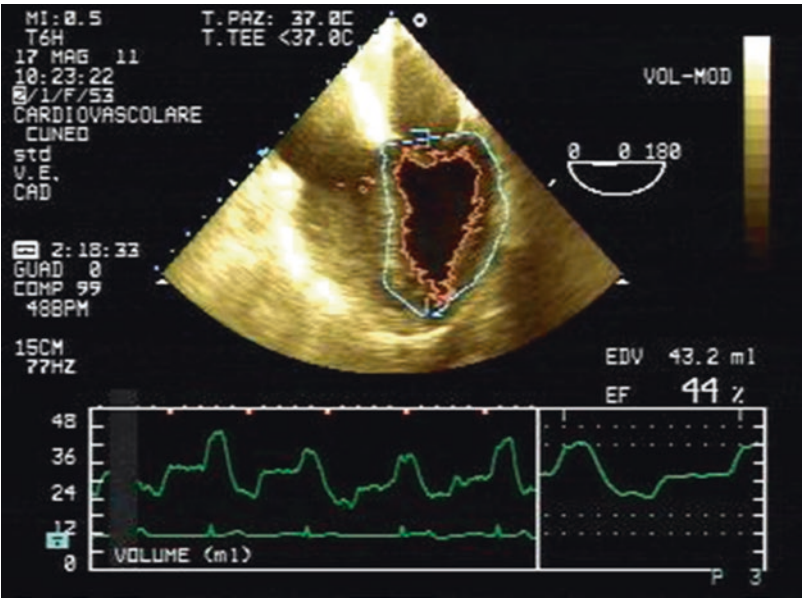
Fig. 26.15 Left ventricular volume and left ventricular EF calculation from 3D dataset
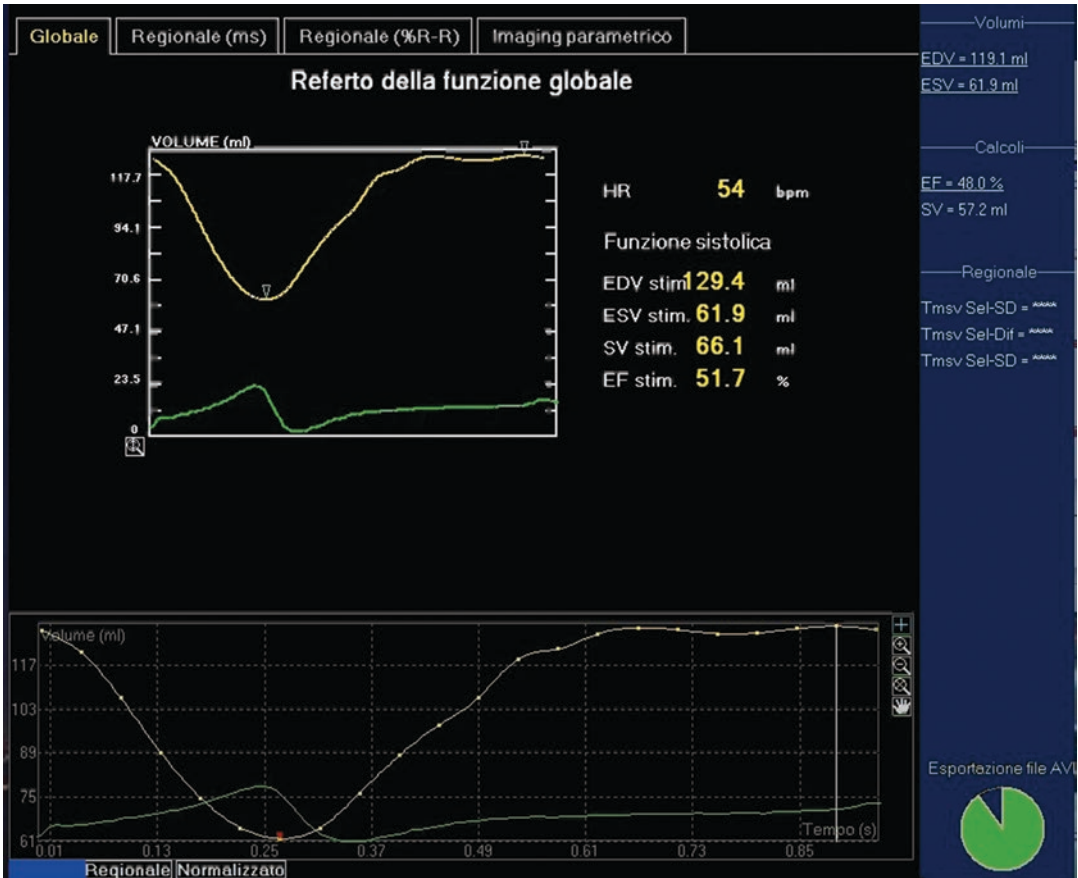
Fig. 26.16   Quantitative panel analysis provided by 3D echocardiography

of ultrasound physics and computerized image processing that has allowed the development of 3D echocardiography.

Real-time 3D echocardiography can currently use three different picture modes: live 3D (a 50° × 30° pyramidal volume), 3D zoom (a truncated pyramid that can be changed in size and in the sections, by the operator), and full-volume 3D (a pyramid volume built by the sum of four to seven images acquired on the ECG trace). This last mode allows one, by aligning the images, to reconstruct the whole left ventricle. Several mathematical algorithms process the image (in which one has to introduce different points of reference oneself and, if necessary, correct the autotracing of the endocardium), provide time-volume curves, and calculate the end-diastolic volume, end-systolic volume, and ejection fraction.

Several studies have demonstrated a high correlation between the volumes calculated by real-time 3D echocardiography and volumes obtained by magnetic resonance imaging (Figs. 26.15 and 26.16).

Further Reading

Ayuela Azcarate JM, et al. Role of echocardiography in the hemodynamic monitorization of critical patients. Med Intensiva. 2012;36(3):220–32.

Boyd JH, Walley KR. The role of echocardiography in hemodynamic monitoring. Curr Opin Crit Care. 2009;15:239–43.

Hüttemann E. Transoesophageal echocardiography in critical care. Minerva Anestesiol. 2006;72:891–913.

Poelaert JI, Schüpfer G. Hemodynamic monitoring utilizing transesophageal echocardiography: the relationships among pressure, flow and function. Chest. 2005;127:379–90.

Porter TR, et al. Guidelines for the use of echocardiography as a monitor for therapeutic intervention in adults: a report from the American society of echocardiography. J Am Soc Echocardiogr. 2015;28:40–56.

Szokol JW, Murphy GS. Transesophageal echocardiographic monitoring of hemodynamic. Int Anesthesiol Clin. 2004;42:59–81.

Vignon P. Hemodynamic assessment of critically ill patients using echocardiography Doppler. Curr Opin Crit Care. 2005;11:227–34.

Contrast Echocardiography in the ICU and OR

27

Paolo Voci, Luigi Tritapepe, Marta Iaconi,
Daria Collacchi, Demetrio Tallarico,
and Luciano Agati

27.1 Ultrasound Contrast Agents

Ultrasound contrast agents can be divided into first-generation and second-generation agents. First-generation hand-agitated saline solutions contain large and unstable air microbubbles which cannot pass through the pulmonary microcirculation and are used only for the opacification of the right side of the heart. These agents have been used for about 40 years to rule out a shunt at the level of the fossa ovalis. Second-generation agents are made of smaller, more standardized and stable microbubbles containing a low-diffusable gas. They can easily cross the pulmonary circulation and provide left ventricular (LV) cavity and LV myocardial opacification. These agents are used for better delineation of the endocardial contour and for myocardial perfusion studies.

P. Voci
Tor Vergata University, Rome, Italy

L. Tritapepe (✉) · M. Iaconi · D. Collacchi
Department of Anesthesia and Intensive Care,
Cardiac Surgery ICU, Policlinico Umberto I Hospital,
Sapienza University of Rome, Rome, Italy
e-mail: luigi.tritapepe@uniroma1.it

D. Tallarico (Retired)
Department of Cardiology I, Policlinico Umberto I
Hospital, Sapienza University of Rome, Rome, Italy

L. Agati
Department of Cardiology II, Policlinico Umberto I
Hospital, Sapienza University of Rome, Rome, Italy

27.2 Intracardiac Shunts

Critically ill patients with unexplained embolic stroke or refractory hypoxemia may have an intracardiac (atrial septal defect or patency of the fossa ovalis, PFO) or an intrapulmonary (pulmonary arteriovenous fistula) shunt. Another rare cause, but from iatrogenic stroke, is anomalous drainage of a persistent left superior vena cava to the left atrium. PFO affects 25–30% of the general population and is usually a virtual, valve-shaped communication between the atria allowing only small and transient passage of blood from the right to the left atrium after a Valsalva maneuver or cough, which temporarily increase right atrial pressure. However, when the pressure in the right atrium permanently exceeds that of the left atrium (as in pulmonary hypertension, right ventricular failure, and severe tricuspid valve regurgitation), the foramen ovale can be widely and constantly opened, producing a hemodynamically significant right-to-left shunt and hypoxemia. Color Doppler imaging may detect intra-atrial shunts, but contrast echocardiography significantly helps in the diagnosis. Agitated saline solution is good enough for this application: 9 mL 0.9 normal saline is mixed with 1 mL blood drawn back or air in a 10-mL syringe and is pushed back and forth between two syringes connected by a three-way stopcock to produce cavitation bubbles. The solution is then forcefully injected into a peripheral vein, with the syringe maintained perpendicular to the injection

Fig. 27.1 Contrast injection to show bubbles' passage through the PFO

site, to prevent injection of large bubbles. Normally, most of the bubbles are trapped in the pulmonary microcirculation, and only a small number of them may occasionally reach the left atrium and ventricle, with a delay of three to seven beats due to the transpulmonary passage (Fig. 27.1).

In PFO, however, the bubbles may cross the atrial septum immediately after right-sided opacification, most often during a Valsalva maneuver, cough, or abdominal compression.

27.3 Improvement of Image Quality

In critically ill patients with poor acoustic windows, endocardial visualization may be inadequate, making the assessment of wall motion, cavity volumes, and ejection fraction difficult. Up to 30% echocardiography studies in critically ill patients are uninterpretable owing to poor image quality. In these patients, there is sufficient evidence that second-generation contrast agents producing LV cavity opacification from a venous injection can dramatically improve delineation of the LV cavity, detection of wall motion abnor-

malities, and correct measurement of ejection fraction (Fig. 27.2). Therefore, contrast echocardiography may be a noninvasive alternative to transesophageal echocardiography for determination of regional and global LV function at rest and during pharmacological stimulation. By the use of second-generation contrast agents, up to 75% of nondiagnostic echocardiograms in the intensive care unit may be diagnostic. Contrast agents also improve detection of endoventricular thrombosis (Fig. 27.3), noncompaction of the left ventricle, and heart rupture and may definitely improve the Doppler signal to detect tricuspid regurgitation, pulmonary artery pressure, aortic transvalvular flow, and pulmonary venous flow.

In critical care settings, segmental wall abnormality suggests an ischemic cause in chest pain assessment or hemodynamic instability, even before elevation of blood cardiac enzymes. The use of contrast ultrasonography has been shown to significantly improve the detection of new segmental abnormality and is now recommended by international guidelines that if two contiguous wall segments cannot be visualized owing to poor image quality in conventional 2D echocardiography, wall motion must be further evaluated with the use of this technique.
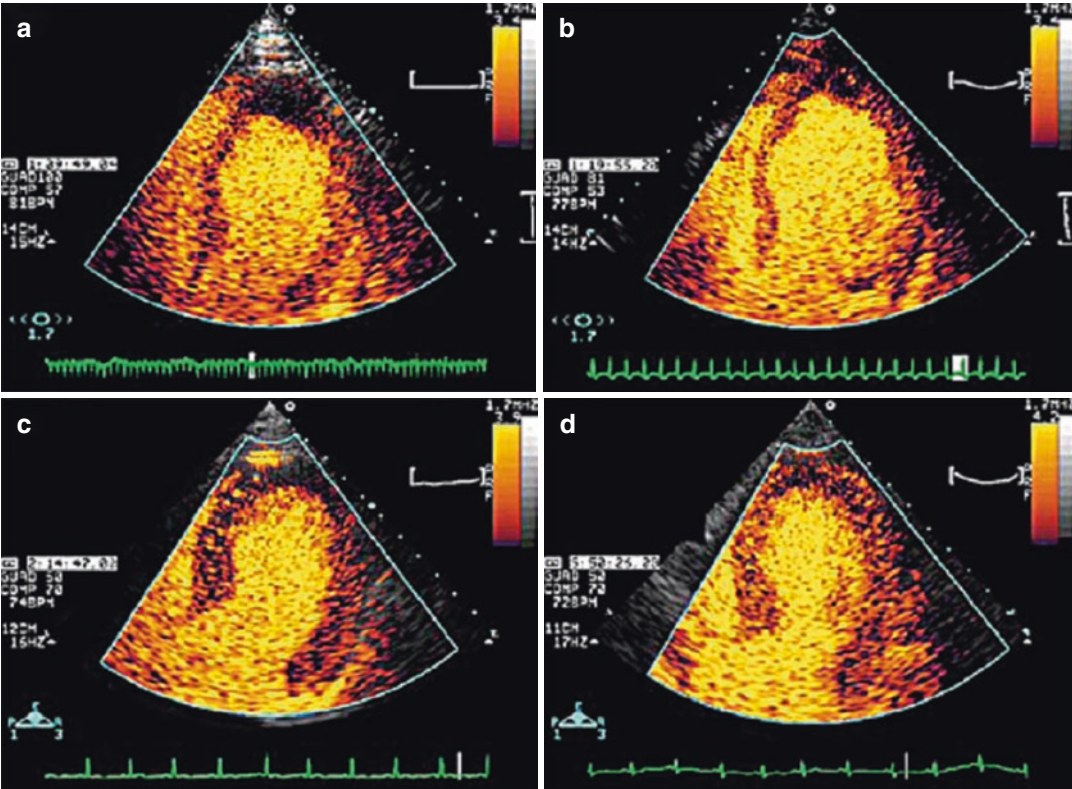
Fig. 27.2 Contrast-enhanced apical four-chamber view in patients with acute myocardial infarction treated with primary coronary intervention (**a**, **b**) or with early primary coronary intervention after lysis (**c**, **d**)
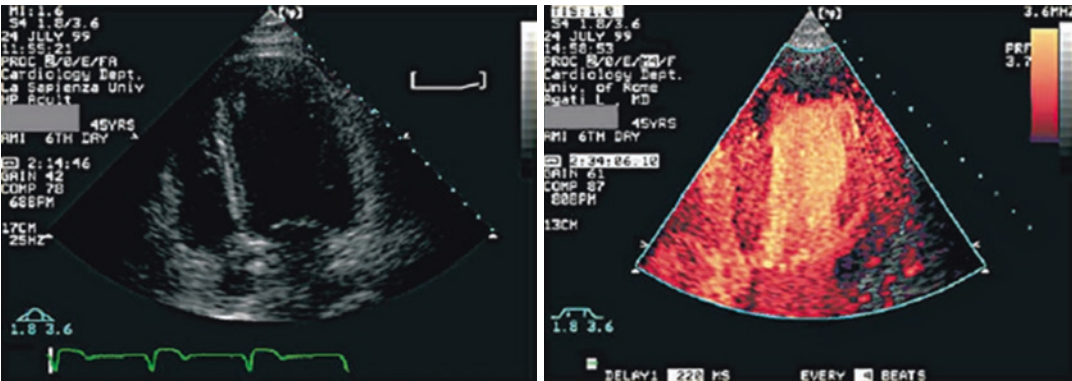
Fig. 27.3 Four-chamber view: the apical thrombus is well visualized only in the contrast-enhanced image (*right*)

27.4   Coronary Flow

Transthoracic imaging of coronary flow is a new imaging modality that can be improved by contrast ultrasonography. The left anterior descending (LAD) coronary artery can be studied at the middle-distal tract in almost all patients. Resting flow measurements may show focal velocity acceleration, suggesting the presence of a coronary stenosis, even though coronary tortuosity may produce

the same effect. Coronary flow reserve (CFR; the ratio between hyperemic and baseline flow velocities) is a useful surrogate of coronary output measurement during maximal microcirculatory vasodilation induced by adenosine, ATP, or dipyridamole, reflecting the functional impact of a coronary stenosis. CFR > 2.5 indicates the absence of a flow-limiting coronary stenosis, whereas CFR < 2 suggests the presence of a flow-limiting coronary stenosis. CFR $\leq$ 1 occurs in coronary subocclusion, when the vasodilator reserve is completely exhausted or coronary steal occurs. In the gray zone ranging from 2 to 2.5, the correlation with angiography is less strong, but usually an intermediate stenosis is found. About 25–30% of patients treated with primary coronary intervention for acute myocardial infarction have a no-reflow or low-reflow phenomenon, despite successful coronary recanalization. These patients may exhibit no significant contractile reserve or functional recovery at follow-up. CFR early after the procedure allows prediction of functional recovery after primary coronary intervention as it is directly proportional to the level of viable myocardium. Perforating branches of the LAD coronary artery can also be visualized as a useful sign of tissue reperfusion and viability after acute anterior myocardial infarction. Graft patency to the LAD coronary artery can be easily imaged, particularly at the suture level, because the mammary artery is not affected by wall motion artifacts, and graft function can be accordingly assessed by vasodilator stress focusing on the LAD coronary artery, not on the graft itself, to prevent the bias introduced by flow competition.

27.5 Myocardial Perfusion

Second-generation contrast agents reach the coronary microcirculation after venous injection and enhance the grayscale level of the LV myocardium. Rate of myocardial blood filling can be assessed by contrast microbubbles (myocardial contrast echocardiography) and myocardial blood flow determined as the product of myocardial blood volume multiplied by veloc-

ity. This technique allows measurement of the extent of the myocardial area at risk subtended by an occluded coronary artery and the detection of the no-reflow phenomenon after reperfusion in acute myocardial infarction and may ultimately predict irreversible LV dysfunction at follow-up.

27.6 Safety and Research Applications

Gas embolism is a potential side effect of galenic contrast agents but has never been a major problem in large series of patients. Caution is recommended in the case of right-to-left shunt at the level of the fossa ovalis. However, the use of ultrasound contrast agents in right-to-left shunt through a patent foramen ovale has been proven in several studies to be safe. Levovist, a hyperosmolar galactose-containing agent, is contraindicated in patients with galactosemia and must be used with caution in patients with severe heart failure. Optison is made of an albumin shell and must not be administered to patients with known or suspected hypersensitivity to blood, hemoderivates, or albumin. SonoVue contains sulfur hexafluoride and is contraindicated in patients with known hypersensitivity to the agent, right-to-left shunt, pulmonary hypertension (more than 90 mmHg), uncontrolled systemic hypertension, adult respiratory distress syndrome, assisted mechanical ventilation, unstable neuropathies, and acute coronary syndromes. No studies have evaluated the safety of intracoronary injection of commercial contrast agents as their rheological behavior has not been studied in the absence of filtering by the pulmonary microcirculation. Therefore, these agents should not be used for intracoronary injection, and they are currently commercially available for delineation of left ventricular endocardial borders. The interaction between the ultrasound beam and microbubbles produces energy with potential effects on tissue, namely, inertial cavitation and acoustic current production. Inertial cavitation refers to formation, growth, and collapse of the gas cavities within a fluid as a result of exposure to ultra-

sound. A high energy level is produced in a very small volume of gas, resulting in a very high but focal temperature increase in the collapsing zone, free-radical generation, and emission of electromagnetic radiation (sonoluminescence). This phenomenon may cause extrasystole, which is frequently seen with sonicated albumin microbubbles and the appearance of contrast agent in the right atrium. Potential membrane damage has been reported in red blood cells in vitro and in animal cells in vivo. An increase in membrane permeability was demonstrated by electron microscopy in cell membranes surrounding oscillating microbubbles, an effect which could be used for local drug delivery using microbubbles as carriers of drugs and genetic material. Early concerns for ultrasound contrast agents used in pulmonary hypertension and in critically ill patients are not supported by several new studies and are now considered safe.

27.7   Intraoperative Ultrasonography

Contrast-enhanced cardioplegia has been shown both experimentally and clinically to detect nonuniform cardioplegia distribution in patients with coronary occlusion and poor collateral circulation, in whom a retrograde administration through the coronary sinus may restore uniform protection and reduce postoperative events. In surgical repair of aortic dissection, contrast agents allow immediate visualization of retrograde aortic perfusion and may prevent severe postoperative neurologic complications in the case of inadvertent false lumen cannulation/perfusion. Evaluation of endocardial borders with intraoperative use of transesophageal echocardiography is usually more accurate than transthoracic examination; however, the use of contrast agents to better delineate the endocardial border is recommended if necessary.

Further Reading

Agati L, Tonti G, Galiuto L, Di Bello V, Funaro S, Madonna MP, Garramone B, Magri F. Quantification methods in contrast echocardiography. Eur J Echocardiogr. 2005;6(Suppl 2):S14–20.

Agati L, Funaro S, Madonna MP, Sardella G, Garramone B, Galiuto L. Does coronary angioplasty after timely thrombolysis improve microvascular perfusion and left ventricular function after acute myocardial infarction? Am Heart J. 2007;154:15127.

Eskandari M, Monaghan M. Contrast echocardiography in daily clinical practice. Herz. 2017;42(3):271–8.

Feinstein SB, Voci P, Segil LJ, Harper PV. Contrast echocardiography. In: Marcus ML, Skorton DJ, Wolf GL, editors. Cardiac imaging. A companion to Braunwald's heart disease. Philadelphia: Saunders; 1991. p. 557–74.

Galiuto L, Garramone B, Scarà A, Rebuzzi AG, Crea F, La Torre G, Funaro S, Madonna MP, Fedele F, Agati L. The extent of microvascular damage during myocardial contrast echocardiography is superior to other known indexes of post-infarct reperfusion in predicting left ventricular remodeling. J Am Coll Cardiol. 2008;51:552–9.

Lang RM, Badano LP, Mor-Avi V, Afilalo J, Armstrong A, Ernande L, et al. Recommendations for cardiac chamber quantification by echocardiography in adults: an update from the American Society of Echocardiography and the European Association of Cardiovascular Imaging. J Am Soc Echocardiogr. 2015;28:1–39.

Pizzuto F, Voci P, Mariano E, Puddu PE, Aprile A, Romeo F. Evaluation of flow in the left anterior descending coronary artery but not in the left internal mammary artery graft predicts significant stenosis of the arterial conduit. J Am Coll Cardiol. 2005;45:424–32.

Porter TR, Xie F. Contrast echocardiography: latest developments and clinical utility. Curr Cardiol Rep. 2015;17(3):569.

Porter TR, Abdelmoneim S, Belcik JT, McCulloch ML, Mulvagh SL, Olson JJ, Porcelli C, Tsutsui JM, Wei K. Guidelines for the cardiac sonographer in the performance of contrast echocardiography: a focused update from the American Society of Echocardiography. J Am Soc Echocardiogr. 2014;27:797–810.

Voci P. The bubbles and the science of life. J Am Coll Cardiol. 2000;36:625–7.

Voci P, Testa G, Tritapepe L. Demonstration of false lumen perfusion during repair of type A aortic dissection. Anesthesiology. 1996;85:926–8.

Voci P, Pizzuto F, Romeo F. Coronary flow: a new asset for the echo lab? Eur Heart J. 2004;25:1867–79.

Echo-Guided Therapy of Myocardial Ischemia

28

Michele Oppizzi, Marco Ancona,
Vittorio Pazzanese, and Rachele Contri

Key Points
- Diagnosis: regional wall motion abnormalities
- Risk stratification: EF < 35%, functional mitral regurgitation, high left atrial and pulmonary pressure and RV dysfunction
- Echo-guided therapy:
  - High heart rate and arterial pressure, FAC or EF > 40%, no mitral regurgitation → deep anaesthesia/analgesia + beta-blocking agents or calcium antagonist + nitrates (if coronary spasm is suspected)
  - High arterial pressure and normal or low heart rate → nitrates
  - Low arterial pressure and FAC or EF > 40%, small LV end-diastolic area, vena cava collapse = hypovolemia → volume expansion
  - Low arterial pressure and FAC or EF < 40% and/or mitral regurgitation (moderate to severe) → inotropic agents, IABP, coronary angiography

M. Oppizzi (✉) · M. Ancona · V. Pazzanese
Department of Cardiology, San Raffaele Hospital,
Milan, Italy
e-mail: oppizzi.michele@hsr.it; ancona.marco@hsr.it; pazzanese.vittorio@hsr.it

R. Contri
Cardiocentro Ticino, Lugano, Switzerland

No controlled clinical trials are currently available on the best treatment of intraoperative myocardial ischemia and infarction (AMI). Therefore, we suggest a personal approach, tailored on hemodynamic and echocardiographic data, which can be summarized in the following scenarios (Fig. 28.1).

28.1 LV Ischemia/Infarction

1. In patients with an *increased mean arterial pressure (MAP) and/or heart rate (HR)*, TEE usually shows a normal end-diastolic area (trans-gastric short-axis view), a fractional area changes (FAC) > 40% (trans-gastric short-axis view) and no or mild mitral regurgitation (four-chamber mid-oesophageal view). In such cases myocardial ischemia can be the manifestation of an inappropriate anaesthetic management. Therefore, the first step is deepening anaesthesia and analgesia.
   - If this manoeuvre is unsuccessful and *both MAP and HR remain high*, heart rate control takes priority. IV beta-blocker with a short half-life such as esmolol is the first choice in most patients with ST segment depression or elevation, whereas diltiazem is preferred whenever coronary spasm is suspected (previous history of rest angina and normal coronary angiography). The effects of both drugs on biventricular function in

ECHODYNAMIC GUIDED THERAPY OF PERIOPERATIVE
MYOCARDIAL ISCHEMIA

LEGENDA:
MAP = mean arterial pressure
HP = heart rate
EDA = end diastolic area
FAC = fractional area changes
MR = mitral regurgitation
NTS = nitrates
ESA = end systolic area
PRBC = packed red blood cells
IABP = intraaortic balloon pump
SG = Swan-Ganz catheter
PCI = percutaneous coronary inteventions

MYOCARDIAL ISCHEMIA

> MAP / HR

< MAP / HR

NORMAL EDA
FAC > 40%
NO MR

FAC > 40%
NO MR

FAC < 40%
MR > 2+

EDA <

ESA <

LV
DYSFUNCTION

CHECK NARCOSIS
CHECK ANALGESIA

HYPOVOLEMIA

< AFTERLOAD

IABP
SG cath.
INOTROPIC AGENTS

MAP >
HR >

MAP >
HR = <

BLEEDING ?
CHECK Ht

SPECIFIC
THERAPY +
NOREPINEPHRINE

ESMOLOL
St depression/elevation
DILTIAZEM
St elevation coronary spasm

NTS

< 30%

> 35%

PRBC

COLLOID
CRISTALLOID

PCI

Fig. 28.1 Echodynamic guided therapy of perioperative myocardial ischemia

the context of ongoing ischemia must be monitored with TEE (trans-gastric short-axis view) to avoid hypotension and heart failure.

- If only *MAP is increased but HR is normal or below normal*, beta-blocker or calcium blockers can be used with caution because of the risks of bradycardia and low-output syndrome. Nitrate infusion is usually well tolerated and is the treatment of choice. Before starting with nitrate infusion, right ventricular (RV) dysfunction, in terms of an enlarged, hypokinetic RV with reduced TAPSE and Sa (mid-oesophageal four-chamber view, trans-gastric short-axis view to visualize the RV), or low left ventricular (LV) preload (small end-diastolic area, EDA; trans-gastric short-axis view) must be ruled out to prevent the risk of severe hypotension. In some patients, the synergistic

effects of a large area of myocardial ischemia combined with an increase in LV afterload due to hypertension result in an acute LV dysfunction by a stunning mechanism that may be detected by TEE (trans-gastric short-axis or mid-oesophageal views). In such cases it is better to start nitrate infusion with a rapid titration to reduce quickly arterial pressure and to administer bolus of furosemide to prevent the development of pulmonary oedema.

2. Among patients with a *decreased MAP/HR* ratio, TEE identifies two groups: the first characterized by a normal LV systolic function (FAC > 40% in the absence of mitral regurgitation) and another characterized by LV systolic dysfunction (FAC < 40%) and/or significant functional mitral regurgitation.

- Many of the patients belonging to the first group have a *reduction in LV end-diastolic*

area. Hypovolemia associated to acute anaemia from surgical bleeding is the cause of hypotension and subsequent subendocardial ischemia (ST segment depression) in most cases. RV dysfunction must be excluded, and other echocardiographic signs supportive of hypovolemia, such as a collapsed inferior vena cava (mid-oesophageal bicaval view), respiratory variations in stroke volume (trans-gastric long-axis view or deep trans-gastric) and a good response to the leg raising manoeuvre, must be confirmed before starting fluid therapy. Rapid volume infusion, based on haematocrit values, is recommended as first step, while LV filling and function (trans-gastric view) are monitored through echocardiography. The indication and timing of coronary intervention should be carefully considered in the light of the frequent presence of multivessel coronary artery disease and the potential risk of bleeding related to dual antithrombotic therapy.

- In a few patients from the first group, *LV end-systolic area is also decreased* at such an extent that during systole LV cavity may become virtual. In these patients a severe afterload reduction is the main mechanism of hypotension. All the possible causes should be evaluated and treated: spinal anaesthesia, improper use of anaesthetic or vasodilating agents and drug interactions with a pre-existing antihypertensive therapy, especially with ACE-I, an acute allergic reaction. Concomitantly, norepinephrine infusion at low or medium dosage is recommended to correct hypotension.

- Patients with a *low MAP/HR ratio with LV dysfunction* and/or functional mitral regurgitation are at higher risk of in-hospital mortality for two reasons: (a) the underlying heart condition: if the arterial pressure is low, then the ischemic area is large or akinetic areas from a previous AMI are present; (b) the therapeutic options are limited: beta-blockers, calcium antagonists and nitrates are contraindicated or may be used at low doses. Patients with severe LV dys-

function have a higher incidence of myocardial ischemia compared to patients with a normal function since they have a lower coronary perfusion pressure (lower arterial pressure, higher LVEDP) and higher myocardial oxygen consumption (more enlarged LV; Laplace law). Most patients with LV dysfunction are on chronic therapy with beta-blockers and ACE-I because of their beneficial effect on long-term survival; nonetheless, it has been well demonstrated that ACE and angiotensin 1 inhibitors potentiate the hypotensive effect of anaesthetic agents and that beta-blockers prevent the compensatory adrenergic responses. Finally, patients with LV dysfunction are more prone to the hemodynamic consequences of myocardial ischemia.

- The mechanisms of hypotension responsible for myocardial ischemia in patients with LV dysfunction are several: an overzealous induction, an interaction between anaesthetic drugs and ACE or angiotensin 1 inhibitors, a LV distension during aortic cross clamping or excessive volume expansion.

- TEE demonstration of severe LV dysfunction associated with myocardial ischemia has important implications for the diagnostic and therapeutic decision-making, i.e. choice of medications and devices and for monitoring. Early coronary angiography followed by percutaneous myocardial revascularization is mandatory. Concomitant percutaneous intra-aortic balloon pump (IABP) insertion through the femoral artery is the treatment of choice because of its beneficial effects on myocardial oxygen balance, but its use may worsen aortic valve regurgitation and may be dangerous in patients with aortic or peripheral vascular disease. Before IABP insertion, severe aortic regurgitation (mid-oesophageal long-axis view of the aorta), aortic dissection and diffuse aortic type 5 atheroma complicated by mobile thrombus (descending aorta views) should be ruled out. During IABP insertion, TE echocardiography (proximal tract of descending

thoracic aorta view) assesses the right positioning of the balloon distal to the left subclavian artery and excludes an uncommon but life-threatening complication, i.e. iatrogenic aortic dissection. When IABP is started, complete balloon inflating and deflating can be seen in the same view (short and long axis). In those patients with a moderate aortic regurgitation, a worsening of the insufficiency (mid-oesophageal long-axis view) and its effects on LV dimensions and function (mid-oesophageal four-chamber or trans-gastric short-axis view) should be identified. An improvement in coronary blood flow in the left anterior descending artery by IABP can be confirmed by skilled echocardiographist (mid-oesophageal short-axis 30° view, a few millimetres above the aortic valve or mid-oesophageal 150° view). After a few minutes from IABP initiation, its benefits on regional wall motion and LV function become visible.

- Inotropic agents, considered to be dangerous in patients with acute myocardial ischemia because of their adverse effects on myocardial oxygen balance, can be used safely provided that an associated LV severe systolic dysfunction is demonstrated by TEE (four-chamber mid-oesophageal or trans-gastric short-axis views). The choice of a specific inotropic agent is based mainly on hemodynamic parameters, but echocardiography may be of additional help. Patients with severe mitral regurgitation (mid-oesophageal views for mitral valve) benefit from vasodilators with low risk of further reduction in systemic arterial pressure because of the improvements in cardiac output and systolic pressure consequent to the reduction of mitral regurgitation; ischemic mitral insufficiency is significantly improved by IABP in many patients. Levosimendan and phosphodiesterase 3 inhibitors are recommended in patients with an associated diastolic dysfunction because of their lusitropic properties, but their use must be cautious in patients with severe LV hypertrophy, especially if LV cavity is reduced (trans-gastric short-axis view), to avoid the risks of preload mismatch, hypotension and worsening of myocardial ischemia, which are amplified by the long half-life of these drugs. Both drugs are contraindicated if LV outflow tract obstruction (by aortic stenosis or hypertrophic cardiomyopathy) is present. Aortic stenosis is well visualized in the upper oesophageal short-axis view for the aortic valve while LV outflow tract obstruction in mid-oesophageal four-chamber or 120° long-axis view of the aorta. The LV outflow gradient can be measured with CWD in the long-axis 120° or in the deep trans-gastric view.

- In the evaluation of LV function, echocardiography is helpful in distinguishing scarred areas, by a previous transmural myocardial infarction, which have no possibility of recovery, from ischemic viable myocardium. Scar areas appear bright and thin (wall thickness < 5 mm); these findings correlate well with the presence of myocardial fibrosis at MRI. The extension of myocardial-scarred areas is useful to anticipate a poor response to inotropic agents.

- The effects of revascularization on regional wall motion and the efficacy of inotropic agents on LV function can be monitored by echocardiography in the mid-esophageal and trans-gastric views. In most patients, regional wall motion abnormalities and LV dysfunction persist for hours to days even after effective myocardial revascularization, due to a reversible stunning phenomenon. Therefore, a lack of early improvement must not be interpreted necessarily as an ominous sign. Insertion of a pulmonary catheter may be considered in these patients to guide the administration of inotropic agents and fluids. Catheter tip is well visualized by ultrasound, so TEE may be useful to guide the pulmonary catheter positioning from the right atrium (mid-oesophageal bicaval view), through the

tricuspid valve, the RV and the pulmonary valve (mid-oesophageal inflow-outflow view of the RV) to the right pulmonary artery (upper oesophageal aorta short-axis view).

- Patients with *large AMI complicated by cardiogenic shock* need emergent myocardial revascularization to reduce high risk of early death. In this scenario, IABP alone has proven to be ineffective to improve further in-hospital survival, and more powerful devices are needed to circulatory support and to reduce multi-organ failure.

- Impella device provides a cardiac output up to 5/l and reduces subendocardial ischemia through LV unloading, so it can be considered the first-choice mechanical support in most patients. Before implantation a comprehensive echocardiographic examination excludes contraindications as severe aortic valve disease or apical thrombosis. During implantation, TEE visualizes the right positioning of the tip of catheter (mid-oesophageal long-axis view) in the LV cavity: pigtail must be angled towards the apex of LV; avoid curling around papillary muscle or subannular apparatus; inlet area should be about 4 cm below the aortic annulus and outlet area above the aortic valve; mosaic pattern at colour Doppler above the aortic valve confirms correct position. During Impella working, TEE is also used to reposition the catheter in case of migration.

- V-A ECMO provides cardiopulmonary support in patients with profound cardiogenic shock complicated by severe hypoxemia, biventricular dysfunction or cardiac arrest. Pre-ECMO TEE assessment focuses on aortic regurgitation (mid-oesophageal long-axis view) that may be worsened by increased afterload induced by initiation of ECMO, embryological remnants in right atrium (mid-oesophageal bicaval view) as prominent Chiari network that might hinder proper advancement of the cannula and the presence of pericardial fluid (mid-oesophageal four-chamber or trans-gastric views). During venous cannulation (mid-oesophageal bicaval view), it must be checked that guidewire goes through inferior to superior vena cava, does not cross tricuspid valve or atrial septum or does not enter into coronary sinus. At the end of the manoeuvres, echocardiography probe is moved to mid-oesophageal four-chamber view to visualize any pericardial effusion suspect of wall perforation by guidewire. Returning to bicaval view, optimal site of venous cannula tip just beyond superior vena cava-atrial junction is well visualized and confirmed.

- After the venous cannulation is completed, the probe is rotated towards the descending aorta to identify the guidewire of the arterial cannula and avoid malposition in a branch vessel.

- After starting ECMO, the proper emptying of both ventricles (trans-gastric short axis) and aortic leaflet opening (mid-oesophageal short and long axis of aortic valve) are checked. Retrograde aortic blood flow from arterial cannula can compete with LV stroke volume worsening previous aortic valve regurgitation or hindering a normal LV emptying, visualized by echo as a close aortic valve. The resulting LV distension not only prevents myocardial recovery but also worsens subendocardial ischemia and may be complicated by pulmonary oedema, intracavitary blood stasis and thrombus formation. To decompress LV may become necessary to implant Impella device or to place a cannula percutaneously in the left atrium or surgically in the left ventricle.

28.2 RV Involvement

An enlarged and hypokinetic RV (mid-oesophageal four-chamber, trans-gastric short- and long-axis views for the RV) with depressed systolic function (reduced TAPSE, Sa, RV FAC) complicated by functional tricuspid valve regurgitation with normal or only mildly elevated pulmonary arterial pressure (mid-oesophageal LV

inflow and outflow views) associated with LV inferior wall akinesia is diagnostic of RV ischemia. It is mandatory that myocardial revascularization of the right coronary artery be performed as soon as possible, especially in cases complicated by cardiogenic shock.

The recognition of RV ischemia is important because, in addition to specific therapy of the underlying cause (i.e. myocardial revascularization), the appropriate treatment strategy is quite different from LV dysfunction. A careful balance between optimized preload and decreased afterload is essential. Drugs (mainly nitrates, diuretics and opioids) and some "not protective" subsets of mechanical ventilation that may reduce RV preload must be avoided.

RV preload optimization is particularly a challenge and differs substantially whether RV afterload is normal or increased.

In most case of RV infarction, PVR are usually normal and adequate preload is maintained by proper fluid loading.

It must be remembered that if RV systolic function is significantly reduced, the inability to fill the LV results in a lack of traditional left-sided predictors of fluid responsiveness (stroke volume variations during passive leg raising).

Initially, a volume challenge of 500–1000 ml should be administered in 15–30′, provided that PAP (mid-oesophageal RV inflow and outflow view) is normal or only mildly increased, LV is not severely dysfunctional (short-axis transgastric view) and mitral regurgitation is no more than moderate (mid-oesophageal four-chamber, commissural, long-axis views). Careful hemodynamic and echocardiographic monitoring is nonetheless required during fluid expansion. If fluid administration is too vigorous and preload increases excessively, the interventricular septum shifts leftwards (trans-gastric short-axis view) and LV stroke volume (deep trans-gastric view) decreases, and no further volume should be administered. If volume loading fails to improve systemic arterial pressure and cardiac output (LVOT pulsed Doppler deep trans-gastric view), inotropic drugs are needed. Some patients have previous (COPD, chronic pulmonary embolism, valvular heart disease) or perioperative (vaso-spastic stimuli such hypoxia, hypercapnia, acidosis, inflammatory injury and atelectasis) pulmonary hypertension. When TEE shows displacement of interventricular septum and systemic venous congestion volume administration is deleterious, high doses of loop diuretics, alone or in combination, are indicated.

Mechanical ventilation, especially if driving pressure (tidal volume/compliance of respiratory system) is high, may increase RV afterload and, according to lung compliance and transpulmonary pressure, may negatively affect RV preload. Therefore a RV-protective ventilation strategy with improving oxygenation, moderate hyperventilation with respiratory alkalosis, strict limitation of PEEP (under 10 mm Hg) and plateau pressure (below 28 cmH$_2$O) and avoidance of acidosis should be used. Patent foramen ovale, especially if a septal aneurysm coexists, may be associated with a right-to-left shunt and a subsequent worsening in hypoxia and therefore should be visualized by TEE (mid-oesophageal bicaval view). The effects of ventilation on RV shape and function are monitored by echocardiography: a leftwards shift of the atrial or ventricular septum (mid-oesophageal four-chamber view), an eccentricity index—defined as the ratio of the anterior-inferior and septal-posterolateral LV cavity dimensions at the trans-gastric short-axis view—greater than 1 at both end-systole and end-diastole and a worsening in tricuspid valve regurgitation (RV inflow-outflow view) indicate an excessive increase in afterload.

The choice of the most appropriate inotropic agent is mainly based on hemodynamic parameters. Dobutamine and milrinone remain the preferred drug in patients with no significant hypotension. In patients with refractory hypotension at risk of worsening coronary perfusion, norepinephrine and IABP are usually beneficial. Levosimendan used as "bailout" therapy in patients with RV infarction complicated by cardiogenic shock not responder to conventional treatment has proven to be effective to reduce RV afterload (PVR) and to improve RV performance (cardiac power index). In some patients who remained in shock despite IABP and optimal medical treatment, RV Impella may be placed

successfully as a bridge to recovery. The optimal position of device with proximal inlet cannula situated in the inferior vena cava (mid-oesophageal bicaval view) and distal outlet placed in the truncus of pulmonary artery (mid-oesophageal RV inflow-outflow) is confirmed by TEE. Most patients (about 80%) with "RV infarction" rapidly recover sufficient RV function to facilitate device explantation.

The effects of inotropic drugs on RV function are immediately visible as an improvement in regional wall motion (mid-oesophageal four-chamber, inflow-outflow, trans-gastric short-axis views) quantified in terms of TAPSE, Sa and RV FAC and a reduction of tricuspid valve regurgitation (mid-oesophageal four-chamber view).

Since the RV poorly tolerates afterload increase, pulmonary vasodilators may be used. The best current evidence supports the combination NO with dobutamine; prostaglandin and sildenafil may be of particular benefit when combined with dobutamine or inodilators. In evaluating the benefits of treatment on RV function, attention must be paid to the ambiguous behaviour of the pulmonary pressure. A decrease in sPAP may be due to a beneficial effect of pulmonary vasodilators on vascular resistances (improvement of RV function), but it may also reflect a worsening of RV performance.

28.3   How to Do It

Myocardial ischemia is best identified in the trans-gastric short-axis views. These cross-sectional views have the advantages of showing the LV territories supplied by all three coronary arteries simultaneously and at the same time of monitoring biventricular filling (end-diastolic area), afterload (end-systolic area) and the effects of ischemia on LV function (fractional area changes).

The trans-gastric views are acquired by advancing the probe into the stomach and anteflexing the tip to obtain the short axis, in which the LV has a circular shape and the RV a crescent-like shape. The image depth is adjusted to include the entire LV, usually at 12 cm. The probe is advanced or withdrawn in order to reach the appropriate level:

basal (at the mitral valve height), mid (at the papillary muscle height) and apical (apex).

Diagnosis of Myocardial Ischemia Myocardial ischemia appears as a reduction in regional wall motion and systolic thickening. Regional systolic thickening is best appreciated by m-mode echocardiography, which has a better temporal and spatial resolution. In short-axis views, only inferior and anterior walls are perpendicular to the m-mode ultrasonic beam; long-axis views are needed to align the beam with the septum and lateral wall. Some limitations of echocardiography in the detection of ischemia should be recognized. Interpretation of regional wall motion may be difficult by the rotation and translation movements of the heart, asynchrony due to left bundle branch block or pacing and tethering of a contiguous zone of myocardial fibrosis.

Site of Ischemia An abnormal motion of the anterior wall (trans-gastric short-axis view) indicates an obstruction of the left anterior descending artery. The outcome of patients with an inferior STEMI depends in large part on the occluded artery: the right coronary (80%) or left circumflex (20%) artery. In-hospital survival is lower in patients with right coronary occlusion due to its associated complications, i.e. RV involvement and conduction disturbances. When the inferior and the posterior wall (posterior-lateral branch) and the ventricular septum are involved, the culprit lesion involves the right coronary artery. Motion abnormalities in the lateral and possibly the posterior walls (posterior-lateral branch) suggest involvement of the left circumflex artery.

Counterclockwise rotation of the biplane probe shows the RV (trans-gastric short-axis view), where kinesis of the RV lateral and anterior wall can be inspected.

Akinesia of these segments, associated with LV proximal inferior wall motion abnormalities, is diagnostic of RV infarction. Akinesia involving the basal segments is indicative of a proximal coronary obstruction and carries a high risk of severe LV (anterior wall) or RV (inferior wall) dysfunction.

In most patients, TEE can be used to visualize the left main coronary artery (visible in the upper oesophageal short-axis view, 1 cm above the aortic valve rotating the probe about 15–30°), the proximal tract of the left anterior descending artery, the circumflex artery (mid-oesophageal 130–160° at the level of left atrioventricular sulcus) and the right coronary artery ostium (mid-oesophageal long-axis view of the ascending aorta 120°). Coronary blood flow can be measured by colour Doppler imaging. The occurrence of the aliasing phenomenon is a marker of flow turbulence due to a significant coronary stenosis. Pulsed Doppler can quantify diastolic velocity. The normal values of peak diastolic velocity are 1.4 m/s in the left main truncus, 0.9 in the LAD and 1.1 in the CCA. In patients with a coronary stenosis, the trans-stenotic blood velocity is significantly increased. The aliasing phenomenon and abnormal coronary Doppler flow patterns of velocities associated with regional wall motion abnormalities are indicative of severe and proximal coronary artery disease. Break of colour mapping, the absence of Doppler spectrum and retrograde diastolic blood flow are echocardiographic criteria of coronary artery occlusion.

Effects of Ischemia on Ventricular Function The effects of myocardial ischemia on global LV systolic function can be quantified by FAC calculation (EDA-ESA/EDA) in the short-axis trans-gastric view at the mid-papillary level or by EF (EDV-ESV/EDV) in the mid-oesophageal four-chamber view. This view is useful to complete the study of wall motion abnormalities, to evaluate the degree of mitral (MV) and tricuspid valve (TV) regurgitation, to study the diastolic function and to measure the left atrial pressure (LAP). By rotating the probe from mid-oesophageal four-chamber to long-axis view at 120°, all walls of the LV can be visualized, and the extension of ischemia can be quantified. Colour Doppler imaging applied to the long-axis view is necessary to exclude an aortic valve regurgitation that would contraindicate IABP use. MV regurgitation is quantified by colour Doppler imaging in the four-chamber, commissural and long-axis views. After completing the estimation of the MV regurgitation, pulsed wave Doppler (PWD) and tissue Doppler (TDI) of MV annulus are performed to evaluate the severity of associated diastolic dysfunction and measure LAP.

In patients with an inferior AMI, RV function is quantified (mid-oesophageal four-chamber view) by m-mode (TAPSE), tissue Doppler evaluation of tricuspid annulus (Sa) and 2D fractional area changes. Withdrawal of the probe to the inflow-outflow view and subsequent application of colour Doppler imaging allow the visualization of tricuspid valve regurgitation; sPAP can be measured through CWD (adding the right atrial pressure).

Finally a study of descending thoracic aorta is performed to detect complicated atheroma dangerous for IABP placement.

Bibliography

Douflè G, Roscoe A, Bilia F, Fan E. Echocardiography for adult patients supported with extracorporeal membrane oxygenation. Crit Care. 2015;2(19):326.

Porter T, Shillcutt SK, Adams MS, Desjardins G, et al. Guidelines for the use of echocardiography as a monitor for therapeutic intervention in adults: a report from the American Society of Echocardiography. J Am Soc Echocardiogr. 2015;28:40–56.

Ranucci M, Pazzaglia A, Tritapepe L, Guarracino F, Al LM e. Fluid responsiveness and right ventricular function in cardiac surgical patients. HSR Proc Intensive Care Cardiovasc Anesth. 2009;1:21–9.

Rudski LG, Lai WW, Afilalo J, Hua L, et al. Guidelines for the echocardiographic assessment of the right heart in adults. A report from the American Society of Echocardiography. J Am Soc Echocardiogr. 2010;23:685–713.

Hypovolemia and Fluid Responsiveness

<div style="text-align:right">**29**</div>

Armando Sarti, Simone Cipani,
and Massimo Barattini

29.1 Introduction

The veins contain around 70% of the body's entire blood volume. They contain a large volume even when their transmural pressure is near zero (venous capacitance). This reserve "unstressed" volume does not produce ongoing flow to the heart. According to Guyton's description of cardiocirculatory function, only the stressed volume within the venous system generates the venous return, which is determined by the difference between the mean systemic filling pressure (the intravascular pressure at cardiac arrest) and right atrial pressure against the resistance to venous flow (Fig. 29.1). The mean systemic filling pressure may increase because of augmented blood volume or the transfer of venous blood from the unstressed to the stressed volume, due to venoconstriction through adrenergic stimulation. In contrast, a reduced mean systemic filling pressure, whether absolute (hypovolemia) or relative (transfer of blood from the stressed to the

unstressed volume due to increased venous compliance), always causes a reduced venous return.

As blood volume decreases, a critical balance may be suddenly disturbed through an increase of intrathoracic pressure often due to mechanical ventilation. Indeed, in clinical practice a compensated hypovolemia is promptly unmasked by severe hypotension just after the institution of positive pressure mechanical ventilation with or without positive end-expiratory pressure.

29.2 Is the Blood Volume Adequate?

Inadequate cardiovascular filling is very common in emergency department and ICU patients. Obvious causes of hypovolemia include external or internal bleeding and loss of circulating body fluid due to insufficient oral or parenteral intake, excessive diuresis, diarrhea, or the redistribution of fluid between the intravascular and extravascular compartments. Inappropriate or excessive diuretic therapy is common in both medical and surgical wards for treating oliguria. The traumatic or surgical insult produces hemorrhages and capillary leakage of fluid and albumin from the vascular space. The clinical picture of severe sepsis and septic shock includes either absolute hypovolemia, due to third space losses, or relative hypovolemia, caused by peripheral redistribution of blood volume. Whether hypovolemia is

A. Sarti (✉)
Department of Anesthesia and Intensive Care,
Santa Maria Annunziata Hospital, Florence, Italy

S. Cipani · M. Barattini
Department of Anesthesia and Intensive Care,
Santa Maria Nuova Hospital, Florence, Italy
e-mail: simone.cipani@uslcentro.toscana.it;
massimo.barattini@uslcentro.toscana.it

Fig. 29.1 Stress volume and unstressed volume. Only the stress volume generates the venous return (VR). See the text for details. Smfp means systemic filling pressure, RAP right atrial pressure, and R resistance to flow
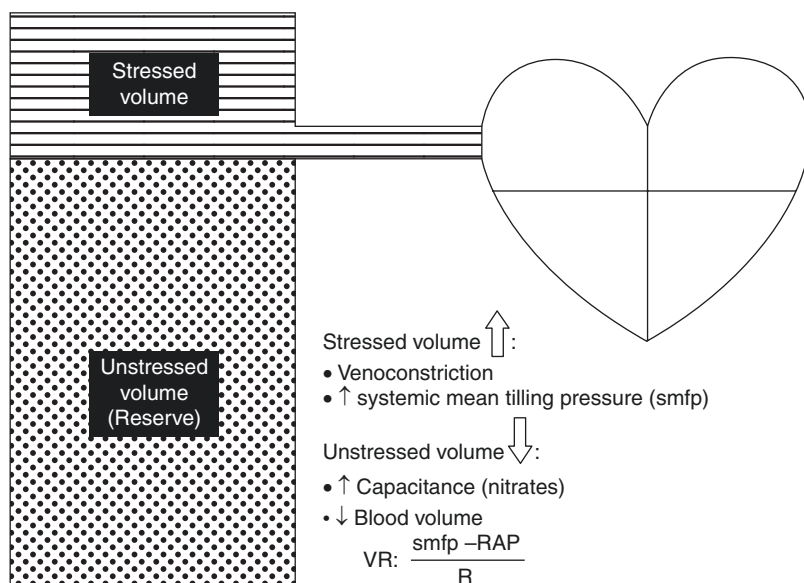
absolute or relative, the heart is not properly filled, and cardiac output decreases. Initially, arterial pressure may not decrease if systemic vascular resistance increases accordingly. However, abrupt hypotension may ensue after an intravenous sedative drug.

Systematic adequate volume expansion in the first few hours of circulatory failure due to severe sepsis and septic shock decreases mortality. Also, uncorrected hypovolemia leads to improper infusion of vasopressors such as norepinephrine, with subsequent organ hypoperfusion and aggravating tissue ischemia.

29.3 Should I Provide a Fluid Bolus?

On the admission of the patient to the emergency department or ICU, the clinical signs of manifest hypovolemia, such as tachycardia, hypotension, oliguria, altered mental status, and mottled or pale skin with augmented capillary refill time, may immediately suggest a positive response to a bolus of fluid infusion. In this case there is initially no need for more sophisticated information. However, for hospitalized patients who experience hemodynamic instability, a favorable response to fluid resuscitation should not be always expected. Indeed, excessive volume expansion may cause interstitial edema in many organs, including the lungs, and is clearly associated with increased morbidity and mortality.

Traditionally, fluid responsiveness has been assessed by graded volume loading, but this may easily lead to fluid overload. Indeed, in septic patients, positive cumulative fluid balance has been shown to be an independent risk factor for death. The end point of fluid resuscitation may often be unclear and hence arbitrary. Occasionally, the futility or worse, the harmfulness of ineffective volume expansion is realized only after multiple fluid boluses have been given.

Therefore, it is not surprising that rapid volume expansion as a first-line therapy is a crucial decision and has a vital key role in the cardiovascular resuscitation of seriously ill patients. Hypotension and signs of tissue hypoperfusion, such as central venous desaturation, increased levels of lactates, augmentation of the venous–arterial carbon dioxide gradient, and oliguria, elicit a possible role for volume expansion. It has been reported that only around 50% of critically ill patients will respond to a volume bolus with significant increase, such as 10–15%, in stroke

volume and cardiac output (fluid responsiveness). The response depends on where the heart of the patient with hemodynamic instability and hypoperfusion is located on the Frank–Starling curve and myocardial contractility reserve (Fig. 29.2). On the steep portion of the curve, the heart will respond to a fluid bolus with an increase of end-diastolic volume, stroke volume, and cardiac output (preload reserve). In contrast, on the flat part of the curve, the heart does not respond with a significantly increased stroke volume (Fig. 29.2) but responds only with fluid overload and rising filling pressure (preload unresponsiveness). For the single patient, the Frank–Starling relationship between preload and stroke volume is not stable but changes with its position with a different ventricular contractility, which can be extremely variable and not easily measured in clinical practice. At a determined preload, many other factors may influence the Frank–Starling curve, such as aortic impedance and the complex effects of mechanical positive pressure ventilation.

Thus, whether to provide a fluid bolus is a critical decision of the utmost importance, particularly in the current practice of intensive care characterized by aging patients with preexistent chronic cardiovascular dysfunction. These patients have a greater chance of being fluid-unresponsive. So the only way to avoid useless or even harmful fluid load is simply to challenge the Frank–Starling relationship to establish the possible positive response to a fluid bolus before giving it, that is, predicting fluid responsiveness. Fluid must be considered as any other drug. Monitoring only arterial blood pressure is not enough, and cardiac output should be monitored as well for any hemodynamically unstable patient. Echocardiography, with all the vital information on cardiovascular functional anatomy it provides, including preload and pump function, has become the best tool to assess volume status, predict fluid responsiveness, and guide fluid therapy in the emergency and ICU setting.

29.4 Hypovolemia

Central venous pressure (CVP) and pulmonary artery occlusion pressure (PAOP) are both generally decreased during manifest hypovolemia, even if previous right ventricular (RV) or left ventricular (LV) dysfunction or valve disease may well alter these measures. A low CVP, such as below 4 cmH$_2$O, may suggest emptiness of the central veins, but no reliable information can be obtained above this pressure. Doppler interrogations of the regurgitation jets of the atrioventricular valves can be used to estimate CVP and PAOP without central venous or pulmonary artery catheters, but their effectiveness as a guide to fluid therapy is insubstantial. Thus, static cardiac filling pressures are poor predictors of preload, and neither CVP nor PAOP can be used to predict fluid responsiveness in patients who breathe spontaneously or in patients on positive pressure ventilation. End-diastolic dimensions are considered better indicators of cardiac preload than filling pressure, but nonetheless they cannot accurately predict fluid responsiveness because the chamber dimensions may be reduced or dilated as a result of many previous or concomitant alterations. It must always be remembered that an assessment of preload is not an assessment of fluid responsiveness, particularly in critically ill patients.
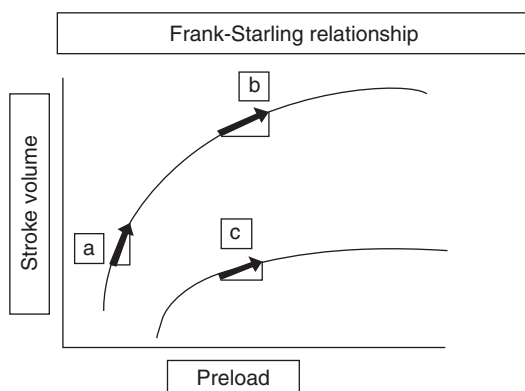
Fig. 29.2 Frank–Starling relationship. Two curves reflecting different heart performance conditions. (*a*) Fluid responsive (a small increase in preload induces a significant increase of stroke volume). (*b*, *c*) Fluid unresponsive (a big increase of preload does not induce a significant increase of stroke volume)

If previous biventricular function is preserved, the echocardiographic appearance of a full-blown picture of hypovolemia is consistent with a small hyperkinetic fast-beating heart. Both end-diastolic and end-systolic dimensions of all cardiac chambers are decreased, with LV cavity end-systolic obliteration. In spontaneously breathing patients, a small inferior vena cava (IVC; transthoracic echocardiography, TTE) or superior vena cava (SVC; transesophageal echocardiography, TEE) is easily visualized with complete inspiratory collapse. In mechanically ventilated patients, small dimensions of the venae cavae with evident respiratory changes are seen at end expiration. All echocardiographic views can show this hypovolemic small-chamber-low-flow imaging:

- No distance is seen during diastole between the septum and the anterior leaflet of the mitral valve in the parasternal long-axis view (TTE) because of the reduced ventricular diameter, as well as the reduced width of the aortic cusps opening in systole with a slowing of aortic closure in diastole.
- In the parasternal short-axis view (TTE) or the transgastric short-axis view (TEE), the section of the left ventricle at the level of the papillary muscles shows reduced LV end-diastolic area (below 5.5 cm^2/m^2) and end-systolic area with a complete, or almost complete, systolic obliteration of the cavity (kissing ventricle) (Fig. 29.3).
- Reduction of all end-diastolic and end-systolic volumes in the apical four-chamber view (TTE) (Fig. 29.4) and mid-esophageal four-chamber view at 0° (TEE) with reduced transmitral flow (E wave).
- Reduced velocity–time integral (VTI) in the RV outflow tract and pulmonary trunk (parasternal short-axis view, TTE, and mid-esophageal ascending aorta view, TEE) and in the LV outflow tract (LVOT) (apical five-chamber or three-chamber view, TTE, and deep transgastric view, TEE) owing to reduced stroke volume.
- Small IVC (subcostal TTE, transgastric 60° off-axis TEE) less than 12 mm in spontane-
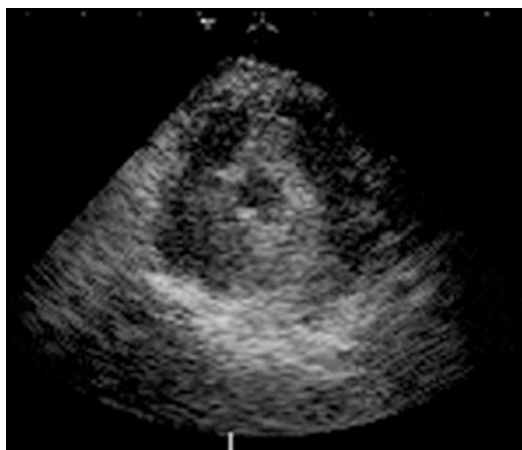
Fig. 29.3 Parasternal short-axis view, papillary muscle level, and transthoracic echocardiography (TTE). Obliteration of the left ventricular (RV) cavity at end-systole (kissing ventricle)
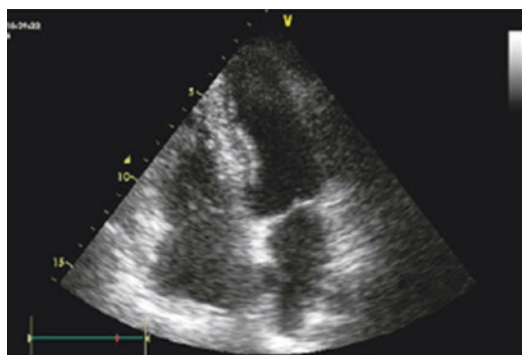
Fig. 29.4 Apical four-chamber view TTE. Reduced volumes of all the cardiac chambers in hypovolemia

ously breathing patients and less than 15 mm in patients with mechanical ventilation and small SVC (mid-esophageal bicaval view, TEE) together with large respiratory changes.

29.5 Passive Leg Raising

Emergency rescuers have raised the lower limbs for years in order to increase heart filling and blood arterial pressure. Passive leg raising (PLR) has been proposed as a preload-modifying maneuver without any potentially harmful fluid infusion. ICU patients are normally kept in a
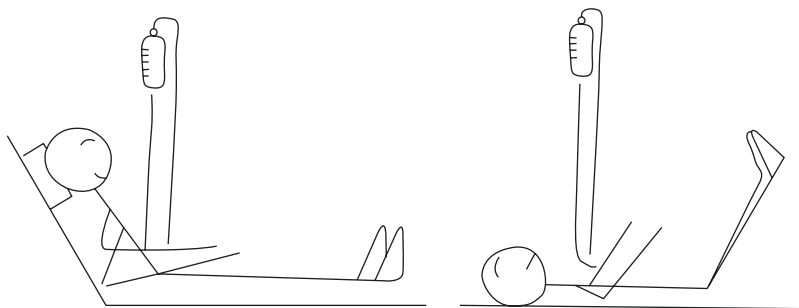
Fig. 29.5 Passive leg raising maneuver. *Left*, the normal position of the ICU patient. *Right*, legs lifted to around 45° and trunk lowered to the horizontal plane. The blood is transferred from the lower part of the body and the abdomen to the thoracic central circulatory compartment (autotransfusion)

semirecumbent position with the trunk lifted to 45° and the legs in the horizontal plane. Lifting the legs to around 45°, while at the same time lowering the trunk to the horizontal plane, induces a gravitational transfer of blood from the lower part of the body and the abdomen to the thoracic central circulatory compartment (Fig. 29.5). LV filling, stroke volume, and then cardiac output will increase if the right ventricle and then the left ventricle are fluid-responsive. This autotransfusion, estimated to be between 300 and 500 ml, is immediately and fully reversed when the trunk is lifted and the legs are laid down. This technique of predicting fluid responsiveness can also be used in spontaneously breathing patients and in the presence of arrhythmias. This is particularly important, since dynamic indices based on oscillation of preload (see below) are not reliable in patients who breathe spontaneously or with atrial fibrillation. An increase of stroke volume greater than 15% after PLR can predict a positive response to a fluid bolus with good sensitivity and specificity. Since the response to PLR is transient, the possible change of stroke volume (or only VTI since the LVOT cross-sectional area does not change acutely) must been assessed using TTE or TEE just after the maneuver and continuing for at least 1 min. Sometimes the PLR maneuver may stress or cause pain to the patient, especially after surgery or trauma. This test may be rather cumbersome and is seldom applied in the clinical practice of some intensivists.

29.6 Fluid Challenge

The response to a quick infusion of a fluid bolus is the easiest approach to check the fluid responsiveness. Usually, 3–4 ml/Kg of crystalloid is infused within a few minutes while measuring any change in cardiac output. An increase more than 10–15% defines the patient as a fluid responder. The fluid bolus can be repeated as long as a sufficient increase in blood flow is observed, ready to stop the infusion if cardiac output does not change to avoid fluid overload. To reduce the risk of overload even more a mini-fluid challenge has been proposed. 100 ml of fluid is infused within 1 min while recording any change of blood flow (VTI) at the left ventricle outflow tract.

29.7 Heart–Lung Interactions

29.7.1 Pulse Pressure, Stroke Volume, and VTI Variation

In spontaneously breathing patients, the systolic arterial pressure falls slightly during inspiration. This is due to increased venous return and ventricular interdependence. A greater fall (more than 10 mmHg) is observed in many clinical conditions, such as hypovolemia, cardiac tamponade, acute severe asthma, massive pleural effusion, anaphylactic shock, and pulmonary embolization (pulsus paradoxus). Mechanical

ventilation with or without positive end-expiratory pressure decreases venous return owing to an increase in intrathoracic pressure if the chest is not opened. During mechanical ventilation, cyclic changes are observed in pulse pressure (reversed pulsus paradoxus). Small changes in arterial pulse pressure during positive pressure ventilation are also frequently caused by ventricular interdependence. In this case, because of diminished LV afterload and enhanced LV pulmonary venous flow (squeezing of blood out of the lungs), the LV systolic ejection transiently increases during the ventilator-derived inspiration relative to the level observed during the expiratory pause (Δup). This Δup effect has been described in congestive heart failure, and it might actually suggest the need for volume reduction rather than expansion.

At the end of positive pressure inspiration, the LV stroke volume (and pulsed wave Doppler VTI at the LVOT, which directly reflects the stroke volume) decreases as a result of depressed RV preload and increased RV afterload and ejection due to increased intrathoracic pressure, which propagates to the left ventricle after a few heartbeats (Δdown) (Fig. 29.6). Disappearance or clear blunting of Δdown during mechanical ventilation is a marker of preload insensitivity (Fig. 29.7). Preload sensitivity and fluid respon-

siveness are thus associated with and are proportional to Δdown, which is linked to the heart operating in the steep portion of the Frank–Starling relationship. This has been demonstrated in both ventilated surgical and septic patients. The entire fluctuation (Δdown plus Δup) (Fig. 29.8) of stroke volume or pulse pressure (ΔPP, maximal–minimal systolic pressure) induced by mechanical breathing (inspiration and expiration) has been similarly validated. Respiratory variations of aortic flow are a robust index of fluid responsiveness in ventilated patients on condition that possible limitations are considered (see below).

29.7.2 Dynamic Arterial Elastance (Eadyn)

Eadyn is the ratio of arterial changes in pressure to changes in volume, thus pulse pressure variation/stroke volume variation (PPV/SVV). A value of Eadyn greater than 0.89 may predict an increase of mean arterial pressure after a fluid bolus with a good sensibility and specificity. Eadyn assessment may be used to distinguish preload-responsive individuals in whom arterial pressure will increase with fluids. As the preload-responder patient shows to be nonpressure-
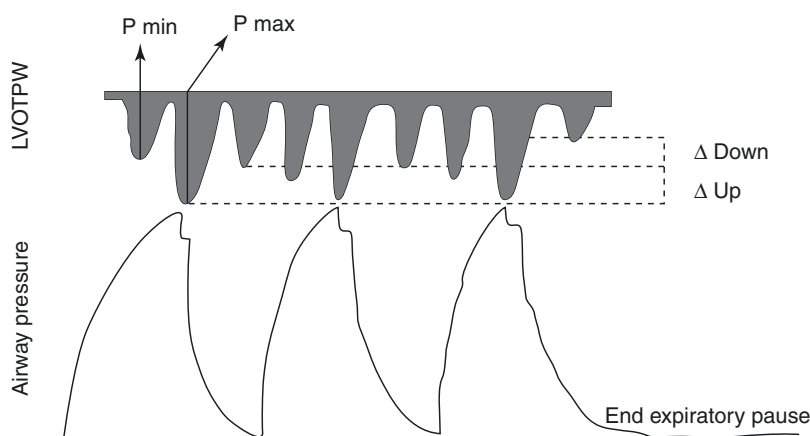
Fig. 29.6 Pulsed wave Doppler velocity–time integral (VTI) at the LV outflow tract recorded continuously during mechanical ventilation. Changes in VTI (below the baseline because the flow runs away from the probe) directly reflect changes in LV stroke volume. Note Δdown and Δup. Δdown reflects fluid responsiveness. $P = \mathrm{VTI_{peak}}$. See the text for details and limitations

Fig. 29.7 Apical five-chamber view, TTE. Pulsed wave Doppler VTI at the LV outflow tract recorded during a mechanical breath. No fluctuation of the VTI (preload insensitivity)
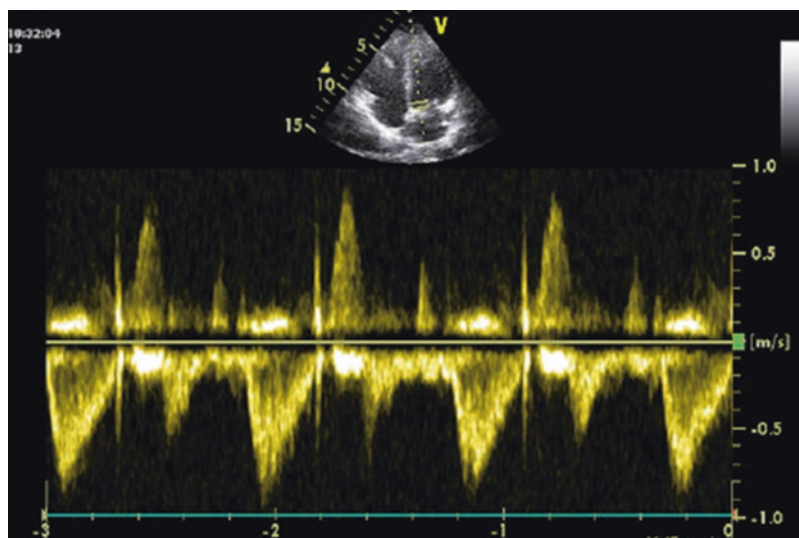
Fig. 29.8 Apical five-chamber view, TTE. Wide VTI fluctuation during a mechanical breath in a clearly fluid-responsive patient. X = VTI 19.1 cm; Y = VTI 29 cm. ΔVTI = 100 × $(\text{VTI}_{max} - \text{VTI}_{min})/(\text{VTI}_{max} + \text{VTI}_{min}/2)$ = 43%. See the text for further details
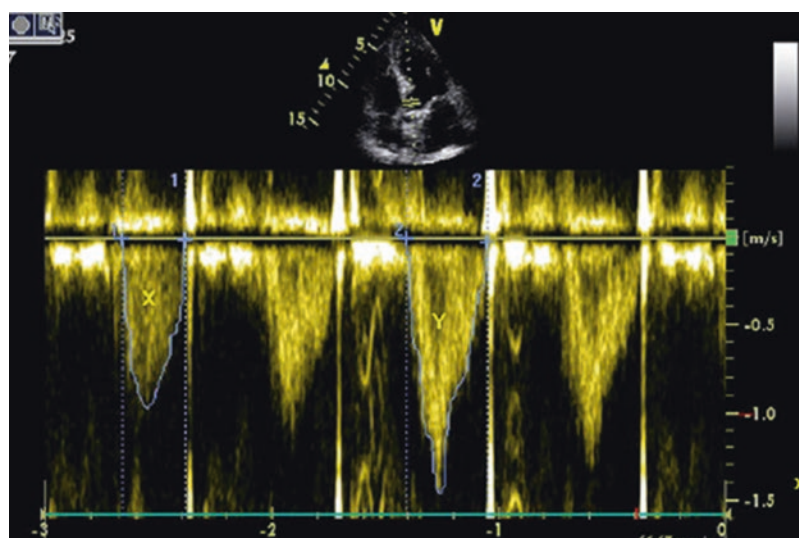
responder (low Eadyn), norepinephrine should be considered first or concomitant with fluid infusion.

29.7.3 End-Expiratory Occlusion Test

Interrupting mechanical ventilation for 15 s at end expiration prevents the cyclic change to central hemodynamics, thus acting as a fluid challenge. More than 5% increase of cardiac index may predict fluid responsiveness with a very good sensitivity and specificity even in ARDS patients. Since the ventilation interruption encompasses many cardiac beats, this test is suitable even for patients with arrhythmias.

29.7.4 Vena Cava Variation

The cyclic effects of positive pressure ventilation are also evident in the geometry of the

venae cavae with increased diameter during inspiration and decreased diameter in the expiratory phase (Fig. 29.9). Ventilator-derived positive intrathoracic pressure will dilate more an incompletely filled IVC because of the transmission of increased pleural pressure and increased transmural pressure, since intra-abdominal pressure only increases partially. It is intuitive that the transmural pressure change of the venae cave will more readily translate into cross-sectional size variations during mechanical ventilation when imposed on a partially empty vessel (hypovolemia). Studies have demonstrated that the amplitude of phasic changes in the diameter of the venae cavae is predictive of an increase of cardiac output after a fluid bolus has been given. The SVC is not influenced by intra-abdominal pressure, and it is only subjected to pleural pressure, directly reflecting the interaction between central volume and intrathoracic pressure. Thus, the wider SVC variation during mechanical ventilation correlates particularly well with fluid responsiveness and is considered more reliable.

Fig. 29.9 Subcostal TTE for the inferior vena cava. Inferior vena cava diameter variation during a mechanical breath. (**a**) Inspiration and (**b**) expiration
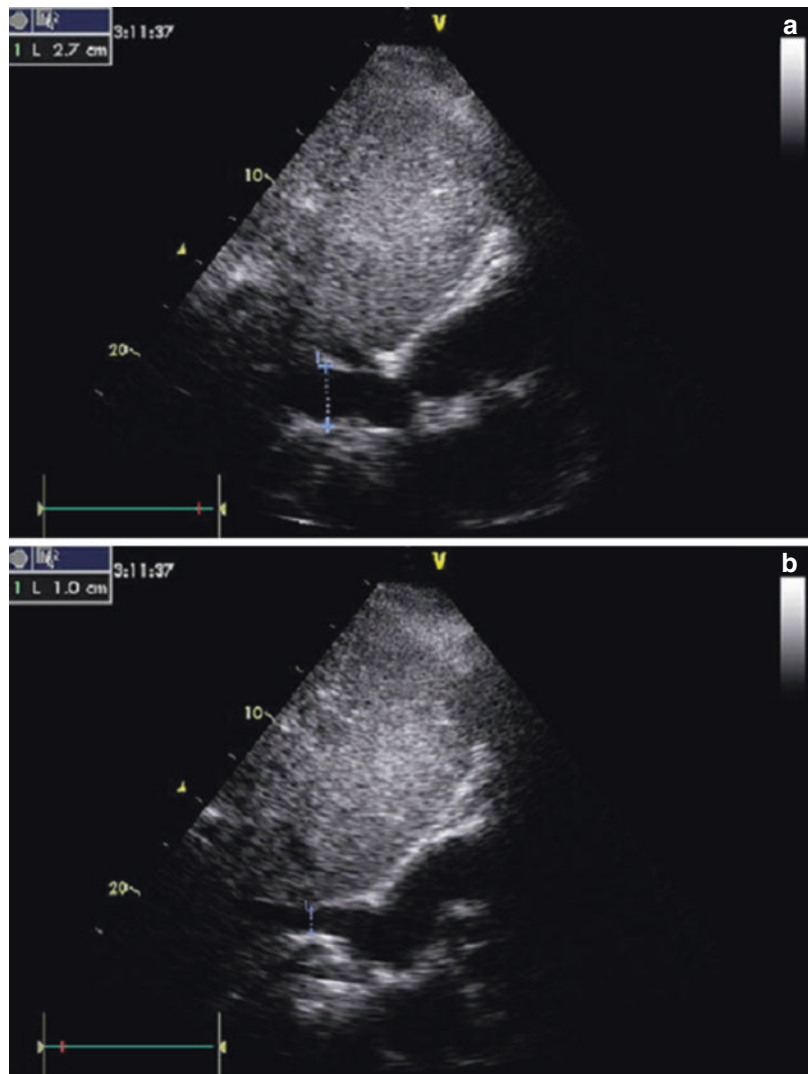
29.8 Screening for the Tolerance to Volume Load and Assessment of the Effect of Fluid Boluses

Low tolerance to fluid load and relative fluid unresponsiveness are expected in patients who present with signs of systemic or pulmonary venous congestion and left and right systolic or diastolic ventricular dysfunction.

An enlarged right ventricle with septal dyskinesia or reduced TAPSE is consistent with right-sided heart dysfunction. The echocardiographic parameters of LV diastolic dysfunction and elevated LV filling pressure are as follows:

- Left atrium enlargement
- *E/A* ratio of the Doppler transmitral flow greater than 1.5
- Deceleration time less than 150 m/s
- *E/E′* (or *E/E*$_a$) ratio greater than 15 at the lateral mitral annulus
- S < D wave of pulsed wave Doppler pulmonary vein flow
- Reversed pulmonary vein flow time (*A*$_r$) greater than atrial systole time (*A*) of the mitral forward flow

These parameters of RV and LV function, as well as the filling patterns, must be assessed before fluid expansion and again during volume loading, after each bolus has been given, to detect early signs of dysfunction and increasing filling pressure.

29.9 Limitations of Fluid Responsiveness Indices Derived from Heart–Lung Interaction

1. Functional hemodynamic parameters can be used only in patients who are on fully and stable mechanical ventilation. No spontaneous respiratory effort should be observed. A tidal volume of 8 ml/kg was shown to be necessary to produce the indices of fluid responsiveness. Patients with acute lung injury or acute respiratory distress syndrome are normally ventilated with lower tidal volumes, but they also exhibit markedly decreased lung compliance. Thus, a lower tidal volume should still generate a large variation of airway and intrathoracic pressure.

2. Respiratory variations in LV stroke volume can be influenced by increasing respiratory rate, whereas SVC variations seem to be unaffected. This may suggest that right and left indices of preload variations can be dissociated. It is important to check also the heart rate. A ratio between heart rate and respiratory rate less than 3.6 is required for a reliable assessment.

3. In RV failure, the inspiratory increase of RV impedance is a major determinant of stroke volume variations. These patients should not be considered fluid-responsive since volume expansion may simply not reach the left ventricle and may only increase RV filling pressure. This is seen particularly in patients on mechanical ventilation who show severe RV dysfunction.

4. Arrhythmias can certainly produce stroke volume variations unrelated to fluid responsiveness. Thus, a regular and stable sinus rhythm is an essential requirement.

5. Acute changes of aortic impedance might alter stroke volume variations. Some animal studies have shown that norepinephrine infusion might reduce the value of dynamic changes, but further study is needed to clear up this point.

6. An increase in intra-abdominal pressure might alter the cyclic variation of the IVC. Theoretically, the SVC seems to be less affected.

If all these limitations cannot be ruled out, the only way to predict fluid responsiveness is by observing the effect of the PLR maneuver on stroke volume.

29.10 Indices of Fluid Responsiveness

29.10.1 Vena Cava Collapsibility

The vena cava collapsibility index (ΔVC) is the percentage variation of the cava diameter during inspiration versus expiration (IVC, subcostal TTE, and SVC, mid-esophageal bicaval TEE):

- $\Delta IVC = 100 \times (IVC_{insp} - IVC_{exp})/IVC_{insp}$ (Fig. 29.9). A variation greater than 18% predicts fluid responsiveness.
- $\Delta SVC = 100 \times (SVC_{insp} - SVC_{exp})/SVC_{insp}$. In this case a variation greater than 36% is used as a predictor.

29.10.2 Stroke Volume Variations

Using pulsed wave Doppler interrogation (apical five-chamber or three-chamber view, TTE, and deep transgastric view at 0°, TEE) at the level of the LVOT (aortic annulus), one can detect the VTI of LV ejection. The product of VTI and LVOT cross-sectional area equals stroke volume.

This method is normally used to measure cardiac output (stroke volume times heart rate) through echocardiography. Considering that the area of the aortic annulus does not change acutely, it is only possible to measure VTI to detect changes in stroke volume. The variation of either the VTI or the peak velocity (P) of LV ejection (the highest level of the VTI curve) can be used to predict fluid responsiveness as follows:

- $\Delta VTI = 100 \times (VTI_{max} - VTI_{min})/(VTI_{max} + VTI_{min}/2)$;
- $\Delta P = 100 \times (P_{max} - P_{min})/(P_{max} + P_{min}/2)$.
- $\Delta VTI > 18\%$ (Fig. 29.8) and $\Delta P > 12\%$ are expressive of fluid responsiveness.

29.11 Final Remarks

The last consensus on circulatory shock and hemodynamic monitoring recommend not to use any ventricular filling pressure or cardiac chamber volume to guide fluid infusion. Apart from extreme conditions, a preliminary full ultrasound assessment of the heart, the lungs, and the great vessels is paramount to obtain a clear picture of
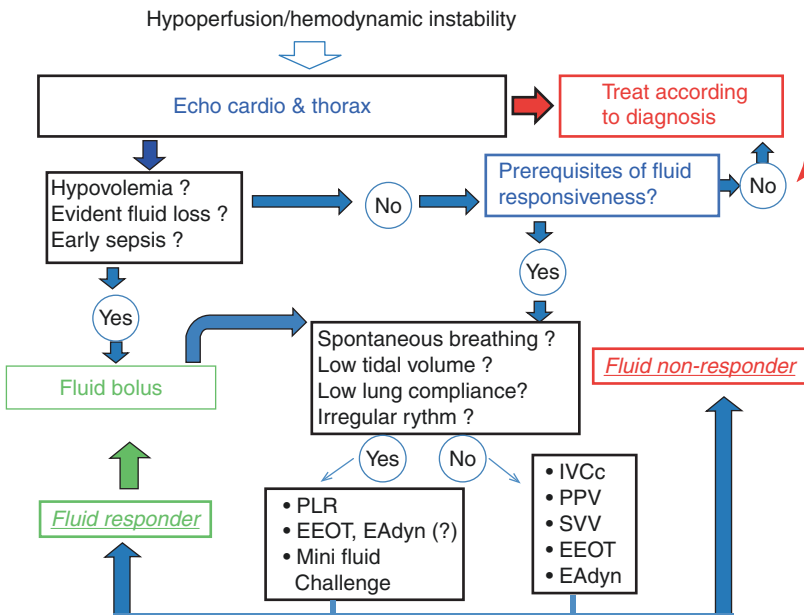
Fig. 29.10 Outline of the approach to hypoperfusion and hemodynamic instability using the dynamic indices of fluid responsiveness

global cardiovascular anatomy and function of any unstable patient before considering any drug or fluid. Hypotension does not necessarily mean the need of fluid infusion. The measure of respiratory variations of aortic blood flow is the most used parameter to predict fluid responsiveness for patient on stable mechanical ventilation. However, the limitations of any technique must always be kept in mind, and different parameters should be considered together to predict the response to a fluid challenge. An outline of the approach to hypoperfusion and hemodynamic instability is shown in Fig. 29.10. Hypotension does not mean always hypoperfusion. The final assessment is the organ and tissue perfusion and function.

Further Reading

Carsetti A, Cecconi M, Rhodes A. Fluid bolus therapy: monitoring and predicting fluid responsiveness. Curr Opin Crit Care. 2015;21:388–94.

Cecconi M, De Backer D, Antonelli M, et al. Consensus on circulatory shock and hemodynamic monitoring. Task Force of the European Society of Intensive Care Medicine. Intensive Care Med. 2014;40:1795–815.

Charron C, Caille V, Jardin F, et al. Echocardiographic measurement of fluid responsiveness. Curr Opin Crit Care. 2006;12:249–54.

De Backer D, Taccone FS, Holsten R, et al. Influence of respiratory rate on stroke volume variation in mechanically ventilated patients. Anesthesiology. 2009;110:1092–7.

Fehil F, Broccard AF. Interactions between respiration and systemic hemodynamics. Part I: basic concepts. Intensive Care Med. 2009;35:45–54.

Feihl F, Broccard AF. Interactions between respiration and systemic hemodynamics. Part II: practical implications in critical care. Intensive Care Med. 2009;35:198–205.

Gerstle J, Shahul S, Mahmood F. Echocardiographically derived parameters of fluid responsiveness. Int Anesthesiol Clin. 2010;48(1):37–44.

Pinsky MR. Heart-lung interactions. Curr Opin Crit Care. 2007;13:528–31.

Teboul JL, Monnet X. Prediction of volume responsiveness in critically ill patients with spontaneous breathing activity. Curr Opin Crit Care. 2008;14:334–9.

Vignon P. Ventricular diastolic abnormalities in the critically ill. Curr Opin Crit Care. 2013;19:242–9.

ARDS, Mechanical Ventilation, and Weaning

30

Federica Marini, Simone Cipani, Armando Sarti, and Carla Farnesi

30.1 Introduction

Acute respiratory distress syndrome (ARDS) is an acute diffuse, inflammatory lung injury, leading to increased pulmonary vascular permeability, increased lung weight, and loss of aerated lung tissue with hypoxemia and bilateral radiographic opacities, associated with increased venous admixture, increased physiological dead space, and decreased lung compliance following a trigger insult.

Nowadays, approximately 5% of hospitalized, mechanically ventilated patients meet the diagnostic criteria for ARDS. As for the severity of the clinical presentation, it has been shown how only 25% of patients have a mild form of ARDS, while the remaining 75% display a moderate or severe form.

The European Society of Intensive Care Medicine convened an international expert panel in 2011 in Berlin, to develop a new definition of the syndrome, which led to the so-called Berlin definition of ARDS. According to this new definition, ARDS is an acute form of diffuse lung injury occurring in patients with a predisposing risk factor, meeting the following criteria:

1. Onset within 1 week of a known clinical insult or new/worsening respiratory symptoms
2. Presence of bilateral opacities on chest X-ray, not fully explained by effusion, lobar/lung collapse, or nodules
3. Diagnosis of respiratory failure not fully explained by cardiac failure or fluid overload
4. Presence of hypoxemia, as defined by a specific threshold of the PaO2/FiO2 ratio measured with a minimum requirement of positive end-expiratory pressure (PEEP) $\geq$5 cm H2O, thus identifying three categories of severity:
   – Mild (200 millimeters of mercury (mm) Hg < PaO2/FiO2 $\leq$ 300 mm Hg)
   – Moderate (100 mm Hg < PaO2/FiO2 $\leq$ 200 mm Hg)
   – Severe (PaO2/FiO2 $\leq$ 100 mm Hg) (Table 30.1)

Lung computerized tomography (CT) is the gold standard for evaluating lung morphology and for assessing the effects of different therapy on lung reaeration. Typical morphological patterns are consolidate regions (homogeneous areas of increased density without vessel and bronchi), ground-glass areas (with augmented density but still recognizable vessel), and normally aerated regions.

F. Marini (✉) · S. Cipani
Anesthesia and Intensive Care Department, Santa Maria Nuova Hospital, Azienda USL Toscana Centro, Florence, Italy
e-mail: federica.marini@uslcentro.toscana.it; simone.cipani@uslcentro.toscana.it

A. Sarti · C. Farnesi
Anesthesia and Intensive Care Department, Azienda USL Toscana Centro, Florence, Italy

Table 30.1 Comparison between AECC definition (1994) and the Berlin definition of acute respiratory distress syndrome (2012)

Characteristic	AECC Definition 1994 [2]	Berlin Definition 2012 [3]
Timing	Acute, without any specification	Maximum within a week after a trigger insult
Imaging	Chest X-ray with bilateral infiltrates	Chest X-ray or CT scan with bilateral infiltrates, not fully explained by effusion, lung collapse or nodules
Non-cardiogenic source of edema	Confirmation of non-elevated left atrial pressure	Respiratory failure not completely explained by excessive volume loading or cardiac failure
Classification	Based on PaO_2/FiO_2	Based on PaO_2/FiO_2 calculated with PEEP ≥ 5 cmH$_2$O
	Acute lung injury: ≤ 300	Mild: 201–300
	ARDS: ≤ 200	Moderate: 101–200
		Severe: ≤ 100
Predisposing condition	Not specified	If none identified, then need to rule out cardiogenic edema with additional data

From "Current Concepts of ARDS: A Narrative Review" Umbrello M. et al.

However, performing a lung CT scan generally requires transportation of the patient to the department of radiology, the presence of trained physicians, and sophisticated cardiorespiratory monitoring. Moreover, radiation exposure limits its repeatability. Ultrasound (US) is increasingly used in the management of the critically ill patient as a noninvasive diagnostic and monitoring tool.

Mechanical ventilation for acute respiratory failure is a routine aspect of patient management in ICU. Ultrasound can assess PEEP-induced changes in lung aeration and thus has the potential to guide recruitment maneuvers. Furthermore, combining the lung with bedside cardiac US can be helpful in differentiating ARDS from cardiogenic pulmonary edema and in assessing right ventricular function.

Lung US has intrinsic patient-dependent limitations, such as obesity or the presence of subcutaneous emphysema which makes the examination difficult.

There is also operator-dependent limitation, even if the learning curve in transthoracic lung US is rather short for residents (<3 wk). Pulmonary processes can be visualized when they come up to the pleura and are accessible via a sound window without subcutaneous emphysema or pneumothorax. Purely central processes cannot be sonographically visualized and therefore cannot be ruled out with this technique.

30.2 Introduction

Chest US in patients with ARDS has been proposed to assess initial abnormalities of lung morphology, monitor the effects of the therapy, and optimize PEEP.

30.3 Pneumonia

The sonographic findings of pneumonia are as follows:

1. Liver-like in the early stage. The echo texture of the consolidated lung is similar to that of the liver.
2. Air bronchogram. Viral or fungal pneumonias are quite often more poorly ventilated and reveal less marked air bronchograms.
3. Air trapping that could be focal or diffuse. Severe airflow obstruction increases airways resistance and causes intrinsic PEEP.
4. Fluid bronchogram is characterized by anechoic/hypoechoic branched tubular structures in the course of the bronchial tree. A persistent fluid bronchogram arouses suspicion of poststenotic pneumonitis and requires bronchoscopic investigation.
5. Blurred, irregular, and serrated margin of a consolidated area is characteristic of pneumonia.
6. Reverberation echos in the margin of the consolidation areas.

7. Hypoechoic abscess formation. Bacterial pneumonias tend to fuse and form abscesses: round or oval and largely anechoic foci. Depending on the formation of a capsule, the margin is smooth and echodense.

30.4   ARDS

In patient with ARDS, a given ultrasound pattern corresponds to a given degree of lung aeration. Four conditions are possible as a progression of consolidation:

- Normal: presence of artifactual horizontal A lines beyond the pleural line.
- Interstitial syndrome: presence of multiple vertical B lines (comet tails) with well-defined spacing corresponds to moderate decrease in lung aeration (regularly spaced B lines 7 mm apart) or to disseminated foci of pneumonia (irregularly spaced B lines).
- Alveolar–interstitial syndrome: presence of coalescent B lines less than 3 mm apart corresponds to more severe decrease in lung aeration resulting from partial filling of alveolar space by edema or confluent bronchopneumonia.
- Alveolar consolidation: presence of lung consolidation characterized by an inspiratory reinforcement – dynamic bronchograms – corresponds to complete loss of lung aeration with persisting aeration of distal bronchioles. The dimension of consolidation does not vary with respiratory movements.

In patients with focal loss of lung aeration, any increase in intrathoracic pressure simultaneously induces hyperinflation of normally aerated lung regions and possible recruitment of non-aerated parts of the lung.

Patients with ARDS can be classified according to the initial distribution of aeration loss:

- Focal loss of aeration: the aeration loss predominates in dependent lung regions.
- Diffuse loss of lung aeration: aeration loss is equally distributed between all lung regions.

The improvement in gas exchange with the use of artificial ventilator techniques is probably related to the number of recruitable alveoli that initially were not involved in gas exchange because of edema or atelectasis. Alveoli that are involved in a consolidation process, such as pneumonia, are less amenable to recruitment.

Heterogeneous distribution of aeration is easily evidenced by lung US: normal pattern in upper anterior and lateral lung regions and consolidation or B lines in lower posterior and lateral ones (dependent lung regions in supine position). Ventilation settings should be the result of a compromise between alveolar recruitment and lung hyperinflation.

The presence of a bilateral B-pattern does not permit a differentiation between ARDS and cardiogenic pulmonary edema. Indeed, in ARDS, more commonly than in cardiogenic pulmonary edema, a nonhomogeneous distribution of B pattern, C (consolidative) pattern, and pleural line abnormalities is observed (Table 30.2).

Table 30.2 Comparison between ultrasonographic findings in ARDS and cardiogenic pulmonary edema

Condition	Thoracic Ultrasound	Cardiac Ultrasound
ARDS	Bilateral B pattern	No change in ventricular function vs. previous examination
	Non-uniform distribution	
	Pleural line abnormalities	No inferior vena cava dilation (diameter <23 mm)
	Reduced in lung sliding	E/e′ ≤ 8
	C pattern	–
Cardiogenic Pulmonary Edema	Bilateral B pattern	New or worsening left ventricular disfunction
	Uniform distribution	Inferior vena cava dilation (≥23 mm)
	Pleural effusion	E/e′ ≥ 14
	Left-sided predominance	–

E/e′ represents the ratio between the peak early diastolic mitral velocity between the tips of mitral leaflets (E wave) and the spectral tissue Doppler-derived peak early diastolic velocity at mitral annulus (E′ wave), thus yielding an accurate estimate of lesft ventricular diastolic function.

From *"Current Concepts of ARDS: A Narrative Review"* Umbrello M. et al. Int. J. Mol. Sci. 2017
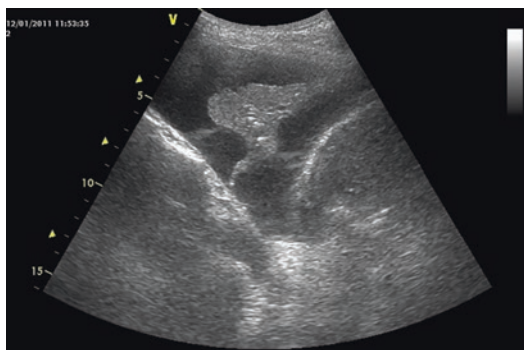
Fig. 30.1 Compression atelectasis caused by voluminous pleural effusion, with floating of the lung

Table 30.3 Ultrasound lung reaeration score.

1 point	3 points	5 points	−5 points	−3 points	−1 point
B1→ N	B2→N	C→N	N→C	N→B2	N→B1
B2→B1	C→B1			B1→C	B1→B2
C→B2					B2→C

B1: Ultrasound lung comets with well-defined and irregular spacing and moderate loss of lung aeration. B2: Abutting ultrasound lung comets and severe loss of lung aeration. C: Alveolar consolidation. N: Normal pattern. (Modified from Bouhemad B. et al.). *First, ultrasound lung aeration was measured in each of the examined lung regions before and after any treatment, and then the score was calculated as the sum of each score characterizing each region of interest. Quantification of reaeration* Quantification of loss of aeration

30.5 Lung Atelectases

Lung atelectases are characterized by partial or complete absence of ventilation:

- The compression atelectasis is caused by voluminous pleural effusion, with floating of the lung. The parenchyma could be partially reventilated during inspiration and recruitment maneuvers and after effusion drainage. Doppler color sonography shows increased branch-like vessel visualization (Fig. 30.1).
- The obstructive atelectasis is marked by a largely homogeneous hypoechoic presentation of lung tissue in terms of hepatization. Effusion is absent or small. The image is similar to that of pneumonia but with significantly less air bronchograms.

30.6 The Ultrasound Lung Reaeration Score

Lung US is a promising tool for assessing PEEP-induced alveolar recruitment, lung re-expansion after pleural drainage, and recovery from ventilator-associated pneumonia. Lung recruitability is higher in patients with diffuse loss of aeration than in patients with focal loss of aeration.

In ARDS, lung consolidation predominates over alveolar interstitial syndrome. In the studies of Bouhemad B. et al., the reaeration score is defined by four stages of aeration, including normal aeration, decreased lung aeration (number and type of B lines), and consolidation.

It is calculated from the changes in the ultrasound pattern of each of the 8 or 12 regions of interest after any treatment or a defined period of therapy. A lung US score of aeration can be calculated as follows; for each given region of interest, points are allocated according to the worst ultrasound pattern observed (normal, 0; well-separated B lines, 1; coalescent B lines, 2; and consolidation, 3). A lung US score ranging between 0 and 36 was calculated as the sum of each region. This score is a global picture of lung aeration and can be regularly monitored. An increase in score indicates a decrease in aeration (Table 30.3).

The ultrasound reaeration score could be appropriate for measuring recruitment resulting from any treatment aimed at increasing lung aeration, such as PEEP, negative fluid balance, patient positioning, or recruitment maneuvers. The score has also been used to compare lung reaeration measured by bedside chest radiography, lung CT, and lung US in patients with ventilator-associated pneumonia treated by antibiotics.

30.7 Mechanical Ventilation

In patients with ARDS, a varying extent of lung recruitability was found, ranging from 0% to 70% of the total lung weight.

Reducing tidal volume during mechanical ventilation decreases mortality in patients with ARDS, but alveolar derecruitment may occur during low-tidal-volume ventilation.

However, selecting the right level of PEEP remains a difficult issue. Alveolar recruitment was defined as the volume of gas penetrating into poorly aerated and non-aerated lung areas after PEEP. In ARDS, the percentage of potentially recruitable lung is extremely variable and is strongly associated with the response to PEEP (Figs. 30.2 and 30.3).

In an ideal model with the inhomogeneous coexistence of areas of hyperinflation, normal inflation, collapse, and areas of consolidation, we have to select the necessary pressure that needs to be applied to the lung in order to overcome the superimposed pressure generated by the lung mass and by the chest wall and recruit the alveolar unit (to inflate the collapsed lung regions) and to maintain these regions open. The selection of the ideal level of PEEP is an issue hard to resolve: if PEEP is too low, some portion of recruitable tissue will collapse, whereas excessive PEEP generates dead space and tissue stretch.

To provide a bedside estimate of the percentage of potentially recruitable lung, it has been shown that at least two of the following three changes in respiratory variables could occur when PEEP was increased from 5 to 15 cm of water:

- An increase in the PaO_2/FiO_2
- A decrease in the $PaCO_2$
- An increase in the respiratory system compliance

Lung US was also compared, by Bouhemad B. et al., with pressure-volume (PV) curve for assessing PEEP that induced lung recruitment in ARDS patients. A highly statistically significant correlation was found between PEEP-induced lung recruitment measured by the PV curve method and the ultrasound reaeration score. The ultrasound reaeration score was accurate for detecting a significant increase in lung aeration associated with a significant increase in arterial oxygenation. Instead, it was less accurate for detecting smaller changes of lung aeration.

So, ultrasonography could be used at the bedside for measuring lung recruitment and is noninvasive and easily repeatable. The quasi-static PV curve method requires deep sedation and muscle paralysis, the patient's disconnection from the ventilator, and specific software on the ventilator to avoid a complex and time-consuming analysis of the data.

Distribution of transthoracic lung ultrasound aeration loss (lung consolidation and B lines) is predominant in the most dependant lung regions (posterior parts of lower lobes). PEEP-induced lung reaeration is predominantly made of the disappearance of B lines in the anterior and lateral
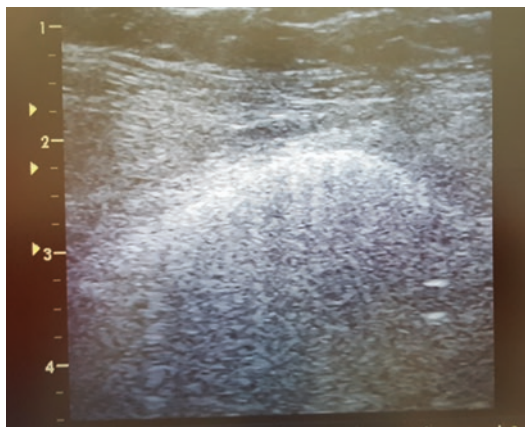
Fig. 30.2 Lung before recruitment maneuvers
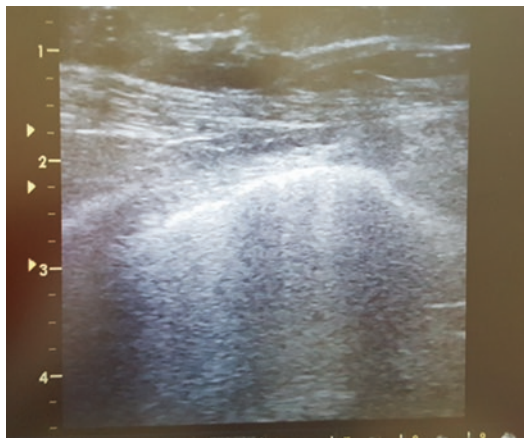
Fig. 30.3 Lung after recruitment maneuvers when PEEP was increased from 5 to 15 cm of water
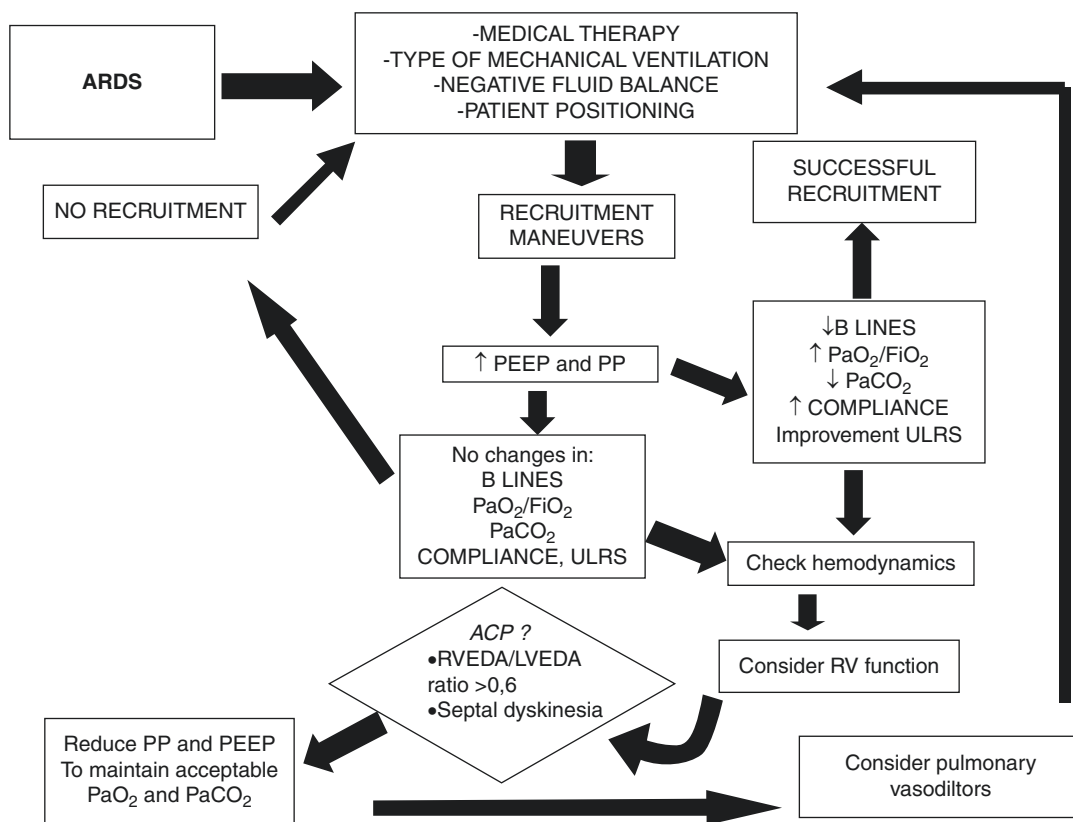
Fig. 30.4 ARDS echo-guided treatment. PP, plateau pressure. PEEP, pulmonary end-expiratory pressure. ULRS, ultrasound lung reaeration score. RVEDA, end- diastolic right ventricular area. LVEDA, end-diastolic left ventricular area. ACP, acute cor pulmonale

parts of the chest wall, whereas consolidation in posterior lung regions was marginally modified by PEEP.

However, lung US cannot detect PEEP-induced lung hyperinflation, so it should not be the sole method for PEEP titration. Ultrasound evidence of PEEP-induced recruitment is insufficient to consider the applied PEEP as optimum (Fig. 30.4).

30.8 Weaning

Once the underlying process necessitating mechanical ventilation has started to resolve, withdrawal of ventilation support should be considered. Many parameters such as neuromuscular state, muscle strength, ability to cooperate, car-diovascular stability, age, comorbidity, and prolonged mechanical ventilation must be taken into account.

Weaning failure is defined as the failure to pass a spontaneous breathing trial or the need of reintubation within 48 h following extubation.

Twenty-six to forty-two percent of critically ill patients with mechanical ventilation fail the first attempt of weaning. Causes of weaning failure are:

- Respiratory failure: increased ventilatory work, reduced compliance from cardiogenic or non-cardiogenic edema, etc.
- Cardiac failure: preexisting cardiac dysfunction, increased metabolic demand, and weaning-induced cardiac dysfunction

- Neuromuscular causes: depression of respiratory center and muscular failure, including the diaphragm
- ICU-acquired weakness
- Metabolic causes: malnutrition, hypoglycemia, electrolytes abnormalities, and anemia
- Neuropsychological causes: anxiety and delirium

Weaning from mechanical ventilatory support is a real cardiovascular stress test. Cardiac dysfunction is a leading cause of weaning failure. During weaning, the support provided by the ventilator is reduced, while the patient progressively takes over the work of breathing. Changes associated with the transition from mechanical ventilation to spontaneous ventilation overload the cardiorespiratory system with increase in venous return (preload), left ventricle (LV) afterload, O_2 consumption, and sympathoadrenergic tone and decrease LV compliance with predictable consequences on heart rate and blood pressure. Hypoxia and high $paCO_2$ may acutely increase pulmonary artery pressure leading to RV impairment and failure. In patients with preexisting heart disease (coronary artery disease and LV insufficiency), these physiological changes associated with spontaneous breathing can trigger LV failure and cardiac ischemia, which in turn may lead to respiratory failure and unsuccessful weaning. The cardiovascular changes are:

- Increases in mean systemic filling pressure due to venoconstriction and associated reduction in venous compliance.
- At the same time, intrathoracic pressure falls.
- Increases in LV afterload.
- Increases of right and left ventricular end-diastolic volumes by the venous return.

All these changes augment myocardial O_2 demand, and the heart must be able to cope with this situation. With diminished cardiovascular reserve, myocardial ischemia may appear with an increase of left ventricular filling pressure. In

a study, the authors demonstrated that weaning failure patients presented left atrium diameter, intraventricular septum thickness, posterior wall thickness, and LV diameter significantly larger than weaning-success patients. These parameters are predictive of a difficult weaning. In another TTE echocardiographic study, patients who failed weaning had low E/E' ratio, reduced stroke volume, and shortened deceleration time. Thus, an altered LV diastolic properties may well contribute to the rise of filling pressure and unsuccessful weaning from mechanical ventilation. In fact, in ventilated ICU patients, a lateral E/E' ratio above 8.0 predicted a pulmonary artery occlusion pressure (PAOP) of more than 18 mmHg with good sensitivity and specificity according to a study. Similarly, other authors showed that an E/A ratio above 0.95 and E/E' ratio above 8.5 at the end of a spontaneous breathing trial could predict a high PAOP in patients difficult to wean.

To summarize:

- Echocardiography is suited to screen patients at risk of weaning failure.
- Patients who exhibit LV ejection fraction less than 35% must be considered at high risk of cardiac-related weaning failure, particularly when LV diastolic dysfunction (shortened deceleration time) and increased filling pressure (elevated E/E') are associated with the systolic dysfunction.
- In patients who ultimately fail weaning due to cardiogenic pulmonary edema, median E/A and E/E' ratios increase when pressure support ventilation is switched to spontaneous breathing trial.
- Echocardiography before, during, and after the weaning process is very helpful to assess hemodynamics and tailor a specific therapy (diuretics, antihypertensive drugs, noninvasive ventilation after extubation, levosimendan) as an attempt to facilitate difficult cardiac-related weaning from positive pressure ventilation (Fig. 30.5).

Fig. 30.5 Echo-guided
weaning algorithm.
PP, plateau pressure.
PS, pressure support
ventilation.
PEEP, pulmonary
end-expiratory pressure.
PAP, pulmonary artery
pressure.
SBT, spontaneous
breathing trial
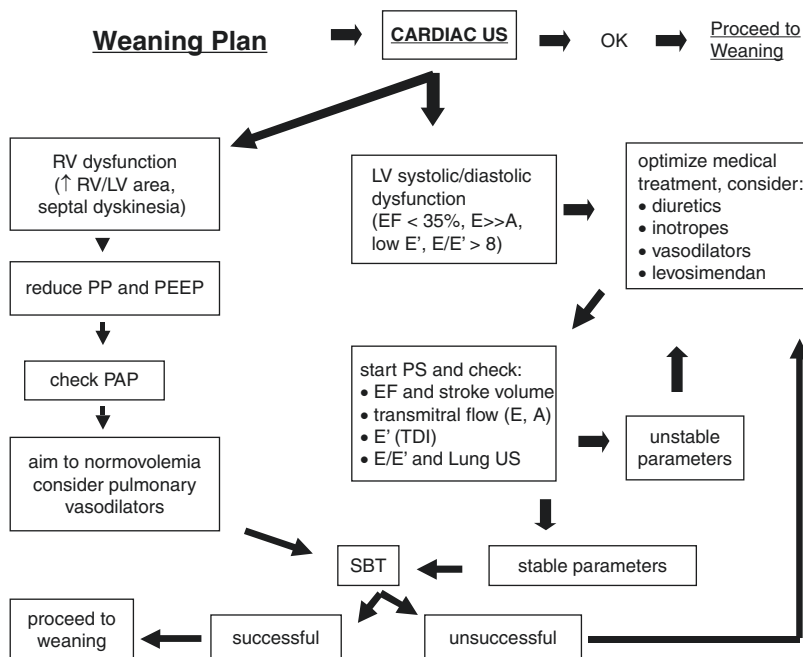
30.9 Mechanical Ventilation, RV Function, and Acute Cor Pulmonale (ACP)

The initial critical care echocardiography evaluation should be performed within 24 h of ICU admission or tracheal intubation to achieve three objectives:

- To rule out any cardiogenic mechanism at the origin of acute respiratory failure.
- To provide a comprehensive assessment of hemodynamic and potentially a better understanding of the mechanism of a potential associated circulatory failure, especially in case of sepsis. In some patients, ACP may already be diagnosed.
- To rule out any significant right-to-left shunting across a patent foramen ovale, especially when the level of hypoxemia seems to be not completely explained by alveolar damage or when increasing PEEP induced unexpected deterioration of the PaO_2/FiO_2 ratio.

Circulatory failure involves more than half of ARDS patients. Among the most severe patients,

two-third to three-fourths of them require the administration of catecholamines over a mean period of 10 days. In many cases, shock is related to sepsis-induced hypovolemia and vasoplegia, nevertheless ARDS induced specific circulatory changes.

In ARDS, two factors combine to produce RV systolic overload:

1. The pathologic features of the syndrome per se, which can be associated with distal occlusion of the pulmonary arterial bed
2. Mechanical ventilation, which increases RV outflow impedance

In addition PEEP may produce increased pulmonary vascular resistance. A high PEEP level represents another potential factor for increased RV outflow impedance. However, when PEEP is able to reaerate part of the lung without over distention, RV impedance may actually decrease.

Mechanical ventilation acts by direct mechanical augmentation of RV afterload in the inflation period. RV impairment may lead to RV dilatation, abnormal septal motion, and low cardiac output. When associated with high inflation pres-

sures, ACP could complicate ARDS. The ventilation respiratory strategy is fundamental for the tolerance of the RV to plateau pressure (PP) and PEEP. In general, the ventilator should be set to the lowest level of positive pressure during both the inspiratory and the expiratory phase of the mechanical breath which is still compatible with acceptable oxygenation and $paCO_2$.

According to a recent study, ACP during the first day of mechanical ventilation depends mainly on PP level:

- A low level of PP, <26 cmH$_2$O, does not generally or almost never produce ACP and is associated with low mortality.
- A PP between 27 and 35 cmH$_2$O is associated with high mortality only if there is concomitant ACP.
- A PP above 35 cmH$_2$O is associated with a high incidence of ACP and mortality.

So, the increase of mortality related with mechanical ventilation (PP level) depends on the presence or not of ACP. The association of the following two echocardiographic findings is fundamental for the diagnosis of ACP in mechanically ventilated patients:

1. End-diastolic right ventricular area (RVEDA)/ end-diastolic left ventricular area (LVEDA), (RVEDA/LVEDA ratio) >0,6, in A4C (TTE) or ME 4C 0° (TEE)
2. Septal dyskinesia in PSSAX TTE or TG 0° TEE

In ARDS, a major cause of ventilator-induced hypotension (and false fluid responsiveness) may not be venous return impairment (unless the patient is hypovolemic), but increased RV afterload. Thus, once the setting of the ventilator is adjusted to the lowest level of positive pressure which guaranties acceptable gas exchange, pulmonary vasodilators, such as nitric oxide,

sildenafil, or prostacyclin, can be used to reduce pulmonary arterial pressure (Fig. 30.5).

Ventilator focus-oriented and RV goal-directed echocardiography has a irreplaceable role on right heart assessment and patient monitoring to guide the setting of mechanical ventilation and any possible use of pulmonary vasodilator agents.

The integrated use of lung, diaphragm, and cardiac ultrasound during spontaneous breathing trial had to be performed to diagnose the cause of weaning failure.

Suggested Reading

Arbelot C, Ferrari F, Bouhemad B, Rouby JJ. Lung ultrasound in acute respiratory distress syndrome and acute lung injury. Curr Opin Crit Care. 2008;14:70–4.

Baron A, et al. Echo-Doppler demonstration of acute cor pulmonale at the bedside in the medical intensive care unit. Am J Respir Crit Care Med. 2002;166:1310–9.

Bouhemad B, Aberlot C, et al. Ultrasound assessment of antibiotic-induced pulmonary reaeration in ventilator-associated pneumonia. Crit Care Med. 2010;38(1):84–92.

Bouhemad B, et al. Bedside ultrasound assessment of positive end-expiratory pressure-induced lung recruitment. Am J Respir Crit Care Med. 2011;183:341–7.

Bouhemad B, et al. Ultrasound for "lung monitoring" of ventilated patients. Anesthesiology. 2015;122:437–47.

Caille V, et al. Echocardiography: a help in the weaning process. Crit Care. 2010;14:R120. http://ccforum.com/content/14/3/R120.

De Robertis E, et al. Ultrasonography during weaning: a support to a comprehensive skillful strategy. Minerva Anestesiol. 2016;82(11):1132–4.

Feihl F, Broccard AF. Interactions between respiration and systemic hemodynamics. Part II: practical implications in critical care. Intensive Care Med. 2009;35:198–205.

The ARDS Definition Task Force. Acute respiratory distress syndrome - the Berlin definition. JAMA. 2012;307(23):2526.

Umbrello M, et al. Current concepts of ARDS: a narrative review. Int J Mol Sci. 2017;18:64. https://doi.org/10.3390/ijms18010064.

Vignon P, et al. Critical care ultrasonography in acute respiratory failure. Crit Care. 2016;20:228.

Hypotension

Luigi Tritapepe, Cecilia Nencini, Giulia Frasacco,
and Demetrio Tallarico

31.1 Introduction

Hypotension is always a symptom of hemodynamic instability, and when physicians talk about hemodynamic instability, they often speak of hypotension. Low systemic arterial pressure frequently develops in critically ill patients. Common causes of hypotension in ICU patients include left ventricular (LV) dysfunction due to myocardial infarction and heart failure due to different causes, such as hypovolemia, sepsis and septic shock, pulmonary embolism, sedation regimen, and mechanical ventilation with aggressive use of positive end-expiratory pressure. Hypotension is a symptom that physicians are often called to treat following the traditional algorithm of hemodynamic stability. This algorithm asks the physician to treat hypotension step by step by answering yes or no to the following question:

Is the patient hypovolemic? If the answer is "yes," you should give fluid until the patient has a central venous pressure (CVP) of about 15 mmHg. If the patient does not respond, you must give inotropes, but if the patient does not have contractile dysfunction, you have to give vasopressors. If you have solved the instability, you are probably a good clinician, or you have chosen the right type of monitoring in a patient without cardiac disease, but in the case of treatment failure, you have to reassess the clinical scenario. Where is the problem?

The diagnosis of hemodynamic instability and hypotension is challenging. In a hemodynamic instability scenario, where diagnosis is not already done or where the patient clinical status has changed or where early or late follow-up is needed, echocardiography examination is fundamental for clinical evaluation and for guiding therapy or management.

Differently from both pressure and volume monitoring, echocardiography is the only diagnostic test that is easy to perform and useful in the early diagnosis of hypotension. After that, according to the causes of instability, an adequate treatment and a tailored hemodynamic monitoring system may be chosen and set up.

The literature describes the use of echocardiography in patients with hypotension.

In the guidelines endorsed by the various societies of physicians published in the *Journal of the American Society of Echocardiography* in 2011, transthoracic echocardiography (TTE)

L. Tritapepe (✉)
Department of Anesthesia and Intensive Care,
Cardiac Surgery ICU, Policlinico Umberto I Hospital,
Sapienza University of Rome, Rome, Italy
e-mail: luigi.tritapepe@uniroma1.it

C. Nencini
Santa Maria delle Croci Hospital, Rome, Italy

G. Frasacco
Policlinico Casilino Hospital, Rome, Italy

D. Tallarico (Retired)
Department of Cardiology, Policlinico Umberto I
Hospital, Sapienza University of Rome, Policlinico
Umberto I Hospital, Rome, Italy

and transesophageal echocardiography (TEE) have a maximal level of appropriateness (class A 9) in the diagnosis of hypotension and hemodynamic instability. Echocardiography can make the difference in terms of time and accurateness. In fact, in skilled hands, it needs only a few minutes to resolve a diagnostic question and to guide the following therapy. Positive-pressure ventilation, high levels of positive end-expiratory pressure, supine position, intrathoracic surgery, and chest trauma all present challenges for adequate image acquisition using TTE. This means that TEE is frequently more useful in the ICU setting and is the first-line echocardiographic examination whenever a patient has an endotracheal tube in situ.

Analyzing the causes of hypotension, we can define the major factors that determine hypotension as problems of preload, contractility, afterload, and impairment of the relationship between the ventricles and between the heart and lungs. Assessment of all these variables may be accomplished with echocardiographic examination. Moreover, echocardiography can identify causes of hypotension that are not clinically suspected and that can alter clinical management, such as LV outflow tract obstruction (LVOTO). An early diagnosis of this condition is particularly important because it does not have other diagnostic possibilities, and an incorrect treatment may result in a fatal outcome.

The best approach is to perform a comprehensive echocardiogram evaluation not only for cardiopathic patients but also for those without a previous history of cardiopathy. A comprehensive examination is less likely to miss an unexpected diagnosis. In this chapter, we want to analyze the causes of hypotension and to describe the utility of echocardiography in detecting the causal abnormalities, especially in the ICU setting and in the operating room.

31.2 Echocardiography in Hypotension

The use of echocardiography in the ICU is increasing. With the use of an abbreviated focus-assessed protocol, TTE has been shown to contribute positively to patient care in 97% of critically ill patients. Normally echocardiography allows the visualization of every cardiac structure and the recognition of the mechanical function of the heart. Ultrasonography can be used to detect the causes of hypotension and to understand why it is refractory to inotropic support or vasopressor infusions. Finally, echocardiography can help physicians in the diagnosis of a wide spectrum of syndromes that may or may not be related to the cardiovascular system.

Hypotension is a common problem in critically ill patients. Immediate treatment is mandatory to avoid prolonged hypotension that may lead to organ ischemia, dysfunction, and poor outcome. Rapid diagnosis and intervention may prevent this deterioration and eventually improve outcome. In the ICU, TTE is the first step in ultrasonography, but in certain cases, it may not be able to provide good image quality because of structures which result in poor penetration of ultrasound, such as air or interposed equipment such as an extensive bandage. The failure rate of the transthoracic approach in the ICU setting has been reported to be between 30% and 40%. TEE is particularly useful in every case of missed diagnosis due to technical impediment, and it is irreplaceable for the evaluation of suspected aortic dissection, malfunctioning of prosthetic heart valves, suspicion of embolization, endocarditis, possible intracardiac shunts, and unexplained hypotension. TEE allows better visualization of the heart in general and especially the posterior structures owing to the proximity of the esophagus without the use of an unfavorable medium. The assessment of hypotension is commonly approached in terms of assessment of heart rate, rhythm, preload, contractility, and afterload. A complete view of all of these variables may be achieved by an echocardiographic study. The first differentiation in the case of hypotension must be made between acute patients with sepsis or trauma and long-term ICU patients. With a basic level of skill, a complete TTE examination may be performed in minutes. Preload, contractility, systolic function, diastolic dysfunction, and pericardial tamponade can be assessed quickly. Specific situations such as pericardial effusion or
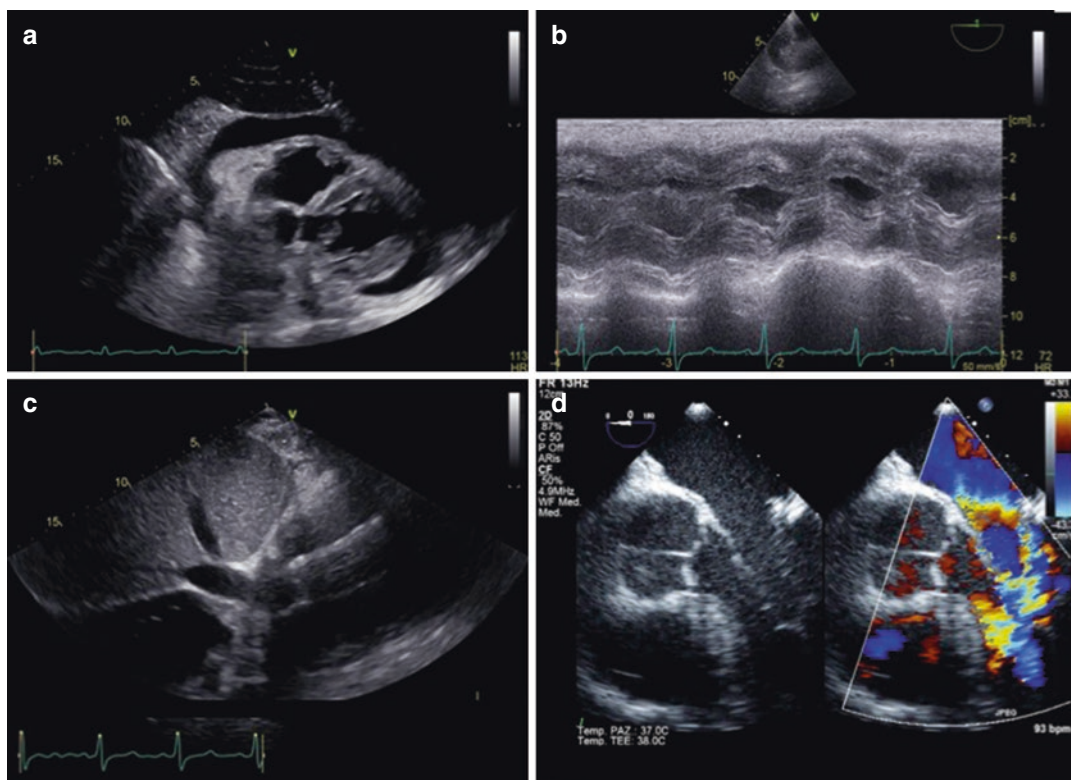
Fig. 31.1 Some causes of unexplained hypotension. Pericardial tamponade (**a**), marked hypovolemia in hypertrophic and hyperkinetic LV (**b**), IVC collapsed (**c**), and LVOTO (**d**)

localized tamponade, pulmonary embolism, LVOTO, unexplained hypoxemia, and aortic dissection, among others, can all be assessed using TEE in a reliable fashion, and their assessment requires an intermediate level of skill (Fig. 31.1).

31.3 Causes of Hypotension

31.3.1 Modification of Preload

Clinical assessment of intravascular volume can be extremely difficult or impossible to achieve in the ICU as well as during major surgery. This is a crucial problem because fluid loading is considered the first step during resuscitation of hemodynamically unstable patients. The literature indicates that only about 50% of hemodynamically unstable patients in the ICU and operating room respond to a fluid challenge. Cardiac filling pressures including the CVP and the pulmonary artery occlusion pressure (PAOP) have traditionally been used to guide fluid management. However, studies performed over the last 30 years have demonstrated that cardiac filling pressures are unable to predict fluid responsiveness. Over the last decade, a number of studies have been reported that have used heart–lung interactions during mechanical ventilation to assess fluid responsiveness. Specifically, the pulse pressure variation derived from analysis of the arterial waveform, the stroke volume variation derived from pulse contour analysis, and the variation of the amplitude of the pulse oximeter plethysmographic waveform have been shown to be highly predictive of fluid responsiveness when certain conditions are maintained (high tidal volume (TV), ventilator–patient synchrony, no spontaneous breathing, and absence of arrhythmias). Although the LV end-diastolic area as determined by TEE is a more accurate measure of preload than either the CVP or the PAOP, it does not

predict fluid responsiveness as well as the dynamic indices. For many years in ICUs, physicians have argued over the best way to assess preload. On one side are those who rely on pressure monitoring, on the other side are those who chose volumetric monitoring. Nevertheless, the Swan-Ganz catheter has continued to be the most popular device, especially in ICUs. The literature describes the systematic failure of preload assessment through static measurement of the pressure, such as the CVP or capillary wedge pressure, but also for volumetric measurements, data are lacking. Dynamic monitoring, which uses the heart–lung interaction to better discover the preload deficit, does not reveal hypotension due to preload reduction. The complexity of every hemodynamic status and of the different abnormalities prevents the applicability of simple algorithms (Fig. 31.2).

TTE and even better TEE provide a snapshot image of the patient and allow us to make a diagnosis either in the presence or in the absence of cardiac disease. First of all, the parasternal short-axis view at the mid-papillary level and the transgastric mid-short-axis view are useful views to quantify the preload of the left ventricle. Short-axis images of the left ventricle provide real-time assessment of ventricular filling, which may not be accurately reflected by the pulmonary capillary wedge pressure. In the presence of a real hypovolemia, we can see a small LV area, in both systole and diastole, and it is possible to note the kissing of papillary muscles that represents the complete collapse of the left ventricle during systole. The diameters of the left ventricle can be measured in M-mode. The criteria for diagnosing hypovolemia include an end-diastolic diameter of less than 25 mm, systolic obliteration of the LV cavity, and a LV end-diastolic area of less than 5.5 cm^2/m^2. Moreover the measurement of LV areas, in both systole and diastole, can solve the question of true or false hypovolemia. In fact, in the case of true hypovolemia, both LV areas are small, whereas in the case of vasodilation with hypotension, only the systolic LV area is small. In general, a hypovolemic patient has a hyperdynamic status with a high ejection fraction.

Patients with chronic cardiac failure have a dilated left ventricle and may be hypovolemic even with a higher LV end-diastolic area. In this case the study of cardiac function can be helpful for the diagnosis.

A new concept is fluid responsiveness instead of volume status or measurement of filling pressures. Fluid responsiveness means that a significant volume expansion, when performed, should induce a significant increase in cardiac output, reflecting the fact that the heart is on the steep portion of the Frank–Starling curve. Echocardiography has been widely demonstrated to predict fluid responsiveness accurately. This is now a complete and noninvasive tool able to determine hemodynamic status precisely in circulatory failure. We can draw the Frank–Starling curve of each patient through the TTE or TEE short-axis view of the left ventricle at different levels of loading, and we can identify a fluid-responder patient when his/her LV short-axis output is not on the flat portion of the curve. In mechanically ventilated patients, it is more useful to evaluate the dynamic indices of the cyclic modification of stroke volume to categorize a fluid-responder patient. A very useful index is the aortic volume–time integral variation with the value of the aortic blood flow peak, measured by TTE in apical three-chamber and apical five-chamber views or by TEE in deep transgastric in transgastric long-axis views with pulsed wave Doppler imaging of the LV outflow tract at the level of the aortic valve. ΔV_{peak} is generally evaluated over each of five consecutive respiratory cycles. Beat-to-beat measurement of aortic blood V_{peak} allows the determination of $V_{peak\ max}$ and $V_{peak\ min}$ over a single respiratory cycle. ΔV_{peak} is calculated as the difference between $V_{peak\ max}$ and $V_{peak\ min}$ divided by the mean of the two values and is expressed as a percentage. A ΔV_{peak} of aortic blood flow greater than 12% indicates a fluid-responder patient. In mechanically ventilated patients perfectly adapted to the respirator (with a tidal volume of at least 8 mL/kg and with no spontaneous respiratory effort), in sinus rhythm and with a normal intraabdominal pressure, respiratory variations in superior vena cava (SVC) and inferior vena
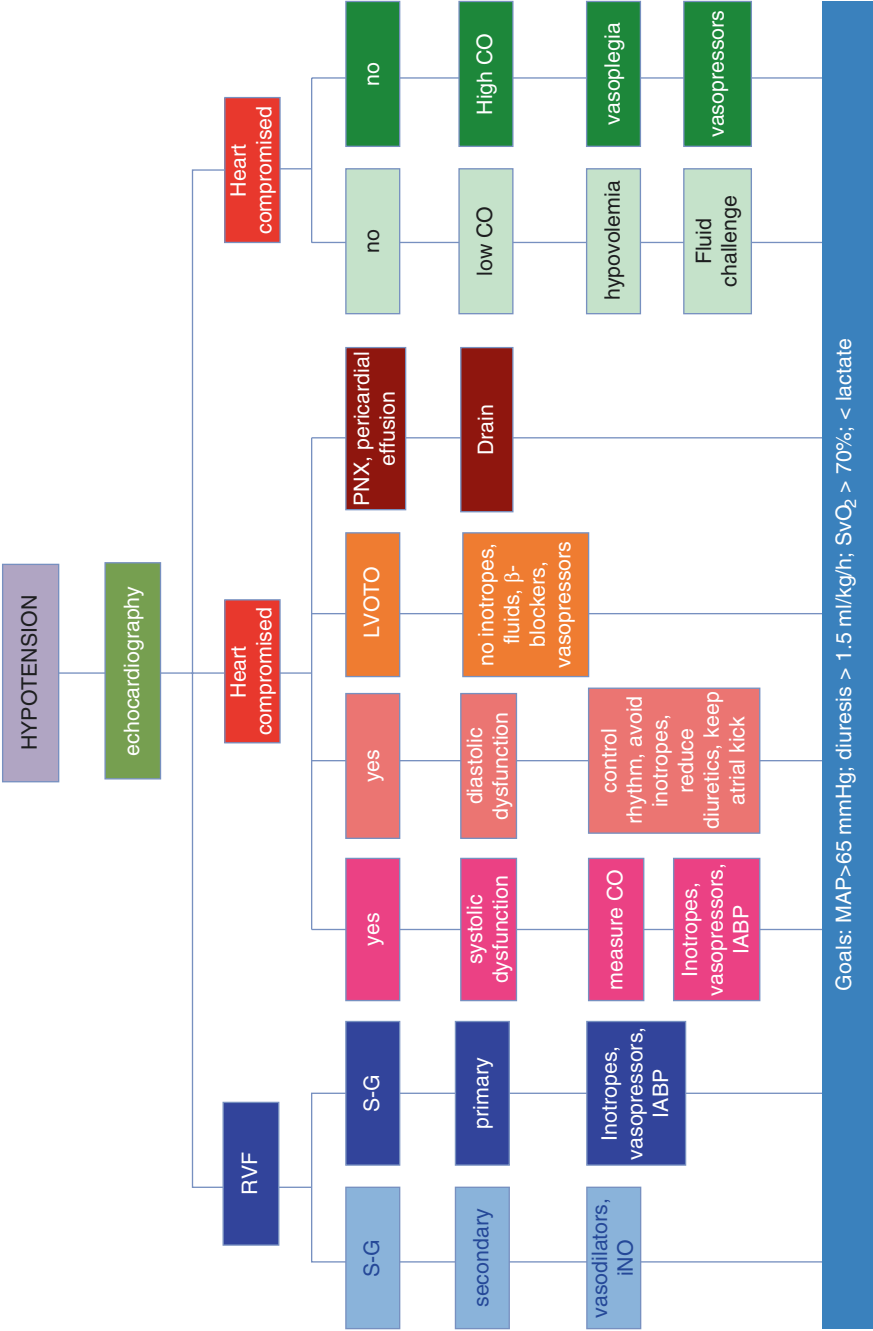
Fig. 31.2 Algorithm for diagnosis and treatment of unexplained hypotension. RVF, right ventricular failure; S-G Swan–Ganz catheter; iNO inhaled nitric oxide, CO cardiac output, IABP intra-aortic balloon pump, LVOTO left ventricular outflow tract obstruction, PNX pneumothorax, MAP mean arterial pressure, SvO2 central/mixed venous oxygen saturation

cava (IVC) diameters have also been validated as parameters of fluid responsiveness. The SVC can be explored with TEE in the bicaval view, where it is represented on the right side of the screen and it is less confounding from the elevations of intraabdominal pressure (SVC is intrathoracic). Simply, the eyeball or even better the M-mode shows the collapse of the SVC in a hypovolemic patient during the respiratory cycle. Volume loading can stop the collapse of the SVC, which has a collapsibility variation of more than 36% in a fluid-responder patient. The SVC collapsibility index is more reliable than the IVC distensibility index in predicting fluid responsiveness. However, the IVC is well recognized in almost all patients in the ICU, and it is simple to visualize when it is not feasible to perform TEE. The IVC distensibility is often measured by a cardiologist to assess the value of the CVP, but the significance of its distensibility in the mechanically ventilated patient is more often used by intensivists. It can be easily visualized in mechanically ventilated patients by echocardiography, using a subxiphoid approach. When the distensibility variation of the IVC rises above 18%, this means that the patient is a fluid responder. To better assess the ventricular loading, we need to know the LV end-diastolic pressure and the left atrial pressure (LAP). We can estimate this pressure by measuring blood and tissue velocities with tissue Doppler imaging of the mitral annulus and transmitral flow. Combining E' from tissue Doppler imaging with the E wave of transmitral flow, we can obtain different values of the ratio E'/E: when this ratio is less than 8, it is indicative of a low LAP and a compliant left ventricle, whereas for values greater than 15, LAP is high and the ventricle is not compliant. Other variables must be researched to precisely assess every intermediate value of LAP.

A temporary test dose of volume expansion can be performed with passive leg raising, which briefly redistributes blood pooled in the lower extremities to the central circulation. If stroke volume is measured before and after the position change, the intensivist can then evaluate the hemodynamic effect of increasing preload. It can

be performed even if the patient is breathing spontaneously and even if the patient is not in sinus rhythm.

31.3.2 Myocardial Function

In the ICU many devices are used to measure cardiac output. Some are invasive, whereas others are noninvasive, but the Swan-Ganz catheter represents the gold standard. Nevertheless, despite the information derived from the pulmonary artery catheter, we need to know more about myocardial function to make a diagnosis. In fact, the measurement of flow does not provide information about the cause.

Measurement of SVC of the right and left ventricles can be reliably performed using both TTE and TEE with PW Doppler. Assessment of CO is important in determining responses to medical and surgical therapies, such as administration of inotropic agents for the treatment of right and left heart failure.

The global systolic function of the left ventricle can be visualized with TTE or TEE by its contractility and by the increase in wall thickness in eyeball mode. It is very important to remember that each contracting myocardial segment moves toward a central point in the short-axis view during systole and simultaneously thickens. If you do not see the increase of wall thickness, the myocardial segment seems to thicken, but it is dragged from neighboring segments. The evaluation of wall motion is crucial in the ICU to verify if it is a new problem that causes hypotension or if it is a worsening of a known disease. This distinction, together with elevation of the level of biomarkers, can show an acute myocardial ischemia, which is treated differently from other forms of myocardial impairment such as stunning and global hypokinesia. Then it is crucial to study the global LV systolic function in terms of qualitative values. Qualitative methods used for assessing global LV systolic function using echocardiography are ejection fraction, fractional shortening, and fractional area change, as well as mitral annular motion, dP/dt using other methods that are not frequently mitral regurgitant jet, and segmental wall motion abnor-

mality assessment using strain-rate imaging. Evaluation of the right ventricle is also essential, as tricuspid regurgitation, right ventricular (RV) overload (greatly increased size), limited tricuspid descent, and poor RV wall contraction may indicate right-sided heart failure. RV dilatation is often associated with LV underfilling and poor cardiac output. The explanation of these measures is given in other chapters in this book. However, it is important, especially in mechanically ventilated patients, to establish if the right ventricle is compromised or not because, despite all the modifications described for the dynamic parameters monitored, the patient will always be nonresponder to fluid challenge. The diastolic function is well described in another chapter in this book, but it is important to underline its role in causing hemodynamic instability. Transmitral flow evaluation combined with measurement of the deceleration time represents the first step in diastolic evaluation. The examination is completed using tissue Doppler imaging of the mitral annulus, which represents an index of diastolic function not closely related to the load condition of the left ventricle. The Doppler imaging of the pulmonary veins helps to clarify the discrepancy from other measurements and to establish the degree of diastolic dysfunction. When patients with hypotension present with various degrees of diastolic dysfunction, they cannot be treated following the algorithms for hypotension with the use of catecholamines.

31.3.3 Modification of Afterload

Afterload is not often measured in the ICU. It is estimated from the clinical conditions such as peripheral vasoconstriction, oligoanuria, and cold extremities. It is measurable, but we can only know the peripheral contribution to afterload because its value is determined more by aortic impedance, aortic elastance, and LV wall stress, which are difficult to obtain in clinical practice. TTE and TEE allow us to extrapolate the reduction of afterload whenever the mean arterial pressure is reduced, but the LV diastolic area is normal, and the left ventricle collapses during systole.

Table 31.1 The major clinical scenarios of hemodynamic instability

Pericardial tamponade
Pulmonary embolism
Left ventricular outflow tract obstruction
Unexplained hypoxemia
Blunt chest trauma
Shock
Aortic dissection

Pulmonary embolism, unexplained hypoxia, and aortic dissection are described extensively in other chapters in this book. Here we will describe pericardial tamponade, LVOTO, blunt chest trauma, and shock

31.4 Different Scenarios of Hypotension

In the ICU, different clinical scenarios result from the physiopathologic causes of hypotension as previously described. These pathologic entities occur frequently, and echocardiography may represent a life-saving tool in many circumstances (Table 31.1).

31.4.1 Pericardial Tamponade

Cardiac tamponade is a true medical emergency, and the overall risk of mortality depends on early diagnosis, treatment, and the underlying cause. The most common cause of tamponade is pericardial effusion. By 2D echocardiography, a pericardial effusion is semiquantitatively described on the basis of the size of the echo-free space seen between the parietal and visceral pericardium at end-diastole as small (<10 mm with 50–100 ml), moderate (10–20 mm with 100–500 ml), and large (>20 mm with >500 ml). M-mode echocardiography shows the persistence of an echo-free space between the epicardium and parietal pericardium throughout the cardiac cycle.

Any condition that increases intrathoracic pressure such as a mediastinal mass or a large bilateral pleural effusion can also increase the pericardial pressure and cause hemodynamic compromise. In the case of pericardial effusion, there is an increase in intrapericardial pressure that rapidly causes a rise in intracardiac pressure, especially in the right side of the heart, where

normally the intracavitary pressures are lower than in the left side. The rapid increase in intra-pericardial pressure causes the diastolic collapse of the right ventricle in the early phase of diastole, whereas during the late phase, it can determine an invagination of the right atrium. Thus, the physiologic process of pericardial tamponade can result in hemodynamic instability with hypotension due to an increased intrapericardial pressure that precludes the cardiac filling and output. Echocardiography is the first-line imaging test in the diagnostic evaluation of pericardial disease.

On TTE and TEE, in 2D views, one sees the presence, the size, the location, the free flowing vs organizing, and the suitability for pericardiocentesis vs windows of pericardial effusion; the diastolic collapse of the right-sided chambers; stasis of agitated saline contrast in right atrium (sluggish flow); the dilatation of the IVC (>2.1 cm) with the loss of its respiratory variations (<50% reduction in diameter during inspiration) reflecting the elevated right atrial pressure; the respiratory increase of interventricular dependence; and the reduction in stroke volume and cardiac output. Although diastolic RV collapse (inward diastolic motion of the RV free wall) occurs later, it is a more specific sign and is best appreciated from the parasternal or subcostal long-axis views. The increase of interventricular dependence can be revealed by pulsed wave and continuous-wave Doppler imaging showing respiratory variations of more than 25% in mitral, aortic, and/or tricuspid flow. This variation of right-sided and left-sided heart inflow is a sign of exaggerated interventricular dependence, which is also a hallmark of pericardial tamponade. The physiologic aspect of these changes during respiration is related to the constriction due to pericardial effusion that impedes the diastolic filling, so during inspiration the intrathoracic negative pressure causes suctioning of the blood from the venae cavae with acceleration of transtricuspid flow and RV dilation. It may be also documented a reciprocal respiratory changes of diastolic forward flow velocity and end-diastolic flow reversal in hepatic veins.

During expiration, the right ventricle is compressed, and the transmitral and transaortic flow are accelerated (tissue Doppler velocities of mitral annulus, color Doppler M-mode of mitral inflow). Flow respiratory variations can be assessed only in spontaneously breathing patients, in regular sinus rhythm (such phasic changes in flow with respiration are reversed or absent in positive-pressure ventilation). An important hemodynamic instability exists when the difference between the highest and the lowest velocity of transtricuspid or transaortic or transmitral flow is more than 25%. The key element of the differential diagnosis is to identify that the patient has a moderate to large pericardial effusion. Cardiac tamponade may be acute or subacute to chronic; it may be either low pressure (occult) or regional, due to a loculated effusion or a compressive pericardial blood clot. A loculated, eccentric effusion or localized hematoma can produce regional tamponade in which only selected (often left-sided) chambers are compressed. So the spectrum of presentation depends on the characteristics of the effusion and the patient's clinical conditions. Regional cardiac tamponade is often seen after cardiac surgery, pericardiotomy, or myocardial infarction. Cardiac tamponade associated with cardiac surgery may occur early (<24 h and often related to surgical bleeding or cardiopulmonary bypass-induced coagulopathy) or late (arbitrarily defined as >5–7 days and it is multifactorial). Although a large pericardial effusion is more likely than a small one to be associated with increased intrapericardial pressure, this depends mainly upon the rate of accumulation (malignant pericardial effusion may lead to minimal hemodynamic compromise; acute RV perforation or ascending aortic dissection may develop cardiogenic shock with only a minimal collection). The amount of pericardial effusion can be estimated by measuring the diameter of the collection. A diameter greater than 1 cm is often considered significant. Also, the hypovolemia presents symptoms and echocardiographic findings similar to those of pericardial tamponade. However, all cardiac chambers are uniformly under filled without compression. In addition, and most importantly, a significant pericardial effusion is notably absent. Pericardial tamponade is well recognized

in the subcostal view but also in the apical four-chamber and parasternal long-axis views. TEE can be useful in the case of saccular compression such as after cardiac surgery when a frank cardiac tamponade can be difficult to diagnose, whereas the left atrial compression is better recognized.

The treatment of cardiac tamponade is urgent pericardiocentesis. An echocardiography-guided approach is recommended as first-line therapy for pericardiocentesis, and it is usually approached from the para-apical region (smallest distance from the skin to effusion in this location). The position of the pericardial needle can be visualized during the procedure and the administration of saline through the pericardiocentesis needle confirms pericardial entry. Echocardiography can additionally confirm the guidewire and pigtail catheter placement into the pericardial space and the collection drainage. Repeat echocardiography within 24 h is indicated to examine for reaccumulation.

31.4.2 Left Ventricular Outflow Tract Obstruction

In the emergency department and in the ICU, dynamic LVOTO occurs more often than is recognized. LVOTO has to be searched for whenever we encounter an unexplained hypotension. The patient who develops LVOTO has various degrees of aortic stenosis, not well-controlled hypertension, cardiac hypertrophy, and a hyperdynamic left ventricle. A particular predisposition is the eccentric hypertrophic interventricular septum associated with a long anterior leaflet of the mitral valve. If volume depletion happens, dynamic LVOTO with systolic anterior motion of the mitral valve and secondary mitral regurgitation develops, resulting in a progressive fall in cardiac output. In this case, the velocity of blood through the LV outflow tract, accelerated by the hypovolemia, tachycardia, or catecholamines, determines a "Venturi effect" on the anterior mitral leaflet that obstructs the outflow tract and causes an aortic stenosis effect and

mitral insufficiency. This situation quickly becomes serious and cannot be diagnosed with traditional monitoring. Indeed, if we monitor the patient with a Swan-Ganz catheter, we note a low cardiac output and a rise in PAOP. Immediately, with the diagnosis of low output syndrome, we administer inotropes, which leads to an irreversible hypotension. There should be a high index of suspicion in such patients, especially where they fail to increase cardiac output in response to escalating inotropic support. Many patients develop an LVOTO during hospitalization in the ICU because they have septic shock and the treatment with catecholamines predisposes them to have a systolic anterior motion of the mitral valve and its chordal apparatus and the resulting consequences.

This dynamic obstruction (systolic anterior motion) can result in cardiovascular collapse, and prompt diagnosis with echocardiography is essential to implement the correct management. Treatment includes the correction of hypovolemia with fluids, the use of vasopressors to raise the LV afterload, and β-blockade to relax the LV obstruction and reduce hypercontractility. Echocardiography, both TTE and TEE, is crucial in the diagnosis and management of therapy. TTE in the apical three-chamber view or the parasternal long-axis view and TEE in the deep transgastric view or mid-esophageal long-axis view at the level of the aortic valve provide the opportunity to immediately and simply make the diagnosis. The most important hallmarks are the presence of a septal bulge due to hypertrophy that is prominent toward the LV outflow tract. This bulge causes a subaortic stenosis, which revealed from the turbulence of the color flow Doppler imaging. The subaortic stenosis is associated with mitral insufficiency, and color flow Doppler imaging shows a typical Y shape due to the contemporary turbulence in the aortic and mitral valves during systole. Continuous-wave Doppler imaging across the LV outflow tract estimates a serious subaortic gradient that can exceed 100 mmHg and has a late-peaking "dagger shape."

31.4.3 Blunt Chest Trauma

Cardiac contusion is usually caused by blunt chest trauma arising from car accidents or falling injuries. The reported incidence of cardiac contusion in patients with blunt chest trauma ranges between 3% and 56% depending on the diagnostic methods. This pathological condition leads to serious hypotension that has to be discriminated from other causes. Echocardiography, together with other examinations and blood samples, is now an important diagnostic tool also in thoracic trauma. The value of TTE in blunt chest trauma is limited because patients with severe chest wall injury often have suboptimal echocardiographic findings. TEE can provide high-quality images when the transthoracic image quality is poor. There are a few reports that blunt chest trauma may lead to acute myocardial infarction caused by coronary artery dissection, thrombosis, or fistula. Echocardiography can be used as a screening tool for ventricular dysfunction, which is one of the most serious complications of cardiac contusion. With respect to myocardial contusion, the right ventricle is nearest to the chest wall, and on echocardiographic examination, its apex can appear damaged, whereas the left ventricle is interested at level of septum and apex. This myocardial contusion is shown as an increase in wall thickness in diastole, alteration of segmental wall contractility, and increased brightness of the ventricular walls. Also, a rapid focused assessment with echocardiography can detect pericardial collection, mediastinal hematomas, aortic intramural hematomas, aortic dissection or transection, and pleural collections (Fig. 31.1).

31.4.4 Shock

Critically ill patients with hypotension and shock need a prompt diagnosis and treatment. Shock can be categorized into hypovolemic, cardiogenic, distributive (e.g., anaphylactic, septic, neurogenic), and obstructive. In all these situations, echocardiogram evaluation is critical to the patient's diagnostic framing, before initiating specific treatment and hemodynamic monitoring.

Hypovolemic shock is caused by a critical decrease in intravascular volume (hemorrhage, inadequate fluid intake, external fluid loss). A reduced venous return (preload) results in decreased ventricular filling and reduced stroke volume. In hypovolemia, echocardiography can rapidly document a small hyperdynamic unloaded ventricle, with a reduced LV end-diastolic area in short-axis frames and "kissing papillary muscles" in M-Mode images. In profound hypovolemia (likely to respond to volume loading by an increase in cardiac output), the inferior vena cava diameter may be small (<10 mm) with inspiratory collapse in spontaneously breathing patients. In mechanically ventilated patients with hypovolemia, the inferior vena cava might also be of small diameter but at end expiration and with variable respiratory change (depending on adaptation to ventilator).

Distributive shock is caused by an insufficient intravascular volume of blood secondary to vasodilation. Septic shock is the commonest cause. It is frequently associated with relative hypovolemia and normal or high cardiac output with ventricular hyperkinesia, even if in some patients, diffuse transient hypokinesia might be observed.

In the presence of chronic or acute heart disease, myocardial impairment may be due to LV (with low CO) or RV systolic dysfunction (due to pulmonary hypertension and/or elevated pulmonary vascular resistance or RV hypokinesia with dilatation) and also diastolic impairment. Septic shock can be also caused by endocarditis. Echocardiography evaluation with TTE and TEE is fundamental for the initial diagnosis and for the evaluation of valvular dysfunction and the subsequent heart impairment. TTE is recommended as the first-line imaging modality in suspected endocarditis (I B), and TEE is recommended in all patients with clinical suspicion of endocarditis and a negative or nondiagnostic TTE or when a prosthetic heart valve or an intracardiac device is present (I B) (ESC 2015 guidelines). TTE and TEE are also recommended during the follow-up (I B-IIa B) and at completion of antibiotic therapy (I C) (ESC 2015 guidelines).

In sepsis accompanying pneumonia or in ARDS, the heart–lung interaction is crucial for the hemodynamic patients' management. In this setting it should consider how mechanical ventilation strategy affects myocardial function and how heart–lung circulation is closely connected.

Emerging studies have suggested the potential use of strain (fractional change in length between two time points, end-diastole (L0) and end-systole (L), and calculated as (L−L0)/ L or ∆L/L0) and speckle tracking to detect ventricular dysfunction in septic shock not appreciated by conventional echocardiography.

Obstructive shock may be caused by mechanical factors that interfere with filling (tamponade, mediastinal masses, inferior or superior vena cava compression or thrombosis, tension PTX, severe asthma, intracardiac tumors, or clot) or emptying (acute massive pulmonary embolism, aortic stenosis, LVOT obstruction) of the heart or great. The resulting low cardiac output leads to hypotension, organ and tissue hypoperfusion, and an increased systemic vascular resistance to compensate.

Cardiogenic shock is a state of inadequate cardiac output to meet tissues' oxygen demands. The commonest cause remains severe LV systolic dysfunction secondary to AMI, with high mortality (50–70%). Other causes include RV dysfunction, mechanical complications of AMI, cardiomyopathy, severe valvular heart disease, myocarditis, myocardial contusion, and acute aortic dissection. Echocardiography is crucial for confirming the diagnosis of the cause of cardiogenic shock (LV or RV dysfunction, RV or LV infarction, acute severe mitral regurgitation, and mechanical complications: LV free wall rupture, ventricular septal rupture, and papillary muscle rupture), for the hemodynamic patient's status assessment (including filling pressures and stroke volume). Therefore, immediate TTE or TEE should be performed when cardiogenic shock is suspected.

31.5 Conclusion

In a setting of hypotension and hemodynamic instability, the first action to take is to diagnose the cause. The echocardiographic examination is crucial in this step for differential diagnosis of the cause of hypotension or shock, by detecting cardiac or non-cardiac aetiologies. Then echocardiography is needed for guiding appropriate therapy (inotropies, vasopressor, fluid challenge, beta-blockers, surgical intervention, etc.), for starting the best hemodynamic monitoring system, and for evaluating subsequent clinical status changes.

Further Reading

2015 ESC Guidelines for the management of infective endocarditis The Task Force for the Management of Infective Endocarditis of the European Society of Cardiology (ESC) Endorsed by: European Association for Cardio-Thoracic Surgery (EACTS), the European Association of Nuclear Medicine (EANM).

Beaulieu Y. Bedside echocardiography in the assessment of the critically ill. Crit Care Med. 2007;35:S235–49.

Chockalingam A, Dorairajan S, Bhalla M, Dellsperger KC. Unexplained hypotension: the spectrum of dynamic left ventricular outflow tract obstruction in critical care settings. Crit Care Med. 2009;37:729–34.

Douglas PS, et al. ACCF/ASE/AHA/ASNC/HFSA/HRS/SCAI/SCCM/ SCCT/SCMR 2011 appropriate use criteria for echocardiography. J Am Soc Echocardiogr. 2011;24:229–67.

Klein AL, et al. American Society of Echocardiography clinical recommendations for multimodality cardiovascular imaging of patients with pericardial disease endorsed by the Society for Cardiovascular Magnetic Resonance and Society of Cardiovascular Computed Tomography. J Am Soc Echocardiogr. 2013;26:965.

Lancellotti P, et al. The use of echocardiography in acute cardiovascular care: recommendations of the European Association of Cardiovascular Imaging and the Acute Cardiovascular Care Association. Eur Heart J Cardiovasc Imaging. 2015;4:3.

Marcelino PA, Marum SM, Fernandes AP, Germano N, Lopes MG. Routine transthoracic echocardiography in a general intensive care unit: an 18 month survey in 704 patients. Eur J Intern Med. 2009;20:e37–42.

Porter TR, et al. Guidelines for the use of echocardiography as a monitor for therapeutic intervention in adults: a report from the American Society of Echocardiography. J Am Soc Echocardiogr. 2015;28:40.

Salem R, Vallee F, Rusca M, Mebazaa A. Hemodynamic monitoring by echocardiography in the ICU: the role of the new echo techniques. Curr Opin Crit Care. 2008;14:561–8.

Subramaniam B, Talmor D. Echocardiography for management of hypotension in the intensive care unit. Crit Care Med. 2007;35:S401–7.

Vignon P. Hemodynamic assessment of critically ill patients using echocardiography Doppler. Curr Opin Crit Care. 2005;11:227–34.

Wasir H, Mehta Y, Mishra YK, et al. Transesophageal echocardiography in hypotensive post-coronary bypass patients. Asian Cardiovasc Thorac Ann. 2003;11:139–42. Legends of figures of the chapter 30.

Suspicion of Pulmonary Embolism

32

Alessandro Locatelli, Ilaria Nicoletti,
and Carla Avallato

32.1 Suspicion of Pulmonary Embolism

Acute pulmonary embolism (PE) consists in the acute obstruction of one or more branches of the pulmonary artery; the obstruction can be total or partial, and the material, usually of thrombotic origin, comes from their site of formation. Venous thrombi, in about half of patients, dislodge from the deep vein of the lower limbs. Sometimes the material can be made up of amniotic fluid, air, or CO_2. In cases of massive PE with cardiogenic shock, the symptoms are clinically obvious, but in most cases, the symptoms are vague, so it is essential to assume clinical suspicion.

Few known factors predispose the development of PE:

- Primary hypercoagulable conditions: the presence of Leiden factor V (resistance to activated protein C with a sharp increase in the risk of developing deep vein thrombosis and PE). Other predisposing factors include the prothrombin gene mutation, protein S deficiency, antithrombin III deficiency, hyperhomocysteinemia, and antiphospholipid antibodies (anticardiolipin antibodies and lupus anticoagulant).
- Acquired hypercoagulable state: all the conditions that promote venous stasis predisposing to thrombosis, for example, prolonged immobilization from surgery, trauma, obesity, smoking, cancer, and use of oral contraception.

The hemodynamic effects are the result of increased pulmonary vascular resistance caused by embolic obstruction and release of neurohumoral substances (thromboxane A2 and serotonin). The abrupt increase in right ventricular (RV) afterload, with increased wall tension, is followed by dilation and dysfunction of the RV. The high wall stress leads to a reduction of right coronary blood flow with increased oxygen requirements and the risk of RV ischemia. The expansion of the right ventricle determines a leftward bowing of the ventricular septum with reduced distensibility and filling of the left ventricle. As a result, left ventricular (LV) filling is compromised, and this may lead to a reduction in cardiac output, hypotension, and hemodynamic instability with the risk of reduced coronary perfusion and myocardial ischemia.

A. Locatelli (✉)
Cardiovascular and Thoracic Anaesthesia,
Santa Croce & Carle Hospital, Cuneo, Italy

Department of Emergency and Critical Care,
Santa Croce & Carle Hospital, Cuneo, Italy
e-mail: locatelli.a@ospedale.cuneo.it

I. Nicoletti · C. Avallato
Department of Emergency and Critical Care,
Santa Croce & Carle Hospital, Cuneo, Italy
e-mail: nicoletti.i@ospedale.cuneo.it;
avallato.c@ospedale.cuneo.it
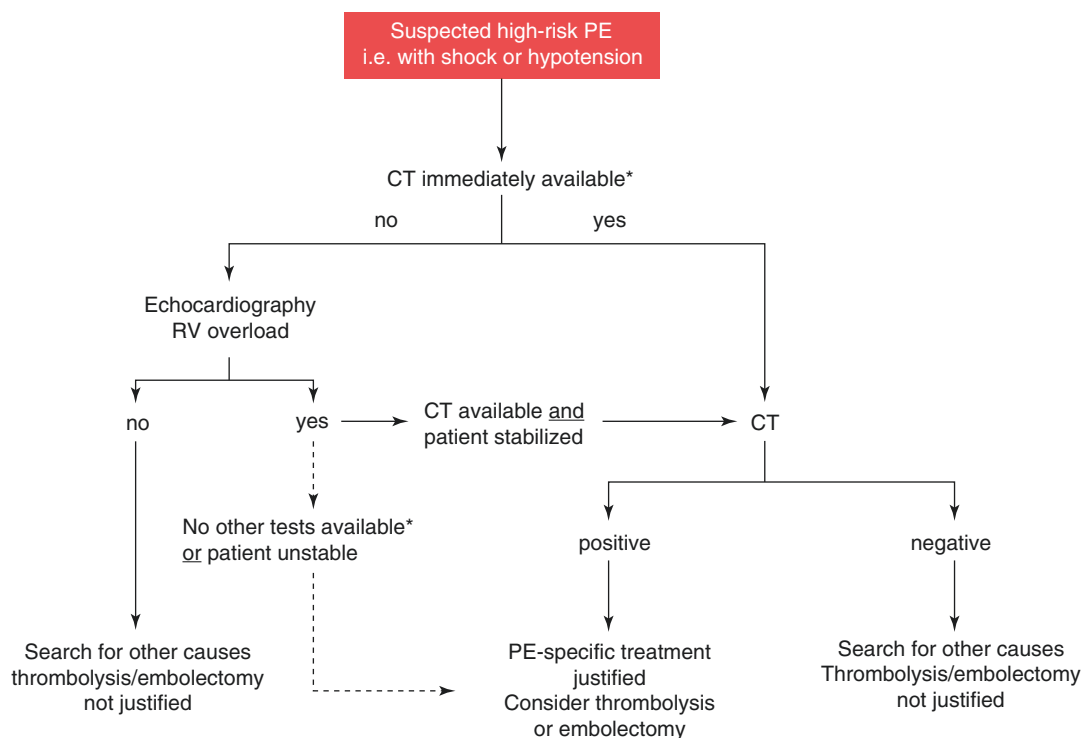
Fig. 32.1 Proposed diagnostic algorithm for patients with suspected high-risk pulmonary embolism (PE), i.e., presenting with shock or hypotension. * CT is considered not immediately available also if the critical condition of a patient allows only bedside diagnostic tests. Transesophageal echocardiography may detect thrombi in the pulmonary arteries in a significant proportion of patients with right ventricular (RV) overload and PE that is ultimately confirmed by spiral CT; confirmation of deep vein thrombosis with bedside compression ultrasonography might also help in decision-making. (From Torbicki et al. 2008)

The contemporary presence of dyspnea, chest pain, haemoptysis, hypoxia, hypocapnia, respiratory alkalosis in the blood gas analysis in a patient with swollen jugular veins, deep thrombosis and predisposing factors, are strongly suggestive of acute PE. If these are associated with a complete or incomplete ECG right bundle branch block, S1Q3T3 complex, and negative T wave from V1 to V4, the probability of PE is very high. Atrial fibrillation, or other atrial arrhythmias, may be associated with acute PE.

The last ESC Guidelines on the diagnosis and management of acute pulmonary embolism (2014) highlight the assessment of clinical probability through two validated scores, Wells rule and revised Geneva score. Both scores take notice of the same indicators (previous PE or DVT, heart rate >100 bpm, surgery or immobilization in the past month, hemoptysis, active cancer, clinical signs of DVT, etc.) and give them a score which identify two or three levels of clinical probability. According to the recent guidelines, there are two different diagnostic routes in case of suspected acute PE depending on the presence of shock or hypotension. In case of suspected PE with shock or hypotension, they suggest diagnostic algorithm showed in Fig. 32.1. In case of suspected PE without shock or hypotension, the algorithm in Fig. 32.2 is proposed.

The algorithm shows the key role of echocardiography in the diagnosis of acute PE, allowing differential diagnosis with acute valvular dysfunction, acute coronary syndrome, aortic dissection, and tamponade. Echocardiography should be performed whenever a CT examination is not readily available or if the patient, admitted to the ICU, can't be moved. The presence or absence of signs of RV overload determines the next diagnostic step.

Fig. 32.2 Diagnostic algorithm for patients with suspected not high-risk pulmonary embolism

Suspected PE no shock no hypotension

Clinical probability of PE evaluation

Low/intermediate clinical probability

High clinical probability

D-Dimero → negative

positive

CT

No PE → no treatment

PE → treatment

CT → PE → treatment

no PE

no treatment or further investigations
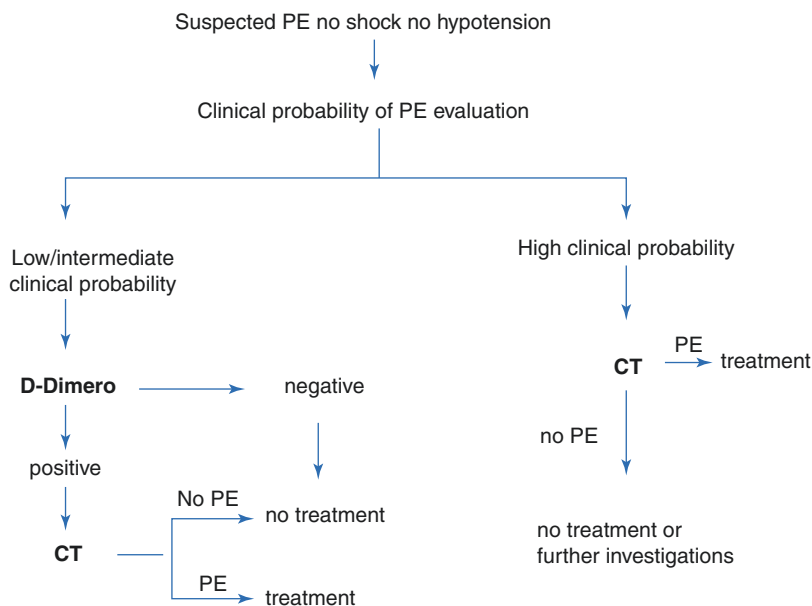
32.2 Role of Echocardiography in PE

Echocardiography is used in the diagnosis, prognosis, and evaluation of pulmonary embolism. It has the advantage of being done easily at the bedside, of having a low cost, and of not being an invasive examination; it can therefore be done several times to monitor hemodynamic status and response to treatment. The echocardiographic signs suggestive of PE are direct and indirect. The direct signs are represented by direct visualization of the thrombus, whereas the indirect ones are mostly related to acute pressure overload in the right ventricle:

- RV dilatation and depressed contractility of the RV free wall compared with the RV apex ("McConnell sign")
- RV free wall hypokinesia or akinesia
- Abnormal interventricular septal motion
- Tricuspid valve regurgitation greater than 2.8 m/s
- Lack or decreased inspiratory collapse of inferior vena cava (IVC)

Transthoracic echocardiography (TTE) can hardly visualize thrombi in the pulmonary artery; however, it is able to provide information on the hemodynamic status, on the RV and LV function, and on pulmonary pressure, and it also allows risk stratification. Transesophageal echocardiography (TEE) has a sensitivity ranging from 60% to 80% and a specificity of 95–100% in the diagnosis of acute PE. It highlights thrombi located in the trunk of the pulmonary artery and the two main branches as well, although the left branch is only visible for a short distance (Figs. 32.3 and 32.4).

TEE has a valuable role in the diagnosis of acute PE in patients who have had a sudden cardiac arrest or acute PE. Floating thrombi in the right atrium are easily detected by TEE. These are classified into three types: types A, B, and C. Type A thrombi have an elongated and serpiginous shape; they originate from peripheral veins and rapidly migrate to the pulmonary circulation. Thrombi of this type are associated with high mortality. Type B thrombi have a globular shape, a broad plant, and are motionless. They also migrate to the pulmonary circulation but have a better prognosis than the other types. Type C is

an intermediate form in its morphology, evolution, and prognosis.

Indirect signs of PE are due to pressure overload on the right ventricle as consequence of obstruction of the pulmonary artery or its branches.

For diagnosis of PE, 2D and Doppler echocardiographic parameters can be observed.

Fig. 32.3 Right branch of pulmonary artery. Upper esophageal long-axis view

32.3 Two-Dimensional Echocardiography

- TTE: Parasternal views (long axis) and apical four-chamber and subcostal four-chamber views
- TEE: Upper esophageal views (trunk of the pulmonary artery and its division into right and left branches) and mid-esophageal views (four-chamber, RV inflow outflow and bicaval views)

The parasternal short-axis view for TTE and the transgastric short-axis view for TEE are useful to investigate the septum and the size of the right ventricle.

The findings in cases of acute RV overload are:

- Expansion of the right ventricle with LV deformity: the expansion can be measured both as the diastolic diameter of the right ventricle (DdRV) and as the relationship
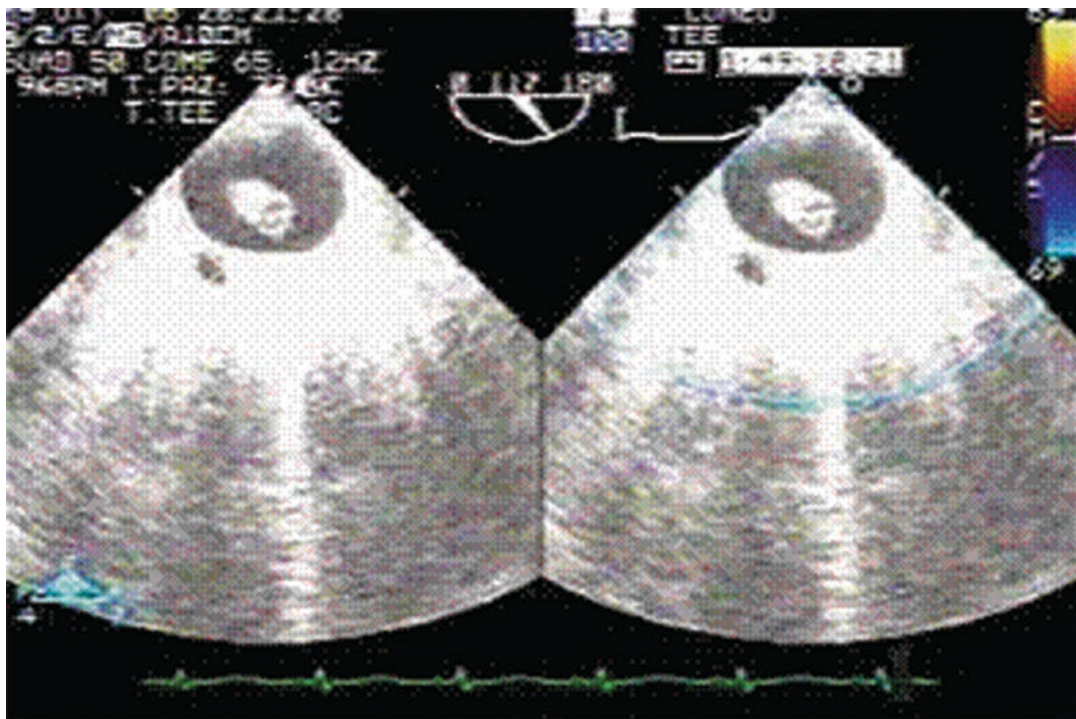
Fig. 32.4 Right branch of pulmonary artery. Upper esophageal short-axis view

between the diastolic diameter of the right ventricle and diastolic diameter of the left ventricle (DdRV/DdLV). The finding of DdRV >30 mm and a DdRV/DdLV ratio of 0.7 or greater in parasternal long-axis and subcostal views and greater than 1 in the apical view is considered pathological. The area ratio of the two ventricles can be used if the images are of good quality. A right ventricle to left ventricle area ratio below 0.6 is normal; if it is greater than 1, a major expansion of the right ventricle is present.

- Right atrial dilation with interatrial septal shift to the left.
- Increased diameter and decreased collapse (less than 40–50%) of the IVC.
- Diastolic dyskinesia of the interventricular septum.
- Normal contraction of the RV apex with hypokinesis of the midportion of the RV free wall (McConnell sign). It has a high negative predictive value. This sign can be visualized from the apical four-chamber view.

32.4 Doppler Echocardiography

- Estimation of pulmonary arterial systolic pressure: The modified Bernoulli equation is applied on the tricuspid valve regurgitation jet to obtain the pressure gradient between the atrium and the right ventricle. Then the estimated right atrial pressure (RAP) is added to this gradient to obtain the pulmonary arterial systolic pressure. The RAP is estimated from the diameter and respiratory variation of the IVC. Usually, if the IVC collapse index is greater than 40–45%, the RAP is estimated to be about 5 mmHg; if the index is between 35% and 40%, the RAP is about 10 mmHg; an index less than 35% means an RAP of about 15 mmHg. Pulmonary arterial diastolic pressure (PAPd) can be estimated from the end-diastolic pulmonary regurgitant jet, which depends on the diastolic pressure difference between the pulmonary artery and the right ventricle. The PAPd is obtained by applying the Bernoulli formula to the velocity of

pulmonary regurgitation and then adding the diastolic pressure of the right ventricle. The RV diastolic pressure (RVPd) equals the RAP if there is no tricuspid valve stenosis ($PAPd = 4V^2_{PRd} + RVPd$).

- Pulmonary acceleration time: this represents the time necessary to reach peak pulmonary velocity and is calculated as the time interval between the beginning of the pulmonary valve flow and its peak velocity. In normal conditions this acceleration time is greater than 90 ms; if it is less than 60 ms, there is pulmonary hypertension. A pulmonary acceleration time of less than 60 ms associated with a tricuspid regurgitation pressure gradient below 60 mmHg (60/60 sign) is highly specific for PE. Another useful sign in the diagnosis of pulmonary hypertension is the shape of pulmonary blood flow; in the case of pulmonary hypertension, pulmonary blood flow has a triangular shape or shows a mesosystolic incision.

The detection of these parameters in a critical patient associated with a clinical suspicion of PE should point toward more specific tests if the condition of the patient allows this. If there is hemodynamic instability, an ultrasound examination compatible with PE can help the start of fibrinolytic therapy.

32.5 Echocardiography and Prognosis of Patients with PE

In the recent Guidelines on acute pulmunary embolism (2014 ESC Guidelines on the diagnosis and management of acute pulmunary embolism, Eur Heart J 35: 3033-3080) patients with PE and haemodinamic instability are regarded as early mortality high risk patients. This score is very complex therefore a semplified form, called sPESI, has been developed. This semplified score identifies two risk levels, low risk (sPESI 0) and intermediate risk (sPESI ≥ 1), of an early adverse outcome. In the last case, a further risk stratification should be done evaluating RV function by

echocardiography or CT angiography and biomarkers as BNP (brain natriuretic peptide) or proBNP and high-sensitivity troponin. Patients with RV dysfunction and elevated cardiac biomarker levels belong to the intermediate-high risk group. In these patients anticoagulation therapy, monitoring and possibly rescue riperfusion is indicated. For intermediate-low-risk patients (one test positive or both negative), anticoagulation and hospitalization are necessary. In patients at low risk, guidelines indicate anticoagulation and early discharge.

32.6 Echocardiography and Therapy for Patients with PE

Early anticoagulation treatment can improve survival: therefore, in patients with a high clinical suspicion and a low bleeding risk, diagnostic investigations should not delay the start of anticoagulation therapy. In patients with clinical suspicion of PE, echocardiography is a quick, accurate, and safe diagnostic tool; it can be used easily at the bedside and is able to show both direct (blood clots in the pulmonary artery or right atrium) and indirect (deterioration of the right side of the heart up to acute lung heart) signs of PE and to guide the therapeutic choice. Ultrasonography is also useful to monitor patients undergoing thrombolytic treatment for thrombosis of the right side of the heart. Thrombolysis is the treatment of choice for massive and submassive PE in patients with hemodynamic instability. It improves lung perfusion, reduces pulmonary hypertension, and improves function of the right side of the heart but is burdened with increased bleeding complications.

Also, echocardiography can give clinical suspicion of chronic thromboembolic pulmonary hypertension. If, after 3 months of anticoagulation therapy, a tricuspid regurgitation velocity more than 2.8 m/s is found, it need to do further investigation as V/Q scan. Echocardiography, however, has some limitations in the diagnosis of PE. It is an operator-dependent method, so the operator's experience and skills are fundamental. The display of thrombi, particularly in the left branch of the pulmonary artery, is obstructed by the interposition of the left bronchus. Furthermore, besides PE, some other diseases that can impair RV function (COPD exacerbations, right IMA, cardiomyopathies, and valvular disease) can be confusing, so it is important to make a differential diagnosis.

Further Reading

Casazza F, Bongarzoni A, Capozi A, Agostoni O. Regional right ventricular dysfunction in acute pulmonary embolism and right ventricular infarction. Eur J Echocardiogr. 2005;6(1):11–4.

Konstantinides S, Torbicki A, Agnelli G, et al. 2014 ESC guidelines on the diagnosis and management of acute pulmonary embolism. Eur Heart J. 2014;35:3033–80.

Leibowitz D. Role of echocardiography in the diagnosis and treatment of acute pulmonary thromboembolism. J Am Soc Echocardiogr. 2001;14:921–6.

Mookadam F, et al. Critical appraisal on the echocardiography in the management of acute pulmonary embolism. Cardiol Rev. 2010;18(1):29–37.

Torbicki A, et al. Right heart thrombi in pulmonary embolism: results from the international cooperative pulmonary embolism registry. J Am Coll Cardiol. 2003;41:2245–51.

Torbicki A, Perrier A, Konstantinides S, Agnelli G, Galiè N, Pruszczyk P, et al. Guidelines on the diagnosis and management of acute pulmonary embolism. The task force for the diagnosis and management of acute pulmonary embolism of the European Society of Cardiology (ESC). Eur Heart J. 2008;29:2276–315.

Suspicion of Acute Aortic Diseases

33

Luigi Tritapepe, Francesca Pacini, Giulia Frasacco, Mario Mezzapesa, and Maurizio Caruso

33.1 Introduction

In this chapter we will consider only the acute diseases of the aorta that quickly endanger the patient. This group of aortic diseases is now called "acute aortic syndrome" (AAS). AAS is a summary term for various acute life-threatening aortic conditions represented by aortic dissection, intramural hematoma, penetrating atherosclerotic ulcer, and thoracic aortic aneurysm rupture, excluding traumatic entities (Fig. 33.1). Although the pathophysiology of these heterogeneous conditions differs, they are grouped because they share common features: (1) similar clinical presentation ("aortic pain"), (2) impaired integrity of the aortic wall, and (3) potential danger of aortic rupture requiring emergency attention. The incidence of AAS is 2.9–3.5 cases per 100,000 individuals per year. An analysis from the International Registry of Acute Aortic Dissections (IRAD) reported a mean age at presentation of 63 years and a male predominance of 65%, yielding an incidence of 16 per 100,000 in

men. Although women were less frequently affected (7 · 9 per 100,000), their outcome was worse because of delayed diagnosis and atypical symptoms. All of these diseases show a certain monotony in terms of symptoms. In fact, the patient complains of severe chest pain radiating to the neck and arms in the case of type A aortic dissection or intramural hematoma and into the abdomen and back in the case of type B aortic dissection. Also, very often, patients may have hypertension or hypertensive emergency with alteration of peripheral pulses which become asymmetric and may have associated aortic valve regurgitation. Depending on the severity of the case, the patient may have hemodynamic instability with splanchnic hypoperfusion, metabolic acidosis, heart failure, and impaired cerebral perfusion. Also, patients may suffer from acute renal failure or respiratory insufficiency, and AAS can present itself as syncope related to cardiac tamponade or to occlusion of cerebral vessels. It may also occur as an acute coronary syndrome that sometimes is mistaken as the main pathologic entity instead of an accompanying syndrome. Therefore, differential AAS diagnoses may include myocardial ischemia/infarction, pulmonary embolism, pericarditis, acute aortic regurgitation without dissection, mediastinal tumors, perforating peptic ulcer, acute pancreatitis, cholecystitis, and musculoskeletal pain. Making a rapid diagnosis in these cases is essential to reduce mortality linked to AAS and especially to

L. Tritapepe (✉) · F. Pacini · M. Mezzapesa
Department of Anesthesia and Intensive Care,
Cardiac Surgery ICU, Policlinico Umberto I Hospital,
Sapienza University of Rome, Rome, Italy
e-mail: luigi.tritapepe@uniroma1.it

G. Frasacco
Policlinico Casilino Hospital, Rome, Italy

M. Caruso
San Giovanni-Addolorata Hospital, Rome, Italy
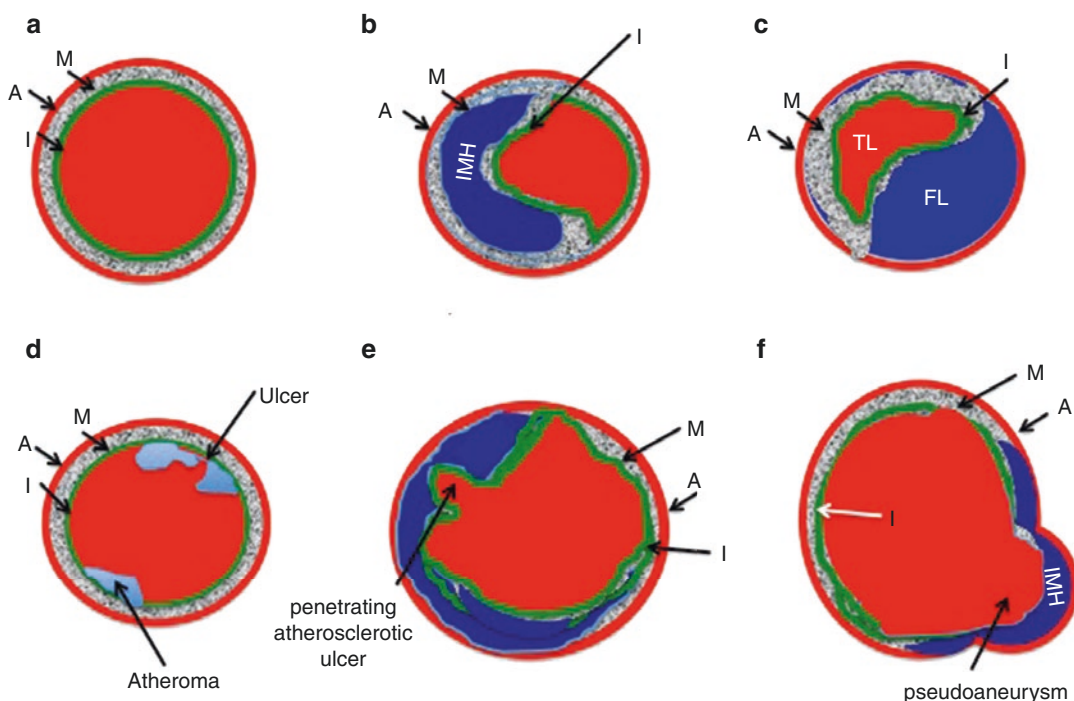
Fig. 33.1 The pathologic entities which determine acute aortic syndrome. (**a**) normal aorta, (**b**) intramural hematoma, (**c**) aortic dissection, (**d**) aortic atheroma and ulcer, and (**e**, **f**) penetrating ulcer with intramural hematoma and pseudoaneurysm. Legend: A, adventitia; M, media; I, intima; IMH, intramural hematoma

reduce morbidity. Normally, the most sensitive and specific imaging techniques are CT and MRI, whereas angiography has lost its diagnostic role. But nowadays echocardiography—transesophageal echocardiography (TEE) and transthoracic echocardiography (TTE)—plays an essential role. The advantages of echocardiography in the assessment of patients with AAS are unquestionable. It is readily available, it can be performed quickly, it offers the unique option to image at the bedside, and it is safe for the diagnosis of AAS.

33.2   TTE and TEE

With TTE, the proximal ascending aorta is visualized in the parasternal long-axis view, also in the modified right parasternal long-axis view, and in the basal parasternal short-axis view but to a lesser extent. The parasternal long-axis view allows us to correctly measure the aortic root diameters. In the parasternal long-axis view,

directly in two dimensions or in M-mode, we can study the aortic root and the proximal ascending aorta at the end of diastole with the aortic leaflets closed. In all patients with suspected aortic disease, the right parasternal long-axis view, even if it is not routinely performed, is recommended for estimating the true size of the ascending aorta. The ascending aorta is also visualized in the apical three-chamber and modified apical five-chamber views; however, in these views, the aortic walls are seen with suboptimal lateral resolution and a false diagnosis could be made or the abnormality may remain unrecognized. The suprasternal view is a crucial tomographic view to visualize, above the right pulmonary artery, the aortic arch and the three supra-aortic trunks (innominate, left carotid, and left subclavian arteries), and again a variable tract of the descending and ascending aorta. Acute ascending aortic AAS (i.e., type A dissection flap) may be visible on TTE with a sensitivity of 80–100% and specificity of 60–90%. However, if there is inconclusive

information or abnormalities are present, another imaging modality (e.g., TEE) is required to either complete or add diagnostic information. A negative TTE, therefore, does not exclude aortic dissection. To avoid a delay in diagnosis, TTE is not the modality of choice in suspected acute aortic syndrome. Its utility, therefore, in the emergency setting is in the rapid assessment of complications of dissection, such as aortic valve dysfunction, pericardial tamponade, or wall motion abnormalities. TEE has been shown to be a very sensitive diagnostic tool in the delineation and management of different aortic diseases. It is a fundamental examination to diagnose aortic syndrome and differentiate other diseases in the case of chest pain. The anatomic proximity of the aorta to the esophagus allows us to have a good view of the aorta, almost entirely. The only invisible tract is the distal portion of the ascending aorta owing to the presence of air in the right main bronchus, whereas the proximal portion of the aortic arch is poorly visible because of the proximity of the trachea, which can cause a virtual blind spot in that area.

In routine practice, TEE evaluation of the aorta is possible through six views (Table 33.1): mid-esophageal ascending aorta short-axis view, mid-esophageal ascending aorta long-axis view, upper esophageal aortic arch short-axis view, upper esophageal aortic arch long-axis view, descending

Table 33.1 Tomographic views for evaluation of the ascending thoracic aorta, the aortic arch, and the descending thoracic aorta

TTE	TEE
PSLAX, PSSAX (Asc + Desc Ao)	ME Asc Ao LAX, ME Asc Ao SAX (Asc Ao)
A4C, A2C, ALAX (Desc Ao)	UE aortic arch, UE aortic arch LAX (arch + Asc Ao)
Suprasternal (arch, Asc + Desc Ao)	Desc Ao LAX, Desc Ao SAX (Desc Ao)
Subcostal (abdominal + Asc Ao)	

TTE transthoracic echocardiography, *TEE* transesophageal echocardiography, *PSLAX* parasternal long axis, *PSSAX* parasternal short axis, *Asc* ascending, *Desc* descending, *Ao* aorta, *A4C* apical four chamber, *A2C* apical two chamber, *ALAX* apical long axis, *ME* mid-esophageal, *LAX* long axis, *SAX* short axis, *UE* upper esophageal

aorta short-axis view, and descending aorta long-axis view. In the mid-esophageal four-chamber view at 0°, the probe should be withdrawn 2 cm and the ascending aorta can then be shown in the short-axis view. This produces a circular image of the aortic root between the left atrium and the right atrium. Rotating the imaging plane to 90° will produce the long-axis view showing the ascending aorta. In this projection, however, the distal ascending aorta cannot be visualized because of the dispersion of echoes due to tracheal air. To view the descending thoracic aorta, we must return to the mid-esophageal four-chamber view and then rotate the probe through 180°, and then we see the aorta, which is positioned behind the esophagus. By slightly shifting the probe back, we can obtain the short-axis view of the thoracic aorta at various levels, making sure to rotate the probe slightly to center the image of the aorta because it runs laterally and then posteriorly to the esophagus at this level. Rotating the imaging plane to 90° will bring into view the long-axis image of the descending aorta. To view the arch, we return to the mid-esophageal four-chamber view at 0° and pull the probe back slowly until the aortic arch is seen. This is displayed in the upper esophageal long-axis view about 20 cm from the mouth rhymes. The proximal part of the aortic arch is not viewable because of air in the trachea; however we have a good view of the arch that shows the proximal portion to the left of the screen, and the distal part on the right with the posterior wall near the probe and at the top of the screen and the anterior wall further down. To obtain short-axis images of the aortic arch, we need to pull the probe back and rotate it 90° clockwise. The left subclavian artery and the left common carotid artery can also be viewed by pulling the probe further back. Study of the thoracic aorta should include wall thickness, tissue characteristics, dimensions, and blood flow patterns by Doppler assessment. The primary aim of TEE is to identify the intimal flap, false lumen, and entry tear, delineate the extent of aortic dissection, and identify intramural hematoma or penetrating atherosclerotic ulcer. TEE has a high sensitivity of 99% and modest to high specificity of 89% for identifying an intimal flap. More information about ultrasonography of the aorta can be found in Chap. 10.

Table 33.2 Acute life-threatening aortic conditions called acute aortic syndrome

Aortic dissection
Intramural hematoma
Penetrating atherosclerotic ulcer
Thoracic aortic aneurysm rupture

Table 33.3 Traditional classification systems

DeBakey
Category I: Dissection tear in the ascending aorta propagating distally to include at least the aortic arch and typically the descending aorta
Category II: Dissection tear only in the ascending aorta
Category III: Dissection tear in the descending aorta propagating most often distally
Category IIIa: Dissection tear only in the descending thoracic aorta
Category IIIb: Tear extending below the diaphragm
Stanford
Type A: All dissections involving the ascending aorta irrespective of the site of tear
Type B: All dissections that do not involve the ascending aorta; note that involvement of the aortic arch without involvement of the ascending aorta in the Stanford classification is labelled as type B

33.3 Acute Aortic Syndrome

Now we review the conditions that fall within the definition of AAS, as illustrated in Table 33.2.

TEE offers considerable advantages in the diagnosis of AAS. The technique has very high sensitivity and specificity, is rapid (5–10 min) and readily available, and does not require the patient to be moved. Echocardiographic study should include transthoracic assessment of the upper third of the ascending aorta, aortic insufficiency quantification, pericardial effusion diagnosis, and assessment of segmental alterations of ventricular contractility. Only in the few cases in which TEE does not permit a definitive diagnosis or where intramural hematoma is suspected would it be advisable to perform MRI or CT. In patients with ascending aorta dissection, TEE offers sufficient information for surgery to be directly indicated. The delay of surgery while conducting other tests may increase the risk of death without any significant advantage.

33.4 Aortic Dissection

Acute aortic dissection occurs when there is a tear or separation of the aortic intima from the media. Flow of blood into the intima–media space allows the tear to propagate as a dissecting hematoma. Aortic dissection classification may be made temporally and in terms of anatomical location. Temporally, the new classification system by Booher and colleagues[2] has four time domains: hyperacute (<24 h), acute (2–7 days), subacute (8–30 days), and chronic (>30 days). Anatomic classification using the DeBakey and Stanford systems drives decisions about surgical and nonsurgical management. The DeBakey classification system categorizes dissections on

the basis of the origin of the intimal tear and the extent of the dissection, and the Stanford system divides dissections according to whether the ascending aorta is involved (type A) or not (type B) involved. (Table 33.3).

Recently, a new classification system has been proposed. It encompasses fundamental anatomical and clinical features to select between medical management, open surgical repair, or endovascular interventions. It has been called DISSECT[3]. The classification has six elements: duration of dissection (D) less than 2 weeks, 2 weeks to 3 months, and more than 3 months from initial symptoms; intimal tear location (I) in the ascending aorta, arch, descending, abdominal, or unknown; size of the aorta (S); segmental extent (SE); clinical complications (C) such as aortic valve compromise, tamponade, rupture, and branch malperfusion; and thrombosis (T) of the false lumen and the extent. On first impression, DISSECT can seem complex and unwieldy; nonetheless, it considers all major prognostic elements.

Demonstration of the presence of an intimal flap that divides the aorta into two lumina, the true and the false (Fig. 33.2), forms the basis of echocardiographic diagnosis of the dissection.

Color Doppler imaging may help to evaluate the dissection when two different flow patterns, separated by the intimal flap, along the aorta, are identified. In the ascending aorta, particularly
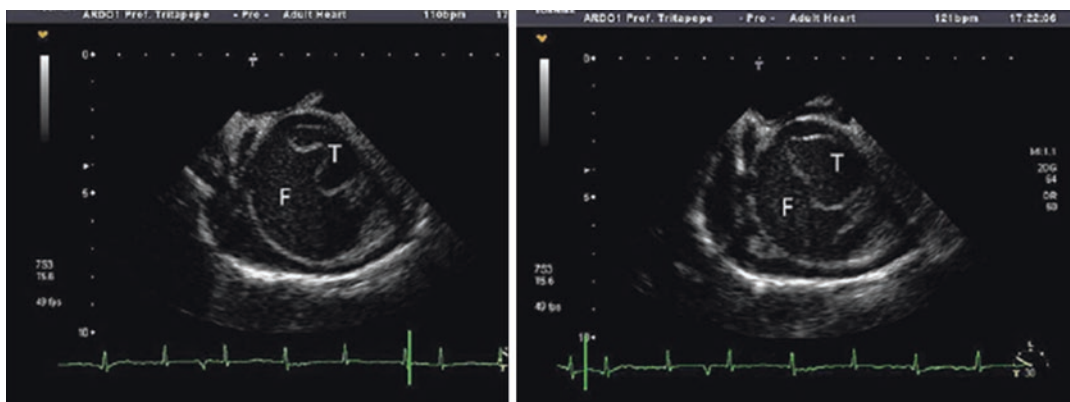
Fig. 33.2 TEE of the aortic dissection. False and true lumen during diastole and systole

when it is dilated, linear artifacts are very common in the images and they may be confused with the intimal flap, which appears in the transverse or longitudinal plane. In most ascending aorta dissections, the movement of the intima is free and does not meet the reverberation criteria. Therefore, assessment of the location and mobility of intraluminal images by M-mode and their longitudinal extent permits correct identification of artifacts in the ascending aorta. Often, the false lumen is thrombosed. The differential diagnosis between total false thrombosis and aneurysm is not always easy by TEE. The high echogenicity on the internal surface, the semilunar form, and the smooth surface increase the probability of it being a thrombosed false lumen. Ascending aorta involvement has high mortality and urgent surgery is indicated; it is of importance to determine the proximal extent of the dissection. Treatment of type A is surgical and that of noncomplicated type B is medical. TEE permits correct assessment of the proximal extent of the dissection, except when it is located in the upper third of the ascending aorta and the proximal half of the aortic arch (Fig. 33.3).

It is very important to localize the intimal tear. With the use of color Doppler imaging, TEE (2D and 3D) permits small communications between true and false lumina, mainly in the descending aorta, to be visualized. It is important to differentiate these secondary communications from the main intimal tear (Fig. 33.4).

The latter is usually identified by two-dimensional echocardiography and tends to measure more than 5 mm and can be located in the proximal part of the ascending aorta in type A dissections and immediately after the origin of the left subclavian artery in type B dissections. With pulsed Doppler imaging, it can be verified that the flow velocity at the tear is usually below 1.5 m/s and the flow goes from the true to the false lumen in systole. In diastole, the velocity is lower and the flow usually goes from the false to the true lumen. In certain circumstances, identification of the false lumen is of special clinical interest. When the aortic arch is involved, the surgeon needs to know whether the supra-aortic vessels originate from the false lumen. Similarly, when the descending aorta dissection affects visceral arteries and ischemic complications arise, it may be important to identify the false lumen prior to surgery or endovascular treatment, such as intima fenestration or endoprosthesis implantation. Percutaneous fenestration of intima may be a therapeutic alternative when the main artery branches originate from the false lumen. On most occasions, the distinction between true and false lumina is easy. The false lumen is usually larger and has less flow than the true lumen. In fact, flow in the false lumen may be absent or in the opposite direction (retrograde) to that of the true lumen. The sluggish flow in the false lumen may result in the presence of spontaneous echo contrast, sometimes referred to as "smoke." The false
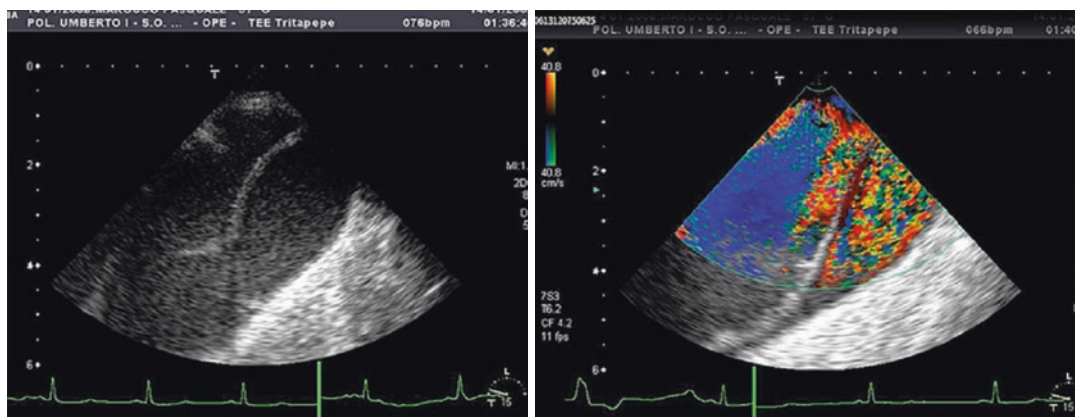
Fig. 33.3 TEE of the aortic arch dissection. False and true lumen without and with color Doppler imaging
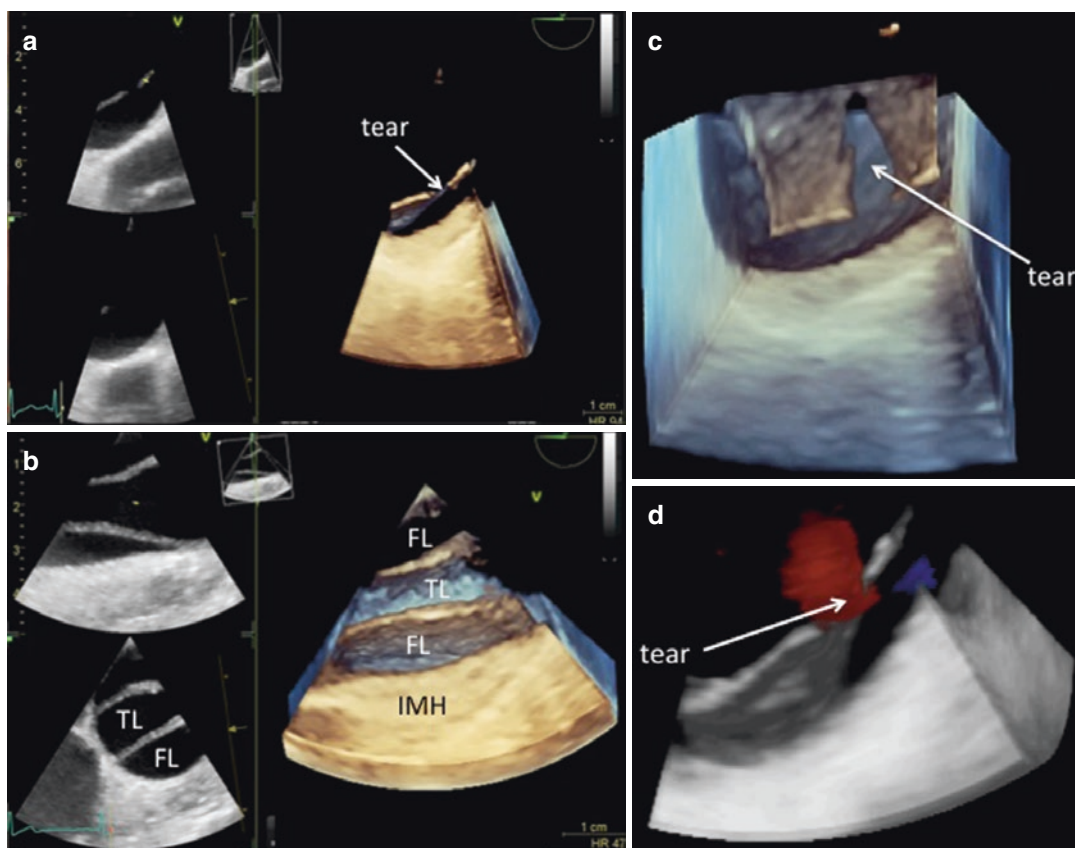
Fig. 33.4 3D TEE of the aortic dissection. False (FL) and true (TL) lumen (**b**) and tears (**a**, **c**, and **d**) are well evident. Note the intramural hematoma (IMH) in the part b of the figure

lumen may also contain variable degrees of thrombus. M-mode shows how the intima moves toward the false lumen at the start of systole by expansion of the true lumen. Partial thrombosis

of the false lumen is frequently present and total thrombosis is occasionally present (Table 33.4).

TEE also is important for the detection of AAS complications. Moderate to severe aortic

Table 33.4 Complications and secondary findings detectable with transesophageal echocardiography

Complications	Secondary findings
Pericardial and pleural effusions	Secondary tears
Aortic rupture	False lumen thrombi
Aortic insufficiency	Intima movement
Arterial branch involvement	Predisposing factors

regurgitation (AR) occurs in approximately 50% of patients with type A aortic dissection. The presence, severity, and mechanism(s) of AR may influence surgical decision-making and aid the surgeon in deciding whether to spare, repair, or replace the aortic valve. A pericardial effusion in an ascending aortic dissection is an indicator of poor prognosis and suggests rupture of the false lumen in the pericardium. Echocardiography is the best diagnostic technique for estimating the presence and severity of tamponade. TEE is capable of imaging the ostia and proximal segments of the coronary arteries in nearly all patients and may demonstrate coronary involvement due to dissection (flap invagination into the coronary ostium and origin of coronary ostium from the false lumen). Color Doppler is useful for verifying normal or abnormal or absent flow into the proximal coronary arteries. Usually, the right coronary artery is more often involved than the left. Another possible complication is the rupture of interatrial septum with development of septal hematoma and/or fistula between aorta and right atrium. Besides, TEE should be performed in the operating room in all patients during repair of type A aortic dissection. Even if the diagnosis has been "established" with a preoperative imaging modality, confirmation by intraoperative TEE before initiating cardiopulmonary bypass will minimize the possibility of a false-positive diagnosis. Once the diagnosis of aortic dissection has been confirmed, the primary purpose of the intraoperative TEE is to detail the anatomy of the dissection and to better define its physiologic consequences. After the repair of a type A aortic dissection, the echocardiographer should systematically reexamine the anatomic features of the aortic valve and proximal aorta to make sure that the surgical correction has been adequate (including exclusion of the entry tear and exclusion of

all proximal communications) and that the aortic valve is competent.

33.5 Aortic Intramural Hematoma

Aortic intramural hematoma (IMH), generally considered to be a variant of aortic dissection, accounts for approximately 10–25% of AAS. Typically, IMH appears as thickening of the aortic wall >0.5 cm in a crescentic or concentric pattern. Diagnosis by TEE is made when a circular or semilunar image, which may contain echolucent zones and which occasionally may be distributed in layers, is observed on the aorta wall. There is no Doppler evidence of communication between the hematoma and the true lumen, but there may be some color Doppler flow within the hematoma. Diagnosis is straightforward in typical cases, but the hematoma may sometimes be mistaken for the presence of an intraluminal thrombus or a dissection with thrombosed false lumen. Other imaging techniques such as CT, which shows an attenuated signal zone, and MRI, with a hyperintense signal, confirm the diagnosis. On occasions, localized zones of the hematoma can be identified which break the intima, giving rise to saccular protrusions that may be confused with penetrating ulcers. In more than 10% of cases, aorta zones with hematoma coexisting with others with classic intima dissection are detected; in these cases, the diagnosis is aortic dissection. In over 60% of hematomas, the location is in descending aorta and is frequently accompanied by other signs of aortic arteriosclerosis. Evolution of the hematoma is highly dynamic. Evangelista et al. described seven evolution patterns: regression, progression to classical dissection with longitudinal propagation, progression to localized dissection, development of fusiform aneurysm, development of saccular aneurysm, development of pseudoaneurysm, and persistence of IMH. Therefore, serial imaging is necessary to rule out progression in patients who receive only medical treatment, because clinical signs and symptoms cannot predict progression. Although there are no established guidelines for the optimal frequency and longitudinal duration

for surveillance imaging of patients with IMH, Evangelista et al., on the basis of the significant dynamic evolution of IMH, recommended imaging at 1, 3, 6, 9, and 12 months from the time of diagnosis. Once stability has been documented, surveillance imaging may be annual.

33.6 Penetrating Aortic Ulcer

The term penetrating aortic ulcer describes the condition in which ulceration of an atherosclerotic lesion penetrates the aortic internal elastic lamina into the aortic media. Although the clinical presentation of PAU is similar to that of classic aortic dissection, PAU is considered to be a disease of the intima (i.e., atherosclerosis), whereas aortic dissection and IMH are fundamentally diseases of the media (degenerative changes of the elastic fibers and smooth muscle cells are paramount), and most patients with aortic dissection typically have little atherosclerotic disease. PAUs may occur anywhere along the length of the aorta but appear most often in the mid and distal portions of the descending thoracic aorta, and they are uncommon in the ascending aorta, arch, and abdominal aorta. Once formed, PAUs may remain quiescent, but the weakened aortic wall may provide a basis for saccular, fusiform, or false aneurysm formation. External rupture into the mediastinum or right or left pleural space may occur but is uncommon. The diagnosis of penetrating ulcer is controversial. The presence of saccular protrusion outside the aorta profile is readily identifiable by contrast angiography and tomography. TEE is less useful in the diagnosis of these protrusions in the aorta profile, although recent studies have suggested its usefulness; nevertheless, it is highly useful for differentiating penetrating arteriosclerotic ulcers from ulcer-like projections secondary to thrombi with crater-like cavities in their surface and hematomas that evolve with disruption located in the intima. Absence of arteriosclerotic plaque in the intima of the aorta wall should lead us to suspect an ulcer-like projection and not a true penetrating ulcer. Both color Doppler echocardiography and contrast echocardiography may be helpful to confirm

the presence of flow within the external saccular protrusion to the aortic intima. Although TEE is highly accurate for the diagnosis of aortic dissection, its sensitivity and specificity in the diagnosis of intramural hematoma and penetrating ulcer have not been reported; thus, it is advisable to perform another imaging technique, particularly MRI, to confirm the diagnosis and provide information on bleeding persistence and the presence of periaortic hematoma.

Further Reading

Armstrong WF, Bach DS, Carey LM, et al. Clinical and echocardiographic findings in patients with suspected acute aortic dissection. Am Heart J. 1998;136:1051–60.

Baliga RR, Nienaber CA, Bossone E, et al. The role of imaging in aortic dissection and related syndromes. JACC Cardiovasc Imaging. 2014;7(4):406–24.

Booher AM, Isselbacher EM, Nienaber CA, et al. The IRAD classification system for characterizing survival after aortic dissection. Am J Med. 2013;126:730.

Dake MD, Thompson M, van Sambeek M, Vermassen F, Morales JP, for the DEFINE Investigators. DISSECT: a new mnemonic-based approach to the categorization of aortic dissection. Eur J Vasc Endovasc Surg. 2013;46:175–90.

Evangelista A, Mukherjee D, Mehta RH, et al. Acute intramural hematoma of the aorta. A mystery in evolution. Circulation. 2005;111:1063–70.

Evangelista A, Flachskampf FA, Erbel R, et al. Echocardiography in aortic diseases: EAE recommendations for clinical practice. Eur J Echocardiogr. 2010;11:645–58.

Evangelista A, Dominguez R, Sebastia C, Salas A, Permanyer-Miralda G, Avegliano G, et al. Long-term follow-up of aortic intramural hematoma: predictors of outcome. Circulation. 2003;108:583–9.

Goldstein SA, Evangelista A, Abbara S, et al. Multimodality imaging of diseases of the thoracic aorta in adults: from the American Society of Echocardiography and the European Association of Cardiovascular Imaging: endorsed by the Society of Cardiovascular Computed Tomography and Society for cardiovascular magnetic resonance. J Am Soc Echocardiogr. 2015;28(2):119–82.

Golledge J, Eagle KA. Acute aortic dissection. Lancet. 2008;372:55–66.

Meredith EL, Masani ND. Echocardiography in the emergency assessment of acute aortic syndromes. Eur J Echocard. 2009;10:i31–9.

Mehta RH, Manfredini R, Hassan F, et al. For the international registry of acute aortic dissection (IRAD) investigators. Chronobiological patterns of acute aortic dissection. Circulation. 2002;106:1110–5.

Nienaber CA, Kische S, Skriabina V, Ince H. Noninvasive imaging approaches to evaluate the patient with known or suspected aortic disease. Circ Cardiovasc Imaging. 2009;2:499–506.

Nienaber CA, Clough RE. Management of acute aortic dissection. Lancet. 2015;385(9970):800–11.

Shiau MC, Godoy MC, de Groot PM, Ko JP. Thoracic aorta: acute syndromes. Appl Radiol. 2010;1:6–16.

Shiga T, Wajima Z, Apfel CC, Inoue T, Ohe Y. Diagnostic accuracy of transesophageal echocardiography, helical computed tomography, and magnetic resonance imaging for suspected thoracic aortic dissection. Arch Intern Med. 2006;166:1350–6.

Willoteaux S, Nedelcu C, Bouvier A, et al. Syndrome aortique: quelle imagerie réaliser. Presse Med. 2011;40:43–53.

Chest Pain

34

Michele Oppizzi, Vittorio Pazzanese,
Roberto Spoladore, and Rachele Contri

Key Points

Pulmonary Embolism
- Suspected diagnosis: arterial pulmonary hypertension, RV enlargement and dysfunction, leftward motion of ventricular septum, tricuspid regurgitation, inferior vena cava dilatation (TTE)
- Diagnosis: thrombus visualization in pulmonary artery truncus (TEE)
- Risk stratification: RV dilatation (RV/LV > 1), patent foramen ovale, and thrombus in transit
- Treatment evaluation: reduction of pulmonary pressure, RV improvement, and normalization of ventricular septal motion

Myocardial Infarction
- Diagnosis: regional wall motion abnormalities

- Risk stratification: EF < 35%, functional mitral regurgitation, high left atrial and pulmonary pressure, RV dysfunction

Takotsubo
- Diagnosis: wall motion abnormalities involving mid and apical segments of the whole LV, beyond the territory of distribution of a single coronary artery, extension of areas of asynergy disproportionate compared to the degree of ST elevation and troponin release
- Risk stratification and echo-guided therapy: low EF -> consider inotropic agents, RV dysfunction -> consider inotropic agents, left ventricular outflow obstruction -> beta-blockers, apical thrombus -> antithrombotics

Aortic Dissection
- Suspected diagnosis: pericardial effusion, aortic enlargement, aortic insufficiency (TTE)
- Diagnosis: intimal flap and tear (TEE)
- Risk stratification: extravasation, aortic regurgitation, and regional wall motion abnormalities
- Echo-guided therapy: type A -> emergent cardiac surgery, type B compli-

M. Oppizzi (✉) · V. Pazzanese · R. Spoladore
Department of Cardiology, San Raffaele Hospital
Milan, Milan, Italy
e-mail: oppizzi.michele@hsr.it; pazzanese.vittorio@hsr.it; spoladore.roberto@hsr.it

R. Contri
Cardiocentro Ticino, Lugano, Switzerland

34.1 Pulmonary Embolism

Echocardiography is an important diagnostic, monitoring, and prognostic tool in the management of patients with PE and guides the choice of the most appropriate therapeutic strategy. In fact, its applications are (a) diagnosis and differential diagnosis, (b) risk stratification, (c) decision-making and echo-guided therapy, and (d) assessment of therapeutic efficacy. Taken all together, clinical, echocardiographic, and biohumoral assessment allows a classification of patients with PE into high, intermediate, and low risk. Patients complicated by hypotension or shock are at high risk with an in-hospital mortality between 15% and 30%. Hemodynamically stable patients (PESI classes III–IV) with marker of RV dysfunction (RV function echo or CT, troponin, BNP) are classified as having an intermediate low risk (one marker) or high risk (both markers), with an early mortality between 3% and 15%. Stable patients (PESI classes I–II) with no RV dysfunction are at low risk with an in-hospital mortality rate of less than 1%.

In the critically ill patients, echocardiography is particularly helpful because it allows a bedside and fast diagnosis, avoiding logistic problems associated with standard radiological diagnostic procedures, and is useful in the differential diagnosis of shock. Moreover, in patients who present with cardiac arrest, particularly in those with pulseless electrical activity, transthoracic (TT) or transesophageal (TE) echocardiographic demonstration of RV enlargement has such a high positive predictive value for PE that it may justify the choice of fibrinolysis or more aggressive treatments.

34.1.1 Diagnosis and Differential Diagnosis

Indirect evidence. Echocardiographic findings suggestive of pressure overload induced by PE include:

1. Arterial pulmonary hypertension
2. RV enlargement and dysfunction
3. Flattening or abnormal leftward motion of the ventricular septum
4. Functional tricuspid regurgitation
5. Inferior vena cava dilation with lack of inspiratory collapse (Fig. 34.1)

1. Pulmonary artery systolic pressure is usually mild to moderate. Acute overloaded RV is often unable to generate a higher pressure. A pulmonary pressure value >50 mm Hg suggests a chronic process or an acute PE superimposed to a chronic lung disease. Severe pulmonary hypertension is associated with the persistence of pulmonary hypertension at follow up.
2. Moderate RV dilatation corresponds to a diastolic RV/LV ratio (diameter or area) between 0.6 and 1, while a severe dilatation corresponds to a diastolic RV/LV ratio > 1. RV/LV ratio is widely accepted as one of the most important and independent factors associated with elevated 30-day mortality. In patients with a known cardiorespiratory disease, speci-
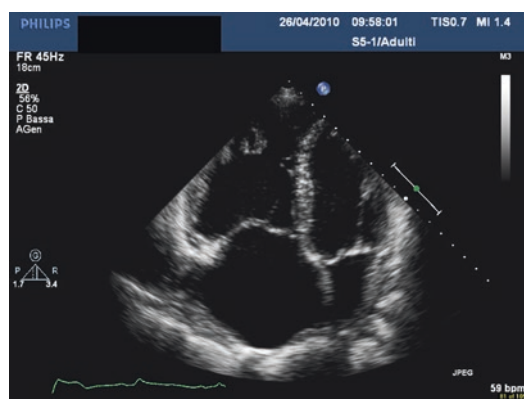
Fig. 34.1 Right ventricular overload

ficity of RV overload criterion decreases from around 80% to 20%.

Several patients with PE have a typical regional pattern of RV dysfunction, characterized by free wall hypokinesis with a normal motion of the apex, known as McConnell's sign. Normal RV apical motion of McConnell's sign is likely due to RV tethering by a normally contracting LV apex. McConnell's sign has a low sensitivity (ranging from 40% to 60%), but its specificity is relatively high (up to 94%) and is associated with an increased clot burden and moderate to severe RV dilatation and dysfunction.

3. Significant RV pressure overload shifts the interventricular septal leftward and reverses septal curvature during systole. This phenomenon may be quantified by eccentricity index, defined as the ratio of the length of two perpendicular minor-axis diameters (anterior-posterior to septal-lateral) of LV short axis. A value more than 1 is abnormal and in one study is associated with poor outcomes in hemodynamically stable patients.

If the patient is hemodynamically stable, the absence of echocardiographic signs of RV overload, which has sensitivity around 60–70%, does not exclude PE, particularly when the clinical suspicion is moderate to high. Nonetheless, it is helpful to identify a low-risk group.

Direct evidence: Signs of RV overload are not specific and may also be found in other cardiac or respiratory diseases as acute respiratory distress syndrome, asthma, chronic obstructive pulmonary disease, pneumothorax, pneumonia, sepsis, myocardial contusion, and cardiac diseases with RV involvement. To have the diagnostic certainty, it is necessary the angio-CT, but TEE may be indicated in critically ill patients that cannot be moved to angiography. TEE visualizes central emboli in about 70% of patients with PE associated with RV dysfunction with high specificity (> 90%).

Differential diagnosis: The absence of signs of RV dysfunction/overload excludes PE as a cause of hypotension, while their presence is highly suggestive of PE and may justify an aggressive approach. Other causes of shock as cardiac tamponade (large pericardial effusion, respiratory variations of transvalvular Doppler, swimming heart), acute valvular regurgitation (severe insufficiency), large myocardial infarction (LV wall motion abnormalities, reduced EF), mechanical complications of acute myocardial infarction (severe mitral regurgitation and papillary rupture, ventricular septal defect), and severe hypovolemia (inferior vena cava collapse) are rapidly detected.

34.1.2 How to Do It

34.1.2.1   Apical 4-Chamber View
(Fig. 34.2)

By 2D echocardiography, an enlarged RV is visualized, and free lateral wall seems severely hypokinetic at inspection. Typically, the RV apex is spared. Atrial and ventricular septa move toward the left ventricle during systole. A movement of the fossa ovalis greater than 1 cm is diagnostic of septal aneurysm, a condition not uncommonly associated with patent foramen ovale (PFO) and with the risk of right to left shunts. After freezing the image, RV and LV end-diastolic diameters and areas are measured. End-diastolic diameter is measured at the midportion of the cavity from the endocardium of the lateral wall to the endocardium of the septum. A RV/LV diameter or area ratio between 0.6 and 0.9/1 indicates a moderate dilatation, while a ratio > 0.9/1 indicates a severe enlargement that is associated with a higher in-hospital mortality. RV end-diastolic and end-systolic areas are quantified, and fractional area change (FAC) is calculated. After unfreezing the image, m-mode is placed on the TV annulus and TAPSE is recorded. A value of RV-FAC < 30% and TAPSE <1.6 confirms RV dysfunction.

Pulmonary arterial systolic pressure is easily estimated by cwd from the velocity of the tricuspid regurgitant jet through the simplified Bernoulli equation. Color flow through the tricuspid valve is activated to visualize a regurgitant jet. Continuous wave Doppler (CWD) is aligned along the jet and velocity is recorded and frozen.

Fig. 34.2 Pulmonary embolism apical 4 chambers view
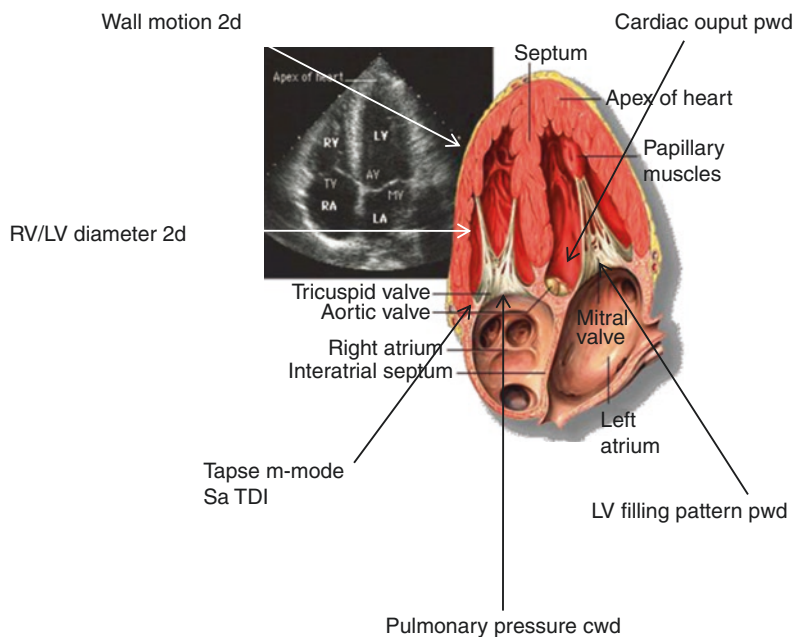
The best envelope is chosen and encircled to measure systolic RA-RV gradient. Right atrial pressure (RAP), estimated from inferior vena cava diameter, is added to the peak gradient to obtain the systolic pulmonary arterial pressure. If spectral Doppler is not well visualized, then 10 ml of agitated saline contrast can be used. Tricuspid regurgitation jet velocities are typically in the range of 2.5–3.5 m/s corresponding to a systolic pulmonary artery pressure (sPAP) of about 40 mm Hg.

The leftward movement of the interventricular septum impairs LV filling, and pulmonary hypertension reduces LV preload. The degree of LV impairment may be evaluated by examination of the diastolic function and cardiac output by positioning pwd first between mitral leaflets and afterward by moving it into the LVOT. E, A waves and DT are measured. A long deceleration time and a E/A ratio > 0.5 are common and indicate an abnormal LV filling. Pwd is obtained at the level of LVOT, immediately under the aortic valve cusps. By tracing the envelope of LVOT, the flow of the velocity-time integral (VTI) is automatically calculated. Stroke volume is obtained by multiplying VTI by aortic area calculated on parasternal long axis.

34.1.2.2 Parasternal Long- and Short-Axis View (Fig. 34.3)

The long-axis view is useful to measure the RV diameter and the aortic area to calculate the stroke volume. RV diameter is measured by m-mode at the end of the diastole. A value >33 mm is considered RV dilatation. Aortic area is calculated from the systolic diameter of LVOT according to the formula. The short-axis view at the level of the left ventricle is ideal to visualize with 2D paradoxical leftward ventricular septal motion and the degree of impairment of LV filling. At end diastole, the anterior-inferior and the septal-lateral diameter can be measured; a ratio between them – eccentricity index – less than 1 is a sign of severe pressure overload. In several cases, moving the probe cranially at the level of the aortic valve allows the visualization of the truncus of the pulmonary artery (PA) and the bifurcation and the proximal tract of right and left PA. In some cases, the thrombus can be identified in the main PA.

34.1.2.3 Subcostal View

The subcostal view is well suited for the measurement of the inferior vena cava diameter. M-mode is placed perpendicular to the vena cava lumen,

Fig. 34.3 Pulmonary embolism parasternal and subcostal view

Leftward motion of ventricular septum 2d

Sfericization index 2d

Right or AP Thrombus 2d

RAP inferior vena cava m-mode
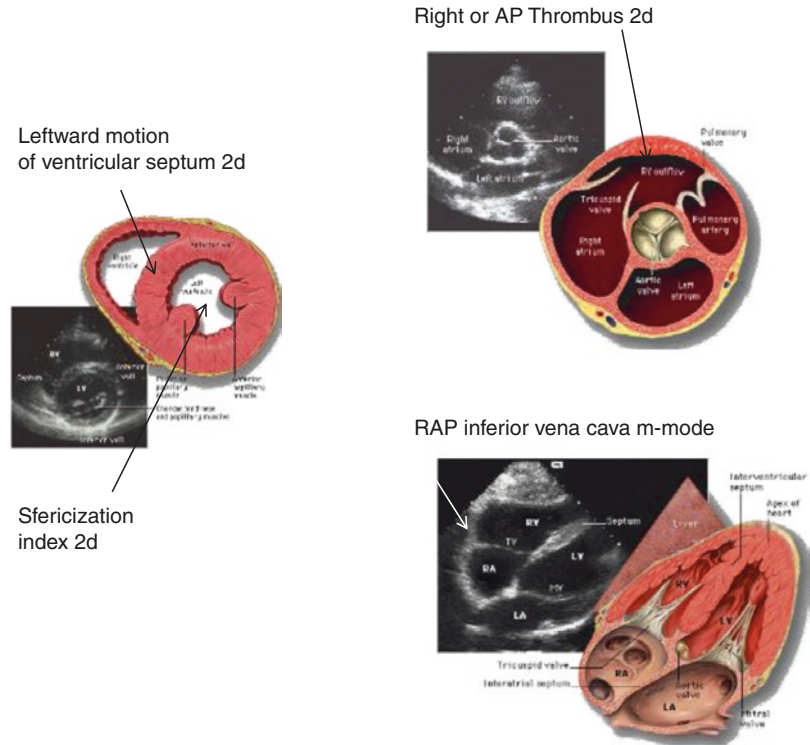
so that its maximal and minimal diameter is measured and right atrial pressure can be calculated according to table.

IVC Diameter cm	SNIFF	RAP mm Hg
<1.5	Collapse	0–5
1.5–2.5	>50%	5–10
	<50%	10–15
>2.5	>50%	15–20
	<50%	> 20

In some cases, by turning the probe clockwise, it is possible to visualize the truncus and the bifurcation of the PA.

TEE is usually needed to confirm the diagnosis of central pulmonary embolism, to assess whether the thrombus is sufficiently proximal to a pulmonary artery to warrant surgical embolectomy, and to visualize any patency of the fossa ovalis. The main views to obtain the visualization of thrombus in the pulmonary artery are the upper esophageal for the pulmonary artery and the mid-esophageal for the RV inflow/outflow tract. In the upper esophageal view, the pulmonary truncus and the right pulmonary artery can

be visualized until branches to the right lung. The proximal tract of left pulmonary artery is obtained by rotation of the probe. The middle portion of the left pulmonary artery is more difficult to investigate because of the interposition of air into the left main bronchus. Nonetheless, the sensitivity of TEE approach remains high (90–95%), because the occurrence of an isolated left pulmonary artery thrombus is uncommon.

Finally, the TE probe is pushed some centimeters downward to achieve the mid-esophageal bicaval view to examine the fossa ovalis. Uncommonly, a thrombus straddling the fossa carrying a high risk of systemic embolism can be visualized.

34.1.3 Risk Stratification and Decision-Making (Fig. 34.4)

Risk stratification achieved by echocardiography and additional to clinical findings has two goals: (1) the recognition of low-risk patients who can
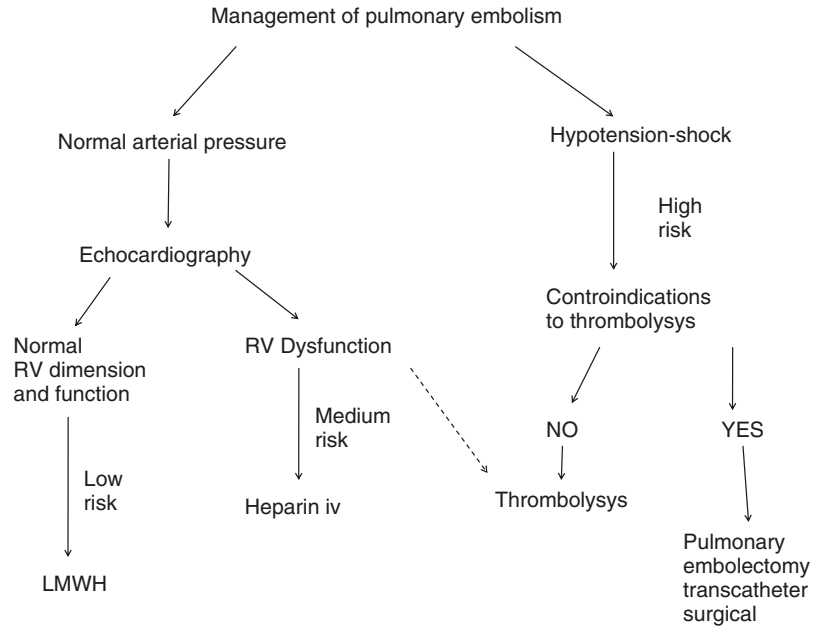
be managed as outpatients and (2) the identification, between hemodynamically stable subjects, of a subgroup with RV dysfunction at intermediate high risk.

Hemodynamically stable patients with normal RV dimensions and function and normal pulmonary artery pressure are a low-risk group with an in-hospital mortality less than 1%. They do not require an ICU admission and could be eligible for early discharge and home treatment with low molecular weight heparin or NOAC.

The optimal management of *stable patients with RV dilatation/dysfunction at intermediate risk is disputable*. In-hospital mortality in these patients is higher than in the previous group, ranging between 5% and 10%, but to date there is no compelling evidence of benefits of fibrinolytic agents on survival. In these patients, the composite primary outcome of early death or hemodynamic decompensation was reduced after treatment with a single intravenous bolus of tenecteplase. However, tenecteplase was also associated with a significant increase in the risk of bleeding. IV heparin is still generally considered the treatment of choice. Thrombolytic therapy may be considered in selected high-risk young patients, if the risk of bleeding is not elevated (Fig. 34.5). A strategy using reduced-dose rtPA seems to be

effective and safe. An alternative approach may consist of local, catheter-delivered, ultrasound-assisted thrombolysis using small doses of a thrombolytic agent. At present, it is not known if an early inotropic treatment of normotensive patients with severe echocardiographic RV dysfunction could decrease the progression toward shock and in-hospital mortality.

In high-risk patients with hypotension or shock, admission in ICU is mandatory, and thrombolytic therapy is the first-line treatment, unless there are absolute contraindications to its use. If thrombolysis is absolutely contraindicated or has failed to improve hemodynamics, surgical or percutaneous pulmonary embolectomy is valuable therapeutic options. In emergency situations, TEE showing the presence of a thrombus in the main pulmonary arteries is the only image modality to indicate this approach.

Echocardiography can also identify two other specific markers of high-risk PE and increased mortality: patent foramen ovale and right heart thrombi. Patent foramen ovale is associated with right to left shunt with two consequences: (a) worsening of hypoxemia, pulmonary hypertension, and RV overload, particularly in patients who have undergone mechanical ventilation, and (b) the risk of cerebral or peripheral embolism due to

Fig. 34.5 Management of pulmonary embolism with RV dysfunction
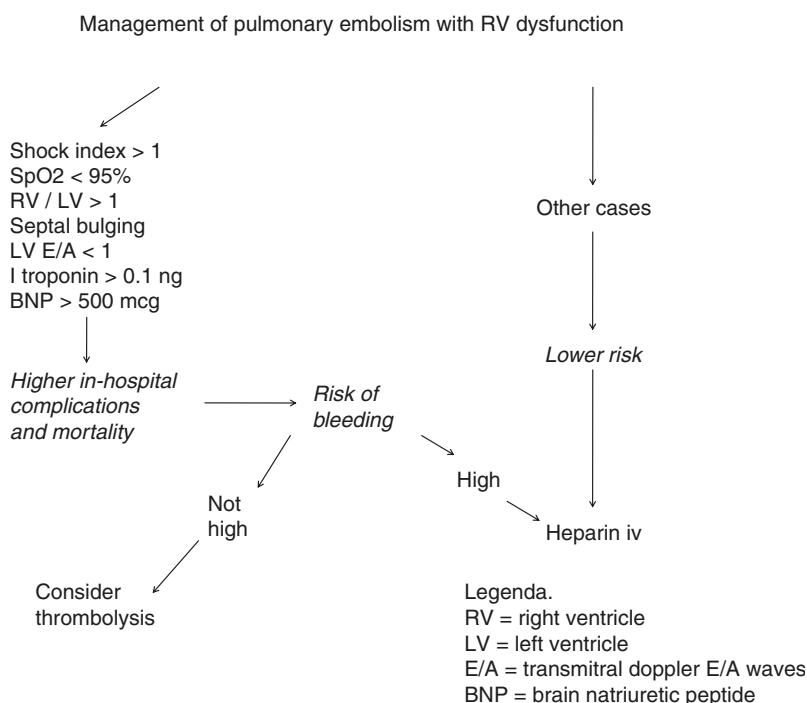
right thrombus crossing to the systemic circulation. Right atrial thrombi are found in more compromised patients and are a marker of worse prognosis (mortality rate of 21% vs 11%; international registry). There are currently no data on the efficacy of thrombolytic treatment in improving prognosis.

34.1.4 Assessment of Treatment

Echocardiography is useful in the evaluation of the efficacy of antithrombotic drugs on thrombus dissolution and to optimize supportive vasoactive treatment on RV function, PA pressure, LV filling, and stroke volume.

34.2 Acute Coronary Syndromes (ACS)

34.2.1 STEMI and NSTEMI

34.2.1.1 Indications
P*atients with suspected acute myocardial infarction (AMI)* have three main indications to TTE:

1. The differential diagnosis between AMI (regional wall motion abnormalities), myocarditis (diffuse hypokinesia), and type A aortic dissection with involvement of right coronary ostium (ascending aorta enlargement, aortic insufficiency, pericardial effusion, inferior wall motion abnormalities) and acute pericarditis (normal wall motion and in some cases pericardial effusion).

2. The diagnosis of STEMI in doubtful cases: in patients with anterior ST depression, TTE allows the identification of the subgroup with posterior STEMI (posterior regional wall motion abnormalities) undergoing early reperfusion. If the baseline ecg is not diagnostic, segmental wall motion abnormalities are highly suggestive of AMI or acute myocarditis.

3. The identification of patients at higher risk: severe depression of LV ejection fraction (< 35%), increased atrial (E/e' ratio > 14) and pulmonary pressure (tricuspid Doppler), pulmonary b-lines (extravascular lung water), RV dysfunction (RV hypokinesia, tapse <18), and coexistence of severe mitral (functional or organic) or aortic valve disease are all signs of

impending hemodynamic worsening. In these patients, urgent PCI, avoidance of IV beta-blockers, and use of diuretics, inotropic agents, and mechanical support should be considered.

34.2.1.2 How to Do It

Diagnosis of ischemia. Myocardial ischemia is characterized by regional wall motion abnormalities, described as hypokinesia, akinesia, and dyskinesia. Each segment is scored from 1 (normal) to 4 (dyskinesia). Hypokinesia is defined as a reduced endocardial motion and wall thickening in systole, akinesia as the absence of inward endocardial motion and systolic thickening, and dyskinesia as outward motion or bulging during systole, usually associated with a thin (thickness < 5 mm), scarred (brighter) myocardium.

Site of ischemia and identification of culprit lesion (Figs. 34.6 and 34.7). From base to apex, the LV is typically divided into three segments: basal, mid-ventricular, and apical. In the parasternal long-axis view, the basal and mid segments of anterior interventricular septum (left anterior descending, LAD) and of the posterior LV (circumflex, CX) wall are visualized. In the short-axis views, all LV segments from base to apex are visible: in clockwise order, the anterior (LAD), lateral (CX), posterior (CX or right coronary-RCA), and inferior (RCA) wall, inferior septum (RCA), and anterior septum (LAD). In the 4-chamber view, the inferior septum (RCA), the anterior apex (LAD), and the lateral wall (CX) are visualized, in the 2-chamber view the anterior (LAD) and inferior wall (RCA), and in the 3-chamber view the anterior septum (LAD) and the posterior wall (CX or RCA). In the subcostal 4-chamber view, the inferior septum (RCA) and lateral wall (CX) are seen.

34.2.2 Takotsubo Syndrome

Takotsubo syndrome (TTS) presents clinically as an ACS but differs from STEMI because epicardial coronary arteries are normal and left
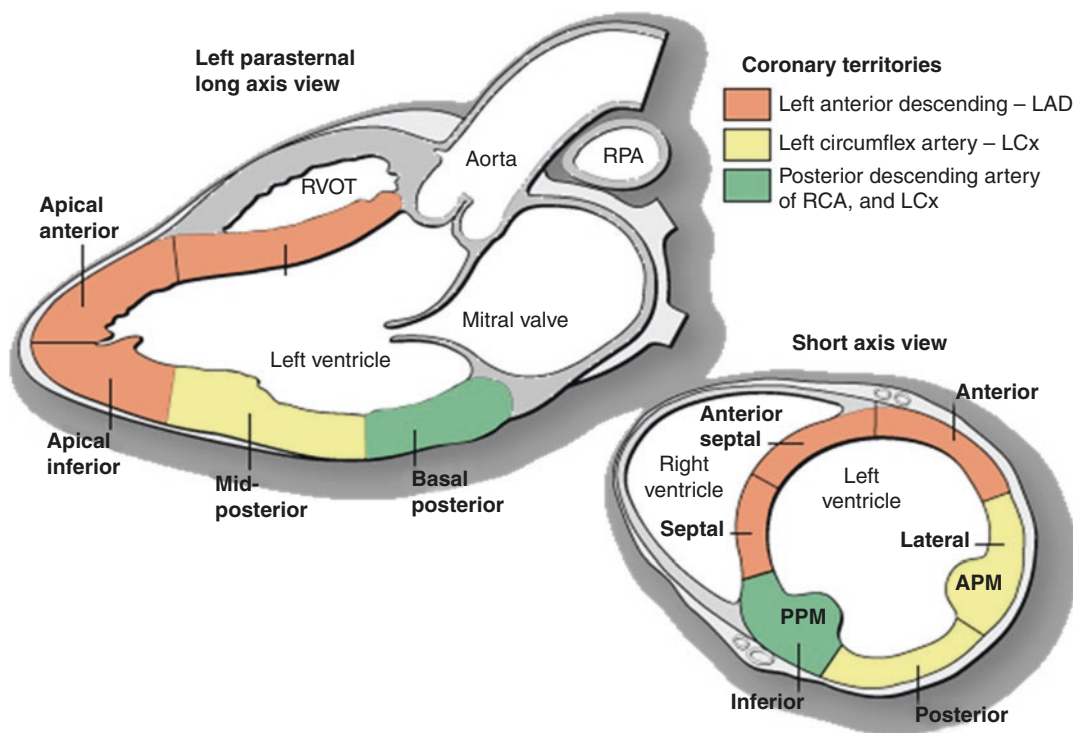
Fig. 34.6 Coronary vascularization parasternal views
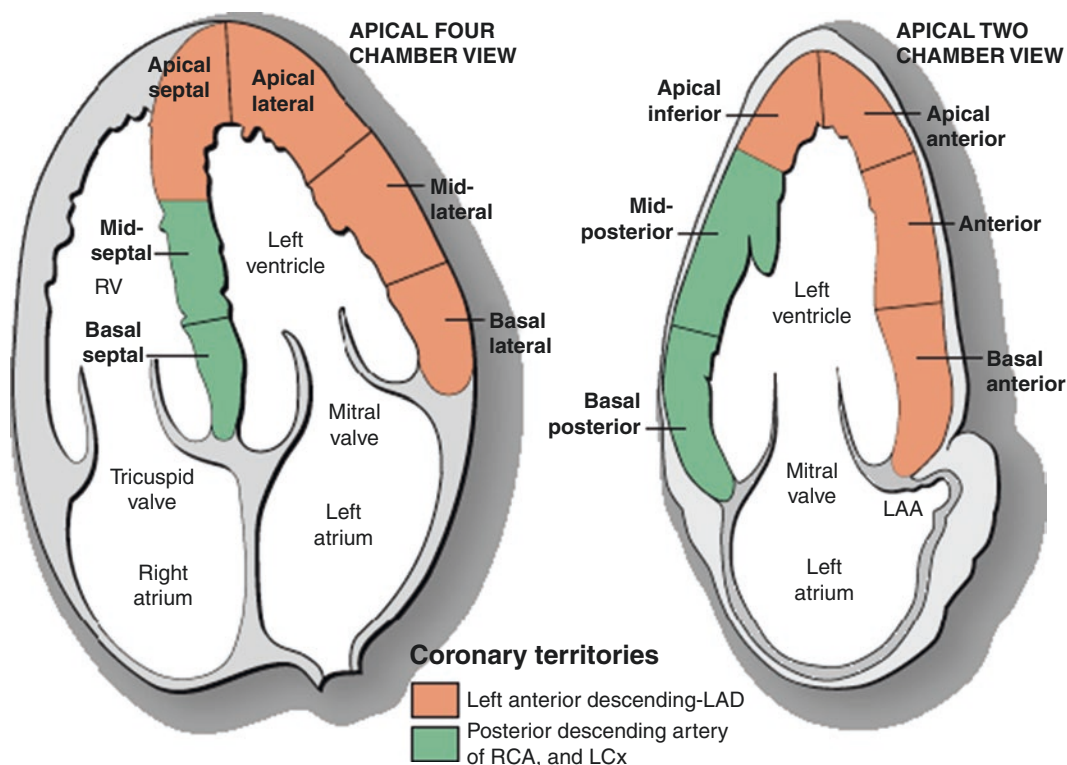
Fig. 34.7   Coronary vascularization apical view

ventricular dysfunction extends beyond a single coronary artery territory and recovers completely within days or few weeks. Despite the absence of coronary artery disease, clinical course is complicated in about 20% of the cases, mostly by acute heart failure and cardiogenic shock, and in-hospital mortality is about 4–5%. TTS is a unique and reversible acute type of LV dysfunction frequently precipitated by a stressful event, whose pathogenesis seems to be related to catecholamine-mediated myocardial stunning. Catecholamine, through multiple mechanisms, e.g. direct toxicity, adrenoceptor-mediated damage, epicardial and microvascular coronary vasoconstriction, and/or spasm, increases cardiac workload, to myocardial damage.

The typical characteristics of TTS are the following:

Clinical features: Postmenopausal women account for 80–90% of cases. A severe emotional or physical stress, an acute illness, or a surgery

procedure usually precedes symptoms in approximately 70% of cases.

Ecg: ST segment elevation usually occurs in the anterior precordial leads. Some ECG criteria may be helpful to discriminate apical ballooning from anterior STEMI: a lesser magnitude of ST segment elevation, no ST segment elevation in V1, ST segment depression in aVR, T wave inversion in anterior leads, and prolongation of QTc interval.

Lab: Increase of troponin is usually mild or moderate and CK are not substantially elevated.

Echocardiography plays a key role in differential diagnosis with anterior STEMI and in identifying the complications.

34.3   Differential Diagnosis

In the classical form of apical ballooning (80% of cases), echo reveals a distinctive pattern: wall

motion abnormalities (hypo or akinesia) involve the mid and apical segments of the whole LV, beyond the territory of distribution of a single coronary artery, sparing the basal segments, which are often hyperkinetic. LV dysfunction assessed by speckle tracking is circular, and mid and apical longitudinal strain is more severely impaired, two findings completely different from anterior STEMI.

Typically, the extension of areas of asynergy is disproportionate when compared to the degree of ST elevation and small troponin release. A reduced ventricular function (mean EF about 40%) is present in most (80%) patients. A cutoff value of wall motion score index >1.75 predicts TTS with a positive predictive value of 100%. Interestingly, a troponin-EF product (EF x peak troponin I level) > 250 had a negative predictive value of 94% and positive predictive value of 88% to differentiate a true STEMI (>250) from TTS (<250).

Using a high-frequency transducer, distal left anterior descending artery may be visualized in a modified 2-chamber view. Color and Doppler flow through the LAD is absent in anterior STEMI whereas is detectable in TTS and it may be helpful when coronary angiography is not feasible.

Some morphological variants are increasingly recognized where hypo/a-kinesis is limited to the mid or basal segments, sparing the apex (defined as "inverted" TTS). Inverted TTS is more common after acute cerebral disease, brain injury, or pheochromocitoma. Speckle tracking changes have more sensitivity than EF impairment, and it may be critical in patients with subarachnoid hemorrhage in which cardiac dysfunction remains a major cause of adverse outcome.

34.4 Complications

The three main complications can be well visualized by TTE:

(1) RV involvement is present in up to 18–34% of patients. The most affected segments are the apical, lateral (apical 4-chamber view), and anterior (parasternal long and short axis). Standard parameters of longitudinal function (TAPSE, Sa) may be reduced but in some cases, because of the hyperkinesis of basal segment, may be falsely normal. RV dysfunction is associated with a lower LVEF (between 35% and 45%) and with a higher incidence of complications such as congestive heart failure, hemodynamic instability, intra-aortic balloon pump requirement, cardiopulmonary resuscitation, and prolonged hospitalization. Many patients with RV involvement have pleural effusions. (2) Dynamic left ventricular outflow tract obstruction (LVOTO) (14–25% of patients) associated with mitral regurgitation due to systolic anterior movement, caused by hyperkinesia of the basal segments. This mechanism is especially observed in patients presenting with hypotension and acute heart failure. Patients at higher risk for LVOTO are elderly women with an abnormal basal-mid septal thickness – the so-called "sigmoid" septum – and with small LV cavity due to concentric hypertrophy, high levels of catecholamine, or acute hypovolemia. In these circumstances, more attention should be paid because of the occurrence of malignant arrhythmias or LV wall rupture. (3) LV mural thrombus formation in the akinetic apical segment is relatively rare (2–8%), but it must be recognized since these patients at high risk of stroke or systemic embolization (up to 30%) require anticoagulation. Mechanical complications, including ventricular septum or papillary muscle rupture, have been rarely reported, but they must be excluded by TTE, especially in patients with hemodynamic instability.

Age > 70 yrs., the extension of regional wall motion abnormalities, regional mid-lateral strain (worse than – 7), the reduction of EF (< 40%), a larger LV and left atrial volumes, an increased LV filling pressure (high E/e' ratio), and the presence of functional mitral regurgitation are predictors of adverse outcome.

Repeated echocardiographic examinations show a complete recovery.

Echo-guided decision-making: Up to now, no trial data are available. Therefore, optimal management has not been definitively established, but supportive therapy usually leads to a relatively prompt and spontaneous recovery. Diagnosis

requires a high index of suspicion, particularly in hospitals not equipped with catheterization laboratories. Inappropriate administration of fibrinolytic drugs may be harmful without conferring any benefits. Beta-blockers and ACEi may be considered in hemodynamically stable patients with LVEF<45% and in patients with atrial or ventricular tachyarrhythmias. LV thrombi that develop 2–5 days after symptom onset may resolve within 2 weeks of therapeutic anticoagulation. In patients with hemodynamically significant LVOTO, treatment with a beta-blocker, eventually associated with norepinephrine, should be considered. In subjects with congestive heart failure, diuretics are usually effective. Cardiogenic shock, after LVOTO has been excluded by echocardiography, is treated empirically with inotropic agents, IABP, and in some cases LVAD.

34.5 Aortic Dissection

Integrated echocardiography (TT and TE) may provide the diagnosis and type (A, B, B retrograde) of aortic dissection and its main complications, quickly, at bedside, with a sensitivity and specificity approaching 100%.

Diagnosis and differential diagnosis. The evaluation starts with TTE approach that is useful to exclude other diagnosis and to suspect type A aortic dissection (Fig. 34.8). Other causes of chest pain such as myocardial infarction (regional wall motion abnormalities), pericarditis (pericardial effusion), and pulmonary embolism (pulmonary hypertension, RV dilatation, and dysfunction) are excluded by TTE. Beware of traps: regional wall motion abnormalities simulating myocardial infarction due to coronary thrombosis, especially when localized to the inferior wall, may be the consequence of the involvement of the ostium of the right coronary artery by type A dissection. This complication is uncommon, but it must be well recognized to avoid the risk of aortic rupture as the consequence of thrombolytic therapy or coronary angiography. Pericardial effusion is usually small in pericarditis, while it is large with signs of cardiac tamponade in aortic dissection.

Echocardiographic signs highly suggestive for type A aortic dissection are dilatation of the ascending aorta, new-onset aortic valve regurgitation, and pericardial effusion. The visualization of an intimal flap separating the true from the false lumen in the ascending (type A), abdominal aorta (type B) or in both (type A) is the diagnostic hallmark of aortic dissection. Sensitivity of TTE is about 85% (type A) and 55% (type B), so TEE approach is usually needed to confirm the diagnosis. TEE also provides more information that is useful for surgical planning. The TEE blind zone, due to the interposition of the trachea between the esophagus and the upper ascending aorta, does not represent a real problem because the probability of dissection confined to this location is extremely low.

Site of intimal tears and classification of dissection. Intimal tears can be localized in 78–100% of patients, usually above the sino-tubular junction (type A) or just distal the origin of the left subclavian artery (type B). Ascending aorta or arch involvement with primary tear beyond left subclavian artery identifies patients with retrograde type B dissection.

Differentiation between true and false lumen. True and false lumen can be identified easily by TEE. True lumen size is usually smaller, has a systolic expansion and systolic antegrade flow, and usually is localized in the inner contour of the aortic arch. False lumen is larger and has low flow, and thrombi are not uncommon.

34.5.1 Complications

Extravasation: Pericardial effusion occurs in up to 20–30% of patients with ascending aorta dissection. It may be due to aortic rupture into the pericardium or to irritation of the visceral pericardial layer secondary to aortic intramural hematoma. Cardiac tamponade is a sign of poor prognosis with in-hospital mortality reaching 50%. Among patients with type B dissection, a left pleural effusion identifies a group at higher risk of aortic rupture. Periaortic hematoma is well visualized only by TEE and appears as a collection of fluid around the aorta, near the site of the acute dissec-
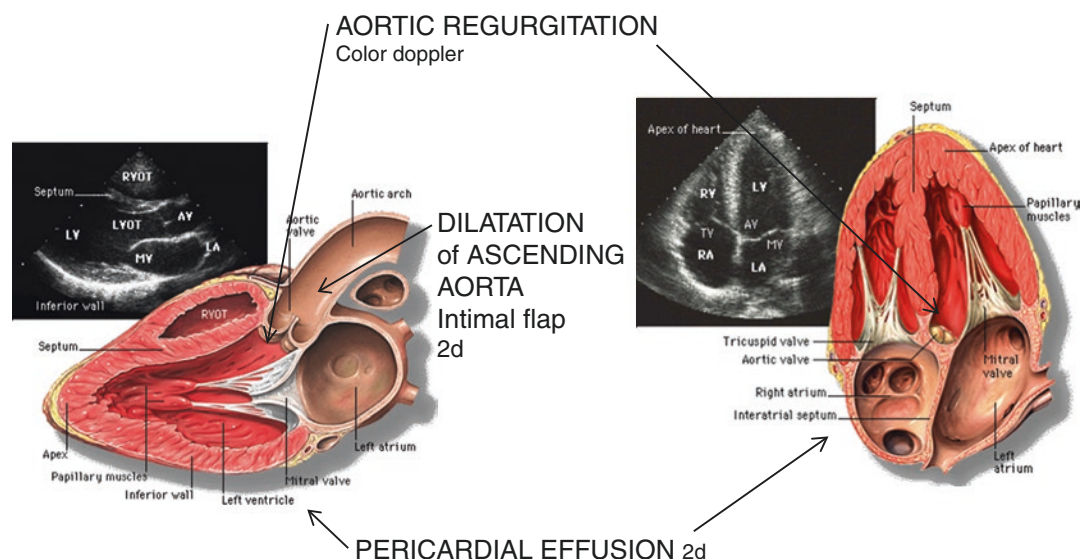
Fig. 34.8 Transthoracic echo in suspected aortic dissection

tion. The hematoma is a harbinger of impending rupture.

Aortic valve regurgitation: Both TTE and TEE can accurately quantify the diameter of the ascending aorta and the degree of aortic regurgitation. TEE usually adds more information on the potential mechanisms of regurgitation, distinguishing valves with geometric distortion amenable to repair (dilatation of sino-tubular junction, prolapse of dissection flap) from those with leaflet prolapse due to destruction of attachments or structural disease (bicuspid or degenerative thickening) that require replacement.

Coronary involvement may be due to the propagation of the dissection to the coronary ostia (usually the right) or, more frequently, to preexisting coronary artery disease. Coronary involvement is suggested by regional wall motion abnormalities. TEE permits to establish whether the coronary ostia originate from the true or false lumen and if the dissection involves the coronary arteries. 3D TEE clearly depicts no coronary involvement better than CT scan. Wall motion abnormalities in the absence of coronary ostia involvement by dissection are indicative of preexisting coronary artery disease. These informations are of invaluable importance in the decision-making to perform myocardial revascu-

larization, considering that coronary angiography is hazardous (risk of aortic rupture, renal failure) and not routinely used.

The aortic arch and the ostia of sovra-aortic vessels are better visualized by TEE. In the evaluation of a surgical approach involving the aortic arch, it is important to assess the presence of an intimal tear in the arch, to distinguish between an entry and a reentry tear, and to establish whether flow in the innominate artery and in the left common carotid artery arises from the true or false lumen.

Real-time 3D TEE provided more detailed informations about the involvement of aortic valve and coronary ostia by dissection flap that may be useful for a better intraoperative management and surgical repair.

34.5.2 How to Do It

34.5.2.1 Transthoracic Echocardiography

In the evaluation of suspected type A aortic dissection, TTE should be performed as soon as possible, with all standard (i.e., left and right parasternal, apical, subcostal, suprasternal and abdominal) and off-axis views, with the patient in the supine and in both the left and right lateral

decubitus to evaluate most part of the thoracic aorta.

Parasternal long-axis view. 2D echocardiographic inspection allows the diagnosis of type A aortic dissection by visualizing the intimal flap within the dilated aorta or indirect signs highly suggestive of aortic dissection: dilatation of the ascending aorta, new onset aortic valve regurgitation, and pericardial effusion.

Pericardial effusion is visualized as a dark space between the echogenic pericardium and the heart. A heart swinging into the pericardial fluid in a patient with pulsus paradoxus is suggestive of cardiac tamponade. The best view to visualize the hemodynamic effects of cardiac tamponade is the apical 4-chamber view.

2D echocardiography inspection permits the immediate visualization of the ascending aorta dilatation. The aortic diameters ("annulus," Valsalva sinuses, sino-tubular junction, and tubular tract) are obtained by m-mode or 2D applied after freezing the image. The severity and the site of dilatation are recorded. Aortic enlargement, due to intramural hematoma consequent to dissection, is usually located in the tubular tract of the ascending aorta. Dilatation involving the sinuses of Valsalva is a common occurrence in younger patients affected by connective tissue diseases. The right parasternal or high left parasternal views allow a better visualization of the ascending aorta in some cases.

By positioning color flow into LVOT, aortic regurgitation is visualized and quantified by the vena contracta method. Direction of the jet may be important to differentiate the various mechanisms of valve regurgitation.

Parasternal short-axis view. At the level of the aortic valve, the morphology of the cusps, the presence of a bicuspid aortic valve, and the diameter of aorta can be assessed. Angulation of the transducer toward the LV apex allows the evaluation of the extension of the pericardial effusion and of LV regional wall motion and function. A swinging heart image caused by cardiac tamponade from aortic rupture may be easily appreciated.

Apical views. Apical views are useful to evaluate pericardial effusion, regional wall motion, LV and RV function, and severity of aortic insufficiency. In the 4-chamber view, the collapse of the right cavities by cardiac tamponade is immediately visualized. LV and RV function are quantified in terms of LV-EF, RV-TAPSE, and RV-FAC. Usually RV and LV function are normal. A depressed EF may be due to acute-severe aortic regurgitation (diffuse hypokinesia), the effect of IV beta-blockers (diffuse hypokinesia), regional wall motion abnormalities consequent a previous AMI (akinesia or scar), or ongoing myocardial ischemia (asynergy without scar). RV dysfunction may be ascribed to acute dissection of the right coronary ostium if it is associated with inferior asynergy in the apical 2-chamber view or to a preexisting lung disease with RV hypertrophy and dilatation. Wall motion abnormalities are investigated in the 4-, 2-, and 3-chamber views. Asynergy of the inferior wall is suggestive of right coronary dissection. Abnormal motion of the other walls is usually associated with coronary artery disease. The presence and the degree of aortic regurgitation are assessed by color Doppler in the 4- and 3-chamber views.

Subcostal and abdominal views. These views easily allow the visualization of pericardial effusion (dd with pleural effusion) and of the swinging heart phenomenon. By rotation of the probe to the vertical position, the abdominal aorta can be seen, and the intimal flap dividing the true from the false lumen can be identified.

Suprasternal view. In the suprasternal view, the arch, the origin of the neck vessels, and the proximal descending aorta can be imaged, and the intimal flap and tear may be visualized.

Pleura. With the patient in the sitting position, placing the probe along the back of the thorax, pleural effusion is an anechoic space between the probe and the lung. Its presence is suggestive of complicated type B dissection.

Transesophageal echocardiography (Fig. 34.9). TEE is the gold standard for the diagnosis of aortic dissection with a sensitivity and specificity reaching 100%.

Medio-esophageal long-axis view for the ascending aorta. TEE examination starts with this view because it allows the diagnosis of type A dissection. In fact, 2D examination shows the

DIAGNOSIS of TYPE A DISSECTION: Intimal flap and tear
DEGREE and SITE of AORTIC DILATATION
DEGREE and MECHANISM of AORTIC REGURGITATION
RIGHT CORONARY OSTIAL OBSTRUCTION

MORPHOLOGY of
the AORTIC VALVE

ARCH INVOLVEMENT
Rentry or entry tear

i. ME AV LAX

h. ME AV SAX

s. UE aortic arch LAX   t. UE aortic arch SAX

DIAGNOSIS of TYPE
B DISSECTION

REGIONAL WALL MOTION
LV / RV FUNCTION

d. TG mid SAX   a. ME four chamber

q. desc aortic SAX
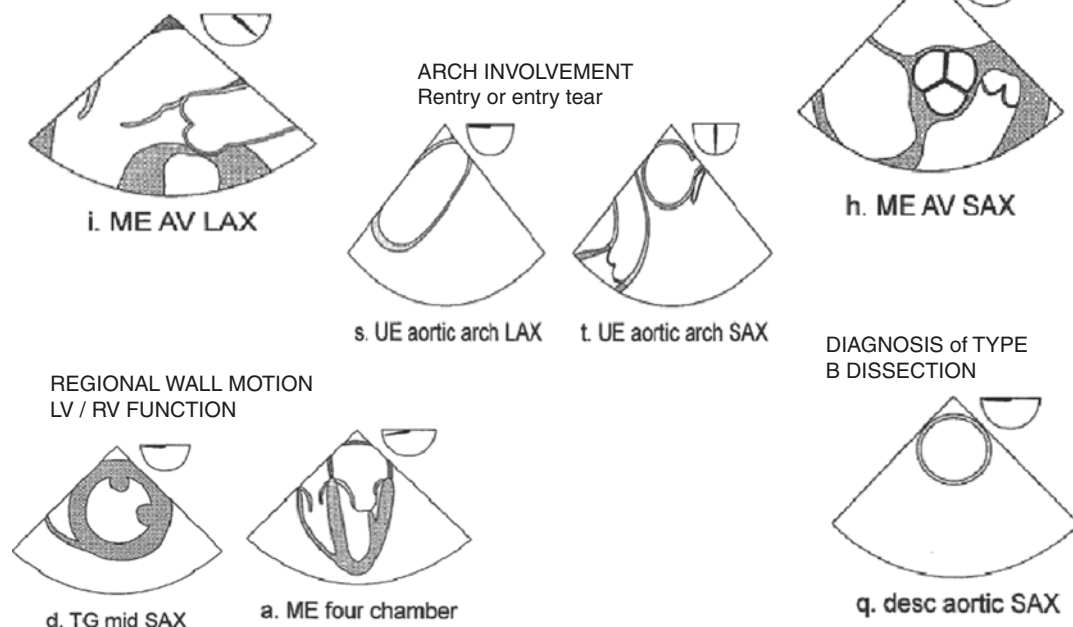
Fig. 34.9 Transesophageal echo in aortic dissection

classic sign of aortic dissection, i.e., the presence of an intimal flap, which appears as a mobile linear echo separating the true from the false lumen. In most cases of type A dissection, a careful examination shows the intimal entry tear which appears as an interruption into the flap crossed by turbulent color flow, located in the tubular tract of ascending aorta usually few centimeters above coronary ostia. The less common extension of the dissection to the sinuses of Valsalva and to the right coronary ostium is easily visualized. When the entry tear is not found in the ascending aorta or the aortic arch, it is usually located in the blind segment.

After freezing the image, all diameters of the ascending aorta should be measured: annulus, Valsalva sinuses, sino-tubular junction, and tubular tract. If the diameter of the Valsalva sinuses exceeds 45 mm, the more complex composite graft operation is required. A careful 2D echocardiography inspection of the morphology and the movements of the valve cusps is helpful in

distinguishing functional from organic regurgitation and to investigate the mechanisms of insufficiency. The presence of a bicuspid valve is suspected from systolic doming of the conjoint cusp. Cusp prolapse and the dissection flap are well visualized. Vena contracta imaged by Doppler color flow mapping predicts the severity of the regurgitation; moreover, information concerning jet direction (central versus eccentric) combined with morphological data are useful to characterize the mechanism of regurgitation.

Medio-esophageal short-axis view of the aortic valve. Short-axis view is complementary but superior to long-axis view in distinguishing a normal from a diseased valve, especially in the evaluation of bicuspid aortic valve. The raphe is well visualized in diastole; in systole, the orifice has a characteristic elliptical shape and "fishmouth" appearance.

Medio-esophageal and trans-gastric short-axis view. These views are useful to evaluate regional wall motion and pericardial effusion.

Descending thoracic aorta. By turning the probe toward the descending aorta, the extension of the dissection to thoracic and abdominal aorta and the presence of reentry tears become visible.

Aortic arch. By withdrawing the probe from the descending aorta, the aortic arch can be well visualized, and it is possible to identify the origin of the neck vessels from the true or false lumen, the extension of the dissection into the ostia of innominate and left carotid arteries, and the presence of a tear. To decide the most appropriate surgical approach, it is fundamental to distinguish the more common reentry (primary tear in ascending aorta) from entry (no tear in ascending aorta) tear.

True lumen vs *false lumen.* The true lumen is usually smaller, the flow is greater, and anterograde during systole and flap moves toward the false lumen. The presences of echo contrast or ongoing thrombosis are specific of false lumen. When the entry tear is large, flow is similar in both lumen.

34.5.3 Timing of Sequence Examination

The primary objectives of the echocardiographist are to identify an intimal flap and delineate the extent of dissection, distinguishing type A, whose treatment is surgical, from type B, whose treatment is medical. The diagnosis of type A dissection and of type B dissection complicated by pleural effusion must be established as soon as possible, cardiac or vascular surgeon must be alerted immediately, and all the necessary procedures propaedeutic to surgery must be carried out without delay. Meanwhile, secondary evaluations must be made to provide important informations for the anesthesiologist and the surgical planning.

The sequence of examination must be tailored on the specific clinical situation.

In *hypotensive patients* (it is always necessary to check arterial pressure on both arms to make sure that is not pseudo-hypotension), it is advisable to start with the subcostal view to visualize at the same time cardiac tamponade and an intimal flap in the abdominal aorta. If both compli-

cations are present, the diagnosis is type A aortic dissection with rupture in the pericardial space, a surgical emergency. More uncommonly, if the intimal flap is visualized but cardiac tamponade is not present, the apical 5-chamber view must follow in search of other more frequent causes of hypotension, such as a massive aortic regurgitation or a severe LV dysfunction.

In *stable patients*, TTE can be performed using the standard sequence of projections or starting from the subcostal and suprasternal views to identify the aortic dissection in the shortest possible time.

After TTE examination has been completed, TEE is needed to confirm the diagnosis of aortic dissection or to identify other types of acute aortic syndromes (hematoma or aortic ulcer), usually poorly visible by TTE, and to provide further information useful for the decision-making.

If the suspicion of type A aortic dissection is high, TEE examination should be performed in an environment where potentially life-saving cardiac surgery can be done without delay. To reduce the catastrophic risk of aortic rupture during esophageal intubation, continuous arterial pressure monitoring and deep sedation are mandatory.

34.5.4 Echo-Guided Decision-Making

The goal of surgery in type A aortic dissection is to replace the tubular tract of the ascending aorta with a supracoronary aortic replacement to prevent early death from aortic rupture, coronary dissection, and aortic valve insufficiency. More complex repairs such as aortic valve replacement, coronary revascularization, composite graft procedure, and arch replacement do not influence in-hospital mortality but improve medium-term event-free survival. Their indications are based, beyond age and concomitant diseases, on the extent of the dissection, the site of the entry tear, and the surgical skill.

Type of dissection. Acute type A aortic dissection is a highly lethal disease with an early mortality rate of 1–2% per hour. In most patients with type A acute aortic dissection, emergent supra-

coronary replacement of the ascending aorta is the only therapeutic option. TEVAR is feasible with promising early results in selected poor candidates for surgical repair. In retrograde type B dissection, medical approach is preferred in stable patients with ascending false lumen thrombosis and ascending aorta diameter < 55 mm; surgical intervention and total arch replacement are suggested for a no thrombosed false lumen, severe dilatation of ascending aorta or aortic arch, and aortic valve regurgitation. Medical therapy is preferred as the initial treatment of type B dissection, but, in the presence of echocardiographic signs of aortic impending rupture (pleural effusion, periaortic hematoma), interventional options (stenting or surgery) must be considered.

True lumen vs *false lumen*. The distinction between the true and false lumen has surgical relevance when the coronary arteries and/or supra-aortic vessels originate from the false lumen (see below). It is also useful to guide safe cannulation in type A and endovascular graft positioning in type B aortic dissection.

Fluid extravasation. Pericardial or pleural effusion and periaortic hematoma are signs of impending aortic rupture. All preoperative procedures must be expedited. Immediate surgery is mandatory. In type B aortic dissection, the presence of a pleural effusion shifts from medical to interventional therapy. Beta-blocking agents (dangerous hypotension) and coronary angiography (time consuming) should be avoided. Smooth induction is recommended. Sternotomy must be performed after femoral or axillary cannulation for extracorporeal circulation.

Aortic regurgitation. If aortic insufficiency is acute (aortic valve of normal morphology) and the degree of regurgitation is severe, there is a high risk of pulmonary edema; beta-blockers are contraindicated, and tracheal intubation might be considered. In elderly or in patients with a history of CAD, vasodilators should be used with caution because of the risk of myocardial ischemia due to further decrease in diastolic aortic pressure. Patients with severe aortic valve regurgitation, even when the cusps are normal, are best

treated by aortic valve replacement (better 5 yrs. event-free survival). More uncommonly (around 5% of cases with calcified or prolapsing bicuspid valve), valve replacement is necessary because of preexisting valve disease. After weaning from cardiopulmonary bypass, TEE is used to evaluate aortic continence after valve-sparing operation.

Aortic root involvement. In the presence of an aneurysm of the aortic root (>45 mm), which usually is associated with Marfan syndrome, or of a dissection involving the sinuses of Valsalva, a skillful surgeon performs a composite graft replacement (around 10% of cases). The choice between the techniques of valve sparing (David operation) and valve replacement (Bentall operation) depends on the morphology of aortic valve and severity of aortic regurgitation. David procedure is preferred when the aortic cusps are normal and the degree of insufficiency is less than severe. In the other cases Bentall operation is recommended.

Tear in the aortic arch. Surgical approach to the aortic arch may be different in reentry and entry tears. Hemiarch replacement, without neck vessels reimplantation, is more easily performed and is indicated when the reentry tear is in the proximal tract of the arch. More complex total resection of the aortic arch with hybrid stent-graft procedures and reimplantation of the neck vessels is preferable in the presence of a primary entry tear involving the great curvature or a dilatation greater than 45 mm. Some skillful surgeons choose to perform extended arch repair also in young patients with Marfan syndrome to reduce the need for later arch resection. Open stent graft is used for tears distal to the left subclavian artery.

Myocardial ischemia. The management of patients with abnormal wall motion abnormalities on TTE has not been standardized. Coronary angiography may be applied, but it is dangerous (false lumen cannulation) and time-consuming (high risk of aortic rupture in the first hours from symptoms onset). Most surgeons perform coronary revascularization based on the site of wall motion abnormalities and intraoperative coronaries inspection.

Suggested Reading

Baliga RR, Nienaber CA, Bossone E, Oh JK, Isselbacher EM, Sechtem U, Fattori R, Raman SV, Eagle K. The role of imaging in aortic dissection and related syndromes. JACC Cardiovasc Imag. 2014;7:406–24.

Citro R, Rigo F, Ciampi Q, D'Andrea A, Provenza G, Mirra M, et al. Echocardiographic assessment of regional left ventricular wall motion abnormalities in patients with tako-tsubo cardiomyopathy: comparison with anterior myocardial infarction. Eur J Echocardiogr. 2011;12:542–9.

Citro R, Rigo F, D'Andrea A, Ciampi Q, Parodi G, Provenza G, et al. Echocardiographic correlates of acute heart failure, cardiogenic shock and in-hospital mortality in tako-tsubo cardiomyopathy. JACC Cardiovasc Imaging. 2014;7:119–29.

Citro R, Lyon AR, Meimoun P, Omerovic E, Redfords B, et al. Standard and advanced echocardiography in Takotsubo cardiomyopathy: clinical and prognostic implications. J Am Soc Echocardiogr. 2015;28:57–74.

Dahlan T, Alenezi F, Samad Z, Rajagopal S. Echocardiography in the risk assessment of acute pulmonary embolism. Semin Resp Crit Care Med. 2016;38:18–28.

Fraser AG, Tan CNH. Perioperative transesophageal echocardiography for aortic dissection. Can J Anesth. 2014;61:362–8.

Fremont B, Pacouret G, Jacobi D, et al. Prognostic value of echocardiographic right/left ventricular end-diastolic diameter ratio in patients with acute pulmonary embolism*. Results from a monocenter registry of 1416 patients. Chest. 2008;133:358–62.

Goldstein SA, Evangelista A, Abbara S, Arai A, Asch FM, Badano LP, et al. Multimodality imaging of disease of the thoracic aorta in adults: from the American society of echocardiography and the European association of cardiovascular imaging. J Am Soc Echocardiogr. 2015;28:119–82.

Intraoperative TEE provides incremental information in many patients leading to change in surgical planning in around fourty percent of cases, Thorsgard ME, Morrisette GJ, Sun B, Eales F, Kshettry V, Flavin T, Tyberg R, Garberich RF. Impact of intraoperative transesophageal echocardiography on acute type-A aortic dissection. J Thorac Cardiovasc Anesth. 2014;28:1203–7.

MacKnight B, Maldonado Y, Augoustides JG, Cardenas R, Patel PA, Ghadimi K, Gutsche JT, Ramakrishna H. Advances in imaging for the management of acute aortic syndromes: focus on transesophageal echocardiography and type A aortic dissection for the perioperative echocardiographer. J CardioThorac Vasc Anesth. 2016;30:1129–41.

Meredith EL, Masani ND. Echocardiography in the emergency assessment of acute aortic syndromes. Eur J Echocardiography. 2009;10:131–9.

Raphaël C, Nicolas P, Yoan L, et al. Speckle tracking analysis allows sensitive detection of stress cardiomyopathy in severe aneurysmal subarachnoid hemorrhage patients. Intensive Care Med. 2016;42(2):173–82.

Slama M, Tribouilloy C, Maizel J. Left ventricular outflow tract obstruction in ICU patients. Curr Opin in Crit Care. 2016;22(3):260–6.

Templin C, Ghadri JR, Diekmann J, Napp LC, Bataiosu DR. Clinical features and outcomes of Takotsubo stress cardiomyopathy. N Engl J Med. 2015;373:929–38.

Torbicki A, Galie N, Covezzoli A, et al. Right heart thrombi in pulmonary embolism: results from the International Cooperative Pulmonary Embolism Registry. J Am Coll Cardiol. 2003;41:2245–51.

Tsai TT, Trimarchi S, Nienaber CA. Acute aortic dissection: perspective from the International Registry of Acute Aortic Dissection. Eur J Vasc Endovasc Surg. 2009;37:149–59.

Wang CJ, Rodriguez-Diaz CA, Trinh MA. Use of real-time three-dimensional transesophageal echocardiography in type A aortic dissections: Advantages of 3D TEE illustrated in three cases. Ann Card Anaesth. 2015;18(1):83–6.

Acute Dyspnea

<div style="text-align:right">

35

</div>

Simone Cipani and Federica Marini

Key Points
- Definition
- Pathogenesis
- Epidemiology
- Diagnostic tool and methodology
- Noncardiogenic dyspnea
- Cardiogenic dyspnea

35.1 Definition of Dyspnea

The American Thoracic Society defines dyspnea as "a subjective experience of breathing discomfort that consists of qualitatively distinct sensations that vary in intensity. It derives from interaction among multiple physiological, psychological, social, and environmental factors, and may induce secondary physiological and behavioral responses."

This condition can be attributed to many disorders involving the airways, pulmonary parenchyma and pleural space, chest wall components (wall or vessels), and heart . It can be caused by many different underlying conditions some of which arise acutely and can be life-threatening. It is very important to identify the cause of dyspnea to undertake the appropriate treatment and therapy. Approximately 85% of all emergency department cases of shortness of breath are due to chronic obstructive pulmonary disease, asthma, cardiac ischemia, pneumonia, cardiogenic pulmonary edema, and interstitial lung disease. Dyspnea is the most common and distressing symptom in patients with acute or subacute decompensated heart failure.

The intensity of the dyspnea reported subjectively does not always correlate with the pulmonary function tested via objective measures. The evaluation of subjectivity of dyspnea is one of main difficulties for the clinician who has to determine the diagnosis and judge the severity of the underlying condition. An important objective of mechanical ventilation (MV) is to assuage this symptom. Dyspnea can, however, persist, reappear, or reincrease after the institution of mechanical ventilation (MV). This can reveal complications (like pneumothorax, pneumonia, cardiac failure, anemia, etc.) or inappropriate ventilator settings.

Generally, isolated ultrasonography of a single organ itself has low accuracy in differentiating acute heart failure from other causes of acute dyspnea. Acute dyspnea (clinical congestion) results from the failure of alveolar capillary membrane (pulmonary congestion), which

S. Cipani · F. Marini (✉)
Department of Anesthesia and Intensive Care,
Santa Maria Nuova Hospital -Azienda USL Toscana
Centro, Florence, Italy
e-mail: simone.cipani@uslcentro.toscana.it; federica.marini@uslcentro.toscana.it

is induced by more stress, following the increase of left ventricular (LV)-filling pressure (hemodynamic congestion). This is one good reason why lung ultrasound should be added to cardiac ultrasound. Cardiopulmonary ultrasound is a portable and reusable resource that may be useful in establishing a diagnosis in patients presenting acute dyspnea in every setting.

35.2 Pathogenesis

The pathogenesis of dyspnea is still not fully clear and is now under continuous investigations. Current explanatory hypotheses are based on the concept of a regulatory circuit that consists of afferent information relayed centrally (from chemoreceptors for pH, carbon dioxide (CO_2), and oxygen (O_2), as well as from mechanoreceptors in the musculature and the lungs (C fibers in the pulmonary parenchyma, J fibers in the bronchi and pulmonary vessels) and a corresponding ventilatory response (Fig. 35.1).

35.3 Epidemiology

Difficult breathing is a common symptom both in general practice and in emergency depart-

Fig. 35.1 Chemical regulation of breathing. CO_2: carbon dioxide. Plasmatic PO_2: blood oxygen partial pressure. Plasmatic PcO_2: blood carbon dioxide partial pressure. Liquor PcO_2: liquor carbon dioxide partial pressure. Arterial PcO_2: arterial blood carbon dioxide partial pressure
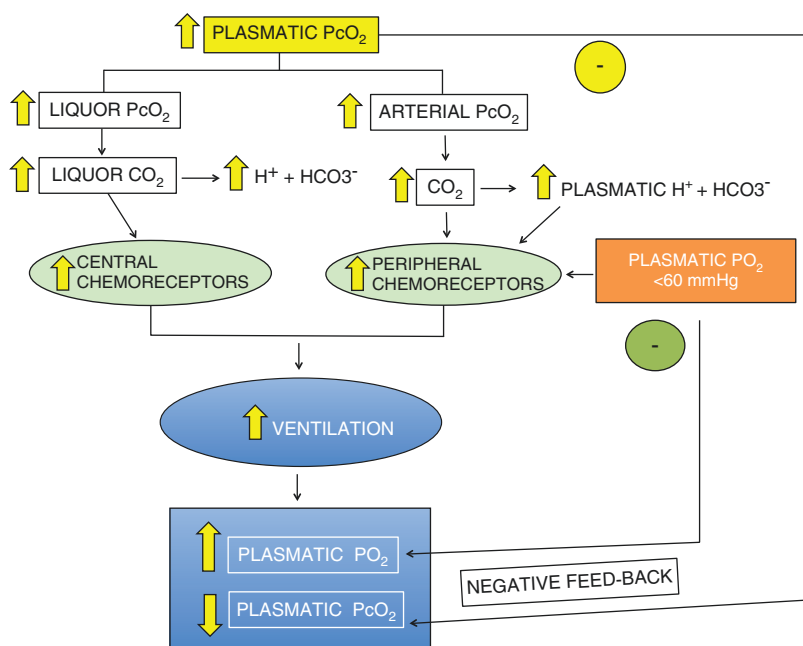
Table 35.1 The more common causes of dyspnea in ED, medical rescue, and general medical practice

Emergency department	Medical rescue	General practice
COPD 16.5%	Heart failure 15–16%	Acute bronchitis 24.7%
Heart failure 16.1%	Pneumonia 10–18%	Acute upper respiratory infection 9.7%
Pneumonia 8.8%	COPD 13%	Other airway infection 6.5%
Acute coronary syndrome 5.3%	Bronchial asthma 5–6%	Bronchial asthma 5–6%
Flutter/atrial fibrillation 4.9%	Acute coronary syndrome 3–4%	COPD 5.4%
Pulmonary embolism 3.3%	Pulmonary embolism 2%	Heart failure 5.4%
Malignant tumor 3.3%	Lung cancer 1–2%	Hypertension 4.3%

ment (ED). Among patients in general practice, 10% complain of dyspnea when walking on flat ground and 25% complain of dyspnea on more intense exertion (climbing stairs). For 1–4% of these patients, dyspnea is their main reason for consulting a doctor.

In the ED, it has been reported that 7.4% of patients complain of dyspnea.

In the intensive care unit (ICU), 47% of mechanical ventilated patients complain of dyspnea.

35.4 Diagnostic Tool and Methodology

Dyspnea can occur for lung disease, heart disease, or both.

Currently, a standard chest radiograph is the first examination performed in patients presenting shortness of breath. Its advantages are the relatively low dose of ionizing radiation administered to the patients and the complete and immediate visualization of the whole chest. However it has also some disavantages; infact we can't administer to some particular patients as pregnant women and often are impossible to acquire in ED posteroanterior and laterolateral projections. The routinely used chest X-ray has a sensitivity of 70% but a specificity of 100% which reflects that there might be a delay in features of frank pulmonary edema to appear on chest X-ray; hence the modality has a low sensitivity. Moreover, this diagnostic tool is often difficult to interpret, imprecise and with high interobserver variability.

In particular conditions standard radiograph is not able to distinguish between atelectasis and pneumonia. Zanobetti et al. have demonstrated high concordance between chest ultrasonograph and standard radiograph in most pulmonary diseases causing dyspnea. When a chest ultrasonograph and chest radiograph reached discordant clinical conclusions, the comparison of these two modalities with a chest tomography (CT) scan as the gold standard demonstrates that ultrasonography is more accurate than radiograph specially diagnosing free pleural effusion. In other pathologies, the two modalities are similarly accurate.

As mentioned previously, chest CT scanning represents the gold standard examination for most pulmonary diseases. Although it's still an important and necessary method to evaluate some patients, CT scanning raises some important issues, such as the high dose of radiation administered to the patient, the need to move the patient into the radiology room, and the lack of CT scanning in some ED.

In the past ultrasound has not been employed for lung evaluation. All diagnostic ultrasound methods are based on the principle that ultrasound is reflected by an interface between media with different acoustic impedance. Infact in normal patients with aerated lungs, the ultrasounds beam finds the lung air and no image is visible, no acoustic mismatch is reflected to the beam because is rapidly dissipated by air. In this condition the only structure detectable is the pleura, visualized as a hyperechoic horizontal line.

When pathological conditions occur in the lung, as air content decreased or increased of extravascular lung water, the acoustic mismatch needed to reflect the ultrasound beams is created and some images appear.

Considering the importance of early and accurate diagnosis, it is crucial to have an easy, inexpensive, noninvasive, reliable, and reproducible method for the diagnosis.

For this reason bedside multiorgan point-of-care US is so important.

35.5 Lung Ultrasound (See Also Chap. 51)

Lung ultrasound (LUS) can be performed easily with any commercially available 2D scanner, with any transducer (phased array, linear array, convex, microconvex). The examination can be performed with any type of echographic platform, from fully equipped machines to pocket-sized ones. The patient can be scanned just laying the probe along the intercostal spaces. In the time many approaches of study have been proposed; starting from the apex to base of the chest (from the second to the fourth space on the left and from the second to the fifth on the right hemi-

Fig. 35.2 Pleural line and A-lines
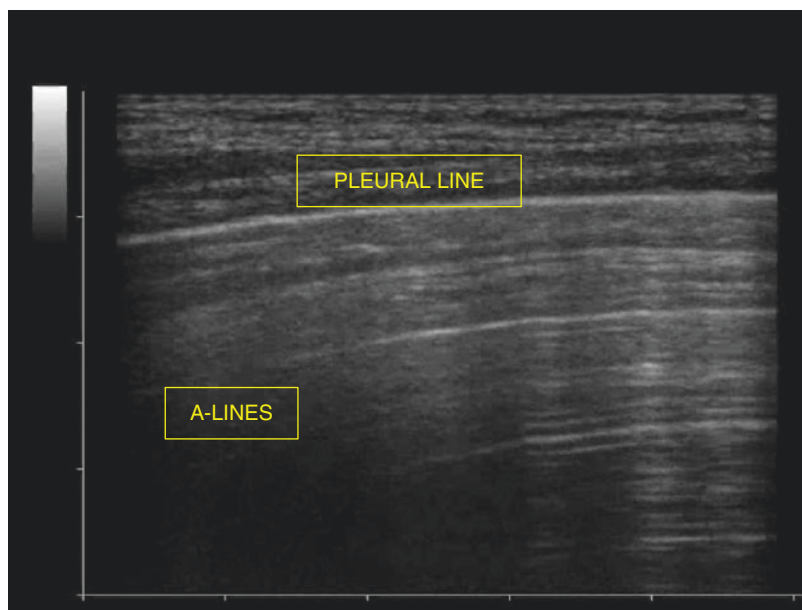
thorax) and from the parasternal to the axillary line, it is possible to perform a complete scan of the lung. LUS limitations are essentially patient dependent. Obese patients are frequently difficult to study because of the thickness of their rib cage and soft tissues. The presence of subcutaneous emphysema or large thoracic dressing alters or precludes ultrasound propagation to the lung periphery.

Normal lung pattern is defined as A-lines (Fig. 35.2) with the lung sliding on the anterolateral chest examination bilaterally, without alveolar consolidation or pleural effusion on posterior examination. A normal lung pattern does not equate a normal lung: LUS could be normal in acute exacerbation of chronic obstructive pulmonary disease, asthma attack, and pulmonary embolism (PE). For this reason, a venous ultrasonography exam is useful (see Chap. 50): the A-pattern plus deep vein thrombosis in the venous analysis has a sensitivity of 81% and a specificity of 99% for pulmonary embolism. Acute PE may lead to right ventricular (RV) pressure overload and dysfunction, which can be visualized by cardiac ultrasound.

35.6 Noncardiogenic Dyspnea

35.6.1 Pleural Disease

Pneumothorax

Patients with pneumothorax present with shortness of breath and pleuritic chest pain. The absence of lung sliding does not have adequate specificity to rule in the disease, as this absence can be observed in severe emphysema, adult respiratory distress syndrome (ARDS), and atelectasis. The lung point (Fig. 35.3) is highly specific for and thus rules in pneumothorax. The presence of lung sliding, B-line, or lung pulse rules out pneumothorax.

Pleural Effusion

Pleural effusion can be identified in posterolateral lung examination. It can cause respiratory difficulty, pleural chest pain, or both. The amount and nature of pleural effusion can be estimated by using an inter-pleural distance or area and sonographic appearances. A large pleural effusion (Figs. 35.4 and 35.5) can cause respiratory embarrassment, hypovolemic shock (especially in a large hemothorax), or even obstructive shock

Fig. 35.3 Lung point in pneumothorax
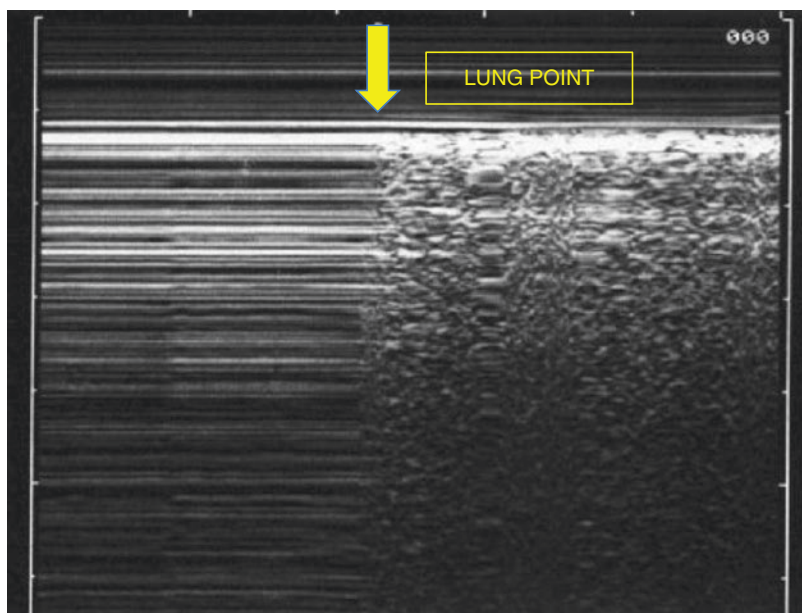
Fig. 35.4 Massive pleural effusion
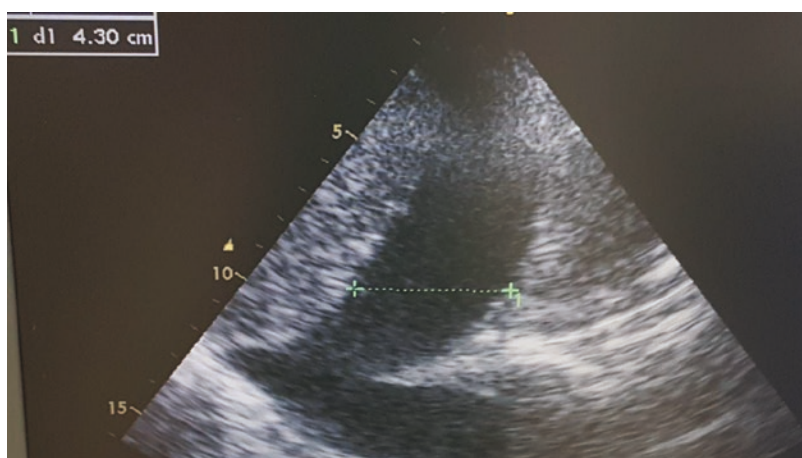
Fig. 35.5 Pleural effusion
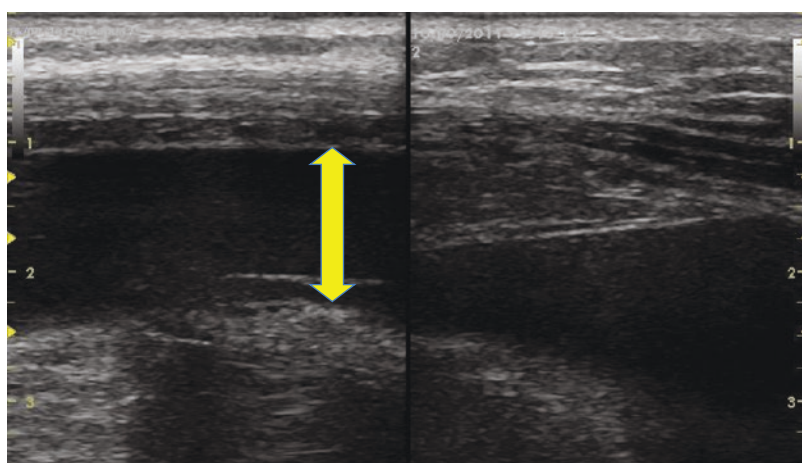
due to compression of the inferior vena cava (IVC) and heart, which induces the diastolic failure.

35.6.2 Parenchymal Disease

Interstitial Syndrome
Interstitial syndrome is divided into diffuse and focal patterns. Diffuse interstitial syndrome is defined as the presence of multiple diffuse bilateral B-lines (Fig. 35.6) with at least two positive scans on each side of the thorax. Causes of diffuse interstitial syndrome include pulmonary edema of various causes, diffuse parenchymal lung disease (pulmonary fibrosis), or interstitial pneumonia. Cardiogenic pulmonary edema is increasingly attributed to heart failure with preserved ejection fraction: it diagnosis relies on identification of elevated left ventricular filling pressure, irrespective of systolic function. The sonographic pattern of diffuse multiple B-lines (Fig. 35.7) is present also in ARDS as well as in car-

Fig. 35.6 Interstitial syndrome: multiple B-lines
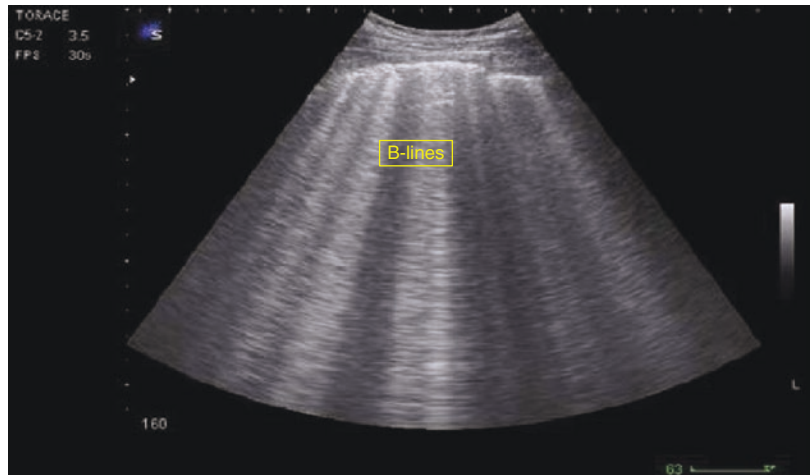
Fig. 35.7 Spared area in a "white lung" (ARDS)
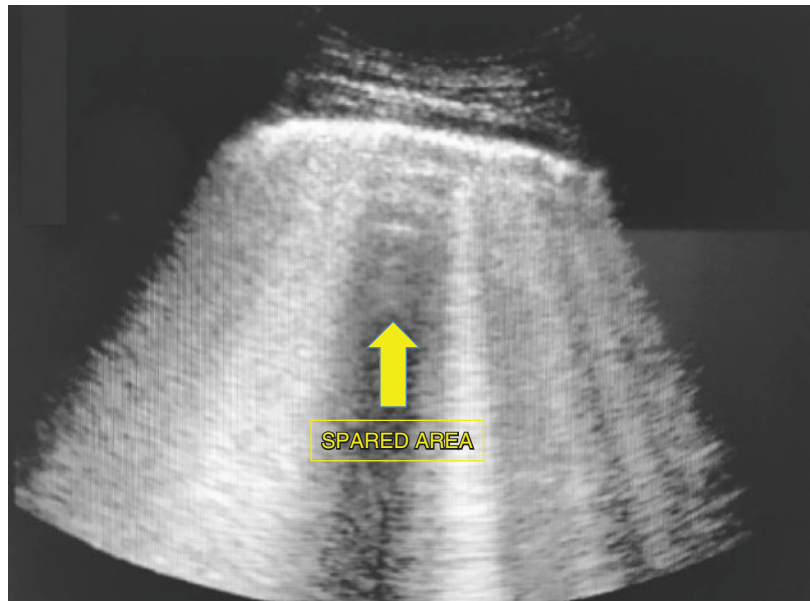
Fig. 35.8 Alveolar consolidation
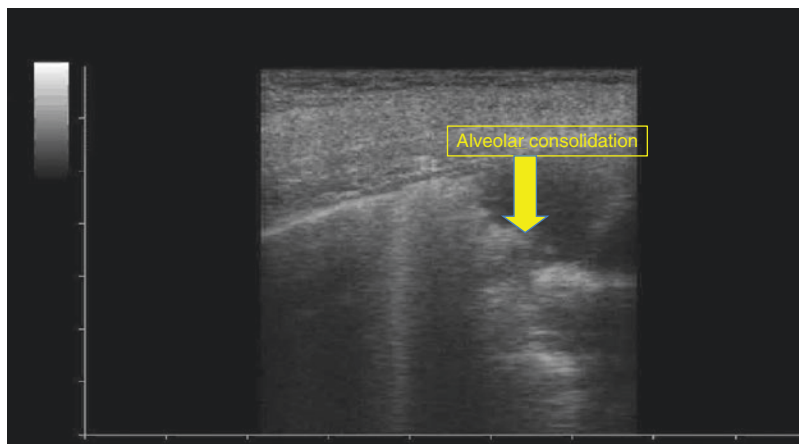
diogenic pulmonary edema. The presence of diffuse interstitial pattern associated with a normal heart indicates a noncardiac cause of pulmonary edema, such as ARDS, interstitial pneumonia, and diffuse parenchymal lung disease (pulmonary fibrosis, in a chronic setting). However there are some clues that may help to differentiate the two clinical conditions. In ARDS we find alterations of the pleura, due to small subpleural consolidation, spared areas (Fig. 35.7), suggestive of non cardiogenic pulmonary edema (ARDS, interstitial pneumonia, and diffuse parenchymal lung disease as pulmonary fibrosis).

Focal (localized) interstitial sonographic pattern is seen in a variety of pathologies of pulmonary origin, such as pneumonia, atelectasis, pulmonary contusion, pulmonary infarction, pleural disease, or neoplasia.

Alveolar Consolidation

The consolidated region of the lung is visualized as an echo-poor or tissue-like pattern, depending on the extent of aeration loss and fluid predominance (Fig. 35.8).

35.7 Dyspnea in Mechanically Ventilated Critically Ill Patients

The determinants of dyspnea in mechanically ventilated patients are multifactorial, with contributions from the intrinsic bronchopulmonary status of the patients, ventilator settings, various care activities, extrinsic physiological stimulations of the ventilatory drive, and non-respiratory factors such as anxiety or pain. An important objective of mechanical ventilation (MV) is to assuage dyspnea. This symptom can, however, persist, reappear, or reincrease after the institution of MV. This can reveal complications (like pneumothorax, pneumonia, cardiac failure, anemia, etc.) or inappropriate ventilator settings. Dyspnea strongly correlated with anxiety, which stresses the clinical relevance of the issue. Reciprocally, dyspnea generates anxiety and relieving dyspnea decreases. Anxiety significantly decreased in those of our patients who reported improvements after adjustments of the ventilator settings. Therefore, relieving dyspnea is likely to have positive effects on anxiety. Pain also stimulates ventilation, and its control could possibly have beneficial effects on dyspnea. There is evidence that dyspnea assessment may be a useful tool to evaluate risk of adverse event. Routine documentation of patient's ratings of dyspnea has the potential to improve symptom management interventions and can lead to better care and better resource allocation. In critically ill patients, bedside visualization of lung morphology and aeration loss is crucial to optimize positive end-expiratory pressure (PEEP) and other therapeutic procedures.

It enables clinicians' easy, rapid, and reliable evaluation of lung aeration and its variations at the bedside. LUS offers information that allows tailoring therapeutics and ventilator settings to each patient for better care.

35.8 Inferior Vena Cava (IVC)

IVC ultrasound is particularly useful in shock assessment. IVC is easily evaluated sonographically, using the liver as a window (Figs. 35.9, 35.10, and 35.11) (see Chap. 29).
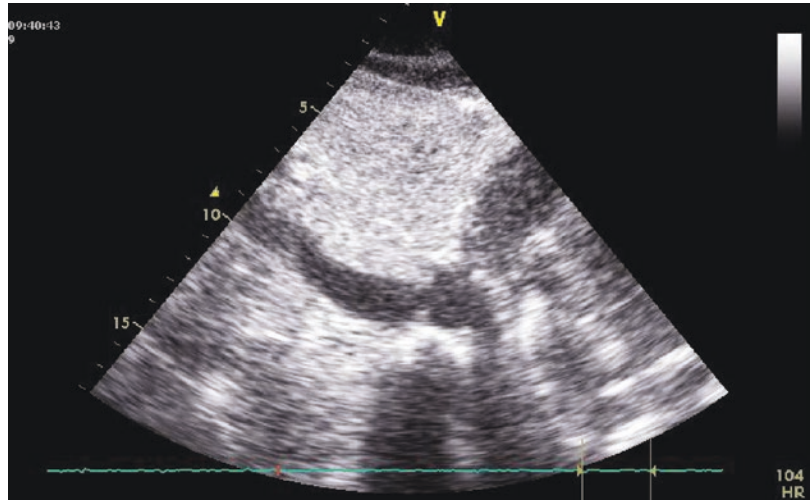
35.9 Cardiogenic Dyspnea

- *Heart failure*
- *Acute coronary syndrome*

As previously mentioned dyspnea is a symptom that often requires medical evaluation and a rapid and accurate diagnosis, because delayed assessment and treatment have a strong association with mortality.

LUS has recently emerged as a noninvasive tool to differentiate acute heart failure from noncardiogenic dyspnea.

Fig. 35.9 B-mode of IVC

Fig. 35.10 M-mode of IVC

Fig. 35.11 IVC using the liver as a window
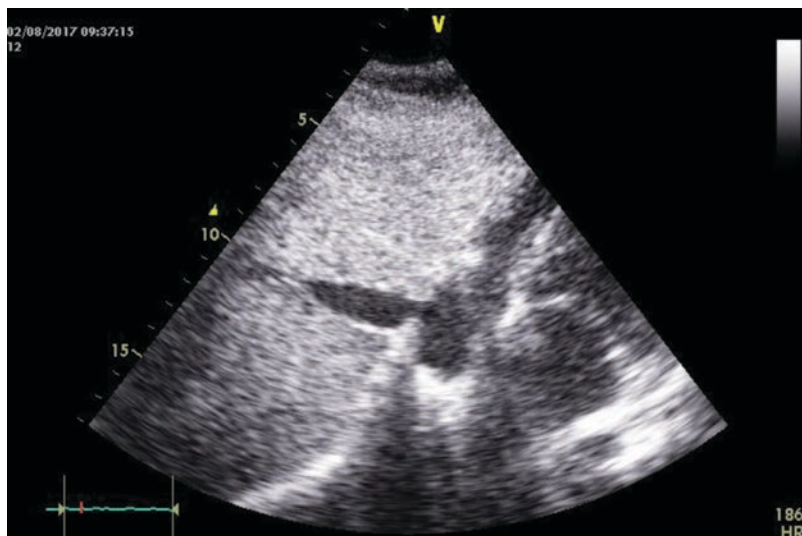
35.9.1 Heart Failure(HF)

HF has been estimated to affect approximately 2% of adults in developed countries, and 8.4% in those aged ≥75 years. Mortality is particularly high in those patients with acute coronary syndrome accompanied by severe heart failure, where the 1 year mortality rate is 30%. In European countries the costs of treating patients with HF have been estimated to consume around 1–2% of the total health-care costs, of which approximately 75% are related to hospitalization. LUS is an important, inexpensive, noninvasive, reliable, and reproducible tool to diagnosis of HF. Along with dyspnea, there are other symptoms including fatigue, diminished exercise tolerance, and fluid retention. The common causes are advanced coronary heart disease, primary cardiomyopathy, hypertension, and valvular heart disease.

There is an important clinical distinction between heart failure with reduced ejection fraction, in which the left ventricular systolic function is less than 40% and the almost equally common heart failure with preserved ejection fraction with elevated cardiac filling pressure. There is also a newly described entity called heart failure with midrange ejection fraction in which signs of diastolic dysfunction are combined with an ejection fraction between 40% and 49%. In all types of

Fig. 35.12 Chest X-ray: congestive chest radiogram in acute decompensated heart failure patient

congestive heart failure, stroke volume and cardiac output are diminished (Fig. 35.12).

Already in 1994, Lange, in a review on the assessment of extravascular lung water (EVLW), had emphasized the importance of detecting the presence of pulmonary edema before it becomes clinically apparent. As previously mentioned, when the air content decreases as in pulmonary edema or fibrosis, the acoustic mismatch needed to reflect the ultrasound beam is created. So in the presence of EVLW, the ultrasound beam finds subpleural interlobular septa thickened by edema. The reflection of the beam creates some comet-tail reverberation artifacts, called B-lines (ultrasound lung comets) (Fig. 35.13). These artifacts

Fig. 35.13 LUS in the same patient; multiple B-lines in interstitial pulmonary edema
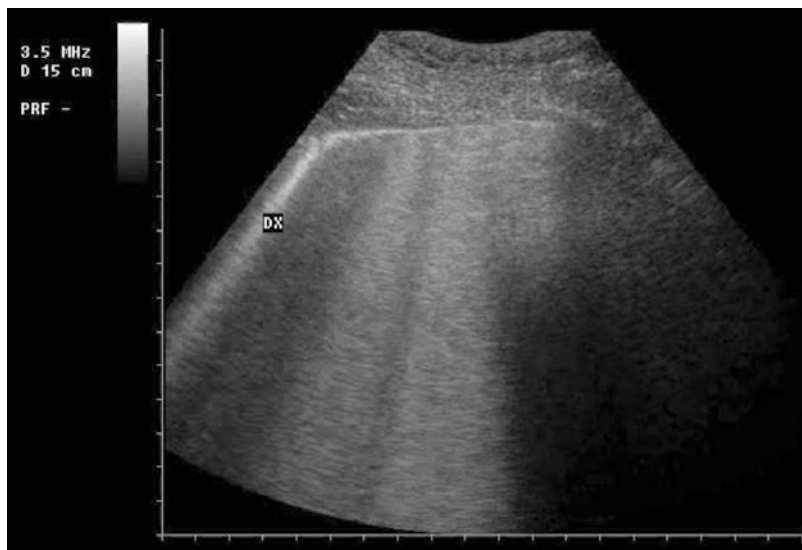
are vertical hyperechoic images that arise from the pleural line synchronously with respiration. Multiple B-lines provide reliable information on interstitial pulmonary edema; this finding associated with congestive chest radiogram, brain natriuretic peptide (BNP) levels, and pulmonary arterial wedge pressure is strongly correlated with a diagnosis of acute decompensated heart failure. Moreover, in critically ill patients, the predominance of an A-line indicates dry interlobular septa and is a strong predictor of normal pulmonary capillary wedge pressure.

35.9.2 Acute Coronary Syndrome

Dyspnea can also be a symptom of coronary stenosis, even if it's not a classic symptom. It can be present simultaneously with angina pectoris, or as the predominant or sole symptom of coronary heart disease, e.g., in a patient with diabetes mellitus. The history, particularly the timing and setting of the onset of dyspnea (stress, cold), often suggests coronary heart disease as a potential cause.

In this particular condition, LUS should be considered as an extension of the echocardiogram, allowing pulmonary congestion diagnosis.

35.10 Conclusion

Ultrasound is central to the evaluation of common causes of dyspnea. While heart failure is a syndrome of clinical signs and symptoms, echocardiography is helpful in the diagnosis and further characterization of patients with suspected acute decompensated heart failure, pericardial effusion with tamponade, and large pleural effusions or causing respiratory distress.

Further Reading

Ahn JH, et al. A novel point of care ultrasound protocol for patients with chest pain, dyspnea or symptomatic hypotension in the emergency department. PLoS One. 2017; https://doi.org/10.1371/journal.pone.0174581.

Berliner D, et al. The differential diagnosis of dyspnea. Dtsch Arztebl Int. 2016;113:834–45.

Gargani L. Lung ultrasound: a new tool for the cardiologist. Cardiovasc Ultrasound. 2011;9:6.

Ha Y-R, et al. Clinically integrated multi-organ point-of care ultrasound for undifferentiated respiratory difficulty, chest pain, or shock: a critical analytic review. J Intensive Care. 2016;4:54.

Schmidt M, et al. Dyspnea in mechanically ventilated critically ill patients. Crit Care Med. 2011;39(9):2059.

Schmidt M, et al. Unrecognized suffering in the ICU: addressing dyspnea in mechanically ventilated patients. Intensive Care Med. 2014;40(1):1–10.

Shah SP, et al. Focused cardiopulmonary ultrasound for assessment of dyspnea in a resource-limited setting. Crit Ultrasound J. 2016;8:7.

Stevens JP, et al. Prevalence and predictive value of dyspnea ratings in hospitalized patients: pilot studies. PLoS One. 2016;11(4):e0152601. https://doi.org/10.1371/journal.pone.0152601.

Vignon P, et al. Critical care ultrasonography in acute respiratory failure. Crit Care. 2016;20:228.

Vizioli L, et al. Accuracy of lung ultrasound in patients with acute dyspnea: the influence of age, multimorbidity and cognitive and motor impairment. Ultrasound Med Biol. 2017;43:1846.

Zanobetti M, et al. Can chest ultrasonography replace standard chest radiography for evaluation of acute dyspnea in the ED? Chest. 2011;139(5):1140–7.

Unexplained Hypoxemia

36

Patent Foramen Ovale Right-to-Left Shunt PFO

Ferdinando Luca Lorini, Bruno Rossetto, and Francesco Ferri

36.1 Introduction

Assessment of unexplained hypoxemia and the inability to wean a patient from ventilatory support are potential uses of echocardiography in the intensive care unit. Causes of hypoxemia that can be diagnosed by echocardiography include intracardiac right-to-left shunting, pulmonary embolus, and disorders of the left ventricle such as left ventricular systolic and/or diastolic dysfunction and mitral valvular abnormalities that can lead to pulmonary edema. If no cardiac abnormality is identified (ventricular or valvular dysfunction), right-to-left shunting must be considered, and the most common cause is patent foramen ovale (PFO).

36.2 Patent Foramen Ovale

The clinical relevance of PFO, a relatively frequent remnant of fetal circulation, has remained obscure for many decades. In fact, before the development of echocardiographic imaging techniques, detection of a PFO during life and clinical diagnosis of paradoxical embolism were rarely possible. In clinical practice, the diagnosis of paradoxical embolism is almost always presumptive and relies on indirect signs such as the presence of a PFO and the diagnosis of arterial embolism. During the past 20 years, initial studies reporting noninvasive detection of right-to-left shunt by contrast echocardiography were followed by extensive clinical research on the association between PFO and several pathological processes, including cryptogenic stroke, peripheral embolism, brain abscesses, decompression sickness, platypnea–orthodeoxia, and fat embolism syndrome. In these studies, PFO was confirmed as a source of paradoxical embolism caused by air, thromboemboli, and fat emboli. Transient right-to-left shunt through a PFO can occur in the presence of normal right-sided hemodynamics. However, patients with submassive and massive pulmonary embolism and those with pulmonary hypertension and right ventricular dysfunction may be at particularly high risk of paradoxical embolism if they happen to have a PFO, with substantial impact on their in-hospital morbidity and mortality. The prevalence of PFO in adults ranged from 25 to 35% in autopsy series and from 5% to 31% in healthy volunteers. The size of the foramen ovale in normal hearts varied between 1 and 19 mm, with a mean of 4.9 mm.

F. L. Lorini (✉) · F. Ferri
Department of Anesthesia and Intensive Care Medicine, ASST Papa Giovanni XXIII, Bergamo, Italy
e-mail: llorini@asst-pg23.it; fferri@asst-pg23.it

B. Rossetto
Department of Anesthesia and Intensive Care Medicine, ASST Gaetano Pini, Milan, Italy

36.3 Diagnosis of PFO

The presence of a PFO generally does not affect the patient's history, clinical findings, ECG, or chest radiograph. Either invasive or noninvasive methods can be used for detection of an intracardiac shunt. Routine right-sided and left-sided cardiac catheterization is generally inadequate for definitive diagnosis of a PFO, and specialized techniques are required for shunt diagnosis. Echocardiography is the primary imaging modality used to diagnose PFO. Transthoracic echocardiography (TTE) and transesophageal echocardiography (TEE) can detect this structure by three different methods:

1. Color Doppler analysis
2. B-mode analysis
3. Contrast echocardiography—microbubbles

36.3.1 Color Flow Analysis

Color flow Doppler analysis with modern multiplane TEE and with variation of the Nyquist limit detects almost all adult PFO. There is no single view for color flow Doppler detection of PFO; the mid-esophageal bicaval and the mid-esophageal four-chamber views are both required for adequate examination. By aligning the Doppler sample volume with the atrial septum, flow across the defect can be recorded. In the usual case, pulsed Doppler imaging will demonstrate low-velocity left-to-right flow extending from mid-systole to mid-diastole, with a second phase of low coincident with atrial systole. Care must be taken to avoid confusing the low-velocity shunt flow with normal venous and atrioventricular valve flows (Figs. 36.1 and 36.2). Color Doppler analysis will show flow across the interatrial septum. Since the pressure gradient between the atria is small, the velocity is low (usually below 1–1.5 m/s) and occurs in late ventricular systole and early in diastole. Calculation of the shunt ratio is usually not necessary. Right ventricular enlargement indicates a hemodynamically significant shunt, being present when the output of the right side of the heart exceeds that of the left side by 50%. It is essential to obtain the right ventricular peak systolic pressure as part of the examination. The best tricuspid regurgitant Doppler signal should be sought from multiple views. By applying the modified Bernoulli equation to the peak velocity of the tricuspid regurgitation jet, one obtains the pressure gradient between the right ventricle and the right atrium.

Fig. 36.1
Transesophageal view of the atrial septum. Color Doppler demonstration of left-to-right flow under mechanical ventilation
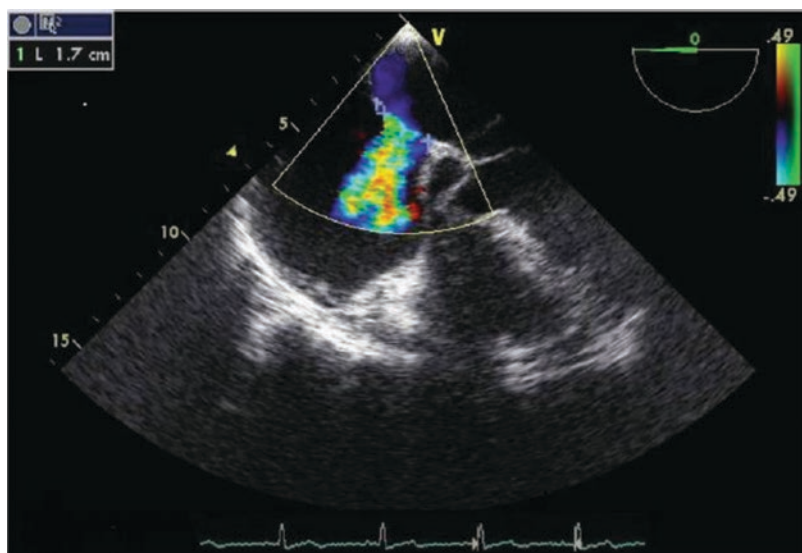
36.3.2 B-Mode Analysis

It is important to recognize normal anatomic variants to avoid confusion. These include atrial septal aneurysm, Eustachian valve (associated with the entrance of the inferior vena cava into the right atrium), and the Chiari network (a strand-like structure that extends from the orifices of the superior vena cava and inferior vena cava). Dropout of echo signal from the foramen ovale occurs when the echo beam is parallel to the interatrial septum in the apical four-chamber view. This gives the false appearance of a septal defect. Whereas TTE can occasionally reveal a PFO, TEE demonstrates the interatrial septum in great detail. Various anatomic components (septum primum, septum secundum, fossa ovalis) can easily be distinguished, and the actual size of the PFO can be defined. The standard TEE views for imaging the atrial septum are as follows:

1. Mid-esophageal four-chamber view (Fig. 36.2). This is useful for demonstrating ostium secundum and ostium primum defects.
2. Mid-esophageal bicaval view. This is useful for demonstrating a sinus venous defect and for identifying anomalous pulmonary veins.
3. Mid-esophageal aortic valve short-axis view (Fig. 36.2). This may need to be rotated

slightly to bring the atrial septum into the center of the image.

TTE is also used. The sensitivity of TTE with agitated saline contrast medium for right-to-left shunts is inferior to that of TEE. However, in dimensional cardiac visualization, the development of contrast-based transmitral Doppler techniques and the use of second-harmonic imaging have improved the diagnostic accuracy of TTE.

36.3.3 Contrast Echocardiography

Contrast echocardiography including a provocative maneuver is the most sensitive modality for PFO detection. This happens by detection of microbubbles from intravenously injected agitated saline in left-sided chambers of the heart that would otherwise be filtered by lung capillaries. The intravenous injection of 5–10 ml agitated saline (or any other sterile solution, including blood) creates a cloud of microcavitations that normally travel with the blood through the right-sided chambers into the pulmonary artery. The microcavitations are trapped in the pulmonary capillaries, and therefore no microcavitations appear in the left side of the heart. With the pres-

Fig. 36.2
Transesophageal aortic valve short-axis view. This may need to be rotated slightly to bring the atrial septum into the center of the image. Color Doppler visualization of left-to-right shunt in a young patient during the Valsalva maneuver
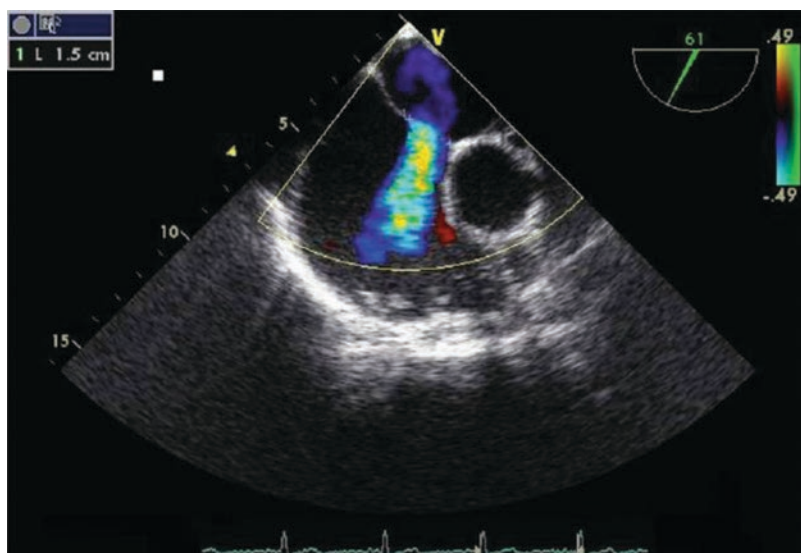
ence of a right-to-left shunt, the microcavitations bypass the pulmonary circulation and appear in the left side of the heart immediately (within one heart beat) after they appear in the right side of the heart. A positive TTE or TEE is considered when at least 1–5 microbubbles can be seen in the left atria or ventricle after 3–5 cardiac cycle following contrast injection. The amount of right-to-left shunting (expressed by the number of microcavitations that appear in the left atrium) can be increased significantly by a "provocative" maneuver that augments venous return to the right atrium and increases right atrial pressure or decreases left atrial pressure. Such maneuvers include the release stage of the Valsalva maneuver, the Müller maneuver, cough, elevation of the lower limbs, and liver compression. The risk of side effects of contrast TEE appears to be low. Nevertheless, several cases of neurological deficiency have already been described after contrast TEE using agitated saline with Valsalva maneuvers. Total PFO detection is only obtained by combining multiple TEE modalities in various atrial views. Thus, a stepwise interrogation of the interatrial septum by multiplane TEE for detection of PFO should include the following:

- Step 1. Two-dimensional imaging of the interatrial septum should be performed in multiple views to rule out any major atrial septal defect.
- Step 2. If step 1 results in negative findings, then color flow Doppler interrogation of the interatrial septum is performed in at least two different views, preferably in the mid-esophageal four-chamber view and the mid-esophageal bicaval view. The Nyquist limit should be serially decreased to approximately 20–40 cm/s.
- Step 3. If step 2 results in negative findings, then contrast echocardiography should be performed with release of positive airway pressure as the provocative maneuver.
- Step 4. If step 3 results in negative findings, contrast echocardiography may be repeated

without a provocative maneuver because this may still facilitate PFO detection.

Transcranial Doppler (TCD) is another imaging modality that can help in the identification of right-to-left shunt. After the injection of agitated saline in the venous system, the TCD is able to detect microbubbles in the intracranial circulation if a right-to-left shunt is present.

36.3.4 Three-Dimensional Echocardiography

Real-time three-dimensional echocardiography (transthoracic or transesophageal) is more accurate than contrast TTE or TEE and can avoid injection of saline contrast medium in a sizable number of patients, especially in those patients with larger PFO who are at higher risk of events and procedure complications. Real-time three-dimensional echocardiography allows fast acquisition of dynamic pyramidal data sets that encompass most of the heart. Acquired data sets can be sliced in several planes and rotated, allowing the observer to visualize cardiac structures such as the interatrial septum "en face" from both the left and the right side with better understanding of its anatomy and its spatial relationship with adjacent structures. Addition of three-dimensional color flow Doppler flow mapping allows one to visualize shunt jets in relation to the anatomy of the interatrial septum and to locate exactly the origin of the jet and the size of the defect. A limitation of real-time three-dimensional echocardiography is that current technology provides a suboptimal spatial and temporal resolution. When smaller defects that have dynamic shunts or shunts elicited only with the Valsalva maneuver/coughing are being imaged, the accuracy of real-time three-dimensional echocardiography may sometimes be hampered by the frame rate.

36.3.5 Closure of Atrial Septal Defects

TEE is also essential for closure of atrial septal defects with an Amplatzer septal occluder. TEE is vital in the recognition of morphologic variations of the atrial septal defects and patient selection. It allows clear visualization of the defect and the device during the procedure, precise measurement of stretch diameters, guidance of deployment, and stable positioning of the device. This is especially important in patients with large or multiple atrial septal defects and those with atrial septal aneurysm. With TEE, incorrect positioning of the device can be detected while it is still screwed to the delivery cable, which allows its early deployment, before any complications occur.

Suggested Reading

Alp N, Clarke N, Banning AP. How should patients with patent foramen ovale be managed. Heart. 2001;85(3):242–4.

Di Tullio MR. Patent foramen ovale: echocardiographic detection and clinical relevance in stroke. J Am Soc Echocardiogr. 2010;23(2):144–55.

Kronzon I, Ruiz CE. Diagnosing patent foramen ovale: too little or too much? JACC Cardiovasc Imaging. 2010;3(4):349–51.

Mahmoud AN, Elgendy I, Agarval N, et al. Identification and quantification of patent foramen ovale-mediated shunts. Interv Cardiol Clin. 2017;6:495–504.

Meier B, Lock JE. Contemporary management of patent foramen ovale. Circulation. 2003;107(1):5–9.

Sharma VK. Diagnostic strategies for patent foramen ovale. Echocardiography. 2010;27(1):100–1.

Tobis JM, Narasihma D, Abudayyeh I. Patent foramen ovale closure for hypoxemia. Interv Cardiol Clin. 2017;6:547–54.

Sepsis and Septic Shock

37

Armando Sarti, Simone Cipani,
and Germana Tuccinardi

37.1 Introduction and Background

Severe sepsis and septic shock are still a common cause for admission to the ICU and are the leading cause of death, despite enormous scientific advances in understanding their complex pathophysiologic processes and biomolecular picture. The natural course of sepsis produces major and different hemodynamic changes depending on the type of immunological response of the patient and the evolution of the disease. All determinants of cardiovascular function, including both central and peripheral blood volume, preload, afterload, and both right and left pump function, may be involved simultaneously or at different times during the progression of the septic insult. Septic shock is often associated with vasoparalysis, microcirculatory dysfunction, and massive fluid leakage into the extravascular compartment. The

pathophysiologic consequences of severe sepsis and septic shock include either absolute hypovolemia, due to third space losses, or relative hypovolemia, caused by abnormal distribution of blood volume between peripheral and central compartments. Regardless of whether hypovolemia is absolute or relative, the heart is not properly filled and both mean arterial pressure and cardiac output decrease. Vasodilation ensues owing to the failure of vasoconstrictor mechanisms. Nitric oxide activity seems to play a major role in the vasoconstriction disturbances. Most endothelial functions are disrupted in sepsis, resulting in a procoagulant, antifibrinolytic, and proadhesive state, altered red blood cell deformability, and sluggish or heterogeneous microvascular flow. Mitochondrial dysfunction occurs inside the cell.

Left ventricular (LV) systolic and/or diastolic dysfunction is common, and right ventricular (RV) dysfunction can also be frequently observed, either primary or secondary to increased pulmonary artery pressure, due to associated acute respiratory distress syndrome (ARDS) and concomitant positive-pressure mechanical ventilation. Myocardial contractility is depressed by circulating substances such as endothelin, endotoxin, and cytokines, in particular IL-1, IL-6, and TNF-α. Myocardial edema and cardiomyocyte apoptosis have even been invoked. LV systolic dysfunction may also reflect impaired adrenergic responsiveness. LV diastolic dysfunction may be

A. Sarti (✉)
Department of Anesthesia and Intensive Care, Santa Maria Annunziata Hospital, Florence, Italy

S. Cipani
Department of Anesthesia and Intensive Care, Santa Maria Nuova Hospital, Florence, Italy
e-mail: simone.cipani@uslcentro.toscana.it

G. Tuccinardi
Department of Pediatric Neuroanesthesia/NeuroICU and PediatricTrauma Center, Meyer Children's Hospital, Florence, Italy

isolated or observed in conjunction with decreased contractility, and it is associated with myocardial edema and augmented cytokine activity, particularly IL-10, IL-8, and TNF-α. Controversy persists over whether LV systolic dysfunction with increased end-diastolic volume might be linked to improved survival, considering LV dilatation as an adaptive mechanism leading to maintained cardiac output. LV diastolic dysfunction is clearly associated with increased mortality. The characteristic hyperdynamic high output and low peripheral resistance circulatory shock is only observed if the patient is readily resuscitated with copious fluid infusions as the heart maintains adequate, or at least acceptable, contractile function and filling properties on both right and left sides. Integrated into the specific bundles of treatment, early broad-spectrum antibiotics and prompt circulatory resuscitation are associated with improved survival. At present, the 2016 Surviving Sepsis Campaign Guidelines consider bedside cardiovascular ultrasound for the reassessment of volume status, after the initial 3-hour bundle. In our opinion, cardiac and lung echography should be performed as soon as possible within the 3-hour bundle to provide clear understanding on myocardial dysfunction and fluid responsiveness.

37.2 Echocardiography in the Clinical Picture of Severe Sepsis and Septic Shock

Since hemodynamic derangement is a dominant feature of severe sepsis and septic shock, bedside echocardiography is paramount for the assessment, management, and frequent reassessment of circulatory failure. In fact, cardiovascular ultrasonography has almost totally replaced right-sided heart catheterization in many ICUs, and a growing number of intensivists now advocate echocardiography as the first-line technique for hemodynamically unstable patients. However, this technique is still complementary to clinical judgment and to all other monitors of hemodynamics.

The initial echocardiography may show unexpected abnormalities of the heart, such as LV diastolic dysfunction, acute cor pulmonale, and pericardial effusion, which can certainly alter the management plan. Moreover, endocarditis as a cause of the sepsis and vegetations on vascular catheters, prosthetic valves, or electrical devices can be diagnosed by echocardiography. Other ultrasonographic techniques may help find the source of infection inside the chest, the abdomen, or the limbs without delay at the bedside (see Chap. 59).

In septic shock patients, Bouferrache et al. have reported a very simple TEE therapeutic protocol to diagnose and then correct hypovolemia, cardiac dysfunction, and vasoplegia in sequence. They also showed that echocardiography is more accurate than the $ScvO_2$-based Surviving Sepsis Campaign approach for elucidating the systolic function of the heart.

Presently, our standard approach is using ultrasonography to evaluate and check again the unstable septic patient after any relevant change or new therapy, while monitoring central venous oxygen saturation by means of a central venous catheter and cardiac output using a continuous semi-invasive method based on arterial trace pulse contour analysis.

37.2.1 Fluid Responsiveness

Volume expansion is a fundamental component of the initial resuscitation of the septic patient (see Chaps. 29 and 31). Restoring blood flow to the organs is essential to prevent microcirculatory dysfunction and hemodynamic collapse. Each minute of tissue hypoperfusion at the onset of the septic insult will be paid for in terms of multiorgan dysfunction later on. On the other hand, considering the ongoing tendency for capillary leakage of severe sepsis and septic shock, once preload has been optimized, further fluid load does not increase delivery of oxygen to the tissues but may only cause adverse consequences, such as pulmonary edema and edema of other tissues, thus enhancing organ dysfunction. Initial fluid loading is always started on a clinical basis. Crystalloids (30 ml/kg bolus) fluid infusion should not be withheld while awaiting more sophisticated information, but it is not easy to

establish the amount of fluid to infuse and for how long to maintain vascular filling. Echocardiography may definitely help to give sufficient fluid (which can be more than generally used) during the early phase of sepsis while restricting the volume load later on.

Traditional static measurements of vascular filling pressures, such as central venous pressure and pulmonary capillary wedge pressure (PCWP), have been found to be unreliable as a guide to volume resuscitation. The clinical picture may suggest severe hypovolemia, which can be clearly confirmed by echocardiography, which shows a small hyperdynamic fast-beating heart with decreased flows and end-diastolic areas or volumes of all cardiac chambers and the inferior (transthoracic echocardiography, TTE) or superior (transesophageal echocardiography, TEE) vena cava. If manifest hypovolemia is not clearly detected, the crucial question regarding whether a volume bolus might increase cardiac output must still be answered. Sonographic dynamic indices of fluid responsiveness based on heart and lung interaction (Chap. 29), which are correlates of pulse pressure variation, have been proposed and validated as a guide to fluid management. The most used ultrasonographically derived parameters for assessment of fluid responsiveness are respiratory variation of vena cava diameter and of stroke volume (see Chap. 29). First, it is very important to fully understand the prerequisite criteria and limitations for applying these measures. Sinus rhythm is required and patients must be fully ventilated (tidal volume of 8 ml/kg) without any spontaneous respiratory effort, even if a reduced tidal volume may still cause enough respiratory variations in patients with decreased lung compliance (ARDS). Abnormal intra-abdominal pressure may interfere with inferior vena cava diameter and respiratory variation. Most important, acute cor pulmonale and RV dysfunction may cause false dynamic signs of fluid responsiveness, owing to adverse effects of the mechanical ventilation on the dilated failing right side of the heart. If these limitations cannot be ruled out, the only way to predict a positive response to a fluid bolus is the measurement of cardiac output before and after passive leg raising. Passive leg raising, as a temporary test of volume

expansion, can be used even in spontaneously breathing patients. The intensivist with competence limited to only basic TTE should rely on respiratory variation and the diameter of the inferior vena cava. Twelve percent as a threshold value for the respiratory variation index of the inferior vena cava can predict an increase of cardiac output of more than 15% with good positive and negative predictive values. More competence in critical care echocardiography allows the skillful intensivist to measure even the diameter and variations (collapsibility index of 36% or more) of the superior vena cava by TEE and to use Doppler interrogation of LV stroke volume variations by both TTE and TEE. A peak velocity variation index greater than 12% and a velocity–time integral greater than 18% can predict a sufficient increase in cardiac output. Crystalloids or albumin fluid challenge should be maintained as long as hemodynamics clearly continues to improve.

37.2.2 Left Ventricular Systolic Dysfunction

"Ejection fraction" (EF) is not synonymous with "contractility" but simply refers to the proportion of blood pumped out of the left ventricle during a cardiac cycle. Thus, a normal or high EF is consistent with low cardiac output, and a very low EF may be found together with a normal cardiac output, according to different end-systolic and end-diastolic volumes. Since traditional echocardiographic indices of systolic function, such as EF, are closely preload and afterload dependent, hypovolemia and decreased afterload due to vasodilatation must first be treated with fluids and/or vasopressors before LV pump dysfunction is established. For the septic patient, an initial normal or even increased EF in the emergency department may only show the unloading effect of reduced systemic vascular resistance on LV performance. Thus, after volume resuscitation and norepinephrine infusion, a further echocardiogram may only show depressed contractility, unmasking the "real" decreased EF, which is frequent after restoring afterload and alerts the clinician to consider inotropic support. In the case of a clinically shocked patient with systolic dysfunction, the PCWP may

be assessed to distinguish genuine cardiogenic shock, characterized by high PCWP ($E/E' > 15$), from septic shock, characterized by normal, near normal, or decreased PCWP ($E/E' < 8$).

Visual estimation of EF is reliable only when performed by the expert echocardiographer intensivist. With competence in only basic TTE, it is preferable to measure EF using endocardial border excursion at the end of diastole and end of systole using both apical four-chamber and apical two-chamber views and averaging the data. Possible regional systolic dysfunction must also be detected, even if precise scoring and accurate localization of regional dysfunction requires an expert second opinion. If regional dysfunction is not observed, the easier-to-measure fractional area change or fractional shortening may be used, with the parasternal short-axis view or the parasternal long-axis view (TTE), respectively, for a quick assessment of systolic function.

The echocardiographer intensivist must also recognize two possible peculiar patterns of systolic dysfunction which lead to a major change of the management plan. Dynamic LV outflow tract (LVOT) obstruction can occur as a consequence of ventricular septal thickening and systolic anterior motion of the anterior mitral leaflet. LV hypertrophy (most often caused by previous hypertension or aortic stenosis), hypercontractility, hypovolemia, and reduced systemic vascular resistance are all predisposing factors. When LVOT obstruction is diagnosed, inotropic support must be stopped immediately, a rapid fluid bolus must be provided, and just in case a pure vasopressor, such as phenylephrine, should be added to the management plan.

Apical ballooning, also referred to as tako-tsubo myopathy, is the other systolic pattern to recognize. Tako-tsubo myopathy is characterized by concomitant hyperdynamic basal and reduced mid-chamber function with akinesis and/or aneurysmal dilatation of the apex. Intense physical or emotional stress may precede apical ballooning, which is associated with increased levels of endogenous or exogenous catecholamines. β-blockers can be considered.

Cardiac output is the final parameter to consider along with the peripheral indices of tissue perfusion which guide the treatment, such as venous hemoglobin desaturation, venous to arterial carbon dioxide gradient, lactate levels and clearance, and organ dysfunction. Among those who survive, all aspects of systolic dysfunction seem to resolve in a few weeks, regardless of severity.

In recent years, speckle tracing echocardiography has been used to provide further understanding on myocardial systolic dysfunction in septic shock. This technique is very useful to unmask both left and right ventricle dysfunction not detected with conventional TTE or TEE echocardiography. Subtle LV systolic dysfunction can be detected by strain imaging in the absence of any ejection fraction changes.

37.2.3 Left Ventricular Diastolic Dysfunction

It must be kept in mind that Doppler analysis of forward mitral flow (E and A waves) is load-dependent. Also, the inflow pattern of the LV filling depends significantly on the age of the patient. Most often, early diastolic relaxation, which is an active energy phenomenon, is involved in sepsis. Reduced LV compliance due to myocardial stiffness can coexist. An E/A ratio of more than 2 is generally associated with a pulmonary artery pressure greater than 18 mmHg. LV diastolic function may be better assessed by the tissue velocity (tissue Doppler imaging) of the longitudinal movement toward the base of the heart of the mitral valve annulus (E'), which is relatively load independent. The E/E' ratio is closely related to the PCWP. Whichever diastolic function is assessed during the initial phase of the sepsis, the measurement must be repeated after volume expansion to avoid excessive fluid load, which increases the risk of pulmonary edema, particularly in the presence of ARDS or if LV function is already depressed prior to the septic insult. New-onset septic diastolic dysfunction may completely reverse if the patient survives. Recent studies show that grade I diastolic dysfunction may be associated with increased mortality. Grades II and III do not seem to be associated with a worse prognosis probably because inadequate fluid resuscitation was previously applied.

37.2.4 Right Ventricular Dysfunction

The right side of the heart may be compromised as well as the left side. RV systolic dysfunction, as diagnosed by speckle tracing, seems to be associated with high mortality in septic shock. The discovery of RV impairment, either primary or secondary, always leads to significant changes in drug therapy and in the mechanical ventilation setting. RV impairment may become manifest only after the institution of positive-pressure mechanical ventilation with or without positive end-expiratory pressure. Severe RV failure may alert the clinician to consider venous thromboembolism as a concomitant or alternative diagnosis. RV end-diastolic dilatation and the RV/LV area ratio in the apical four-chamber view allow the diagnosis of dysfunction, together with septal paradoxical motion (dyskinesia) or flattening, which is more related to pressure overload. The assessment of pulmonary artery systolic pressure by the Doppler velocity of tricuspid regurgitation is crucial to distinguish a RV primary involvement as a direct effect of all circulating factors of sepsis from a secondary involvement, due to increased afterload caused by chronic obstructive pulmonary disease, or factors such as acidosis, hypoxia, ALI/ARDS, and positive-pressure mechanical ventilation. Inotropic support is considered for primary systolic dysfunction, together with vasopressors, to sustain coronary perfusion pressure, whereas specific steps should be taken to reduce afterload, as in the presence of pulmonary hypertension. Pulmonary vasodilators, such as oxygen, nitric oxide, sildenafil, and prostacyclin, can be used to reduce pulmonary pressure. At the same time, mechanical ventilation is adjusted to reduce as much as possible the inspiratory plateau pressure and the positive end-expiratory pressure, while maintaining arterial oxygen content and preventing excessive respiratory acidosis.

37.2.5 Vasopressors and Inotropes

Echocardiography, with all the information it provides on the entire cardiovascular function, may greatly help guide the rational use, if any, of vasopressors, inotropes, and vasodilators. Serial echo-cardiographic examinations are necessary to reassess the hemodynamic profile of the septic patient during the progression of the disease and after any relevant management change. Norepinephrine is the first-line vasopressor of choice. When the arrhythmic risk is high, it will be certainly more appropriate to use norepinephrine than dopamine. Recent findings show that vasopressin may be considered to restore systemic arterial pressure if norepinephrine treatment fails or if high, potentially dangerous doses need to be used. Some authors now suggest vasopressin even before considering norepinephrine infusions. However, both vasopressin infusion to increase arterial pressure and dobutamine infusion to increase cardiac output imply adequate previous vascular filling. A good response to dobutamine infusion is a reduction of heart rate. Epinephrine is administered to sustain cardiovascular function if other drugs fail to restore pump function and arterial pressure. The calcium sensitizer levosimendan seems able to improve both systolic and diastolic ventricular function on both sides of the heart without increasing oxygen consumption. However, this agent stimulates the endothelial release of nitric oxide and thus it might be speculated that this could exacerbate the sepsis-related fall of systemic vascular resistance and the tendency for hypotension. Both levosimendan and dobutamine seem to improve microvascular flow.

The LV ejection velocity–time integral is closely related to stroke volume since the LVOT cross-sectional area does not change acutely, and it can therefore be monitored to detect any inotropic change as long as both preload and afterload stay stable. Cardiac output is the final central determinant of tissue perfusion. It may be manipulated with fluids and drugs according to all the relevant clinical and hemodynamic data to reach peripheral therapeutic goals, such as:

- Adequate mixed venous oxygen saturation (above 70%)
- Central venous–arterial carbon dioxide gradient below 6 mmHg
- Acceptable diuresis
- Decreasing lactate level
- Recovery of organ function
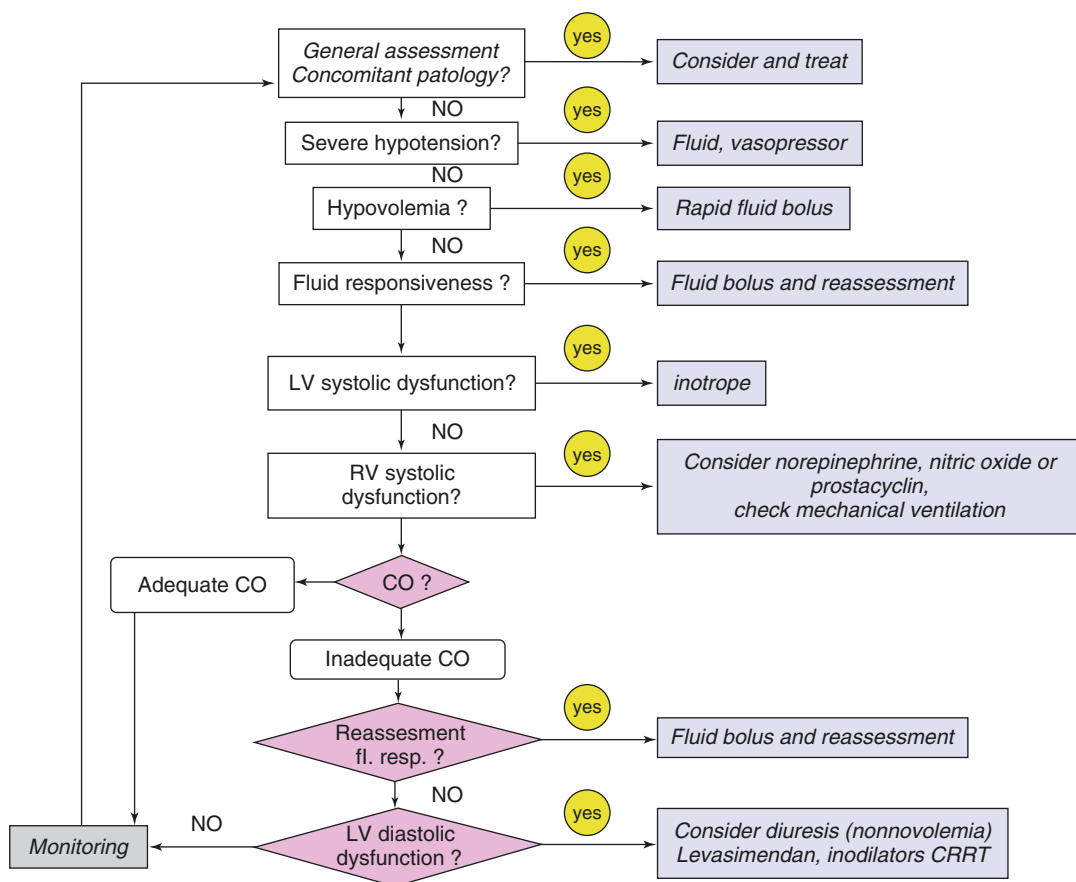
Fig. 37.1 Echo-guided assessment and management of the septic patient. See the text for details. *LV* left ventricular, *RV* right ventricular, *CO* cardiac output, *fl resp* fluid responsiveness, *CRRT* continuous renal replacement therapy

Figure 37.1 shows an algorithm for the assessment and the management plan of the septic unstable patient based on the echocardiographic findings.

Further Reading

Bouferrache K, et al. Initial resuscitation guided by the Surviving Sepsis Campaign recommendations and early echocardiographic assessment of hemodynamics in intensive care unit septic patients: a pilot study. Crit Care Med. 2012;40:2821–7.

Funk D, Sebat F, Kumar A. A systems approach to the early recognition and rapid administration of best practice therapy in sepsis and septic shock. Curr Opin Crit Care. 2009;15:301–7.

Gerstle J. Echocardiographically derived parameters of fluid responsiveness. Int Anesthesiol Clin. 2010;48:37–44.

Griffee MJ, Merkel MJ, Wei KS. The role of echocardiography in hemodynamic assessment of septic shock. Crit Care Clin. 2010;26:365–82.

Howell MD, Davis AM. JAMA clinical guidelines synopsis. Management of sepsis and septic shock. JAMA Published online. 2017;317:847.

Rhodes A, et al. Surviving sepsis campaign: international guidelines for management of sepsis and septic shock: 2016. Crit Care Med. 2017; https://doi.org/10.1097/CCM.0000000000002255.

Shahul S, et al. Detection of myocardial dysfunction in septic shock: a speckle-tracking echocardiography study. Anesth Analg. 2015;121:1547–54.

Chest Trauma

38

Echocardiography in Cardiovascular Thoracic Injuries

Fabio Sangalli, Serena Calcinati, Lucia Galbiati, and Roberto Fumagalli

Trauma is a major cause of morbidity and mortality worldwide and represents the leading cause of death for those between 1 and 41 and the fifth leading cause of death overall. Chest trauma, either blunt or penetrating, occurs in almost two thirds of multiple trauma patients and contributes 15–35% of the burden of trauma-related deaths. These injury mechanisms may result in pneumothorax, hemothorax, pulmonary contusion, or injuries to the mediastinal structures. Although pulmonary parenchymal injuries such as contusion and laceration represent the most common intrathoracic lesions – occurring in 30–70% of blunt thoracic trauma victims – mortality from chest trauma is usually due to aortic or great vessel injury, and though only about 15% of chest trauma patients requires operative intervention, a considerable number of preventable deaths occur due to inadequate or delayed treatment of an otherwise remediable injury.

Echocardiography, particularly transesophageal echocardiography (TEE), is a key component of the diagnostic process. It carries a higher sensitivity and specificity than transthoracic echocardiography, ranging in experienced hands between 91% and 100% and between 98% and 100%, respectively (Table 38.1). Besides providing accurate and real-time information on the

Table 38.1 Indications for echocardiography in the trauma patient

Problem	Class of evidence
Serious blunt or penetrating chest trauma	I
Mechanically ventilated patients with multiple trauma or chest trauma	I
Hemodynamically unstable polytrauma patients without obvious chest injury but with a mechanism of trauma suggesting potential cardiac or aortic injury (i.e., deceleration or crush injury)	I
Widening mediastinum or suspicion of postinjury aortic damage	I
Trauma patients with suspicion of preexisting valvular or myocardial disease	I
Evaluation of hemodynamics in multiple trauma or chest trauma patients with PAC monitoring data that are disparate from the clinical scenario	IIa
As a follow-up study to victims of serious blunt or penetrating injury	IIa
Suspected myocardial contusion in hemodynamically stable patients with a normal ECG	III

F. Sangalli (✉) · S. Calcinati · L. Galbiati
Department of Anaesthesia and Intensive Care, ASST
Monza – San Gerardo Hospital – University of
Milano-Bicocca, Monza, MB, Italy
e-mail: f.sangalli@asst-monza.it

R. Fumagalli
Department of Anaesthesia and Intensive Care, ASST
Grande Ospedale Metropolitano Niguarda Ca'
Granda – University of Milano-Bicocca,
Milano, MI, Italy
e-mail: roberto.fumagalli@unimib.it

morphological and functional aspects of the heart and great intrathoracic vessels, it allows point-of-care examination and can be performed without interrupting ongoing measures to stabilize the patient. The speed and portability of echocardiography make it an attractive alternative to other imaging technologies such as computed tomography (CT), arteriography, and magnetic resonance imaging (MRI) (Table 38.2). Although the sensitivity and specificity of TEE have been reported as comparable to CT imaging in diagnosing traumatic aortic injury (TAI), TEE furthermore allows the identification of associated cardiac injuries and is more sensitive than CT in the detection of intimal lesions. TEE nowadays represents the primary diagnostic tool in unstable patients in most institutions where an experienced echocardiographer is available.

Ultrasound also plays a role in the differential diagnosis of pulmonary lesions and may allow to discriminate between them and to evaluate the effects of therapeutic interventions. Lung ultrasonographic techniques are described elsewhere in this manual.

38.1 Blunt and Penetrating Chest Trauma

Chest trauma is generally classified into blunt or penetrating, as different mechanisms of injury are involved (Table 38.3, Fig. 38.1).

Blunt chest trauma to the heart and intrathoracic great vessels – although relatively rare, accounting for less than 5% of trauma-related vascular lesions – carries an extremely high mortality, representing the second leading cause of trauma-related death after head injury. The actual incidence is very likely underestimated, as up to 80% of patients with TAI die before reaching the hospital and traumatic aortic rupture accounts for nearly 18% of all deaths related to motor vehicle accidents. A timely and accurate diagnosis and lifesaving interventions are essential to reduce the burden of preventable deaths due to inadequate or delayed management.

In penetrating trauma, injury comes as a result of the extrinsic violation of the thoracic cavity integrity. Two different mechanisms contribute to the damage: direct injury from the intrusion and

Table 38.2 Imaging techniques in chest trauma

	TEE	CT	MRI	Angiography
Pros				
Portability (bedside)	X	–	–	–
Rapidity	X	X	–	–
No radiation	X	–	X	–
Visualization of the entire aorta and branches	–	X	X	X
Specific advantages	Evaluation of cardiac function and cardiac valves, flow in the true/false lumen			
Cons				
Invasive	–	–	–	X
Requires experienced operator/interpreter	X	–	X	–
	–	–	X	X
	–	X	–	X
Expensive	Aspiration in the non-intubated patient	Potential renal damage from contrast	Long acquisition time	Retrograde extension of dissection
Requires contrast	Damage to visceral structures (very rare)		Not widely available 24h/7	False negative if false lumen is completely thrombosed
Specific risks			Contraindicated in patients with metal prostheses	Potential renal damage from contrast

Table 38.3 Classification of chest trauma

	Mechanism of injury	Frequent causes	Structures involved	Clinical pictures
Blunt	Compression between the spine and sternum Abrupt intrathoracic pressure shifts Shearing from rapid deceleration Upward displacement of intra-abdominal organs Blast injuries	Motor accidents Crush fractures Falls Kicks Sports injuries Explosions	Anterior structures (right chambers and aorta) more commonly involved	Cardiac contusion Rupture of myocardial free walls or interventricular septum Tamponade Aortic lesion (ranging from intramural hematoma to aortic rupture) Intrathoracic herniation of abdominal organs
Penetrating	Direct injury from penetrating object Damage to adjacent structures is directly related to the amount of energy exchange (i.e., mainly to the missile velocity)	Stab wounds Impalement Low- and high-velocity missiles	Dependent on the site of penetration, the velocity, and the intrathoracic path of the penetrating object	Penetrating injuries to the ventricles or the atria Tamponade
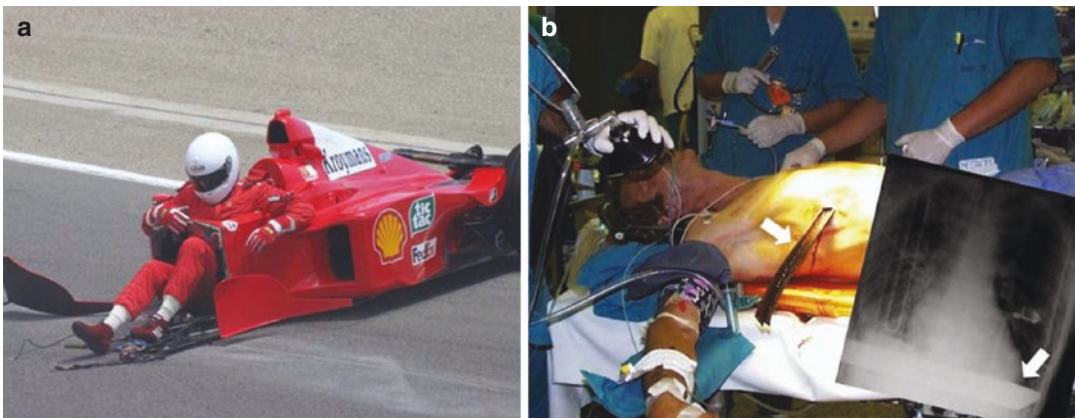
Fig. 38.1 Examples of blunt (**a**) and penetrating (**b**) chest trauma patients

damage to adjacent structures due to the exchange of energy between the penetrating object and the surrounding tissue; this latter harm is directly proportional to the amount of energy exchanged, which is in turn in direct relationship with the speed of the missile.

lesions, although nearly all possible cardiovascular lesions have been reported in trauma patients (Fig. 38.2). The most frequent and life-threatening clinical scenarios derived from these lesions are hemorrhagic shock, cardiac tamponade, and cardiac rhythm disturbances.

38.2 Cardiovascular Lesions in Chest Trauma

The most common trauma-related intrathoracic lesions are represented by traumatic aortic injury, myocardial contusion, cardiac rupture, and valve

38.2.1 Traumatic Aortic Injury

TAI is a rare but very lethal condition and represents the most commonly diagnosed injury in unstable chest trauma patients. Deceleration injuries from high-speed motor vehicle collisions and

Fig. 38.2 Post-traumatic heart dislodgement, with a rotation of the cardiac chambers in the right chest (arrow)
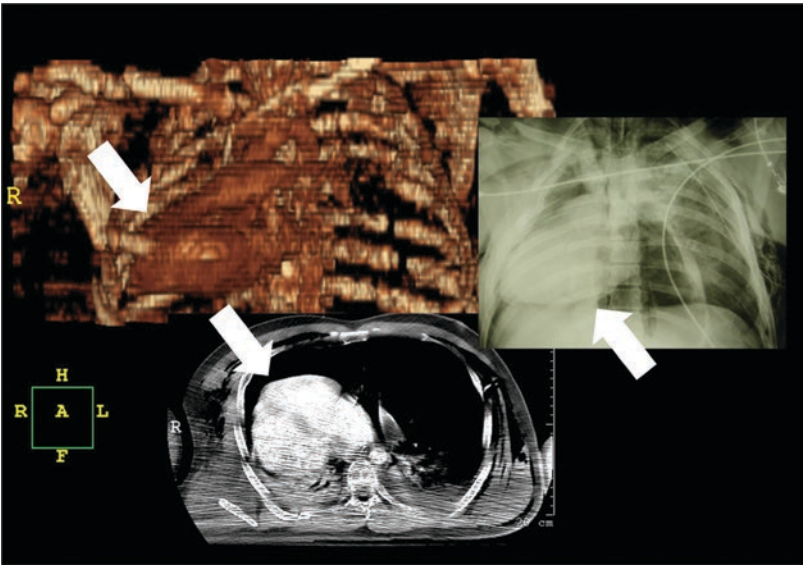
Table 38.4 Classification of TAI

Grade 1	TAI consisting of superficial lesions; conservative management is safe and effective
Grade 2	Subadventitial injuries requiring repair (immediate or delayed depending on clinical conditions)
Grade 3	Aortic transection with blood extravasation or aortic obstruction with ischemia; requires prompt repair

falls from a height represent the most frequent causal mechanisms. As already mentioned, roughly 80% of the patients die at the scene, and up to 50% of those who make it to the hospital die within 24 h if not promptly diagnosed and treated. The outcome of patients depends primarily on the extent of the lesion and on the rapidity of appropriate care (Table 38.4).

Most lesions are localized at the level of the aortic isthmus, between the left subclavian and the first intercostal arteries; this is due to the relative mobility of the ascending aorta with respect to this region, which is partially fixed by the ligamentum arteriosum, postnatal remnant of the duct of Botallus (Fig. 38.3).

Three factors contribute to aortic rupture: shear stress, bending stress, and torsion stress. As deceleration occurs, the aortic isthmus is placed under tension by the gradient created between the mobile aortic arch and the relatively fixed
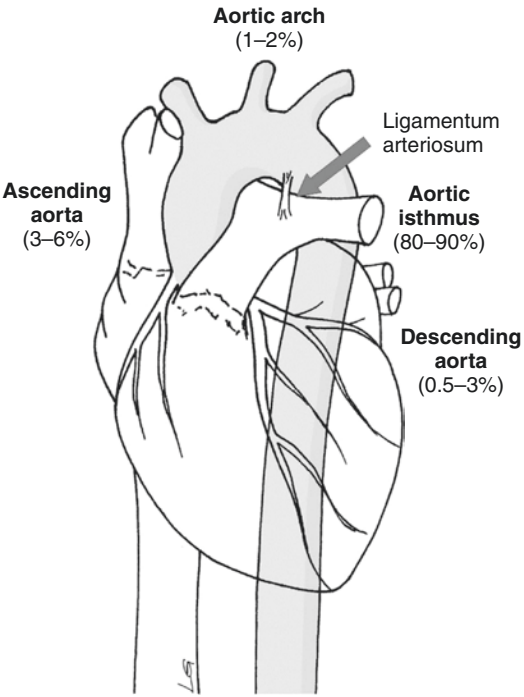
Fig. 38.3 Schematic drawing of the thoracic aorta, indicating the relative topographic distribution of traumatic aortic lesions

descending aorta, with an ensuing shear stress that can lead to rupture or tear. Bending stress results from the hyperflexion of the aortic arch produced by the downward traction exerted by

the heart, while anteroposterior compression of the chest with the heart displaced to the left leads to torsion stress. The combination of these three forces generates maximum stress to the inner aortic layer at the level of the ligamentum arteriosum (aortic isthmus), which represents the point of greatest fixation.

The second most common location for traumatic aortic injury is the supravalvular portion of the ascending aorta, followed by the diaphragmatic hiatus. Once again, these two regions represent points of relative fixation of the aorta and are hence subject to intense shear forces in case of abrupt deceleration.

A traumatic lesion may be classified as (1) intimal hemorrhage, (2) intimal hemorrhage with laceration, (3) medial laceration, (4) complete laceration of the aorta, (5) false aneurysm formation, and (6) periaortic hemorrhage.

Most patients with free rupture die at the scene, whereas patients with a contained rupture who reach the hospital alive often exhibit inconsistent symptoms, due to the variety of clinical presentations. For this reason it is of paramount importance to keep a high index of suspicion in all trauma patients with a potential TAI, even though they do not present evident signs of chest trauma.

38.2.1.1 Echocardiographic Findings

As mentioned above, TAI represents a wide spectrum of possible lesions, ranging from intimal lesion to intramural hematoma, pseudoaneurysm, aortic dissection, and aortic rupture.

Whereas complete aortic transection leads to on-scene death in most patients, cases with an incomplete rupture may reach the hospital alive. When the tear does not extend to the adventitial layer of the aortic wall, a pseudoaneurysm will develop. Contained rupture is generally visualized by TEE as a discontinuity of the aortic arch from the descending aorta, with torn and mobile ends often visible (Fig. 38.4). Perivascular hematoma is generally present, while flow to and from the pseudoaneurysmal space is inconsistent (Fig. 38.5). Doppler may detect a gradient across the lesion when the transection causes a flow obstruction.

Less severe trauma to the aorta may lead to intimal tearing, with the development of intramural hematoma; this scenario is generally characterized by stable hemodynamic conditions and presents a more benign course. Echocardiographic signs are similar to those occurring in spontaneous dissection, consisting of an aortic wall thickening (more than 7 mm is generally considered diagnostic) and/or an echolucent appearance within the aortic wall. Differential diagnosis with atherosclerotic lesions is not always straightforward, unless a tear is clearly visible. The site of the tear should be accurately inspected for perivascular hematoma – which represents a risk factor for a quickly progressive lesion – and for the patency of epiaortic vessels.

Fig. 38.4 TEE short-axis aortic view at the level of the aortic isthmus in a young man with incomplete post-traumatic aortic transection. The ruptured aortic wall is visible within the lumen of the vessel (arrow)
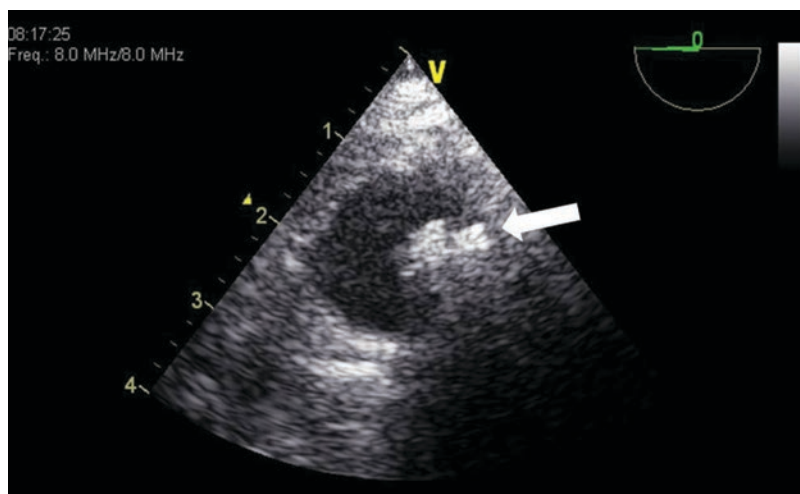
Fig. 38.5 In the same patient from Fig. 38.3, color Doppler demonstrates flow to and from the pseudoaneurismatic sac (arrow)
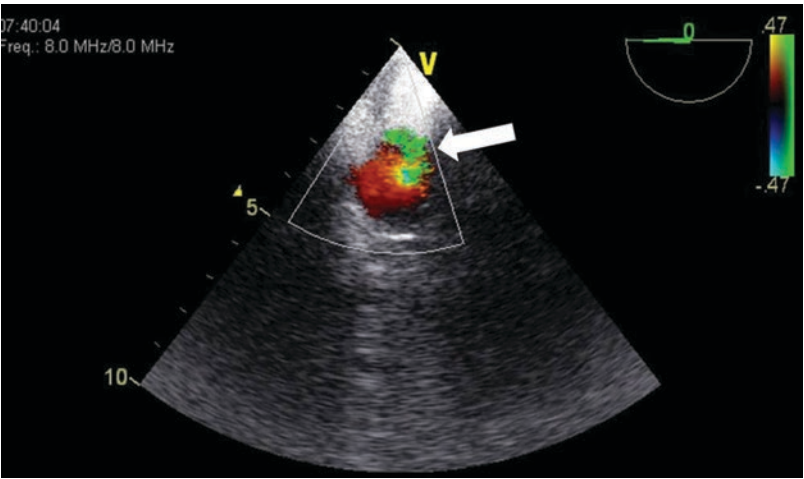
Table 38.5 Essential information gained by TEE in TAI patients

Proximal extent of dissection
Entry tear(s) location
Pericardial effusion and/or tamponade
Presence, mechanism, and severity of aortic regurgitation
Involvement of coronary ostia
Patency of epiaortic vessels
Systolic and diastolic ventricular function
Additional cardiac alterations

Information gained with TEE that is essential in the management of the patient do not differ from the setting of aortic dissection and are reported in Table 38.5.

The main limitation of TEE in the diagnosis of TAI is due to the "blind spot" caused by the trachea and the right main bronchus that makes the distal ascending aorta and the proximal arch very difficult to scan. The incidence of TAI in this region has been reported up to 20% of all TAIs, requiring a watchful attention and possibly a second imaging modality (i.e., CT scan) if the likelihood of aortic trauma is high.

Besides its fundamental role in the diagnostic stage of TAI, TEE also plays a key role during the operative period. Not only it allows ongoing monitoring of cardiac function and hemodynamics, but it also represents a consistent aid in the evaluation of the intraoperative and early postop-erative results of both surgical and endovascular interventions.

In the last decade, the endovascular treatment of traumatic aortic lesions gained an increasing role both in the acute and in the subacute settings. TEE, together with angiography, plays a pivotal role in the intraprocedural distinction of the true from the false lumen, guidewire positioning, graft positioning and deployment, patency of epiaortic branches, and periprosthetic leaks (Fig. 38.6, Table 38.6).

38.3 Blunt Cardiac Injury

Cardiac injury may come as a result of direct blows, athletic trauma, industrial crush, blasts, rapid deceleration, or falls from a height. A direct blow to the precordium creates a force that compresses the myocardium against the spine.

A significant chest wall trauma predicts a blunt cardiac injury in 13% of patients.

Because of the relatively free anteroposterior movement of the heart, the momentum generated from a rapid deceleration accident maintains the heart in a uniform, straight-line motion, resulting in a direct strike against the internal sternum. Several forces may be involved in BCI, including compression of the heart between the spine and sternum, abrupt pressure fluctuations in the chest and abdomen, shearing from rapid
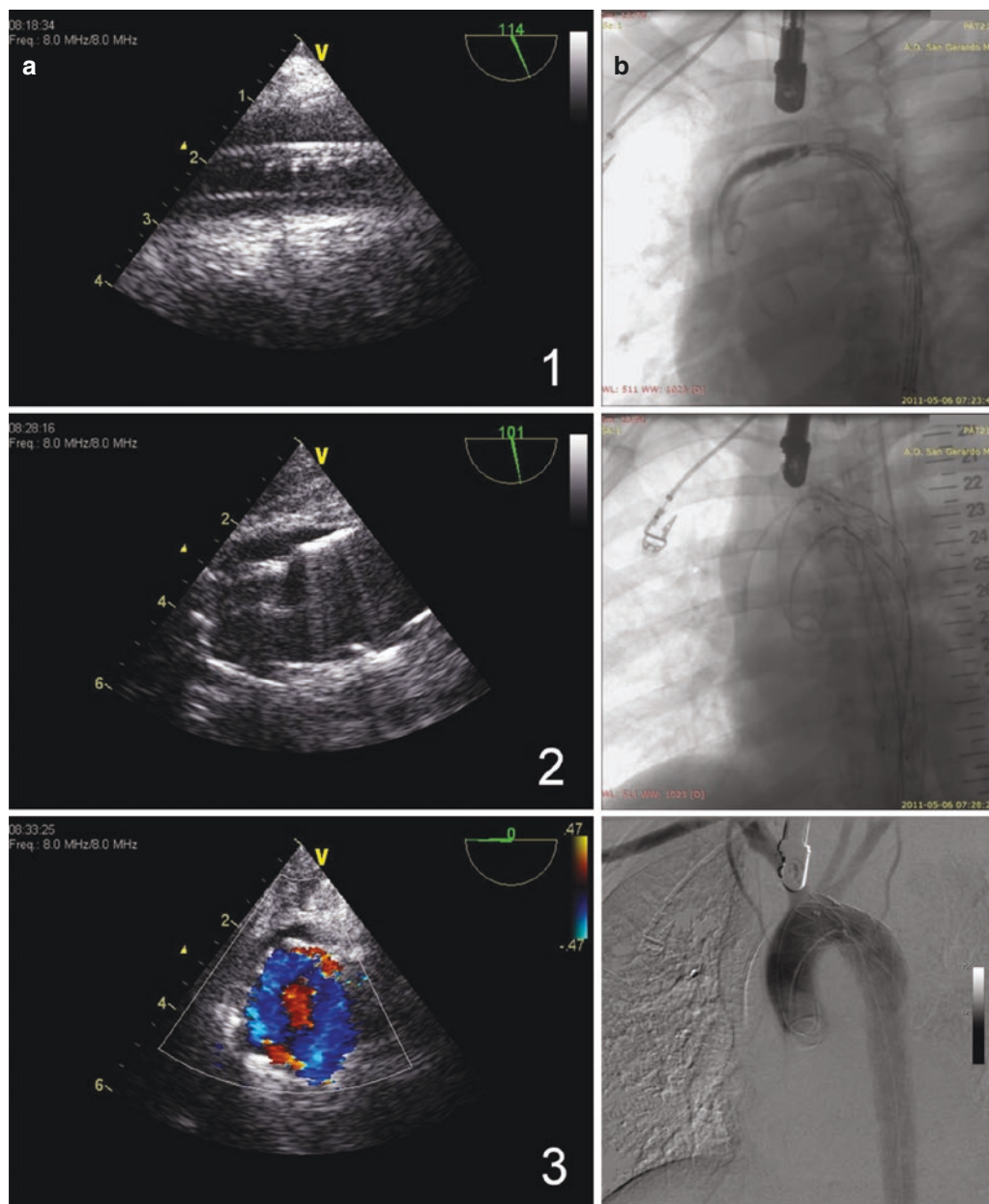
Fig. 38.6 Intraoperative echocardiographic (panel A) and angiographic (panel B) monitoring during endovascular repair of a traumatic lesion of the aortic isthmus. The graft is advanced in the descending aorta to cover the lesion, with the distal landing zone just distal from the emergence of the left subclavian artery (1); the graft is subsequently deployed in the correct position (2); and, finally, the procedure is verified for proper positioning, patency of the epi-aortic vessels, and the absence of significant leaks (3)

deceleration, and blast injury. In addition, fragments from rib fractures can directly traumatize the heart.

Blunt cardiac injury (BCI) includes cardiac contusion and concussion (commotio cordis), cardiac chamber rupture (free wall, septa, papillary muscles, and chordae tendineae), and valvular disruption. The right heart is most commonly injured, probably due to its position closest to the anterior chest wall. In autopsy series, ventricular

Table 38.6 Classification of endoleaks

Type I	Endoleak originating from either the proximal (Type Ia) or distal (Type Ib) end of the stent graft
Type II	Retrograde flow into the area of exclusion via side branches, i.e., intercostal arteries, inferior mesenteric artery, or lumbar arteries
Type III	Endoleak due to graft defect or between stent graft components
Type IV	Endoleak due to graft porosity

injuries predominate, while other findings such as valvular tear or rupture, septal tears, and coronary artery thrombosis do not, but these are far less common.

38.3.1 Myocardial Contusion

The absence of a clear definition and accepted gold standard for testing makes the diagnosis of cardiac contusion difficult. This also leads to the wide variability of reported prevalence in the literature, ranging from 3% to 56%. Suggestive symptoms may be unrelated to BCI, while mild injuries may be clinically asymptomatic. Moreover, some of the other criteria used in the definition of myocardial contusion, such as dysrhythmias and troponin release, may be related to the patient's preexisting conditions or to traumatic lesions remote from the chest.

Bradycardia may also result from direct compression or traction on the vagus nerve.

Despite the lack of a clear clinical indication, the association of a significant thoracic trauma with suggestive symptoms and/or dysthymias should trigger an echocardiographic examination.

38.3.1.1 Echocardiographic Findings
As significant cardiac contusion resembles myocardial ischemia and infarction, echocardiography is useful in detecting global and regional wall motion abnormalities, diastolic alterations, and associated lesions such as thrombi, pericardial effusions, and valvular lesions.

38.3.2 Cardiac Rupture

Cardiac rupture represents the most devastating form of BCI. As for complete aortic transection, most patients who sustain rupture of a heart chamber do not reach the hospital alive. Delayed rupture of the heart also may occur weeks after blunt trauma, probably as a result of necrosis of a contused or infarcted area of the myocardium.

The immediate ability of the patient to survive cardiac rupture depends mostly on the integrity of the pericardium. An intact pericardium or a very small pericardial tear may protect from immediate exsanguination. These patients may survive for variable periods, but they eventually develop significant hemopericardium and pericardial tamponade.

Atrial rupture occurs far less often than the ventricular rupture, most likely due to anatomy and lower compliance, and presentation may be delayed and less acute. Right atrial rupture is seen in about 10% of wall ruptures from blunt trauma and left atrial rupture less often.

Septal injury appears to be rare and its presentation variable. Septal injury may involve insignificant tears or frank rupture and may be associated with valvular injury. Signs of acute heart failure may be present.

Isolated valvular injury is likewise rare. The aortic valve is most often injured (Fig. 38.7), followed by the mitral and tricuspid valves. The lesion may consist of a tear of the leaflet or a partial- or full-thickness tear of the papillary muscle or chordae tendineae. Presentation may vary depending upon the lesion but falls somewhere on the spectrum of acute valvular insufficiency with right- or left-sided heart failure. Treatment for septal and valvular injury is generally surgical, and timing depends upon the stability of the patient and associated lesions.

38.3.2.1 Echocardiographic Findings
Focused assessment with sonography for trauma (FAST, discussed elsewhere in this book) allows to detect significant pericardial effusions in unstable trauma patients. Once

Fig. 38.7 Traumatic disruption of the aortic valve. The aortic cusps show a diastolic flail in the left outflow tract
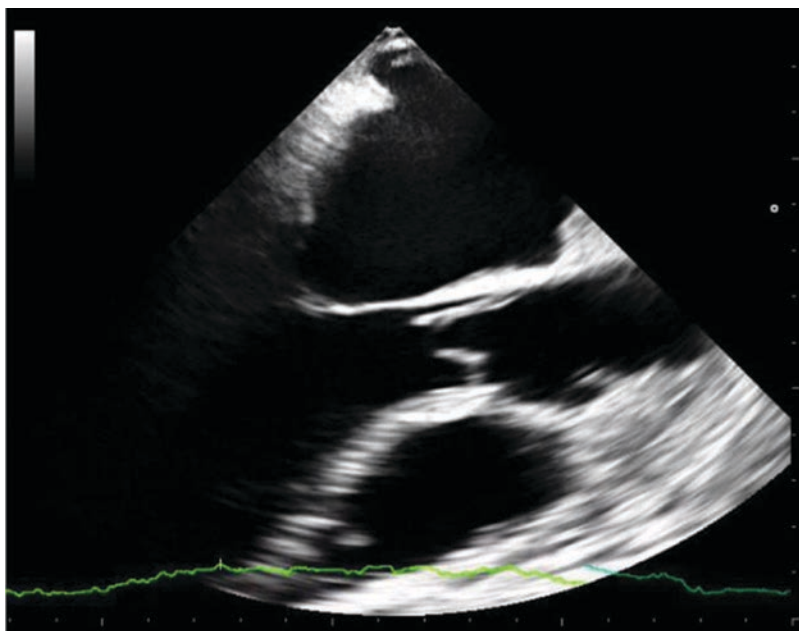
pericardial tamponade is ruled out, echocardiography (particularly TEE) permits to identify wall motion abnormalities, to determine the need for fluid resuscitation or inotropic support and identify other lesions requiring intervention. Of particular interest is the recognition of pericardial effusion and its monitoring, in order to anticipate and avoid cardiac tamponade. The identification of free wall discontinuations may be challenging, since those are frequently subtle fistular fissures across the myocardial layers, rather than linear ducts. Doppler flow imaging and/or the intravenous injection of a small amount of echogenic contrast medium may be helpful when the diagnosis is particularly demanding. The same considerations apply to septal lesions; in this latter case, the presence, direction, and magnitude of intracardiac shunts should be clarified, and signs of right heart volume overload should be noted. For right chambers, a small volume of colloid solution shaked well with a small amount of air to form microbubbles may work as intravenous contrast medium, whereas when the microbubbles need to persist across the pulmonary circulation and reach the left chambers, a contrast agent is indicated. These media contain small (1–8 μm)

engineered microbubbles filled with a high molecular weight perfluorocarbon which have substantial persistence in the bloodstream (contrast effect lasting up to 10 min). It should be noted that this indication is off-label for all FDA-EMEA-registered contrast agents.

Traumatic valvular injuries encompass a wide spectrum of possible lesions from small fissures or perforations in the valve leaflets, to complete disruption of the valve structure. The echocardiographic investigation of such lesions reflects the usual evaluation of cardiac valves carried out in the standard echocardiographic examination. Signs of volume or pressure overload associated with these lesions should be inspected as well.

38.4 Diagnostic Algorithm in the Chest Trauma Patient

In order to approach trauma patients in a consistent and reproducible way, the implementation of a diagnostic protocol is of paramount importance, as it allows to minimize individual judgment and time loss in such a challenging situation. The diagnostic algorithm reported in

Fig. 38.8 The algorithm for the management of chest trauma patients in use at the authors' institution

Diagnostic algorithm in chest trauma patients

* Endovascular procedure when feasible
** Intraoperative angiography in O.R.
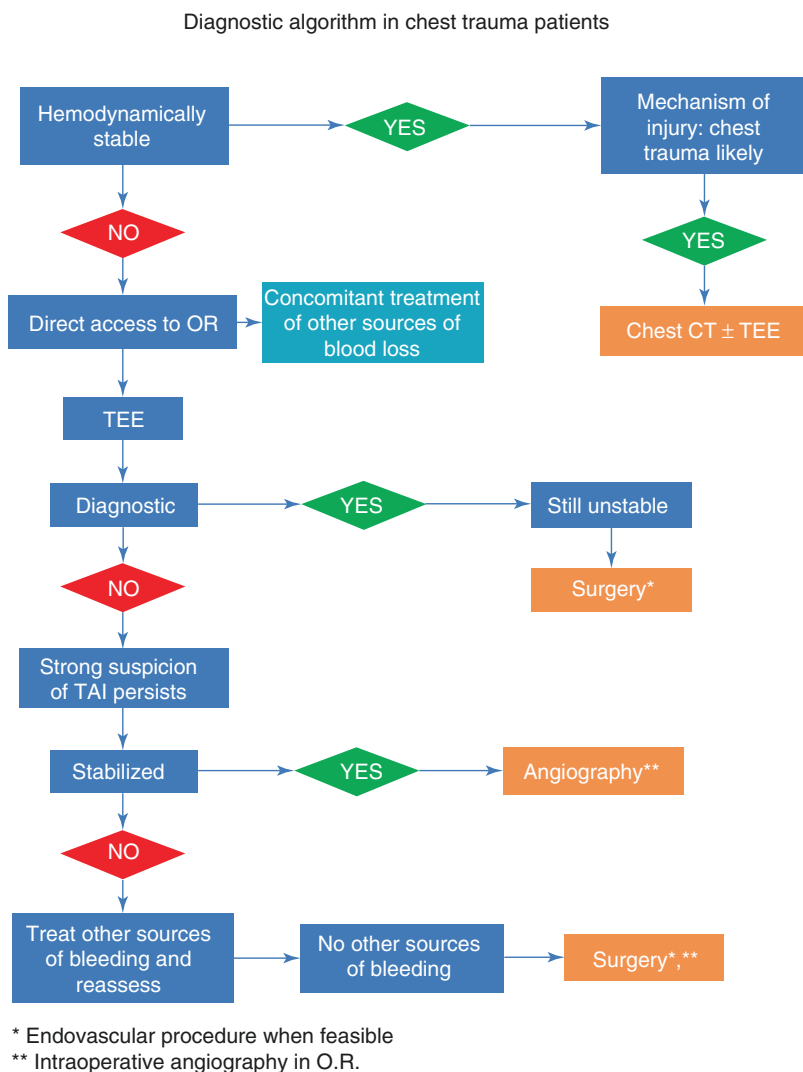
Fig. 38.8 represents the guideline currently applied at our institution.

38.5 Cardiac Ultrasound in Traumatic Cardiac Arrest

Traumatic cardiac arrest brings an extremely poor prognosis, particularly in patients presenting with non-shockable rhythms.

Whereas TEE does not generally add much in asystolic patients, it has a role in those presenting with pulseless electrical activity (PEA). In this population the first role of echocardiography is to differentiate between true PEA (i.e., organized activity on ECG without evidence of cardiac motion) and pseudo-PEA (presence of cardiac motility which is not able to generate a clinically appreciable pulsatile activity), as the latter yields a far better prognosis when the cause leading to cardiac arrest is promptly recognized and adequately treated. The second role of echocardiography in this setting is hence to investigate the likely cause of cardiac arrest and monitor therapeutic interventions.

38.6   Summary

Although the involvement of the chest in trauma is quite common, serious injuries are relatively rare.

Nevertheless, lesions to the heart and great intrathoracic vessels carry an extremely high mortality, which is attributable to a delayed recognition and treatment in a number of patients.

Echocardiography – namely, TEE – represents, in experienced hands, an invaluable tool in the acute management of chest trauma patients, as it allows continuation of ongoing resuscitative maneuvers and provides point-of-care diagnostic and monitoring capabilities on the morphological and functional status of intrathoracic cardiovascular structures (Table 38.7).

TEE furthermore represents a fundamental aid during the operative moment to assess the adequacy of therapeutic interventions, particularly in the setting of endovascular aortic surgery, where its integration with intraoperative angiography allows optimal control of the procedure.

Although in stable patients CT still presents some advantages on the morphological evaluation of the thoracic aorta, it needs nonetheless integrative information that only TEE can provide on the heart morphology and function and on the hemodynamic status.

Caution is advised in the introduction of the transesophageal probe in patients with proven or suspected cervical spine trauma.

We can state that TEE and CT represent complementary diagnostic techniques in the stable patient, whereas in the unstable critically injured patient, TEE proves superior in terms of portability and lifesaving information gained.

Table 38.7 Advantages and disadvantages of TEE in chest trauma patients

Advantages:
Excellent visualization of the aortic isthmus (most common location of traumatic aortic injury)
Can be obtained at the bedside and avoids transportation to CT in unstable patients
Allows simultaneous evaluation of injuries to the heart and great vessels and cardiac function
Disadvantages:
Blind spot on the distal ascending aorta and proximal arch due to interposition of the right main stem bronchus
Requires adequate training and yields a certain degree of operator dependency
Might be unobtainable or unsafe in patients causing injuries to the face, pharynx, upper airways, and esophagus
Particular caution must be paid in patients with known or suspected
Benefit should be weighed against possible risks in such patients

Suggested Reading

American College of Surgeons. ATLS – Advanced Trauma Life Support Student Course Manual. ISBN 78-0-9968262-3-5. 2018.

Evangelista A, Flachskampf FA, Erbel R, et al. Echocardiography in aortic diseases: EAE recommendations for clinical practice. Eur J Echocardiogr. 2010;11:645–58.

Goldstein SA, Evangelista A, Abbara S, et al. Multimodality imaging of diseases of thoracic aorta in adults: from the American Society of Echocardiography and the European Association of Cardiovascular Imaging. J Am Soc Echocardiography. 2015;28:119–82.

Hiratzka LF, Bakris GL, Beckman JA, et al. 2010 ACCF/AHA/AATS/ACR/ASA/SCA/SCAI/SIR/STS/SVM Guidelines for the diagnosis and management of patients with thoracic aortic disease: a report of the American College of Cardiology Foundation/American Heart Association Task Force on Practice Guidelines, American Association for Thoracic Surgery, American College of Radiology, American Stroke Association, Society of Cardiovascular Anesthesiologists, Society for Cardiovascular Angiography and Interventions, Society of Interventional Radiology, Society of Thoracic Surgeons, and Society for Vascular Medicine. Circulation. 2010;121:e266–369.

Meredith EL, Masani ND. Echocardiography in the emergency assessment of acute aortic syndromes. Eur J Echocardiogr. 2009;10:i31–9.

Neschis DG, Scalea TM, Flinn WR, Griffith BP. Blunt aortic injury. N Engl J Med. 2008;359:1708–16.

Ting JYS. Blunt traumatic aortic injury. A review of initial diagnostic modalities and a proposed diagnostic algorithm. Eur J Trauma. 2003;29:129–38.

Acute Atrial Fibrillation and Other Arrhythmias

39

Piercarlo Ballo

Key Points

- Atrial fibrillation (AF) is commonly observed in daily practice. It is associated with worse outcome, particularly with regard to the risk of systemic thromboembolism and hemodynamic deterioration.
- Transthoracic echocardiography plays a primary role in the clinical management of patients with AF, providing clinically useful information on AF etiology, underlying cardiac disease, and risk stratification.
- This is also true in the setting of acute AF, where rapid decisions among the possible options for clinical management must be taken.
- Transesophageal echocardiography also has a major role in this context, as the first-choice technique to rule out intracardiac thrombosis for subjects in whom an early cardioversion strategy is planned.

P. Ballo (✉)
Cardiology Unit, Santa Maria Annunziata Hospital, Florence, Italy
e-mail: piercarlo.ballo@uslcentro.toscana.it

39.1 Introduction

Atrial fibrillation (AF) is one of the most commonly observed arrhythmias in daily practice. Its overall prevalence is about 0.4% in the general population but raises to 9% in those aged ≥80 years. These values will probably increase in the next years, as a result of the advancing age of the population, with a significant socio-economic health burden. From a clinical point of view, AF is associated with increased mortality and morbidity, with systemic thromboembolism – particularly stroke – and hemodynamic deterioration being the most relevant complications. AF may also lead to reduced quality of life and impaired exercise capacity. Transthoracic echocardiography (TTE) plays a major role in the clinical management of patients with AF, allowing a detailed assessment of cardiac structure and function and providing information for risk stratification, with a potentially important impact on the issue of anticoagulation. Transesophageal echocardiography (TEE) is often used to rule out intracardiac thrombosis for patients in whom an early cardioversion strategy is planned. New echocardiographic techniques such as speckle tracking have further expanded the potential applications of echocardiography in this context. Lastly, echocardiography plays a key role in some interventional techniques such as cath-

eter ablation and left atrial appendage (LAA) occlusion.

In this chapter, we briefly review the role of echocardiography in the assessment and management of patients with acute AF. Most of the information provided also applies to other sustained supraventricular arrhythmias, for which the clinical management (e.g., in terms of anticoagulation) is often similar. Although we focused on the assessment of the morphologic and functional evaluation of the left atrium and the LAA – which plays a major role in this context – it should be pointed out that a comprehensive echocardiographic examination provides a number of other important data for the management of patients with AF, which include LV size and systodiastolic function, right-sided chamber size and function, pulmonary vein flow patterns, valve disease, myocardial and pericardial diseases, and others.

39.2 Transthoracic Echocardiography

39.2.1 Assessment of LA Size

Assessment of LA size is a rapid, simple, but very relevant part of the echocardiographic evaluation in patients with AF. In patients with no significant mitral valve disease, an enlarged LA size often reflects the presence of increased LA pressure, as well as LA dysfunction due to atrial tissue myopathy. The magnitude of LA enlargement in these cases is a marker of the severity and duration of LV diastolic dysfunction. Increased LA size is a major risk factor for incident AF and stroke and is associated with adverse cardiovascular outcomes in a number of pathophysiological conditions, as well as in the general population. LA anteroposterior is classically measured by M-mode imaging at end-systole from the parasternal long-axis view at the level of the aortic sinuses, using the leading-edge to leading-edge technique (Fig. 39.1). This measurement has the advantages of being reproducible and having elevated temporal resolution and has been extensively validated in clinical studies. LA diameter measurement can also be per-

formed using two-dimensional images, to facilitate the orientation of the ultrasonic beam perpendicularly to the posterior LA wall, although this approach provides lower temporal resolution. Whatever the approach used, care is needed in interpreting LA diameter as an index of true LA size, since this would imply the incorrect assumption of a constant ratio between LA dimensions along different geometrical axes. Indeed, because of the anatomical confinement afforded by the spine and sternum in the anteroposterior axis, the left atrium often enlarges asymmetrically with a preferential dilatation along the other two geometrical axes. As a result, the use of the simple LA diameter as a measure of LA size can lead to a significant underestimation, particularly in dilated atria. Therefore, it is preferable to avoid the use of LA diameter alone when assessing LA size.

LA area can be measured from apical views at end-systole, choosing the frame prior to mitral valve opening and tracing the LA endocardial borders after careful optimization of the image by dedicated acquisitions, to avoid foreshortening of the LA chamber. In this measurement, the LAA and the confluences of the pulmonary veins should be excluded, whereas a straight line representing the mitral annulus plane should be taken as the inferior aspect of LA border (Fig. 39.2). A similar technique is used to estimate LA volume, which to date is recommended by the 2015 ASE/EACVI chamber quantification guidelines as the most reliable measure of LA size. LA volume is also a better prognostic predictor than LA diameter in various cardiac diseases. LA volume is calculated from biplane planimetry of the LA chamber using the method of disks, which is similar to that used for the calculation of LV volumes. This method can also be applied using a single-plane approach when biplane planimetry is not possible, taking into account that apical four-chamber volumes generally provide values that lead to values that usually are 1–2 mL/m^2 smaller than apical two-chamber volumes. Alternatively, LA volume can be measured using the biplane area-length method, in which a formula including the two planimetric areas and LA length (defined as the shortest of the two LA lengths measured in the two- and four-chamber
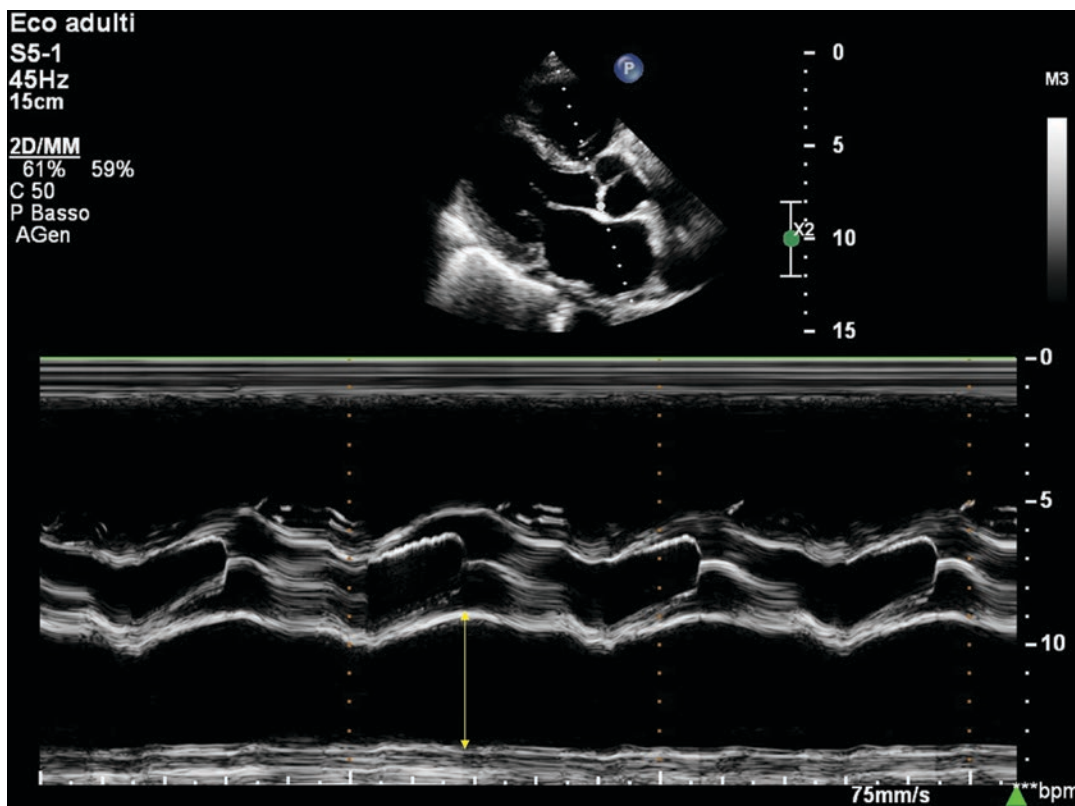
Fig. 39.1 M-mode measurement of left atrial diameter

apical views) is used. After indexation to body surface area, a LA volume index of 34 mL/m² is to date considered the upper limit of the normal range. 3D echocardiography is a promising technique for the assessment of LA volume, providing estimates that correlate better with cardiac magnetic resonance and computed tomography than those obtained by 2D imaging. Unfortunately, despite the increasing availability of 3D software, to date the relative paucity of normative data, the need of adequate training to obtain and interpret images, and the lack of a standardized approach make this approach still difficult to be used for routine practice.

39.2.2 Assessment of LAA by TTE

Although the LAA is usually best imaged by TEE, it can also be visualized by TTE using various approaches, particularly the parasternal short-axis view at the level of great vessels, a modified apical four-chamber view with anterior angulation, or the apical two-chamber view (Fig. 39.3). However, even when the acoustic windows are good, TTE images do not allow to exclude the presence of thrombus with adequate confidence. Tissue Doppler imaging of the LAA myocardial motion has been proposed as an alternative technique to provide additional information for prognostic stratification in patients with AF, since lower LAA myocardial velocities are associated with spontaneous echo contrast, increased probability of thrombus, and history of ischemic cerebral events. However, a well-known major limitation of tissue Doppler is that it is unable to discriminate active and passive movements, so that it is subject to tethering and translation effects. 2D strain imaging by speckle tracking is a technique that can overcome these
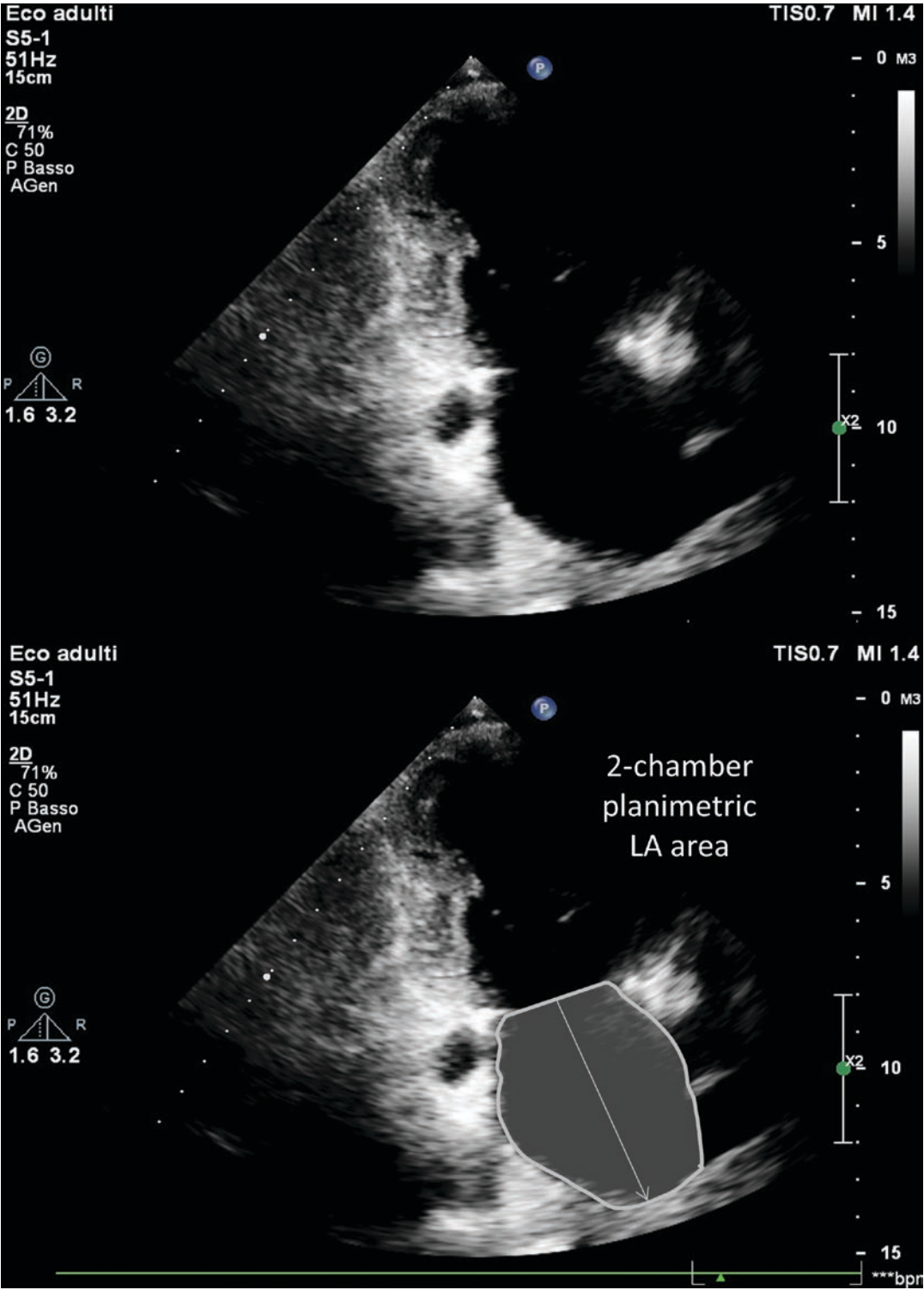
Fig. 39.2 Two-dimensional planimetry of left atrial (LA) chamber area from the apical two-chamber view. From the biplane measurement of LA areas, LA volume is then calculated using the method of disks or the area-length approach
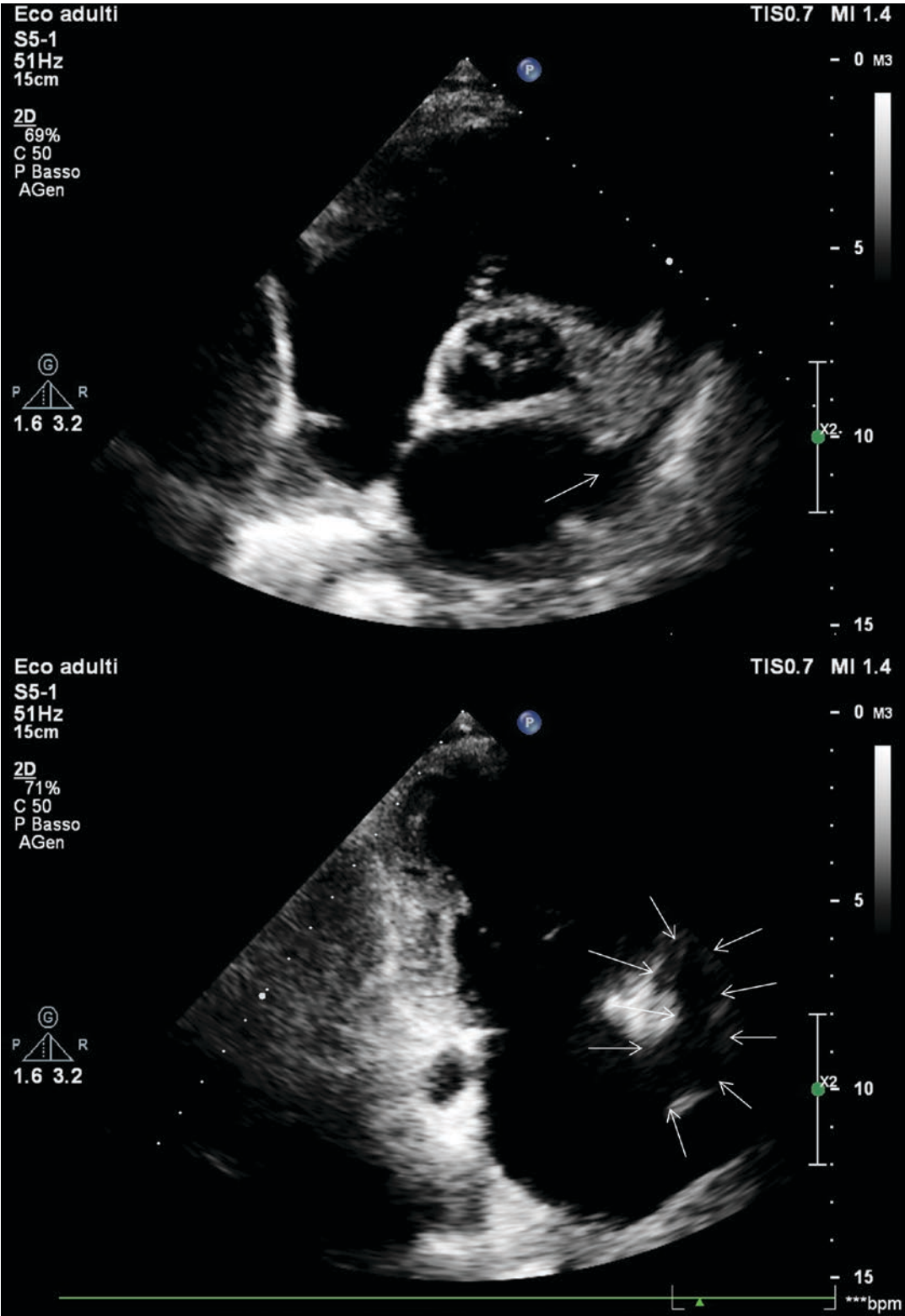
Fig. 39.3 Visualization of the left atrial appendage by transthoracic echocardiography. *Top panel*: short-axis view at the level of the aortic valve. *Bottom panel*: apical two-chamber view

limitations providing information about LA myocardial deformation dynamics. Although most of its applications to the study of the left atrium have been focused on the study of LA function (see above), some studies have explored its potential utility for the study of LAA function, showing a good correlation of various LAA strain parameters with the emptying and filling velocities even when 2D strain assessment is obtained using the transthoracic approach. The use of contrast agents has been shown to increase the ability of TTE to identify a thrombus in the LAA. In the CLOTS trial, TTE was found to be useful for the detection of LAA thrombus using harmonic imaging combined with intravenous contrast, whereas LAA myocardial velocities by tissue Doppler were useful to predict the severity of spontaneous echo contrast and to detect sludge or thrombus. Lastly, 3D echocardiography can provide interesting information for the visualization and quantitative analysis of the LAA, giving data that correlate well with those obtainable by computed tomography. LAA end-diastolic volume and LAA cauliflower phenotype detected by 3D echocardiography have also been found to be predictors of thromboembolic events, independent of the $CHA_2DS2VASc$ score, in patients with non-valvular AF.

39.2.3 Assessment of LA Function

TTE also provides relevant data about LA function. Three components of LA function have been classically assessed: the reservoir function, which occurs during the ventricular systole and the isovolumetric relaxation, when the left atrium receives the pulmonary venous flow; the conduit function, which occurs in early diastole after mitral valve opening, when the blood moves from the left atrium to the left ventricle; and the booster pump function, which occurs in late diastole when the left atrium actively contracts, giving a contribution to LV filling. The LA contraction contributes up to 30% of total LV stroke volume in normal subjects, and this proportion is further increased in patients with abnormal relaxation patterns. The atrial contribu-

tion to LV filling, which is particularly important in patients with LV dysfunction, disappears with the onset of AF, which is typically associated with a loss of atrial booster pump function. This leads to an increase in the pressure gradient between the left atrium and the left ventricle during early diastole, necessary to maintain an adequate stroke volume. However, if this compensation mechanism is not sufficient, symptomatic deterioration can occur.

The standard approach of TTE to LA function is based on the assessment of LA phasic function by the volumetric method. Three LA volumes are measured at different phases of the cardiac cycle, using the electrocardiographic support. The maximal LA volume is measured at end-systole, at the end of the T wave, before mitral valve opening. The minimal LA volume is measured at the onset of the QRS, at the mitral valve closure; and the so-called pre-A LA volume is measured at the onset of the P wave. Measures expressing the efficiency of each of the three components of LA function – such as the LA passive emptying volume and fraction, the conduit volume, the LA active emptying volume and fraction, and the LA total emptying volume and fraction – can be calculated from these LA volumes. Unfortunately, the 2D volumetric approach to LA function is rather time-consuming and not particularly suitable for daily practice. Moreover, the lack of atrial contraction in AF prevents the calculation of some of these indexes. The peak velocity of the A wave in the transmitral inflow is an alternative simple and easy-to-measure index of LA mechanical function expressing the booster pump component (Fig. 39.4, top panel), but again it cannot be measured in patients with AF, in whom no valid LA contraction occurs. This is also true for other indexes utilizing the A wave velocity, such as LA ejection force and kinetic energy. However, the peak A velocity, together with other similar indexes such as the velocity-time integral of the A wave and its ratio to that of the total diastolic transmitral flow, has been proposed to assess progressive LA function recovery in patients with AF after successful cardioversion or ablation. Tissue Doppler imaging of LV longitudinal motion, which is an established technique
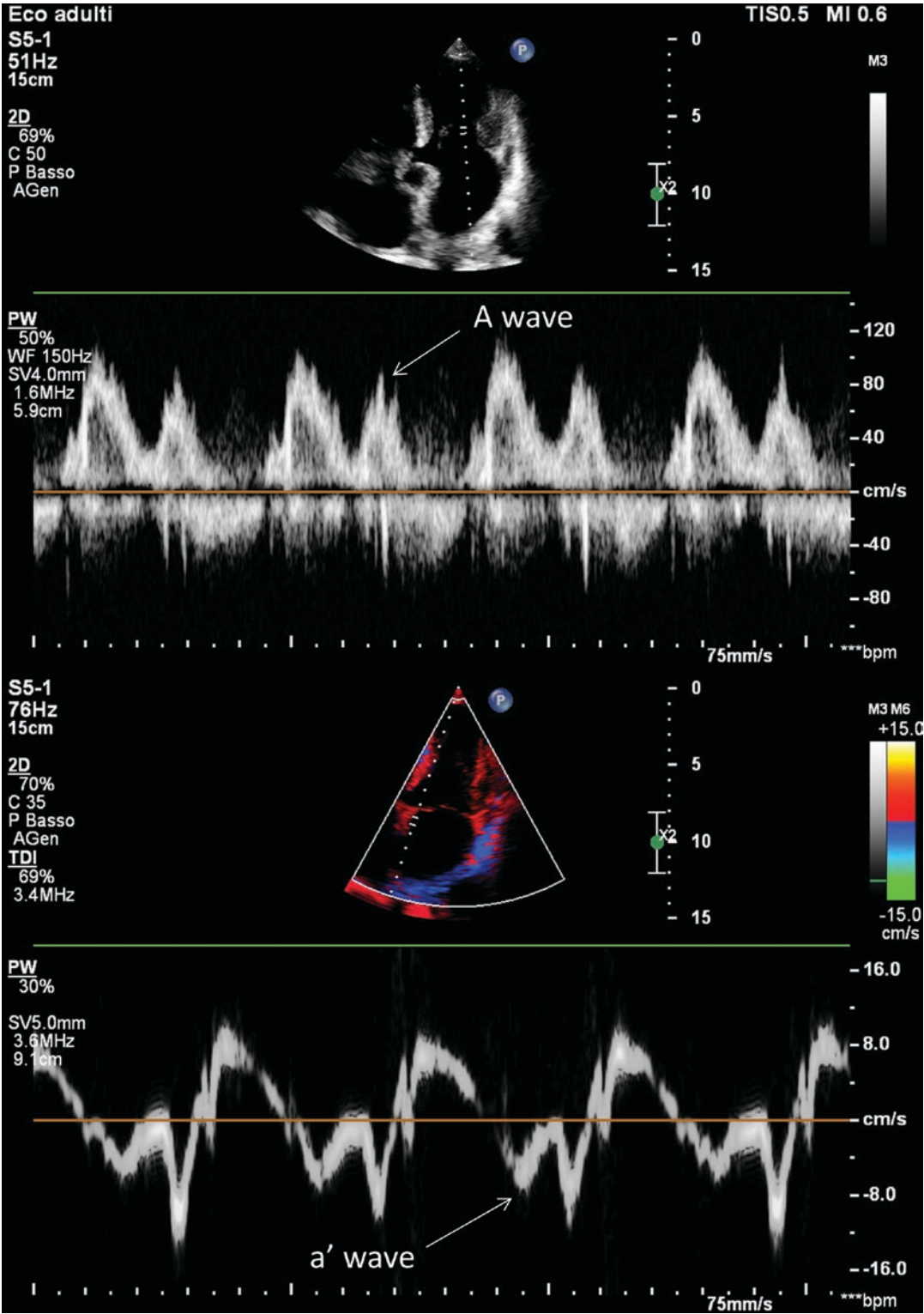
Fig. 39.4 Atrial waves in standard Doppler imaging of mitral inflow (top) and tissue Doppler imaging of mitral annulus motion (bottom)

for the assessment of LV diastolic function, also allows measurement of the peak velocity of the mitral annulus in late diastole (a' velocity) (Fig. 39.4, bottom panel). This has been proposed as marker of atrial function that correlates with LA systolic fractional area and volume change. In addition to the impossibility of using this measure in AF patients, unfortunately the abovementioned limitations of tissue Doppler imaging reduce the clinical utility of these measures.

2D strain imaging of the left atrium by speckle tracking is a very promising technique for the assessment of LA function. As already mentioned, the speckle tracking technique provides measures of myocardial deformation that are relatively insensitive to passive motion and tethering effects. Its application to the study of LA function provides two main indexes, the peak atrial longitudinal strain, measured at the end of the reservoir phase, and the peak atrial contraction strain, mostly expressing the LA booster function (Fig. 39.5). The assessment of LA strain by speckle tracking has been shown to provide useful information for the prediction of AF in many scenarios. In patients with AF, LA strain has been used to assess LA recovery after electrical cardioversion.

39.2.4 Clinical Utility of TTE in Patients with Acute AF

Echocardiography should be considered as a key part of the routine evaluation in patients with AF. The current 2016 ESC guidelines for the management of patients with atrial fibrillation recommend TTE in all AF patients to guide treatment decisions (class I, level of evidence C), pointing out that TTE should be used to identify structural diseases (e.g., valvular, myocardial, pericardial diseases) and to assess LV size and systodiastolic function, left atrial (LA) size, and right heart morphology and function. All these data are of primary importance to assess AF etiology, to choose the most appropriate strategy by guiding therapeutic choices, and to stratify the risk of patients with AF. Similar recommendations are given by the 2014 AHA/ACC AF guideline for the management of patients with AF.

A major clinical application of echocardiographic data for the management of acute AF patients is related to the choice of the rate control strategy, which is a primary issue in the management of AF patients, being often sufficient to improve AF-related symptoms. Rate control can be achieved, both in the acute setting and for
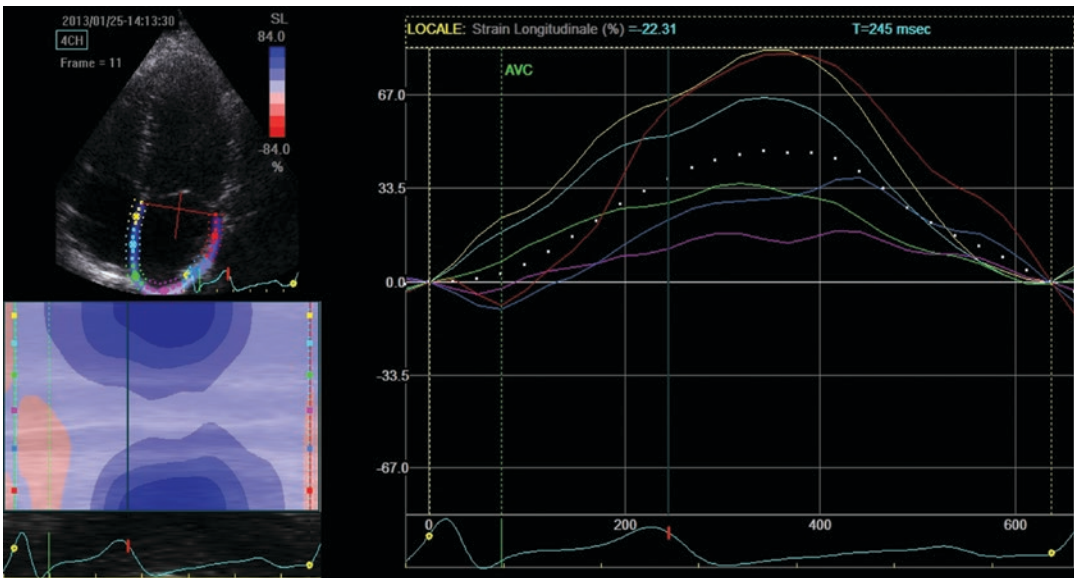
Fig. 39.5 Two-dimensional left atrial strain curves, assessed by speckle tracking imaging. The dotted white line is the average strain curve

long-term therapies, using several medication classes, including beta-blockers, digoxin, non-dihydropyridine calcium channel blockers (vera-pamil and diltiazem), or combination therapy. Some antiarrhythmic agents also show rate-controlling effects (e.g., amiodarone, dronedar-one, and sotalol), but they are mostly used for rhythm control therapy. For patients with AF who require acute heart rate control, who often present with high ventricular rate and potential risk of hemodynamic deterioration and for whom a decision about the best clinical management must be rapidly made, the ESC algorithm recommends TTE, together with the clinical assessment of signs of heart failure, as a first step for the evaluation of LV function, to guide the pharmacological management and to determine further decisions. In this algorithm, different practical recommendations are given according to the presence of an ejection fraction higher or lower than 40%. It should be stressed that, in these patients, a correct assessment of LV function may be sometimes difficult, as the high and irregular rate may play as a confounder for a correct definition of LV systodiastolic function. Nonetheless, TTE provides invaluable information and can also guide the successive management, with a particular impact on the choice of the antiarrhythmic prophylaxis or the need of early cardioversion. TTE also plays a primary role in the ESC algorithm for long-term heart rate control.

TTE in this context also provides important data for risk stratification. It is well known that LA size is a major determinant of AF risk. In the Framingham study, a 5 mm increase in LA diameter was associated with a nearly 40% increased risk of AF occurrence. In a large cohort study, a value of >50 mm was associated with a fourfold increase in the risk of developing AF. LA volume is also a predictor of AF and is a superior prognostic marker as compared to LA diameter. Similarly, in the specific population with acute AF, for which after stabilization a decision on rhythm or rate control has to be made, a larger LA size is associated with higher probability of AF cardioversion failure and AF relapse. On the other hand, in patients for whom a cardioversion strategy is considered appropriate, it should be pointed out that,

because AF favors further LA dilatation, prompt cardioversion and adequate restoration and maintenance of sinus rhythm may interrupt and potentially reverse this process. As previously mentioned, the information given by LA size should be complemented by those provided by a comprehensive TTE examination, in order to decide the best strategy and to obtain a correct risk stratification in both the acute phase and the long-term management of patients with AF. The assessment of LA strain by speckle tracking can add further data for the prognostic stratification. Evidences suggest that a lower peak atrial longitudinal strain may be a predictor of AF cardioversion failure and that it provides incremental value for embolism and stroke risk stratification over the CHA_2DS_2-VASc score in patients with AF.

39.3 Transesophageal Echocardiography

39.3.1 Assessment of the LAA

The risk of systemic embolism is an issue of major importance in patients with AF, which is estimated to account for a considerable proportion of all cases of cardiogenic thromboembolism. In this regard, it must be highlighted that cardioembolic infarction is usually the most severe ischemic stroke subtype, showing a low probability of symptom-free at hospital discharge, an elevated risk of recurrences, and a high mortality rate. Therefore, stroke prevention is one of the primary goals of the management of patients with AF. Compared to TTE, TEE has a higher sensitivity and specificity for detection of thrombi in the left atrium and particularly in the LAA, with values of approximately 95% to 100%.

By TEE, the LAA is best visualized in the mid-esophageal view, starting at 0°. Multiple views using the multiplane function (i.e., moving the beam angle) should be obtained for a comprehensive assessment of LAA cavity. A common approach is to begin the imaging of the LAA in the mid-esophageal aortic valve short-axis view (30–60°) and then to continue by anteflexing the

probe and gradually rotating the multiplane angle over the entire range from 0° to 180°. A relatively high interindividual variability of LAA shape exists, and then the angle allowing the best visualization of the LAA complex shape and potentially multilobed architecture varies between subjects (Fig. 39.6). Live 3D TEE is able to provide additional information of the complex LAA anatomy.

Importantly, identification of LAA thrombus by TEE can sometimes be difficult even in patients with adequate image quality, particularly at the tip of the LAA. A number of factors, including artifacts, prominent pectinate muscles, and trabeculae, can mimic the presence of thrombus. Careful assessment from multiple views is mandatory in these cases to discriminate thrombus (Fig. 39.7). Even when no thrombus is found, the detection of LA or LAA spontaneous echo contrast is a major predictor of ischemic strokes.

Spontaneous echo contrast results from low blood flow velocities, particularly in the LAA, and is characterized by the so-called smoke effect. The detection of spontaneous echo contrast in the LAA is associated with a considerably higher risk of thromboembolic event in comparison with patients without it.

TEE also allows assessment of LAA function. Pulsed Doppler imaging of LAA flows is obtained by placing the sample volume in the proximal third pf LAA cavity, keeping the gain relatively low to minimize the artifacts due to LAA myocardial wall. In normal subjects with sinus rhythm, a typical quadriphasic flow pattern is observed, including an *early diastolic emptying velocity, a late diastolic emptying velocity (LAA contraction flow), a systolic LAA filling velocity, and systolic reflection waves* (Figs 39.8 and 39.9). *In patients with AF, usually the pattern is characterized by irregular* sawtooth waves of
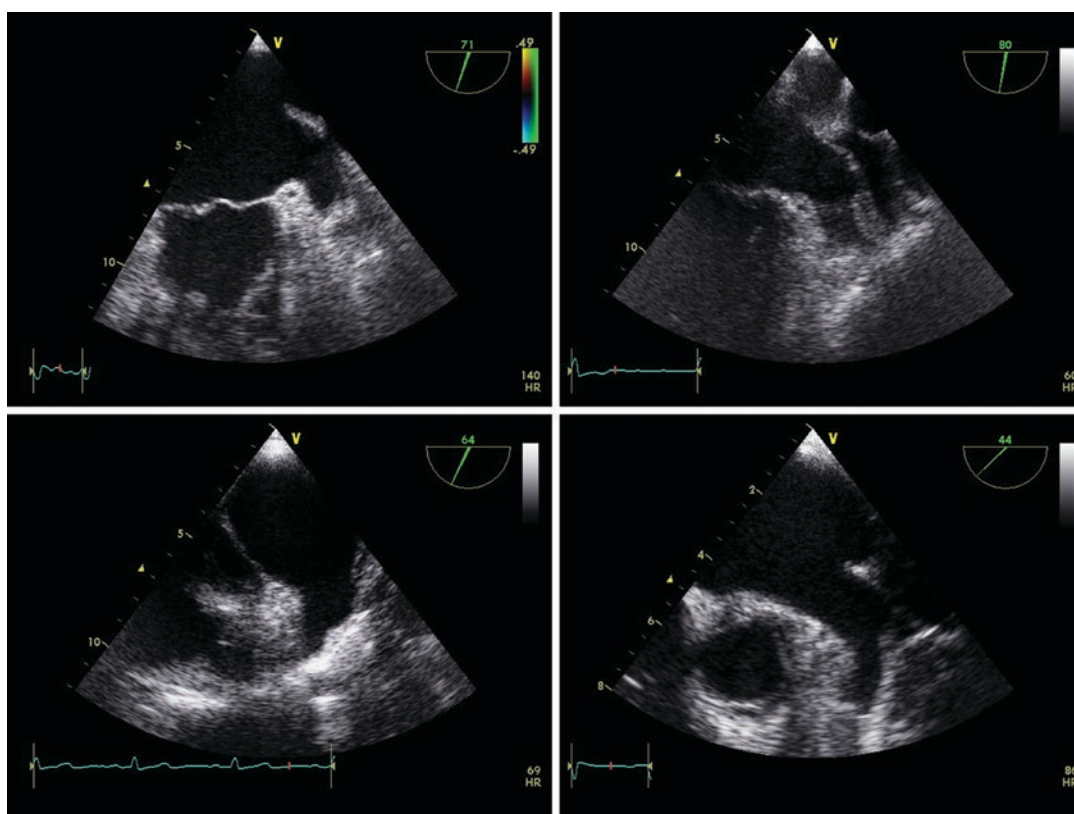
Fig. 39.6 Examples of left atrial appendage shape variability in different individuals, as shown by transesophageal echocardiography in the mid-esophageal view
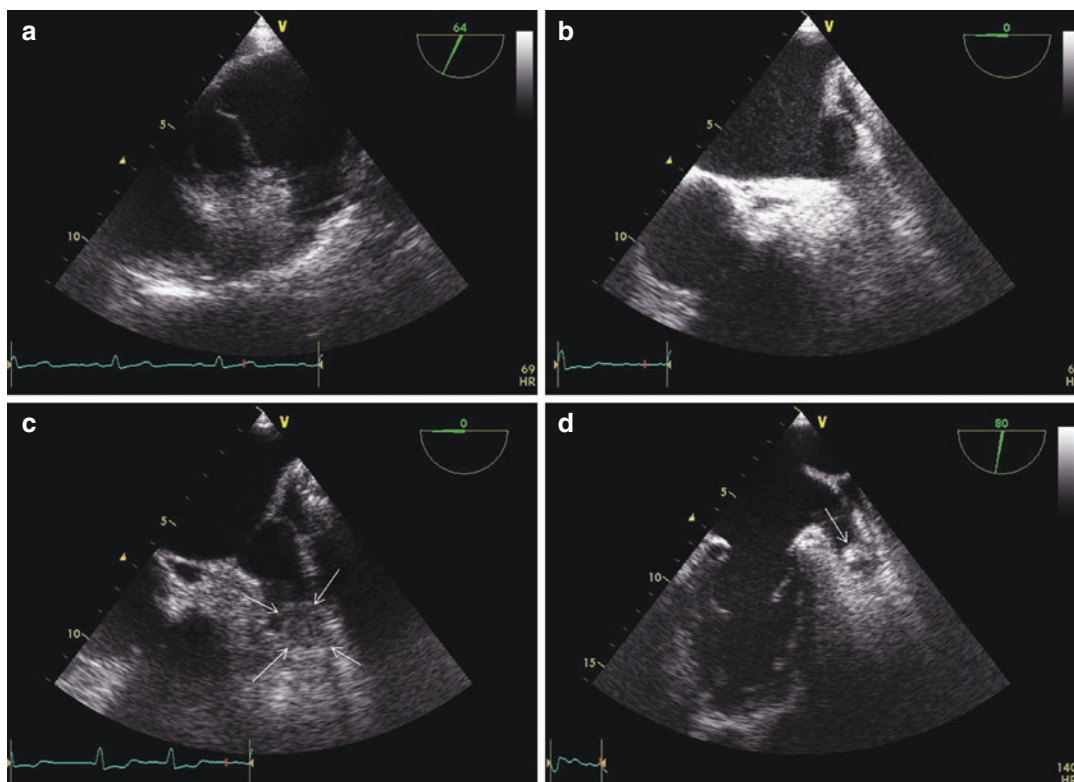
Fig. 39.7 Transesophageal echocardiography showing different findings in the left atrial appendage: artifacts (panel **a**), spontaneous echo contrast (panel **b**), and thrombus (panels **c** and **d**)

varying amplitude and regularity, depending on the active LAA contraction, with irregular early diastolic emptying waves. Low emptying flow velocities (<20 cm/s) in patients with AF are associated with the presence of spontaneous echo contrast and thrombus, whereas velocities >40 cm/s are associated with higher probability of successful cardioversion and sinus rhythm maintenance at 1 year.

39.3.2 TEE-Guided Electrical Cardioversion

The 2016 ESC guidelines for the management of patients with atrial fibrillation confirm that electrical cardioversion can be safely performed in patients with a definite duration of AF <48 h (class IIa, level of evidence B). This is a standard procedure in clinical practice, aimed at restoring sinus rhythm, improving functional capacity, and

relieving symptoms. Because of the risk of stroke or other systemic embolism due to preexisting intracardiac thrombus in patients with longer AF duration or with AF of unknown onset, those for whom an early cardioversion strategy is planned are routinely submitted to TEE. This technique allows to visualize the LA chamber and the LAA with a high image quality in the majority of patients, providing a useful tool for the identification of LA or LAA thrombus. Compared to the conventional approach, the advantages of the TEE-guided early cardioversion strategy include early improvement in symptoms, lower AF duration and more rapid recovery of LA function, higher probability of sinus rhythm restoration and maintenance, shorter period of anticoagulation, and relatively better cost-effectiveness. In the ACUTE study, early TEE-guided cardioversion was found to be a clinically effective alternative strategy to conventional routine anticoagulation followed by elective cardiover-
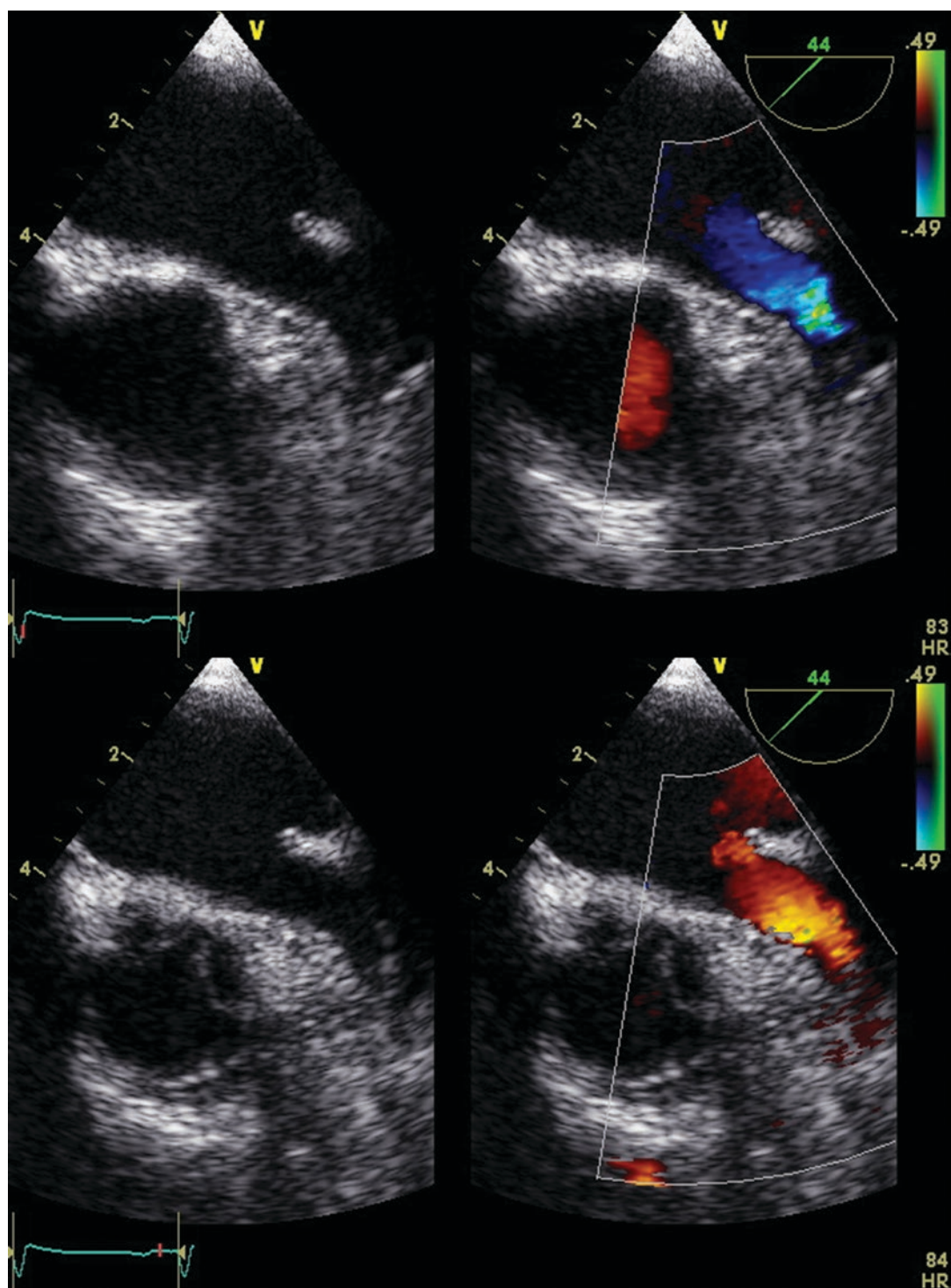
Fig. 39.8 Left atrial appendage (LAA) flows using color Doppler imaging by transesophageal echocardiography. During systole, there is blood flow entering the LAA (systolic filling). During late diastole, there is blood flow moving out of the LAA (late diastolic emptying), as a result of LAA contraction

Fig. 39.9 Left atrial appendage (LAA) Doppler flows in a normal subject, as obtained using pulsed Doppler by transesophageal echocardiography. The classical quadriphasic pattern is shown (see text)
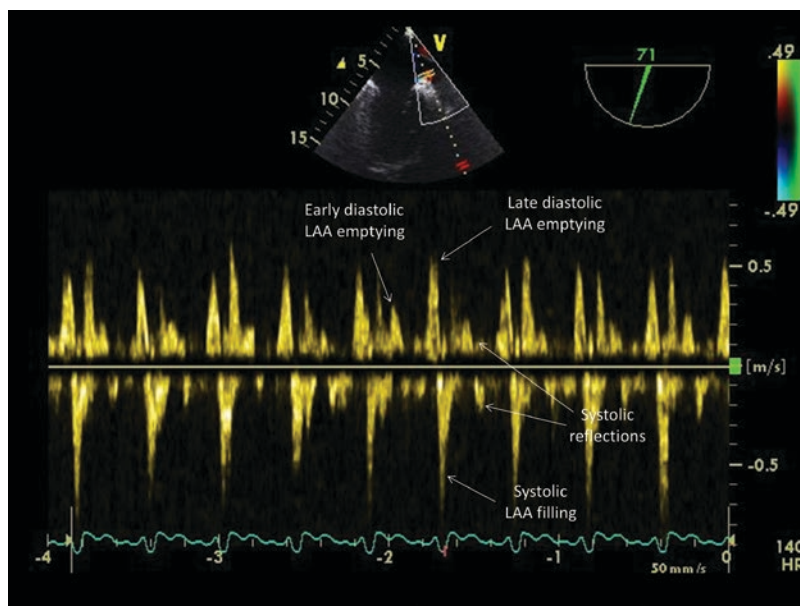
sion, showing similar efficacy with no excess of thromboembolic events, and a reduction in hemorrhagic events as a result of the shorter duration of anticoagulant therapy. On the other hand, it is mandatory that TEE in this context is performed by adequately trained operators. The potential complications of TEE, although relatively rare, should also be taken into account. Moreover, thromboembolic events after AF cardioversion can occur despite a negative TEE for thrombus, as a consequence of undetected small thrombi or new thrombus development after cardioversion due to LAA stunning in patients with inadequate anticoagulation. To date, TEE-guided early electrical cardioversion should be considered a valid, relatively safe, and reasonable choice especially for patients with relevant symptoms or in whom pharmacological adequate rate control is difficult.

Further Reading

Arboix A, Alio J. Acute cardioembolic cerebral infarction: answers to clinical questions. Curr Cardiol Rev. 2012;8:54–67.

Aune E, Baekkevar M, Roislien J, Rodevand O, Otterstad JE. Normal reference ranges for left and right atrial volume indexes and ejection fractions obtained with real-time three-dimensional echocardiography. Eur J Echocardiogr. 2009;10:738–44.

Bai W, Chen Z, Tang H, Wang H, Cheng W, Rao L. Assessment of the left atrial appendage structure and morphology: comparison of real-time three-dimensional transesophageal echocardiography and computed tomography. Int J Cardiovasc Imaging. 2017;33:623–33.

Barnes ME, Miyasaka Y, Seward JB, Gersh BJ, Rosales AG, Bailey KR, et al. Left atrial volume in the prediction of first ischemic stroke in an elderly cohort without atrial fibrillation. Mayo Clin Proc. 2004;79:1008–14.

Benjamin EJ, Dagostino RB, Belanger AJ, Wolf PA, Levy D. Left atrial size and the risk of stroke and death - the Framingham Heart-Study. Circulation. 1995;92:835–41.

Bernard-Brunet A, Saint Etienne C, Piver E, Zannad N, Pagés JC, Fauchier L, et al. Incomplete recovery of mechanical and endocrine left atrial functions one month after electrical cardioversion for persistent atrial fibrillation: a pilot study. J Transl Med. 2014;12:51.

Black IW, Fatkin D, Sagar KB, Khandheria BK, Leung DY, Galloway JM, et al. Exclusion of atrial thrombus by transesophageal echocardiography does not preclude embolism after cardioversion of atrial fibrillation. A multicenter study. Circulation. 1994;89:2509–13.

Bogousslavsky J, Cachin C, Regli F, Despland PA, Van Melle G, Kappenberger L. Cardiac sources of embolism and cerebral infarction--clinical consequences and vascular concomitants: the Lausanne Stroke Registry. Neurology. 1991;41:855–9.

Bouzas-Mosquera A, Broullon FJ, Alvarez-Garcia N, Mendez E, Peteiro J, Gandara-Sambade T, et al. Left atrial size and risk for all-cause mortality and ischemic stroke. Can Med Assoc J. 2011;183:E657–64.

Boyd AC, Thomas L. Left atrial volumes: two-dimensional, three-dimensional, cardiac magnetic resonance and computed tomography measurements. Curr Opin Cardiol. 2014;29:408–16.

Brodsky MA, Allen BJ, Capparelli EV, Luckett CR, Morton R, Henry WL. Factors determining maintenance of sinus rhythm after chronic atrial fibrillation with left atrial dilatation. Am J Cardiol. 1989;63:1065–8.

Cameli M, Lisi M, Reccia R, Bennati E, Malandrino A, Solari M, et al. Pre-operative left atrial strain predicts post-operative atrial fibrillation in patients undergoing aortic valve replacement for aortic stenosis. Int J Cardiovasc Imaging. 2014;30:279–86.

Candan O, Ozdemir N, Aung SM, Dogan C, Karabay CY, Gecmen C, et al. Left atrial longitudinal strain parameters predict postoperative persistent atrial fibrillation following mitral valve surgery: a speckle tracking echocardiography study. Echocardiography. 2013;30:1061–8.

Candan O, Gecmen C, Kalayci A, Dogan C, Bayam E, Ozkan M. Left atrial electromechanical conduction time predicts atrial fibrillation in patients with mitral stenosis: a 5-year follow-up speckle-tracking echocardiography study. Int J Cardiovasc Imaging. 2017 [Epub ahead of print];33:1491.

Chen Z, Bai W, Li C, Wang H, Tang H, Qin Y, et al. Left atrial appendage parameters assessed by real-time three-dimensional transesophageal echocardiography predict thromboembolic risk in patients with nonvalvular atrial fibrillation. J Ultrasound Med. 2017;36:1119–28.

Cherian TS, Shrader P, Fonarow GC, Allen LA, Piccini JP, Peterson ED, et al. Effect of atrial fibrillation on mortality, stroke risk, and quality-of-life scores in patients with heart failure (from the outcomes registry for better informed treatment of atrial fibrillation [ORBIT-AF]). Am J Cardiol. 2017;119:1763–9.

Costa C, González-Alujas T, Valente F, Aranda C, Rodríguez-Palomares J, Gutierrez L, et al. Left atrial strain: a new predictor of thrombotic risk and successful electrical cardioversion. Echo Res Pract. 2016;3:45–52.

Donal E, Lip GY, Galderisi M, Goette A, Shah D, Marwan M, et al. EACVI/EHRA Expert Consensus Document on the role of multi-modality imaging for the evaluation of patients with atrial fibrillation. Eur Heart J Cardiovasc Imaging. 2016;17:355–83.

Ersboll M, Anderson MJ, Valeur N, Mogensen UM, Waziri H, Moller JE, et al. The prognostic value of left atrial peak reservoir strain in acute myocardial infarction is dependent on left ventricular longitudinal function and left atrial size. Circ Cardiovasc Imaging. 2013;6:26–33.

Go AS, Hylek EM, Phillips KA, Chang Y, Henault LE, Selby JV, et al. Prevalence of diagnosed atrial fibrillation in adults: national implications for rhythm management and stroke prevention: the AnTicoagulation and Risk Factors in Atrial Fibrillation (ATRIA) Study. JAMA. 2001;285:2370–5.

Guron CW, Hartford M, Rosengren A, Thelle D, Wallentin I, Caidahl K. Usefulness of atrial size inequality as an indicator of abnormal left ventricular filling. Am J Cardiol. 2005;95:1448–52.

Hesse B, Schuele SU, Thamilasaran M, Thomas J, Rodriguez L. A rapid method to quantify left atrial contractile function: Doppler tissue imaging of the mitral annulus during atrial systole. Eur J Echocardiogr. 2004;5:86–92.

January CT, Wann LS, Alpert JS, Calkins H, Cigarroa JE, Cleveland JC Jr, et al. American College of Cardiology/American Heart Association Task Force on Practice Guidelines. 2014 AHA/ACC/HRS guideline for the management of patients with atrial fibrillation: a report of the American College of Cardiology/American Heart Association Task Force on Practice Guidelines and the Heart Rhythm Society. J Am Coll Cardiol. 2014;64:e1–76.

Kedia G, Habibzadeh MR, Kudithipudi V, Molls F, Sorrell VL. Using traditional measurement of left atrial diameter to predict the left atrial volume index. Echocardiography. 2008;25:36–9.

Kirchhof P, Benussi S, Kotecha D, Ahlsson A, Atar D, Casadei B, et al. ESC guidelines for the management of atrial fibrillation developed in collaboration with EACTS. Eur Heart J 2016. 2016;37:2893–962.

Kizer JR, Bella JN, Palmieri V, Liu JE, Best LG, Lee ET, et al. Left atrial diameter as an independent predictor of first clinical cardiovascular events in middle-aged and elderly adults: the Strong Heart Study (SHS). Am Heart J. 2006;151:412–8.

Klein AL, Grimm RA, Murray RD, Apperson-Hansen C, Asinger RW, Black IW, et al. Assessment of cardioversion using transesophageal echocardiography investigators. Use of transesophageal echocardiography to guide cardioversion in patients with atrial fibrillation. N Engl J Med. 2001;344:1411–20.

Lam CS, Rienstra M, Tay WT, Liu LC, Hummel YM, van der Meer P, et al. Atrial fibrillation in heart failure with preserved ejection fraction: association with exercise capacity, left ventricular filling pressures, natriuretic peptides, and left atrial volume. JACC Heart Fail. 2017;5:92–8.

Lane DA, Skjøth F, Lip GYH, Larsen TB, Kotecha D. Temporal trends in incidence, prevalence, and mortality of atrial fibrillation in primary care. J Am Heart Assoc. 2017; 6.

Lang RM, Badano LP, Mor-Avi V, Afilalo J, Armstrong A, Ernande L, et al. Recommendations for cardiac chamber quantification by echocardiography in adults: an update from the american society of echocardiography and the European association of cardiovascular imaging. Eur Heart J Cardiovasc Imaging. 2015;16:233–71.

Le Tourneau T, Messika-Zeitoun D, Russo A, Detaint D, Topilsky Y, Mahoney DW, et al. Impact of left atrial volume on clinical outcome in organic mitral regurgitation. J Am Coll Cardiol. 2010;56:570–8.

Lee SR, Choi EK, Han KD, Cha MJ, Oh S. Trends in the incidence and prevalence of atrial fibrillation and estimated thromboembolic risk using the CHA(2)

DS(2)-VASc score in the entire Korean population. Int J Cardiol. 2017;236:226–31.

Lester SJ, Ryan EW, Schiller NB, Foster E. Best method in clinical practice and in research studies to determine left atrial size. Am J Cardiol. 1999;84:829–32.

Leung DY, Black IW, Cranney GB, Hopkins AP, Walsh WF. Prognostic implications of left atrial spontaneous echo contrast in nonvalvular atrial fibrillation. J Am Coll Cardiol. 1994;24:755–62.

Lloyd-Jones DM, Wang TJ, Leip EP, Larson MG, Levy D, Vasan RS, et al. Lifetime risk for development of atrial fibrillation: the Framingham Heart Study. Circulation. 2004;110:1042–6.

Lonborg JT, Engstrom T, Moller JE, Ahtarovski KA, Kelbaek H, Holmvang L, et al. Left atrial volume and function in patients following ST elevation myocardial infarction and the association with clinical outcome: a cardiovascular magnetic resonance study. Eur Heart J Cardiovasc Imaging. 2013;14:118–26.

Manning WJ, Silverman DI, Katz SE, Riley MF, Doherty RM, Munson JT, et al. Temporal dependence of the return of atrial mechanical function on the mode of cardioversion of atrial fibrillation to sinus rhythm. Am J Cardiol. 1995;75:624–6.

Mascioli G, Lucca E, Michelotti F, Alioto G, Santoro F, Belli G, et al. Severe spontaneous echo contrast/auricular thrombosis in "nonvalvular" AF: value of thromboembolic risk scores. Pacing Clin Electrophysiol. 2017;40:57–62.

Mattioli AV, Vivoli D, Bastia E. Doppler echocardiographic parameters predictive of recurrence of atrial fibrillation of different etiologic origins. J Ultrasound Med. 1997;16(10):695–8.

Mitusch R, Garbe M, Schmucker G, Schwabe K, Stierle U, Sheikhzadeh A. Relation of left atrial appendage function to the duration and reversibility of nonvalvular atrial fibrillation. Am J Cardiol. 1995;75:944–7.

Mochizuki A, Yuda S, Fujito T, Kawamukai M, Muranaka A, Nagahara D, et al. Left atrial strain assessed by three-dimensional speckle tracking echocardiography predicts atrial fibrillation recurrence after catheter ablation in patients with paroxysmal atrial fibrillation. J Echocardiogr. 2017;15:79–87.

Moller JE, Hillis GS, Oh JK, Seward JB, Reeder GS, Wright RS, et al. Left atrial volume - a powerful predictor of survival after acute myocardial infarction. Circulation. 2003;107:2207–12.

Mor-Avi V, Lang RM, Badano LP, Belohlavek M, Cardim NM, Derumeaux G, et al. Current and evolving echocardiographic techniques for the quantitative evaluation of cardiac mechanics: ASE/EAE consensus statement on methodology and indications endorsed by the Japanese Society of Echocardiography. Eur J Echocardiogr. 2011;12:167–205.

Mor-Avi V, Yodwut C, Jenkins C, Kühl H, Nesser HJ, Marwick TH, et al. Real-time 3D echocardiographic quantification of left atrial volume: multicenter study for validation with CMR. JACC Cardiovasc Imaging. 2012;5:769–77.

Obokata M, Negishi K, Kurosawa K, Tateno R, Tange S, Arai M, et al. Left atrial strain provides incremental

value for embolism risk stratification over CHA_2DS_2-VASc score and indicates prognostic impact in patients with atrial fibrillation. J Am Soc Echocardiogr. 2014;27:709–716.e4.

Omran H, Jung W, Rabahieh R, Wirtz P, Becher H, Illien S, et al. Imaging of thrombi and assessment of left atrial appendage function: a prospective study comparing transthoracic and transoesophageal echocardiography. Heart. 1999;81:192–8.

Poulsen MK, Dahl JS, Henriksen JE, Hey TM, Hoilund-Carlsen PF, Beck-Nielsen H, et al. Left atrial volume index: relation to long-term clinical outcome in type 2 diabetes. J Am Coll Cardiol. 2013;62:2416–21.

Psaty BM, Manolio TA, Kuller LH, Kronmal RA, Cushman M, Fried LP, et al. Incidence of and risk factors for atrial fibrillation in older adults. Circulation. 1997;96:2455–61.

Recommendations for Cardiac Chamber Quantification by Echocardiography in Adults. An update from the American Society of Echocardiography and the European Association of, Cardiovascular Imaging. Eur Heart J Cardiovasc Imaging. 2016;17:412.

Saha SK, Anderson PL, Caracciolo G, Kiotsekoglou A, Wilansky S, Govind S, et al. Global left atrial strain correlates with CHADS(2) risk score in patients with atrial fibrillation. J Am Soc Echocardiogr. 2011;24:506–12.

Sallach JA, Puwanant S, Drinko JK, Jaffer S, Donal E, Thambidorai SK, et al. Comprehensive left atrial appendage optimization of thrombus using surface echocardiography: the CLOTS multicenter pilot trial. J Am Soc Echocardiogr. 2009;22:1165–72.

Shah SJ, Bardo DM, Sugeng L. Real-time three-dimensional transesophageal echocardiography of the left atrial appendage: initial experience in the clinical setting. J Am Soc Echocardiogr. 2008;21:1362–8.

Shih JY, Tsai WC, Huang YY, Liu YW, Lin CC, Huang YS, et al. Association of decreased left atrial strain and strain rate with stroke in chronic atrial fibrillation. J Am Soc Echocardiogr. 2011;24:513–9.

Stefanadis C, Dernellis J, Stratos C, Tsiamis E, Tsioufis C, Toutouzas K, et al. Assessment of left atrial pressure-area relation in humans by means of retrograde left atrial catheterization and echocardiographic automatic boundary detection: effects of dobutamine. J Am Coll Cardiol. 1998;31:426–36.

Sunbul M, Oguz M, Dogan Z, Atas H, Bozbay M, Cincin A, et al. Heart failure and mortality in patients with nonvalvular atrial fibrillation started on novel oral anticoagulant therapy: a single-center experience. Clin Appl Thromb Hemost. 2017;23:454–9.

Sundbøll J, Hováth-Puhó E, Adelborg K, Ording A, Schmidt M, Bøtker HE, et al. Risk of arterial and venous thromboembolism in patients with atrial fibrillation or flutter: a nationwide population-based cohort study. Int J Cardiol. 2017;241:182–7.

Thomas L, Levett K, Boyd A, Leung DY, Schiller NB, Ross DL. Changes in regional left atrial function with aging: evaluation by Doppler tissue imaging. Eur J Echocardiogr. 2003;4:92–100.

Thomas L, Thomas SP, Hoy M, Boyd A, Schiller NB, Ross DL. Comparison of left atrial volume and function after linear ablation and after cardioversion for chronic atrial fibrillation. Am J Cardiol. 2004;93:165–70.

Transesophageal echocardiographic correlates of thromboembolism in high-risk patients with nonvalvular atrial fibrillation. The stroke prevention in atrial fibrillation investigators committee on echocardiography. Ann Intern Med. 1998;128:639–47.

Tsang TS, Barnes ME, Bailey KR, Leibson CL, Montgomery SC, Takemoto Y, et al. Left trial volume: important risk marker of incident atrial fibrillation in 1655 older men and women. Mayo Clin Proc. 2001;76:467–75.

Tsang TSM, Barnes ME, Gersh BJ, Bailey KR, Seward JB. Left atrial volume as a morphophysiologic expression of left ventricular diastolic dysfunction and relation to cardiovascular risk burden. Am J Cardiol. 2002;90:1284–9.

Tsang TSM, Barnes ME, Gersh BJ, Takemoto Y, Rosales AG, Bailey KR, et al. Prediction of risk for first age-related cardiovascular events in an elderly population: the incremental value of echocardiography. J Am Coll Cardiol. 2003;42:1199–205.

Tsang TS, Abhayaratna WP, Barnes ME, Miyasaka Y, Gersh BJ, Bailey KR, et al. Prediction of cardiovascular outcomes with left atrial size: is volume superior to area or diameter? J Am Coll Cardiol. 2006;47:1018–23.

Uretsky S, Shah A, Bangalore S, Rosenberg L, Sarji R, Cantales DR, et al. Assessment of left atrial appendage function with transthoracic tissue Doppler echocardiography. Eur J Echocardiogr. 2009;10:363–71.

Van Gelder IC, Crijns HJ, Van Gilst WH, Hamer HP, Lie KI. Decrease of right and left atrial sizes after direct-current electrical cardioversion in chronic atrial fibrillation. Am J Cardiol. 1991;67:93–5.

Vaziri SM, Larson MG, Benjamin EJ, Levy D. Echocardiographic predictors of nonrheumatic atrial fibrillation. The Framingham Heart Study. Circulation. 1994;89:724–30.

Zhu M, Wang M, Ma X, Zheng D, Zhang Y. The value of left atrial strain and strain rate in predicting left atrial appendage stasis in patients with nonvalvular atrial fibrillation. Cardiol J. 2018;25(1):87–96. [Epub ahead of print].

Ultrasound-Guided Nursing

40

Marco Sozzi, Dorella Donati, and Stella Neri

40.1 Introduction

In today's nursing practice, ultrasound plays a fundamental role.

In critical care apart from having the clinical skills and competencies, some specialities use echography on a regular basis to augment their clinical skills.

Cross hierarchical (nursing staff of different rankings/seniority) and multidisciplinary working between medical specialities will only lead to improvements in quality of care and outcomes for our critical care patients.

By including ultrasound competencies (knowledge and technique) in the medical student and advanced nursing curriculum, it will lead to better skilled clinical staff.

Ultrasound imaging is useful in a multitude of clinical scenarios in nursing.

It provides data for the formulation of a nursing diagnosis and the subsequent nursing activity plan. It is a validated tool for the monitoring of the progression of diseases, with which nurses can proactively modify their management plan.

Nurses can use the ultrasound for various routine techniques and daily nursing activities, i.e. bladder catheterization or to access peripheral veins.

Moreover ultrasound can reduce the risk of infection and contamination during certain diagnostic procedures, e.g. taking a blood culture. Ultrasound is particularly useful in assessing correct placement of the catheter post bladder catheterization. Ultrasound enhances the success rate of phlebotomy and successful placement of intravenous lines in obese or very fragile patients.

To support my above statements, the following chapter will give one greater insight in the various ways using ultrasound that can support and be fully integrated in daily nursing activities.

40.2 Bladder Catheter: Volume Calculation, Measurement Choice, Position Check and Malfunction Check

As for urinary function, bladder ultrasound has multiple uses in nursing, such as volume calculation, choice of the device in relation to prostate and bladder content, detection of bladder catheter malfunction, daily diuretic counting in the absence of catheter and determination of bladder globe.

M. Sozzi (✉) · S. Neri
Department of Critical Care, Ospedale Santa Maria Nuova, Florence, Italy
e-mail: marco.sozzi@uslcentro.toscana.it; stella.neri@uslcentro.toscana.it

D. Donati
Intensive Care Unit (Rianimazione e Terapia Intensiva), Santa Maria Nuova, Florence, Italy
e-mail: dorella.donati@uslcentro.toscana

40.2.1 Volume Calculation

The volume of the bladder content can easily be calculated by measuring the maximum three diameters: the lateral in lateral projection, the back anterior and the caudal skull in sagittal projection. Then multiply each other and then multiply again by 0.52.

40.2.2 Choice of Device

The choice of the bladder catheter may be based on a preliminary bladder ultrasound study. If the bladder content is totally anecdotal, a catheter 14–16 Fr can be used. If the contents are anechogenic with moderately echoreflecting points (pus, sediment), you will have to use a 16–18 Fr catheter. If the content is predominantly ecorephlettent, structural aspect (clots) uses 18–20 Fr. If the bladder content is not perfectly anecdotic, you can think of a three-way catheter for flushing (Figs. 40.1 and 40.2). The evaluation of prostate salience will give you indications of the type of difficulty that you will encounter in the catheter insertion. A sagittal scan displays the prostate: if there is no bladder salience or symmetric salience up to 1.5 cm, no specific catheter is required, and if the salience is greater than 1.5 cm or asymmetric with the third lobe, the use of curved tip catheters is recommended.

40.2.3 Check the Positioning of the Bladder Catheter

The position of the bladder catheter head can be assessed ecographically. With transverse and longitudinal scans in the overlapping area, it is possible to evaluate the presence of the bladder catheter head, which appears as a moderately hyperechogenic circle with the anechogenic interior. To ensure that the image is actually the bladder catheter headset, you can try to deflate it and inflate it under following the ultrasound images (Fig. 40.3).

40.2.4 Malfunction of the Bladder Catheter

If you have any doubts about the functioning of a bladder catheter, echographic images can help you to detect a stagnant bladder. If you see a moderately echogenic circular image with internal anechoic content (headset fluid) immersed in a variable quantity of anechogenic material (the bladder stagnation), the bladder catheter is actually malfunctioning. You will need to replace or resolve the problem. If, however, in the absence of drained urine there is no presence of the same in the bladder, the problem upper of bladder (Fig. 40.4).

Fig. 40.1 If on viewing the bladder by ultrasound sediment is seen, one should consider a three-way catheter. Image with 3.5 mhz convex probe with vertical scan
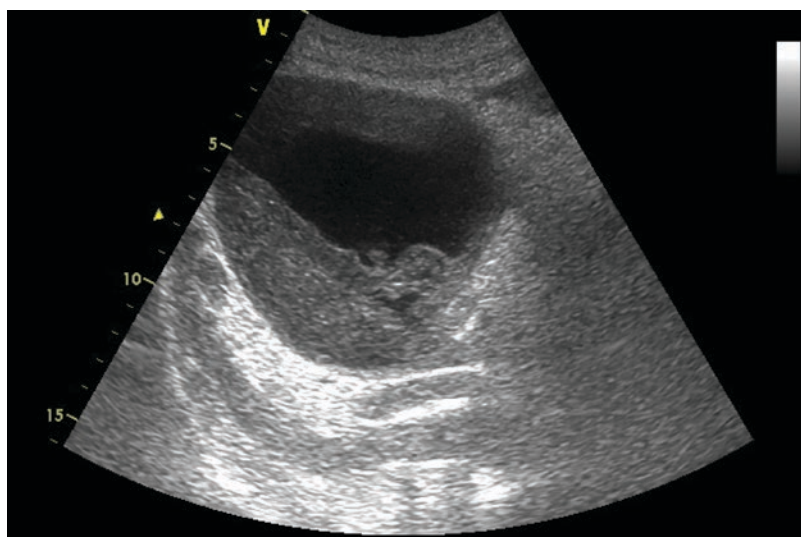
Fig. 40.2 Sediment in the bladder in horizontal scan. Convex probe 3.5 mhz
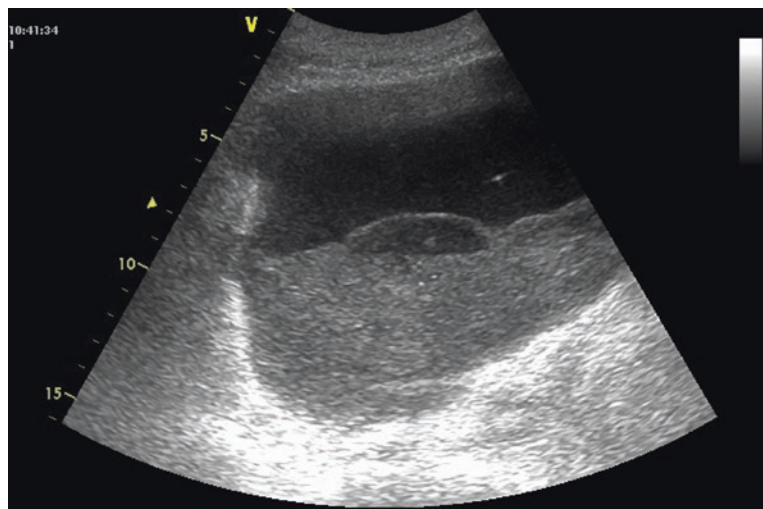
Fig. 40.3 Vesicle catheter not working. One can see the dilated balloon of the catheter and bladder stagnation, indicated by increased volume of urine in the bladder. Convex probe 3.5 mhz
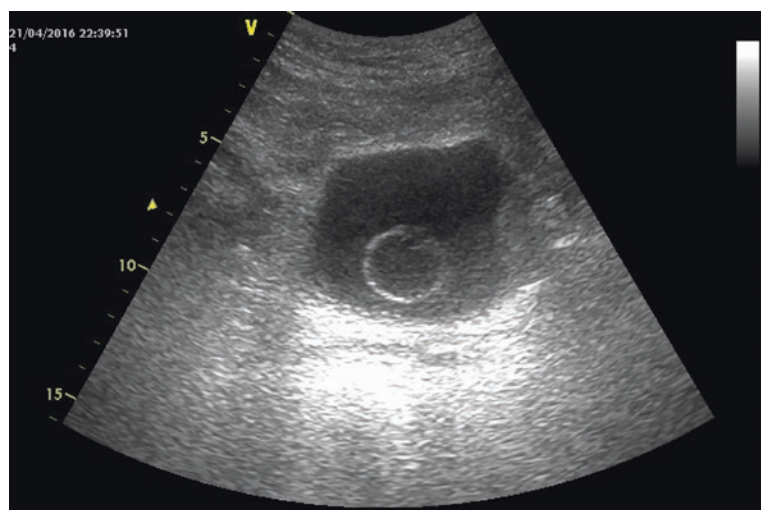
Fig. 40.4 Vesicle catheter working. You can see only the dilated balloon of the catheter. Sonda convex 3.5 mhz
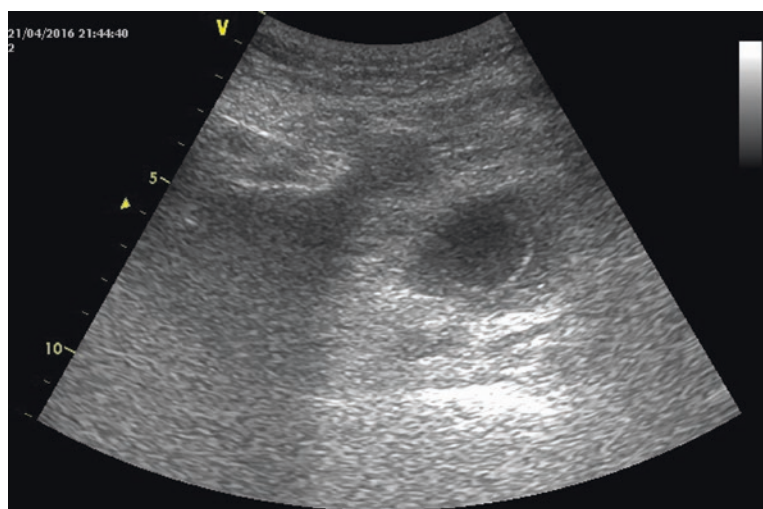
40.3 Peripheral Venous Blood Drawing, Cannulation, Blood Culture, Arterial Blood Withdrawal and Reclining, Central Venous Catheter Position Check and Control of Incannulated Veins

Ultrasound imaging is very useful in the finding of a vein or an artery for the drawing of blood or for the incannulation as in patients with a difficult access (poor vascular access, children, obesity, oedema, sepsis). Ultrasound reduces the number of punctures and redirectioning of the needle and therefore the risk of contamination and discomfort.

40.3.1 Peripheral Venous Blood Drawing and Cannulation

As far as the cannulation or the blood drawing of a peripheral vessel is concerned, the patient's vein is first assessed without and then with ultrasound. Additionally this gives you the possibility to assess the best insertion site; furthermore you can understand whether the vein you have chosen is compressible or not (not trumped/trumped). Even when the vein is visible and/or palpable, it is not easy to determine if it is trumped or not. If it is trumped, you will have to choose a different vein. For insertion with a sterile technique, a linear probe is recommended. Once you have

selected the vein, you disinfect the site, and then the catheter will be introduced eco-driven. You can choose both the short-axis off-axis approach and the long-axis plan. The first one is optimal for blood drawings as it is easier to reach the vein with inclination even close to 60° for veins with depths greater than 2–3 cm. For the peripheral cannulation, the long-axis plan is preferable. In fact the needle will have an inclination of about 30–45°, and it will be easier to follow the course of the needle from the point of insertion through the skin to the vein (ultrasound images). Alternatively, you can use the first approach with the bend to bend or move the probe to follow the needle tip to get the perfect moment when the tip itself meets the vein (Fig. 40.5).

40.3.2 Blood Culture

The taking of blood samples for blood cultures from venous peripheral and arterial blood is at risk for being contaminated. In fact the operator needs to palpate the preselected vein several times before piercing the vessel and has to redirect the needle after piercing the skin. The use of an eco-led technique is useful in preventing sample contamination during blood sampling, reducing the redirections of the needle during the procedure. Furthermore, a preliminary ultrasound study is helpful in choosing the best sample site. This will give you the safety of not having to change it, even if the vein

Fig. 40.5 The needle tip is visible into the vessel. Short axis, out of plane. Linear probe 12 mhz
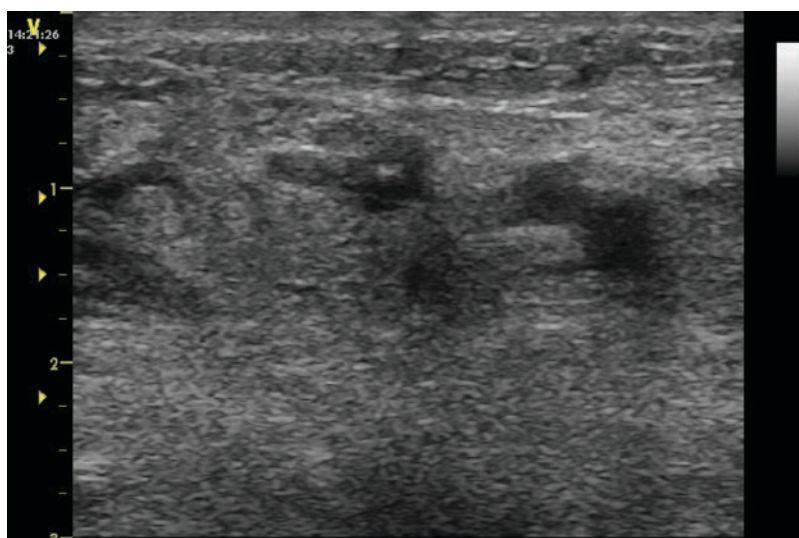
is not palpable and/or not visible. Once the site is detected, disinfection is performed, and the sampling is carried out using sterile gloves and coats. Venipuncture is performed as described above.

40.3.3 Arterial Blood Withdrawal and Reclining

The ultrasound guide is helpful in case of arterial blood withdrawal and chafing. In regard to arterial blood withdrawal in cases when the artery is hardly palpable as in obese patients, infants, septic patients or hypotensive patients,

the ultrasound guide will ensure greater success at first attempt. Before taking an arterial sample or inserting an arterial catheter, it is necessary to evaluate the perennial ulnar collateral circulation. In addition to the classical, modified Allen test or other tests, it is possible to evaluate the perennial ulnar artery with the ultrasound before stinging the radial artery. Studies on the use of an ultrasound technique for ulnar collateral assessment are limited but encouraging. To verify the viability of ulnar and radial arteries, you have to ensure their pulsativeness during compression with a linear probe. Otherwise you can use the Doppler colour (Figs. 40.6 and 40.7). The use of

Fig. 40.6 Flow highlighted by Doppler colour in the ulnar artery. Linear probe 12 mhz
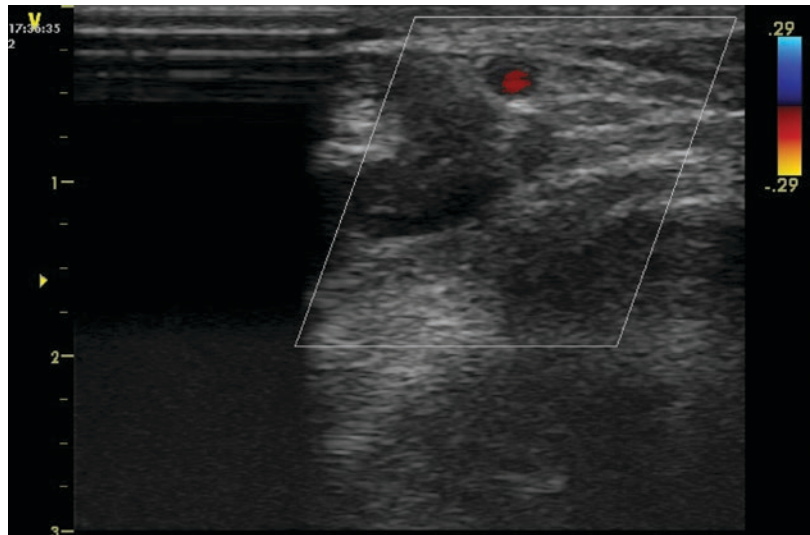
Fig. 40.7 Flow highlighted by Doppler colour in the radial artery. Linear probe 12 mhz
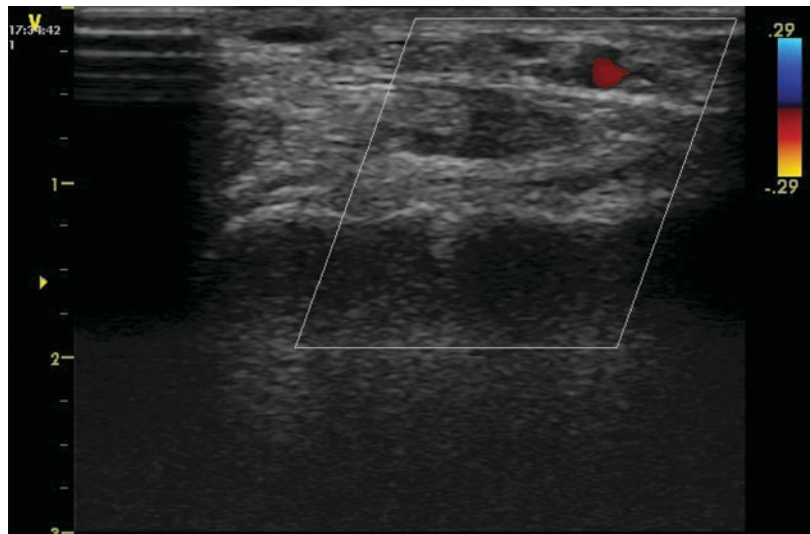
the ultrasound guide for arterial swelling significantly increases the success of the first attempt. Once the pertinence of the collateral vessel is checked, you can start with the arterial cannulation using gloves, cap and a fenestrated sterile drape. You can use both a long-axis in-plane approach and a short-axis out-of-plane approach. It allows you to insert a catheter in a more proximal portion than the usual one.

40.3.4 Central Venous Catheter Position Check

In order to verify the right position of the tip of the central venous catheter, you can use the same technique as for visualizing the cava vein (see Chap. 29). The optimal position is at the cavoatrial junction. To view this portion, use a sector probe and subcostal projections. The portion to be displayed is the one which is close to the right atrium. Transverse and longitudinal projections may be used to display the tip of the catheter. A flush of 1–5 cc of saline solution or 1 cc of an air-emulsified colloid solution may be ultrasonically seen as a fluctuating hyperechogenicity in the vein (Figs. 40.8 and 40.9). This technique can be useful both in the case of insertion of a central

line and when you have any doubt about the possible displacement of the device.

40.3.5 Control of Incannulated Veins

In order to quickly detect the possible incompatibility of the incannulated veins, you can assess their compressibility in the upstream and downstream sections of the insertion site (see Chap. 50). In case of incompatibility, to reduce the risk of thrombosis and of other complications, the infusions have to be suspended and the catheter removed. To do this, glide the linear probe along the affected vein starting from the insertion site both downstream and upstream. Compress the vein with the probe until it collapses. With PICC and midline devices, go up to the succlavia vein and for CVC to the neck portion (Figs. 40.10 and 40.11).

40.4 Monitoring of the Inferior Cava Vein (ICV)

The measurement of the ICV diameters during respiration, as already described in the text, is a useful data to target fluid therapy (see Chap. 29). This measurement can be performed by specifi-

Fig. 40.8 The tip of the central line can be detected by ultrasound, subcostal. The catheter is visible like in the cavo-atrial junction. Sectorial probe 5 mhz
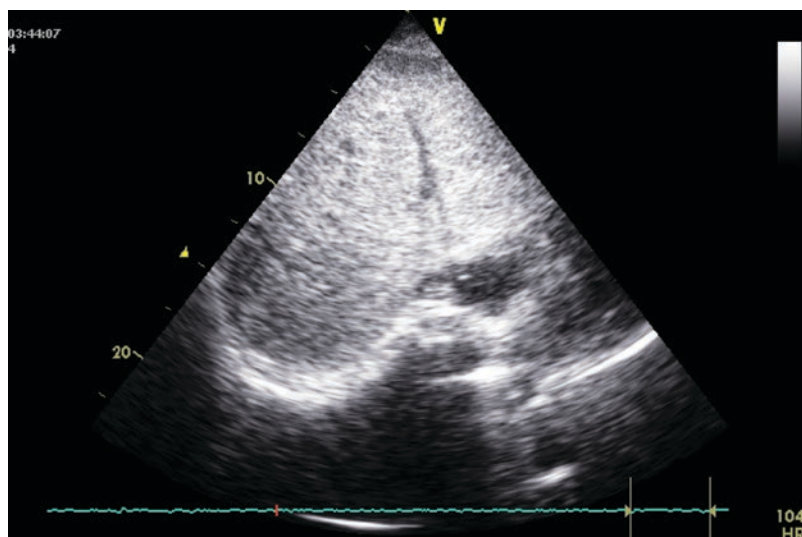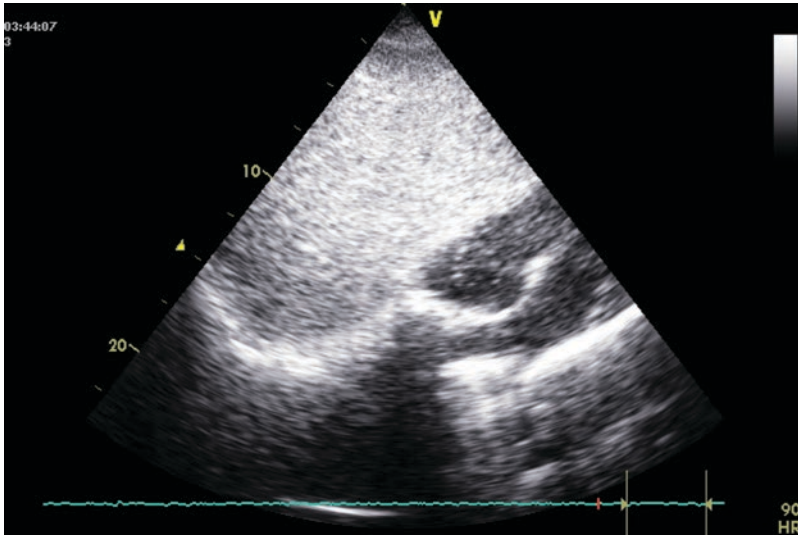
Fig. 40.9 To confirm the hyperechoic point is the catheter, you can inject 3–5 cc of saline solution or 1 cc of colloid solution mixed with a little bit of air. If you see immediately the flush on the monitor, you can be sure about the catheter tip position. If you note a delay, then it can indicate that the catheter is far from the cavo-atrial vein. However, if one immediately sees the flush in the right atria, it indicates that the catheter tip is too long. Sectorial probe 5 mhz

Fig. 40.10 Brachial veins and arteria are shown in this image. Linear probe 12 mhz
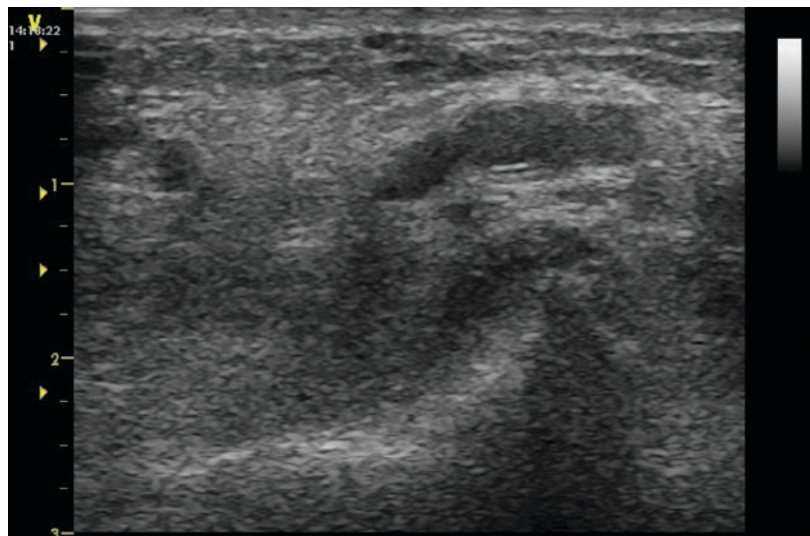
cally trained nurses. The use of protocols may be useful for the timing of the measurement, for example, at regular intervals, after IV fluid intake, at time 0. This technique is particularly helpful when it is not possible to measure central venous pressure.

40.5 Prevention of Intradialytic Hypovolemia

The ultrasound measurement of the ICV may be an important data to prevent the risk of intradialytic hypotension. This kind of nursing

Fig. 40.11
Compressing by the probe, only the artery is visible. This excludes thrombosis from the vessel. Linear probe 12 mhz
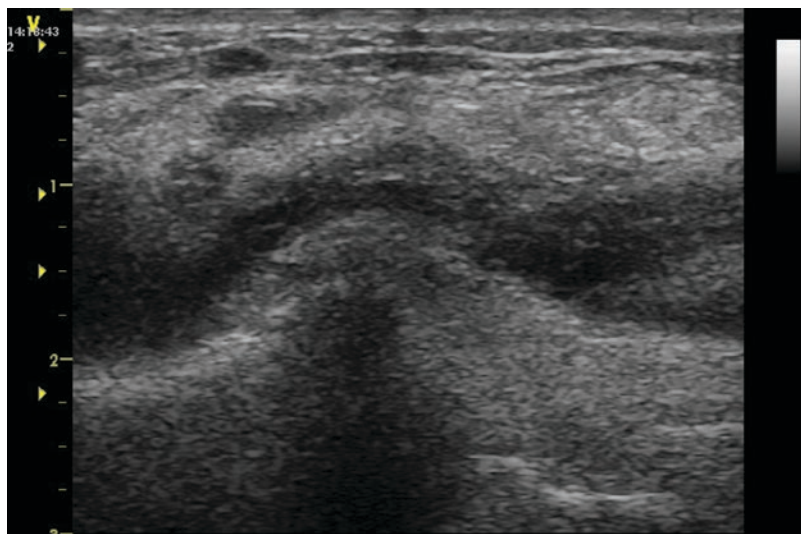
assessment performed before, during and after the dialytic treatment may help to define the ultrafiltration goal, reducing the risk of intra-dialytic hypotension and to understand patient's volemia after the treatment.

40.6   Lung Echography

Lung ultrasound images may be useful both in critical and in noncritical settings. In patients with left cardiac insufficiency, it is possible to assess therapy efficacy and to promptly act in order to avoid reacutization of the respiratory condition. In the ER, lung ultrasound can support classification of priority. In fact patients with respiratory insufficiency associated with cardiac failure or due to cardiac failure alone can be quickly identified and treated immediately.

40.6.1 Dry Lung/Wet Lung

By chest ultrasound you will be able to view the wet lung and the dry lung (see Chaps. 30 and 51). This allows immediate assessment of respiratory problems (e.g. triage in the emergency department) and understanding if therapy is effective or not in respiratory aetiology. The dry lung has transversal lines called lines A. The lung with lines B (vertical reversals in the pleura and arriving to the lower edge of the screen) indicates the presence of the wet lung. To understand the severity of the wet lung, you will need to see if the lines B are 1 cm apart or if they are close and confluent. In relation to the first images, you can see whether the patient is getting worse or better before the clinical manifestation.

40.6.2 Sliding

Whenever the chest is evaluated through ultrasound, the presence of the sliding of the pleura can also be evaluated (see Chap. 51). This will quickly detect the presence of PNX and immediately alert the physician or emergency team.

40.7   Verification of Correct Placement of the Nasogastric Tube (NGT)

To confirm the correct placement of a NGT, it is possible to use a convex probe. In the oesophagogastric junction, the NGT is directly visualized with longitudinal and angled scans of the epigastrium. Visualization of the NGT in separate scans of the fundus and the antrum of the stomach can be attempted. Visualization of the correct place-

ment can be confirmed by injecting a blend of air (10 cc) and water (40 cc) into the NGT which will result in images with dynamic fogging only in patient with orotracheal tube.

Further Reading

1. http://onlinelibrary.wiley.com/doi/10.1111/jorc.12191/abstract;jsessionid=368A16CD4468AAE0A42B306DB6B699A8.f03t02.
2. https://www.ncbi.nlm.nih.gov/pmc/articles/PMC4030119/ http://www.albertahealthservices.ca/assets/wf/lab/wf-lab-prc-performing-bc-collection.pdf.
3. https://www.ncbi.nlm.nih.gov/pmc/articles/PMC4915310/(emocoltura).
4. https://www.researchgate.net/profile/Matthew_Lyon3/publication/227635369_Emergency_Nurses'_Utilization_of_Ultrasound_Guidance_for_Placement_of_Peripheral_Intravenous_Lines_in_Difficult-access_Patients/links/53d246640cf228d363e92e8b.pdf.
5. http://journals.lww.com/online/Abstract/2009/03000/Randomized_Controlled_Trial_of_Ultrasound_Guided.5.aspx. Randomized Controlled Trial of Ultrasound-Guided Peripheral Intravenous Catheter Placement Versus Traditional Techniques in Difficult-Access Pediatric Patients.
6. Doniger SJ, Ishimine P, Fox JC, Kanegaye JT. Pediatr Emerg Care. 2009;25(3).
7. Brzezinski M, Luisetti T, London M. Radial artery cannulation: a comprehensive review of recent anatomic and physiologic investigations. Anesth Analg. 109(6):176381. https://doi.org/10.1213/ANE.0b013e3181bbd416. https://www.ncbi.nlm.nih.gov/pubmed/19923502.
8. Gargani L, Gheorghiade M, Picano E, et al. Ultrasound lung comets for the differential diagnosis of acute cardiogenic dyspnea: a comparison with natriuretic peptides. Eur J Heart Fail. 2008;10(1):70–7. (comete).
9. Ricci D, Benetton M. Use of ultrasound by nurses: a review. Scenario. 2014;31(2). (generale).
10. Storti M, Musella L, Cianci V. Nurse-performed FAST ultrasound in the Emergency Department: a systematic review. Prof Inferm. 2013;66(1):5–16.
11. Garavaglia MT, et al. Accuratezza diagnostica dell'ecografia per la valutazione del corretto posizionamento del sondino naso-gastrico nell'adulto: una revisione sistematica N.14/2015 IJN.
12. http://onlinelibrary.wiley.com/doi/10.1111/jorc.12191/abstract; jsessionid=368A16CD4468AAE0A42B306DB6B699A8.f03t02 (cava dialisi).
13. Brennan JM, Ronan A, Goonewardena S, Blair JE, Hammes M, Shah D, Vasaiwala S, Kirkpatrick JN, Spencer KT. Handcarried ultrasound measurement of the inferior vena cava for assessment of intravascular volume status in the outpatient hemodialysis clinic. Clin J Am Soc Nephrol. 2006;1(4):749–53.
14. https://www.ncbi.nlm.nih.gov/pmc/articles/PMC3477076/.
15. https://wp.aniarti.it/wp-content/uploads/2016/congresso/10/m/-MOGGIA.pdf.
16. https://www.ncbi.nlm.nih.gov/pubmed/24052186.
17. https://www.ncbi.nlm.nih.gov/pubmed/2405218.
18. Giornale Italiano di Nefrologia / Anno 23 n. 1, 2006 / p. 22–8.

Multiorgan Donor and Transplanted Patient

41

Ferdinando Luca Lorini and Lorenzo F. Mantovani

41.1 Evaluation of Donor Patient

Up to the present, worldwide physicians have made a considerable effort to increase the number of transplants under the circumstances of extremely severe organ donor shortage. There is a mandatory need to increase up to the maximum the disponibility of grafts' availability. In this setting the preharvesting evaluation of the candidate and the right management of the donor organ function and haemodynamics are of the utmost importance.

Usually a transthoracic exam is performed, but according to evidence that all those patients are mechanically ventilated (with worsening of echo window) and due to extreme importance of exclusion of inadequate grafts, we think that in the absence of major contraindications, a transoesophageal examination should be always assessed.

Ideally a transplantation medical consultant doctor or an expert transplant cardiologist should evaluate the patient before the procedure, but this is often impossible due to evident logistic difficulties in many countries, and sometimes even a nonexpert cardiologist is not immediately available. In this setting the role of the intensivist is usually of pivotal importance. We can identify two aspects of the heart evaluation:

1. Function of the graft itself
2. Exclusion of direct heart damage

Moreover it should be underlined that the possibility of comparing pre-transplantation images with post-transplantation ones gives a great chance of a rapid identification of early postoperative dysfunction of the graft.

41.2 Function of the Graft

The assessment of a good cardiac function in multiorgan donor is of utmost importance considering the role of the heart to perfuse and supply the whole human body. Finding of an ineffective cardiac function should alert clinician in order to better investigate real availability of other potential grafts.

The exam should certainly include the evaluation of standard echocardiographic parameters, the area and distribution of ventricular regional wall motion abnormalities.

The presence of an eventual atrial or ventricular defect should always be excluded, but remember that in case of atrial defect, a surgical intraoperative closure is an option.

Obviously we recommend the standard evaluation of all the heart valves with a careful attention

F. L. Lorini (✉) · L. F. Mantovani
Department of Anaesthesia and Intensive Care, ASST Papa Giovanni XXIII, Bergamo, Italy
e-mail: llorini@asst-pg23.it

to the presence/absence of relevant valvular disease including valvular calcification. Anyway it should be reminded that finding of a bicuspid aortic valve does not contraindicate the use of a donor heart. In the case of valvular disease associated with haemodynamic abnormalities, the donor heart may still be used for heart transplantation. In some occasions bench repair or replacement of a donor aortic valve or repair of an incompetent mitral valve has been performed with favourable outcomes.

The myocardial function and the coronary tree of the patient should be evaluated as far as possible, especially in patients with relevant risk of such a disease defined as current or history of hyperlipidemia, hypertension, diabetes, and smoking and older than 50 years of age, but we recommend whenever possible this kind of evaluation for all patients. Discreet wall motion abnormalities on echocardiography or left ventricular ejection fraction (LVEF) <40% despite optimization of haemodynamics with inotropic support should lead to exclusion of graft.

Evaluation of left anterior descending coronary artery flow should be obtained whenever possible; examination should include evaluation of end-systolic and end-diastolic left ventricular diameters from M mode or 2D imaging, EF evaluation and measurements of thickness of the ventricular septum and left ventricular posterior wall and as stated before an accurate observation of eventual ventricular regional wall motion abnormalities. Another crucial evaluation is the measure of donor heart size expressed as LV diameter; it usually correlates very well with the LV mass index; this is very important especially in case of an eventual donor-recipient body mass index mismatch superior to 20%. We should always consider that there is a poor relationship between echocardiographic adult heart size and body weight. In such a case, the postoperative course of this kind of patient should be carefully monitored, and inotropic support and haemodynamic monitoring should be prolonged.

The presence of a LV hypertrophy in donor heart suggests the need of an early administration of cardioprotective agents (ACEi, angiotensin receptor blockers and calcium antagonist) in the postoperative course. Scientific publications dealing with this subject concluded that early mortality after transplantation is increased only if donor wall thickness is greater than 14 mm and associated with ECG abnormalities.

Finally it should be reminded that a relative increase of LV wall thickness compared with previous measurements is a very precocious sign of antibody-mediated rejection in the postoperative period.

Evaluation of mitral inflow obtained by pulsed wave Doppler echocardiography sampling volume between mitral leaflet tips during diastole, peak early (E) and late (A) transmitral filling velocities with their ratio (E/A) and deceleration time of E should be always assessed, but it should be remembered that very often, discordances between the parameters of E and E/A and the degree of valvular regurgitation between donor and recipient were attributable to the difference of volume status pre- and post-transplantation, so abnormalities in the donor heart should not forbid harvesting itself.

In the clinical decision perspective, the role of echocardiography prior to graft harvesting seems to be fundamental in the presence of LV dysfunction in donor: LV dysfunction is a common finding in patients with intracranial pathologies (about 20%) with the singular feature of regional wall abnormalities covering multiple coronary territories without associated coronary disease. In a peculiar way, the apical LV function is often preserved despite other regional abnormalities (probably due to a paucity of norepinephrine content leading to less sensibility to the catecholamine storm especially during subarachnoid haemorrhage). So it is recommended a further evaluation by means of coronary angiography when this kind of feature is found; moreover in case of negative result after coronary angiography, it should be reminded that this kind of ventricular dysfunction has been proven to be reversible even many days after transplantation (30 days). To distinguish donor cases likely to be transient, it seems useful to perform a dobutamine stress echocardiography associated with troponin I plasma level; some preliminary studies suggest that a reversible dysfunction after stress test associated with low troponin level should lead to a successful transplantation of organ. Another interesting issue is to perform a

prolonged donor management in order to obtain a series of echocardiographic exams showing an improvement in LV function. All the above statements are very important especially in evaluation of urgent transplantation in sick paediatric patients due to lack of donor hearts.

In conclusion it has been demonstrated that an expert operator can obtain a good preoperative evaluation with a 5–10 min standard examination by means of recording thickness of the ventricular septum and left ventricular posterior wall and end-systolic and end-diastolic LV diameters from M mode or 2D imaging. LV EF is measured with a two- and four-chamber view by biplane Simpson's method.

41.3   Exclusion of Direct Heart Damage

Obviously this is perhaps the other important issue in evaluating a donor's heart. This kind of evaluation is made in order to exclude marked heart damage often caused by direct or indirect chest trauma: the exam should exclude direct lesion of heart structures like atrial or ventricular rupture and related acute cardiac tamponade or pericardial effusion, acute valve regurgitation due to lesion of valve apparatus (especially mitral valve acute papillary muscle lesion but even aortic lesion in case of aorta direct or indirect damage) and myocardial direct lesion leading to acute myocardial infarction. Even iatrogenic lesions (great vessels or heart lesion especially following resuscitation procedures or placement of intravascular monitoring infusion lines or devices) should always be excluded. Always be reminded that heart lesions are not infrequent following deceleration trauma, a situation often leading to brain death and consequently to transplantation.

41.4   Perioperative and Postoperative Monitoring During Cardiac and Lung Transplantation

Intraoperative echocardiography has become a standard procedure during most cardiac proce-

dures including heart transplantation; it can provide help to identify intracardiac thrombosis and a real-time assessment of the cardiac allograft during de-airing, weaning from cardiopulmonary bypass and after implantation of the donor heart as the chest is closed. Biventricular function, especially right ventricular function, valve function and surgical anastomoses should always be assessed if possible. Particularly attention should be given to exclude acute rejection, right ventricular failure or tamponade any time acute haemodynamics instability arises.

Another specific issue to seek for is the presence of tricuspid regurgitation. The adverse impact of significant tricuspid regurgitation on mortality or need for retransplantation has been stressed in the paediatric heart transplantation so far that a prophylactic donor tricuspid annuloplasty (De Vega) was proposed in order to prevent postoperative valve regurgitation specially if a biatrial anastomosis technique is used.

Usually the newly transplanted heart allograft typically has a good LV systolic function, so observation of an early acute LV dysfunction following heart transplantation is particularly worrisome and should always be investigated to exclude early rejection or poor graft quality or preservation. More frequently we can see the presence of a RV postoperative early dysfunction, often predictable in patients with high preoperative pulmonary vascular resistance, excessive perioperative bleeding with massive transfusion, pulmonary oedema, poor RV protection during implantation, significant donor-recipient mismatch or more infrequently acute right coronary air embolization.

As a matter of fact, even heart allograft with excellent early function typically shows a worsening of ventricular function over the first 12 postoperative hours, primarily due to ischaemia time, reperfusion and myocardial oedema; this results in both systolic and diastolic dysfunction. Intraoperatively, it is not uncommon to see an increase in wall thickness and mass and a restrictive cardiac filling pattern (by means of a transmitralic Doppler evaluation) in early postoperative period; echocardiographic seriated monitoring is very useful to lead clinician decision to discrimi-

nate between transient benign course associated with a good cardiac output status and impaired cardiac function with poor cardiac output with need for prolonged inotropic support, IABP or RVAD/LVAD assistance. Anyway it seems there is a substantial evidence that isovolumetric relaxation time < 90 milliseconds and ratio of pulsed Doppler E/A major than 1.7 could be significant predictors of acute cardiac allograft rejection, even if each single echocardiographic feature is not able to confirm rejection alone, and this kind of diagnosis should be confirmed by clinical, haematochimic clues, keeping in mind that right heart endomyocardial biopsy stand as gold standard yet.

Another important issue to consider is the surgical technique used during heart transplantation: orthotopic cardiac transplantation has most commonly been performed with biatrial anastomoses according to Lower and Shumway technique; more recently, bicaval and total techniques have been devised to improve cardiac anatomy and physiology. The bicaval technique leaves a large cuff of the recipient's atria and leads to a marked atrial enlargement and altered geometry with a predisposition to intracavitary thrombus formation.

Observation of an elevated E/A transmitralic ratio could be explained as the result of an impaired overall atrial function after standard left atrial anastomosis rather than from a truly restrictive pattern. In this case the observation of a "pseudorestrictive" pattern associated with elevated E/A ratios and paradoxically normal early diastolic mitral annular motion velocities avoids misdiagnosis of an advanced diastolic dysfunction status often associated with acute rejection as stated above.

Recent findings suggest a potential new role for the echocardiographic study in post-transplant patients: there is some evidence that an improvement in the postoperative dedicated echocardiographic routine examination could lead to a minor necessity for myocardial biopsy (EBM) to detect graft rejection. EBM is an invasive procedure related to some potential severe complications (i.e. cardiac tamponade), so a valid alternative to it would be of maximum interest. According to some recent studies, TDI analysis of LV, particularly of the late diastolic "a" velocity, could be well related with a high degree of suspicion of cardiac rejection (more the 3A according to EBM classification). Such an evaluation could be useful in screening high-risk patients for EBM. RV TDI also seems to be well related to early post-surgical RV dysfunction too.

3D echocardiography technology is in process of evaluation to better understand its potential for prediction of post-transplant graft failure: the superiority of 3D in appreciation of geometry and volume of cardiac chambers puts this technique ahead compared to 2D for a better and earlier understanding of acute and chronic evolution in transplanted hearts.

Key Points in Heart Transplantation Echo

Preoperative Evaluation
1. Finding of an ineffective cardiac function should alert clinician in order to better investigate real availability of other potential grafts.
2. Discreet wall motion abnormalities on echocardiography or left ventricular ejection fraction (LVEF) <40% despite optimization of haemodynamics with inotropic support should lead to exclusion of graft.
3. The presence of a LV hypertrophy in donor heart suggests the need of an early administration of cardioprotective agents.

Intraoperative Evaluation
1. An early acute LV dysfunction following heart transplantation is particularly worrisome and should always be investigated to exclude early rejection or poor graft quality or preservation.
2. More frequently we can see the presence of a RV postoperative early dysfunction, often predictable in patients with high preoperative pulmonary vascular resistance.

Postoperative Evaluation
1. In early postoperative period, echocardiographic seriated monitoring is very useful to lead clinician decision.
2. There is a substantial evidence that reduction of pressure half time (PHT) and TDI, isovolumetric relaxation time < 90 milliseconds and ratio of pulsed Doppler E/A major than 1.7 evaluation of late diastolic "a" velocity could be significant predictors of acute cardiac allograft rejection, but no single predictor or combination was powerful enough to eliminate surveillance by endomyocardial biopsies.
3. 3D technology is promising for best appreciation of early and late cardiac graft rejection (evaluation of chambers geometry and volumes).

41.5 Heterotopic Heart Transplantation (Fig. 41.1)

In this technique the donor heart is placed without recipient cardiectomy. Initially it was a technique developed in the pre-cyclosporine era for patients whose myocardium was expected to recover; nowadays it is a technique adopted for patients with severe pulmonary hypertension because the preconditioned native right ventricle should cope better with the high transpulmonary pressure gradients; moreover it permits use of undersized allografts, and it is sometimes used in size mismatch patients, expanding the donor pool.

The allograft is placed right to the native heart in the right chest at an angle close to 90° to it. Both left and right donor atria are connected to recipient's atria, and both aortas are anastomosed. The donor pulmonary artery may be connected to the donor right atrium (LV assist configuration) or to the pulmonary artery by means of interposed graft (biventricular configuration); physiologically we have a situation in which native and donor atria share systemic and pulmonary venous return. The donor pulmonary artery and aorta are anastomosed to the respective native vessels, each receiving blood from both native and donor ventricles.

Clinical experience demonstrates that due to the huge space occupied by the two anastomosed hearts, it is often very difficult to obtain a single image comprehensive of all the anatomical field, so it is very important to identify correctly the single structures, so in this case, transoesopha-

Fig. 41.1 *NLV* native left ventricle, *GRA* graft right atrium, *GRV* graft right ventricle
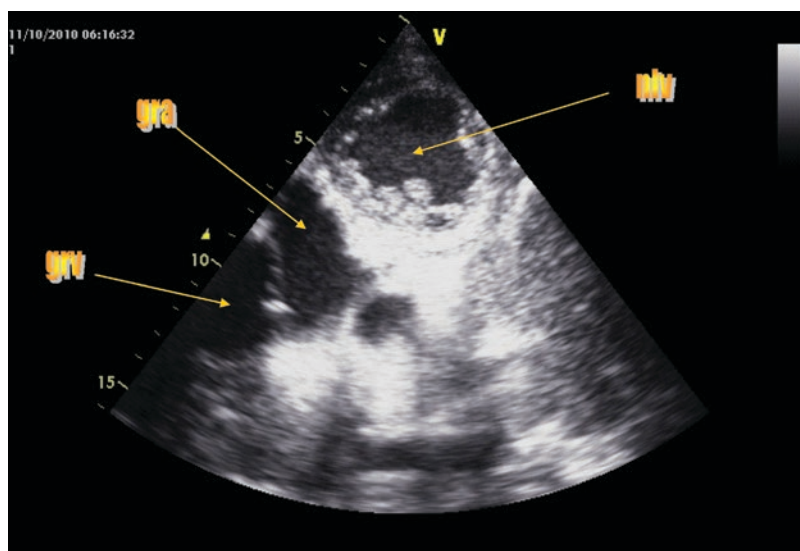
geal echocardiography requires correct identification of chambers in a step-by-step examination, considering the different orientations of the two hearts in the chest and their expected function and keeping in mind the 90° orientation between native and donor chambers. Often it is possible to find smoke-like effect in the native atria and dilatation and poor contractility obviously in the native left ventricle.

41.6 Lung Transplantation

Due to the close interrelation between the heart and lung, the TOE evaluation is considered an invaluable tool for intraoperative monitoring during anaesthesia in this kind of surgical procedure. Induction and mechanical ventilation can exacerbate a pre-existing pulmonary hypertension leading to an acute right ventricular failure. Preoperative severe emphysema (always present in alpha 1 antitrypsin deficiency) can lead to acute pneumatic tamponade. Intraoperative hypoxemia due to one-lung ventilation can exacerbate cardiac ischaemia, so TOE became the right tool to inform the anaesthesiologist about necessity for extracorporeal intraoperative support. During the reperfusion of the lung, there is the possibility of coronary air embolism; moreover TOE is routinely used to assess eventual thrombi, vascular strictures and permeability of pulmonary venous vascular sutures.

41.7 Conclusion

In conclusion it can undoubtedly be assessed that TOE stands as a fundamental tool for both standard monitoring and diagnosis in the surgery transplantation environment.

It could make the difference in saving or preserving grafts due to its early warning capacity, affording the decision-making process to be as fast as possible in virtue of its bedside utilization compared with more complex diagnostic procedures requiring the moving of the patient.

A well-planned evaluation strategy in the preoperative, intraoperative and postoperative setting plays a key role in successful anaesthesia and in the intensive care unit management.

Suggested Reading

1. Hashimoto S, Kato TS, Komamura K, Hanatami A, et al. The utility of echocardiographic evaluation of donor hearts upon the organ procurement for heart transplantation. J Cardiol. 2011;57:215–22.
2. Venkateswaran RV, Bonser RS, Steeds RP. The echocardiographic assessment of donor heart function prior to cardiac transplantation. Eur J Echocardiogr. 2005;6:260–3.
3. Chair Costanzo MR, Co-Chairs Dipchand A, Sterling R, et al. The international society of heart and lung transplantation guidelines for care of heart transplants recipients. Task Force 1: perioperative care of the heart transplant recipient. 2010. ISHLT.
4. Sun JP, Abdalla IA, Asher CR, Greenberg NL, Popovic ZB, Taylor DO, Starling RC, Thomas JD, Garcia MJ. Non invasive evaluation of orthotopic heart transplant rejection by echocardiography. J Heart Lung Transplant. 2005;24(2):160–5.
5. Serra E, Feltracco P, Barbieri S, et al. Transoeshophageal echocardiographic during lung transplantation. Transplant Proc. 2007;39(6):1981–2.

New-Onset Cardiac Murmur in the Unstable Patient

42

Michele Oppizzi, Marco Ancona, and Vittorio Pazzanese

There are several different clinical scenarios and causes of haemodynamic instability associated with cardiac murmur of new onset, including:

- *Mechanical complications of acute myocardial infarction*:
  - Free wall rupture
  - Ventricular septal defect (VSD)
  - Papillary muscle rupture
- *Left ventricular outflow tract obstruction (LVOTO)*:
  - Systolic anterior motion (SAM)
- *Mitral regurgitation due to spontaneous rupture of chordae tendineae*
- *Endocarditis*:
  - Mitral regurgitation (MR)
  - Aortic regurgitation (AR)
- *Aortic dissection*
- *Prosthetic valve dysfunction*

42.1 Mechanical Complications of Acute Myocardial Infarction (AMI)

Patients at high risk of mechanical complications are usually elderly female patients with first STEMI without a history of previous angina with late presentation to emergency department and too late or no reperfusion.

42.1.1 Free Wall Rupture

Clinical Scenario Free wall rupture typically appears within few days from the onset of STEMI in the population previously mentioned. Within few days from infarction, these patients suddenly develop a circulatory collapse, usually associated with bradycardia. Free wall rupture represents an emergency, because it leads to cardiac tamponade and death. At physical examination cardiac tamponade manifests as distension of neck veins, pulsus paradoxus and muffled heart sounds. ECG might demonstrate the presence of Q waves and persistence of ST segment elevation in the settings of low voltages. Occasionally ruptures of the septum or papillary muscle are associated.

Echo Diagnosis TTE is sufficient to diagnose a free wall rupture. Blood pericardial effusions commonly cause cardiac tamponade: the right ventricle and both atria appear compressed, and

M. Oppizzi (✉) · M. Ancona · V. Pazzanese
Department of Cardiology, San Raffaele Hospital, Milano, Italy
e-mail: oppizzi.michele@hsr.it; ancona.marco@hsr.it; pazzanese.vittorio@hsr.it

diastolic filling is impaired (swimming heart image). Typically the presence of (a) pericardial effusion (2D; apical, parasternal or subcostal views); (b) an akinetic wall, usually inferior (two chambers) or lateral (four chambers); and (c) hyperkinesis of other segments in patients with circulatory collapse must raise the suspicion of free wall rupture. Increased contraction of remote walls produces a high intra-ventricular pressure; late thrombolysis converts ischaemic into haemorrhagic necrosis causing rupture of infarcted wall. Free wall rupture occurs between viable and necrotic myocardium. A large anterior AMI in the left anterior descending territories usually is not associated with free wall rupture because it causes a severe left systolic dysfunction: the ventricle is not able to generate a high intra-ventricular pressure sufficient to determine wall rupture.

The diagnosis is confirmed by a turbulent systolic flow (colour Doppler) through the akinetic wall, usually in mid-ventricular position of the anterior or lateral wall. In some patients the rupture is incomplete or closed by a cloth and is not well visualised by echo. In this setting the use of contrast echocardiography can be considered, in order to confirm the active replenishment.

Echo-Guided Therapy Free wall rupture is a surgical emergency; in the absence of prompt treatment, this condition is usually fatal. During surgery, the pericardial effusion is evacuated, and pledgeted sutures close myocardial tear.

42.1.2 VSD

Clinical Scenario Symptoms of VSD include a sudden relapse of chest pain, shortness of breath and a rapid worsening in the patient's haemodynamic status that evolves in cardiogenic shock. In patients who have not been treated with reperfusion therapy, symptoms usually appear after 3 to 7 days from the infarct, while rupture occurs earlier (median 24 h) if thrombolytic therapy has been used. A parasternal thrill is palpable in half of the patients, and a harsh, loud and holosystolic new-onset murmur becomes audible along the

sternal border and radiates to the right parasternal area. Signs of left and right heart failure are both present. In patients with cardiogenic shock, it can be difficult to identify a thrill or a murmur, and therefore shock may be erroneously attributed to extension of the AMI. Definitive treatment is the surgical closure of the VSD with a patch; in few selected patients, it is possible to close the VSD by placing a device percutaneously.

How to Do It and Echo-Guided Therapy Echocardiography is useful in diagnosing septal rupture, to define the site, to estimate left to right shunt, to quantify right and left ventricular function and to assess the possibility to close it percutaneously.

VSD appears by colour Doppler as a turbulent systolic flow from left to right ventricle through the akinetic ventricular septum and is more commonly associated with hyperkinesia of other walls. Such findings are diagnostic of a VSD: sensitivity and specificity of colour Doppler are about 100%. The size of the defect ranges from a few millimetres to several centimetres. So larger VSD appears at 2D as an echo dropout across the septum. In patients with an anterior AMI, the defect is simple (discrete with direct communication at the same level on both sides of the septum) and apically located, and it can be well visualised in the four-chamber view. In patients with an inferior AMI, the defect is more complex (irregular and serpiginous), and it involves the basal portion of inferior-posterior septum, close to the tricuspid and mitral valves; it may be imagined in the basal septum in the four-chamber TT or TE views and in the parasternal short-axis views. Sometimes, multiple septal perforations are present. Given the high mortality rate for patients treated conservatively, the diagnosis of VSD is itself an indication for emergent surgery, even when the patient is stable.

In most cases the right ventricle appears dilated in the four-chamber and long-axis views as a consequence of left to right shunt and/or right ventricular infarction. Right atrial pressure inferred from the inferior vena cava diameter and its degree of collapse in the subcostal view may be high. Right ventricular infarction is suspected

in patients with bradycardia complicating an inferior AMI, and it is confirmed by ST elevation in the right precordial leads (V3R–V4R) and reduced indexes of right ventricular function: diffuse hypokynesia, a tricuspid annular plane systolic excursion (TAPSE) <1.8 cm and a systolic velocity at Tissue Doppler Imaging <10 cm/s. A posterior location of the VSD and right ventricular dysfunction, particularly if complicated by an increase in right atrial pressure, are echocardiographic predictors of poor outcome. Cardiogenic shock more commonly develops in patients with RV dysfunction. Surgical closure of a complex posterior VSD is more technically demanding and carries a higher risk of recurrence. Percutaneous closure is not always feasible. In-hospital mortality for anterior defects amounts to 10–15% and 30–35% for anterior and for posterior VSD, respectively.

The estimation of left to right shunt can be obtained by measuring the ratio between the right and left cardiac output as recorded with pulsed Doppler (PWD) on the right and left ventricular outflow tracts: its clinical relevance has recently declined because early surgery is now recommended in all patients, irrespective of the amount of the shunt. On the other hand, it is valuable in patients who develop a recurrent defect after surgical closure: in these patients redo surgery is indicated when the shunt fraction is >1.5.

Left ventricular function, quantified by EF in the four-chamber view, is usually mildly reduced. The preoperative haemodynamic status is a more powerful predictor of outcome when compared to LV ejection fraction.

Simultaneous significant mitral regurgitation secondary to papillary muscle infarction or dysfunction may occur in up to 20% of patients with VSD. It is well visualised and quantified in the apical four- and two-chamber view and in the parasternal long-axis view. If the regurgitation is severe, concomitant valve repair or replacement is indicated.

In the operating theatre, TEE is used after the weaning from cardiopulmonary bypass in order to assess the completeness/efficacy of the septal and of the mitral valve repair, if performed, and the response of right and left ventricular function

to inotropic and mechanical support. In the postoperative period, TTE is recommended to guide the weaning from drugs or devices and if a VSD recurrence (new-onset murmur, haemodynamic worsening) is suspected.

42.1.3 Papillary Muscle Rupture

Clinical Scenario The population at risk of papillary muscle rupture is the same described for the other mechanical complications of AMI. Complete resection of papillary muscle is incompatible with life. Partial papillary muscle rupture is usually due to a small inferior infarction involving the posterior-medial papillary muscle. Rupture of the posterior-medial papillary muscle is three times more frequent than anterior-lateral papillary muscle, because the former is vascularised only by the right coronary artery, while the latter usually has a double vascularisation from the LAD and circumflex coronary artery. Clinical manifestations of papillary muscle rupture are similar to those of VSD with an abrupt onset of shortness of breath and hypotension, but the incidence of papillary muscle rupture is lower (about 1%), the onset is earlier (median 1 day), pulmonary oedema is more common and more severe, while signs of right heart failure, such as jugular veins distension, are missing. Physical examination reveals no thrill, and the cardiac murmur is softer and radiated to the left axilla.

How to Do It TTE (apical and parasternal views) with colour Doppler immediately identifies the MR (usually eccentric and severe), regional reduced indexes of right ventricular function, wall motion abnormalities (usually the inferior wall) and a hyperdynamic cardiac motion consequent to acute volume overload. The anterior or, more commonly, the posterior mitral valve leaflet, consequent to the rupture of the head of the medial or of the lateral papillary muscle, respectively, flails into the left atrium. TTE can often visualise the papillary muscle's head protruding in the left atrium, but in some patients, TEE (mid-oesophageal views for mitral valve and trans-

gastric long-axis views) is needed to confirm the diagnosis.

Echo-Guided Therapy Partial papillary muscle rupture is a surgical emergency. The option between repair and replacement is based on surgical preference and skills and not on echocardiographic data.

42.2 LVOTO and SAM of the Mitral Valve

Clinical Scenario LVOTO is a dynamic, functional, obstruction due to systolic movement of the anterior mitral leaflet (SAM) into the outflow caused by suction (Venturi's effect) or pushing (drag forces) of the anterior leaflet. These forces are generated by a combination of (a) *predisposing anatomic features of the LV*, such as moderate to severe hypertrophy of the basal ventricular septum, in some cases associated with an anteroposition of the papillary muscles, a small LV cavity and a hyperkinetic LV and (b) *predisposing conditions such* as a hyperdynamic state and/or a preload reduction (Fig. 42.1)

LVOTO is typical of hypertrophic obstructive cardiomyopathy (HOCM). However, it has also been described in patients with hypertensive heart disease, especially in elderly women, in pheochromocytoma, apical ballooning syndrome, after mitral valve repair or cerebral haemorrhages and in those situations characterised by high catecholamine levels and/or low LV preload (hypovolemia, use of nitrates, pericardial effusion, etc.).

SAM causes two different problems:

- *Obstruction of LVOT* which, if severe, may lead to a reduction in cardiac output, hypotension, myocardial ischaemia and to cardiac arrest by ventricular fibrillation
- *MR* which increases left atrial and pulmonary capillary pressure leading to dyspnoea, pulmonary oedema and hypoxemia

When a high-risk patient meets a high-risk condition, the prerequisites for the perfect storm are present. A typical scenario is a patient who becomes hypotensive with or without ST changes or pulmonary oedema. If haemodynamic doesn't respond to volume expansion, catecholamine is the first choice of therapy, but drugs are not effec-

Fig. 42.1 Left ventricular outflow obstruction
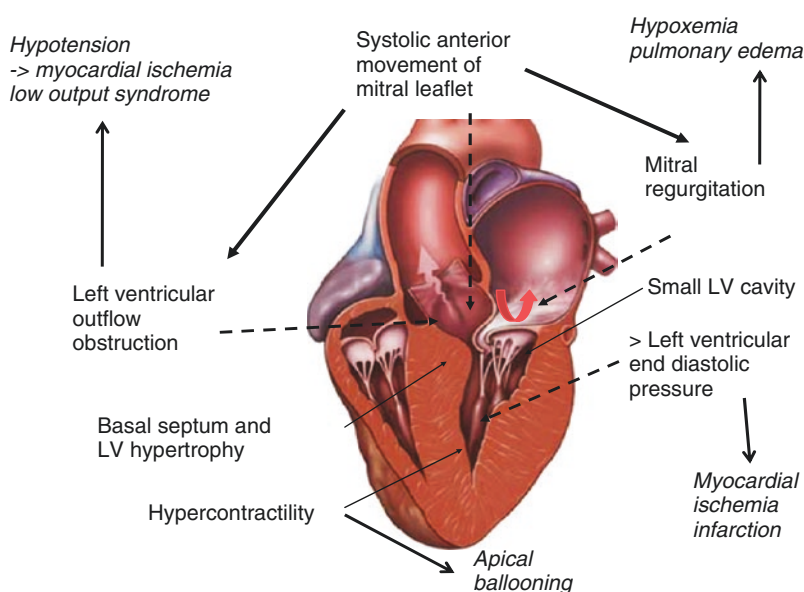
tive, and arterial pressure remains low. So the anaesthesiologist decides to position the Swan-Ganz (SG) catheter: but haemodynamic data from pulmonary catheter are dangerously misleading, because low cardiac output (due to LVOTO) and high left atrial pressure (due to MR) are interpreted as the consequences of a severe systolic LV dysfunction. Adrenergic agents are increased and furosemide is started. LVOTO is worsened with a positive feedback, and if the loop is not interrupted by an echo-guided diagnosis, cardiac arrest eventually occurs.

How to Do It   The diagnosis of LVOTO by SAM can only be performed by echocardiography, which can also quantify the gradient. SAM can be easily diagnosed both with TTE and TEE. At first you have to identify, with 2D echocardiography, the anterior mitral leaflet being suctioned during systole into the LVOT. The more useful views are the parasternal long-axis, apical five-chamber view and mid-oesophageal long-axis for the aorta at 120°. In these views colour Doppler imaging typically shows two contemporary turbulent systolic flows: one directed into the LVOT, i.e. the obstruction, and the other directed posteriorly in

the left atrium, i.e. the MR, both caused by SAM. In the apical five-chamber or deep transgastric views, continuous-wave Doppler (CWD) allows the quantification of the obstruction through the measurement of the gradient. The systolic gradient due to SAM has a typical *dagger-shaped* morphology, increasing during systole and reaching its peak in end-systole (Fig. 42.2). Its morphology is very different from that of aortic stenosis, whose peak is in mid-systole. A peak gradient value higher than 30 mmHg defines a critical gradient.

Pay attention: MR and turbulent flow of LVOT obstruction can be very close, and it can be difficult to understand which flow is being measured by CWD. To discriminate between them, remember the dagger-shaped morphology of LVOT obstruction and the higher velocity of MR flow.

Echo-Guided Therapy   The diagnosis of LVOTO in the setting of a hypotensive patient is critical: in this clinical condition, every positive inotropic agent must be avoided, because they worsen the obstruction. Volemic expansion, preload and afterload increase by the use of norepinephrine, and low doses of beta-blockers are the appropriate treatment of SAM (Fig. 42.3).

Fig. 42.2 LVOT gradient by continuous wave Doppler
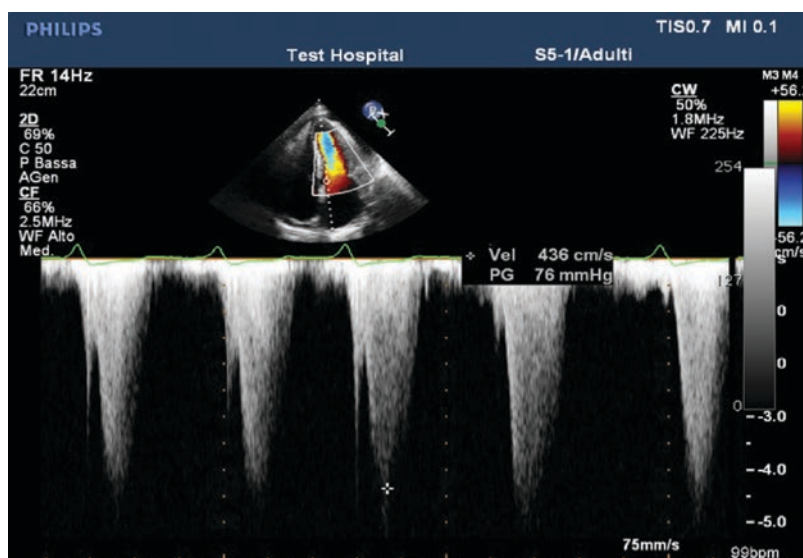
Fig. 42.3 Echo guided treatment of left ventricular outflow obstruction

SYSTOLIC ANTERIOR MOVEMENT of MITRAL LEAFLET

NOREPINEPHRINE

MITRAL REGURGITATION

LEFT VENTRICULAR OUTFLOW OBSTRUCTION

ADD VOLUME CAUTIOUSLY

BETABLOCKERS

SMALL LV CAVITY

HYPERCONTRACTILITY

AVOID / STOP ADRENERGIC AGENTS
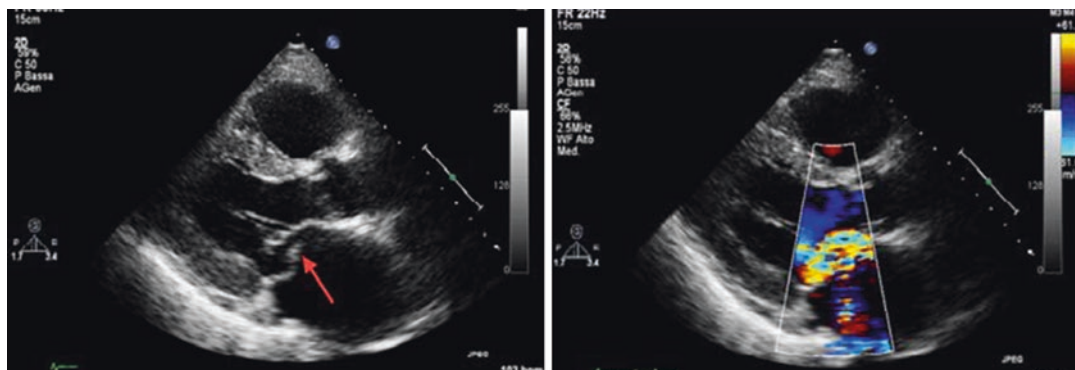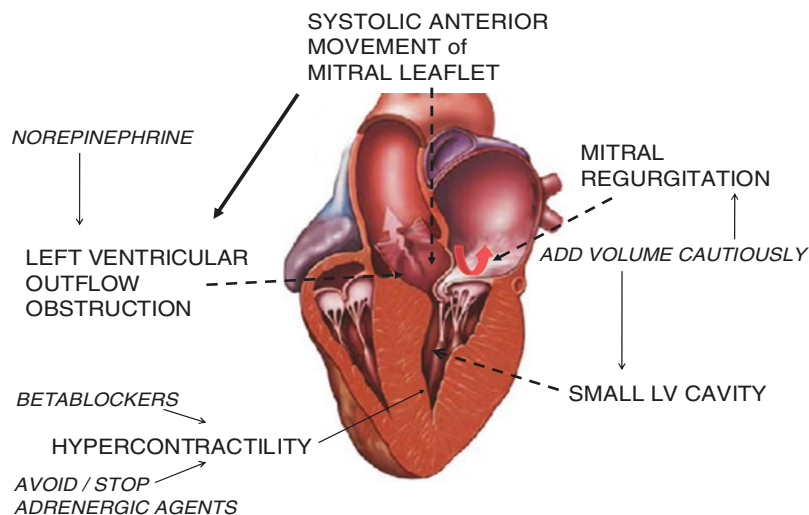
Fig. 42.4 Posterior leaflet chordal rupture parasternal long axis view

42.3 Mitral Regurgitation Due to Spontaneous Rupture of Chordae Tendineae

Spontaneous rupture of chordae tendineae (flail) in patients affected by myxomatous degeneration of mitral valve gives rise to an acute MR which can quickly decompensate the patient.

Echocardiographic Findings (Fig. 42.4) At 2D the leaflet losses the normal concavity towards the left ventricle, becoming flat or with concavity directed at the left atrium, with a free movement during systole, giving the eversion of the leaflet.

- Direct visualisation of ruptured chordae tendineae protruding in atrium during systole.
- Regurgitant jet is usually severe (colour Doppler) and holosystolic (colour M-mode). As in mitral valve prolapse, jet directs in a direction, which is opposite to that of the leaflet whose chordae are ruptured (e.g. ruptured of the chordae of the posterior leaflet determines an anteriorly directed jet).

How to Do It Usually TTE (parasternal long-axis and four-chamber views) allow the diagnosis of suspicion. TEE is necessary to confirm the diagnosis through the direct visualisation of the chordal rupture (Fig. 42.5).
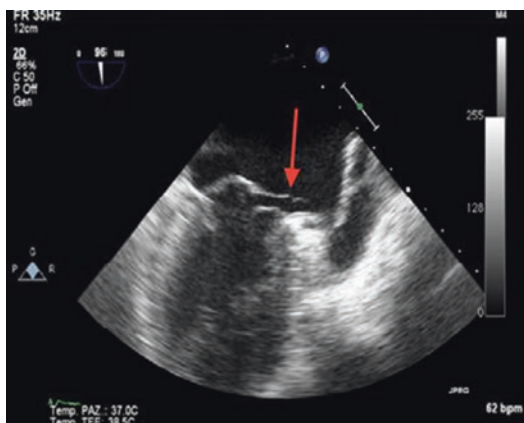
Fig. 42.5 Posterior leaflet chordal rupture 2 chambers TEE view

Caveat Chordae tendineae rupture near the commissure gives rise to a markedly eccentric regurgitation jet which can be easily underestimated at TTE: it appears as a horizontal jet spreading over the opposite leaflet. A TEE should be performed in order to confirm the diagnosis of chordae tendineae rupture.

42.4 Endocarditis

Hypotension and acute congestive heart failure are not uncommon in infective endocarditis as a result of sepsis status and/or haemodynamic complications: severe mitral or aortic regurgitation, prosthetic detachment or obstruction, cardiac shunts or cardiac tamponade from fistula formation. TTE sensibility for infective endocarditis is suboptimal especially in patients with prosthetic valves and/or periannular complications: TEE must be performed in high-risk populations. Infective endocarditis complicated by acute congestive heart failure is an indication for urgent surgical treatment.

Native Valve Endocarditis
Vegetation is the echocardiographic hallmark of infective endocarditis. It appears at 2D examination as an echogenic, irregularly shaped mass, usually oscillating with high-frequency movement, independent from that of cardiac valve and typically attached to ventricular layer of aortic cusps or to atrial layer of mitral leaflets (Fig. 42.6). Sometimes primary aortic vegetations can be responsible for the so-called kiss lesion on the anterior mitral leaflet. Other cardiac masses (Libman Sacks lesions, marantic endocarditis, myxomatous valve, chordal rupture, Lambl's excrescences) may mimic vegetations, but only spontaneous chordal rupture may cause acute severe regurgitation with haemodynamic instability.

Native valve endocarditis can cause acute regurgitation in three different ways: perforation, fistula formation (aortic valve) and chordal rupture (mitral valve).

*Perforation* is the most common lesion causing regurgitation: it appears early, usually in the first week after the onset of fever. At echocardiography, it can be diagnosed as a regurgitant flow originating from the body of the leaflet or cusp and not from the coaptation zone. *Fistula* is due to spread of infection to perivalvular tissue with the development of an aorto-cavitary communication creating intracardiac shunt: it can result in acute overload of LV or RV. It is uncommon in aortic valve endocarditis; the incidence is a little bit higher in patients with aortic prosthetic valve. Fistula is well visualised by colour Doppler in parasternal or mid-oesophageal short-axis views of aortic valve like a turbulent jet between periaortic tissue and a cardiac cavity. LV or RV appears hyperkinetic because of acute overload. Patients with infective endocarditis complicated by fistula formation are, despite surgery, at increased risk of adverse outcome including heart failure and death (up to 40%). Fistula may break itself into the pericardial sac causing cardiac tamponade.

Prosthetic Valve Endocarditis
Infective endocarditis on prosthetic valve begins on the valvular cuff and usually extends to periannular tissue resulting in prosthetic dehiscence and abscess and fistula formation. It can be difficult to visualise vegetations and extra-annular complications with TTE due to shadowing of the prosthetic valve, so TEE is usually needed.

There are three possible echocardiographic findings:

MEDIOESOPHAGEAL LONG AXIS VIEW

MEDIOESOPHAGEAL 4 CHAMBERS VIEW

VEGETATION on the RIGHT CUSP
of the AORTIC VALVE

ABSCESS of ANTERIOR LEAFLET of
MITRAL VALVE with SEVERE
REGURGITATION
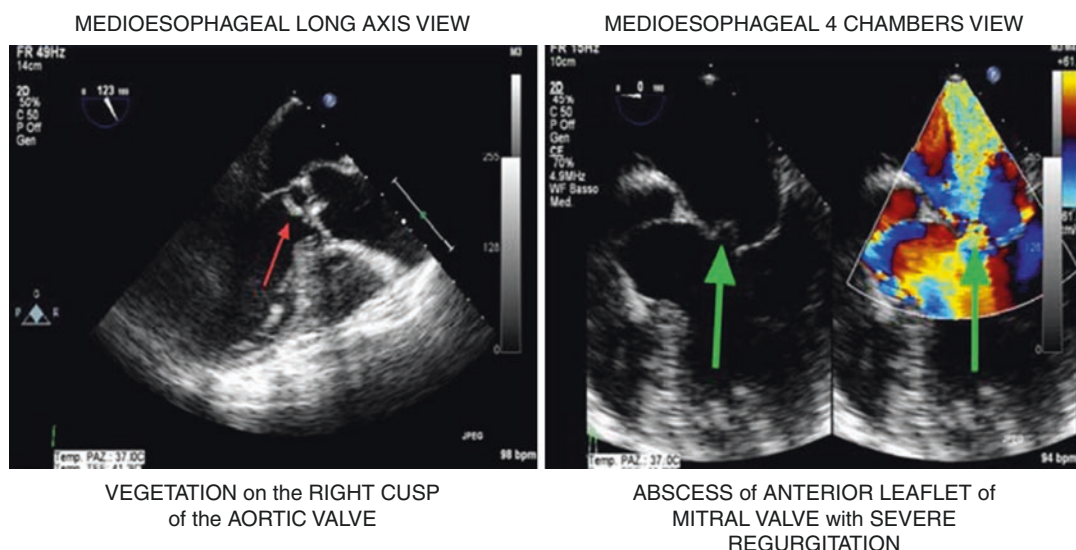
Fig. 42.6 Aortic and mitral valve endocarditis

1. *Vegetations* are attached to the prosthetic annulus.
2. *Prosthetic detachment* appears as a paraprosthetic regurgitating jet. It is responsible for the development of severe regurgitation and sometimes of haemolysis. Extensive detachment can produce a "rocking" motion of the of the entire valve apparatus.
3. *Paraprosthetic abscesses* appear as anechoic cavity surrounding the prosthesis. Echocardiographic appearance is usually nonhomogeneous. In many cases there is evidence at colour Doppler of a flow within the echo-free space, but this fact is not mandatory. They are typical of prosthetic aortic valves and usually localised posteriorly, i.e. in the left or right fibrous trigone. They can fistulise in the surrounding cavity/cavities, such as the left atrium for posterior abscesses, right atrium for lateral abscesses and the pulmonary artery for anterior abscesses.

Vegetations and abscesses, when isolated, do not determine haemodynamic instability. On the contrary, an acute prosthetic detachment causing severe aortic or mitral regurgitation can drive to acute heart failure.

How to Do It The aortic native valve can be well evaluated at TTE in the long-axis parasternal view, while the mitral valve can be studied also in the apical four-chamber view.

It is mandatory to perform a TEE in the prosthetic valve setting when the clinical suspicion for endocarditis is high. Native and prosthetic aortic valves can be evaluated in the mid-oesophageal short- and long-axis view: the short axis allows the evaluation of abscesses and detachments. Native and prosthetic mitral valves should be studied in every mid-oesophageal view.

Differential Diagnosis It can be difficult to distinguish vegetation from a mitral valve flail on TTE. TEE allows a simple discrimination between the two. In prosthetic mechanical valve, it can be challenging to discriminate between vegetations and thrombi localised at the prosthetic annulus: thrombi are usually bigger and are associated with spontaneous echo contrast.

42.5 From Echo Images to Diagnosis: A Practical Approach

In the unstable patient in whom a new-onset cardiac murmur is present, three different echocardiographic settings might be responsible for the instability: a new mitral regurgitation, a new aor-

tic regurgitation and a prosthetic malfunction. A practical overview of the differential diagnosis and the aetiology of these murmurs is described here.

42.5.1 New-Onset Mitral Regurgitation (Fig. 42.7)

Mitral regurgitation (MR) appears at colour Doppler imaging as a turbulent systolic flow directed from the left ventricle through the left atrium. All the causes of new-onset MR must be excluded: endocarditis, SAM, papillary muscle rupture as complication of acute myocardial infarction or flail mitral leaflet. You have to proceed step by step in order to discriminate between them.

Firstly, the *left ventricular outflow tract* (LVOT) must be inspected: normally there is a systolic nonturbulent flow. A turbulent flow in the LVOT associated to the MR is indicative of SAM:

the anterior leaflet of the mitral valve, during systole, is suctioned by a Venturi effect through the LVOT, causing an obstruction; if the anterior leaflet is displaced in the LVOT, it cannot ensure an adequate coaptation and therefore causes MR. This mechanism causes a reduction of the cardiac output, through the obstruction of the LVOT, and increases left atrial pressure through MR.

In order to confirm the diagnosis of SAM, you have to:

- *Evaluate the gradient on the LVOT*: SAM typically gives a dagger-shaped gradient whose peak value is greater than 30 mmHg.
- *Evaluate the direction of the MR jet*, which is typically directed posteriorly.

Once a LVOT obstruction caused by SAM has been excluded, the morphology of mitral valve leaflet should be evaluated, particularly at the concavity of the leaflet. When the valve is closed,
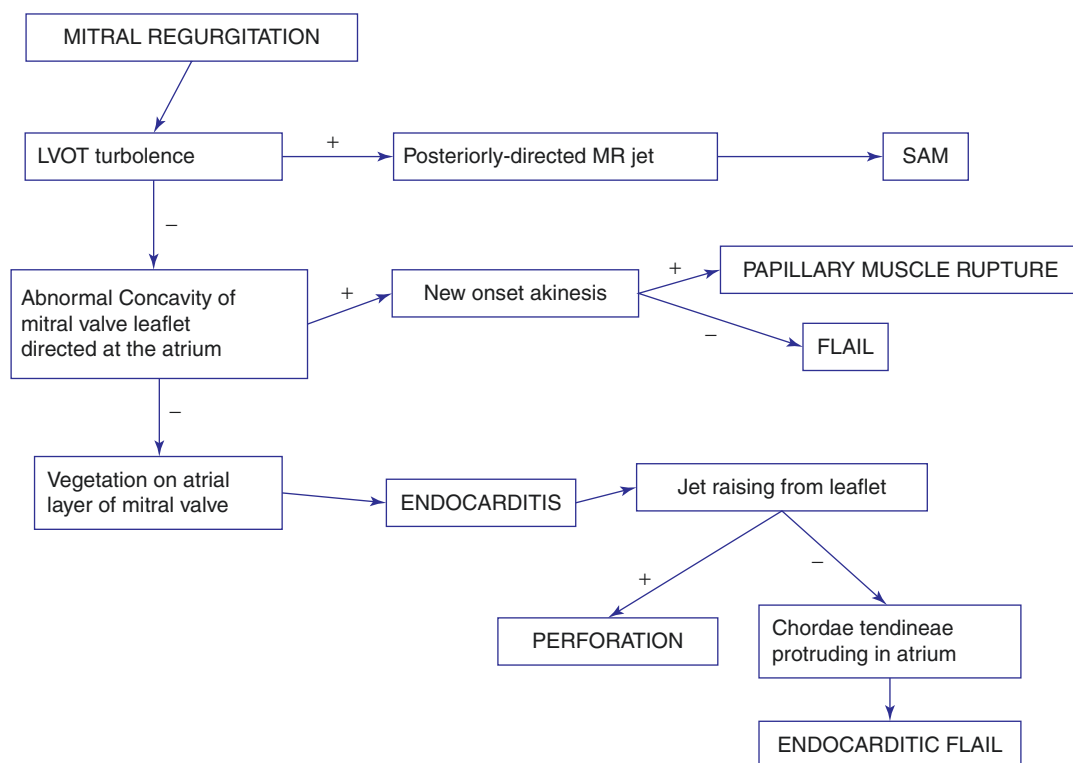
Fig. 42.7 Diagnostic algorhytm for mitral regurgitation

mitral leaflet concavity is normally directed to the ventricle, and the chordae tendineae attached to the leaflet are visible. There are two pathological conditions in which the mitral leaflet concavity during systole is directed to the atrium, determining a leaflet eversion that causes MR: papillary muscle rupture as a complication of an acute myocardial infarction and a flail mitral leaflet. Therefore, in an unstable patient with MR and a mitral leaflet with an abnormal concavity directed to the atrium, the differential between these two diagnoses must be performed. In order to do so, attention should be focused on *left ventricular wall kinesis*. An akinetic wall could be the consequence of an acute myocardial infarction that might have caused, after a few hours from the beginning of symptoms, the rupture of the papillary muscle. In this case the head of the papillary muscle attached to the mitral leaflet through the chordae tendineae is visible, moving during systole in the left atrium. If the left ventricular kinesis is normal, myocardial infarction can be excluded as the cause of the papillary muscle rupture. In the case of a MR with an abnormal concavity of the leaflet directed to the atrium, the likely diagnosis is flail mitral leaflet. Chordae tendineae rupture can be difficult to visualise at TTE, and therefore you may need a TEE to confirm your diagnosis.

Once LVOT obstruction, flail and papillary muscle rupture have been excluded, another cause of new-onset MR causing haemodynamic instability should be considered, i.e. *infective endocarditis*. It is characterised by the presence of fluctuant vegetation attached to the atrial layer of the mitral valve; it can cause MR by two different mechanisms: perforation or chordal rupture. The origin of the regurgitant jet discriminates between them. In fact, when the jet originates from the leaflet, perforation is the culprit mechanism, while when the jet originates from the coaptation zone in the presence of chordae tendineae protruding in atrium during systole, it's obviously caused by chordal rupture. TTE sensitivity in the diagnosis of endocarditis is about 75%: when clinical suspicion is high, TEE should be performed.

When an acute MR in an instable patient is diagnosed, you have to understand the right mechanism of insufficiency in order to institute the right treatment. The diagnostic process consists of three steps: (1) look at the LVOT, (2) look at the morphology of the valve and (3) look for vegetations.

42.5.2 New-Onset Aortic Regurgitation (Fig. 42.8)

Aortic regurgitation (AR) is characterised at colour Doppler imaging by a turbulent diastolic flow from the ascending aorta to the left ventricle through the aortic valve. Remember the causes of

Fig. 42.8 Diagnostic algorhytm for aortic regurgitation
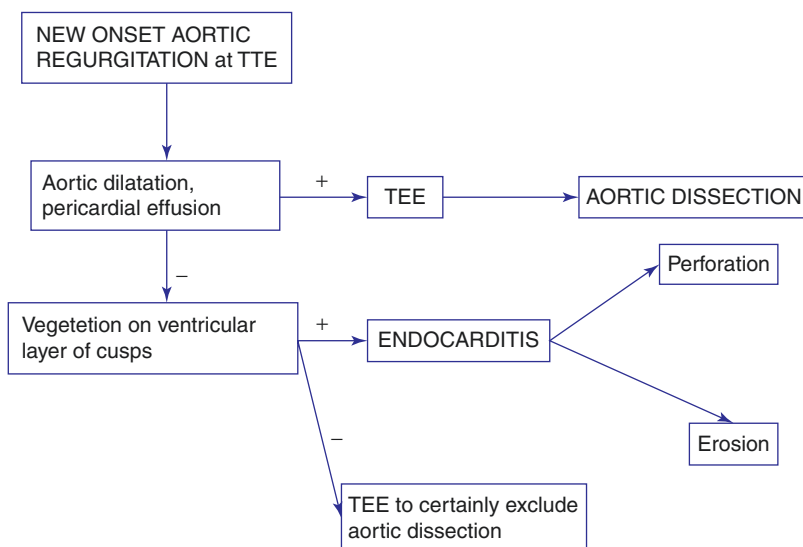
new-onset AR: type A aortic dissection and infective endocarditis.

In the unstable patient with acute AR, *type A aortic dissection must be excluded first* since it is a surgical emergency, and if not treated, it has 50% mortality in the first 24 h. TTE shows direct signs of dissection of the ascending aorta, such as the visualisation of the tear with the true and the false lumen, or sign that is indicative of dissection, such as a dilated ascending aorta or the presence of a pericardial effusion. TTE sensitivity in diagnosing ascending aorta dissection is only 70%, while TEE sensitivity reaches 100%.

Firstly *look for direct sign of dissection at TTE*, using also the sovra-jugular view, which allows a better visualisation of the aortic arch: in the presence of direct signs of dissection, the heart surgeon must be alerted as soon as possible.

When direct signs of dissection are not present, look for *indicative sign*: if you find them, confirm the diagnosis of dissection by TEE as soon as possible. If you don't find neither direct nor suspect sign of dissection, look for other causes of acute AR, such as endocarditis: it's characterised by a fluctuant vegetation attached to the ventricular layer of aortic cusps. As in MR, endocarditis can cause AR by perforation or erosion.

As the mortality of type A aortic dissection is high, you must be sure that this diagnosis is excluded in the setting of an acute AR: if it's not possible to understand the cause of an acute AR, it's mandatory to perform a TEE in order to increase the sensibility of your examination. If you highly suspect a dissection, it's advisable to call the anaesthetist and perform the TEE under sedation, in order to avoid dangerous hypertensive peaks that can cause aortic rupture.

42.5.3 Prosthetic Dysfunction
(Fig. 42.9)

In an unstable patient with a prosthetic mechanical valve, two pathologic processes should be excluded: prosthetic obstruction or paraprosthetic leaks. In patients with a prosthetic biologi-

cal valve, thrombosis is unlikely; therefore, only paraprosthetic leaks should be excluded.

How to Do It Obstruction is generally due to either thrombosis, more common in mitral or tricuspid prosthesis, or pannus, more common in aortic side.

Obstruction is likely when:

1. The excursion of mobile elements by (M-mode) is reduced.
2. Mean gradient at CWD on the prosthetic valve is more than >35 mmHg for aortic prosthesis and >10 mmHg for mitral prosthesis. For each valve, comparison with previous (ideally at time of implant) velocities should be undertaken.
3. Doppler velocity index (DVI) is <0.25 for aortic prosthesis and >2.5 for mitral prosthesis. DVI is calculated as the ratio of peak LVOT velocity (PWD) and peak trans-prosthetic velocity (CWD) for aortic prosthesis, and it is the ratio between peak trans-prosthetic velocity (CWD) and peak LVOT velocity (PWD) for mitral prosthesis.

Gradient measurements are more easily obtained by TTE, while the direct visualisation of thrombosis is more likely visualised by TEE.

If a prosthetic mechanical valve presents normal mobile elements excursion with a gradient comprised within the normal limits for that spe-
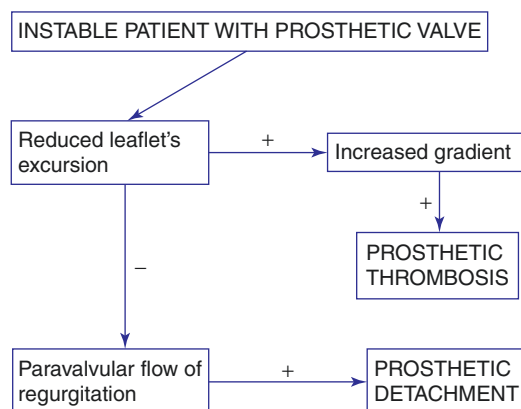
Fig. 42.9 Diagnostic algorhytm for prosthetic valve dysfunction

cific mechanical valve, thrombosis is excluded, and a paraprosthetic leak may be suspected. Leakage is diagnosed by excessive motion of the sewing ring (ECO 2D) and by a paravalvular turbulent flow of regurgitation (colour Doppler). In aortic prostheses the quantification of the severity of regurgitation is usually difficult to judge, and short-axis view should be used. The extent of circumferential leakage more than 20% indicates a severe regurgitation. Paraprosthetic leaks in mechanical mitral valve can be missed at TTE due to shadowing of the prosthesis. A TEE is needed to confirm and to accurately evaluate the extension of the paraprosthetic leaks. Acute paraprosthetic leakage is usually due to infective endocarditis.

Suggested Reading

Beaulieu Y. Bedside echocardiography in the assessment of the critically ill. Crit Care Med. 2007;35(suppl):S235–50.

Habib G, Badano L, Tribouilloy C. Recommendation for the practice of echocardiography in infective endocarditis. Eur J Echo. 2010;11:202–19.

Konoske R, Whitener G, Nicoara A. Intraoperative evaluation of paravalvular regurgitation by transesophageal echocardiography. Anesth Analg. 2015;121:329–36.

Lancellotti P, Price S, Edvardsen T. The use of echocardiography in acute cardiovascular care. Eur Heart J Acute Cardiovasc Care. 2015;4:3–5.

Lancellotti P, Pibarot P, Chambers J. Recommendations for the imaging assessment of prosthetic heart valves. Eur Heart J Cardiovasc Imaging. 2016;17:589–90.

Lester SJ, Wilansky S. Endocarditis and associated complications. Crit Care Med. 2007;35(suppl):S384–91.

Price S, Nicol E, Gibson DG, Evans TW. Echocardiography in the critically ill: current and potential roles. Int Care Med. 2006;32:48–59.

Slama M, Tribouilloy C, Maizel J. Left ventricular outflow tract obstruction in ICU patient. Curr Opin Crit Care. 2016;22(3):260–6.

ICU Echocardiography and Noninvasive Haemodynamic Monitoring

43

Giulia Frasacco, Mario Mezzapesa,
Giovanni Carriero, Fernando Piscioneri,
and Luigi Tritapepe

43.1 Introduction

Our challenge is to achieve the most adequate haemodynamic monitoring for a specific setting, optimizing cardiovascular function and improving patient outcome.

Haemodynamic monitoring provides dynamic measures of cardiovascular system changes, in real time.

A combination of clinical examination, prior assessment of therapeutic strategy and the treatment response is often called "dynamic or functional monitoring".

Many different tools are available. Every system has its own features and also its limitations.

Devices that measure systemic blood pressure, heart rate and cardiac output can be extremely basic and noninvasive, but these are less accurate for some critical settings (e.g. poor peripheral perfusion and vasoconstriction).

Minimally invasive (arterial catheter) and more invasive (central venous line and pulmonary artery catheter) devices directly allow mea-

suring of cardiac output. They can require time for positioning and lead to some complications.

Between these two categories of devices, there are some monitoring systems that indirectly measure the CO and the fluid responsiveness. They can be used in less critical patients, providing a cardiac output monitoring.

43.2 Arterial Pressure

Arterial blood pressure (AP) measurement is a cornerstone of haemodynamic assessment.

Despite being easy to conduct, the arterial blood pressure and the heart rate measures are very difficult to evaluate. Even if a very low blood pressure value is often matched with tachycardia, a normal value is not always a haemodynamic stability index.

Hypotension can be due to an autonomic nervous system inability to balance a decreased cardiac output and an anomalous oxygen delivery.

The severity of the hypotension state can be different according to the patient's age, sedative drug effects on haemodynamic status, pain control and patient comorbidities. Under general condition, during a decreased CO, baroreceptor activity tries to increase the sympathetic tone, leading to an increase in heart rate and vascular tone to restore the mean arterial pressure. Hence, patients could have sudden haemodynamic

M. Mezzapesa · G. Carriero F. Piscioneri
L. Tritapepe (✉)
Department of Anesthesia and Intensive Care,
Cardiac Surgery ICU, Policlinico Umberto I Hospital,
Sapienza University of Rome, Rome, Italy
e-mail: luigi.tritapepe@uniroma1.it

G. Frasacco
Policlinico Casilino Hospital, Rome, Italy

instability with a low CO, before the hypotension appears.

Arterial blood pressure alone is a late marker of haemodynamic instability; if we consider simultaneously the heart rate, we can have more information of the haemodynamic status.

During low blood flow or fluid loss, HR and noninvasive AP can detect haemodynamic changes.

The gold standard for arterial blood pressure monitoring is the invasive measure method, especially in patients with haemodynamic derangement, needing controlled hypotension or increased organ perfusion or multiple arterial blood gas analysis.

43.3 Measure of Volemia

Central venous catheters especially the pulmonary artery catheter (PAC) are the most invasive monitoring systems. They provide characteristic haemodynamic data as no other systems can.

Although not perfect, the pulmonary artery catheter has long been considered an optimal device of haemodynamic monitoring. Recent clinical trials have not confirmed the clinical effectiveness of its use.

However in these trials, no clinical targets were selected, and data have been often misunderstood. It is important to emphasize that the PAC insertion did not affect patient mortality, and it is the unique system that can continuously monitor the cardiac output, the mixed venous oxygen saturation (SvO_2), the intrathoracic vascular pressure and the oxygen delivery (DO_2).

If DO_2 is inadequate, tissue oxygen extraction is increased, with a consequent SvO_2 reduction (<70%). In this setting with low SvO_2 and high intrathoracic vascular resistances, the cardiac output detects the instability status, leading to a specific therapy. A high CO value with low MAP can show a distributive shock status. On the other hand, a low cardiac output shows hypovolemic shock (low right atrial pressure/CVP and low Pcwp), cardiogenic shock (high CVP and high Pcwp), obstructive shock (CVP > Pcwp) and high main pulmonary artery pressure (MPAP).

In the presence of haemodynamic instability, the key issue is to determine if the cardiac output will increase with fluid administration (preload-dependent patient).

The assessment of preload and fluid responsiveness is crucial also in cardiogenic shock.

Static pressures (CVP and Pcwp) traditionally have been used to guide fluid management, but they are poor predictors of fluid responsiveness: low value shows a "poor fluid filling" and high value an "adequate fluid filling".

Since they were rigorously designed, pulmonary artery occlusion pressure and central venous pressure fail to predict ventricular filling volume or fluid responsiveness, with 50% reliability.

Dynamic measures such as stroke volume variation (SVV) are more accurate than static measurements to assess the fluid responsiveness in mechanically ventilated patient, during anaesthesia.

Stroke volume is the difference between the maximum and the minimum stroke volume over the main stroke volume measured at the same time, over consecutive mechanical breaths. During positive pressure ventilation, the increase in the intrathoracic pressure is associated with decreased venous return to the right ventricle (RV) and consequent RV cardiac output reduction (RV is preload-dependent). After 2–3 beats time, left ventricle (LV) stroke volume decreases due to a reduced RV filling. These changes in LV stroke volume are most marked in hypovolemic patients. Given that, the pulse pressure variation (PPV) varies from beat to beat according to the SVV, so the PVV measure reflects the stroke volume variation (Fig. 43.1).

Stroke volume variation and pulse pressure variation are specific and sensitive predictors of fluid responsiveness.

A SVV > 15% in patients during mechanically ventilation with tidal volume > 8 ml/kg or SVV > 10% with tidal volume 6 ml/kg predict fluid responsiveness.
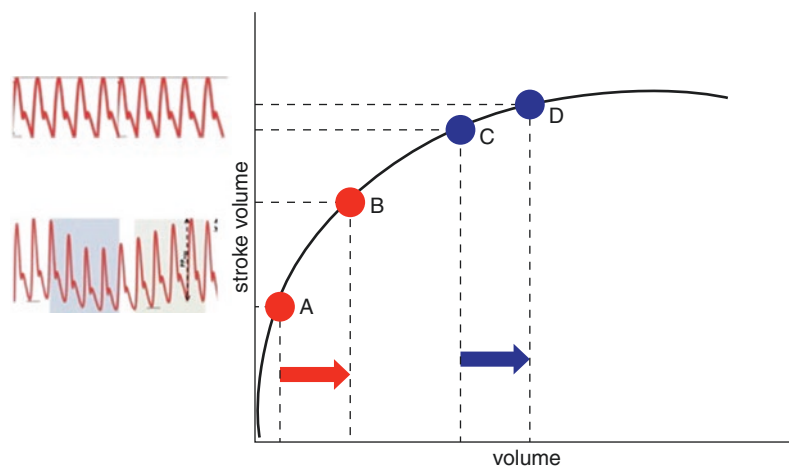
Fig. 43.1 Dynamic indices (PPV, SVV, SPV) predict fluid responsiveness of the patient. In the picture the same volume replacement (fluid challenge) determines two different situations: the patient with variation of haemodynamic indices passes from point A to B in the Starling curve with an important increase of stroke volume, whereas the patient without any variation of dynamic indices moves from C to D without any increase of stroke volume

43.4   Pulse Contour Analysis

Pulse contour analysis requires positioning an arterial line/catheter, generally in the radial or femoral artery. There are five devices providing continuous CO measurement using the arterial pressure waveform. Three of these systems require calibration with the thermodilution method. These monitoring tools assume that the pulse pressure is linked to the stroke volume. However, this relationship is not so easy to understand, and the amplitude of the differential pressure, in a specific stroke volume, depends on the aortic compliance, which does not have a linear trend.

After years of study, available data seem sufficient to characterize the relationship between the pressure waveform and the aortic compliance, but only recent technologies have allowed the construction of functional devices, which use complex algorithms to analyse the pulse pressure waveform that correlates with the stroke volume. Such algorithms can explain the influence of waves reflected from the periphery, the magnitude of which is influenced by the systemic vascular resistance.

Different monitoring tools, with different algorithms and with or without an initial calibration, use this technology for the measurement of CO, SVV and PPV.

Among non-calibrated systems, which achieved success for their easy use, a special mention should be for a system provided by a transducer, easily and quickly connectable to any arterial line already placed, allowing the measurement of CO. It does not need calibration for calculating the CO, but it is necessary to insert patient's age, height, sex and weight into the system, to determine the cardiac output from the pulse contour analysis.

Overall, these devices are very effective in predicting the preload responsiveness. Protocols guided by the SVV or PVV monitoring for the haemodynamic optimization all lead to improvements in surgical setting; but in the ICU, these devices show some limitations.

The presence of arrhythmias or atrial fibrillation is a bias in the measurement of SVV and PPV; in fact they are a result of cyclical changes in the ventricular filling, rather than cyclical changes due to mechanical ventilation. In these situations, the dynamic indices are unable to predict the preload/fluid responsiveness.

43.5 Totally Noninvasive Systems

A completely noninvasive system, providing a continuous cardiac output (CCO) measures, uses an inflatable cuff placed on the patient's finger to measure blood pressure and to determine the stroke volume through the systolic single-beat pulse, calculated on impedance. Some researchers have shown how this system is a reliable method, when compared to invasive systems for the determination of cardiac output (in specific clinical setting, e.g. intermediate-risk pregnant); this may be preferable.

Another noninvasive monitoring system is the plethysmographic variability index (PVI) used as a continuous measure of vascular reactivity volume, with the highest values which correspond to a greater reactivity. The examination of the plethysmographic trace, using a modified pulsossimetric probe, allows to determine the perfusion index. The perfusion index (PI) is a numerical value determined by the strength of the detected infrared signal. The signal strength correlates with the amount of volume at the sampling site. Changes in this index may indicate regional changes in the patient volume status. For these reasons, it is not indicated as a noninvasive monitoring system to evaluate the fluid responsiveness

and the patient's volemic status, in low cardiac output state, in severe peripheral vascular disease or in spontaneous ventilation: (pleth variability index (PVI)% = [(Pimax-PImin) / Pimax] x100%).

These systems are poorly applicable in ICU patients in which rapid changes in vascular tone are not detectable by completely noninvasive monitoring.

43.6 Echocardiography

Echocardiography examination can easily lead to a noninvasive evaluation of the haemodynamic patient status, especially in critically ill patients in the intensive care unit.

The transthoracic echocardiography rapidly allows to identify a pericardial or pleural effusion; to evaluate right and left ventricle contractility or the presence of hypokinesia due to ischaemia; and to identify any valve abnormalities or obstructive heart failure which lead to haemodynamic impairment. With more experience, clinicians can perform a general assessment of the left ventricle ejection fraction, the right ventricle function, the patient's volume status (Fig. 43.2) and the cardiac output quantification.

Fig. 43.2 Evaluation of end-diastolic area to assess the volume request, painting the Starling's curve based on the LV SAX

PRELOAD ASSESSMENT ON EDA EVALUATION

Stroke volume

preload
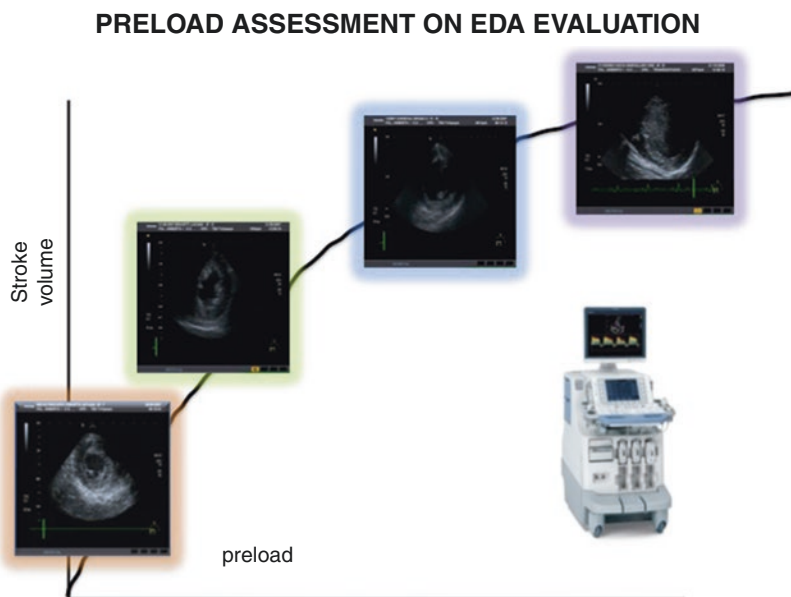
The echocardiographic examination is often performed in the perioperative period rather that in the intraoperative time, especially in noncardiac surgery. Nevertheless, the evaluation of the inferior vena cava (ICV) has been used, even during anaesthesia, as a measure of patient's volume status and as a predictor of preload responsiveness.

The diameter of the ICV can be easily measured from the subcostal view, in the long-axis view (TTE) or in the deep TG view (TEE). Measures less than 2 cm, with a greater inspiratory collapse of 50%, are related to intravascular volume depletion, while measures greater than 2 cm, with a less than 50% inspiratory collapse, suggest an adequate volume or the inability of the right heart to accept further volume (Fig. 43.3).

A transient and reversible increase in preload (passive leg raising), demonstrated by the distensibility of the ICV, can be used as a surrogate of a fluid challenge (distensibility index (DI): (ICV max - min ICV)/ICV (max) = DI% x100).

A DI > 18% identifies patients responding to fluids challenge with a sensitivity and specificity of 90%.

Some limitations related to the echocardiographic technique include the inability to obtain adequate projections because of patient habitus or positioning and because of the operator's skills. This becomes even more evident in patients receiving intensive care, where the supine position, the impossibility of movement, patient co-operation and mechanical ventilation prevent an optimal acoustic window.

Transoesophageal echocardiography (TEE) is not a conventional monitoring device. It can be performed by an experienced sonographer, and it may require a specialized cardiologist evaluation.

A standard TEE examination is based on 20 views for the assessment of the global ventricular function, the volume status, the valve evaluation, the aorta vessel, the pericardium and the pleura evaluation.

With the development of technologies and indication of TEE, the views necessary to perform a comprehensive examination have expanded. An additional 8 views have been added (multiple LAX and SAX views for all valves, all cardiac chambers and great vessels) with a total of 28 views. In addition, the degree of rotation and manipulation of the probe such as right or left flexion, anteflexion or retroflexion and turning may be required in individual patients. Each view can be also performed as a 3D image with advance 3D echocardiographs.

Fig. 43.3 MMode and 2D evaluation of IVC diameter and its modifications during the respiratory cycle
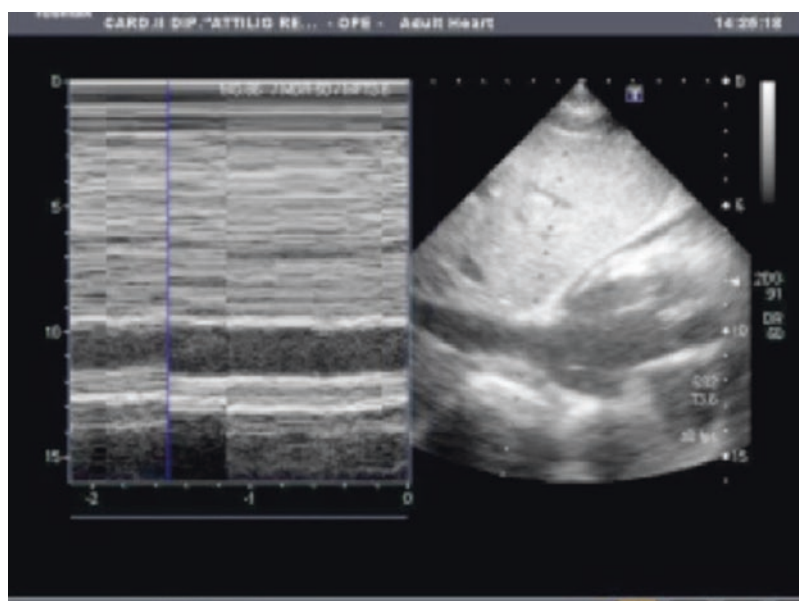
TEE assessment is crucial for routine intraoperative monitoring in cardiac surgery and should be also used in high-risk patient with haemodynamic instability and undiagnosed pathology. However, the use of TEE may change with the routine use of a miniaturized transoesophageal probe which allows left ventricular function and filling status assessment, through the trans-gastric left ventricle short axis.

43.7 Cardiac Output Measured by Echocardiography

Two-dimensional echocardiography is a noninvasive TTE or semi-invasive TEE method for the assessment cardiac anatomy and function. When Doppler technique or the volumetric method (difference of end-systolic and end-diastolic volume) is added, it is possible to measure stroke volume and CO. The anatomic sites for measuring velocity likely affect CO measurement, and the guidelines from the American Society of Echocardiography recommend that the left ventricular outflow tract (LVOT) is used for measurements of CO (considering LVOT diameter and LVOT velocity time integral VTI with Doppler).

Doppler techniques can be used to quantify cardiac flow, volume and pressure. Basic haemodynamic formulas are used for these calculations. If performed properly, these relatively noninvasive techniques correlate well with other more invasive methods. As in any Doppler measurement, parallel beam alignment is crucial and cannot be overemphasized.

Traditionally, LVOT diameter measurements are made in mid-systole in ME AV LAX at an angle of 120° to 140° with TEE or in apical five-chamber views with TTE; at the same time during the cardiac cycle, the LVOT flow velocity (VTI) measurements are made (in deep trans-gastric level with TEE-TG five-chamber view – or in apical five-chamber views in TTE). In some of the patients, image quality is suboptimal during systole, and the LVOT is not clearly delineated, whereas it is clearly seen and easily measured at the end of diastole.

Blood flow velocity (VTI) in the LVOT is measured by positioning the pulse-wave Doppler sample volume in the centre of the LV outflow tract just proximal to the AV. The spectral Doppler is used with the LV outflow tract or annular diameter to calculate the LV stroke volume. The CO is calculated by multiplying LV stroke volume for the heart rate (Fig. 43.4).

A minimum level of training experience is required to use echocardiography as a quantitative monitoring tool, regardless of the clinical scenario for which it is being applied. Although a basic level of training experience in TTE is sufficient to monitor LV dimensions and IVC collapsibility, additional level of training experience with both TTE and TEE is required to ensure accurate Doppler and advanced haemodynamic pressure measurements in intensive care units, emergency departments and surgical suites. Because echocardiographic monitoring is currently used in a wide range of clinical settings, it is imperative that the person using quantitative echocardiography to guide therapeutic decision-making (whether an anaesthesiologist, a cardiologist or an emergency room physician with a good level of experience) understands the interobserver variability of each of the quantitative measurements and has the technical expertise required to ensure the serial measurements are obtained accurately.

There are many opportunities for operators to err and miscalculate in TTE-derived CO measurements, but if taken properly, these measurements compare favourably with the thermodilution techniques of PAC.

Measurements of CO using TTE require time for measurement and calculations, where contour analysis and PAC CO measurements, once calibrated, can be continuous and automatic. In a dramatically dynamic situation, it is unrealistic to be constantly measuring and remeasuring parameters in order to calculate CO using TTE. PAC and contour analysis can measure CO in a continuous fashion. When evaluating echocardiography, it is important to bear in mind that it provides valuable information about the cardiac anatomy, cardiac function, valve pathology, imaging of
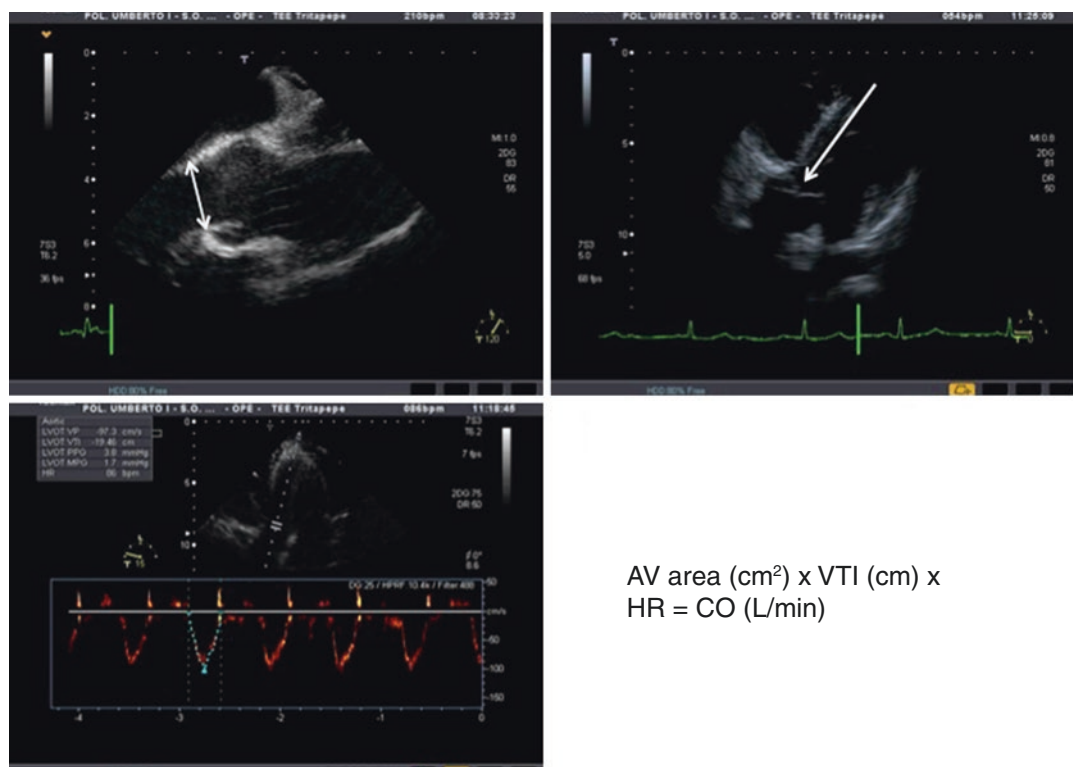
AV area (cm^2) x VTI (cm) x
HR = CO (L/min)

Fig. 43.4 Measurement of CO by measuring the diameter of the aortic outflow tract and the aortic VTI with pulse Doppler

blood flow and assessment of systolic and diastolic function of the heart.

There are many assumptions made using Doppler quantification. These assumptions play a part in the degree of inaccuracies that result.

1. One assumption is that the area measured for the calculation of SV is constant throughout systole. The aortic valve is not closed one moment and completely opens the next, which means that flow is not constant throughout a cardiac cycle.
2. Errors in diameter measurements are quadrupled in that the formula requires squaring the diameter. Therefore very small errors in measurement make a dramatic difference in the calculation.
3. To guarantee accuracy, parallel blood flow is required in any of these calculations. In addition, the area and flow measurements must be made at the same anatomical site. Depending

on whether and how much the heart is rotated in the patient, these two criteria (parallel flow and anatomical site measurements) may not be easily achieved.

Erroneous CO measurements could potentially lead to erroneous clinical decisions including inappropriate use of fluid or inotropic drugs. This may potentially harm patients. As echocardiography is widely used in the clinical setting and promoted by experts, it is imperative to ensure that its validation is based on high-quality studies using the Bland-Altman analysis when assessing the agreement.

The importance of measuring the CO with TTE is to categorize the patient in a class of low cardiac output, normal cardiac output and high cardiac output, so to choose the most appropriate continuous monitoring of CO.

During the evaluation, assessment of RV size and function may offer insights into the presence

or consequences of pathology, such as RV infarction, pulmonary embolus, pericardial effusion and extracardiac pathology such as masses that may be impinging on the right ventricle.

The LV regional myocardial function is assessed on the basis of the observed wall thickening and endocardial motion of the myocardial segment. Regional wall motion abnormalities may occur in a variety of conditions, such as coronary artery disease, myocarditis, sarcoidosis and stress-induced (takotsubo) cardiomyopathy. Abnormal motion patterns of the interventricular septum may be found postoperatively or in the presence of a left bundle branch block or RV epicardial pacing, as well as RV dysfunction caused by RV pressure or volume overload. Echocardiographic quantification of regional myocardial function is currently based on DTI or speckle-tracking echocardiographic techniques.

Furthermore echocardiography allows patient volemic status assessment by IVC measurement, LV short-axis view and VTI variability in response to a fluid challenge.

So in critically ill patients, echocardiogram examination may help physicians in diagnosing haemodynamic instability causes and may guide in therapeutic choices and in treatment response monitoring.

Further Reading

Barbier C, Loubières Y, Schmit C, Hayon J, Ricôme JL, et al. Respiratory changes in inferior vena cava diameter are helpful in predicting fluid responsiveness in ventilated septic patients. Intensive Care Med. 2004;30:1740–6.

Bellomo R, Uchino S. Cardiovascular monitoring tools: use and misuse. Curr Opin Crit Care. 2003;9:225–9.

Hahn RT, et al. Guidelines for performing a comprehensive transesophageal echocardiographic examination: recommendations from the American Society of Echocardiography and the Society of Cardiovascular Anesthesiologists. J Am Soc Echocardiogr. 2013;26:921–64.

Harvey S, Harrison DA, Singer M, et al. Assessment of the clinical effectiveness of pulmonary artery catheters in management of patients in intensive care (PAC-man): a randomised controlled trial. Lancet. 2005;366:472–7.

Lang RM, et al. Recommendations for cardiac chamber quantification by echocardiography in adults: an update from the American Society of Echocardiography and the European Association of Cardiovascular Imaging. Eur Heart J Cardiovasc Imaging. 2015;16:233–71.

Monnet X, Rienzo M, Osman D, et al. Esophageal Doppler monitoring predicts fluid responsiveness in critically ill ventilated patients. Intensive Care Med. 2005;31:1195–201.

Parks JK, Elliott AC, Gentilello LM, et al. Systemic hypotension is a late marker of shock after trauma: a validation study of advanced trauma life support principles in a large national sample. Am J Surg. 2006;192:727–31.

Perera P, Mailhot T, Riley D, Mandavia D. The RUSH exam: rapid ultrasound in shock in the evaluation of the critically ill. Emerg Med Clin North Am. 2010;28:29–56.

Pinsky MR, Payen D. Functional hemodynamic monitoring. Crit Care. 2005;9:566–72.

Reeves ST, Finley AC, Skubas NJ, Swaminathan M, Whitley WS, et al. Basic perioperative transesophageal echocardiography examination: a consensus statement of the American Society of Echocardiography and the Society of Cardiovascular Anesthesiologists. J Am Soc Echocardiogr. 2013;26:443–56.

Shah MR, Hasselblad V. Stevenson LW et al. Impact of the pulmonary artery catheter in critically ill patients: meta-analysis of randomized clinical trials. JAMA. 2005;294:1664–70.

Stover JF, Stocker R, Lenherr R, et al. Noninvasive cardiac output and blood pressure monitoring cannot replace an invasive monitoring system in critically ill patients. BMC Anesthesiol. 2009;9:6.

Van de Vijver K, Verstraeten A, Gillbert C, et al. Validation of non-invasive hemodynamic monitoring with Nexfin in critically ill patients. Crit Care. 2011;15:P75.

Vincent JL, Pinsky MR, Sprung CL, et al. The pulmonary artery catheter: in medio stat virtus. Crit Care Med. 2008;36:3093–6.

Arterial Ventricular Coupling (AVC)

44

Simone Cipani, Francesco Maria Traina,
and Armando Sarti

Key Points
- Preload
- Afterload
- Contractility
- Determinants of stroke volume
- Bedside assessment of AVC

44.1 Introduction

The heart is anatomically and functionally linked to the vascular tree, and their interplay, described as arterial ventricular coupling (AVC), results in one of the cardiovascular performance parameters that can influence the efficiency of the system and the magnitude of energy transmitted from the heart to the circulatory system.

S. Cipani (✉)
Department of Anesthesia and Intensive Care, Santa Maria Nuova Hospital, Florence, Italy
e-mail: simone.cipani@uslcentro.toscana.it

F. M. Traina
University of Florence, Medical School Largo Brambilla, Florence, Italy
e-mail: francesco.traina@stud.unifi.it

A. Sarti
Department of Anesthesia and Intensive Care, SS Maria Annunziata Hospital, Florence, Italy

The heart and blood vessels have the important function of oxygenating the tissues through stroke volume (SV) and oxygen delivery (DO_2).

The circulatory system can be compared to the three hydraulic elements of "Windkessel" model, where the aorta, thanks to its viscoelastic properties, receives energy at each systole and stores and releases it in the diastolic phase, ensuring a continuous arterial blood flow. This provides pressure and flow to peripheral organs, in different physiological (rest and exercise) and pathological conditions because of the constant modulation of arterial system compliance, "stiffness," and resistance to ensure adequate left ventricular performance. Cardiac output is the final result of this complex dynamic modulation.

The myocardial pump function and the performance of the entire cardiovascular system are determined by *preload*, *afterload*, *and contractility*.

44.2 Preload

In the healthy subject, the size of the heart muscle and stroke volume depend on the muscle length at the beginning of contraction (preload), muscle tension during contraction, and muscle contractility in terms of shortening and speed according to preload and afterload. In the heart preload is represented by the end-diastolic volume. The increase in preload as a result of increased venous

Fig. 44.1 Increased preload as a result of increased venous return increases the end-diastolic volume and stroke volume

Myocardial Contractility
- Intramyocardial [Ca2]
- Cardiac adrenergic nerve activity
- Circulating catecholamines
- Cardiac rate
- Exogenous inotropic agents
- Myocardial ischemia
- Myocardial cell death (apoptosis)
- Alterations of sarcomeric and cytoskel-etal proteins
- Myocardial fibrosis
- Chronic overexpression of neurohormones
- Ventricular remodeling
- Cardiomyopathies

return increases the end-diastolic volume and then stroke volume (Fig. 44.1) if the heart is fluid-responsive. This mechanism allows a constant myocardium inflow and outflow blood volume.

Determinants of Stroke Volume
Ventricular Preload
- Blood volume
- Distribution of blood volume.
  1. Body position
  2. Intrathoracic pressure
  3. Intrapericardial pressure
  4. Venous tone
  5. Pumping action of skeletal muscles
- Atrial contraction

Ventricular Afterload
- Systemic vascular resistance
- Elasticity of arterial tree
- Arterial blood volume
- Ventricular wall tension:
  1. Ventricular radius
  2. Ventricular wall thickness

44.3 Afterload

Afterload is the force which is opposed to ventricular fiber shortening along the ventricular ejection phase. This parameter expresses both the ejection pressure and the left ventricular chamber capacity to emptying, affecting the heart oxygen consumption.

The determining factors of afterload are:

- Systemic vascular resistance
- Wall stress
- Aortic impedance

44.3.1 Systemic Vascular Resistance

Systemic vascular resistance is not a reliable afterload parameter since it is a measure of the vascular tone expressing only the non-pulsatile component of the peripheral load, without taking into account the impedance and the elastance of the vessels. In this way it is assumed that the cardiovascular system represents a continuous current, generating constant pressure and flow to the tissues throughout the heart cycle. However, the left ventricular chamber is a noncontinuous, pulsatile pump characterized by

an internal load constituted by pressure and geometry and an external load constituted by pulsatile and non-pulsating components. Hence, evaluating the afterload only through systemic resistances represents a monocular view of the cardiac work.

44.3.2 Wall Stress

It is another afterload parameter dependent on the shape, diameters, and wall thickness of the left ventricle. It is represented by the integral of the parietal tension of the left ventricle on the time.

σ(wall stress) : pressure × diameter/wall thickness

44.3.3 Aortic Impedance

The aorta and the big blood arteries are anatomical structures capable of accumulating energy during systolic phase with a subsequent release in the diastolic phase, thus transforming a pulsated flow in a constant one.

Briefly, vascular impedance is represented by:

- The vessel impedance which depends on the vessel flexibility and viscosity.
- Pressure and flow wave which are reflected in the opposite sense from the vascular periphery.
- Density and viscosity of the blood.

In synthesis, a complete vision of the afterload must include the vascular resistances (small arteries and arterioles), the arterial compliance, and the vascular impedance. This is the three components model of Windkessel, necessary to represent the arterial system. In this model if the vascular parameters and the frequency are constant, the end-systolic pressure linearly increases with the systolic ejection with a proportional relation to the resistance offered by the arterial tree. In such way, it is possible to represent the characteristics of the arterial system through the relationship between the pressure (end-systolic pressure) and volume (stroke volume); this relationship defines the *arterial elastance (Ea). Ea indicates the variation of arterial pressure in response to the variation of stroke volume.*

Since it's a mathematical relationship, every increase of the end-systolic pressure leads to a natural decrement of the stroke volume if contractility remains constant.

44.4 Contractility

During systole, left ventricle (LV) contraction leads to the storage of potential energy, which, when released, provides the restoring force that aids left ventricle filling. An increase in LV contractility leads to higher restoring forces and more effective suction from the left atrium.

Among the determinants of the cardiac function, contractility is surely a parameter difficult to determine in operation of the extreme variability of loading conditions. Such parameter can be defined as the intrinsic strength of the cardiac muscle. Contractility has a linear relation with an independent loading index: *the inclination of end-systolic pressure-volume relationship (ESPVR).* In fact, such inclination increases with the increase of the contractility and decreases in case of myocardial depression (Fig. 44.2).

The slope of such relationship (ESPVR) is defined as *ventricular elastance (Ees).* As previously mentioned, this parameter is a load-independent index of the myocardial contractility and represents left ventricular inotropic efficiency. *Ees indicates the variations of left ventricular end-systolic volume in response to the variation of arterial pressure.* The myocardial contractility, index of systolic function, can be influenced by numerous factors (biochemical characteristics of the myocytes, geometric remodeling, synchronic contraction) that can severely influence left ventricular performance.
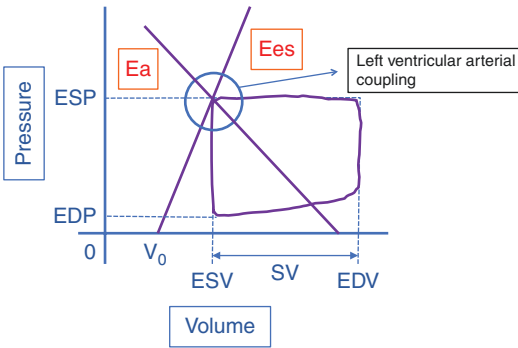
Fig. 44.2 The line of the end-systolic pressure-volume relationship (**ESPVR**) intercepting the axis of the volume at the point V0 and describing left ventricle elastance (**Ees**). **Ea** is the arterial elastance showing the variation of arterial pressure (**ESP**) in response to the variation of stroke volume. The intersection of the **Ea** slope and the **Ees** slope represents the **left ventricular coupling (AVC).** **V0** volume axis intercept of the end-systolic pressure volume relationship, **ESV** end-systolic volume, **EDV** end-diastolic volume, **ESP** end-systolic pressure, **EDP** end-diastolic pressure, **SV** stroke volume

44.5   Arterial Ventricular Coupling

The performance of the cardiovascular system depends on the interaction of the left ventricle and arterial system. All conditions which include an appropriate coupling of these components are important to quantify the efficiency of myocardium. Normally there is a reasonable matching of ventricular elastance to aortic elastance. This minimizes the amount of work done by the heart in transferring energy and blood from the ventricle to the aorta.

Arterial ventricular coupling can be expressed as the ratio of *arterial elastance* (Ea) to *left ventricular elastance* (Ees), where Ea is an integrated index of net arterial load that is imposed to left ventricle work; it represents the complex association of different arterial properties (compliance, stiffness, and outflow resistance). Ees is an index of contractility and systolic stiffness of the heart.

Mechanical energy transferred from the heart to the vessels generates flow and is maximal when the two elastances are approximately equal. This ratio also reflects cardiac energetics; indeed the balance between myocardial oxygen con-

sumption and the mechanical energy required appears to be optimal when the heart and vessels are coupled (heart pumps blood into the vessels with volume and rate that matches the capability of the arterial system to produce flow). As previously mentioned, the reciprocal influence of arterial and ventricular elastance can be explained by the anatomical and the functional connection of the heart with the arterial tree. Systo-diastolic stiffness of LV increases in parallel with arterial stiffness in various pathological conditions in order to preserve the maximum efficiency of cardiovascular system. In the presence of hypertension, Ea increases and Ees rises to respond to the increased afterload through increased contractility and then cardiac remodeling. It allows systolic wall stress normalization and the preservation of LV systolic function. Over time cardiac remodeling generates loss of contractile and diastolic reserve resulting in higher risk of development of heart failure with preserved ejection fraction especially in women.

Recent studies have examined the impact of hypertension on AVC and its components. The data show an important increase of Ea and Ees in hypertensive patients compared with normotensive controls, while the coupling ratio seems to remain similar. However the increase of these AVC components with a preserved ratio can be dangerous: a stiffer heart-arterial system generates a greater systolic pressure change for a given change in stroke volume, resulting in greater blood pressure liability and increased sensitivity to fluid changes. This altered coupling also influences myocardial perfusion by elevating the proportion of coronary flow during systole, thus worsening the impact of regional coronary ischemia.

So in the managing of the critical illness patient, the intensivist must keep in mind many pathological conditions that cause alterations in myocardial contractility and vascular tone, resulting in a decoupling of this important relationship. In the same way, a contractility or arterial tone that is too high or too low decouples this link, leading to cardiac failure (Fig. 44.3) independent of myocardial ischemia or the toxic effects of sepsis (Fig. 44.4).

Fig. 44.3 Critically ill patient with hypotension; note the increased slope of Ea as result of increased peripheral vascular resistance. Ees is reduced by a severe systolic dysfunction (↓↓ SV). **Ea/Ees > 1, suboptimally coupled.** Green loop, normal coupling
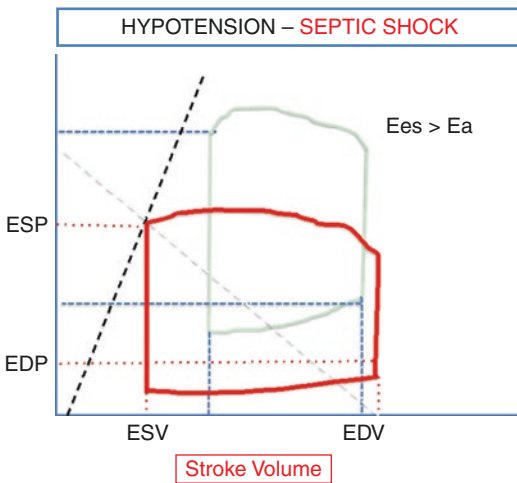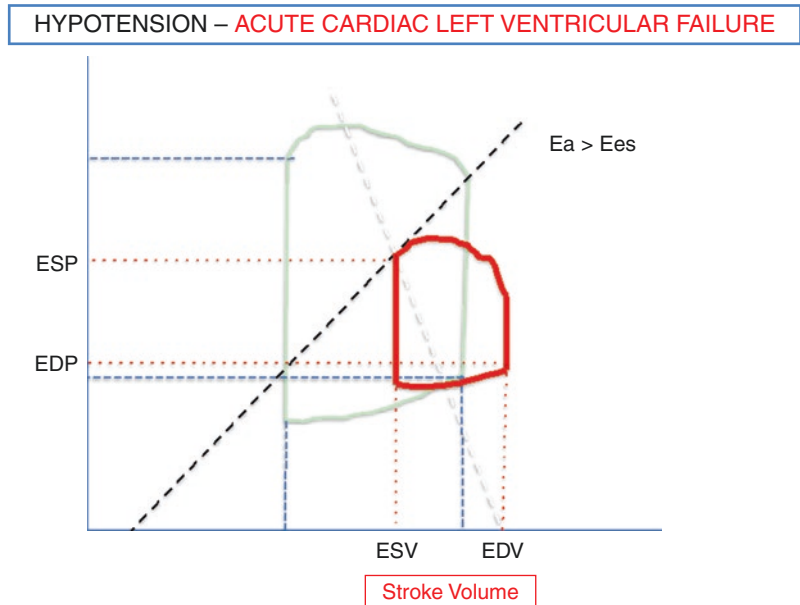
Fig. 44.4 Critically ill patient with hypotension; note the increased slope of Ees as result of increased systolic function (↑↑ SV) in the absence of adequate afterload (septic shock). **Ea/Ees < 1, suboptimally coupled.** Green loop, normal coupling

44.6 AVC: Bedside Assessment

Several noninvasive approaches to evaluate AVC have been proposed.

Effective *arterial elastance* (*EA*) approximates the arterial afterload faced by the LV dur-ing systole. It can be estimated noninvasively as follows. *End-systolic pressure (ESP)/stroke volume* (SV), where end-systolic pressure is derived as mean arterial pressure and stroke volume is calculated by echocardiography (SV: LVOT cross-sectional area × VTI). *EA* is affected by the peripheral vascular resistance, arterial compliance, and cardiac cycle durations. The normal resting value of *EA is 2.2 ± 0.8 mm Hg/mL.*

LVelastance (*ELV in mm Hg/mL*) is an index of contractility that is load-independent. It is determined noninvasively as follows: *end-systolic pressure/(end-systolic volume V0)*, where V0 represents the volume (*x* axis) intercept of the end-systolic pressure-volume relationship (Fig. 44.2). To derive this interception volume, at least one other point of the ESPVR should be obtained. This would require changes in diastolic filling that are often not feasible in critically ill patients. In a number of studies, it has simply been assumed that V0 = 0. This simplification allows to obtain an easy, bedside assumption: *ESP/ESV*, where end-systolic pressure is obtained as mean arterial pressure and the end-systolic volume by echocardiography or as difference among EDV (end-diastolic volume) and SV. *ELV normal resting value is 2.3 ± 1 mm Hg/mL. Therefore, the EA/ELV ratio is normally 1.0 ± 0.36.* EA and ELV increase

proportionately with age in normal men, and their ratio remains unchanged. Normal women show a higher increase in ELV with ageing, so the ratio decreases slightly.

Guarracino et al. evaluate Ees through the measure of ejection fraction, stroke volume, systolic time interval, and pre-ejection time coupled with systolic and diastolic arterial pressure measurements. Ea can be defined as the capability of the arterial vessels to modulate their resistance when left ventricular stroke volume increases. Ea is calculated as end-systolic pressure/stroke volume. See Further Readings.

Pittarello et al. propose to evaluate AVC starting from a short-axis window of LV evaluating end-diastolic diameter, end-systolic diameter, and R-R interval for heart rate.

44.7 Conclusion

AVC represents an important parameter of interaction between the heart and peripheral vascular system. When the relationship between these two entities is 1, this means a good cardiovascular performance.

In such condition the left ventricle furnishes a stroke volume with the lowest energetic consumption. Such parameter represents therefore an effectiveness index of mechanical performance of the ventricular left chamber and of the dynamic modulation of the cardiovascular system. So the evaluation of the cardiovascular function through arterial ventricular match is able to furnish a further comprehension in pathophysiological terms for the patient with serious hemodynamic instability.

Further Reading

1. Sorbara, et al. ICU Echocardiography and noninvasive Hemodynamic monitoring. In: Sarti A, Lorini FL, editors. Echocardiography for Intensivist: Springer.
2. Guarracino F, et al. Ventriculo-arterial decoupling in acutely altered hemodynamic states. Crit Care. 2013;17:213.
3. Wang J, et al. Current perspectives on cardiac function in patients with diastolic heart failure. Circulation. 2009;119:1146–57.
4. Faconti L, et al. Arterial-ventricular coupling and parameters of vascular stiffness in hypertensive patients: role of gender. JRSM Cardiovasc Dis. 2017;6:1–8.
5. Pittarello D, et al. Alterations in left ventricular-arterial coupling and mechanical efficiency produced by remifentanil during cardiac anesthesia. Minerva Anestesiol. 2001;67:133–47.

Non-cardiac Surgery: Perioperative Echocardiography and Lung Echography

45

Stefano Romagnoli, Cosimo Chelazzi, and Zaccaria Ricci

Key Points

- Perioperative echocardiography may be performed either by transthoracic (TTE) or transesophageal (TEE) approach.
- TEE is the most powerful cardiovascular diagnostic technique available during the intraoperative phase, while TTE is optimal for cardiac assessment in non-intubated patients for cardiovascular risk stratification and investigation of hemodynamically unstable patients.
- TTE/TEE in the non-cardiac perioperative setting aims at the identification of the etiology of acute hemodynamic derangement secondary to the surgical event.
- Echocardiography can be performed by anesthesiologists or by critical care physicians provided they are adequately trained for this purpose.

- Chest ultrasound examination is an invaluable tool in evaluating lung parenchyma and pleural spaces. It allows to detect common causes of perioperative respiratory failure.

45.1 Introduction

Over the past decades, ultrasonography has undergone a progressive evolution in technology and reduction in costs. This has favored its clinical application and acceptance throughout perioperative medicine. The population undergoing non-cardiac surgery is older than in the past. Furthermore, the surgical complexity and the number of comorbidities of surgical patients are increasing. Accordingly, the number of patients with cardiovascular diseases are rising. Perioperative echocardiography, defined as ultrasonography of the heart and large vessels, may be performed either by a transthoracic (TTE) or transesophageal (TEE) approach. TEE is the most powerful cardiovascular diagnostic technique available during the intraoperative phase, while TTE is considered an irreplaceable tool for cardiac assessment in non-intubated patients, its clinical application ranging from preoperative cardiovascular risk

S. Romagnoli (✉) · C. Chelazzi
Department of Anesthesia and Critical Care, Azienda Ospedaliero-Universitaria Careggi, Florence, Italy
e-mail: stefano.romagnoli@unifi.it

Z. Ricci
Pediatric Cardiac Intensive Care Unit, Department of Pediatric Cardiac Surgery, Bambino Gesù Children's Hospital, Rome, Italy

stratification to the postoperative quick assessment of hemodynamically unstable patients. With the information provided by echocardiography, trained clinicians can manage the hemodynamics of surgical patients and possibly improve their outcome. Classic echocardiographic examination acquires all acoustic views from all standard windows. Although echocardiography began as a specific domain of the cardiologist, during the last years, it has gained new fields of clinical application for anesthesiologists and critical care physicians. Hence, echocardiography in the non-cardiac perioperative setting is not focused on specific and refined cardiac diagnoses (i.e., valve morphology, detailed myocardial function identification): differently, it aims at the identification of the etiology of acute hemodynamic derangement secondary to the surgical event. Therefore, if "classic" echocardiography is usually performed by a certified sonographer or cardiologist, perioperative echocardiography can be performed by anesthesiologists or by critical care physicians (including intensivists, fellows, residents) provided they are adequately trained for this purpose. In settings where major non-cardiac surgery is performed (i.e., liver resections, transplants, pancreatic surgery, esophagostomies), both TTE and TEE expertise should be available, as fundamental elements of modern anesthesiology approach to major non-cardiac surgery.

Chest ultrasound examination is nowadays a widely diffused practice and an invaluable tool in evaluating lung parenchyma and pleural spaces. It allows to detect several different and common clinical entities such as pleural effusion, pneumothorax, and areas of parenchymal consolidation. It is easily feasible, relatively easy to learn, and cheap. It allows also to guide the insertion of pleural drains. Thus, chest ultrasound is considered as a must-to-have clinical skill for anesthesiologists and intensivists. Together with heart ultrasound, they provide many useful clinical information that can direct diagnosis and treatment of acute hypoxia and/or hypotension.

45.2 Preoperative Echocardiography: Risk Stratification and Hemodynamic Assessment

Cardiac disease is a potential source of perioperative complications in any non-cardiac surgical patient. Preoperative echocardiography has been utilized for decades in patients with (and without) cardiac diseases scheduled for non-cardiac surgery to aid in risk stratification and cardiovascular/hemodynamic assessment/optimization. In most patients, TTE is still performed for screening (i.e., risk stratification), even if resting echocardiography has a relatively weak evidence in predicting postoperative outcomes notwithstanding the baseline cardiac conditions and functional status. The indications for preoperative resting or stress TTE are now described by the European Society of Cardiology/European Society of Anesthesiology (ESC/ESA) guidelines on cardiovascular assessment and management of heart diseases in non-cardiac surgery. These guidelines represent the official position of the ESC/ESA on various aspects of perioperative cardiac care. According to ESC/ESA, in non-cardiac surgical patients, non-invasive cardiac testing should be considered for patients with previous coronary artery revascularization and/or for patient counselling, change of perioperative management in relation to type of surgery, anesthetic technique, and long-term prognosis. Echocardiography is a costly and time-consuming procedure. Therefore, the ESC/ESA guidelines have delivered the following restriction in terms of TTE in asymptomatic patients without signs of cardiac disease or electrocardiographic abnormalities: (1) "rest echocardiography may be considered in patients undergoing high-risk surgery (class IIb; level C)"; (2) "routine echocardiography is not recommended in patients undergoing intermediate or low-risk surgery (class III; level C)". Recommendations on imaging stress testing before surgery in asymptomatic patients are the following: (1) "imaging stress testing is recommended before high-risk surgery in patients with

Table 45.1 Clinical risk factors according to the revised cardiac risk index – ESC/ESA guidelines 2014

Ischemic heart disease (angina pectoris and/or previous myocardial infarction)[a]
Heart failure
Stroke or transient ischemic attack
Renal dysfunction (serum creatinine > 170 μmol/L or 2 mg/dL or a creatinine clearance < 60 ml/min/1.73 m^2)
Diabetes mellitus requiring insulin therapy

[a]According to the universal definition of myocardial infarction

more than two clinical risk factors and poor functional capacity (<4 Metabolic Equivalent of Tasks; METs) (class I; level C)" (clinical risk factors are listed in Table 45.1); (2) "imaging stress testing may be considered before high- or intermediate-risk surgery in patients with one or two clinical risk factors and poor functional capacity (<4 METs) (class IIb; level C)"; "imaging stress testing is not recommended before low-risk surgery, regardless of the patient's clinical risk (class III; level C)". Guidelines recommend preoperative cardiac stress testing only if the results are likely to modify the perioperative management. In modern perioperative medicine, anesthesiologists and intensivists should always be able to perform cardiac ultrasound.

45.3 Intraoperative and Postoperative Transesophageal Echocardiography

TEE is a standard practice monitoring tool during cardiac surgery. During the last years, it has been increasingly used also for non-cardiac surgical patients, despite a definitive evidence supporting its use is still lacking.

TEE is rapidly available, minimally invasive, and provides a number of crucial information: by enabling direct visualization of the chambers of the heart, its valves, and the major connecting vessels (aorta, pulmonary artery, pulmonary veins, and vena cave), it provides potential diagnostic data on a number of acute cardiac alterations including acute myocardial infarction, new
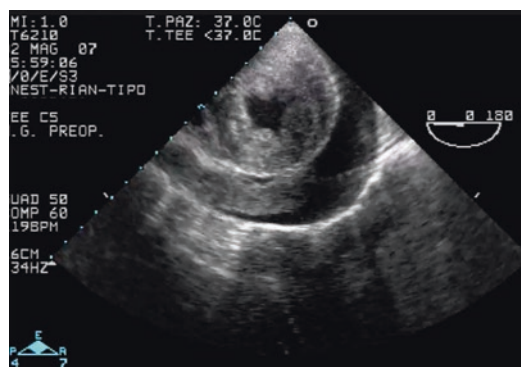
Fig. 45.1 Pericardial effusion in patient with gastric cancer. Transesophageal echocardiography. Left ventricle short-axis view

regional wall motion abnormalities, low ejection fraction, valvular diseases, right ventricular dysfunction, cardiac tamponade (Fig. 45.1), new vegetation (Fig. 45.2), intracardiac thrombus, acute pulmonary embolism, gas embolism during laparoscopic/robot-assisted surgery, dynamic left ventricle outflow tract (LVOT) obstruction (Fig. 45.3), and pulmonary hypertension. These all are conditions potentially occurring during and/or after non-cardiac surgery. Although TEE is in general a safe procedure, serious adverse events can occur, and the risk of complications is closely related with the experience of the operator and the presence of esophageal or gastric diseases. Therefore, specific training of users is essential to avoid inaccurate interpretation, and benefits of perioperative TEE should always be weighed against its risks.

While TEE is not indicated for routine use during non-cardiac surgery, it is strongly recommended if acute/severe hemodynamic instability or life-threatening abnormalities develop during or after surgery (Table 45.2). The leading indications for TEE examination in non-cardiac surgery are hemodynamic instability and massive blood loss, during which TEE may be a crucial tool to diagnose the cause of the hemodynamic impairment and to guide volume resuscitation (see the next paragraph). According to the *Practice Guidelines for Perioperative Transesophageal Echocardiography* published in 2010 by the American Society of

Anesthesiologists and the Society of Cardiovascular Anesthesiologists, "TEE may be used when the nature of the planned surgery or the patient's known or suspected cardiovascular pathology might result in severe hemodynamic, pulmonary, or neurologic compromise. If equipment and expertise are available, TEE should be used when unexplained life-threatening circulatory instability persists despite corrective therapy." The more recent ESC/ESA guidelines on non-cardiac surgery clearly indicate that "transesophageal echocardiography is recommended when acute sustained severe haemodynamic disturbances develop during surgery or in the peri-operative period (class I; level C)" and that TEE monitoring "may be considered in patients at increased risk of significant hemodynamic disturbances during and after high-risk non-cardiac surgery (class IIb – level C)" and "may be considered in patients who present severe valvular lesions dur-

ing high-risk non-cardiac surgery procedures accompanied by significant haemodynamic stresses (class IIb – level C)." Finally, TEE "should be considered in patients who develop ST-segment changes on intra-operative or peri-operative ECG monitoring (class IIa – level C)" and "may be considered in patients at high risk of developing myocardial ischemia, who undergo high-risk non-cardiac surgery (class IIb – level C)."

Another common and important setting for TEE monitoring application is video-laparoscopic surgery or robotic-assisted surgery in which abdominal pressure is usually increased with carbon dioxide (capnoperitoneum) up to 8–12 mmH_2O. In this case, the cardiovascular loading conditions during general anesthesia may differ profoundly from those existing in the preopera-
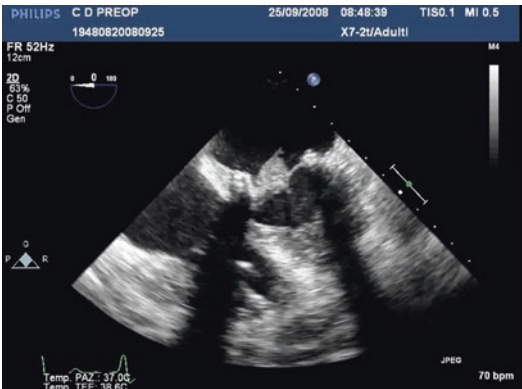
Fig. 45.2 Endocarditis on previous mitral valve plasty

Table 45.2 Common conditions, indications and requirements for perioperative echocardiography

Main indications: hemodynamic assessment (LV systolic and diastolic function; LVOT obstruction; pericardial space; volume optimization)
Performed in the OR (TEE) or at the bedside (TTE) by the anesthesiologist and ICU physician respectively
Interpretation in light of the clinical setting and additional hemodynamic information (BP, CVP, PPV, SVV, IVC diameter and collapsibility etc)
24/7 availability
Immediate diagnostic/therapeutic impact

Abbreviations: *LV* left ventricle, *LVOT* left ventricular outflow tract, *TEE* transesophageal echocardiography, *TTE* transthoracic echocardiography, *BP* blood pressure, *CVP* central venous pressure, *PPV* pulse pressure variation, *SVV* stroke volume variation, *IVC* inverior vena cava
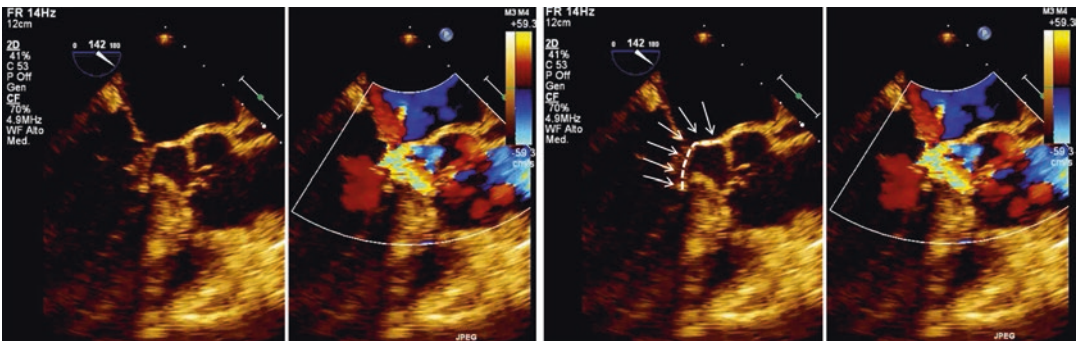
Fig. 45.3 Intra-operative dynamic left ventricular outflow tract (LVOT) during hemorrhage. 2D echo examination shows the close approximation of the anterior mitral valve leaflet (dashed line and arrows) to the interventricular septum. Color Doppler will demonstrate turbulent flow through the LVOT. See text for details

tive period. In these conditions, patients with limited cardiac reserve, or those with severe aortic stenosis, may benefit from TEE monitoring to maintain an appropriate preload and myocardial function that is of critical importance for hemodynamic stability.

45.4   Echocardiography in Perioperative Shock

Shock, a life-threatening, generalized form of circulatory failure associated with inadequate oxygen delivery to the cells, is traditionally divided into distributive, hypovolemic, cardiogenic, and obstructive. In major surgery of high-risk patients, a combination of these may occur. For example, a hemorrhagic shock may lead to LVOT obstruction (Fig. 45.3) or insufficient myocardial perfusion eventually causing variable degrees of systolic and/or diastolic dysfunction and/or persistently reduced vascular tone. This results in a combination of hypovolemic, cardiogenic, and distributive shock. The prompt identification of the leading cause of the shock is fundamental to properly treat the acute patients in both operating rooms and intensive care units. A rapid and detailed physical examination is the first step in the diagnosis of circulatory shock. Any information on the recent clinical status (previous or actual surgery, history of cardiac diseases, etc.) and other available hemodynamic data (e.g., arterial pressure, central venous pressure, pulse pressure variation, stroke volume variation, arterial elastance, dP/dt_{max}, cardiac output, stroke volume, heart rate) may help the physician in the etiological diagnosis of shock. If not immediately available, initial clinical management should start prior of heart ultrasound since timing is crucial to success; however, without a rapid improvement of hemodynamic status, echocardiography should be performed without further delay, due to its undisputed superiority in providing structural and functional information on valves, myocardium, and big vessels. A fast-basic assessment, also called Rapid Assessment by Cardiac Echo (RACE), should be performed. RACE allows an overall evaluation of left ventricular contractility, including ejection fraction (subjective evaluation is reasonably accurate only with experience), regional wall motion abnormalities, right heart failure, intravascular volume status (Fig. 45.4), and pericardial tamponade (Fig. 45.1). A recent survey among 284 German intensivists demonstrated that ultrasonography was used by 99% to diagnose and treat the type of circulatory shock. Echocardiography just after surgery can be made difficult by suboptimal position of the patient and clinical conditions (i.e., entrapped air after abdomen and/or chest open surgery, subcutaneous emphysema, or chest tubes); however, data from literature report high success rates of adequate acquisition of ultrasound
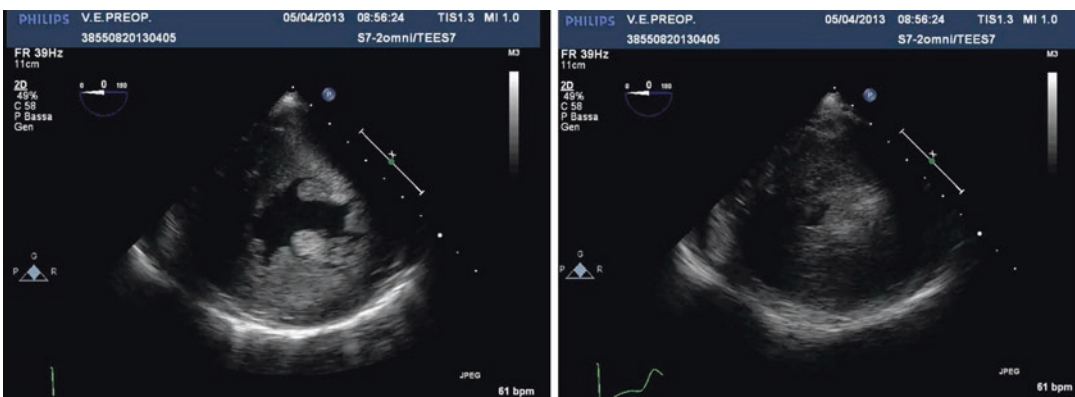

Fig. 45.4 Kissing walls or papillary kissing. Severe left ventricle hypertrophy. End-diastole (left) – End-systole

images with TTE for the specific purpose in most cases even in mechanically ventilated patients.

Arterial hypotension is a frequent trigger for fluid administration, but fluid overload and positive fluid balance have been demonstrated to negatively impact the outcome of surgical patients. Echocardiography is useful to detect fluid responders in low CO states. Severe hypovolemia is associated with the collapse of the LV walls at end-systole (named "kissing walls" or "papillary kissing"; Fig. 45.4). Although not common, a possible cause of shock in perioperative patients is the dynamic LVOT obstruction due to hemorrhage since tachycardia, hypovolemia, and inotropes are predisposing factors (Fig. 45.3). On the opposite, fixed bowing, without alternate swing, of the atrial septum into the right atrium throughout the cardiac cycle indicates elevated left atrial pressures, and fluids are not necessary and potentially harmful. Although these signs are nonspecific for intravascular fluid status, they help the clinician towards a proper treatment. A more precise identification of fluid responders can be reached with the measurement of cardiac output (CO) and inferior (by means of TTE) or superior (by means of TEE) vena cava collapsibility (IVC and SVC, respectively). These measures are recognized as quantitative dynamic parameters useful to address fluid responsiveness in daily practice. Techniques to measure CO and vena cava collapsibility are beyond the present chapter as the reader may refer to dedicated chapters. The IVC diameter must always be evaluated in combination with the heart and thoracic examinations because right heart failure, pericardial effusion, or tension pneumothorax all make the use of IVC less reliable as an index of volemia. If TEE is performed, the SVC during mechanical ventilation can be used to identify fluid responders. Importantly, to performing TTE/TEE during emergency conditions can be more challenging compared to elective settings with the potential risk to miss abnormalities. The interpretation of contractile state needs to consider the effects of vascular impedance, which is increased during vasoactive drug administration, or the effects of inotropes. Therefore, the clinicians should be aware of the limitations associated with use of TTE/TEE and thoracic ultrasounds in such conditions and may benefit from invasive "external" CO monitoring and pulse contour analysis.

45.5 Lung Echography and Thoracic Ultrasound

The use of thoracic ultrasound in everyday clinical practice is becoming increasingly common, having been incorporated into standards of care for many specialties. Bedside lung ultrasound has proved to be more informative than portable chest X-ray for detecting and quantifying common conditions of critically ill patients and patients with surgical complications including pneumothorax, infiltrates, pulmonary edema, and pleural effusion. The most common complications after surgery are bleeding, sepsis, and pulmonary complications (i.e., atelectasis, infiltrates, pleural effusions). Postoperative pulmonary complications (PoPCs) have been demonstrated to be a burdening issue by the recently published large cross-sectional LAS VEGAS study on almost 10,000 patients that showed an incidence of PoPCs of 19%. According to the ARISCAT score (Assess Respiratory Risk in Surgical Patients in Catalonia risk score), patients at increased risk of PoPCs were over 2500 out of the 10,000 patients ventilated for surgery, and the rate of PoPCs was 19.2 versus 7.0% (RR 3.16, (95% CI) 2.76 to 3.61; $p < 0.001$). The most frequent PoPCs were unplanned supplemental oxygen administration, followed by respiratory failure, and need for invasive mechanical ventilation. Severe PoPCs (total PoPCs excluding unplanned supplemental oxygen administration) occurred in 2.8% of all patients and in 14.5 versus 1.6% (RR 3.98 (95% CI 3.09 to 5.12), $p < 0.001$) of patients at increased versus low risk of PoPCs, respectively. Thus, thoracic-pulmonary ultrasound examination represents an important diagnostic tool in non-cardiac surgery for a goal-directed diagnosis and treatment of PoPCs.

In case of dyspnea after surgery, portable chest X-ray may be done; it takes time, and it is frequently performed with the patient in the supine position, because of surgery, mechanical

ventilation, or hypotension. This makes accurate imaging and interpretation more difficult. Ultrasound may lead to quicker and more accurate diagnosis, avoiding any delay in treatment for many thoracic and pulmonary diseases. Benefits of the examination speed and accuracy are of outmost importance: the opportunity of examining patients without moving them from the surgical ICU beds is not negligible especially when mechanical ventilation is necessary.

Thoracic ultrasound after surgery is typically performed by anesthesiologists, intensivists, residents, fellows, and attending physicians. This allows for the rapid detection of either fluid or air within the pleural cavity with great accuracy. As an example, ultrasound diagnosis of pneumothorax is based on the absent sliding sign (i.e., the movement of the visceral pleura as it glides over the parietal pleura in a normally aerated and ventilated lung) and the absent seashore sign (M-mode depiction of pleural movements in a single section of the thorax). The presence of lung pulse can safely rule out pneumothorax in the absence of lung sliding with high sensitivity. Sensitivity and specificity of lung ultrasound in the diagnosis of pneumothorax had been reported to vary from 86–100% to 97–100%, respectively, whereas 28–75% and 100% were the rates reported for chest x-ray. In patients with poor LV systolic and/or diastolic function, with or without fluid overload and surgical sepsis, lung ultrasound can contribute to the diagnosis of pulmonary edema. B-lines are horizontal hyperechoic beams extending parallel to the pleura to the deep edge of the screen. B-line pattern correlates with thickened interlobular septa or ground-glass areas on computed tomography.

Critically ill surgical patients may have pleural fluid effusion, either transudate or exudate. Ultrasound examination can provide qualitative/quantitative informations of the intrathoracic fluid. This examination can be repeated as many times as necessary. Moreover, in patients with effusions, ultrasound-guided insertion of chest drains or punctures is useful to reduce the rate of procedural complications.

Another frequent PoPC is represented by atelectasis. General anesthesia may cause atelectasis within the first few minutes of induction in the most dependent part of the lungs, especially when pneumoperitoneum is necessary for surgery. Conventional chest x-ray may not detect small atelectasis, and computed tomography could be unfeasible or unnecessary in the perioperative phases. Lung ultrasound allows for the evaluation of efficacy of recruitment maneuvers, PEEP application, or physiotherapy. Importantly, postoperative atelectasis can progress to pneumonia as a continuum of pathophysiological events. Lung ultrasound helps the physician to identify and treat them. Distinguishing atelectasis from infiltrates can be difficult. The finding of sonographic air bronchograms suggests an infiltrative process with alveolar consolidation.

Additional applications of thoracic lung ultrasound include checking for correct positioning of the endotracheal tube above the carina after intubation (e.g., by bilateral pleural sliding during ventilation) and verification of correct lung exclusion before initiating one-lung ventilation for thoracic surgery after placement of a double-lumen endotracheal tube. Thoracic ultrasound assessment of double-lumen tube placement has been found to be as specific and sensitive as fiberoptic bronchoscopy to verify correct lung exclusion. During thoracic surgery, endobronchial intubation or dislodgement of the endotracheal tube can be easily identified by lung ultrasound.

Bilateral lung sliding could be very informative in case of intraoperative or postoperative desaturation. If echocardiography is associated with lung ultrasound, the source behind most of the acute intraoperative and postoperative desaturations can be quickly clarified. Pneumothorax, endobronchial intubation, bronchospasm, atelectasis, pulmonary edema, and pulmonary embolism are all examples of acute entities that can be rapidly diagnosed with lung-and-heart concomitant ultrasound.

45.6 Conclusions

The ESC and the ESA have released detailed guidelines on cardiovascular assessment and management in non-cardiac surgery providing the

clinician with a useful guide for an oriented and cost-effective use of preoperative and intraoperative application of TTE and TEE.

Although its use is increasing over time, intraoperative echocardiography is still limited by the necessary training and expertise and because rarely electively needed in non-cardiac surgery. Nonetheless, TTE and TEE could be of crucial importance when hemodynamic derangement occurs acutely during or after surgery. Clinicians need adequate training on how and when to perform cardiac US and need to be aware of the learning curve. Today, echocardiography is regarded as a mandatory part of perioperative and critical care training. Bedside point-of-care thoracic ultrasound may be used to evaluate surgical patients presenting with desaturation, dyspnea, or shortness of breath, as it is of great aid to diagnose and treat a variety of acute or emergent conditions.

Further Reading

Barbier C, Loubieres Y, Schmit C, et al. Respiratory changes in inferior vena cava diameter are helpful in predicting fluid responsiveness in ventilated septic patients. Intensive Care Med. 2004;30:1740–6.

Cecconi M, De Backer A, Antonelli M, et al. Consensus on circulatory shock and hemodynamic monitoring. Task force of the European Society of Intensive Care Medicine. Intensive Care Med. 2014;40:1795–815.

Corcoran JP, Tazi-Mezalek R, Maldonado F, Yarmus LB, Annema JT, Koegelenberg CFN, St Noble V, Rahman NM. State of the art thoracic ultrasound: intervention and therapeutics. Thorax. 2017; [Epub ahead of print].

Expert Round Table on Ultrasound in ICU. International expert statement on training standards for critical care ultrasonography. Intensive Care Med. 2011;37(7):1077–83.

Koster G, van der Horst ICC. Critical care ultrasonography in circulatory shock. Curr Opin Crit Care. 2017;23(4):326–33.

Kristensen SD, Knuuti J, Saraste A, Anker S, Bøtker HE, De Hert S, Ford I, Gonzalez Juanatey JR, Gorenek B, Heyndrickx GR, Hoeft A, Huber K, Iung B, Kjeldsen KP, Longrois D, Luescher TF, Pierard L, Pocock S, Price S, Roffi M, Sirnes PA, Uva MS, Voudris V, Funck-Brentano C, Authors/Task Force Members. 2014 ESC/ESA guidelines on non-cardiac surgery: cardiovascular assessment and management: The Joint Task Force on non-cardiac surgery: cardiovascular assessment and management of the European Society of Cardiology (ESC) and the European Society of Anaesthesiology (ESA). Eur J Anaesthesiol. 2014;31(10):517–73.

McLean AS. Echocardiography in shock management. Crit Care. 2016;20:275.

Practice Guidelines for Perioperative Transesophageal Echocardiography. An Updated Report by the American Society of Anesthesiologists and the Society of Cardiovascular Anesthesiologists Task Force on Transesophageal Echocardiography. Anesthesiology. 2010;112:1084–96.

Saporito A, Lo Piccolo A, Franceschini D, Tomasetti R, Anselmi L. Thoracic ultrasound confirmation of correct lung exclusion before one-lung ventilation during thoracic surgery. J Ultrasound. 2013;16(4):195–9.

Shillcutt SK, Brakke TR, Thomas WR, Porter TR, Lisco SJ. The development of a perioperative echocardiography consult service: the Nebraska experience. J Cardiothorac Vasc Anesth. 2015;29(3):777–84.

Shillcutt SK, Markin NW, Montzingo CR, Brakke TR. Use of rapid "rescue" perioperative echocardiography to improve outcomes after hemodynamic instability in noncardiac surgical patients. J Cardiothorac Vasc Anesth. 2012;26(3):362–70.

The LAS VEGAS investigators. Epidemiology, practice of ventilation and outcome for patients at increased risk of postoperative pulmonary complications. LAS VEGAS - an observational study in 29 countries. Eur J Anaesthesiol. 2017;34:492–507.

Perioperative Echocardiography for Aortic Procedures

46

Ilaria Blangetti and Alessandro Locatelli

Key Points

TOE for vascular surgery

- Anatomical and functional cardiac assessment
- Aortic assessment
- Periprocedural decision-making
- Complex endovascular approaches

46.1 Anatomical and Functional Cardiac Assessment

ESC/ESA Guidelines recommendations on noncardiac surgery [1] underline that cardiac monitoring with TOE in high-risk patients helps clinicians to:

- Assess ventricular function.
- Identify cardiac valve disease.
- Guide fluid administration.
- Guide administration of vasoactive and inotropic drugs.
- Allow early recognition of myocardial ischemia.

Table 46.1 From 2014 ESC/ESA Guidelines on noncardiac surgery [1]

Indications	Class and level of recommendation
Patients with ST alterations	IIa level C
Patients at high risk for myocardial infarction during and after high-risk surgery	IIb level C
Patients with progression from mild to severe valvular regurgitation	I level C
Patients at high risk for hemodynamic instability during and after high-risk surgery	IIb level C
Patients with severe valvular disease undergoing high-risk surgery with hemodynamic stress	IIb level C

Recommendations for intraoperative TOE monitoring are resumed in Table 46.1.

Valve disease and systo-diastolic myocardial function get worse during aortic cross clamping and declamping; TOE allows to manage at best these critical phases of surgical time.

Figure 46.1 shows worsening of mitral regurgitation during abdominal aortic cross clamping.

46.2 Aortic Assessment

TOE is the ultrasound technique of choice in thoracic aorta assessment.

I. Blangetti (✉) · A. Locatelli (✉)
Department of Emergency and Critical Care, Santa Croce e Carle Hospital, Cuneo, Italy
e-mail: blangetti.i@ospedale.cuneo.it; locatelli.a@ospedale.cuneo.it
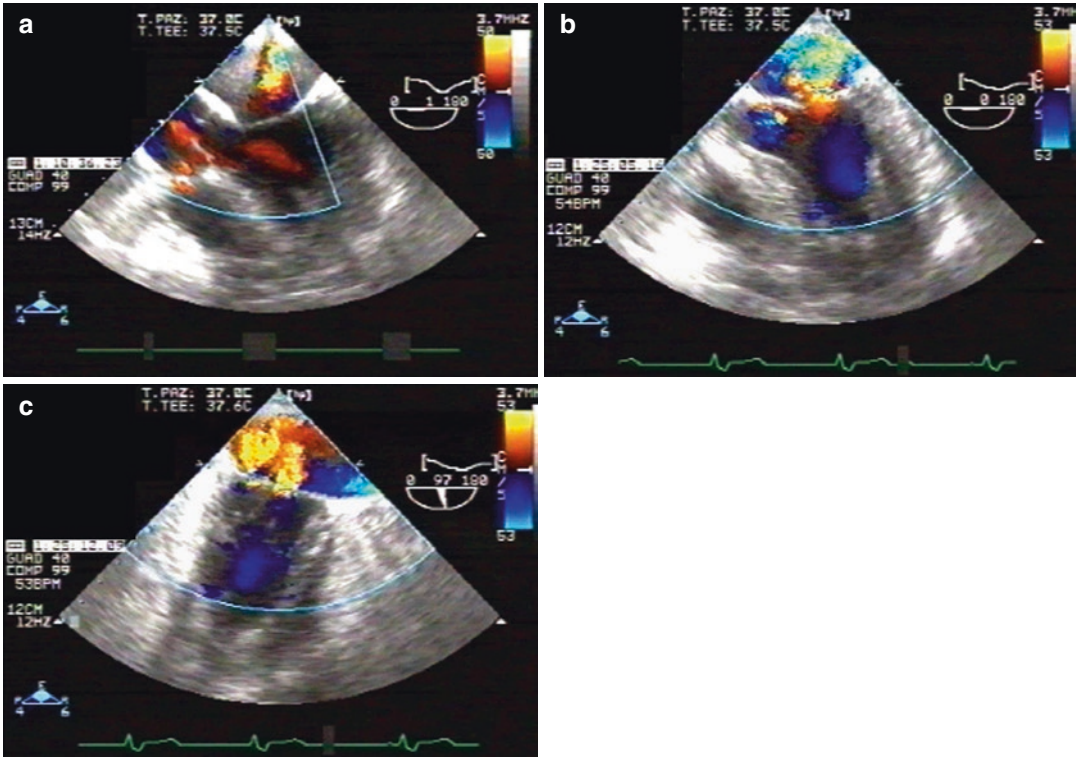
Fig. 46.1 Mitral regurgitation during aortic cross clamping. (a) Before clamping. (b–c) After clamping

46.2.1 Aortic Views

High-quality images can be obtained with TOE for the use of multiplane high-frequency transducers, and because of the close proximity of the oesophagus to the thoracic aorta, in particular ascending and descending thoracic aorta are well visualized (green zones in Fig. 46.2).

X-Plane mode allows aorta visualization in short axis contemporarily to long axis. Real-time 3D technology brings simultaneous multiplane imaging; three-dimensional reconstructions provide high grade of accuracy.

46.2.2 Relationship Between the Aorta and Oesophagus

Thoracic aorta is anterior to the oesophagus in ascending tract and aortic arch, is lateral to the
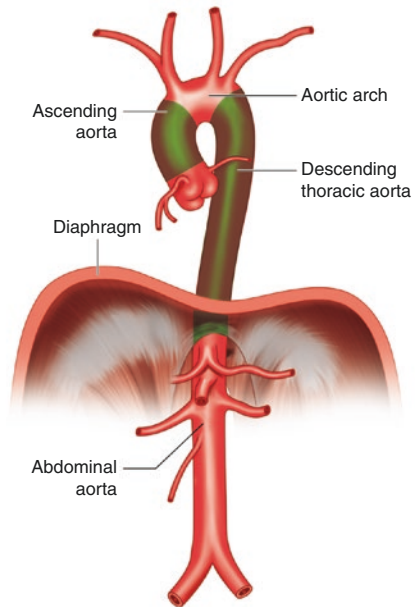
Fig. 46.2 Aortic segments well visualized by TOE (green zones)

oesophagus in the mid-thorax, and finally becomes posterior when diaphragmatic hiatus is passed.

Because of changing in relationship between the oesophagus and aorta, it's essential to know the probe position in the oesophagus for a correct identification of the aortic wall (Fig. 46.3).

The American Society of Echocardiography (ASE) and the Society of Cardiovascular Anaesthesiologists (SCA) in 2013 [2] suggest 28 views for comprehensive TOE examinations; 10 aortic views are reported in the following images (Fig. 46.4a, b).

46.2.3 Limits of Aortic Views

- Poor visualization of distal ascending aorta and aortic arch because of interposition of the trachea and left main bronchus (BLIND SPOT). It could be possible to overcome these limits inflating a balloon with 20–50 ml of saline in the trachea.
- Difficulties in correct definition of anterior-posterior wall on thoracic descending aorta because of changing in relationship between the oesophagus and aorta.
- Poor visualization with PTFE stent-graft (US are absorbed and reflected).
- Poor visualization of sub-diaphragmatic aortic tract.

46.2.4 Aortic Diameter

Measurement of aortic diameter has to be reproducible and precise. The American Society of Echocardiography recommends to measure the aorta at the end of diastole, from the leading edge of anterior root wall to the leading edge of posterior root wall and perpendicular to the long axis of the aorta.

46.2.5 Landmarks in Thoracic Descending Aorta

It's difficult to identify precise landmarks in descending aorta; usually, distance from incisors

Fig. 46.3 Probe position in oesophagus and corresponding aortic walls

Aorta to the left-upper

Aorta to the left

Aorta posteriorly

a
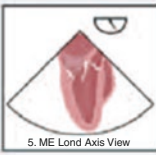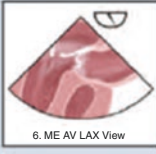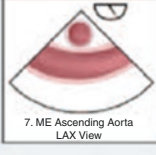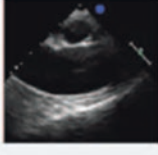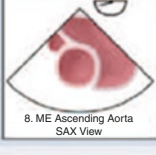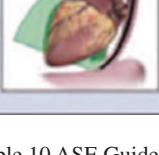
Imaging plane	3D Model	2D TEE Image	Acquisition Protocol	Structures Imaged
5. ME Lond Axis View			**Transducer Angle:** ~ 120 - 140° **Level:** Mid-esophageal **Maneuver** (from prior image): NA	Left atrium Left ventricle LVOT RVOT Mitral valve (P_2-A_2) Aortic valve Proximal ascending aorta
6. ME AV LAX View			**Transducer Angle:** ~ 120 - 140° **Level:** Mid-esophageal **Maneuver** (from prior image): Withdrawl + anteflex	Left atrium LVOT RVOT Mitral valve (A_2-P_2) Aortic valve Proximal ascending aorta
7. ME Ascending Aorta LAX View			**Transducer Angle:** ~ 90 - 110° **Level:** Upper-Esophageal **Maneuver** (from prior image): Withdrawl	Mid-ascending aorta Right pulmonary artery
8. ME Ascending Aorta SAX View			**Transducer Angle:** ~ 0 - 30° **Level:** Upper-Esophageal **Maneuver** (from prior image): CW	Mid-ascending aorta (SAX) Main/bifurcation pulmonary artery Superior vena cava
21. Deep TG G-Chamber View			**Transducer Angle:** ~ 0 - 20° **Level:** Transgastric **Maneuver** (from prior image): Left-flex, Advance, Anteflex	Left ventricle Left ventricular outflow tract Right ventricle Aortic valve Aortic root Mitral Valve
24. TO LAX View			**Transducer Angle:** ~ 120 - 140° **Level:** Transgastric **Maneuver** (from prior image): CCW	Left ventricle Left ventricular outflow tract Right ventricle Aortic valve Aortic root Mitral Valve

Fig. 46.4 (**a**) From Table 10 ASE Guidelines and Standards [2]. (**b**) From Table 10 ASE Guidelines and Standards [2]

b
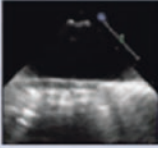
Imaging Plane	3D Model	2D TEE Image	Acquisition Protocol	Structures Imaged
25. Descending Aorta SAX View			**Transducer Angle:** ~ 0 - 10° **Level:** Transgastric to Mid-esophageal **Maneuver** (from prior image): Neutral flexion	Descending aorta Left thorax Hemiazygous and Azygous veins Intercostal arteries
26. Descending Aorta LAX View			**Transducer Angle:** ~ 90 - 100° **Level:** Transgastric to Mid-esophageal **Maneuver** (from prior image): Neutral flexion	Descending aorta Left thorax
27. UE Aortic Arch LAX View			**Transducer Angle:** ~ 0 - 10° **Level:** Upper Esophageal **Maneuver** (from prior image): Withdrawl	Aortic arch Innominate vein Mediastinal tissue
28. UE Aortic Arch SAX View			**Transducer Angle:** ~ 70 - 90° **Level:** Transgastric to Mid-esophageal **Maneuver** (from prior image): NA	Aortic arch Innominate vein Pulmonary artery Pulmonary valve Mediastinal tissue

Fig. 46.4 (continued)

is used. Aortic isthmus, left subclavian artery and celiac artery can be used as markers for anatomical location of aortic disease. During interventional procedure It can be useful to visualize landmarks on radiological images during interventional procedures.

46.2.6 Aortic Disease

In acute aortic syndrome (AAS), TOE confirms the diagnosis, determines the sites of involvement, delineates the extension and detects complications. Acute aortic syndrome includes aneurysms, dissections (AD), penetrating atherosclerotic

ulcer (PAU) and intramural hematoma (IMH) (see Chap. 11).

Aortic wall anomalies are usual findings in vascular patients; TOE can define its localization, morphology, size and grade of mobility.

Aortic atheroma can be well visualized with real-time 3D technology; morphological features and location have to be considered because of the possible source of embolism (Fig. 46.5).

TOE has been described by the authors of this chapter as an intraoperative diagnostic tool for the unknown source of peripheral embolism, and decisional algorithm has been proposed.
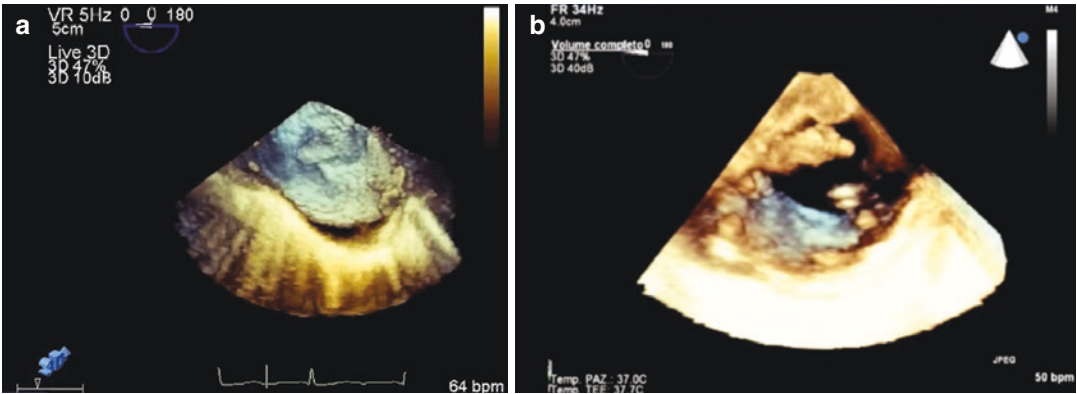
Fig. 46.5 Atheroma in live 3D a. aortic arch b. descending aorta
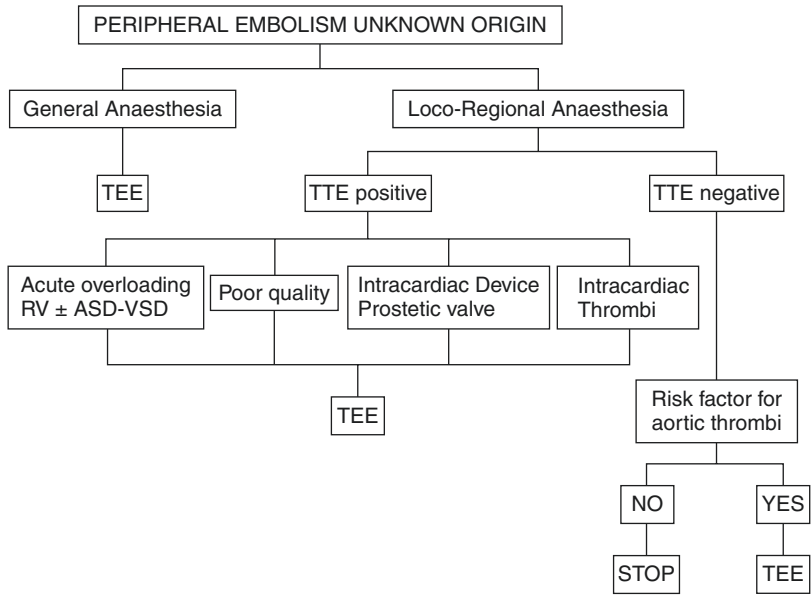
46.3 Periprocedural Decision-Making

Thoracic endovascular aortic repair (TEVAR) is a therapeutic option for treatment of aortic disease as aneurysm and dissection because of less morbidity and mortality in comparison to open surgery.

Indications for endovascular aortic procedures are explained in details in 2014 ESC guidelines on the diagnosis and treatment of aortic diseases [3].

Summary of TEVAR indications is available in the following table (Table 46.2).

Goals of endovascular treatment are:

Table 46.2 2014 ESC guidelines on the diagnosis and treatment of aortic disease [3]

Type of disease	Class and level of recommendation
Descending aortic aneurysm	IIa C
Complicated type B AD	I C
Uncomplicated type B AD	IIa B
Complicated type B IMH	IIa C
Complicated type B PAU	IIa C
Contained rupture of thoracic aortic aneurysm	IC
Traumatic aortic injury	IIa C

Table 46.3 Z zones

Z zones	Location
Zone 0	Ascending aorta and proximal arch to innominate artery
Zone 1	Between innominate artery and left common carotid artery
Zone 2	Between left common carotid artery and left subclavian artery
Zone 3	Left subclavian artery along curved portion of distal arch
Zone 4	Descending aorta starting at level of fourth thoracic vertebra

- The complete exclusion of the aneurysm's sac or the aortic wall injury
- The false lumen thrombosis in type B dissection with sealing of primary entry tear

The role of TOE during TEVAR is well defined since several years, TOE is essential in monitoring endovascular aortic treatment and in detecting possible complications. Echocardiographic reports can influence procedural planning and have to be correctly interpreted and reported.

46.3.1 Aortic Z Zones

In the endovascular era, thoracic aorta has been described in terms of zones not cones. Five Z zones have been identified (Table 46.3) (Fig. 46.6).

46.3.2 Confirmation of Aortic Disease

At the beginning of the procedure, TOE could help the clinician to specify and to confirm:

- Type of disease/abnormalities (Fig. 46.7).
- Relationship between aortic neck and healthy wall vessel.

Fig. 46.6 Z zones. (From Vallabhajosyula P, Szeto WY, Desai N, Komlo C, Bavaria JE. Type II arch hybrid debranching procedure. *Ann Cardiothorac Surg*. 2013;2(3):378–86. doi: https://doi.org/10.3978/j.issn.2225-319X.2013.05.08)

- Size of hematoma in traumatic aortic injury and retrograde expansion.
- Relationship between aortic wall disease and previous prosthesis (Fig. 46.8 elephant trunk prosthesis and thoracic aortic hematoma).
- Identification of aortic flap: dissection flaps in acute dissections are "oscillating" while thicker, echo-dense and relatively immobile in chronic dissection.
- Detection of entry tears and localization of re-entry tears (Fig. 46.9).
- Flap invagination in aortic branches.

46.3.3 Landing Zone

An appropriate landing zone for stent-graft delivery should be available proximally and distally to aortic disease. Landing zone has to be evaluated to exclude the presence of protruding aortic plaques that can't allow a correct adhesion between stent-graft and aortic wall.

It's essential to visualize left subclavian artery and its distance from aortic disease.

Fig. 46.7 Thoracic aortic aneurysm and thrombus

46.3.4 True Lumen and False Lumen in Aortic Dissection

TOE can differentiate true lumen (TL) from false lumen (FL) [4]

Key Points
- FL in the descending thoracic aorta is usually larger than TL (Fig. 46.10)
- Systolic expansion of the TL and diastolic expansion of the FL (Fig. 46.11)
- Rapid anterograde systolic flow in TL
- Sluggish, absent or retrograde flow in FL
- Communication flow from true to false lumen in systole
- Contrast echo flow early and fast in TL

Fig. 46.8 Elephant trunk prosthesis (red arrow) and thoracic aortic hematoma
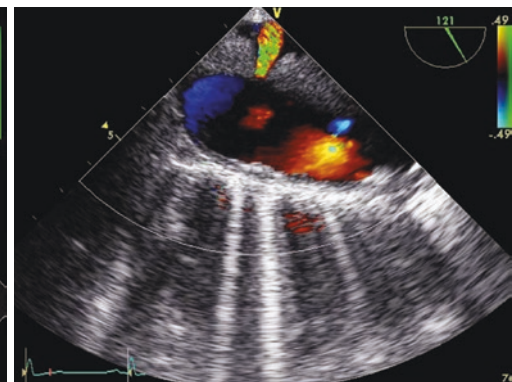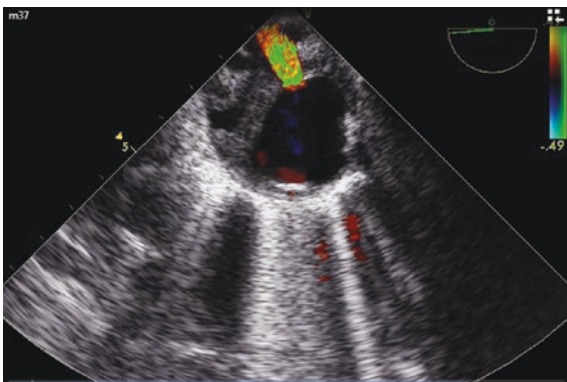
Fig. 46.9 The same tear in short axis (0°) and long axis (120°)
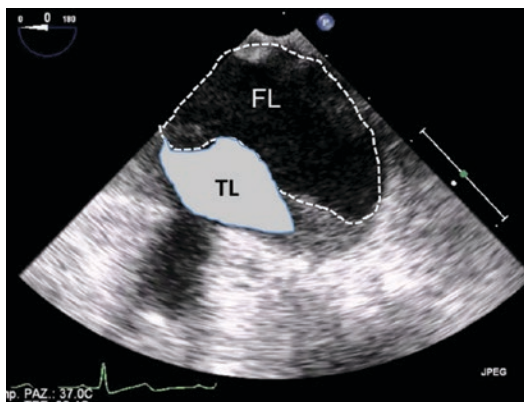
Fig. 46.10 FL (false lumen) and TL (true lumen) in aortic dissection
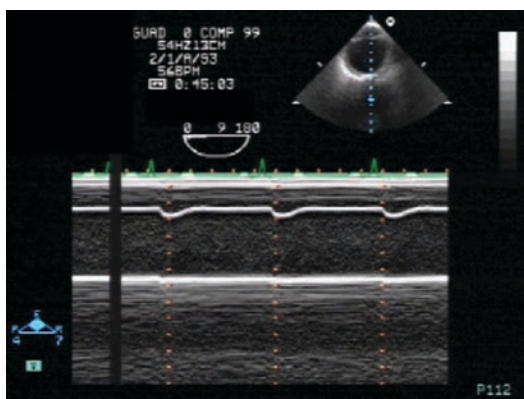
Fig. 46.11 Systolic expansion of the TL

46.3.5 Guidewires

Guidewire is bright and echo-dense at view. and it's possible to follow its positioning with TOE [4].

Key Points
- Visualize guidewire to be inserted in TL, and follow its positioning throughout descending aorta to be sure it remains in the TL (Fig.46.12).
- Visualize guidewire position in prostheses of the previous aortic surgery.
- Avoid guidewire's movements near ATS plaque for risk of embolization.
- Visualize ascending aorta and aortic valve to be sure guidewire has not been positioned in the left ventricle.
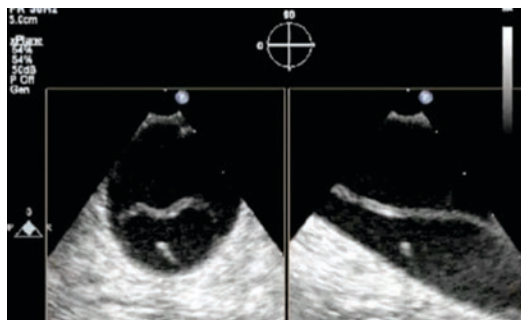
Fig. 46.12 Guidewire inserted in true lumen

46.3.6 Device Deployment Monitoring

It's possible to obtain good quality of echo-images during device deployment; the probe is positioned at the level of the landing zone and X-plane mode is used.

This procedure is not always allowed because of interference of probe itself on radiologic imaging.

46.3.7 Post-procedural Examinations

After stent-graft deployment, TOE is useful to verify:

- Stent-graft position in aorta and complete device expansion
- Thrombosis of false lumen and distal re-entry tears in aortic dissection
- Presence of endoleaks and indications and monitoring of ballooning or deployment of another stent (Fig. 46.13) (Table 46.4).

Type I and III endoleaks has to be treated as soon as possible.

The use of a colour flow Doppler with a scale of 25 cm/s and PWD is recommended to be more precise in endoleak's diagnosis. A velocity higher than 50 cm/s is highly suspicious of endoleak.

Recently, contrast-enhanced TEE (cTEE) has been used for this purpose; persistent leaks and incomplete expansion of device are better visualized with contrast (Fig. 46.14).

- Patency of aortic branches
- Other complications: retrograde dissection and pleural effusion (Fig. 46.15)
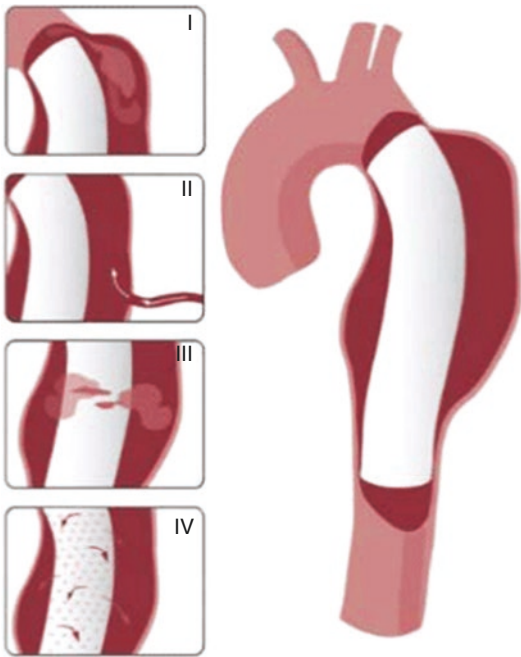
Fig. 46.13 Type of endoleaks

Table 46.4 Definition from Society of Vascular Surgery (SVS)

Classification of endoleaks	Characteristics
Type I	Gap between the graft and the vessel wall at "seal zones." IA, proximal zone; IB, distal zone
Type II	Retrograde flow from side branches
Type III	Defect or misalignment between the components of endografts
Type IV	Porosity
Type V	Endotension

46.4 Complex Endovascular Approaches

Endovascular repair for thoraco-abdominal aneurysms has been proposed using fenestrated or branched aortic grafts.

Hybrid techniques for complex aortic arch surgery are now available; it's a combination of open supra-aortic vessel debranching and endovascular exclusion of aortic disease.

TOE can be useful also in these settings, although aortic arch and abdominal aorta have been defined "blind zone," with the following purposes:

• Detect ATS plaques in ascending aorta to guide where surgical anastomosis for TSA has to be performed.
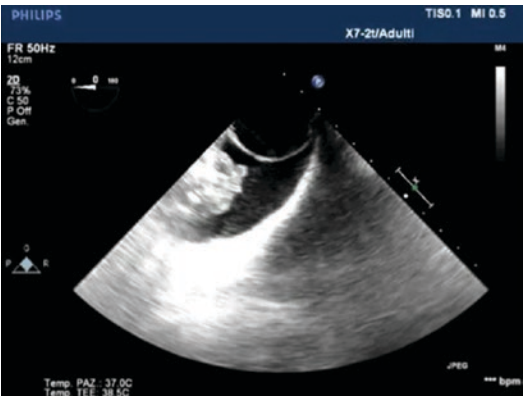
Fig. 46.15 Pleural effusion
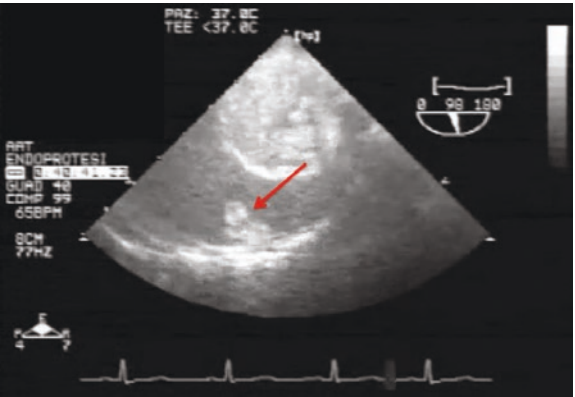
Fig. 46.14 Echo contrast preparation and endoleak visualization (red arrow)

- Visualize supra-aortic vessels' flow after surgical debranching (Fig. 46.16).
- Detect pleural or pericardial effusion.
- Visualize visceral aortic branch flow before procedure to localize their position.
- Visualize visceral aortic branches flow after stent deployment to control stent patency.

46.4.1 Aortic Branches Views

46.4.1.1 Supra-aortic Trunk
Aortic arch vessels originate directly from the aortic arch; sometimes, it's possible to visualize at least part of them.

Probe has to be positioned in four-chamber view and to be turned to the left until the aorta appears in short axis. Withdrawing the probe, the aortic arch appears at 0° in long axis, and the left subclavian artery (LSA) and left carotid artery (LCA) could be visualized [5]. Brachiocephalic trunk is difficult to visualize because of trachea interposition.

46.4.1.2 Visceral Vessels
- *Celiac trunk*:
  The celiac trunk (CT) is the first major branch of abdominal aorta arising inferior to the aortic hiatus of the diaphragm, where the distance between the probe and aorta increases. Probe has to be positioned in the stomach and turned to the left until the aorta appears in short axis. CT is the vessel originating at 1 o'clock of the aorta, it divides promptly in two branches, and it moves away from the aorta [5] (Fig. 46.17).
- *Superior mesenteric artery*:
  Superior mesenteric artery (SMA) can be found at few centimetres below TC; it originates at 3 o'clock remaining adjacent to the aorta [5].
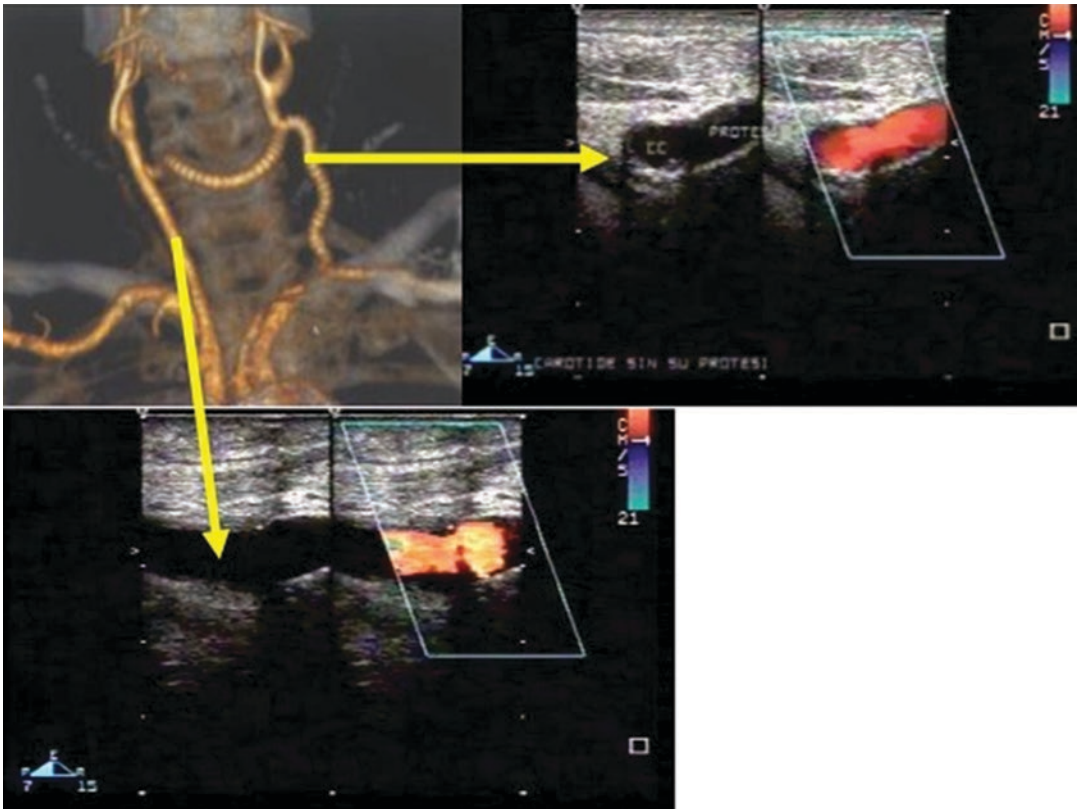
Fig. 46.16 Supra-aortic vessels' flow after surgical debranching (2D and CFD)

Flow pattern in aortic branches is resumed in Table 46.5.

46.4.2 Intravascular Ultrasound (IVUS)

IVUS is a new imaging methodology using an ultrasound probe placed on a catheter allowing a 360° intravascular image. IVUS allows to visualize arteries' wall from the inside, and it could be used complementary to other imaging modalities.
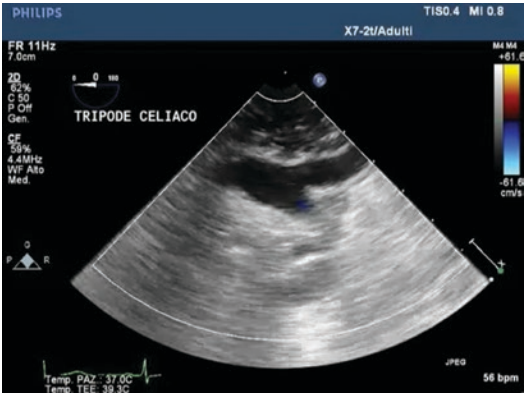
Fig. 46.17 Celiac trunk
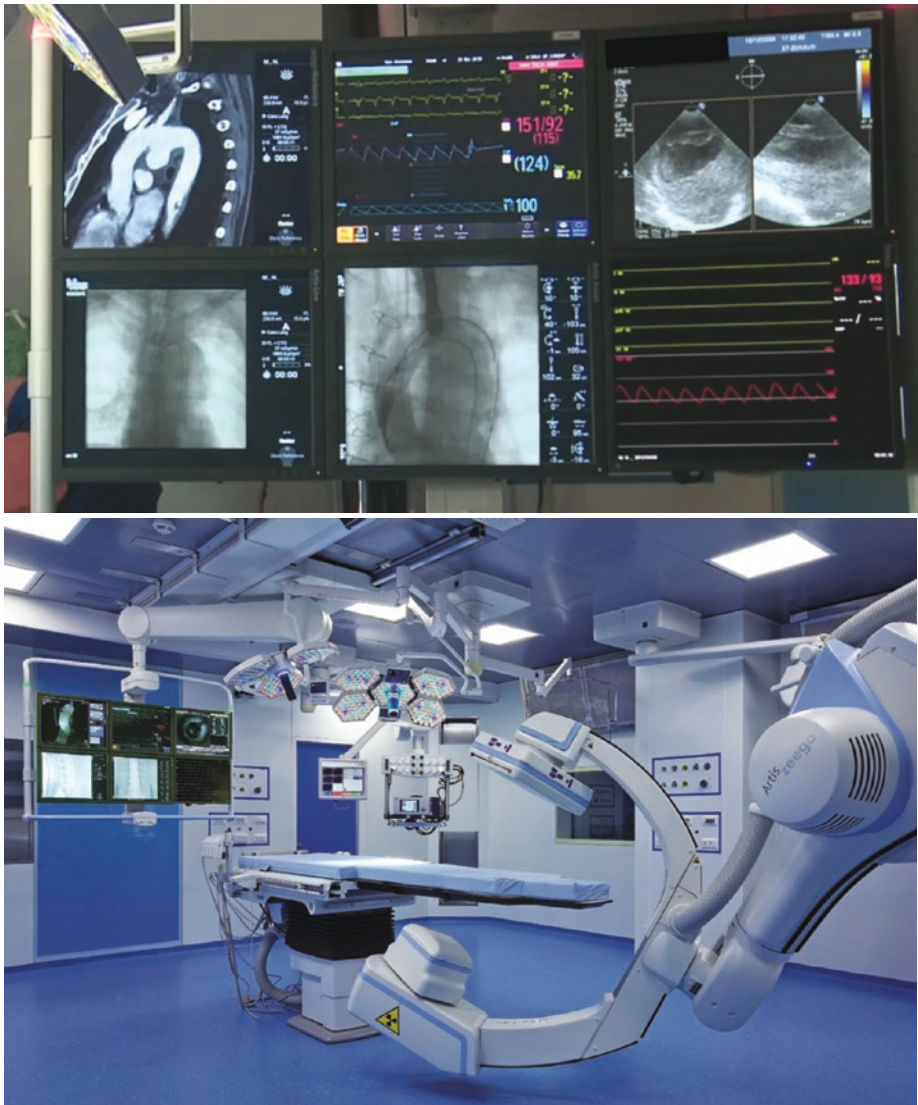
Fig. 46.18 Hybrid operative room of Cuneo Hospital and imaging screen with echo

Table 46.5 Flow pattern in aortic branches

Aortic branches	Flow pattern
Left subclavian artery	High resistance: systolic anterograde flow, short early diastolic reversal flow
Carotid artery	Low resistance: anterograde flow presents as systole so in diastole
Celiac trunk	Low resistance
Superior mesenteric artery	Low resistance

46.4.3 Conclusions

TOE plays an important role for intraoperative management of vascular patients, as for diagnosis so for monitoring.

Anaesthesiologist who performs TOE has to be skilled not only to obtain high-quality images but also to integrate echo informations into clinical decision-making process.

TOE images should be visualized in a multimedia screen by all the specialists involved in the procedures; this could be possible in a hybrid operating room that has all the characteristics to be the right place to perform endovascular and hybrid procedures (Fig. 46.18).

References

1. Kristensen SD, Knuuti J, Saraste A, Anker S, Bøtker HE, Hert SD, Ford I, Gonzalez-Juanatey JR, Gorenek B, Heyndrickx GR, Hoeft A, Huber K, Iung B, Kjeldsen KP, Longrois D, Lüscher TF, Pierard L, Pocock S, Price S, Roffi M, Sirnes PA, Sousa-Uva M, Voudris V, Funck-Brentano C, Authors/Task Force Members. 2014 ESC/ESA guidelines on non-cardiac surgery: cardiovascular assessment and management the joint task force on non-cardiac surgery: cardiovascular assessment and management of the European Society of Cardiology (ESC) and the European Society of Anaesthesiology (ESA). Eur Heart J. 2014;35:2383–431.
2. Hahn RT, Abraham T, Adams MS, Bruce CJ, Glas E, Lang RM, Reeves ST, Shanewise JS, Siu SC, Stewart W, Picard MH. Guidelines for performing a comprehensive transesophageal echocardiographic examination: recommendations from the American Society of Echocardiography (ASE) and the Society of Cardiovascular Anesthesiologists (SCA). J Am Soc Echocardiogr. 2013;26(9):921–64.
3. Erbel R, Aboyans V, Boileau C, Bossone E, Di Bartolomeo R, Eggebrecht H, Evangelista A, Falk V, Frank H, Gaemperli O, Grabenwöger M, Haverich A, Iung B, Manolis AJ, Meijboom F, Nienaber CA, Roffi M, Rousseau H, Sechtem U, Sirnes PA, von Allmen RS, Vrints CJ. 2014 ESC guidelines on the diagnosis and treatment of aortic diseases. Eur Heart J. 2014;35:2873–926.
4. Evangelista A, Flachskampf FA, Erbel R, Antonini-Canterin F, Vlachopoulos C, Rocchi G, Sicari R, Nihoyannopoulos P, Zamorano J, Document Reviewers, Pepi M, Breithardt OA, Plonska-Gosciniak E. Echocardiography in aortic diseases: EAE recommendations for clinical practice. Eur J Echocardiogr. 2010;11:645–58.
5. Salerno P, Jackson A, Shaw M, Spratt P, Jansz P. Transesophageal echocardiographic imaging of the branches of the aorta: a guide to obtaining these images and their clinical utility. J Cardiothorac Vasc Anesth. 2009;23(5):694–701.

Obstetric Echocardiography

47

Ferdinando Luca Lorini and Chiara Viviani

47.1 Introduction

Maternal cardiovascular disease complicates approximately 0.2–4% of all pregnancies in western industrialized countries, and it is the major cause of maternal death during pregnancy. Women are increasingly seeking pregnancy at a later age characterized by cardiovascular risk factors (diabetes, obesity, hypertension), resulting in more frequent cardiac events. Furthermore, surgery of congenital heart disease has improved, so as an increased number of women with congenital problems contemplate pregnancy.

47.2 Haemodynamic Changes/ Physiologic Alterations

Pregnancy is a physiological state that induces adaptation of the cardiovascular system to meet the increased metabolic demands of the mother and foetus and to ensure adequate uteroplacental circulation for foetal growth and development. These changes, which occur during labour and delivery and in the postpartum period, can mimic cardiac disease so that an understanding of both

haemodynamic alterations and anatomic changes is the key to interpret the echocardiograms in pregnant patients. Further, the normal haemodynamic changes can precipitate cardiac symptoms in previously stable women or may exacerbate symptoms in those with mild baseline symptoms.

Cardiac output increases by about 30–50% by the end of the first trimester, primarily due to an increase in stroke volume and in circulating blood volume. Between the second and third trimesters, cardiac output shows a peak, owing to a 15–20% increase in heart rate and a fall in afterload via decreased total vascular resistance. Arterial blood pressure decreases early in pregnancy, characterized by decreases in DBP exceeding those in SBP. The mean arterial pressure gradually falls, with the largest decrease occurring at 16–20 weeks. BP then begins to rise during the mid-third trimester to levels approaching pre-pregnancy BP values.

During labour and delivery, pain and uterine contractions result in additional increases in cardiac output (20% with each contraction), heart rate, blood pressure and systemic vascular resistance. Because of contribution of pain and anxiety to the increase in heart rate and blood pressures, pain control may help mitigate the haemodynamic changes. Immediately following delivery, relief of caval compression and auto-transfusion from the emptied and contracted uterus results in a further increase in preload with

F. L. Lorini (✉) · C. Viviani
Department of Anesthesia and Intensive Care Medicine, ASST Papa Giovanni XXIII, Bergamo, Italy
e-mail: llorini@asst-pg23.it; cviviani@asst-pg23.it

venous return of blood to the maternal circulation (approximately 500 mL). This effect can cause cardiac output to increase by 60–80%. Delivery of the placenta increases afterload by removing this low-resistance vascular bed. Most haemodynamic changes of pregnancy resolve by 2 weeks postpartum.

47.3 Heart Remodelling

During normal pregnancy, the progressive and marked increase in left ventricular stroke volume (as a high-output state) can result in an increased velocity across valves, which may falsely increase systolic or diastolic gradients. The normal flow murmur of pregnancy is typically soft (grade 1 or 2), located at the pulmonic region, associated with a normal first and second heart sound, and is not accompanied by a diastolic murmur or signs of heart failure. As the heart enlarges, the mitral, tricuspid and pulmonary annuli dilate and small functional atrioventricular regurgitations may appear through these valves. As left ventricular volume increases and the position of the mitral valve leaflets changes with respect to one another, pre-existing mitral regurgitation due to mitral valve prolapse may actually improve during pregnancy. During gestation, a small pericardial effusion haemodynamically non-significant is not necessarily indicative of pathology.

47.4 Echocardiography

Echocardiography is, by far, an important tool during pregnancy and the preferred diagnostic exam to evaluate pregnant women with cardiac disease due to its availability, accuracy and safety with no risk of radiation to the mother and the foetus. A transthoracic echocardiogram provides both qualitative and quantitative information; in addition it can help to stratify maternal risk during pregnancy and consequently to choose the correct management. Depending on the underlying cardiac abnormality, serial echo examinations rather than a single study may be indicated.

The following conditions are indications to perform an echocardiogram in a pregnant woman:

1. Cardiac complaints including shortness of breath and palpitations out of proportion to what is expected in a normal pregnancy to exclude a diagnosis of a new cardiac disease
2. Pre-existing hypertension to evaluate systolic and diastolic cardiac function
3. Known heart disease (congenital heart disease, cardiomyopathy, ischemic heart disease, valvular heart disease, arrhythmia) to exclude residual defects that need intervention and to evaluate maternal risk
4. Known aortic root dilatation to stratify risk of rupture and decide management
5. Stroke of unknown aetiology
6. A prior history of chemotherapy or radiation in a woman to evaluate cardiac function

MRI (without gadolinium) should be considered if echocardiography is insufficient for diagnosis, and it can be safely performed after the first trimester.

47.4.1 Echocardiographic Findings

The echocardiographic changes during pregnancy are based on the morphological and physiological adaptation of the human heart to transient preload and afterload changes. The main features are detailed in Table 47.1.

Healthy pregnancy is associated with prolonged cardiac volume overload secondary to increased blood volume that results in a reversible "physiologic" eccentric left ventricular (LV) hypertrophy with the aim of preserving adequate oxygen supply. Starting from as early as 12 weeks of gestation, LV wall thickness increases by about 15–25% to minimize wall stress and maintain myocardial oxygenation; LV wall mass increases by about 50% above pre-pregnancy values mainly during the third trimester (increase in both LV mass and left ventricle mass index). The LV mass increases result from the increased LV end-diastolic and end-systolic diameters (about 12% and 20%, respectively), increased LV posterior wall diastole and systole (about 22%

Table 47.1 Echocardiographic findings during pregnancy

Echocardiographic variables	Changes during pregnancy
Left ventricular dimension and volume	Increases
Left ventricular wall thickness and left ventricular mass	Increases
Left ventricular ejection fraction	Unchanged
Left ventricular fractional shortening	Unchanged
Left ventricular radial and longitudinal strain rate	Increases
Aortic root diameter	Mildly increases
Right ventricular dimension and volume	Increases
Right ventricular ejection fraction	Unchanged
Left atrial size and volume	Increases
Stroke volume (as measured using pulsed wave Doppler)	Increases
Mitral E wave velocity	Increases and then decreases
Mitral A wave velocity	Increases
Peak pulmonary artery systolic pressure estimated using tricuspid regurgitation jet	Unchanged

and 13%, respectively) and intraventricular septal thickness during diastole and systole (about 15% and 19%, respectively). Similar to the LV, the right ventricle (RV) increases in size throughout pregnancy because of increased preload. Sphericity index decreases during pregnancy, indicating a more spherical shape of the left chamber towards the third trimester. This physiologic cardiac remodelling resolves in the first weeks postpartum.

47.4.1.1 Left Atrium

Left atrium acts as a reservoir, a conduit and a booster pump during the cardiac cycle. The left atrium dimensions and function are enhanced gradually in pregnancy, as an adaptive response to increased preload. These changes cause a gradually improved atrial contribution to ventricular filling, so as to maintain adequate LV stroke volume and cardiac output. These findings result in a slightly lower tissue Doppler *E* velocity and ascended tissue Doppler *A* wave. The speckle-tracking echocardiography as well shows an improved left atrium reservoir and booster pump function; concerning the conduit function the speckle-tracking echocardiography shows it is decreased. However, all these changes are reversible.

47.4.1.2 Left Ventricular Function

The data regarding systolic LV function during normal pregnancy are conflicting. The debate is still open whether the LV function deteriorates as a consequence of the physiological changes during pregnancy (comparable to exercise-induced cardiac remodelling) or has no changes or is enhanced in pregnancy. Regarding diastolic function, E wave and A wave are increased, as a result of the over preload and increased blood volume. The E/A ratio and E'/A' ratio decrease, while the E/E' remains into normal range.

47.4.1.3 Right Ventricular Function

There are too few echocardiographic studies that evaluate RV function during normal pregnancy.

47.5 Hypertensive Disorders

Paradigmatic examples of the utility of echocardiography in pregnancy are the hypertensive disorders. Echocardiography has the potential to categorize patients with gestational hypertension or preeclampsia into high- and low-risk groups. Women with increased LV mass are more likely to have complications. Reduced *e'* and therefore elevated E/e' may be an early predictor of preeclampsia. Echocardiography can also help to identify the small numbers of women with LV systolic dysfunction who are more likely to deteriorate during pregnancy or postpartum. In addiction the use of 3D speckle tracking confirms the known LV remodelling and changes in LV function and allows additional detection of earlier abnormal radial and longitudinal strain values in early preeclampsia compared to late preeclampsia.

47.6 Valvular Heart Diseases

The main features are detailed in Table 47.2.

47.7 Congenital Heart Diseases

The main features are detailed in Table 47.3.

Table 47.2 Management of pregnant women with valvular diseases

Valvular disease	Pathophysiology	Considerations	Diagnostic assessment	Management	Labour and delivery
Mitral stenosis (MS)	Elevated transmitral gradient due to the physiological rise in blood volume, cardiac output and heart rate Increase in left atrial pressure and left atrial dilatation can cause arrhythmias Cardiac complications: dyspnoea, decreased exercise capacity, orthopnoea, paroxysmal nocturnal dyspnoea, pulmonary oedema or less frequently arrhythmias	Gradient and PAP have a prognostic value (do not directly reflect the severity of MS during pregnancy) Guidelines advise against pregnancy for a woman with valve area <1.1 cm^2 or who has significant pulmonary hypertension Haemodynamic deterioration more often happens towards the end of the second or beginning of the third trimester, when maternal blood volume and cardiac output peak	Echocardiography to confirm the diagnosis and to determine the severity of the stenosis and assessment of pulmonary pressures, right ventricular function, mitral regurgitation and the configuration of the subvalvular apparatus Monthly/bimonthly clinical and echocardiographic follow-up, depending on haemodynamic tolerance Trimester evaluation and prior to delivery in mild MS Invasive diagnostic testing is rarely indicated	NYHA class II to IV symptoms or severe pulmonary hypertension (defined as pulmonary artery pressure >75% of systemic pressure) should be referred for prophylactic percutaneous mitral balloon valvotomy (PMBV) or open commissurotomy before conception Medical therapy directed at the treatment of volume overload (diuretics) and to attenuate the increases in heart rate and prolong the diastolic filling period (β-blockers)	Vaginal delivery (shortening of the second stage of labour and assisted delivery) in mild MS and in moderate or severe MS in NYHA I/II without pulmonary hypertension Epidural analgesia to reduce fluctuations in HR and CO Caesarean section for obstetrics considerations and in moderate or severe MS in NHYA III/IV or with pulmonary hypertension despite medical therapy Invasive haemodynamic monitoring for women with moderate to severe MS or symptoms of heart failure During the first two stages, successive uterine contractions lead to an increase in atrial pressures The most vulnerable time is immediately after delivery: an abrupt increase in venous return, and therefore left atrial pressure, may lead to acute pulmonary oedema (haemodynamic monitoring for 12–24 h after the delivery)
Aortic stenosis (AS)	Increased gradient across the aortic valve due to an increase in stroke volume and in CO and a fall in peripheral resistance The clinical consequences of the increased aortic gradient depend on the degree of pre-existing LV hypertrophy and LV systolic function	Mild-to-moderate AS with preserved LV function usually is well tolerated during pregnancy Symptoms (dyspnoea, angina pectoris, syncope) usually become apparent late in the second trimester or early in the third trimester	Echocardiography can confirm diagnosis, detect LV hypertrophy and estimate ejection fraction and LV dimensions Monthly/bimonthly cardiac evaluations in severe AS Women with EF <55% are at high risk for developing heart failure during pregnancy In case of a congenital maternal AS, foetal echocardiography is indicated	Exercise testing is recommended in asymptomatic patient before pregnancy (to evaluate exercise tolerance, BP response, arrhythmias) Medical therapy (preload reduction) Aortic valve replacement and palliative aortic balloon valvuloplasty (with associated maternal and foetal risk)	Vaginal delivery with assisted second stage of labour in non-severe AS, avoiding a decrease in peripheral vascular resistance in case of regional analgesia Caesarean delivery with general anaesthesia is recommended in severe symptomatic AS (intrapartum increases in CO related to contractions may significantly increase the risk of cardiac events) Haemodynamic monitoring is strongly recommended for labour and delivery in moderate and severe AS

Mitral and aortic regurgitation	Reduced regurgitant volume due to the physiological fall of systemic vascular resistance, both from widespread vasodilatation and by virtue of the low-resistance placental circulation. The increase in blood volume is likely only to cause a modest increase in pressure of an already dilated left atrium	Generally well tolerated. Severe regurgitation with LV dysfunction is poorly tolerated (high risk of heart failure)	Doppler echocardiography is useful in diagnosis, evaluation of the structure of the valve and subvalvular apparatus (papillary muscle, chordae tendineae), assessment of left ventricular size and function, left atrial size and left atrial appendage thrombosis. Every trimester follow-up in mild/moderate regurgitation, more often in severe regurgitation	Medical therapy. Surgical repair. Women with pulmonary arterial pressure greater than 50 mm Hg are at increased risk for complications	Vaginal delivery. Epidural analgesia and shortened second stage in symptomatic patients
Pulmonary stenosis (PS)		Generally well tolerated. Severe stenosis may result in RV failure and arrhythmias. Increased incidence of maternal obstetrics complications, particularly hypertension-related disorders including (pre-)eclampsia	In mild and moderate PS (low-risk lesions): follow-up once every trimester. In severe PS: monthly/ bimonthly cardiac evaluation including echocardiography (RV function)	Balloon valvuloplasty should be performed in severe stenosis (peak Doppler gradient >64 mmHg)	Vaginal delivery in non-severe PS or severe PS in NYHA class I/II. Caesarean section in severe PS and in NYHA class III/IV
Pulmonary regurgitation		Independent predictor of maternal complication, especially in case of concomitant impaired ventricular function		Pre-pregnancy valve replacement in symptomatic women or in RV abnormal function due to severe pulmonary regurgitation	
Tricuspid regurgitation					Vaginal delivery

Table 47.3 Management of pregnant women with congenital heart diseases

	WHO* class 1	WHO *class II	WHO *class III	WHO* class IV
Type of lesion	Mild pulmonary stenosis Small patent ductus arteriosus (PDA) Repaired atrial septal defect (ASD) Repaired ventricular septal defect (VSD) Repaired PDA Repaired total anomalous venous drainage	Unrepaired ASD Unrepaired VSD Repaired tetralogy of Fallot (TOF) Repaired aortic coarctation (COAO)	Systemic right ventricle (RV): e.g. atrial switch with Mustard or Senning for TGA Fontan operation for univentricular heart Complex CHD repaired Cyanotic CHD	Pulmonary hypertension Native severe aortic coarctation
Physiopathology	As normal pregnancy	Left to right shunt (ASD, VSD) Risk of pulmonary hypertension (ASD, VSD) Obstruction to pulmonary flow with high pressure in RV (TOF repaired) RV function (ASD, TOF) Arrhythmias (ASD, TOF) Hypertension (COAO)	Right to left shunt RV function Arrhythmias Coronary problems (in particular TGA) Embolism	
Echo	As normal pregnancy	Every trimester, to rule out residual lesions and evaluate heart function	Every 2 weeks or monthly, to rule out residual lesions and evaluate heart function	
Pregnancy	Not avoided	Low to moderate risk	High risk	Counsel to avoid pregnancy
Delivery	Vaginal delivery	Vaginal delivery		
Management	Not necessarily in a specialized centre with a specialized team	Counselling and first visit in a specialized centre with a congenital grown up (GUCH) unit. If not high risk pregnancy or residual lesion, delivery can happen also in a centre without a specialized team	Only in specialized centre with a GUCH unit	

General considerations:

Vaginal delivery is preferable and safer

Labour may be induced with good pain control (incremental epidural analgesia)

Labour can be conducted with the mother in left lateral position to avoid inferior caval compression and maintain venous return

Maternal ECG monitor should be performed to detect any arrhythmia during labour and puerperium

Continuous pulse oximetry is useful

Intra-arterial monitors can be an option in some circumstances (e.g. cyanotic heart disease)

Caesarean section (preferably planned) in case of:

Obstetric consideration

Patient on Coumadin (to avoid risk of foetal intracranial haemorrhage)

Severe obstructive lesions (to minimize the haemodynamic perturbations)

Aortopathy with unstable aorta (to minimize the haemodynamic perturbations)

Severe pulmonary hypertension

The duration of postpartum monitoring must be individualized. For WHO class III or IV should be continued at least 24 h after delivery in an ICU

Suggested Reading

Castleman JS. Echocardiographic structure and function in hypertensive disorders of pregnancy a systematic review. Circ Cardiovasc Imaging. 2016;9:1–13.

Greutmann M, Pieper PG. Pregnancy in women with congenital heart disease. Eur Heart J. 2015;36:2491–9.

Liu S, et al. Echocardiography in pregnancy: part 1. Curr Cardiol Rep. 2016;18:92.

Melchiorre K, et al. Cardiac structure and function in normal pregnancy. Curr Opin Obstet Gynecol. 2012;24:413–21.

Regitz-Zagrosek V, et al. ESC guidelines on the management of cardiovascular diseases during pregnancy. Eur Heart J. 2011;32:3147–97.

Waksmonski CA. Cardiac imaging and functional assessment in pregnancy. Semin Perinatol. 2014;38:240–4.

Warnes CA. Pregnancy and delivery in women with congenital heart disease. Circ J. 2015;79:1416–21.

Part V

Ultrasound in the ICU: Other Applications

Echocardiography and Advanced Life Support

48

Simone Cipani, Rita Cammelli, Sara Felici, and Mauro Cavuta

Key Points
- Unstable patient
- Sudden cardiac arrest
- Shockable rhythms
- Non-shockable rhythms

48.1 Unstable Patient

Echocardiography has shown to be an essential diagnostic tool in the critically ill patient's assessment. In this scenario the initial fluid therapy, such as is recommended in the actual guidelines, not always provides the desired results and maintains a considerable incidence of cardiorespiratory failure. Echocardiography can counsel us on these patients' clinical handling, not only the initial fluid therapy but also on the best-suited election of the vasoactive-inotropic treatment and the early detection of complications.

The Intensive Care Society recommends Focused Intensive Care Echocardiography (FICE) certification as a basic competency for intensivists. Operators are taught to be able to assess left and right ventricular function, the presence of pericardial effusion, the inferior vena cava size, and any valve thickening or unusual morphological appearance. There are some important protocols (FEEL and FOCUS) that are aimed at teaching basic echocardiogram skills for the acute setting.

As the intensivist is faced with periarrest conditions, rapid and safe interpretation of the clinical picture may improve patient outcome. Physical examination has been shown to be unreliable in differentiating hypovolemic from cardiogenic causes of hypotension. Goal-directed echocardiography most frequently aims to rapidly identify and differentiate the cause of hemodynamic instability and/or the cause of acute respiratory failure.

Faced with a patient with hemodynamic instability, dyspnea, and hypotension, what kind of informations are obtainable with a goal-directed echocardiography scan?

1. *Systolic and diastolic function:* an apical four-chamber or parasternal short-axis (PSSAX) view on medium papillary muscles may show significant reduction of systolic and diastolic function. This condition can explain coronary artery disease (CAD), acute

S. Cipani (✉) · R. Cammelli · S. Felici
Department of Anesthesia and Intensive Care, Santa Maria Nuova Hospital, Florence, Italy
e-mail: simone.cipani@uslcentro.toscana.it; rita.cammelli@uslcentro.toscana.it; sara.felici@uslcentro.toscana.it

M. Cavuta
Department of Anesthesia and Intensive Care, SS Maria Annunziata Hospital, Florence, Italy
e-mail: mauro.cavuta@uslcentro.toscana.it

coronary syndrome, systemic hypoperfusion with oliguria, or dyspnea for a reduced compliance of the left ventricle (increased of left sections' filling pressure).

2. *Low systolic and diastolic volumes:* a quick scan with the apical four-chamber may show significant reduction of systolic and diastolic volumes of the left ventricle (kissing ventricle) and a reduced size of all the other cavities with limited opening of valvular structures. With the subcostal window, a reduced diameter (less than 1 cm in spontaneous breath and <1.5 cm in mechanical ventilation) of the vena cava together with a complete inspiratory collapse allows us to confirm the diagnosis of hypovolemia, justifying an aggressive immediate fluid resuscitation.

3. *Pericardial effusion and tamponade:* the diagnosis of tamponade can be suspected in case of jugular turgor, tachycardia, tachypnea, pulsus paradoxus, hypotension, and cardiac arrest, but the ultrasonographic assessment may greatly help to establish the right diagnosis and confirm this suspicion in the presence of hemodynamic instability. The echocardiographic findings are essentially pericardial effusion, interference with diastolic filling and compression of the right sections resulting in decreased cardiac output, and marked respiratory excursion in Doppler right-sided heart preload and ejection. Moreover, ultrasound-guided pericardial drainage is much safer than any blind technique.

4. *Acute cor pulmonale:* the quick ultrasonography assessment may document significant dilatation of the right sections. This imaging assumes a high probability of pulmonary embolism in the absence of significant valvular disease or previous ventricular or pulmonary diseases (check with subcostal view the end-diastolic thickening of the right ventricle free wall; if <0.5 cm normal value; if >0.5 cm can be expression of a chronic increase of pulmonary pressures). Acute cor pulmonale ensues as more than two thirds of the pulmonary arterial bed is blocked because of an embolus.

The diagnosis of thromboembolism has a clear therapeutic implication (immediate thrombolysis).

5. *Lung ultrasound:* dyspnea is a frequent symptom in critically ill patient that often requires medical evaluation and a rapid, precise assessment, because inappropriate diagnosis and treatment have a strong association with mortality. It can be performed easily with any commercially available 2D scanner, with any transducer (phased array, linear array, convex, microconvex). Lung ultrasound has recently emerged as a noninvasive tool to differentiate acute heart failure from non-cardiogenic dyspnea.

48.2 Sudden Cardiac Arrest (SCA)

Sudden cardiac arrest (SCA) is one of the leading causes of death in Europe. Depending on how SCA is defined, about 55–113 per 100,000 inhabitants a year or 350,000–700,000 individuals a year are affected in Europe. On initial heart rhythm analysis, about 25–50% of SCA victims have ventricular fibrillation (VF), a percentage that has declined over the last 20 years. It is likely that many more victims have VF or rapid ventricular tachycardia (VT) at the time of collapse, but by the time the first electrocardiogram (ECG) is recorded by emergency medical service, their rhythm has deteriorated to asystole. It's fundamental an immediate recognition of loss of consciousness and to start cardiopulmonary resuscitation (CPR) as soon as possible because "time is brain." The recommended treatment for VF cardiac arrest is immediate bystander CPR and early electrical defibrillation. Most cardiac arrests of non-cardiac origin have respiratory causes, such as drowning (among them many children) and asphyxia. Rescue breaths as well as chest compressions are critical for successful resuscitation of these victims (Fig. 48.1).
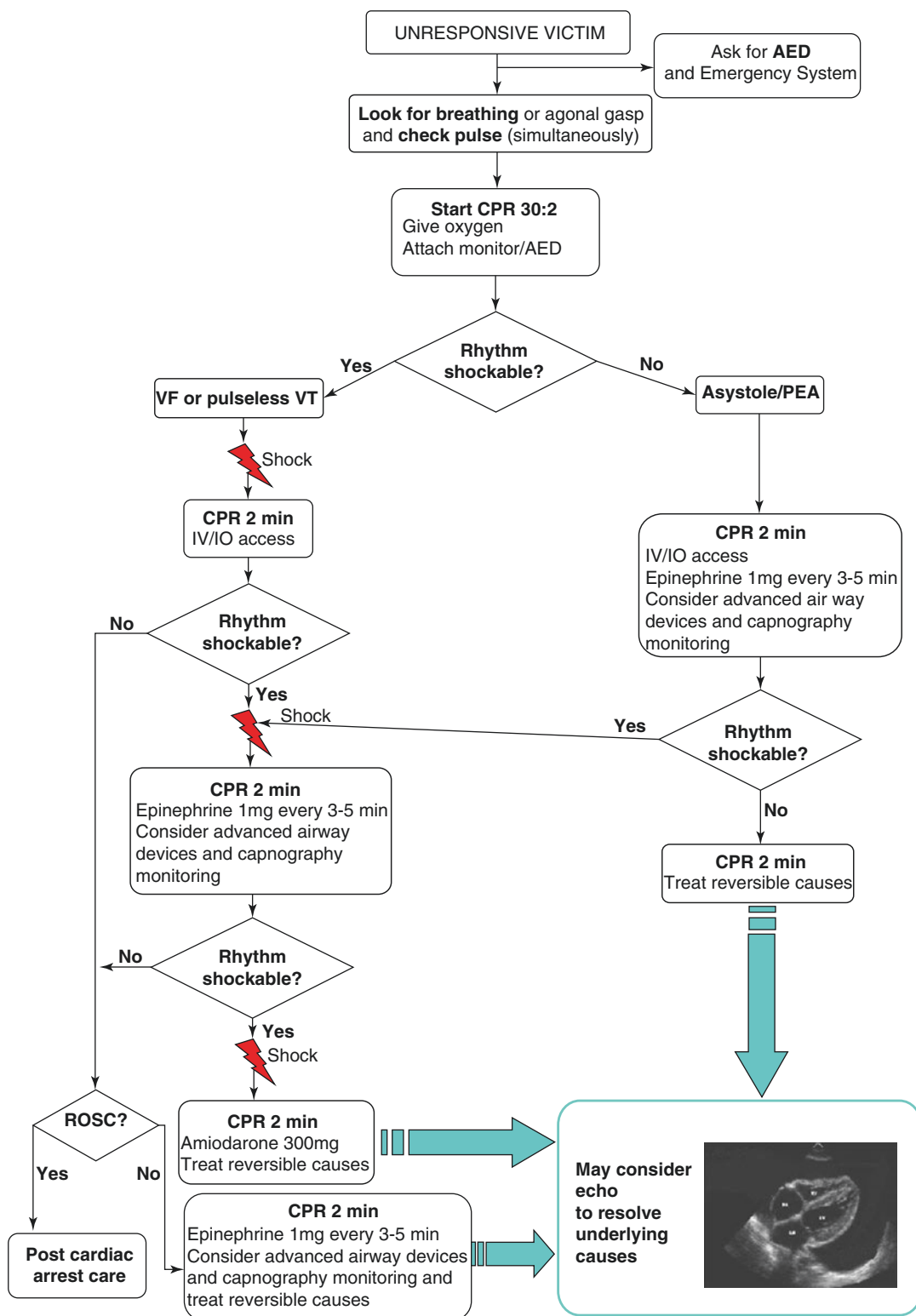
Fig. 48.1 Algorithm for sudden cardiac arrest

48.3 Shockable Rhythms

A cardiac arrest can present anywhere, any time on the street or at home, but also in the emergency department, medical ward, intensive care unit, operating theatre, catheterization suite, or imaging department. Therefore, optimal performance depends on rigorous pre-event interdisciplinary collaborative planning and practice. Excellent outcomes can occur after well-choreographed, high-quality CPR with effective chest compressions, ventilation, and early defibrillation. Hospital leaders have the opportunity to optimize outcomes with rigorous resuscitation programs that include the cycle of quality improvement: measurement of performance and outcomes, comparison, interventions to improve outcomes, and continuous measurement of performance and outcomes after interventions. It is very important to know that the pathophysiological bases of cardiac arrest differ depending on whether this occurs outside the hospital (OHCA, out-of-hospital cardiac arrest) or inside the hospital (IHCA, in-hospital cardiac arrest). OHCA generally starts with a shockable rhythm (ventricular fibrillation/pulseless ventricular tachycardia) due to an acute event. IHCA is attributed to a progressive deterioration of vital functions related to hypoxia, systemic hypoperfusion, and electrolyte imbalance. Its onset is generally characterized by a non-defibrillable rhythm (asystolia or pulseless electrical activity, PEA). As mentioned in the last American Heart Association guidelines (2015), the management of cardiac arrest by any cause must be aimed at resolving the underlying cause (hypoxemia, hypovolemia, electrolyte imbalance, coronary thrombosis, pulmonary thrombosis, hypertensive pneumothorax, cardiac tamponade). Despite the wide implementation of structured basic life support and advanced cardiac life support training and quality improvement activities, the outcome of patients with a shockable rhythm is 40% (survival rate); patients with PEA have an even lower survival rate (6%). Given the high mortality rate of non-shockable rhythms, close vital parameters and prompt correction of underlying causes of cardiac arrest are crucial.

Overall, less than 8% survived an OHCA. Recently, POC (point-of-care ultrasound) focused echocardiography has been used to aid in diagnosing correctable causes of cardiac arrest, prediction outcome, and decision-making of termination resuscitation.

48.4 Non-shockable Rhythms

As previously mentioned non-shockable rhythms are characteristic of in-hospital cardiac arrest (IHCA). The incidence of PEA has increased during the recent two decades. While intensivists struggle to cope with this challenging issue, PEA still carries out a low survival rate. Actually, few studies have assessed the role of transthoracic echocardiography along with CPR, and its real effect to improve survival remained doubtful.

48.5 Conclusion

Currently, the optimal approach to manage patients in PEA cardiac arrest state is detecting the reversible causes including hypovolemia, cardiac tamponade, pulmonary emboli, tension pneumothorax, acidosis, electrolyte imbalance, and hypothermia. However, differentiating all etiologies solely based on physical examination is ineffective and inaccurate. Point-of-care focused echocardiography can be used to identify reversible causes of PEA and predict short-term outcome. In these patients with a low pretest probability for return of spontaneous circulation (ROSC), the absence of spontaneous cardiac movement on echocardiography can predict a low likelihood of survival and guide the decision of resuscitation termination.

Further Reading

Chardoli M, et al. Echocardiography integrated ACLS protocol versus conventional cardiopulmonary resuscitation in patients with pulseless electrical activity cardiac arrest. Chin J Traumatol. 2012;15(5):284–7.

Gray R, et al. Diagnostic echocardiography in an unstable intensive care patient. Echo Res Pract. 2015;2(1):K11–6.

Mark S, et al. Adult advanced cardiovascular life support 2015 American Heart Association guidelines update for cardiopulmonary resuscitation and emergency cardiovascular care. Circulation. 2015;132(suppl 2):S444–64.

Walley P, et al. A practical approach to goal-directed echocardiography in the critical care setting. Crit Care. 2014;18(6):681.

Ultrasound-Guided Central and Peripheral Vein Cannulation

49

Fulvio Pinelli and Antonio Franco

49.1 Introduction

During the last 30 years, there has been an increasing use of ultrasound (US) guidance for central and peripheral vascular access. Multiple studies have demonstrated that US-guided cannulation improves safety, efficiency, and efficacy compared to "blind" techniques (landmarks), and guidelines strongly recommend its use in clinical practice. In fact, the use of echography has several advantages over the old fashion and no more recommended "blind" technique. Allowing the evaluation of vessel depth, the relationship with other structures as arteries and nerves, and needle visualization, US reduce both immediate and long-term complications related to venipuncture. In particular, evidence exists that US significantly reduce mechanical complications related to central venous catheter procedures, such as arterial puncture, pneumothorax, hemothorax, and malposition. US-guided venipuncture not only minimizes immediate complications but also reduces long-term complications, such as catheter-related blood stream infections (CRBSI)

and thrombosis. This is because US reduce a number of attempts, time of the procedure, and therefore the contamination risk of the insertion site during positioning. Moreover, they limit by the maximum extent the endothelial damage and the risk of hematoma, which are both related to an increased risk of insertional thrombosis. In addition, to reduce the risk of thrombosis, US allow the evaluation of the vein with the greater diameter, in respect to catheter dimensions.

49.2 Terminology

Central vascular access devices (CVADs) are identified by localization of the catheter tip at the inferior third of superior vena cava, cava-atrial junction (CAJ), and superior third of right atrium. Thus, according to the new nomenclature proposed by the World Congress of Vascular Access (WoCoVA) based on the insertion site, we are able to classify CVADs in CICC (centrally inserted central catheters), PICC (peripherally inserted central catheters), and FICC (femorally inserted central catheters). FICC, even if its tip is not "central" since it lays in inferior vena cava, can be considered "central" for infusion purposes. All other cases in which vascular access tip does not lay at the CAJ or in the inferior vena cava have to be considered peripheral (e.g., a midline is a peripheral catheter).

F. Pinelli
Center for Vascular Access, Department of Anesthesia and Intensive Care, Careggi University Hospital, Florence, Italy

A. Franco (✉)
Anesthesia and Intensive Care Department, Santa Maria Nuova Hospital, Florence, Italy
e-mail: antonio.franco@asf.toscana.it

Fig. 49.1 Right internal jugular vein (*RIJV*) overlapping the carotid artery (*CA*). (From Sarti A. Ecocardiografia per l'intensivista. Springer Verlag Italia srl, Milano, 2009, with permission of the publisher and the author)
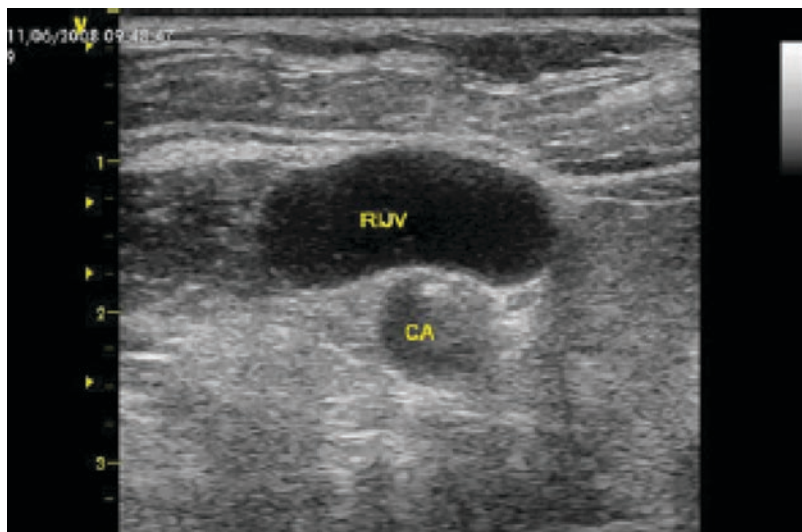
49.3 Indications

For safe administration of solutions with pH greater than 9 or lower than 5 as well as an osmolality above 600–800 mOsm/L, guidelines strongly recommend CVADs. CVADs are also indicated for monitoring purposes (central venous pressure, central venous oxygen saturation, pulmonary artery pressure, etc.), in the case of multiple infusates or patient's instability, frequent blood samplings, and hemodialytic treatment. In all other cases, a peripheral access may be indicated.

49.4 Principles of Vein Echo-Anatomy and US-Guided Venipuncture Technique

US-guided insertion of CVADs implies (1) recognition of the principal vascular and nerve structures in the region of venipuncture and (2) knowledge of appropriate US-guided venipuncture techniques.

Linear echographic probes with a length of 28–36 mm and a frequency of 7.5–13 MHz accomplish vessel visualization, since neck/chest veins and, even more, arm veins are quite superficial (1–2 cm deep the internal jugular, 3–4 cm axillary, 0.5–2 cm arm veins). In short axis, veins appear as compressible, circular, hypo-echogenic structures with hyper-echogenic borders. Compressibility distinguishes a vein from an artery.

For central vein cannulation, neck and chest vein diameters and depth are systematically evaluated. In particular, internal jugular vein is visualized at mid (Fig. 49.1) and low neck, just above the clavicle, in its short axis. The probe tip is then tilted toward the chest to explore the brachiocephalic vein in its long axis. Afterward, the operator slides the probe laterally onto the supraclavicular fossa, to visualize subclavian and external jugular (long axis). Once done, the axillary vein in its short and long axis (Fig. 49.2) is explored below the clavicle.

Appropriate veins for US-guided peripheral cannulation and suitable for PICC or midline insertion are located at the median third of the arm. They are the (1) basilic vein, which runs rectilinearly along the bicipital-humeral fossa, away from arterial and nervous structures; (2) brachial veins, inside of the vascular-nervous bundle of the arm (here, at an echographic exam, they typically appear as circular images located on each side of the brachial artery: the resulting image is often referred as the "Mickey Mouse" head, where brachial artery is the face and the brachial veins are the ears (Fig. 49.3); and (3) cephalic vein.

Fig. 49.2 Right axillary vein (*RAxV*) in the long axis and a little lower the pleural line (*PL*). (From Sarti A. Ecocardiografia per l'intensivista. Springer Verlag Italia srl, Milano, 2009, with permission of the publisher and the author)
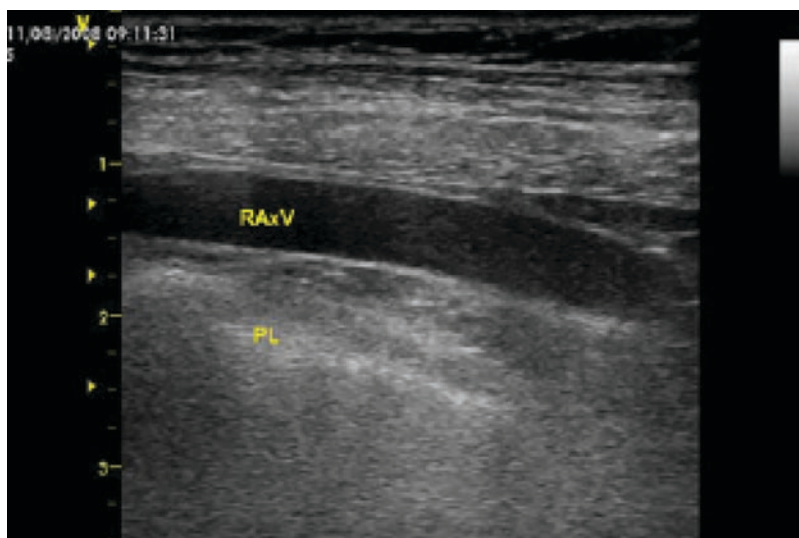
Fig. 49.3 Arm veins and brachial artery with a Mickey Mouse shape. *OA* brachial artery, *BV* basilic vein, *BrV* brachial vein. (From Sarti A. Ecocardiografia per l'intensivista. Springer Verlag Italia srl, Milano, 2009, with permission of the publisher and the author)
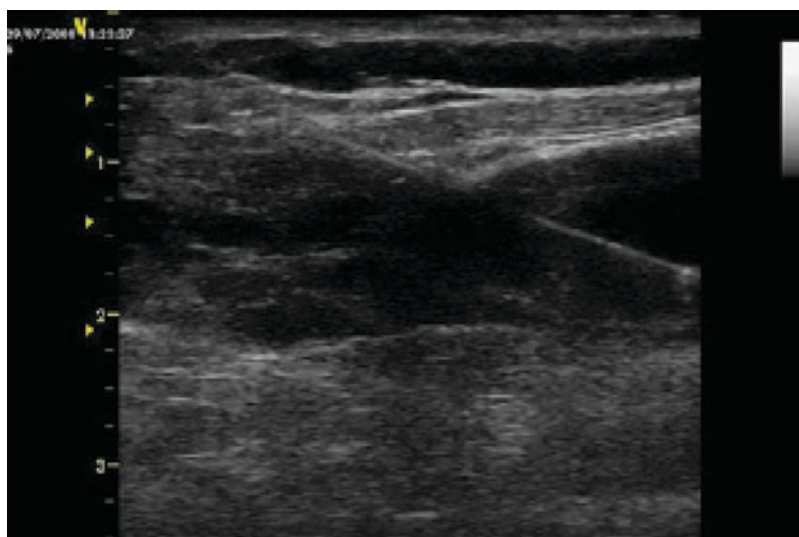
In order to apply properly US-guided venipuncture techniques, it is fundamental to understand spatial relationships between the vein, the probe, and the needle. In terms of vein to probe spatial relationship, we identify short-axis (the principal axis of the vein is perpendicular to the echo beam) and *long-axis* visualization (the principal axis of the vein is parallel to the echo beam). *Short axis* has the advantage of a "panoramic view" of the target vein but also of the adjacent structures (nerves, arteries, etc.). In terms of needle to probe spatial relationship, it is possible to distinguish *in-plane* (when the needle trajectory is all inside the echo beam plane) versus *out-of-plane* venipuncture (when the needle trajectory is out of the echo beam plane). The obvious advantage of in-plane venipuncture is the possibility to visualize the whole needle during its advancement, reducing the risk of accidental damage of other structures. Theoretically, every combination is possible between short axis/long axis and in-plane/out-of-plane. However, clinical experience has selected only three US-guided approaches: (1) in-plane long-axis venipuncture (typically used in cases, it is of utmost importance to avoid trespassing the vein and hitting the pleura, like in

anonymous and subclavian vein venipuncture); (2) out-of-plane short-axis venipuncture (typically used for deep arm veins); and (3) in-plane short-axis venipuncture (the so-called Jernigan infero-lateral approach as modified by Pittiruti) which is limited to internal jugular vein.

49.5   Procedure

In this section, we describe the most used central and peripheral US-guided venipuncture approaches.

Patients should receive clear and comprehensive oral and written information on catheter risks/benefits and explanations on catheter care. Signed consent should be obtained prior to catheter insertion. It is generally accepted that the platelet count should be >50 · 10^3/L and the international normalized ratio (INR) <1.5, prior to the insertion of a catheter other than a PICC or a midline.

A preliminary bilateral ultrasound study is performed following criteria described above. The ergonomic positioning of the operator, probe, and screen with regard to the patient is of utmost importance. The screen must be positioned in front, and not on the side, of the operator. In order to facilitate the cannulation of the vessel, the probe must be held with the non-dominant hand and the benchmark (usually located on the left side of the screen) on the same side of the operator. According to guidelines, the operator must perform surgical handwashing and use maximal sterile barriers (cap, mask, sterile gown, and gloves). After disinfection with 2% chlorhexidine in isopropyl alcohol, the operative field is covered with sterile drapes, and the ultrasound probe also must be covered with a sterile sheath.

Internal Jugular Vein (IJV) Cannulation The patient lies supine, face turned in the direction opposite the side of the procedure. In the Jernigan-Pittiruti approach, the probe is placed just above the clavicle and parallel to it. This approach guarantees both the advantage of the short axis in terms of panoramic view and the advantage of the in-plane technique, i.e., the thorough visualization of the needle. Moreover, it allows a very convenient exit site in terms of patient comfort and nursing, maximizing at the same time the distance of the hubs from oral/nasal secretions and hair. Puncture is performed just behind the clavicular head of the sternocleidomastoid muscle with an angle of slightly less than 90° to the vessel, with the needle sliding under this muscle to find the IJV in the space between the sternal and clavicular heads. On the ultrasound screen, the needle is visualized passing through the various planes until it reaches the target, where it pushes the vein's intimal wall inward toward the lumen ("curtain sign") and then punctures it (Fig. 49.4). Blood return should then be obtained into the syringe connected to the

Fig. 49.4 Needle into the vein with a "curtain" sign. (From Sarti A. Ecocardiografia per l'intensivista. Springer Verlag Italia srl, Milano, 2009, with permission of the publisher and the author)
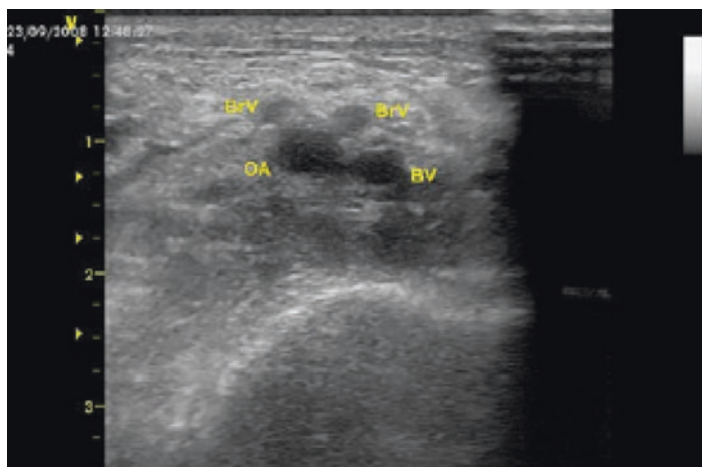
needle. After this, in order to facilitate the insertion of the guide wire, the needle will be moved with great caution and under ultrasound vision toward the vein's major axis. At this point guidewire is inserted 10–15 cm and its position in the anonymous veins checked with US before proceeding to put the dilator and insert the catheter. In our series, this technique has virtually eliminated the risk of pneumothorax.

Axillary Vein Cannulation Although the subclavian vein is not well visible echographically, moving the probe from mid-clavicle to the shoulder, it is possible to visualize the axillary vein. Axillary vein venipuncture can be performed either with a long-axis in-plane technique or with a short-axis out-of-plane technique. Although the former has the advantage of visualizing the needle all the way through, it obliges to a very lateral venipuncture and a too close to the shoulder exit site. Therefore, the latter is preferable, paying attention to the vein's relationship with the axillary artery and pleura. In fact, in order to minimize risk of damaging these structures, a micro-introducer kit is preferable in this approach. In particular, it is advisable to use a 22-gauge echogenic needle, a 0.018 inches nitinol guidewire, and a 5.5 French micro-dilator. Moreover, needle tip should be carefully advanced with a 45–60° inclination, avoiding trespassing the vein. Also, too deep (i.e., > than 3–3.5 cm) or too collapsible veins should be avoided. In order to achieve a better exposition of the vein, it is possible to position the patient's arm slightly abducted. This approach, in expert hands, has several advantages: (1) safe exit site (i.e., far from nasal and oral secretion) especially for those patients with tracheostomy, (2) very good nursing, and (3) patient's comfort. Moreover, in case of accidental puncture of the artery, in respect to subclavian vein, a compression is easier to perform.

For CICC, at the end of the procedure, US can also be used to confirm the absence of pneumothorax by positioning the beam longitudinally in the anterior region of the thorax and looking for the sliding sign. The pleural line is a fundamental sign in chest echography; it is located deeply under rib shadows and is visualized as an echogenic line. It glides with an apparently single movement that is related to lung excursion during breathing (gliding or sliding sign). The gliding sign disappears in the presence of pneumothorax.

Femoral Vein Cannulation The femoral vein is the last choice for higher risk of infectious and thrombotic complications. Guidelines strongly recommend this approach only in emergency situations and to remove the cannula within 48 h. With the probe positioned under the inguinal ligament, it is possible to visualize deep and superficial femoral arteries, the common femoral vein and the saphenous-femoral cross in their short axis. The needle is advanced out-of-plane to the femoral vein.

Arm Vein Cannulation Although the use of echography is fundamental for CICC positioning, it is mandatory for PICC and midline. Patient's arm lies abducted on a table with the operator positioned so that the dominant hand is always lateral to the patient and the probe is held with the non-dominant hand. Veins suitable for cannulation are carefully evaluated in terms of depth, diameter (before applying plastic tourniquet), and relationship with arteries and nerves. The vein of choice is the basilic vein, because it is larger, empties directly into the axillary vein without valves, and has no structures at risk in its proximity (median nerve, brachial arteries). Brachial veins are the second choice, while the cephalic vein is the third one, because it is usually smaller and more superficial and because it empties in axillary vein forming nearly a perpendicular angle. It is often used in obese patients, in which it becomes deeper and more stable. The catheter diameter is carefully chosen in order to respect the ratio catheter/vessel of 1/3. The median third of the arm is the preferred region for venipuncture not only because here veins become deeper and larger but also because it represents a very convenient exit site. In fact, it is far from flexion areas such as the elbow and the axilla and also because it is the less contaminated part of the body. A short-axis/out-of-plane technique is used

Table 49.1 How to position probe and screen with regard to patient

Vein	Operator position	Screen position	
Right IJV	Behind the patient head on the right	On the patient left side	The probe must always be aligned with itsreference on the same side of screenreference
Left IJV	Behind the patient head on the left	On the patient right side	
Right sub V	On the patient right side	Next to patient head to the left	
Left sub V	On the patient left side	Next to patient head to the right	

in this approach. US are also useful in PICC insertion as a tip navigation tool, as they allow the operator to check the catheter do not take wrong roads (as the internal jugular or the contra-lateral subclavian veins) (Table 49.1).

49.6 Conclusion

US-guided peripheral and central cannulation reduces the risk of immediate and long-term complication compared to the traditional "land-mark technique." A prerequisite for the applica-tion of this technology is knowledge of basic vein echo-anatomy and US venipuncture techniques. Internal jugular, axillary, and femoral veins are the most used veins for US-guided CICC place-ment. Basilic and brachial veins are the choices in the case of PICC or midline insertion.

Suggested Reading

Brass P, Hellmich M, Kolodziej L, et al. Ultrasound guid-ance versus anatomical landmarks for internal jugu-lar vein catheterization. Cochrane Database Syst Rev. 2015a;(1):CD006962.

Brass P, Hellmich M, Kolodziej L, et al. Ultrasound guid-ance versus anatomical landmarks for subclavian or femoral vein catheterization. Cochrane Database Syst Rev. 2015b;9(1):CD011447.

Ding W, Shen Y, Yang J, et al. Diagnosis of pneumothorax by radiography and ultrasonography: a meta-analysis. Chest. 2011;140(4):859–66.

Gorsky L, et al. Infusion therapy standards of practice. J Infus Nurs. 2016;(1S):39.

Karakitsos D, Labropoulos N, De Groot E, et al. Real-time ultrasound-guided catheterization of the internal jugular vein: a prospective comparison with the land-mark technique in critical care patients. Crit Care. 2006;10(6):R162.

Lamperti M, Bodhenam AR, Pittiruti METAL. International evidence-based recommendations on ultrasound-guided vascular access. Intensive Care Med. 2012;38(7): 1105–11.

O'Grady NP, Alexander M, Burns LA, et al. Healthcare infection control practices advisory committee (HICPAC). CDC guidelines for the prevention of intravascular catheter-related infections. Clin Infect Dis. 2011;52(9):e162–93.

Sarti A. Ecocardiografia per l'intensivista. Milano: Springer Verlag Italia srl; 2009.

Essential Ultrasound for Venous Thrombosis

50

Federica Marini, Silvia Laviola, Paola Pieraccioni, and Armando Sarti

50.1 Essential Ultrasound for Venous Thrombosis

Deep vein thrombosis (DVT) is a life-threatening complication in intensive care unit (ICU) patients, and DVT incidence is used as a marker of quality care. DVT is a common, serious, often under-recognized diagnosis in the critically ill patient. The prevalence and incidence of pulmonary embolism in the ICU remain unclear.

ICU patients share similar general risk factors for DVT with other patients: age, immobilization, obesity, patient history of personal or familial VTE (venous thromboembolism), past history of cancer, sepsis, stroke, respiratory or heart failure, pregnancy, trauma, or recent surgery.

Additional, specific risk factors for the ICU population are mechanical ventilation, by decreasing venous return and requiring sedation and immobilization that increase the risk of VTE. Although critically ill patients with DVT had a longer duration of mechanical ventilation than those who did not, the causal relationship between length of mechanical ventilation and VTE is unclear. Central venous catheterization is another important risk factor for ICU-acquired DVT, especially when inserted in femoral veins, with a catheter-related thrombosis ranged from 2.2% up to 69%.

Vasopressor administration was found to be an independent risk factor for DVT certainly explained by reduced absorption of subcutaneous heparin-linked vasoconstriction of peripheral blood vessel.

Platelet transfusion and high level of platelets have been identified as risk factor of VTE certain related to increased platelet activation and adherence to vessel walls with subsequent fibrin clot formation, as described in inflammatory processes and sepsis.

The level of risk of VTE in critically ill patients also depends on the underlying illness leading to ICU admission. The importance of any of these clinical risk factors is not completely determined, nor is the role of inherited or acquired coagulation system abnormalities (Table 50.1).

Point-of-care ultrasonography performed at the bedside by critical care physicians is easy and immediate.

F. Marini (✉) · S. Laviola
Anesthesia and Intensive Care Department, Santa Maria Nuova Hospital, Azienda USL Toscana Centro, Florence, Italy
e-mail: federica.marini@uslcentro.toscana.it; silvia.laviola@uslcentro.toscana.it

P. Pieraccioni
Department of Anesthesia and Intensive Care, Santa Maria Nuova Hospital, Florence, Italy

A. Sarti
Department of Anesthesia and Intensive Care, Santa Maria Annunziata Hospital, Florence, Italy

Table 50.1 Venous thromboembolism risk factor

General VTE risk factor	ICU-acquired risk factor
Age	Sepsis
Past history of VTE	Respiratory or cardiac failure
Past history of cancer	Vasopressor use
Immobilization	Pharmacological sedation
Obesity (BMI ≥ 35)	Mechanical ventilation
Pregnancy	Central venous catheter
Trauma, spinal cord injury	End-stage renal failure
Recent surgery	
Stroke	
Thrombophilic state	
Hormone therapy	

50.2 Lower Deep Vein Thrombosis

Lower extremity deep venous thrombosis (DVT) is a major national health problem, with an overall age and sex incidence more than 1 per 1000 annually. Because the incidence is so high and the progression from DVT to pulmonary embolism can lead to significant morbidity and mortality, the ability to rule in or rule out DVT in the emergency department and ICU is paramount.

Focused ultrasound is a sensitive and specific tool for the assessment of patient at risk of DVT. The probe of choice to perform the examination is a 5–10 MHz linear. Two sonographic findings are diagnostic of a venous thrombosis:

- Non-compressibility of the venous segment
- Echogenic intraluminal material

50.3 Compression Strategy

DVT was diagnosed by bilateral lower limb compression ultrasonography (CUS).

Two methods are commonly used: compression and duplex.

- Compression ultrasound works by the principle that normal veins collapse when extrinsic pres-

sure is applied by the sonographer. Using B-mode 2-D imaging and a high-frequency linear transducer, the examiner locates the vessel of interest and performs a compression maneuver using a transverse plane. Considering the adjacent artery as a reference point, full compression of the vein with minimal deformation of the artery indicates the absence of thrombus. If a vein is compressible, the walls of the vessel will join together under direct probe pressure resulting in the disappearance of the vessel lumen (Fig. 50.1).
- Duplex and triplex ultrasound combines compression ultrasound with pulse-wave Doppler (duplex) and both pulse-wave and color Doppler (triplex).

50.4 Intraluminal Material

Most acute thrombi are hypoechoic and not well visualized. If a thrombus is identified within the vessel lumen, a compression maneuver is not necessary and may even be harmful as excessive compression may dislodge the thrombus (Fig. 50.2).

Grayscale images should be recorded without and with compression at each of the following levels, at a minimum. The femoral and popliteal veins should be imaged to the fullest extent possible, and images should be recorded at each of the following level:

- Common femoral vein, medial over the artery (Fig. 50.3).
- Junction of common femoral vein with the great saphenous vein. The proximal deep femoral and proximal great saphenous veins should also be examined.
- Proximal deep femoral vein separately or along with the proximal femoral vein.
- Proximal, mid, and distal femoral vein.
- Popliteal vein: the patient's leg should be positioned at a 45° flexion angle at the knee, and the transducer is placed in the popliteal fossa. The popliteal vein is examined distally to the tibioperoneal trunk.
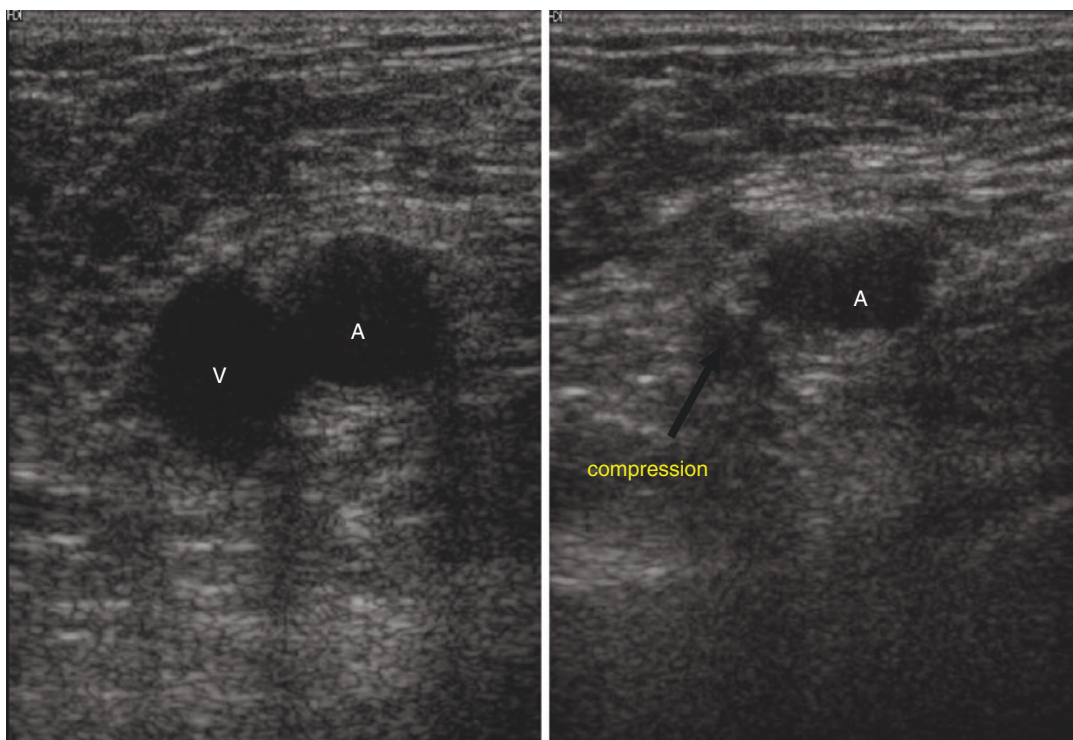
Fig. 50.1   Full compression of the vein indicates the absence of thrombus
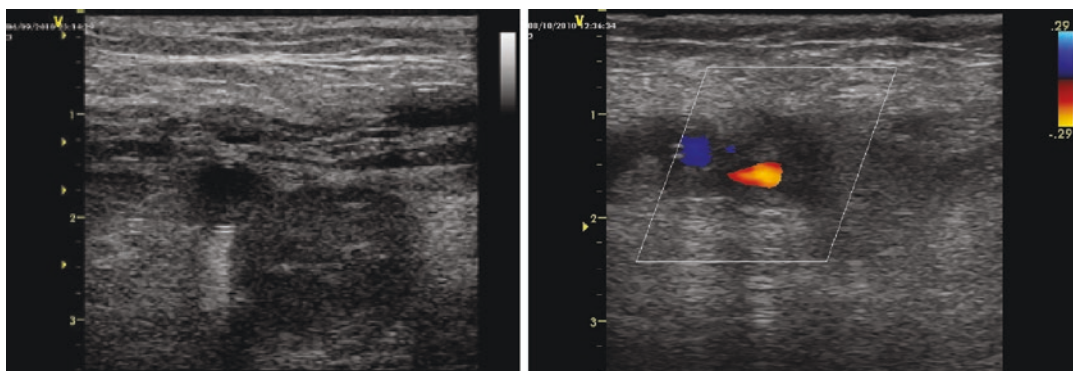
Fig. 50.2   Common femoral vein with a thrombus inside

Venous compression is applied every 2 cm or less in the transverse (short axis) plane with adequate pressure on the skin to completely obliterate the normal vein lumen.

At a minimum (even if the examination is otherwise unilateral), right and left common femoral or right and left external iliac venous spectral Doppler waveforms should be recorded to evaluate for asymmetry or loss of respiratory phasicity.

Both sides should be assessed with similar patient posture so symmetry can be assessed.
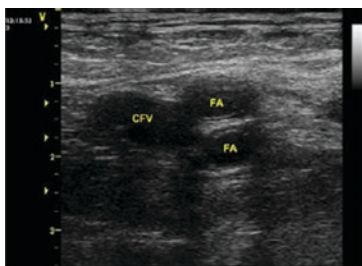
Fig. 50.3 The image shows the common femoral vein (CFV) and the superficial and deep femoral artery (FA) medially

A popliteal venous spectral Doppler waveform of the symptomatic leg should also be obtained. All spectral Doppler waveforms should be obtained from the long axis.

Color or spectral Doppler evaluation can be used to support the presence or absence of an abnormality.

Other vascular and nonvascular abnormalities, if found, should be recorded but may require additional imaging for diagnosis or further characterization. Anatomic variations such as duplications should be noted.

50.5 Vein Thrombosis of the Upper Extremities

Approximately 10% of all cases of vein thrombosis involve the upper extremities, resulting in an annual incidence of 0.4–1 case per 10,000 people. The incidence is increased due to the routine use of central venous catheters and possible cardiac pacemakers and defibrillators.

Axillary and subclavian veins are often involved. Secondary forms, such as catheter-associated thrombosis, cancer-associated thrombosis, surgery or trauma of the arm or shoulder, pregnancy, use of oral contraceptives, and ovarian hyperstimulation syndrome, are more common than primary form (e.g., the venous thoracic outlet syndrome).

Symptoms of deep vein thrombosis of an upper extremity include discomfort, pain, paresthesias, and weakness of the arm. Upper extremity evaluation consists of assessment of subclavian, innominate, jugular, and axillary veins. Duplex Doppler or color Doppler techniques are used to assess venous compressibility, wall thickening, spontaneous venous flow, cardiac and respiratory phasicity of flow, and venous filling defects. Venous compression is applied to accessible veins in the transverse plane with adequate pressure on the skin to completely obliterate the normal vein lumen. Supine position is preferred. Symmetrical posture to prevent false asymmetry, if possible, is preferred.

For each normal examination, at a minimum, grayscale images should be recorded without and with compression at each of the following levels:

- Internal jugular vein
- Peripheral subclavian vein
- Axillary vein
- Brachial vein in the upper arm
- Cephalic vein in the upper arm
- Basilic vein in the upper arm
- Focal symptomatic areas, if present

Color and spectral Doppler images are recorded at each of the following levels using the appropriate color technique to show filling of the normal venous lumen.

Compression ultrasonography, which relies on the finding that a thrombosed vein cannot be compressed, is the preferred imaging test also for patients with suspected deep vein thrombosis of the upper extremity. However, the proximal subclavian and brachiocephalic veins are difficult to visualized because of overlying bony structures. When a proximal subclavian or brachiocephalic thrombosis is suspected, duplex ultrasonography of distal arm veins may reveal an abnormal Doppler pattern with reduced variability or no variability in flow velocity during a Valsalva maneuver.

Complications of deep vein thrombosis, which are less common in the upper extremities than in the lower extremities, include pulmonary embolism, recurrence at 12 months, and the post-thrombotic syndrome. Thrombosis of the axillary and subclavian veins and residual thrombosis at 6 months are associated with an increased risk of post-thrombotic syndrome; the risk is lower for catheter-associated thrombosis as the catheter has been removed under appropriate anticoagulant treatment.

Vascular US is rapid, repeatable, bedside easy-to-perform assessment. The learning curve for intensivist is steep and rapid. Doppler US is currently the goal standard for the diagnosis of venous thrombosis in the emergency and ICU practice.

Suggested Reading

Boddi M, et al. Follow-up after four-year quality improvement program to prevent inferior limb deep vein thrombosis in intensive care unit. Thromb Res. 2014;134:578–83.

Di Bello C, Koenig S. Diagnosis of deep venous thrombosis by critical care physicians using compression ultrasonography the open. Critical Care Med J. 2010;3:43–7.

Fields M, Munish G. Venothromboembolism. Emerg Med Clin N Am. 2008;26:649–83.

Geerts W, Selby R. Prevention of venous thromboembolism in the. ICU Chest. 2003;124:357S–63S.

Kucher N. Deep-vein thrombosis of the upper extremities. N Engl J Med. 2011;364:861–9.

Minet C, et al. Venous thromboembolism in the ICU: main characteristics, diagnosis and thromboprophylaxis. Crit Care. 2015;19:287.

Allen LM, et al. Peripheral Venous Ultrasound Examinations. AIUM practice parameter —peripheral venous ultrasound by the American Institute of Ultrasound in Medicine. 2015.

Lung and Pleural Ultrasonography in Emergency and Intensive Care

51

Federica Marini, Francesca Covani Frigieri, and Diletta Guarducci

For many years, US (ultrasound) was not used for the lung evaluation. Despite of the great use that US has had on various medical disciplines, the dominant opinion of the sonographers, which persists in part, is the incompatibility of the use of US on ventilated organs; according to conventional notions through an organ lung full of air, the US cannot pass. Curiously, this innovation developed from veterinary experiences, when Rantanen described, as the absence of the pleural sliding, the pneumothorax (PNX) in horses [1].

The following year (1987), Wernecke published a study on humans, identifying the absence of sliding in eight subjects with radiological evidence of PNX [2].

In 1997, Lichtenstein proposed the evidence of "comet tails" as a sign of pulmonary interstitial syndrome opening the way for the US definition of interstitial syndrome and pulmonary edema [3].

Over the past 10 years, the knowledge of the use of US for the study of the lung have increased enormously and collected data not only for the evaluation of the pleural space but also for the definition of certain aspects of pathology of the lung.

The pleuropulmonary US, therefore, is becoming an important tool for a more comprehensive approach to the patient, from the early stages of the physical examination; positive characteristics of US are its repeatability, its noninvasiveness, the possibility of being carried out at the bedside, and its ability to give sufficiently accurate and dichotomic answers to medical queries.

Critically ill patients admitted to the intensive care unit (ICU) frequently have limited mobility as a result of their underlying pathology or the invasive devices used for monitoring. Mobilization of ICU patients has long been recognized as a critical issue with high risk for potential complications and adverse events [4, 5].

Significant hemodynamic and respiratory complications may occur during transport to the radiology department in as many as 40–50% of critically ill ventilated patients, so lung US is very useful and is gaining popularity among intensivists (Table 51.1).

Lung US (LUS) can be performed on the whole chest, just laying the probe in the intercostal spaces, avoiding the ribs. The probe can be positioned both longitudinally, perpendicular to the ribs, and obliquely, along the intercostal spaces (Fig. 51.1). The longitudinal approach allows visualization of so-called bat-sign: in a longitudinal view, the "bat-sign" identifies the upper and lower ribs and, a little deeper, the

F. Marini (✉) · F. C. Frigieri · D. Guarducci
Anesthesia and Intensive Care Department, Santa
Maria Nuova Hospital, Azienda USL Toscana Centro,
Florence, Italy
e-mail: federica.marini@uslcentro.toscana.it;
francesca.covanifrigieri@uslcentro.toscana.it;
diletta.guarducci@uslcentro.toscana.it

Table 51.1 Advantages of lung ultrasound in evaluation of critically ill patient

Easy to learn
Fast, noninvasive, and easily reproducible
Portable device and bedside examination
Widely available
Reduces exposure to radiation
Good accuracy
Low cost
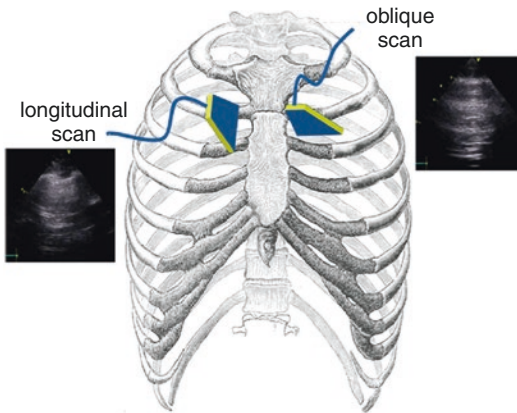
Fig. 51.1 Longitudinal and oblique approach to lung ultrasound. (Gargani and Volpicelli [7])

pleural line. The oblique approach allows visualizing a larger part of the pleural line, which is not interrupted by the rib shadows [6].

Different probes can be suitable for LUS; the choice of the more suitable one depends on the patient size and the suspected pathology. Linear probes have high superficial definition and low penetration capacity due to their high frequency; they are therefore suitable in thin parietal wall patients, mainly in anterior fields, and in pleural pathologies evaluation (i.e., pneumothorax). Convex probes are more suitable to deep pathologies examination (consolidations and pleural effusions). Microconvex probes are more flexible and can be suitable for both superficial and deep pathology evaluation due to their wide frequency range.

LUS is also patient dependent. Obesity, subcutaneous emphysema, and the presence of large thoracic dressings preclude propagation of ultrasound beams from the skin to the lung. LUS cannot detect lung overinflation resulting from an increase in intrathoracic pressures.

51.1 Patient Position

Patient is usually examined in supine/semi-recumbent position with arm abducted to facilitate examination of anterior and lateral chest wall. Lateral decubitus position or minimal tilting with upper limb moved anteriorly is required to expose lateral and posterior chest wall for examination. Dorsal region of lower lobes is better appreciated in lateral decubitus position.

51.2 Echographic Patterns

Echography has elevated sensitivity and specificity for acute pleural diseases such as pneumothorax, hemothorax, and pleural effusions.

In a normally aerated lung, the only detectable structure is the pleura, visualized as a hyperechoic horizontal line. It is debated whether this line represents an artifact due to a reflection phenomenon at the interface between alveolar air and the soft tissues of the thoracic wall or it images the real pleura. The pleural line moves synchronously with respiration: this dynamic horizontal movement is called *lung sliding* and therefore excludes the possibility of pneumothorax. In M-mode images, lung sliding is seen as the "seashore sign," with the static chest wall as waves and the normal lung parenchyma as a beach. This sign highlights the difference between the moving pleura and the motionless chest wall. Beyond the pleural line, normally aerated lungs are seen as artifacts; there are some hyperechoic, horizontal lines arising at regular intervals from the pleural line, the A-line (Fig. 51.2 and Table 51.2). Although A-lines constitute a basic artifact of the normally aerated lung, they are also seen in pneumothorax without lung sliding.

51.3 Pathological Findings

51.3.1 B-Lines

B-lines are hyperechoic lines perpendicular to the pleural lines extending to the bottom of the screen without fading and moving synchronously
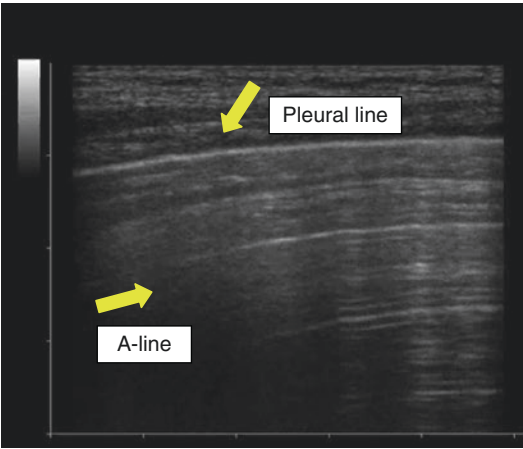
Fig. 51.2 Pleural line and A-lines

Table 51.2 Commonly used terminology in lung US

Terminology	Meaning
Lung sliding	Movement of visceral pleura against parietal pleura during respiration. May exclude pneumothorax
A-lines (Fig. 51.2)	Reverberation artifacts in normal lung
B-lines, comet-tail artifacts, lung rockets	Vertical hyperechoic reverberation artifacts that arise from pleural line. The number of vertical B-lines depends on the degree of lung aeration loss
Consolidation	Massive loss of lung aeration. Hypoechoic tissue structure
Lung pulse	Small movement of the visceral on the parietal pleura induced by heartbeat

with lung sliding. The number of B-lines depends on the degree of lung aeration loss. Their number increases with decreasing air content. The presence of multiple B-lines is directly related to the degree of interlobular septal thickening and the sonographic sign of lung interstitial syndrome. A positive region is defined by the presence of three or more B-lines in a longitudinal plane between two ribs. Fewer than two B-lines can be detected in dependent lung regions even in normally aerated lungs. The sum of B-lines found on each scanning site yields a score, denoting the extent of extravascular fluid in the lung (Fig. 51.3 and Table 51.3) [9].
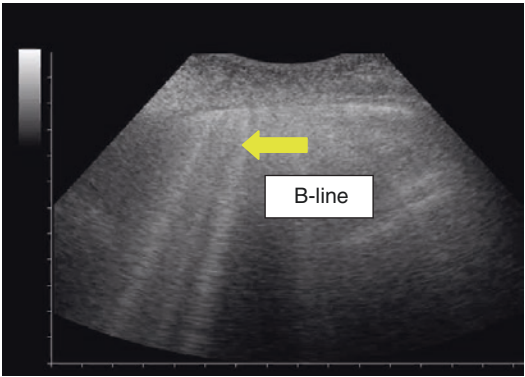
Fig. 51.3 B-lines

Table 51.3 Scoring of B-lines

Score	Number of B-lines	Extravascular lung water
0	≤5	No sign
1	6–15	Mild degree
2	16–30	Moderate degree
3	>30	Severe degree

Modified from Picano et al. [8]

In addition, the number of B-lines is directly proportional to the worsening of functional class of heart failure, to the extravascular lung water content, to brain natriuretic peptide levels, and to the severity of diastolic dysfunction for any degree of systolic dysfunction. Therefore, the presence of B-lines in nondependent lung regions is useful for the differential diagnosis between cardiogenic and noncardiogenic dyspnea.

51.3.2 Interstitial Syndrome

In interstitial syndrome, aeration is impaired due to an increase in interstitial fluid, while some lung aeration is preserved. If B-lines are focally observed, pneumonia/pneumonitis, atelectasis, pulmonary contusion, pulmonary infarction, or neoplasm should be considered. If multiple diffuse B-lines are observed, pulmonary edema of various causes, interstitial pneumonia/pneumonitis, or diffuse parenchymal lung disease should be considered.

Regularly spaced B-lines suggest septal or interstitial edema. Coalescent B-lines are suggestive of alveolar edema (Fig. 51.4).
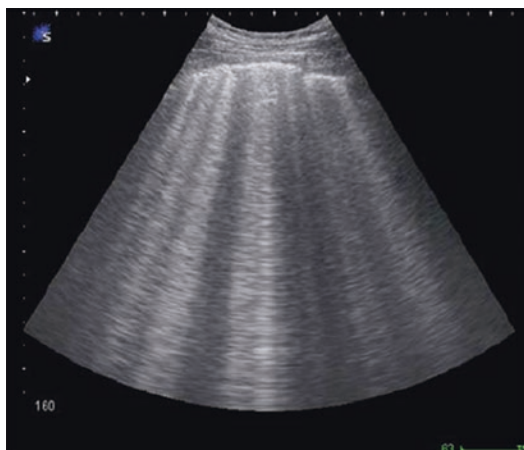
Fig. 51.4 Interstitial syndrome

Fig. 51.5 Lung consolidation

51.3.3 Consolidation

Pulmonary consolidation consists of a loss of aeration, which generates a visible area of parenchyma, similar to the liver texture, with irregular margin. Hyperechoic punctiform images can be seen within the consolidation; these images vary according to the respiratory cycle (changing location, size, or shape) and correspond to the finding of air bronchograms. Bronchograms along with shred line are characteristic of lung consolidation caused by pneumonia. Inhomogeneous unilateral/bilateral and focal/multifocal positive areas for B-lines with pleural abnormalities (thickened, fragmented pleura and subpleural consolidation) and reduced or absent lung sliding are seen in LUS in interstitial and bronchopneumonia (Fig. 51.5).

51.3.4 Acute Respiratory Distress Syndrome (ARDS)

Compromised alveolar capillary membrane leads to increased capillary permeability, and diffuse flooding of alveoli takes place. ARDS usually presents dishomogeneous and irregular pattern, featuring many anterior subpleural consolidations and fragmented pleural line, intense hyperlucent multiple B-lines alternating with spared areas in both lungs. The reduction or absence

of lung sliding with pleural line abnormalities is also present. The "spared areas" of normal parenchyma are characteristic and help to differentiate it from other causes of alveolar-interstitial syndrome involving both lungs and in cardiogenic pulmonary edema, where B-lines are usually detected in more homogenous distribution.

51.3.5 Pneumothorax

There is a collection of air between visceral and parietal pleura: this results in the absence of lung sliding. In M-mode only horizontal lines are seen because dynamic pleural sliding is absent. The presence of B-line rules out pneumothorax because this artifact arises at visceral pleura. The characteristic "lung point" is the point at which a partially collapsed lung is in contact with the chest wall: there is a transition area from any sliding or moving B-lines into an area of sliding. The absence of lung sliding, B-lines, lung pulse, and presence of lung point are four characteristic sonographic signs of pneumothorax. The lung pulse refers to the subtle rhythmic movement of the visceral upon the parietal pleura with cardiac oscillations. Lung point will not be present if the lung is completely collapsed; in this case, the absence of ruling out signs associated to the clinical context should be suggestive enough. The presence of lung sliding effectively rules out pneumothorax with high negative predictive value of 99.2–100%. However, the absence

Fig. 51.6 Pneumothorax

Fig. 51.7 Pleural effusion and lung atelectasis

of lung sliding is not specific for pneumothorax. This characteristic is also present in pathological conditions such as ARDS, atelectasis, pleural adhesions, pulmonary fibrosis, and single-lung intubation (Fig. 51.6).

51.3.6 Pleural Effusion

Pleural effusion is usually seen on LUS as an anechoic or hypoechoic space between the visceral and parietal pleura. In supine patients, the optimal site for evaluation is at the posterior axillary line above the diaphragm. In this position, diaphragmatic movement, which is the swaying of the atelectatic lung within the pleural effusion, can be visualized. The nature of the pleural effusion, whether transudate or exudate, cannot be accurately predicted using LUS. However, a few signs can be helpful. Most transudates and some exudates appear anechoic: the presence of internal echoes in this anechoic space is suggestive of exudate or hemorrhage which can be confirmed by thoracentesis. Hemothoraxes generally have a typical corpusculated aspect. Septated fluids are usually observed in infected exudates and in malignant effusions. LUS also helps to guide bedside thoracentesis also in patients receiving mechanical ventilation. During LUS exam, it is important to describe pleural effusion characteristics, the degree of lung atelectasis, and a semiquantitative estimate of the fluid (Figs. 51.7 and 51.8 and Table 51.4).

Fig. 51.8 Pleural effusion

Table 51.4 Pleural effusion

Distance (centimeters)	Volume (millimeters)
1.5 cm	250–300 ml
1.5–4.5 cm	300–1000 ml
>4.5 cm	>1000 ml

51.4   Monitoring Lung Disease

In critically ill patients, bedside visualization of lung morphology and aeration loss is crucial to optimize positive end-expiratory pressure (PEEP) and other therapeutic procedures (e.g., antibiotic therapy). It must be performed according to a systematic protocol of examination to explore lung region and obtain a comprehensive picture of the lung. These patterns can be used to express aeration and its variation as a score (Table 51.5) [10].

Table 51.5 Image US characteristics in lung pathologies

Lung pathology	Lung US	Distribution

Normal lungs	Hyperechoic pleural line: present
	Lung sliding: present
	    A-line: present
	    Isolated B-line may be seen
		Both lungs
		In laterobasal areas

Asthma/COPD	A profile ↓ lung sliding, if hyperinflation is present	In affected areas
Interstitial/ bronchopneumonia	Pleural line and lung sliding: present Lung sliding: normal/may be ↓ Pleural line and subpleural abnormalities: present A-line: present B-lines: significant and spaced/crowed	In affected lung May be bilateral or unilateral Focal/multifocal/inhomogeneous
Pulmonary edema	Hyperechoic pleural line and lung sliding: present Pleural line and subpleural abnormalities: absent A-line: present B-lines: significant and ≥2 bilateral regions	Both lungs Homogeneous Dependent areas
ALI/ARDS	Pleural line: present Lung sliding: present/may be ↓ Pleural line and subpleural abnormalities: present A-line: present B-lines: significant but irregularly spaced	Both lungs Inhomogeneous Spared areas of normal appearance
Pneumonia consolidation	Pleural line and lung sliding: absent Dynamic air/fluid bronchogram: present Tissue like echo-texture of consolidated lung	In affected lung May be bilateral or unilateral Focal/multifocal/inhomogeneous
Atelectasis	Pleural line and lung sliding: absent Tissue like echo-texture of atelectic lung Dynamic air/fluid bronchogram: absent Image characteristics depend on aeration	In affected lung

Pneumothorax	Hyperechoic pleural line: present
	Lung sliding: absent
	    A-line: present
	    B-lines: absent
	    Lung point: present
	    Lung pulse: absent
		In affected lung

Pleural effusion	Hyperechoic pleural line and lung sliding: absent Anechoic (dark) space present Hyperechoic lung line present if underlying lung is aerated	In affected hemithorax

References

1. Rantanen NW. Diseases of the thorax. Vet Clin North Am Equine Pract. 1986;2(1):49–66.
2. Wernecke K, et al. Pneumothorax: evaluation by ultrasound--preliminary results. J Thorac Imaging. 1987;2(2):76–8.
3. Lichtenstein D, et al. The comet-tail artifact. An ultrasound sign of alveolar-interstitial syndrome. Am J Respir Crit Care Med. 1997;156(5):1640–6.
4. Voigt LP, et al. Review of a large clinical series: intrahospital transport of critically ill patients: outcomes, timing, and patterns. J Intensive Care Med. 2009;24:108–15.

5. Braman SS, et al. Complications of intrahospital transport in critically ill patients. Ann Intern Med. 1987;107:469–73.

6. Volpicelli G, et al. International Liaison Committee on Lung Ultrasound (ILC-LUS) for International Consensus Conference on Lung Ultrasound (ICC-LUS). International evidence-based recommendations for point-of-care lung ultrasound. Intensive Care Med. 2012;38:577–91.

7. Gargani L, Volpicelli G. How I do it: lung ultrasound. Cardiovasc Ultrasound. 2014;12:25.

8. Picano E, et al. Ultrasound lung comets: a clinically useful sign of extravascular lung water. J Am Soc Echocardiogr. 2006;19:356–63.

9. Picano E, et al. Ultrasound of extravascular lung water: a new standard for pulmonary congestion. Eur Heart J. 2016;37:2097–104.

10. Bouhemad B, et al. Ultrasound for "lung monitoring" of ventilated patients. Anesthesiology. 2015;122(2):437–47.

Ultrasound and Morbidly Obese Patient

52

Pavoni Vittorio, Poli Claudio, and Cipani Simone

Key Points
- Obese patient
- Obesity and cardiovascular system
- Role of echocardiography
- Echocardiographic parameters in obese patient
- Effect of bariatric surgery

52.1 Introduction

The prevalence of significant obesity continues to rise in both developed and developing countries and is associated with an increased incidence of a wide spectrum of medical and surgical pathologies.

Obesity is a condition of excessive body fat. An individual must be considered obese when the amount of fat tissue is increased such an extent that physical and mental health are affected and life expectancy reduced. Accurate measurement of body fat content is difficult and requires sophisticated techniques. Useful estimates, however, can be obtained by evaluating weight for a given height and then comparing that figure with an ideal body weight (IBW), originated from life insurance studies. For general clinical purposes, IBW can be estimated from the formula IBW (kg) = height (cm) – x, when x is 100 for adult males and 105 for adult females.

The body mass index (BMI) is a measure of the relationship between height and weight, and it is calculated as follows: BMI = body weight (kg)/height^2 (in metres). A BMI of <25 kg/m^{-2} is considered normal; a person with a BMI of 25–30 kg/m^{-2} is considered overweight, but at low risk of serious medical complications, while those with a BMI >30, >35, and >55 kg/m^{-2} are considered obese, morbidly obese and super-obese, respectively.

Morbidity and mortality rise sharply when the BMI is >30 kg/m^{-2}.

Morbidly obese individuals are at greater risk of mortality from diabetes, cardiorespiratory and cerebrovascular disorders and certain forms of cancer.

Other factors such as the pattern of adipose tissue distribution may be better predictor of health risk. It is now becoming clear that it is not only the amount of fat that is important in determining risk but also its anatomical distribution. In the central or android type of distribution, which is more common in males, fat is predominantly distributed in the upper body and may be associated with increased deposits of intra-abdominal or visceral fat. In the peripheral or gynaecoid type, fat is more typically distributed around the hips,

P. Vittorio (✉) · P. Claudio · C. Simone
Department of Anesthesia and Intensive Care,
Santa Maria Nuova Hospital, Florence, Italy
e-mail: vittorio.pavoni@uslcentro.toscana.it;
simone.cipani@uslcentro.toscana.it
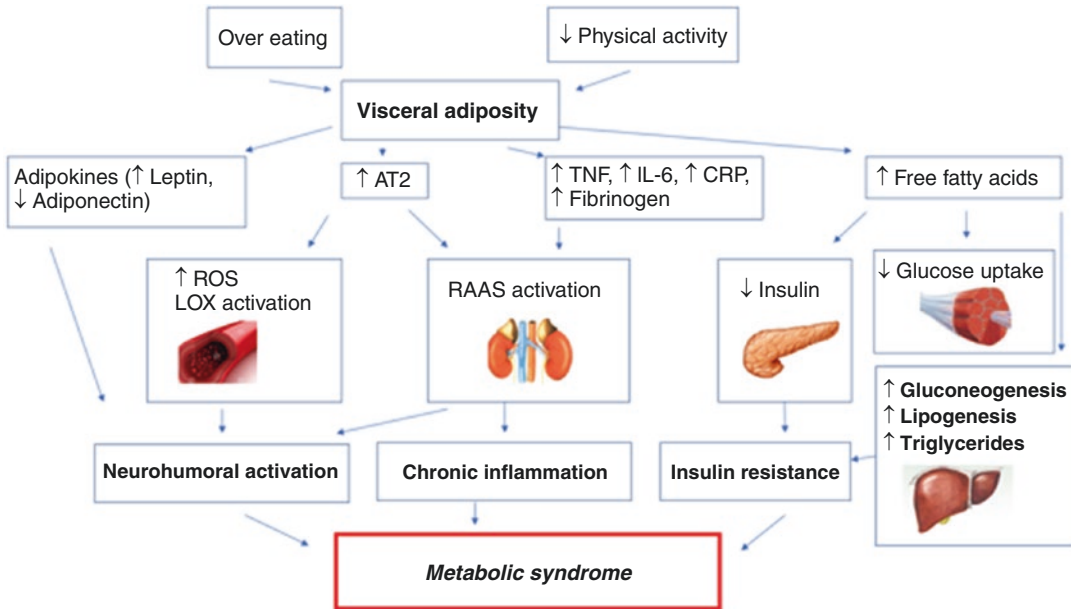
Fig. 52.1 Metabolic syndrome and pathophysiological mechanisms (AT2 angiotensin II type 2 receptor, CRP C-reactive protein, IL-6 interleukin 6, LOX lectin-like oxidized low density, RAAS renin-angiotensin-aldosterone system, ROS reactive oxygen species, TNF tumour necrosis factor)

buttocks or thighs; this is the more usual female pattern of distribution. Central adipose tissue is metabolically more active than fat in the peripheral distribution and is associated with more metabolic complications, such as dyslipidaemias, glucose intolerance and diabetes mellitus, and a higher incidence of mortality from ischaemic heart disease.

Metabolic syndrome (MetS) is a cluster of metabolic abnormalities that includes hypertension, central obesity, insulin resistance and atherogenic dyslipidaemia. MetS is strongly associated with an increased risk of developing atherosclerotic cardiovascular diseases (CVD).

The pathogenesis of MetS involves both genetic and acquired factors that play a role in the final pathway of inflammatory that lead to CVD. Visceral adiposity has been demonstrated to be a primary trigger for most of the pathways involved in MetS.

Activation of various pro-atherogenic pathways in MetS culminates in a final common pathway of chronic inflammation that leads to clinical manifestations of MetS. Systemic oxidant stress induced by obesity and insulin resistance leads to increased activation of downstream signalling cascades that cause atherogenesis and tissue fibrosis (Fig. 52.1).

52.2 Obesity and the Cardiovascular System

Cardiovascular disease dominates the morbidity and mortality in obesity. There are multiple factors that increase the susceptibility to CVD including metabolic dysregulation, abnormal cardiac remodelling, endothelial dysfunction, premature coronary disease, increased sympathetic tone and pulmonary hypertension and arrhythmias.

Obesity increases metabolic demand by causing a greater increase in fat-free mass compared to fat mass, despite the fact that adipose tissue comprises a greater portion of the total body weight. A significant volume of fluid is present in the interstitial space of adipose tissue, which is about 10% of the tissue wet weight. Despite the increase in cardiac output with total fat mass,

the perfusion per unit of adipose tissue decreases with increasing obesity. This is because the blood flow is regulated by β1-adreno-receptors that mediate vasodilation, whereby skeletal muscle blood flow is regulated mainly by β2-receptors. Therefore, the blood flow is actually lower in adipose tissue than in skeletal muscle even though adipose tissue comprises a greater portion of the total body weight and contains a larger portion of fluid. The net result is an increase in blood flow and an increased total blood volume produced by obesity.

The increase in total blood volume is associated with a concomitant increased cardiac output mostly from an increase in the cardiac stroke volume. In turn, the left ventricular filling pressure increases disproportionately incrementally due to the Frank-Starling curve being shifted to the left. At any given level of activity, the cardiac workload is increased for subjects with obesity because of the increased venous return that occurs during exercise. With the volume overload that occurs with increased blood return to the heart, there is left ventricle chamber dilation. Eccentric hypertrophy is a process by which new sarcomeres lengthen in series with existing sarcomeres to dilate the chamber radius of the heart. Eccentric hypertrophy is an adequate, compensatory response to the early volume overload.

There is an increased prevalence of left ventricular hypertrophy (LVH) in individuals with obesity which is associated with left ventricular diastolic dysfunction.

LVH is an important predictor of cardiovascular risk and sudden death in obese patients.

Diastolic dysfunction is an abnormality of the myocardium to return to the unstressed length and force. It is due to an incremental increase in left ventricle filling pressures and volume (preload) with concomitant chamber dilation. Progressive chamber dilation leads to increased wall stress with subsequent increases of myocardial mass and LVH of the eccentric or concentric type. The development of the concentric type of LVH results from an increased wall thickness relative to chamber size. In contrast, in eccentric LVH, chamber enlargement is more prominent than the increase in wall thickness. Left ventricular

diastolic dysfunction may progress as a result of increased stiffness and/or decreased ventricular relaxation as the ventricular chamber is unable to accept an adequate volume during diastole.

At this point, there is usually development of left ventricular systolic dysfunction and left ventricular failure. The processes of increased filling pressures, stroke volume and cardiac output are adequate, compensatory changes, up to the point of dysfunction of the left ventricle with ensuing heart failure. Left ventricular failure can lead to pulmonary venous hypertension; pulmonary artery hypertension, which in turn results in right ventricular hypertrophy; and right ventricular failure and pulmonary oedema.

The capacity of the dilated ventricle to hypertrophy is limited so, when left ventricular wall thickening fails to keep pace with dilatation, systolic dysfunction ensues (obesity cardiomyopathy).

Obesity cardiomyopathy is a distinct clinical entity that was described in necropsy studies and was reported for the first time by Smith and Willius in 1933. The first studies using echocardiographs began in 1978 and were conducted by Alexander.

The combination of cardiac hypertrophy and direct fatty infiltration creates a substrate of arrhythmias. The most common arrhythmia observed is atrial fibrillation (AF), and the dose-dependent link between obesity and AF is well established. Pathak and colleagues have quoted an increased risk of 3–7% for developing AF for each incremental unit of BMI.

Patients who are obese also have an elevated incidence of ventricular dysrhythmias, raising the risk of sudden cardiac death.

Obesity is the leading cause of nonischaemic sudden cardiac death in young people, responsible for approximately 25% of cases.

A 2008 study of more than 100.000 patients with acute coronary syndrome demonstrated that morbid obesity is the most powerful risk factor for premature cardiovascular events, lowering the age of first coronary syndrome by a mean of 12 years. By contrast, smoking lowered the age of first coronary syndrome by a mean of only 9.7 years.

With an increasing morbidly obese population, cardiologists are seeing an increase in young patients with ST-segment elevation myocardial infarction (STEMI). A 2011 study into the high prevalence of obesity in young patients with STEMI founded that almost 80% of young patients (men aged less than 45 years, women less than 55 years) who experienced a STEMI were obese.

Furthermore, the cardiovascular problem is often compounded by superimposed hypertension. Hypertension appears to be related both to obesity and to central distribution of body fat. Subjects with high abdominal adipose tissue distribution have higher total peripheral resistance and lower cardiac output and react with increased systemic vascular resistance to psychosocial stress; this suggests that the abdominal fat distribution is associated with structural, endocrine or both aberrations with important circulatory effects (Fig. 52.2).

Ventricular hypertrophy and dysfunction worsen with increasing duration of obesity and improve to some extent with weight loss.

The morbidly obese tolerate exercise badly with any increase in cardiac output being achieved by increasing the heart rate, without an increase in stroke volume or ejection fraction.

This is often accompanied by an increase in the filling pressures.

Changing position from sitting to supine is associated with significant increases in cardiac output, pulmonary capillary wedge pressure and mean pulmonary artery pressure, together with reductions in heart rate and peripheral resistance.

Morbidly obese individuals often have very limited mobility and may appear to be asymptomatic even they have cardiovascular diseases. Symptoms such as angina or dyspnoea may occur only occasionally. The patient should be evaluated thorough cardiovascular examination, in particular for evidence of hypertension and cardiac failure. Signs of cardiac failure, such as added heart sounds, hepatomegaly, peripheral oedema and pulmonary crackles, may be difficult to elicit in the morbidly obese patients, and investigations with instrumental examinations are necessary.

52.3   Role of Echocardiography

Echocardiography plays a major role in quantifying left heart chamber dimensions, which are thought to increase proportionally with increasing body size.
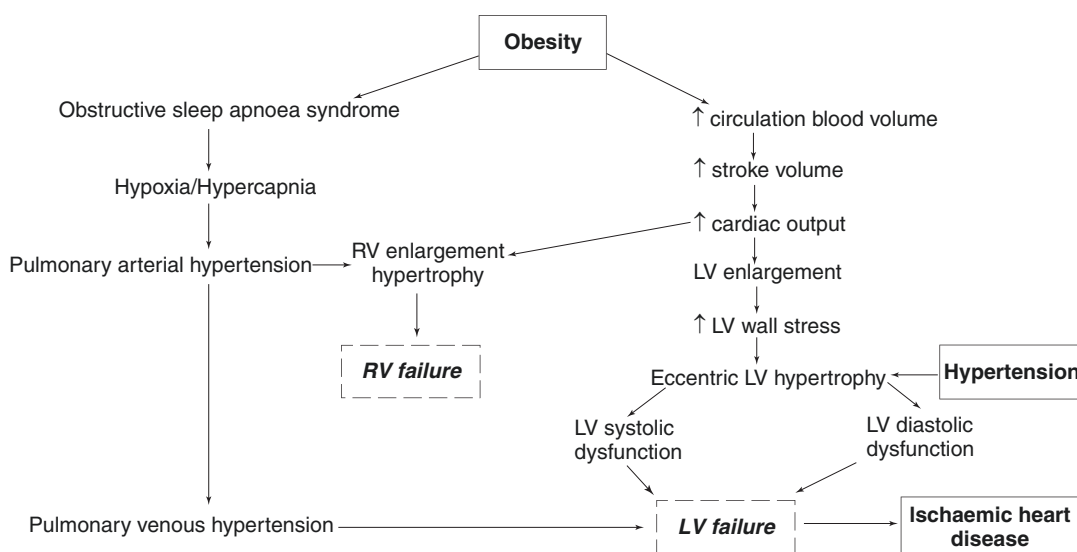
Fig. 52.2 The aetiology of cardiovascular diseases in obesity. LV left ventricular, RV right ventricular

To accurately differentiate pathologic cardiac conditions from normal obesity-related increases in cardiac dimensions, it is important to normalize chamber size with an appropriate body size variable. However, the accurate scaling of left heart chamber size in the obese population remains a challenge.

The role of normalization is to facilitate inter- and intragroup comparisons of cardiac dimensions while eliminating the effects of differences in patients' size.

To determine an accurate normalization model, two elements need to be selected: (1) a mathematical model (isometric model vs allometric) and (2) the body size measurement involved in the model, such as height, weight, body surface area (BSA) and BMI.

The American Society of Echocardiography suggests an isometric scaling method to normalize the measured cardiac chamber sizes. The method is based on the assumption of a linear relationship between the cardiac chamber size variable (Y, the dependent variable) and the body size variable (X, the independent variable) such as BSA or height, resulting in $Y = aX$, where a is a scaling factor. Conventional isometric method has been criticized because of their incompatibility with geometric relationship (two-dimensional body size vs three-dimensional cardiac chamber size), and few studies have shown if their normalization process effectively removed the correlation of their scaled data with the size variable used.

The allometric method based on nonlinear assumption has been suggested to be more appropriate in normalizing cardiac dimensions. This method would allow for a nonlinear relationship between the cardiac chamber size variable (Y) and the body size variable (X). This would assume the form $Y = aX^b$, where b is a scaling exponent. An allometric approach using an optimal scaling exponent for normalization could effectively remove the effect of body size on cardiac chamber sizes.

A large study in obese individuals founded that normalizing left heart chamber measurement using the allometric scaling method is superior to using the isometric method in removing the effect of body size variables.

Body mass index has been used as an obesity index in many other studies. However, its ability to predict or to be associated with hypertension, metabolic syndrome or left ventricular hypertrophy has been questioned.

A clinical study suggested that a cutoff point for waist circumference/stature ratio (in cm) with regard to left ventricular hypertrophy is 0.56 and recommends a waist circumference such as to stay below this measurement. It is the simplest and best obesity index for identifying echocardiographic left ventricular hypertrophy, mainly in women.

Ultrasound study is a useful tool for evaluating cardiac alterations in overweight and obese, but sometimes it is difficult to have good echo views because of the body size. When a good echo study is mandatory, transoesophageal echocardiography instead of a transthoracic echocardiography must be preferred.

52.4 Cardiac Remodelling in Obesity

The left heart chambers' dimensions are thought to increase proportionally with body size increasing.

Obese individuals have larger left atrial anteroposterior dimension (parasternal long-axis view) and left atrial area and volume (apical 4CH and 2CH view) due both to augmented preload and to altered left ventricle (LV) filling properties (see diastolic dysfunction). Also LV diameter (left ventricular end-diastolic dimension in parasternal long-axis view) and volume (left ventricular end-diastolic volume apical 4CH and 2CH view) are increased in obese. The increased end-diastolic volume in obesity has been interpreted as activation of Frank-Starling mechanism compensatory to augmented preload.

Wall thickness (that is strictly related to frequently associated hypertension and augmented afterload) may be similar to nonobese subjects or increased.

In obese people Framingham study described LV hypertrophy (usually concentric pattern, sometimes eccentric, as noted previously): the

extent of cardiac remodelling is related with severity and duration of obesity, and it is additive, but not synergistic, with associated hypertension. In obese patients the hypertrophy often exceeds the level needed to compensate the increased preload and afterload. In case of severe hypertrophy of basal anterior interventricular septum, clinical conditions as hypovolaemia and tachycardia may exacerbate left ventricular outflow tract obstruction leading, if not recognized, to life-threatening conditions (Figs. 52.3 and 52.4).
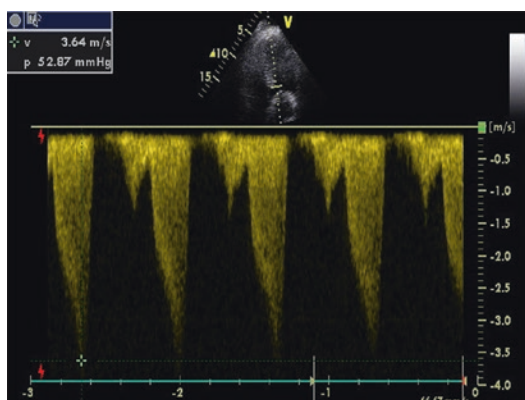
Fig. 52.3 Apical five-chamber (A5C) CW on left ventricular outflow tract (LVOT). (Note the high pressure gradient across the aortic valve)
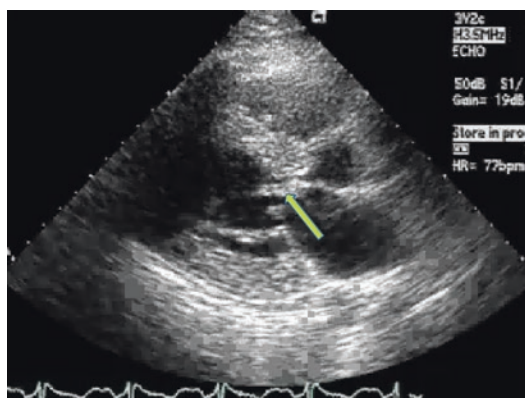
Fig. 52.4 Parasternal long axis on obese patient (Note the severe hypertrophy of anterior interventricular septum and posterior wall. Yellow arrow: anterior mitral cuspid that slams with anterior interventricular septum, hemodynamic outflow tract obstruction)

52.5 Systolic Function in Obesity

The augmented preload in obesity leads to a higher cardiac output (both stroke volume and heart rate increase). The contractility indices (ejection fraction B-mode, fractional shortening M-mode) are normal or higher in obese patients. However obese people may fail to increase their ejection fraction during exercise.

Furthermore improved echocardiography (i.e. tissue Doppler and speckle tracking at basal septal level) suggests that all obese patients have a degree of systolic dysfunction, although subclinical.

52.6 Diastolic Dysfunction in Obesity

LV diastolic dysfunction, often an asymptomatic condition, reflects an impairment of the LV filling properties and is a predictor of future developing of heart failure in still asymptomatic patients. While cardiac remodelling and systolic function are not strictly associated with obesity and overweight, it is evident that an increased BMI is related with worsening of LV diastolic function and increasing of the LV filling pressure, regardless of other cardiovascular risk factors .

The "cardiomyopathy of obesity" is manifested by LV diastolic dysfunction and LV remodelling.

For echocardiographic assessment of the diastolic function, it is necessary to study the transmitral flow in apical four-chamber view (A4C) sampling at the level of mitral valve leaflet tips with pulsed wave Doppler, studying the early *E wave* (protodiastolic rapid ventricular inflow) and the late *A wave* (telediastolic atrial systole) mitral inflow. It is necessary to measure their velocity peak (normally *E* wave 60–120 cm/s and *A* wave 40–80 cm/s) and to calculate their *E/A ratio* (normally 0.96–2.2), identifying the diastolic pattern (normal, impaired relaxation, pseudonormal and restrictive). Normally the *E/A* ratio decreases with age: it is higher in young people and lower in

Table 52.1 Diastolic dysfunction: effects of overweight, obesity and bariatric surgery on echocardiographic parameters

	Lean normal values	Overweight BMI > 25	Obese BMI > 30	Post-bariatric surgery
LV end-diastolic dimension cm.	Women 3.9–5.3 Men 4.2–5.9	⇑	⇑ ⇑	⇓
Peak E wave cm/s	60–120	⇑	⇑ ⇑	⇓ or ⇔
Peak A wave cm/s	40–80	⇑	⇑ ⇑	⇓
E/A ratio[a]	2.2 (young) 0.96 (age > 60)	⇓ or ⇔	⇓ or ⇔	⇑
TDI: Peak E′ wave cm/s[b]	Lateral 10–12 Septal 8–10	⇓	⇓ ⇓	⇑
E/E′ ratio[b]	<8 normal 8–15 "grey zone" >15 pathological	⇑	⇑ ⇑	No data available

[a]Normally the *E/A* ratio decreases with age, higher in young people and lower in older people. The variations in obesity depend mainly on patients' age and associated or not hypertension

[b]Note in the report if *E′* is an average value between septal and lateral *E′* waves or if it is only the lateral *E′* wave value

older people. However it is important to remember that the use of mitral inflow parameters alone as diastolic function index is strongly limited by their preload dependence.

So more reliable information about LV relaxation properties are obtained by tissue Doppler imaging (TDI), in A4C view, sampling the mitral annulus at the lateral and septal side, measuring the peak early diastolic velocities *(E′ waves)* and then averaging the data. The septal *E′* value is influenced by right ventricle movements ("tethering effect"), so in intensive care patients, it is better and faster to measure only the lateral side. The calculated *E/E′ ratio* (ratio between flow and tissutal velocities, Doppler measured) is a very good and rapid index of LV filling pressures, i.e. diastolic function. If the ratio *E/E′* is less than 8, the left ventricular filling pressures are normal. If the ratio *E/E′* is greater than 15, the left ventricular filling pressures are augmented. If the ratio *E/E′* is in the range 8–15, we are in a "grey zone" of uncertain estimate.

You must note in the report if *E′* is an average value between septal and lateral *E′* waves or if it is only the lateral *E′* wave value.

In overweight and obese patients, *E* and *A* waves increase, *E/A* ratio is stable or decreases (it depends mainly on patients' age and associated or not hypertension), *E′* wave decreases and *E/E′* ratio increases (Table 52.1).

52.7 Effects of Bariatric Surgery on Left Ventricular Geometry and Function

Several studies on effects of bariatric surgery on the mean changes in bi-dimensional echocardiographic parameters, with a follow-up from 3 to 36 months, demonstrate a significant reduction in wall thickness and an improvement in systolic function (only in those patients who had systolic function severely depressed preoperatively). On the other side bariatric surgery positively modulates the echocardiographic markers of diastolic

dysfunction: end-diastolic dimensions decrease, E/A ratio increases, A wave reduces and tissutal Doppler peak E' waves increase. These data are heterogeneous, but it is noticeable that the greatest improvements are in those patients who have been obese for a longer duration of time. The positive effects of bariatric surgery on cardiovascular risk are based not only on weight loss but also on improving blood lipid biochemistry, hypertension, type 2 diabetes mellitus and so on: comprehensive and larger studies are still needed.

Further Reading

Adabag S, Huxley RR, Lopez FL, et al. Obesity related risk of sudden cardiac death in the atherosclerosis risk in communities study. Heart. 2015;101:215–21.

Alauddin A, Neterissian S, Lisbona R, NacLean LD, Forse RA. Assessment of cardiac function in patients who were morbidly obese. Surgery. 1990;108:809–20.

Alexander JK. Obesity and cardiac performance. Am J Cardiol. 1964;14:860–5.

Alexander JK, Woodard CB, Quinones MA. Heart failure from obesity. In: Mancini M, Lewis B, Contaldo F, editors. Medical complications of obesity. London: Academic Press; 1978. p. 178–87.

Alpert NA, Hashimi NW. Obesity and the heart. Am J Med Sci. 1993;306:117–23.

Alpert MA, Terry BE, Kelly DL. Effect of weight loss on cardiac chamber size, wall thickness and left ventricular function in morbid obesity. Am J Cardiol. 1985;55:783–6.

Alpert NA, Singh A, Terry BE. Effect of exercise on left ventricular function and reserve in morbid obesity. Am J Cardiol. 1989;63:1478–82.

Alpert NA, Terry BE, Lambert CR, et al. Factors influencing left ventricular systolic function in nonhypertensive morbidly obese patients, and effect of weight loss induced by gastroplasty. Am J Cardiol. 1993;71:733–7.

Alpert NA, Lambert CR, Panayiotou H, et al. Relation of duration of morbid obesity to left ventricular mass, systolic function, and diastolic filling, and effect of weight loss. Am J Cardiol. 1995;76:1194–7.

Ashrafian H, le Roux CW, Darzi A, Athanasiou T. Effects of bariatric surgery on cardiovascular function. Circulation. 2008;118:2091–102.

Ashwell M, Chinn S, Stalley S, Garrow JS. Female fat distribution: a simple classification based on two circumference measurement. Int J Obes. 1982;6:143–52.

Azevedo A, Ramos E, von Hafe P, Barros H. Upperbody adiposity and risk of myocardial infarction. J Cardiovas Risk. 1999;6:32l–5.

Basoor A, Cotant JF, Randhawa G, et al. High prevalence of obesity in young patients with ST elevation myocardial infarction. Am Heart Hosp J. 2011;9:37–40.

Bjorntop P. Visceral obesity: a "civilization syndrome". Obes Res. 1993;1:206–22.

Bjorntorp P. Obesity. Lancet. 1997;350:423–6.

Bray GA. Pathophysiology of obesity. Am J Clin Nutr. 1992;55:488S–94S.

Brodksy JB. Anesthetic management of the morbidly obese patient. Int Anesthesiol Clin. 1986;24:93–103.

Dewey FE, Rosenthal D, Murphy DI Jr, et al. Does size matter? Clinical applications of scaling size and function for body size. Circulation. 2008;117:2279–87.

Drenick EJ, Fisler JS. Sudden cardiac arrest in morbidly obese surgical patients unexplained after autopsy. Am J Surg. 1988;155:720–6.

Eckel RH. Obesity and heart disease: a statement for healthcare professionals from the Nutrition Committee, American Heart Association. Circulation. 1997;96:3248–50.

Franzosi MG. Should we continue to use BMI as a cardiovascular risk factor? Lancet. 2006;368:624–5.

Garfinkel L. Overweight and cancer. Ann Intern Med. 1985;103:1034–6.

Garrison RJ, Castelli WP. Weight and thirty-year mortality of men in the Framingham study. Ann Intern Med. 1985;103:1006–9.

Grundy SM, Hansen B, Smith SC, et al. American Heart Association, National Heart, Lung, and Blood Institute, American Diabetes Association. Clinical management of metabolic syndrome: report of the American Heart Association/National Heart, Lung, and Blood Institute/American Diabetes Association conference on scientific issues related to management. Arterioscler Thromb Vasc Biol. 2004;24(2):e19–24.

Gutgesell HP, Rembold CM. Growth of the human heart relative to body surface area. Am J Cardiol. 1990;65:662–8.

Hsieh SD, Yoshinaga H. Abdominal fat distribution and coronary heart disease risk factors in me-waist/height ratio as a simple and useful predictor. Int J Obes Relat Metab Disord. 1995;19:585–9.

James WP. Assessing obesity: are ethnic differences in body mass index and waist classification criteria justified? Obes Rev. 2005;6:179–81.

Jern S, Bergbrant P, Hansson L. Relation of central hemodynamics to obesity and body fat distribution. Hypertension. 1992;19(6 Pt 1):520–7.

Kaltman AJ, Goldring RM. Role of circulatory congestion in cardiorespiratory failure of obesity. Am J Med. 1976;60:645–53.

Lang RM, Biering M, Devereux RB, Flachskampf FA, et al. Chamber quantification writing group, American Society of Echocardiography's Guidelines and Standards Committee, European Association of Echocardiography. Recommendations for chamber quantification: a report from the American Society of Echocardiography's Guidelines and

Standards Committee and the European Association of Echocardiography, a branch of the European Society of Cardiology. J Am Soc Echocardiogr. 2005;18:1440–63.

Lapidus L, Bengtsson C, HallstrOm T, Bjorntorp P. Obesity, adipose tissue distribution and health in women — results from a population study in Goteborg, Sweden. Appetite. 1989;12:25–35.

Larsson B, Svardsudd K, Welin L, Wilhelmsen L, BjSrntorp P, Tibblin G. Abdominal adipose tissue distribution, obesity, and risk of cardiovascular disease and death: 13 year of follow up of participants in the study of men born in 1913. Br Med J. 1984;288(6428):1401–4.

Lauer MS, Anderson KM, Levy D. Separate and joint influences of obesity and mild hypertension on left ventricular mass and geometry: the Framingham heart study. J Am Coll Cardiol. 1992;19:130–4.

Lauer MS, Anderson KM, Larson MG, et al. A new method for indexing left ventricular mass for differences in body size. Am J Cardiol. 1994;74:487–91.

Lavie CJ, Milani RV, Ventura HO. Obesity and cardiovascular disease: risk factor, paradox, and impact of weight loss. J Am Coll Cardiol. 2009;53(21):1925–32.

Lesser GT, Deutsch S. Measurement of adipose tissue blood flow and perfusion in man by uptake of 85Kr. J Appl Physiol. 1967;23:621–30.

Linde B, Chisolm G. The interstitial space of adipose tissue as determined by single injection and equilibration techniques. Acta Physiol Scand. 1975;95:383–90.

Madala MC, Franklin BA, Chen AY, et al. Obesity and age of first non-ST segment myocardial infarction. J Am Coll Cardiol. 2008;52:979–85.

Messerli FH. Cardiomyopathy of obesity: a not-so-Victorian disease. N Engl J Med. 1986;314:378–80.

Moller JE, Hills GS, Oh JK, et al. Left atrial volume: a powerful predictor of survival after acute myocardial infarction. Circulation. 2003;107:2207–12.

National Institutes of Health Consensus Development Conference Statement. Health implications of obesity. Ann Intern Med. 1985;103:147–50.

Noheria A, Teodorescu C, Uy-Evanado A, et al. Distinctive profile of sudden cardiac arrest in middle-aged vs. older adults: a community-based study. Int J Cardiol. 2013;168:3495–9.

Oberg B, Rosell S. Sympathetic control of consecutive vascular sections in canine subcutaneous adipose tissue. Acta Physiol Scand. 1967;71:47–57.

Pathak RK, Mahajan R, Lau DH, et al. The implications of obesity for cardiac arrhythmia mechanisms and management. Can J Cardiol. 2015;31:203–10.

Paul DR, Hoyt JL, Boutros AR. Cardiovascular and respiratory changes in response to change of posture in the very obese. Anesthesiology. 1976;45:73–8.

Perry AC, Applegate EB, Allison MD, Jackson ML, Miller PC. Clinical predictability of the waist-to-hip ratio in assessment of cardiovascular disease risk factor in overweight, premenopausal women. Am J Clin Nutr. 1998;68:1022–7.

Poirier P, Cornier MA, Mazzone T, et al. Bariatric surgery and cardiovascular risk factors: a scientific statement from the American Heart Association. Circulation. 2011;123:1683–701.

Rodrigues LS, Baldo MP, Cunha R, et al. Anthropometric measures of increased central and overall adiposity in association with echocardiographic left ventricular hypertrophy. Hypertens Res. 2010;33:83–7.

Rosell S, Belfrage E. Blood circulation in adipose tissue. Physiol Rev. 1979;59:1078–104.

Russo C, Jin Z, Homma S, Rundek T, Elkind MSV, Sacco RL, Di Tullio MR. Effect of obesity and overweight on left ventricular diastolic function: a community based study in elderly cohort. J Am Coll Cardiol. 2011;57(12):1368–74.

Sluysmans T, Colan SD. Theoretical and empirical derivation of cardiovascular allometric relationship in children. J Appl Physiol. 2005;99:445–57.

Smith HL, Willius FA. Adiposity of the heart. Arch Intern Med. 1933;52:911–31.

Tanner JM. Fallacy of per weight and per surface area standards, and their relation to spurious correlation. J Appl Physiol. 1949;2:1–15.

Vasan RS. Cardiac function and obesity Framingham Heart Study. Heart. 2003;89(10):1127–9.

Yao GH, Vallurupalli N, Cui J, Hiser WL, et al. Allometric model improves scaling of left atrial size in obese population: the use of body weight containing variables is challenged. Echocardiography. 2011;28:253–60.

Zile MR, Brutsaert DL. New concepts in diastolic dysfunction and diastolic heart failure: Part I. Circulation. 2002;105:1387–93.

Zong P, Zhang L, Shaban N, et al. Left heart chamber quantification in obese patients: how does larger body size affect echocardiographic measurement? J Am Soc Echocardiogr. 2014;27(12):1267–74.

Ultrasound Exam Approach in Trauma Patients

53

Gianfranco Giannasi

53.1 Introduction

E-FAST (extended focused assessment with sonography for trauma) is an ultrasound "bedside" diagnostic exam performed in trauma patients during the primary survey in the emergency unit by consultants trained in sonography.

The exam must be completed in less than 5 min without interfering with resuscitation maneuvers and must satisfy specific diagnostic questions (the presence of free air or liquids).

E-FAST consists of six US windows, two thoracic and four abdominal, by researching on two simple and reliable US signs:

1. The pleural "gliding sign" for the diagnosis of PNX
2. The presence of an "anechoic area", suggesting hemothorax

E-FAST is particularly indicated in unstable blunt trauma to the chest and abdomen.

In many trauma centers, E-FAST has been extended even further to include questioning of the IVC during respiration as a noninvasive means of volume status assessment. In trauma, the simplest approach is to evaluate IVC in hypo-

tensive patients to see if there is a substantial collapse with small diameter (1.5 cm), indicating volume depletion and probably peritoneal hemorrhage. If, instead, the diameter of the vena cava is enlarged and there is no change in inspiratory and expiratory diameters, the patient has an obstructive shock due to pericardial effusion with cardiac tamponade, massive pneumothorax, or pleural effusion with massive hemothorax.

In hemodynamically stable patients, CT scan is more accurate in identifying solid organ injury in the intra- and retroperitoneal space. In stable patient with CT, negative E-FAST may be applied in follow-up. In pregnancy, the method also offers the possibility to assess fetus status.

More recently, a new ultrasound technique using second-generation contrast agents, named contrast-enhanced ultrasound (CEUS), has been developed. This technique allows the entire vascular phase to be performed in real time, increasing ultrasound capability to detect parenchymal injuries, enhancing some qualitative findings, such as lesion extension, margins, and its relationship with capsule and vessels.

CEUS has been demonstrated to be near sensitive as contrast-enhanced CT in the detection of traumatic injuries in patients with low-energy isolated abdominal trauma, with sensitivity and specificity levels ranging to 95%.

Several studies have demonstrated its ability to detect lesions affecting the liver, spleen, pancreas, and kidneys and also to recognize active

G. Giannasi (✉)
San Giovanni di Dio Hospital, Florence, Italy

USL Toscana Centro, Florence, Italy
e-mail: gianfranco.giannasi@uslcentro.toscana.it

Fig. 53.1 Trimodal distribution of trauma deaths

	First peak	Second peak	Third peak
Time from injury:	Minutes	Minutes to few hours	Days to weeks
Location:	At scene, en route to medical facility	Emergency department Operating room	Critical care unit
Cause of death:	Laceration of brain or brainstem, high spinal cord injury, injury to heart, aorta, or other large vessels	Subdural or epidural hematoma, hemo- pneumothorax, ruptured spleen, liver laceration, pelvic fracture, injuries associated with exten- sive blood loss	Sepsis, multiple organ dysfunction syndrome (MODS)

bleeding as hyperechoic bands appearing as variable-sized round or oval spots. Its role seems to be actually relevant in pediatric patients, thus avoiding a routine exposure to ionizing radiation.

Nevertheless, CEUS is strongly operator dependent, and it has some limitations, such as the cost of contrast media, lack of panoramicity, the difficulty to explore some deep regions, and the poor ability to detect injuries of the urinary tract. On the other hand, it is timesaving, and it has several advantages, such as its portability, the safety of contrast agent, avoiding ionizing radiation exposure, and therefore its repeatability, allowing follow-up of conservatively approached traumas, especially in cases of fertile females and pediatric patients.

In the United States and Europe, trauma is the fourth leading cause of death after heart disease, cerebrovascular diseases, and tumors, and the leading cause of death in the population under 40 years old, with predominance of blunt trauma (approximately 80%).

In most countries where reliable, epidemiological studies have been conducted among the various causes of trauma, road traffic accidents are the main responsible for mortality and morbidity, probably due to the high kinetic energy that characterizes them, followed by falls, drown-

ings, burns, assault, self-inflicted wounds, and, in some areas, gunshot wounds. In severe trauma (injury severity scores, ISS, >15), mortality varies with cases but appears closely related to the economic level of the country in which it occurs, ranging from 19% to 63%.

Deaths for trauma follow a trimodal distribution (Fig. 53.1):

1. About half of the deaths are reported in the first few minutes (deaths and triage) for severe injury of the central nervous system, heart, and aorta.
2. A further 30% are recorded within 24 h after hospitalization (early intrahospital deaths) typically related to hemorrhagic shock, intracranial hemorrhage, and pneumothorax.
3. The remaining 20% of deaths finally takes place days or weeks after hospitalization (delayed intrahospital deaths) due to sepsis, ischemic, and thromboembolic complications.

Prevention obviously plays a major role, with a possible 50% reduction of deaths.

The improvement of healthcare organizations with a more appropriate management of trauma would affect the remaining half of the cases (intrahospital deaths).

Table 53.1 The ABCDE approach with important assessment points and examples of treatment options

Assessment		Treatment
A – Airways	Voice Breath sounds	Head tilt and chin lift *Oxygen (15 l/min)* *Suction*
B- Breathing	Respiratory rate (12–20 min) Chest wall movements Chest percussion *Lung auscultation* *Pulse oximetry (97–100%)*	Seat comfortably Rescue breaths *Inhaled medications* *Bag-mask ventilation* *Decompress tension pneumothorax*
C- Circulation	Skin color, sweating Capillary refill time (<2 s) Palpate pulse rate (60–100 min) *Heart auscultation* *Blood pressure (systolic 100–140 mmHg)* *Electrocardiography monitoring*	*Stop bleeding* *Elevate legs* *Intravenous access* *Infuse saline*

D- Disability	Level of consciousness
	AVPU
	    Alert
	    Voice responsive
	    Pain responsive
	    Unresponsive
	Limb movements
	Pupillary light reflexes
	Blood glucose
		Treat airway
		breathing, and
		circulation
		problems
		Recovery position
		Glucose for
		hypoglycemia

E- Exposure	Exposure skin Temperature	*Treat suspected cause*

In summary, the strengthening of healthcare organizations will improve the management of the airway investigation and the treatment of thoracic injuries and hemorrhagic shock (ABC).

The rescuer should complete the primary evaluation according to the ABCDE (Table 53.1) in less time as possible (golden hour), recognizing and treating the most serious emergency situations without a complete diagnosis, which will be performed later on (secondary survey).

In many countries, the ATLS program is the standard treatment of trauma patients and the basic training element for the extra- and intra-hospital emergency services: its introduction has actually improved trauma management and significantly reduced mortality.

Thoracic trauma is the major cause of mortality, accounting for approximately 25–33% of deaths. Less than 10% of blunt trauma of thorax and approximately 15–30% of penetrating injuries require thoracotomy.

Immediately life-threatening conditions are airway obstruction, pneumothorax, hemotho-rax, pneumothorax with flail chest, and massive (defined by the rapid accumulation of 1500 ml of blood or a third or more of circulating blood volume in the pleural cavity) and pericardial effusion.

Abdominal trauma is responsible for the deaths in 10% of cases, and the hemorrhagic shock is its main mechanism. A delay in transferring a patient with hypovolemic shock caused by bleeding to the operating room is associated with a worst prognosis. The results of autopsy studies show that abdominal injuries with hemoperitoneum are among the most frequent causes of death.

Thoracic or abdominal injuries can be caused by trauma with two mechanisms:

1. Compression mechanism, sometimes by means of safety equipments worn (belts, helmet).
2. Deceleration mechanism: the fixed parts of the body are stimulated by a movement different from moving parts – the mechanism

causes frequent hepatic and splenic injuries to the fixing ligaments.

The dynamics of the event correlates statistically with the gravity of internal injuries in the thoracic-abdominal trauma. High-risk circumstances of injury are:

- The ejection from the vehicle
- Its overturning
- The death of one of the passengers of the same vehicle
- Collision with severe damage to the vehicle
- The impact movement against fixed obstacle
- Vehicle-pedestrian impact
- Failure to use protective equipment
- The fall from height more than 6 meters
- Aggression

53.2 Management of Thoracoabdominal Trauma

Patients with penetrating thoracoabdominal trauma require surgical therapy in the absence of further investigations, with the exception of a quick ultrasound evaluation of the pericardium (single view) in suspected cases of hemopericardium in order to address immediate pericardiocentesis.

The extension of ultrasound examination aimed to evaluate penetrating trauma, when it is possible, seems feasible in these patients: a positive examination will address to a surgical solution, while a negative one authorizes attending for a more sophisticated imaging examination and/or for clinical observation.

However, in the presence of hemodynamic instability, patient transfer to radiology for an additional examination is not appropriate while strongly appropriate for bedside assessment to decide an immediate transfer to the operating room for definitive treatment.

In blunt thoracoabdominal trauma, pneumothorax (PNX) has a prevalence of 20%, while the more frequent internal injuries are spleen rupture (40–50%), liver (35–45%), and retroperitoneal

hematoma (15%). Therefore, any patient who has undergone a major thoracoabdominal blunt trauma should be suspected of having an abdominal and endothoracic lesion and investigated for the presence of PNX, hemothorax, hemopericardium, hemoperitoneum, or injury of the abdominal organs. In young patients' victims of trauma, non-specific signs of bleeding after the loss of at least 30% of the circulating blood volume, such as agitation and tachycardia, may be observed.

The aim of primary assessment of a trauma patient after resuscitation maneuvers consists in deciding which patient requires immediate surgery.

Before the onset of computer tomography (CT) for emergency diagnosis of abdominal blunt trauma or injury, it was necessary to perform diagnostic peritoneal lavage (DPL, diagnostic peritoneal lavage). This procedure is sensitive for the detection of hemoperitoneum but less useful to detect not retroperitoneal lesions or blood loss. It is also invasive and associated with a significant rate of complications (1–5%); it cannot be repeated and causes the release of free air and fluid in the peritoneal cavity, potential obstacle to subsequent ultrasound investigations; moreover, it requires a 20 min average execution time of expert personnel. However, we must not forget that it does not give any indication of the extent and the source of the abdominal effusion, important to plan a conservative treatment, such as arterial emobolization, in traumatic intraperitoneal organ lesions at low risk of excessive hemorrhage.

CT is accurate, sensitive, and noninvasive but is relatively expensive and involves some delay in the execution, patient transport, the use of contrast, and exposure to ionizing radiation. In particular, with respect to this point, it should be noted how radiation exposure is less acceptable in pregnancy and pediatric age.

Focused ultrasound in trauma or "focused goal-directed," known by the acronym FAST, is performed by the emergency physician for clinical evaluation completion (Fig. 53.2). Versatility and the diagnostic accuracy in the hands of well-trained experts is a must, although we should also mention its limits, especially

Fig. 53.2 The four-window US for the original FAST scan: *A* = right upper quadrant that may be helpful to see pleural space, Morrison's pouch, liver, and right kidney; *B* = left upper quadrant that may be helpful to see pleural space, spleen, and left kidney; *C* = suprapubic view that may be helpful to see bladder and free liquid suggested peritoneal hemorrhage; *D* = subxiphoid view of the heart for pericardial effusion

related to the inexperience of the operator. In the hands of an emergency physician, however, this method, aimed to answer some simple and decisive questions for the management of critically ill patients, gradually is assuming an increasingly important role.

While it is characterized by a lower sensitivity with respect to DPL and CT for hemoperitoneum detection, and undergoing an obstacle caused by intestinal flatulence, fat, and finally subcutaneous emphysema to explore retroperitoneal space, it stands as a noninvasive method that can be performed at bedside. It also allows a careful follow-up of the patient as quick and repeatable and does not avoid other diagnostic procedures. It requires a training period, less than the training period for the peritoneal lavage, and standardized protocols (such as FAST) with sequential ultrasound scans, to increase the diagnostic sensitivity.

Abdominal ultrasound examination can be misleading in the case of patients with other endoperitoneal fluid collections (patients who have already undergone a diagnostic peritoneal lavage, patients with ascites or ruptured ovarian cysts or pelvic inflammatory processes). It must be considered that the FAST technique has a lower sensitivity if the intraperitoneal liquid (blood) is less than 500 ml, because a single negative exam does not exclude small collections or mesenteric vascular lesions or injuries of hollow organs or diaphragmatic minor lacerations. The use of FAST in the 24 h follow-up of stable patients increases the sensitivity of the method of 30–40%. For this a FAST check after 6 h is appropriate, before considering as a negative examination, and on the other hand, the ATLS recommendations suggest a FAST check after 30 min.

53.3 Evolution of FAST

FAST in the investigation of abdominal trauma was initially introduced in Europe in the early 1980s, with some Italian, French, and German studies, and later has spread throughout the world. It aims to discriminate patients requiring immediate surgery from patients who can be observed or that require further investigation.

In the United States, until the 1990s, this procedure was scarcely used, as deemed more inaccurate than CT; an important problem was the unavailability of experienced personnel because it is unreliable if performed by inexperienced personnel.

The acronym FAST appears for the first time in literature in 1996 and affirms the use of ultrasound in blunt abdominal trauma unstable, with the aim to identify the hemoperitoneal effusion: it immediately arises as an alternative to diagnostic peritoneal lavage.

In 2004, it was proposed a further extension of FAST, aimed to the search of pneumothorax (PNX): ultrasound examination becomes extended FAST (E-FAST) (Fig. 53.3). The E-FAST is an ultrasound examination performed at the patient's bedside directly from the emergency doctor and differs significantly from the comprehensive exam performed in radiology.
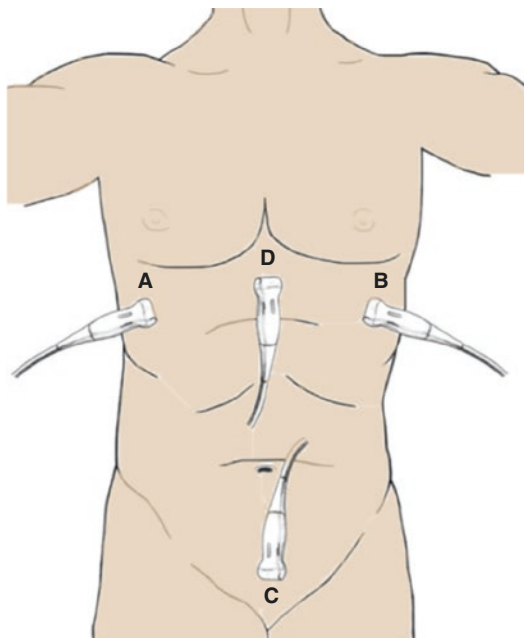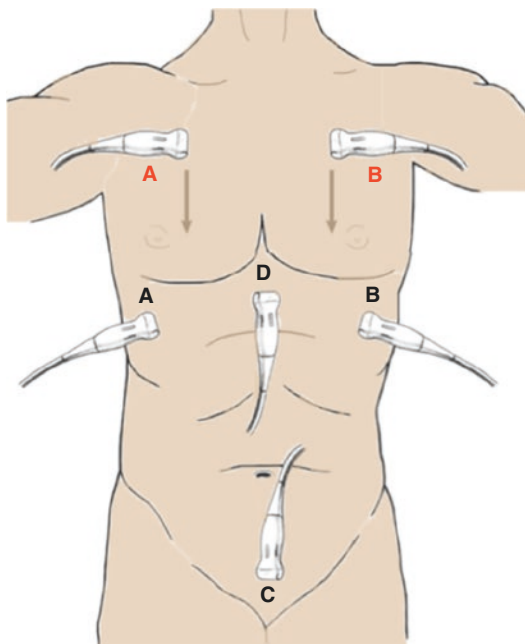
Fig. 53.3 The six-window US for the E-FAST scan. Abdomen: *A* = right upper quadrant that may be helpful to see the pleural space, Morison's pouch, liver, and right kidney; *B* = left upper quadrant that may be helpful to see pleural space, spleen, and left kidney; *C* = suprapubic view that may be helpful to see bladder and free liquid suggested peritoneal hemorrhage; *D* = subxiphoid view of the heart for pericardial effusion. *Thorax*: *A* = right parasagittal view of the lung for pneumothorax, *B* = left parasagittal view of the lung for pneumothorax

The E-FAST (Fig. 53.3) is a targeted examination representing a study of clinical ultrasound signs, while traditional radiological examination represents an organ or apparatus study (ultrasound images). The clinical ultrasound signs are divided in three groups: artifactual, anatomical, and functional. Moreover E-FAST must answer short and precise diagnostic questions (is there air? is there liquid?).

The procedure, now well standardized, is based on clinical ultrasound signs:

1. The absence of gliding sign, a baseline level for diagnosis of pleural PNX, possibly associated with the absence of lines B and to the relief of the lung point (functional) (Fig. 53.4a)
2. B-lines in an area of the lung parenchyma with pleural thickening of the line or not,

indicative of early pulmonary contusion (artifactual) (Figs. 53.4b and 53.5)
3. The presence of pleural effusion suggestive for hemothorax (anatomical) (Fig. 53.6)

The ultrasound examination can also provide an estimation, though approximate, of PNX extent (complete or minimum) (Fig. 53.7) and of the degree of blood effusion (quantitative assessment). In case of hypertensive or occult PNX, the sensitivity and the negative predictive value of ultrasonography in the latest cases are ranged, respectively, from 59% to 98% and from 94% to 99%.

Clinical signs of pericardial effusion with tamponade, represented by Beck's triad (hypotension, jugular turgor, and muffled heart sounds) in addition to dyspnea and tachycardia, being non-specific, are often interpreted with delay. Targeted ultrasound examination, even with a single subcostal scan, has diagnostic sensitivity and specificity equal to 100% (Fig. 53.8).

The E-FAST procedure, integrated into trauma management, finds its natural place at the end of the primary survey (ABCDE evaluation) (Table 53.1).

However, in the unstable patient, requiring immediate resuscitation maneuvers, targeted ultrasound examination with single scans (single view) can become decisive in identifying and resolving any problem drastically encountered in previous phases ABCD.

A = Airway During the evaluation of a patient's airway, breezy but with poor gas exchange might have a not well-positioned tracheal tube: observation of "gliding sign" and/or lines B moving bilaterally on the chest, parasternal positions, is the indirect method to diagnose a correct tracheal intubation. The B-lines (vertical comet tail artifacts from pleural line) are absent in PNX but present (sign of the "lights on the lake") after intubation failure.

On the other hand, if it is an emergency cricothyrotomy for glottal obstruction or airway supraglottal, ultrasound assistance reduces the execution time, improves success rate through the preliminary evaluation of the cervical anat-
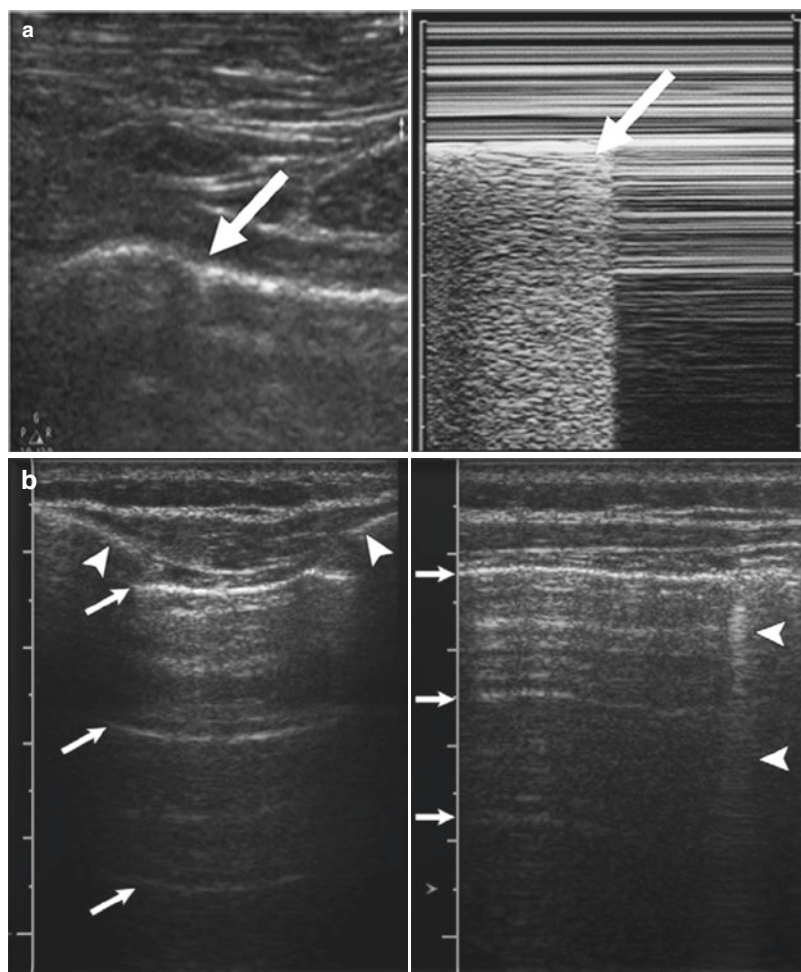
Fig. 53.4 (**a**) Lung point in M-mode. On the left the echogenic interface between the parietal and visceral pleural is seen, and posteriorly there is a granular appearance to the normal lung, the "seashore sign." To the right are numerous lines, termed the "barcode sign," representing pneumothorax. The white arrow indicates the interface between the normal lung and pneumothorax: the "lung point." (**b**) Normal lung. (A) Parasagittal view of the lung between the ribs shows shadowing at the anterior ribs (arrowheads). The most anterior echogenic line (arrow just below arrowhead) is the junction of the parietal and visceral pleura, where motion of sliding lung is observed. There are also A-lines (lower two arrows), which are equally spaced reverberation artifacts and decrease in echogenicity with depth. (B) Scan between ribs shows the most echogenic line (anterior arrow), or the junction of parietal and visceral pleura which represents the "sliding lung" sign in real time. Multiple reverberation artifacts are noted (posterior arrows). A B-line or "comet tail" artifact is also seen (arrowheads)

omy, and reduces the risk of abnormally shaped vases, sting finally confirming needle placement in the trachea, especially in obese or with abnormalities in the neck.

B = Breath Character assessment of breathing, tachypnoic patient or dyspnoic that desaturates, especially with suspected trachea asymmetry and/or hemothorax, deserves an immediate double view chest ultrasound to exclude a hypertensive PNX. Ultrasound bilateral rule approach in seconds direct you to the 14 g needle decompression maneuver by thoracentesis intensive care, to insert a chest tube as soon as possible.

C = Circulation The condition circulation represents the initial application of FAST, which, to recall, was born in its first version to assess the

Fig. 53.5 The states of lung contusion. (**a**) Initial appearance of B-lines; (**b**) B-lines divergent (black and white lung); (**c**) B-lines convergent (white lung); (**d**) thickening lung
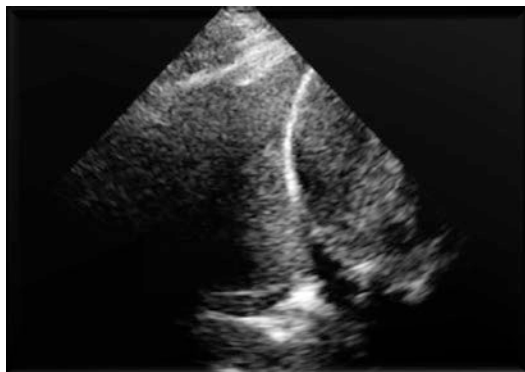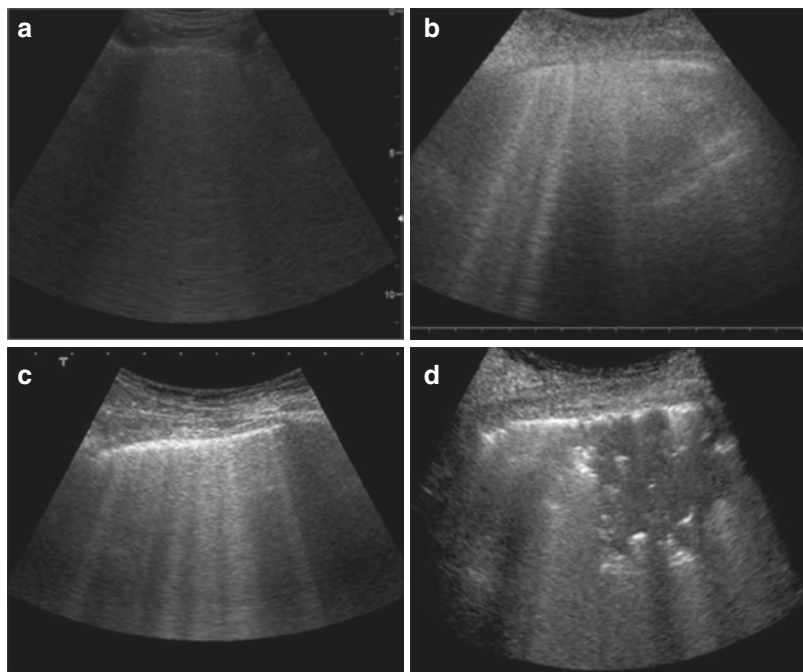
Fig. 53.6 Massive hemothorax. The ultrasound scan is made with cardiac probe

Fig. 53.7 Search for lung point in right pneumothorax

condition of hemorrhagic shock in trauma (hemo-pericardium has also been reported, hemothorax, hemoperitoneum).

On the other hand, in almost all medical and surgical emergencies, hypovolemia should be considered as the cause shock, until proven otherwise. Unless there are clear signs of cardiogenic shock, it is appropriate to administer intravenous fluids to all patients with cold extremities and tachycardia. Patient in shock should immediately be scored

using the E-FAST (also a hypertensive PNX can cause hemodynamic alterations), which would direct toward immediate resuscitation maneuvers, providing assistance in the event of hypertensive PNX (decompression), cardiac tamponade (pericardiocentesis), and thoracentesis (hemothorax) or by performing laparotomy (hemoperitoneum). It was estimated that the mortality of the patient with multiple trauma increases 1% every 3 min delay. Ultrasound examination can also collect more
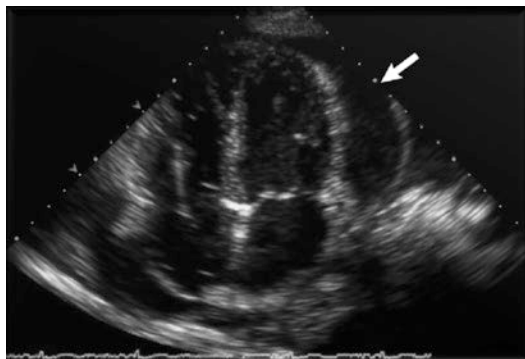
Fig. 53.8 Pericardial effusion: four-chamber view of the heart demonstrates moderate-size pericardial effusion (arrow)

information about circulation (empty hyperkinetic heart, inferior vena cava empty) and provide assistance for difficult venous access positioning, until simple arterial and/or venous sampling.

D = Disability In assessing the state of consciousness and neurological injuries, ultrasound can integrate the study of intracranial hypertension. The variation of the optic nerve transverse diameter has been suggested as a possible indicator of endocranic hypertension.

To visualize the ocular structures, we must align the beam toward optic nerve and with the size of diameter of the optic nerve so perpendicular to the vertical axis of the scan.

The diameter of the optic nerve, measured at 3 mm from the eyeball, normal is less than 6 mm in diameter 5 mm: > is related to intracranial hypertension.

E = Exposure Resolved immediately threatening situations or excluded in the ABCD; the sonographic evaluation finds its full application in the management of the critically ill patient with multiple trauma, in an attempt to identify a potentially life-threatening situation and integration of clinical parameters so far collected. On the other hand, at this stage, pending or immediately upon completion of secondary and evaluation of laboratory and instrumental investigations, the ultrasound examination can find additional applications:

- Evaluating possible fractures of the sternum, ribs, and long bones (Fig. 53.12)
- Locating pulmonary bruises in the evolution and during follow-up
- PNX control after decompression with chest tube or occult PNX
- Search for potential sources of abdominal organs and insidious parenchymal lesions of internal bleeding (liver, splenic, renal contusions and hematomas)
- Study of soft tissues for the presence of hematoma, subcutaneous emphysema, muscle and tendon injuries, eye injuries, and foreign bodies
- Guiding any regional anesthesia

To sum up, if FAST in primordial version is placed in phase C of the primary survey of trauma looking for internal bleeding (unstable patients with suspected hemorrhagic shock), its extended version (E-FAST), adding the study of PNX, can be placed in the patient who has gone through the ABCD steps without requiring resuscitation maneuvers at the end of the primary survey (proposed E = Ecography?).

Finally, E-FAST with the further extended study of bone tissue and superficial and internal organs can be used to improve patient secondary survey.

53.4   Evaluation of Inferior Vena Cava

At many trauma centers, FAST has been extended even further to include interrogation of the IVC during respiration as a noninvasive means of volume status assessment.

The most common cause of hypotension in trauma patients is hypovolemic shock from hemorrhage, but injuries to the heart or central nervous system may result in cardiogenic and neurogenic, or distributive, shock. These different forms of shock may be differentiated by performing US of the IVC. There is a general relationship between the IVC diameter and the central venous pressure; this forms the basic science of the way the IVC is measured, as a smaller diameter of the IVC may indicate volume depletion.

US of the IVC is performed with the patient in the supine position using the same low-frequency convex probe as for the abdominal views. A sub-xiphoid approach is made with the transducer in sagittal orientation (Fig. 53.9). Superiorly, the IVC enters the right atrium at the cava-atrial junction. The IVC diameter is measured 2 cm below the cava-atrial junction (Table 53.2). Inspiratory and expiratory diameters are obtained for comparison (Table 53.3). The use of M-mode has been advocated by some to be a more precise method to measure the IVC. Interpretation of IVC US is based on the diameter and degree
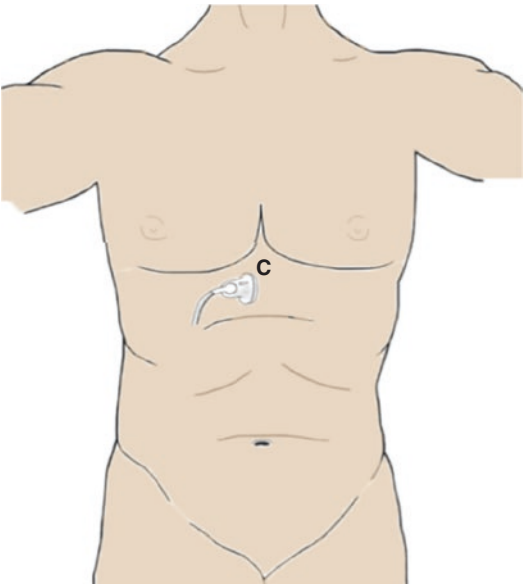
Fig. 53.9 The additional window US that may be helpful in the trauma in hypotensive patient for evaluated the vein cave: *C* = a longitudinal scan for view of the IVC

Table 53.2 IVC diameter change and correlation with central venous pressure

Expiratory IVC diameter (cm) and respiratory change	Estimated CVP (cm H$_2$O)
<1.5	
Total collapse	0–5
1.5–2.5	
>50% collapse	6–10
<50% collapse	11–15
>2.5	
<50% collapse	16–20
No change	>20

CVP central venous pressure

Table 53.3 Normal variation of IVC diameter with spontaneous breathing in an otherwise healthy patient

This spontaneous change may not be present in certain disease states or positive pressure ventilation
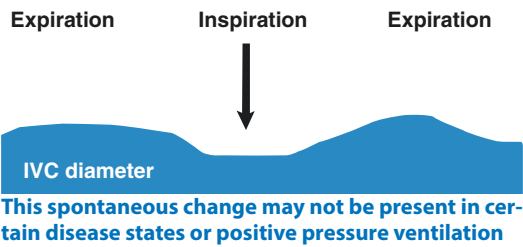
of inspiratory collapse of the IVC in non-intubated patients or intubated patients not receiving positive-pressure ventilation. The normal expiratory diameter of the IVC is 1.5–2.5 cm, and in the patient with normal volume, the IVC collapses during inspiration to less than 50% of its expiratory diameter. The caval index is calculated as a percentage with the formula: [(IVC expiratory diameter 2 IVC inspiratory diameter)-IVC expiratory diameter]x100. An index approaching 100% indicates almost complete collapse and likely volume depletion, whereas an index closes to 0% indicates minimal tricuspid regurgitation may also increase IVC diameter and render an inaccurate estimate of shock. Additionally, the IVC can be difficult to detect in hypotensive trauma patients with hypovolemic shock owing to its reduced diameter. As the initial FAST sonogram represents a snapshot in time, serial examinations performed in stable blunt trauma patients may be useful. Examination after stabilization gives the sonographer more time for a comprehensive scan. With active intraperitoneal hemorrhage, the collapse, suggesting volume overload. Ferrada and co-workers studied 101 hypotensive acute trauma patients who underwent IVC US and reported poor prognosis for those patients with a collapsed IVC.

For trauma, the simplest approach is to evaluate the IVC in hypotensive patient to see if it has substantial collapse with small diameter (1.5 cm), indicating volume depletion and probably peritoneal hemorrhage (Fig. 53.10). If, instead, the diameter of the vena cava is enlarged and there is no change in inspiratory and expiratory diameters, the patient has an obstructive shock due to pericardial effusion with cardiac tamponade,

Fig. 53.10 Collapse >50% of vein cave in traumatic patient with hemorrhagic shock. (**a**) The heart little and hyperkinetic. (**b**) The normal lung. (**c**) The massive hemoperitoneal
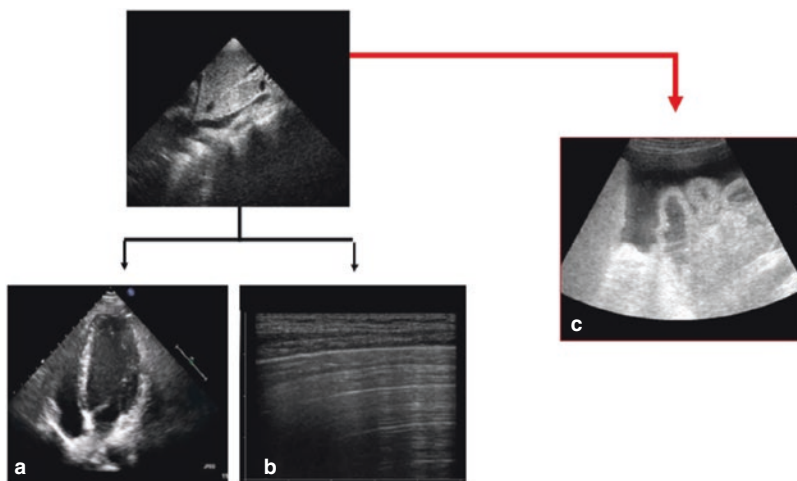
Fig. 53.11 Vein cave enlarged in traumatic patient with hemorrhagic shock. (**a**) Cardiac tamponade. (**b**) Massive pneumothorax. (**c**) Massive hemothorax
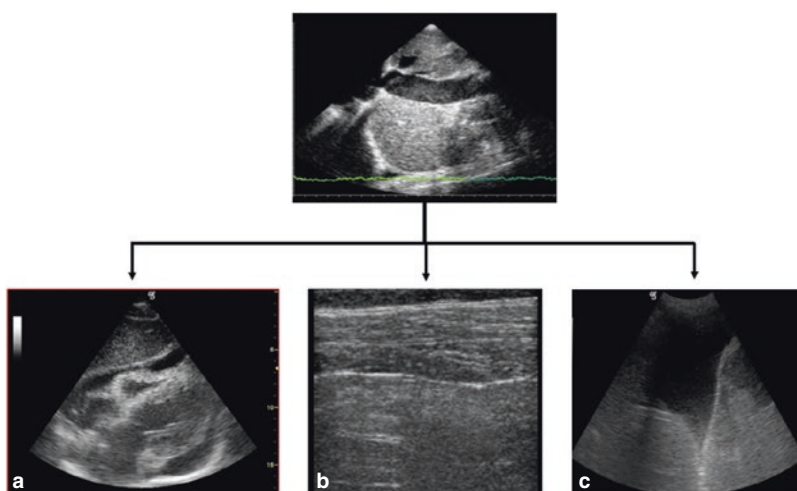
massive pneumothorax, or pleural effusion with massive hemothorax (Fig. 53.11).

IVC evaluation has also been shown to be useful in gauging fluid responsiveness in patients requiring volume resuscitation or transfusion of blood products.

For IVC US, there are diagnostic limitations for its use in the estimation of shock in intubated patients with positive-pressure ventilation, as the IVC diameter will be increased. Severe chronic obstructive pulmonary disease, pulmonary hypertension, right-sided heart failure, cardiac tamponade, and tricuspid regurgitation may also increase IVC diameter and render an inaccurate estimate of shock (Fig. 53.12).

53.5   The Technique and Ultrasound Semiology of Pneumothorax

In pneumothorax (PNX), the presence of air in the pleural cavity is not directly provable by ultrasonography. Its presence is indirectly confirmed by the lack of baseline shift with pleural respiratory acts (absence of gliding sign).

On the other hand, ultrasound documentation of this sign confirms the stored contact between visceral pleura and parietal pleura and excludes the presence of PNX with almost absolute diagnostic accuracy. The presence of plaques of

Fig. 53.12 Second survey in stable traumatic patient. (**a**) No composite fracture of sternum. (**b**) No composite fracture of the rib. (**c**) Composite fracture of rib
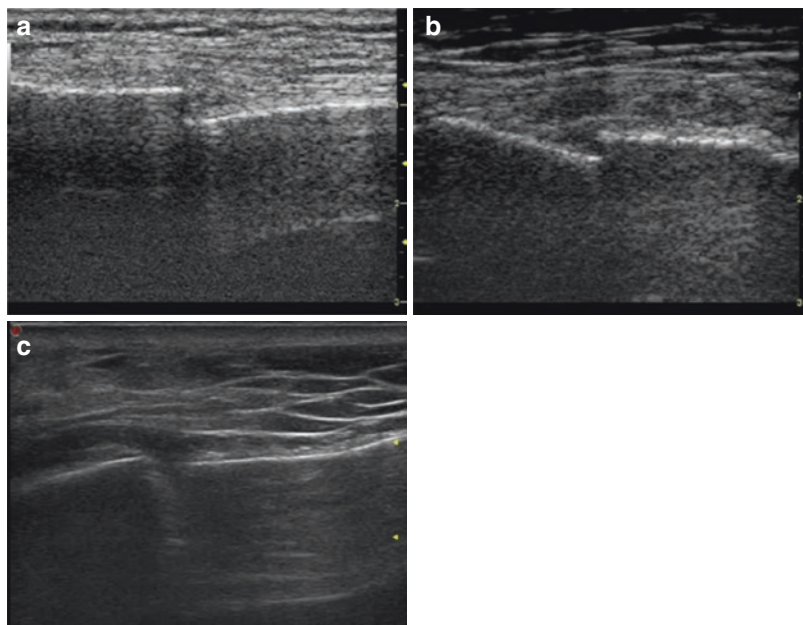
fibro-chest, pulmonary fibrosis, or atelectasis may give way to false-positives.

The ultrasound examination second sign is the presence of vertical artifacts (lines B): attributable to the so-called tails of a comet (comet tails), the lines are always moving from pleural line artifacts consensual iterating over this (Fig. 53.5). Detectable in normal subjects only in approximately 50% of cases, you are able to exclude the presence of PNX with negative predictive value equal to 100%.

The extension of PNX is measurable by locating a third ultrasound sign: the "lung" point "(pulmonary point sign) (Fig. 53.7). Even the lung point is a dynamic sign. It represents the point where contact between the pleural slips back, documented by the sliding of the visceral pleura on that parietal, flanked in the same image from the pattern typical of PNX ("A-line sign pattern") (Fig. 53.4a).

The ultrasonographic findings of PNX in the parasternal regions were defined as the "deep sulcus sign." The area of the "deep sulcus" is that corresponding to the projection of the anterior thoracic edges cardio-phrenic mediastinal and furrow, bounded above by the second front-fee costs, below the diaphragm and laterally by axillary lines below mammary cranial lines. The

demonstration of the sliding of the visceral pleura on parietal pleura during respiratory movements (gliding sign) can be effectively demonstrated with M-mode (Fig. 53.4a).

53.6   Ultrasound of Pouring Blood

Pouring free semiotics into preformed cavities (whether it be hemopericardium, hemothorax, or hemoperitoneum) initially appears like the anechoic ascitic effusion; after a few hours, following blood clot onset, the sonographic appearance changes and tends to appear unevenly through the country, with thin hyperechoic echoes scattered and settled in part sloping; then it becomes again anechoic for the lysis of clots, thereby showing a collection often bounded by an echoic wall, in whose context for red cell sedimentation phenomena of the solid part tends to stratify in the sloping, forming a liquid-solid level, anechoic-parenchyma.

Quantitative ultrasound, while it may also detect small amounts limited to a few ml, detects safely diffuse deposit only if it is greater than 300 ml.

The forums where more often in the peritoneal cavity bleeding tends to be located adjacent to the

Fig. 53.13 Spleen
contusion
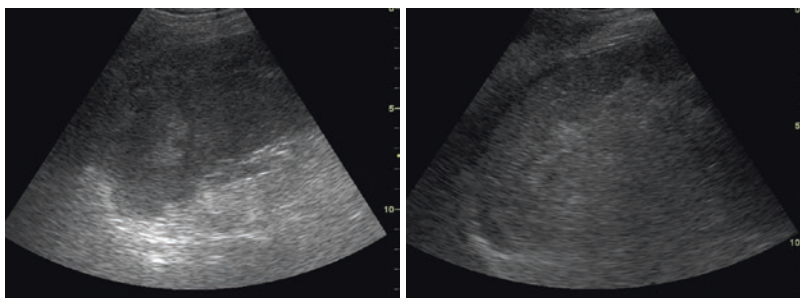
Fig. 53.14 Liver
contusion
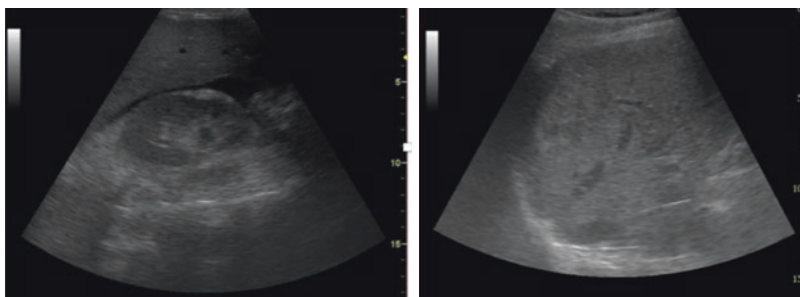
organ of origin are the withdrawal (Figs. 53.13
and 53.14) and from multiple slopes: typically,
the Morrison's pouch for sovramesocolic and
Douglas hemorrhages (women) or recto-vesical
space (men) to those of sotto mesocolic origin.

53.7   Examination Technique

Bedside ultrasonography examination in emer-
gency trauma room is different from the com-
prehensive exam in radiology. The goal, when
using the E-FAST technique (Fig. 53.3), is to
answer a few questions. The examination must
be completed within minutes (less than 5 min)
without interfering hypotensive resuscitation
maneuvers but in a patient with a massive hemo-
peritoneum can be highlighted with a single
pocket level scanning so far 90% of cases in a
Morrison less than 20 s. In case of hemoperi-
toneum in Morrison Pocket and spleno-renal
is more frequently involved than the pelvic
digging.

In unstable patients or in suspected abdomi-
nal injury, it may be appropriate to evaluate the
Morrison space, most involved in intraperitoneal
organ hemorrhages.

In the stable patient or with manifest breath-
ing difficulty, the exam sequence starting from
the chest should be followed.

The probe is convex operating at 3–6 MHz,
which can be used for both thoracic scans than
for abdominal scans, with the only difference of
point to low levels of depth (6–8 cm) in the study
of PNX and high levels (12–20 cm) in abdomi-
nal scans. The complete examination includes
the sequential study of six regions, two thoracic
(A and B) and four abdominal (A, B, C, and D)
for examining ten sites or mnemonic 10 P rule
(Fig. 53.3).

- *Position A*. The left parasternal region for the
  evaluation of longitudinal scan PNX
- *Position B*. The right parasternal region, sym-
  metrical to the former
- *Position A*. The region of hypochondrium
  region-flank, to inspect in coronal and trans-
  verse scans periepathic regions with hepatore-
  nal pouch (Morrison), pleural sloping level
  (within cost-phrenic), or colic and paracolic
  parieto-region
- *Position B*. Hypochondrium region-left flank,
  to inspect in coronal and transverse scans
  perisplenic pocket wide regions spleno-renal,

Fig. 53.15 The laceration of the left kidney before and after CEUS exam
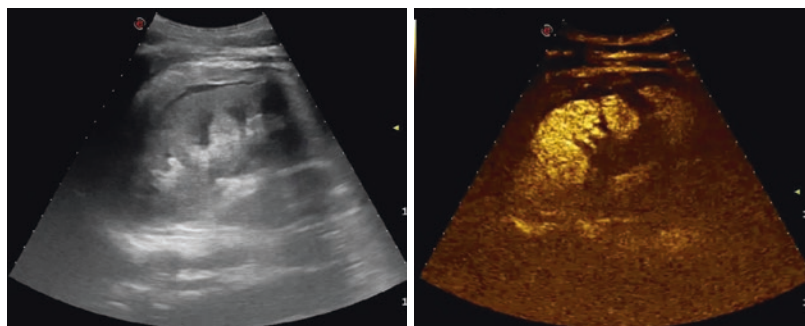
Fig. 53.16 The laceration of inferior pole of spleen before and after CEUS exam
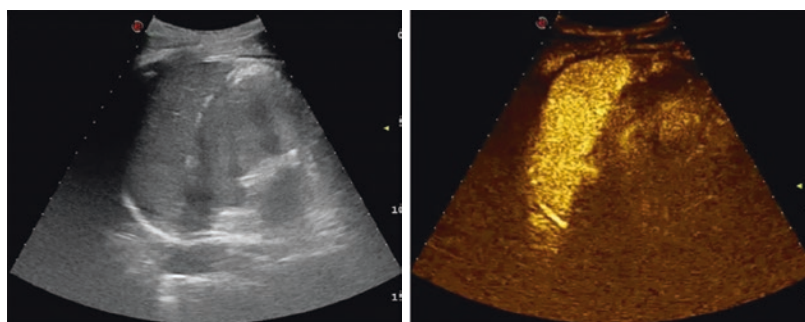
sloping left pleural (seno phrenic cost), and the left paracolic or parieto-shower colic region
- *Position C*. The hypogastric region using the pubic to study with longitudinal and transverse scans of the pelvis, which is primarily recto-uterine space in woman (Douglas) or recto-vesical space in man
- *Position D*. The epigastric region, to examine the pericardium in ascending, preferably subcostal transverse scan (long axis)
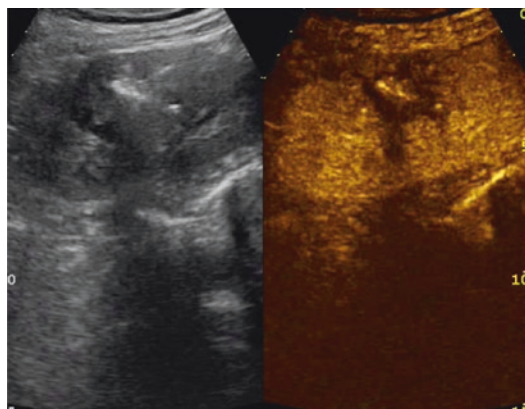
53.8 Contrast-Enhanced Ultrasound (CEUS)

US is highly sensitive in the assessment of abdominal trauma, particularly in the detection of intra-abdominal fluid with a percentage varying from 63% to 99% (Figs. 53.13 and 53.14); the sensitivity of US is significantly reduced in the diagnosis of traumatic parenchymal lesions, and currently, in the evaluation of patients with abdominal trauma, CT is the reference standard.

Fig. 53.17 The injury of right kidney complicated by abscess in traumatic event after 7 days

The introduction in clinical practice of CEUS has improved the sensitivity of the US in the detection and assessment of the traumatic parenchymal lesions extension (Figs. 53.15, 53.16, and 53.17). In addition, CEUS exceeded the limits of the B-mode US and the US color and power-Doppler and expanded the applications of the method especially in abdominal trauma in children.

The first results in literature indicate the use of CEUS in patients with blunt abdominal trauma after the FAST or the US, in hemodynamically stable patients with a history of low-energy trauma. CT is reserved in cases of severe trauma, with clinical suspicion of multiple organ lesions and cases with inconclusive CEUS.

The first-generation contrast agents consisted of air-filled microbubbles: they were particularly fragile, and their quick and easy break involved a large inter- and intraindividual variation of the signal amplification with short duration of contrast effect.

The second-generation contrast agent (SonoVue), used in our experience, is represented by inert gas-filled microbubbles and denser than air (sulfur hexa- fluoride) and delimited by stabilized phospholipids membranes giving high strength and flexibility. Sulfur hexafluoride is eliminated via the respiratory system, while the membrane phospholipids are metabolized in the liver.

The contrast agent eco-amplifiers are able to modify the acoustic impedance of tissues, interacting with ultrasound beams and increasing the echogenicity of blood.

The contrast media (CM) ultrasound (USCA, ultrasound contrast agent) consists of microbubbles containing inert gases and surrounded by membrane stabilizers.

This CM is well tolerated (side effects-based incidence of anaphylactoid reactions has 0.001%), non-nephrotoxic, and with short half-life (approximately 12 min), but particular caution should be exercised in patients with cardiac and pulmonary disease.

These are characterized by strong power echogenic microbubbles sufficiently small in size (<7 ìm) able to pass through capillaries but unable to cross the endothelial fenestrations with persistence in the blood stream for a relatively long time. In fact, unlike the CM used in CT or MRI, which spread rapidly in the extravascular interstitial space, the ultrasound contrast agent used in pharmacokinetics has the characteristic to remain confined to the vessel lumen, without spreading to interstitial level, and therefore are not filtered in the kidney.

The CM is administered intravenously by bolus injection using needles 18–20 Gauge followed by a bolus of approximately 10 ml of saline solution.

53.9 The CEUS Technique

The CEUS technique involves the continuous insonation of the region of interest after the injection of CM with real-time and continuous evaluation of all the contrastrographic phases (arterial phase, venous phase, and late phase).

The CEUS enhancement patterns in each phase are similar to that of CT or MRI; however, due to the different pharmacokinetics of the CM, the late phase of CEUS does not correspond to equilibrium phase as described for the extracellular CM used in CT.

The CEUS findings are related to the contrast material distribution and are defined as homogeneous, heterogeneous, or absent. On the other hand, it is difficult to define the degree of enhancement qualitatively when the parenchyma is considered.

The appearance of a normal abdominal parenchymal organ is homogeneous and hyperechoic in the absence of distortions of the echogenicity, and vascular structures are clearly distinguishable.

Trauma can cause various parenchymal changes: bruises, lacerations, bleeding, heart attack, or arteriovenous fistulas. According to the mechanism of injury, bruises show different aspects, ranging from a simple edematous area, not well-defined with ultrasound contrast media, to hypoechoic areas characterized by reduced or no perfusion.

The lacerations appear as bands of linear or branched marked hypoechogenicity sharply defined and the clinical course usually perpendicular to the surface of the organ (and dependent on the force lines of the trauma) and may be associated with capsular discontinuity of the profile (Fig. 53.15).

The intraparenchymal hematoma is valuable as a heterogeneously hypoechoic area with poorly defined contours in the context of which vascular structures are not recognizable;

subcapsular hematoma appears as a lenticular area of absent enhancement surrounding parenchyma in which, if actively stocked, extravasation CM is recognizable.

The spreading of contrast material within the peritoneal or retroperitoneal space is indicative of active bleeding.

The complete avulsion of the vascular pedicle of an organ (e.g., spleen or kidney) is realized with the complete absence of parenchyma enhancement in abdominal examination. It is fundamental for differential diagnosis of traumatic parenchymal lesions respect to other pathological conditions, possible causes of hypoechoic in ultrasound with contrast medium: e.g. calcifications (clearly visible with conventional imaging), pseudoaneurysm, non-traumatic focal parenchymal lesions.

53.9.1 Spleen

The spleen is the most frequently affected intra-abdominal traumtized organ. Its exploration may be limited by the interposition of ribs and the bloating of the splenic flexure, particularly at the level of inaccessible sites such as the upper pole and the phrenic subregion, especially in non-collaborative patients (inability to vary the respiratory phases or decubitus).

The splenic arterial phase of enhancement (early start at 12–18 s) has a relatively long duration with an uneven aspect of organ called "zebra" (due to the movement of two circuits with red pulp and white pulp), which makes it difficult if not impossible, the identification of tissue damage. Venous phase (approximately 40–60 s after i.v. contrast means injection) is accurate in the detection of traumatic lesions of the spleen (Fig. 53.16); in the venous phase, the normal parenchyma presents a homogeneous contrast enhancement of sufficiently long duration (about 5–7 min).

Compared to the left kidney, which exhibits early enhancement but brief, the spleen appears less echogenic and hyperechoic during the arterial phase during the late stage.

Since the spleen acts as a filter for microbubbles, the splenic vein and its tributaries exhibit washout about 3 min after the start of contrast means, thus resulting in only a tenuous enhancement of the vessels due to intrasplenic entrapment. In this case, the venous vascular structures, quickly hypoechoic, create problems of differential diagnosis with posttraumatic parenchymal perfusion defects; in fact, Valentine et al. recommend, when in doubt, a second evaluation with a second bolus of contrast agent.

For adults, dose range is between 0.6 and 1.2 ml. For children, the dose in ml is calculated using the following formula: age/20.

53.9.2 Liver

The liver is the second intraperitoneal parenchymal organ involved in trauma. In CEUS examination, the arterial phase appears about 10–20 s after the injection of contrast means, lasts approximately 15 s, and is quickly followed by the venous phase, which lasts about 2 min. The late phase lasts until complete clearance of the microbubbles from liver parenchyma (4–6 min) and does not correspond to the equilibrium phase described for the extracellular contrast media used in CT or MR.

For adults, dose range is between 1.2 and 2.4 ml. For children, the dose in ml is calculated using the following formula: age in years/10.

CEUS in the healthy liver parenchyma shows diffuse and homogeneous hyperechoic in absence of echotexture distortions. Parenchymal injuries are hardly appreciable with examination and occur at CEUS as areas of reduced or absent perfusion better highlighted during the late phase.

The full exploration of the liver can be affected from the large liver surface to explore and limited to the study of not easily accessible areas (dome and lateral segments), particularly in uncooperative patients (inability to vary the respiratory phases or decubitus) by interposition of ribs and bloating stomach and bowels. In addition, the entity hematoma or hepatic laceration is not easily found in the acute phase as yet isoechoic compared with adjacent healthy parenchyma. For these reasons, the CT examination remains the imaging modality of reference, particularly in high-energy trauma victims.

53.9.3 Kidney

Renal trauma is relatively frequent and represents about 5% of abdominal traumas.

The kidneys show different degrees of enhancement in the cortex and the pyramids; the cortex almost immediately enhances very brightly and evenly, while the pyramids enhance diffusely from the periphery to the center over about 30 s. The homogeneous phase of the kidneys generally lasts 2–2.5 min: this homogeneous phase (venous phase or nephrographic phase) is still the most effective for detection of traumatic injuries. The recommended dose is the same as used for the study of the spleen (0.6 ml or ml of SonoVue: age in years/20).

It is necessary to investigate the kidneys separately with two different boluses of contrast media. The full exploration of both kidneys is usually hard: the left kidney is sometimes obscured by superimposed bowel gas and ribs on images from US evaluations.

Similarly to the liver and spleen, kidney contusion lesions appear as a hypoechoic area without clear delimitation; laceration usually appears as a linear or branched hypoechoic band, perpendicular to the surface of the organ (Fig. 53.15). A subcapsular hematoma appears as a nonhomogeneous collection surrounding the kidney. In the case of renal hilum tear, a total absence of parenchymal enhancement is found at CEUS. The rapid enhancement can generate interpretation questions that can possibly be solved only with a second injection of contrast agent.

An injection of a dose too high of contrast media will have a negative effect due to the intense enhancement, potentially masking the presence of lacerations. Moreover, as much as no microbubble excretion into urinary tract is found, CEUS evaluation detects only indirect signs (abdominal fluid) in the event of accidental bladder, ureter, or collecting system failure. For the above limits, CT remains the method of choice for staging of renal damage.

53.10 Conclusion

Clinical ultrasound in the emergency department performed in the trauma room by consultants in emergency medicine with training in bedside sonography and goal-directed, for historical reasons, has its main application in multiple trauma, and FAST (today in new capacity known as E-FAST) is its most common protocol expression.

The E-FAST is today considered to be irreplaceable in the evaluation at the integrative technique assistance (point of care) from the scene of the accident and inpatient transport, as proposed in PH-EUS (PreHospital – Emergency US) and FASTER (Focused Assessment by Sonography in Trauma during Emergency Retrieval) protocols, to complete the intrahospital management, emergency room (shock room) observation, emergency medicine, and intensive care departments.

However, it should be pointed out that urgent sonographic evaluation in thoracoabdominal trauma victims must always be performed with respect to patient's clinical situation. Only if correctly included in the global assessment, anamnesis, objective data, and laboratory tests, E-FAST can provide useful data in guiding clinician's decision in the multiple trauma management.

Its comfort in a stable patient and its easy use can be considered as further extensions of E-FAST. The chest can be thoroughly investigated in order to identify sternal or rib bone lesions, extension, and evolution of occult PNX evaluated after treatment, while the lung parenchyma lends itself to the study of potential bruises.

Long limb bones also can be evaluated to rule out fractures, especially if guided by patient's symptoms.

The evolution of intracranial hypertension can be measured through the evaluation of thickness of optic nerve sheathing using high frequency trans orbital linear probe scans (Fig. 53.18). In the abdominal area, organ lesions can be searched.

CEUS introduction in clinical practice increases the sensitivity and accuracy of US; however, it has some limitations in parenchymal and retroperitoneum injuries evaluation. With respect to parenchymal injuries CEUS, similar to US, some locations are poorly inaccessible (e.g., hepatic dome and the upper pole of the spleen). CEUS is enabled to evaluate simultaneously abdominal parenchyma. In order to overcome this limitation, some authors propose to split contrast material in two or more boluses to study one or at most two ipsilateral parenchyma.

Fig. 53.18 The optic nerve sheath visualized by ultrasonography by insonation across the orbit in the axial plane
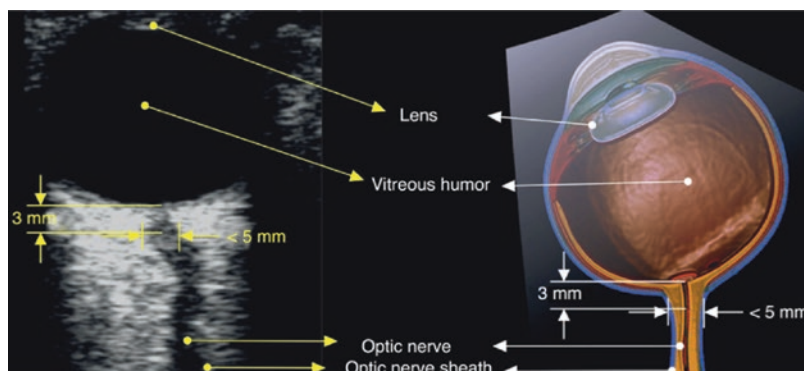
According to this diagnostic strategy, the kidney must be the first organ to be studied because of the early and short enhancement peak (first 2 min), and the same bolus (volume of about 2.4 ml) can be used for the study of the liver or the spleen in relation to the late reaching of a homogeneous enhancement (2–4 min after injection of contrast material) respectively, for the right or left abdominal quadrants.

The study of the renal excretory cavity is not a limit to the examination of the urinary tract in the multiple trauma patient, due to the lack of renal flow out of contrast means used in US. CEUS should be performed by high-level competence operators.

Additional limitations of CEUS are the absence of three-dimensional scanning, the lack of whole-body exploration, and extreme difficulty in detecting traumatic bowel and mesenteric lesions, and operator dependence makes the technique "subjective."

CT remains the imaging of choice in trauma due to its high sensitivity and specificity and the relatively noninvasive and rapid execution.

In multiple trauma patients, CEUS was proposed as a first-level examination, after E-FAST, in order to reduce the number of CT exams. US B-mode is able to demonstrate the presence of intra-abdominal fluid in most cases but is poorly sensitive in detecting posttraumatic organ damage; some authors recommend CEUS in completion of E-FAST or the US for the evaluation of liver, spleen, and kidney trauma, while others reserve CEUS in case of low-energy abdominal traumas.

In order to reduce radiation exposure dose, particularly in young or children, CEUS has an important role in the follow-up of conservatively treated traumatic injuries of the abdominal parenchymal organs (liver, spleen, and kidneys) diagnosed by CT.

Currently available data about the diagnostic accuracy of E-FAST are less full-bodied than in adults: there is no indication of reduced sensitivity of the method to identify internal bleeding in the period immediately after trauma, while the sensitivity is high in further controls and in hypotensive patients, however, like the adult.

A peculiar well-established application is the use of E-FAST in traumatized pregnant women: in these cases, the targeted clinical ultrasound examination, in addition to preserve all the diagnostic validity described above, allows to avoid dangerous exposure of fetus to ionizing radiation and provides guidance on the viability of the same.

Suggested Readings

1. Mock CN, Jurkovich GJ, Amon-Kotei D, Arreola-Risa C, Maier RV. Trauma mortality patterns in three nations at different economic levels: implications for global trauma system development. J Trauma. 1998;44:804–12.
2. American Institute of Ultrasound in M, American College of Emergency P. AIUM practice guideline for the performance of the focused assessment with sonography for trauma (FAST) examination. J Ultrasound Med. 2014;33:2047–56.
3. Smith ZA, Wood D. Emergency focused assessment with sonography in trauma (FAST) and haemodynamic stability. Emerg Med J. 2014;31:273–7.

4. Quinn AC, Sinert R. What is the utility of the Focused Assessment with Sonography in Trauma (FAST) exam in penetrating torso trauma? Injury. 2011;42:482–7.

5. Tam MMK. Occult pneumothorax in trauma patients: should his be sought in the focused assessment with sonography for trauma examination? Emerg Med Australas. 2005;17:488–93.

6. Udobi KF, Rodriguez A, Chiu WC, et al. Role of ultrasonography in penetrating abdominal trauma: a prospective clinical study. J Trauma. 2001;50:475–9.

7. Whitson MR, Mayo PH. Ultrasonography in the emergency department. Crit Care. 2016;20:227; Ding W, Shen Y, Yang J, He X, Zhang M. Diagnosis of pneumothorax by radiography and ultrasonography: a meta-analysis. Chest. 2011;140:859–866.

8. Alrajhi K, Woo MY, Vaillancourt C. Test characteristics of ultrasonog- raphy for the detection of pneumothorax: a systematic review and meta-analysis. Chest. 2012;141:703–8.

9. Subcommittee A, American College of Surgeons' Committee on T, International Awg. Advanced trauma life support (ATLS(R)): the ninth edition. J Trauma Acute Care Surg. 2013;74:1363–6.

10. Testa A. Manuale di Ecografia Clinica in Urgenza, (ed.) Verduci Editore, Roma; 2008. p. 247–252.

11. American College of Emergency Physicians. Emergency ultrasound imaging criteria compendium. Ann Emerg Med. 2006;48:487–510.

12. Blackbourne LH, Soffer D, McKenney M, et al. Secondary ultrasound examination increases the sensitivity of the FAST exam in blunt trauma. J Trauma. 2004;57:934–8.

13. Ollerton JE, Sugrue M, Balogh Z, D'amours SK, Giles A, Wyllie P. Prospective study to evaluate the influence of FAST on trauma patient management. J Trauma. 2006;60:785–91.

14. Kirkpatrick AW, Sirois M, Laupland KB, et al. Hand-held thoracic sonography for detecting post-traumatic pneumothorax:the extended focused assessment with sonography for trauma (EFAST). J Trauma. 2004;57:288–95.

15. Soldati G, Testa A, Sher S, et al. Occult traumatic pneumothorax: diagnostic accuracy of lung ultrasonography in the emergency department. Chest. 2008;133:204–11.

16. Kirkpatrick AW. Clinician-performed focused sonography for the resuscitation of trauma. Crit Care Med. 2007;35(Suppl):S162–72.

17. Roy CL, Minor MA, Brookhart MA, Choudhry NK. Does this patient with a pericardial effusion have cardiac tamponade? JAMA. 2007;297:1810–8.

18. Tayal VS, Beatty MA, Marx JA, Tomaszewski CA, Thomason MH. FAST (focused assessment with sonography in trauma) accurate for cardiac and intraperitoneal injury in penetrating anterior chest trauma. J Ultrasound Med. 2004;23:467–72.

19. Soyuncu S, Cete Y, Bozan H, Kartal M, Akyol AJ. Accuracy of physical and ultrasonographic examination by emergency physicians for the early diagnosis of intraabdominal haemorrhage in blunt abdominal trauma. Injury. 2007;38:564–9.

20. Soudack M, Epelman M, Maor R, et al. Esperience with focused abdominal sonography for trauma (FAST) in 313 pediatricpatients. J Clin Ultrasound. 2004;32:53–61.

21. Liu M, Lee CH, P'eng FK. Prospective comparison of diagnostic peritoneal lavage, computed tomographic scanning and ultrasonography for the diagnosis of blunt abdominal trauma. J Trauma. 1993;35:267–70.

22. Weaver B, Lyon M, Blaivas M. Confirmation of endotracheal tube placement after intubation using the ultrasound sliding lung sign. Acad Emerg Med. 2006;13:239–44.

23. ALS Advanced Life Support. Manuale di rianimazione cardiopolmonare avanzata. IRC. 2 edizione. Masson S.p.A. Milano; 2014.

24. Clarke JR, Trooskin SZ, Doshi PJ, Greenwald L, Mode CJ. Time to laparotomy for intra-abdominal bleeding from trauma does affect survival for delays up to 90 minutes. J Trauma. 2002;52:420–5.

25. Blaivas M, Theodoro DL, Sierzenski P. Elevated intracranial pressure detected by bedside emergency ultrasonography of the op-tic nerve sheath. Acad Emerg Med. 2003;10:376–81.

26. Tayal VS, Neulander M, Norton HJ, et al. Emergency department sonographic measurement of optic nerve sheath diameter to detect findings of increased intracranial pressure in adult head injury patients. Ann Emerg Med. 2007;49:508–14.

27. Soldati G, Testa A, Silva FR, Carbone L, Portale G, GentiloniSilveri N. Chest ultrasonography in lung contusion. Chest. 2006;130:533–8.

28. Soldati G, Testa A, Pignataro G, et al. The sonographic deep sulcus sign in traumatic pneumothorax. Ultrasound Med Biol. 2006;32:1157–63.

29. Lichtenstein D. Pneumothorax and introduction to ultrasound signs in the lung. In: Lichtenstein D, editor. General ultrasound in the critically ill. Berlin: Springer; 2005. p. 105–15.

30. Rose JS, Bair AE, Mandavia D, et al. The UHP ultrasound protocol: a novel ultrasound approach to the empiric evaluation of the undifferentiated hypotensive patients. Am J Emerg Med. 2001;19:299–302.

31. Nielsen K, Lauridsen JR, Laursen CB, Brabrand M. Physicians using ultrasound in Danish emergency departments are mostly summoned specialists. Scand J Trauma Resusc Emerg Med. 2015;23:51.

32. Simonson JS, Schiller NB. Sonospirometry: a new method for noninvasive estimation of mean right atrial pressure based on two-dimensional echographic measurements of the inferior vena cava during measured inspiration. J Am Coll Cardiol. 1988;11(3):557–64.

33. Kircher BJ, Himelman RB, Schiller NB. Noninvasive estimation of right atrial pressure from the inspiratory collapse of the inferior vena cava. Am J Cardiol. 1990;66(4):493–6.

34. Juhl-Olsen P, Frederiksen CA, Sloth E. Ultrasound assessment of inferior vena cava collapsibility is not a valid measure of preload changes during triggered

positive pressure ventilation: a controlled cross- over study. Ultraschall Med. 2012;33(2):152–9.

35. Goldam K, Saul T, Lewiss R. Focus on: inferior vena cava ultrasound. ACEP News. 2011.

36. Ferrada P, Vanguri P, Anand RJ, et al. Flat inferior vena cava: indicator of poor prognosis in trauma and acute care surgery patients. Am Surg. 2012;78(12):1396–8.

37. Neri L. Prehospital trauma care ultrasound. In: Prehospital trauma care. Bologna: Italian Resuscitation Council Edizioni; 2007. p. 325–9.

38. Valentino M, Serra C, Zironi G, et al. Blunt abdominal trauma: emergency contrast-enhanced sonography for detection of solid organ injuries. Am J Roentgenol. 2006;186:1361–7.

39. Catalano O, Lobianco R, Raso MM, Siani A. Blunt hepatic trauma: evaluation with contrast-enhanced sonography. J Ultrasound Med. 2005;24:299–310.

40. Catalano O, Lobianco R, Sandomenico F, et al. Real-time contrast-enhanced sonographic imaging in emergency radiology. Radiol Med. 2004;108(5–6):454–69.

41. McGahan JP, Horton S, Gerscovich EO, et al. Appearance of solid organ injury with contrast-enhanced sonography in blunt abdominal trauma: preliminary experience. AJR. 2006;187:658–66.

42. Cokkinos D, Antypa K, Stefanidis K, et al. Contrast-enhanced ultrasound for imaging blunt abdominal trauma – indication, description of the technique and imaging review. Ultraschall in Med. 2012;33:60–7.

43. Valentino M, Serra C, Zironi G, et al. Blunt abdominal trauma: emergency contrast-enhanced sonography for detection of solid organ injuries. AJR. 2006;186:1361–7.

44. Thorelius L. Emergency real-time contrast-enhanced ultrasonography for the detection of solid organ injuries. Eur Radiol Suppl. 2007;17:107–12.

45. Catalano O, Aiani L, Barozzi L, et al. CEUS in abdominal trauma: multi- center study. Abdom Imaging. 2009;34:225–34.

46. Valentino M, Serra C, Pavlica P, et al. Contrast-Enhanced Ultrasound for blunt abdominal trauma. Semin Ultrasound CT MR. 2007;28(2):130–40.

47. Valentino M, Pavlica P, Barozzi L. Ecografia con mezzo di contrasto nei traumi addominali. Diagnostica per immagini del trauma maggiore. Masson. 2010;20:211–6.

48. Claudon M, Cosgrove D, Albrecht T, et al. Guidelines and good clinical practice recommendations for contrast enhanced ultrasound (CEUS) – update 2008. Ultraschall in Med. 2008;29:28–44.

49. Esposito F, Di Serafino M, Sgambati P, Mercogliano F, Tarantino L, Vallone G, Oresta P. Ultrasound contrast media in paediatric patients: is it an off-label use? Regulatory requirements and radiologist's liability. Radiol Med. 2012;117(1):148.

50. Brenner DJ, Hall EJ. Computed tomography – an increasing source of radiation exposure. NEJM. 2007;357:2277–84.

51. Levy IA, Noble VE. Bedside ultrasound in pediatric emergency medicine. Pediatrics. 2008;121:1404–12.

52. Brown MA, Sirlin CB, Farahmand N, Hoyt DB, Casola G. Screening sonography in pregnant patients with blunt abdominal trauma. J Ultrasound Med. 2005;24:175–81.

Color Duplex Ultrasonography in the Study of the Stenosis of Renal Arteries

54

Gianfranco Giannasi and Antonio Mannarino

54.1 Introduction

Renal artery stenosis (RAS) essentially recognizes two types: the atherosclerotic form responsible for about 90% of all cases and fibromuscular dysplasia (FMD), which represents a significantly less significant proportion (less than 10%).

Atherosclerotic RAS is born as an extension of the atherosclerotic process that from the abdominal aorta generally involves the ostium or the first proximal portion of the renal artery.

The range of the age involved is >60 years with mild prevalence of male sex, often associated with signs of atherosclerosis in other vascular districts.

Atherosclerotic RAS may present asymptomatically or be associated with high blood pressure with or without chronic renal failure. FMD is actually a complex of diseases characterized by the fibrous degeneration of the muscle tissue of the renal artery.

The most common form is the multifocal with the typical angiographic appearance of "string of beads" at the median and distal level of the

renal artery. There is then a unifocal form, less frequent. Classically FMD has a prevalence of female sex in the youth age range (<50 years). Clinically FMD presents with hypertension and a preserved renal function, although with a high frequency (up to 60%), it can reduce the parenchyma thickness and the size of the affected kidney. Both types of stenosis may be unilateral or bilateral. These clinical differences indicate which artery segments should be studied with greater accuracy for the diagnosis of RAS.

The ideal imaging procedure for RAS should identify the main renal arteries as well as the accessory vessels, localize the site of stenosis or disease, provide evidence for the hemodynamic significance of the lesion, and identify associated pathologies (e.g., abdominal aortic aneurysm, renal mass, etc.) that may have an impact on the treatment of RAS.

Angiography, once considered the "gold standard" for arterial imaging, is invasive and expensive and carries a small but not negligible risk of severe complications such as adverse contrast media reactions, cholesterol embolization, or arterial dissection. Owing to its invasive character and the substantial costs involved, angiography is not used as a screening method but as a guide for therapeutic transluminal angioplasty.

Furthermore, angiography provides no information on the functional significance of the stenosis. Thus, in recent years many less invasive or noninvasive diagnostic methods, such as captopril

G. Giannasi (✉)
Emergency Medicine, San Giovanni di Dio Hospital, USL Toscana Centro, Florence, Italy
e-mail: gianfranco.giannasi@uslcentro.toscana.it

A. Mannarino (✉)
Nephrology Department, San Giovanni di Dio Hospital, USL Toscana Centro, Florence, Italy
e-mail: antonio.mannarino@uslcentro.toscana.it

renal scintigraphy, color duplex ultrasonography (CDUS), computed tomography angiography (CTA), and magnetic resonance angiography (MRA), have been tested and compared to arteriography. Among these different methods, CDUS has been selected by many institutions as the principal screening tool used to detect RAS.

54.2 Anatomic Finding

Right renal artery originates from the anterior surface of the abdominal aorta, then posterior to the left renal vein (LRV), and the inferior cava vein (ICV). The left renal artery originates from the posterolateral surface of the abdominal aorta and passes back to the LRV (Fig. 54.1).

In the renal hilum, the arteries are divided into a back and anterior branch, which in turn, at the intrarenal site, give rise to segmental vessels. From the segmental vessels, the interlobular vessels originate, which after a straight course along the kidney pyramids toward the periphery of the kidney, flow into the arcuate arteries at the base of the pyramids and the cortical-medullary junction. Arcuate arteries spread interlobular arteries, which represent the most distal circulation highlighted in color Doppler (CD) (Fig. 54.2).

The kidney veins are tributary to the ICV and begin in front of the arteries. The LRV slides into the aorto-mesenteric fork and enters the ICV; the right renal vein starts directly from the kidney to ICV. Anatomical variants are very common in renal circulation. Thirty percent of subjects have the presence of renal arteries more often one but sometimes two or three), one-sided or bilateral, usually from the aorta. Renal arteries in another 15% of the subjects show early bifurcation in two branches. Anatomical variants are also present in the venous district: the most common are the LRV with posterior course between the aorta and the vertebral body and the circumaortic LRV with one branch coursing anteriorly and another branch posteriorly to the aorta (Fig. 54.3).

54.3 Examination Techniques and Normal Finding

Renal artery scanning is very difficult, and it requires a great amount of skill due to the depth of the arteries, the motion imposed by respiration, and intraabdominal gas.

The patients should therefore be examined early in the morning if at all possible after a 12-h overnight fast and preceded if possible by a fiberless diet for a couple of days. This will

Fig. 54.1 Axial gray scale image showing the renal arteries arising from the aorta. The right artery passes underneath the ICV and the narrow portion of LRV; the left artery courses posteriorly to the hilar tract of LRV. The SMA lies before the LRV and aorta

Fig. 54.2 Color Doppler image showing intrarenal vessels. Arteries are encoded red (the flow is directed toward the probe), and the veins are encoded blue. From the hilum to the periphery of the kidney, it is possible to distinguish in descending order of size the intrarenal vasculature: the segmental, interlobar, arcuate, and interlobular vessels
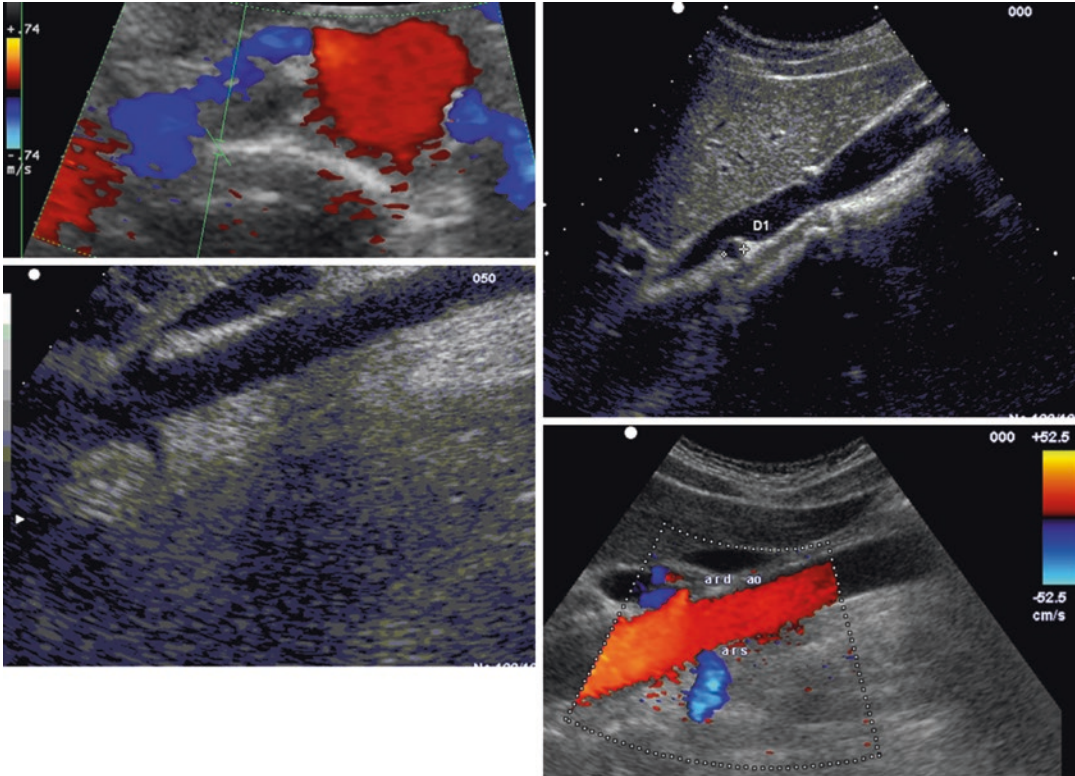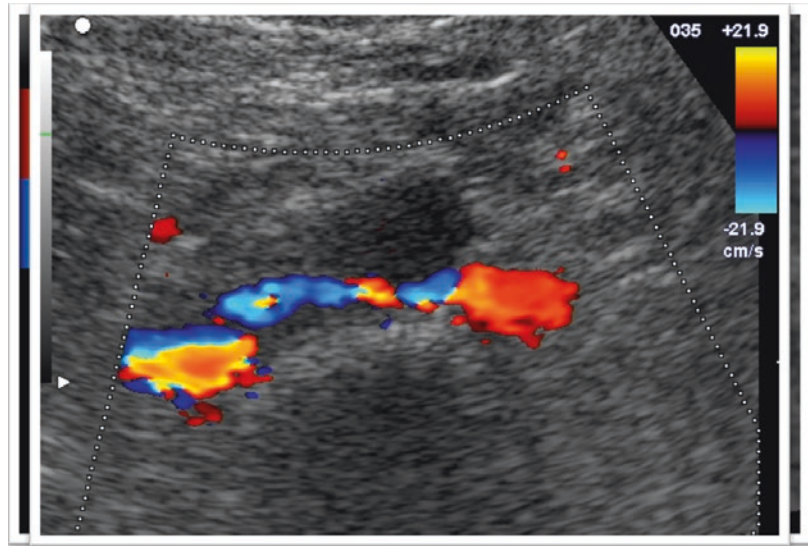
Fig. 54.3 Transverse color Doppler view shows the retroaortic course of the LRV before reaching the ICV

diminish the amount of bowel gas and also ensure that the stomach is empty.

The color duplex ultrasonography (CDUS) of the kidney arteries requires a well-coded examination strategy. However, the risks of an incomplete examination are always present because renal arteries, located on a deeper floor than the probe, may be unavailable even for patient-specific characteristics (obesity, meteorism difficulty in maintaining apnea).

The procedure begins with the patient in the supine position and the head of the bed elevated about 30°. A low-frequency scanner (2.5–5.0 MHz) is used to depict the abdominal aorta and renal arteries.

The two main approaches for imaging the renal arteries are through the anterior abdominal wall and the flank. Which approach is used depends on the specific portion of the renal vasculature being investigated. In most cases the anterior approach is used to evaluate the main renal arteries.

The flank approach may be used to image both the intrarenal vasculature and the main renal arteries. Each of these windows has limitations, which are dependent on individual body habitus and several other variables, such as the ability of the patients to hold their breath. In selected cases the posterior approach can be used.

54.4 Transverse Scan (Front)

With the probe transversely in the middle epigastric region, the ultrasound anatomical window of the origin of the renal arteries results from the detection in B mode of three structures: aorta, superior mesenteric artery (SMA), and left renal vein (LRV). Once these three structures have been identified, the plan of the origin of the renal arteries is about 1–1.5 cm from the SMA: the right renal artery from the anterolateral aortic surface and the left renal artery from the posterolateral surface, posteriorly to LRV.

The proximal course of the right renal artery is often perpendicular to the ultrasound beam, and, on the one hand, it represents the best possible approach in B mode; on the other hand, it obstructs the display on CD and the correct use of the Doppler angle (with Doppler angle 90°, the Doppler shift is zero). By moving the probe slightly to the middle of the median line and tilting the probe toward the right of the patient, the right artery view is displayed on CD with a favorable Doppler angle (<60°).

The PRF setting for high flows minimizes aliasing and allows the definition of the artery edges from those of the LRV and ICV, both

placed before the artery. The optimum CD display in the middle section is less adequate because the distance of the Doppler gate is greater and this reduces the PRF used to accurately measure high flow rates. In B mode, the left renal artery is generally more difficult to detect. The landmark for locating the left renal artery is the LRV well-known as a large caliber vessel (about 1 cm).

The CD is activated, and the probe is placed slightly in the median line; the probe is tilted toward the left of the patient; the proximal portion of the left renal artery appears well with a good Doppler angle (30–45°) with code color blue (flow away from the probe), behind the LRV, clearly visible with code color red (flow toward the probe). The average length of the artery is more difficult to detect due to the presence of artifacts in the colon.

54.5 Posterior Side Scan (Lumbar)

This scan initially examines the B mode of the kidney. The patient is placed in the contralateral decubitus with respect to the kidney to be examined. This mode displays the coronary scan of the kidneys (i.e., passing through the hilum of the kidneys).

On the right it is also possible to carry out a longitudinal scan of the kidney with the supine patient by placing the probe at the middle axillary line level.

Since each patient's anatomy is unique, the operator needs to freely change the position of the probe to have the best possible viewing with longitudinal, oblique, and transverse scans.

Examination in B mode allows to detect any signs of chronic parenchymal disease but does not provide specific diagnostic elements for the diagnosis of renal artery stenosis. However, the following parameters are evaluated:

- Kidney size expressed by the largest longitudinal diameter measured in sagittal scan (normal value 9–12 cm)
- Measured parenchymal thickness (normal value >14 mm)

- Echogenicity of parenchyma: hypoechogenic to liver or spleen, isoechogenic, hyperechogenic, and severely hyperechogenic (Hricak scale 0–3, normal value 0–1)
- Any scarring of the cortical profile (to be differentiated from fetal lobes)
- Presence of any solid masses/cysts
- Urinary stones and/or urinary tract obstruction

When the difference between the longitudinal diameters of the two kidneys is>1.5 cm, there is a renal asymmetry, which causes suspicion for the presence of RAS.

After examining in B mode, a CD evaluation is performed which allows in many cases to examine renal arteries with a favorable Doppler angle (<60° and often <30–45°) for the whole length. This operation is easier on the right where it is possible to exploit as the hearing aid window as well as the kidney also the liver. Visualize the kidneys you have to look for the aorta, then open the Doppler gate and optimize the shape of the box in relation to the district to be scanned, keeping it small in order to increase the frame rate.

With fine tilting movements of the probe, it goes for the research of kidney arteries, which can be visualized for much or for their entire course (the right measures about 7 cm, the left about 5 cm in length).

However, if the course is tortuous, it is only possible to highlight segments apparently unrelated to each other, and the examination may not disclose aliasing and flux accelerations since the hemodynamic variations caused by stenosis tend to dissolve to 1–2 cm from stenosis.

54.6   Aortic Coronal Scan

With the patient on the left lateral decubitus, the probe is placed under the rib arch in the sagittal position, and the aorta and ICV are found along the major axis.

In B mode it is possible to highlight the right renal artery transversally and posteriorly to the ICV and the presence of any accessory arteries. The color gate is activated, and probe swinging movements are indicated until both renal arteries are seen arising from the aorta with a favorable Doppler angle (<30°) to measure the flow velocities in the kidney, arteries, and aorta. This aspect is characteristic and is described as a "banana peel view."

When the transverse approach is found to be unsuccessful (obesity, marked meteorism), this scanning may allow a good evaluation of at least the proximal portion of the kidney arteries (Fig. 54.4).

54.7   Diagnostic Criteria of RAS

54.7.1 Direct Evaluation of Renal Artery

In B mode, in many cases, it is possible to measure the diameter of the renal arteries by using transverse abdominal scanning and limited to the right artery, using aortic coronal scanning. In B-mode ultrasound, the diameter of the renal arteries is measurable about 5 mm.

Variations in flow velocity are the basis of Doppler diagnosis of stenosis. For this purpose, the peak systolic velocity (PSV) and the renal aortic PSV ratio (RAR) are used.

For the study of renal arteries, the low-frequency Doppler (2–3 MHz) probe is used to improve the penetration of the US beam, and a high-frequency PRF (3–4 kHz) is set.

The kidney arteries are displayed with a homogeneous color code (red or blue according to the direction of flow to the probe) with different degrees of saturation in relation to the extent of the shift (Fig. 54.5). If the CD shows focal points with the typical "mosaic" appearance, it is aliasing.

The Doppler waveform does not allow in this case to accurately measure the PSV because the waveform has the severed systolic peaks with the tips that appear on the opposite side of the baseline line. To reduce any aliasing, you can do it in several ways: increase the PRF up to the maximum limit set by the depth of the district to be investigated, act on the baseline, use a lower transmission frequency, and act on the Doppler angle.

Fig. 54.4 Normal arteries in different patients. (**a**) Transverse color Doppler view of the aorta (encoded red) and the origin of both renal arteries (encoded blue). The ICV is located anteriorly to the right artery on the left of the image; (**b**) sagittal ultrasound image in B mode showing the ICV in the long axis and the right renal artery in the short axis in the passage underneath the ICV; (**c**) coronal ultrasound image in gray scale demonstrating the aorta in the long axis with the origin of both renal arteries; and (**d**) coronal scan in color Doppler showing the aorta (ao), the right renal artery (ard), and the left renal artery (ars). This image has been described as the banana peel view
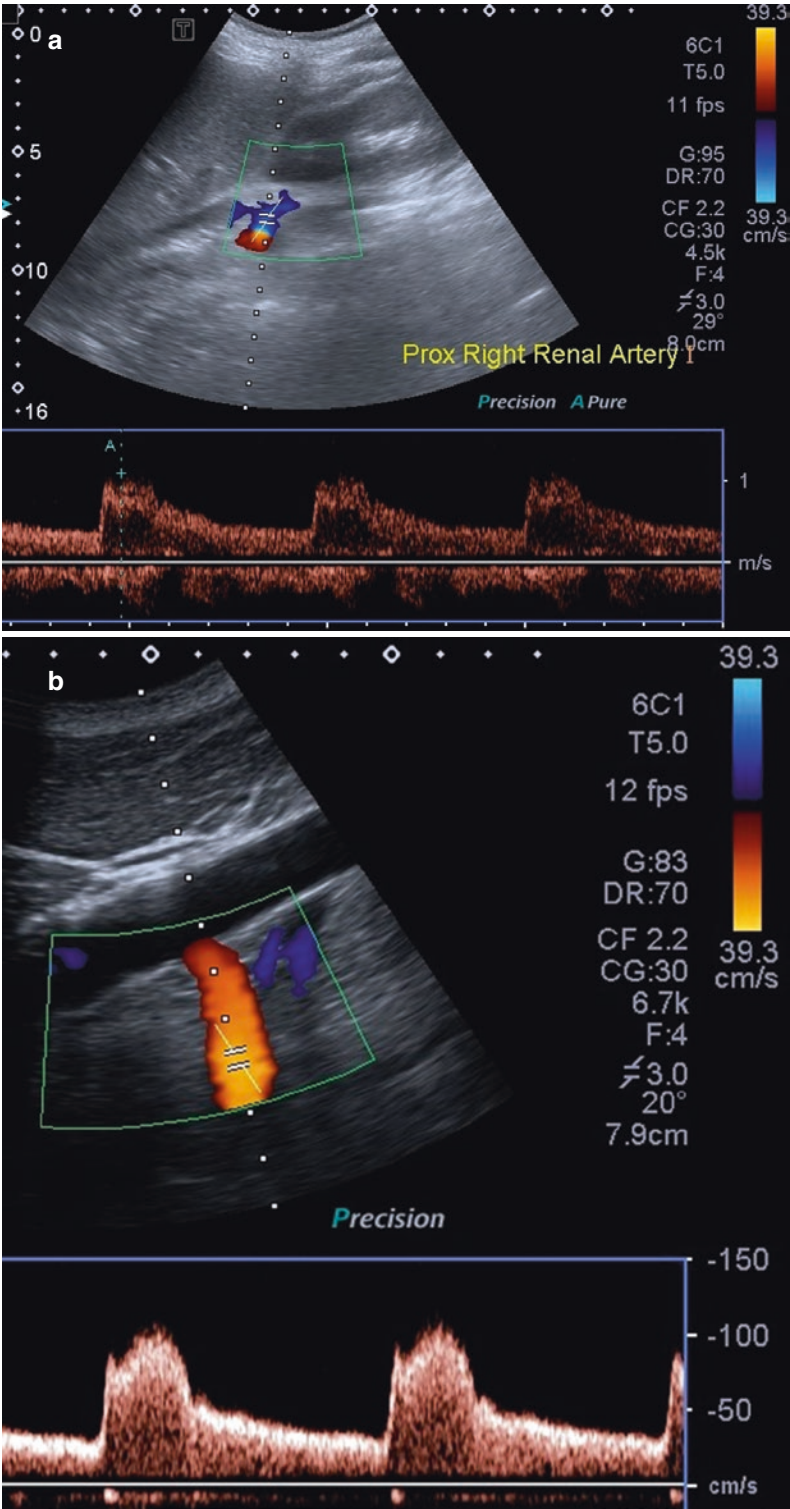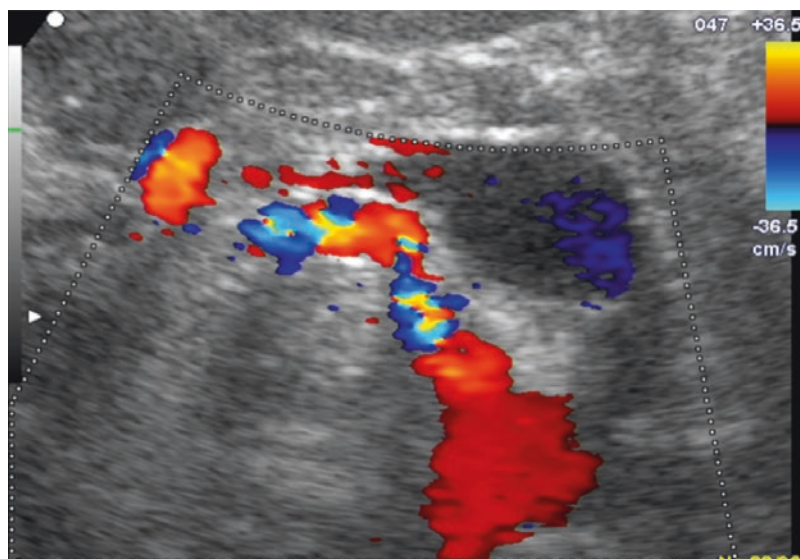
The Doppler equation explains what is said: Doppler shift = $2v * Ft * \cos \Theta / c$ (where v = flow rate; Ft = transmission frequency; $\cos \Theta$ = insonance angle; c = US transmission speed in tissues). The other important adjustment in the survey is the correct Gain setting: if too high, the Doppler path has a mirror image on the other side of the baseline; if too low, the path becomes less obvious until it disappears. After performing all the adjustments, the Doppler sampling of the PSV is carried out at the origin, proximal, mid, and distal tracts or any aliasing focal points present.

The Doppler angle must be <60° because angles >60% cause an overhang of speed. Incorrect alignment of the angle correction cursor also causes errors in speed measurement. In normal subjects PSV values <150 cm/s and RAR <2. Flow velocities 200 cm/s indicate the presence of hemodynamic stenosis (stenosis diameter >60%) (Fig. 54.6).

Various Doppler validation studies with angiographic controls have shown for this cutoff a sensitivity around 90% with a specificity of about 50% with a positive predictive value (PPV) of 60% and a negative NPV of 95%. Of course, if the PSV is used, the cutoff value of 300 cm/s increases the specificity with values up to 90% and reduces the sensitivity (about 60%) (Fig. 54.7).

The presence of a turbulence distal to a stenotic focal strength strengthens the diagnosis of hemodynamic stenosis. The ultrasound examination of renal arteries is complemented by the evaluation of the abdominal aorta, which is examined from the origin to the carrefour, for the search for ectasia of the lumen/aneurysms and for the presence of atheroma of the vessel walls. With longitudinal or coronal scan, PSV is then measured which usually has a value of about 60 cm/s (if the PSV is <40 cm/s, it is not possible to calculate the RAR).

Arterial hypertension causes an increase in speed in all vessels, and for this reason RAR can more accurately represent an increase in the flow rate in the renal artery. The cutoff of the RAR of 3.5 offers a good diagnostic accuracy (sensitivity around 80% and specificity around 90%) for diagnosing RAS.

Accessory kidney arteries, present in 25–30% of subjects, are frequently not displayed in CDUS, and this theoretically sets limits to the diagnostic accuracy of the examination. In fact, the presence of an isolated hemodynamic stenosis of an accessory artery is a rare occurrence (in 1–1.5% of patients with documented RAS in angiography). It may also be helpful to note that no accessory artery has been documented if the artery diameter measured in B mode at least 5.5 mm, while the presence of an accessory branch was probable if the artery measured <4.1 mm.

Fig. 54.6 Renal artery stenosis. Main renal artery analysis in different patients. (**a**) Subcostal scan performed with the patient into a left decubitus position. Color Doppler view of the aorta and the right renal artery shows two focal zones of aliasing and stenosis in the tract underneath the ICV and (**b**) traverse color Doppler of the aorta and the origin of the right renal artery. The pulsed Doppler waveform shows elevated PSV (328 cm/s)
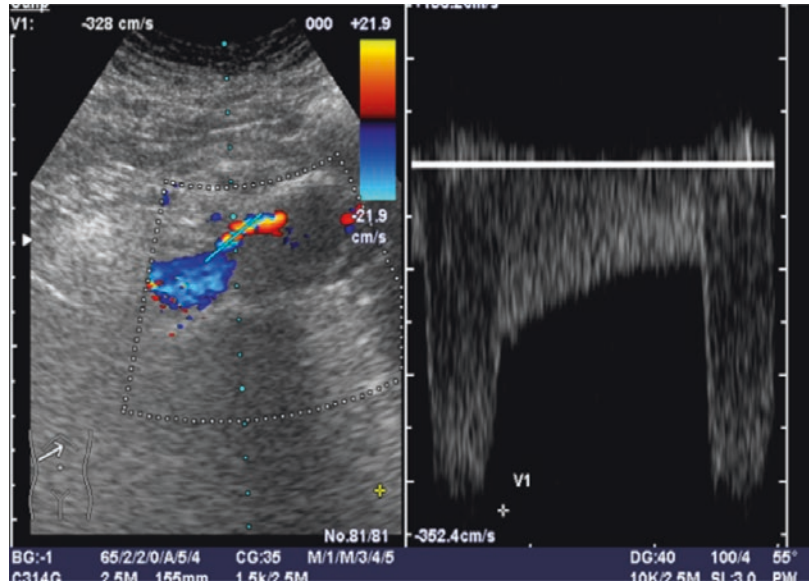
Fig. 54.7 Fibromuscular dysplasia. Transverse color Doppler view showing at the mid tract of left renal artery a focal zone of aliasing and a pulsed Doppler waveform with elevated PSV (>300 cm/s)
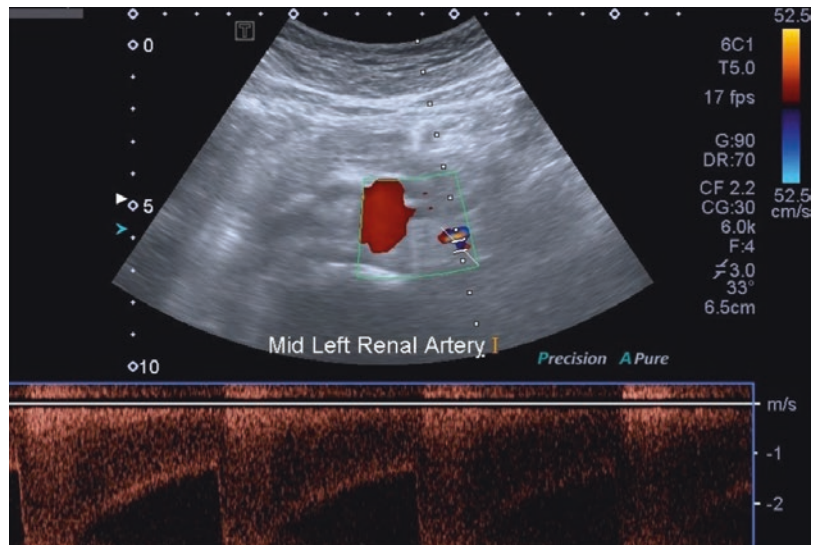
54.8 Indirect Signs of Renal Artery Stenosis (Downstream of Stenosis)

The search for indirect signs of stenosis is certainly a quicker procedure than direct study of kidney arteries. However, you should know some rules to take into account in this lumbar scan:

- A high-frequency probe (3.5–5 Mhz) is used to achieve a high Doppler shift.
- The position of probe along the rear axillary line so that it has a sagittal scan of the kidney as far as possible from the skin surface without the liver or spleen interposed.
- The CD highlights segmental and interlobular vessels with a Doppler angle <15–30°.
- A sufficiently large sample volume is used in relation to the size of the vessel to be investigated.
- The PRF, set for low flow (1.5 kHz), is adjusted so that the spectral signal size is slightly higher than half in the rate scale represented.

Locate the vessel to be investigated, with the patient in apnea for a few seconds, with the slider well aligned with the long axis of the vessel.

Flow in the kidney vessels is of the continuous type diastolic with low diastolic resistance. The most important and generally evaluated parameters are three:

- Acceleration time (AT)
- Presence of the early systolic peak (ESP)
- Resistance indices (RI)

The normal renal waveform is characterized by an ESP (not always present), by a phase of systolic plateau and diastolic phase (Fig. 54.8).

The AT parameter, whose reference value is <70 ms, defines the time interval between the start of the systole and the early systolic peak when present, if absent, from the onset of the systole to the first deflection point of the spectral waveform.

The RI parameter is the expression of the peripheral resistances and the diastolic rate of the tissue flow and is expressed by the S-D/S ratio where S is the systolic peak velocity and D is the diastolic rate. The reference value is between 0.5 and 0.69. Normally, the RI difference between the two kidneys (ΔRI) is <0.06. Simplifying the intrarenal level, three types of renal waveforms can be identified:

- Type 1, normal and biphasic with rapid systolic rise and the presence of ESP
- Type 2a, normal and biphasic with late systolic peak and AT within normal limits
- Type 2b, pathological and biphasic with late systolic peak and pathological AT
- Type 3, pathological and monophasic where it is evident in addition to the systolic delay (tardus), also the reduction of PSV (parvus)

Multiple sampling at the two renal poles and mesorenal site should normally be performed. The presence of ESP plays an important role when present because at least in normal renal kidney, it is possible to exclude with a good approximation the presence of stenosis of the renal artery.

However, it should be taken into account that subjects with nephrosclerosis may exhibit an
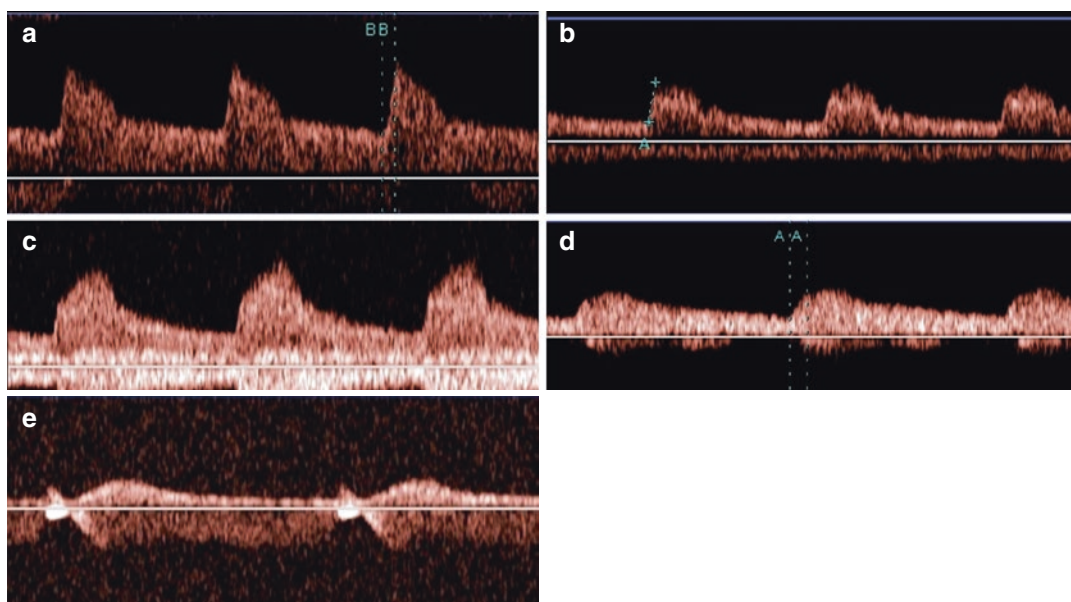
Fig. 54.8 Intrarenal waveforms. (**a**) Normal waveform with early systolic peak detected on each waveform; (**b** and **c**) two examples of normal waveform with late systolic peak and normal acceleration time; (**d**) abnormal waveform late systolic peak and slowed systolic acceleration; (**e**) abnormal waveform with monophasic systolic appearance (tardus parvus)

accentuated ESP that cannot disappear even in the presence of RAS. If you cannot highlight the early systolic peak (ESP), check that the Doppler angle is <30° before concluding that ESP is absent. At this point, a proper measurement of the AT becomes the only useful indirect sign of stenosis to the possible presence of an indirect sign of stenosis. The ΔRI >0.05 is an indirect sign of stenosis because in the stenotic kidney, the reduction of PSV results in a reduction in RI relative to the non-stenotic kidney, but especially in the elderly, ΔRI may also be an expression of a different degree of parenchymal damage between the two kidneys. Even with these limitations, AT and ΔRI parameters, at least in young subjects with normal RI kidneys, have a good specificity (about 90%) with a lower sensitivity for detecting RAS (about 50%).

54.9   Conclusion

The ultrasound diagnosis of RAS is based on both the direct study of renal arteries and the evaluation of the spectral trace detected downstream of intrarenal stenosis.

Evaluation in B mode of the kidney completes the clinical evaluation of the RAS by providing useful elements for the correct patient diagnostic framing.

The direct criteria used to diagnose RAS are PSV with cutoff of 200 cm/s and RAR with cutoff of 3.5.

The indirect criteria normally used are the AT with cut off of 70 ms and the ΔRI >0.05.

In older subjects, the study of indirect signs of stenosis is less reliable, and the examination takes advantage of the direct signs of RAS.

In all cases strict compliance with the principles of proper examination execution and dedication to this survey should be fair (40 min). The B-mode examination combined with CD evaluation allows a correct morphological functional evaluation of the kidney in relation to the staging of ischemic nephropathy nephrovascular or other associated nephropathy possibly present.

References

1. Scoble JE. Atherosclerotic nephropathy. Kidney Int. 1999;56(Suppl. 71):S106–9. [PubMed].
2. Coen G, Calabria S, Lai S. Atherosclerotic ischemic renal disease. Diagnosis and prevalence in an hypertensive and/or uremic elderly population. BMC Nephrol. 2003;4:2. [PMC free article] [PubMed].
3. Plouin PF, Rossignol P, Brobrie G. Atherosclerotic renal artery stenosis: to treat conservatively, to dilate, to stent, or to operate? J Am Soc Nephrol. 2001;12:2190–6. [PubMed].
4. Mailloux LU, Husain A. Atherosclerotic ischemic nephropathy as a cause of chronic kidney disease: what can be done to prevent end-stage renal disease? Saudi J Kidney Dis Transpl. 2002;13(3):311–9. [PubMed].
5. Safian RD, Textor SC. Renal-artery stenosis. N Engl J Med. 2001;344:431–42. [PubMed].
6. Bloch MJ, Basile J. The diagnosis and management of renovascular disease: a primary care perspective. J Clin Hypertens. 2003;5(3):210–8. [PubMed].
7. Strandness DE. Doppler and ultrasound methods for diagnosis. Semin Nephrol. 2000;20(5):445–9. [PubMed].
8. Zubarev AV. Ultrasound of renal vessels. Eur Radiol. 2001;11:1902–15. [PubMed].
9. Meola M, Petrucci I. Color Doppler sonography in the study of chronic ischemic nephropathy. J Ultrasound. 2008;11(2):55–73. [PMC free article] [PubMed].
10. Korst MB, Joosten FB, Postma CT, Jager GJ, Krabbe JK, Barentsz JO. Accuracy of normal-dose contrast-enhanced MR angiography in assessing renal artery stenosis and accessory renal artery stenosis and accessory renal arteries. Am J Roentgenol. 2000;174:629–34. [PubMed].
11. Krumme B. Renal Doppler sonography – Update in clinical nephrology. Nephron Clin Pract. 2006;103:c24–8. [PubMed].
12. Moghazi S, Jones E, Schroepple J. Correlation of renal histopathology with sonography findings. Kidney Int. 2005;67:1515–20. [PubMed].
13. Lee HY, Grant EG. Sonography in renovascular hypertension. J Ultrasound Med. 2002;21:431–41. [PubMed].
14. Zucchelli PC. Hypertension and atherosclerotic renal artery stenosis: diagnostic approach. J Am Soc Nephrol. 2002;13:S184–6. [PubMed].
15. Radermacher J, Chavan A, Schäffer J. Detection of significant renal artery stenosis with color Doppler sonography: combining extrarenal and intrarenal approaches to minimize technical failure. Clin Nephrol. 2000;53(5):333–43. [PubMed].
16. Hua HT, Hood DB, Jensen CC, Hanks SE, Weaver FA. The use of color flow duplex scanning to detect significant renal artery stenosis. Ann Vasc Surg. 2000;14:118–24. [PubMed].

17. Olin JW, Piedmonte MR, Young JR, DeAnna S, Grubb M, Childs MB. The utility of duplex ultrasound scanning of the renal arteries for diagnosing significant renal artery stenosis. Ann Intern Med. 1995;122:833–8. [PubMed].

18. Bokhari SW, Faxon DP. Current advances in the diagnosis and treatment of renal artery stenosis. Rev Cardiovasc Med. 2004;5:204–15. [PubMed].

19. Williams GJ, Macaskill P, Chan SF. Comparative accuracy of renal duplex sonographic parameters in the diagnosis of renal artery stenosis: paired and unpaired analysis. Am J Roentgenol. 2007;188:798–811. [PubMed].

20. Hoffmann U, Edwards JM, Carter S, Goldman ML, Harley JD, Zaccardi MJ. Role of duplex scanning for the detection of atherosclerotic renal artery disease. Kidney Int. 1991;39(6):1232–9. [PubMed].

21. Bude RO, Forauer AR, Caoili EM, Nghiem HV. Is it necessary to study accessory arteries when screening the renal arteries for renovascular hypertension? Radiology. 2003;226:411–6. [PubMed].

22. Labropoulos N, Ayuste B, Leon LR Jr. Renovascular disease among patients referred for renal duplex ultrasonography. J Vasc Surg. 2007;46:731–7. [PubMed].

23. Chain S, Luciardi H, Feldman G, Berman S, Herrera RN, Ochoa J. Diagnostic role of new Doppler index assessment of renal artery stenosis. Cardiovasc Ultrasound. 2006;25(4):4. [PMC free article] [PubMed].

24. Aytac SK, Yigit H, Sancak T, Ozcan H. Correlation between the diameter of the main renal artery and the presence of an accessory renal artery. Sonographic and angiographic evaluation. J Ultrasound Med. 2003;22:433–9. [PubMed].

25. Soares GM, Murphy TP, Singha MS, Parada A, Jaff M. Renal artery duplex ultrasonography as a screening and surveillance tool to detect renal artery stenosis: a comparison with current reference standard imaging. J Ultrasound Med. 2006;25:293–8. [PubMed].

26. Souza de Oliveira IR, Widman A, Molnar LJ, Fukushima JT, Praxedes JN, Cerri GG. Color Doppler ultrasound: a new index improves the diagnosis of renal artery stenosis. Ultrasound Med Biol. 2000;26:41–7. [PubMed].

27. Li JC, Wang L, Jiang YX, Dai Q, Cai S, Lv K. Evaluation of renal artery stenosis with velocity parameters of Doppler sonography. J Ultrasound Med. 2006;25:735–42. [PubMed].

28. Garcìa-Criado A, Gilabert R, Nicolau C, Real MI, Muntañá X, Blasco J. Value of Doppler sonography for predicting clinical outcome after renal artery revascularization in atherosclerotic renal artery stenosis. J Ultrasound Med. 2005;24(12):1641–7. [PubMed].

29. Li JC, Jiang YX, Zhang SY, Wang L, Ouyang YS, Qi ZH. Evaluation of renal artery stenosis with hemodynamic parameters of Doppler sonography. J Vasc Surg. 2008;48:323–8. [PubMed].

30. Grenier N, Hauger O, Cimpean A, Pérot V. Update of renal imaging. Semin Nucl Med. 2006;36:3–15. [PubMed].

31. Demirpolat G, Ozbek SS, Parildar M, Oran I, Memiş A. Reliability of intrarenal Doppler sonographic parameters of renal artery stenosis. J Clin Ultrasound. 2003;31:346–51. [PubMed].

32. Hausberg M, Lang D, Barenbrock M, Kosch M. What do Doppler indices of renal perfusion tell us for the evaluation of renal disease? J Hypertension. 2005;23(10):1905–11. [PubMed].

33. Rabbia C, Valpreda S. Duplex scan sonography of renal artery stenosis. Int Angiol. 2003;20:101–15. [PubMed].

34. Patriquin HB, Lafortune M, Jequeier JC. Stenosis of the renal artery: assessment of slowed systole in the downstream circulation with Doppler sonography. Radiology. 1992;184(2):479–85. [PubMed].

35. Soulez G, Oliva VL, Turpin S, Lambert R, Nicolet V, Therasse E. Imaging of renovascular hypertension: respective values of renal scintigraphy, renal Doppler US, and MR angiography. RadioGraphics. 2000;20:1355–68. [PubMed].

36. Saeed A, Bergström G, Zachrisson K. Accuracy of colour duplex sonography for the diagnosis of renal artery stenosis. J Hypertension. 2009;27(8):1690–6. [PubMed]s].

Ultrasound for Percutaneous Tracheostomy

55

Percutaneous Tracheostomy Ultrasound Guided

Massimo Barattini, Gabriele Gori, and Alessandra Nella

Percutaneous dilatational tracheostomy (PDT) is nowaday a standard technique for critically ill patients who require long-term ventilation. In our experience we use a conservative approach because we have a large number of postsurgical patients, so weaning from mechanical ventilation is often reached easily. For medical patients with severe acute respiratory failure, neurosurgical patients, and in the case of septic shock, we perform PDT after 10 days [1].

PDT was first described by Ciaglia et al. in 1985 [2]. Since then, the Ciaglia technique with all its new variations is still widely used and performed everyday in ICU in the world. If we exclude Fantoni's translaryngeal tracheostomy, all PDT uses the Seldinger's technique, which is based on the use of a guide wire introduced through a needle. PDT has become a standard technique and today supersedes open surgical tracheostomy for all but the most complicated cases [3, 4].

PDT is considered a minimally invasive procedure that is performed at patient's bedside in ICU and has many advantages. First it avoids transferring critically ill patients to the operating room to perform surgical tracheostomy; second its cost is lower than open surgical tracheostomy.

Nevertheless we must always remember that PDT remains one of the few procedures performed in ICU where serious adverse events are reported, including death [5]. For this reason the use of bronchoscopy and ultrasound (US) guide technique can assure a more safety procedure with respect to blind puncture of the trachea.

The most appropriate level for puncturing the trachea is between the first and second tracheal ring [6]; upper punctures may lead to stenosis and lower to bleeding.

Complications may be considered as minor (minor bleeding is a bleeding that is controlled by compressing the wound), intermediate (oxygen desaturation, hypoxia, cuff perforation, cranial guide wire migration), and major (major bleeding where pressure-compressed wound dressing or electrocauterization is used to control bleeding or blood transfusion is required; tracheal tube erosion into adjacent vasculature in case of late bleeding complications, which are thought to be related to initial tracheal tube malposition; lesion of posterior trachea wall with pneumomediastinum). Incidents are reported as technical (multiple punctures, tracheal tube cuff puncture), intra-procedural (desaturation, minor bleeding, hypotension), and postprocedural (hematoma at the puncture site, skin infection) [3].

Bronchoscopic guidance during the procedure has been widely used for several reasons. Bronchoscopic transillumination is useful to indicate the puncture site (vision of needle), confirm

M. Barattini (✉) · G. Gori · A. Nella
Department of Anesthesia and Intensive Care,
Santa Maria Nuova Hospital, Florence, Italy
e-mail: massimo.barattini@uslcentro.toscana.it;
gabriele.gori@uslcentro.toscana.it;
alessandra.nella@uslcentro.toscana.it

the needle position, insert the guide wire, confirm its position, and control real-time dilatation and positioning of the tracheostomy tube. However, it does not identify the vascular structures and thyroid gland and doesn't prevent complications linked to local puncture lesions [7, 8].

Pre-procedural and real-time intra-procedural US-guided technique provides additional assistance during PDT. Sonographic evaluation of neck anatomy and vessels before performing PDT has been shown to predict PDT success [9] and improve the safety of the procedure avoiding, for instance, lesion of aberrant vessels during puncture first of all [10].

The incidence of risky conditions for a PDT procedure was significantly higher in patients with short necks (distance between cricoid cartilage and sternal notch ≤3 cm) than in other patients, and this characteristic is also common in obese patients. The physical landmarks of the neck should be clearly identified to assess a suitable puncture location for PDT; in this kind of patients, this method is not easy to perform; thus US examination of neck region is useful. The use of US before PDT is also useful in the case of short necks, deviated tracheas, massive goiters, edema, subcutaneous emphysema, and difficulties in the positioning of unconscious patients which are the principal complicating factors. Preoperative US examination of the neck shows trachea, thyroid (bleeding structures such as the thyroid isthmus, a thickened (≥10 mm) thyroidal isthmus, inferior thyroid vessels), and vascular aberrations (anterior jugular). After these analyses US examination often modifies the puncture site chosen on the basis of anatomical palpation data [11].

US can also provide information about variations in neck anatomy and measure the distance between the skin and trachea [10] and could be used to identify the level of seal penetration, to confirm the withdraw level of the endotracheal tube cuff to prevent cuff perforation during the initial puncturing and could prevent posterior tracheal wall damage by the estimation of the penetration length of the seeking needle according to the US-quantified tracheal depth. Finally US could help visualize the caudal advancement of the guide wire when it is introduced through the

seeking needle at PDT; cranial guide migration could be eliminated (6).

We use linear probe 6–13 MHz, GE Vivid-i US machine (GE Healthcare Japan Corporation, Tokyo); other centers use 5.0–10.0 MHz microconvex probes.

Two operators are involved in the procedure: one deals with the airway management, while the other performs the US-guided PCT (an assistant and an operator). Deep sedation of the patient is provided by propofol 2% (2–4 mg/kg/h), fentanyl (1–2 mg/kg), and remifentanil (0,10 mcg/kg/min) according to hemodynamic state; muscular relaxation is achieved by rocuronio 0,6–1 mg/kg because of possibility of immediate reversal by sugammadex in the case of severe complication. Patient is mechanically ventilated with 8 ml/kg tidal volume; RR is 12–14 b/m and Fio2 100%. Patient's neck is placed in hyperextension and under direct bronchoscopic visualization; tracheal tube is withdrawn until the tip is just below the level of the vocal cords to prevent cuff's perforation by the seeking needle and allowing visualization of the cricoid and first, second, and third tracheal rings. US control of right placement of the tube and its cuff is ensured by detecting the shaft's echogenic US "double-line" appearance at the anterior margins of the tracheas (Fig. 55.1). Consecutive inflations and deflations of the balloon with real-time US visualization are used to ensure a definite cuff balloon level.

Fig. 55.1 Sagittal US confirmation of endotracheal tube in 60-year-old female patient in the ICU. The "echogenic double line" indicates the tube shaft

Prior to PDT, a US examination of the neck region with longitudinal section is performed to locate the cricoid cartilage, the tracheal rings, and the puncture site (Fig. 55.2).

US transversal section is performed to identify arteries, veins, thyroid, trachea, and endotracheal tube and measures the thickness of the skin to the anterior tracheal wall (Figs. 55.3, 55.4, and 55.5). If altered structures are noted, puncture level is changed by the operator (either more cranial or more caudal), preferred to prevent possible complications.

After skin sterilization, a second operator performed the PDT using the single-stage dilator technique with US guidance. Local anes-

thesia (lidocaine 2% 4 mL) of the skin and subcutaneous tissues is performed before puncture, and local anesthetic spread can be observed using US. Then a puncture needle with a saline-filled syringe is introduced perpendicularly to the skin and advanced until the needle is seen to pass the anterior trachea wall during air aspiration. Then the needle is angled caudally to prevent retrograde passage of the guide wire. The needle can be visualized in an "out-of-plane" mode (i.e., the needle path is determined by the presence of a distinct acoustic shadow ahead of the needle) on a transversal section of the neck region (Fig. 55.6) or "in-plane." In this case the all needle pathway is visualized, and this can avoid damage to posterior trachea wall [12].

The insertion routes are determined by identifying the slight echogenicity of the needle, and,

Fig. 55.2 Longitudinal US visualization of trachea for "in-plane" approach. Numbers starting from the top indicate tracheal cartilage rings. * cricoid cartilage. Arrow optimal puncture site for standard PDT
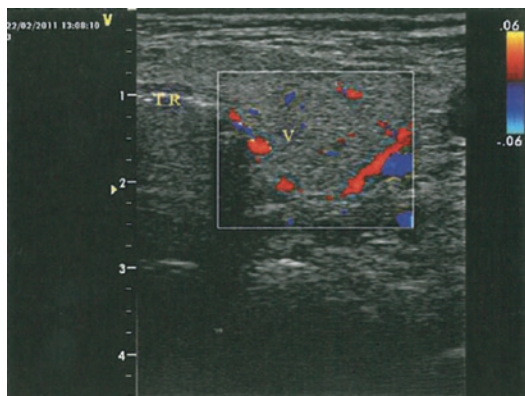
Fig. 55.4 Blood vessels around tracheal ring, short axis

Fig. 55.3 Thyroid gland over the tracheal ring

Fig. 55.5 Transversal US measure of the distance between the skin and trachea

Fig. 55.6 Transversal US vision of trachea with "out-of-plane" needle visualization. Note that you can't directly visualize the needle but only its acoustic shadow ahead

in most cases, tilting the needle is used to aid in its recognition when necessary. The advancement of the needle tip is limited on the basis of the previously measured tracheal depth to avoid posterior tracheal wall injuries.

The guide wire is introduced, the needle is removed, and a small horizontal incision is performed at the point of puncture. The guide wire is visualized as a hyperechoic signal on transversal and longitudinal sections.

The caudal advancement of the guidewire through the tracheal lumen is ensured by demonstration of the guidewire's penetration angle in the sagittal US plane. The small dilator is then used to create the initial stoma followed by the single-stage curve dilator over the guide wire. The tracheostomy tube fitted over an appropriate loading tube is passed through the stoma. US provides information on the correct positioning of the puncture site and the guide wire before the dilatation of the trachea and then placement of the tracheostomy tube.

With this technique anatomical palpation data (short neck, palpated goiter, deviation of the trachea, vessels, puncture site and cricoid-manubrium distance in centimeters) and US data (thyroid, tracheal deviation, aberrant vessels, puncture site, subcutaneous tissue thickness in cm defined by the distance between the skin and the anterior wall of the trachea measured perpendicularly to the skin at the puncture level, tracheal diameter in cm) can be compared to assure a major safety for the patient.

Using US a good level of anatomical knowledge of the neck is required, and all of the practitioners must had been trained by a radiologist on the anatomy of the neck as revealed by US. Another difficulty is to identify the cuff of the endotracheal tube. Visualization of the balloon is partly improved by using a double-contrast technique (i.e., a balloon inflated with water). However, this technique is nonoptimal because the air around the tracheal tube could act as an artifact for US. A learning curve might well be required before the technique can be incorporated into routine use.

Tracheal visualization during PDT could be realized by real-time US using long axis instead of short axis.

This technique could be realized using a linear 6–13 MHz ultrasound transducer under musculoskeletal preset. In this approach, after a first rapid short-axis view of the trachea, useful to determinate its midline position, the US probe is rotated 90° counterclockwise to visualize the trachea in long axis. Now thyroid cartilage, cricoid cartilage, and tracheal rings 1–5 are visualized. The needle is positioned at 45° angle to the skin, pointing caudally from edge of the transducer. A perfect alignment between needle and probe is crucial. Under real-time US guidance in long-axis view, the introducer needle is inserted into the first or second ring space and confirmed with air aspiration. The procedure is then completed as shown before. At the end US is useful for evaluating postprocedural immediate complications too. A rapid evaluation for postprocedural pneumothorax could be realized rapidly. Bilateral lung US is performed at the end of the procedure to document the presence of bilateral lung sliding.

References

1. Andriolo BN, Andriolo RB, Saconato H, et al. Early versus late tracheostomy for critically ill patients. Cochrane Database Syst Rev. 2015;(1):CD007271.
2. Ciaglia P, Firsching R, Syniec C. Elective percutaneous dilatational tracheostomy. A new simple bedside procedure: preliminary report. Chest. 1985;87:715–9.
3. Grant CA Dempsey G, Harrison J, et al. Tracheo-innominate artery fistula after percutaneous tracheostomythree case reports and a clinical review. BJA. 2006;96:127–31.

4. Krishnan K, et al. The current pratice of tracheostomy in the United Kingdom: a postal survey. Anaesthesia. 2005;60:360–4.
5. Gilbey P. Fatal complications of percutaneous dilatational tracheostomy. Am J Otolaryngol. 2012;33(6):770–3.
6. Yavuz A, Yılmaz M, Göya C, et al. Advantages of US in percutaneous dilatational tracheostomy: randomized controlled trial and review of the literature radiology. Radiology. 2014;273:3.
7. Guinot P-G, Zogheib E, Petiot S, et al. Ultrasound-guided percutaneous tracheostomy in critically ill obese patients. Crit Care. 2012;16:R40.
8. Even-Tov E, Koifman I, Rozentsvaig V, et al. Pre-procedural ultrasonography for tracheostomy in critically ill patients: a prospective study. IMAJ. 2017;19:337–40.
9. Flint AC, Midde R, Rao VA, Lasman TE, et al. Bedside ultrasound screening for pretracheal vascular structures may minimize the risks of percutaneous dilatational tracheostomy. Neurocrit Care. 2009;11:372–6.
10. Tremblay LN, Scales DC. Ultrasound-guided tracheostomy–not for the many, but perhaps the few… or the one. Crit Care. 2011;15(2):147.
11. Rudas M. The role of ultrasound in percutaneous dilatational tracheostomy. AJUM. 2012;15(4):143–8.
12. Farshidpanah VADS, Lu S, et al. Real-time Sonographically guided percutaneous dilatational tracheostomy using a long-axis approach compared to the landmark technique. J Ultrasound Med. 2014;33:1407–15.

Transcranial Doppler Ultrasonography in Emergency and Intensive Care

56

Mauro Pratesi and Daniele Cultrera

<div style="border:1px solid #000; padding:10px;">

Key Points
- Normal patterns
- Pathological patterns
- Acute ischemic stroke
- Left-right shunt
- Severe cranial trauma

</div>

56.1 Transcranial Eco Color Doppler (TCCD): Normal and Pathological Patterns

The use of ultrasounds as a method of studying intracranial structures has become possible since the 1980s, with remarkable enrichment of information by color coding of the Doppler signal in the 1990s. As all ultrasound methods, also this one is inexpensive, repeatable in very close times, and performable at bedside, and it provides real-time information on flow velocities and parameters derived from the flow curves' morphology.

Currently (as of now), the study of intracranial arterial circulation is based on two ultrasound methods: (1) transcranial Doppler (TCD) by using two-way pulse emission probes at variable depths between 25 and 125 mm, and thanks to the depth of the sounded vessel and the direction of the flow, it is possible to locate the vessel and (2) transcranial eco color Doppler (TCCD) by combining images obtained in B-mode with the color method through pulsed Doppler method; the TCCD allows to visualize the vessel and thus optimize the Doppler sound-proofing angle.

Intracranial vessels can be studied with ultrasonic with low frequency probes (2–2.5 MHz) at pulsed emission; this method presents some problems since the ultrasonic beam undergoes (takes on an) energy attenuation in the passage through the skull (skeletal bone with trabecules containing bone marrow covered by external and internal compact bone); this attenuation is caused by many factors: the presence of multiple interfaces, Circumcentred endocranial surface, age (better compatibility and tissue coherence in younger patients than in the elderly), sex, and ethnicity (minimum thickness in the Caucasian male and maximum in black female).

The elective examination must be preceded by a complete bilateral study of extracranial carotid-vertebral districts.

M. Pratesi (✉)
Former Director SC Emergency Medicine, Santa Maria Nuova Hospital, Florence, Italy
e-mail: mauro.pratesi@uslcentro.toscana.it

D. Cultrera
SS Anestesia e Rianimazione Ospedale Santa Maria Nuova, Florence, Italy
e-mail: daniele.cultrera@uslcentro.toscana.it

The three transcranial acoustic windows most commonly used are temporal, occipital, and ocular.

- The *temporal window* is placed above the zigomatic arch and allows an insonance, using the axial or coronal plane access. With the axial access, we use two scans. In the first one, the mesencephalic plane, the most used in acute, is obtained by displaying in B mode the "butterfly" represented by the mesencephalus; from this position, small adjustments allow with the color to visualize the middle cerebral arteries (M1) and anterior (A1) and posterior cerebral arteries in the pre- and post-connective segment (P1 and P2), sometimes the anterior and posterior adjoining stretches and, in particular favorable cases, contralateral cerebral arteries. Again from the axial access, by moving the probe more cranial, it's possible to get the diencephalic scan plane; this plane is characterized in B mode by a "binary" image representing the third ventricle; the color activation allows this scan to display the most distal tracts of the middle (M2), anterior (A2), and posterior cerebral artery (P2). With the coronal plane, which is obtained by rotating the transducer by 90° from the axial position, the longitudinal intracranial tract of siphon of internal carotid is displayed together with the origin of M1 and A1 while posteriorly the top of basilar artery with the initial tract of P1.

- The *occipital window* uses as intracranial access path the foramen magnum, through which the access to the vertebral arteries (V4) to their confluence in basilar artery is possible; from this access can also be sounded the posteroinferior cerebellar arteries (PICAs) that originate right before the confluence of the vertebral arteries and are carried laterally and then from the latter (opposite flow than that vertebral arteries).

  This window can be used with a central or lateral access and with patient both supine but also, if possible, sitting; it is an access that needs to be researched and adapted to the patient's anatomical and clinical features.

- The *ocular window* allows to study ophthalmic and internal carotid arteries inside the siphon. It is the least used because the ultrasound beam that hits the retina can cause damages; in addition, the introduction of the TCCD often renders the information provided superfluous. From this window we can study the anterior compensation circle that is characterized by a displacement flow from the probe with increased diastolic rate indicating a tight stenosis or occlusion of the internal carotid before the ophthalmic origin. The middle cerebral artery (MCA) begins at a depth of 25–60 mm, with a high flow (approximately 80% of the carotid flow), directed towards the probe and has an entirely explorable course; the flow characteristic is a positive diastolic phase, as in all intracranial circulatory arteries, expression of a continuous cerebral spraying (peak velocity of about 116 cm/s). The flow rate on the MCA is detected in the first stroke of its course, within 10 mm of the origin (M1) before its division (M2, M3). The anterior cerebral artery (ACA) is located at a depth of about 70 mm and has a flow in the distance, maximum speed of about 90 cm/s; heads forward and medially (A1), it connects with the contralateral via the front communicator and then continues surrounding the corpus callosum (A2).

- The posterior cerebral artery (PCA) is found about 50–80 mm from the surface, curved around the cerebral peduncles with pre-communicating P1 segment with direct flow to the probe and P2 post-communicating segment with flow away from the probe. The P1 tract may be hypoplastic, but if visible it is the place where the sample volume for the velocity determination is preferentially placed. The vertebral arteries in their V4 segment are on the sides of the spinal cord at a depth of 50–70 mm with flow away from the probe to the basilar artery confluence at a depth of about 65–70 mm; the flow velocities can be asymmetric with the most common left prevalence and maximum peak of 66 cm/s. Shortly before the confluence of the two vertebral arteries, the posterior inferior cerebellar artery

(PICA) originates; the other two cerebellar arteries originate from basilar artery and, respectively, inferior anterior cerebellar artery (AICA) from the middle tract and the superior cerebellar artery from the top.

For better sounding of these vases for some years, echo-enhancers have been used such as (1) Levovist (I generation) consisting of galactose + palmitic acid, which gives rise to microbubbles and increases backward diffusion, (2) SonoVue (II generation) composed of sulfur hexafluoride, and (3) Perflutren (III generation) consisting of lipid microspheres and gas.

56.1.1 TCCD: Clinical Use

Clinical use of the TCCD allows the intracranial circulation to be visualized with a noninvasive, inexpensive, and practicable examination at bedside; the informations provided by this examination are:

- Evaluate both anterior and posterior arterial compensation, remembering that Willis's circle is incomplete in 1/4 of the cases. The most frequent compensation is anterior that occurs in the case of occlusion or tight stenosis of the internal carotid arteria; when it is present, a reduced systolic flow rate on the homolateral MCA can be detected with increased diastolic flow and pulse index and with reverse flow on the ACA and the homolateral ophthalmic.
- Identify intracranial vascular stenosis by detecting a segmental acceleration of the flow with aliasing to color-Doppler and B-mode hyperechogenicity. The speed of acceleration (PSV) at the stenosis point provides an estimate of the degree of stenosis (see table).

Intracranial stenosis: diagnostic criteria

Arteria	Stenosis <50% (PSV)*	Stenosis ≥50% (PSV)*
ACA	≥120 cm/s	≥155 cm/s
ACM	≥155 cm/s	≥220 cm/s
ACP	≥100 cm/s	≥145 cm/s
Basilar	≥100 cm/s	≥140 cm/s

Arteria	Stenosis <50% (PSV)*	Stenosis ≥50% (PSV)*
Vertebral	≥90 cm/s	≥120 cm/s
ACI	≥104 cm/s	≥180 cm/s

*PSV Peak systolic flow velocity. Baumgartner RW et al. *Stroke* 1999;30:87–92

The qualitative and quantitative evaluation of the stenosis downstream curve provides a validated indication of the degree of stenosis according to the criteria of the TIBI score. This score is used and validated by the TCD, but it can also be used with TCCD, and it is based on the morphology of the velocity curve downstream of stenosis or acute obstruction; the score is divided into five classes (0: absent flow, minimal flow, blunted flow, dampened flow, stenotic flow, and normal flow):

- To follow the trend of acute cerebral ischemia especially during thrombolytic treatment is surely the most widely used of TCCD; this examination provides the treatment progress in real time; it serves to select candidates for thrombolysis, to evaluate the possible recanalization of the occluded vessel, and then to evaluate the trend of thrombolysis. Ultrasound also serves to enhance the thrombolysis itself (sonothrombolysis): it consists in performing the acoustic oscillation for 2 h continually of the arterial occlusion zone during infusion of rt-PA. Actually many studies have used the TCD with 2 MHz probe fixed to the temporal window with a little helmet. (studio CLOTBUST, Alexandrov 2004);
  - Detection of vascular abnormalities >2 cm in diameter (aneurysm) with well-defined colorimetric pattern.
  - Evaluation of the presence of cerebral microembolization (MES) in patients with high embolic risk, such as carotid endarterectomy and endoluminal revascularization by carotid stenting and especially with potentially embolic cardiopathy. MES relief is helpful to the clinician for therapeutic choices; today it is possible to make good quality recordings with outpatient TCD (Holter TCD) and quantify the number of MESs with automatic reading programs.
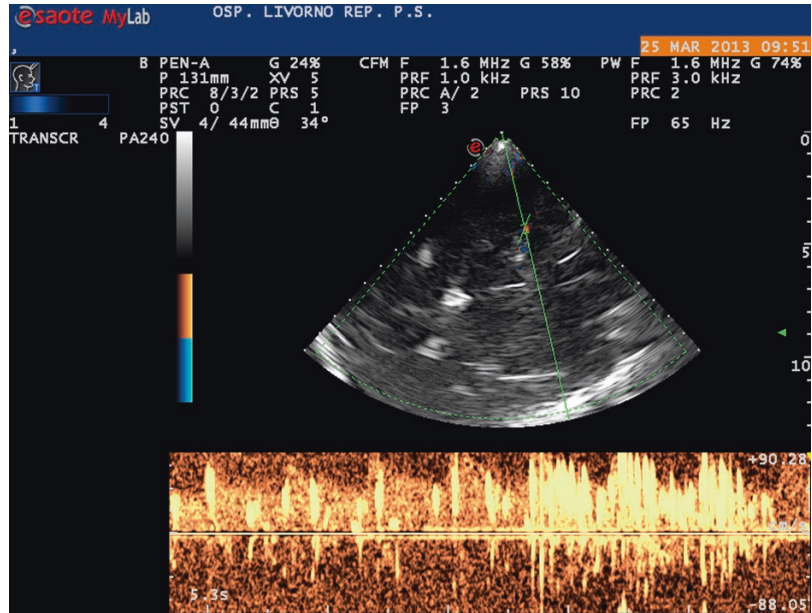
– Evaluation of the patent foramen ovale (PFO) through dynamic test with contrast medium (CM) consisting of a mixture of physiological solution (9 cc) and air (1 cc). At the same time as rapid CM bolus administration, MCA flow is evaluated both at rest and during Valsalva's maneuver; the microemboli relief (MES) demonstrates the presence of left-right shunt (Fig. 56.1).

– Evaluation of cerebral death by detection of precise flow patterns formed progressively by early diastolic phase reduced (IR increase), reverberant flow, presence of only systolic points, no flow signal (Fig. 56.2).

56.2 TCCD in Clinical Management and Therapeutic Choices

The use of ultrasounds in the evaluation of the cerebral circulation is an examination that is closely linked to the clinic both in its indication and in its use. Hoping that this examination provides indications of insufficient neurological examination in an uncertain and uninterpreted patient is one of the most common misuse of the method; TCCD is instead an examination to which precise questions should be asked: where is the blockage of this patient with acute stroke localized? Does this coma patient have an occlusion of basilar artery? Does this young patient who has had a TIA has a PFO?

Usually the answer to these questions is precise and useful for clinical practice.

56.2.1 Acute Ischemic Stroke

It is surely the most extensive and appropriate use of this method since it (1) provides the site of the lesion and (2) monitors the response to thrombolytic therapy by documenting the timing and modes of reperfusion. A great contribution to the development, diffusion, and rapidity of this examination at this stage was provided by the introduction of ultrasonic contrast media that allows to precisely appreciate the location of the thrombus and the activation of the collateral circles. Although the systemic thrombolytic treatment (TS) is useful and indicated in all pathogenetic subclasses and independent of the localization of obstruction, it is useful to determine an intracranial vascular study, but it is not currently possible to delay TS treatment time (*Stroke* 2013; 44:

Fig. 56.2 Cerebral death: reversing flow expression of stopping of cerebral circulation
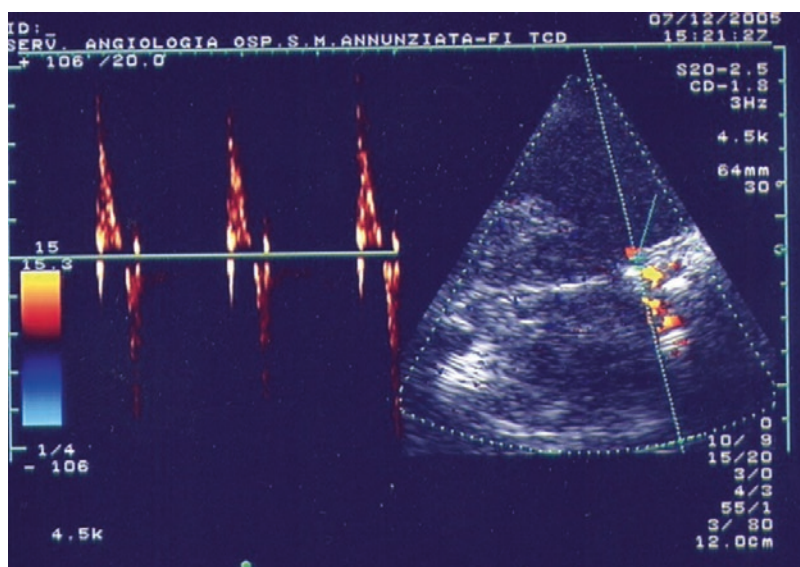
884 Recommendation 4) to perform diagnostic methods. This data has allowed TCCD diffusion as a method that can be done at bedside without delaying the treatment. All major studies of acute stroke patients undergoing neuroscientific study (DIAS, NAIS, ELIGIBLE) showed close correlation between type and localization of intracranial occlusion and prognosis.

The main types of occlusion are:

1. Isolated occlusion of internal or external intracranial carotid artery (ICA) with preserved middle cerebral artery (MCA) and anterior cerebral artery (ACA): this occlusion may be paucisintomatic if the anterior compensation (with inversion on the ipsilateral ACA) or the posterior occurs; if that does not happen (hypoplasia or stenosis), a severe stroke occurs.

2. T-occlusion: where distal ICA, MCA, and ACA are occluded; ICA may be closed by the extracranial level or only in its intracranial distal portion; even in the latter case its presence is also susceptible to the supra-aortic trunk eco Doppler (SAT) in which there is a marked reduction in systolic flow to the bullet with the disappearance of the stump-flow. The T-occlusion patient has a severe stroke with high NIH and usually does not respond satisfactorily to the TS (Figs. 56.3 and 56.4). Moreover, this framework has to be treated because conservative treatment has bad prognosis. In addition to TS therapy in these patients, if there is no early recanalization, an endovascular treatment (TEV) must be performed.

3. Tandem occlusion: where an ICA steno-occlusion usually associates an MCA occlusion in the M1 tract; this is suspected when associating the MCA blocking frame with an ipsilateral ACA flow reversal with extracranial ICA eco color Doppler SAT with high resistances. Even this type of injury responds poorly to TS, so a TEV must be provided.

4. Isolated MCA occlusion: acute diagnosis and MC intake are relatively simple and fast especially if they affect the M1 segment, while occlusion of downstream segments, M2, is suspected when there is a reduction (>21%) of the flow velocity in M1 and the increase of the IP compared to the MCA contralateral. The response to the TS treatment is good (Figs. 56.5 and 56.6) in the case of M2 obstruction, while patients with occlusion of the M1 tract, if they do not resume early, should be directed to TEV.

5. Basilar artery occlusion may have slow and progressive clinical neurologic deficiency or

Fig. 56.3 T-occlusion detected prior to TS treatment (h: 23.54)

Fig. 56.4 One hour after the end of the thrombolytic treatment, ACA had been recanalized, while the MCA remained occluded; the patient exhibited severe hemiplegia (h 1.50)
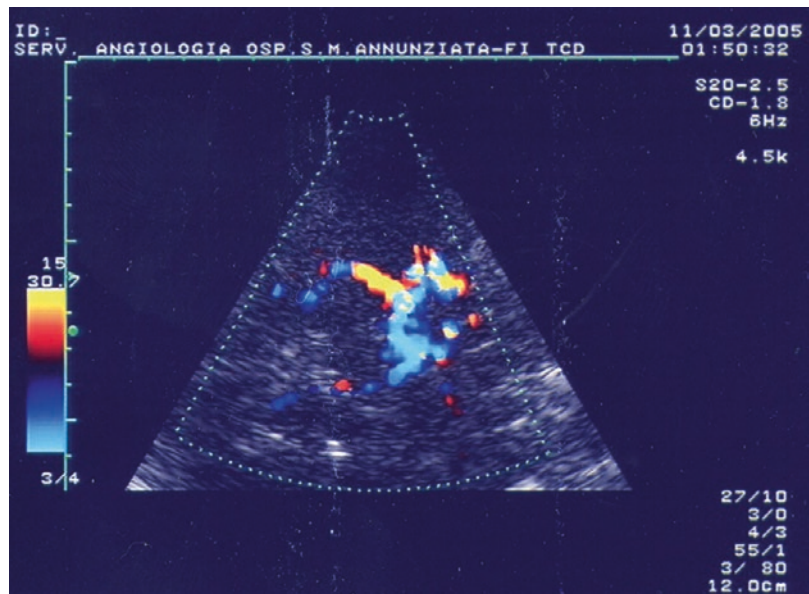
may occur dramatically with sudden coma. Diagnosis in the event of obstruction is usually clear as both high-throughput on both the vertebral arteries in V2 are detected and despite the fact that the MC is unable to display the baseline. In a coma patient, therefore excluding the obstruction of a basilar artery is one of the first tasks; this is possible with angioTC, but it can also be done with an ultrasound probe. Diagnosis must be done

early to establish a disintegrating treatment; otherwise the conservative treatment will be useless. TEV is the recommended treatment even if not demonstrated; the TS must be executed if the TEV is not available immediately.

So the TCCD allows us to understand not only the location of the obstruction but also the course of the treatment and the prognosis of our patient compared to the ongoing treat-

Fig. 56.5 MCA occlusion in M1 (h 14,33)

Fig. 56.6 After 25 min of TS, there is the reopening of the MCA with stomatology resolution
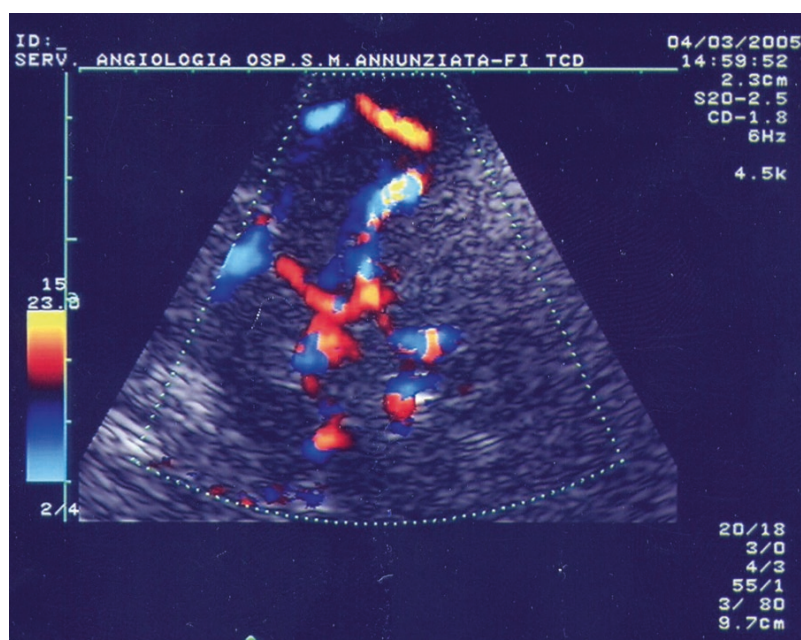
ment. An interesting therapeutic strategy is the one suggested by Sekoranja (*Stroke* 2006; 37: 1805–1809) that using TCCD monitoring with TS checks the action at 30 min of treatment and if the recanalization is not obtained performs the remaining thrombolytic treatment intra-arterial (switch therapy). The results obtained were really good.

The TS fails in 45% of the treated patients and gets the vessel's recanalization in a surprisingly low percentage between 20% and 30% depending on the occlusion and extension of it. The use of ultrasounds (US) in order to increase the effect of thrombolytic agents and speed the thrombus lysis has been evaluated in various studies: this treatment is called sonothrombolysis (ST).

Fig. 56.7 High PI sign of severe endocranial hypertension

US increases penetration of circulating r-TPA (recombinant tissue plasminogen activator) in the thrombus, promotes fibrin polymer rupture, and improves the affinity of r-tPA for fibrin itself. In addition, the US accelerates enzymatic fibrinolysis through nonthermal mechanisms and by a fluid movement inside and around the thrombus. A recent Cochrane review of all randomized trials published on ST reports a significant reduction in mortality and disability at 3 months in patients treated with ST. One thing that surely strikes is the unquestionable improvement obtained by ST in the recanalization of the vessel due to stroke, compared with r-tPA alone therapy. The study concludes with a new wide trial confirming this data. The study should be done with TCD with a 2 MHz probe that sounds the occluded vessel as close to the occlusion for 1 h continuously during the administration of thrombolytic e.v. treatment. The TCD is held in place by the commercially available cartridges that have preferred this method to TCCD. The TCCD may be useful before the beginning of the ST treatment to identify the depth of the origin of the obstruction, since it is easier to acquire with this method. Limit of this treatment is the yet limited spread of practitioners with this method available 24 h for 7 days.

The Alexandrov group tried to overcome this limit by designing and proposing a CLOTBUST-Hands Free (ongoing) study that contains 18 transducers that sound all over the brain and therefore do not require an expert hand.

56.2.2 Left-Right Shunt

It is a condition that causes cyanosis if permanent and may be due to congenital heart disease or arteriosclerotic venous thromboembolic fistulas. A common cause is the permeability of the patent foramen ovale (PFO) that is due to the incomplete septum primum welding with the septum secundum and is a condition that usually does not activate any shunt as the higher pressures in the left atrium impose a closure, valve, and septum. Conversely, if the gradient between the two atria is reversed, the primary septum is disjointed in the front portion of the foramen ovale, giving rise to a left-right short-circuit communication. This type of shunt can be caused by coughing or with Valsalva's maneuver. Right-sided shunt can cause paradoxical embolism, TIA or stroke, migraine, and severe hypoxic respiratory failure (s. Platypnea-

orthodeoxia). Various ultrasound techniques can be used to diagnose the PFO and to identify and quantify the right-to-left shunt. All techniques are based on the use of contrast media, which have the characteristic of not crossing the pulmonary filter. The contrast media used are obtained by using two syringes connected to a three-way tap, which is required for rapid mixing of the components, resulting in the formation of microbubbles. The most commonly used solution consists of 9 ml of physiological solution mixed with 0.5–1 ml of air. TCCD with injected saline solution is a widely used diagnostic technique for evaluating left-right shunt. The exam consists of evaluating any high intensity signals (MESs), determined by the microbubbles of the contrast medium, which reach the level of the cerebral circulation. Commonly, the examination is conducted by sounding the middle cerebral artery, with repeated tests both at rest and during Valsalva's maneuver. The TCCD has a diagnostic susceptibility essentially equivalent to the transesophageal echocardio (TEE). According to our experience, the TCD allows better quantification of the right-left shunt, resulting in the patient's ability to perform a valid Valsalva's maneuver. It is recommended to follow the scale proposed by Serena and Blersch to quantify the shunt: level 1, 0 MES; level 2, 1–10 MES; level 3, > 10 MES; and level 4, curtain effect. Levels 3 and 4 quantify significant shunts (Fig. 56.1). Given the high sensitivity and low invasiveness, this exam is referred to as a first-rate exam; with negative results you determine the term of the spell, while if positive it is recommended to perform a TEE.

56.2.3 Severe Cranial Trauma

Defined as a trauma that results in a Glasgow Coma Score <8, it has as a diagnostic indication the TC Skull possibly repeated after a few hours. The development of endocranial hypertension is the factor that determines the major secondary ischemic brain damage. TCCD or TCD can help in monitoring perfusion and help in early detection of its reduction in order to establish early anti-edema therapy. Through TCD it was seen that pulsatility index values>1.4, telediastolic velocity <20 cm/s, and medium speed <30 cm/s in early detection of subjects with severe cerebrovascular trauma (*Intensive Care Medicine* 2007: 33; 645–651).

Further Reading

1. Malferrari G, Sanguigni S, Accorsi F, Eco color doppler transcranico; Mattioli 2006, Baumgartner RW, Mattle HP, Schroth G. Assessment of ≥50% and <50% intracranial stenoses by transcranial color-coded duplex sonography. Stroke. 1999;30:87–92.
2. Andrei V, Alexandrov MD, Carlos A, Molina MD, Grotta JC, et al. Ultrasound-Enhanced Systemic Thrombolysis for acute ischemic stroke. N Engl J Med. 2004;351:2170–21.
3. Malferrari G, Bertolino C, Casoni F, Zini A, Sarra VM, Sanguigni S, Pratesi M, Lochner P, Coppo L, Brusa G, Guidetti D, Cavuto S, Marcello N. The eligible study: ultrasound assessment in acute ischemic stroke within 3 hours. Cerebrovasc Dis. 2007;24:469–76.
4. LuckaSekoranja JL, Yilmaz H, Lovblad K, Temperli P, Comelli M, Sztajzel RF. Intravenous versus combined (intravenous and intra-arterial) thrombolysis in acute ischemic stroke a transcranial color-coded duplex sonography–guided pilot study. Stroke. 2006;37:1805–9.
5. Komar M, Olszowska M, Przewłocki T, Podolec J, Stępniewski J, BartoszSobień RB, Kabłak-Ziembicka A, Tomkiewicz-Pająk L, Podolec P. Transcranial doppler ultrasonography should it be the first choice for persistent foramen ovale screening? Cardiovasc Ultrasound. 2014;12:16.
6. Ract C, Le Moigno S, Bruder N. Transcranial Doppler ultrasound goal-directed therapy for the early management of severe traumatic brain injury. Intensive Care Med. 2007;33(4):645–51.

Ultrasonography of the Optic Nerve

57

Daniele Cultrera and Mauro Pratesi

In recent years, the international scientific community has accepted that optic nerve sheath diameter (ONSD) ultrasound is a safe, valid, and noninvasive method of measuring intracranial pressure (ICP), with high sensitivity and specificity. Recent studies have shown that due to the anatomical relationship of the optic nerve complex to the subarachnoid space within the brain, an increase in ICP results in increased optic nerve sheath and hence an increase in ONSD [1]. The proximal portion of the optic nerve complex has been found to be most sensitive to changes in ICP, and studies have taken ONSD measurements at a retrobulbar position 3 mm behind the globe [2]. This portion demonstrates the optimum sonographic contrast of the hypoechoic optic nerve complex within the echogenic retrobulbar fat and provides a noninvasive means of detecting raised ICP. Recently other studies have also observed that alterations in ONSD strongly correlated with neuroimaging findings on cranial computed tomography (CT) in patients with elevated ICP [1–3]. An interesting article in 2015 has highlighted the correlation between ultra-

sound and magnetic resonance imaging in the measurements of ONSD. The authors found a close correlation between the two methods [4]. In severe head injury, intracranial bleeding, and idiopathic intracranial hypertension, several studies showed close association between optic nerve sheath diameter (ONSD) and raised ICP [5–7].

Raised ICP can be detected with an increase in ONSD due to the presence of continuity of meninges and subarachnoid space around the optic nerve [8, 9]. It is very important to detect and treat raised ICP in such crucial situations. Intraventricular catheters have been considered as gold standard in measuring ICPs. Their usage is limited by cost and is associated with complications like infection and bleeding. Assessment of ICP and its monitoring with radiological imaging modalities requires transportation, which increases the risk and endangers the lives of critically ill patients [10]. A sure benefit of ultrasound is a cost-effective treatment modality which does not require transportation of the patient. It is helpful bedside noninvasive method in measuring ONSD. It can be repeated at regular intervals which help in close monitoring of ICP as well. Raised intracranial pressure (ICP) is usually associated with increased morbidity, mortality, and poor neurological outcomes. The etiology could be varied on stroke, liver failure, meningitis, meningoencephalitis, metabolic encephalopathy, and postresuscitation syndrome. Increased ICP is common in

D. Cultrera (✉)
SS Anestesia e Rianimazione Ospedale Santa Maria Nuova, Florence, Italy
e-mail: daniele.cultrera@uslcentro.toscana.it

M. Pratesi
Former Director SC Emergency Medicine, Santa Maria Nuova Hospital, Florence, Italy
e-mail: mauro.pratesi@uslcentro.toscana.it

neurocritically ill patient [11]. The sequelae of increased ICP can cause severe disability or death if not recognized and managed immediately [12–15]. Early detection and prompt treatment of raised ICP in such situations are essential. However, it may pose challenges at the same time [15, 16]. Invasive ICP monitoring is the gold standard. It is associated with complications such as infection, bleeding, and being expensive. Regular assessment and comparison by computed tomography (CT)/magnetic resonance imaging (MRI) in these critically ill patients are fought with dangers of transporting to radiology [17, 18]. The use of bedside ocular ultrasonography in measuring optic nerve sheath diameter (ONSD) can be a useful method for detecting raised ICP. It has the advantage of being a noninvasive, portable, easily performed at bedside in minimum time. It can be repeated for re-evaluation without risk of radiation.

57.1 Measurement of the Optic Nerve Sheath Diameter

A clear barrier is placed over the patient's eyelid, followed by application of a generous amount of ultrasound gel. Measurements should be taken in multiple planes. The optic nerve sheath is measured at a depth of 3 mm behind the orbit. The procedure consists in placing a linear probe (more than 7.5 MHz) over the closed eye of the supine patient in the axial plane (Fig. 57.1) with a sterile gel coating on the probe. The optic nerve sheath is identified as two hyperechoic lines behind the globe. The measurement is done using electronic calipers 3 mm behind the papilla (Fig. 57.2). In healthy people the measurement of ONSD is under 5 mm (Fig. 57.3).

Fig. 57.1 Probe position

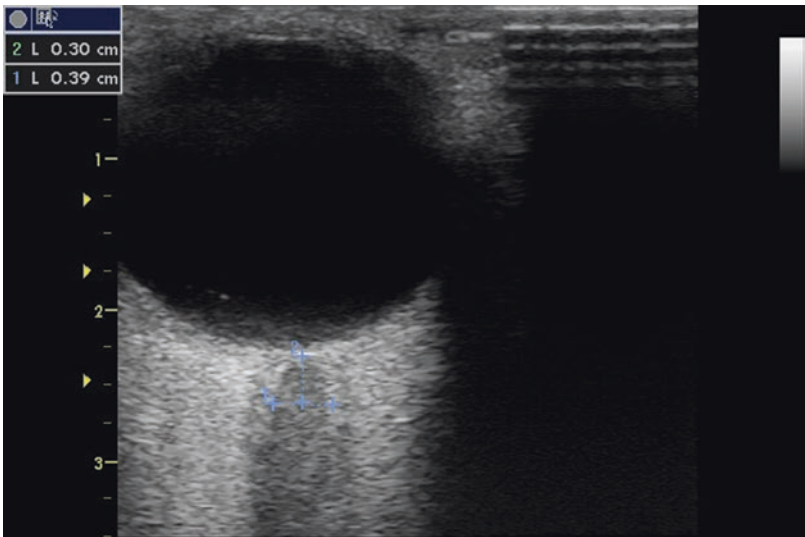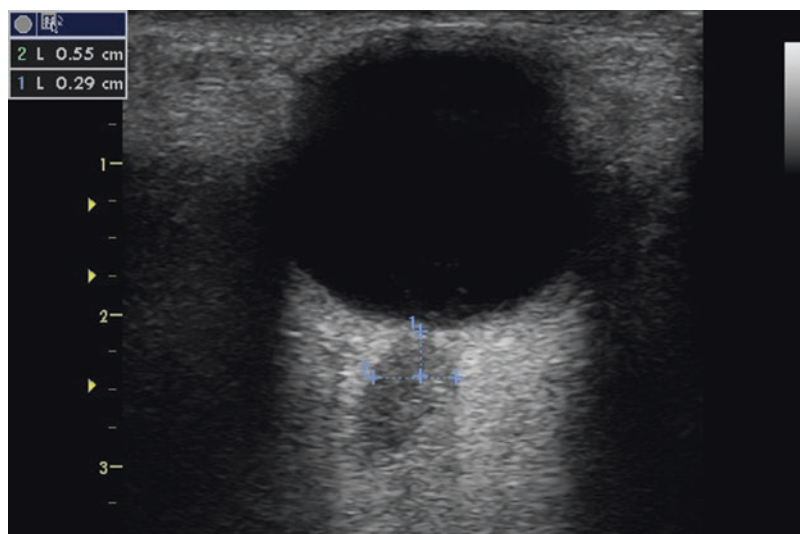**Fig. 57.2** Measurement of the optic nerve sheath

Fig. 57.3 Abnormal ONSD

References

1. Goel RS, Goyal NK, Dharap SB, Kumar M, Gore MA. Utility of optic nerve ultrasonography in head injury. Injury. 2008;39(5):519–24.
2. Girisgin AS, et al. The role of optic nerve ultrasound for the diagnosis of elevated intracranial pressure. Emerg Med J. 2007;24:252–4.
3. Karakitsos D, et al. Transorbital sonographic monitoring of optic nerve diameter in patients with severe brain injury. Transplant Proc. 2006;38(10):3700–6.
4. Shirodkar CG, Munta K, Rao SM, Mahesh MU. Correlation of measurement of optic nerve sheath diameter using ultrasound with magnetic resonance imaging. Indian J Care Med. 2015;19(8):466–70.
5. Bäuerle J, Nedelmann M. Sonographic assessment of the optic nerve sheath in idiopathic intracranial hypertension. J Neurol. 2011;258:2014–9.
6. Geeraerts T, Merceron S, Benhamou D, Vigué B, Duranteau J. Non-invasive assessment of intracranial pressure using ocular sonography in neurocritical care patients. Intensive Care Med. 2008;34:2062–7.
7. Geeraerts T, Newcombe VF, Coles JP, Abate MG, Perkes IE, Hutchinson PJ, et al. Use of T2-weighted magnetic resonance imaging of the optic nerve sheath to detect raised intracranial pressure. Crit Care. 2008;12:R114.
8. Killer HE, Jaggi GP, Flammer J, Miller NR, Huber AR, Mironov A. Cerebrospinal fluid dynamics between the intracranial and the subarachnoid space of the optic nerve. Is it always bidirectional? Brain. 2007;130(Pt 2):514–20. [PubMed].
9. Hansen HC, Helmke K. Validation of the optic nerve sheath response to changing cerebrospinal fluid pressure: ultrasound findings during intrathecal infusion tests. J Neurosurg. 1997;87:34–40.
10. Beckmann U, Gillies DM, Berenholtz SM, Wu AW, Pronovost P. Incidents relating to the intra-hospital transfer of critically ill patients. An analysis of the reports submitted to the Australian incident monitoring study in intensive care. Intensive Care Med. 2004;30:1579–85.
11. Hylkema C. Optic nerve sheath diameter ultrasound and the diagnosis of increased intracranial pressure. Crit Care Clin North Am. 2016;28(1):95–9.
12. Pickard J, et al. Management of raised intracranial pressure. J Nurol Neurosurg Psychiatr. 1993;56:845–58.
13. Price DD, et al. Trauma ultrasound feasibility during elicopter transport. Air Med J. 2000;19(4):144–6.
14. Sayed M, et al. Prehospital emergency ultrasound: a review of current clinical applications, challenges, and future implications. Emerg Med Int. 2013;2013:531674.
15. Sippel S, et al. Review article: use of ultrasound in the developing world. Int J Emerg Med. 2011;4:72.
16. Nelson BP, et al. Use of ultrasound by emergency medical services: a review. Int J Emerg Med. 2008;1(4):253–9.
17. Shirodkar CG, et al. Optic nerve sheath diameter as a marker for evaluation and prognostication of intracranial pressure in Indian patients: an observational study. Indian J Crit Care Med. 2014;18(11):728–34.
18. Beckmann U, et al. Incidents relating to the intrahospital transfer of critically ill patients. An analysis of the reports submitted to the Australian incident monitoring study in intensive care. Intensive Care Med. 2004;30:1579–85.

Muscle Ultrasound for the ICU Patient

58

Duccio Conti and Laura Salucci

Key Points
- Although further evidence is needed, US is increasingly used to interpret the association of muscle composition and functional or clinical outcome.
- US muscle can help physician to early diagnose ICU-AW. This is fundamental for the optimization of nutritional status, pharmaceuticals, exercise/rehabilitation, or some combination of strategy.
- Diaphragmatic ultrasound (DU) is a useful method for the evaluation of critical care patients and can predict the success of extubation in ventilated patients.
- US is an important tool for physicians in the early diagnosis and management of traumatic and infection muscle disease.

In the second part of the century, the US imaging became widely available to study the morphology of abdominal organs, heart, and vessels. In the last few years, it became routinely used in the ICU. In this context, muscle ultrasound represents the last heat for physicians. Many start to believe that US is an unfeasible method because it is noninvasive, sensitive, inexpensive, safe, and available at bedside and allows repeated measurements.

Muscle US may be utilized in ICU to evaluate both quality and loss of mass in limb muscles, to directly assess diaphragmatic function (weakness, paralysis, detection of atrophy, contractility), and for diagnosis and evaluation of traumatic and infection muscles disease (edema, hematoma, fasciitis, myositis).

58.1 Sarcopenia, ICU-Acquired Weakness and Muscle US

The concept of sarcopenia appeared for the first time in the late 1980s. It is defined as a progressive loss of skeletal muscle mass, strength, and function occurring primarily as a consequence of aging. Sarcopenia is a major contributing factor to frailty and is associated with serious consequences, functional limitations, comorbidities, and mortality. This condition can be classified as primary (age-related) or secondary, due to certain medical problems including malnutrition, inactivity, and chronic disease (i.e., heart failure). Although this term is especially used in geriatric patients, a similar condition to secondary sarcopenia has been reported in ICU patients, called ICU-acquired weakness (ICU-AW). ICU-AW is defined as bilateral symmetrical limb weakness

D. Conti (✉) · L. Salucci
Anaesthesia and Intensive Care Unit, Santa Maria Annunziata Hospital, Florence, Italy
e-mail: duccio.conti@uslcentro.toscana.it;
laura.salucci@uslcentro.toscana.it

resulting from axonal polyneuropathy or myopathy or a combination of both (critical illness neuromyopathy).

Muscle wasting occurs early and rapidly during the stay in ICU, with subsequent impaired function and disruption of muscle architecture. Retrospectively, it was demonstrated that muscle mass at ICU admission is an independent predictor of mortality in mechanical ventilated critically ill patients. ICU-AW is associated with respiratory muscle weakness, mechanical ventilation with prolonged weaning period, and persistent functional disability after discharge. It is advisable to recognize as soon as possible the onset of ICU-AW, to optimize nutritional and pharmaceutical therapy and physiokinesitherapy (FKT) program or some combination of strategy.

To date, there is no gold standard assessment method in ICU to diagnose ICU-AW. Bioelectrical impedance analysis, dual X-ray absorptiometry, and TC or handgrip strength to evaluate muscle strength are not suitable in ICU because of immobilization, routine use of sedative medications, and life-threatening illnesses. In this context muscle US may be a useful method to assess muscle quality and loss of mass among critical care patients. In addition to the advantages of US at bedside, there exists an excellent interobserver reliability, irrespective of the expertise level, for the quantitative analysis of muscle parameters. The recent VALIDIUM study has demonstrated a moderate correlation between quadriceps muscle thickness with US and cross-sectional area (CSA) of skeletal muscles measured with CT scan at level of the third lumbar vertebra. In addition, a very good correlation with quadriceps muscle assessed by MRI was previously demonstrated for US on long-term patients. Numerous studies have observed a linear relationship between muscle thickness (MT) and muscle cross-sectional area (CSA) in the quadriceps, tibialis anterior, and adductor.

Although the use of US for muscle composition tool has dramatically increased over the last 10 years, further evidence and standardized protocols are needed to ensure the validity of these measures in interpreting the association of muscle composition and functional or clinical outcome. There are several steps in US skeletal muscle protocols that should be considered and could add error to estimates including patient position, landmarking, pressure applied by the probe, and caliper placement on the image.

ICU-AW affects preferentially the lower limb muscles. US B-mode images can be acquired for gastrocnemius, tibialis anterior (TA), and quadriceps muscle layer thickness. During the first days of an ICU admission, an evaluation of the four muscles that form the quadriceps complex, rectus femoris (RF) (predominantly of type II fibers), vastus intermedius (VI) (predominantly of type I fibers), vastus lateralis (VL), and medialis can be performed to assess the rate of muscle wasting and the association with subsequent impaired function. US measurement of the rectus femoris muscle is highly reproducible, can demonstrate changes in muscle thickness and loss of muscle mass, and is preferentially measured during the ICU stay.

Images are acquired with patients in the supine position and with their knee in passive extension and neutral rotation. A suitable amount of US coupling gel is used to facilitate acoustic contact and minimize transducer pressure on the skin.

It is possible to obtain images with a hand-carried US unit using a linear array transducer (>10 MHz). The probe is placed on the anterior aspect of the thigh, perpendicular or longitudinal to its long axis at the border between the lower third and upper two-third between the anterior superior iliac spine (ASIS) and the upper pole of the patella or at the half distance between the ASIS and the upper pole of the patella (Fig. 58.1). Lateral imaging is obtained 5 cm laterally from the first imaging point. Operators should adjust the image gain and contrast for each probe and patients. To avoid the overestimation or underestimation of muscle measure, it is advisable to scan the muscle image at three or four different measurement points in both legs without moving the probe. The average of the scores is used for final analyses.

The cross-sectional thickness of the muscle is measured as the distance between the superficial and deep aponeurosis. The orientation of the fibers of RF is predominantly parallel to their

fascia. In this muscle no pennation angle, defined as an angle between muscles fibers and the deep fascia of the muscle, can be determinate differently to other quadriceps muscles (VI,VL).

Placing the probe perpendicular to the long axis of the thigh, the cross-sectional area can be obtained (Fig. 58.2). The quadriceps muscle

Fig. 58.1 Image acquisition with a hand-carried ultrasound unit. The transducer is placed perpendicular (or longitudinal) to the skin without exerting compression, at the half distance between the anterior superior iliac spine (ASIS) and the upper pole of the patella (1) or at the border between the lower third and upper two-third between the ASIS and the upper pole of the patella (2)

appears as a semicircle centered at the femur. When the image quality is optimal, the operator freezes the image of the muscle on the US monitor. Using the movable cursor, the inner echogenic line of the rectus fascia is outlined, and the cross-sectional area is automatically calculated by the US planimetric software.

Actually ICU-specific cut points that identify patients with low muscle mass are needed, and studies report only site-specific cut points for older patients with the following thresholds of muscle thickness: RF, 20 mm in men and 16 mm in women; vastus lateralis, 17 mm in men and 15 mm in women; and tibialis anterior, 23 mm in men and 22 mm in women.

In critical care setting, there is growing interest in the use of US for the assessment of changes in quality muscle (echogenicity). After the first 10 days of critical illness, echogenicity often increases, matching worsened muscles condition and impaired strength and worsening clinical function. Echo intensity (EI), defined as the mean pixel intensity in the muscle, can be determined by grayscale analysis using the standard histogram function (Adobe Photoshop
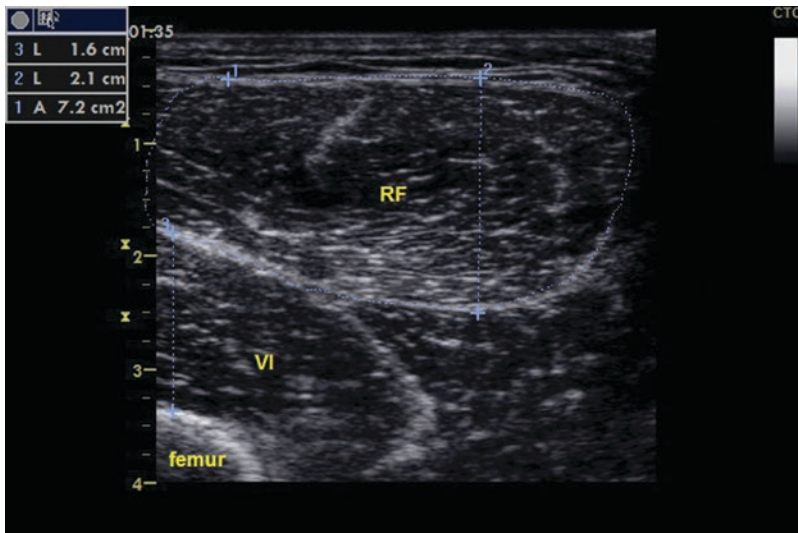
Fig. 58.2 Assessment of quadriceps femur thickness using ultrasound with the transducer placed perpendicular to the long axis of the thigh in a healthy man. The dotted circular line represents the region of the muscle used in the calculation of cross-sectional area (1). The thickness of each muscle is measured from subcutaneous tissue to the inner edge of the rectus femoris (RF) muscle (2) or from the femur to the inner edge of the vastus intermedius (VI) muscle (3)
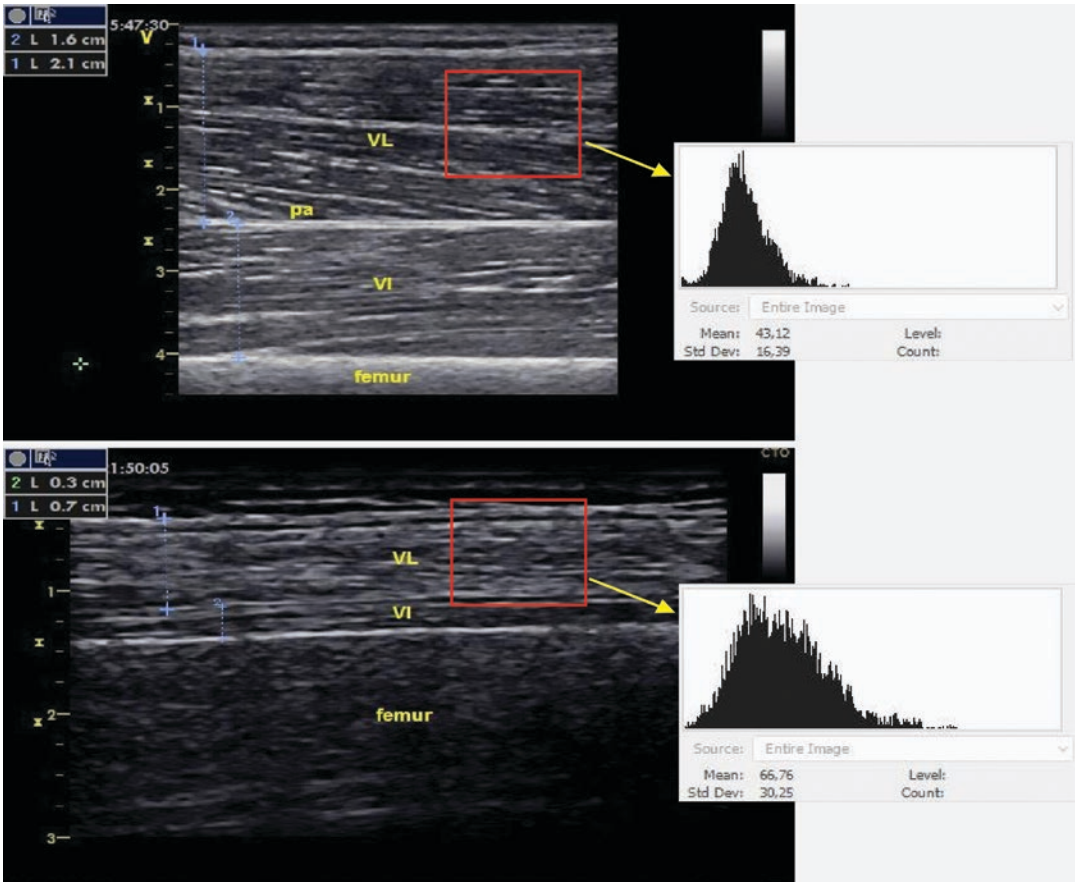
Fig. 58.3 Examples of longitudinal ultrasound images of quadriceps. Top panel: measurement of pennation angle (pa) and muscle thickness in a healthy man. Bottom panel: patient with critical illness with extremely reduced muscle thickness and increased echo intensity. The square boxes indicate the region of interest (ROI) selected over the vastus lateralis (VL) of both ultrasound images. Corresponding histograms for computerized quantitative grayscale analysis are shown. The bottom ultrasound image shows greater hyperechoic properties in comparison to the top one, evidencing wider distribution, shift to the right and large grayscale histogram values. The grayscale value of bottom image is 66.67, suggesting a higher proportion of fat and fibrotic infiltration in comparison to the top image (43.12)

program) (Fig. 58.3). EI could be evaluated in a region of interest (ROI) that represents as much of the muscle as possible without any bone-surrounding fascia and artifacts. The value of EI in the ROI is expressed in values between 0 (= black) and 255 (= white), with higher values indicating more hyperechoic material. The comparatively hyperechoic image characteristics can highlight changes of muscle quality. The normal muscle is relatively hypoechoic (dark). In critical care patients, changes in muscle echogenicity are probably due to muscle necrosis and infiltration of fatty and connective tissue in replacement of muscle fibers. In addition, in the acute stage of septic patients, changes in muscle echotexture are related to muscle edema due to capillary leak.

In septic patients, US echogenicity can be graded according to the Heckmatt score. This score differentiates echogenicity of cross section of tibialis anterior muscles in four grades:

1. Normal echo intensity with starry-night aspect and distinct bone in healthy control
2. Increased echo intensity with normal bone echo (day 4)

3. Increased echo intensity with reduced bone signal echo (day 14)
4. Increased echo intensity with loss of bone signal echo (day 14)

The interpretation of US results from ICU patients can be affected by several factors: variability in hydration status, challenges in acquiring height and limb length (for normalizing muscle thickness or area), bias in the type of patients, as well as the extent that edema confounds muscle measure.

58.2 Diaphragm Ultrasound

The diaphragm is a fundamental respiratory muscle for spontaneous breathing in humans. A substantial number of critical patients during stay in ICU develop striated muscle weakness and diaphragm dysfunction (DD), which seems to occur more rapidly compared to general limb muscle. Many factors, including inflammation, malnutrition, pharmacological agents, and mechanical insults such as cardiac and upper abdominal surgery, contribute to this problem, but mechanical ventilation (MV) affects independently the diaphragm. The expression "ventilator-induced diaphragmatic dysfunction" (VIDD) describes the effects of mechanical ventilation and respiratory muscle unloading on the diaphragm. DD is associated to prolonged mechanical ventilation and directly correlates to weaning failure.

Gold standard methods to assess diaphragmatic function are twitch magnetic phrenic nerve stimulation or measurement of transdiaphragmatic pressure with esophageal and gastric balloons. These methods are difficult to obtain at the bedside and not routinely available. Diaphragmatic ultrasound (DU) in ICU is a non-ionizing imaging technique widely available and has an excellent intra- and interobserver reproducibility. DU is useful to evaluate diaphragm dysfunction (weakness, paralysis) and can predict the success of extubation in ventilated patients, quantifying morphologic assessment (detection of atrophy) and functional evaluation of the muscle (contractility).

Two acoustic windows can be used to study the diaphragm:

1. *Diaphragm thickness* is measured at the apposition zone, on the midaxillary line, 0.5–2 cm below the costophrenic sinus. The diaphragm is displayed placing the transducer perpendicular to the chest wall. The diaphragm is imaged with a linear high-frequency probe (>10 MHz) at the depth of 1.5–3 cm. It appears as a structure with three distinct layers; two parallel echogenic lines can be identified: the nearest line represents the parietal pleura and the deeper one is the peritoneum. The diaphragm is the less echogenic structure between these two lines. Maximum diameters are measured between diaphragmatic pleural line and peritoneal line (Fig. 58.4). In health subjects during spontaneously breathing, at the apposition zone, the normal thickness of the diaphragm, evaluating usually in M-mode, is 1.7 ± 0.2 mm and increases to 4.5 ± 0.9 mm during breath at total lung capacity (TLC). The thickening fraction ([TF = thickness at end-inspiration- thickness at the end-espiration]/thickness at the end-espiration) is an index of diaphragm thickening. In mechanically ventilated patients, during spontaneous breathing, a TF >30% can be used as an index of weaning success with a positive predictive value of 91%.

2. *Diaphragmatic motion* can be assessed in the subcostal position with visualization of the posterior diaphragmatic third. Placing an abdominal or cardiac probe (2–5 MHz) perpendicular to the chest wall between the midclavicular and anterior axillary lines can provide images from the subcostal area. The liver and the spleen may be used as acoustic windows for the right/left hemidiaphragm. The diaphragm is represented as an hyperechoic line (produced by the tight adherence of the pleura to the muscle). During normal breathing, the inspiratory diaphragmatic movement is caudal, and the diaphragm moves toward the probe; in expiration, the diaphragm moves away from the probe because of its cranial movement. The diaphragmatic inspiratory

Fig. 58.4 Diaphragm ultrasonography (US) at the zone of apposition in (**a**) B-mode and (**b**) M-mode during quiet breathing in healthy woman. Maximum diameters are measured between diaphragmatic pleural line (d) and peritoneal line (p). Non-echogenic central diaphragmatic tendon (#) is indicated. (1) Thickness at end expiration. (2) Thickness at end inspiration
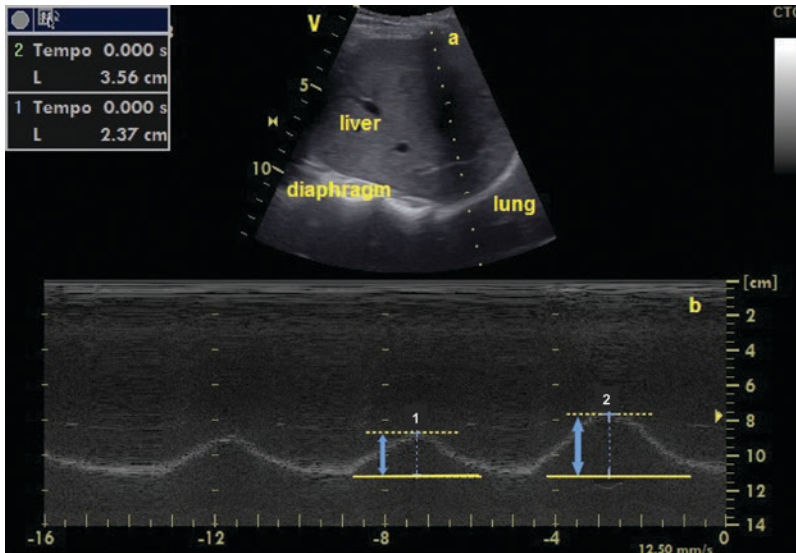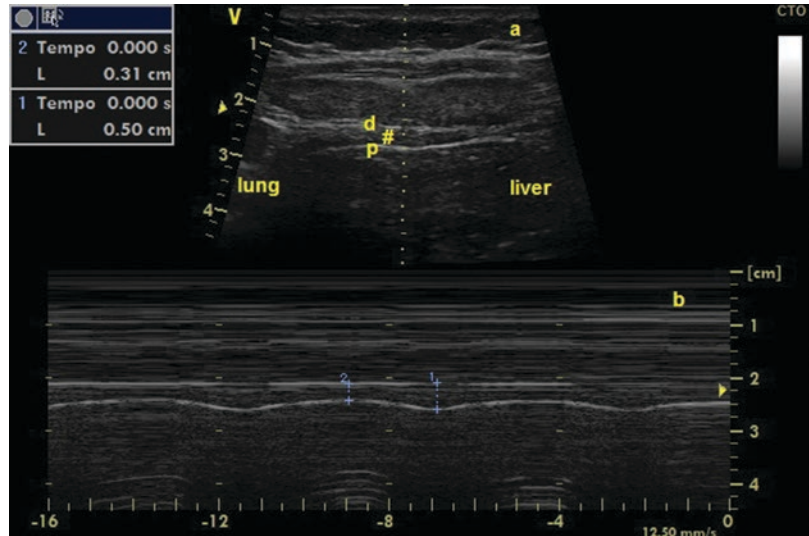
Fig. 58.5 Diaphragm ultrasonography (US) from the right subcostal position with a 3.5–5 MHz probe in (**a**) B-mode and (**b**) M-mode during quiet (1) and deep breathing (2). The diaphragmatic dome should be assessed per- pendicularly, and the liver/spleen may be used as sound windows for right/left hemidiaphragm. Inspiratory dia- phragmatic position (solid line), expiratory position (dashed line), and excursion (arrow) are indicated

excursion in healthy subjects during spontane- ous breathing, measured in M-mode, is 1.34 ± 0.18 cm (Fig. 58.5). The diaphragmatic dome downward motion at rest should be ≥ 1 cm and represents a lower limit in healthy subjects.

During unilateral or bilateral diaphrag- matic paralysis, M-mode imaging shows a paradoxical (i.e., cranial) or absence of active movement. If there is a paralysis, the dia- phragm moves passively cranially instead of following normal caudal movement. The M-mode diaphragmatic trace of its movement direction (cranial or caudal) allows to recog- nize diaphragmatic weakness from paralysis.

There are some difficulties and limitations in the evaluation of diaphragmatic sonography;

particularly in the ICU, poor acoustic windows with poor quality of images have been reported to occur with a prevalence of 2–10%. The sonographer should place the probe as perpendicular as possible to the excursion line to minimize inaccuracy of measure. For better assessment of diaphragmatic excursion, it is advisable a brief recording (5–10 min.) during spontaneous breathing. In contrast, if the patient is under assisted ventilation, the measured excursion represents the force of diaphragmatic contraction by itself added to the passive displacement of the diaphragm by pressure generated by the ventilator. In this way, it is possible to get a better evaluation of the patient-ventilator interaction.

Both thickness and thickening fraction can be affected by several factors; mean thickness values are about 1.5–2 mm, and therefore it is necessary to use a high-frequency probe (vascular probe 10 Mhz). The distance that is measured is very small, and therefore small operator-dependent variations could affect the measure. In addition, there can be technical difficulties with some obese patients.

58.3 Muscles Trauma and Infection Ultrasound

In addition to ICU-acquired weakness and to diaphragm dysfunction, ICU muscle diseases can be classified in traumatical, inflammatory, or infective.

Especially in trauma patients, US is a useful method to evaluate the anatomy and pathology of muscle injuries. The developing of imaging techniques has led to a three-grade clinical severity grading system with features of US appearance.

Grade I – hypoechoic area length, <20% cross-sectional area involvement, and focal increased echogenicity with no architectural distortion.

Grade II – presence of an-echoic gap with "bell clapper" sign, more than 50% muscle involvement and with extent of 20–50% cross-sectional area involvement.

Grade III – full-thickness tear of muscle or fascia, with extravasation of collection away from injured part of muscle can detect complete discontinuity of muscle fibers with disruption of muscle architecture, "bell clapper" sign, associated hematoma and >50% of muscle involvement with >50% of cross-sectional area.

In many patients admitted to the ICU, clinical history should help in differentiating between abscesses and hematomas since both often have similar appearances on US. Doppler may be useful to see increased vascularity. Often, it could be difficult to definitively diagnose a fluid collection as a hematoma on the basis of the sonographic appearance alone. Furthermore, both hematomas and abscesses may appear similar as regards their US characteristic. They both transmit sound well (reflect well the echoes) and have internal echoes and irregular walls. The echointensity of blood clots in a hematoma changes with age and usually reduces (Fig. 58.6). In patients with history of a bleeding disorder or anticoagulant therapy, rectus sheath hematomas may develop following severe bouts of sneezing, coughing, or convulsions. These hematomas are usually painful.

Infection myositis can result from microbial invasion (bacterial, viral, fungal, parasitic organisms) of subcutaneous tissue through external trauma or from direct spread from hematogenous seeding in intravenous drug users or immunocompromised hosts. As with CT, US (probe 2–12 MHz) can be used to assess muscle parenchymal abnormalities that are reflected in changes of the echotexture of the muscle. Focal inflammation can be detected as echo-poor regions within the musculature and hypo- or hyperechogenic swelling. Calcifications may be visible and often seen as brightly echogenic foci with acoustic shadowing. These findings can be associated with subcutaneous fat thickened and hyperechoic, indicating overlying inflammation and cellulitis.

US is a convenient and noninvasive bedside method and can be used to help in the differential diagnosis between necrotizing fasciitis (NF), cellulitis, and deep venous thrombosis.

NF is a rare, life-threatening soft-tissue infection with high mortality (up to 70%) and represents a medical and surgical emergency. It is characterized by rapidly spreading and progressive necrosis of deep fascia and subcutaneous tissue since to systemic failure. NF is often

Fig. 58.6 Ultrasound image of an 89-year-old woman after total hip replacement complicated by postoperative bleeding and subsequent embolization of an iliac artery branch. Assessment of thigh images was obtained using a linear transducer placed perpendicular to the long axis. (**a**) The hematoma (X) is characterized by internal echoes and irregular walls with reduction of the echointensity due to advanced age. (**b**) Ultrasound findings below the hematoma reveal thickening of superficial fascia (fasciitis), cellulitis, and edema with swelling of the subcutaneous tissue (+). Parenchymal abnormalities with changes in echotexture, reduction of thickness, and hypo- or hyperechogenic areas (X)
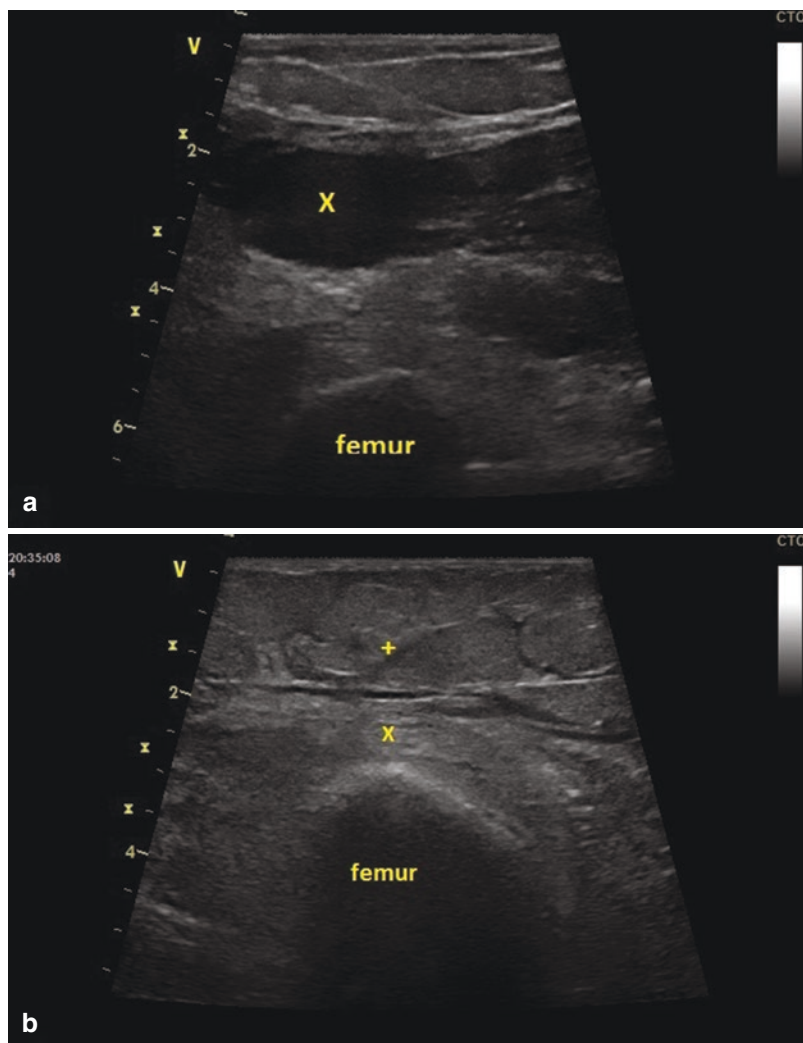
underestimated because of the initial difficulties to differentiate it from cellulitis. Only early diagnoses can decrease mortality. The gold standard modality for diagnosis is operative exploration ("finger test") and frozen biopsy. The imaging tests are an invaluable diagnostic adjunct, with magnetic resonance imaging (MRI) the recommended modality. US findings are thickening of deep fascia (>4 mm fasciitis), turbid fluid collections along the deep fascia suggestive of myositis, muscle hypo- or hyperechogenic swelling, findings of cellulitis, and swelling of the subcutaneous tissue.

US may be helpful to delineate subtle muscle hernias and in the early detection of compart-ment syndrome that is fundamental for early surgical treatment. This severe complication of traumatic, inflammatory or infective disease can result in loss of affected extremity, and the assessment can be effectively accomplished using US Doppler.

Suggested Reading

Kizilarslanoglu MC, Kuyumcu ME, Yesil Y, Halil M. Sarcopenia in critically ill patients. J Anesth. 2016;30:884–90.

Kuo GP, Carrino JA. Skeletal muscle imaging and inflammatory myopathies. Curr Opin Rheumatol. 2007;19:530–5. Review.

Matamis D, Soilemezi E, Tsagourias M, Akoumianaki E, Dimassi S, Boroli F, Richard JC, Brochard L. Sonographic evaluation of the diaphragm in critically ill patients. Technique and clinical applications. Intensive Care Med. 2013;39:801–10.

Paris M, Mourtzakis M. Assessment of skeletal muscle mass in critically ill patients: considerations for the utility of computed tomography imaging and ultrasonography. Curr Opin Clin Nutr Metab Care. 2016;19:125–30.

Zambon M, Greco M, Bocchino S, Cabrini L, Beccaria PF, Zangrillo A. Assessment of diaphragmatic dysfunction in the critically ill patient with ultrasound: a systematic review. Intensive Care Med. 2017;43:29–38.

Fever of Unknown Origin and Ultrasound

59

Diletta Guarducci and Armando Sarti

Key Points
- Fever of unknown origin: definition
- Instruments for measuring body temperature
- Noninfectious causes of fever in the intensive care units
- Infectious causes of fever in the intensive care units
- Fever of unknown origin ultrasound assessment

59.1 Fever of Unknown Origin: Definition

Fever is a common problem in intensive care unit (ICU) patients. The presence of fever frequently results in the performance of diagnostic tests and procedures that significantly increase medical costs and expose the patient to unnecessary invasive diagnostic procedures and inappropriate use of antibiotics.

Fever of unknown origin (FUO) is defined as fever at or above 101 °F (38.3 °C) that remains undiagnosed after 3 days and for a time ≥2 days after incubation of microbiological cultures.

D. Guarducci (✉) · A. Sarti
Department of Intensive Care, S. M. Annunziata Hospital, Florence, Italy
e-mail: mariadiletta.guarducci@uslcentro.toscana.it

Normal body temperature is generally considered to be 37.0 °C (98.6 °F) with a circadian variation of between 0.5 and 1.0 °C.

59.1.1 Instruments for Measuring Body Temperature

The definition of fever is arbitrary and depends on the purpose for which it is defined. The Society of Critical Care Medicine practice parameters define fever in the ICU as a temperature >38.3 °C (>101 °F).

A variety of methods are used to measure body temperature, combining different sites, instruments, and techniques:

1. The mixed venous blood in the pulmonary artery is considered the optimal site for core temperature measurement; however, this method requires placement of a pulmonary artery catheter.
2. Infrared ear thermometry has been demonstrated to provide values that are a few tenths of degree below temperatures in the pulmonary artery. This is the technique of choice for most ICU patients.
3. Rectal temperatures obtained with a mercury thermometer or electronic probe are often a few tenths of a degree higher than core temperature. Access to the rectum may be limited by patient position, with an associated risk of rectal trauma.

4. Oral measurements are influenced by events such as the presence of respiratory devices delivering warmed gases.
5. Axillary measurements substantially underestimate core temperature and lack reproducibility.

The main diagnostic dilemma is to exclude noninfectious causes of fever and then determine the site and likely pathogens of those patients with infections. ICU patients frequently have multiple infectious and noninfectious causes of fever. Therefore they necessitate a systematic and comprehensive diagnostic approach.

Fever in the ICU is one reason for performing whole body ultrasound in a sequential way.

59.1.2 Infectious and Noninfectious Causes of Fever in the ICU

A large number of noninfectious disorders result in tissue injury with inflammation and a febrile reaction. For reasons that are not entirely clear, most noninfectious disorders usually do not lead to a fever >38.9 °C (102 °F); therefore, as the temperature increases above this threshold, the patient should be considered to have an infectious etiology as the cause of the fever.

In Table 59.1 are listed many noninfectious disorders that should be considered in ICU patients

Table 59.2 lists the most important sites of infection in ICU patients.

The Flowchart 59.1 shows which sites must be investigated by ultrasound in a patient with fever unknown (FUO).

59.2 Noninfectious Causes

59.2.1 Atelectasis

The role of atelectasis as a cause of fever is unclear; however, atelectasis probably does not cause fever in the absence of pulmonary infection.

The dynamic air and fluid bronchogram are used to distinguish atelectasis from pneumonia.

Table 59.1 Common noninfectious causes of fever in the ICU

Postoperative fever (48 h postoperative)
Posttransfusion fever
Drug fever
Pancreatitis
Acalculous cholecystitis
Ischemic bowel
Aspiration bowel
ARDS
Transplant rejection
Deep venous thrombosis/thrombophlebitis
Hematoma
GI bleed
Adrenal insufficiency
Neoplastic fever
Atelectasia

Table 59.2 Common infectious causes of fever in the ICU

Ventilator-associated pneumonia (VAP)
Sinusitis
Catheter-related sepsis
Clostridium difficile diarrhea
Infective endocarditis and myocarditis
Intra-abdominal processes
Cholecystitis
Urinary sepsis

The remark of lung pulse without lung sliding is found in the atelectasis. Lung pulse is a dynamic lung ultrasound sign. It can be described as the association of absent lung sliding with the perception of heart activity at the pleural line (see Chap. 30).

59.2.2 Acute Respiratory Distress Syndrome (ARDS)

Acute respiratory distress syndrome (ARDS) is a clinical syndrome characterized by:

1. Inflammatory pulmonary edema
2. Severe hypoxemia
3. Stiff lungs
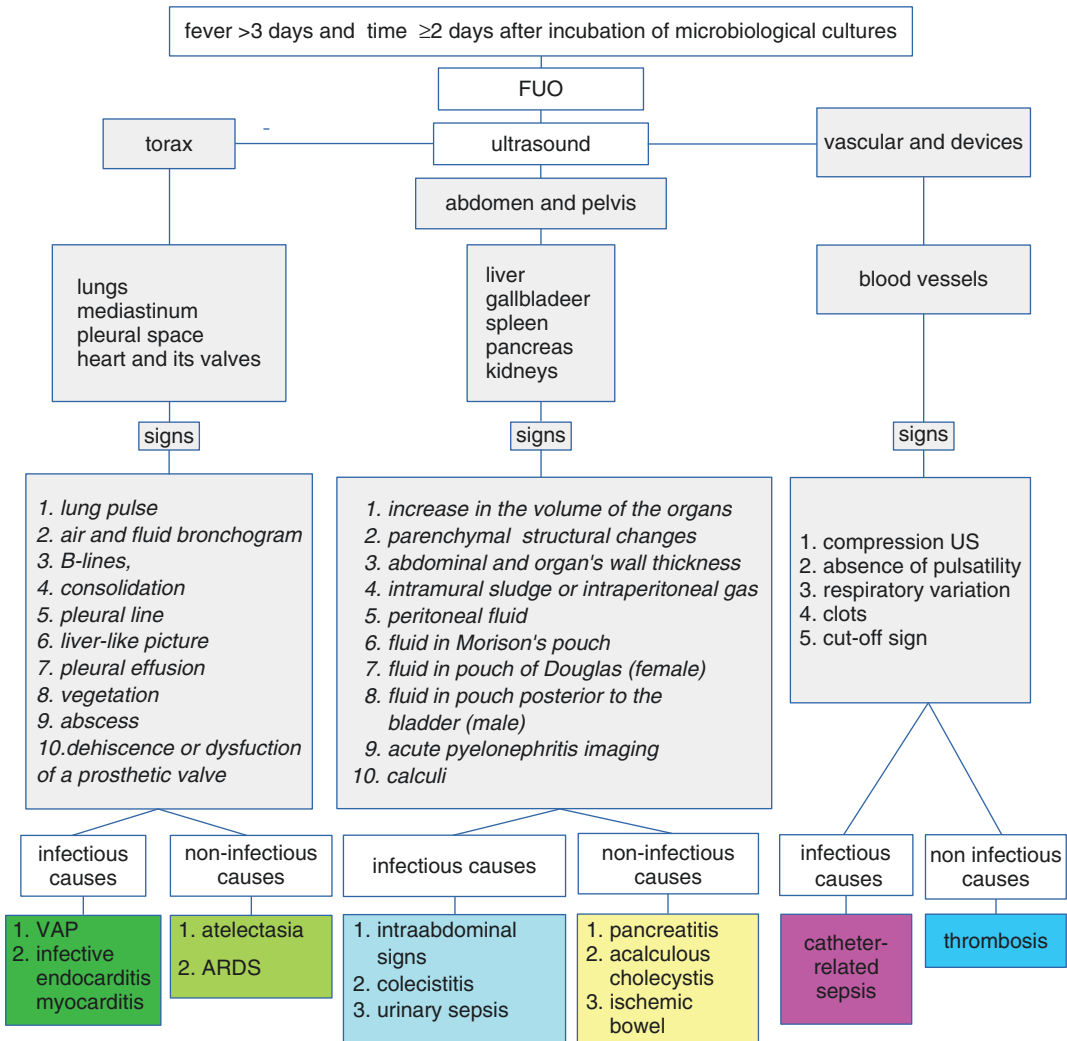4. Diffuse endothelial and epithelial injury

In all of the patients with ALI/ARDS the lung ultrasonographic picture is characteristic:

fever >3 days and time ≥2 days after incubation of microbiological cultures

FUO

torax — ultrasound — vascular and devices

abdomen and pelvis

lungs
mediastinum
pleural space
heart and its valves

liver
gallbladeer
spleen
pancreas
kidneys

blood vessels

signs

signs

signs

1. lung pulse
2. air and fluid bronchogram
3. B-lines,
4. consolidation
5. pleural line
6. liver-like picture
7. pleural effusion
8. vegetation
9. abscess
10. dehiscence or dysfuction of a prosthetic valve

1. increase in the volume of the organs
2. parenchymal structural changes
3. abdominal and organ's wall thickness
4. intramural sludge or intraperitoneal gas
5. peritoneal fluid
6. fluid in Morison's pouch
7. fluid in pouch of Douglas (female)
8. fluid in pouch posterior to the bladder (male)
9. acute pyelonephritis imaging
10. calculi

1. compression US
2. absence of pulsatility
3. respiratory variation
4. clots
5. cut-off sign

infectious causes

non-infectious causes

infectious causes

non-infectious causes

infectious causes

non infectious causes

1. VAP
2. infective endocarditis myocarditis

1. atelectasia
2. ARDS

1. intraabdominal signs
2. colecistitis
3. urinary sepsis

1. pancreatitis
2. acalculous cholecystis
3. ischemic bowel

catheter-related sepsis

thrombosis

Flowchart 59.1 FUO ultrasound assessment

(a) *B-lines:* vertical artifact, also called "comet-tail artifact," extending to the edge of the screen, moving within pleural line synchronously with inspiration and effacing A-lines. In ARDS b when the b-lines are bilateral and more than 3 the lung is defined "fully white lung."

(b) Spared areas: *areas of normal lung that are observed in at least one intercostal space, surrounded by areas of B-lines or white lung.*

(c) Consolidations: *consolidations may be located in the posterior lung fields, especially at the base.*

(d) Pleural line: *it is often involved. The pleural line appeared irregular, thickened, and coarse for the presence of multiple small subpleural consolidations. Involvement of the pleural line is not homogeneous and follows faithfully the distribution and the degree of the ARDS. "Lung sliding" is reduced.*

(e) Liver-like picture: *areas of "hepatization."*

59.2.2.1 Pancreatitis

US permits pancreas visualization in about 75–93% of the cases. The US examination cannot replace more efficient examination methods such

as CT or MRI, especially in the case of patients in whom parenchymal necrosis or abscesses of the abdominal cavity have to be detected.

CT scans should be used if the following occur:

1. Complications
2. Severe pain
3. Sepsis/shock
4. Prolonged intestinal paresis

If these signs are not present, US correlated with clinical data is usually conclusive.

The examination techniques are:

1. External
2. Endocavitary
3. Intraoperative

The external examination is the most frequently used.

The diagnosis of acute pancreatitis includes:

1. The increase in the volume of the pancreas region
2. Structural changes in the parenchyma
3. Significant decrease in echoes

59.2.2.2 Acalculous Cholecystitis

The diagnosis of acalculous cholecystitis should be considered in every critically ill patient who has clinical findings of sepsis with no obvious source.

It is an important "noninfectious" cause of fever in critically ill patients. Rapid diagnosis is essential because ischemia may progress rapidly to gangrene and perforation, with consistent increase in the already high morbidity and mortality.

The main signs are:

1. Wall thickness ≥3 mm is reported to be the most important diagnostic feature on ultrasound examination, with a specificity of 90% and a sensitivity of 100%.
2. Pericholecystic fluid.
3. Intramural sludge.

59.2.2.3 Ischemic Bowel

It represents a complex of diseases caused by impaired blood perfusion to the small and/or large bowel including:

1. Acute arterial mesenteric ischemia (AAMI)
2. Acute venous mesenteric ischemia (AVMI)
3. Nonocclusive mesenteric ischemia (NOMI)
4. Ischemia/reperfusion injury (I/R)
5. Ischemic colitis (IC)

At present, the reference diagnostic modality for intestinal ischemia is contrast-enhanced CT. In ICU not all patients with suspected bowel ischemia can be subjected to these examinations, so US could constitute a good imaging method as first examination in these patients with suspected bowel ischemia to rule out other abdominal pathologies.

AAMI In early phase of bowel ischemia, US examinations may show SMA (superior mesenteric artery) occlusion and bowel spasm. In late phase: fluid-filled luminal, bowel wall thinning, and evidence of extraluminal fluid.

AVMI In initial phase US may reveal thrombus, mural thickening, and edema of the affected bowel. In late stage US reveals mural thickening of the involved segment, intramural or intraperitoneal gas, and peritoneal fluid.

NOMI In the early phase, US findings are aspecific and poorly indicative. In the late phase, when there is severe necrosis of bowel wall, fluid collections and intramural gas could be found.

I/R As consequence of reperfusion, US may show fluid-filled lumen, bowel wall thickening, evidence of some extraluminal fluid, and decreased peristalsis.

IC US could be useful in the evaluation of location and length of the injured colonic segment and could also detect the wall thickening and stratification and the abnormal echogenicity of pericolic fat and the peritoneal fluid. Color

Doppler can be useful in differentiating between wall thickening from inflammatory or ischemic disease.

Thrombosis

Ultrasound is a useful diagnostic tool in the evaluation of patients presenting with signs and symptoms suggestive of a deep vein thrombosis (DVT) (see Chap. 50).

1. "Cut-off sign" is an abrupt loss of the high contrast interface between the venous lumen and the posterior venous wall.
2. Compression perpendicular to achieve complete collapse of the vein. The lumen of the vein must disappear completely in order to exclude the presence of a clot.
3. A clot may be seen as echogenicity within the lumen. However, in many instances the only evidence of a DVT will be the inability to compress the vein fully.

59.3 Infectious Causes

59.3.1 Ventilator-Acquired Pneumonia (VAP)

There is still no definitive validated diagnostic gold standard procedure in the diagnosis of VAP. The limited sensitivity of chest radiography has been well described, so early diagnosis of VAP remains a challenge to the intensivist.

The use of lung ultrasound, in combination with clinical and microbiologic data, can improve early diagnosis of VAP: US specificity is 88% and positive predictive value 86%.

The main signs are:

1. Small subpleural consolidations or lobar/hemilobar consolidations.
2. Bronchial tree filled with air and secretions appear as hyperechoic linear/arborescent bronchograms within lobar/hemilobar consolidations, moving synchronously with respiratory acts.
3. Pleural effusion.
4. Liver-like picture.

The presence of a consolidation pattern may represent pneumonia or atelectasis. Observing respiratory variance in air bronchograms, sonographic fluid and air bronchogram can help distinguish between them.

When pneumonia is complicated by lung abscess, it is identified at US as:

1. Hypoechoic lesion with a well-defined or irregular wall
2. Anechoic center sometimes with internal echoes and septations

59.3.2 Endocarditis and Myocarditis

It is clear that echocardiography has assumed a crucial role in the diagnosis of the endocarditis and myocarditis, particularly when blood cultures are negative.

The major echographic criteria for endocarditis are:

1. Vegetation
2. Abscess
3. New dehiscence of a prosthetic valve

Other echocardiographic features are not main criteria for endocarditis but may be suggestive of the diagnosis.

They include:

1. Valve destruction
2. Prolapse, aneurysm, and/or perforation of a valve

The Flowchart 59.2 shows the respective indications of Transthoracic (TTE) or transoesophageal echocardiography (TEE).

59.3.3 Myocarditis

Cardiac function may be monitored by serial echocardiograms.

In myocarditis echocardiographic findings include:

Flowchart 59.2 Task Force on the Prevention, Diagnosis, and Treatment of Infective Endocarditis (IE) of the European Society of Cardiology. *transthoracic echocardiography (TTE). **transesophageal echocardiography (TEE)
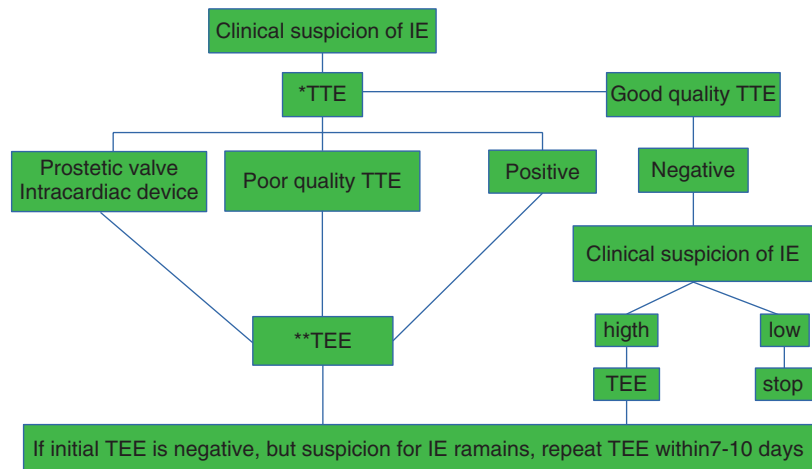
1. Wall motion abnormalities
2. Systolic dysfunction
3. Diastolic dysfunction

Echocardiographic characteristics are widely illustrated in the Chap. 24.

59.3.3.1   Abdominal Sepsis

The diagnostic approach to identify abdominal problems will differ depending upon the hemodynamic stability of the patient. So patients who have low systolic blood pressures may be too unstable to undergo studies that require moving from the ICU. Intra-abdominal pathology may be detected by ultrasound.

When critically ill patients are stable, computerized tomography (CT) is the imaging modality of choice for most intra-abdominal processes.

An exception to the use of CT scanning is evaluation of suspected biliary pathology, which is best imaged by ultrasound. It will identify calculous and acalculous cholecystitis and may show changes in the gallbladder or common bile duct associated with biliary obstruction.

Fluids must be sought at many sites:

1. Morison's pouch
2. Pouch of Douglas (posterior to the uterus) in the female
3. Pouch posterior to the bladder in the male
4. Between spleen and diaphragm
5. Around the liver

59.3.3.2   Cholecystitis

US has the best sensitivity and specificity for evaluating patients with suspected gallstones.

CT is the imaging modality of choice in the event of complications such as gangrenous cholecystitis, bile peritonitis, or biliary ileus.

The ecographic evaluation is useful for a percutaneous biliary drainage.

The main findings of acute calculous cholecystitis on US include:

1. The presence of stones.
2. Distension of the gallbladder lumen (length > 10 cm).
3. Gallbladder wall thickening (>3.5 mm) and a hyperemic wall. Thickening of the gallbladder wall in the absence of cholecystitis may be observed in systemic conditions, such as liver, renal, and heart failure.
4. A positive US Murphy sign: pain is provoked by either the transducer or the sonographer's palpation under guidance, in the exact area of the gallbladder.
5. Pericholecystic fluid.

59.3.3.3   Urinary Sepsis

Ultrasound scan is especially valuable for emergency imaging in patients with severe lower back pain and fever.

It can define:

1. Kidney size and renal scars.
2. Evaluation of prostate gland.
3. Various complications of acute pyelonephritis such as emphysematous pyelonephritis, renal abscess, and perirenal abscess.
4. Calculi are detected as echogenic structures with acoustic shadowing.
5. Cystitis: it is a clinical diagnosis; in most patients, imaging is not required.

However we can use ultrasonography to exclude secondary causes of cystitis.

Common to all forms of cystitis are:

- Bladder wall
- Mucosal thickening
- Irregularity
- Mucosal ulceration of varying intensity

Catheter-Related Sepsis (CRS)

CRS is closely related to catheter-related central vein thrombosis in ICU patients.

Many authors have reported a strong vulnerability to microbial colonization, probably resulting from ligands in the thrombus that promoted microbial adherence.

59.4   Sinusitis and Neutropenic Enterocolitis (NEC)

Separately we remember two important diseases:

1. Sinusitis
2. Neutropenic enterocolitis (NEC)

59.4.1 Sinusitis

The suspicion of maxillary sinusitis (MS) is generally established by the presence of fever without a clear clinical cause.

Sinus ultrasound has similar accuracy as sinus X-ray in the diagnosis of acute MS. US mode B compared to the CT is accurate in critical patients with 91% sensitivity and 92.5% specificity. So US mode B can be proposed as the first-line imaging method for the diagnosis of MS.

We can see two main imaging:

1. Normal ultrasound: an echographic line generated by the anterior sinusal wall that determines a posterior acoustic shadow
2. Sinusitis finding: presence of signs of sinusal occupation represented by the visualization of the posterior area of the maxillary sinus as an echogenic line

59.4.2 Neutropenic Enterocolitis (NEC)

NEC is not a widespread disease in ICU; however patients may die within hours from the onset of acute symptoms. So a swift diagnosis is imperative.

NEC is a life-threatening complication of chemotherapy in leukemic and solid tumor patients. Early diagnosis is crucial to start conservative medical treatment which appears the optimal strategy.

The initial symptoms are aspecific and very often consist of a combination of:

1. Crampy abdominal pain
2. A palpable mass and tenderness in the right lower quadrant with rebound tenderness (a sign of peritonism)
3. Fever
4. Diarrhea

Sepsis and signs of septic shock are life-threatening complications.

NEC should be always suspected in neutropenic patients with abdominal pain, fever, and diarrhea.

The characteristic sonographic features of NEC are:

1. Thickening (>4 mm) or dilation of small and/or large intestine
2. Transmural inflammatory reaction areas of different echogenicity caused by edema, necrosis, and/or circumscript hemorrhages
3. Intramural air suggests an infection with anaerobic bacteria
4. Pericolic fluid is a sign of possible perforation

The mortality rate associated with NEC is relatively high 50–100% in some reports: A swift diagnosis lowers the mortality to 14.5%.

Further Reading

Badea R. Ultrasonography of acute pancreatitis -an essay in. Images Rom J Gastroenterol. 2005;14:83–9.

Blaivas M. Lung ultrasound in evaluation of pneumonia. J Ultrasound Med. 2012;31:823–6.

Burke A. Fever of unknown origin: a clinical approach. Med J Med. 2015;128:1138.e1–1138 e15.

Dietrich CF. Sonographic signs of neutropenic enterocolitis. World J Gastroenterol. 2006;12:1397–402.

Habib G, et al. Recommendations for the practice of echocardiography in infective endocarditis. Eur J Echocardiogr. 2010;10:202–19.

Landò F, et al. Value of B-mode ultrasound for the diagnosis of maxillary sinusitis in critic patients. Revista De Imagenol. 2010;14:37–42.

Jitendranath L, et al. Work-up of fever of unknown origin in adult patients. Hosp Physician. 2005;9:15.

Marik PE. Fever in the ICU. Chest. 2000;117:855–69.

Sartelli M. A focus on intraabdominal infections. World J Emerg Surg. 2010;5:1–20.

Schenck EJ, et al. Ultrasound and management of the pneumonia current opinion in infectious. Diseases. 2016;29:223–8.

Shyr-Chyr C, et al. Accuracy of ultrasonography in the diagnosis of peritonitis compared with the clinical impression of the surgeon. Arch Surg J. 2000;135:170–3.

Habib G, Lancellotti P, Antunes MJ, Bongiorni MG, Casalta JP, Del Zotti F, Dulgheru R, El Khoury G, Erba PA, Iung B et al European Heart Journal, 2015, 36, Issue 44, 3075–3128.

Vandenbussche T. Value of antral puncture in the intensive care patient with fever of unknown origin. Laryngoscope. 2000;110:1702–6.

Zierler BK. Ultrasonography and diagnosis of venous thromboembolism. Circulation. 2004;109:9–14.

US-Guided Regional Analgesia in the ICU

60

Stefano Secchi, Juri Valoriani, and Paolo Cecconi

Most patients admitted to the intensive care unit need analgesia and sedation. It is estimated that 50–70% of patients have had a painful experience during hospitalization. Nonetheless, 95% of the physicians and 80% of nurses believe that analgesia is adequate. There are many causes of pain in the intensive care unit: the traumatic and/or surgical pathology that causes hospitalization, nursing, mobilization and prolonged immobilization, physiotherapy, invasive diagnostic, and therapeutic procedures. A multimodal approach to pain therapy should include treatment of the cause of pain and reduce discomfort related to the position, to invasive devices and to physiotherapy. The methods of pain assessment include various objective scales: visual analogue scale (VAS), visual rating scale (VRS), and numerical rating scale (NRS). In case the patient is uncooperative, facial expression, upper limbs, and compliance with ventilation should be evaluated according to Behavioral Pain Scale (BPS). State of agitation and physiological stress (blood pressure, heart rate, respiratory rate, intracranial pressure, diaphoresis) should be evaluated too. A proper pain control allows better ventilation

and weaning, early mobilization, lower levels of circulating catecholamines, and lower oxygen consumption. The regional analgesia, using single-injection regional blocks and continuous neuraxial and peripheral catheters, allows the maintenance of analgesia without centrally acting drugs or using low doses (opioids) and also the suspension of daily sedation. Several complications like delirium, mental status changes, and gastrointestinal dysfunction can therefore be reduced or minimized. There are contraindications like coagulation disorders, hemodynamic instability, and difficulty in neurological evaluation which could require an assessment of risks and benefits.

## 60.1 Regional Anesthesia/ Analgesia

Regional anesthesia was born with anatomical knowledge, using paresthesias and drowning the nerve with the local anesthetic.

In 1962 electrical neurostimulation (ENS) is introduced allowing the reduction of nerve damage and further spread of regional anesthesia. In 1999 the stimulated catheter is introduced.

With the use of ultrasounds, the approach to regional anesthesia changes: you no longer need any cutaneous landmarks; you can see the nerve fiber to block and what is in the surroundings.

S. Secchi (✉) · J. Valoriani · P. Cecconi
Anesthesia and Intensive Care Department, Santa Maria Annunziata Hospital, Azienda USL Toscana Centro, Florence, Italy
e-mail: stefano.secchi@uslcentro.toscana.it;
juri.valoriani@uslcentro.toscana.it;
paolo.cecconi@uslcentro.toscana.it

Fig. 60.1 Linear probe: ultrasound scan of the posterior chest wall showing the transversal process (TP), external intercostal muscle (EIM), pleura, and paravertebral space (PVS)
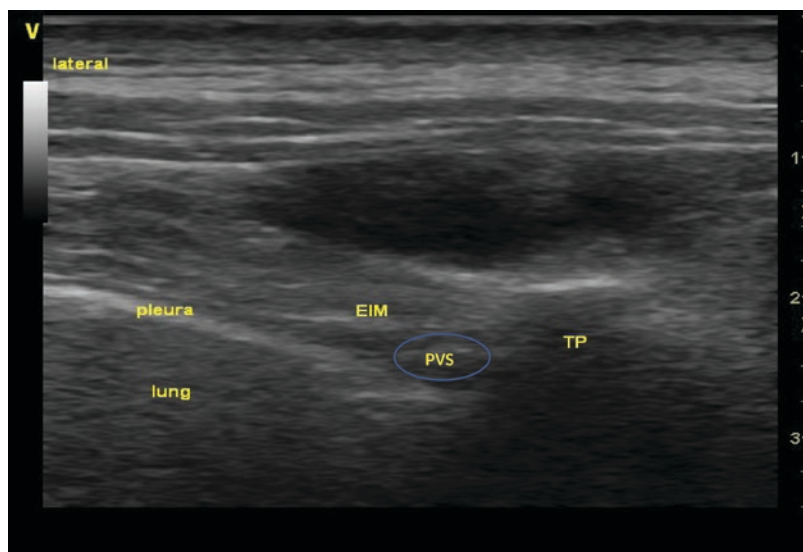
The advantage of ultrasound is that it enhances the possibility to see anatomic variability present in nature and the course of the needle with improved performance. Ultrasounds permit faster block performances or fewer attempts of needle redirection, a faster initial onset of block, and a reduced dose of local anesthetic. Nonetheless, nerve injuries are not excluded.

Security is a mixture of craftsmanship, materials, and good judgment. The three hinges to reduce the incidence of lesion are:

- Ultrasound
- Electrical neurostimulation
- Injection pressure control

In his classic text, *Regional Anesthesia: its technic and clinical application*, Labat concludes "Regional Anesthesia is an art. Remembering that even expert may fail, we should try often and again observing scrupulously its principles until we succeed."

60.2 Paravertebral Block

Thoracic paravertebral block is a possible alternative to epidural analgesia. Paravertebral space is well defined laterally to the spine; it is bounded anteriorly by the parietal pleura, medially by the face of the vertebral body (transversal process, TP), and posteriorly by the internal intercostal membrane and external intercostal muscle (EIM) (Fig. 60.1). The patient is placed in lateral decubitus, in a sitting or prone position. You are using a high-frequency linear probe. You can start with a transverse interspinous space scan, and then move sidewise until the transverse process appears in the middle of the screen. Then you slightly rotate the probe on the coronal plane, and move caudally until paravertebral space target appears.

60.2.1 Paravertebral Block Out of Plane

The puncture site is 1 cm below the long axis of the probe, orientating the needle toward cranial direction to reach the parietal pleura. The tip of the needle should go beyond the internal intercostal membrane (IIM) where local anesthetic will be injected slowly. The block provides adequate analgesia in the land between the upper and lower body segments.

60.2.2 Paravertebral Block in Plane

You can use two scans:

1. Paravertebral longitudinal scan: you seek two adjacent transverse processes, and then you move medially until you visualize the internal intercostal membrane and the pleura.

   The needle is inserted 1 cm below the short axis of the probe.

2. Transverse scanning previously described: the puncture site is 1 cm off the minor axis of the probe. The disadvantage of this approach is that the needle moves toward the intervertebral foramina and the epidural space.

60.3 Intercostal Nerve Block

• Directions: pain from rib fractures and postoperative pain control.

The patient is positioned sideways, sitting or prone. You are using a high-frequency probe which allows you to see the ribs, the intercostal muscles, and the pleura (Fig. 60.2).

It exploits the costal angle area at about 7 cm from the interspinous line. In this point the rib is thicker and the costal groove is wider and the lateral nerve branch has not yet separated.

You place the probe on the sagittal plane, and you view two adjacent ribs in short axis. The block is executed with the needle visualization in long axis. When the needle point exceeds the internal intercostal muscle, after testing negative suction, inject a test dose of local anesthetic just by looking at the spread.

There are studies that compare the peripheral nerve block with epidural analgesia for patients with rib fractures. Truitt MS. concludes that the use of peripheral nerve blocks improves lung function and pain control and shortens hospital stay. Britt T. does not detect differences with epidural analgesia in the incidence of pneumoniae or respiratory failure; he rather points out fewer complications and contraindications.

60.4 Epidural Analgesia

Continuous epidural analgesia remains the most commonly utilized regional analgesia technique in ICU. There are several studies that show benefits regarding outcome parameters like mortality, length of ICU stay, length of ventilator support, rate of nosocomial pneumoniae, improving

Fig. 60.2 Linear probe. The intercostal space, external intercostal muscle (EIM), internal intercostal muscle (IIM), and intercostal nerve (IN)
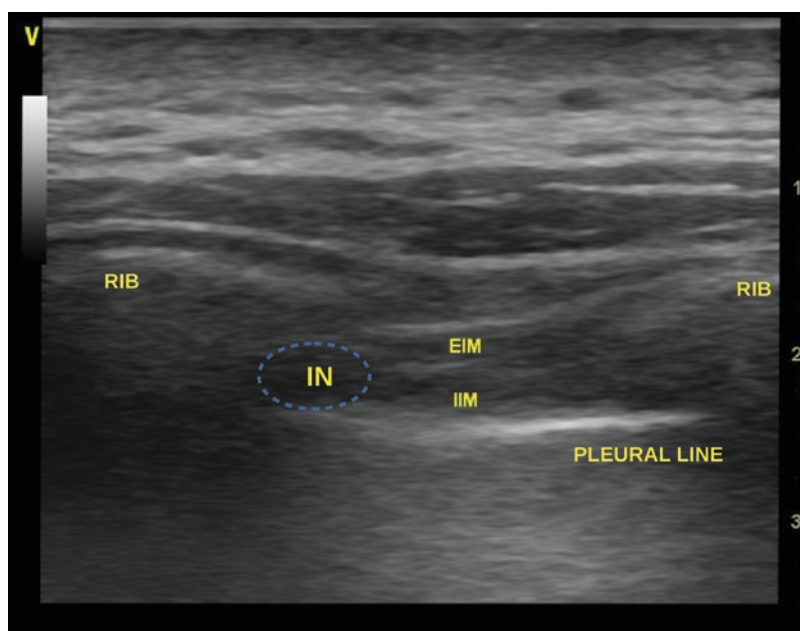
pulmonary function test, incidence of ileus, improved analgesia, and patients' satisfaction.

Indications for epidural catheters in ICU:

1. Chest trauma and surgery (multiple rib fracture, esophageal surgery)
2. Cardiac surgery
3. Abdominal surgery
4. Orthopedic surgery of pelvis and lower extremities
5. Paralytic ileus, pancreatitis, cancer pain, pelvic malignancies, peripheral vascular diseases of lower extremities

Contraindications:

1. Uncooperative patient
2. Raised intracranial pressure
3. Coagulophathy
4. Bacteremia and sepsis
5. Local infections at the puncture site
6. Severe hypovolemia and acute hemodynamic instability
7. Obstructive ileus
8. Lack of physicians' experience

From NICE guidance in 2008:

> evidence on ultrasound-guided catheterization of the epidural space is limited in amount, but suggests that it is safe and may be helpful in achieving correct placement.

In expert hands, the use of ultrasound for epidural needle insertion was shown to reduce the number of puncture attempts, improves the probability of success on the first attempt, reduces the need to puncture multiple levels, and improves patient comfort during the procedure.

60.4.1 US Imaging of the Lumbar Spine

US imaging of the spine requires the use of a low frequency convex probe that has a large acoustic window and a high penetrance. The patient is positioned in the sitting or lateral position, the lumbosacral spine maximally flexed. The transducer is placed 1–2 cm lateral to the spinous process (*paramedian sagittal plane*) with its orientation marker directed cranially. The US visibility of neuraxial structure can be improved if the vertebral spine is viewed in the paramedian oblique sagittal plane. The transducer is positioned 2 cm lateral to the midline in the sagittal axis, and it is tilted slightly medially (*paramedian oblique sagittal scan* Fig. 60.3). The sacrum is identified as a flat hyperechoic structure.

When the transducer is slid in a cranial direction, a gap is seen between the sacrum and the lamina of the L5 vertebra, which is the L5-S1 interlaminar space. The L3-L4 and L4-L5 interlaminar space can be located by counting upward. You see a sawtooth picture (Fig. 60.4).

The interlaminar space is the gap between two adjoining laminas, and it is the acoustic window, through which the neuraxial structures are visualized within the spinal canal. The ligamentum flavum (LF) appears as a hyperechoic band, the posterior dura is the next hyperechoic structure anterior to the ligamentum flavum, and the epidural space is the hypoechoic area between the LF and the posterior dura. The LF, the epidural space, and the dura mater are called posterior complex. Intrathecal space is uniformly hypoechoic.

The anterior dura, the back surface of the vertebral body, and the posterior ligament are visible as a single hyperechoic line called anterior complex. When the US probe is positioned over the spinous process (*median transverse approach*) and the lamina, they are seen as a hyperechoic reflection anterior to which there is a dark acoustic shadow that obscures the underlying spinal canal. If the transducer is slid slightly cranially or caudally, it is possible to see a picture of a bat (Fig. 60.5). In the transverse interspinous view, the posterior dura, the thecal sac, and the anterior complex can be visualized. The articular processes and the transverse processes are visualized laterally. Medial-transverse approach can be used to examine rotational deformities of the vertebra. US imaging of the thoracic spine is more challenging than imaging of the lumbar spine. The sonographic appearance of the neuraxial

Fig. 60.3 Convex probe: paramedian sagittal sonogram of the lumbosacral junction
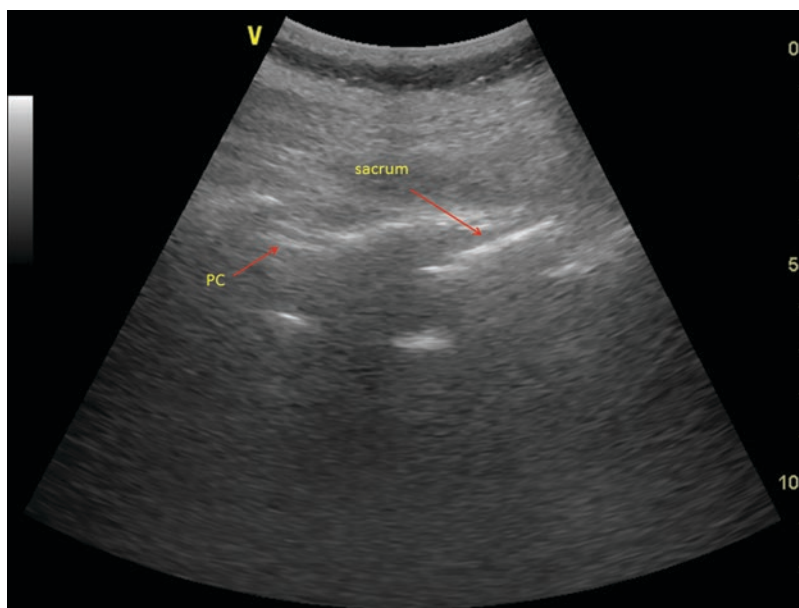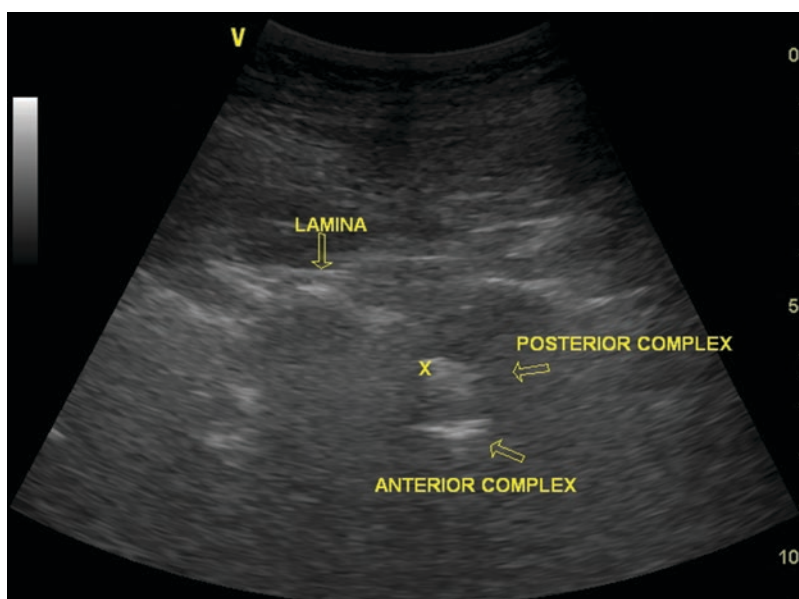

Fig. 60.4 Paramedian sagittal sonogram of the lamina showing the L3-L4 interlaminar space, x = epidural space

structures is comparable to that in the lumbar region, but in the midthoracic region, there is a narrower acoustic window with limited visibility of the underlying neuraxial anatomy.

Grau reports that the transverse axis produces the best images of the neuraxial structures and that the epidural space is best visualized in the paramedian scan.

Sonographic evaluation prior to the procedure:

• Allows you to choose the most suitable level of puncture in patients with difficult landmarks
• Allows the estimation of the depth of the epidural space and of any anatomical abnormalities of the spine

Fig. 60.5 Convex probe: median transverse scan: articular process. The ligamentum flavum is the first echogenic structure visible from the skin. Deeply, you can see the perimedullar structures
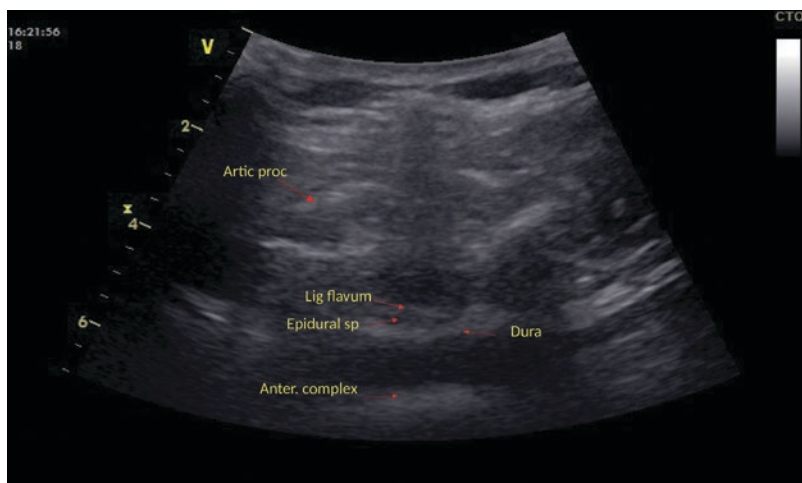
Elsharkawy describes a technique that uses color Doppler and M-mode US to determine the position of the epidural catheter.

60.5 Nerve Block

60.5.1 Analgesia for the Upper Limb

A detailed description of anatomy of the brachial plexus is beyond the purpose of this book.

The most used techniques of analgesia for the upper limb are interscalene, supraclavicular, infraclavicular, and axillary blocks. Each of these blocks presents unique challenges and indications. We briefly review the sonographic anatomical landmark, indication, and complication of these approaches to the brachial plexus.

60.5.2 Ultrasound-Guided Interscalene Brachial Plexus Block

- Indications: shoulder and arm analgesia and surgery.
- Ultrasound anatomy: with a plane probe, explore the supraclavicular region, and locate the subclavian artery with nervous structure around. Move the probe cranially, following

the nerve trunks. The probe needs to be stopped at the best position for each patient.
- Purpose: direct view of spread of local anesthetic around superior and middle trunks of the brachial plexus (in-plane view).

Patient in semi-lateral, semi-sitting, or supine position, with the patient head turned away from the side to be blocked.

The interscalene approach to the brachial plexus blockade results in analgesia and anesthesia of the shoulder and upper arm (Fig. 60.6).

60.5.3 Ultrasound-Guided Supraclavicular Brachial Plexus Block

- Indications: arm, elbow, forearm, and hand analgesia and surgery.
- Transducer position: supraclavicular region.
- Purpose: direct view of spread of local anesthetic around the brachial plexus, lateral and superficial to the subclavian artery (Fig. 60.7).

Patient in supine or semi-sitting position with the patient head turned away from the side to be blocked.

This block produces analgesia and anesthesia of the upper limb below the shoulder.

Fig. 60.6 Linear probe, in-plane technique interscalene brachial plexus block. The carotid artery (CA), anterior scalene muscle (ASM), middle scalene muscle (MSM), sternocleidomastoid muscle (SCM), and brachial plexus (BP). This approach to the brachial plexus allows analgesia and/or anesthesia of the shoulder and arm
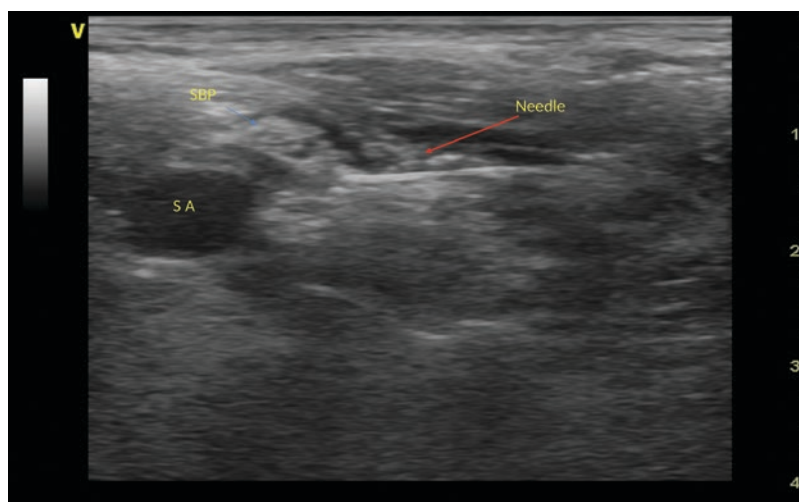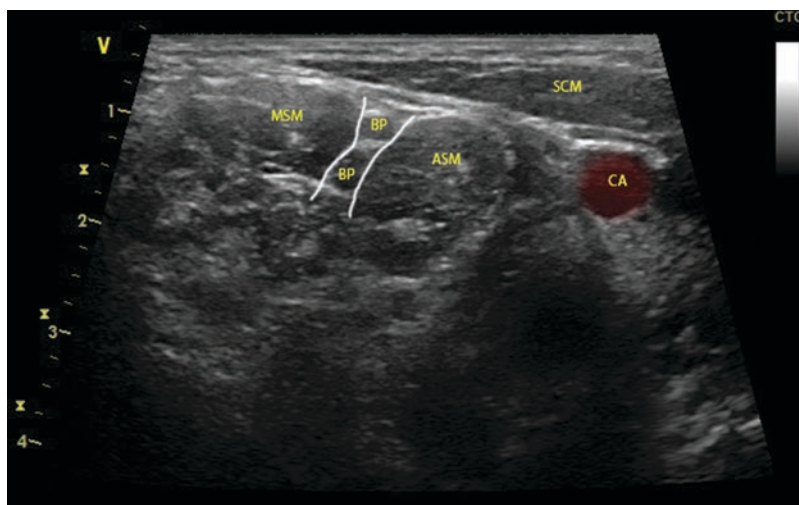

Fig. 60.7 Linear probe: in-plane technique supraclavicular approach to the brachial plexus. The subclavian artery (SA) and supraclavicular brachial plexus (SPB). Local anesthetic spread can be appreciated around the nervous structures. Doppler exploration of the area, before the block is recommended in order to look for blood vessels. This technique is useful for analgesia and anesthesia of the entire upper limb, except for the medial aspect of the arm

60.5.4 Ultrasound-Guided Infraclavicular Brachial Plexus Block

- Indications: arm, elbow, forearm, and hand analgesia and surgery.
- Transducer position: approximately parasagittal, just medial to coracoid process, inferior to clavicle.
- Purpose: local anesthetic spreads around the axillary artery.

Patient in supine position with the head turned away from the side to be blocked. Arm is abducted to 90° and the elbow flexed.

This block produces analgesia and anesthesia of the upper limb below the shoulder.

The skin of the medial portion of the arm receives sensitive innervation from T2 and is never anesthetized by any approach to brachial plexus block.

Comparison of supraclavicular brachial plexus block (SC-BPB) and infraclavicular brachial plexus block (IC-BPB) is recently published in a systematic review of randomized controlled trials.

The SC-BPB, in respect to IC-BPB, is associated to a more frequent incidence of phrenic nerve palsy (PNP) (34% vs 3%, by measuring diaphragmatic function using M-mode ultrasonography). Clinically relevant PNP is not described. However a patient history of pneumonectomy or severe respiratory disease must be taken into account when choosing between these anesthetic approaches. Horner syndrome incidence is 32.1% for SC-BPB vs 3.2% for IC-BPB. No treatment is required because of the temporary nature of the syndrome.

Pneumothorax is a feared complication of these approaches to BPB, reaching 4% in case of blind SC-BPB and 1% in case of blind IC-BPB. Ultrasonography dramatically reduces, but not zeroes, even in expert hands, this complication.

In today's available literature, there are no differences between these two approaches to the brachial plexus for performance time, onset and duration of sensory block, and incidence of successful blockade. However, two studies report incomplete ulnar block in the case of SC-BPB. These reports are not confirmed by other studies. IC-BPB was associated with incomplete radial block in many reports, if performed with a single-injection technique. The use of double or triple injection technique reduces drastically the radial sparing. It may be difficult, with a single-injection technique, to reach the posterior cord of the brachial plexus at infraclavicular region. Another possible issue to explain the radial sparing in IC-BPB, even with the use of ultrasonography and performing an injection posterior to the axillary artery, was the leak of local anesthetic in the thoracoscapular space.

60.5.5 Ultrasound-Guided Axillary Brachial Plexus Block

- Indications: forearm and hand analgesia and surgery.
- Transducer position: linear probe, just distal to pectoralis major insertion (Fig. 60.8).

Patient in supine position and abduction of the arm 90°.

Fig. 60.8 Linear probe, in-plane technique. Axillary brachial plexus block. The axillary artery (AA) and brachial plexus (BP). This approach to the brachial plexus produces analgesia and anesthesia of the upper limb from elbow to hand. In order to accomplish this procedure, you need to look for musculocutaneous nerve that leaves the brachial plexus proximally
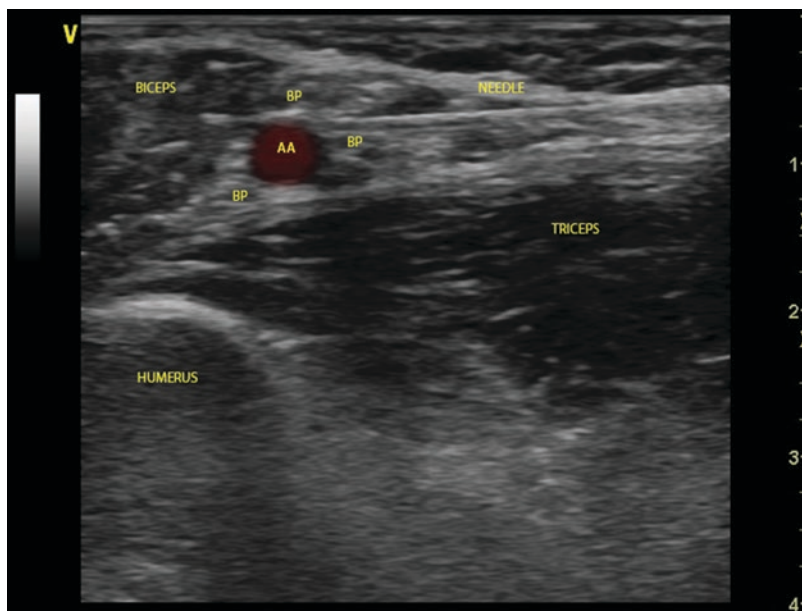
Fig. 60.9 Fascia iliaca block: local anesthetic (LA). The iliac muscle (IM). This block can be performed in order to obtain analgesia and seldom anesthesia of the inferior limb in the area reached by local anesthetic. Femoral nerve and femorocutaneous nerve can usually be blocked. The purpose of this block is to view local anesthetic spread underneath the fascia iliaca
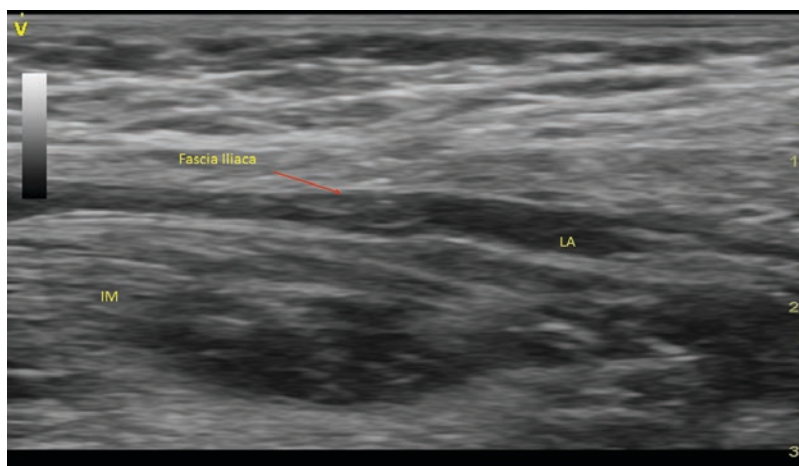
This block produces analgesia and anesthesia of the mid-arm down to the hand.

60.6   Inferior Limb

60.6.1 Ultrasound-Guided Femoral Nerve Block

- Indications: anesthesia and analgesia of anterior thigh, femur, and knee surgery.
- Transducer position: linear probe, transverse, close to femoral crease.
- Purpose: spread of local anesthetic around the femoral nerve.

  Patient position and distribution of blockade:

- Patient in supine position. This block produces analgesia and anesthesia of the anterior and medial thigh down to knee included. It produces also anesthesia of a variable portion of skin on the medial leg and foot.

60.6.2 Ultrasound-Guided Fascia Iliaca Block

- Indications: anterior thigh and knee surgery and analgesia for hip and knee procedures.
- Transducer position: linear probe, transverse, close to the femoral crease, and lateral to the femoral artery.

- Purpose: local anesthetic spread underneath fascia iliaca (Fig. 60.9). This block is usually performed with high volume (40 ml) and low concentration of local anesthetic (e.g., ropivacaine 0.2%). Traditionally, it was believed that the local anesthetic could spread proximally toward the lumbosacral plexus.
- Patient positioning: supine position.

60.6.3 Ultrasound-Guided Popliteal Sciatic Block

- Indications: foot and ankle analgesia and surgery.
- Transducer position: usually linear probe, transverse, on the lateral aspect of thigh, or over popliteal fossa.

  Patient position and distribution of blockade:

- In supine position and in oblique or lateral decubitus, a slight knee flexion is required.
- This block produces anesthesia of the lower limb below the knee, except a portion of skin innervated by the saphenous nerve (Fig. 60.10).

60.6.4 TAP (Transversus Abdominis Plane) Block

- Indications: analgesia for laparotomy, appendicectomy, cesarean delivery, and alternative

Fig. 60.10 Linear probe: in-plane technique, popliteal sciatic nerve block. Sciatic nerve (SN). It can be visible local anesthetic spread around the nerve. This approach is indicated for analgesia and anesthesia below the knee
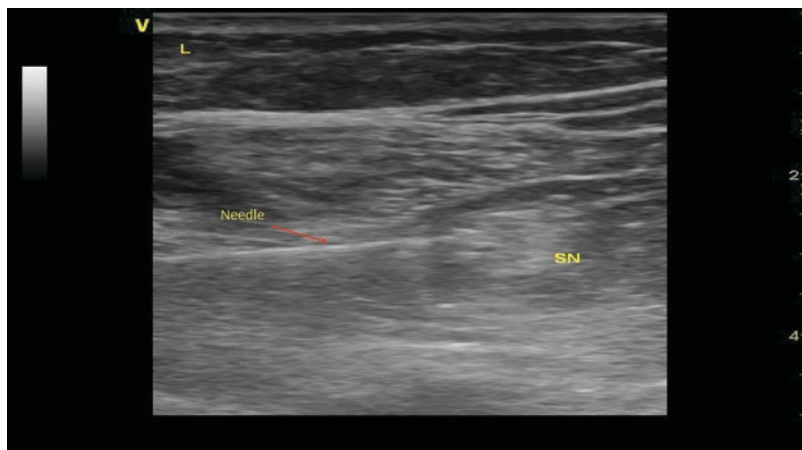
to epidural anesthesia for operation on the abdominal wall.

- Transducer position: transverse on the abdomen, at the anterior axillary line, and between the costal margin and the iliac crest.
- Purpose: spread of local anesthetic between the internal oblique muscle and transverse muscle.
- Supine position. The extension of the block is not consistently reproduced in clinical practice. It can be usually reached a block from T10 to L1.

60.7 Complications and Side Effects of Peripheral Nerve Blocks

- Failed blocks: this event, usually, reflects an inadequate time period elapsing between injection of the anesthetic and the start of the operation. A reason for a slow induction is the anatomical disposition of the septa, with the relative lack of communication pathways between compartments.
- Nerve injuries: one of the most feared complications of regional anesthesia; it is relatively rare with an incidence of 2.4–4/10000 blocks. However transient neurological symptoms lasting up to 2 weeks are frequently observed (8.2–15%). Most evidence arises from animal studies, especially for mechanical pressure and chemical toxicity. Neurological function

after a PNB has to be considered as a spectrum from normal function to complete nervous damage. Neurological damage in PNB is multifactorial; the multiple risk factors are classified in host factors (comorbidity), agent (chemical insults, mechanical, pressure) and environmental (US+ENS, US/ENS guidance, safe practice). The final event, the development of nervous damage, is the result of a chain of interactions.

- Infection: perineural catheter (PNC) infection is defined as signs of systemic infection (leukocytosis, positive blood cultures, fever, markers infection/inflammation) in a patient with signs of catheter entry site inflammation or evidence of cellulitis, abscess, and pyomyositis. Most studies report an incidence <1%. Life-threatening infections are rare. One report of a lethal infection is published in literature after a one-shot axillary block. Otherwise, catheter tip colonization is most common, ranging from 6% to 57%.
- Pathogenesis of PNC infection: three mechanisms have been proposed – (1) catheter bloodstream infection from a distant foci, (2) catheter infection after drug contamination, and (3) pathogen penetration. It probably represents the major role in catheter infection, in a way not dissimilar from CVC infection.
- Risk factors for PNC infection and prevention: diabetes mellitus, postoperative hyperglycemia in nondiabetic patients, drug abuse, coexisting malignancies, immunosuppression,

trauma, and ICU stay. PNC location (axillary> femoral> interscalene) and catheter life (>48 h) seem to be considered as independent risk factors; however evidence is inconsistent. Skin disinfection and a strict aseptic technique are strongly recommended. Antiseptic dressing, micropore filters, catheter tunneling, and aseptic preparation of the drug that needs to be infused are also useful in preventing PNC infection.

- Vascular lesion: may be avoided with use of ultrasound technique.
- High spinal block: interscalene block may be complicated by injection of local anesthetic in epidural space or subarachnoid space.
- Toxic reactions: these usually occur after reabsorption of local anesthetic.

Bibliography

Arcand G, Williams SR, Chouinard P, et al. Ultrasound-guided infraclavicular versus supraclavicular block. Anesth Analg. 2005;101:886–90.

Britt T, Sturm R, Ricardi R, Labond V. Comparative evaluation of continuous intercostal nerve block or epidural analgesia on the rate of respiratory complications, intensive care unit, and hospital stay following traumatic rib fractures: a retrospective review. Local Reg Anesth. 2015;8:79–84.

Capdevila X. Infectious risk of continuous peripheral nerve blocks. Anesthesiology. 2009;110(1):182–8.

Ehieli E, Yalamuri S, Brudney CS, Pyati S. Analgesia in the surgical intensive care unit. Postgrad Med J. 2017;93(1095):38–45.

Grau T, Leipold RW, Conradi R, Martin E, Motsch J. Efficacy of ultrasound imaging in obstetric epidural anesthesia. J Clin Anesth. 2002;14(3):169–75.

Hajiesmaeili MR, Motavaf M, Safari S. Regional analgesia in intensive care unit. Anesth Pain Med. 2013;3(2):263–5.

Jakobsson J, Johnson MZ. Perioperative regional anaesthesia and postoperative longer-term outcomes. F1000Res. 2016 Oct 11;5. pii: F1000 Faculty Rev-2501. eCollection 2016. Review. PubMed PMID: 27785357; PubMed Central PMCID: PMC5063036.

Klaastad O, Lilleås FG, Røtnes JS, Breivik H, Fosse E. A magnetic resonance imaging study of modifications to the infraclavicular brachial plexus block. Anesth Analg. 2000;91:929–33.

Nicolotti D, Iotti E, Fanelli G, Compagnone C. Perineural catheter infection: a systematic review of the literature. J Clin Anesth. 2016;35:123–8.

Nseir S. Fatal streptococcal necrotizing fasciitis as a complication of axillary brachial plexus block. Br J Anaesth. 2004;92:427–9.

Park S-K, Lee S-Y, Kim WH, Park H-S, Lim Y-J, Bahk J-H. Comparison of supraclavicular and infraclavicular brachial plexus block: a systemic review of randomized controlled trials. Anesth Analg. 2017;124:636–44.

Perna P, Gioia A, Ragazzi R, Volta CA, Innamorato M. Can pre-procedure neuroaxial ultrasound improve the identification of the potential epidural space when compared with anatomical landmarks? A prospective randomized study. Minerva Anestesiol. 2017;83(1):41–9.

Rawal N. Epidural technique for postoperative pain: gold standard no more? Reg Anesth Pain Med. 2012;37(3):310–7.

Sandhu NS, Capan LM. Ultrasound-guided infraclavicular brachial plexus block. Br J Anaesth. 2002;89:254–9.

Schulz-Stübner S, Boezaart A, Hata JS. Regional analgesia in the critically ill. Crit Care Med. 2005;33(6):1400–7. Review PubMed PMID: 15942362.

Sondekoppam RV, Tsui BCH. Factors associated with risk of neurologic complications after peripheral nerve blocks: a systematic review. Anesth Analg. 2017;124:645–60.

Wiebalck A, Grau T. Ultrasound imaging techniques for regional blocks in intensive care patients. Crit Care Med. 2007;35(5 Suppl):S268–74.